



INSTITUTE FOR DEFENSE ANALYSES

User-Oriented Measures of Effectiveness for the Evaluation of Transport and Dispersion Models

Steve Warner, Project Leader
Nathan Platt
James F. Heagy
Institute for Defense Analyses
Alexandria, Virginia

Scott Bradley
George Bieberbach
Logicon Advanced Technology
Alexandria, Virginia

Gayle Sugiyama
John S. Nasstrom
Kevin T. Foster
David Larson
Atmospheric Sciences Division
Lawrence Livermore National Laboratory
Livermore, California

January 2001

Approved for public release;
distribution unlimited.

IDA Paper P-3554
Log: H 00-002142

Form SF298 Citation Data

Report Date ("DD MON YYYY") 01012001	Report Type Final	Dates Covered (from... to) ("DD MON YYYY")
Title and Subtitle User-Oriented Measures of Effectiveness for the Evaluation of Transport and Dispersion Models		Contract or Grant Number
		Program Element Number
Authors Dr. Steve Warner Dr. Nathan Platt Dr. James F. Heagy		Project Number
		Task Number
		Work Unit Number
Performing Organization Name(s) and Address(es) Institute for Defense Analyses 1801 N. Beauregard St. Alexandria, VA 22311		Performing Organization Number(s)
Sponsoring/Monitoring Agency Name(s) and Address(es)		Monitoring Agency Acronym
		Monitoring Agency Report Number(s)
Distribution/Availability Statement Approved for public release, distribution unlimited		
Supplementary Notes		
Abstract		
Subject Terms		
Document Classification unclassified		Classification of SF298 unclassified
Classification of Abstract unclassified		Limitation of Abstract unlimited
Number of Pages 815		

This work was conducted under contract DASW01 98 C 0067, Task DC-9-1767, for the Defense Threat Reduction Agency. The publication of this IDA document does not indicate endorsement by the Department of Defense, nor should the contents be construed as reflecting the official position of that Agency.

**© 2000, 2001 Institute for Defense Analyses, 1801 N. Beauregard Street,
Alexandria, Virginia 22311-1772 • (703) 845-2000.**

**This material may be reproduced by or for the U.S. Government pursuant
to the copyright license under the clause at DFARS 252.227-7013
(NOV 95).**

INSTITUTE FOR DEFENSE ANALYSES

IDA Paper P-3554

**User-Oriented Measures of Effectiveness
for the Evaluation of Transport and
Dispersion Models**

Steve Warner, Project Leader
Nathan Platt
James F. Heagy
Institute for Defense Analyses
Alexandria, Virginia

Scott Bradley
George Bieberbach
Logicon Advanced Technology
Alexandria, Virginia

Gayle Sugiyama
John S. Nasstrom
Kevin T. Foster
David Larson
Atmospheric Sciences Division
Lawrence Livermore National Laboratory
Livermore, California

PREFACE

The Institute for Defense Analyses (IDA) prepared this paper for the Defense Threat Reduction Agency (DTRA), in partial fulfillment of the task “Support for DTRA in the Validation Analysis of Hazardous Material Transport and Dispersion Prediction Models.” The objective of this effort was to conduct analyses and special studies associated with the verification, validation, and accreditation (VV&A) of hazardous transport and dispersion prediction models. This task involves the comparison of two models: DTRA’s Hazard Prediction and Assessment Capability (HPAC) and Lawrence Livermore National Laboratory’s (LLNL) National Atmospheric Release Advisory Center (NARAC) modeling system. An additional component of this task, addressed in this report, is the exploration and development of validation and accreditation measures of effectiveness for transport and dispersion models.

The IDA Technical Review Committee was chaired by Thomas P. Christie and consisted of John N. Bombardt Jr., Arthur Fries, Jeffrey H. Grotte, David A. McWhorter, and Jozsef A. Toth. The authors would like to thank Allan Reiter (DTRA), Leon Wittwer (DTRA), and Don Ermak (LLNL) for their comments, critiques, and support throughout this effort.

The LLNL work was performed under the auspices of the U.S. Department of Energy by University of California Lawrence Livermore National Laboratory under contract No. W-7405-Eng-48.

USER-ORIENTED MEASURES OF EFFECTIVENESS FOR THE EVALUATION OF TRANSPORT AND DISPERSION MODELS

TABLE OF CONTENTS

SUMMARY	1
A. Background	1
B. Purpose	1
C. User-Oriented Measures of Effectiveness (MOEs).....	1
D. Conclusions Based on the Examination of MOE Estimates	8
E. Outline of This Paper	12
1. INTRODUCTION	1-1
A. Background	1-1
1. Brief HPAC Description.....	1-3
2. Brief NARAC Description	1-3
B. Description of the <i>Prairie Grass</i> Field Trial Experiment	1-4
C. Near-Term Planned Comparisons	1-6
References.....	1-R-1
2. METHODOLOGIES.....	2-1
A. Background	2-1
B. Comparative Measures	2-3
1. Measures of Effectiveness.....	2-3
a. User-Oriented Measure of Effectiveness: MOE 1	2-4
b. A Two-Dimensional MOE: MOE 2	2-8
c. Interpretation of MOE 2	2-8
d. Relationship Between MOE 1 and MOE 2	2-12
e. Two Estimates of “Area” Size.....	2-13
f. Application of Probit Curves as a “Lethality/Effects Filter” ..	2-15
2. Statistical Measures	2-18
3. Estimation of Confidence Intervals	2-21
C. Trial Conditions That Were Examined	2-23
1. <i>Prairie Grass</i> Field Trial Data Were Collected Along Five Arcs..	2-23
2. Stability Category Groupings	2-26
3. Thresholds for Sampler Observations	2-26
4. Comment: Value of Graphics Tools	2-28
References.....	2-R-1
3. RESULTS, ANALYSES, AND DISCUSSION.....	3-1
A. Comparisons of HPAC and NARAC Predictions with MOEs.....	3-1
1. MOE 1	3-1

a.	Across All Trials	3-1
b.	As a Function of Range.....	3-3
c.	As a Function of Stability Category	3-3
2.	MOE 2	3-4
a.	Across All Trials	3-4
b.	As a Function of Range.....	3-6
c.	As a Function of Stability Category	3-9
	d. Lethality/Effects Filter Results.....	3-12
3.	HPAC Predictions: Excursions.....	3-15
a.	With and Without Surface Deposition	3-15
b.	With Different Values Defining Dispersion for the Lightest Wind Conditions.....	3-19
4.	NARAC Predictions: Excursions	3-23
a.	With and Without Surface Deposition	3-23
b.	With Different Dispersion Parameter Values: Sigma-v Experimental and Sigma-v Calculated.....	3-27
B.	A Few Comments on the “Standard” Statistical Measures	3-29
C.	Conclusions: Value of MOEs	3-35
	References.....	3-R-1

Appendix A – Acronyms

Appendix B – Initial Conditions for HPAC and NARAC Predictions

Appendix C – HPAC Predictions Compared to *Prairie Grass* Trials

Appendix D – NARAC Predictions Compared to *Prairie Grass* Trials

Appendix E – Comparisons of HPAC and NARAC Predictions

Appendix F – Comparisons of HPAC Predictions: With and Without Surface Deposition

Appendix G – Comparisons of HPAC Predictions: With Different Values of Dispersion During the Lightest Wind Conditions

Appendix H – Results and Analyses: Supplemental Figures for MOEs

Appendix I – Results and Analyses: Supplemental Figures and Tables for Standard Statistical Measures

Appendix J – Some Comments on the Estimation of Plume Width and Direction

Appendix K – *Prairie Grass* Field Trial Data Anomalies That Were Corrected

Appendix L – Comparisons of NARAC Predictions: With and Without Surface Deposition

Appendix M – Comparisons of NARAC Predictions: With Different Values of Dispersion (Sigma-v Experimental and Calculated)

Appendix N – Task Order Extract

LIST OF FIGURES

1.	Conceptual View of 3 Comparative Dimensions	2
2.	Two-Dimensional MOE: MOE 2	4
3.	Illustration of Critical Threshold Area (AE1) Estimates of A_{OV} , A_{FN} , and A_{FP}	5
4.	Illustration of AE2 Procedure	5
5.	Nominal Lethality/Effects Filter Illustrated.....	7
6.	MOE 2 Comparisons of HPAC and NARAC Predictions of 51 <i>Prairie Grass</i> Trials	9
7.	MOE 2 Comparisons of HPAC and NARAC Predictions of 51 <i>Prairie Grass</i> Trials as a Function of Stability Category Grouping	10
1-1.	Example Dosages (in mg-sec/m ³) and Field Trial Setup.....	1-5
2-1.	Illustration of A_{FN} , A_{FP} , and A_{OV}	2-4
2-2.	MOE 1 as a Function of A_{FN} and A_{FP} ($C_{FN} = C_{FP} = 1.0$)	2-6
2-3.	MOE 1 as a Function of C_{FN} and C_{FP}	2-7
2-4.	MOE 2 as a Function of A_{FN} and A_{FP}	2-9
2-5.	2D MOE: Interpretation of Model Comparisons.....	2-11
2-6.	Relationship Between MOE 1 and MOE 2: $C_{FN} = 1$, $C_{FP} = 1$	2-12
2-7.	Relationship Between MOE 1 and MOE 2: $C_{FN} = 5$, $C_{FP} = 0.5$	2-12
2-8.	Illustration of AE1	2-14
2-9.	Illustration of AE2	2-15
2-10.	Nominal Lethality/Effects Filter Illustrated.....	2-16
2-11.	Lethality/Effects Filter as an Extension of AE2	2-17
2-12.	<i>Prairie Grass</i> Trial 7 as a Function of Arc: Stability Category is 1	2-24
3-1.	MOE 1, AE1, All Trials: For 51 Trials and Two Sets of User Coefficients .	3-2
3-2.	MOE 1, AE2, All Trials: For 51 Trials and Two Sets of User Coefficients .	3-2
3-3.	MOE 1, AE1 and AE2: By Arc Range ($C_{FN} = C_{FP} = 1$)	3-3
3-4.	MOE 1, AE1 and AE2: By Stability Category Grouping ($C_{FN} = C_{FP} = 1$)....	3-4
3-5.	MOE 2, AE1 and AE2, All Trials: For 51 <i>Prairie Grass</i> Trials	3-5
3-6.	MOE 2, AE1 and AE2: As a Function of Arc Range.....	3-6
3-7.	MOE 2, AE1 and AE2: As a Function of Stability Category Grouping.....	3-10
3-8.	MOE 2, Lethality/Effects Filter: As a Function of Stability Category Grouping	3-13
3-9.	MOE 2, Demonstration of Highly Toxic Material Lethality/Effects Filter (at Threshold = 3 mg-sec/m ³): As a Function of Stability Category Grouping	3-14
3-10.	MOE 2, AE2: HPAC Predictions With and Without Surface Deposition....	3-17
3-11.	MOE 2, AE1 and AE2: $uu(\text{calm}) = 0.0$ Versus $uu(\text{calm}) = 0.25$	3-20
3-12.	HPAC Predictions for Trial 58 With Two Values of $uu(\text{calm})$: SCG 6 (“Stable”) at the 5 Arc Ranges.....	3-22
3-13.	MOE 2, AE2: NARAC Predictions With and Without Surface Deposition .	3-25
3-14.	MOE 2, AE2: NARAC Predictions Using Calculated and Experimental Sigma-v.....	3-28
3-15.	FB, NMSE, MG, and VG: HPAC and NARAC ArcMax Comparisons to <i>Prairie Grass</i> Trials	3-29

3-16.	FB, NMSE, MG, and VG: HPAC and NARAC CWI Dosage Comparisons to <i>Prairie Grass</i> Trials.....	3-31
3-17.	FB as a Function of Range: HPAC and NARAC W_{ec} Comparisons to <i>Prairie Grass</i> Trials.....	3-31
3-18.	HPAC and NARAC Predictions for <i>Prairie Grass</i> Trials 28 and 45	3-33
3-19.	Bias as a Function of Range: HPAC and NARAC CentDir Comparisons to <i>Prairie Grass</i> Trials.....	3-34

LIST OF TABLES

1-1.	List of <i>Prairie Grass</i> Trials That Were Used in HPAC/NARAC Comparison.....	1-6
2-1.	Distance Between Samplers by Arc	2-25
2-2.	Stability Category Groupings (SCG) Used in This Study	2-26
2-3.	Sample Sizes Used for Model Comparisons to <i>Prairie Grass</i> Field Trials...	2-27
3-1.	Number of Arc Range Comparison Differences That Are Statistically Resolved	3-8
3-2.	Number of Arc Range Comparison Differences <i>Between</i> Models That Are Statistically Resolved.....	3-9
3-3	MOE 1 AE2 Comparisons for HPAC Predictions of <i>Prairie Grass</i> Field Trials: With and Without Surface Deposition	3-18
3-4	MOE 1 AE2 Comparisons for NARAC Predictions of <i>Prairie Grass</i> Field Trials: With and Without Surface Deposition	3-26
3-5	MOE 1 AE2 Comparisons for NARAC Predictions of Prairie Grass Field Trials: Calculated and Experimental Sigma $-v$	3-28

SUMMARY

A. BACKGROUND

In 1999, IDA conducted a study for the Office of the Secretary of Defense that, in part, explored military user requirements for hazard predictions.¹ During that study, it became apparent that there was a need for measures that clearly communicate to the user the relative worth of a model's predictions.

During fiscal year 2000, a series of studies in support of the Defense Threat Reduction Agency (DTRA) was begun. The goal of these studies is to improve the verification, validation, and accreditation (VV&A) of hazard prediction and assessment models and capabilities. These studies are part of a larger joint VV&A effort that DTRA and the Department of Energy, via the Lawrence Livermore National Laboratory (LLNL), are conducting. This joint effort includes comparisons of the LLNL and DTRA transport and dispersion (T&D) modeling systems, NARAC and HPAC, respectively.²

B. PURPOSE

The purpose of this paper is to introduce and describe a family of novel user-oriented MOEs, focusing on their interpretation and usage. The application of these MOEs to the comparison of HPAC and NARAC predictions of the 1956 *Prairie Grass* field trial observations is also described in this paper.³

C. USER-ORIENTED MEASURES OF EFFECTIVENESS (MOEs)

There is an enduring user need for measures that meaningfully communicate the relative worth (and validity) of a model's predictions when applied in a given regime

¹ *NBC Hazard Prediction Model Capability Analysis*, IDA Document D-2245, September 1999.

² NARAC = National Atmospheric Release Advisory Center and HPAC = Hazard Prediction and Assessment Capability.

³ The 1956 *Prairie Grass* field trials represent one of the best-characterized short-range transport and dispersion experiments. In addition, these trials correspond to a baseline against which many transport and dispersion models have been compared. Therefore, these field trials were chosen for this initial study. Additional descriptions of the *Prairie Grass* field trials can be found in Chapter 1, Section B and Chapter 2, Section C.

(e.g., short-range chemical agent or longer-range biological agent, unstable or stable meteorological conditions). For a user-oriented measure, we desire the following properties:

- Clear-cut interpretation for consistent utility and relatively widespread communication potential
- Sensitivity to real changes in model performance (e.g., can detect differences between various models)
- Robustness with respect to small measurement errors and uncertainties.

The key objective for an interpretive user-oriented MOE is its ability to communicate simply (and appropriately) the relative performance of a model in a given application. It is important that other measures, for instance, the other statistical measures described later in this paper, also be examined for any set of data that is to be described. In order for such a user-oriented MOE to have widespread credibility, the conclusions communicated by the MOE should be consistent with the conclusions one would obtain from a detailed review of other statistical measures and graphical representations. Where there are inconsistencies, the differences should be highlighted and understood.

A fundamental feature of any comparison of hazard prediction model output to observations is the over- and under-prediction regions. We define *false negative* where a hazard is observed but not predicted, and *false positive* where a hazard is predicted but not observed. Figure 1 shows the observed and predicted area at the same dosage level for some nominal situation. Numerical values in three-dimensional space characterize this conceptual view. These values are associated with estimates of the false negative region (A_{FN}), the false positive region (A_{FP}), and the overlap region (A_{OV}).

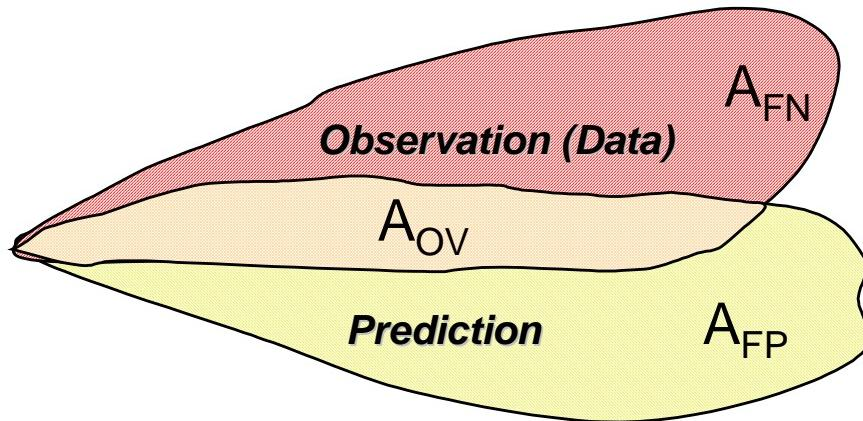


Figure 1. Conceptual View of 3 Comparative Dimensions

The first measure that we describe, MOE 1, combines the area of overlap, the area of false negative, and the area of false positive to form a single value as shown in equation 1.

$$MOE\ 1 = \frac{A_{OV}}{(A_{OV} + C_{FN}A_{FN} + C_{FP}A_{FP})}. \quad (1)$$

In this equation, C_{FN} and C_{FP} represent user coefficients that weight the relative importance of the false positive and false negative areas. The coefficient values chosen should be related to the specific model application being examined and the particular user's risk tolerance. If we consider $C_{FN} = C_{FP} = 1$, that is, equal weights for false positive and false negative areas, then this MOE simply is the fraction of the total area that constitutes overlap between the model and the prediction. A perfect model would have an MOE value of 1 (i.e., all overlap) and a perfectly terrible model would have an MOE value of 0 (i.e., no overlap).

The second measure that we consider, MOE 2, has two dimensions. The x-axis corresponds to the ratio of overlap area to observed area and the y-axis corresponds to the ratio of overlap area to predicted area. These mathematical definitions can be algebraically rearranged (equation 2 below) and we then recognize that the x-axis corresponds to *1 minus the false negative fraction* and the y-axis corresponds to *1 minus the false positive fraction*.

$$MOE\ 2 = \left(\frac{A_{OV}}{A_{OB}}, \frac{A_{OV}}{A_{PR}} \right) = \left(\frac{A_{OV}}{A_{OV} + A_{FN}}, \frac{A_{OV}}{A_{OV} + A_{FP}} \right) = \left(1 - \frac{A_{FN}}{A_{OB}}, 1 - \frac{A_{FP}}{A_{PR}} \right) \quad (2)$$

where A_{FN} = area of false negative, A_{FP} = area of false positive, A_{OV} = area of overlap, A_{PR} = area of the prediction, and A_{OB} = area of the observation. Consistent with the above algebraic rearrangement, Figure 2 shows the area of false negative decreasing from left to right.

We imagine associating a given user and application with specific risk tolerances, r_1 and r_2 , therefore accepting from a given prediction a certain false positive and false negative fraction. These risk tolerances define in the MOE space an acceptable or desirable region for model performance.

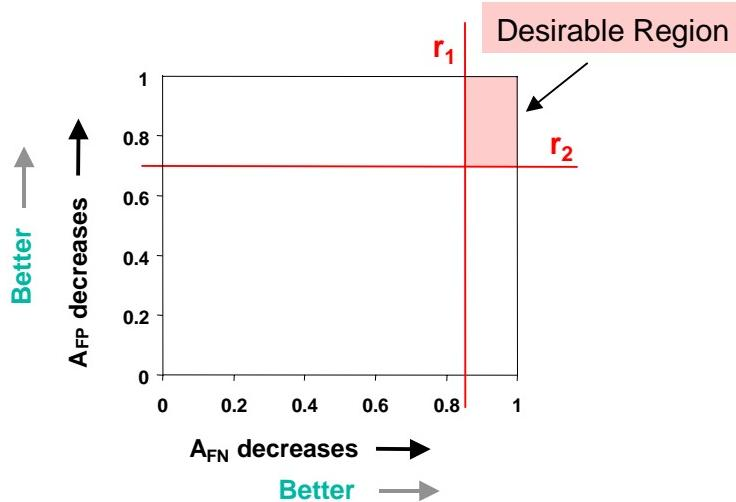


Figure 2. Two-Dimensional MOE: MOE 2

The various areas described in equations 1 and 2 can be estimated from field trial observations and model predictions. For example, we considered the distance traversed by samplers along an arc at which both the observations and predictions led to dosages above some selected threshold, as a natural estimate of the overlap “area.” An analogous methodology was used to estimate A_{FN} and A_{FP} . We denote estimates determined in this way with the label “AE1.” The AE1 estimate represents a natural analog to a hazard area at a given critical threshold. However, it should be noted that a perfect MOE score based on AE1 does *not* imply perfect agreement between the observed and predicted values at all measurement locations, since only the points above a particular threshold dosage value are considered. Figure 3 illustrates this procedure.

Next, we considered the summed dosages. For example, for A_{FP} , all of the samplers with *predictions of greater value than the observations* can be considered. One then sums the differences between the predicted and observed dosages at those samplers to generate A_{FP} . Based on the samplers that contained *observed values that were larger than the predicted values*, one can similarly compute A_{FN} . A_{OV} is calculated by considering all samplers and summing the dosages associated with the minimum predicted or observed value. We refer to this procedure as AE2 and it is illustrated in Figure 4.⁴

⁴ Theoretically, the computation of AE2-based values does not require the use of a threshold. However, field trial data will always have uncertainties associated with the smallest observations – that is, experimental resolution. Therefore, AE2-based computations that use field trial data require a defined threshold.

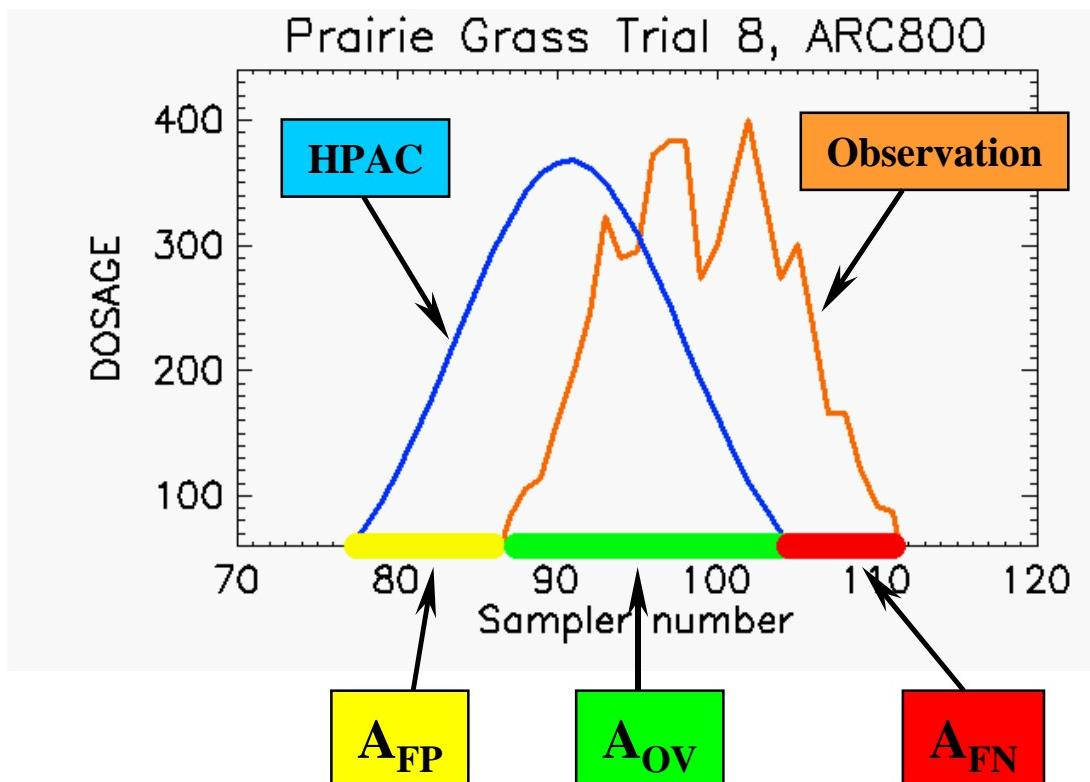


Figure 3. Illustration of Critical Threshold Area (AE1) Estimates of A_{OV} , A_{FN} , and A_{FP}

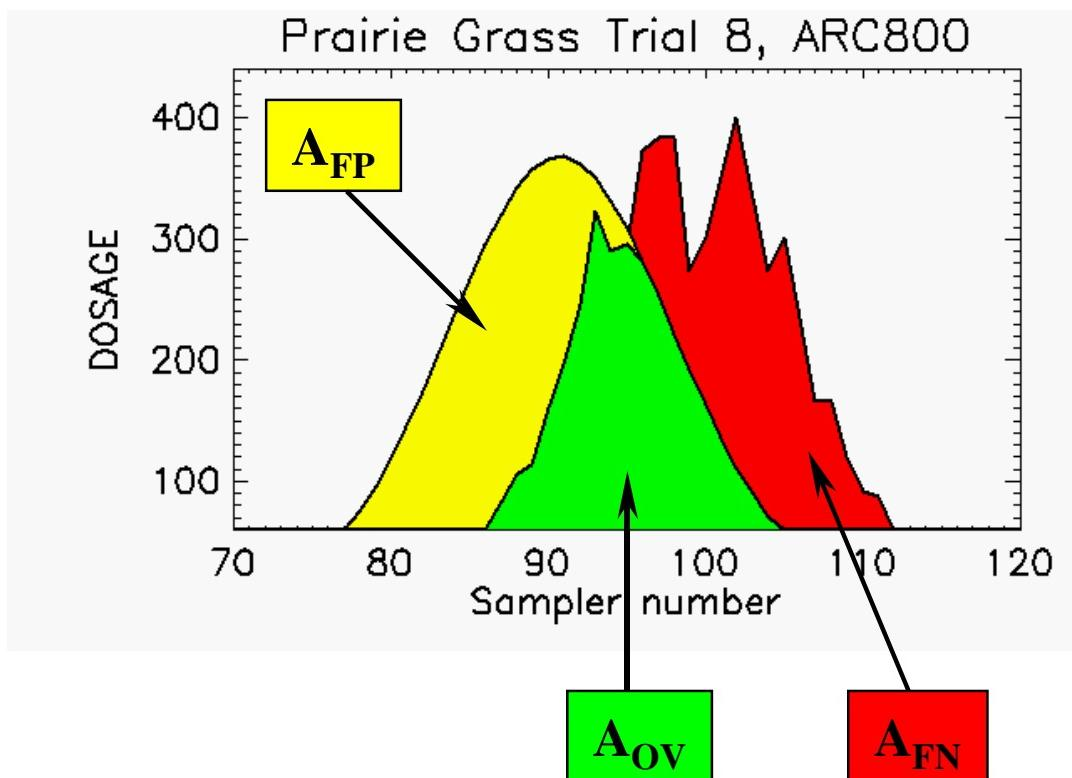


Figure 4. Illustration of AE2 Procedure

AE2 is based on comparison of observed and predicted values at every point and is a measure of under- and over-prediction. A perfect MOE score based on AE2 implies an exact match between observed and predicted values. We consider AE2-based MOEs to correspond to validation measures that can have diagnostic potential. In contrast, an AE1-based MOE, if it includes a user-defined critical threshold, can serve as an operational or accreditation measure.

We also interpreted the area estimates (i.e., A_{OV} , A_{FN} , and A_{FP}) in terms of a filter that considered the effects of a presumably toxic agent on an exposed population.⁵ First, the lethality or effects of the agent being studied and the dosages at a given sampler are examined. For example, standard probit curves might be used to assess the lethality/effects of exposure at a given sampler. Next, the dosages are converted into a fractional lethal/effects exposure, that is, the fraction of an exposed population, at that dosage level, expected to become a casualty.⁶ For example, if the observed or predicted dosage were LD_{50} (lethal dosage for 50 percent of the exposed population), then half of the exposed population would be expected to die.

Figure 5 provides a nominal illustration of this calculation. First, the observed dosage at sampler 17 is “10 LD_{50} ” ($10 \times LD_{50}$) and the predicted dosage (by HPAC in this illustration) is 1,000 LD_{50} s. These differences can be converted into the fraction of the exposed population that would be expected to become a casualty. Assume that for the probit curve associated with the hypothetical agent, a dosage of $10 \times LD_{50}$ means that 90 percent of the population is exposed to a lethal dosage, while a dosage of $1,000 \times LD_{50}$ implies 99.99 percent of the population accumulates a lethal dosage. For the overlap area, A_{OV} – that is, $10 LD_{50}$ s – 0.90 of the exposed population would be expected to accumulate a lethal dosage. At this sampler, the model overpredicts the observation and the area of false positive, A_{FP} , corresponds to an additional 0.10 lethal exposure population fraction. Then for each trial (or arc or sampler), estimates of A_{OV} , A_{FN} , and A_{FP} can be obtained in this way.⁷

⁵ As applied here, we assumed a spatially uniform exposed population.

⁶ Determining actual casualty levels for a specific scenario would also need to include factors such as the means of exposure (respiratory or percutaneous) and other parameters relating to that exposure (e.g., breathing rate and the effect of clothing).

⁷ Chapter 2, Section B.1.f provides additional details.

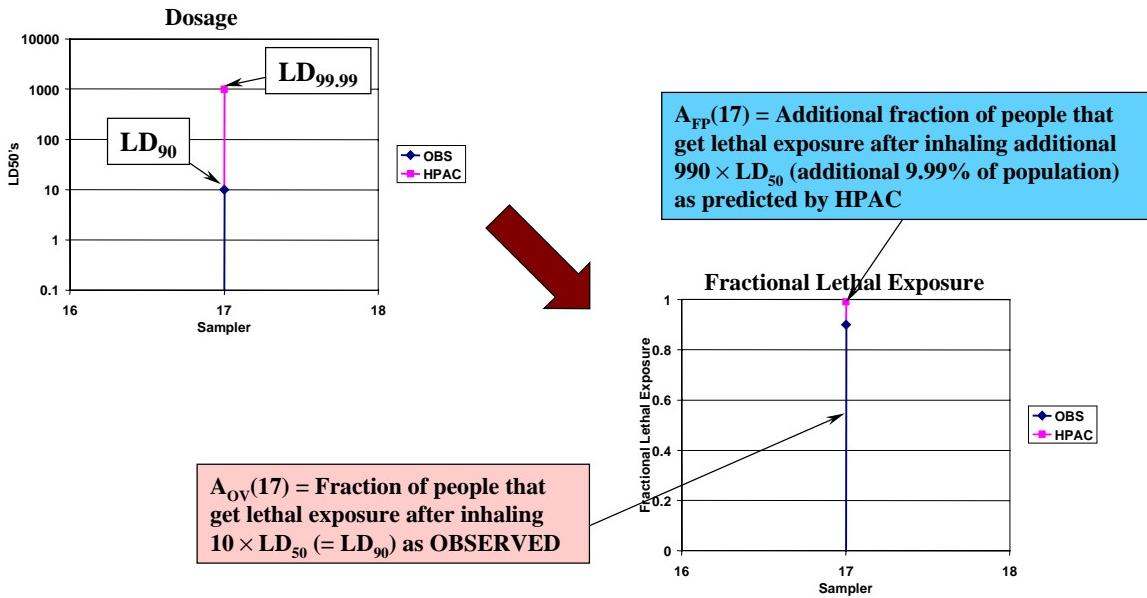


Figure 5. Nominal Lethality/Effects Filter Illustrated

By accounting for the lethality/effects of a given hazard, this measure *operationally* weights the over- or under-prediction of a model (with respect to a set of observations). Therefore, differences between observations and predictions that would lead to additional deaths or casualties are considered more important than those that, perhaps, lead to very different dosages, but a similar fraction of lethal/effects exposure. In a sense, the above process filters our interpretation of the above areas (i.e., A_{ov} , A_{fp} , and A_{fn}) through the appropriate lethality/effects “lens.” Hence, we refer to MOE results obtained in this way as “lethality/effects-filtered.”

Perhaps the key feature of the MOEs described in this paper is their inclusion of directional effects. That is, in order to “score” well in terms of these MOEs, the hazard prediction modeling system must predict the shape *and* location (e.g., direction) of the plume accurately. One advantage of these MOEs is that mean value and probabilistic outputs can be directly compared. Therefore, a modeling system that creates a probabilistic plume, that is meant to encompass many possible plume realizations, can be scored with this MOE.⁸

In addition to the two MOEs described above, eight other statistical measures were computed for the model comparisons described in this paper. Two observed/predicted values were considered for the calculation of each of these statistical

⁸ An upcoming IDA paper describes the results of the application of MOEs to probabilistic outputs generated by HPAC.

measures. First, for each arc the maximum dosage was considered – ArcMax. Next, the crosswind-integrated dosage (CWI) was examined. The statistical measures computed include fractional bias (FB), geometric mean bias (MG), normalized mean square error (NMSE), geometric mean variance (VG), correlation coefficient (R), fraction of predictions within a factor of 2 (FAC2), fraction of predictions within a factor of 5 (FAC5), and fraction of predictions within a factor of 10 (FAC10).⁹

D. CONCLUSIONS BASED ON THE EXAMINATION OF MOE ESTIMATES¹⁰

The two-dimensional (2D) measure (MOE 2), with false positive and false negative fractions considered orthogonal, consistently resolved important model performance features. MOE 2 was useful in identifying and describing differences between HPAC and NARAC predictions of the *Prairie Grass* trials.¹¹

Figure 6 compares MOE 2 estimates for HPAC and NARAC predictions. The x-axis corresponds to decreasing false negative fraction, from left to right, and the y-axis corresponds to decreasing false positive fraction, from bottom to top.¹² Each colored area in the figure represents the estimated 95th percent confidence region for the given MOE 2 point estimate.¹³ The complete separation of these two regions implies that the differences between the HPAC and NARAC MOE 2 point estimates are statistically significant.

⁹ In addition, NMSE and FB were computed for an estimate of the plume width and the root mean square error (RMSE) and bias were computed for the centerline direction. Appendix J provides additional details.

¹⁰ The *Prairie Grass* simulations used for this study were performed using a protocol designed to allow analysis of differences in dispersion model physics. As much as possible, meteorology, resolution, and user skill level differences were minimized. As such, the results identified interesting differences in the models, but should not be viewed as a conclusive comparison of the HPAC-NARAC results in terms of their best possible performance against the *Prairie Grass* data set.

¹¹ This section illustrates the main results and conclusions of this analysis based on MOE 2. MOE 1 results were similar and consistent, albeit not always as informative. Chapter 3, Section A.1 and Appendix H provide detailed MOE 1 results and comparisons.

¹² As described in equation 2, $1-A_{FN}/A_{OB}$ (x-axis) and $1-A_{FP}/A_{PR}$ (y-axis) can be algebraically rearranged to give A_{OV}/A_{OB} and A_{OV}/A_{PR} , respectively. Throughout this paper – the main body and appendix H – we typically refer to the x- and y-axis as decreasing false negative (i.e., $1-A_{FN}/A_{OB}$) and decreasing false positive ($1-A_{FP}/A_{PR}$), respectively. This labeling scheme tends to emphasize the false positive and false negative aspects of the MOE.

¹³ These 95th percent confidence regions are based on 1,000 bootstrap samples. See Chapter 2, Section B.3 for additional details.

The HPAC MOE 2 AE1 threshold area estimate (0.80, 0.85) lies somewhat closer than the corresponding NARAC estimate (0.94, 0.62) to the best possible value of (1,1). The AE2 estimates, in which the “areas” are based on the summed crosswind dosages, show similar results albeit with the NARAC estimate (0.74, 0.71) closer to (1,1) than the HPAC estimate (0.60, 0.79). Figure 6 indicates that the NARAC predictions exhibit a smaller false negative fraction relative to the HPAC predictions, at least on average. Similarly, the HPAC predictions show smaller false positive fractions relative to the corresponding NARAC predictions. One reasonable implication is that the NARAC-predicted plumes are, on average, wider than the HPAC-predicted plumes, at least as the models were employed in this study. This was verified by examining graphical representations of the predicted and observed plumes and by computing standard statistical measures (as described in the main body and appendices).

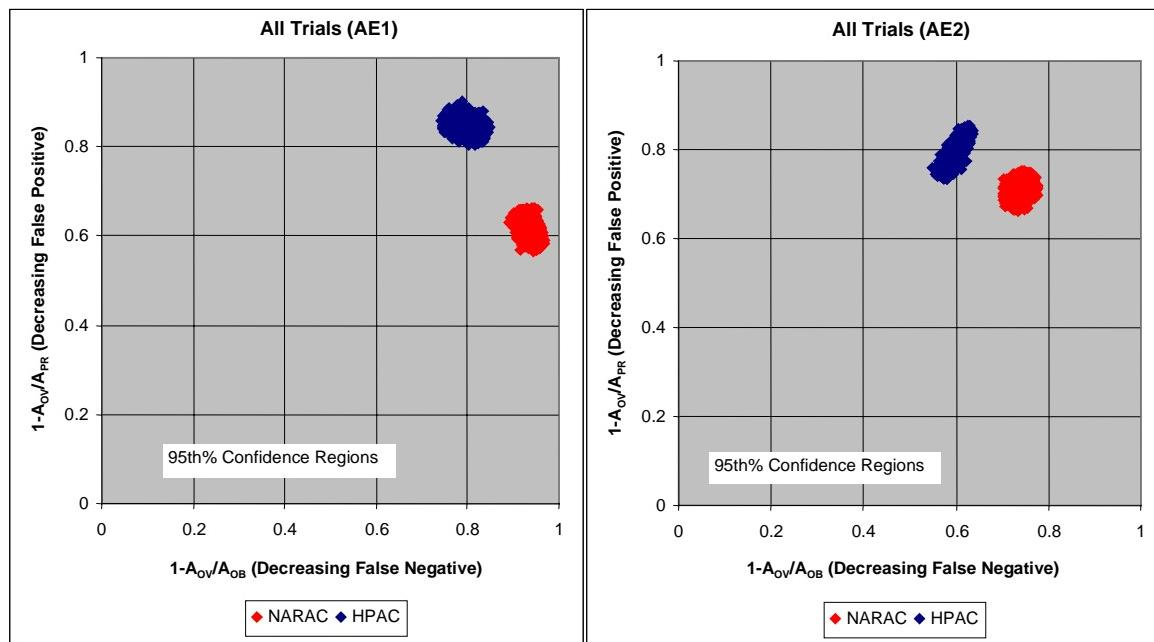


Figure 6. MOE 2 Comparisons of HPAC and NARAC Predictions of 51 Prairie Grass Trials

Variances in a given model’s prediction performance as a function of arc range and stability condition were easily detected and typically led to statistically significant conclusions. Figure 7 presents confidence region estimates for MOE 2 as a function of meteorological stability category grouping (SCG). For this figure, three independent meteorological stability category groupings were examined: unstable to very unstable (SCG = 1,2); near neutral to somewhat stable (SCG = 3,4,5); and stable to very stable (SCG = 6,7). The same 51 trials that were described in Figure 6 are included in Figure 7 albeit categorized by SCG.

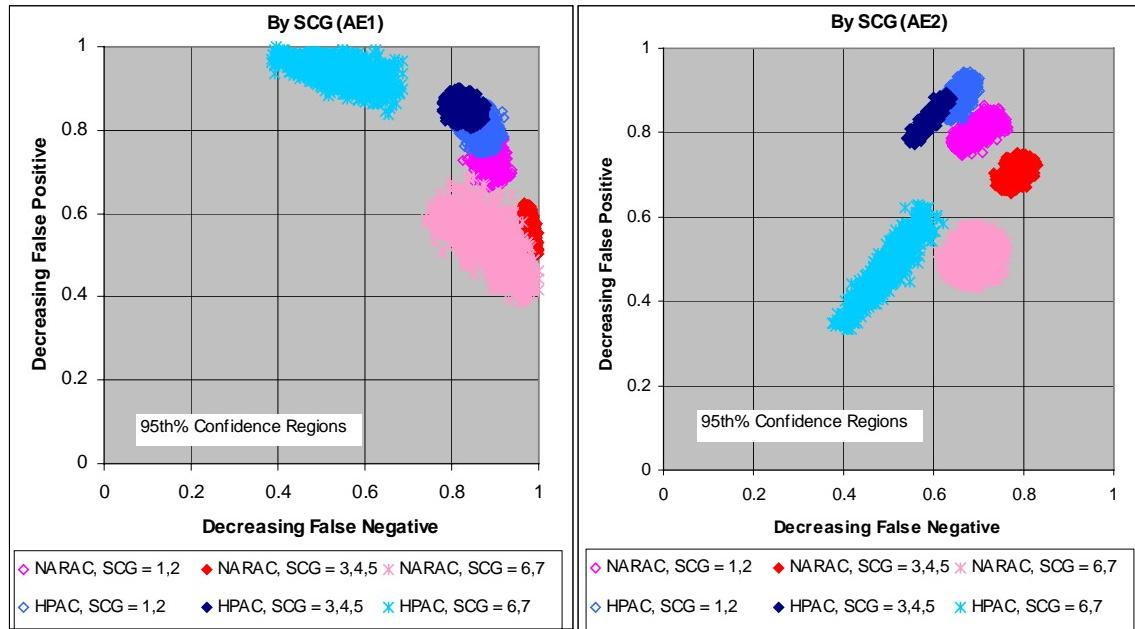


Figure 7. MOE 2 Comparisons of HPAC and NARAC Predictions of 51 Prairie Grass Trials as a Function of Stability Category Grouping

With respect to HPAC and NARAC comparisons, the MOE 2 (AE1 and AE2) results are most similar for the trials conducted during the more unstable conditions (SCG = 1,2) with the NARAC predictions generating slightly larger false positive fractions and slightly smaller false negative fractions. This trend is magnified for the near-neutral trials (SCG = 3,4,5). The biggest separation is associated with the MOE 2 AE1 estimates for the stable trials (SCG = 6,7).¹⁴ For both the neutral and the stable conditions, the NARAC predictions generate relatively little area (AE1) associated with false negatives (i.e., along the x-axis the confidence region lies close to 1). The HPAC predictions of the neutral and stable trials lead to larger false negative but smaller false positive fractions (AE1).

The MOE 2 AE2 results (summed dosage-based “areas”) for stable trials, indicate decreased false negative fractions associated with NARAC predictions relative to HPAC predictions and similar false positive fractions for both sets of predictions. However, the HPAC predictions of the stable trials (SCG = 6,7) show a wider range of false negative and false positive values (relative to the NARAC predictions). This can be seen in the

¹⁴ A separate independent grouping of stability categories (SCGs = 1,2,3; 4; and 5,6,7) was also examined with similar results. See Chapter 3 and Appendix H. A more physically-based arrangement would be to group the near-neutral categories, 3 and 4, together. The conclusions of this paper were not substantially affected by this regrouping.

strong directionality (i.e., elliptical eccentricity) associated with the stable trials' confidence region for the HPAC prediction. This result is consistent with a few narrow plume predictions and observations being slightly offset in direction. Therefore, for those few trials, both false positive and false negative fractions are increased at the expense of the overlap fraction.¹⁵

Both HPAC and NARAC appear to perform the best, with respect to being closest to the best case (1,1) value, for the relatively unstable trials. Similarly, both models performed worst, as measured by MOE 2, for the trials that were conducted under the more stable conditions.¹⁶

Based on relatively small changes in HPAC inputs, we were also able to discern prediction performance differences (between HPAC runs) after examining the computed MOE 2 estimates. These changes in HPAC inputs included adding a mechanism for SO₂ deposition and, separately, modifying a default value associated with dispersion assumptions during the lightest wind conditions. Similarly, changes to NARAC inputs (i.e., the inclusion of a surface deposition mechanism and changes to a dispersion parameter – sigma-v) led to detectable differences in MOE 2 results. Furthermore, we found that the 2D MOE (MOE 2) allowed for straightforward communication of the impact of these modest input changes.

We found that the lethality/effects filter can be used to compute MOE values, and can be characterized as a “tunable dial” that can relate the goodness of a prediction for agents of greatly varying toxicity (e.g., biological versus chemical agents or threshold versus lethal effects for a chemical agent). This feature may make this methodology of particular value with respect to user accreditation. For instance, the specific application and user will dictate the agent type, effect, and downwind distance of interest, therefore defining how the lethality/effects dial should be tuned.

Overall the 2D MOE revealed the following with respect to comparisons of HPAC and NARAC predictions under the specified model intercomparison protocol:

¹⁵ For MOE 2 AE2, using the default uu(calm) input value, vice the baseline uu(calm) value, improved the HPAC stable trials' point estimate and greatly reduced the associated elliptical eccentricity and confidence region size.

¹⁶ For these data, we found that the conclusions based on the standard statistical measures were consistent with those based only on the MOEs. Chapter 3, Section B provides a few additional comments on the usage and value of these standard statistical measures.

- HPAC and NARAC predictions of the relatively unstable *Prairie Grass* trials were most similar. Predictions of the most stable trials led to the biggest differences.
- In a sense, the NARAC predictions, as run, were more conservative than the HPAC predictions. In general, NARAC predictions led to substantially smaller false negative fractions, but at the expense of larger false positive fractions. This was most true for the predictions of the neutral and stable trials. In contrast, HPAC predictions showed substantially smaller false positive areas, but at the expense of larger false negative areas. A review of Appendix E confirms this interpretation.

This study also used a variety of other statistical and graphical measures of model performance. Examination of plots of measured and predicted dosages as a function of distance helped support conclusions. Statistical measures for derived quantities – such as ArcMax, CWI dosage, plume horizontal spread, and mean plume direction – were of some value in confirming the underlying reasons for the MOE results. MOE results (for both AE1 and AE2) include the effects of directional error by pairing observed and predicted dosage in space (and time). Separate comparisons of ArcMax, CWI dosage, plume spread, and mean plume direction (which do not measure mean wind direction error) can allow for the isolation of errors due to the dispersion modeling methods from those due to mean wind advection modeling errors (particularly directional). The results of this study show that these MOEs are a potentially valuable tool, but that no single measure can be used exclusively in evaluating and analyzing model performance.

E. OUTLINE OF THIS PAPER

This paper is divided into three chapters and fourteen appendices. Chapter 1 provides a brief introduction and Chapter 2 describes this study's methodologies. Chapter 2 defines and develops two user-oriented MOEs, MOE 1 and MOE 2, and discusses a few statistical measures that have often been used for the evaluation of transport and dispersion models. Chapter 3 provides the results of the application of these MOEs to the comparison of HPAC and NARAC predictions of the *Prairie Grass* field trials.

Appendix A provides an acronym list and Appendix B presents some details associated with the model predictions that were used for this study's comparisons. Appendices C, D, E, F, G, L, and M present comparisons, by sampler arc, of *Prairie Grass* field trial observations and model predictions. Detailed model comparison results, using MOEs and standard statistical measures, are deposited in Appendices H and I,

respectively. Appendix J briefly describes some details of our methodology, and possible alternatives, for estimating a plume width and direction (associated with a given arc) and Appendix K describes a few corrections that were applied to the field trial data set that we used. Finally, Appendix N includes an extract from the pertinent task order.

CHAPTER 1

INTRODUCTION

1. INTRODUCTION

A series of studies in support of the Defense Threat Reduction Agency (DTRA) was begun in Fiscal Year 2000. The goal of these studies is to improve the verification, validation, and accreditation (VV&A) of hazard prediction and assessment models and capabilities (e.g., HPAC and NARAC)¹. These studies are part of a larger joint VV&A effort that DTRA and the Department of Energy (DOE), via the Lawrence Livermore National Laboratory (LLNL), are conducting. This joint effort includes comparisons of the LLNL and DTRA transport and dispersion (T&D) modeling systems, NARAC and HPAC, respectively, and their predictions. IDA's role is to conduct independent analysis and special studies associated with this VV&A effort. This role includes conducting comparisons between the models, providing analysis and discussions associated with these examinations, and exploring and developing measures of effectiveness (MOE) that can aid hazard prediction model validation and accreditation.²

This paper develops novel user-oriented MOEs and applies them to the comparison of two hazard prediction models. The usage and interpretation of these MOEs and their resulting values are described for short-range field trial data. In addition, “standard” statistical measures are computed and some comparisons to the proposed MOEs are provided.

A. BACKGROUND

We refer to this joint VV&A effort as a *cooperative comparison*. That is, DTRA and LLNL have set up a funded team that works closely together to provide comparable model runs and analysis. The two models have, over the years, been developed independently and against different requirements. Further, we speculate that it is more efficient for the various agencies to learn about other government models and tools in a cooperative (joint effort) manner. Recent newsletter articles have suggested the value and challenges of hazard prediction model VV&A [Ref. 1-1] and concluded that joint

¹ NARAC = National Atmospheric Release Advisory Center and HPAC = Hazard Prediction and Assessment Capability.

² Appendix N of this document contains an extract from the pertinent Fiscal Year 2000 task order.

efforts in the Chemical and Biological (CB) warfare modeling and simulation arena are expected to bring a certain synergy to the community [Ref. 1-2].

Future studies are expected to include comparisons of model algorithms, VV&A efforts, and reporting methods. Careful comparisons to relatively simple, previously collected, field trial data have been completed. In addition, comparisons of model outputs over a small set of controlled input conditions have also been completed. We refer to this first set of comparisons as model-to-field trial comparisons (or simply MFT). The second set of examinations is referred to as model-to-model-only comparisons (MMO).³ This paper documents some of the methodology, results, and analyses associated with the first in a series of MFT studies, with an emphasis on the presentation and application of user-oriented MOEs. The field trial that was selected for this comparison is the 1956 *Prairie Grass* experiment [Ref. 1-4] described briefly later in this chapter.

It is anticipated that even these simple MFT and MMO comparisons should lead to the identification of differences in model behavior and the quantification of the potential magnitude of such differences under a variety of conditions.⁴ Importantly, these initial studies are expected to serve as the basis for future more complex comparisons (e.g., more complex weather and the inclusion of significant terrain features). To that end, the methodologies and reporting techniques described here represent a “template” for future studies.

For this study, we adopt Department of Defense definitions for verification, validation, and accreditation as shown below [Ref. 1-6]:

- **Verification** – The process of determining the degree to which a model or simulation implementation accurately represents the developer’s conceptual description and specification. Verification also evaluates the extent to which the model or simulation has been developed using sound and established software engineering techniques.⁵ [DOD Directive 5000.59]
- **Validation** – The process of determining the degree to which a model or simulation is an accurate representation of the real world from the perspective of the intended uses of the model or simulation. [DOD directive 5000.59]

³ An initial MMO comparison has recently been completed [Ref. 1-3].

⁴ A recently completed MMO-like study, which included HPAC, demonstrated the potential for these types of studies to identify, clarify, and communicate differences, including operational differences, between models [Ref. 1-5].

⁵ This effort does not examine software engineering technique issues.

- **Accreditation** – The official certification that a model or simulation is acceptable for use for a specific purpose. [DOD Directives 5000.59 and 5000.59-P]

1. Brief HPAC Description

HPAC is composed of a suite of software modules that can generate source terms for hazardous releases, retrieve and prepare meteorological information for use in a prediction, model the transport and dispersion (T&D) of the hazardous release over time, and plot and report the results of these calculations. HPAC has been applied to various national defense problems including military studies and operational planning.

For hazardous material T&D, HPAC uses the Second-Order Closure Integrated Puff (SCIPUFF) model and an associated mean wind field model. SCIPUFF, which is a Lagrangian model for atmospheric dispersion that uses the Gaussian puff numerical method – an arbitrary time-dependent concentration field is represented by three-dimensional Gaussian distributions – bases its turbulent diffusion parameterization on second-order closure theories. This methodology provides a link between measurable velocity statistics and the predicted dispersion rates. This “second-order” feature implies that concentration variance can also be computed, and this uncertainty estimate can be used as the basis for a probabilistic description of the dispersion prediction.⁶

This study examines the most recently released HPAC software version, 3.2 [Ref. 1-8].

2. Brief NARAC Description

The ADAPT/LODI⁷ modeling system is used for both real-time operational applications and detailed assessments of events involving atmospheric releases of hazardous material at the Department of Energy’s (DOE) National Atmospheric Release Advisory Center (NARAC) at Lawrence Livermore National Laboratory (LLNL). The ADAPT meteorological data assimilation model constructs fields of such variables as the mean winds, pressure, precipitation, temperature, and turbulence, using a variety of interpolation methods and atmospheric parameterizations [Ref. 1-9]. Non-divergent wind

⁶ See Reference 1-7 for several reports that provide details of HPAC design, functionality, capabilities, and V&V.

⁷ ADAPT = Atmospheric Data Assimilation and Parameterization Techniques. LODI = Lagrangian Operational Dispersion Integrator.

fields are produced by an adjustment procedure based on the variational principle and a finite-element discretization.

The LODI dispersion model solves the 3-D advection-diffusion equation using a Lagrangian stochastic, Monte Carlo method [Ref. 1-10]. LODI includes methods for simulating the processes of mean wind advection, turbulent diffusion, radioactive decay and production, first-order chemical reactions, wet deposition, gravitational settling, dry deposition, and buoyant/momentum plume rise. The models are coupled to NARAC databases providing topography, geographical data, chemical-biological-nuclear agent properties and health effects, real-time meteorological observational data, and global and mesoscale forecast model predictions.

B. DESCRIPTION OF THE PRAIRIE GRASS FIELD TRIAL EXPERIMENT

Prairie Grass field trials were conducted during the summer of 1956 in north central Nebraska near the town of O'Neil.⁸ The primary objective of *Project Prairie Grass* was to determine the rate of diffusion of a neutrally-buoyant tracer gas as a function of meteorological conditions. These experiments involved continuous ten-minute releases of sulfur dioxide (SO_2) from a near-surface point source. Downwind SO_2 concentrations were sampled along five concentric, semi-circular arcs located 50, 100, 200, 400, and 800 meters away from the gas source.

The sampling network utilized midget impingers mounted at a height of 1.5 meters along five arcs. In addition, limited vertical sampling was carried out along the 100-meter arc by means of impingers mounted at nine levels on six lightweight towers. Electrically operated vacuum units suitably positioned within the sampling network provided aspiration for the impingers. During the diffusion experiments, air was drawn into the impingers through short sections of capillary tubing and bubbled through a dilute hydrogen-peroxide solution. Sulfur dioxide present in the air samples combined with the hydrogen peroxide to form sulfuric acid. Ten-minute averaged SO_2 concentrations were determined from laboratory measurements of the electrical conductivity of the aspirated solutions. The samplers were arranged at 2-degree intervals along the 50, 100, 200, and 400-meter arcs (91 samplers per arc), and at 1-degree intervals for the 800-meter arc (i.e., 181 samplers along the 800-meter arc).

⁸ See References 1-4 and 1-11.

The meteorological conditions (wind speed and direction) were measured at a number of weather stations. Figure 1-1 shows the setup and typical concentrations recorded at the *Prairie Grass* field trials. Surface weather observations at a 2-meter height were recorded at the “Source,” “North450,” “MIT 3L,” and “MIT AREA” weather stations. The “A&M TWR” surface tower provided wind speed and direction at seven levels (0.3, 0.5, 1.0, 2.0, 4.0, 8.0, and 16.0 meters) above the surface. In addition, the “Rawinsond” radiosonde was used to provide meteorological conditions at upper levels.

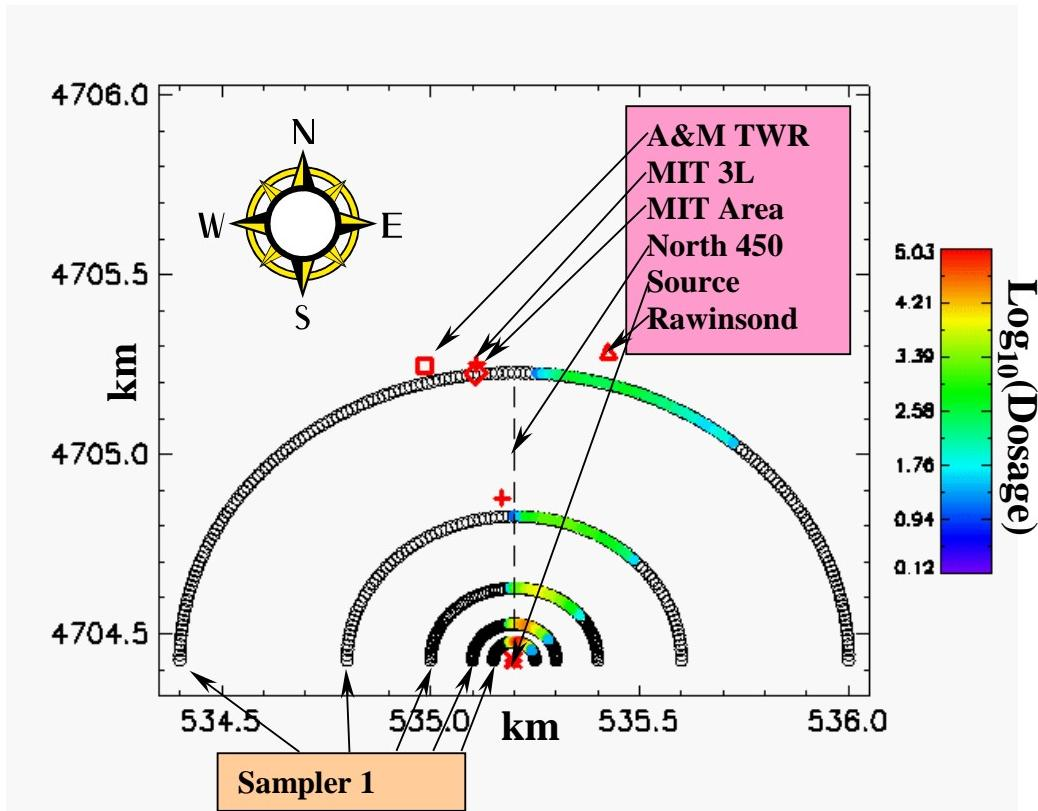


Figure 1-1. Example Dosages (in $\text{mg}\cdot\text{sec}/\text{m}^3$) and Field Trial Setup⁹

Approximately 70 experiments were carried out in a wide variety of weather conditions. Some of the trials (30, 31, 63, and 64) did not include correction factors for the compensation of the evaporative loss of impinger solution during aspiration.¹⁰ Other

⁹ The dosages shown here were obtained from *Prairie Grass* field trial 61. The color intensity corresponds to the logarithm of dosage at the samplers. Dosages are calculated by multiplying ten-minute averaged SO_2 concentrations, as reported in the *Prairie Grass* field trials, by 600 seconds. The source release point is at (535.2 km, 4704.427 km). The sampling network is oriented on a West-East grid, with the middle sampler pointing toward the north. Sampler 1 corresponds to the west-most sampler. Red symbols denote locations of the meteorological stations.

¹⁰ See Reference 1-4, pages 200-201.

Prairie Grass trials have significant portions of meteorological data missing. For these reasons, 19 trials were removed from this comparison. Appendix B gives further details for the elimination of the *Prairie Grass* trials. Table 1-1 lists trials that were used in this HPAC/NARAC comparison.

Table 1-1. List of *Prairie Grass* Trials That Were Used in HPAC/NARAC Comparison

{5, 7, 8, 9, 10, 11, 12, 13, 14, 15, 16, 17, 18, 19, 20, 21, 22, 23, 24, 25, 26, 27, 28, 32, 33, 34, 35, 36, 37, 38, 39, 40, 41, 42, 43, 44, 45, 46, 48, 49, 50, 51, 54, 55, 56, 57, 58, 59, 60, 61, 62}
--

On some trials, critical information associated with a specific sampler arc was missing. The 50-meter arc of trial 62 did not include a correction factor for the compensation of the evaporative loss. The 200-meter arc of trial 50 and the 100-meter arc of trial 57 had vacuum lines disconnected.¹¹ We eliminated these three arcs from our HPAC/NARAC comparisons.

Computer-ready data files of the *Prairie Grass* field trials were provided by Lawrence Livermore National Laboratory [Ref. 1-12]. Appendix K provides a list of data anomalies that we discovered during our analysis of the *Prairie Grass* field trial data and the “corrections” that we applied.

C. NEAR-TERM PLANNED COMPARISONS

Follow-on analyses, planned for the near-term, will describe the results of comparisons of these models to field trial data collected during the *Dugway Proving Ground Phase I* experiment [Ref. 1-13]. Further analysis that considers the usage of hazard prediction models with more limited weather inputs and probabilistic outputs is planned and will include the application of the proposed user-oriented MOEs. We expect that future examinations will include field trial data collected over longer ranges and complex terrain.

¹¹ See Reference 1-4, pages 79-80.

REFERENCES

- 1-1. Merkle, P. B., "Analysis and Validation: A Perspective for Hazard Models," *Chemical and Biological Defense Information Analysis Center (CBIAC) Newsletter*, Spring 1998, Vol. 4, No. 2.
- 1-2. Gibbs, R. L., "Improving the Development Process for Chemical and Biological Warfare Modeling and Simulation," *CBIAC Newsletter*, Fall 1999, Vol. 5, No. 4.
- 1-3. Warner S., Heagy, J. F., Platt, N., Bradley, S., Bieberbach, G., Larson, D., Sugiyama, G., Nasstrom, J. S., and Foster, K. T., *Evaluation of Transport and Dispersion Models: An Initial Comparison of Hazard Prediction and Assessment Capability (HPAC) and National Atmospheric Release Advisory Center (NARAC) Predictions*, IDA Paper P-3555, in preparation.
- 1-4. Barad, M. L. (Editor), *Project Prairie Grass, A Field Program in Diffusion*, Geophysical Research Papers No. 59, Volumes I and II, DTIC #AD-152572/AFCRC-TR-58-235(I), Air Geophysical Laboratory, Hanscom Air Force Base, MA, 1958.
- 1-5. Warner, S., Carpenter, J. N., Cook, J. M., Miller, R. S., and Hegemann, B. E., *NBC Hazard Prediction Model Capability Analysis*, IDA Document D-2245, September 1999.
- 1-6. Director, Operational Test and Evaluation and Director, Test, Systems Engineering and Evaluation OUSD(A&T), *Simulation, Test and Evaluation Process: STEP Guidelines*, 4 December 1997.
- 1-7. Bradley, S., Mazzola, T., Ross, R., Srinivasa, D., Fry, R., and Bacon, D., *Verification and Validation of HPAC 3.0*, for Defense Special Weapons Agency, June 1998, and references therein; Sykes, R. I., "HPAC/SCIPUFF: Kamisiyah Modeling Issues," *3rd Annual GMU/DTRA Transport and Dispersion Modeling Workshop*, Fairfax, VA, 28-29 July 1999; and Nappo, C. J., Eckman, R. M., Shankar Rao, K., Herwehe, J. A., and Gunter, L., *Second Order Closure Integrated Puff (SCIPUFF) Model Verification and Evaluation Study*, Air Resources Laboratory, NOAA, May 1998.
- 1-8. DTRA, *The HPAC User's Guide: Version 3.2*, October 1999.
- 1-9. Sugiyama, G. and Chan, S. T., "A New Meteorological Data Assimilation Model for Real-Time Emergency Response," *10th Joint Conference on the Applications of Air Pollution Meteorology*, Phoenix, AZ (11-16 January 1998), Am. Met. Soc., Boston, MA, 285-289.

- 1-10. Ermak, D. L. and Nasstrom, J. S., "A Lagrangian Stochastic Diffusion Method for Inhomogeneous Turbulence," *Atmospheric Environment*, 2000 and Nasstrom, J. S., Sugiyama, G., Leone, J. M. Jr., and Ermak, D. L., "A Real-Time Atmospheric Dispersion Modeling System," *American Meteorological Society's 11th Joint Conference on the Applications of Air Pollution Meteorology*, Long Beach, CA, 9-14 January 2000.
- 1-11. Haugen, D. A. (Editor), (1959) *Project Prairie Grass, A Field Program in Diffusion*, Geophysical Research Paper, No. 59, Volume III, Report AFCRC-TR-58-235, Air Force Cambridge Research Center.
- 1-12. The sampler data in the arcs were obtained from Doug Murray of TRC, while the 100-meter arc tower data were transcribed by LLNL (private communication, July 2000).
- 1-13. Biltoft, C., *Phase 1 of Defense Special Weapons Agency Transport and Dispersion Model Validation*, DPG-FR-97-058, Meteorology and Obscurant Division, West Desert Test Center, U. S. Army Dugway Proving Ground, Dugway, UT, July 1997.

CHAPTER 2

METHODOLOGIES

2. METHODOLOGIES

This chapter provides a description of the methodologies used to compare HPAC and NARAC predictions to the *Prairie Grass* field trial observations. In particular, two new user-oriented MOEs are defined and discussed. Standard statistical measures, which have been used to compare hazard prediction model output with field trial experiments in the past, are also described. In addition, the conditions associated with the *Prairie Grass* field trial observations that were used to compare the models are presented in this chapter.¹

A. BACKGROUND

In general, model validation efforts include specific measures of effectiveness that are needed to define a metric by which field trial observations and predictions can be compared. It would also be helpful if model accreditation were to include measures of effectiveness that relate “operational” use of the model to field trial experiments. Such MOEs would give a certain degree of confidence to users with respect to how closely the model approximates the real world in their particular situation.

In this paper, we introduce a family of novel MOEs that could aid both validation and accreditation efforts. For the most part, the analyses and discussion described in this paper are associated with validation. However, the application of these MOEs begins to address issues associated with user accreditation.

All methods of evaluating model performance have both strengths and limitations.² Any single statistical or graphical measure of model performance involves explicit and implicit judgments as to the most important aspect(s) of model performance (e.g., the peak concentration, the integrated dose, the plume arrival time, the location of affected populations, or the correspondence between calculated and measured values at all locations). Statistical measures can also be sensitive to details of the comparison calculations, including the selection and/or elimination of data (e.g., the removal of data

¹ Appendix B contains additional details that describe the inputs for the HPAC and NARAC predictions.

² For example, see Ref. 2-1.

based on a specified threshold value), the data transformations applied (e.g., the use of logarithmic data transformations, time or space averaging), and the criteria used to pair data (e.g., the pairing of observed and predicted values at the same point in space and time, the elimination of directional effects by the use of derived quantities such as the integrated dose or the peak value). The weakness of any single measure can be exacerbated by the limited resolution of the plume provided by sparsely distributed observations (in time or space) and the strong correlation of values across the entire plume, which limits the validity of assumptions about data independence. Therefore, overall model performance analysis should involve many measures and is an iterative process in which selected statistical and graphical analyses are used to formulate specific questions, identify differences in model results, and test trends.

Graphical comparisons (e.g., overlays of measurements on two-dimensional predicted plume plots, plots of predicted and observed dosages along sampler arcs, time-histories of predicted and observed dosages at a given sampler location) may be the most generally useful and easily interpretable methods of evaluation. These types of plots allow the user to detect patterns that are not easily reduced to statistical or numerical comparisons and to both formulate and verify conclusions about plume direction, plume spread, and peak concentrations. However, comparisons based on graphical patterns can be sensitive to the choice of contour values or dosage ranges, particularly when comparing data that range over several orders of magnitude. In addition, graphical evaluations, by their very nature, tend to be subjective and less quantitative.

Statistical measures potentially allow for more objective quantitative evaluation of model performance. They also allow overall performance for a large number of data points to be assessed, along with the statistical significance of differences. However, standard statistical measures (e.g., fractional bias, geometric bias, normalized mean square error) suffer from various shortcomings, including a potential over-sensitivity to either low or high data values. All such measures can be heavily influenced by the criteria used to eliminate and/or combine data (e.g., choice of thresholds, methods for handling zero values). Typically, the most robust approach is the use of statistical measures in conjunction with insight gained from examination of graphical plots of observed and predicted data.

In general, a single method of evaluation or statistical measure should not be used in isolation. Application of any measure requires a clear understanding and documentation as to the purpose, meaning, and limitations of the comparison criteria, as well as the methodology by which it was calculated. Multiple measures need to be

available to meet different user needs and to conduct different types of analysis. In general, the most robust and perhaps the only valid conclusions concerning model differences are those supported by a number of complementary measures.

B. COMPARATIVE MEASURES

Several recent comparisons of T&D model predictions to field data and other models have demonstrated a variety of measures and issues [Refs. 2-2 through 2-10]. In particular, it has been pointed out [Ref. 2-10] that the relative advantages of different statistical measures of performances with respect to accurately communicating model behavior is dependent, at least in part, on the distribution of the variables of interest. In this study, we compute several statistical measures of performance and user-oriented measures of effectiveness (MOE) and base our conclusions on a review of all of these measures.

The rest of this section provides a detailed description of the two MOEs we examined and a brief description of the statistical measures we computed.

1. Measures of Effectiveness

Interest in developing application-specific MOEs is ultimately related to the desire to improve the potential for validation and user accreditation.³ Typical measures, or figures of merit (FOM), use ratios or differences between predicted and observed quantities (e.g., dosages or plume centerline). In general, these FOMs do not necessarily reflect specific user application-based concerns.

Perhaps the key objective for an interpretive user-oriented MOE, is its ability to communicate simply (and appropriately) the relative performance of the model in a given application. It is important that other measures, for instance, the statistical measures described later in this paper, also be examined for any set of data that is to be described. In order for such an MOE to have widespread credibility, the conclusions communicated to the user via the MOE should be consistent with the conclusions one would obtain from a detailed review of other statistical measures and graphical representations. Where there are inconsistencies, the differences should be highlighted and understood.

In the next six subsections, we define and explore two MOEs that have the potential to address user-specific requirements directly.

³ See Appendix N, “Task Order Extract” and Reference 2-11.

a. User-Oriented Measure of Effectiveness: MOE 1

A fundamental feature of any comparison of model output to observations is the over- and under-prediction regions. We can define false negative where a hazard is observed but not predicted and false positive where a hazard is predicted but not observed.

Figure 2-1 shows the observed area at a given dosage level and the predicted area at the same dosage level for some hypothetical situation. Numerical values in three-dimensional space characterize this conceptual view. These values are associated with estimates of the false negative region (A_{FN}), the false positive region (A_{FP}), and the overlap region (A_{OV}). Figure 2-1 illustrates, conceptually, A_{OV} , A_{FN} , and A_{FP} .

The first measure that we describe considers the ratio of the area of overlap (A_{OV}) to the total area (A_T). A_{OV} is the area in which both the prediction and the observation agree in some manner; for example, both the predictions and the observations show dosages above a certain level. Graphically, A_{OV} might correspond to the intersection of the two areas for which a certain dosage is exceeded.

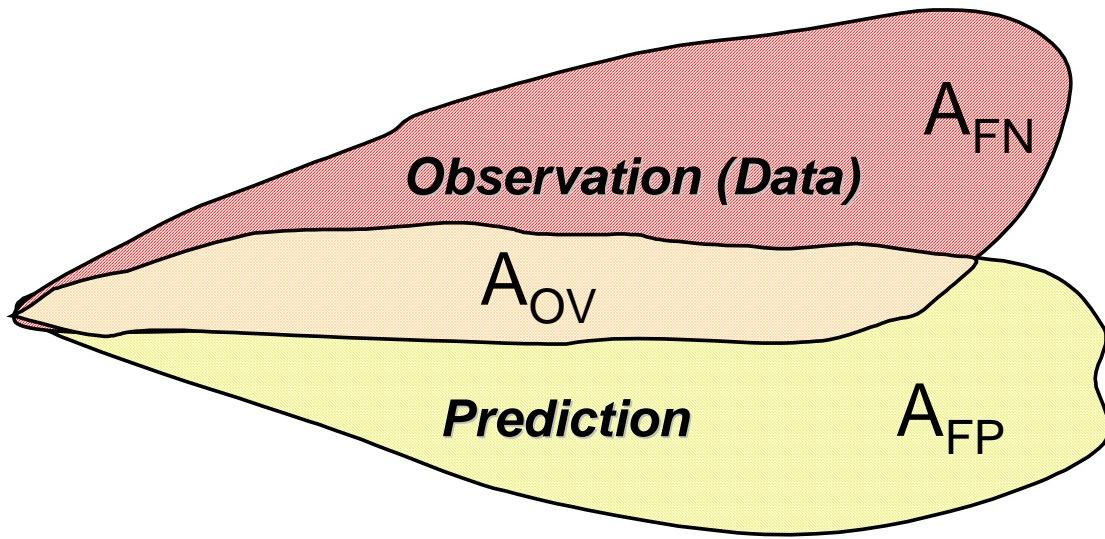


Figure 2-1. Illustration of A_{FN} , A_{FP} , and A_{OV}

A_T includes the overlap area (A_{OV}), the area in which a certain dosage level was predicted but not observed (“false positive”), and the area in which a certain dosage was observed but not predicted (“false negative”). Equation 2-1 describes this MOE. This measure for evaluating transport and dispersion models has been previously described [Refs. 2-12 and 2-13].

$$\frac{A_{OV}}{A_T} = \frac{A_{OV}}{(A_{OV} + A_{FN} + A_{FP})} \quad (2-1)$$

where A_{FN} is the false negative area and A_{FP} is the false positive area.

Typical operational users of transport and dispersion models might consider false positives and false negatives quite differently. For many applications, false positives would be much more acceptable to the user than false negatives (which could result in decisions that directly lead to death or injury). It has been suggested that equation 2-1 be modified with “tunable” coefficients that allow a user to weight the relative importance of false negatives and false positives [Ref. 2-14]. Equation 2-2 illustrates this modification, with C_{FN} defined as the false negative coefficient and C_{FP} defined as the false positive coefficient.

$$\frac{A_{OV}}{(A_{OV} + C_{FN}A_{FN} + C_{FP}A_{FP})} \quad (2-2)$$

where $C_{FN}, C_{FP} > 0$.

It may be true that, for some comparisons of predictions and observations, the weightings for false negatives and false positives are considered irrelevant or set equal ($C_{FN} = C_{FP}$).⁴

Figure 2-2 describes the behavior of MOE 1 ($C_{FN} = C_{FP} = 1.0$) as a function of A_{FN} and A_{FP} . For the computation of the values shown in Figure 2-2, A_T was normalized to 1.0. That is, $A_T \equiv A_{OV} + A_{FN} + A_{FP} \equiv 1.0$. Thus, the values of A_{FN} and A_{FP} shown on the x- and y-axis correspond to the fraction of the total area that is represented by false negative and false positive, respectively.

It can be seen that MOE 1 with $C_{FN} = C_{FP} = 1.0$, varies linearly from 0.0 to 1.0 as A_{FN} and A_{FP} decrease. A perfect one-to-one correspondence between a model’s predictions and observations would result in an MOE 1 value of 1.0.

⁴ As developed here, the implicit coefficient associated with A_{OV} is 1.0. Therefore, the notion of equal weights for A_{FN} and A_{FP} (i.e., $C_{FN} = C_{FP}$) is insufficient for the complete specification of this MOE. That is, the precise MOE values will depend on the values chosen for C_{FN} and C_{FP} and not just their ratio.

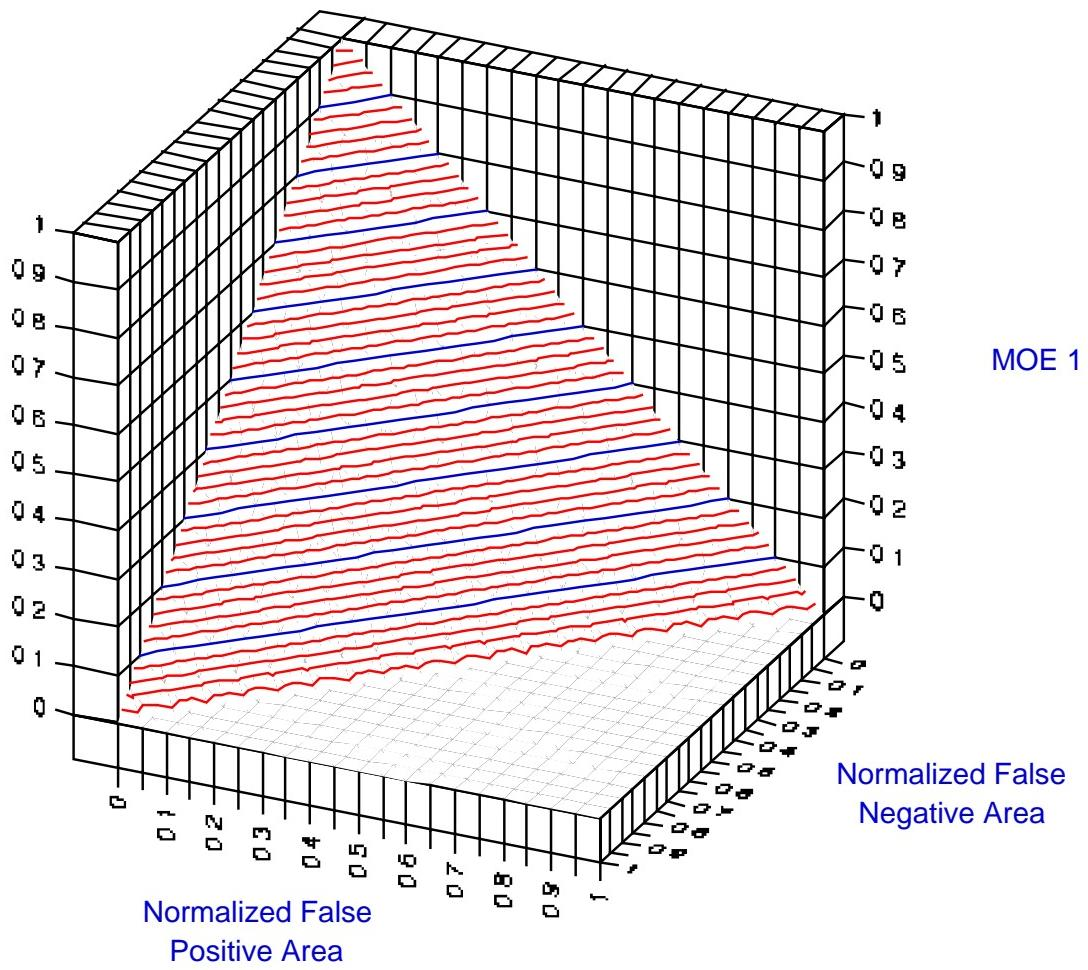


Figure 2-2. MOE 1 as a Function of A_{FN} and A_{FP} ($C_{FN} = C_{FP} = 1.0$)

Figure 2-3 illustrates the shape of this MOE when the coefficients are varied. The somewhat extreme weighting (i.e., 100 to 1) of false negative relative to false positive and overlap area shown in the bottom plot of Figure 2-3 illustrates the potential for significant nonlinear behavior of this measure. We expect that measures that perform linearly (or nearly linearly) over a large range will have greater utility than those that do not, at least with respect to the communication of model performance. It is also true that highly nonlinear measures could amplify relatively small changes in a data set, perhaps due to a minor measurement/transcription error. Therefore, such a nonlinear measure might not be considered robust.

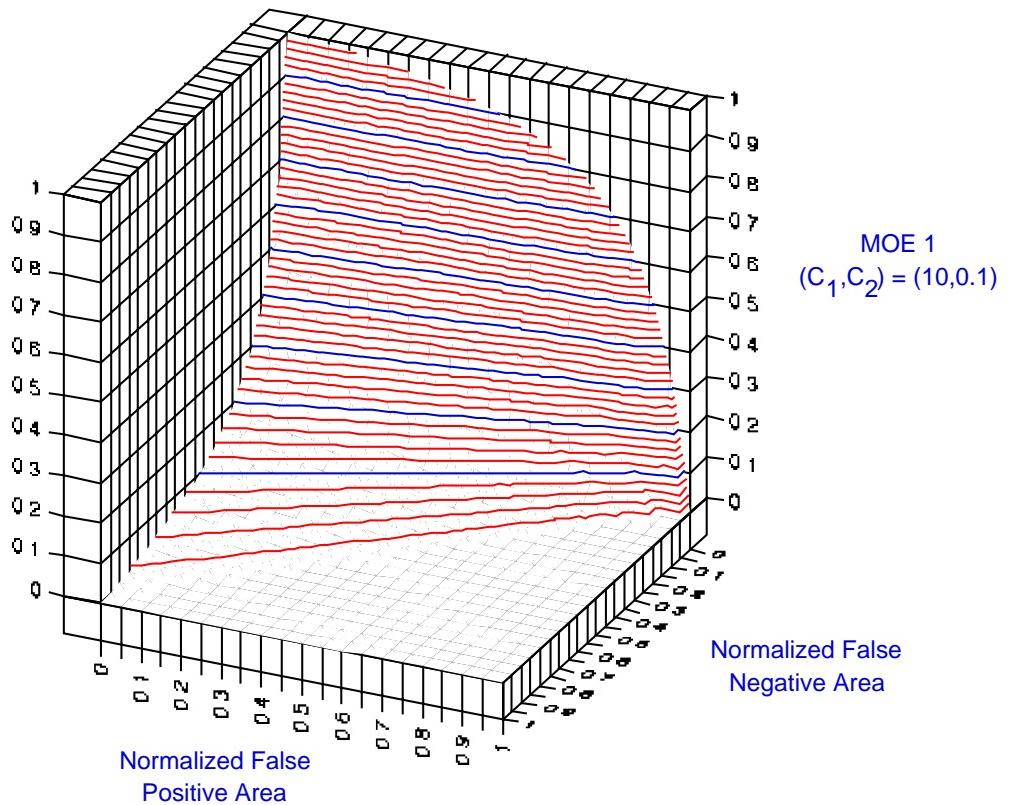
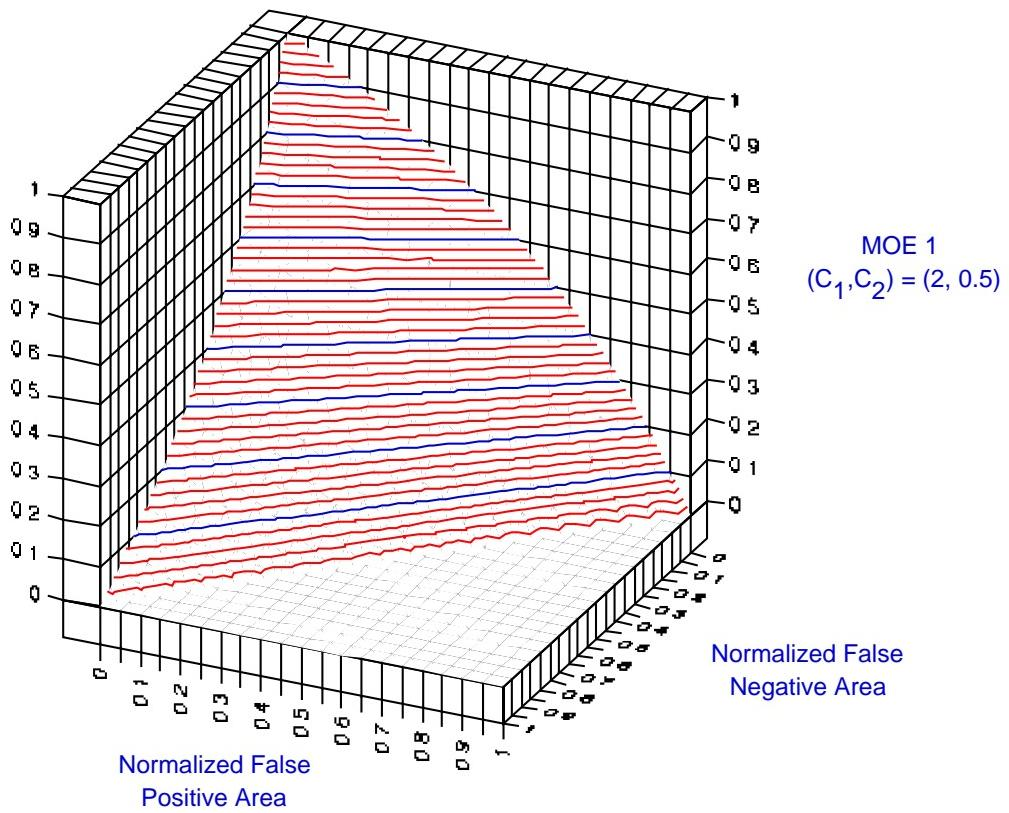


Figure 2-3. MOE 1 as a Function of C_{FN} and C_{FP}

b. A Two-Dimensional MOE: MOE 2

The second MOE that we consider is two-dimensional. That is, it is represented by a pair of numbers (x,y). First, we consider the ratios of the overlap area (A_{OV}) to the observed and predicted areas. Equation 2-3 describes these ratios as a point in two-dimensional space.

$$(r_1, r_2) = \left(\frac{A_{OV}}{A_{OB}}, \frac{A_{OV}}{A_{PR}} \right) \quad (2-3)$$

where A_{OB} is the area associated with the observations and A_{PR} is the area associated with the prediction. Inspection of Figure 2-1 suggests the relationships $A_{OB} = A_{OV} + A_{FN}$ and $A_{PR} = A_{OV} + A_{FP}$. Substituting these equalities into the denominator of equation 2-3, followed by algebraic rearrangement leads to Equation 2-4 – our preferred definition of MOE 2.

$$(r_1, r_2) = \left(\frac{A_{OV}}{A_{OV} + A_{FN}}, \frac{A_{OV}}{A_{OV} + A_{FP}} \right) = \left(1 - \frac{A_{FN}}{A_{OB}}, 1 - \frac{A_{FP}}{A_{PR}} \right). \quad (2-4)$$

A model prediction that is in perfect agreement with an observation, that is, all overlap area and no false positive or false negative, will have an MOE 2 value of (1,1). A model prediction that entirely misses the observed cloud, perhaps because of an errant wind direction, would have no overlap and an MOE 2 value of (0,0).

c. Interpretation of MOE 2

MOE 2 separates, orthogonally, the two fundamental features of any transport and dispersion *predictive* model – “false negatives” and “false positives.” The user or specific application determines the acceptability of a given false positive or false negative fraction. In practice, one expects that, for a given model, various underlying assumptions about input uncertainties (for example) can affect the relative ratio of A_{FN} and A_{FP} . Without some fundamental improvement to the model, one expects that decreases in A_{FP} will lead to increases in A_{FN} . Similarly, decreases in A_{FN} will be achieved only at the expense of increases in A_{FP} (without some fundamental model improvement, for example better weather data).⁵

⁵ More accurate weather data, for example, a more accurate wind direction, might improve both the false negative and false positive behavior of a prediction. That is, the 2D MOE value would move along the diagonal up and to the right (Figure 2-4).

Figure 2-4 illustrates the potential of MOE 2 for assessing application- or user-specific worth for a T&D model. The axes of the figure are as shown in equation 2-4. Along the x-axis, the fraction of the false negative area (A_{FN}) decreases from left to right. That is, model performance improves as this value gets larger. Similarly, as the values move up the y-axis, a decrease in A_{FP} is indicated.

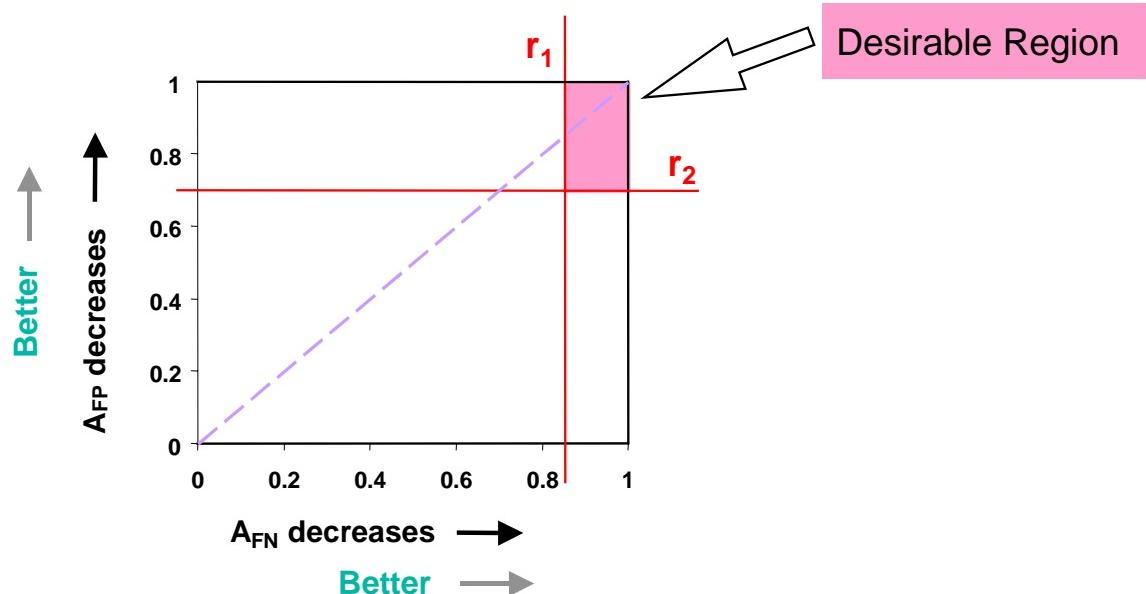


Figure 2-4. MOE 2 as a Function of A_{FN} and A_{FP}

We imagine a given user and application being associated with some risk tolerances, r_1 and r_2 , and therefore accept from a given prediction a certain false positive or false negative fraction. In essence, these risk tolerances define, in the MOE space, an acceptable or desirable region for model performance.

We envision that users may have very different requirements. For example, one application may concern estimating the hazardous area to a population and deciding how many people to evacuate. Clearly, large amounts of false negative area would not be acceptable – many people might be unnecessarily exposed. Alternatively, too large an area of false positive would be inefficient and perhaps dangerous if it implied the evacuation of a large population. A similar argument can be made for the use of a model to predict the release of hazardous material from an attack on an enemy CB facility. Again, a low false negative fraction would be required, but a large false positive fraction could greatly limit the target set, and adversely impact the wartime strategy.

Finally, one can imagine, for instance, a CB ballistic missile attack in the vicinity of a U.S. military unit. In such a case, an immediate goal of a friendly chemical

reconnaissance unit would be to locate the hazardous area, perhaps with only limited information, and ensure that future troop movements avoid this area. For this mission then, this reconnaissance unit would *want* to encounter the chemical agent quickly in order to start mapping the hazardous location. Unlike the other scenarios discussed above, a T&D predictive system with a relatively high false negative fraction, but with a very low false positive fraction, might be considered quite satisfactory for this application.

An additional feature associated with this 2D MOE is highlighted by the dashed purple line that lies along the diagonal in Figure 2-4. Setting $r_1 = r_2$, we can derive from equation 2-4 the equation shown below.

$$1 = \frac{r_1}{r_2} = \frac{\left(\frac{A_{OV}}{A_{OV} + A_{FN}} \right)}{\left(\frac{A_{OV}}{A_{OV} + A_{FP}} \right)} = \frac{\left(\frac{A_{OV}}{A_{PR}} \right)}{\left(\frac{A_{OV}}{A_{OB}} \right)} = \frac{A_{OB}}{A_{PR}}. \quad (2-5)$$

Therefore, MOE 2 values lying on the diagonal line represent cases where the total predicted and observed plume areas are of equal size. For example, an estimate of (1,1), at the top of diagonal, corresponds to a predicted and observed plume of the same size that exactly coincide – that is, perfect overlap. A 2D MOE estimate of (0,0), at the lower end of the diagonal, implies plumes that miss each other completely – that is, no overlap (perhaps due to incorrect wind direction information).⁶ As MOE values traverse this diagonal, from (0,0) to (1,1), the suggestion is, at least for equally shaped plumes, that the wind field model components (e.g., direction and speed) have improved (i.e., the amount of overlap is increasing).

MOE 2 values along the axis (1,y) imply no false negative fraction. That is, the prediction totally includes the observation (e.g., a probabilistic output that considered an ensemble of initial conditions might be represented on this axis). Along the axis defined by (x,1), the suggestion is that the predicted area fits totally within the observed area, with the false negative fraction described by 1-x.

In the end, the credibility and usefulness of MOEs designed to incorporate user/application-specific needs will require review by the user – as part of the

⁶ Mathematically, at exactly (0,0) nothing can be inferred about the sizes of the plumes. However, at any point arbitrarily close to (0,0) and along the diagonal, it will be true that the predicted and observed area sizes will be equal with almost no overlap.

accreditation process. We believe that measures that clearly present the “tradeoffs” associated with false negatives and false positives stand the best chance to satisfy the user’s accreditation needs.

Figure 2-5 suggests an additional interpretation of the 2D MOE. In this figure, the multi-pointed gold star represents the estimate of MOE 2 for some set of fictional model predictions and field trial observations. The point estimate, perhaps the vector mean value of several similar trials, would be found at the center of this star, and the overall size of the star represents the uncertainty associated with the point estimate of MOE 2. If a second set of model predictions were compared to “Model A” with MOE 2, several conclusions might be anticipated. The second model estimate might be found in the region shaded orange (lower left). This would imply that Model A performs significantly better; both its false positive and false negative fractions are lower. Alternatively, the second model might lead to an estimate in the green region (upper right) – an indication that Model A is the poorer performer (for this set of field trial observations). Finally, the new model predictions might lead to an MOE 2 value that is located within the gray region. The implication here is that a user would have to make a determination as to the tradeoff between false positive and false negative before deciding which model was most appropriate for his/her specific application.

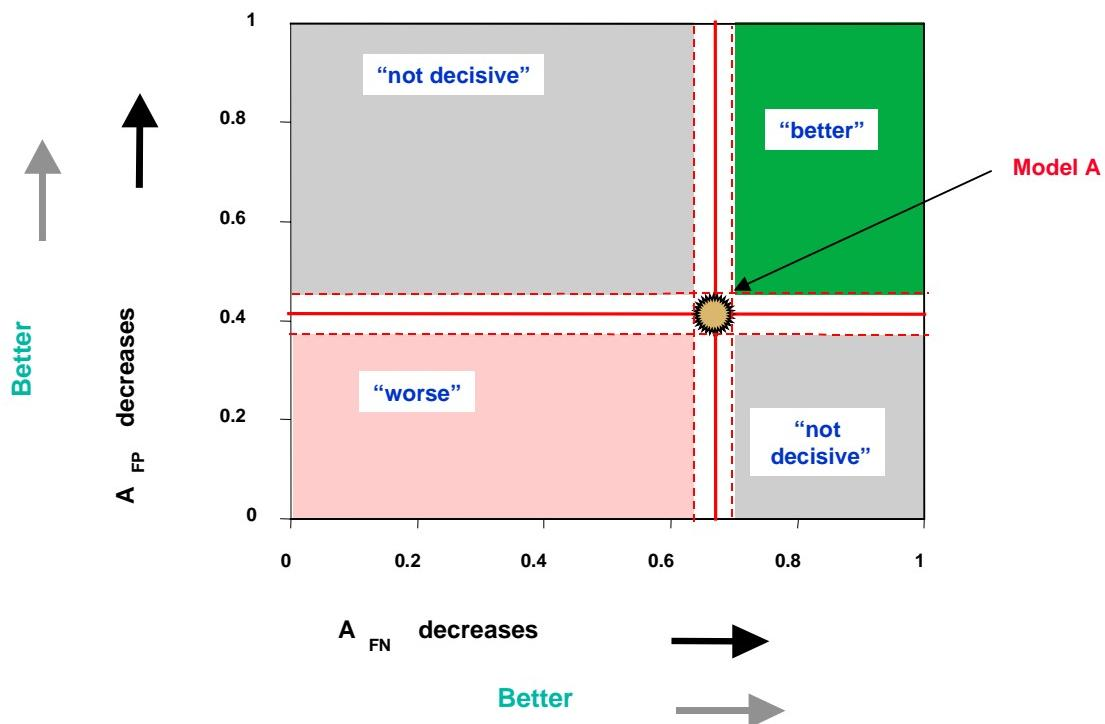


Figure 2-5. 2D MOE: Interpretation of Model Comparisons

d. Relationship Between MOE 1 and MOE 2

The two MOEs described previously, one- and two-dimensional, are related. Equation 2-6 relates the x- and y-axes of the 2D MOE to the one-dimensional MOE.

$$MOE\ 1 = \frac{xy}{(xy + C_{FN}y(1-x) + C_{FP}x(1-y))}. \quad (2-6)^7$$

Figure 2-6 shows MOE contours (i.e., isolines for MOE 1) for $C_{FN} = C_{FP} = 1$. Similarly, Figure 2-7 illustrates the case where A_{FN} is weighted by a factor of 10 relative to A_{FP} and 5 relative to A_{OV} (i.e., $C_{FN} = 5$ and $C_{FP} = 0.5$).

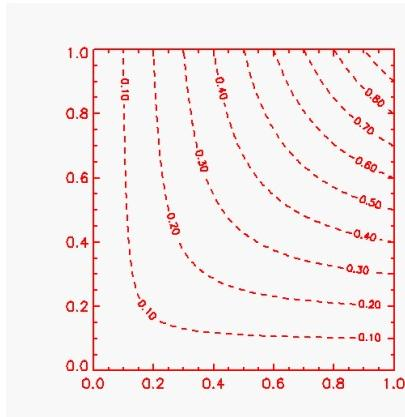


Figure 2-6. Relationship Between MOE 1 and MOE 2: $C_{FN} = 1$, $C_{FP} = 1$

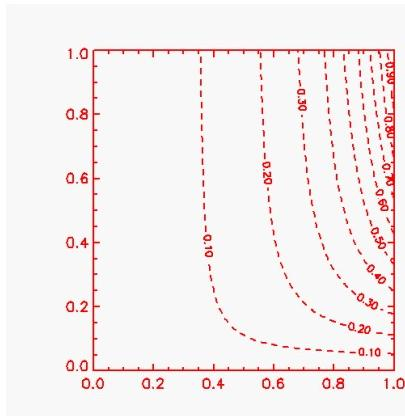


Figure 2-7. Relationship Between MOE 1 and MOE 2: $C_{FN} = 5$, $C_{FP} = 0.5$

⁷ This equation is derived by first recognizing that for the 2D MOE, $x = \frac{A_{OV}}{(A_{OV} + A_{FN})}$, $y = \frac{A_{OV}}{(A_{OV} + A_{FP})}$ and, therefore, $A_{FN} = \left(\frac{1-x}{x}\right)A_{OV}$ and $A_{FP} = \left(\frac{1-y}{y}\right)A_{OV}$. These definitions of A_{FN} and A_{FP} are then substituted into equation 2-2. Following algebraic rearrangement, equation 2-6 is obtained.

The above two figures show that estimates of the 2D MOE can be directly converted to estimates of MOE 1. For example, a 2D MOE point estimate of (0.5,0.5) implies, according to Figure 2-6 (and equation 2-5), an MOE 1 value of 0.33 for $C_{FN} = C_{FP} = 1.0$. Similarly, inspection of Figure 2-7 shows that for $C_{FN} = 5$ and $C_{FP} = 0.5$, a 2D MOE point estimate of (0.5,0.5) suggests an MOE 1 value of about 0.15.

e. Two Estimates of “Area” Size

A 1998 comparison of long-range dispersion model predictions included an MOE similar to the one-dimensional measure (MOE 1) that was described previously. In that case [Ref. 2-13], the measure was referred to as the figure-of-merit in space and did not include weighting coefficients (C_{FN} and C_{FP}). Long-range observations (across Europe) from the European Tracer Experiment (ETEX) were used to develop contours (isolines) at given concentrations using logarithmic interpolation of the ground-level sampled values. This measure was deemed an effective index for describing model performance at a fixed time, although it was suggested that this figure-of-merit in space was sensitive to the type of interpolation scheme used.

Often, field trial observations are represented by dosages at specific sampler locations, perhaps along an arc or line. Therefore, a direct estimate of the area that contains a given concentration or dosage is not available. When using the above MOEs for comparisons to observations, an approach to estimating the “area” size and location must be developed.

Below we describe two different methods that can be used to develop “area” estimates from *Prairie Grass* observations.

1) Area Estimate 1 (AE1)

AE1 is illustrated in Figure 2-8 for the 800-meter arc samplers of *Prairie Grass* field trial 8. First, we define a threshold dosage of interest. In the figure, a threshold of 60 mg·sec/m³ is used. One then can develop an area estimate, referred to here as AE1, say for the false positive, by computing the distance covered by the samplers in which there is a prediction but no observation above threshold. Similarly, distances for the overlap region and false negative region can be computed. These *distances* are naturally related to actual areas. That is, the AE1 estimate represents a natural analog to a hazard area at a given critical threshold.

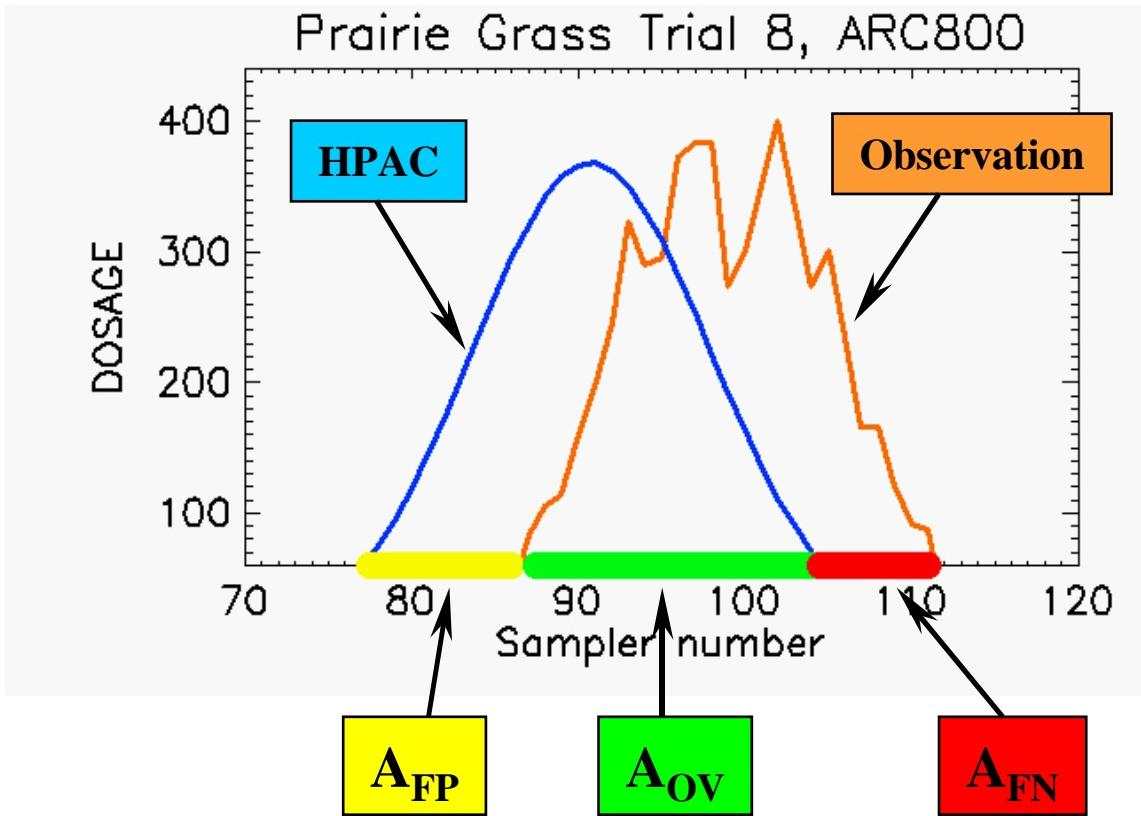


Figure 2-8. Illustration of AE1

2) Area Estimate 2 (AE2)

AE2, illustrated in Figure 2-9, can be computed by integrating the areas under the associated curves. For example, for A_{fp} (as shown in Figure 2-9), one first considers all of the samplers at which the *prediction is of greater value than the observation*. Next, one simply sums the differences between the predicted and observed dosages at those samplers. Based on the samplers that contained *observed values that were larger than the predicted values*, one can similarly compute A_{fn} . A_{ov} is calculated by considering all samplers and summing the dosages associated with the minimum predicted or observed value. A_{ov} , A_{fp} , and A_{fn} are computed as shown in Figure 2-9 and are somewhat related to crosswind integrated (CWI) dosages. However, AE2 involves point-to-point comparisons and includes directional effects, unlike CWI dosages.

It should be noted that the terms “false negative” and “false positive,” as defined in Figure 2-1 and used in AE1, are not strictly applicable to AE2. A more accurate description is that AE2 measures the degree of under-prediction and over-prediction of dosages integrated along the sampler arc. Unlike an MOE using AE1, a perfect MOE

score based on AE2 indicates “exact” agreement between measured and predicted dosages at every sampler location.⁸

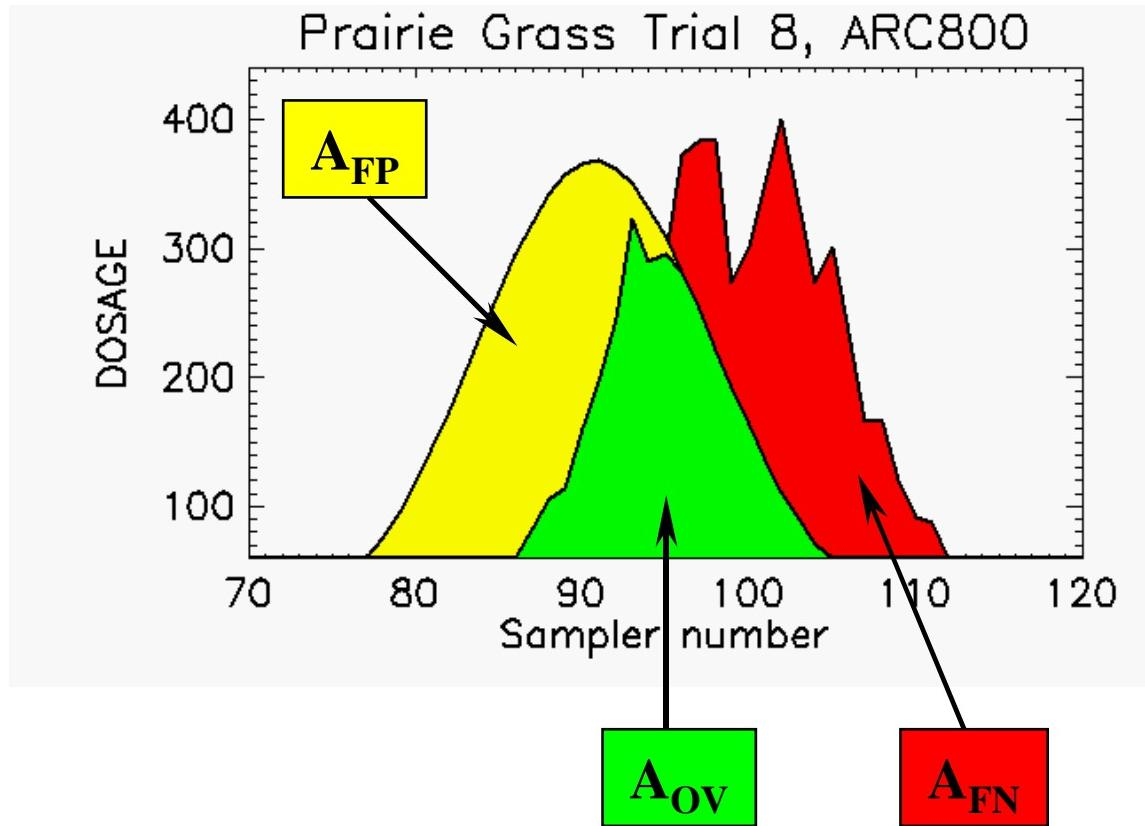


Figure 2-9. Illustration of AE2

f. Application of Probit Curves as a “Lethality/Effects Filter”

Next, we interpret observations and predictions by considering the lethality or effects of a presumed agent. First, the lethality/effects of the agent being studied and the dosages at a given sampler are examined. For example, standard probit curves might be used to assess the lethality/effects of a given exposure.⁹ Next, the dosages are converted

⁸ Theoretically, the computation of AE2-based values does not require the use of a threshold. However, field trial data will always have uncertainties associated with the smallest observations – that is, experimental resolution. Therefore, AE2-based computations that use field trial data require a defined threshold. Thus, for a perfect MOE 2 AE2 value of (1,1), exact agreement at samplers above some threshold can be inferred.

⁹ Lethality and effects models may be subject to poorly known thresholds and probit slopes (assuming a probit model). There may be uncertainties in the knowledge of the source purity and unknown correction factors for applying data to a general population versus military personnel. Determining actual casualty levels for a specific scenario would also need to include factors such as the means of exposure (respiratory or percutaneous) and other parameters relating to that exposure (e.g., breathing rate and the effect of clothing).

into a fractional lethal/effects exposure, i.e., that fraction of an exposed population, at that dosage level, that would be expected to become a casualty. For example, if the observed or predicted dosage were LD_{50} (lethal dosage for 50 percent), then half of the population would be expected to die.

Figure 2-10 provides a nominal illustration of this calculation. First, the observed dosage at sampler “17” is $10 LD_{50}s$ ($10 \times LD_{50}$) and the predicted dosage (by HPAC in this illustration) is $1,000 LD_{50}s$. These differences can be converted into the fraction of the exposed population that would be expected to become a casualty. Assume that for the probit curve associated with the hypothetical agent, a dosage of $10 \times LD_{50}$ means that 90 percent of the population is exposed to a lethal dosage, while a dosage of $1000 \times LD_{50}$ implies 99.99 percent of the population accumulates a lethal dosage. The $10 LD_{50}s$ observed dosage indicates that 0.90 of the exposed population would be expected to accumulate a lethal dosage. In this case, the model overpredicts the observation and the area of false positive, A_{FP} , corresponds to an additional (approximately) 0.10 lethal exposure population fraction.¹⁰ Then for each trial (or arc or sampler), estimates of A_{ov} , A_{FN} , and A_{FP} can be obtained in this way.

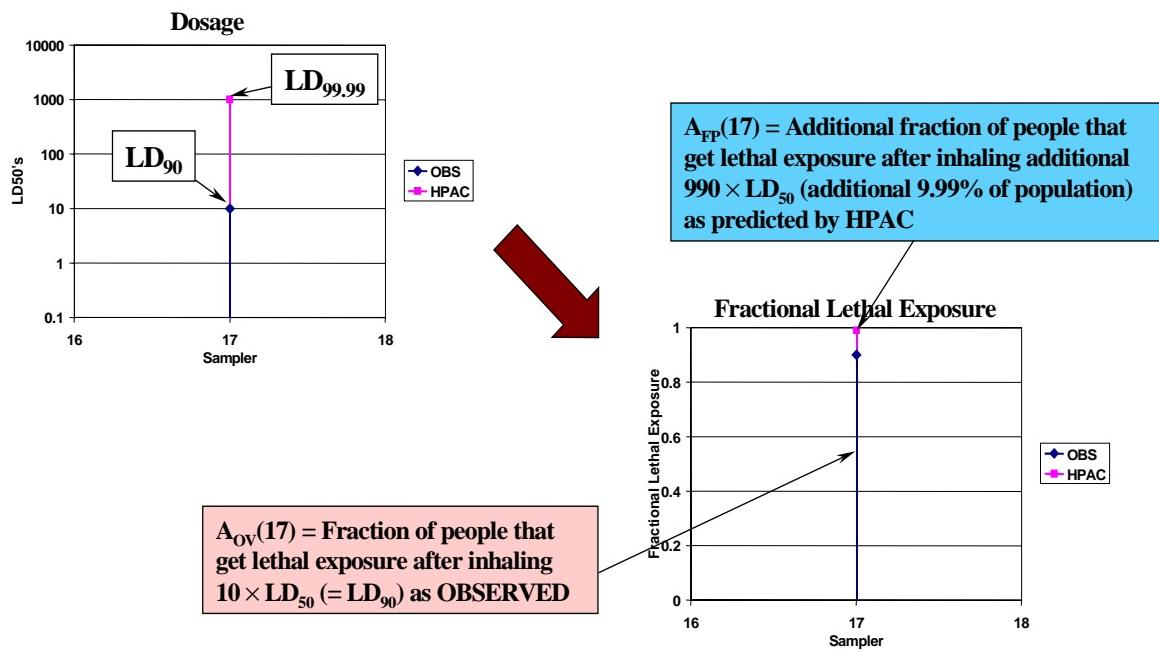


Figure 2-10. Nominal Lethality/Effects Filter Illustrated

¹⁰ In this study, the underlying population distribution was assumed to be spatially uniform for the computation of the lethality/effects-filtered MOEs.

In a sense, the above process filters our interpretation of the above areas (i.e., A_{OV} , A_{FP} , and A_{FN}) through the appropriate lethality/effects “lens.” Hence, we refer to MOE results obtained in this way as “lethality/effects-filtered.”

Figure 2-11 suggests that these lethality/effects-filtered results can be viewed as an extension of AE2. By accounting for the lethality/effects of a given hazard, this measure *operationally* weights the over- or under-prediction of a model (with respect to a set of observations). Therefore, differences between observations and predictions that would lead to additional deaths or casualties are considered more important than those that, perhaps, lead to very different dosages but a similar fraction of lethal/effects exposure.

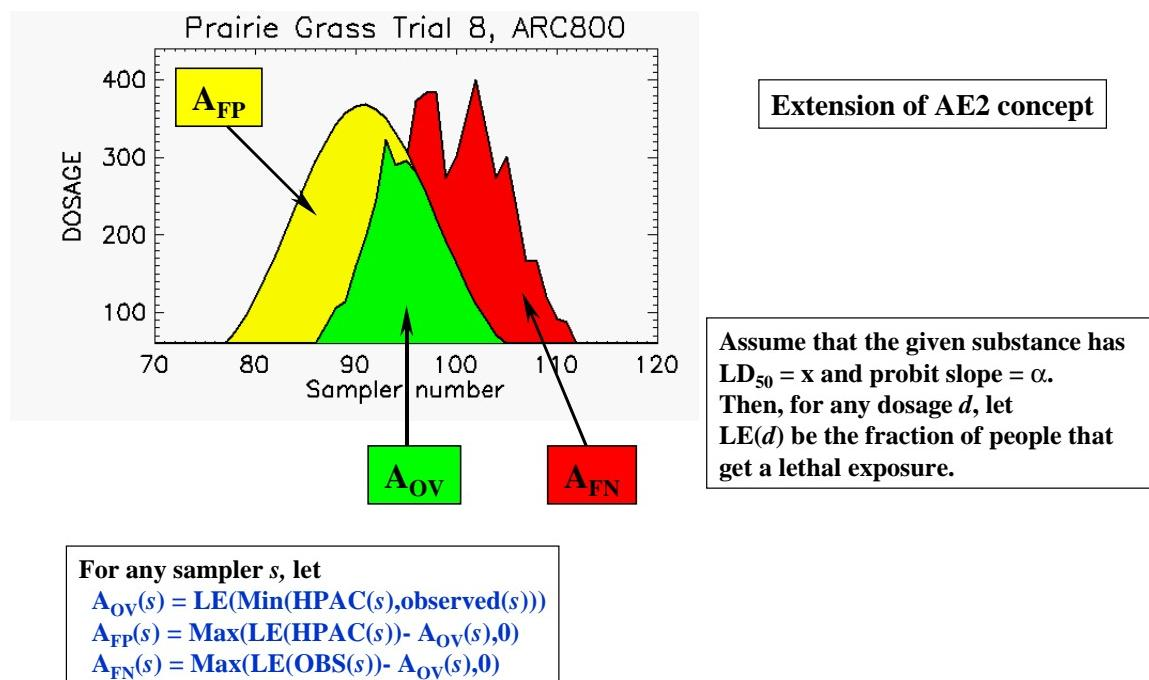


Figure 2-11. Lethality/Effects Filter as an Extension of AE2

For this comparison to *Prairie Grass* trials, the tracer agent was sulfur dioxide, SO_2 . Because this agent is considered relatively non-toxic, one cannot *directly* compute lethality/effects filter-based MOEs. Of course, for some assumed lethality/effects levels, one can apply the above methodology to the *Prairie Grass* observations (as we do in Chapter 3 in order to demonstrate the utility of this method).¹¹

¹¹ In Chapter 3, the relationship between lethality/effects-filtered MOE results and AE1/AE2 results will be described.

2. Statistical Measures

In addition to the MOEs described above, eight other statistical measures of performance were computed for the model comparisons described in this paper. Two derived parameters were considered for the calculation of each of these statistical measures. First, for each arc the maximum dosage was considered – ArcMax. Next, the crosswind-integrated (CWI) dosage was examined.

The statistical measures include fractional bias (FB), geometric mean bias (MG), normalized mean square error (NMSE), geometric mean variance (VG), correlation coefficient (R), fraction of predictions within a factor of 2 (FAC2), fraction of predictions within a factor of 5 (FAC5), and fraction of predictions within a factor of 10 (FAC10). These measures are defined below:

$$FB = \frac{(\bar{C}_o - \bar{C}_p)}{0.5(\bar{C}_o + \bar{C}_p)} \quad (2-7)$$

$$MG = \exp\left(\overline{\ln C_o} - \overline{\ln C_p}\right) = \exp\left(\overline{\ln\left(\frac{C_o}{C_p}\right)}\right) \quad (2-8)$$

$$NMSE = \frac{(\bar{C}_o - \bar{C}_p)^2}{\bar{C}_o \bar{C}_p} \quad (2-9)$$

$$VG = \exp\left(\overline{(\ln C_o - \ln C_p)^2}\right) = \exp\left[\overline{\left(\ln\left(\frac{C_o}{C_p}\right)\right)^2}\right] \quad (2-10)$$

$$R = \frac{(\bar{C}_o - \bar{C}_o)(\bar{C}_p - \bar{C}_p)}{\sigma_{C_p} \sigma_{C_o}} \quad (2-11)$$

$$FAC(x) = \text{fraction of data for which } \frac{1}{x} \leq \frac{C_p}{C_o} \leq x \quad (2-12)$$

where C = observation/prediction of interest (e.g., dosage), C_p corresponds to model prediction, C_o corresponds to observations, \bar{C} implies the average, σ_C = standard deviation, and for this study $x = 2, 5$, and 10 . We consider these statistical measures to be *somewhat standard* since several relatively recent reports known to the authors [Refs. 2-2 and 2-10] make use of these measures.

FB and MG measure the systematic bias in a model (relative over-prediction or under-prediction). NMSE and VG measure the scatter associated with the predictions

relative to observations. Because FB and NMSE are based on a linear scale, they can be overly influenced by infrequently occurring high observed or predicted dosages.¹² Alternatively, MG and VG arise from a logarithmic scale and can be influenced, perhaps unduly, by a few low observed or predicted dosages. Our approach is to compute all of these measures and recognize the inherent limitations of each. It is expected that, taken together, the eight measures described above can provide good insight into the relative performance of a given model.¹³

An additional issue exists for the measures that are computed on a logarithmic scale. Situations in which the observation or prediction is exactly 0.0 cannot be directly dealt with – $\log(0)$ is undefined. Typical approaches to this problem have included leaving those observation/prediction pairs that include a zero out of the calculation – an undoubtedly biased approach – or somewhat arbitrarily setting zeros equal to some minimum value. In general, tests for sensitivity to the exclusion of data will need to be performed to allow for robust conclusions. Of course, MG and VG estimates might be very sensitive to the choice of this minimum value.¹⁴

In addition to the ArcMax and the CWI dosage, estimates of the plume width and centerline direction were also derived for each arc. We defined the width of the plume by “cutting” equal crosswind integrated dosages from the sides of the plume. Given a particular fraction of the crosswind integrated dosage that we want to capture inside the plume (e.g., 0.75), we can find the maximal index k_{left} , and minimal index k_{right} (from the left and right, respectively) such that:

¹² In fact, our initial observation of large NMSE values (with associated very large estimated confidence intervals) led us to carefully re-examine the *Prairie Grass* field trial computer files that had been provided to us. A few apparently spurious peaks in the data were identified and their origins were investigated. The inclusion of these few peaks (i.e., ArcMax values) resulted in large NMSE and very large associated confidence intervals. As a result of this investigation, we found a few places where a decimal point had been misplaced in converting the “hardcopy” of the *Prairie Grass* field trial sampler data into computer format. Additionally, we concluded that two “spurious” peaks that were recorded in the hardcopy of the report were due to incorrect placement of the decimal point by the authors of that report. Appendix K details these findings and corrections.

¹³ Perfect agreement with a set of observations would result in MG, VG, R, FAC2, FAC5, and FAC10 = 1.0; and FB and NMSE = 0.0.

¹⁴ For this study, we do not report point-to-point comparisons. That is, we only present statistical measures associated with single characterizations of each sampler arc, for example, ArcMax and CWI dosage. The values of ArcMax and CWI dosage for the valid *Prairie Grass* field trials were always greater than zero. Therefore, we do not encounter the problem of “zeros” in this study and can directly compute measures such as MG and VG.

$$\begin{aligned} k_{left} &= \max \left\{ k \mid \sum_{i=1}^k D_i \leq \frac{1-0.75}{2} = 0.125 \right\} \\ k_{right} &= \min \left\{ k \mid \sum_{i=k}^N D_i \leq \frac{1-0.75}{2} = 0.125 \right\} \end{aligned} \quad (2-13)$$

where D_i is a dosage collected at sampler i .

Then, we define width for this equal-cuts-off-the-sides method (W_{ec}) as:

$$W_{ec} = r\theta \times (k_{right} - k_{left}) \quad (2-14)$$

where r is the distance in meters to the arc and θ is the angular separation (in radians) between the samplers. W_{ec} is estimated in units of meters. For this study, we considered widths that included 75 percent of the CWI dosage associated with the given arc (as in equation 2-13).

We defined the centerline direction (CentDir) in the following way. We considered the point that divides the plume into two equally weighted plumes (i.e., this is a median-based calculation). We define the median of mass (MOM) centerline of the plume for any given arc by finding the sampler with index MOM, (s_{MOM}), such that:

$$MOM = \min \left\{ k \mid \sum_{i=1}^k D_i > 0.5 \sum_{i=1}^N D_i \right\}. \quad (2-15)$$

CentDir is measured in units of degrees.¹⁵ Additional comments and discussion of alternative methodologies for estimating the plume width and direction for *Prairie Grass* field trial data can be found in Appendix J of this document.

For W_{ec} , we computed the NMSE and FB.¹⁶ For CentDir, we computed the root mean square error (RMSE) and bias as defined below:¹⁷

$$RMSE = \sqrt{\overline{(C_o - C_p)^2}} \quad (2-16)$$

$$Bias = \overline{C_o} - \overline{C_p}. \quad (2-17)$$

¹⁵ Because the angular separation of the samplers for the 50- through 400-meter arcs is 2 degrees, the precision with which CentDir MOM can be known is 2 degrees. For the 800-meter arc, the angular separation, and, hence precision, is 1 degree.

¹⁶ Since W_{ec} values did not vary by large amounts (e.g., orders of magnitude), we do not present logarithm-based measures (i.e., MG and VG) in this case.

¹⁷ NMSE and FB were deemed inappropriate for use with CentDir. In particular, the normalizing feature of these measures (i.e., the denominators) requires an absolute scale which is absent in this measure of direction. For example, if CentDir (in degrees) is measured from the North, one would expect the NMSE and FB values to differ when compared to measurements done, for instance, from the South.

3. Estimation of Confidence Intervals

In order to assess the significance of a particular result, we computed confidence intervals (95 and 80 percent) for each measure. For these calculations, we adopted the bootstrap (resampling) procedures that have been applied in recent air quality model evaluation studies [Refs. 2-15 and 2-16]. We used a modified version of the *BootCode*.¹⁸ In addition, for use in this study, the following modifications were made to the *BootCode* software:

- **The random number generator was modified.** The unmodified *BootCode* requires a separate file that contains the “official” list of random numbers. This file has 10,000 random numbers, which are reused in a circular fashion (i.e., 10,001st random number is the same as the first, and the 10,002nd is the same as the second). This random number generation methodology appears to be an artifact associated with this software’s development on personal computers in the mid-1980s. That is, such a procedure was computationally acceptable.

From a statistical point of view, this procedure can be problematic. To compute bootstrap confidence intervals, 1,000 “resamples” are typically required. Using the same “random numbers” via the circular procedure described above can lead to correlation and confidence intervals that are not as exact as one might expect based solely on the number of resamplings. To see this, consider the following “worst case-like” situation. Assume that the input data set contains 250 points and that 1,000 resamplings, each of size 250, are completed. This implies that the original 10,000 numbers will be used exactly 25 times. In fact, the confidence intervals in this example will really be based on 40 resamplings and not 1,000. Whenever more than 10,000 random numbers are required, this correlation problem *will* exist, although generally to a smaller degree than in the example shown above.

Our modification to the *BootCode* allows the random numbers to be chosen from a modern random number generator, based on a *Numerical Recipes* [Ref. 2-17] formulation. This modification refills the original 10,000 random numbers with a new set when the end of the list is reached.

- **Additional blocking features were added.** This modification allows confidence interval information to be output for each defined block. For

¹⁸ The *BootCode* software (Sigma Research Corporation, S. R. Hanna) as modified by LLNL to output FAC 5 and FAC10.

example, if data are blocked by range, then confidence interval information is output at each range.¹⁹

- **The percentile method, rather than the bootstrap-t method, was used for confidence interval estimation.** The *BootCode* calculates two types of confidence intervals: “robust” and “seductive.” Robust intervals appear to be based on the bootstrap-t procedure and the seductive intervals are based on the percentile method [Ref. 2-18]. The authors of the *BootCode* recommend using the robust intervals.²⁰ Basically the bootstrap-t method (also known as robust) allows one to estimate the mean and variance and then, based on a Student’s t-distribution, generate confidence limits. This technique was employed instead of the percentile (or seductive) method because it was known that the tails of the given distribution might be less accurately known than the mean and variance. The percentile method directly uses the tails of the distribution to generate, for instance, the 95th percent confidence interval. The concern with less accurate tails is that estimates of confidence intervals based on them might be inaccurate or biased. Hence, the recommendation to use the bootstrap-t procedure.

However, the t-distribution may not be appropriate for the given statistic. For example, using the recommended *BootCode* procedures, we often found that estimates of the lower bound limits for NMSE were negative – a physically implausible situation. Similarly, estimated upper limits on correlation, R, could be above 1.0.

A simple fix to this problem would be to allow the user to choose an appropriate distribution depending on the statistic being examined (e.g., perhaps log-normal in some cases). The *BootCode* software that we had did not easily allow for this decision. In addition, considering the varied potential users of this software, allowing such decisions by all users may not be deemed “operationally robust” (i.e., some users might make incorrect decisions).

We decided simply to use the percentile method for all calculations of confidence intervals – essentially to avoid implausible confidence intervals on NMSE. We also note that the amount of bias resulting from a bootstrap procedure can be estimated by comparing the bootstrap sample estimates to the original point estimate. Furthermore, if substantial bias is identified, then

¹⁹ In addition, a minor modification to the *BootCode* allowed us to compute approximate confidence intervals for RMSE and bias.

²⁰ See page 2271 of Reference 2-2 and page 1386 of Reference 2-16.

a straightforward bias correction procedure, known as the bias-corrected and accelerated (BC_a) method, can be applied.²¹

Bootstrap techniques, similar to those described above for the statistical measures, were also used to assign approximate confidence regions to MOE 2 estimates. We used our own resampling routines (vice the *BootCode*) for these computations.²² For each trial prediction/observation (and each individual arc), an MOE 2 value, (x,y), was computed. For a given set of comparisons, for example, all 50 meter arcs, the vector mean of these values corresponded to the MOE 2 point estimate. Approximate confidence regions were computed by re-sampling *pairs* of MOE 2 “observations” (i.e., individual trial (x,y) vectors). This procedure, resampling in pairs, maintains the appropriate correlation inherent in the data set.

C. TRIAL CONDITIONS THAT WERE EXAMINED

Logicon R&D Associates or IDA prepared the HPAC predictions and LLNL personnel prepared the NARAC predictions. Appendix B of the paper provides tables that describe additional input details associated the NARAC and HPAC predictions.

1. Prairie Grass Field Trial Data Were Collected Along Five Arcs

Some of the *Prairie Grass* field trials were removed from the HPAC/NARAC comparison. (See Appendices B and K for further details.) That left 51 field trials that formed a basis for our HPAC/NARAC comparisons. Each *Prairie Grass* trial contains data for five semicircular arcs of samplers positioned at an altitude of 1.5 meters, and six towers containing samplers at various altitudes located at the 100-meter arc. In this study, only samplers located at semicircular arcs at the height of 1.5 meters were considered. Figure 2-12 depicts a typical *Prairie Grass* trial result for the five arcs that were used in the analyses.

Table 2-1 lists the number of samplers in each of the semicircular arcs, angular separation between samplers in the arc, and the Cartesian distance between samplers in

²¹ See page 184 of Reference 2-18. As an aside, Reference 2-18, page 160, footnote 1 states in part, “In practice, however, the bootstrap-t can give somewhat erratic results, and can be heavily influenced by a few outlying data points. The percentile based methods of the next two chapters are more reliable.”

²² The routines used are based on in-house modified versions of spreadsheet software available at <http://web.nps.navy.mil/~orfacpag/resumePages/gaver/bootstrap.htm>.

the arc. For each arc, a single value²³ (for either the user-oriented MOEs or the “standard” statistical measures) is calculated, thus yielding five separate values per trial.

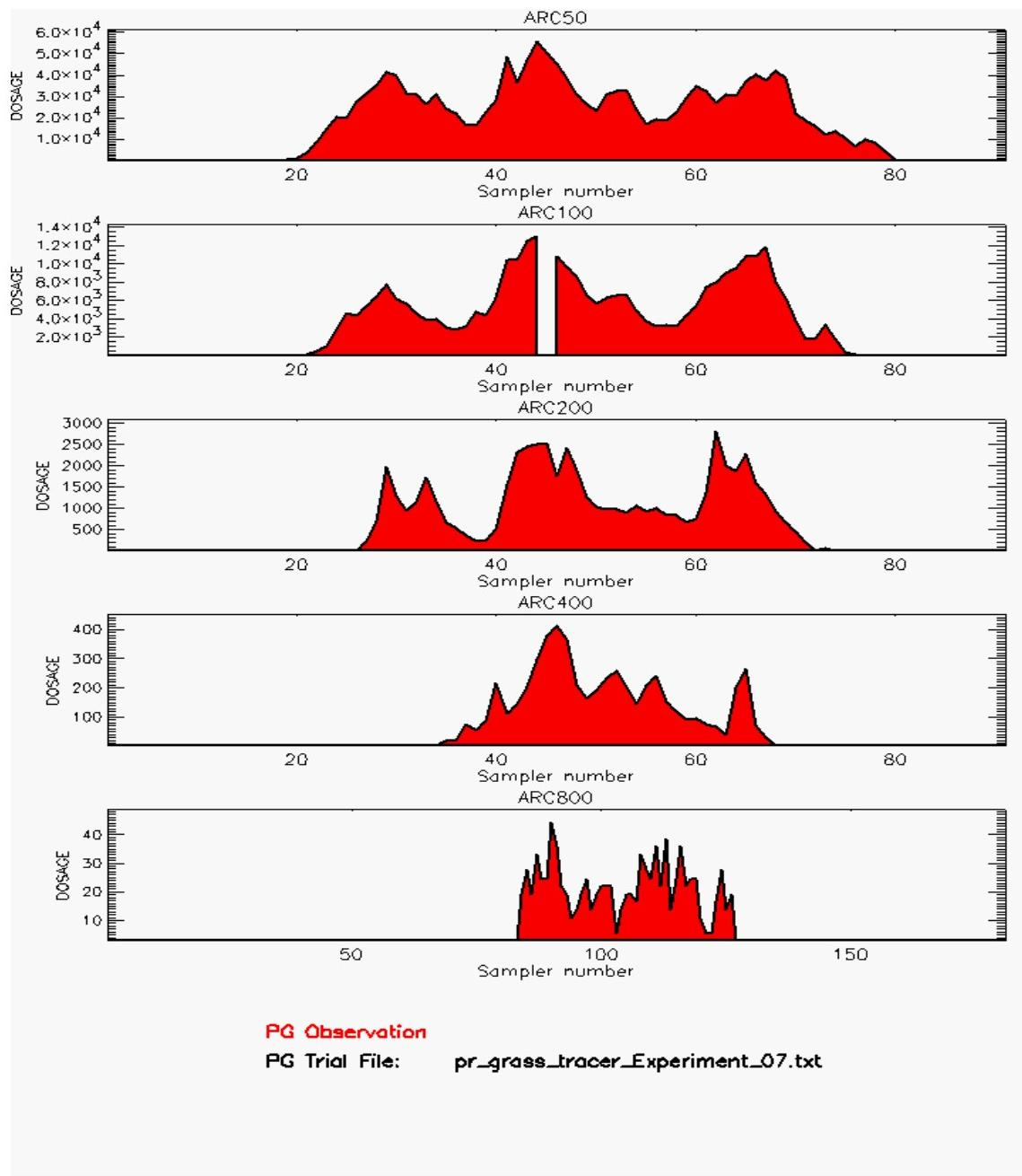


Figure 2-12. Prairie Grass Trial 7 as a Function of Arc: Stability Category is 1²⁴

²³ For the one-dimensional MOE (MOE 1), this is a single number, while for the two-dimensional MOE (MOE 2) this is represented by a pair of numbers.

²⁴ The value for sampler 45 of the 100-meter arc is missing. Dosage units are in mg-sec/m³. Dosage times a breathing rate (in m³/sec) equals dose (in mg).

These values are combined into separate groupings that are then used in the comparisons. This structure of the *Prairie Grass* field trials gives a natural way of comparing results by arc range.

Table 2-1. Distance Between Samplers by Arc

Arc	Number of Samplers	Angular Separation, degrees	Cartesian Separation, meters
50-meter	91	2	1.75
100-meter	91	2	3.49
200-meter	91	2	6.98
400-meter	91	2	13.96
800-meter	181	1	13.96

Importantly, the user-oriented MOEs presented in the previous subsection are closely related to actual area measures.²⁵ Thus, there is a natural way to combine MOEs calculated for each individual arc into a single MOE value that is associated with a particular trial. To do so, we associate each sampler with a short line segment centered at the sampler location and having the same length as the inter-sampler distance for that arc. Then for AE1, given some specified threshold, we multiply the number of samplers in each individual arc used to define A_{OV} , A_{FN} , and A_{FP} by the inter-sampler distance. Adding the values for the five arcs together forms the A_{OV} , A_{FN} , and A_{FP} estimates for the entire (all arcs) trial. Similarly, for AE2, we combine crosswind-integrated dosages for each individual arc together by multiplying them by the inter-sampler distance for each individual arc.²⁶

²⁵ In Chapter 3, we provide an example that compares MOE values based on AE1 to those based on “actual” areas. In that case, the actual areas are based on logarithmic interpolation. Briefly, the interpolation procedure is as follows: 1) values obtained at the samplers are transformed into log space; 2) Delaney triangulation of the physical space between inner and outer arcs is performed in terms of sampler location; 3) for each resulting triangle, the data values within a triangle are linearly interpolated; 4) the interpolated values are transformed back to linear space. Steps 2) and 3) are done efficiently within the Interactive Data Language (IDL) software.

²⁶ By defining the function $f(i) = \begin{cases} 1 & \text{if dosage at sampler } i > \text{threshold} \\ 0 & \text{otherwise} \end{cases}$, we recognize that, for AE1,

A_{OV} , A_{FN} , and A_{FP} are integrals over the sub-arcs that contain samplers with observations above the defined threshold. Similarly, AE2 and lethality/effects filter-based estimates correspond to integrals over sub-arcs. Hence, there is a natural way of combining arcs at different ranges, as long as the integration preserves the distance units. This is achieved by converting each integral from the “number of samplers” units to physical length units (e.g., meters).

2. Stability Category Groupings

Stability category assignments, that were developed by Irwin [Ref. 2-19] for the *Prairie Grass* trials, were used to group trials with similar characteristics in terms of atmospheric stability. There are seven stability categories ranging from “very unstable” (category 1) to “very stable” (category 7). Because of the relatively small sample sizes involved, we used two different procedures to combine categories together, as depicted in Table 2-2. Comparing results obtained by these categorizations of the data, allowed for the examination of the statistical spread to assess the effects of the relatively small sampling sizes for some groupings. Table 2-3 lists the *Prairie Grass* data sample sizes that were used in the model comparisons.

Table 2-2. Stability Category Groupings (SCG) Used in This Study²⁷

	SCG Set 1	SCG Set 2
Unstable	1,2	1,2,3
Neutral	3,4,5	4
Stable	6,7	5,6,7

3. Thresholds for Sampler Observations

SO_2 concentrations were estimated in the following way. First, SO_2 was captured at the impingers (samplers). These impingers were later filled with a hydrogen peroxide (H_2O_2) solution. This caused the SO_2 and H_2O_2 to form sulfuric acid (H_2SO_4). Next, the concentration of sulfuric acid was estimated by measuring the electrical conductivity. Based on the computed sulfuric acid concentration, an estimate of the original SO_2 concentration was derived.

The reported sampler minimal averaged concentration value for the *Prairie Grass* field trials is 0.005 mg/m^3 , which corresponds to a minimal dosage of 3 mg-sec/m^3 . However, to obtain averaged concentration values for samplers inside the gas plume, it was necessary to estimate the “background” averaged concentrations for SO_2 . To do so, some samplers were placed outside of the limits of the time-mean gas plume. In general, this small background concentration level was almost entirely due to a trace amount of sulfuric acid that had been added during the preparation of the dilute hydrogen peroxide

²⁷ A more physically-based arrangement would be to group the near neutral categories, 3 and 4, together.

Table 2-3. Sample Sizes Used for Model Comparisons to Prairie Grass Field Trials²⁸

SCG	All Arcs	50-Meter	100-Meter	200-meter	400-meter	800-meter
1	6	6	6	6	6	4 ²⁹
2	11	10 ³⁰	11	10 ³¹	11	11
3	9	9	8 ³²	9	9	9
4	10	10	10	10	10	10
5	7	7	7	7	7	7
6	6	6	6	6	6	5 ³³
7	2	2	2	2	2	2
Total	51	50	50	50	51	48
First procedure used to combine stability categories						
1-2	17	16 ²²	17	16 ²³	17	15 ²¹
3-4-5	26	26	25 ²⁴	26	26	26
6-7	8	8	8	8	8	7 ²⁵
Second procedure used to combine stability categories						
1-2-3	26	25 ²²	25 ²⁴	25 ²³	26	24 ²¹
4	10	10	10	10	10	10
5-6-7	15	15	15	15	15	14 ²⁵

-
- ²⁸ Sub-groupings for the comparisons include all arcs (highlighted in pink); sub-grouping by range (highlighted in red); sub-grouping by all arcs and stability group (highlighted in gray); and sub-grouping by range and stability group (highlighted in turquoise). Sample sizes highlighted in red and turquoise are applicable to the “standard” statistical measures and user-oriented MOEs that we computed while gray and pink highlighted entries apply to the user-oriented MOEs only.
- ²⁹ The 800-meter arcs of trials 7 and 16 have maximum values below the data threshold of 60 mg ·sec/m³. These two arcs were included only for calculations done with a cutoff threshold set to 3 mg ·sec/m³.
- ³⁰ The 50-meter arc of trial 62 has a missing correction factor for the compensation of the evaporative loss of the impinger solution during aspiration [Ref. 2-20, p. 201].
- ³¹ The 200-meter arc of trial 50 was replaced by “missing values” because the vacuum line to sampler 62 became disconnected during the run [Ref. 2-20, p. 80].
- ³² The 100-meter arc of trial 57 was replaced by “missing values” because the vacuum line to sampler 47 was believed to have become disconnected [Ref. 2-20, p. 80].
- ³³ The 800-meter arc of trial 39 has too many samplers that are missing. Of 19 samplers that recorded non-zero values, 13 have missing values. The HPAC prediction fit completely within this missing value region. In this case, we replaced the whole arc with “missing values.”

solution. Because of this, as the limit of the sampling technique was approached, the uncertainty of the averaged SO₂ concentration determination increased rapidly. For concentrations less than 0.1 mg/m³ (60 mg-sec/m³), this uncertainty was estimated to be 25 percent.³⁴

The mechanism described above was considered the chief source of uncertainty associated with estimates of SO₂ concentrations and, hence, dosages. For this reason, we chose 0.1 mg/m³ (60 mg-sec/m³) as the data cutoff threshold.³⁵

4. Comment: Value of Graphics Tools

The majority of the computer software used to manipulate the field trial and prediction data, and calculate the user-oriented MOEs, was written in Interactive Data Language (IDL) [Ref. 2-21]. This computer language provides a flexible platform for the interactive investigation and manipulation of the data with an emphasis on graphics. One of the valuable lessons that we learned early on was that the best way to analyze or compare data quickly is to find a suitable format to graph it. To that extent, a prerequisite for the best kind of user-oriented MOE (and perhaps also for a “standard” statistical measure) is that it should be able to describe all of the major nuances of the plots that are easily discernible by the human eye. For this analysis, Appendices C, D, E, F, G, L, and M – graphical plots of the observations and predictions – represent invaluable tools with respect to confirming our interpretations of the MOE results.

³⁴ See Reference 2-20, p. 77.

³⁵ In Section A.2.d of Chapter 3, we briefly set the data cutoff threshold to 3 mg-sec/m³. This was done to allow for the demonstration (only) of a lethality/effects filter as applied to a highly toxic substance.

REFERENCES

- 2-1 Ermak, D. L. and Merry, M., "A Methodology for Evaluating Heavy-Gas Dispersion Models, Report UCRL-21025, Lawrence Livermore National Laboratory, Livermore, CA, 1988
- 2-2 Hanna, S. R., Chang, J. C., and Strimaitis, D. G., "Hazardous Model Evaluation With Field Trial Observations," *Atmos. Environ.*, Vol. 27A, No. 15, 2265-2285, 1993.
- 2-3 Biltoft, C., *Phase 1 of Defense Special Weapons Agency Transport and Dispersion Model Validation*, DPG-FR-97-058, Meteorology and Obscurant Division, West Desert Test Center, U. S. Army Dugway Proving Ground, Dugway, UT, July 1997.
- 2-4 Biltoft, C., *Dipole Pride 26: Phase II of Defense Special Weapons Agency Transport and Dispersion Model Validation*, DPG-FR-98-001, Meteorology and Obscurant Division, West Desert Test Center, U. S. Army Dugway Proving Ground, Dugway, UT, 1998.
- 2-5 Bradley, S., "HPAC 3.1 Validation Using DIPOLE PRIDE 26 Field Trial Data," *3rd Annual GMU/DTRA Transport and Dispersion Modeling Workshop*, Fairfax, VA, 28-29 July 1999.
- 2-6 Thuillier, R. H., "Tracer Experiments and Model Evaluation at Diablo Canyon Nuclear Power Plant," *Proc. of the ANS Topical Meeting on Emergency Response-Planning, Technologies, & Implementation*, Amer. Nuc. Soc., 1988.
- 2-7 Nasstrom, J. S., Sugiyama, G., Leone, J. M. Jr., and Ermak, D. L., "A Real-Time Atmospheric Dispersion Modeling System," *American Meteorological Society's 11th Joint Conference on the Applications of Air Pollution Meteorology*, Long Beach, CA, 9-14 January 2000.
- 2-8 Hines, E. L., *HPAC Versus VLSTRACK Operational Comparison*, SAIC Report, 1999.
- 2-9 Warner, S., Carpenter, J. N., Cook, J. M., Miller, R. S., and Hegemann, B. E., *NBC Hazard Prediction Model Capability Analysis*, IDA Document D-2245, September 1999.
- 2-10 Chang, J. C., Franzese, P., and Hanna, S. R., *Evaluation of CALPUFF, HPAC, and VLSTRACK with the Dipole Pride 26 Field Data*, Institute for Computational Sciences and Informatics, George Mason University, August 1999.

- 2-11. Warner, S., Platt, N., and Heagy, J. F., "User-Oriented Measures of Effectiveness," *4th Annual George Mason University Transport and Dispersion Modeling Workshop*, Fairfax, VA, 11-13 July 2000; IDA Briefing, *September 1, 2000 Status/Update: IDA Support to DTRA*, for DTRA, 1 September 2000; and IDA Briefing, *February 14, 2000 Status/Update: IDA Support to DTRA*, for DTRA, 14 February 2000.
- 2-12. Rowland, R. H. and Thompson, J. H., *A Method for Comparing Fallout Patterns*, DNA-2919F, April 1972.
- 2-13. Mosca, S., Graziani, G., Klug, W., Bellasio, R., and Bianconi, R., "A Statistical Methodology for the Evaluation of Long-Range Dispersion Models: An Application to the ETEX Exercise," *Atmos. Environ.*, Vol. 32, No. 24, 4307-4324, 1998.
- 2-14. Reiter, A., *HPAC Verification and Validation*, Technical Exchange Meeting (DOE/DP-23 and DOD/DTRA) 3 June 1999.
- 2-15. Hanna, S. R., "Air Quality Model Evaluation and Uncertainty," *JAPCA*, Vol. 38, 406-412, 1988.
- 2-16. Hanna, S. R., "Confidence Limits for Air Quality Model Evaluations, as Estimated by Bootstrap and Jackknife Resampling Methods," *Atmos. Environ.*, Vol. 23, No. 6, 1385-1398, 1989.
- 2-17. Press, W. H., Teukolsky, S. A., Vetterling, W. T., and Flannery, B. P., *Numerical recipes in Fortran 77: The Art of Scientific Computing*, Second Edition, Cambridge University Press, Chapter 7: Random Numbers, 1992.
- 2-18. Efron, B. and Tibshirani, R. J., "An Introduction to the Bootstrap," *Monographs on Statistics and Applied Probability* 57, Chapman and Hall, 1993.
- 2-19. Irwin, J.S., and Rosu, M-R., "Comments on a Draft Practice for Statistical Evaluation of Atmospheric Dispersion Models," *Proceedings of the 10th Joint Conference on the Applications of Air Pollution Meteorology*, American Meteorological Society, Boston, pp. 6-10, 1998.
- 2-20. Barad, M. L. (Editor), *Project Prairie Grass, A Field Program in Diffusion*, Geophysical Research Papers No. 59, Volumes I and II, DTIC #AD-152572/AFCRC-TR-58-235(I), Air Geophysical Laboratory, Hanscom Air Force Base, MA, 1958.
- 2-21. *Interactive Data Language (IDL)* developed by Research Systems, Inc, www.rsinc.com.

CHAPTER 3

RESULTS, ANALYSES, AND DISCUSSION

3. RESULTS, ANALYSES, AND DISCUSSION

This chapter provides the results of comparisons, done with user-oriented MOEs, of HPAC and NARAC predictions to *Prairie Grass* field trial observations. This chapter includes a few comparisons of these models using standard statistical measures. Additional details of these comparisons are given in Appendices C, D, E, F, G, H, I, J, K, L, and M.

A. COMPARISONS OF HPAC AND NARAC PREDICTIONS WITH MOEs

This section is divided into four parts. The first part describes results based on MOE 1. The next part discusses the 2D MOE (MOE 2) results. The third part provides analyses and discussion associated with two HPAC prediction excursions. Finally, two NARAC excursion prediction comparisons are described.

1. MOE 1

a. Across All Trials

Figure 3-1 compares MOE 1 values based on the threshold area estimate AE1 for HPAC and NARAC predictions for two different C_{FN}/C_{FP} values and a dosage threshold of 60 mg-sec/m³. In this figure, the mean value and the 50th, 80th, and 95th percent confidence intervals for the point estimates are shown.¹

On the left, false positive (i.e., A_{FP}) and false negative (i.e., A_{FN}) are equally weighted (e.g., $C_{FN} = C_{FP} = 1$). For these predictions and this measure, the HPAC predictions achieve a larger MOE 1 value. This difference is statistically significant. The right side of Figure 3-1 illustrates the results when A_{FN} is weighted at ten times the amount of A_{FP} (i.e., $C_{FN} = 5$, $C_{FP} = 0.5$).² Under these conditions, the NARAC predictions achieve the statistically larger value of MOE 1. The implication is that, on

¹ In the figure, LCL = Lower Confidence Limit and UCL = Upper Confidence Limit.

² Perhaps this situation corresponds to a user that is much more concerned with accidental exposure relative to unnecessary evacuation.

average at a threshold dosage of 60 mg-sec/m^3 , the NARAC predictions are more conservative than the HPAC predictions (tend to overpredict relative to HPAC).³

Figure 3-2 shows a similar comparison for MOE 1 using the summed dosages, AE2, to estimate A_{OV} , A_{FN} , and A_{FP} . HPAC and NARAC results are similar for the equally weighted case. This suggests that the predictions of dosage appear consistent between the models. The increased user weighting of A_{FN} (right side of Figure 3-2) leads to an improved MOE 1 value for NARAC relative to HPAC. These conclusions are consistent with the MOE 1 AE1 results of Figure 3-1.

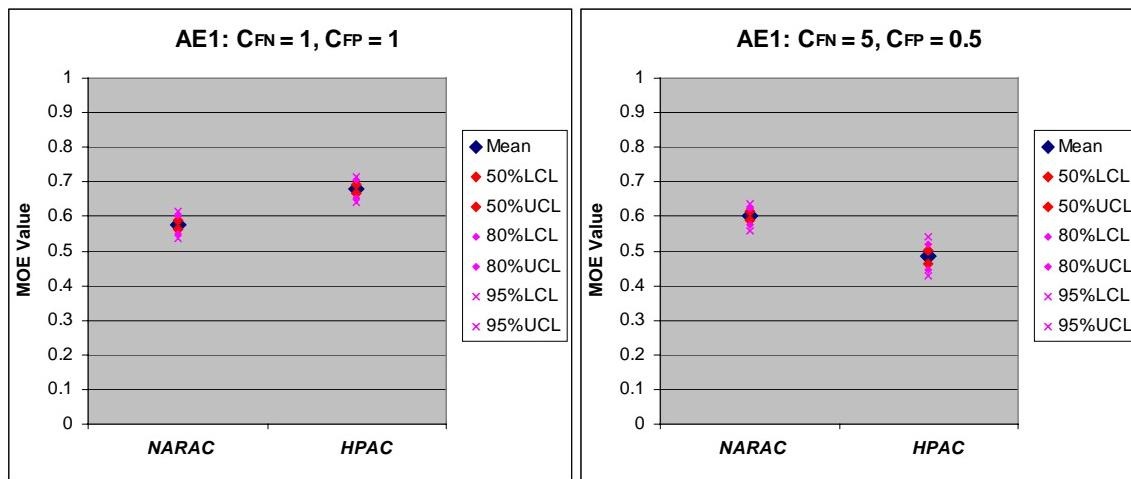


Figure 3-1. MOE 1, AE1, All Trials: For 51 Trials and Two Sets of User Coefficients

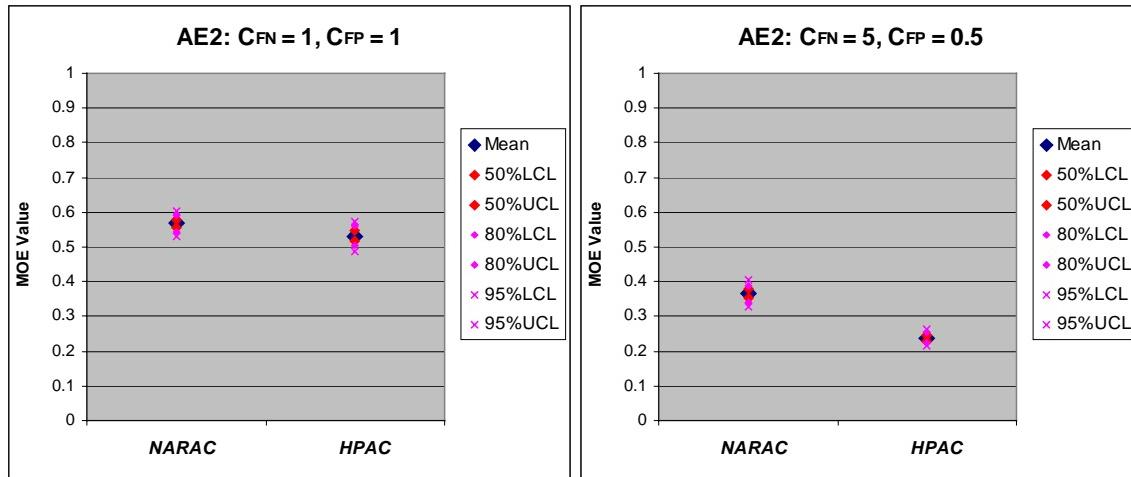


Figure 3-2. MOE 1, AE2, All Trials: For 51 Trials and Two Sets of User Coefficients

³ An inspection of the plots deposited in Appendix E confirms this interpretation.

b. As a Function of Range

Figure 3-3 shows MOE 1 comparisons for HPAC and NARAC, as a function of range, for equal weighting of false positive and false negative areas. Similar behavior, a decrease in MOE 1 value at the longest range, is observed for both models (and with both area estimates – AE1 and AE2).

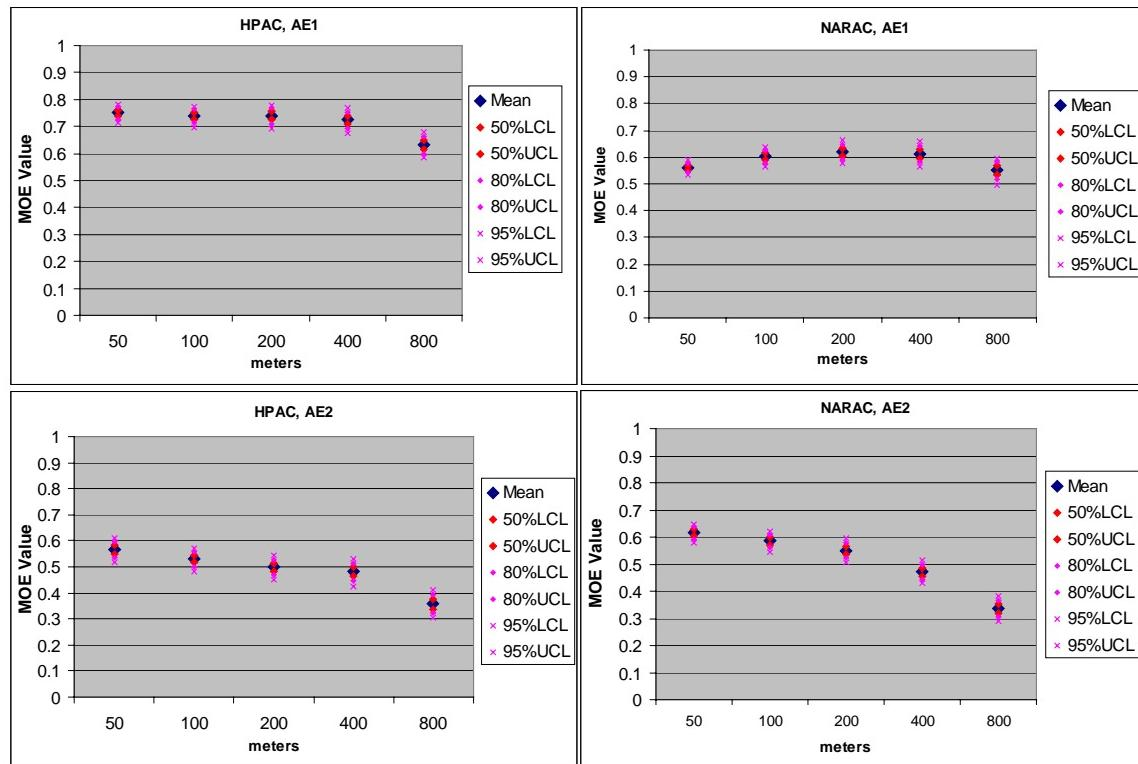


Figure 3-3. MOE 1, AE1 and AE2: By Arc Range ($C_{FN} = C_{FP} = 1$)

c. As a Function of Stability Category

Figure 3-4 shows the computed MOE 1 values for AE1 and AE2 as a function of the stability category grouping (SCG). Individual stability categories for the 51 *Prairie Grass* trials used in this comparison are based on Reference 3-1. Two independent sets of SCGs are shown in Figure 3-4 – 1,2; 3,4,5; 6,7 and 1,2,3; 4; 5,6,7.⁴ Additional comparisons of HPAC and NARAC MOE 1 estimates for the different SCGs and at each arc distance (i.e., SCG \times arc range) are provided in Appendix H.

⁴ For example, the SCG labeled “1,2” implies that the very unstable and unstable trials were combined. A more physically-based arrangement would be to group the near neutral categories, 3 and 4, together. The conclusions of this paper are not substantially affected by this re-grouping.

Stable trials are typically characterized by plumes with relatively narrow crosswind widths and sharp peaks. Unstable trials are represented by wider crosswind plumes with lower relative peak values.

As measured by MOE 1, the performance of both HPAC and NARAC decreases significantly for the more stable trials (6,7 and 5,6,7). For both models and for both MOE 1 estimates (i.e., AE1 and AE2), the models achieve the highest values for the neutral or unstable trials. The relatively small sample size associated with the more stable trials (sample size for SCG 6,7 = 8) is reflected in the larger confidence intervals associated with the point estimates.

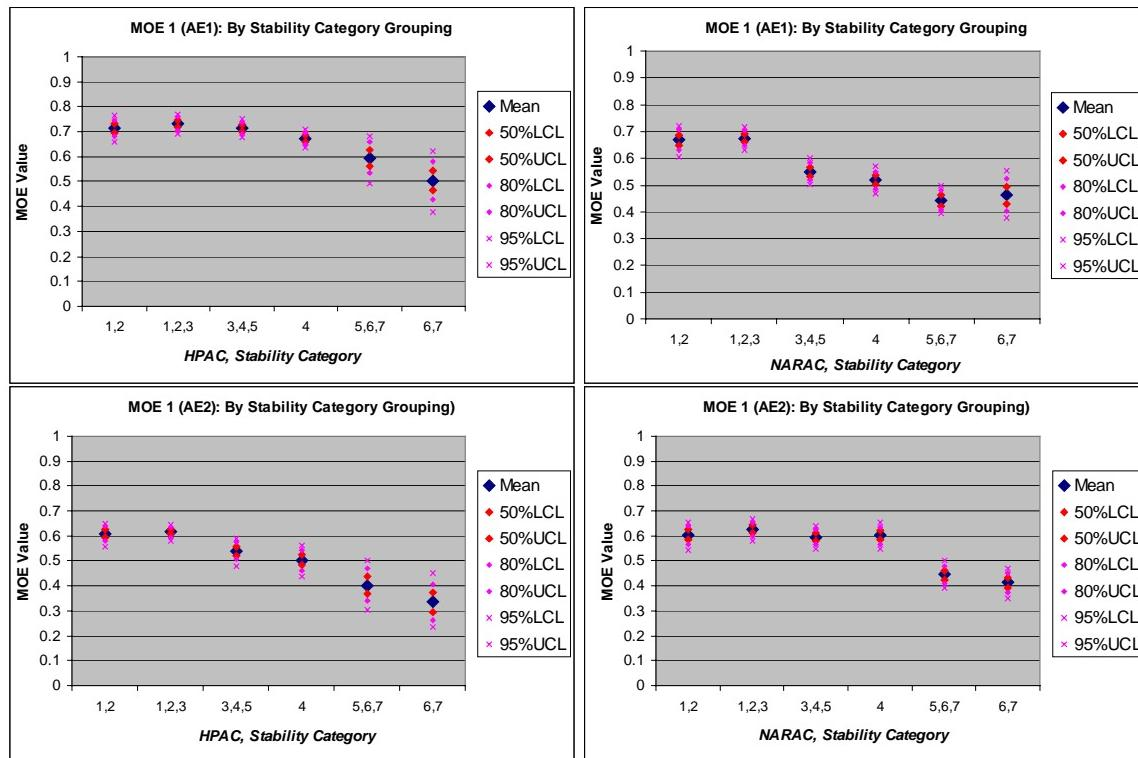


Figure 3-4. MOE 1, AE1 and AE2: By Stability Category Grouping ($C_{FN} = C_{FP} = 1$)

The next section invokes the two-dimensional MOE and further develops the differences between HPAC and NARAC predictions as a function of SCG.

2. MOE 2

a. Across All Trials

Figure 3-5 illustrates our estimates of MOE 2. Each point shown in the figure represents a bootstrap estimate of MOE 2. A total of 1,000 bootstrap resamplings were

computed and 950 points are shown for each estimate. The area covered by these 950 points corresponds to the approximate 95th percent confidence region. The point estimates for MOE 2 reside at approximately the center of the colored confidence regions.

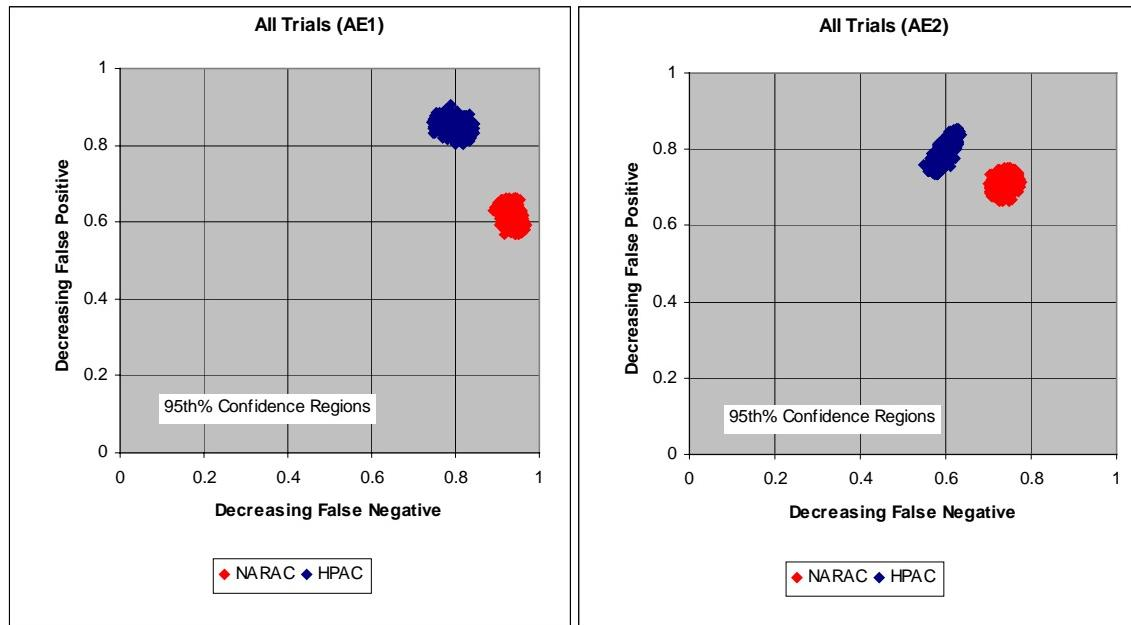


Figure 3-5. MOE 2, AE1 and AE2, All Trials: For 51 Prairie Grass Trials

Using the critical threshold area estimate, the HPAC MOE 2 AE1 value of (0.80, 0.85) lies somewhat closer than the corresponding NARAC estimate (0.94, 0.62) to the best possible value of (1,1).⁵ According to the left side chart in Figure 3-5, the NARAC predictions exhibit a smaller false negative fraction relative to the HPAC predictions. The HPAC predictions show a smaller false positive fraction relative to the corresponding NARAC predictions. These conclusions are statistically significant (i.e., the 95th percent confidence regions are completely separated). The AE2 estimates, in which the “areas” are based on the summed crosswind dosages, show similar results

⁵ As briefly mentioned in Chapter 2 (footnote 24), we also computed MOE 2 using interpolated areas (e.g., in m²) to estimate A_{FP}, A_{FN}, and A_{Ov}. There was very little change in the estimates and confidence regions for MOE 2 based on interpolated areas relative to AE1 – hence, our occasional reference to AE1 as a natural area estimate (at least for the *Prairie Grass* field trial data). The point estimates for HPAC MOE 2 based on AE1 and interpolated area were (0.796, 0.850) and (0.818, 0.848), respectively. Similarly, for NARAC, the estimates were (0.935, 0.616) and (0.937, 0.615), respectively. A future IDA paper will document, compare, and contrast a few area interpolation schemes.

(right side chart in Figure 3-5) but with the NARAC estimate (0.74, 0.71) somewhat closer than the HPAC estimate (0.60, 0.79) to the best possible value (1,1).

b. As a Function of Range

Figure 3-6 compares MOE 2 confidence regions as a function of arc range. There is evidence that both models' performance degrades at the longer ranges. For both models and for both AE1 and AE2 estimates, the results for the 800-meter arc are significantly degraded relative to the 50-meter arc. For the critical threshold area estimate, MOE 2 AE1, the chart on the left side of Figure 3-6 illustrates that as the range increases, relative to the 50-meter arc, the HPAC prediction tends toward increased false positive with minimal increases in false negative. For the NARAC predictions, as the range increases the results tend toward increased false negative with at first minor decreases in false positive fraction. The 50- and 800-meter arcs, for NARAC MOE 2 AE1, have similar false positive fractions.

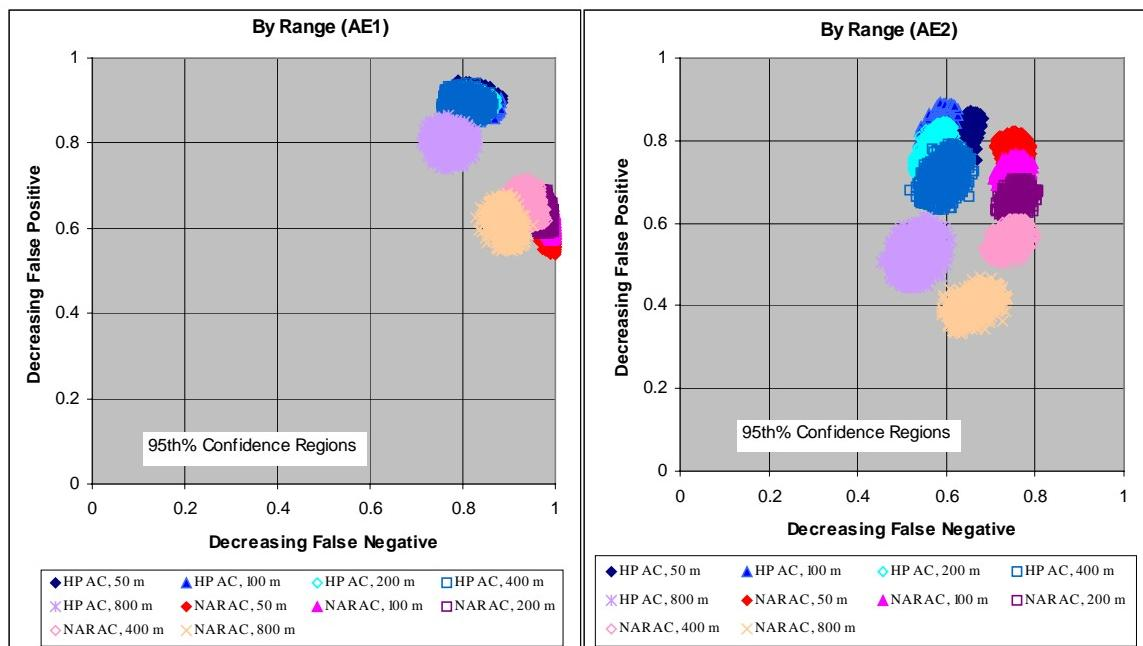


Figure 3-6. MOE 2, AE1 and AE2: As a Function of Arc Range

For these data, MOE 2 AE2 provides complete separation of confidence regions, indicating statistically significant differences, between the results for most arcs. For example, for the NARAC MOE 2 AE2 estimates, the 95th percent confidence regions are generally separate (with the exceptions of the 50-/100-meter, 100-/200-meter, and 200-/400-meter comparisons). That is, of the ten possible arc range comparisons for NARAC

predictions of the *Prairie Grass* trials, MOE AE2 reveals statistically significant differences in seven instances.

For the HPAC predictions, a similar examination of the AE2-based MOE 2 95th percent confidence regions, suggests that the 800-meter arc result is significantly different from the other four arc range results. Thus, four of the ten possible arc range comparisons for the HPAC predictions suggest statistically significant differences – the four involving the 800-meter arc.

We also considered some standard statistical measures. Figure I-7 in Appendix I presents results based on standard statistical measures (FB and NMSE) for CWI dosage.⁶ **Figure I-7** shows that no statistically significant separation or trend can be detected for NMSE as a function of arc range for the NARAC or HPAC predictions. FB for CWI dosage (also Figure I-7) shows a trend of increased NARAC over-prediction at the longer arc ranges (consistent with the increasing false positive fraction shown for MOE 2 AE2). However, none of the NARAC FB values by range for CWI dosage are different in a statistically significant sense. Similarly, just one of the HPAC comparisons results in a statistically significant conclusion (the 100-/800-meter comparison, i.e., the 95th percent confidence regions are completely separate).

Standard statistical measures that consider the logarithms, MG and VG, de-emphasize the largest concentration values, by increasing the weight of the contribution of the outer arcs and the tails of the distribution on the inner arcs, relative to statistical measures that do not use logarithms. For MG values, **Figure I-8** shows a trend toward increasing over-prediction with increased range for NARAC CWI dosage with six (of ten possible) arc range comparisons different in a statistically significant sense. That is, the NARAC MG CWI dosage results for all four comparisons involving the 800-meter arc and the 50- and 100-meter comparisons to the 400-meter arc are significantly different. Figure I-8 also shows VG values for NARAC CWI dosage. In this case, four comparisons suggest statistically significant differences –100-/800-meter, 200-/800-meter, 400-/800-meter, and 100-/400-meter.

As previously mentioned for HPAC, both MOE 2 AE1 and MOE 2 AE2 resolve statistically significant performance differences between the 50- and 800-meter arcs.

⁶ The calculations of MOE 2 AE2 and CWI dosage involve the summing of dosages across an arc. However, unlike MOE 2 AE2, the standard statistics for CWI dosage do not include errors in the spatial position of observed and predicted plumes. Therefore, the CWI standard statistical measures and the AE2-based MOE assess somewhat different aspects of model performance.

Furthermore, for MOE AE2, the performance at the 800-meter arc is completely separated from all of the other arcs. The statistical measures of FB, NMSE, and VG show no statistically significant performance differences between any arc ranges for HPAC CWI dosage. For the HPAC CWI dosage parameter, statistically significant differences in MG (Figure I-8) are apparent for the 50-/100-meter, 50-/800-meter, 100-/800-meter, 100-/400-meter, and 200-/800-meter comparisons.

We also examined statistical results based on ArcMax (Figures I-1 and I-2) and found only a few significant differences between arc ranges for FB, NMSE, MG, and VG. Table 3-1 summarizes the results in terms of the number of arc range comparisons, out of ten possible, that led to statistically significant differences (i.e., the 95th percent confidence regions or intervals were completely separated). The standard statistical measure results are highlighted in red and the MOE 2 results are highlighted in blue.

Table 3-1. Number of Arc Range Comparison Differences That Are Statistically Resolved

Derived Value	Measure	NARAC Predictions	HPAC Predictions
ArcMax	FB	0	0
	NMSE	3	0
	MG	4	0
	VG	0	0
CWI Dosage	FB	0	0
	NMSE	0	0
	MG	6	5
	VG	4	0
AE1-Based	MOE 2	2	3
AE2-Based	MOE 2	7	4

Of the measures shown in Table 3-1, MOE 2 AE2 and MG CWI dosage show the most statistically significant differences in model performance as a function of arc range between 50 and 800 meters.

We also considered comparisons at each range *between* models (i.e., HPAC 50-meter arc versus NARAC 50-meter arc, HPAC 100-meter arc versus NARAC 100-meter arc and so on). There are five possible comparisons between models as a function of arc range. Table 3-2 lists the number of statistically resolvable differences between models (out of a possible 5). By “statistically resolvable,” we mean that the 95th percent confidence regions or intervals are completely separate.

As can be seen in Table 3-2, the MOEs (MOE 2 AE1 and AE2) perform the best with respect to detecting differences between models. The MG CWI dosage measure resolves differences between the models at all but the 50-meter arc range (Figure I-7).

Table 3-2. Number of Arc Range Comparison Differences Between Models That Are Statistically Resolved

Derived Value	Measure	Number
ArcMax	FB	1
	NMSE	0
	MG	1
	VG	0
CWI Dosage	FB	3
	NMSE	0
	MG	4
	VG	2
AE1-Based	MOE 2	5
AE2-Based	MOE 2	5

Later in this chapter we describe results for a direct measure of the plume width, W_{ec} . This parameter is developed and described in Chapter 2 and Appendix J. Examination of FB(W_{ec}) led to statistically significant differences between the models at *all* 5 arc ranges (Figure 3-17).⁷

c. As a Function of Stability Category

Figure 3-7 provides MOE 2 results for two sets of stability category groupings. The top two charts of Figure 3-7 present AE1 results and the bottom two charts provide AE2 results. The charts on the left side show results for SCGs 1,2,3; 4; and 5,6,7. The charts on the right present results for SCGs 1,2; 3,4,5; and 6,7.

First, we consider the AE1 estimates (top charts). With respect to HPAC and NARAC comparisons, the MOE 2 results are most similar for the trials conducted during the more unstable conditions (1,2 and 1,2,3) with the NARAC predictions generating slightly larger false positive fractions and slightly smaller false negative fractions. This trend is greatly magnified for the more neutral trials (3,4,5 and 4). The biggest separation

⁷ No statistically significant differences *between* ranges for a given set of model predictions are seen for W_{ec} .

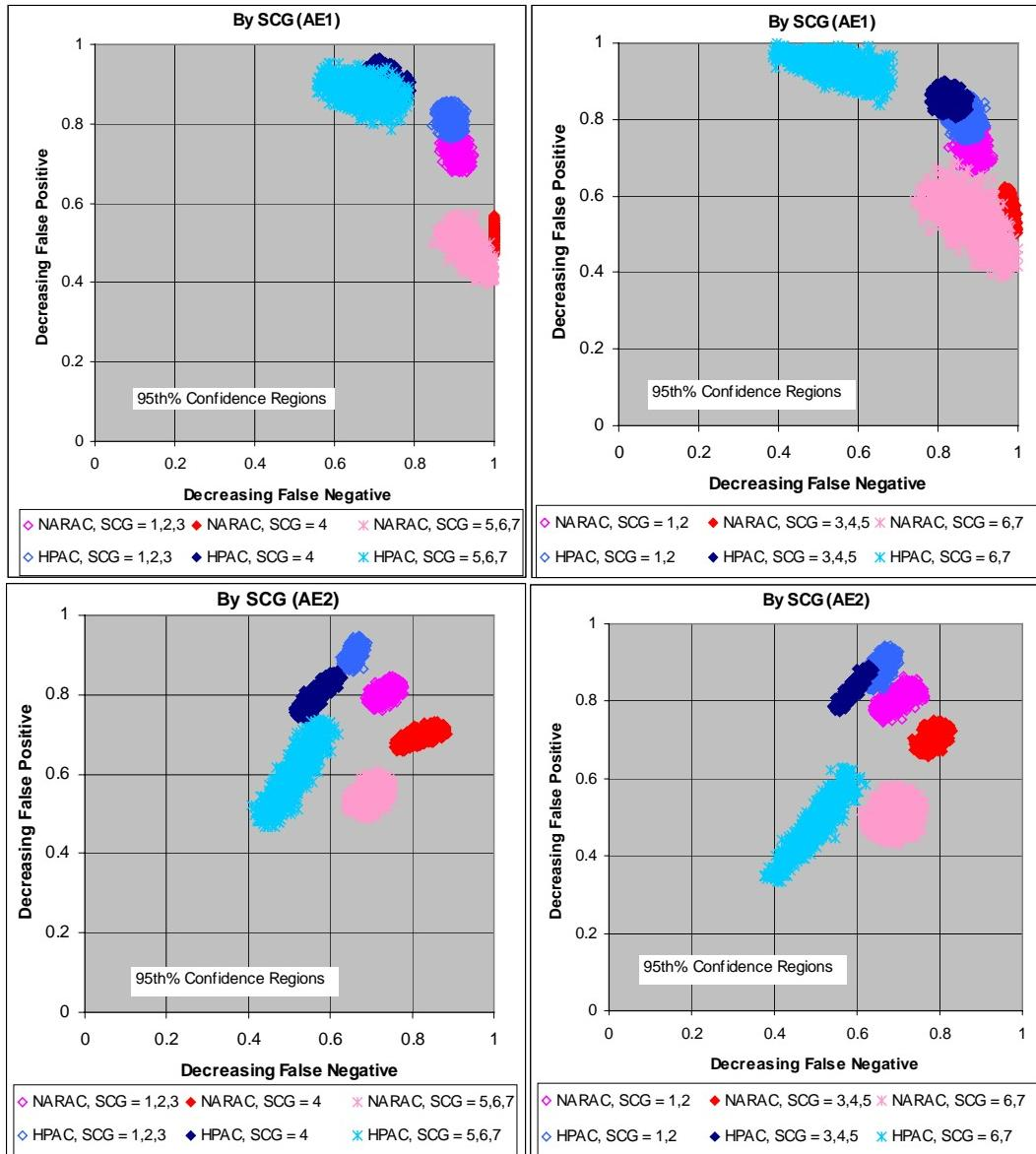


Figure 3-7. MOE 2, AE1 and AE2: As a Function of Stability Category Grouping

is associated with the relatively stable trials (5,6,7 and 6,7).⁸ For both the neutral and the stable conditions, the NARAC predictions generate relatively little fraction associated with false negative (i.e., along the x-axis the confidence region lies close to 1). The HPAC predictions of the neutral and stable trials lead to larger false negative but smaller false positive fractions. The HPAC and NARAC SCG-associated results appear to be the “mirror image” of one another (with the symmetry axis lying on the diagonal that

⁸ The larger confidence regions associated with the stable trials labeled 5,6,7 and 6,7 are due, in part, to the correspondingly smaller sample size.

approximately cuts between the two unstable confidence regions). Both HPAC and NARAC appear to perform the best, with respect to being closest to the best-case (1,1) value, for the relatively unstable trials. Similarly, both models performed worst, as measured by MOE 2, for the trials that were conducted under the more stable conditions.

The bottom two charts show almost complete separation of confidence regions as a function of model used and SCG. As was true for MOE 2 AE1, MOE 2 AE2 implies higher false negative fractions for HPAC predictions relative to NARAC. For the relatively neutral and unstable trials the HPAC predictions have lower false positive fractions than the NARAC predictions. For the stable trials, HPAC and NARAC show similar false positive fractions for MOE 2 AE2. Both HPAC and NARAC appear to perform the best, with respect to being closest to the best-case (1,1) value for MOE 2 AE2, for the relatively unstable trials. Similarly, both models performed worst, as measured by MOE 2 AE2, for the trials that were conducted under the more stable conditions.

With respect to performance comparisons of the sort described in [Figure 2-5](#), the differences between HPAC and NARAC for each of the stability category groupings and for AE1- and AE2-based MOE 2 estimates would be considered “not decisive.” That is, there is no case where one model appears to have the clear advantage – statistically significant decreased false positive and decreased false negative fractions relative to the other model.

Investigation showed that the large somewhat elliptical shape associated with HPAC stable-condition prediction confidence regions is due, in part, to slight errors in the transport direction. For the stable cases, the HPAC plumes are very narrow and there are a few trials for which the HPAC prediction is about the right size and shape but the centerline appears off by a few degrees (perhaps due to limited wind direction information).⁹ If the direction of the prediction and the actual plume is identical, the overlap is maximized and the false positive and false negative areas are minimized. Therefore, improved wind direction information can improve both the false positive and false negative aspects of MOE 2. Similarly, somewhat incorrect wind direction information should lead to degraded MOE 2 values along both the false positive and false negative axes. However, for a very narrow plume, even slight errors in direction can greatly increase the false positive and false negative areas at the expense of overlap.

⁹ See, for example, Appendix C [Figures C-27a](#) and [C-47a](#).

Therefore, transport or perhaps wind direction errors, can explain the elliptical shape and its orientation (i.e., major axis along the (0,0) to (1,1) line) shown by some of the confidence regions.

The above consideration, transport errors, describes a mechanism that can correlate the two axes of MOE 2. For predictions that have perfect wind direction information and hence accurate transport directions, another feature – the relative predicted and actual plume width – could lead to a correlation. In this case, predictions that are too wide lower false negative and raise false positive values. Similarly, predictions that are too narrow increase false negative areas at the expense of false positive areas. Such a mechanism would likely lead to an elliptical confidence region whose major axis would be oriented along the (1,0) to (0,1) line.

d. Lethality/Effects Filter Results

Figure 3-8 presents some sample results using a lethality/effects filter (as described in Chapter 2) in lieu of AE1 and AE2. The charts on the left side of Figure 3-8 use a probit curve with $LD_{50} = 100 \text{ mg-sec/m}^3$ and a slope of 6. The charts on the right side of Figure 3-8 use a probit curve with $LD_{50} = 5,000 \text{ mg-sec/m}^3$ and a slope of 12.¹⁰

Interestingly, a quick comparison of Figures 3-7 and 3-8 reveals that they are quite similar and appear to convey almost identical information. That is, the AE1 charts of Figure 3-7 correspond to the $LD_{50} = 100$ charts of Figure 3-8. Likewise, the AE2 and $LD_{50} = 5,000$ charts appear similar.

This relationship should not be a surprise. For example, for very toxic substances (or low threshold values of interest), the filter simply computes a high fraction of lethality/effects wherever there is essentially *any* false negative dosage. For a uniformly distributed exposed population, this scales (they are related by a constant) directly to the critical threshold area (AE1) value for A_{FN} . A similar comment applies to the false positive and overlap areas. Therefore, MOE 2 values computed with a very toxic

¹⁰ The results in this section represent a *demonstration* of the use of lethality/effects filters. In fact, lethality and effects models may be subject to poorly known thresholds and probit slopes (assuming a probit model). There may be uncertainties in the knowledge of the source purity and unknown correction factors for applying data to a general population versus military personnel. Determining actual casualty levels for a specific scenario would also need to include factors such as the means of exposure (respiratory or percutaneous), other parameters relating to that exposure (e.g., breathing rate and the effect of clothing), and the specification of a particular source material. We note here that, *a priori*, there is no reason that a more detailed lethality or effects model could not be used within the above lethality/effects-filter framework.

lethality/effects filter lead to results comparable to AE1-based calculations. A similar conclusion would be attained if one considered simply a threshold effect for a chemical agent (e.g., the onset of ocular or nasal irritation for a nerve agent).

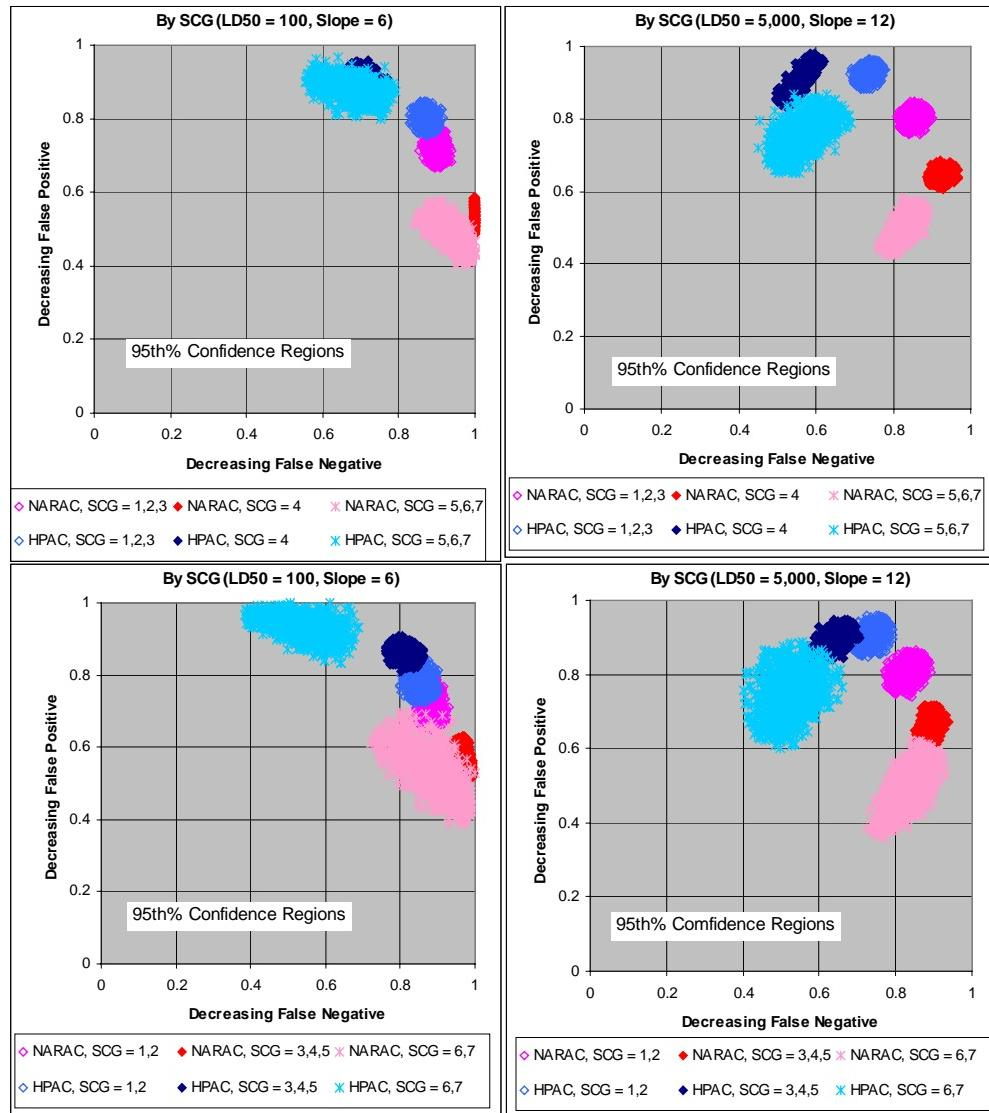


Figure 3-8. MOE 2, Lethality/Effects Filter: As a Function of Stability Category Grouping

The relationship between AE2-based MOE 2 values and estimates based on less toxic filters (e.g., $LD_{50} = 5,000$ vice 100) is somewhat more complicated. There is a regime of toxicity, for example, thousands of mg-sec/m³, where the lethality/effects-based calculations lead to results very similar to the AE2-based estimates (based on the *Prairie Grass* field trial observations). In this regime, false negative dosages, for instance, appear to be nearly linearly related to additional unpredicted exposures that lead to death or some effect. Therefore, the computed areas for the lethality/effects filter and

AE2 computations are related by a constant. However, there must exist some level of toxicity where essentially none of the material causes any effect (or perhaps just the peak along the centerline causes an effect). Near this low level of toxicity, the relationship between AE2-based and lethality/effects filter-based MOE 2 computations breaks down.

Practically, the lethality/effects filter represents a tunable dial that relates AE1 to AE2. In addition, if probit slopes or other effects models associated with agents of interest are used, this filter places MOE 2 results in an appropriate operational context – that is, fractions of affected populations are considered.

The MOE 1 and MOE 2 results presented to this point involve an initial threshold setting of 60 mg·sec/m³.¹¹ We also computed these MOEs using a threshold value of 3 mg·sec/m³. Overall, the HPAC/NARAC comparative results were substantially the same for the two threshold values. However, this lower threshold value allowed us to demonstrate the lethality/effects filter results using probit curves that modeled much more toxic agents. For example, we examined LD₅₀ values of 3 and 10 mg·sec/m³ as shown in Figure 3-9. As expected the results appear similar to those presented for MOE 2 AE1. We conclude that the above lethality/effects filter can be used to compute MOE values, and that this “tunable dial” not only connects AE1 to AE2, but more importantly, can relate the goodness of a prediction for agents of greatly varying toxicity (e.g., biological versus chemical agents or threshold versus lethal effects for chemical agents).

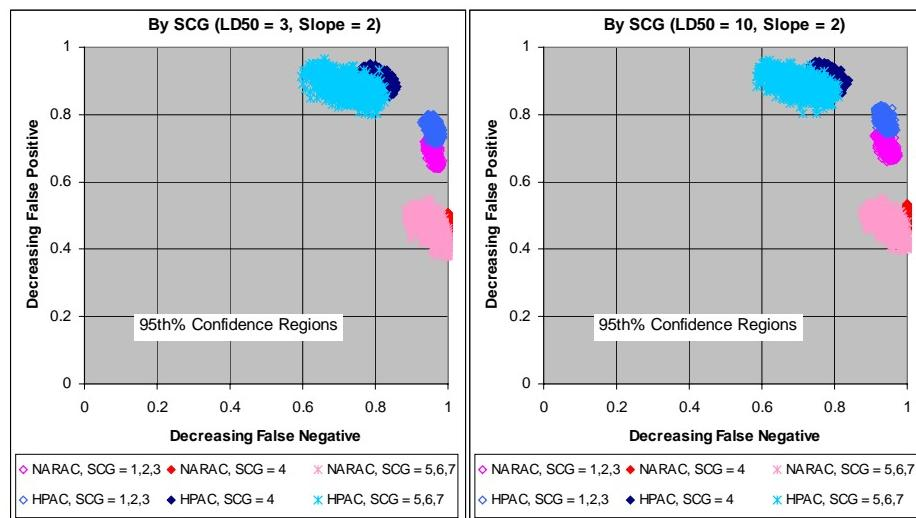


Figure 3-9. MOE 2, Demonstration of Highly Toxic Material Lethality/Effects Filter (at Threshold = 3 mg·sec/m³): As a Function of Stability Category Grouping

¹¹ See Chapter 2, Section C.3 for an explanation of this choice.

3. HPAC Predictions: Excursions

This section describes the results of comparisons of the baseline HPAC predictions of *Prairie Grass* trials to two excursions. First, we reran the HPAC predictions using a defined deposition velocity.¹² This allowed the prediction to consider surface deposition of some of the SO₂.

In the second excursion, the HPAC input parameter labeled uu(calm) was changed from 0.0 to 0.25. Essentially, this parameter sets a lower limit on the plume dispersion during the lightest wind conditions. For the *Prairie Grass* field trials that were conducted over flat, mowed fields in Nebraska, these lightest wind conditions were typically associated with the most stable conditions. The *baseline* uu(calm) value, 0.0, was suggested just prior to this study by the SCIPUFF developer.¹³ The uu(calm) value of 0.25 corresponds to the nominal HPAC *default* value.

a. With and Without Surface Deposition

Including surface deposition should lead to the removal of some SO₂, although perhaps only a small amount of material. Therefore, with respect to using the summed dosages (AE2) to estimate A_{FP}, A_{FN} and A_{OV} for MOE 2, we expect that the decreases in predicted material would, overall, lead to decreases in false positive and increases in false negative fractions relative to the “no deposition” predictions. However, if deposition is a physically important effect for the *Prairie Grass* field trials and it is well modeled, then the “deposition” results should lead to reduced false positive and reduced (or perhaps only slightly increased) false negative fractions relative to the “no deposition” predictions.

Figure 3-10 compares two sets of HPAC predictions using MOE 2 AE2 – with and without surface deposition included in the computation. In addition to a comparison of results with all 51 trials, this figure also presents results as a function of arc range and SCG.

In all cases, the inclusion of surface deposition in the HPAC prediction (the blue confidence regions in Figure 3-10) led to slightly increased false negative and slightly decreased false positive areas. For any individual comparison (e.g., 400-meter arc), the confidence regions for the two MOE 2 estimates have considerable overlap. The

¹² See Appendix B for additional details.

¹³ This recommendation was made by Ian Sykes (ARAP) after a brief review of initial comparative results (on 13 July 2000).

difference in MOE 2 values for the “deposition” and “no deposition” predictions are quite small, and not necessarily statistically significant. However, with respect to A_{FP} and A_{FN} , the same differences are seen for all trials and for all conditions examined (all ranges and all SCGs).

We confirmed that this trend was not simply due to the statistical fluctuations associated with our bootstrap sample size – 1,000. To do this, we simply re-estimated the confidence regions associated with each of the two sets of HPAC predictions (i.e., with and without a surface deposition mechanism included). The difference in confidence region location between runs for the same HPAC set of predictions was much less than the differences between sets of predictions. That is, the re-estimated regions fell approximately on top of the original estimates of the confidence regions.

Next, we considered the following. In *all* cases, we confirmed that the point estimates for MOE AE2 for the “with deposition” predictions led to increased false negative and decreased false positive relative to the “without deposition” trials. This “diagonal movement” of the HPAC MOE 2 estimates might be due to random fluctuations (because of the relatively small number of trials upon which the MOE 2 AE2 point estimates were based). In this case, one would consider four equally likely directions for the “with deposition” trials to have moved – increased A_{FN} /increased A_{FP} , increased A_{FN} /decreased A_{FP} , decreased A_{FN} /increased A_{FP} , and decreased A_{FN} /decreased A_{FP} . However, for all five arc distances and for all six stability category groupings the predictions done “with deposition” led to increased false negative and decreased false positive. Given the equally likely multinomial choice-of-four described above, one can compute the likelihood that all three independent SCGs (e.g., 1,2; 3,4,5; and 6,7) would lead to the same choice that we previously hypothesized. For this situation one expects a 1 in 64 (4^3) chance (i.e., significance level $\alpha = 0.016$) of observing all three independent SCGs with the same choice (given it is due to random fluctuations). If one considered the five arc ranges as independent samples, a similar procedure leads to a 1 in 1,024 (4^5) chance ($\alpha < 0.001$). Thus, at the $\alpha = 0.05$ significance level, we can reject the null hypothesis that the consistent trends that we detect are due solely to random fluctuations.

We note, however, that the magnitudes of the MOE 2 differences between the “with deposition” and “without deposition” trials are smaller than the uncertainty associated with the individual point estimates. An inspection of the comparative figures of Appendix F shows just how small the differences in HPAC “deposition” and “no deposition” *Prairie Grass* predictions are.

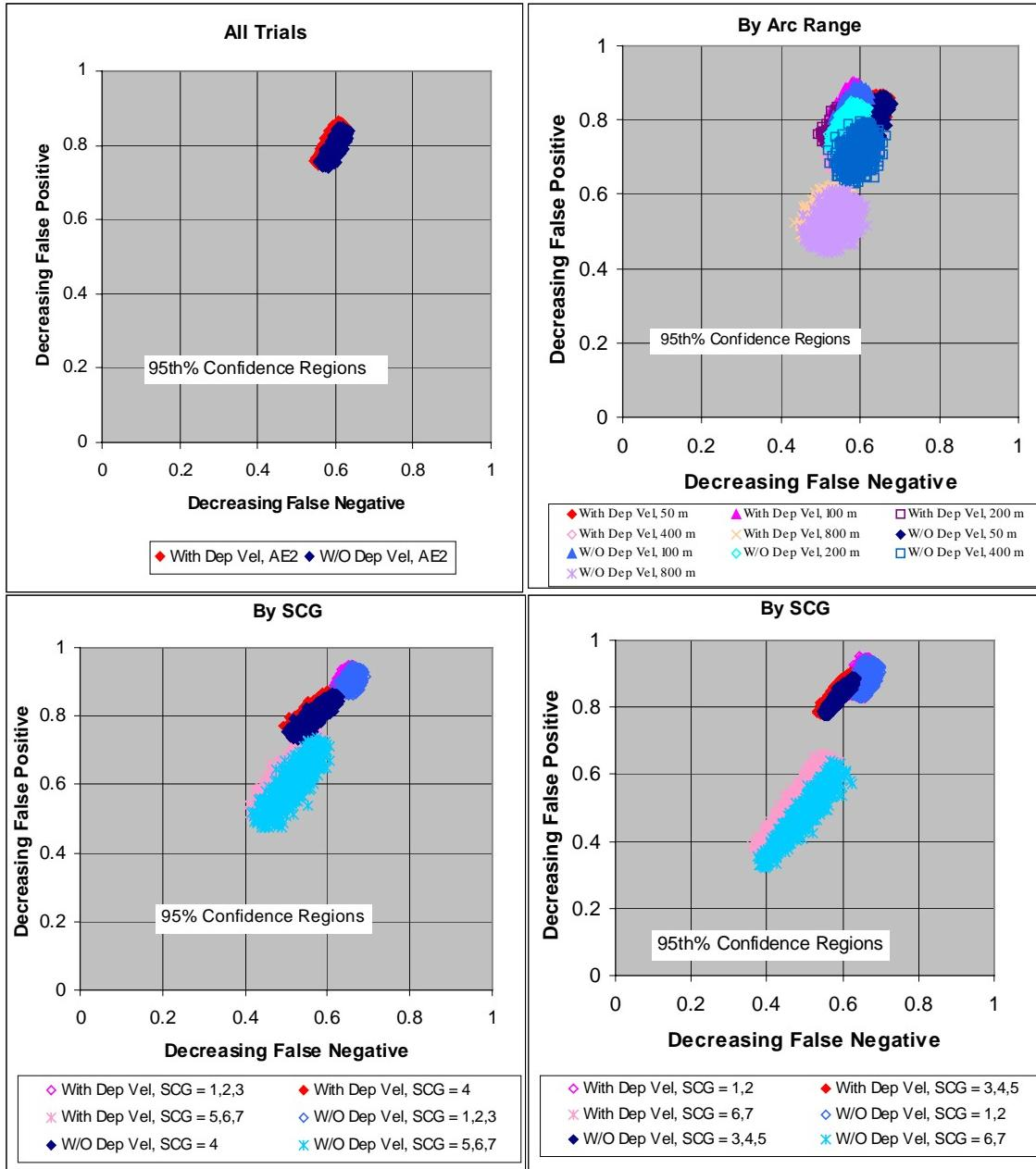


Figure 3-10. MOE 2, AE2: HPAC Predictions With and Without Surface Deposition

At this point, we might ask if the decrease in false positive fraction is greater than the increase in false negative fraction associated with the inclusion of surface deposition. In fact, MOE 1, with equal weightings for A_{FN} , A_{FP} , and A_{OV} (i.e., $C_{FN} = C_{FP} = 1.0$), allows for exactly this assessment. Recall Figure 2-6.

Table 3-3 compares MOE 1 AE2 values for HPAC predictions done with and without surface deposition. The numbers in parentheses correspond to the 95th percent

confidence intervals associated with the given point estimate. The larger MOE 1 AE2 value for each comparison is highlighted in blue boldfaced text.

Table 3-3. MOE 1 AE2 Comparisons for HPAC Predictions of Prairie Grass Field Trials: With and Without Surface Deposition

Trial Type	With	Without
All	0.532 (0.487 – 0.573)	0.528 (0.483 – 0.571)
Range = 50 m	0.566 (0.513 – 0.610)	0.564 (0.512 – 0.609)
Range = 100 m	0.530 (0.483 – 0.568)	0.523 (0.480 – 0.561)
Range = 200 m	0.499 (0.453 – 0.540)	0.494 (0.449 – 0.538)
Range = 400 m	0.481 (0.427 – 0.529)	0.476 (0.425 – 0.524)
Range = 800 m	0.357 (0.304 – 0.412)	0.357 (0.302 – 0.406)
SCG = 1,2	0.610 (0.556 – 0.651)	0.604 (0.550 – 0.645)
SCG = 1,2,3	0.617 (0.581 – 0.646)	0.612 (0.575 – 0.639)
SCG = 3,4,5	0.541 (0.481 – 0.589)	0.536 (0.482 – 0.584)
SCG = 4	0.504 (0.436 – 0.561)	0.501 (0.437 – 0.555)
SCG = 5,6,7	0.403 (0.314 – 0.500)	0.403 (0.308 – 0.500)
SCG = 6,7	0.335 (0.230 – 0.458)	0.341 (0.238 – 0.458)

For most conditions shown in the Table 3-3, the “with deposition” predictions led to marginally better MOE 1 AE2 values (indicating associated larger decreases in false positive fraction than the corresponding increases in false negative fraction). The exceptions to the above statement are the results for the 800-meter arc and for the more stable trials. In fact, for the small sample size SCG = 6,7 trials (sample size = 8), the “without deposition” MOE 1 AE2 value is slightly larger than the “with deposition” result. Inspection of Figures F-24 (trial 32, SCG = 6), F-47 (trial 58, SCG = 6), and F-48 (trial 59, SCG = 5),¹⁴ suggest a possible cause of this result. In each of these cases, the baseline HPAC prediction (“without deposition”) led to an under-prediction of a very narrow peak. The “with deposition” predictions simply removed material from the predicted peak (particularly at the 800-meter arc), therefore leading to a larger AE2-based false negative fraction or area.

The above mechanism (perhaps active in just a few of the trials) would result in a greater increase in false negative fraction than decrease in false positive fraction, on

¹⁴ Page F-1 describes the meanings of the various shadings in the Appendix F figures.

average (i.e., for the MOE 1 AE2 value which is the vector mean for all trials being considered). This is exactly what is implied when considering both MOE 2 AE2 and MOE 1 AE2 together for the “with deposition” and “without deposition” HPAC predictions of the more stable trials.

For all of the differences shown in Table 3-3 the 95th percent confidence intervals overlap (as can be seen in the table). We also inspected the 80th percent confidence intervals and found the same result (i.e., in all cases the intervals overlap). Thus, the differences between individual comparisons shown in Table 3-3 are not considered statistically significant. Therefore, although the trend suggested by MOE 1 AE2 is toward improvement with the inclusion of a surface deposition mechanism, with the exceptions of the 800-meter arc and the more stable trials, we consider these results marginal at best.

In conclusion, although differences were detected, the addition of a deposition mechanism to the modeling did not lead to a clear improvement in the MOE 2 value for the HPAC predictions. Furthermore, inspection of MOE 1 AE2 values, with the assumption of equal weighting of false positive and false negative fractions, suggested, at best, marginal *overall* (MOE 1 AE2 (All Trials) = 0.532 versus 0.528) improvement with the inclusion of a surface deposition mechanism.

b. With Different Values Defining Dispersion for the Lightest Wind Conditions

Figure 3-11 provides the confidence regions associated with MOE 2 AE1 and AE2 estimates for two sets of HPAC predictions with differing values of uu(calm). This figure compares results for all trials and as a function of SCG. For the trials conducted during neutral and unstable conditions, the two types of HPAC predictions yield identical estimates and confidence regions. Comparisons of individual trial predictions confirm that the actual predictions were identical. However, for the trials conducted under the relatively stable conditions, which was also when the wind speed was smallest, the setting of uu(calm), not surprisingly, had a large impact on the predictions. This impact is reflected in the estimates of MOE 2 AE1 and MOE 2 AE2 shown in Figure 3-11.

For the stable trials, the HPAC predictions that were completed using the default value of uu(calm) of 0.25, result in substantially wider plumes and, hence, decreased A_{FN} and increased A_{FP} at least for AE1 estimates. This result is statistically significant for MOE 2 AE1. The HPAC MOE 2 AE1 result for the stable trials with the default setting of uu(calm) is much more similar to the NARAC result described earlier (e.g., compare

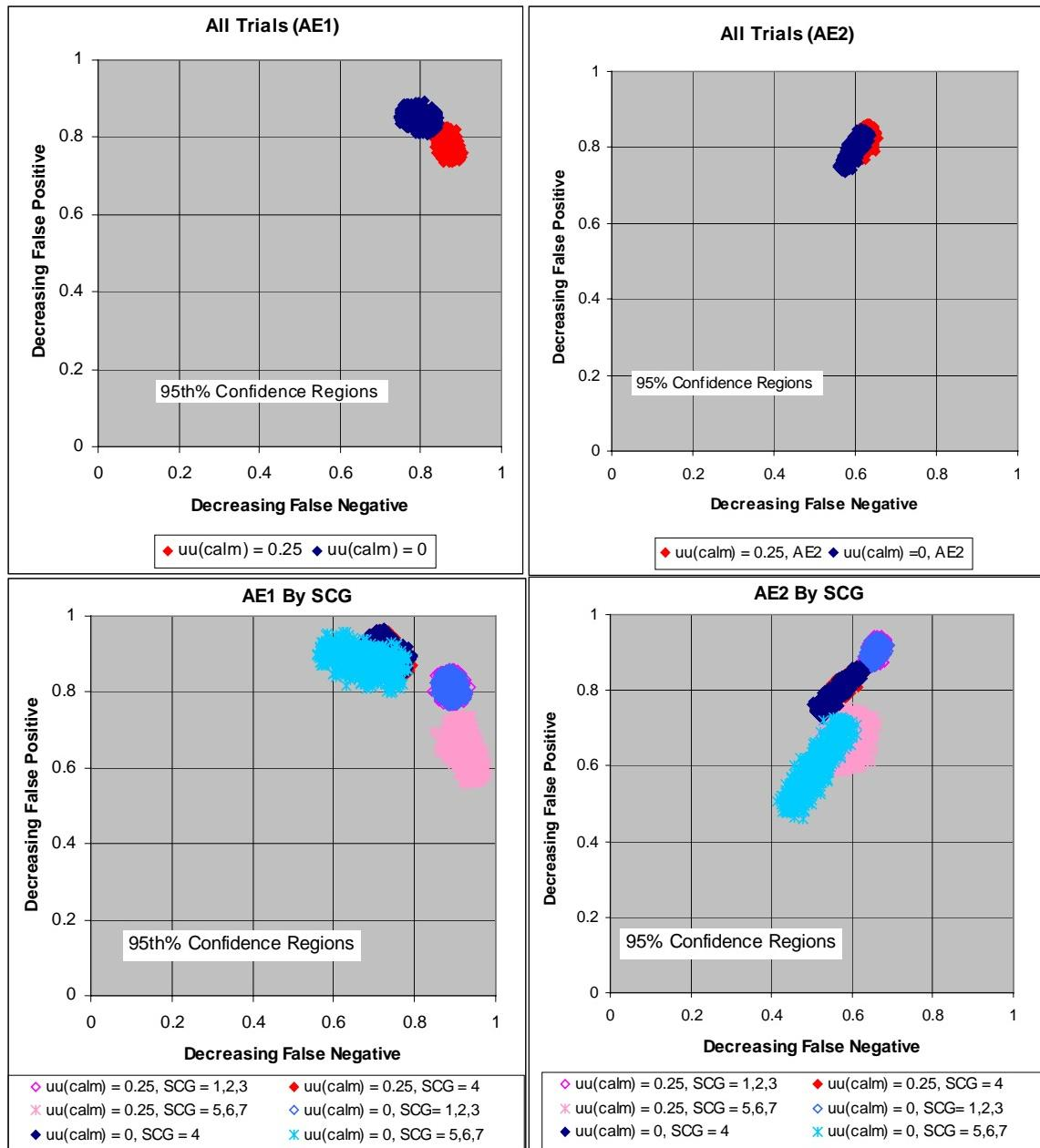


Figure 3-11. MOE 2, AE1 and AE2: uu(calm) = 0.0 Versus uu(calm) = 0.25

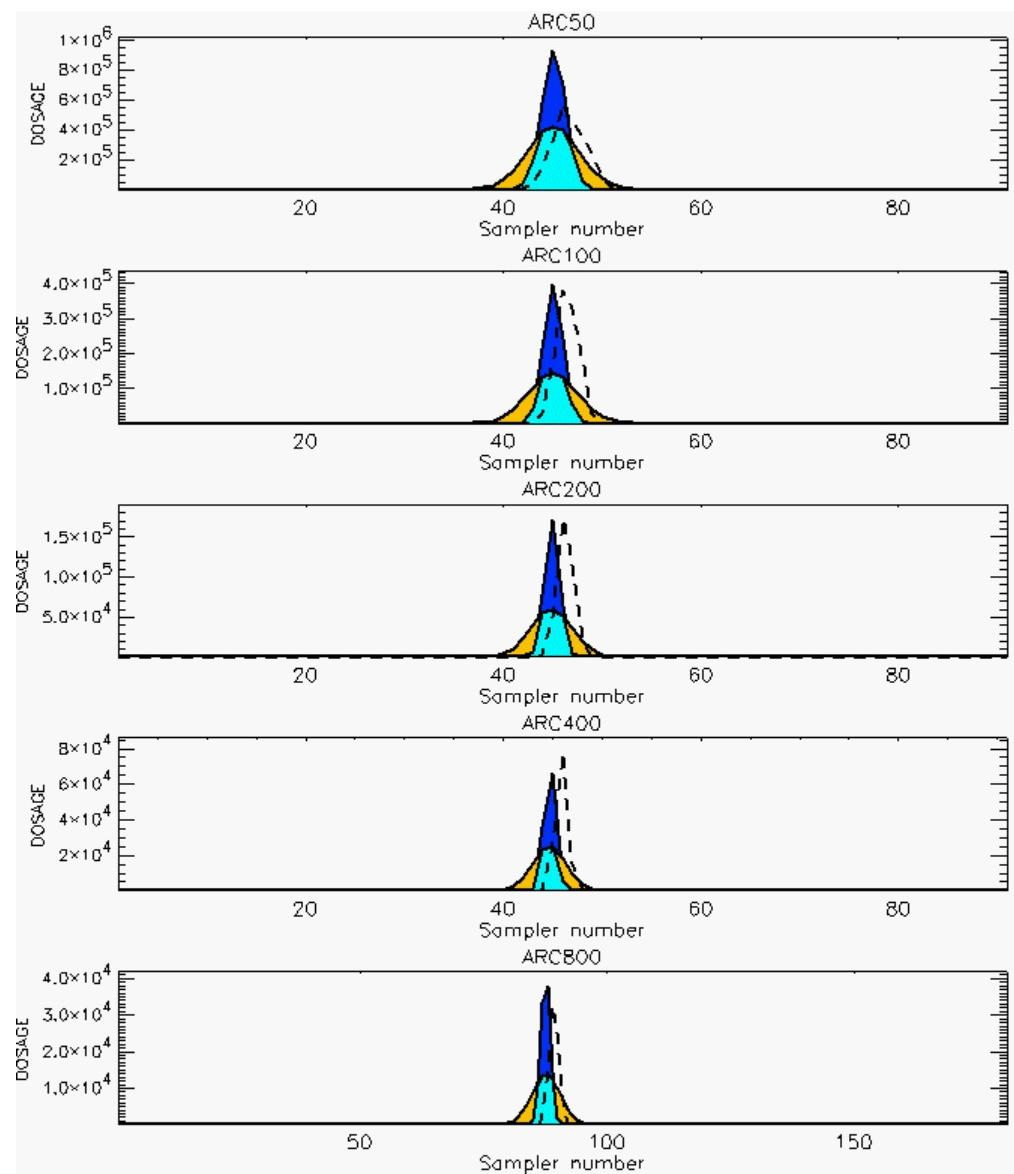
to [Figure 3-7](#), top, left chart). The MOE 2 estimates based on AE2, shown in Figure 3-11, suggest decreased A_{FN} and little change (or perhaps a slight decrease) in A_{FP} . Based on these results, one can conclude that the default value, $uu(\text{calm}) = 0.25$, leads to slightly improved predictions for the *Prairie Grass* trials relative to the baseline value of $uu(\text{calm}) = 0.0$. In this sense, at least for the *Prairie Grass* field trials, the usage of the default value for $uu(\text{calm})$ is validated relative to the value of 0.0.

Similarly, we can consider the MOE 1 AE2 results for HPAC predictions of the more stable trials done with the default and baseline $uu(\text{calm})$ values. The MOE 1 AE2 values for the default and baseline $uu(\text{calm})$ predictions of the SCG = 5,6,7 trials were 0.456 (95th percent confidence interval of 0.393 to 0.521) and 0.403 (95th percent confidence interval of 0.311 to 0.498), respectively. The MOE 1 AE2 values for the default and baseline $uu(\text{calm})$ predictions of the SCG = 6,7 trials were 0.446 (95th percent confidence interval of 0.394 to 0.503) and 0.335 (95th percent confidence interval of 0.228 to 0.455), respectively. Examination of MOE1 AE1 results showed a similar trend. In no case were the 95th percent confidence intervals separated. However, these MOE 1 results do tend to confirm an improvement for the HPAC predictions of the *Prairie Grass* field trials that used the default value of $uu(\text{calm})$.

Figure 3-12 provides an example of the differences between the two HPAC predictions for a trial that was conducted during stable conditions. The suggestion, at least for stable trials, is that differences between HPAC and NARAC predictions obtained when using the default setting of $uu(\text{calm})$ are minimized relative to the baseline $uu(\text{calm})$ value predictions. However, differences between HPAC and NARAC predictions of neutral and unstable *Prairie Grass* trials persist.

Appendix G provides comparisons of these two sets of HPAC *Prairie Grass* predictions for all of the trials. Of course, for the higher wind speed neutral and unstable trials, the two sets of HPAC predictions were identical.

Dark Blue: $uu(\text{calm}) = 0$ Over-Prediction Relative to $uu(\text{calm}) = 0.25$
Light Blue: $uu(\text{calm}) 0.25$ and $uu(\text{calm}) = 0$ Prediction Overlap
Tan: $uu(\text{calm}) = 0.25$ Over-Prediction Relative to $uu(\text{calm}) = 0$
Dotted Line: Trial Observation



PG Prediction1 to Prediction2 Comparison

PG Trial File: pr_grass_tracer_Experiment_58.txt

PG Prediction File 1: HPAC\nodeposition\pg_58_noxd.out

PG Prediction File 2: HPAC\noxd_uu calm_0250\pg_58_noxd.out

Figure 3-12. HPAC Predictions for Trial 58 with Two Values of $uu(\text{calm})$: SCG 6 (“Stable”) at the 5 Arc Ranges

4. NARAC Predictions: Excursions

This section describes the results of comparisons of the NARAC predictions of *Prairie Grass* trials for two excursions. First, two sets of NARAC predictions were prepared. Both sets used an experimentally determined value for the NARAC input sigma-v – a parameter related to the dispersion.¹⁵ One of these runs included a defined deposition velocity thus including in the prediction surface deposition of some of the SO₂.¹⁶ Therefore, these first two sets of NARAC predictions allow for the comparison of predictions “with” and “without” surface deposition.

Next, we compare two sets of NARAC predictions of the *Prairie Grass* field trials that do not include a mechanism for surface deposition of SO₂. One of these sets includes the experimentally determined value for the parameter sigma-v. The second set uses the calculated value for sigma-v and is identical to the set of predictions that were used for the comparisons to HPAC apart from the change in wind fields for four trials as discussed in footnote 13.

a. With and Without Surface Deposition

Including surface deposition should lead to the removal of some SO₂, although perhaps only a small amount of material. Therefore, with respect to using the summed dosages (AE2) to estimate A_{FP}, A_{FN} and A_{OV} for MOE 2, we expect that the decreases in predicted material would, overall, lead to decreases in false positive and increases in false negative areas relative to the “no deposition” predictions. This is exactly the same hypothesis that we applied to the HPAC surface deposition prediction excursions. Again, we note however, that if deposition is a physically important effect for the *Prairie Grass* field trials *and* it is well-modeled, then the “deposition” results should lead to reduced false positive and reduced (or perhaps only slightly increased) false negative fractions relative to the “no deposition” predictions.

¹⁵ The input weather for these two sets of predictions differed slightly from the original baseline NARAC predictions that were compared to HPAC. For trials 35, 39, 51, and 59, the rawinsonde data were included in the surface wind field computation and the non-divergent adjustment was suppressed. This improved the plume direction for cases in which there was large vertical and/or horizontal wind shear, but had minimal effect in other cases. These input weather changes resulted from an examination of differences between NARAC, HPAC, and field trial plume directions for individual trials and arcs. Figures E-27a, E-31a, E-42a, and E-48a show the differences between NARAC, HPAC, and field trial plume directions for the four original baseline trials (i.e., before the changes to NARAC wind field computations described in this footnote). Additional details associated with the NARAC predictions can be found in Reference 3-2.

¹⁶ See Appendix B for additional details.

Figure 3-13 presents AE2-based MOE 2 comparisons for NARAC predictions with and without the inclusion of a surface deposition mechanism. In addition to a comparison of results with all 51 trials, this figure also presents results as a function of arc range and SCG.

In all cases, the inclusion of surface deposition in the NARAC prediction (the reddish confidence regions in Figure 3-13) led to slightly increased false negative and slightly decreased false positive areas. For any individual comparison (e.g., 400-meter arc), the confidence regions for the two MOE 2 estimates have considerable overlap. With respect to A_{FP} and A_{FN} , the same differences are seen for all trials and for all conditions examined (all ranges and all SCGs). As was true for the HPAC deposition prediction excursion, this consistency leads us to conclude that MOE 2 AE2 is able to discern the difference in NARAC *Prairie Grass* predictions due to the inclusion of a surface deposition mechanism.¹⁷

The magnitudes of the MOE 2 differences between the “with deposition” and “without deposition” trials are smaller than the uncertainty associated with the individual point estimates. An inspection of the comparative figures of Appendix L shows just how small the differences in NARAC “deposition” and “no deposition” *Prairie Grass* predictions are. These results are consistent with those previously described for the HPAC surface deposition prediction excursions.

Additional inspection of the figures of Appendix L, presented on the logarithmic scale (the odd-numbered pages in Appendix L), show the occasional over-prediction of dosages by the “with deposition” predictions relative to the “without deposition” predictions. The level of over-prediction is quite small and typically appears to occur on the “edges” of the predicted plume (near the threshold cutoff value). This is most likely due to statistical error in the NARAC Monte Carlo dispersion simulations in these regions caused by the lower number of particles used to calculate dosages toward the edges of the plumes.

At this point, as we did for the HPAC predictions, we might ask if the decrease in false positive fraction is greater than the increase in false negative fraction associated with the inclusion of surface deposition. Again, we use MOE 1 AE2 (with $C_{FN} = C_{FP} = 1.0$) to aid this assessment

¹⁷ Other measures, including scatterplots of observed and predicted values, showed similar trends. [Ref. 3-2.]

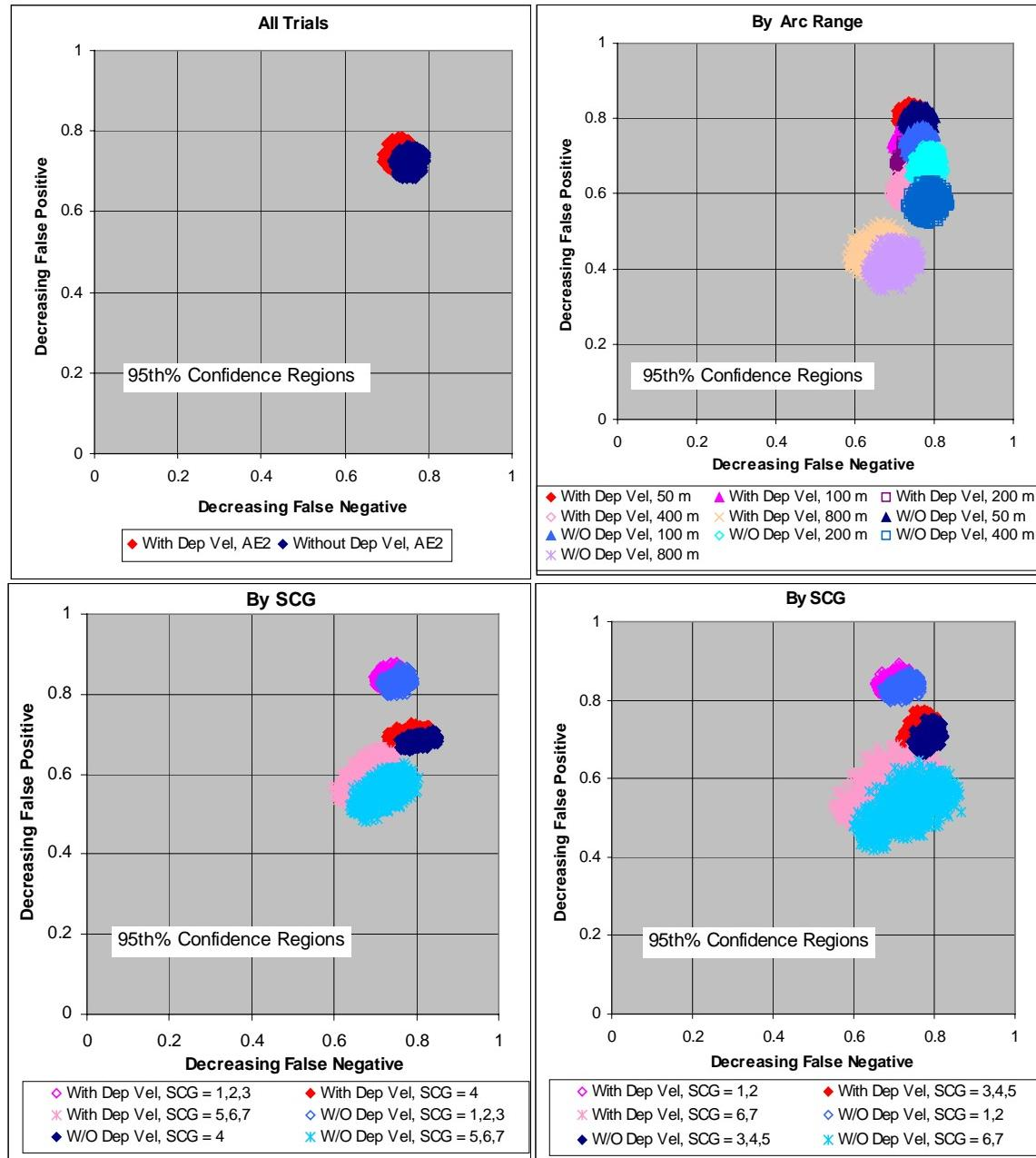


Figure 3-13. MOE 2, AE2: NARAC Predictions With and Without Surface Deposition

Table 3-4 compares MOE 1 AE1 values for NARAC predictions done with and without surface deposition. The numbers in parentheses correspond to the 95th percent confidence intervals associated with the given point estimate. The larger MOE 1 AE2 value for each comparison is highlighted in blue boldfaced text.

**Table 3-4. MOE 1 AE2 Comparisons for NARAC Predictions of Prairie Grass Field Trials:
With and Without Surface Deposition**

Trial Type	With	Without
All	0.586 (0.551 – 0.616)	0.584 (0.547 – 0.616)
Range = 50 m	0.629 (0.593 – 0.663)	0.623 (0.586 – 0.654)
Range = 100 m	0.600 (0.563 – 0.634)	0.593 (0.557 – 0.627)
Range = 200 m	0.573 (0.529 – 0.614)	0.570 (0.531 – 0.611)
Range = 400 m	0.501 (0.455 – 0.544)	0.509 (0.465 – 0.554)
Range = 800 m	0.351 (0.302 – 0.398)	0.363 (0.314 – 0.412)
SCG = 1,2	0.632 (0.589 – 0.673)	0.624 (0.582 – 0.667)
SCG = 1,2,3	0.655 (0.619 – 0.691)	0.649 (0.611 – 0.682)
SCG = 3,4,5	0.598 (0.554 – 0.641)	0.596 (0.549 – 0.640)
SCG = 4	0.587 (0.551 – 0.622)	0.587 (0.547 – 0.624)
SCG = 5,6,7	0.463 (0.404 – 0.522)	0.470 (0.406 – 0.529)
SCG = 6,7	0.446 (0.354 – 0.525)	0.460 (0.356 – 0.541)

For most conditions shown in the Table 3-4 the “with deposition” predictions led to a marginally improved MOE 1 AE2 value (indicating associated larger decreases in false positive fraction than the corresponding increases in false negative fraction). The exceptions to the above statement are the results for the 400-meter arc, the 800-meter arc and for the more stable trials. In fact, for the SCG = 5,6,7 and SCG = 6,7 the “without deposition” MOE 1 AE2 value is slightly larger than the “with deposition” result.

For all of the differences shown in Table 3-4, the 95th percent confidence intervals overlap (as can be seen in the table). We also inspected the 80th percent confidence intervals and found the same result (i.e., in all cases the intervals overlap). Thus, the differences between individual comparisons shown in Table 3-4 are not considered statistically significant. Therefore, although the trend suggested by MOE 1 AE2 is toward improvement with the inclusion of a surface deposition mechanism, at least at the shorter ranges and with the exception of the more stable trials, we consider these results marginal at best.

As was the case with the HPAC “with and without deposition” prediction comparisons the cause for the stable trials exception described above can be discerned from a look at some of the individual trial results. Figures L-23a (trial 28, SCG = 5), L-24a (trial 32, SCG = 6), and L-48a (trial 59, SCG = 5),¹⁸ suggest the same possible

¹⁸ Page L-1 describes the meanings of the various shadings in the Appendix L figures.

cause for this result as was hypothesized for the HPAC comparisons. In each of these cases, the baseline NARAC prediction (“without deposition”) led to an under-prediction of a very narrow peak. The “with deposition” predictions simply removed material from the predicted peak (particularly at the 400- and 800-meter arc), therefore leading to a larger AE2-based false negative fraction or area.

In conclusion, although differences were detected, the addition of a deposition mechanism to the modeling did not lead to a clear improvement in the MOE 2 value for the HPAC predictions. Furthermore, inspection of MOE 1 AE2 values, with the assumption of equal weighting of false positive and false negative fractions, suggested, at best, marginal *overall* (MOE 1 AE1 (All Trials) = 0.586 versus 0.584) improvement with the inclusion of a surface deposition mechanism.

b. With Different Dispersion Parameter Values: Sigma-v Experimental and Sigma-v Calculated

Figure 3-14 compares NARAC predictions of *Prairie Grass* as a function of SCG. MOE 2 AE2 results are shown for predictions using experimentally observed sigma-v values input to the NARAC modeling system and for sigma-v calculated by the NARAC modeling system. For the neutral/near neutral trials (SCG = 4 and 3,4,5) the confidence regions for the MOE 2 AE2 point estimate overlap almost entirely. That is, there does not appear to be any difference. For both the stable and unstable trials, the predictions using the experimentally observed sigma-v appear to be a small improvement, moving toward decreased false negative and decreased false positive fractions. These improvements in MOE 2 AE2 appear small, on the order of the uncertainty in the estimate. For example, the larger 95th percent confidence regions associated with the NARAC “Sigma-v Exp” predictions of the stable trials (SCG = 6,7 and 5,6,7) completely contain the “Sigma-v Calc” predictions. It is not surprising that the use of the experimentally measured sigma-v value improves the NARAC model predictions. The relatively close agreement between the NARAC results with and without the experimentally observed sigma-v suggests that the NARAC parameterizations used to calculate sigma-v are reasonable.

Table 3-5 compares MOE 1 AE2 estimates for NARAC predictions done with the experimental and calculated sigma-v values. These values are for $C_{FN} = C_{FP} = 1.0$ (i.e., equal weighting of A_{FN} , A_{FP} , and A_{OV}). The numbers in parentheses correspond to the 95th percent confidence intervals associated with the given point estimate. The larger MOE 1 AE2 value for each comparison is highlighted in blue boldfaced text.

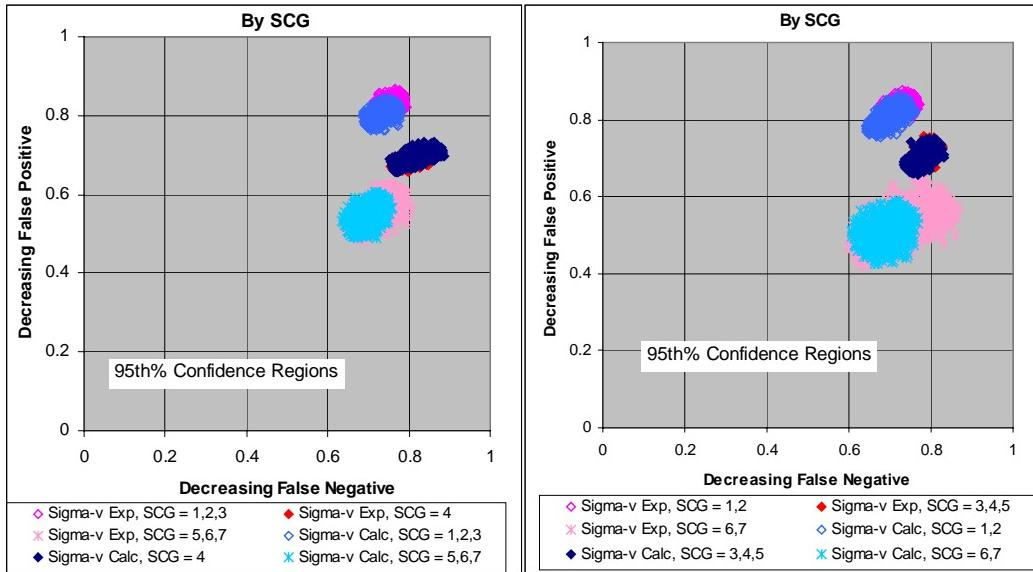


Figure 3-14. MOE 2, AE2: NARAC Predictions Using Calculated and Experimental Sigma-v

Table 3-5. MOE 1 AE2 Comparisons for NARAC Predictions of Prairie Grass Field Trials: Calculated and Experimental Sigma -v

Trial Type	Experimental	Calculated
All	0.586 (0.553 – 0.619)	0.569 (0.530 – 0.604)
Range = 50 m	0.629 (0.592 – 0.661)	0.615 (0.576 – 0.648)
Range = 100 m	0.600 (0.563 – 0.635)	0.585 (0.546 – 0.623)
Range = 200 m	0.573 (0.527 – 0.619)	0.550 (0.505 – 0.592)
Range = 400 m	0.501 (0.457 – 0.544)	0.471 (0.429 – 0.517)
Range = 800 m	0.351 (0.303 – 0.395)	0.336 (0.285 – 0.378)
SCG = 1,2	0.632 (0.588 – 0.671)	0.604 (0.545 – 0.658)
SCG = 1,2,3	0.655 (0.619 – 0.691)	0.628 (0.583 – 0.669)
SCG = 3,4,5	0.598 (0.549 – 0.642)	0.596 (0.547 – 0.636)
SCG = 4	0.587 (0.552 – 0.621)	0.603 (0.551 – 0.652)
SCG = 5,6,7	0.463 (0.402 – 0.517)	0.445 (0.396 – 0.504)
SCG = 6,7	0.446 (0.353 – 0.527)	0.413 (0.355 – 0.469)

For most of the trial types considered in Table 3-5, the predictions that used the experimental sigma-v led to marginally improved MOE 1 AE2 values. The SCG = 4 trials' predictions, based on a sample size of 10, represent the exception. In all cases, comparisons led to overlap between 95th (and 80th) percent confidence intervals. That is, no individual comparison appears to be statistically significant. Appendix M provides individual trial comparisons for the sigma-v experimental and sigma-v calculated NARAC predictions.

B. A FEW COMMENTS ON THE “STANDARD” STATISTICAL MEASURES

In addition to the MOEs described in the previous sections, we computed the values of several standard statistical measures. In large part, the goal of these computations was to allow for comparisons of conclusions based on MOE values to conclusions based on standard statistical measure examinations. These measures, which include FB, NMSE, MG, VG, R, FAC2, FAC5, and FAC10, are described in Chapter 2, Section A.2. Appendix I provides detailed results (via plots and tables) associated with these measures.

Figure 3-15 provides comparisons (to field trial observations) of HPAC and NARAC predicted ArcMax for the measures FB, NMSE, MG, and VG. The display on the left presents point estimates and 95th percent confidence intervals for FB and NMSE. The display on the right presents point estimates and 95th percent confidence intervals for MG and VG. The blue parabolas correspond to limiting curves – since NMSE and VG for a model can be due to mean bias and random error, there are minimum values of NMSE and VG for a given FB and MG, respectively.¹⁹

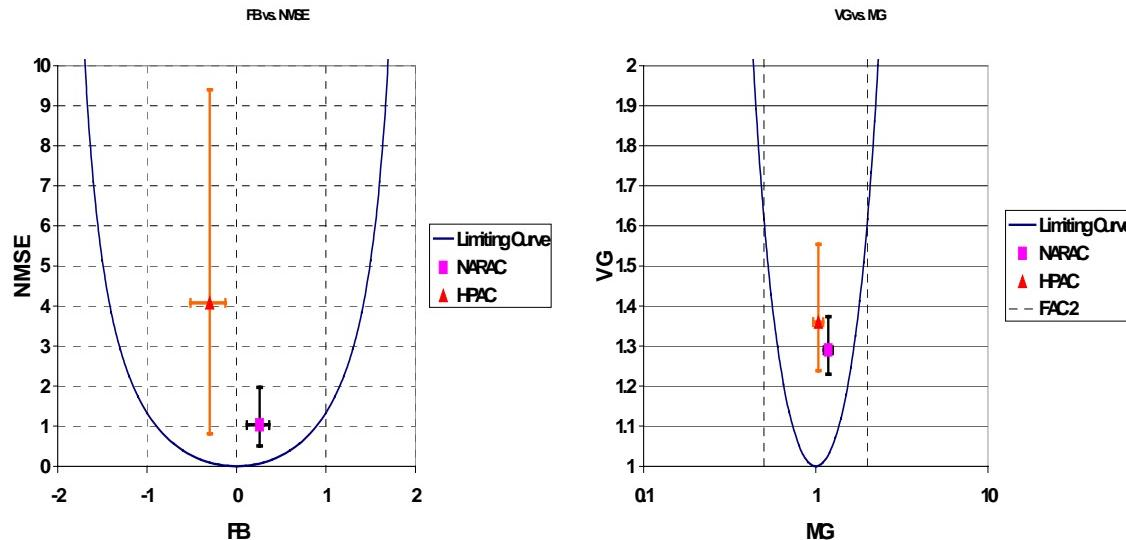


Figure 3-15. FB, NMSE, MG, and VG: HPAC and NARAC ArcMax Comparisons to Prairie Grass Trials

The x-axis for the plots above describes the overall bias with respect to a model’s ability to predict the ArcMax. The vertical lines at MG = 1 and -1 in the VG versus MG plot coincide with a result that indicates a factor-of-two difference between the prediction

¹⁹ See Appendix I for a brief discussion.

and the observation. FB values greater than 0.0 or MG values greater than 1.0 imply, on average, an under-prediction by the model. Similarly, FB values less than 0.0 or MG values less than 1.0 suggest an over-prediction, on average, by the model.

Both plots imply that NARAC tends to underpredict the peak (ArcMax) – NARAC FB = 0.26 (with a 95th percent lower confidence limit of 0.12) and NARAC MG = 1.18 (with a 95th percent lower confidence limit of 1.11). For HPAC, the FB value of –0.30 (with a 95th percent upper confidence limit of –0.12) implies that the HPAC predictions, on average, overpredict the ArcMax. The HPAC MG value, 1.04 (with a 95th percent confidence interval of 0.97 to 1.11) is not significantly different from 1.0. The confidence intervals for HPAC and NARAC MG and FB estimates are completely separated, indicating that predictions of the two modeling systems are significantly different from each other.

With respect to NMSE and VG, both measures of variance, there is no statistical difference (see the 95th percent intervals) between the two models' predictions. The larger confidence interval associated with the HPAC NMSE estimate *is due to just a few large values.*²⁰

Figure 3-16 provides comparisons (to field trial observations) of HPAC and NARAC predicted CWI (crosswind integrated) dosage for the measures FB, NMSE, MG, and VG. These plots indicate that HPAC tends to underpredict CWI dosage (HPAC FB = 0.16 [0.00 to 0.26]²¹ and HPAC MG = 1.20 [1.14 to 1.25]). Based on MG, NARAC tends to overpredict CWI dosage (NARAC MG = 0.82 [0.79 to 0.85]). The NARAC FB value of –0.06 [-0.18 to 0.02] is not significantly different from 0.00. The MG results for HPAC and NARAC are significantly different.

With respect to VG(CWI dosage) the results for the two models are similar given the uncertainty estimates.

In addition to the above standard measures that dealt with ArcMax and CWI dosage, we examined an estimate of the plume's width, W_{ec} , as described in Chapter 2. Figure 3-17 presents the FB values as a function of range for W_{ec} . The triangles and diamonds correspond to the point estimates for $FB(W_{ec})$, the solid red lines correspond to

²⁰ This sort of limitation for this measure, NMSE, was described in Chapter 2. Most of the variance in NMSE is associated with a few stable trials, particularly the 50- and 800-meter arcs. See [Figures I-1](#) and [I-3](#).

²¹ Numbers in brackets correspond to the 95th percent confidence interval.

the 80th percent confidence intervals, and the solid blue lines correspond to the 95th percent confidence intervals. The negative NARAC FB values imply that the observed plume was, on average, narrower than the NARAC-predicted plume. Similarly, the positive FB values associated with the HPAC calculations imply that the observed plume was, on average, wider than the HPAC predictions. For three of the arc ranges, 200, 400, and 800 meters, the NARAC W_{ec} values include the perfect FB value of 0.0. The NARAC-predicted W_{ec} values are in better agreement with the observations than the *baseline* HPAC-predicted values.

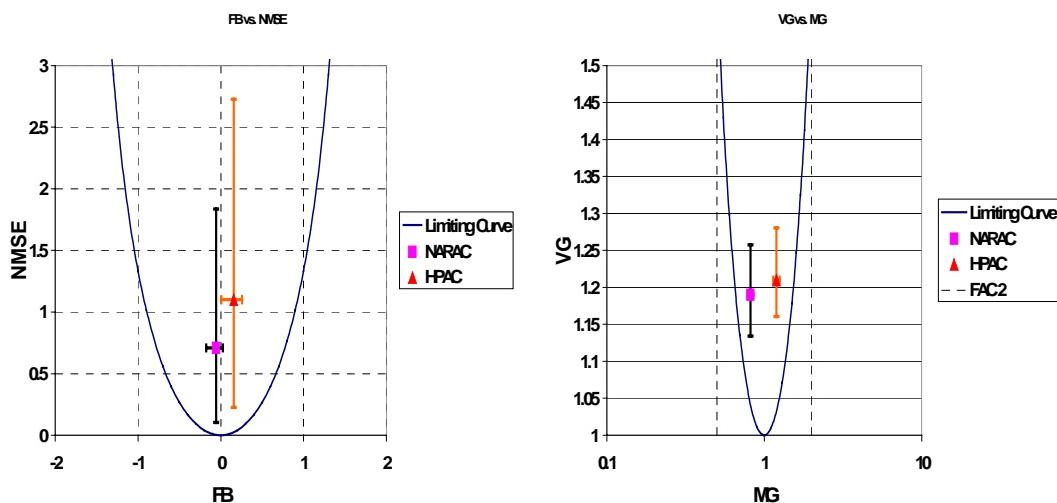


Figure 3-16. FB, NMSE, MG, and VG: HPAC and NARAC CWI Dosage Comparisons to Prairie Grass Trials

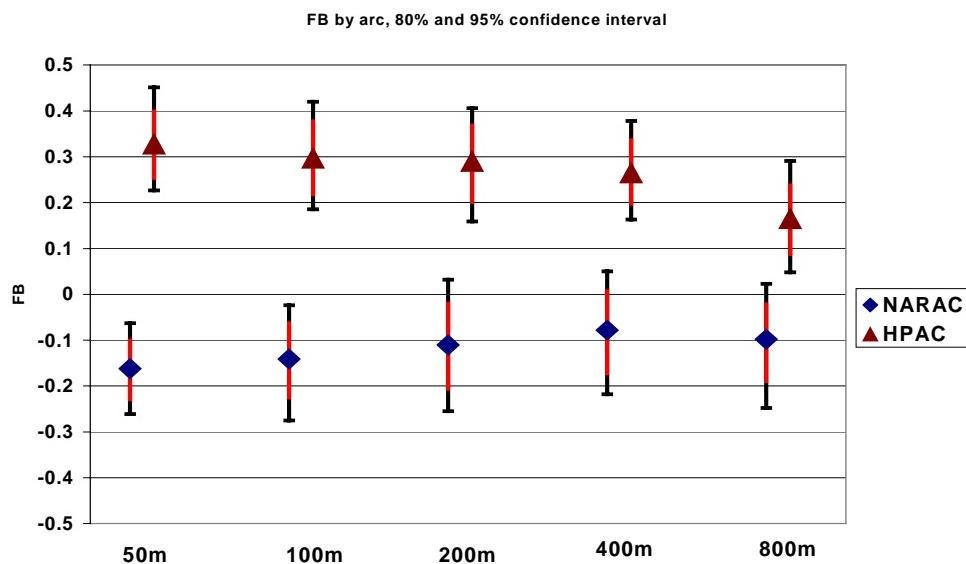


Figure 3-17. FB as a Function of Range: HPAC and NARAC W_{ec} Comparisons to Prairie Grass Trials

Figures I-16, I-17, and I-18 (Appendix I) provide additional comparisons of HPAC and NARAC FB (W_{ec}) and NMSE (W_{ec}) as a function of range and stability category. Figure I-17 suggests that HPAC under-predictions of W_{ec} are due mainly to the stable trials (SCG = 6,7). However, HPAC predictions done with the default uu(clam) value of 0.25 lead to a substantial reduction in the under-prediction of W_{ec} for the stable trials.²²

The above results suggest that, on average and as the models were run, HPAC produces narrower and sharper plumes relative to NARAC's wider plumes. Figure 3-18 provides two examples that tend to confirm this explanation. A more complete inspection of the figures of Appendix E supports this contention. This conclusion is consistent with our findings based on examinations of MOEs – the NARAC predictions led to larger false positive fractions (i.e., wider plumes at a given threshold) and the HPAC predictions led to larger false negative areas (i.e., narrower plumes).

With respect to comparisons of the standard statistical measures and the MOEs, we have the following comments:

- For these data, the conclusions based on the MOEs and the standard statistical measures were consistent.
- Individual standard statistical measures were, in general, less likely to detect statistically significant differences (e.g., as a function of arc range) relative to the MOEs. This may be due to the fact that the MOEs are based on point-to-point comparisons and include directional effects. The standard statistical measures that we examined did not include these effects.

Perhaps the most important difference between the MOEs and standard measures included in this paper is related to information content of the parameters that were examined. The statistical measures that we used were applied to ArcMax, CWI dosage, and W_{ec} . That is, each arc was characterized by a peak, a total dosage, and a width. Information associated with the relative direction of the observed and predicted plumes was not included in the standard measure analysis. For some applications, assessing model performance in this way may be perfectly acceptable, for instance, if one is only interested in the dispersion features of the model. However, if transport (e.g., direction) and dispersion are of interest, then the measures cited above could not be used.

²² See Figures G-8, G-9, G-24, G-27, G-28, G-31, G-32, and G-47 (SCG = 6, 7 trials).

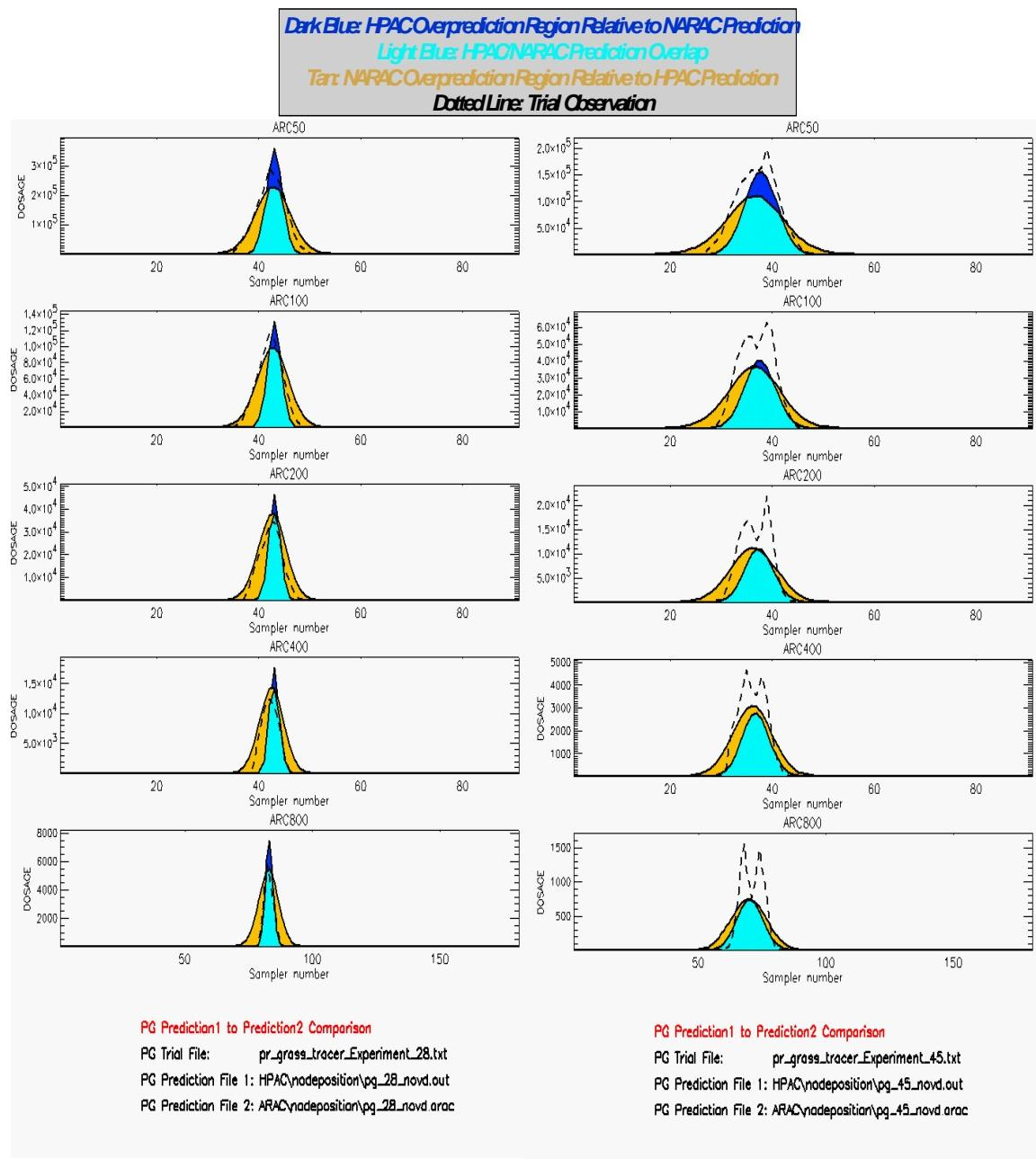


Figure 3-18. HPAC and NARAC Predictions for Prairie Grass Trials 28 and 45

As described earlier, the MOEs directly allow for assessments that include differences in predicted and observed directions. Of course, for such measures, it will be important to sort out the causes of substantial differences between predictions and observations. Whereas an incorrect wind direction measurement would have no impact on measures that considered ArcMax or CWI dosage, such an error could dramatically

change the result of an MOE 1 or MOE 2 calculation. Additional research could be done to compare the MOEs against statistical measures that incorporate directional effects.

To further explore the above, we examined CentDir – that is, the centerline direction (in degrees) as described in Chapter 2 and Appendix J. The calculated bias and RMSE values associated with the CentDir parameter are deposited in Appendix I. Figure 3-19 presents an interesting result. First, the precision by which the CentDir parameter was measured is at best equal to the angular separation between samplers (i.e., 1 degree for the 800-meter arc and 2 degrees for the rest of the arcs). The point estimates and confidence intervals shown in Figure 3-19 suggest that the observations and predictions (both HPAC and NARAC) have about the same centerline direction, within the precision of this measurement, out to about 400 meters. Interestingly, the 800-meter bias values (and the overall trend shown) suggest that there may be a systematic error associated with the *Prairie Grass* field trial wind direction measurements.

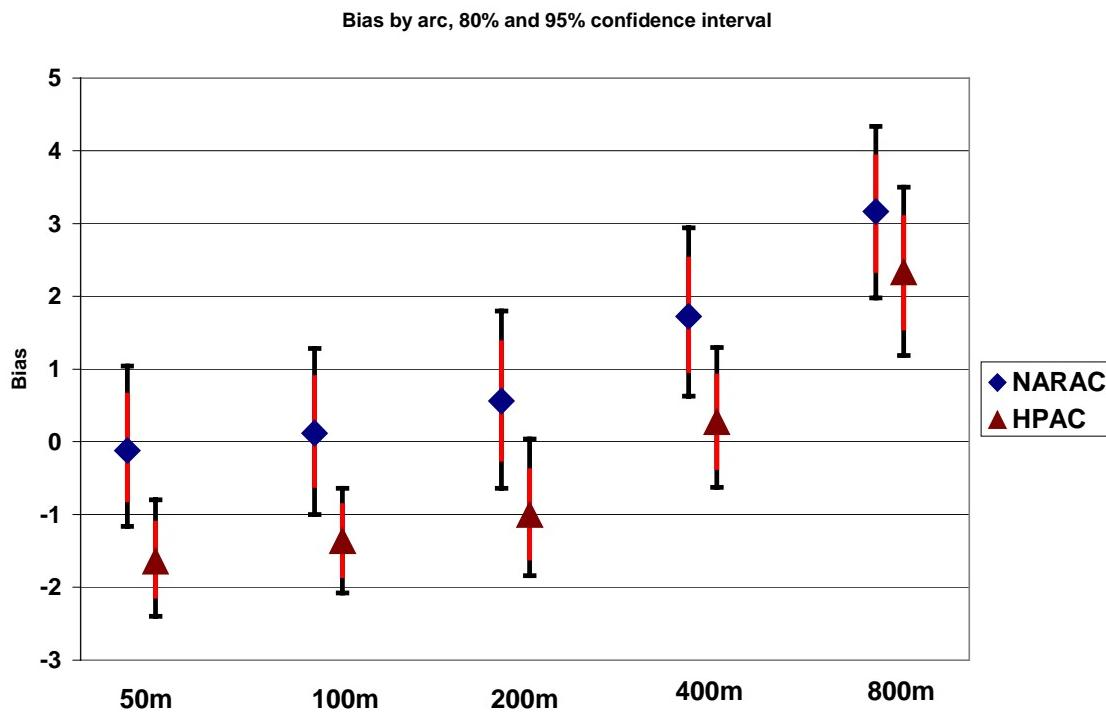


Figure 3-19. Bias as a Function of Range: HPAC and NARAC CentDir Comparisons to *Prairie Grass* Trials

C. CONCLUSIONS: VALUE OF MOEs

In this chapter, novel user-oriented MOEs have been used to compare *Prairie Grass* field trial observations to HPAC and NARAC predictions. These MOEs provide a useful tool for examining differences in model performance. This application has demonstrated their relative ease of use, at least for a short-range field trial. These measures can communicate numerically what plume plots show graphically.

Our user-oriented MOEs are defined in terms of false positive, false negative, and overlap regions. The choice of area estimate allows the MOEs to be used to compare different quantities, for example, the degree of under-/over-prediction for a critical threshold area (AE1) or for spatially integrated dosages (AE2). The MOEs can also be interpreted by first applying an effects model, e.g., a probit curve. This methodology allows a user to evaluate a model's performance directly in terms of an exposed or potentially exposed population.

The two-dimensional measure (MOE 2), with false positive and false negative fractions considered orthogonal consistently appears to resolve important features. MOE 2 was useful in identifying and describing differences between HPAC and NARAC predictions of the *Prairie Grass* trials. Variances, in a given model's prediction performance as a function of arc range and stability condition, were easily detected and, often, led to statistically significant conclusions. Examination of MOE 2 values and trends allowed us to discern prediction performance differences, based on changes in HPAC inputs (i.e., including a mechanism for SO₂ deposition and, separately, modifying the uu(calm) default value). Similarly, input changes to NARAC predictions (i.e., including a mechanism for SO₂ deposition and, separately, modifying the sigma-v value) led to detectable differences in prediction performance (i.e., movement in MOE 2 space). Furthermore, we found that the 2D MOE (MOE 2) allowed for straightforward communication of the impact of these modest input changes in terms of false positive and false negative fractions.

We found that a lethality/effects filter can be used to compute MOE values, and can be characterized as a “tunable dial” that can relate the goodness of a prediction for agents of greatly varying toxicity (e.g., biological versus chemical agents or threshold versus lethal effects for a chemical agent). This feature may make this methodology of particular value with respect to user accreditation. For instance, the specific application and user will dictate the agent type, effect, and downwind distance of interest, therefore defining how the lethality/effects dial should be tuned.

Overall the 2D MOE revealed the following with respect to comparisons of HPAC and NARAC predictions under the specified model intercomparison protocol:

- HPAC and NARAC predictions of the relatively unstable *Prairie Grass* trials were most similar. Predictions of the most stable trials led to the biggest differences.
- In a sense, the NARAC predictions, as run, were more conservative than the HPAC predictions. In general, NARAC predictions led to substantially smaller false negative areas, but at the expense of larger false positive areas. This was most true for the predictions of the neutral and stable trials. In contrast, HPAC predictions showed substantially smaller false positive areas, but at the expense of larger false negative areas. A review of Appendix E confirms this interpretation.

This study also used a variety of other statistical and graphical measures of model performance. Examination of plots of measured and predicted dosages as a function of distance helped support conclusions. Statistical measures for derived quantities – such as ArcMax, CWI dosage, plume horizontal spread, and mean plume direction – were of some value in confirming the underlying reasons for the MOE results. MOE results (for both AE1 and AE2) include the effects of directional error by pairing observed and predicted dosage in space (and time). Separate comparisons of ArcMax, CWI dosage, plume spread, and mean plume direction (which do not measure mean wind direction error) can allow for the isolation of errors due to the dispersion modeling methods from those due to mean wind advection modeling errors (particularly directional). The results of this study show that MOEs are a potentially valuable tool, but that no single measure can be used exclusively in evaluating and analyzing model performance.

Additional work can be pursued to further develop, improve, and demonstrate the value of the new MOEs. It might be valuable to compare the new MOEs to standard statistical measures that are applied to dosage observations and predictions that are paired in space and time, since this is the approach used when determining the area estimates for the new MOEs. Similarly, since the MOEs differentiate over-predictions from under-predictions, this might also be done for the standard statistical measures in order to determine the unique features of the MOEs. In particular, it would be of interest to understand further how much of the differences identified by the MOEs are due to plume directional errors.

Further study of the sensitivity of MOE AE1 to the choice of critical threshold dosage could be of some value. In particular, the AE1-based MOEs, to the degree that

they allow the user to set the threshold of interest, may best be characterized as corresponding to operational or accreditation measures.²³

At this point, it appears possible to extend, or possibly adapt, the new MOEs, to evaluations that consider longer-range field trial observations. These extensions and/or adaptations are to be explored in the near future. Additional study, to compare and contrast differing interpolation schemes to estimate actual area sizes from field trial data, is underway.

Future efforts will also focus on developing a quantitative framework from which a user can describe his/her risk tolerances. In this way, the 2-dimensional space associated with MOE 2 can be divided into acceptable and unacceptable regions for a given user.

²³ The AE1 methodology, as described previously, is identical to the application of a lethality/effects filter in which the lethality/effects model is simply a step function (i.e., a critical threshold). The threshold value of 60 mg-sec/m³ that was used throughout this report is higher than a typical threshold effects dosage for the occurrence of ocular effects for nerve agents.

REFERENCES

- 3-1. Irwin, J. S. and Rosu, M-R., "Comments on a Draft Practice for Statistical Evaluation of Atmospheric Dispersion Models," *Proceedings of the 10th Joint Conference on the Applications of Air Pollution Meteorology*, American Meteorological Society, Boston, pp. 6-10, 1998.
- 3-2. Sugiyama, G., Nasstrom, J., Foster, K., and D. Larson, *NARAC Prairie Grass Simulations*, UCRL-ID in preparation.

APPENDIX A
ACRONYMS

APPENDIX A

ACRONYMS

2D	Two-dimensional
A _{OB}	Area Associated With the Observations
ADAPT	Atmospheric Data Assimilation and Parameterization Techniques
AE1	Area Estimate 1
AE2	Area Estimate 2
A _{FP}	False Positive Area
A _{FN}	False Negative Area
A&M	Texas A&M University
A _{OV}	Area of Overlap
A _{PR}	Area Associated With the Prediction
ARAC	Atmospheric Release Advisory Center
ARAP	Aeronautical Research Associates of Princeton
ArcMax	Maximum dosage along an arc
A _T	Total Area
BC _a	Bias-corrected and accelerated
cal	calories
CB	Chemical and Biological
CBIAC	Chemical and Biological Defense Information Analysis Center
cc	Fractional Cloud Cover
CentDir	Centerline Direction
C _{FN}	false negative coefficient
C _{FP}	false positive coefficient
cm	centimeters
C _o	predicted dosages/concentrations or for this study dosages/concentrations predicted by HPAC
COM	Center of Mass
C _p	observed dosages/concentrations or for this study dosages/concentrations predicted by NARAC
CWI	Crosswind Integrated
DOD	Department of Defense
DOE	Department of Energy
DPG	Dugway Proving Ground
DTRA	Defense Threat Reduction Agency

ETEX	European Tracer Experiment
FAC2	fraction of predictions within a factor of 2
FAC5	fraction of predictions within a factor of 5
FAC10	fraction of predictions within a factor of 10
FB	Fractional Bias
FOM	Figure of Merit
GMU	George Mason University
h	boundary layer height
H_o	Sensible Heat Flux
H_2O_2	Hydrogen Peroxide
H_2SO_4	Sulfuric Acid
HPAC	Hazard Prediction and Assessment Capability
hr	hour
IDA	Institute for Defense Analyses
IDL	Interactive Data Language
kg	kilogram
L	Monin-Obukhov length scale
LCL	Lower Confidence Limit
LD_{50}	Lethal Dosage (for 50 percent of the population)
$\text{LE}(d)$	Lethal Exposure fraction – for a dosage , d , the fraction of people that die
LLNL	Lawrence Livermore National Laboratory
LODI	Lagrangian Operational Dispersion Integrator
μ	microns
m	meters
MFT	Model-to-Field Trial
MG	geometric mean bias
mg	milligrams
min	minutes
MIT	Massachusetts Institute of Technology
MMD	Mass Median Diameter
MMO	Model-to-Model-Only
MOE	Measure of Effectiveness
MOL	Monin-Obukhov Length
MOM	Median of Mass
m/s	meters per second
N	Neutral
NARAC	National Atmospheric Release Advisory Center (same as ARAC)

NMSE	Normalized Mean Square Error
NOAA	National Oceanic and Atmospheric Administration
R	correlation coefficient
r_c	canopy resistance
RMSE	Root Mean Square Error
ROC	Receiver Operating Characteristic
σ	sigma
S	Stable
SCG	Stability Category Grouping
SCIPUFF	Second-Order Closure Integrated Puff
sec	seconds
SO_2	Sulfur Dioxide
θ_o	Air Temperature
T_{avg}	Conditional Averaging
T&D	Transport and Dispersion
TWR	Tower
U	Unstable
u_*	Friction Velocity
UCL	Upper Confidence Limit
VG	geometric mean variance
V&V	Verification and Validation
VV&A	Verification, Validation, and Accreditation
W	University of Wisconsin
W_{ec}	Width as estimated by the equal-cuts-off-the-sides method
WMD	Weapons of Mass Destruction
ZI	boundary layer height
z_i	boundary layer height
z_o	surface roughness height
z_r	reference height for the deposition velocity

APPENDIX B
INITIAL CONDITIONS FOR HPAC AND NARAC PREDICTIONS

APPENDIX B

INITIAL CONDITIONS FOR HPAC AND NARAC PREDICTIONS

This appendix describes the initial input parameters that were used for HPAC and NARAC predictions of the *Prairie Grass* field trials [Ref. B-1 and B-2].

1. PRAIRIE GRASS COMPARISON PROTOCOL

This section of the appendix is extracted from draft documentation [Ref. B-3]. The preparation of initial input parameters for the simulations consisted of two parts. First, meteorological (e.g., wind speed, wind direction, and temperature at various observation stations) and sulfur dioxide (SO_2) release information was manually transcribed from the hardcopy of the *Prairie Grass* field trial report into computer-ready files. Second, data from various tables in the hardcopy of the report was used to derive (or fit) additional input parameters as required for each of the simulation models.

A typical meteorological input data file for a particular field trial is shown in Figure B-1. The first line description of the trial includes the experiment number followed by the fractional cloud cover (in tenths),¹ air temperature at an altitude of 2 meters (in degrees Celsius),² net radiation (in $\text{cal}/\text{cm}^2\text{-sec}$),³ sensible heat flux (in $/\text{cm}^2\text{-sec}$),⁴ latent heat flux (in $/\text{cm}^2\text{-sec}$),⁵ and friction velocity (in meters/second).^{6,7}

¹ See Reference B-1, Volume I, Table 3.1.

² See Reference B-1, Volume II, Table 8.1.

³ See Reference B-1, Volume II, Table 8.1.

⁴ See Reference B-1, Volume II, Tables 9.2 and 10.1.

⁵ See Reference B-1, Volume II, Tables 9.2 and 10.1. In the first line, the “W” between the latent heat flux and the friction velocity values stands for the origin of the sensible/latent heat flux observations. If this character is blank, then the sensible/latent heat flux is taken from Reference B-1, Volume 2, Table 9.2 (Texas A&M observations), and if this character is W, the sensible/latent heat flux is taken from Reference B-1, Volume 2, Table 10.1 (University of Wisconsin observations).

⁶ The friction velocity was calculated from the $u'w'$ and $v'w'$ data in Reference B-2, Table 17.3.

⁷ For some trials, an additional data field between the air temperature and the net radiation fields is populated with a value. In these cases, this value corresponds to the insolation (in $\text{cal}/\text{cm}^2\text{-sec}$). See Reference B-1, Volume II, Table 8.1.

Experiment	24	0	21.89	-0.00115	0.03	0.02	W	0.404
560730045000	RAWINSON			2.00	3.80	130.00	-99999.00	
560730045000	RAWINSON			290.00	13.30	150.00	-99999.00	
560730045000	RAWINSON			600.00	14.40	160.00	-99999.00	
560730045000	RAWINSON			930.00	13.70	190.00	-99999.00	
560730045000	RAWINSON			1270.00	14.20	210.00	-99999.00	
560730051000	SOURCE			2.00	6.22	141.00	7.10	
560730051000	NORTH450			2.00	5.76	142.00	6.20	
560730051500	A&M TWR			0.25	3.82	-99999.00	-99999.00	
560730051500	A&M TWR			0.50	4.61	-99999.00	-99999.00	
560730051500	A&M TWR			1.00	5.21	146.00	-99999.00	
560730051500	A&M TWR			2.00	5.86	-99999.00	-99999.00	
560730051500	A&M TWR			4.00	6.62	-99999.00	-99999.00	
560730051500	A&M TWR			8.00	7.64	-99999.00	-99999.00	
560730051500	A&M TWR			16.00	8.65	-99999.00	-99999.00	
560730051500	MIT 3L			2.00	-99999.00	135.40	6.40	

Figure B-1. Meteorological Input File for *Prairie Grass* Field Trial 24

The rows that follow the first line include the following information. The first column presents the date and time (year/year/month/month/day/day/hour/hour/minute/minute/second/second). The next column describes the meteorological station, and the columns that follow provide the altitude (meters above ground level), wind speed (m/sec), wind direction (in degrees from North), and the standard deviation of the wind direction (σ_θ in degrees). Values of “-99999” denote missing (or unmeasured) data points.

Table B-1 characterizes the input parameters used for the *Prairie Grass* simulations and was derived from Reference B-3. In addition, a surface roughness length value of 0.008 meters was specified for the *Prairie Grass* field trials.

A description of the column headings and meanings of symbols appearing in Table B-1 follows.

- **Trial** refers to the *Prairie Grass* field trial number. The cases marked by a diamond,♦, in the Trial field were eliminated from the comparison runs because of missing data. Specifications of the reasons for the elimination of individual cases are given in Table B-2.
- **Year/Month/Day/Time** refers to the date/time stamp in YYYYmmdd hhmm format.
- **Experimental Data (Raw)** signifies that data was taken (or derived) from the raw observations available in the *Prairie Grass* report.
- The air temperature, θ_o , is the value at a height of 2 meters (above ground level) in degrees Celsius [Ref. B-1, Table 8.1, Volume II].

Table B-1. Table of Input Parameters Provided by LLNL

Trial	Year/Month /Day/Time	Experimental Data (Raw)				Experimental Data (Fit)			Vel_d
		θ_o	H_o	u_*	cc	u_*	L	h	
1♦	1956JUL03 1700	22.12			9	0.19	-8.6	871	
2♦	1956JUL03 2100	23.87	-0.048		9	0.13	-14	1042	
3♦	1956JUL06 0400	19.83			3			73	
4♦	1956JUL06 0700	17.50			1			194	
5	1956JUL06 2000	30.17		0.357	0	0.39	-28	1100	0.0042
6♦	1956JUL06 2300	30.80		0.309	0	0.44	-84	969	0.0043
7	1956JUL10 2000	30.27	-0.430	0.291	0	0.31	-9.8	2639	0.0041
8	1956JUL10 2300	31.10	-0.205	0.313	0	0.31	-18	1913	0.0041
9	1956JUL11 1600	27.39	-0.331	0.376	3	0.46	-31	533	0.0043
10	1956JUL11 1800	30.45	-0.382	0.277	3	0.32	-11	1064	0.0041
11	1956JUL14 1400	25.01	-0.21*		0	0.50	-66	201	0.0044
12	1956JUL14 1600	29.67	-0.38*		0	0.52	-47	682	0.0044
13	1956JUL23 0200	20.39	0.01*	0.042	2	0.09	3.4	82	0.0026
14	1956JUL23 0400	16.25	0.01*		0	0.05	1.6	91	0.0018
15	1956JUL23 1400	21.44	-0.208	0.290	0	0.23	-7.6	120	0.0038
16	1956JUL23 1600	25.61	-0.322	0.229	0	0.24	-5.2	1136	0.0039
17	1956JUL24 0200	27.44	0.00*	0.181	7	0.21	48	141	0.0037
18	1956JUL24 0400	23.52		0.109	1	0.20	25	159	0.0036
19	1956JUL25 1700	28.59	-0.326	0.423	3	0.39	-28	849	0.0042
20	1956JUL25 1900	32.49	-0.692		2	0.60	-62	894	0.0045
21	1956JUL26 0400	28.60	0.053	0.342	10	0.38	172	325*	0.0042
22	1956JUL26 0600	26.42	0.092	0.474	6	0.46	204	390*	0.0043
23	1956JUL30 0300	23.40	0.04*	0.411	0	0.39	193	350*	0.0042
24	1956JUL30 0500	21.89	0.03*	0.404	0	0.38	248	83	0.0042
25	1956AUG01 1900	23.62	-0.131		10	0.20	-6.2	736	0.0037
26	1956AUG02 1800	29.21	-0.370	0.435	9	0.43	-32	1052	0.0043
27	1956AUG02 2000	31.43	-0.445	0.492	7	0.42	-30	1396	0.0043
28	1956AUG03 0600	24.22		0.151	0	0.16	24	141	0.0034
29♦	1956AUG03 0800	25.36				0.23	36	122	0.0038
30♦	1956AUG03 1900	33.53	-0.432		0	0.46	-39	2055	0.0043
31♦	1956AUG03 2100	34.25	-0.280		2	0.51	-67	1855	0.0044
32	1956AUG07 0200	22.93	0.049	0.067	1	0.13	8.3	112	0.0031
33	1956AUG07 1900	28.73	-0.322			0.50	-51	541	0.0044
34	1956AUG07 2100	30.19	-0.450		2	0.60	-76	1101	0.0045
35S♦		22.28	0.039	0.244	2	0.24	53		
35	1956AUG12 0330	19.73	0.009		1	0.11	6.8	64	0.0029
36	1956AUG12 0530	18.94	0.028	0.085	0	0.10	7.8	120	0.0028
37	1956AUG12 0900	20.65		0.324	3	0.29	95	279	0.0040
38	1956AUG12 1100	19.82	0.036	0.275	8	0.28	99	345	0.0040
39	1956AUG14 0430	20.47	0.043	0.091	0	0.14	9.8	167	0.0032
40	1956AUG14 0630	20.29	0.034			0.11	8.0	148	0.0029
41	1956AUG14 0900	20.20	0.050	0.253		0.23	35	298	0.0038
42	1956AUG14 1100	21.49	0.078	0.362		0.37	120	252	0.0042
43	1956AUG15 1800	33.05	-0.401	0.366	10	0.35	-16	1493	0.0041
44	1956AUG15 2000	35.43	-0.449	0.311	8	0.40	-25	2447	0.0042
45	1956AUG15 2300	35.04	-0.104	0.277	9	0.39	-87	1990	0.0042
46	1956AUG16 0045	32.74	0.064	0.241	9	0.34	114	250*	0.0041
47	1956AUG20 1600	17.73	-0.21*		3			1243	
48S♦	Not used		-0.218		6	0.21	-7.8		
48	1956AUG21 1500	18.40	-0.345		1	0.51	-63	491	0.0044
49	1956AUG21 1700	23.29	-0.464		1	0.45	-28	932	0.0043

Table B-1. Table of input parameters provided by LLNL (cont'd)

Trial	Year/Month /Day/Time	Experimental Data (Raw)				Experimental Data (Fit)			Vel_d
		θ_o	H_o	u_*	cc	u_*	L	h	
50	1956AUG21 2000	28.64	-0.542		1	0.44	-26	1697	0.0043
51	1956AUG21 2130	29.80	-0.409		1	0.45	-40	2332	0.0043
52◆	1956AUG24 1717	24.96	-0.511		0			1154	
53◆	1956AUG25 0200	17.39	0.067	0.051	0	0.17	10	73	0.0034
54	1956AUG25 0400	18.68	0.058	0.212	0	0.24	40	285	0.0038
55	1956AUG25 0700	16.75	0.077	0.349	0	0.37	124	405	0.0042
56	1956AUG25 0900	15.29	0.041	0.199	0	0.29	76	444	0.0040
57	1956AUG25 2330	34.11	-0.082		0	0.46	-194	1836	0.0043
58	1956AUG26 0130	23.64		0.065	3	0.11	6.4	66	0.0029
59	1956AUG26 0430	23.60	0.050	0.103	5	0.14	11	248	0.0032
60	1956AUG26 0630	25.75	0.068	0.196	7	0.28	58	295	0.0040
61	1956AUG27 1700	31.63	-0.500	0.218	3	0.51	-38	581	0.0044
62	1956AUG27 2000	30.75	-0.173	0.246	8	0.34	-30	109	0.0041
63◆	1956AUG28 0200							263	
64◆	1956AUG28 0500							368	
65	1956AUG30 0130	24.96		0.271	2				
66	1956AUG30 0330	20.19		0.170	0			159	
67	1956AUG30 0630	20.55		0.218	0			197	
68	1956AUG30 0830	20.65		0.116	0			141	

- The sensible heat flux, H_o , is in cal/cm²-min and, in general, was taken from the Texas A&M data in Reference B-1, Table 9.2, Volume I. The * indicates that the values were taken from the University of Wisconsin data in Reference B-1, Table 10.1, Volume II.
- Friction velocity, u_* (m/s), was derived from $u_*^2 = \frac{1}{4}(\overline{u'w'}^2 + \overline{v'w'}^2)^{1/2}$ and data found in Table 17.3, Volume III of Reference B-2.
- The fractional cloud cover, cc, are given in tenths [Ref. B-1, Table 3.1, Volume I].
- Experimental Data (fit)** signifies that data were numerically fitted. The parameter values in these columns were used in the simulations instead of the raw experimental observations. This was done in order to resolve accuracy questions associated with the raw measured values. A more reliable approach for estimating u_* (friction velocity in m/s) and L (Monin-Obukhov length scale in meters) is based on fits to the temperature and wind speed profiles [Ref. B-4]. An almost complete set of friction velocity and Monin-Obukhov lengths derived using this approach are found in Reference B-5. The boundary layer height, h (meters), is determined from the temperature soundings. The * in the boundary layer height column signifies that the standard default was used [Ref. B-3].
- Deposition velocity, Vel_d , was determined according to the following formula [Ref. B-6]:

$$Vel_d = \frac{k u_*}{\log(z_r/z_o)} + 2.6 + k u_* r_c - \Psi$$

where

$$\Psi = \begin{cases} \exp(0.598 + 0.39 \log(-z_r/L) - 0.90 [\log(-z_r/L)]^2) & L < 0 \\ -5 z_r/L & L > 0 \end{cases}$$

Here L is the Monin-Obukhov length (m), u_* is the friction velocity (m/s), z_r is the reference height for the deposition velocity (m), and z_o is the surface roughness height (m). The canopy resistance r_c is given by:

$$r_c = \begin{cases} 0.0 \text{ sec/m} & \text{wet surface} \\ 70.0 \text{ sec/m} & \text{actively growing vegetation} \\ 200.0 \text{ sec/m} & \text{vegetation subject to small water stress} \end{cases}$$

The canopy resistance was set to 200.0 s/m corresponding to the fairly arid soil conditions of Nebraska and the surface roughness height was set to 0.008m. The reference height for deposition was set to $z_r = 0.5$ m. The experimental fit values for friction velocity, u_* , were derived from Reference B-5 but were scaled by the ratio of 0.40/0.35 to compensate for the use of a different choice of the von Karman constant [Ref. B-3].

Table B-2 [Ref. B-3] describes the reasons for the elimination of the trials that had missing data. Five additional experiments were eliminated from the comparisons, as described in Table B-3 [Ref. B-3].

Table B-2. Trials That Were Eliminated from the Comparison Because of Missing Data

Trial	Reason for elimination of case from simulations
1	Missing all or part of tower winds (stations "SOURCE" and "NORTH450")
2	Missing all or part of tower winds (stations "SOURCE" and "NORTH450")
3	Missing all or part of tower winds (stations "SOURCE" and "NORTH450")
4	Extremely diffuse concentration measurements
6	Missing all or part of tower winds
29	Missing all or part of tower winds
30	Missing sampler concentration correction factors
31	Missing sampler concentration correction factors
35S	Missing rawinsonde data
48S	Missing rawinsonde data and directions (stations "SOURCE" and "NORTH450")
52	Missing all or part of tower winds
53	Missing all or part of tower winds
63	Missing all or part of tower winds and missing concentration data
64	Missing all or part of tower winds and missing concentration data

Table B-3. Additional Trials That Were Eliminated from the Comparison

Trial	Reason for elimination of case from baseline simulations
65-68	Source height is different for these cases so no turbulence fit data was reported
47	Maximum concentration < 0.5mg/m^3

2. HPAC SIMULATION SETUP

The data discussed in section 1 of this appendix were used to produce two profiles for the HPAC simulations. HPAC’s “Upper Air Observations” profile was created from the “Rawinson” radiosonde and “A&M TWR” tower data. HPAC’s “Surface Observations” profile was derived from the rest of the meteorological data shown in Figure B-1. Figures B-2 and B-3 depict the two types of HPAC meteorological input parameter files that were created from the information available from the file shown in Figure B-1.

```
# TYPE:          OBSERVATION
# TIMEREference: UTC
PROFILE
7 3
ID      YYMMDD  HOUR     X           Y           MOL8      ZI9
      HOURS   KM        KM         M          M
Z       WSPD     WDIR
M       M/S      DEG
-9999.00
ID: 000001  560730  4.83    535.425  4705.287  248.00   83.00
      2.00    3.80    130.00
      290.00   13.30   150.00
      600.00   14.40   160.00
      930.00   13.70   190.00
      1270.00   14.20   210.00
ID: 000002  560730  5.25    534.985  4705.247  248.00   83.00
      0.25    3.82    146.00
      0.50    4.61    146.00
      1.00    5.21    146.00
      2.00    5.86    146.00
      4.00    6.62    146.00
      8.00    7.64    146.00
      16.00   8.65    146.00
```

Figure B-2. HPAC’s “Upper Air Observations” Profile for Trial 24¹⁰

The HPAC-derived wind profiles (described previously), the surface roughness height (0.008m), and the *L* and *h* values of Table B-1 (whose column headings are highlighted in red) were used to generate the HPAC predictions. In addition, for the

⁸ The Monin-Obukhov Length (denoted here by MOL) was provided by LLNL and is shown in Table B-4.

⁹ The boundary layer mixing height (denoted here by ZI) was provided by LLNL and is shown in Table B-4

¹⁰ Station ID 000001 corresponds to “Rawinson” radiosonde and Station ID 00002 corresponds to “A&M TWR”. Note that for “A&M TWR,” the wind direction at all heights is assumed to be identical to the wind direction at the height of 1 meter.

HPAC predictions that considered an SO₂ deposition mechanism, the *Vel_d* values (whose column heading is highlighted in blue) were used.

```
# TYPE:          OBSERVATION
# TIMEREference: UTC
SURFACE
10
ID    YYMMDD   HOUR   X           Y           Z           WSPD  WDIR  MOL  ZI
      HOURS  KM       KM       M       M/S   DEG   M     M
-9999.00
KSRC 560730 5.17    535.200 4704.427 2.00    6.22 141.00 248.00 83.00
KNRT 560730 5.17    535.170 4704.877 2.00    5.76 142.00 248.00 83.00
KMTT 560730 5.25    535.109 4705.251 2.00 -9999.00 135.40 248.00 83.00
```

Figure B-3. HPAC's “Surface Observations” Profile for Trial 24¹¹

¹¹ Station IDs “KSRC”, “KNRT” and “KMTT” denote the stations “SOURCE”, “NORTH450” and “MIT 3L” from Figure B-1, respectively.

REFERENCES

- B-1. Barad, M. L. (Editor), *Project Prairie Grass, A Field Program in Diffusion*, Geophysical Research Papers No. 59, Volumes I and II, DTIC #AD-152572/AFCRC-TR-58-235(I), Air Geophysical Laboratory, Hanscom Air Force Base, MA, 1958.
- B-2. Haugen, D. A. (Editor), *Project Prairie Grass, A Field Program in Diffusion*, Geophysical Research Paper, No. 59, Volume III, Report AFCRC-TR-58-235, Air Force Cambridge Research Center, 1959.
- B-3. Sugiyama, G., Nasstrom, J., Foster, K., and D. Larson, *NARAC Prairie Grass Simulations*, UCRL-ID in preparation.
- B-4. Nieuwstadt, F., "The Computation of the Friction Velocity u_* and the Temperature Scale T_* from Temperature and Wind Velocity Profiles by Least-Squares Methods," *Boundary Layer Met.*, **14**, pp. 235-246, 1977.
- B-5. Van Ulden, A. P., "Simple Estimates for Vertical Diffusion from Sources Near the Ground," *Atmos. Envir.*, **12**, pp.2125-2129, 1978.
- B-6. Weseley and Hicks, J., *Air Poll. Control Assoc.*, **27**, 11, 1977.

APPENDIX C
HPAC PREDICTIONS COMPARED TO *PRAIRIE GRASS TRIALS*

APPENDIX C

HPAC PREDICTIONS COMPARED TO *PRAIRIE GRASS* TRIALS

This appendix presents graphical comparison of HPAC predictions with no SO₂ surface deposition to *Prairie Grass* field trials [Ref. C-1]. Vertical plot units are dosage units of mg-sec/m³. Horizontal plot units are sampler numbers as presented in the *Prairie Grass* field trials with sampler number 1 oriented to the west, the middle sampler (45 or 90) oriented to the north, and the last sampler (91 or 181) oriented to the east of the SO₂ gas release source. Only data values greater than the cutoff threshold of 3 mg-sec/m³ (0.005 mg/m³) are presented for both field trial data and HPAC predictions. This cutoff threshold value corresponds to a minimum value reported in *Prairie Grass* field trials.

Comparisons of HPAC predictions and *Prairie Grass* field trial observations are presented on both linear and logarithmic dosage scales. Each graphical comparison consists of five plots (one for each arc) with the top plot depicting the 50-meter arc, the second plot depicting the 100-meter arc, the third plot depicting the 200-meter arc, and so on. The last panel (just above the figure caption) contains information about the data files used to produce these plots. The *Prairie Grass* field trial file name contains a two-digit number corresponding to the trial number. The HPAC prediction file name contains the moniker “nodeposition,” denoting that SO₂ surface deposition was not considered in these predictions, and a one- or two-digit number reflecting the *Prairie Grass* field trial being predicted. Odd-numbered pages contain figures on the linear dosage scale while even-numbered pages contain figures on the logarithmic dosage scale.

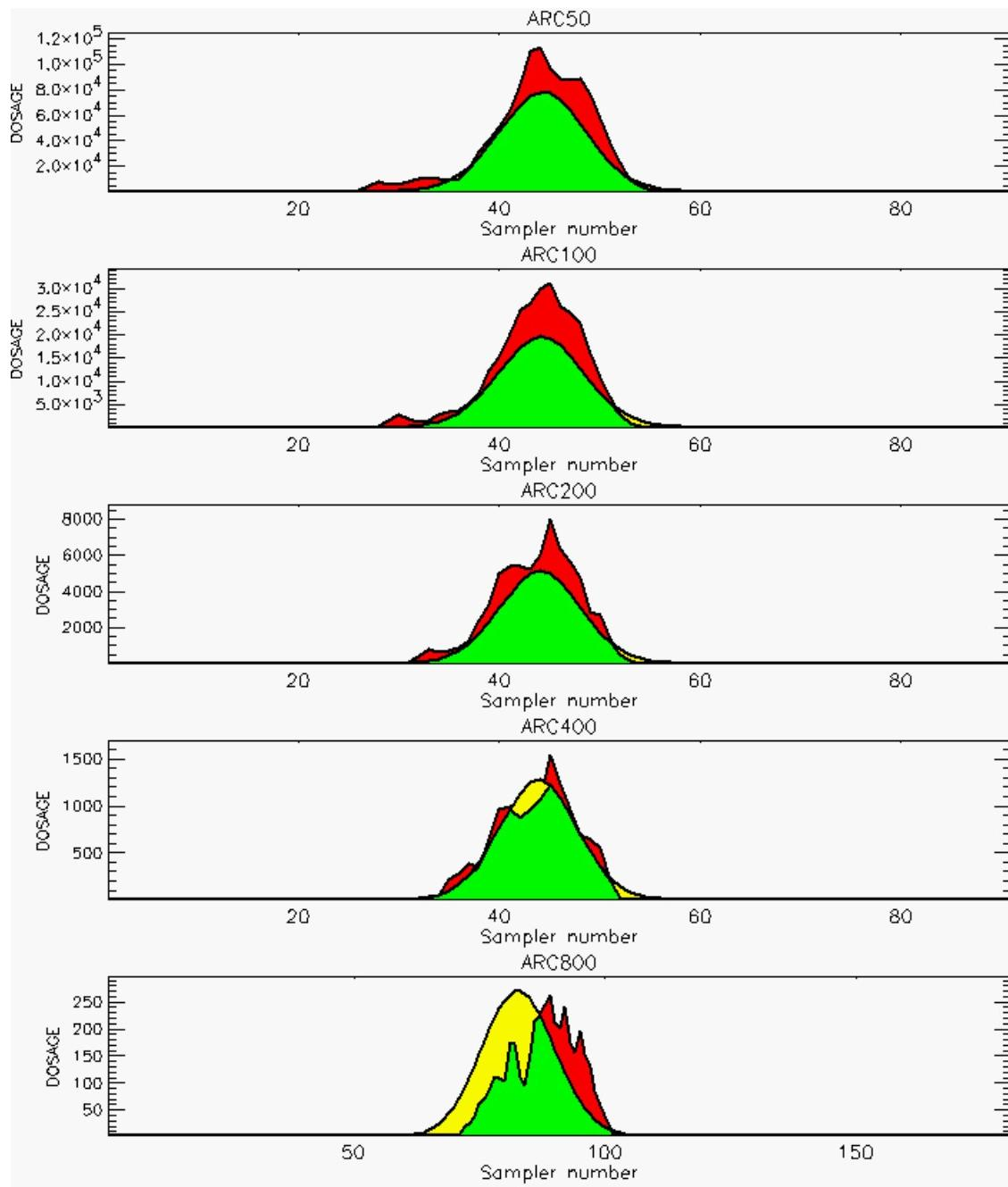
The meanings of the colors used in the plots are described below:

- Red — trial dosages that are higher than the prediction
- Green — trial dosages that overlap with the prediction
- Yellow — prediction dosages that are higher than the trial
- White — trial sampler observation is missing.

These shadings correspond to AE2 as described in Chapter 2.

Samplers with missing values, or spurious maximum that were fixed by moving the decimal point, are noted in the figure captions [Ref. C-2] (see also Appendix K).

Irwin stability categories that were used in our analyses are denoted in the figure captions. These stability category assignments are based on Reference C-3.

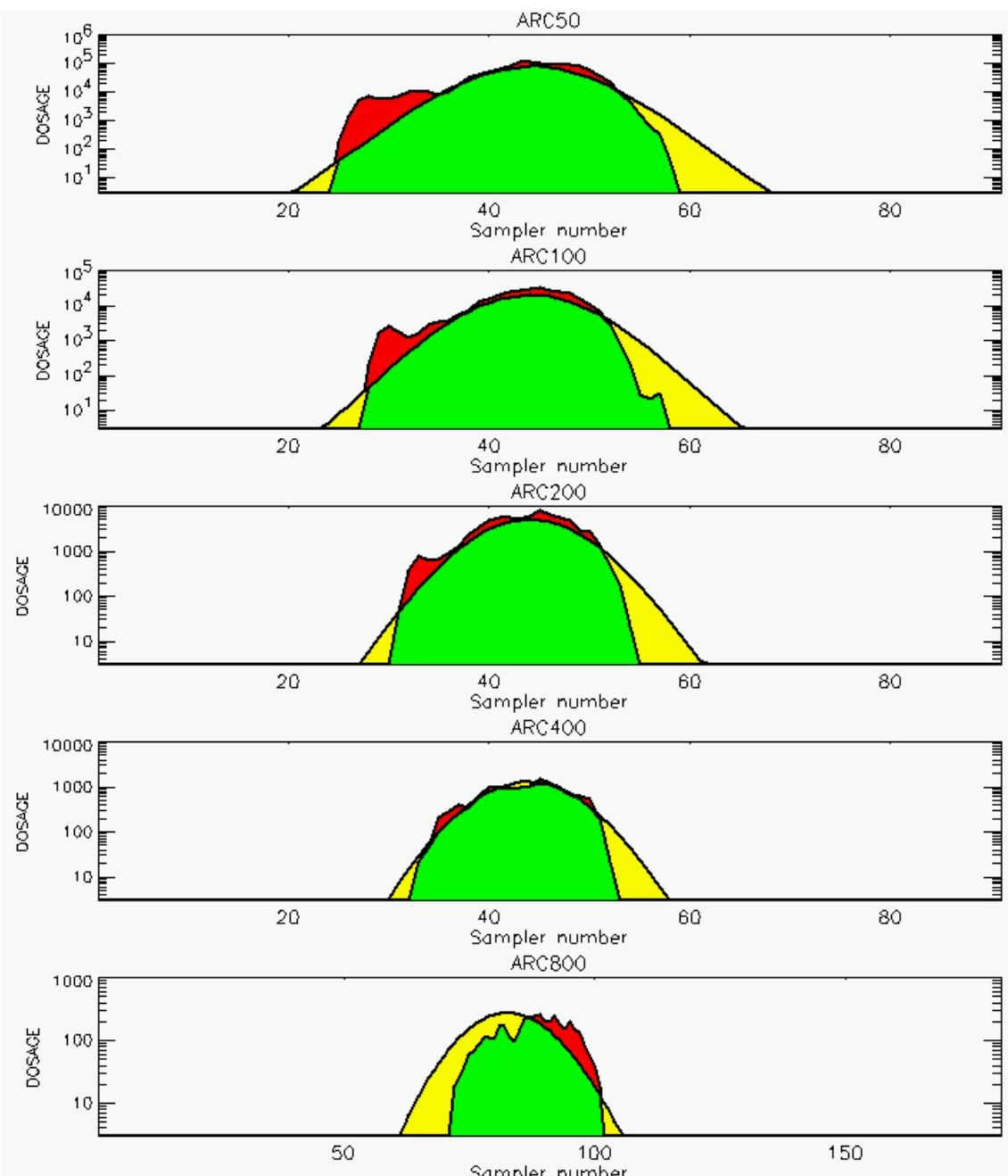


PG Observation to Prediction Comparison

PG Trial File: pr_grass_tracer_Experiment_05.txt

Prediction File: HPAC\nodeposition\pg_5_noxd.out

Figure C-1a. HPAC Predictions to Trial 5 on Linear Scale: Stability Category is 2

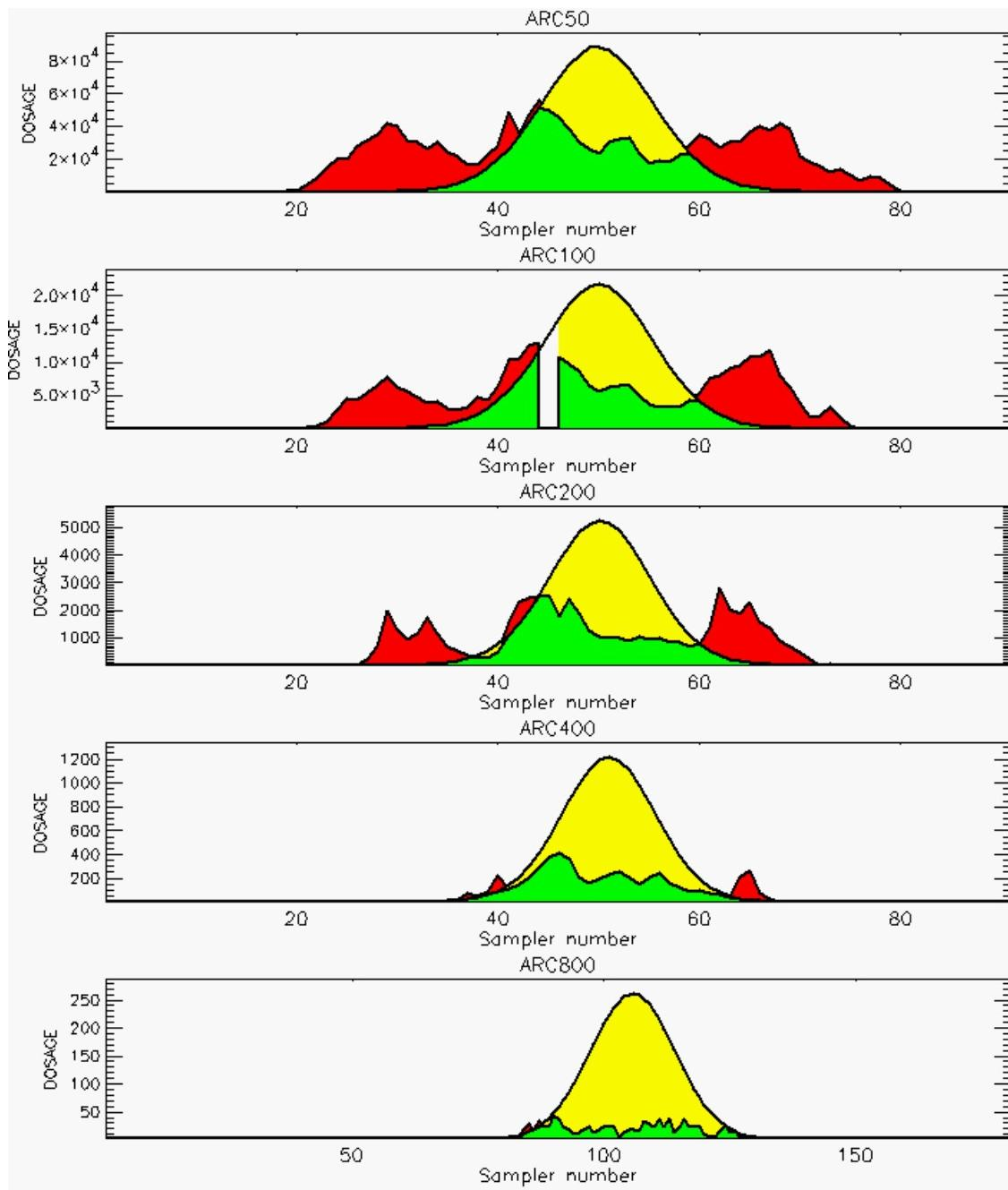


PG Observation to Prediction Comparison

PG Trial File: pr_grass_tracer_Experiment_05.txt

Prediction File: HPAC\nodeposition\pg_5_noxd.out

Figure C-1b. HPAC Prediction to Trial 5 on Logarithmic Scale: Stability Category is 2

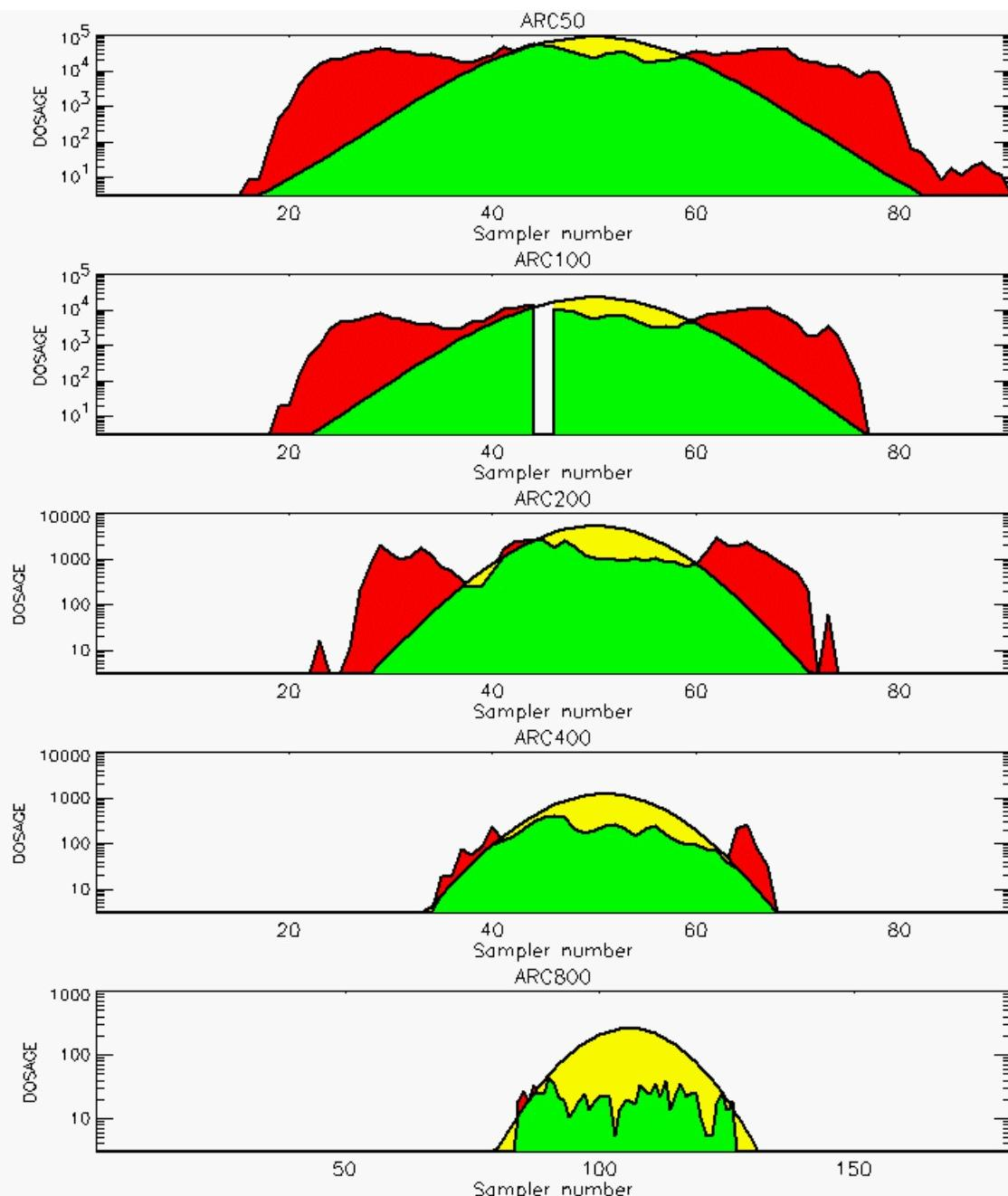


PG Observation to Prediction Comparison

PG Trial File: pr_grass_tracer_Experiment_07.txt

Prediction File: HPAC\nodeposition\pg_7_novd.out

**Figure C-2a. HPAC Prediction to Trial 7 on Linear Scale: Stability Category is 1
(Value for Sampler 45 of 100-Meter Arc is Missing)**

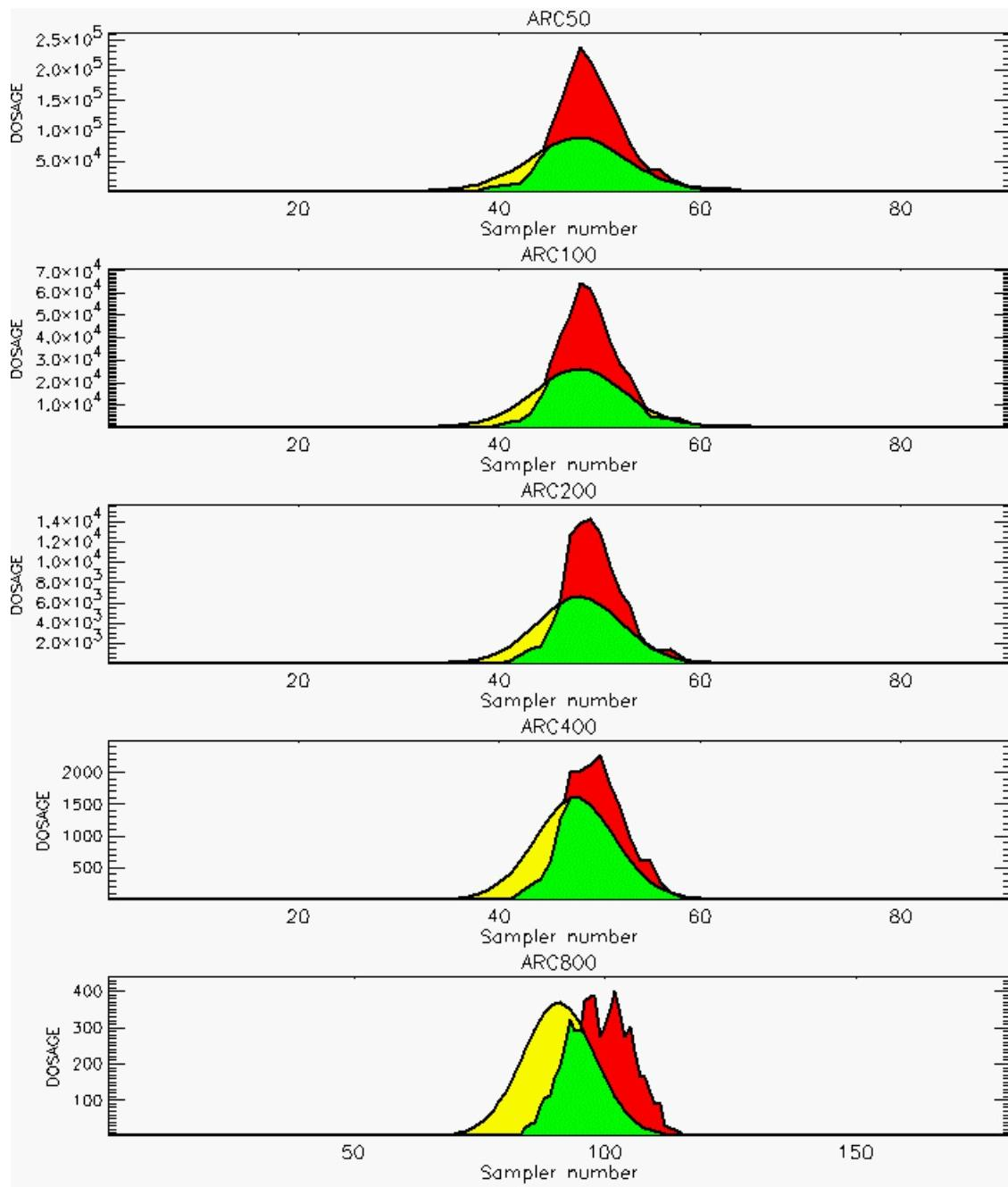


PG Observation to Prediction Comparison

PG Trial File: pr_grass_tracer_Experiment_07.txt

Prediction File: HPAC\nodeposition\pg_7_noxd.out

**Figure C-2b. HPAC Prediction to Trial 7 on Logarithmic Scale: Stability Category is 1
(Value for Sampler 45 of 100-Meter Arc is Missing)**

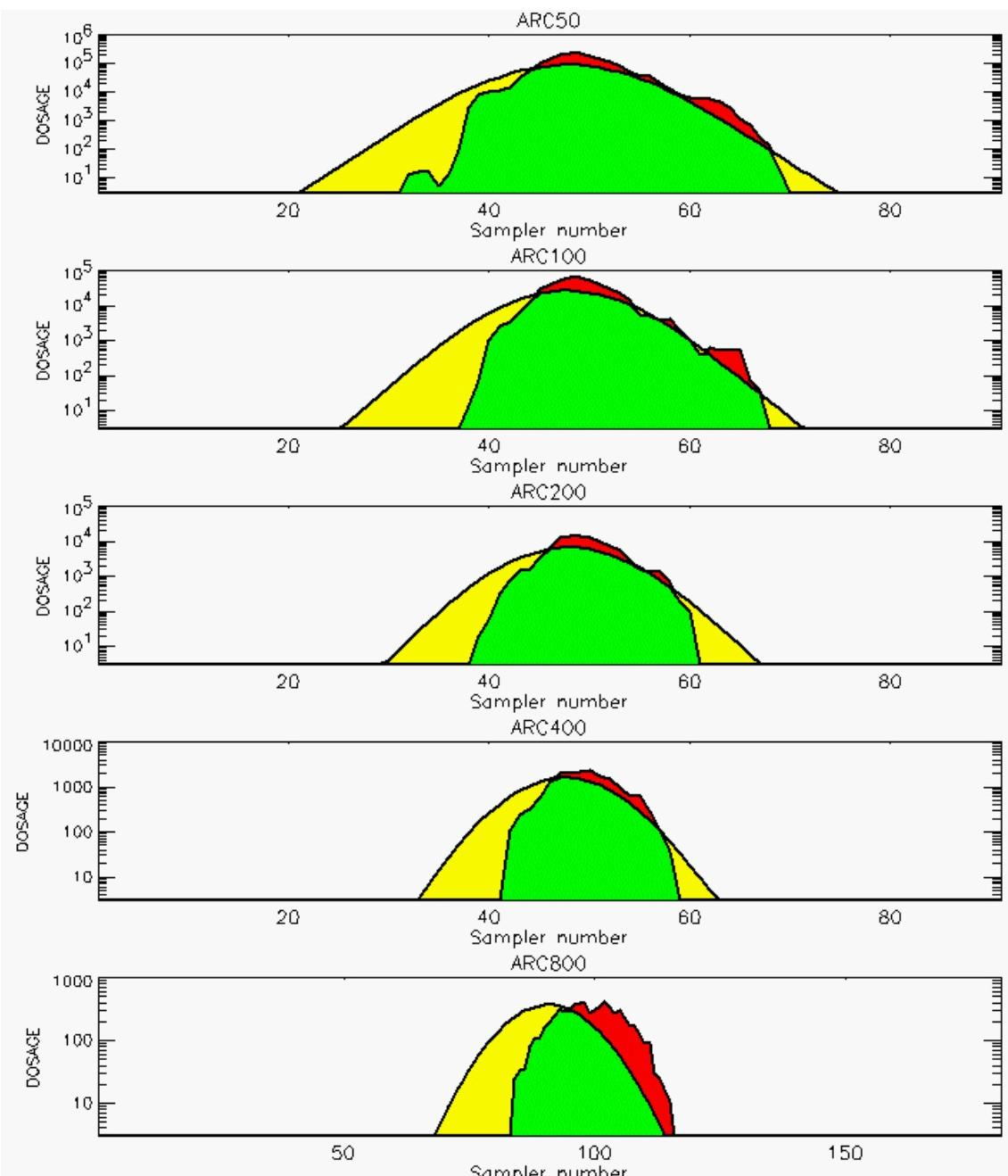


PG Observation to Prediction Comparison

PG Trial File: pr_grass_tracer_Experiment_08.txt

Prediction File: HPAC\nodeposition\pg_B_noxd.out

Figure C-3a. HPAC Prediction to Trial 8 on Linear Scale: Stability Category is 2

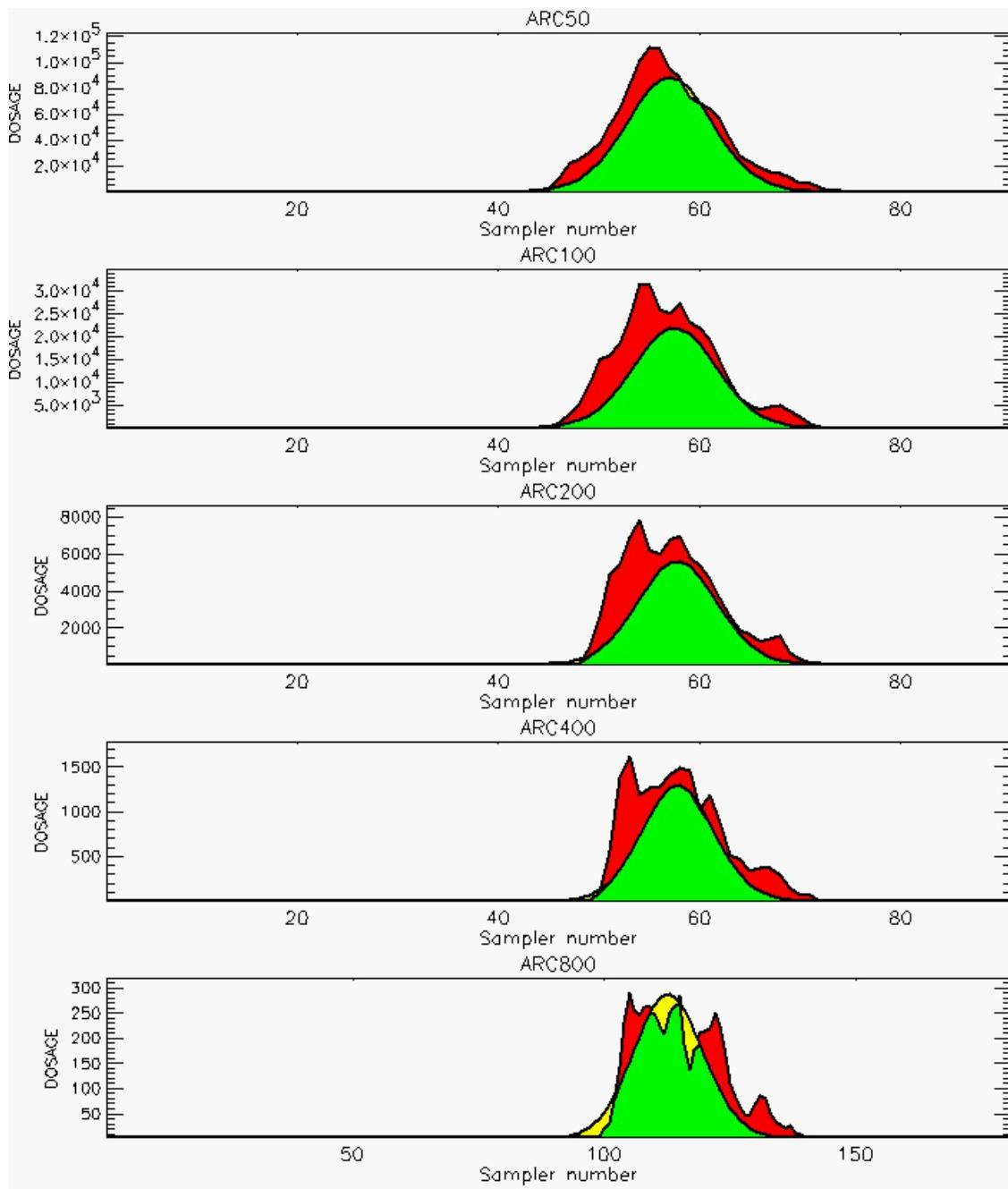


PG Observation to Prediction Comparison

PG Trial File: pr_grass_tracer_Experiment_08.txt

Prediction File: HPAC\nodeposition\pg_B_noxd.out

Figure C-3b. HPAC Prediction to Trial 8 on Logarithmic Scale: Stability Category is 2

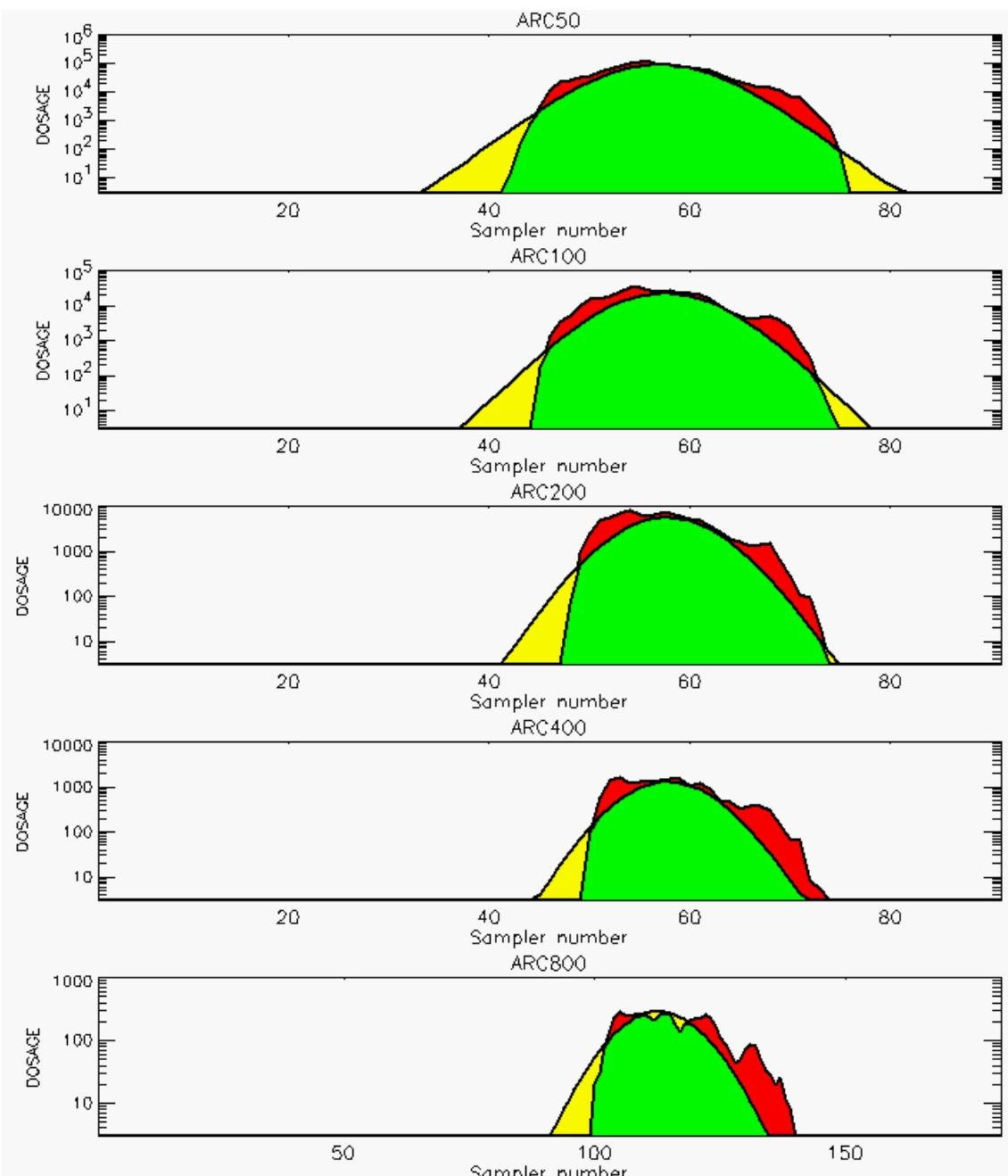


PG Observation to Prediction Comparison

PG Trial File: pr_grass_tracer_Experiment_09.txt

Prediction File: HPAC\nodeposition\pg_9_novd.out

Figure C-4a. HPAC Prediction to Trial 9 on Linear Scale: Stability Category is 2

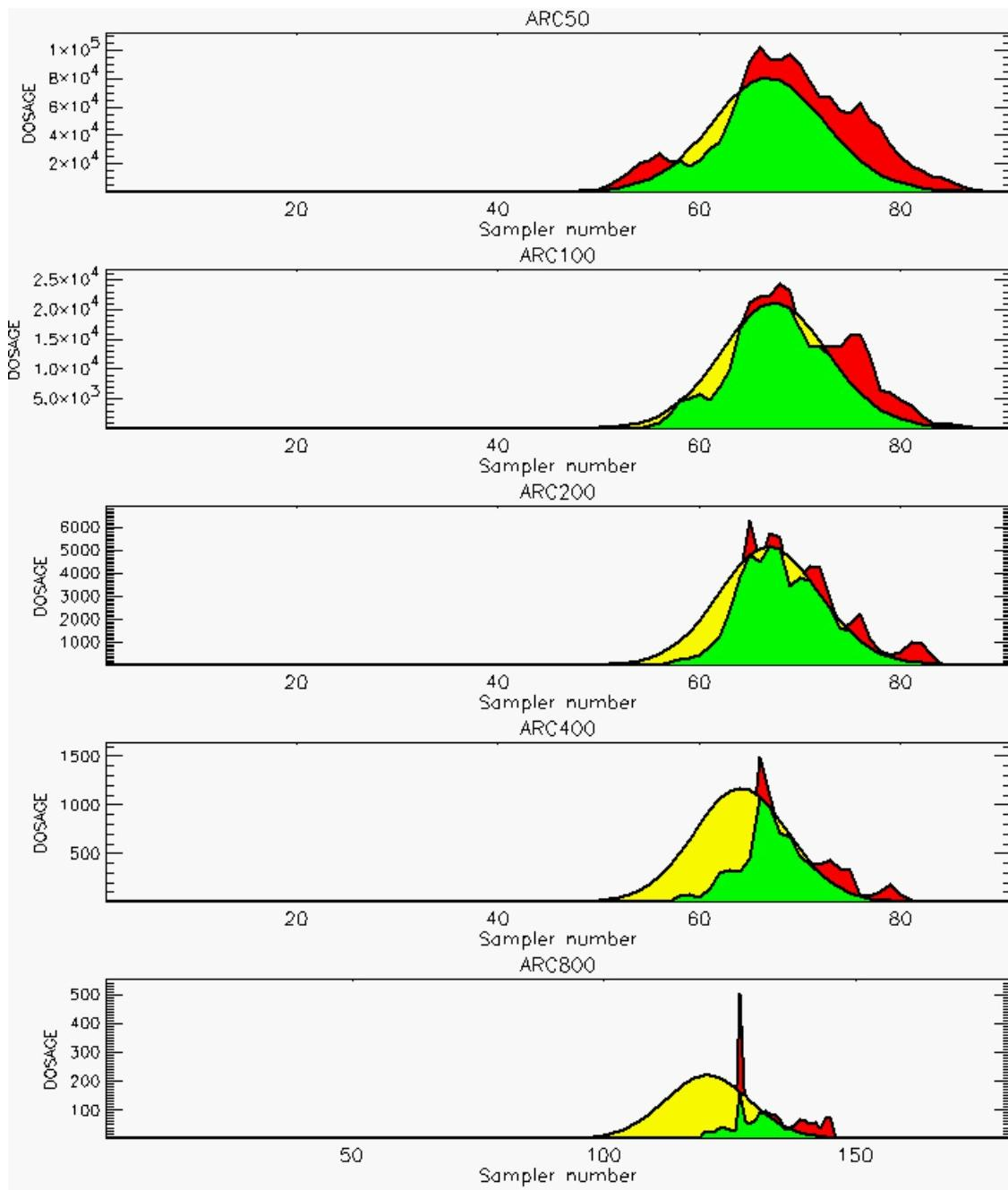


PG Observation to Prediction Comparison

PG Trial File: pr_grass_tracer_Experiment_09.txt

Prediction File: HPAC\nodeposition\pg_9_noxd.out

Figure C-4b. HPAC Prediction to Trial 9 on Logarithmic Scale: Stability Category is 2

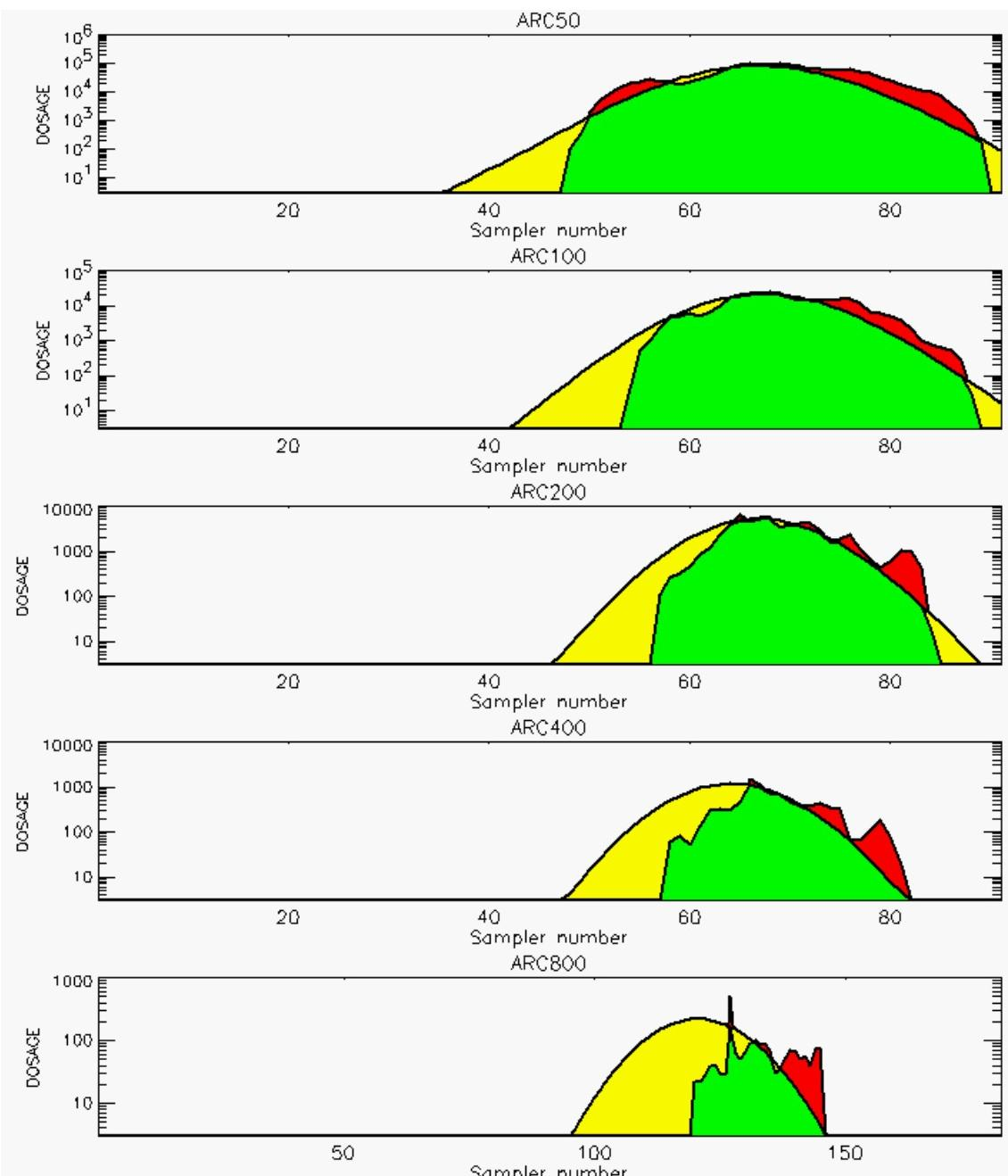


PG Observation to Prediction Comparison

PG Trial File: pr_grass_tracer_Experiment_10.txt

Prediction File: HPAC\nodeposition\pg_10_noxd.out

Figure C-5a. HPAC Prediction to Trial 10 on Linear Scale: Stability Category is 1

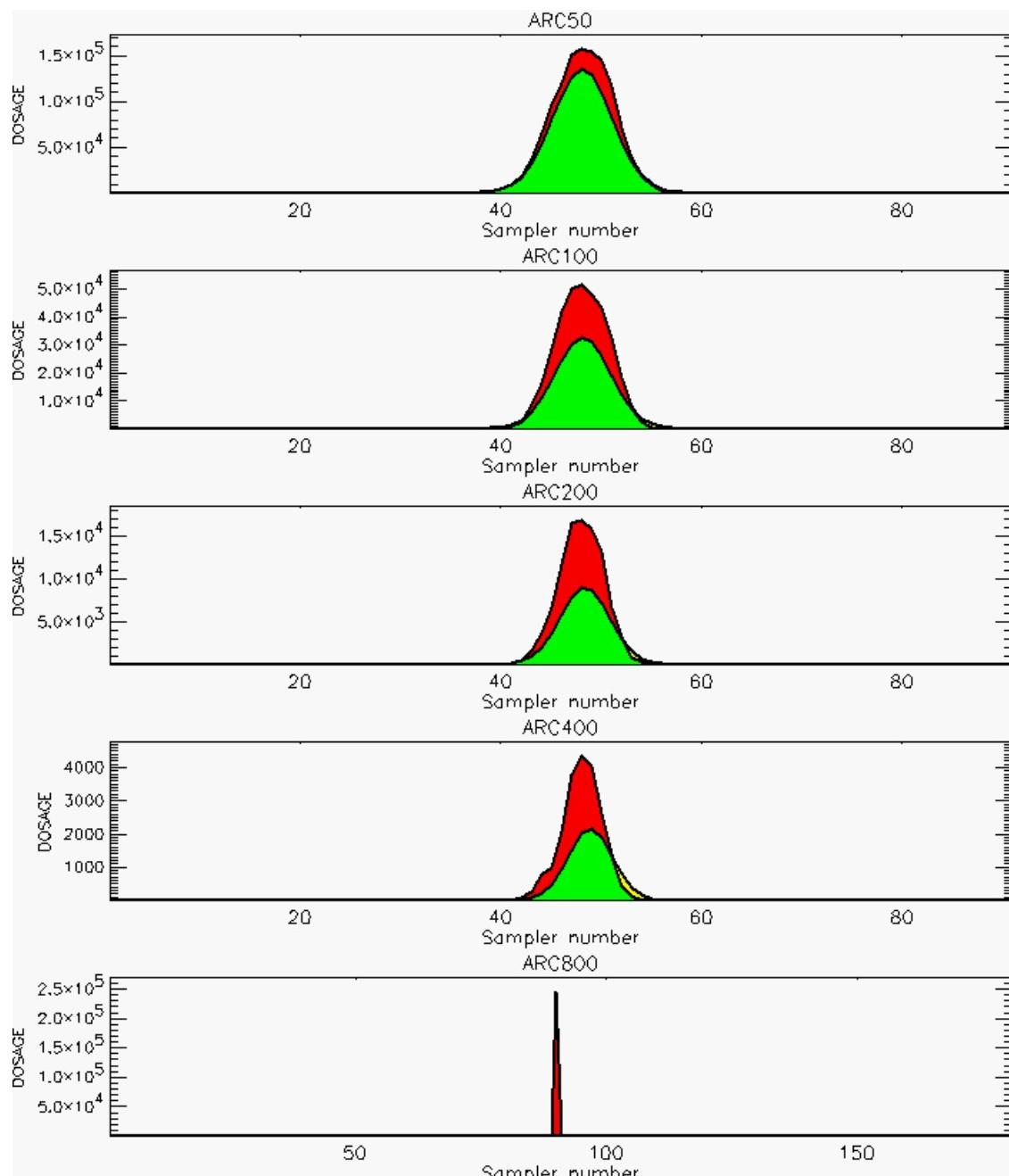


PG Observation to Prediction Comparison

PG Trial File: pr_grass_tracer_Experiment_10.txt

Prediction File: HPAC\nodeposition\pg_10_noxd.out

**Figure C-5b. HPAC Prediction to Trial 10 on Logarithmic Scale:
Stability Category is 1**

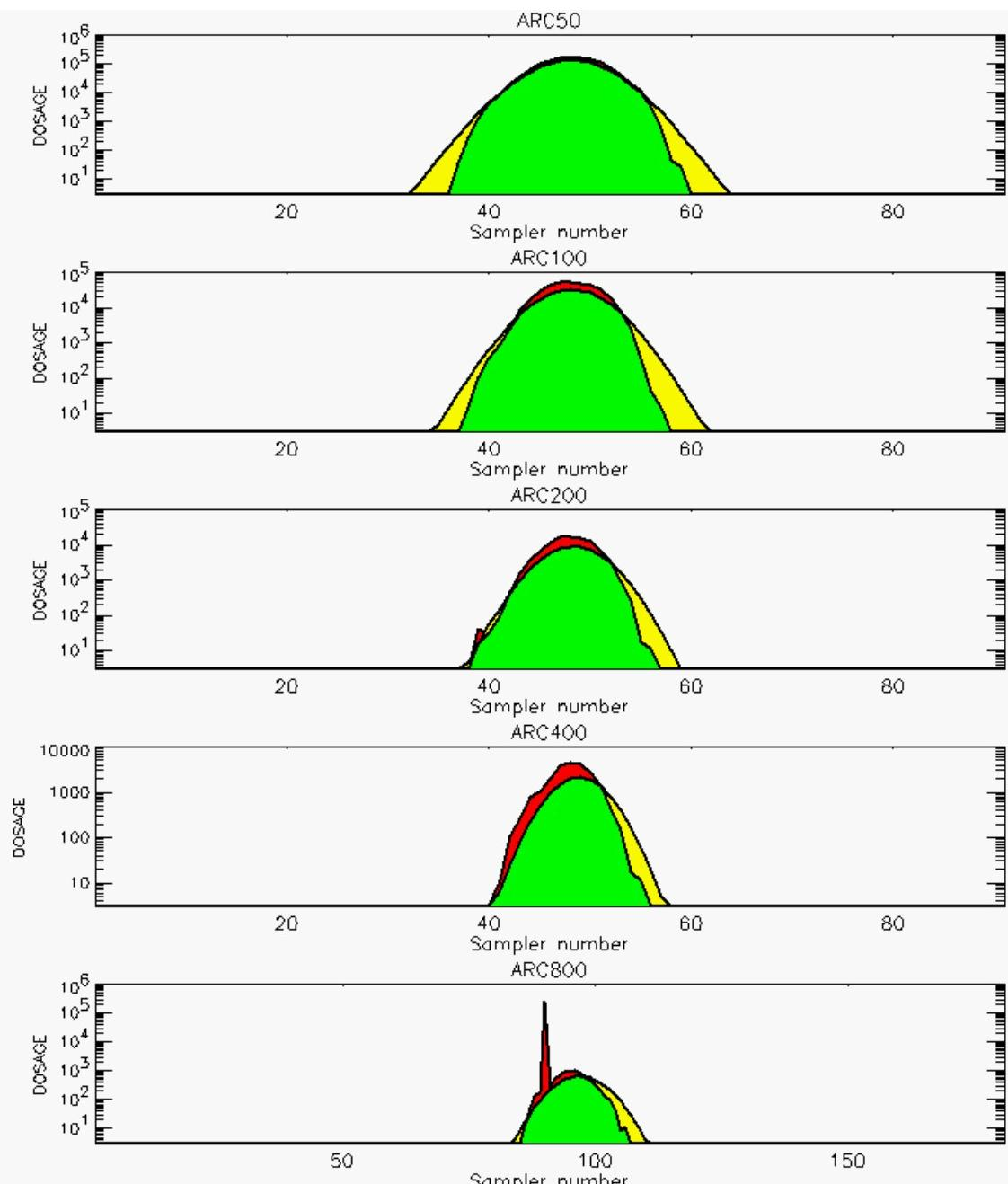


PG Observation to Prediction Comparison

PG Trial File: pr_grass_tracer_Experiment_11.txt

Prediction File: HPAC\nodeposition\pg_11_noxd.out

**Figure C-6a. HPAC Prediction to Trial 11 on Linear Scale:
Stability Category is 3 (Value for Sampler 90 of 800-Meter Arc is Considered “Spurious”
and is Fixed by Moving Decimal Point)**

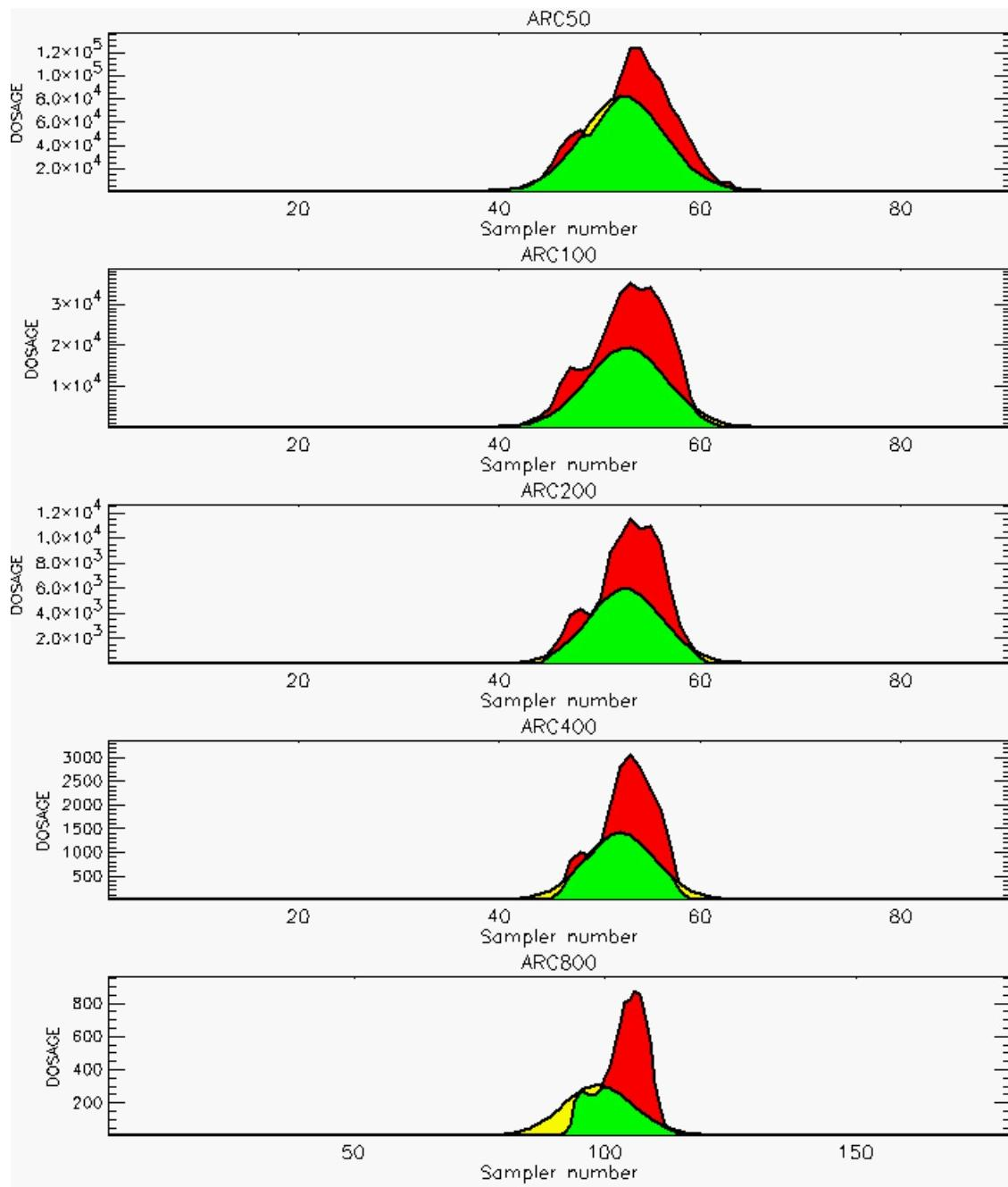


PG Observation to Prediction Comparison

PG Trial File: pr_grass_tracer_Experiment_11.txt

Prediction File: HPAC\nodeposition\pg_11_noxd.out

**Figure C-6b. HPAC Prediction to Trial 11 on Logarithmic Scale:
Stability Category is 3 (Value for Sampler 90 of 800-Meter Arc is Considered "Spurious"
and is Fixed by Moving Decimal Point)**

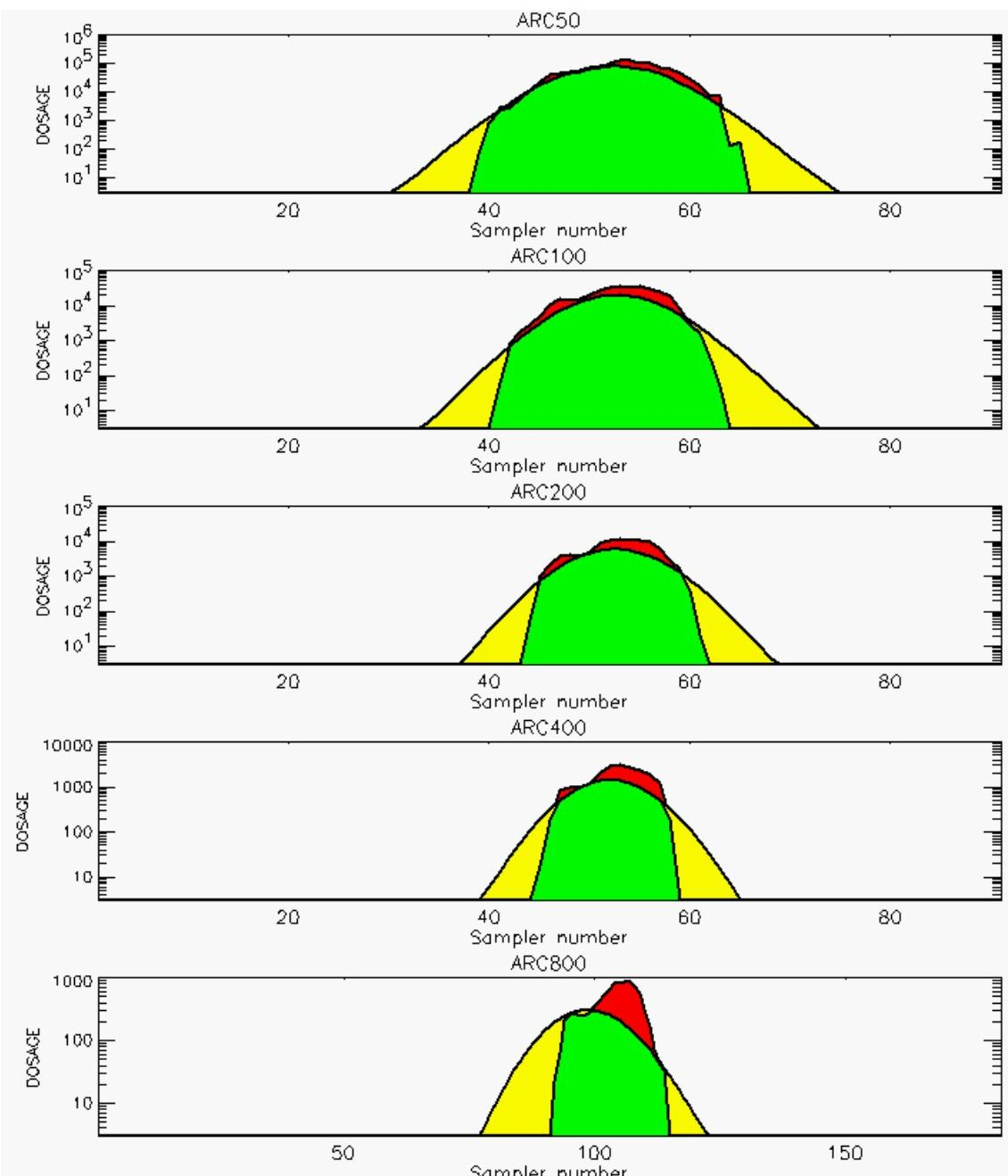


PG Observation to Prediction Comparison

PG Trial File: pr_grass_tracer_Experiment_12.txt

Prediction File: HPAC\nodeposition\pg_12_noxd.out

Figure C-7a. HPAC Prediction to Trial 12 on Linear Scale: Stability Category is 3

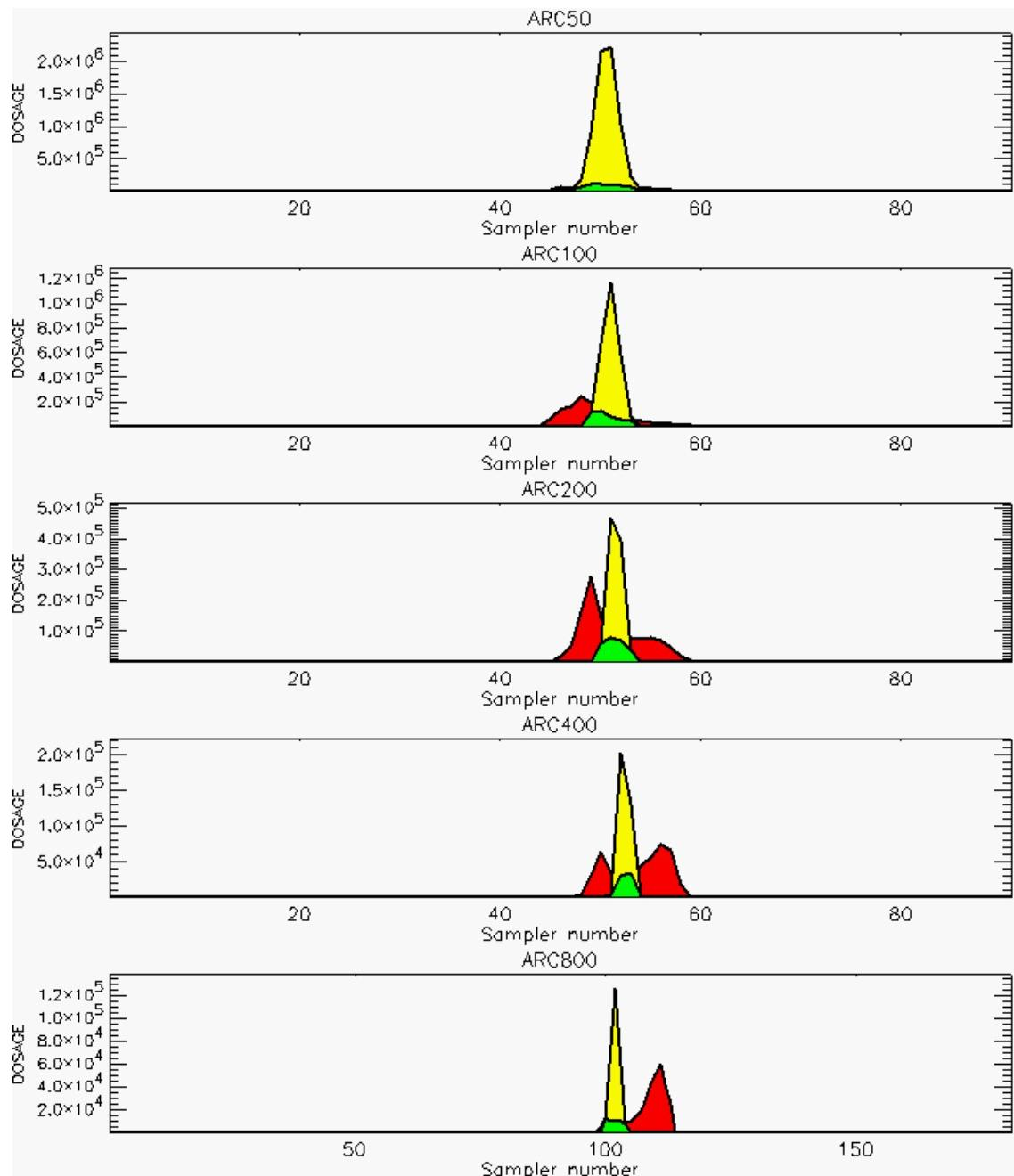


PG Observation to Prediction Comparison

PG Trial File: pr_grass_tracer_Experiment_12.txt

Prediction File: HPAC\nodeposition\pg_12_noxd.out

**Figure C-7b. HPAC Prediction to Trial 12 on Logarithmic Scale:
Stability Category is 3**

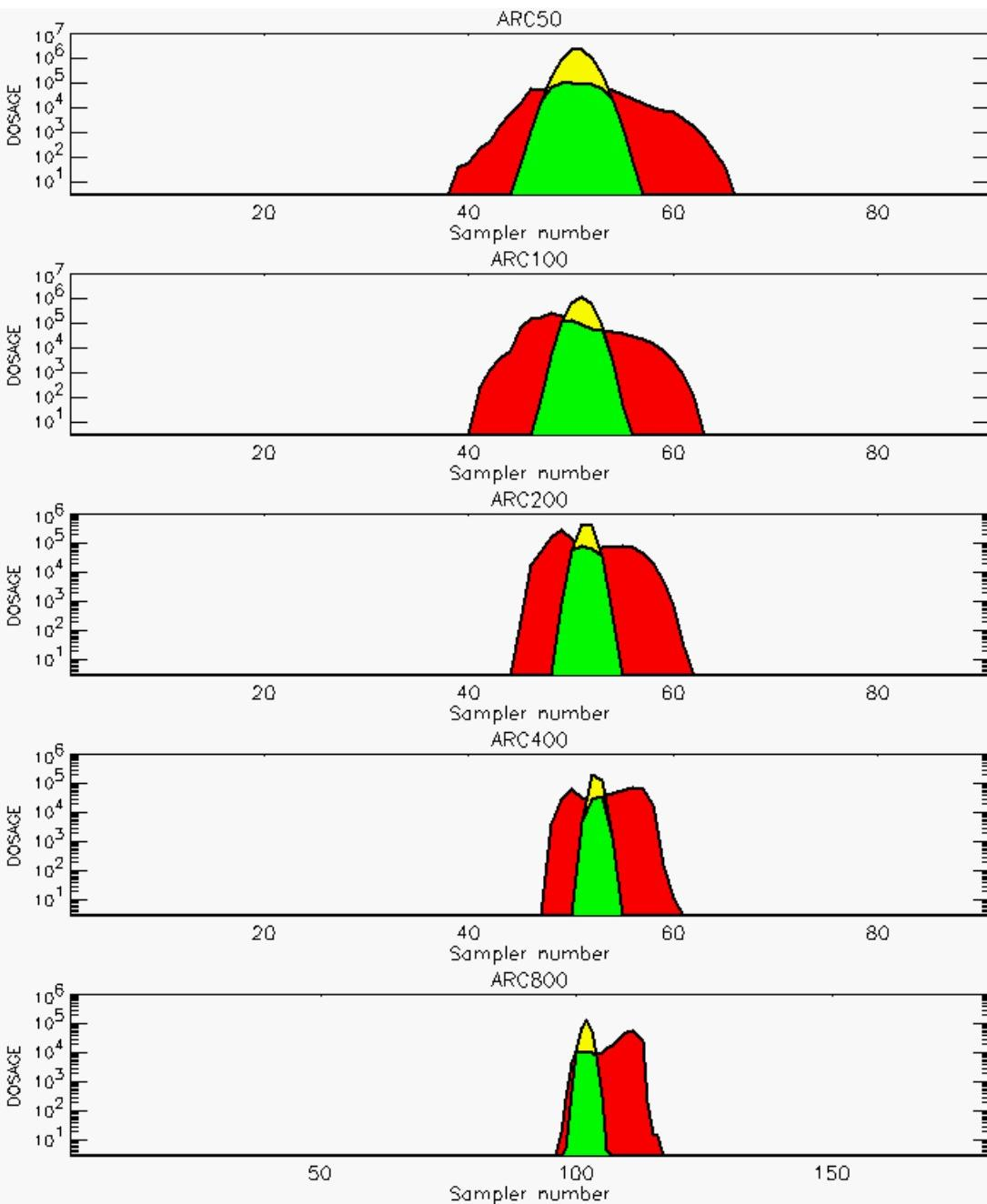


PG Observation to Prediction Comparison

PG Trial File: pr_grass_tracer_Experiment_13.txt

Prediction File: HPAC\nodeposition\pg_13_noxd.out

Figure C-8a. HPAC Prediction to Trial 13 on Linear Scale: Stability Category is 7

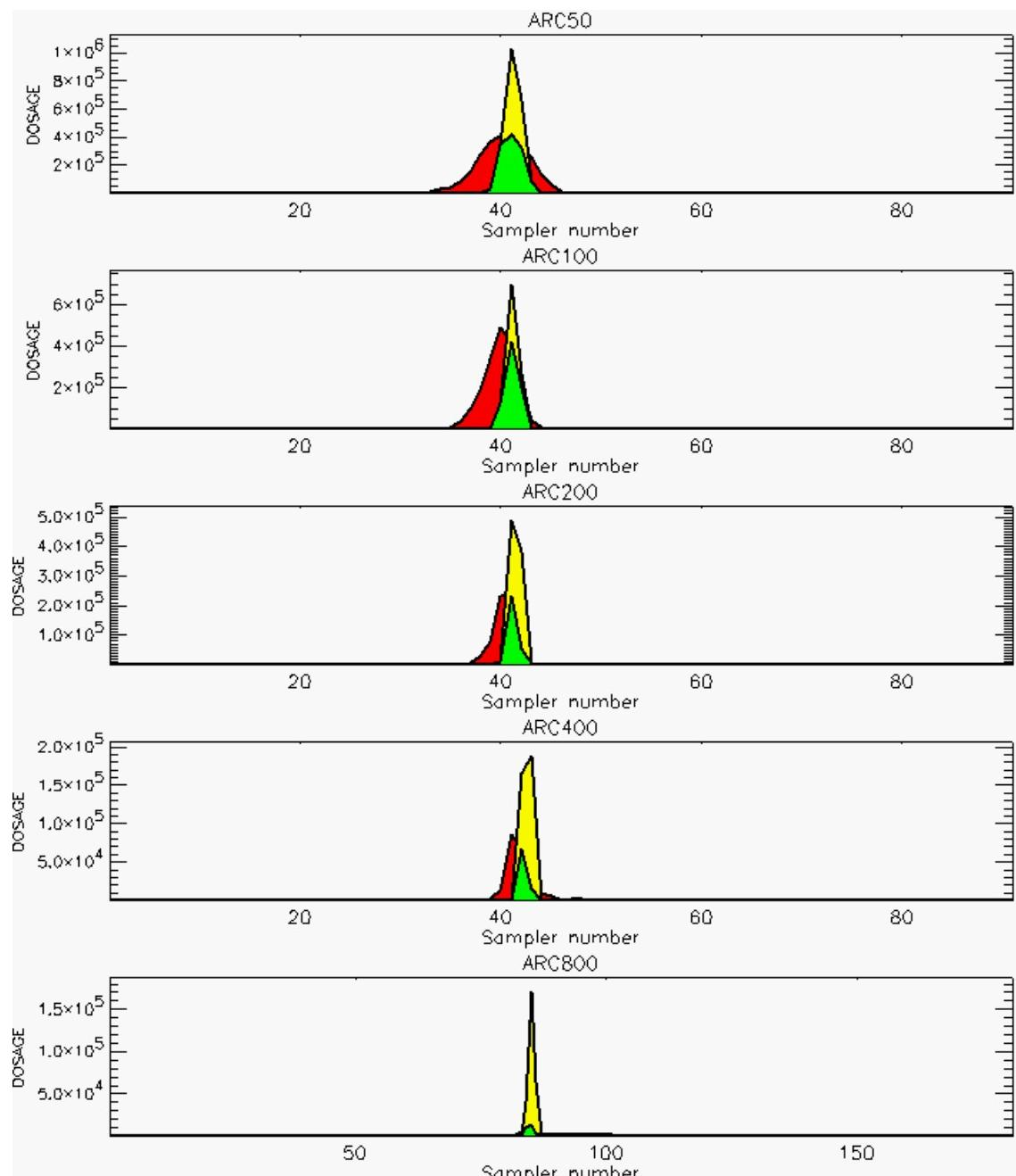


PG Observation to Prediction Comparison

PG Trial File: pr_grass_tracer_Experiment_13.txt

Prediction File: HPAC\nodeposition\pg_13_noxd.out

**Figure C-8b. HPAC Prediction to Trial 13 on Logarithmic Scale:
Stability Category is 7**

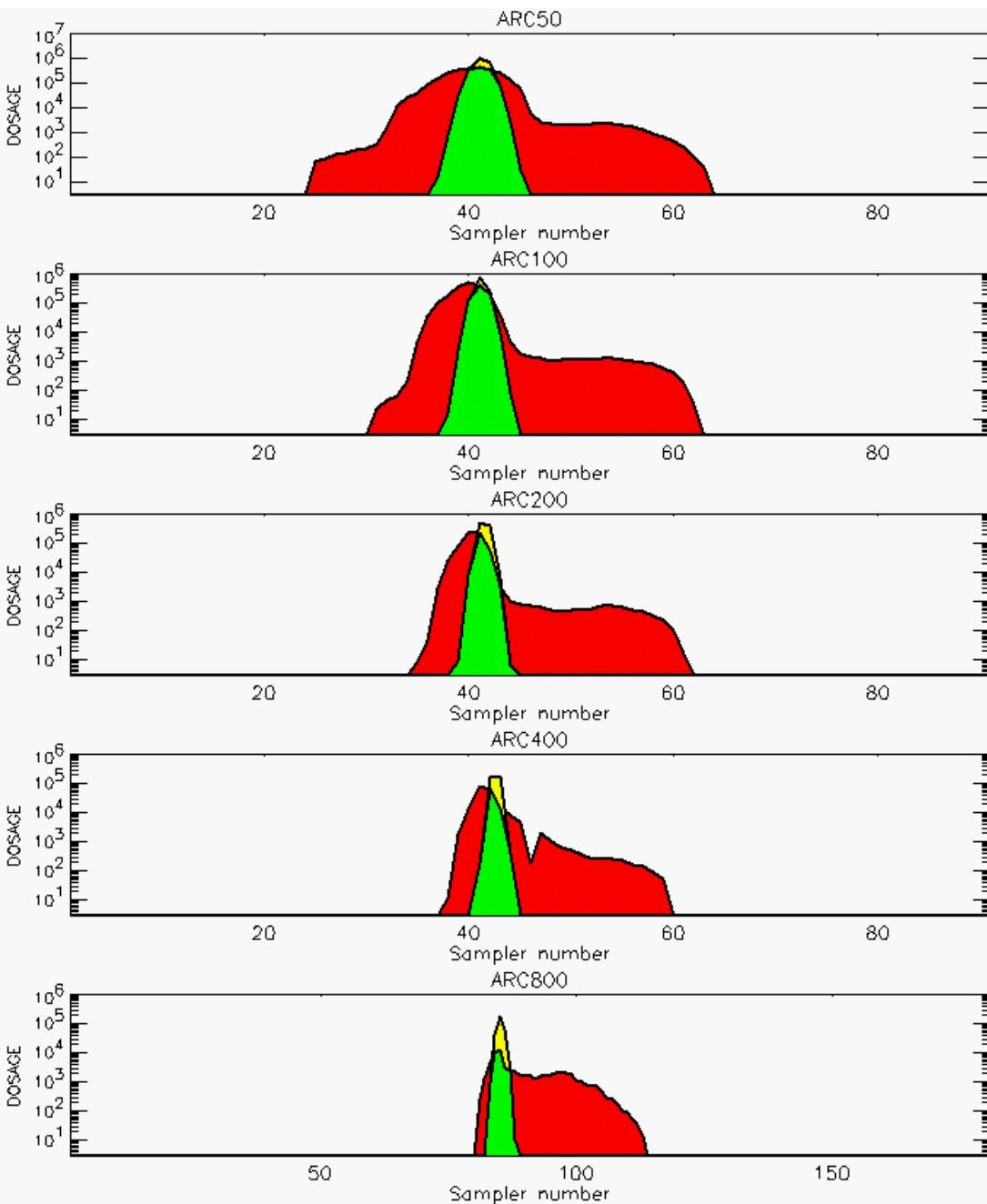


PG Observation to Prediction Comparison

PG Trial File: pr_grass_tracer_Experiment_14.txt

Prediction File: HPAC\nodeposition\pg_14_noxd.out

Figure C-9a. HPAC Prediction to Trial 14 on Linear Scale: Stability Category is 7

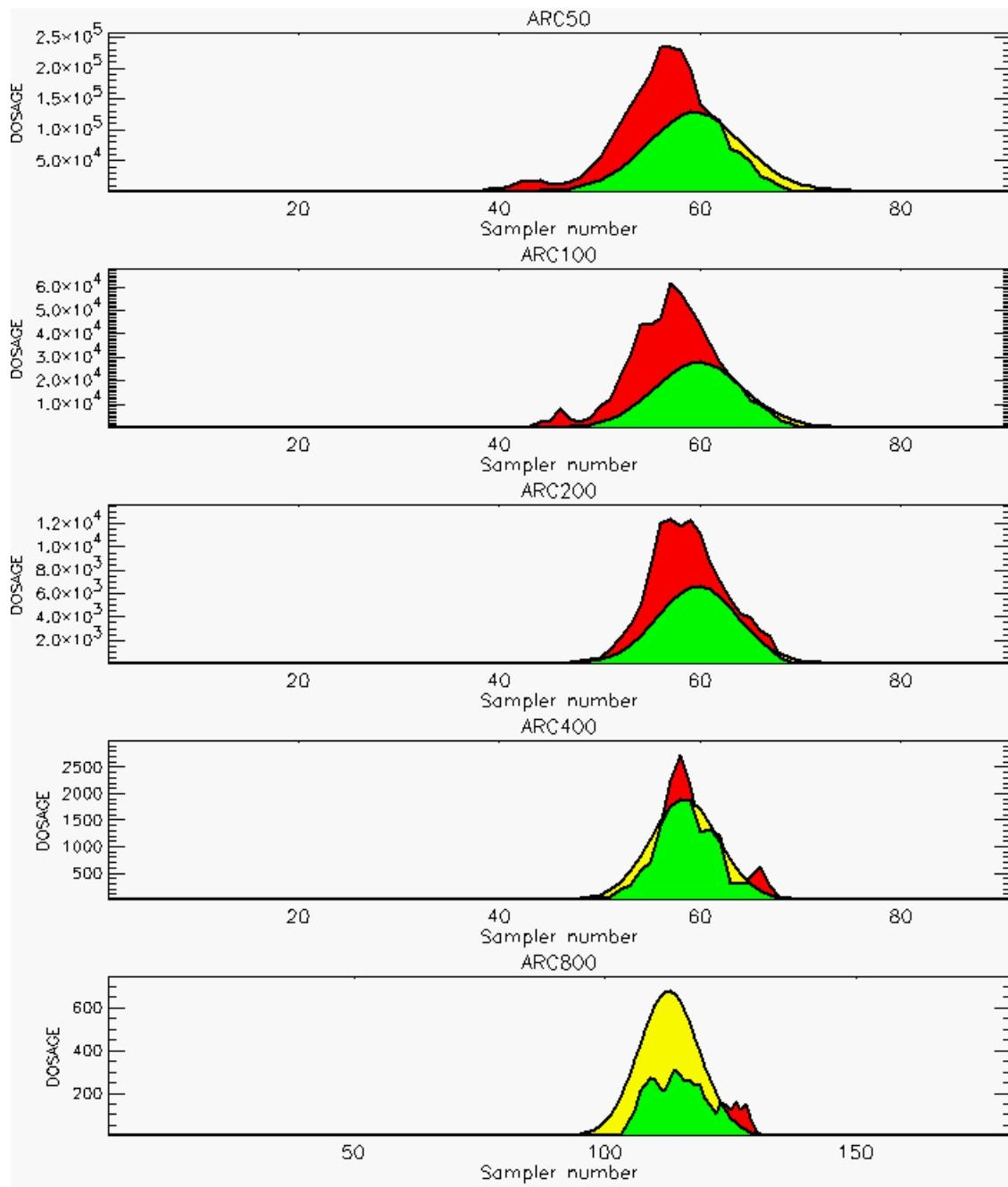


PG Observation to Prediction Comparison

PG Trial File: pr_grass_tracer_Experiment_14.txt

Prediction File: HPAC\nodeposition\pg_14_noxd.out

**Figure C-9b. HPAC Prediction to Trial 14 on Logarithmic Scale:
Stability Category is 7**

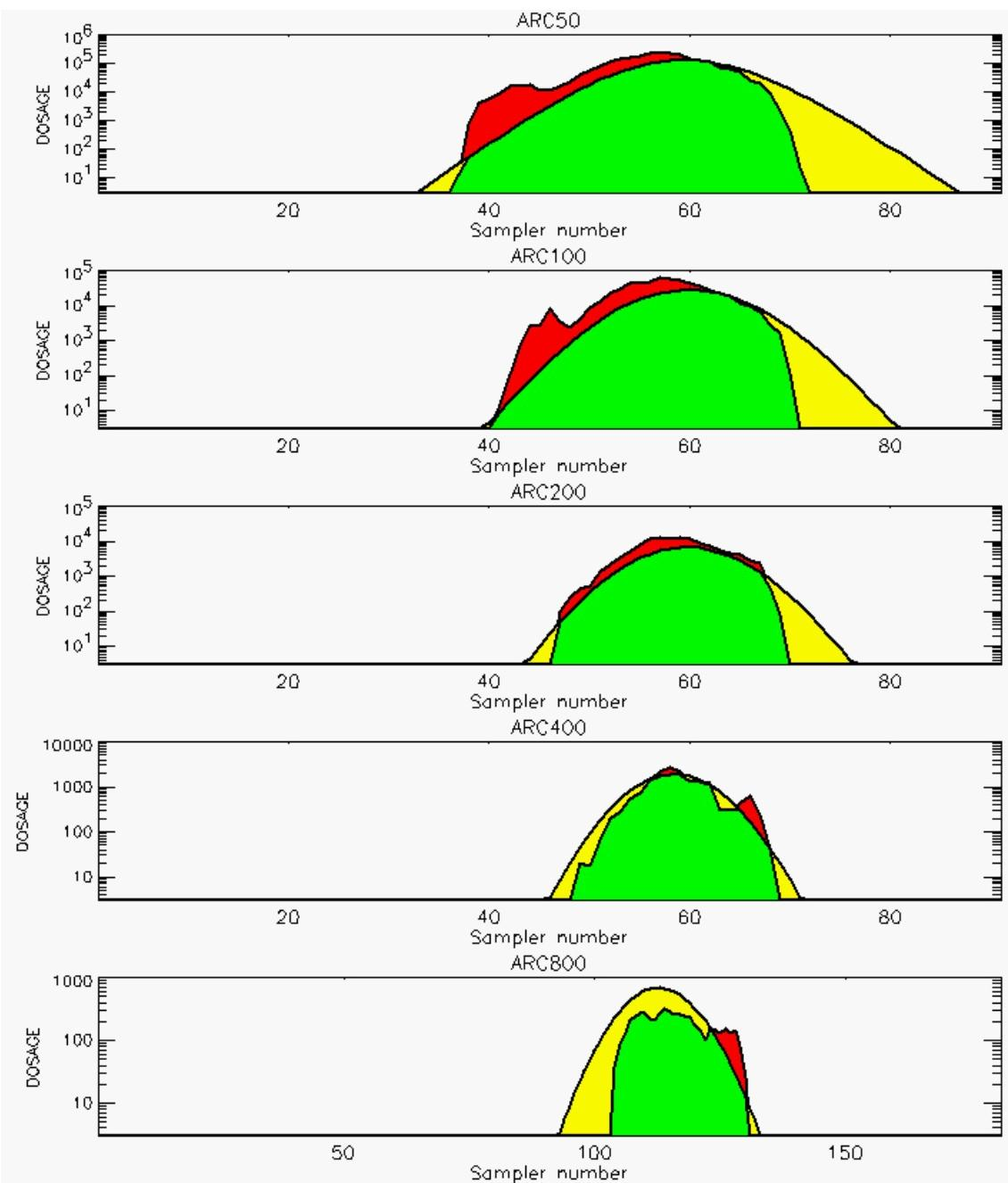


PG Observation to Prediction Comparison

PG Trial File: pr_grass_tracer_Experiment_15.txt

Prediction File: HPAC\nodeposition\pg_15_noxd.out

Figure C-10a. HPAC Prediction to Trial 15 on Linear Scale: Stability Category is 1

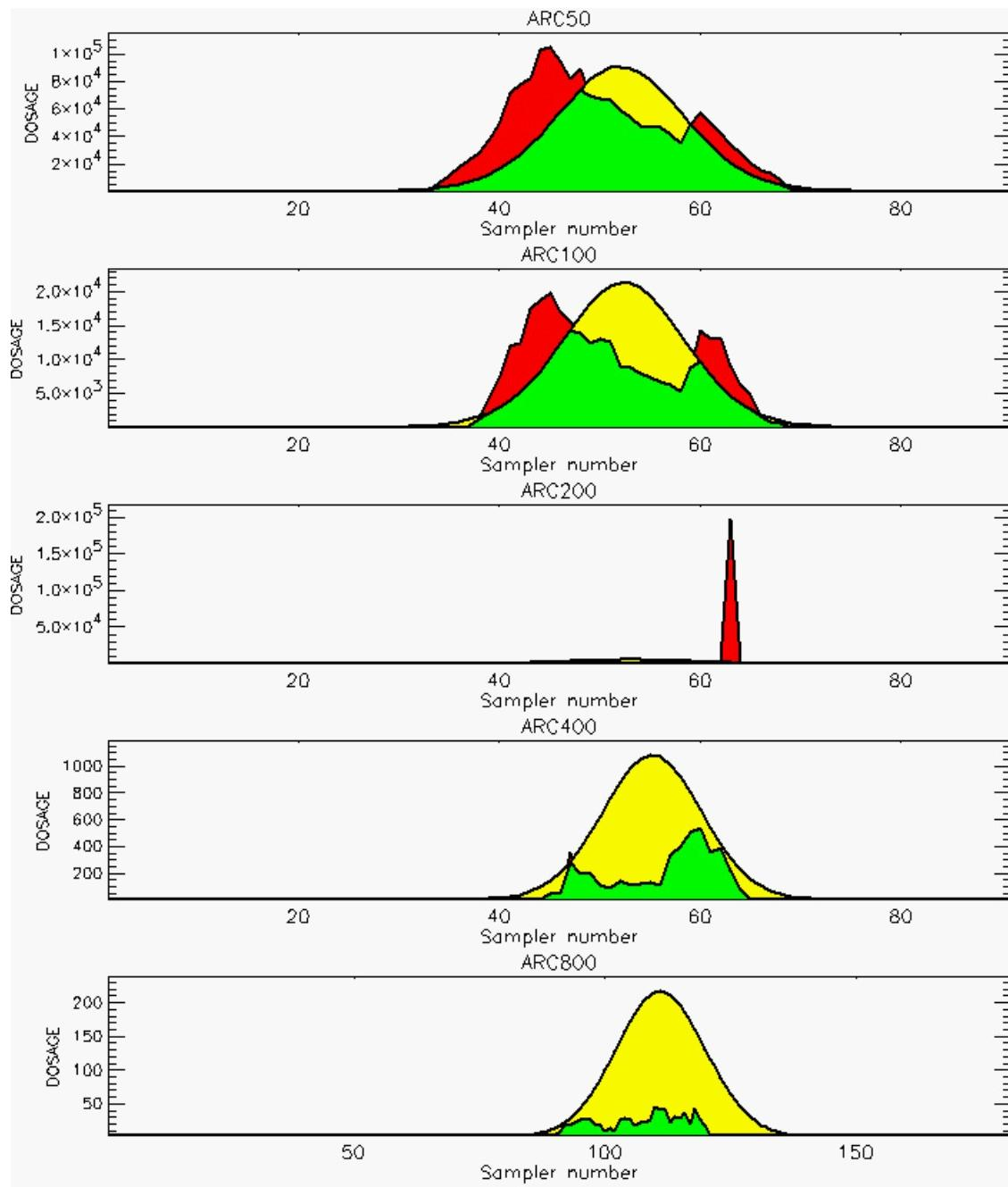


PG Observation to Prediction Comparison

PG Trial File: pr_grass_tracer_Experiment_15.txt

Prediction File: HPAC\nodeposition\pg_15_noxd.out

**Figure C-10b. HPAC Prediction to Trial 15 on Logarithmic Scale:
Stability Category is 1**

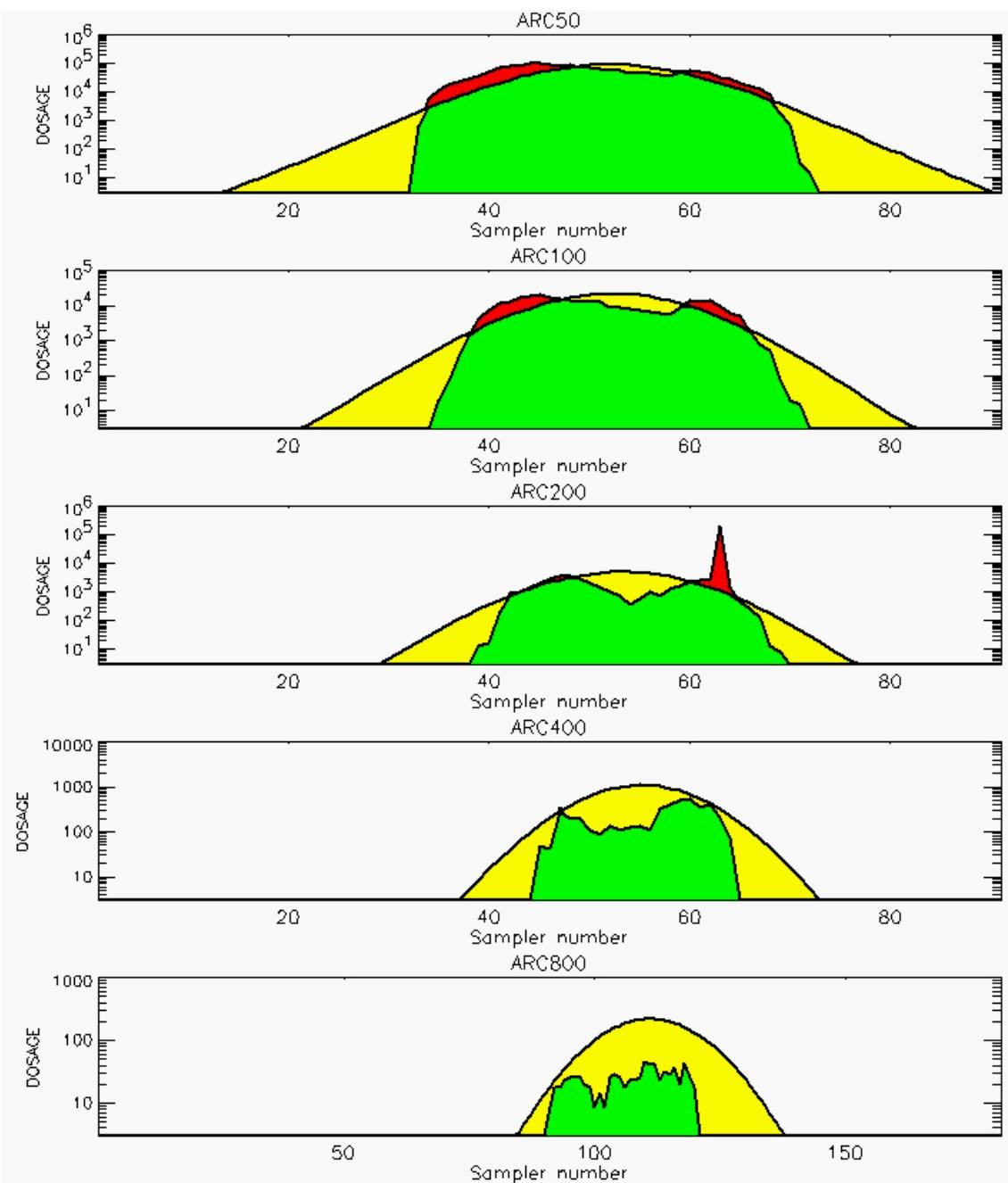


PG Observation to Prediction Comparison

PG Trial File: pr_grass_tracer_Experiment_16.txt

Prediction File: HPAC\nodeposition\pg_16_noxd.out

Figure C-11a. HPAC Prediction to Trial 16 on Linear Scale: Stability Category is 1 (Value for Sampler 63 of 200-Meter Arc is Considered “Spurious” and is Fixed by Moving Decimal Point)

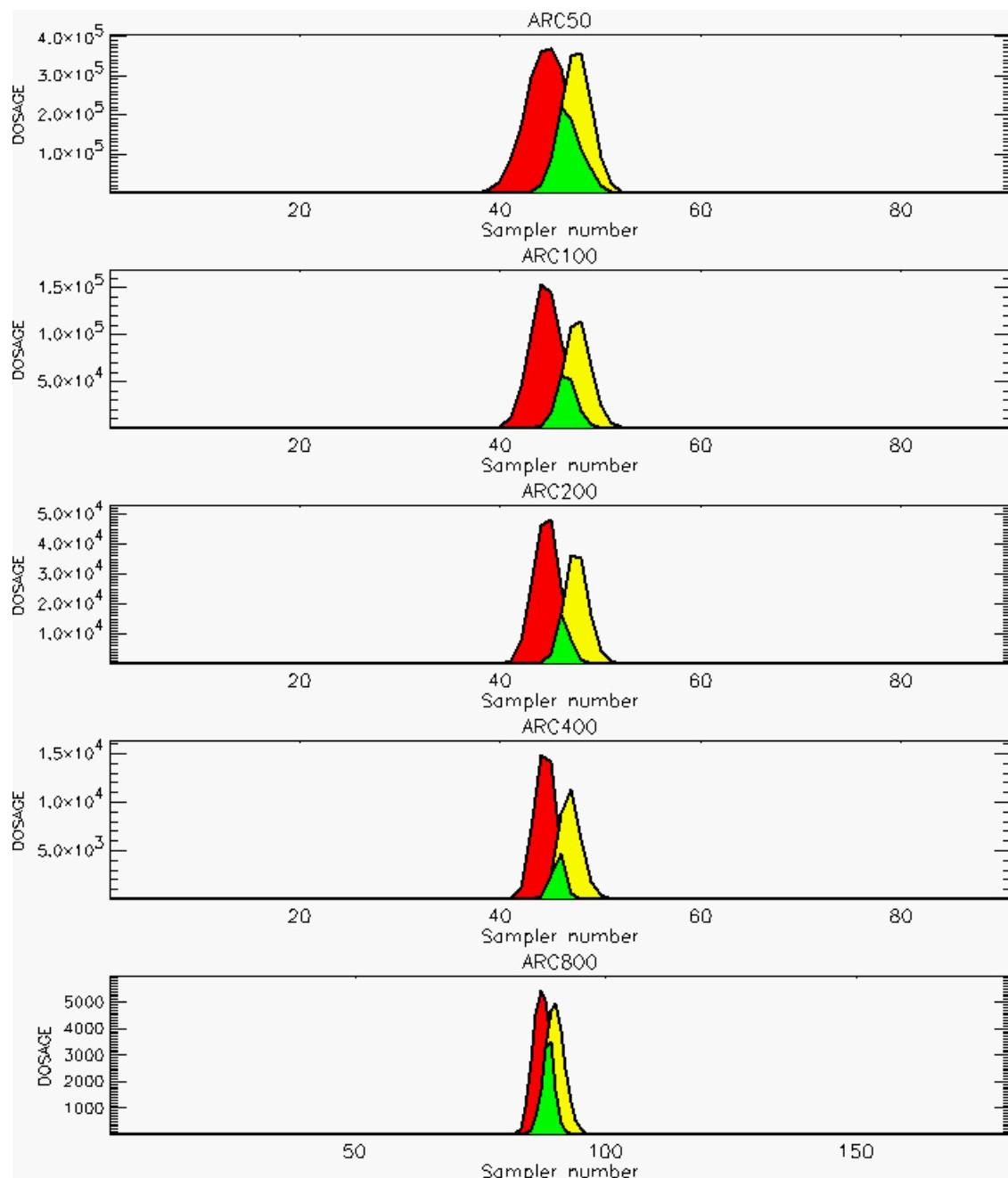


PG Observation to Prediction Comparison

PG Trial File: pr_grass_tracer_Experiment_16.txt

Prediction File: HPAC\nodeposition\pg_16_noxd.out

**Figure C-11b. HPAC Prediction to Trial 16 on Logarithmic Scale:
Stability Category is 1 (Value for Sampler 63 of 200-Meter Arc is Considered "Spurious"
and is Fixed by Moving Decimal Point)**

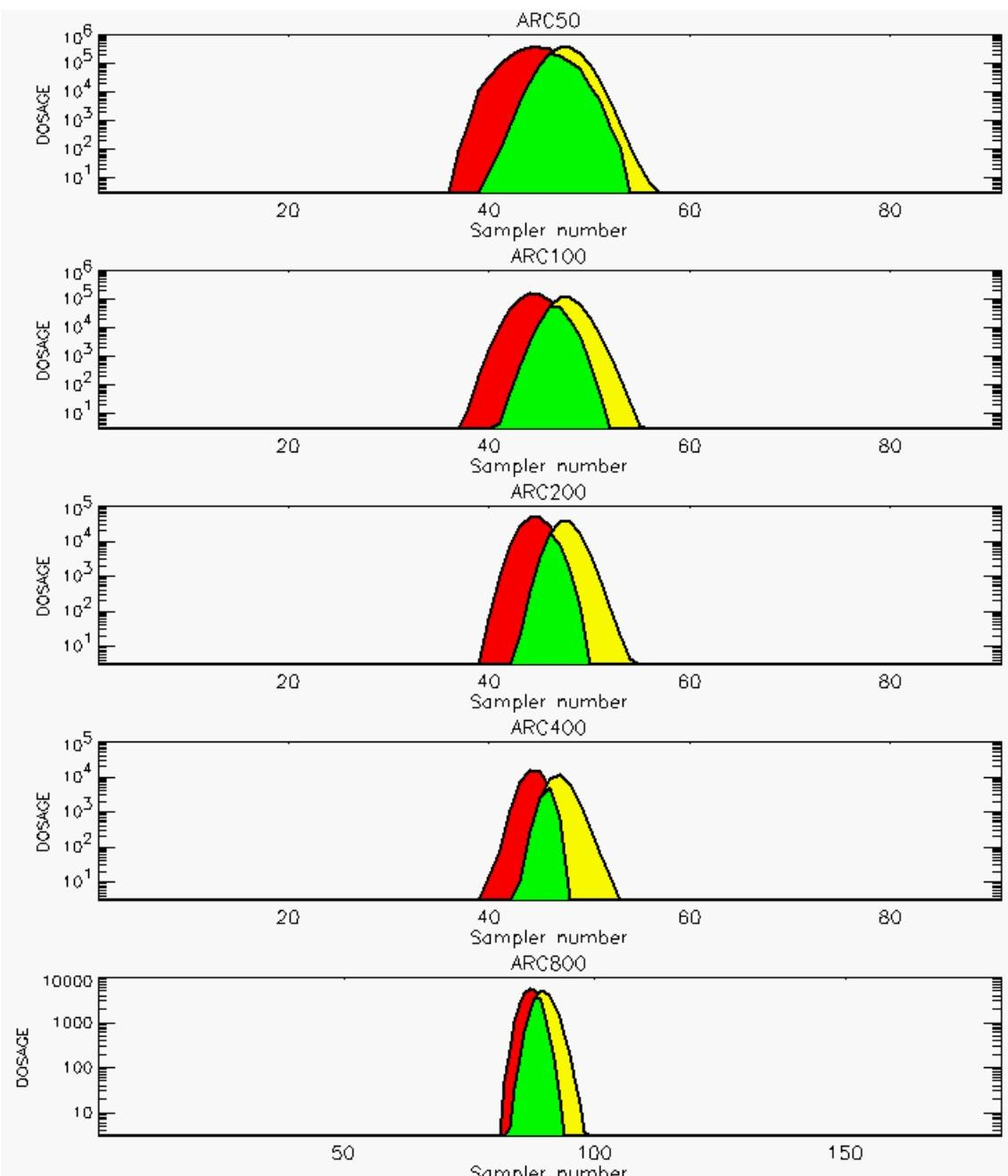


PG Observation to Prediction Comparison

PG Trial File: pr_grass_tracer_Experiment_17.txt

Prediction File: HPAC\nodeposition\pg_17_noxd.out

Figure C-12a. HPAC Prediction to Trial 17 on Linear Scale: Stability Category is 5

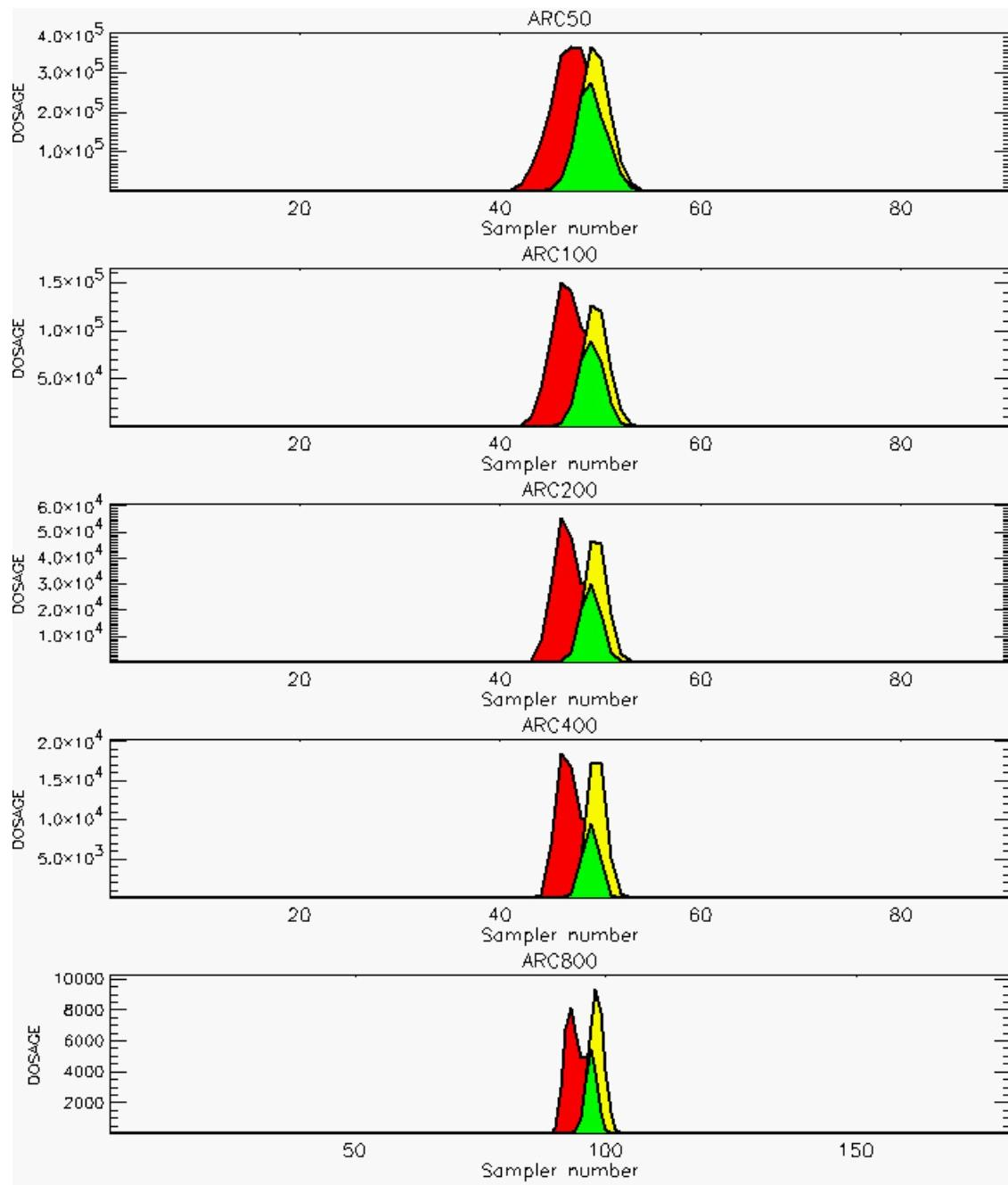


PG Observation to Prediction Comparison

PG Trial File: pr_grass_tracer_Experiment_17.txt

Prediction File: HPAC\nodeposition\pg_17_noxd.out

**Figure C-12b. HPAC Prediction to Trial 17 on Logarithmic Scale:
Stability Category is 5**

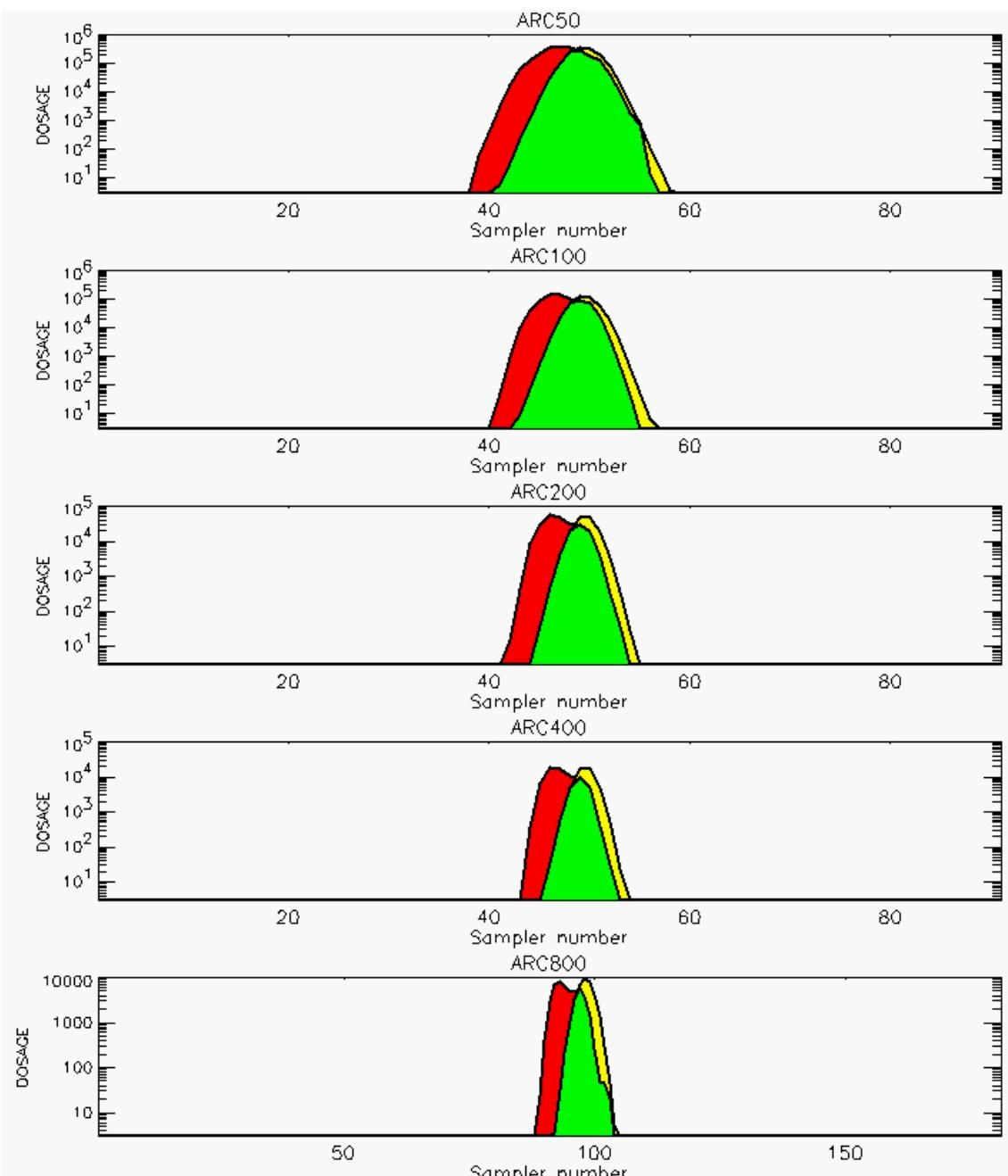


PG Observation to Prediction Comparison

PG Trial File: pr_grass_tracer_Experiment_18.txt

Prediction File: HPAC\nodeposition\pg_18_noxd.out

Figure C-13a. HPAC Prediction to Trial 18 on Linear Scale: Stability Category is 5

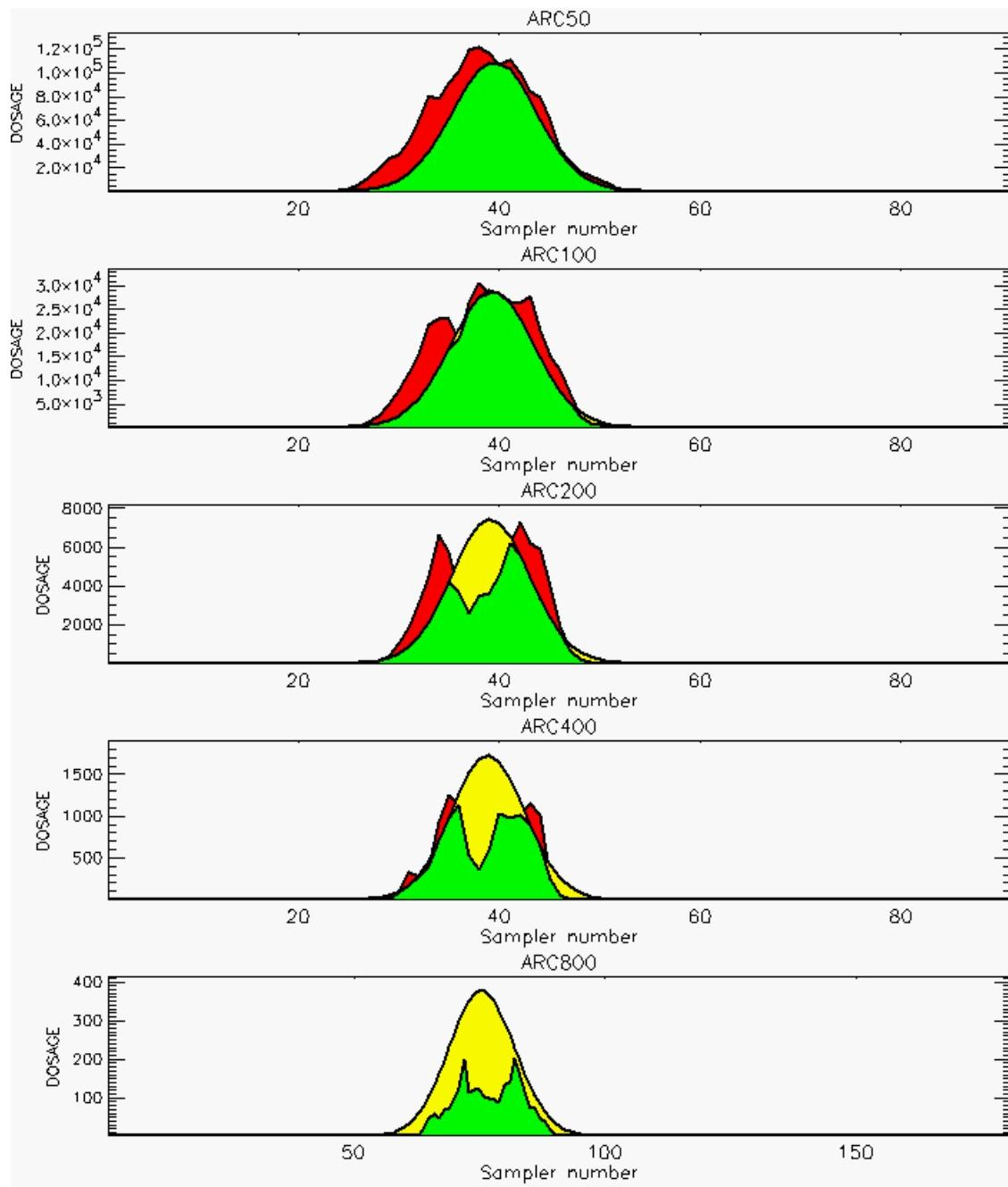


PG Observation to Prediction Comparison

PG Trial File: pr_grass_tracer_Experiment_18.txt

Prediction File: HPAC\nodeposition\pg_18_noxd.out

**Figure C-13b. HPAC Prediction to Trial 18 on Logarithmic Scale:
Stability Category is 5**

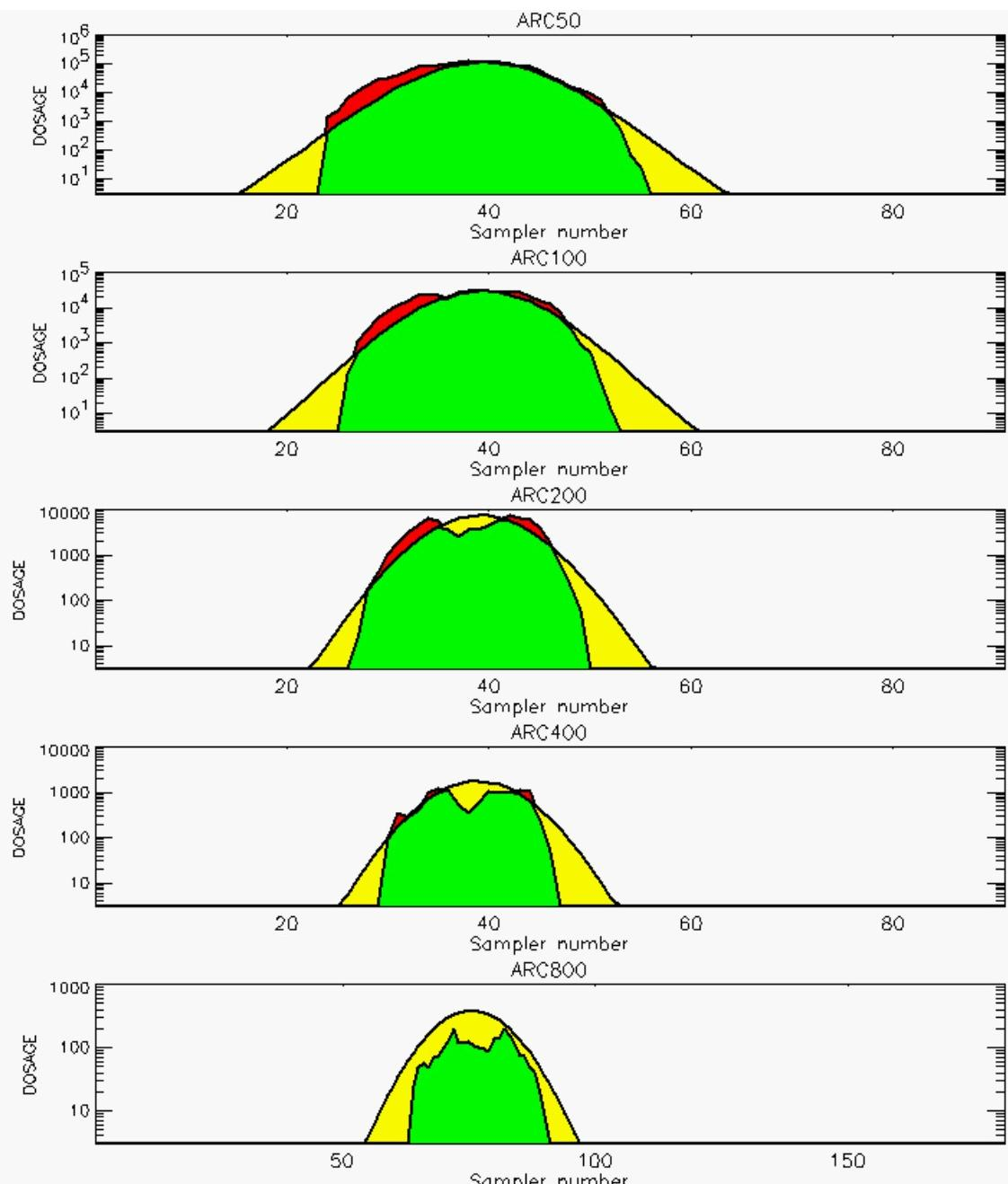


PG Observation to Prediction Comparison

PG Trial File: pr_grass_tracer_Experiment_19.txt

Prediction File: HPAC\nodeposition\pg_19_noxd.out

Figure C-14a. HPAC Prediction to Trial 19 on Linear Scale: Stability Category is 2

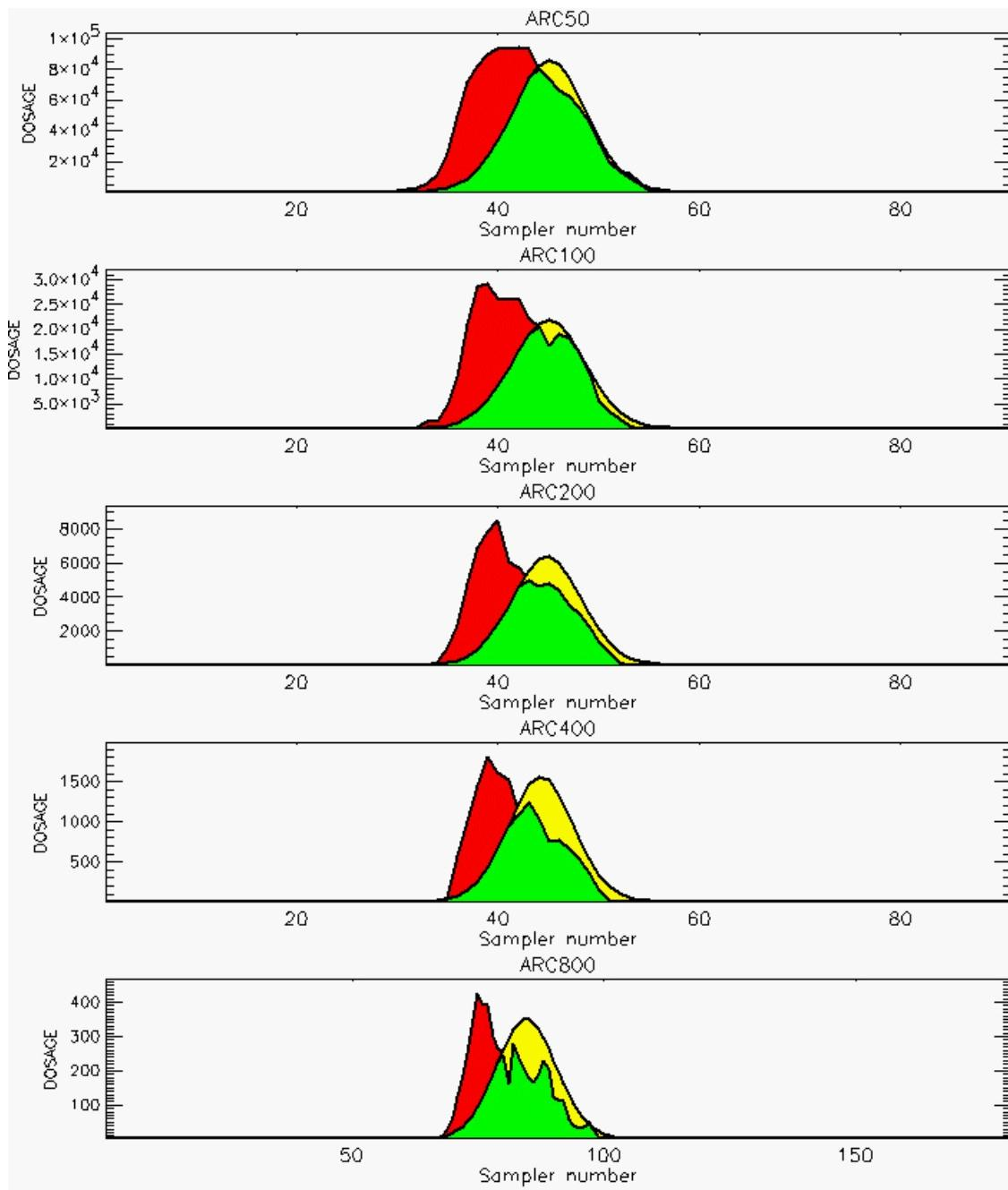


PG Observation to Prediction Comparison

PG Trial File: pr_grass_tracer_Experiment_19.txt

Prediction File: HPAC\nodeposition\pg_19_noxd.out

**Figure C-14b. HPAC Prediction to Trial 19 on Logarithmic Scale:
Stability Category is 2**

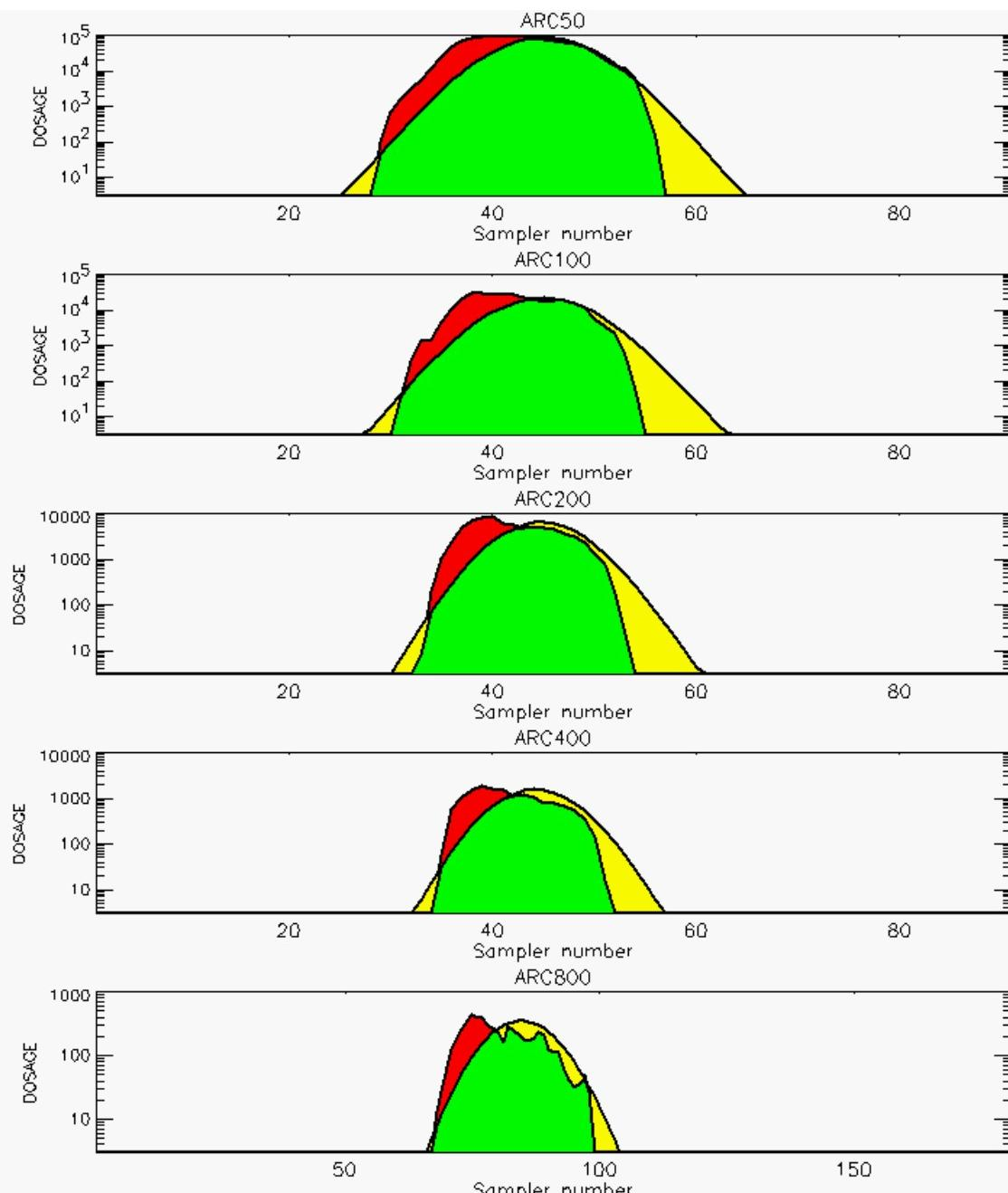


PG Observation to Prediction Comparison

PG Trial File: pr_grass_tracer_Experiment_20.txt

Prediction File: HPAC\nodeposition\pg_20_noxd.out

Figure C-15a. HPAC Prediction to Trial 20 on Linear Scale: Stability Category is 3

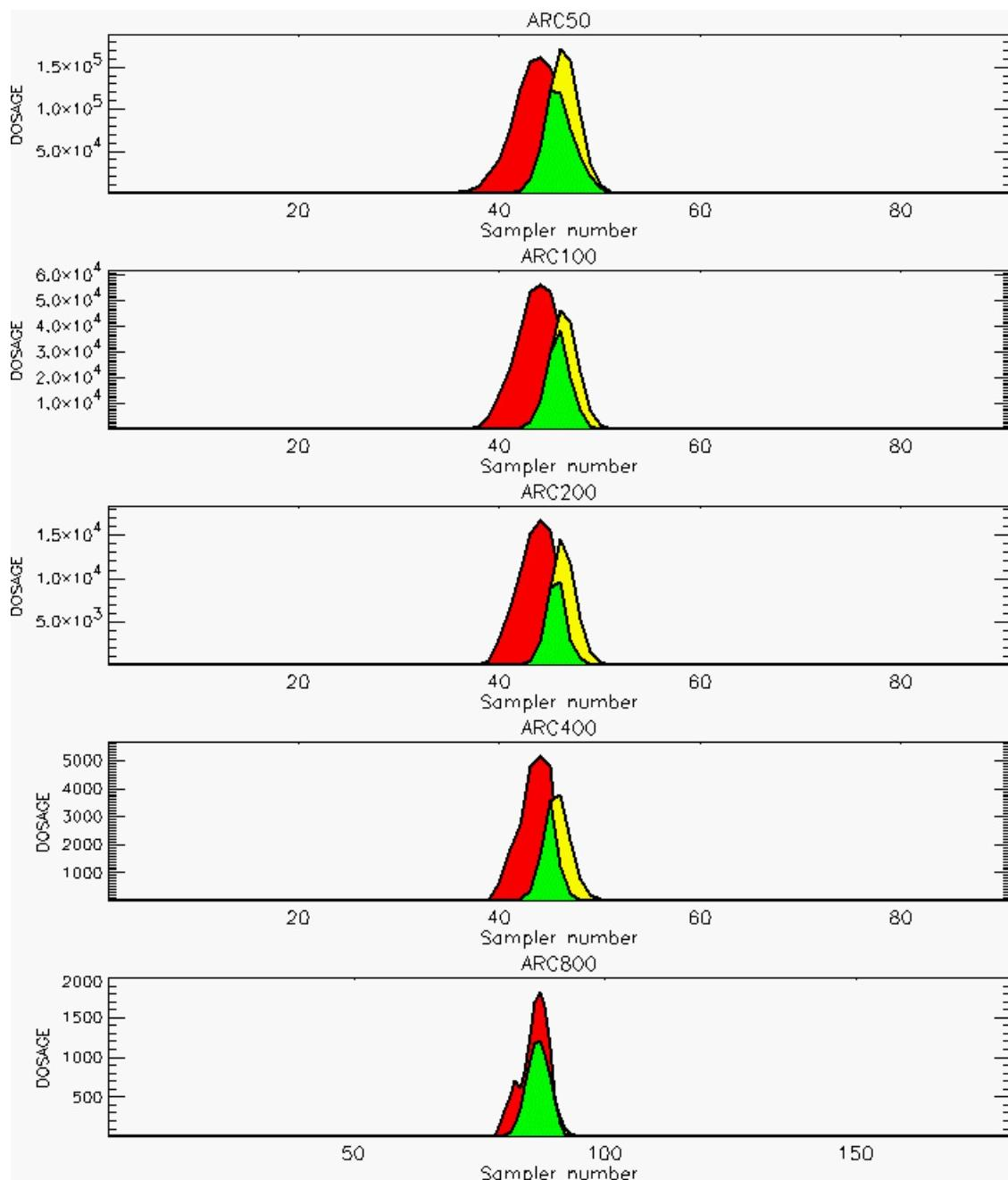


PG Observation to Prediction Comparison

PG Trial File: pr_grass_tracer_Experiment_20.txt

Prediction File: HPAC\nodeposition\pg_20_noxd.out

**Figure C-15b. HPAC Prediction to Trial 20 on Logarithmic Scale:
Stability Category is 3**

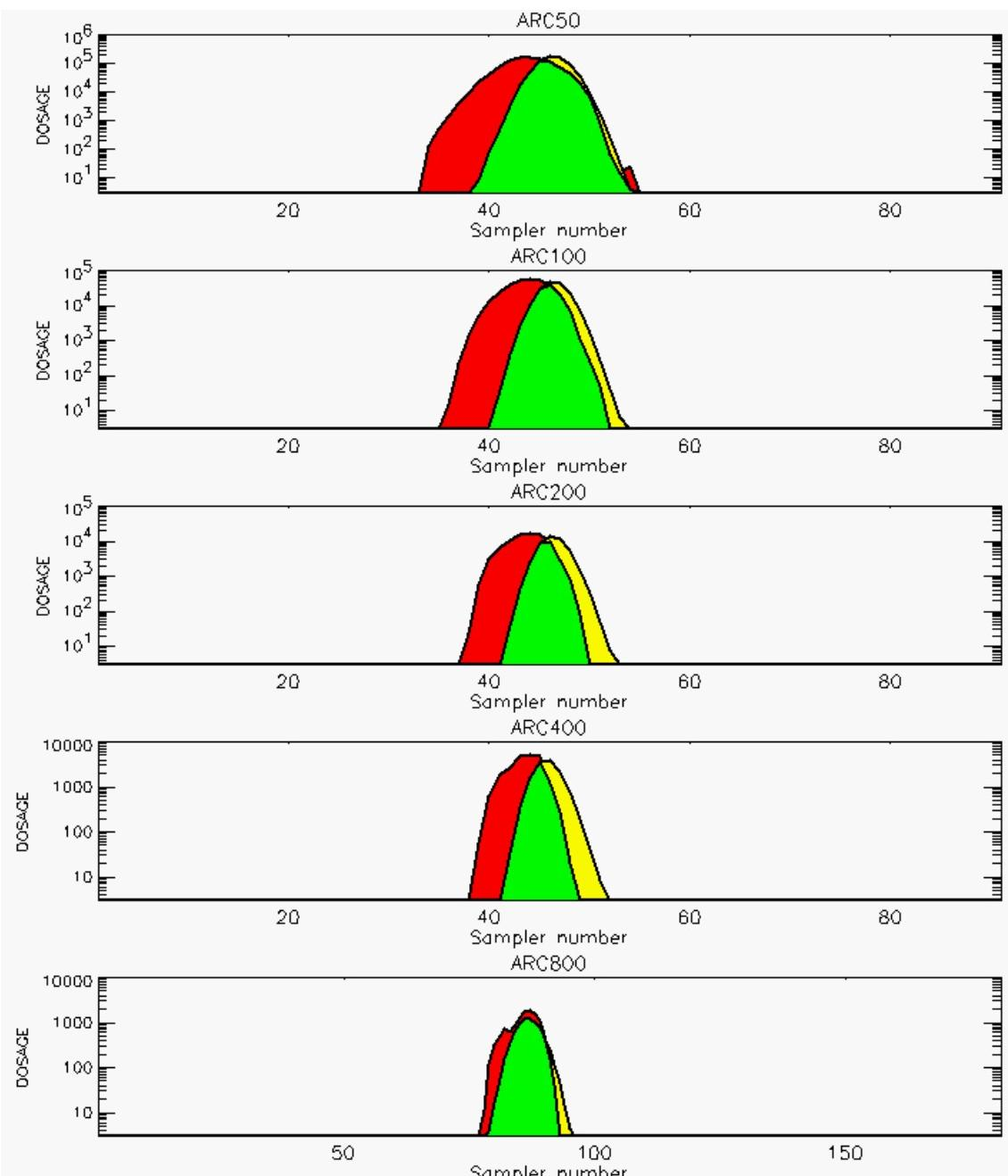


PG Observation to Prediction Comparison

PG Trial File: pr_grass_tracer_Experiment_21.txt

Prediction File: HPAC\nodeposition\pg_21_noxd.out

Figure C-16a. HPAC Prediction to Trial 21 on Linear Scale: Stability Category is 4

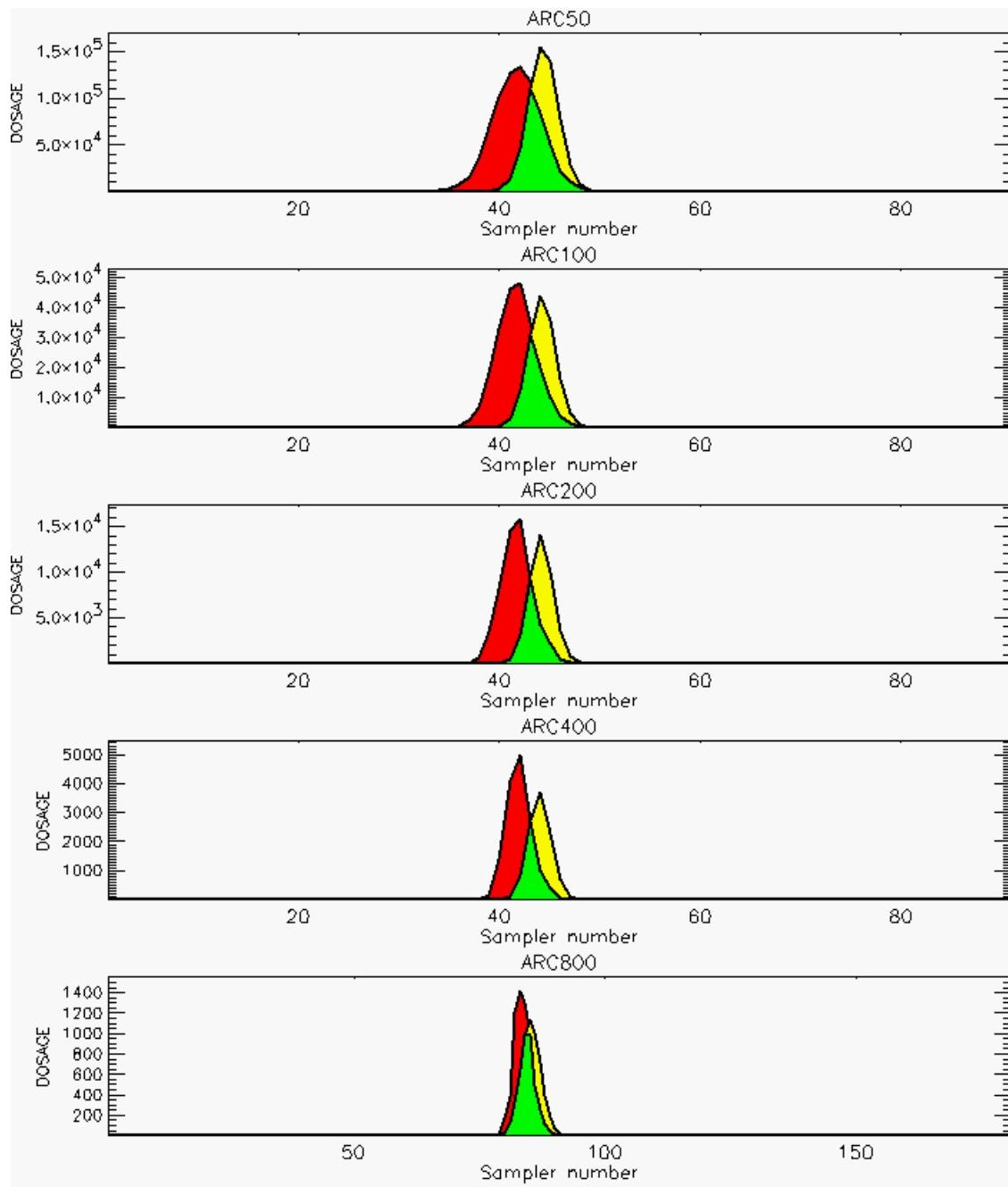


PG Observation to Prediction Comparison

PG Trial File: pr_grass_tracer_Experiment_21.txt

Prediction File: HPAC\nodeposition\pg_21_noxd.out

**Figure C-16b. HPAC Prediction to Trial 21 on Logarithmic Scale:
Stability Category is 4**

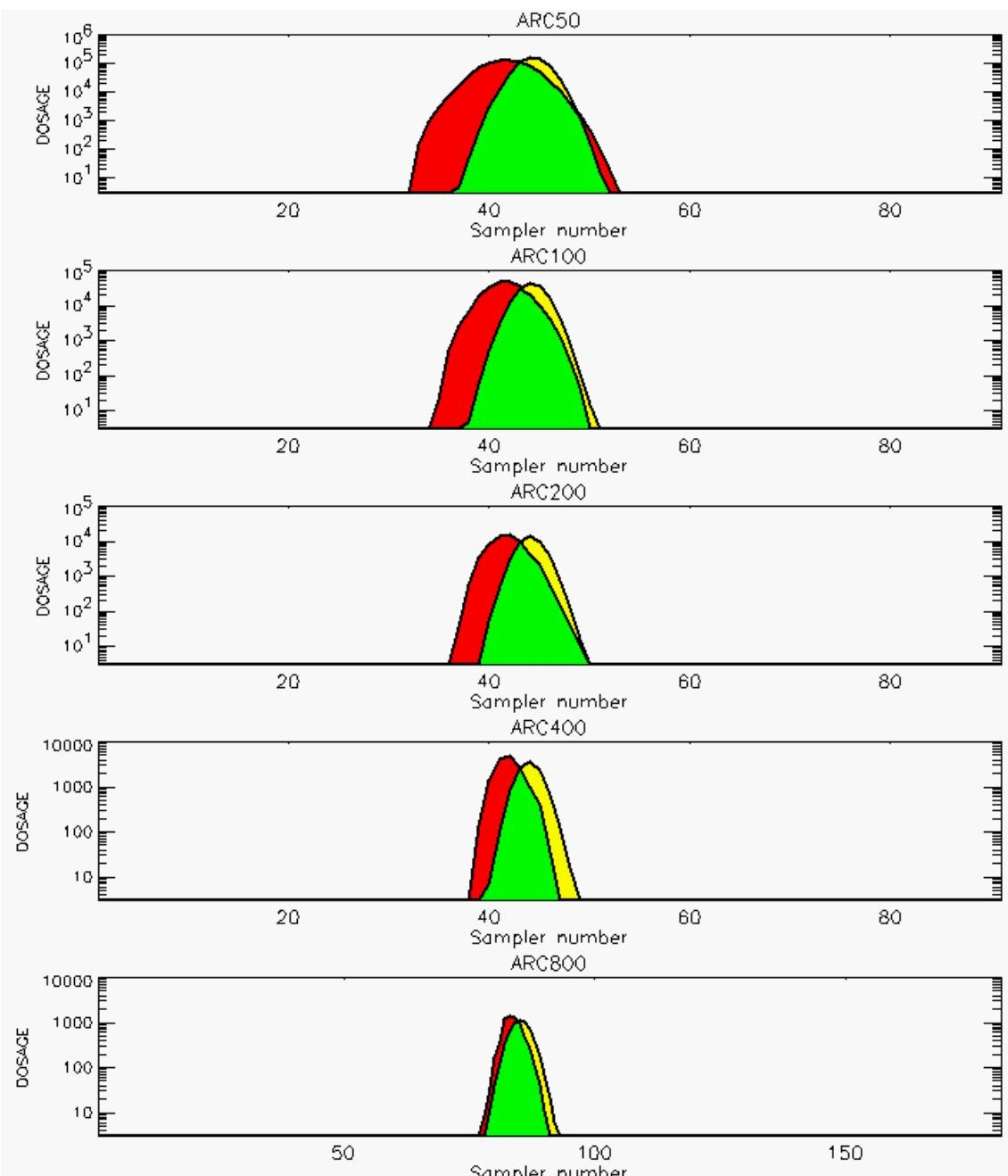


PG Observation to Prediction Comparison

PG Trial File: pr_grass_tracer_Experiment_22.txt

Prediction File: HPAC\nodeposition\pg_22_noxd.out

Figure C-17a. HPAC Prediction to Trial 22 on Linear Scale: Stability Category is 4

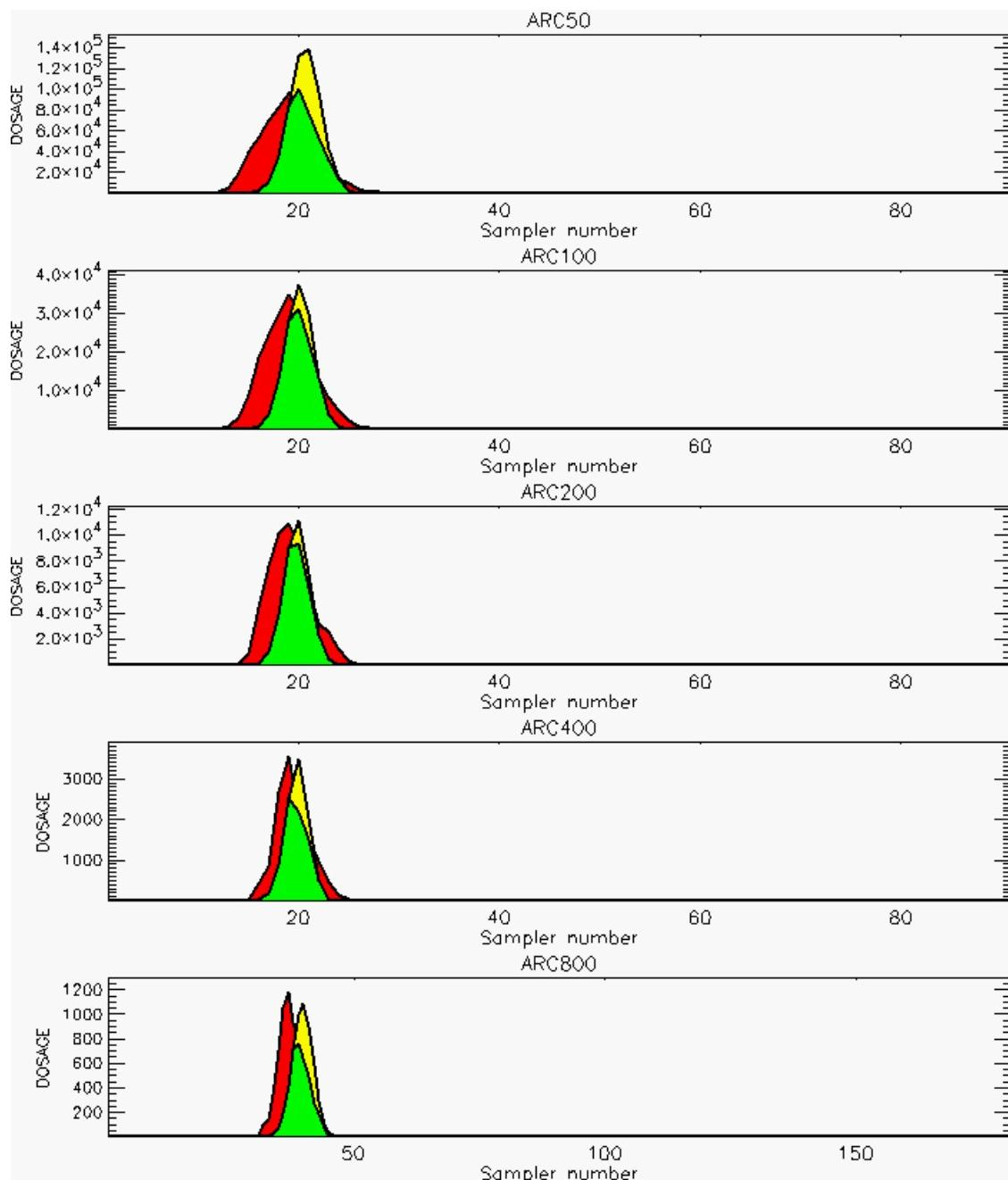


PG Observation to Prediction Comparison

PG Trial File: pr_grass_tracer_Experiment_22.txt

Prediction File: HPAC\nodeposition\pg_22_noxd.out

**Figure C-17b. HPAC Prediction to Trial 22 on Logarithmic Scale:
Stability Category is 4**

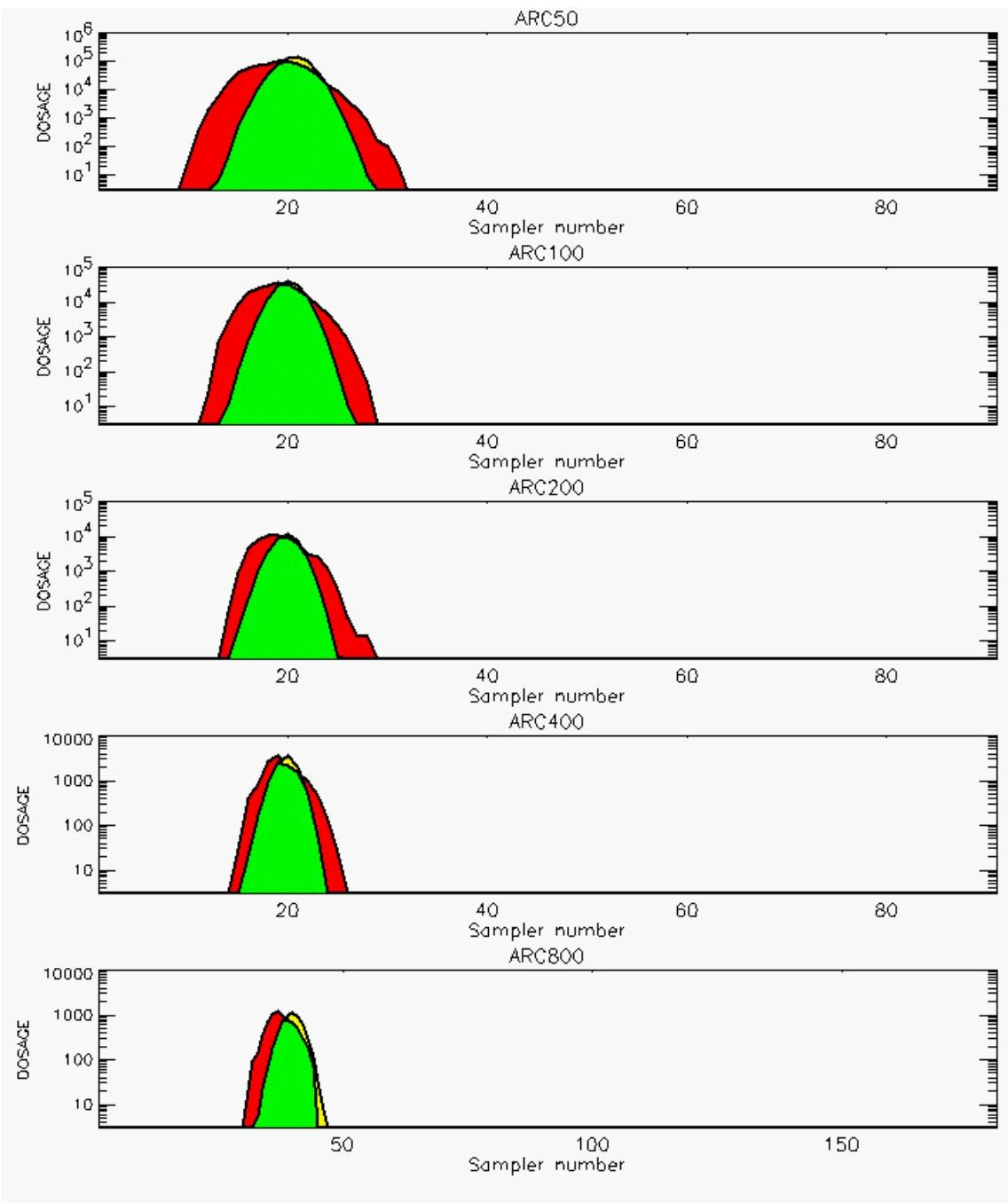


PG Observation to Prediction Comparison

PG Trial File: pr_grass_tracer_Experiment_23.txt

Prediction File: HPAC\nodeposition\pg_23_noxd.out

Figure C-18a. HPAC Prediction to Trial 23 on Linear Scale: Stability Category is 4

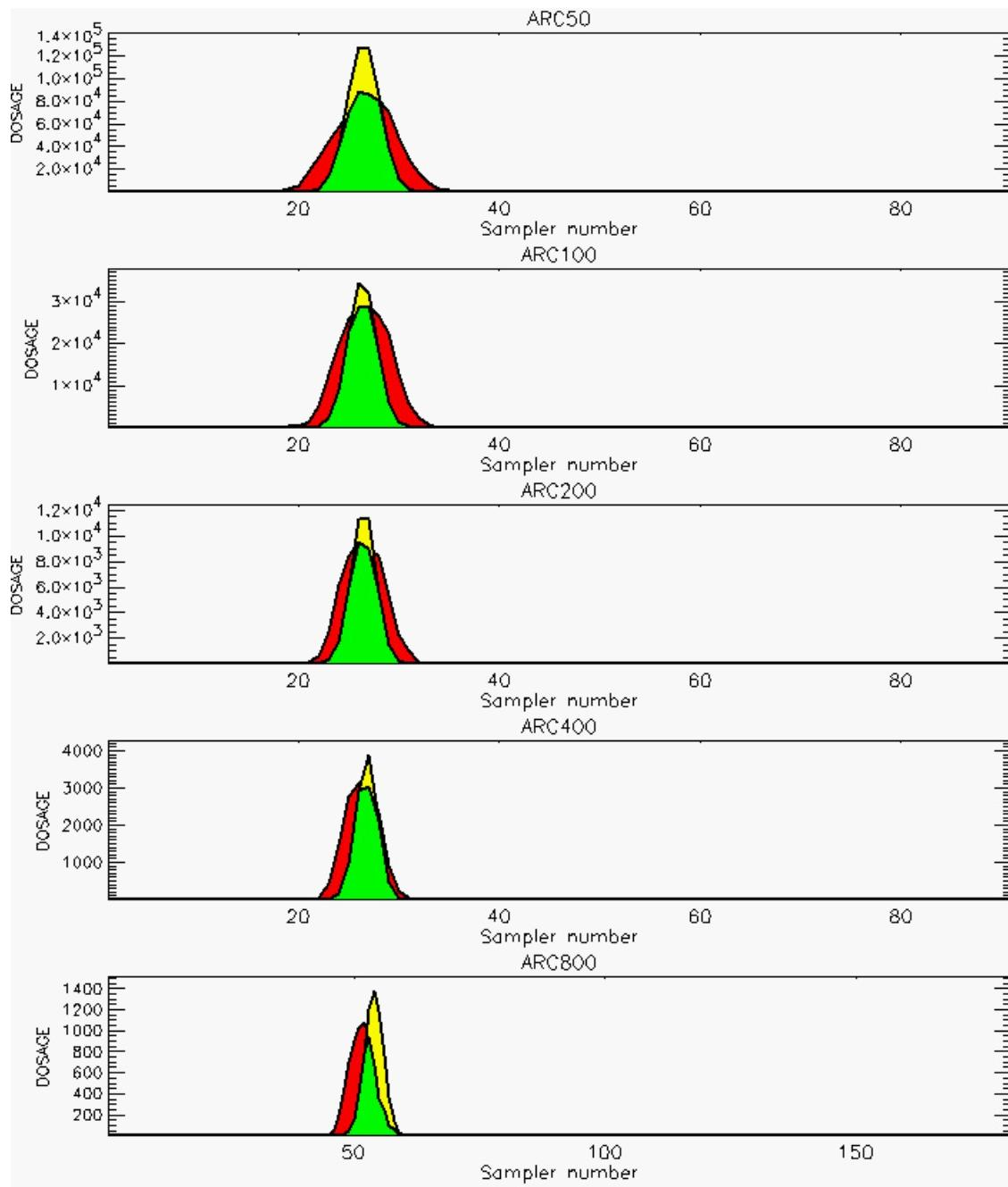


PG Observation to Prediction Comparison

PG Trial File: pr_grass_tracer_Experiment_23.txt

Prediction File: HPAC\nodeposition\pg_23_noxd.out

**Figure C-18b. HPAC Prediction to Trial 23 on Logarithmic Scale:
Stability Category is 4**

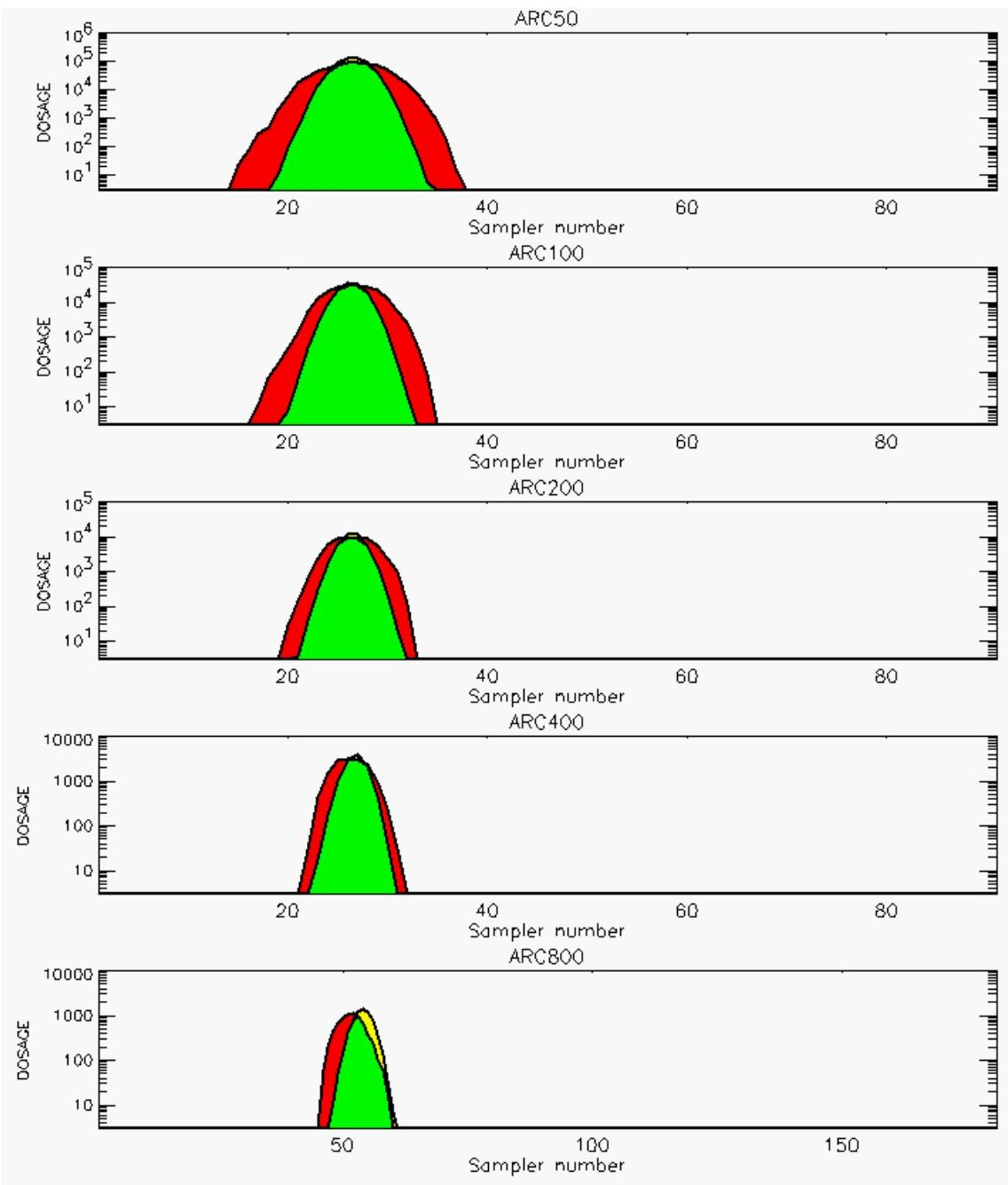


PG Observation to Prediction Comparison

PG Trial File: pr_grass_tracer_Experiment_24.txt

Prediction File: HPAC\nodeposition\pg_24_noxd.out

Figure C-19a. HPAC Prediction to Trial 24 on Linear Scale: Stability Category is 4

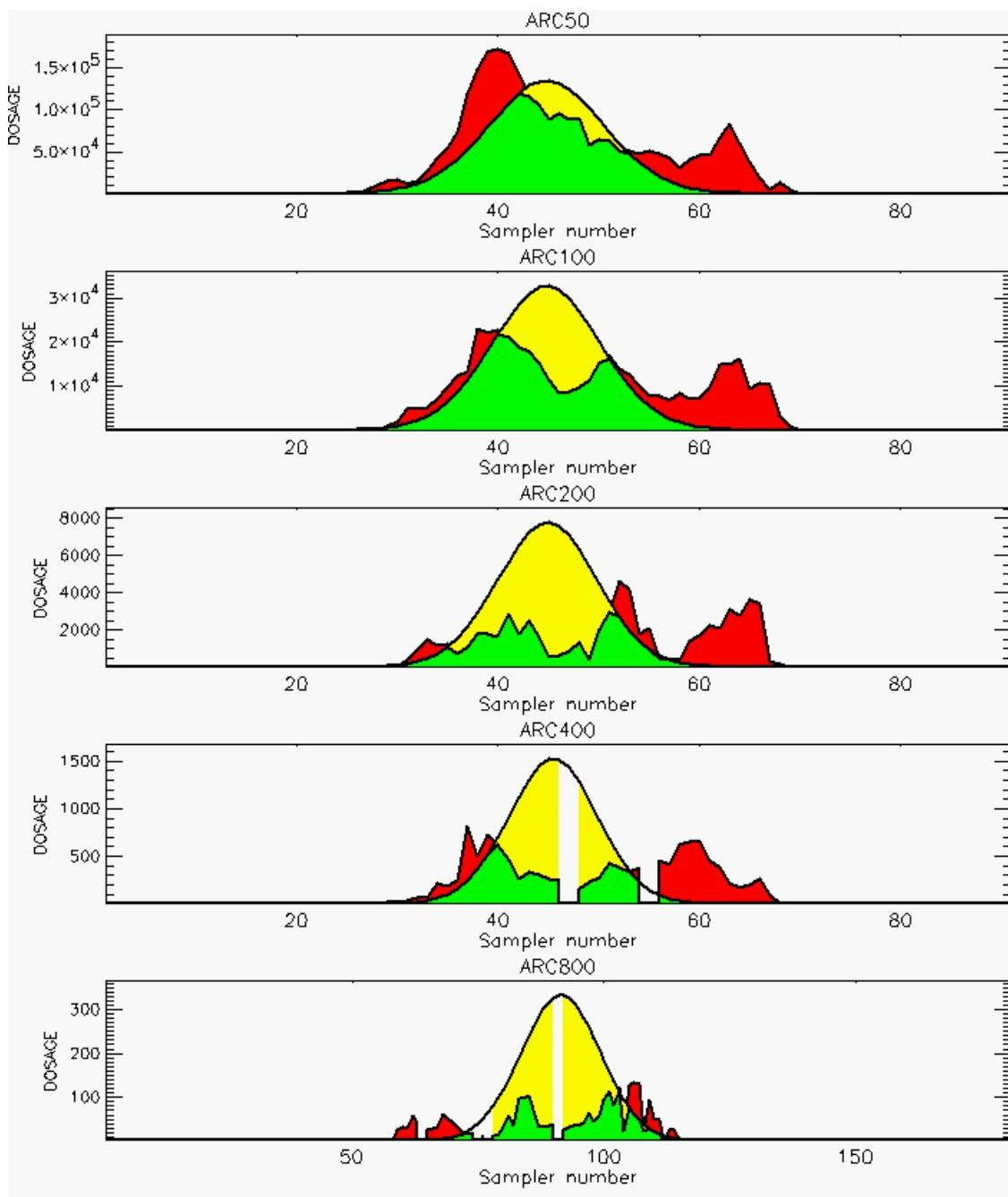


PG Observation to Prediction Comparison

PG Trial File: pr_grass_tracer_Experiment_24.txt

Prediction File: HPAC\nodeposition\pg_24_noxd.out

**Figure C-19b. HPAC Prediction to Trial 24 on Logarithmic Scale:
Stability Category is 4**

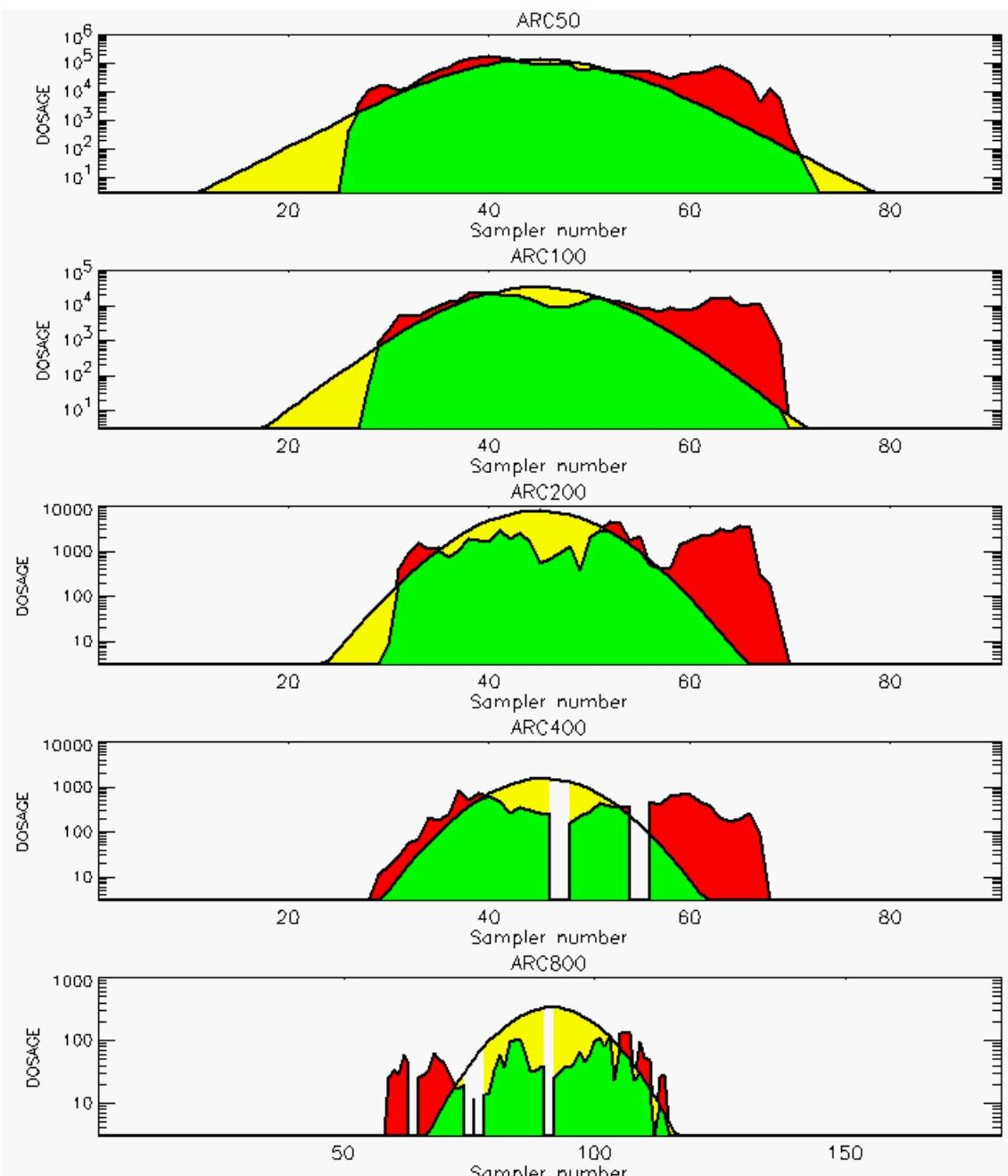


PG Observation to Prediction Comparison

PG Trial File: pr_grass_tracer_Experiment_25.txt

Prediction File: HPAC\nodeposition\pg_25_noxd.out

Figure C-20a. HPAC Prediction to Trial 25 on Linear Scale: Stability Category is 1 (Values for Samplers 47 55 of 400-Meter Arc and 64, 75, 77, 91 of 800-Meter Arc are Missing)

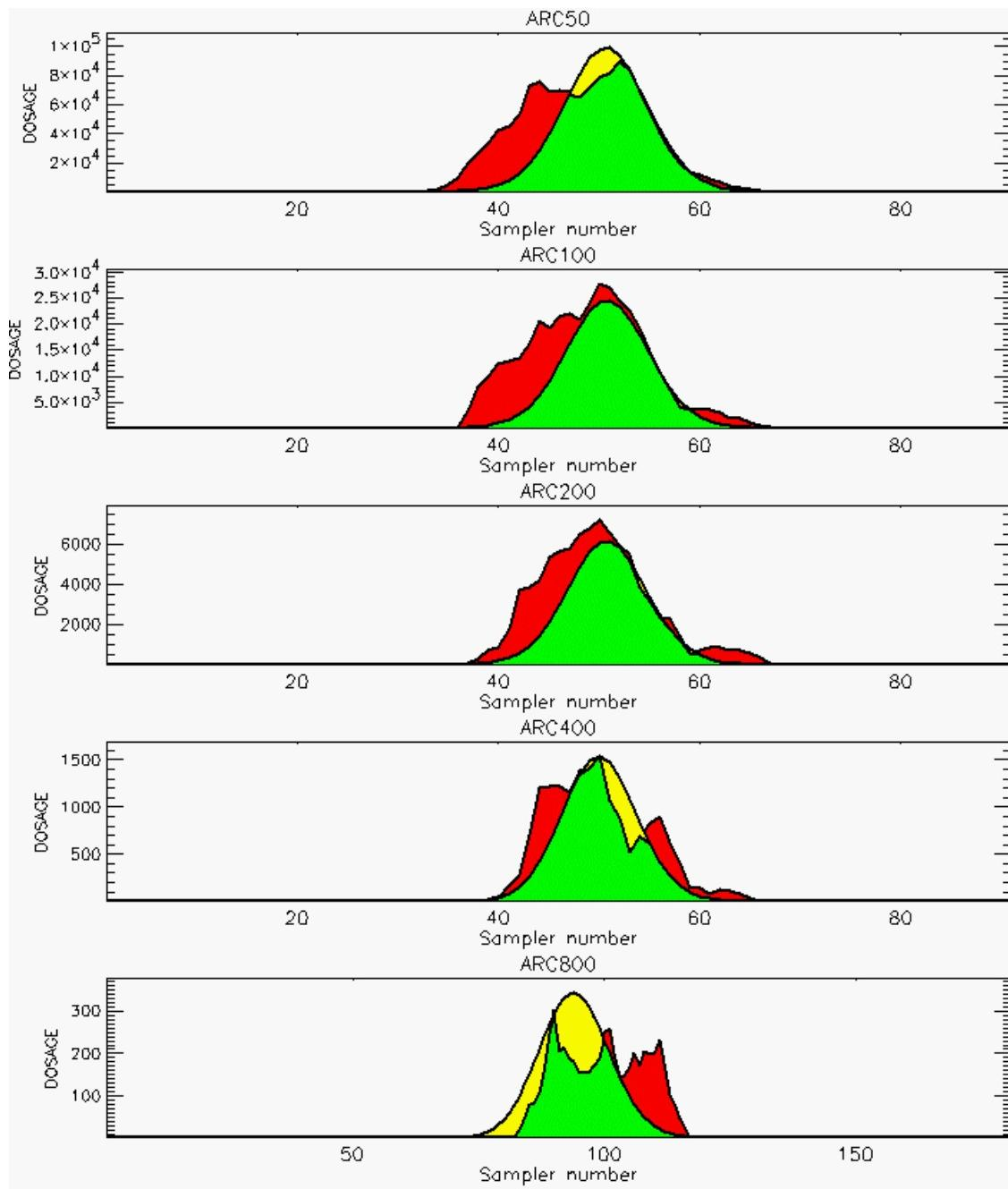


PG Observation to Prediction Comparison

PG Trial File: pr_grass_tracer_Experiment_25.txt

Prediction File: HPAC\nodeposition\pg_25_noxd.out

**Figure C-20b. HPAC Prediction to Trial 25 on Logarithmic Scale:
Stability Category is 1 (Values for Samplers 47 55 of 400-Meter Arc and 64, 75, 77, 91 of
800-Meter Arc are Missing)**

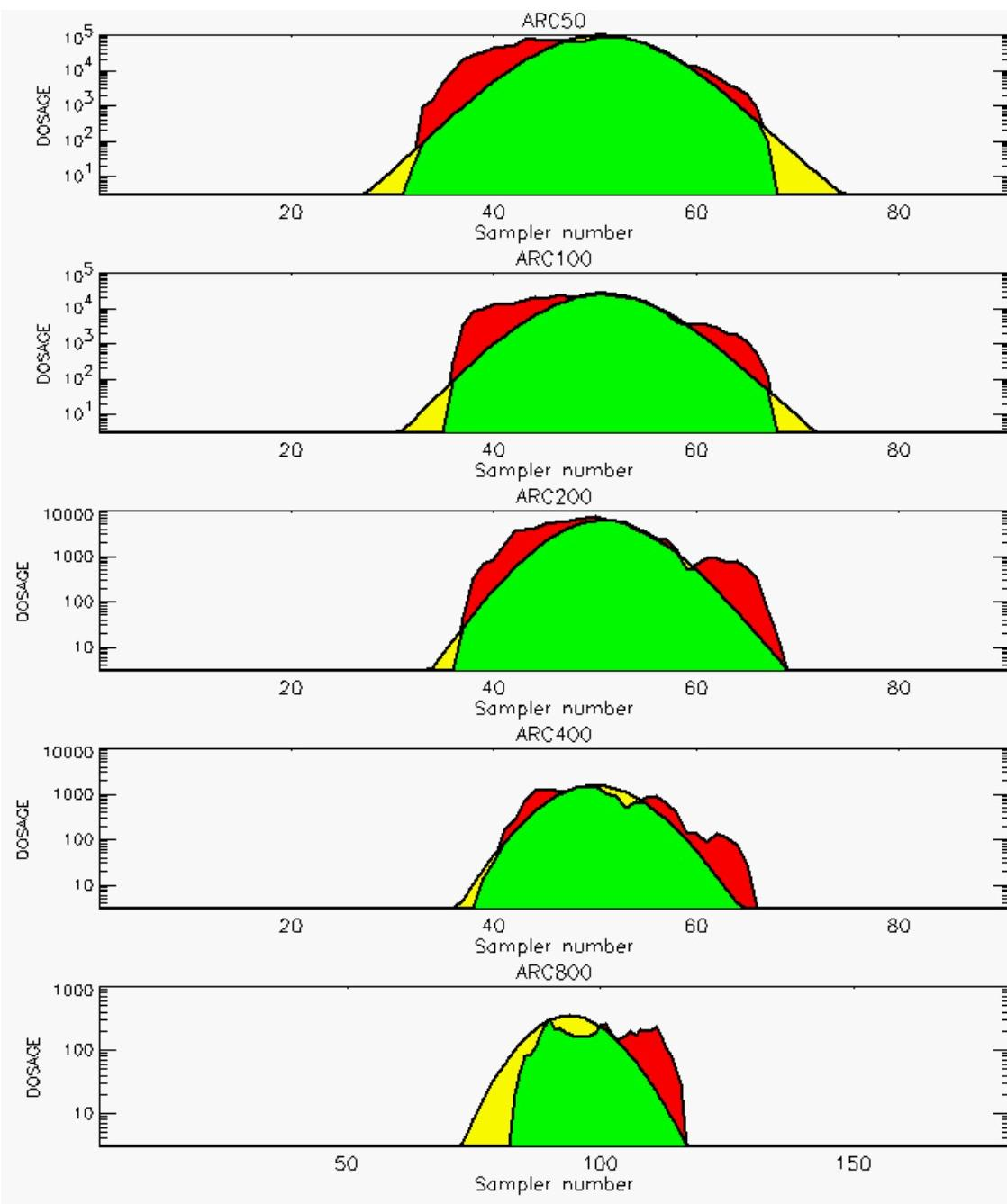


PG Observation to Prediction Comparison

PG Trial File: pr_grass_tracer_Experiment_26.txt

Prediction File: HPAC\nodeposition\pg_26_noxd.out

Figure C-21a. HPAC Prediction to Trial 26 on Linear Scale: Stability Category is 2

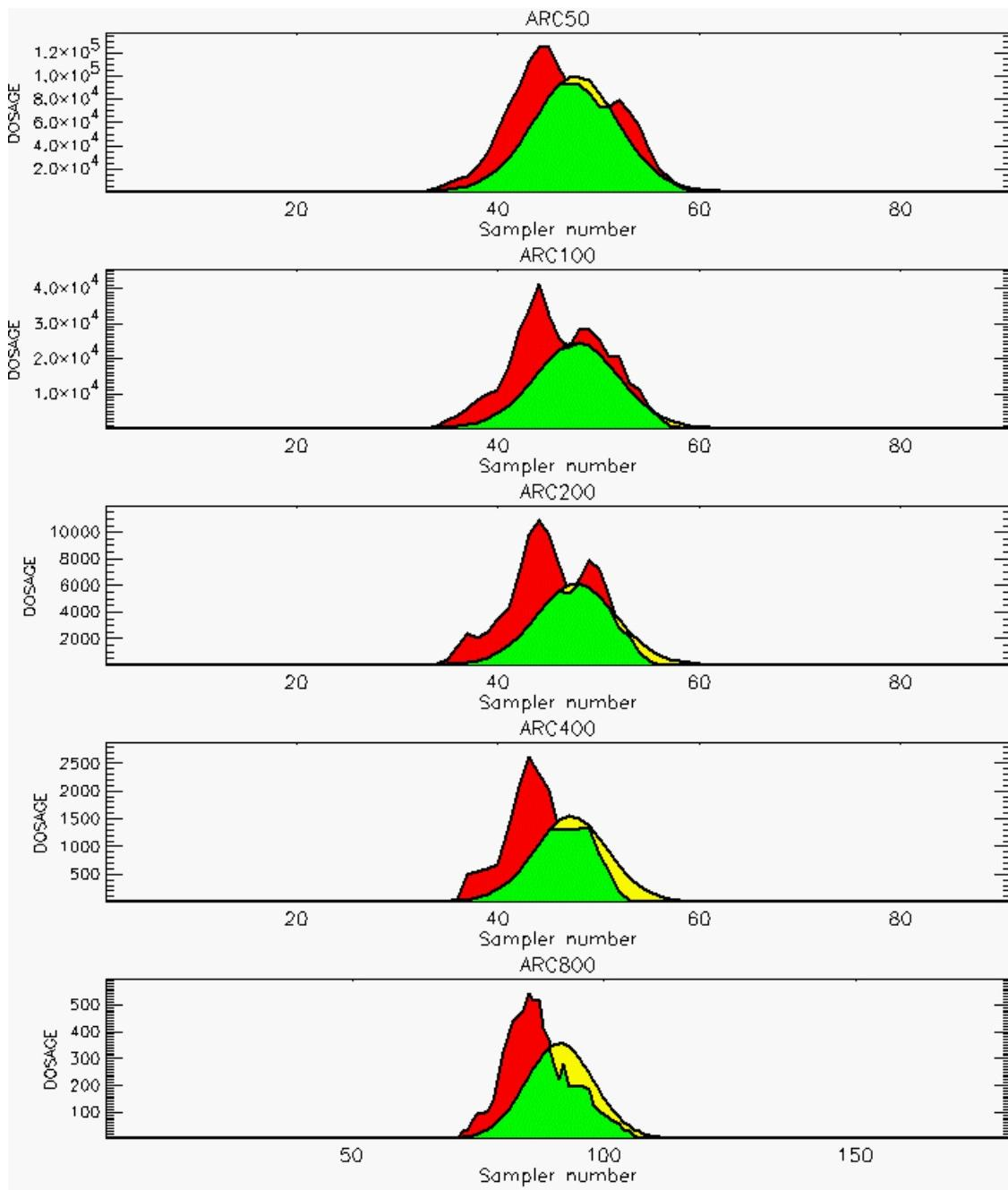


PG Observation to Prediction Comparison

PG Trial File: pr_grass_tracer_Experiment_26.txt

Prediction File: HPAC\nodeposition\pg_26_noxd.out

**Figure C-21b. HPAC Prediction to Trial 26 on Logarithmic Scale:
Stability Category is 2**

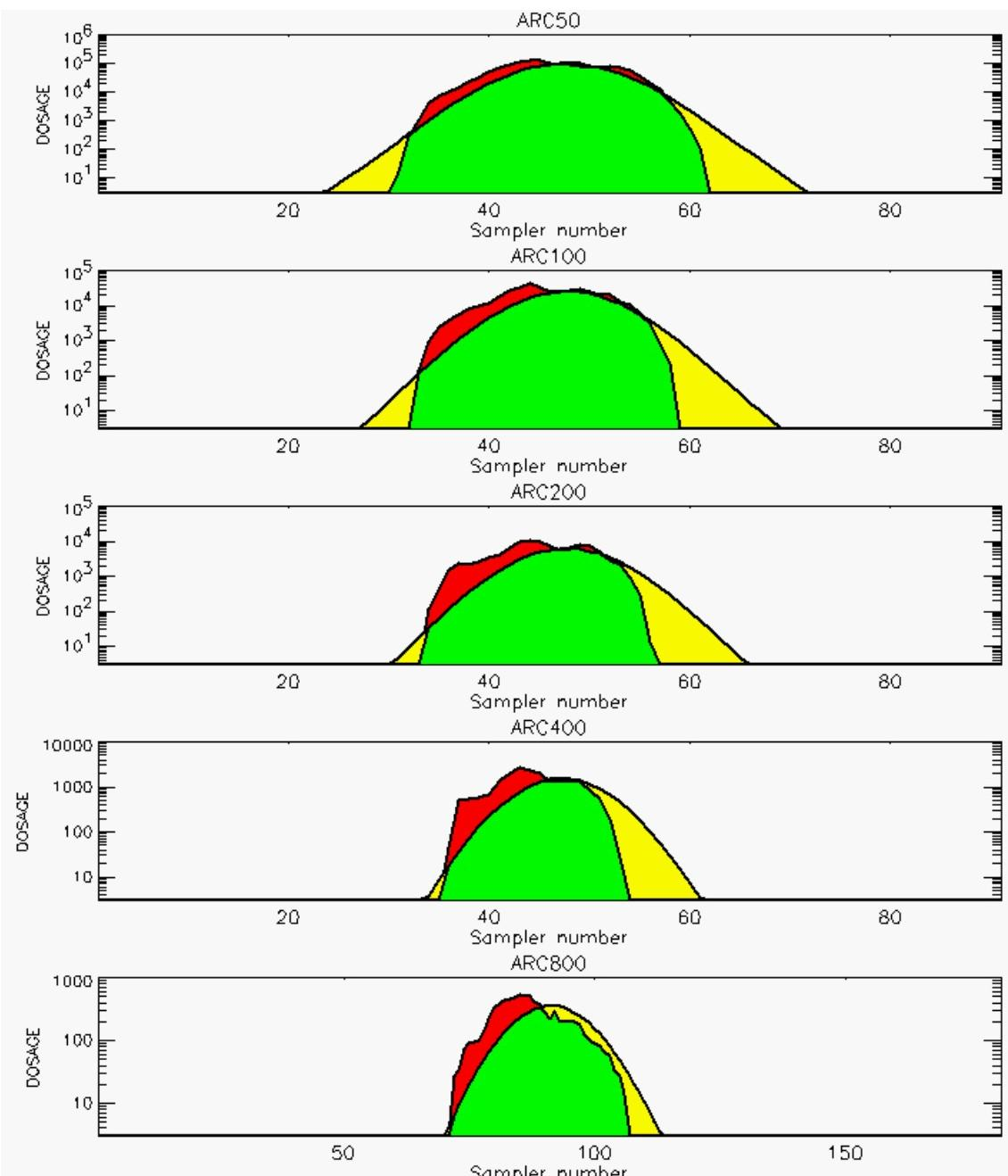


PG Observation to Prediction Comparison

PG Trial File: pr_grass_tracer_Experiment_27.txt

Prediction File: HPAC\nodeposition\pg_27_noxd.out

Figure C-22a. HPAC Prediction to Trial 27 on Linear Scale: Stability Category is 2

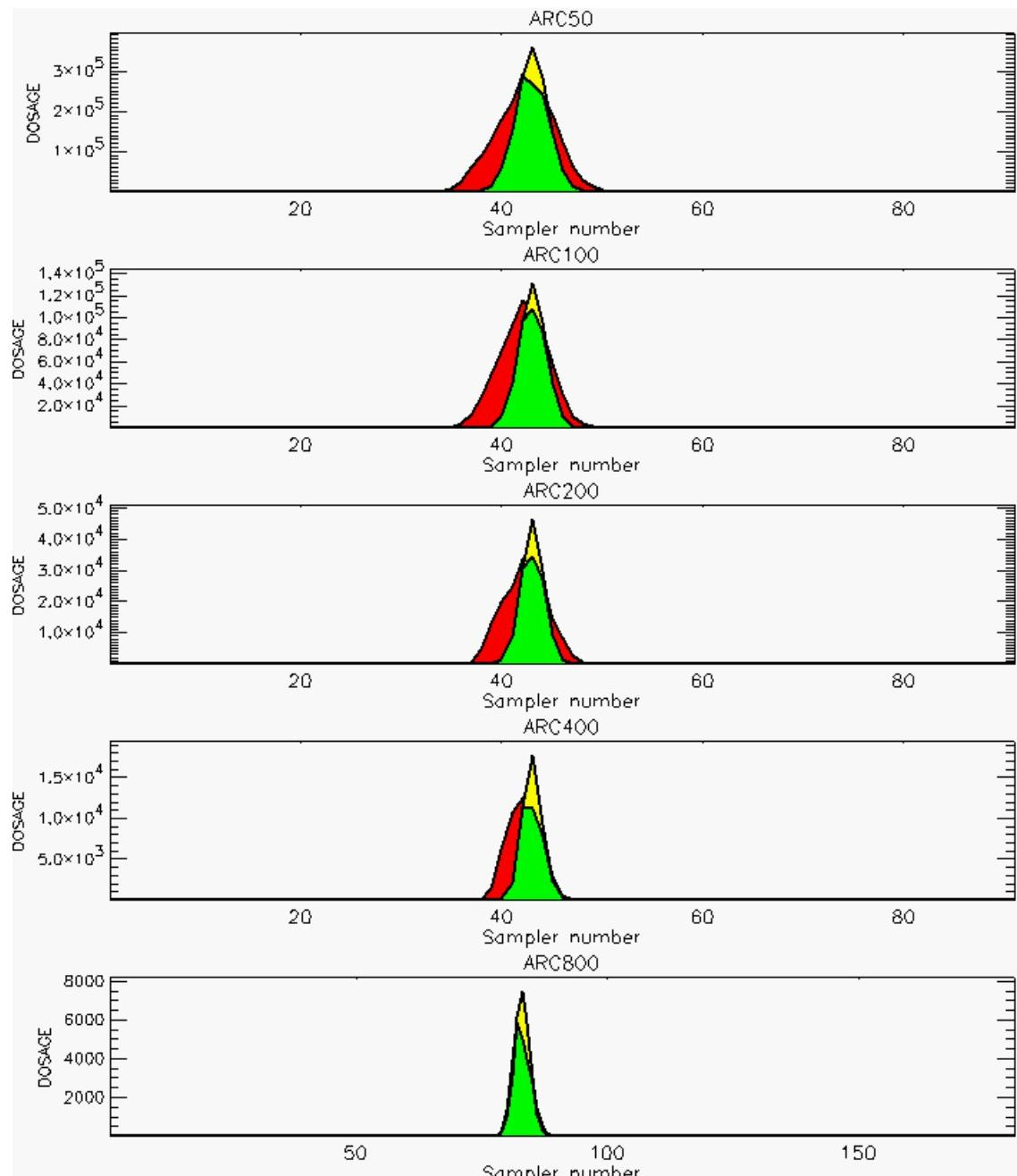


PG Observation to Prediction Comparison

PG Trial File: pr_grass_tracer_Experiment_27.txt

Prediction File: HPAC\nodeposition\pg_27_noxd.out

**Figure C-22b. HPAC Prediction to Trial 27 on Logarithmic Scale:
Stability Category is 2**

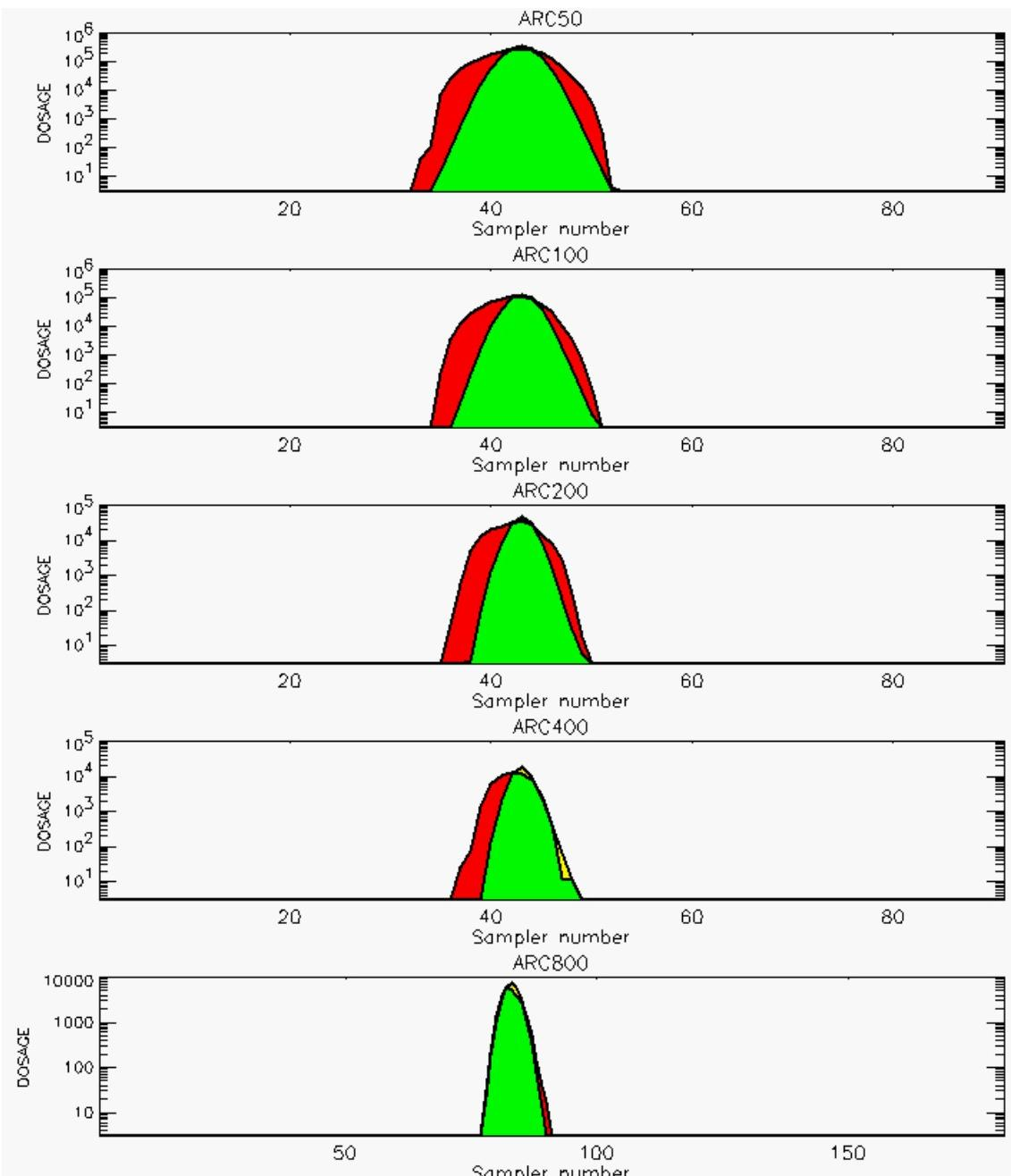


PG Observation to Prediction Comparison

PG Trial File: pr_grass_tracer_Experiment_28.txt

Prediction File: HPAC\nodeposition\pg_28_noxd.out

Figure C-23a. HPAC Prediction to Trial 28 on Linear Scale: Stability Category is 5

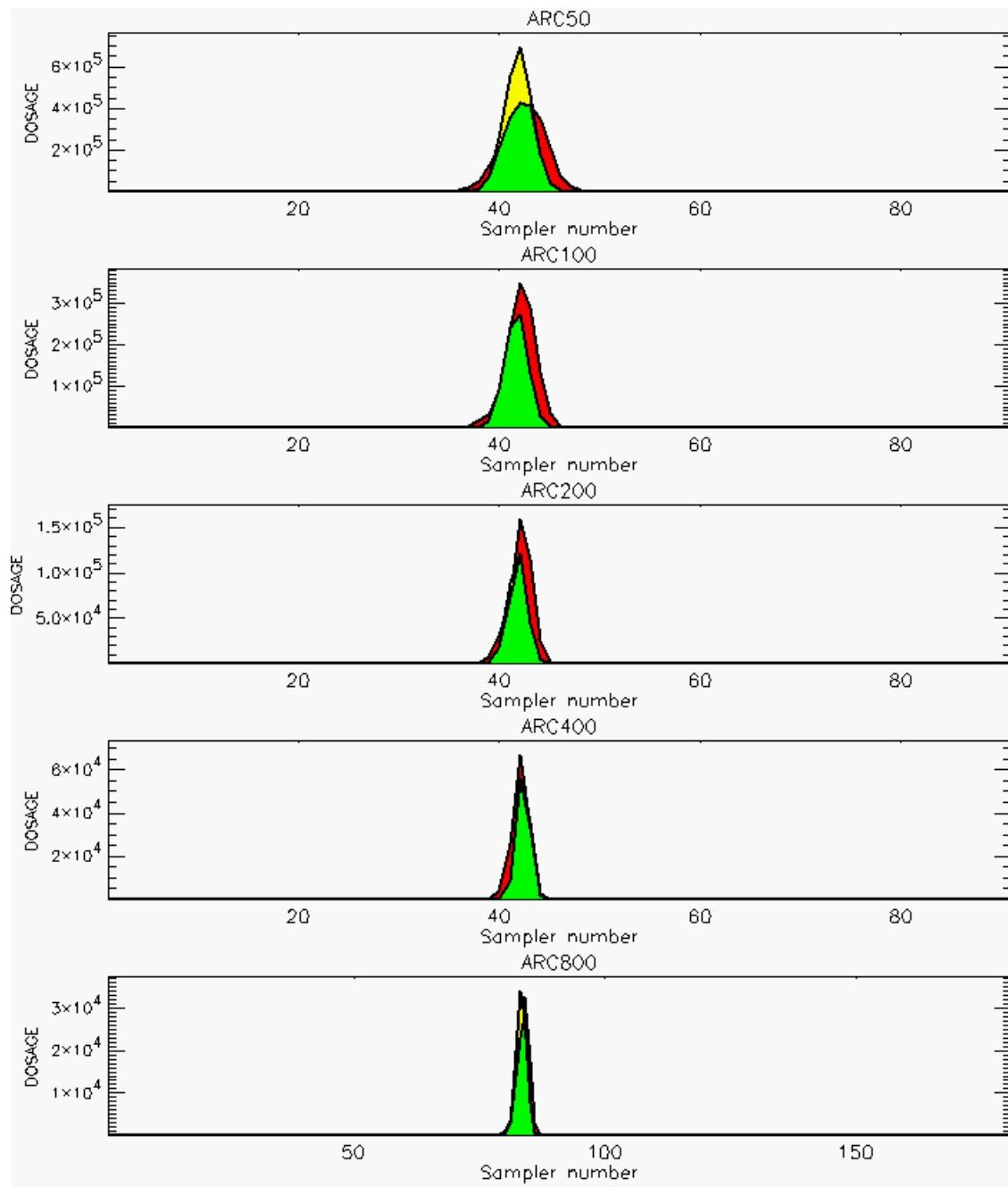


PG Observation to Prediction Comparison

PG Trial File: pr_grass_tracer_Experiment_28.txt

Prediction File: HPAC\nodeposition\pg_28_noxd.out

**Figure C-23b. HPAC Prediction to Trial 28 on Logarithmic Scale:
Stability Category is 5**

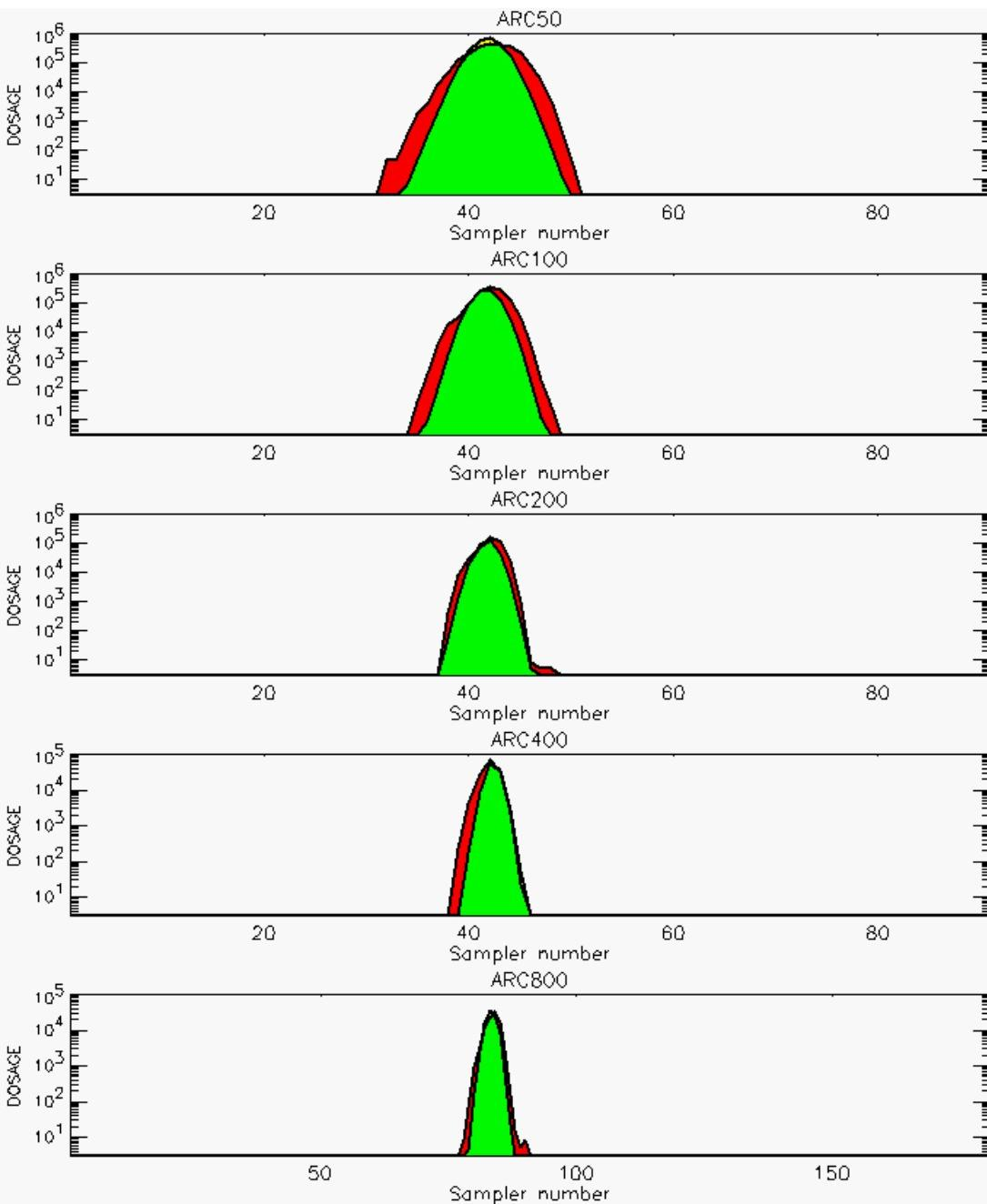


PG Observation to Prediction Comparison

PG Trial File: pr_grass_tracer_Experiment_32.txt

Prediction File: HPAC\nodeposition\pg_32_noxd.out

Figure C-24a. HPAC Prediction to Trial 32 on Linear Scale: Stability Category is 6

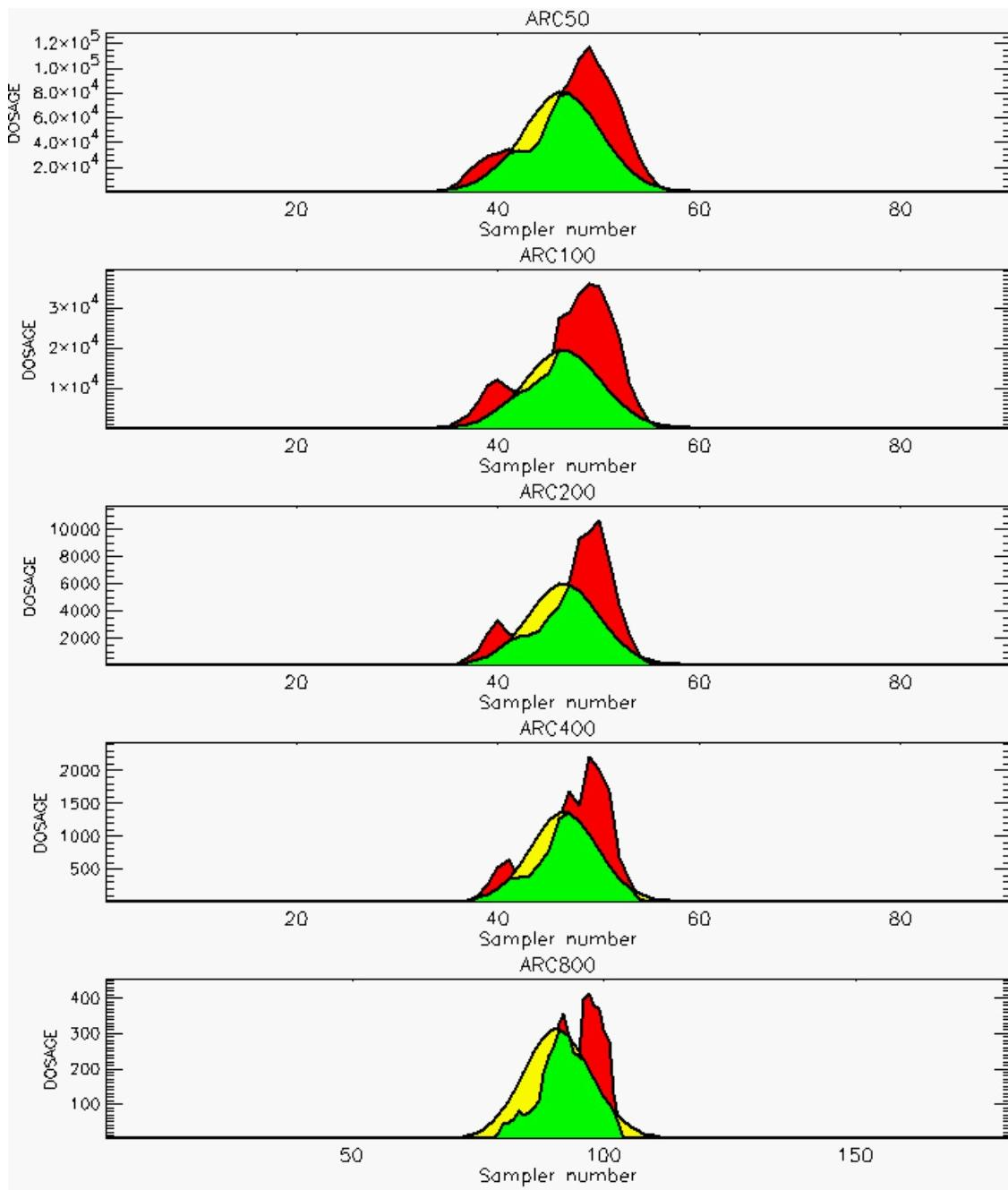


PG Observation to Prediction Comparison

PG Trial File: pr_grass_tracer_Experiment_32.txt

Prediction File: HPAC\nodeposition\pg_32_noxd.out

**Figure C-24b. HPAC Prediction to Trial 32 on Logarithmic Scale:
Stability Category is 6**

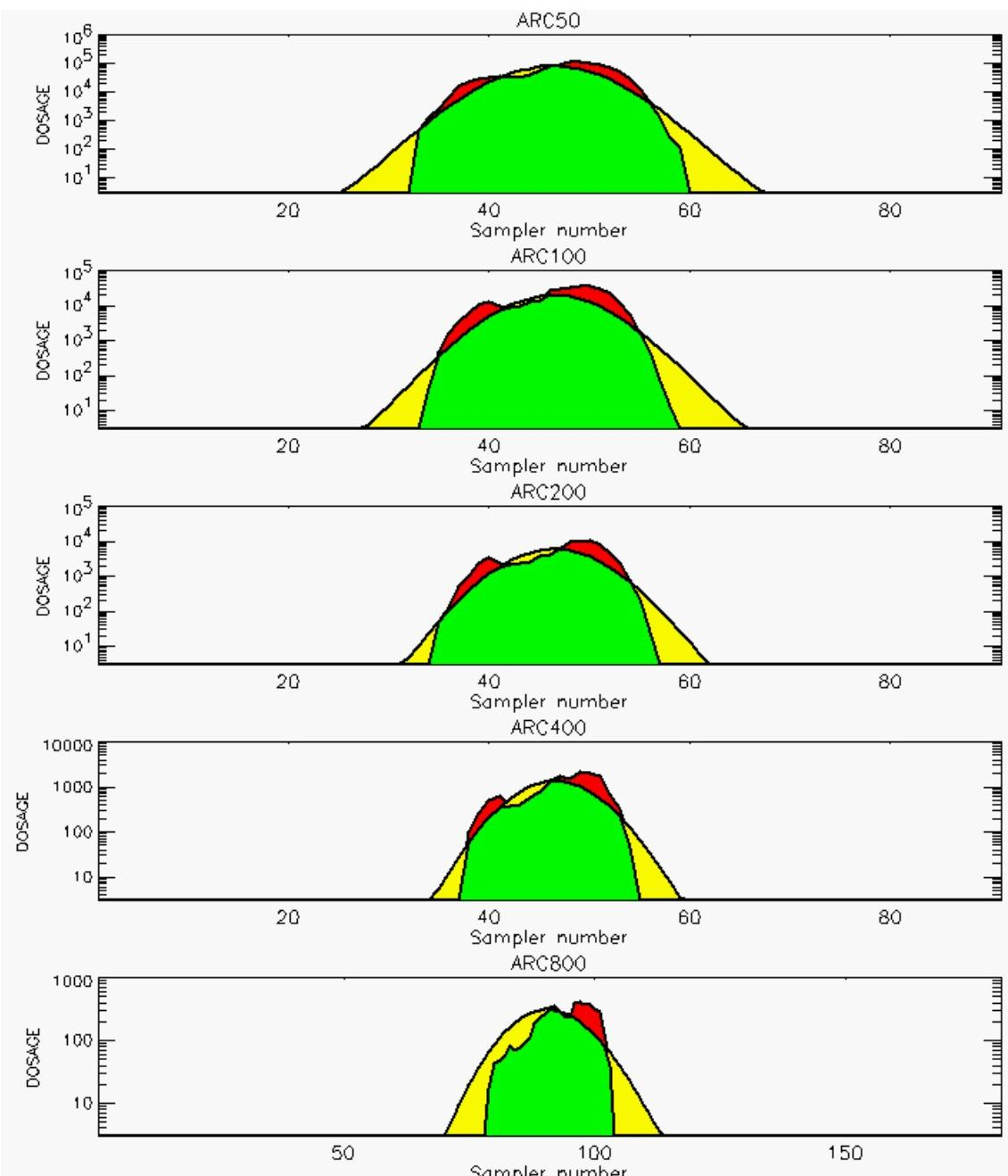


PG Observation to Prediction Comparison

PG Trial File: pr_grass_tracer_Experiment_33.txt

Prediction File: HPAC\nodeposition\pg_33_noxd.out

Figure C-25a. HPAC Prediction to Trial 33 on Linear Scale: Stability Category is 3

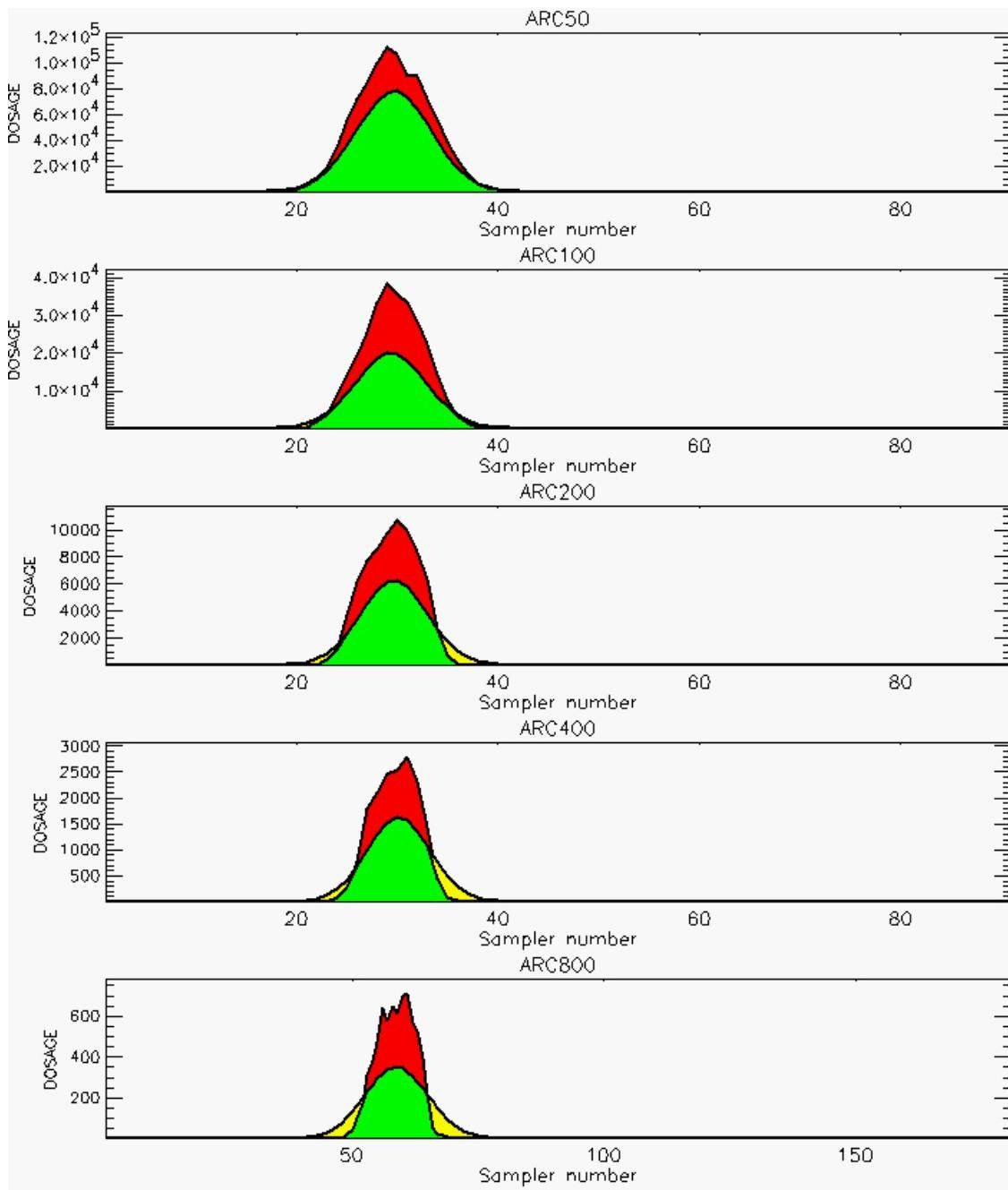


PG Observation to Prediction Comparison

PG Trial File: pr_grass_tracer_Experiment_33.txt

Prediction File: HPAC\nodeposition\pg_33_noxd.out

**Figure C-25b. HPAC Prediction to Trial 33 on Logarithmic Scale:
Stability Category is 3**

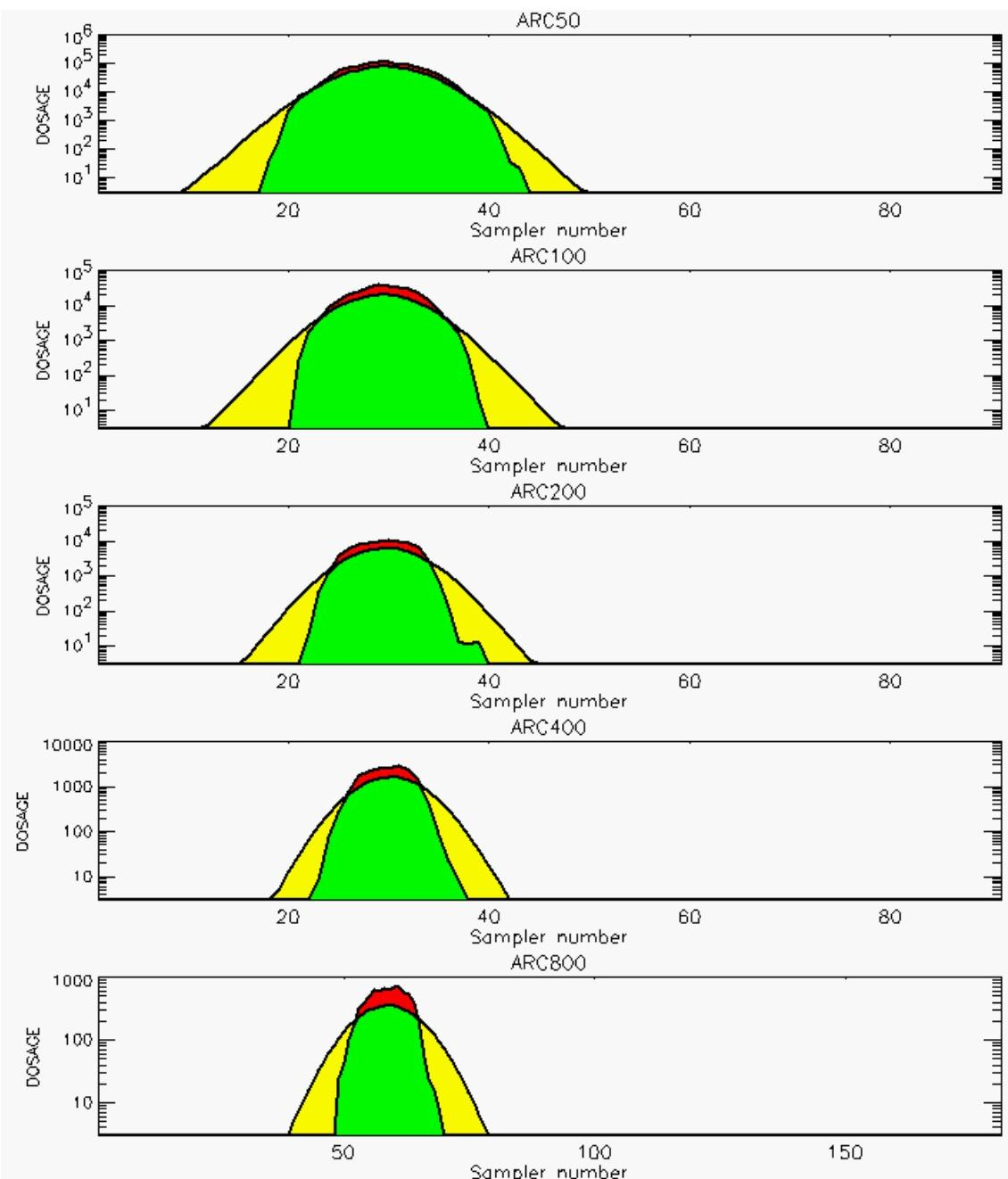


PG Observation to Prediction Comparison

PG Trial File: pr_grass_tracer_Experiment_34.txt

Prediction File: HPAC\nodeposition\pg_34_noxd.out

Figure C-26a. HPAC Prediction to Trial 34 on Linear Scale: Stability Category is 3

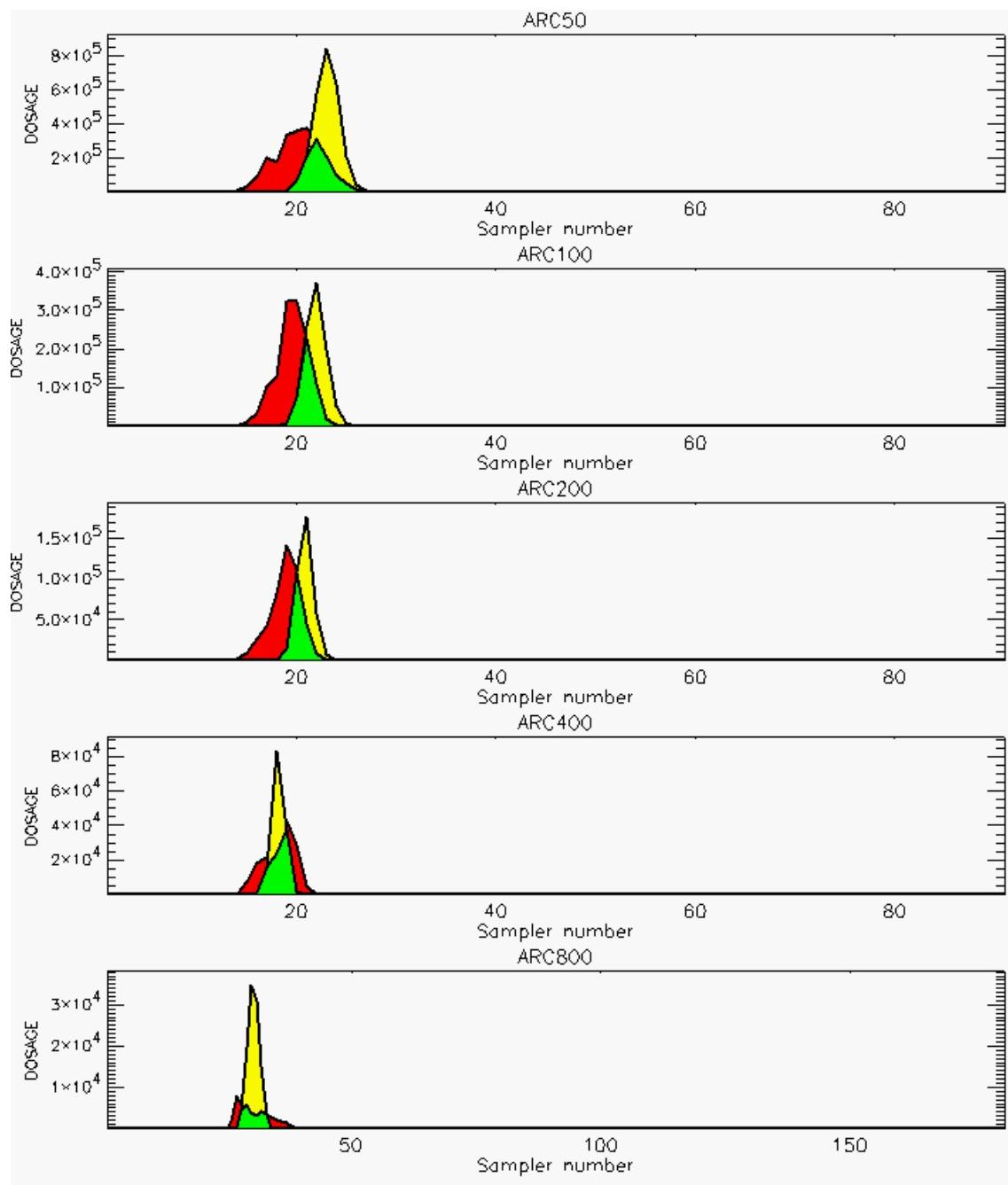


PG Observation to Prediction Comparison

PG Trial File: pr_grass_tracer_Experiment_34.txt

Prediction File: HPAC\nodeposition\pg_34_noxd.out

**Figure C-26b. HPAC Prediction to Trial 34 on Logarithmic Scale:
Stability Category is 3**

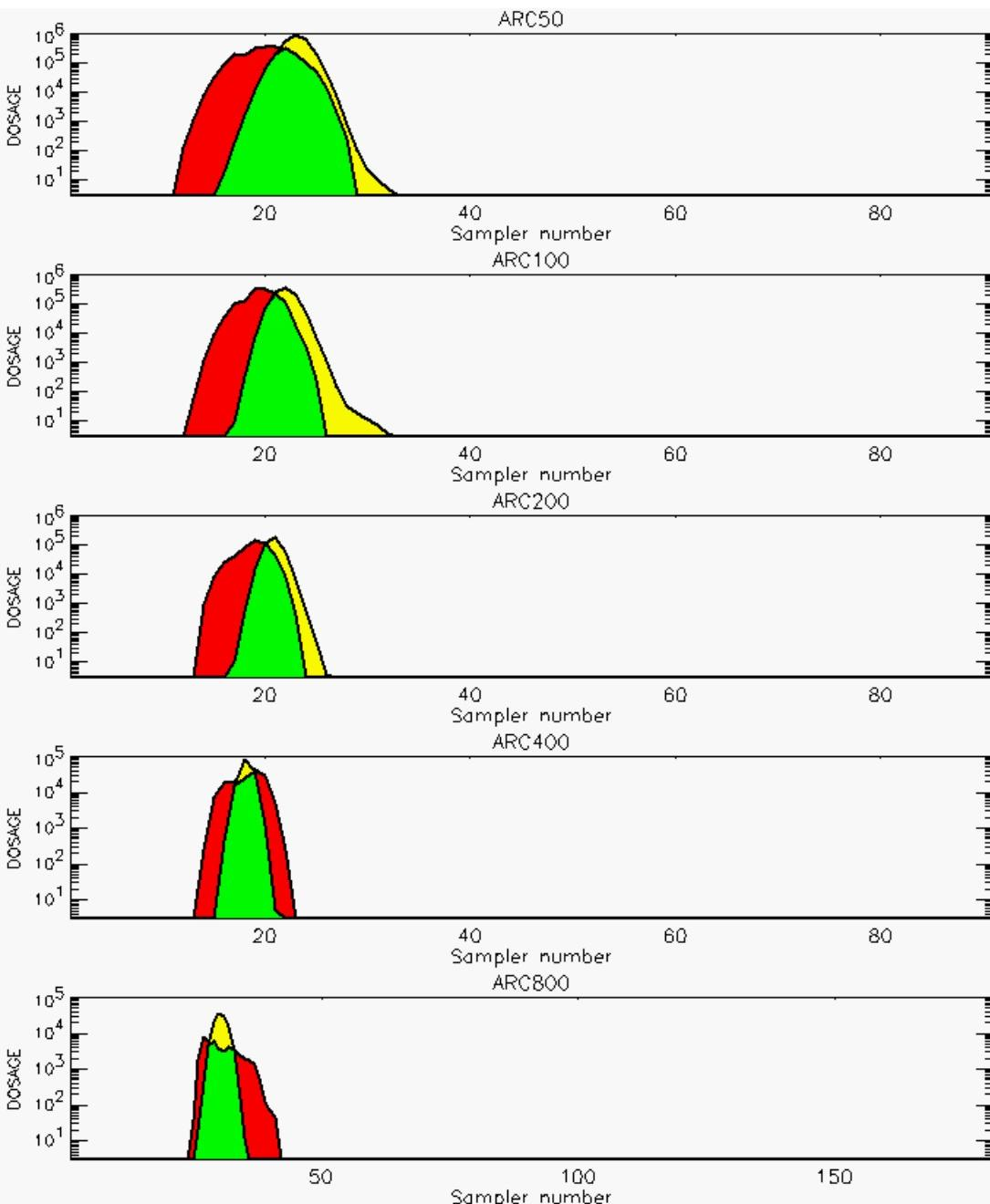


PG Observation to Prediction Comparison

PG Trial File: pr_grass_tracer_Experiment_35.txt

Prediction File: HPAC\nodeposition\pg_35_noxd.out

Figure C-27a. HPAC Prediction to Trial 35 on Linear Scale: Stability Category is 6

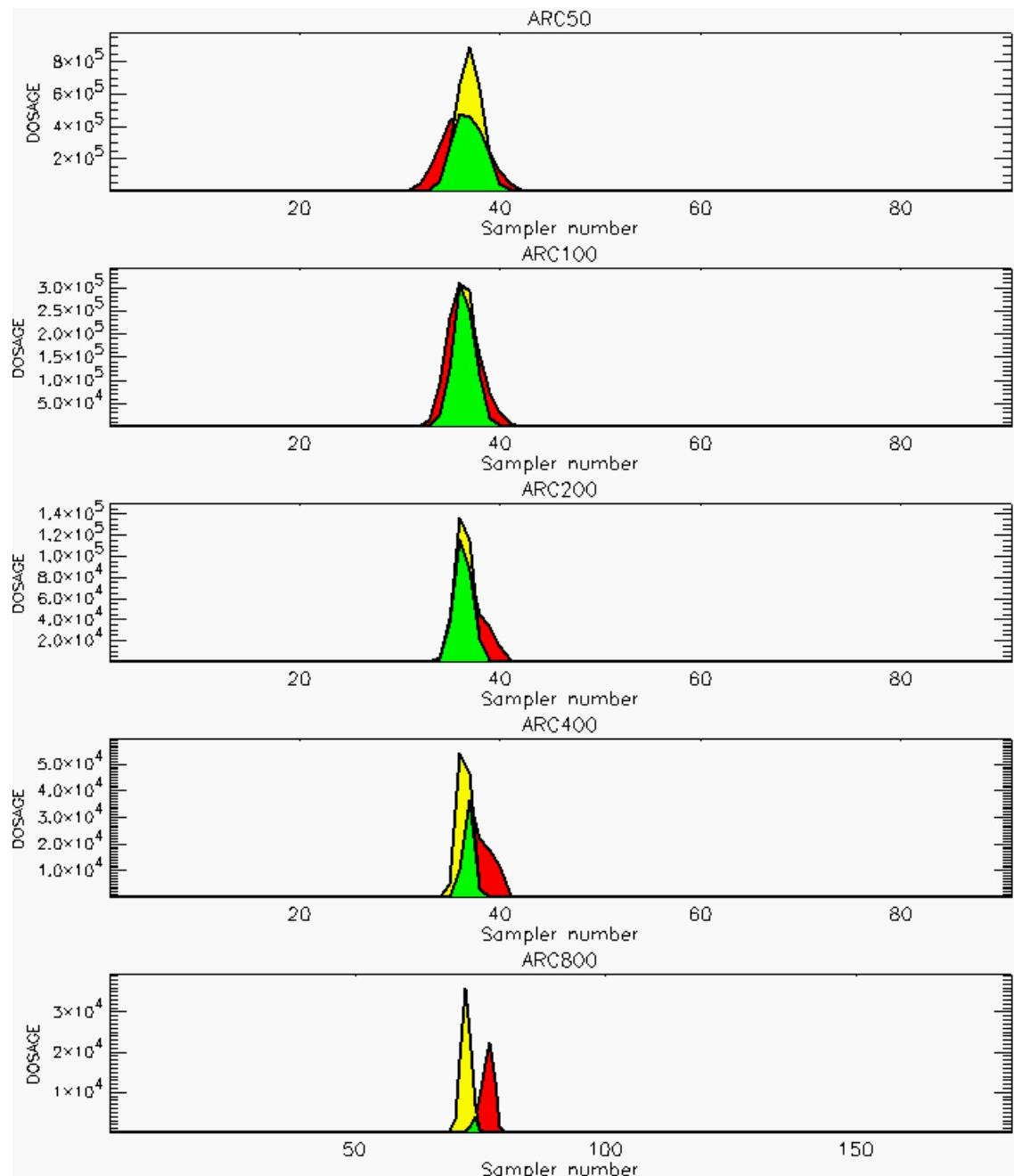


PG Observation to Prediction Comparison

PG Trial File: pr_grass_tracer_Experiment_35.txt

Prediction File: HPAC\nodeposition\pg_35_noxd.out

**Figure C-27b. HPAC Prediction to Trial 35 on Logarithmic Scale:
Stability Category is 6**

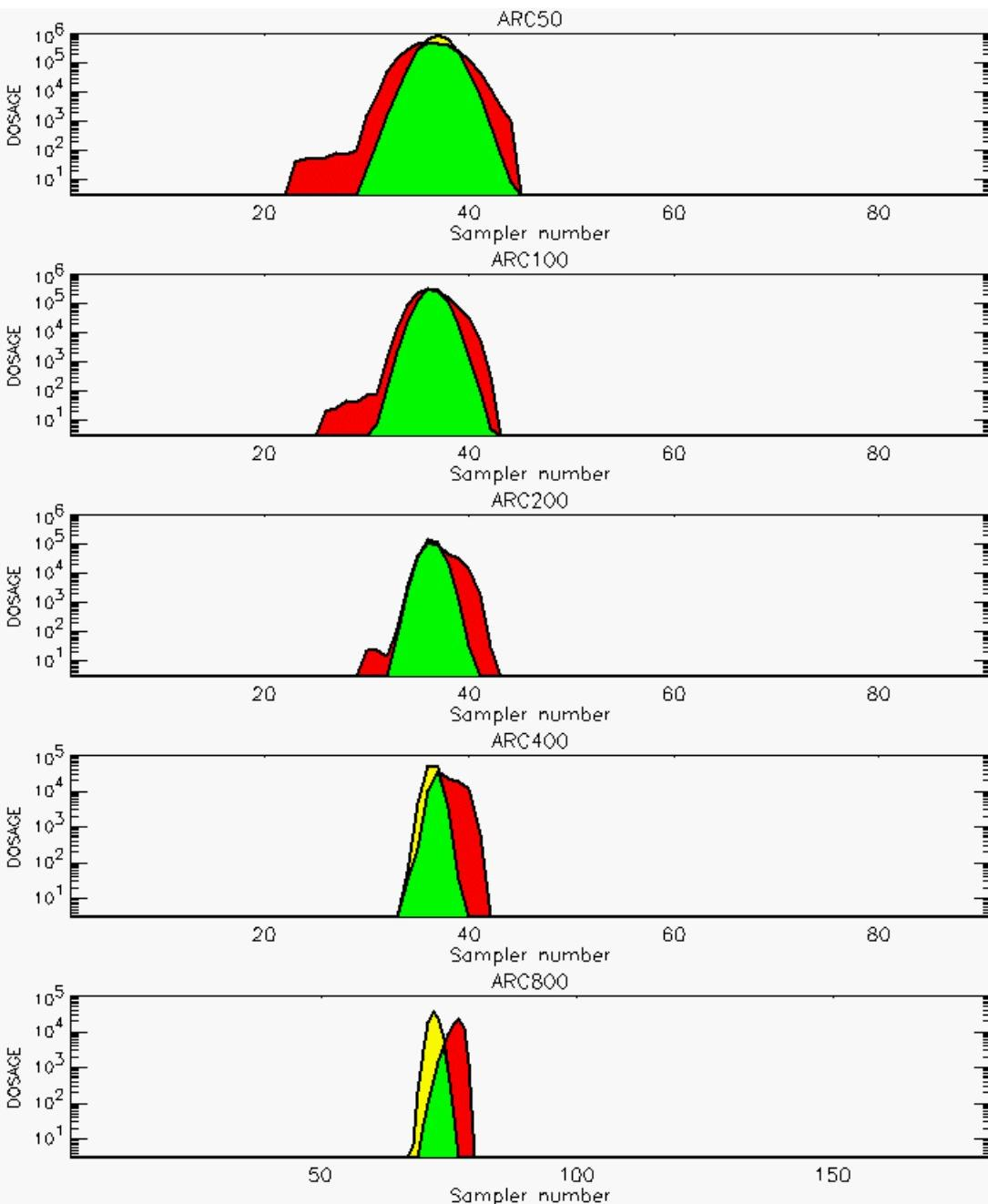


PG Observation to Prediction Comparison

PG Trial File: pr_grass_tracer_Experiment_36.txt

Prediction File: HPAC\nodeposition\pg_36_noxd.out

Figure C-28a. HPAC Prediction to Trial 36 on Linear Scale: Stability Category is 6

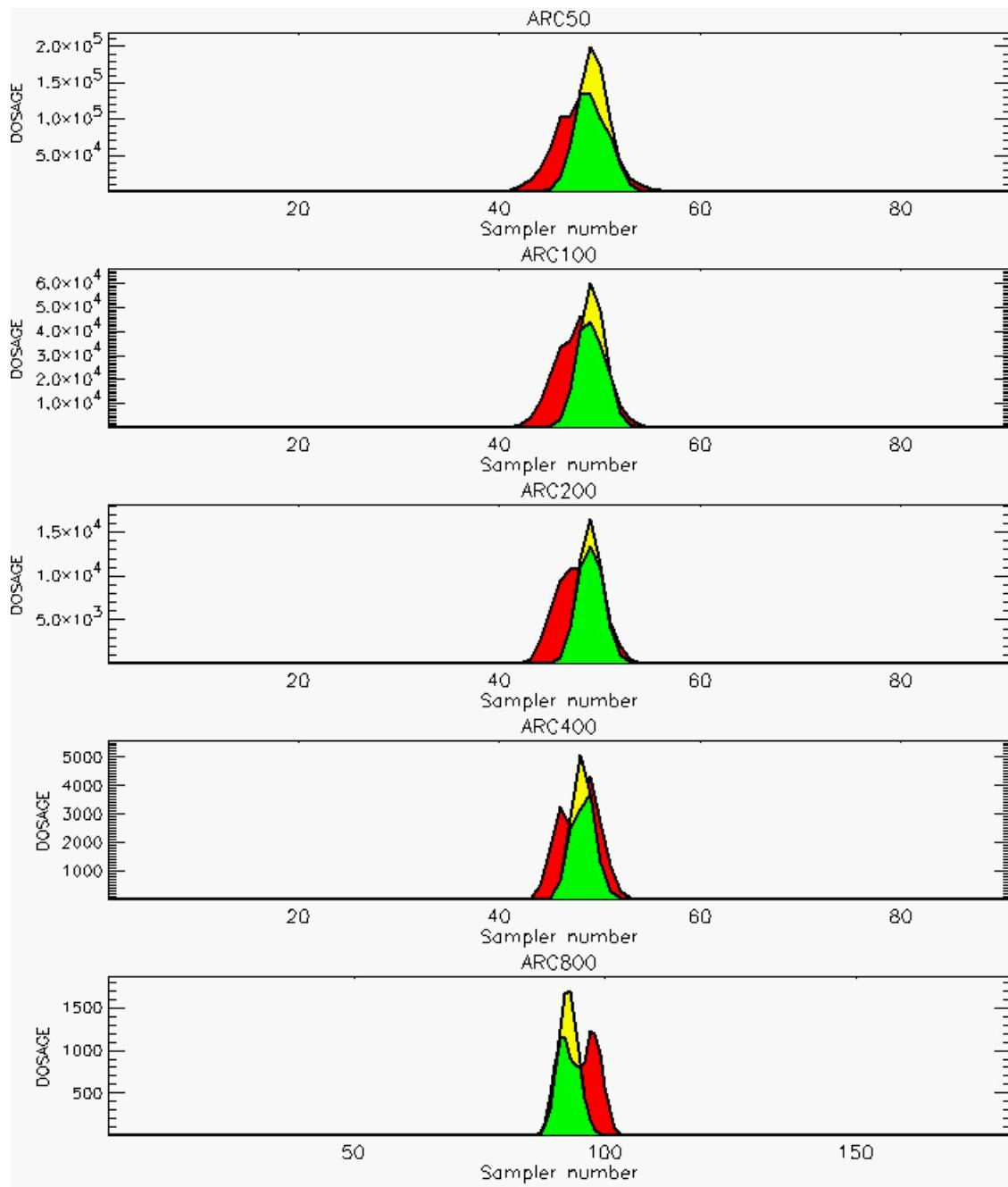


PG Observation to Prediction Comparison

PG Trial File: pr_grass_tracer_Experiment_36.txt

Prediction File: HPAC\nodeposition\pg_36_noxd.out

**Figure C-28b. HPAC Prediction to Trial 36 on Logarithmic Scale:
Stability Category is 6**

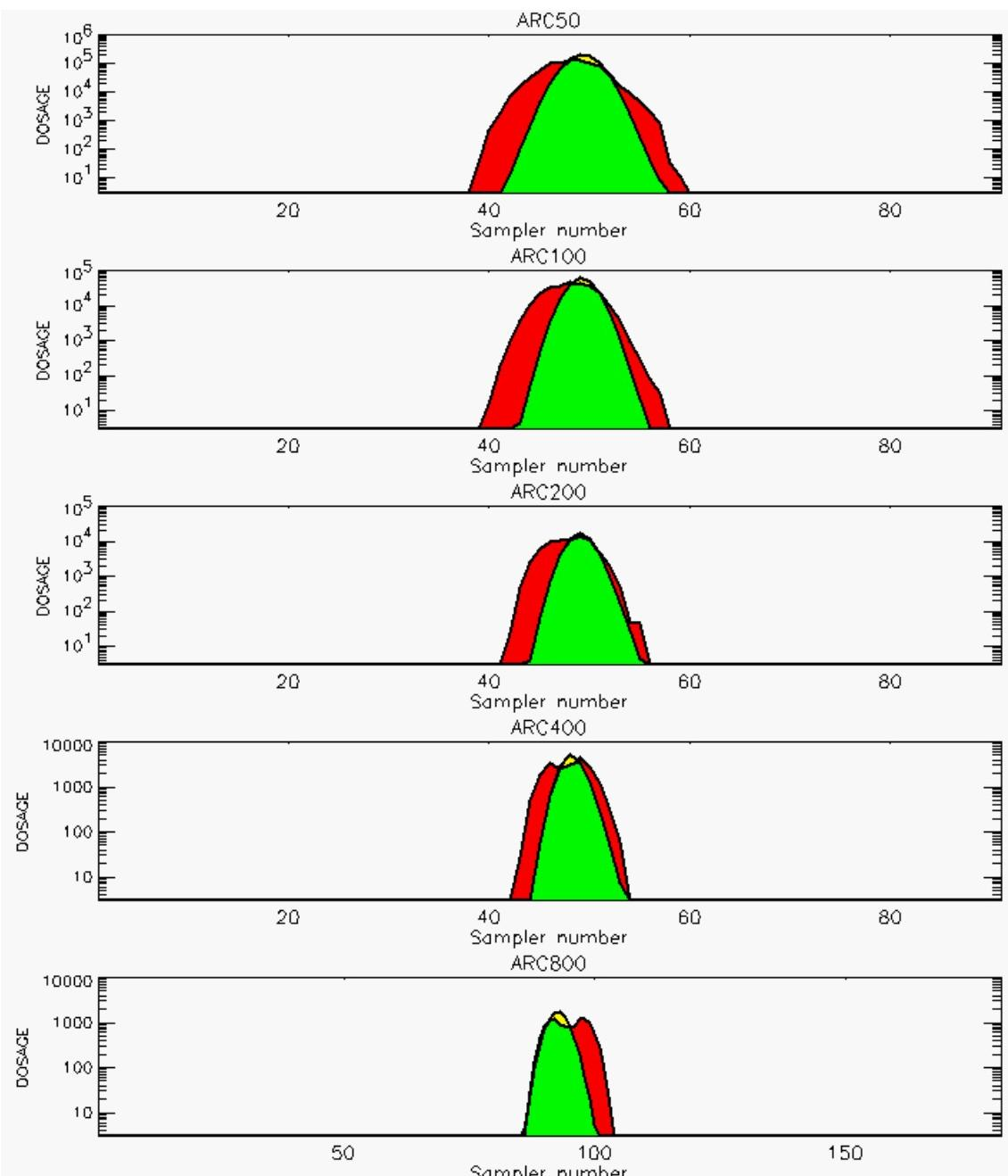


PG Observation to Prediction Comparison

PG Trial File: pr_grass_tracer_Experiment_37.txt

Prediction File: HPAC\nodeposition\pg_37_noxd.out

Figure C-29a. HPAC Prediction to Trial 37 on Linear Scale: Stability Category is 4

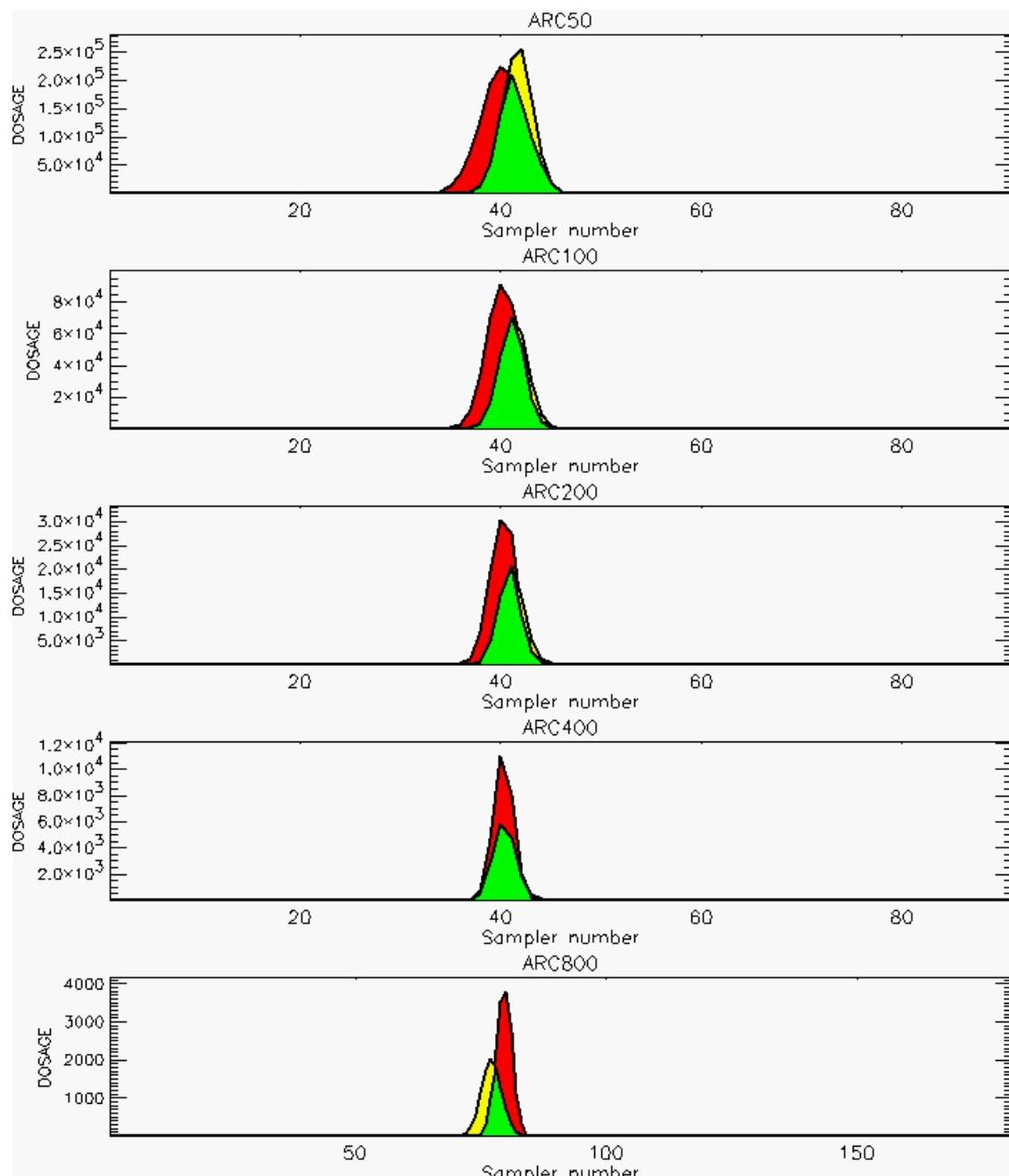


PG Observation to Prediction Comparison

PG Trial File: pr_grass_tracer_Experiment_37.txt

Prediction File: HPAC\nodeposition\pg_37_noxd.out

**Figure C-29b. HPAC Prediction to Trial 37 on Logarithmic Scale:
Stability Category is 4**

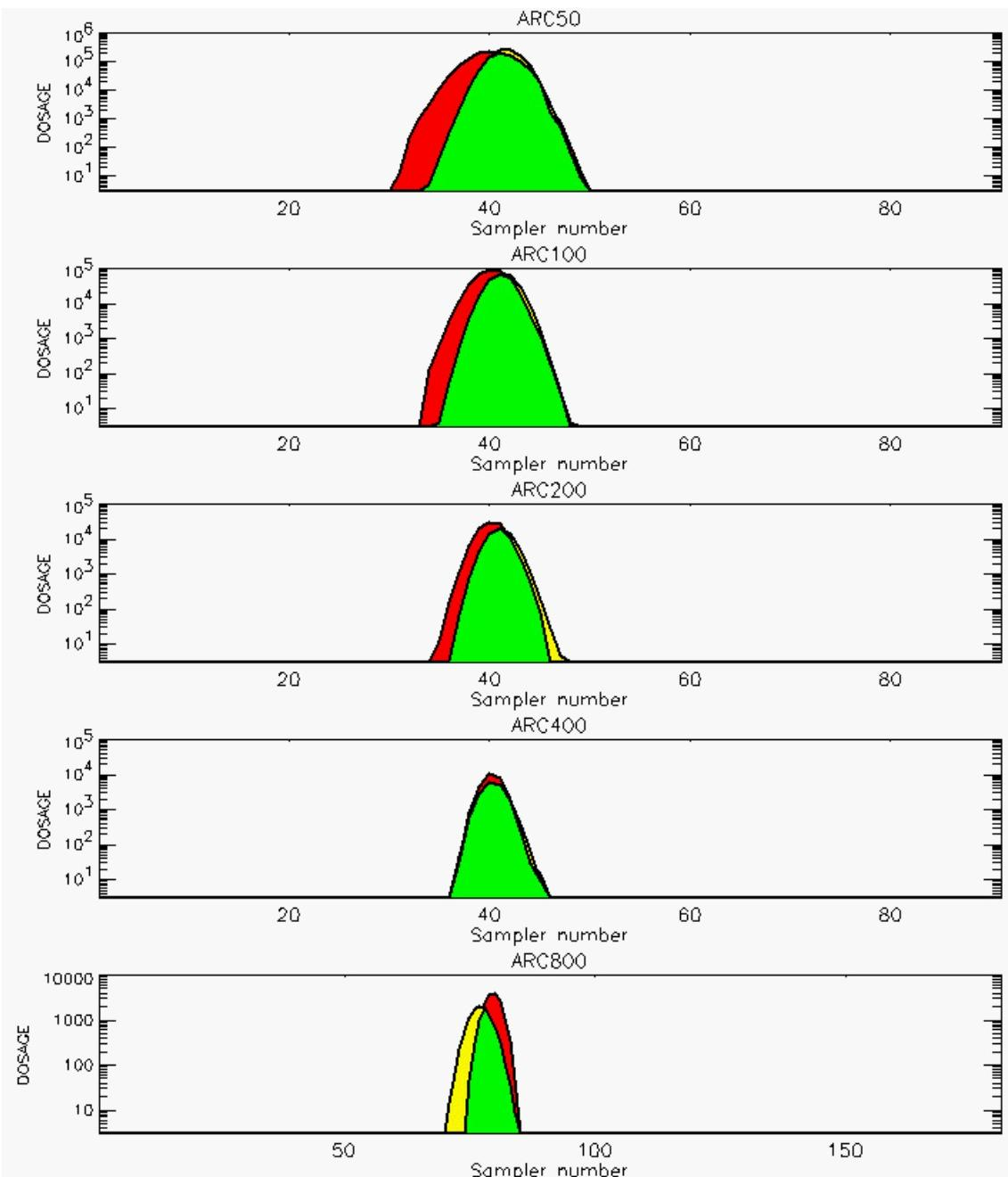


PG Observation to Prediction Comparison

PG Trial File: pr_grass_tracer_Experiment_38.txt

Prediction File: HPAC\nodeposition\pg_38_noxd.out

Figure C-30a. HPAC Prediction to Trial 38 on Linear Scale: Stability Category is 4

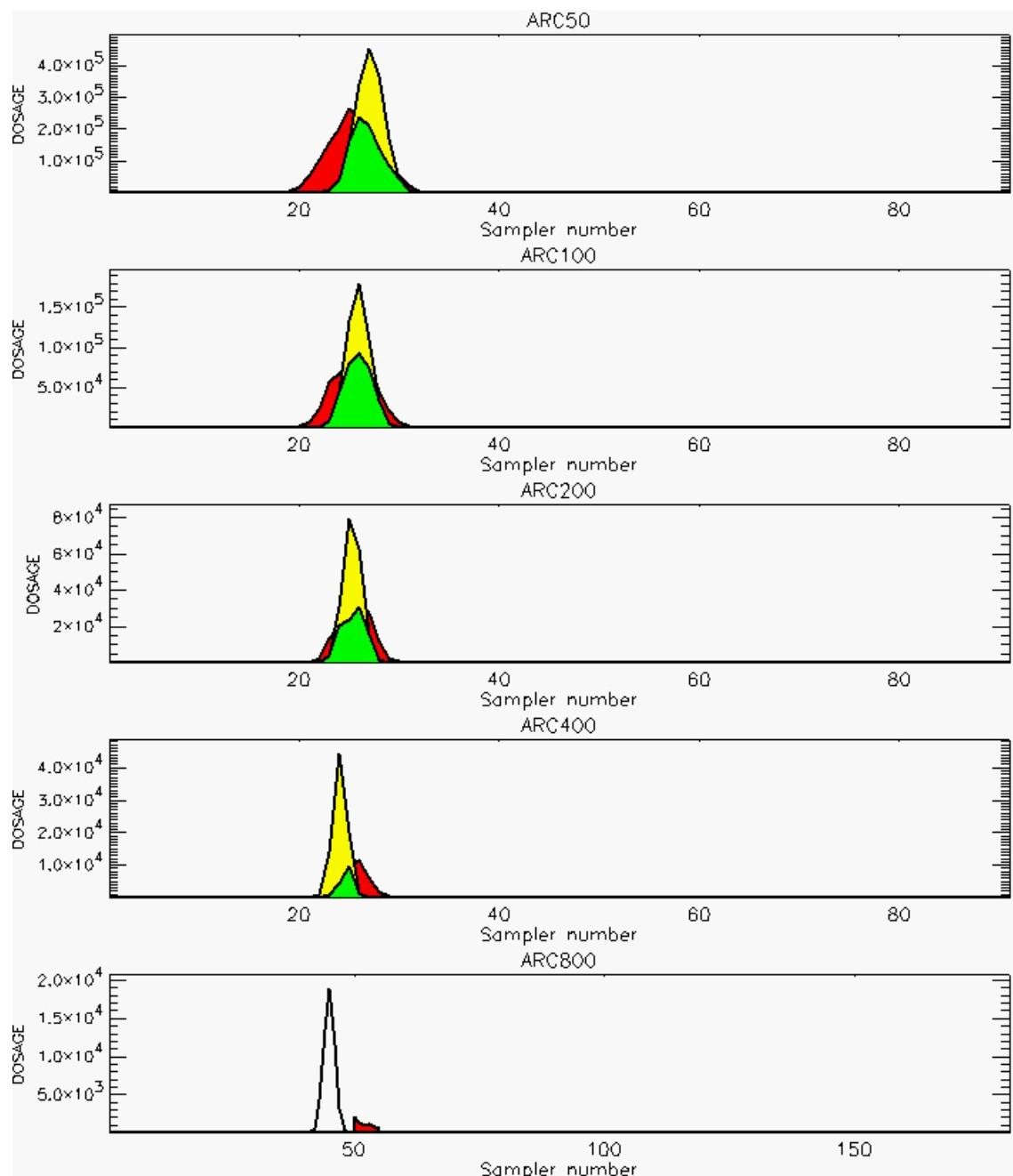


PG Observation to Prediction Comparison

PG Trial File: pr_grass_tracer_Experiment_38.txt

Prediction File: HPAC\nodeposition\pg_38_noxd.out

**Figure C-30b. HPAC Prediction to Trial 38 on Logarithmic Scale:
Stability Category is 4**

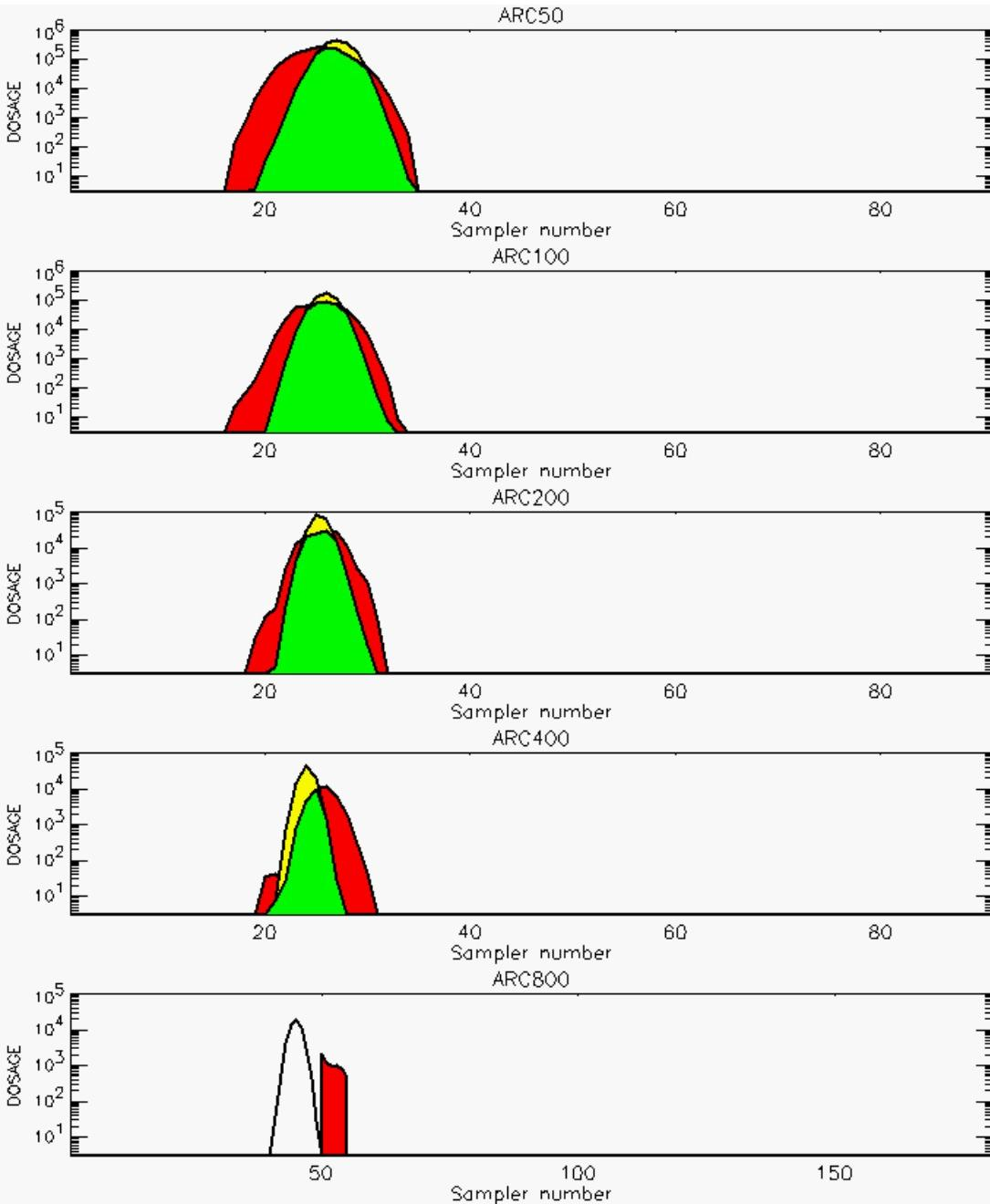


PG Observation to Prediction Comparison

PG Trial File: pr_grass_tracer_Experiment_39.txt

Prediction File: HPAC\nodeposition\pg_39_noxd.out

Figure C-31a. HPAC Prediction to Trial 39 on Linear Scale: Stability Category is 6 (Values for Samplers 40-49, 56-58 of 800-Meter Arc are Missing)

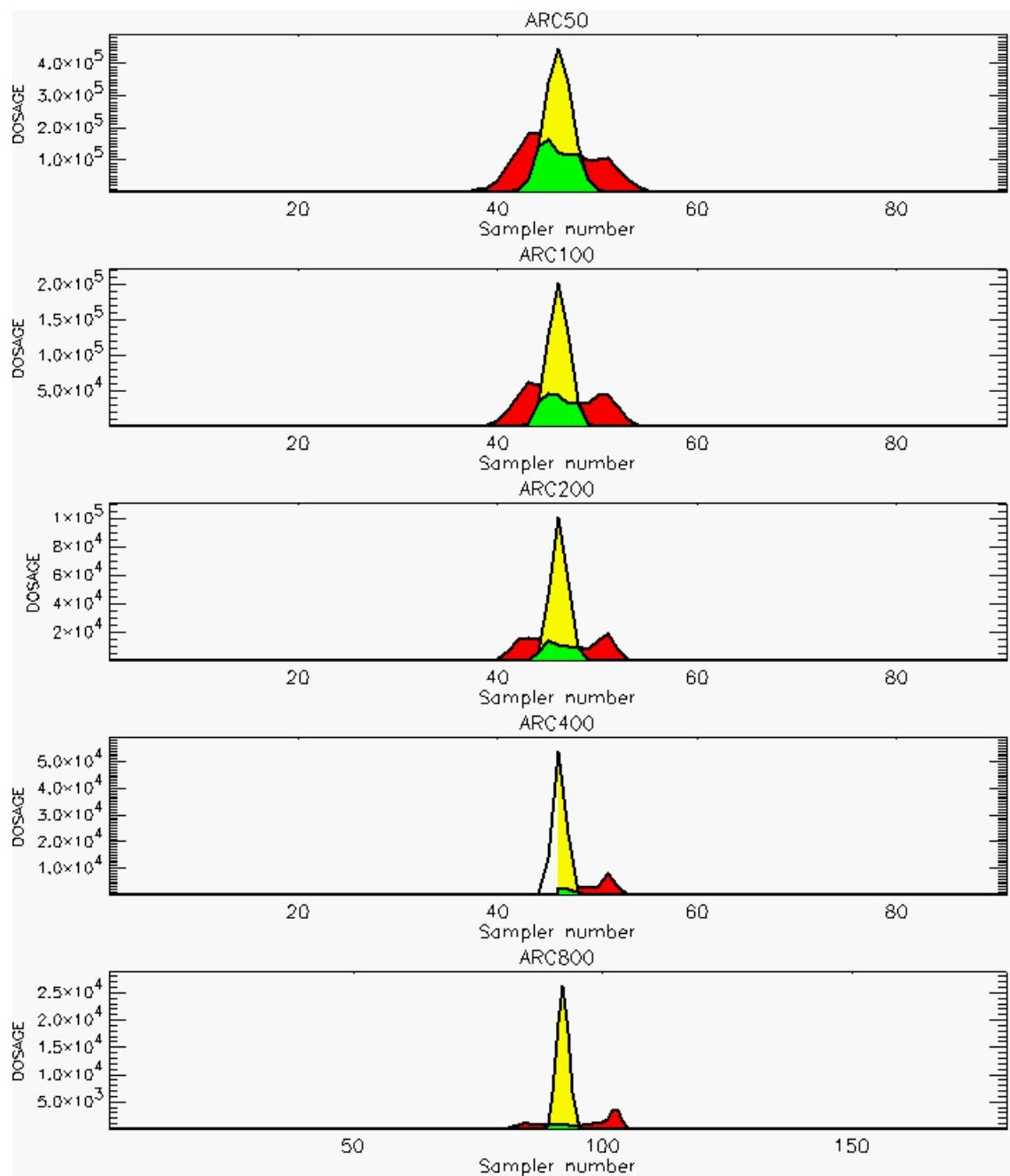


PG Observation to Prediction Comparison

PG Trial File: pr_grass_tracer_Experiment_39.txt

Prediction File: HPAC\nodeposition\pg_39_noxd.out

**Figure C-31b. HPAC Prediction to Trial 39 on Logarithmic Scale: Stability Category is 6
(Values for Samplers 40-49, 56-58 of 800-Meter Arc are Missing)**

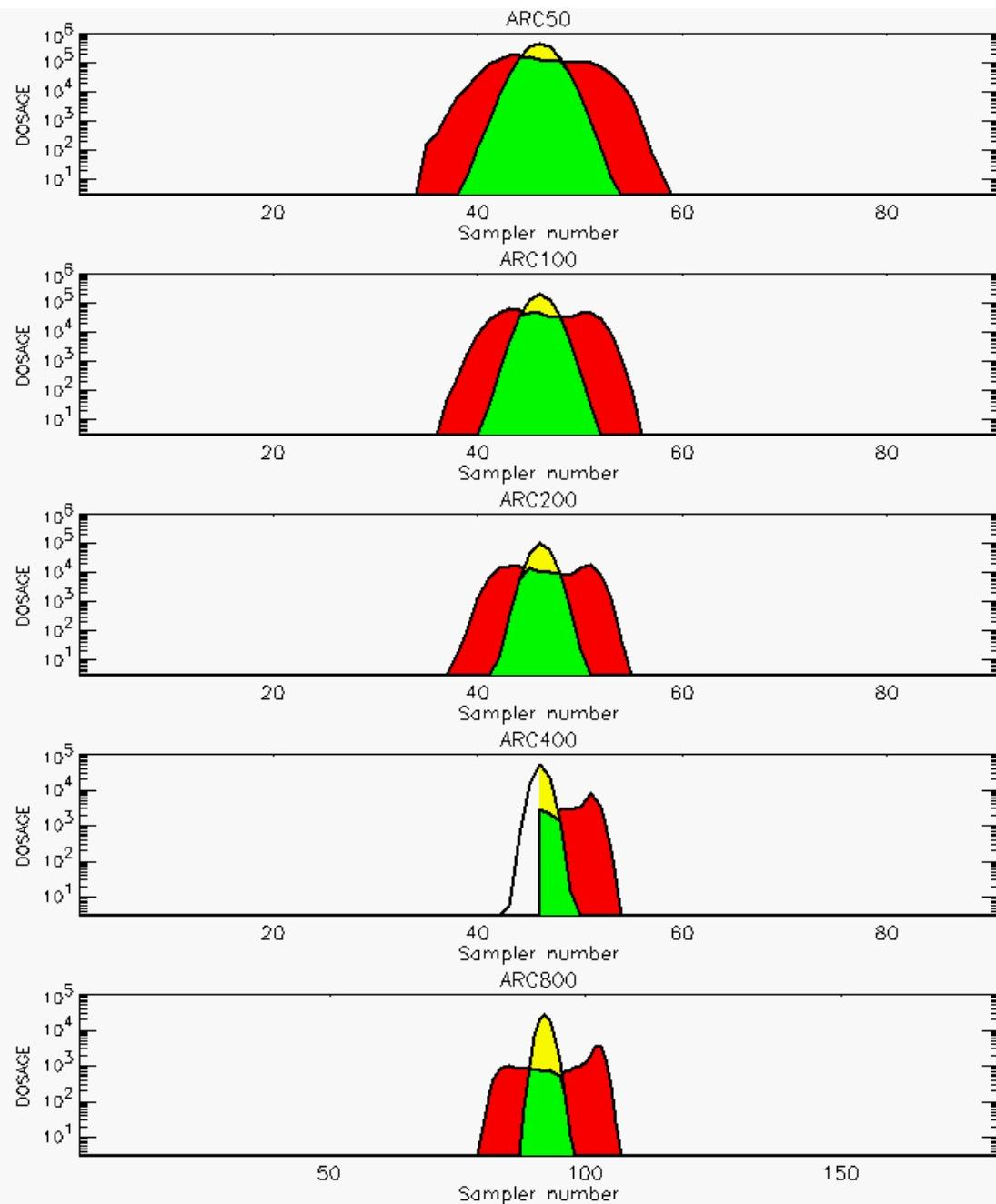


PG Observation to Prediction Comparison

PG Trial File: pr_grass_tracer_Experiment_40.txt

Prediction File: HPAC\nodeposition\pg_40_noxd.out

Figure C-32a. HPAC Prediction to Trial 40 on Linear Scale: Stability Category is 6 (Values for Samplers 39-45 of 400-Meter Arc are Missing)

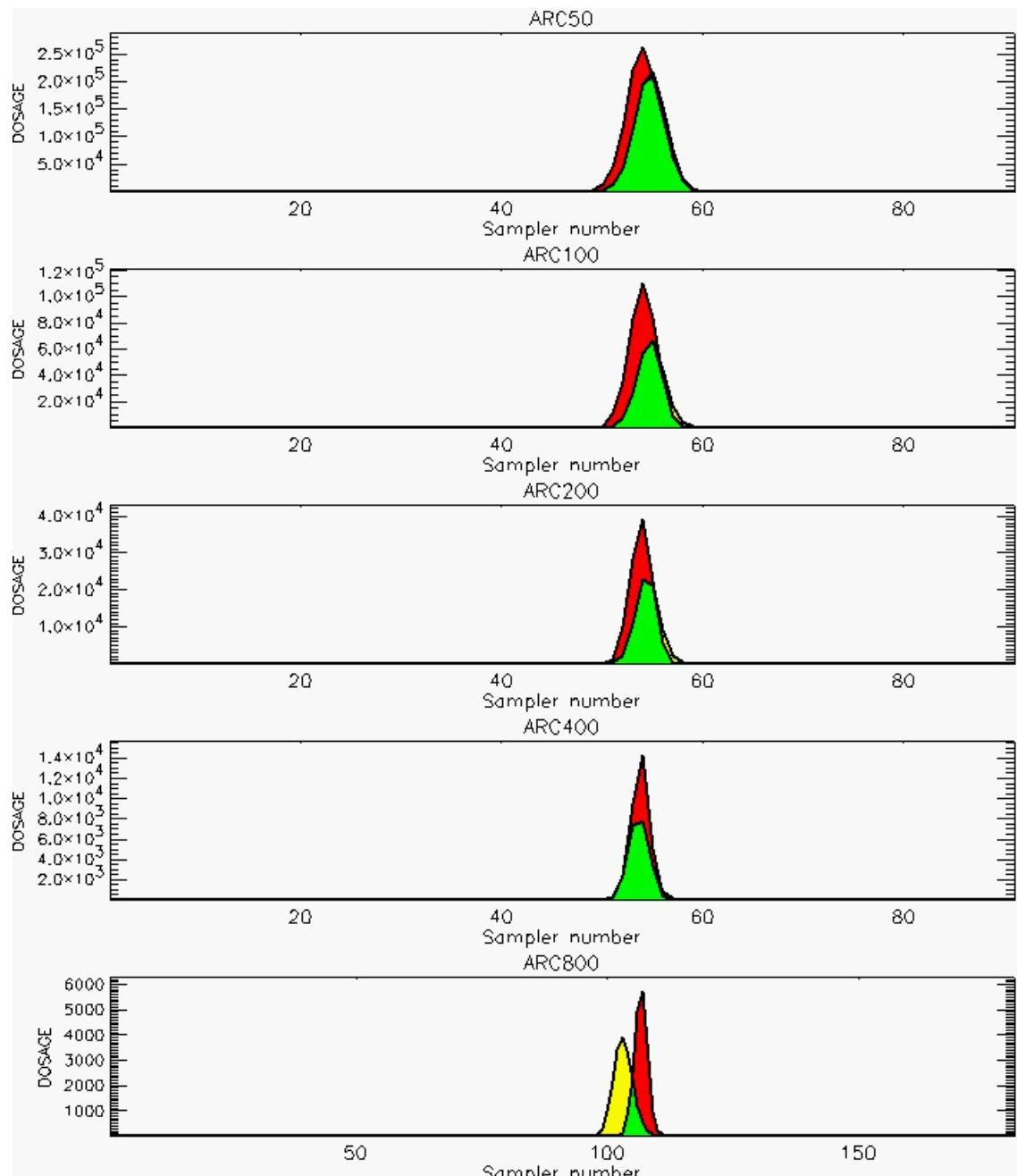


PG Observation to Prediction Comparison

PG Trial File: pr_grass_tracer_Experiment_40.txt

Prediction File: HPAC\nodeposition\pg_40_noxd.out

**Figure C-32b. HPAC Prediction to Trial 40 on Logarithmic Scale: Stability Category is 6
(Values for Samplers 39-45 of 400-Meter Arc are Missing)**

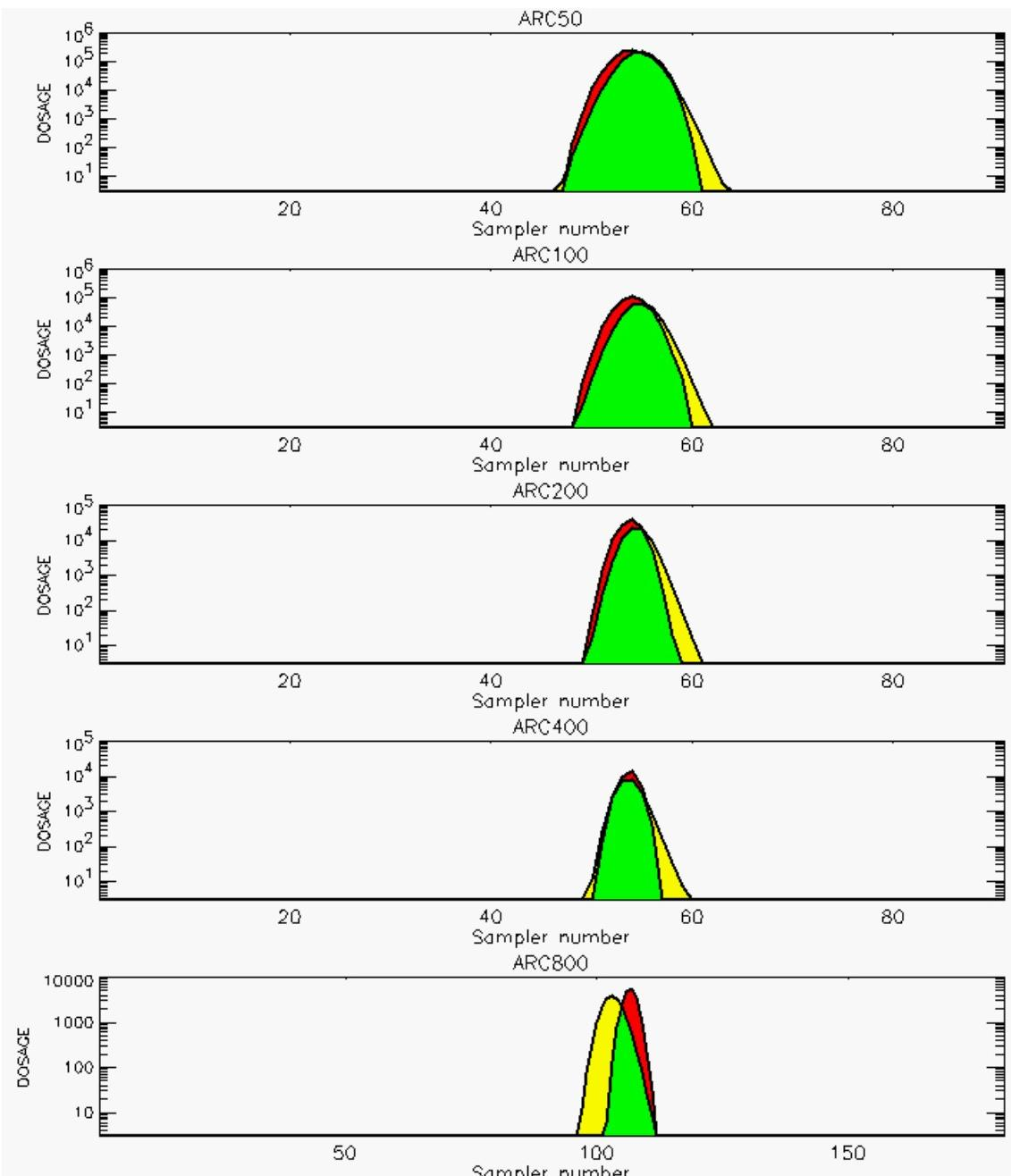


PG Observation to Prediction Comparison

PG Trial File: pr_grass_tracer_Experiment_41.txt

Prediction File: HPAC\nodeposition\pg_41_noxd.out

Figure C-33a. HPAC Prediction to Trial 41 on Linear Scale: Stability Category is 5

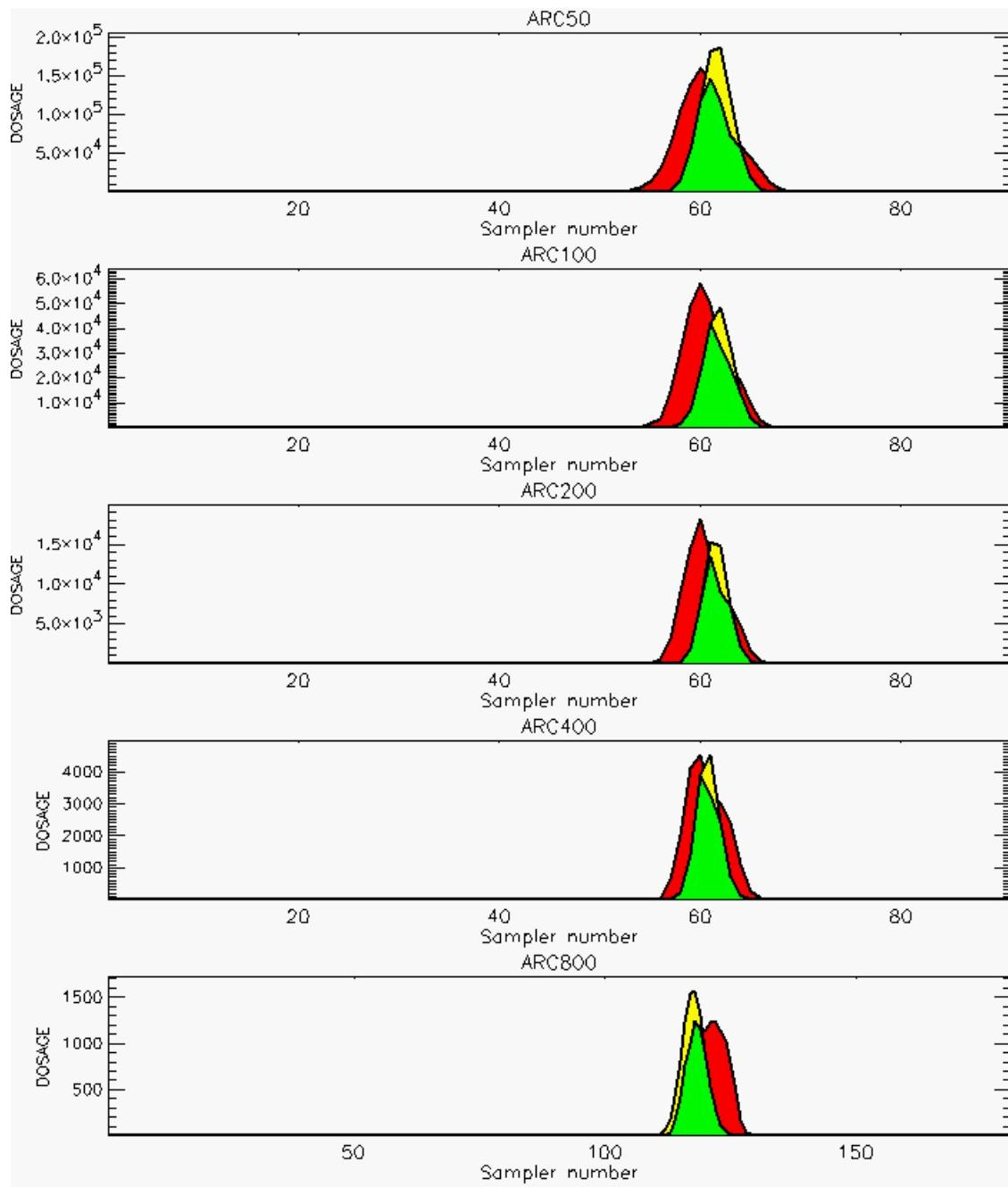


PG Observation to Prediction Comparison

PG Trial File: pr_grass_tracer_Experiment_41.txt

Prediction File: HPAC\nodeposition\pg_41_noxd.out

**Figure C-33b. HPAC Prediction to Trial 41 on Logarithmic Scale:
Stability Category is 5**

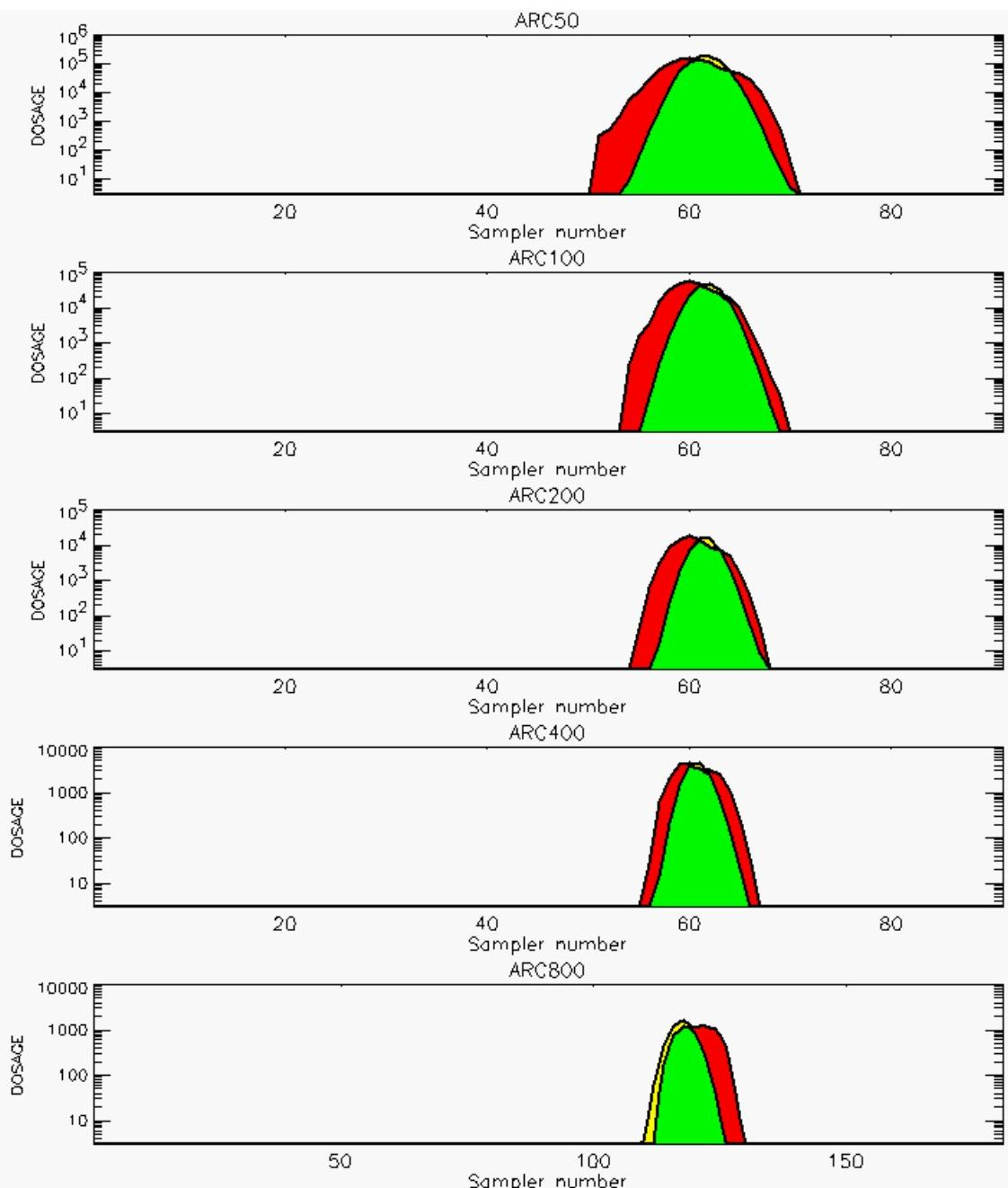


PG Observation to Prediction Comparison

PG Trial File: pr_grass_tracer_Experiment_42.txt

Prediction File: HPAC\nodeposition\pg_42_noxd.out

Figure C-34a. HPAC Prediction to Trial 42 on Linear Scale: Stability Category is 4

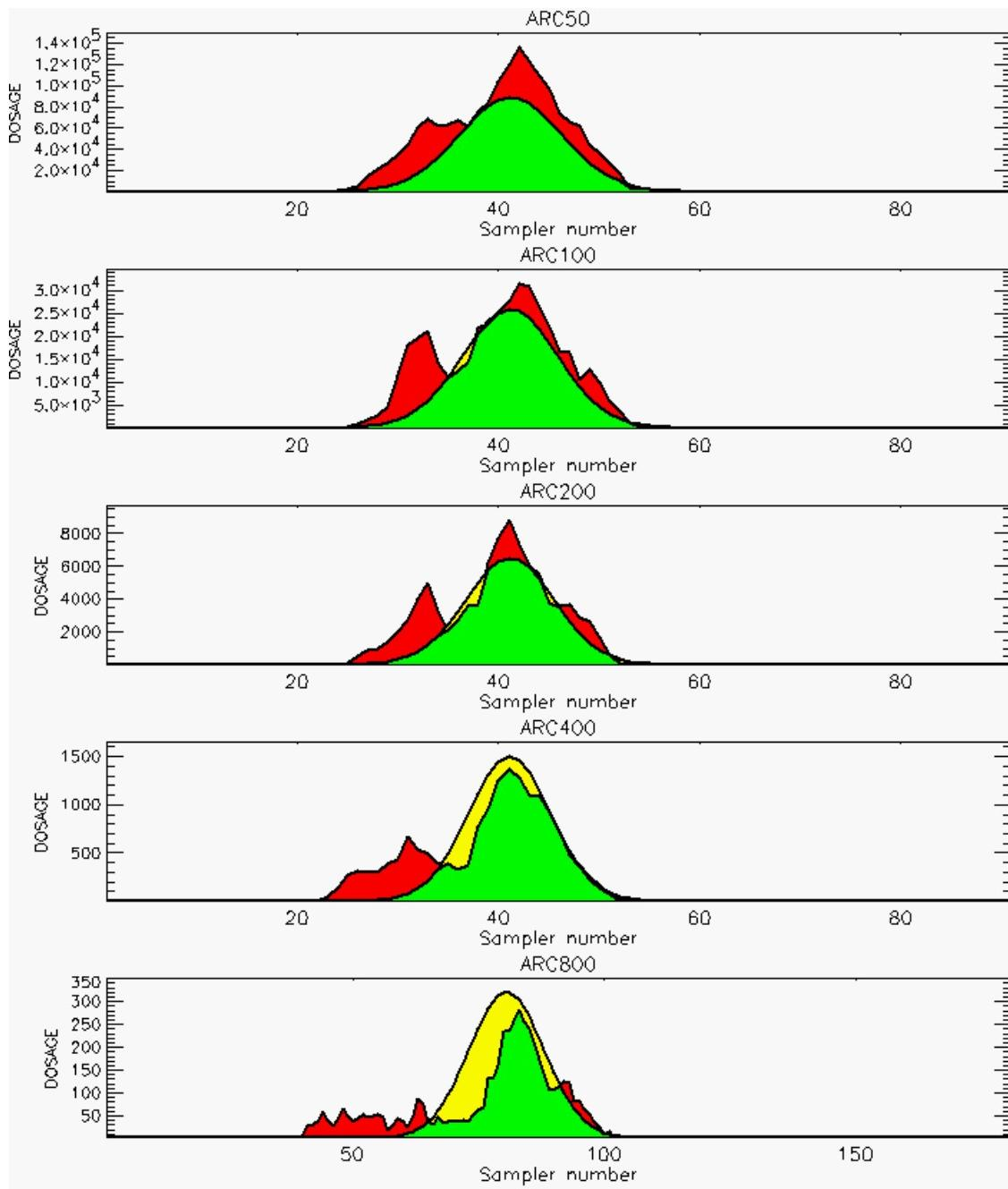


PG Observation to Prediction Comparison

PG Trial File: pr_grass_tracer_Experiment_42.txt

Prediction File: HPAC\nodeposition\pg_42_noxd.out

**Figure C-34b. HPAC Prediction to Trial 42 on Logarithmic Scale:
Stability Category is 4**

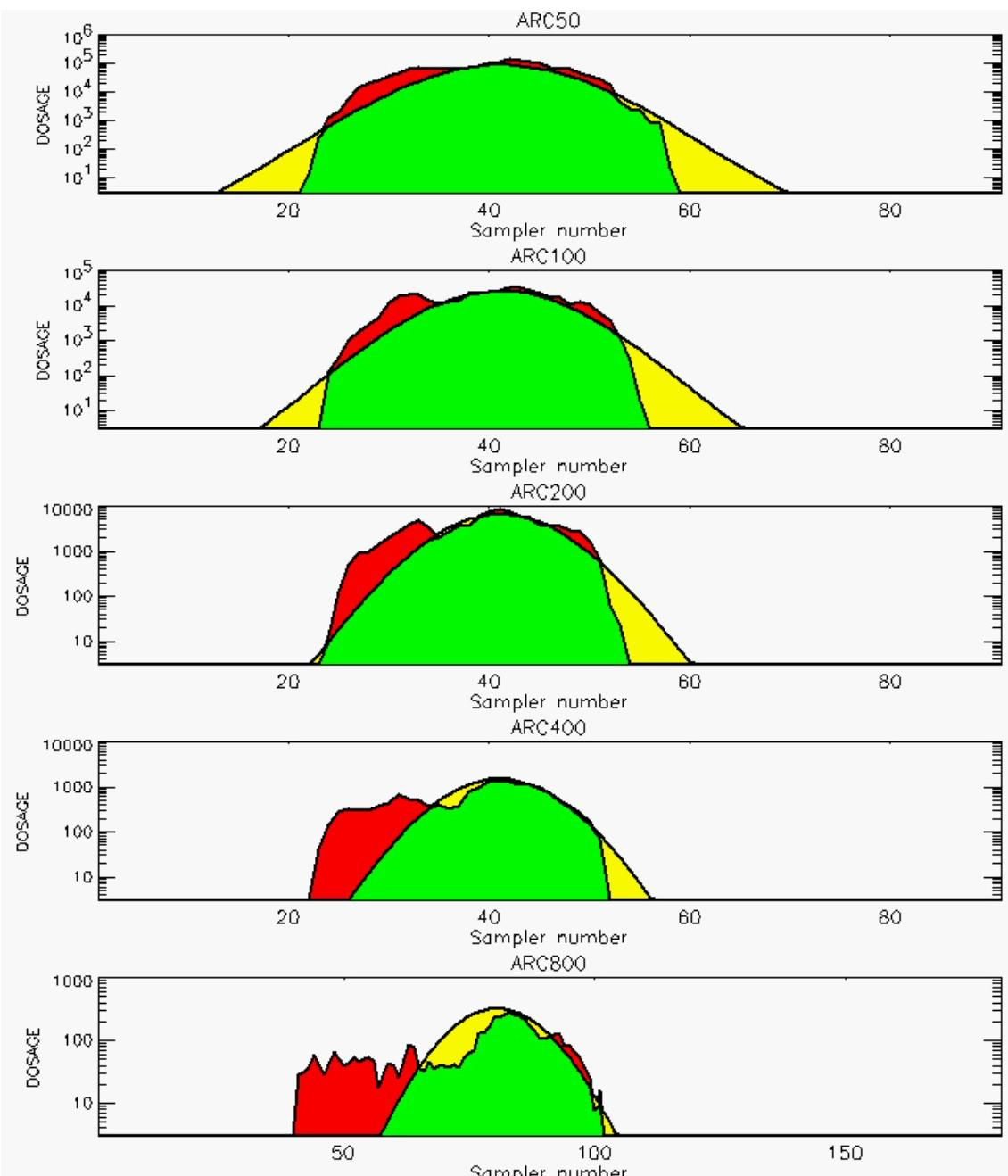


PG Observation to Prediction Comparison

PG Trial File: pr_grass_tracer_Experiment_43.txt

Prediction File: HPAC\nodeposition\pg_43_noxd.out

Figure C-35a. HPAC Prediction to Trial 43 on Linear Scale: Stability Category is 1

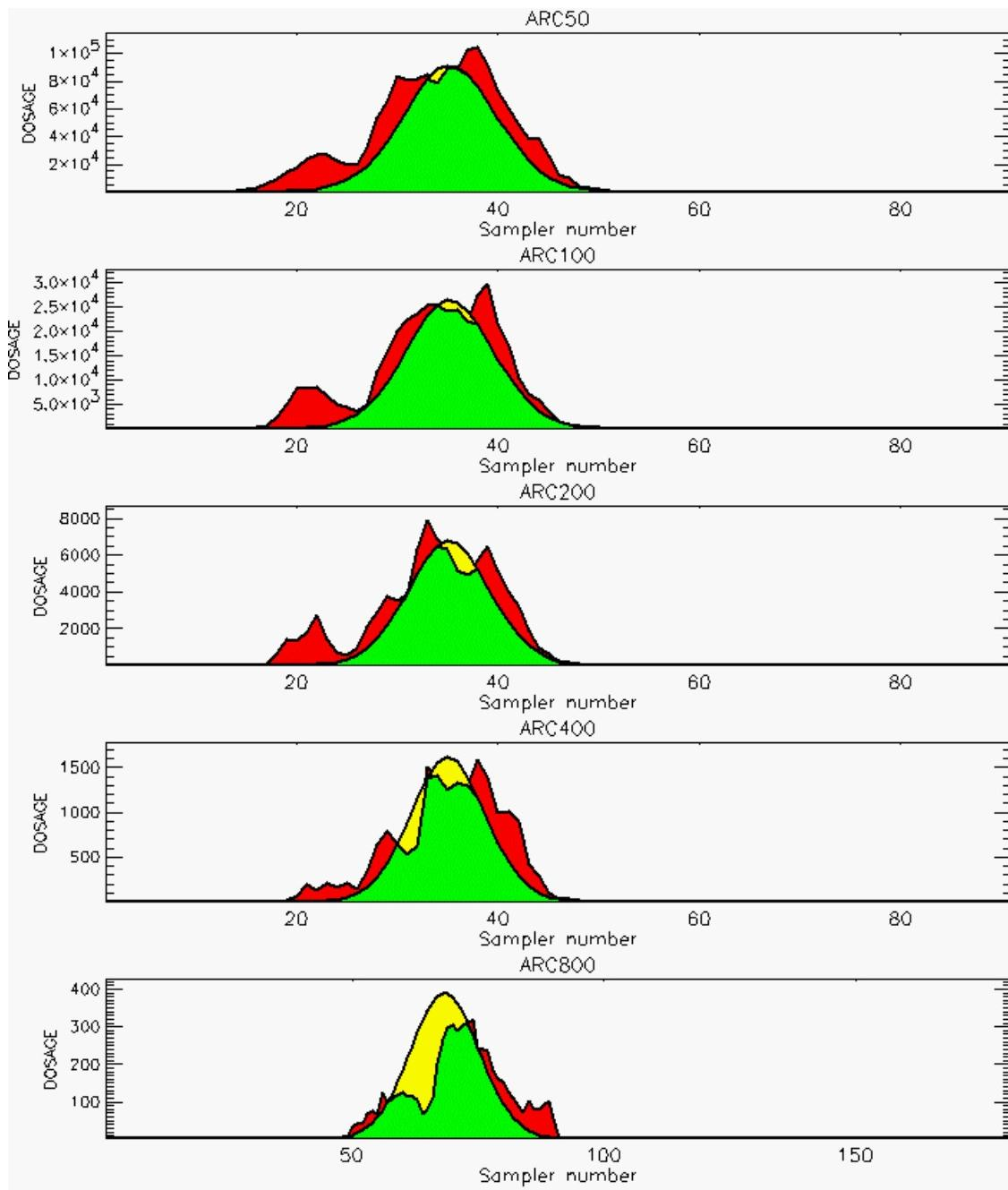


PG Observation to Prediction Comparison

PG Trial File: pr_grass_tracer_Experiment_43.txt

Prediction File: HPAC\nodeposition\pg_43_noxd.out

**Figure C-35b. HPAC Prediction to Trial 43 on Logarithmic Scale:
Stability Category is 1**

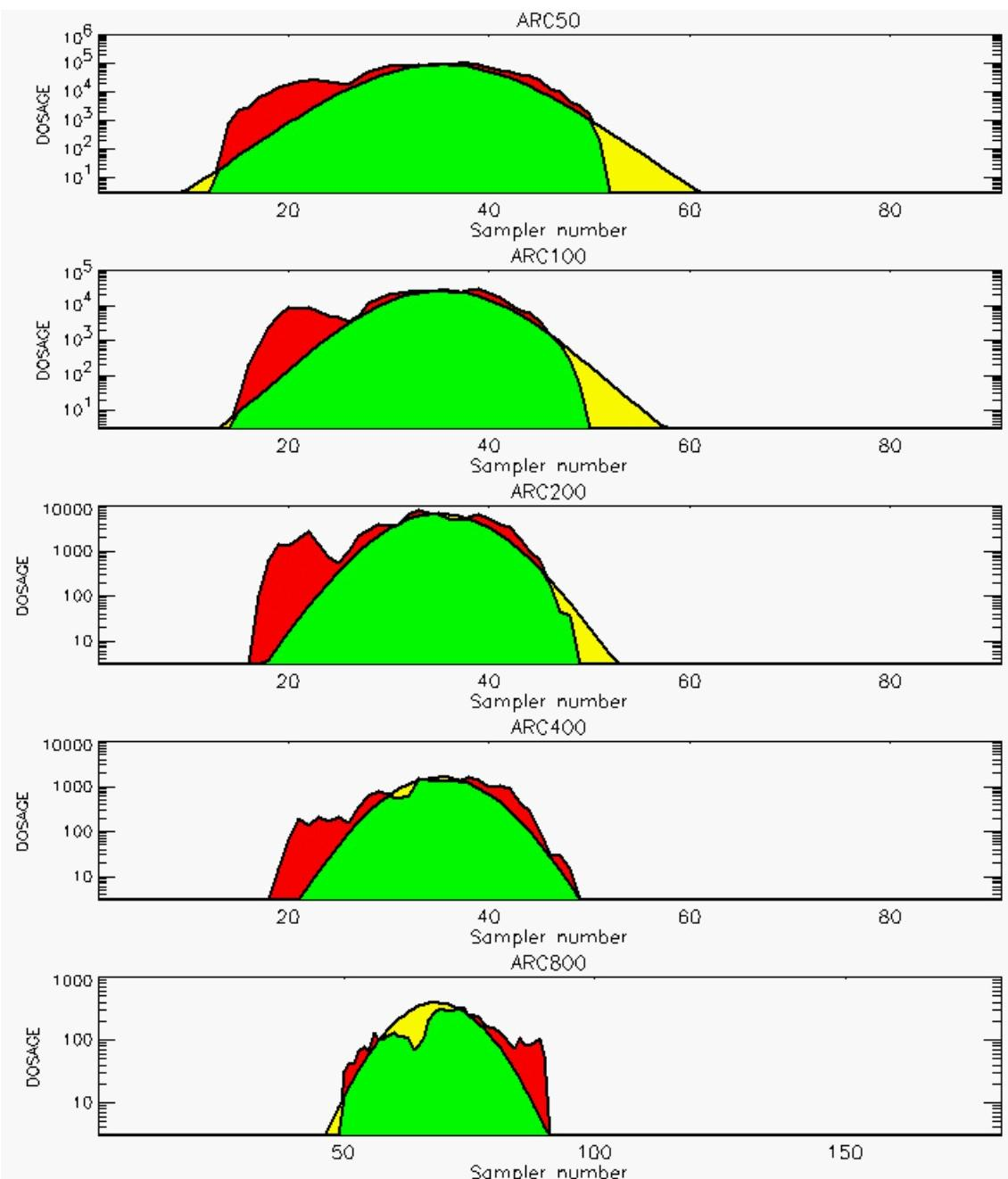


PG Observation to Prediction Comparison

PG Trial File: pr_grass_tracer_Experiment_44.txt

Prediction File: HPAC\nodeposition\pg_44_noxd.out

Figure C-36a. HPAC Prediction to Trial 44 on Linear Scale: Stability Category is 2

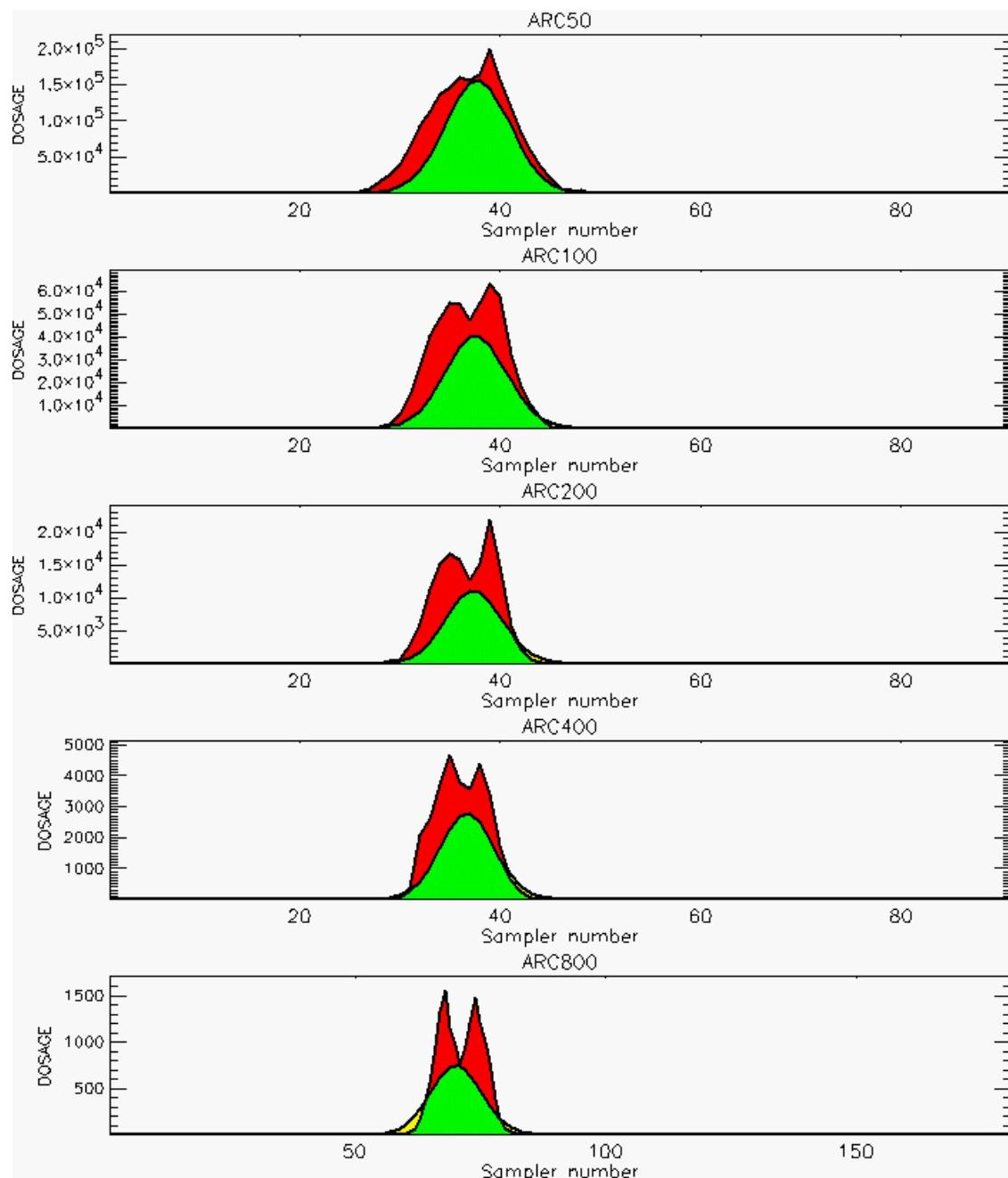


PG Observation to Prediction Comparison

PG Trial File: pr_grass_tracer_Experiment_44.txt

Prediction File: HPAC\nodeposition\pg_44_noxd.out

**Figure C-36b. HPAC Prediction to Trial 44 on Logarithmic Scale:
Stability Category is 2**

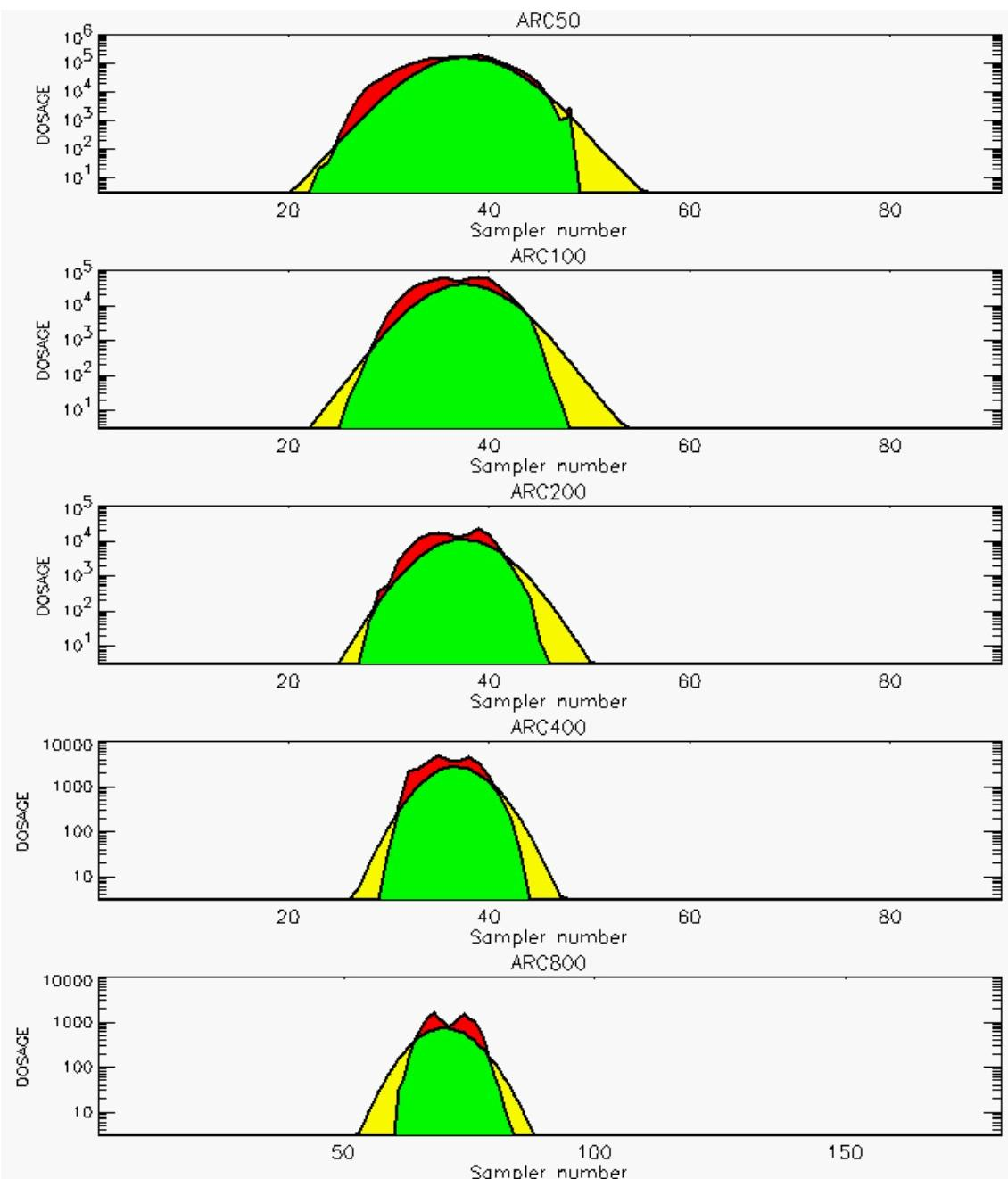


PG Observation to Prediction Comparison

PG Trial File: pr_grass_tracer_Experiment_45.txt

Prediction File: HPAC\nodeposition\pg_45_noxd.out

Figure C-37a. HPAC Prediction to Trial 45 on Linear Scale: Stability Category is 3

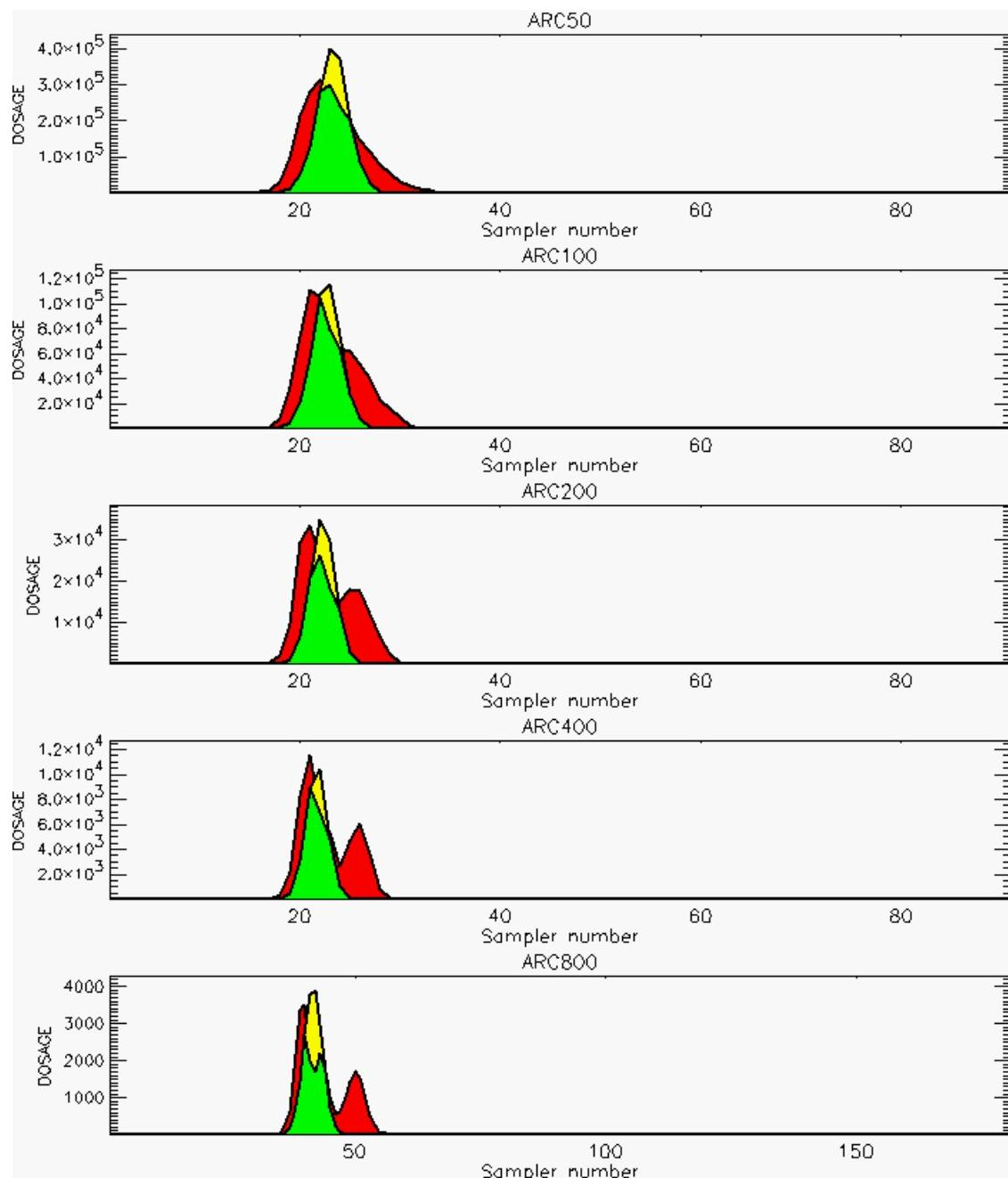


PG Observation to Prediction Comparison

PG Trial File: pr_grass_tracer_Experiment_45.txt

Prediction File: HPAC\nodeposition\pg_45_noxd.out

**Figure C-37b. HPAC Prediction to Trial 45 on Logarithmic Scale:
Stability Category is 3**

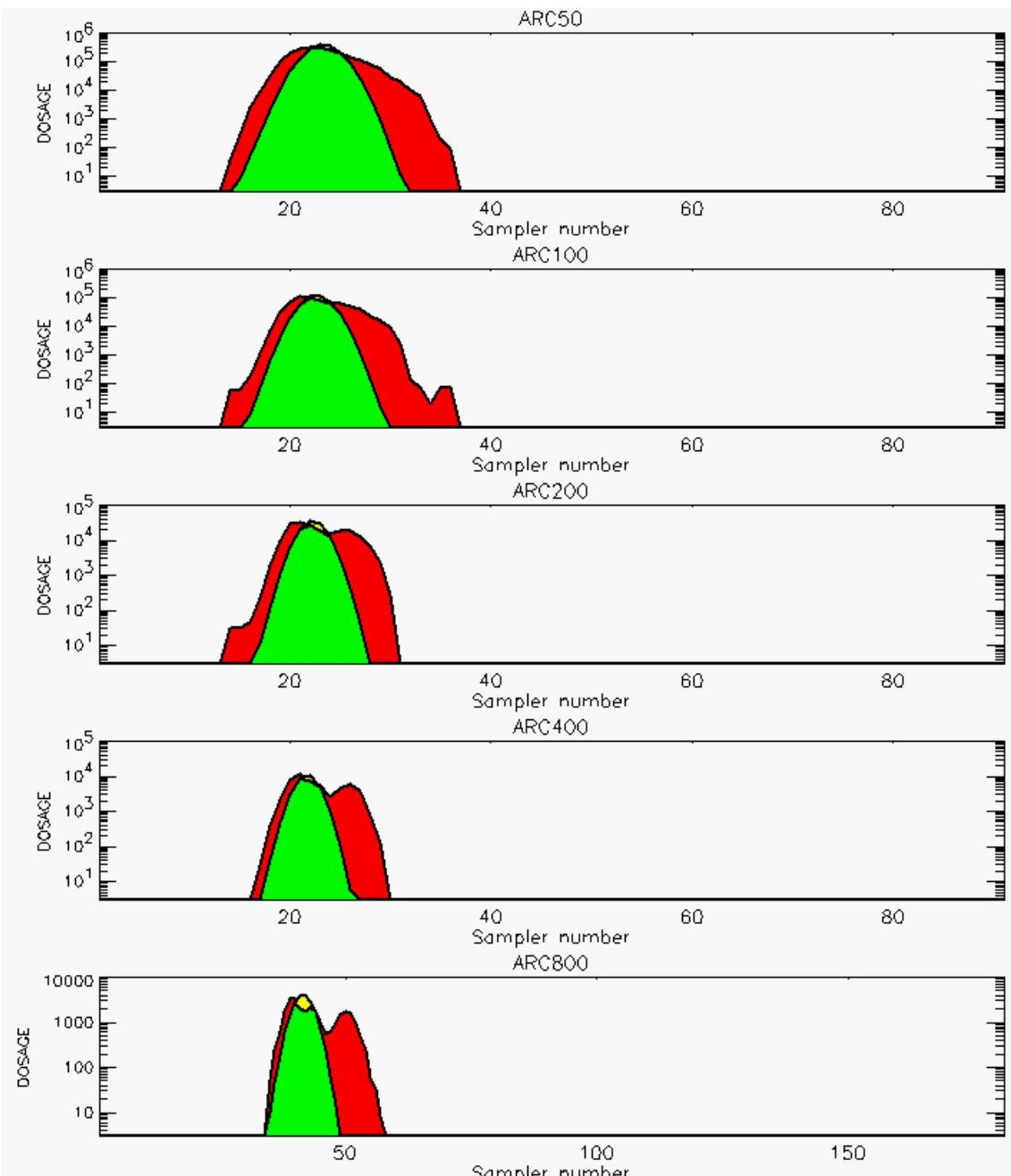


PG Observation to Prediction Comparison

PG Trial File: pr_grass_tracer_Experiment_46.txt

Prediction File: HPAC\nodeposition\pg_46_noxd.out

Figure C-38a. HPAC Prediction to Trial 46 on Linear Scale: Stability Category is 4

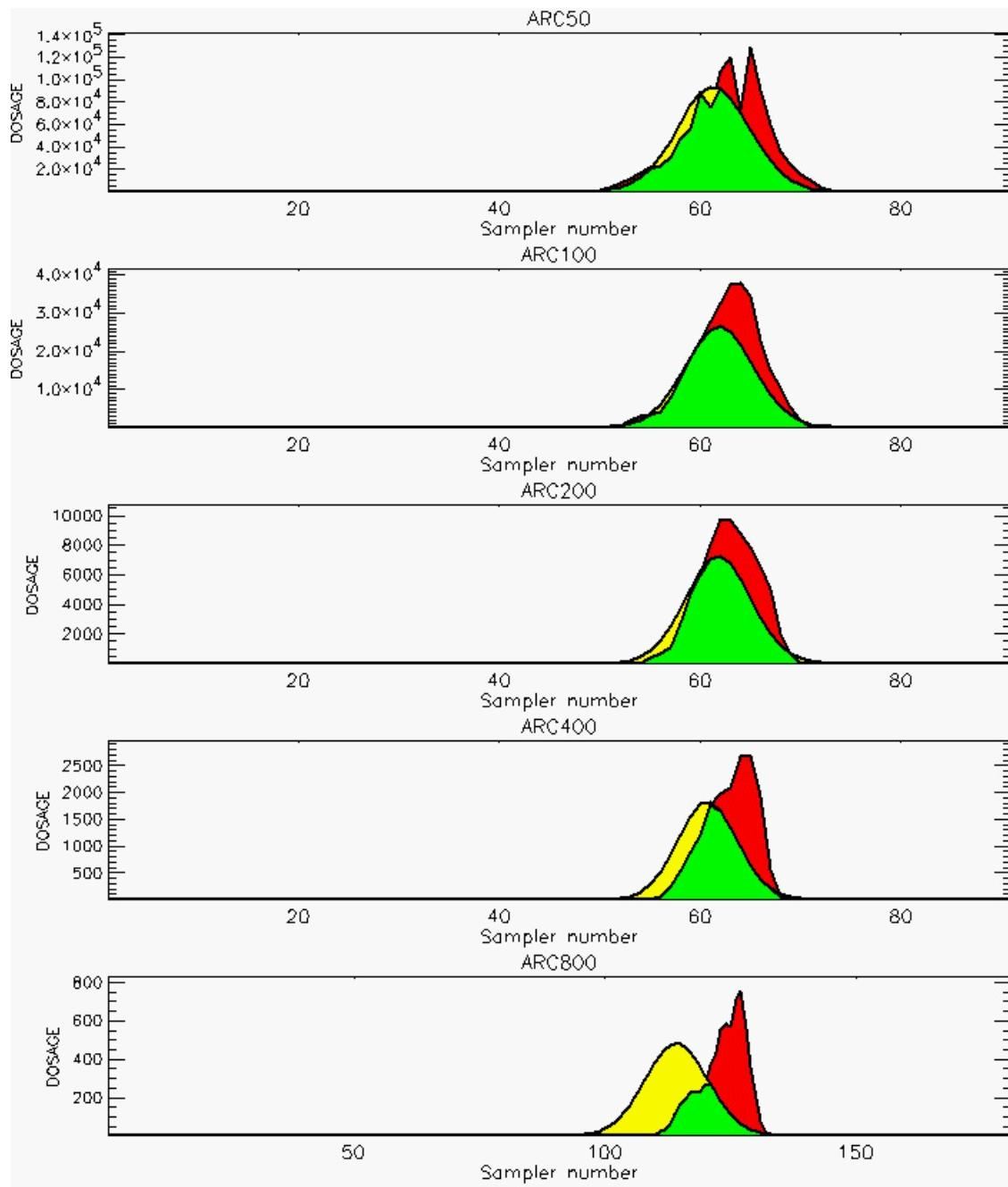


PG Observation to Prediction Comparison

PG Trial File: pr_grass_tracer_Experiment_46.txt

Prediction File: HPAC\nodeposition\pg_46_noxd.out

**Figure C-38b. HPAC Prediction to Trial 46 on Logarithmic Scale:
Stability Category is 4**

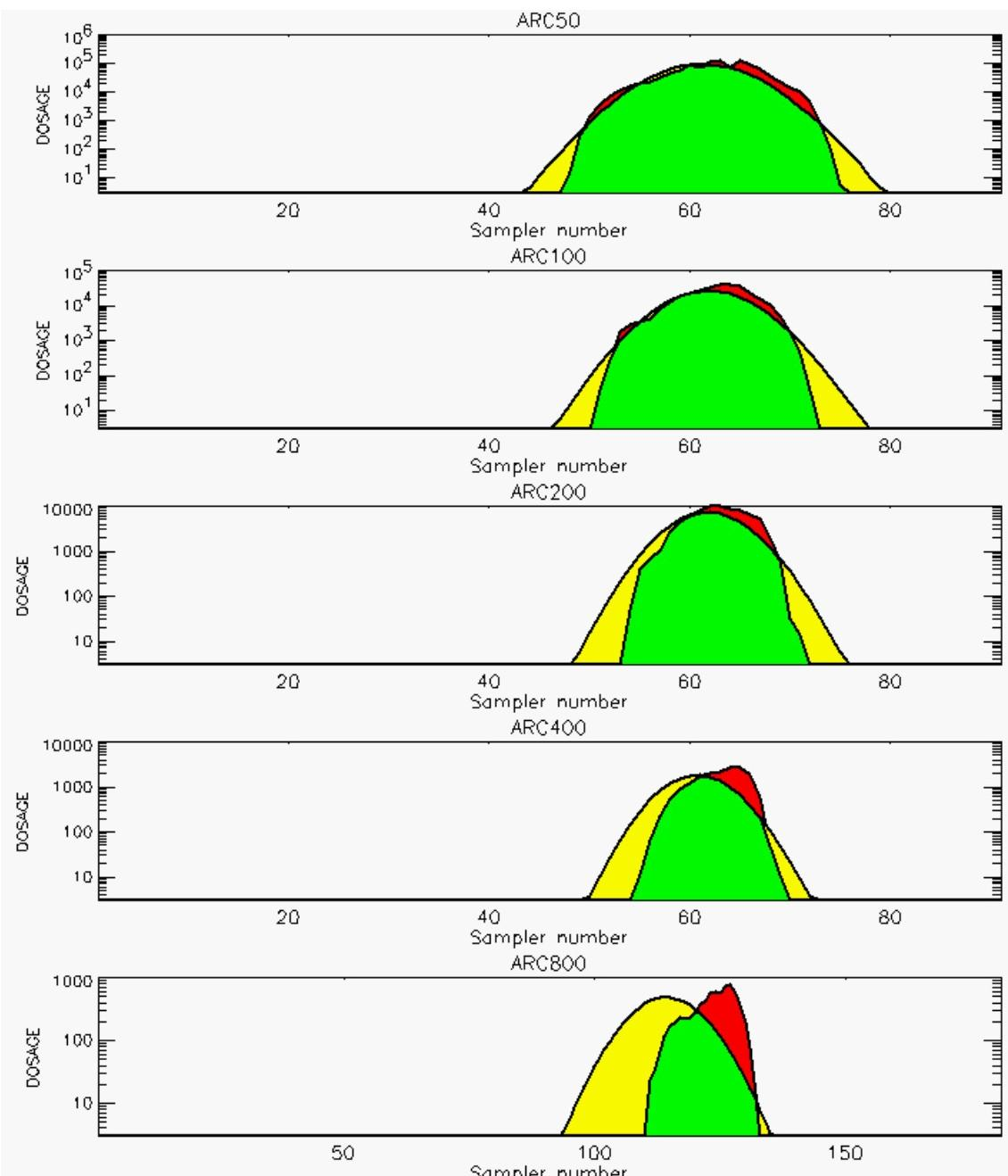


PG Observation to Prediction Comparison

PG Trial File: pr_grass_tracer_Experiment_48.txt

Prediction File: HPAC\nodeposition\pg_48_noxd.out

Figure C-39a. HPAC Prediction to Trial 48 on Linear Scale: Stability Category is 3

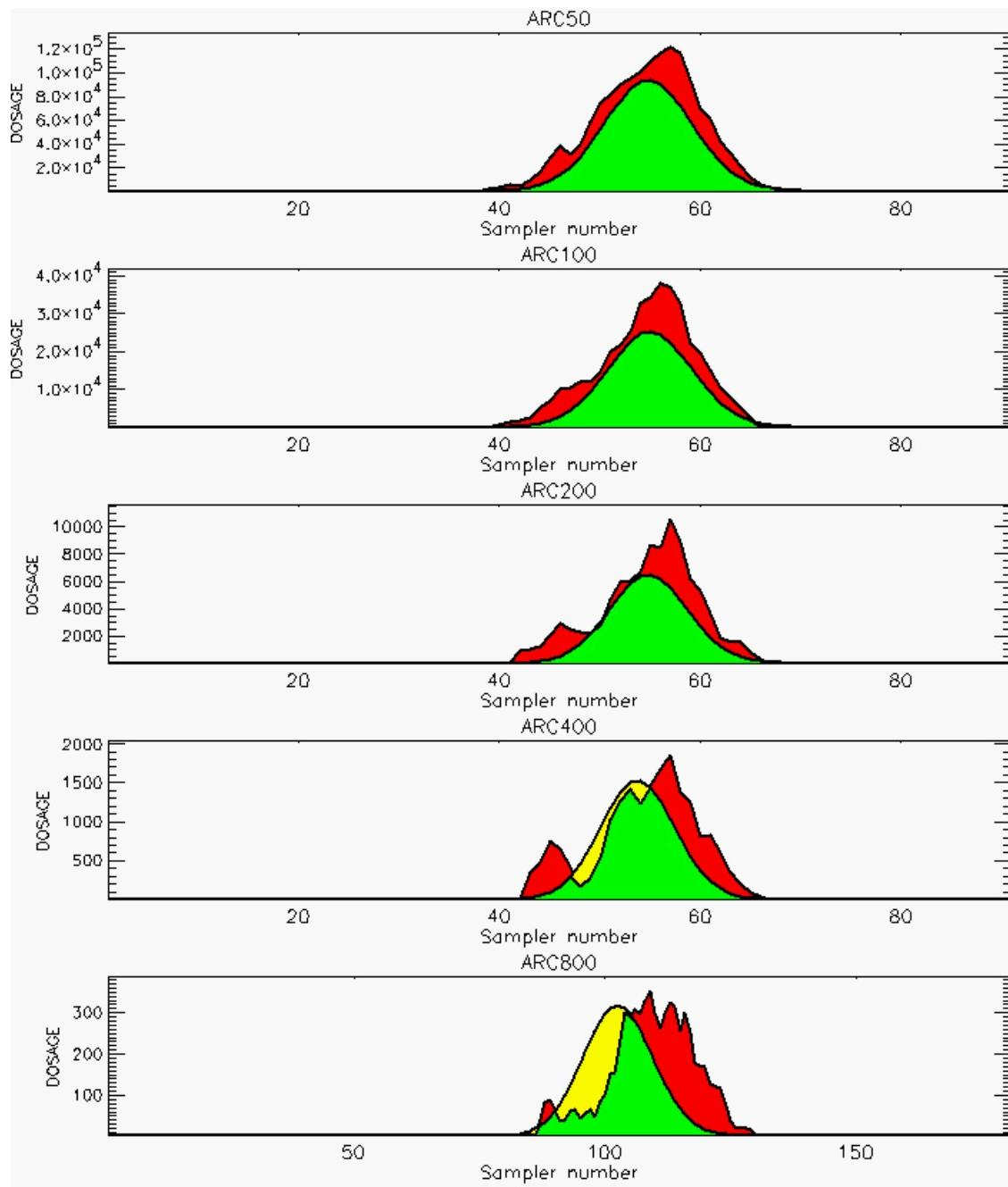


PG Observation to Prediction Comparison

PG Trial File: pr_grass_tracer_Experiment_48.txt

Prediction File: HPAC\nodeposition\pg_48_noxd.out

**Figure C-39b. HPAC Prediction to Trial 48 on Logarithmic Scale:
Stability Category is 3**

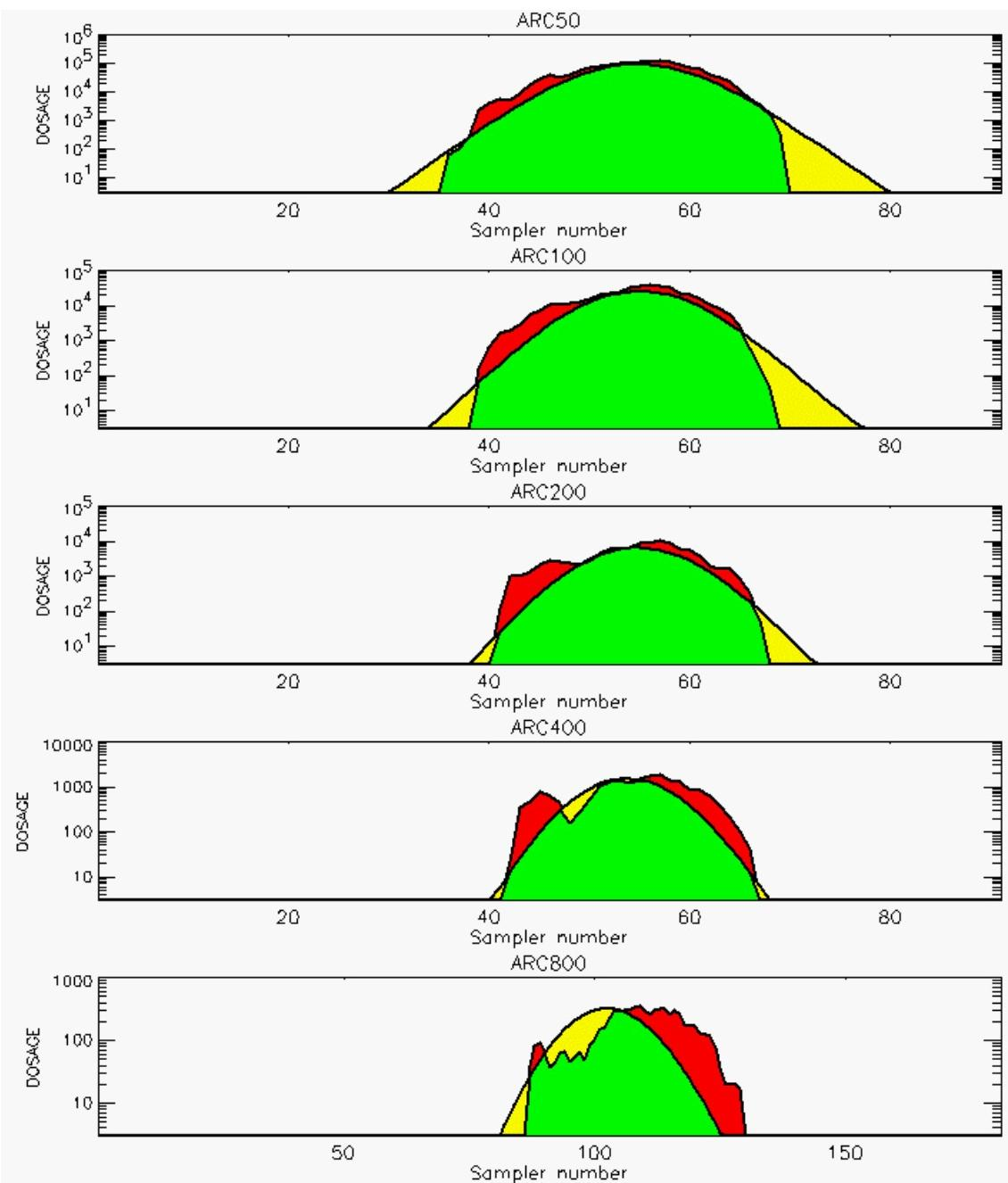


PG Observation to Prediction Comparison

PG Trial File: pr_grass_tracer_Experiment_49.txt

Prediction File: HPAC\nodeposition\pg_49_noxd.out

Figure C-40a. HPAC Prediction to Trial 49 on Linear Scale: Stability Category is 2

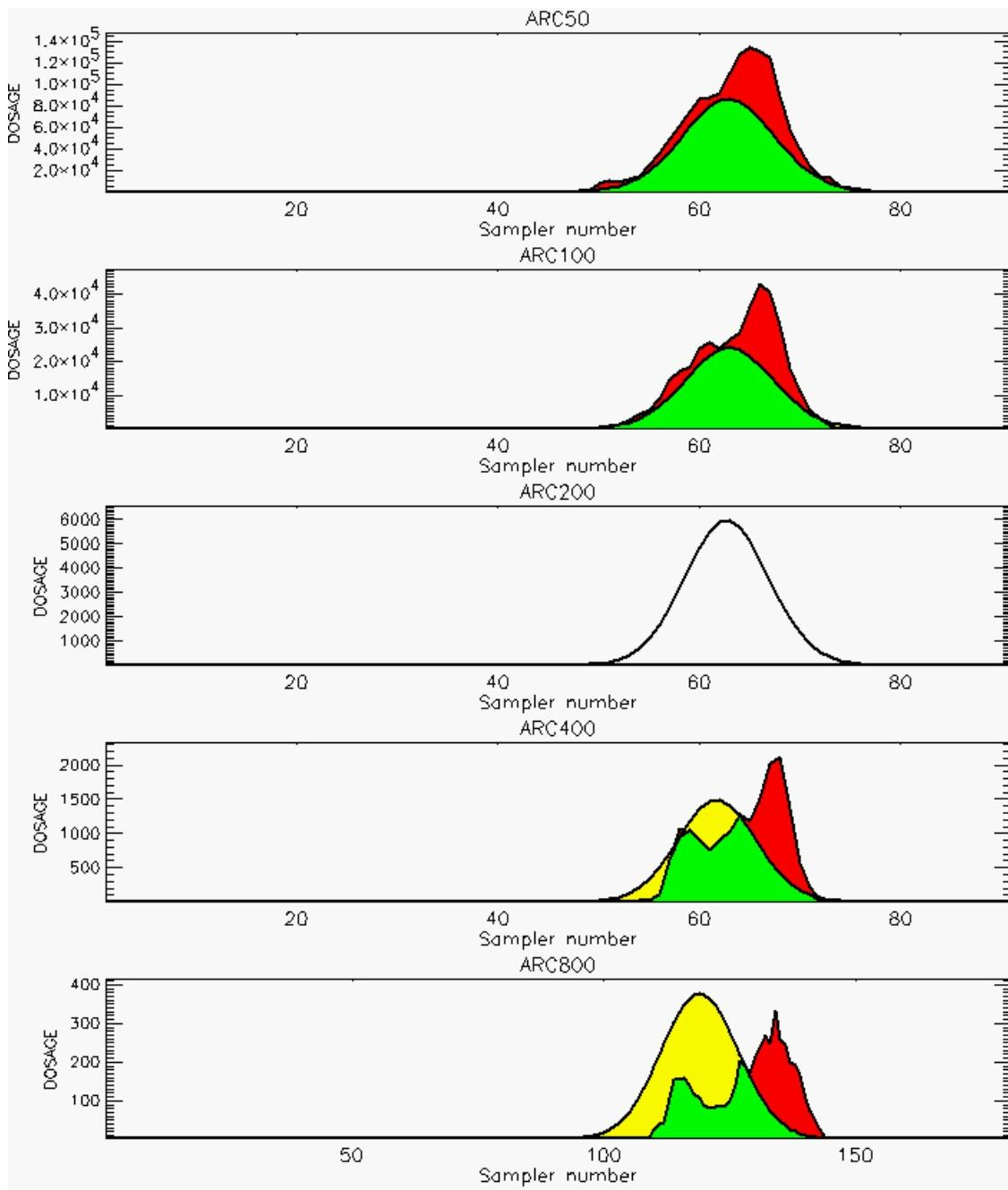


PG Observation to Prediction Comparison

PG Trial File: pr_grass_tracer_Experiment_49.txt

Prediction File: HPAC\nodeposition\pg_49_noxd.out

**Figure C-40b. HPAC Prediction to Trial 49 on Logarithmic Scale:
Stability Category is 2**

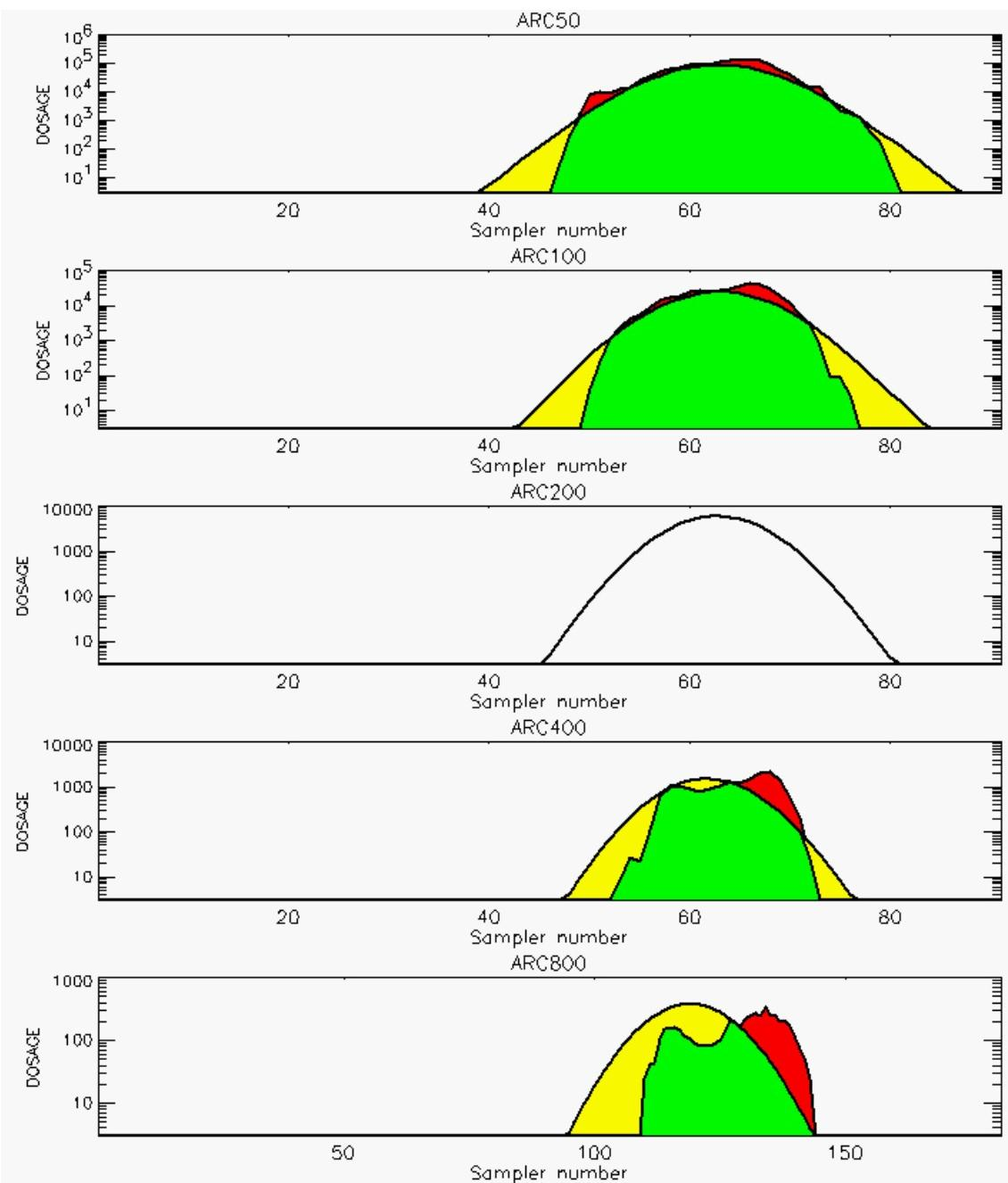


PG Observation to Prediction Comparison

PG Trial File: pr_grass_tracer_Experiment_50.txt

Prediction File: HPAC\nodeposition\pg_50_noxd.out

Figure C-41a. HPAC Prediction to Trial 50 on Linear Scale: Stability Category is 2 (Values for Samplers of 200-Meter Arc are Replaced by Missing Values [Ref. C-2])

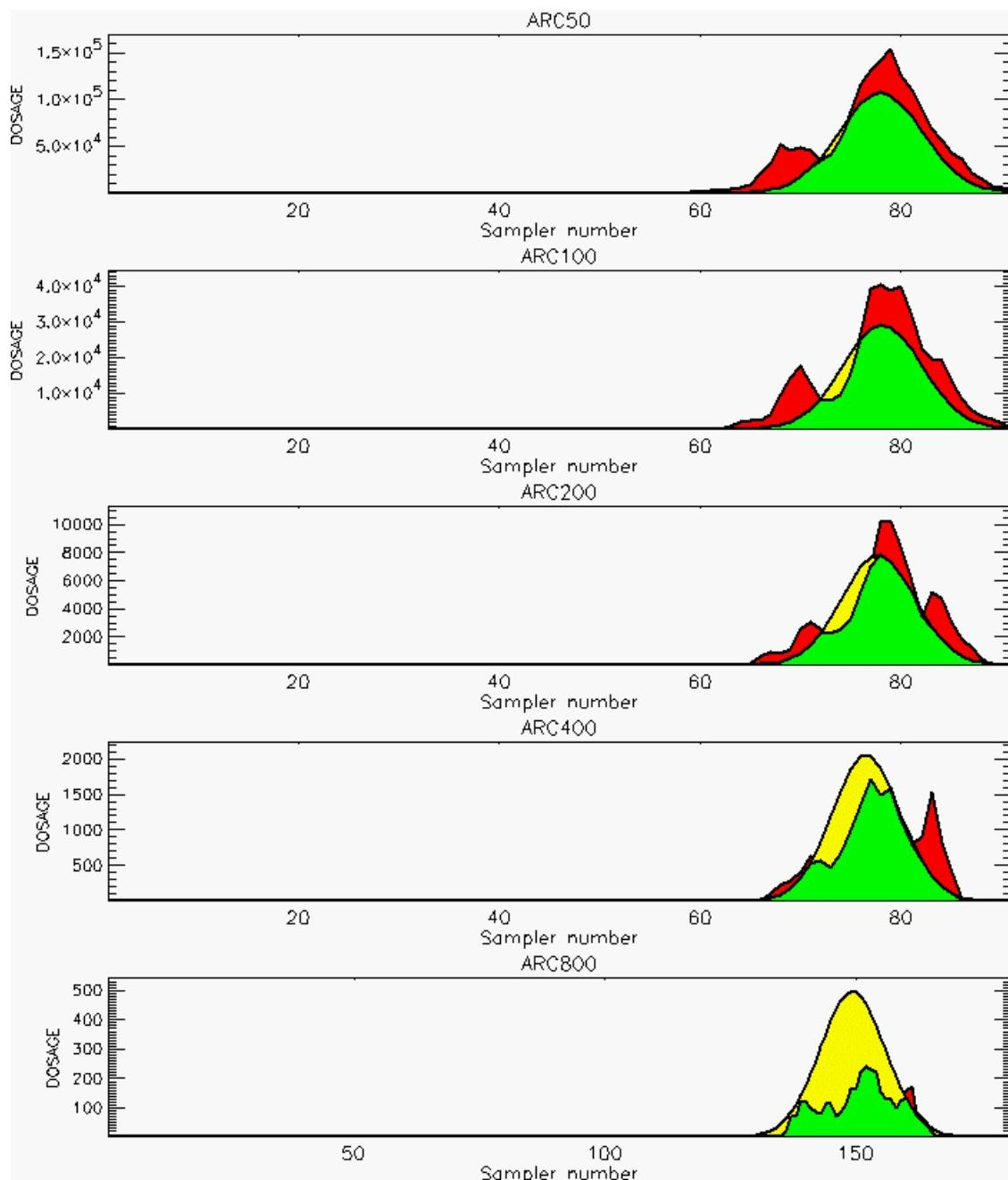


PG Observation to Prediction Comparison

PG Trial File: pr_grass_tracer_Experiment_50.txt

Prediction File: HPAC\nodeposition\pg_50_noxd.out

Figure C-41b. HPAC Prediction to Trial 50 on Logarithmic Scale: Stability Category is 2 (Values for Samplers of 200-Meter Arc are Replaced by Missing Values [Ref. C-2])

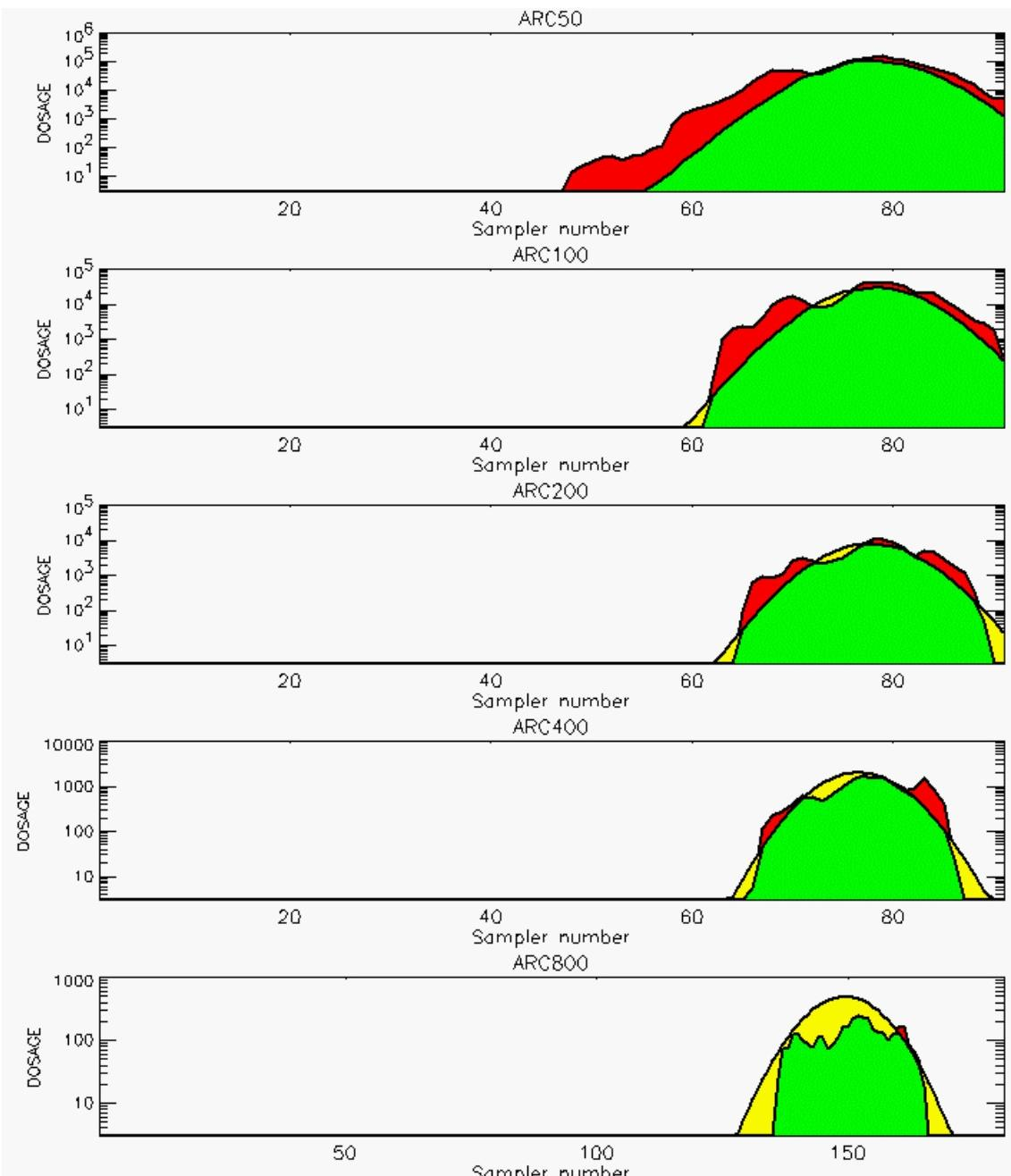


PG Observation to Prediction Comparison

PG Trial File: pr_grass_tracer_Experiment_51.txt

Prediction File: HPAC\nodeposition\pg_51_noxd.out

Figure C-42a. HPAC Prediction to Trial 51 on Linear Scale: Stability Category is 2

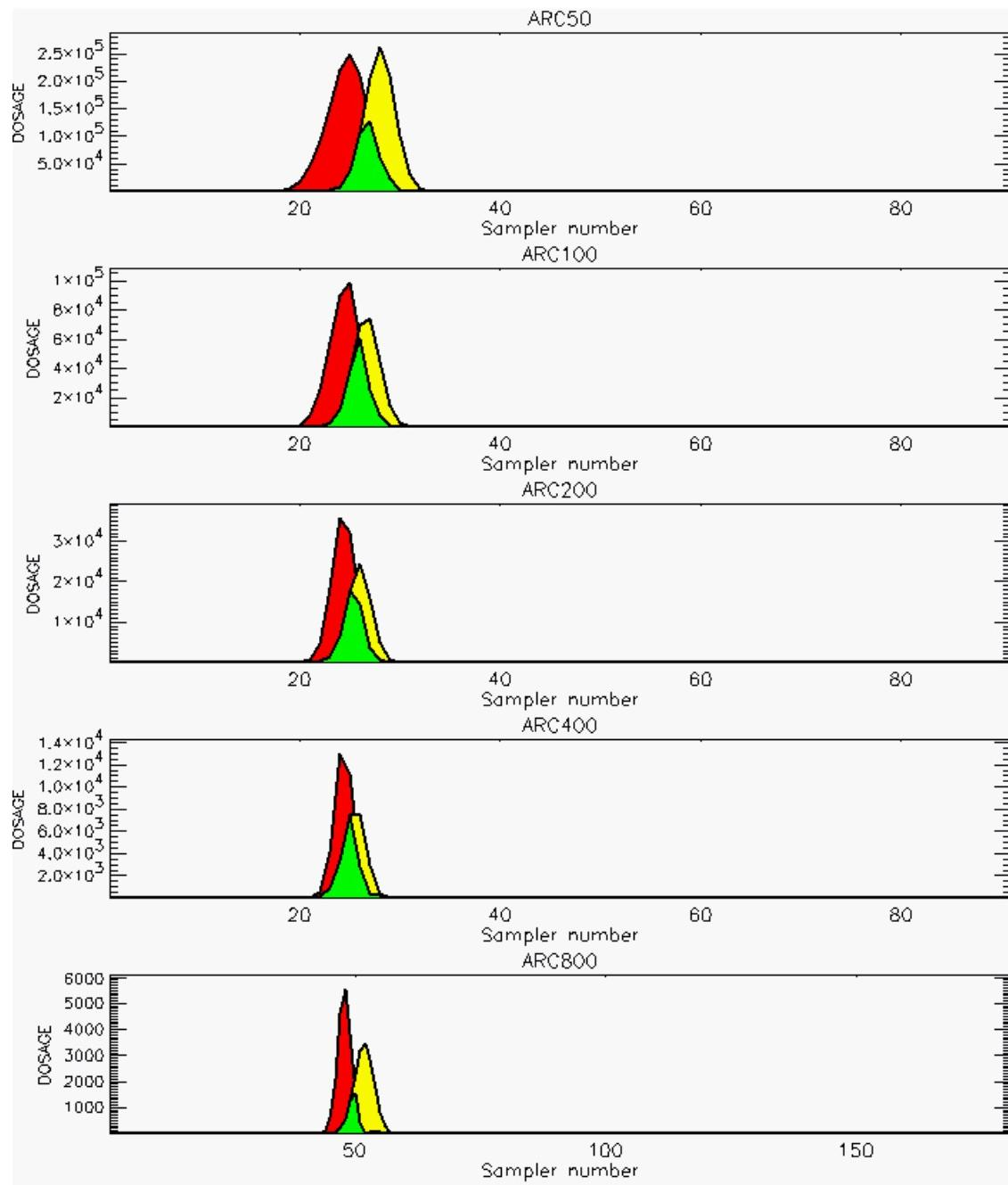


PG Observation to Prediction Comparison

PG Trial File: pr_grass_tracer_Experiment_51.txt

Prediction File: HPAC\nodeposition\pg_51_noxd.out

**Figure C-42b. HPAC Prediction to Trial 51 on Logarithmic Scale:
Stability Category is 2**

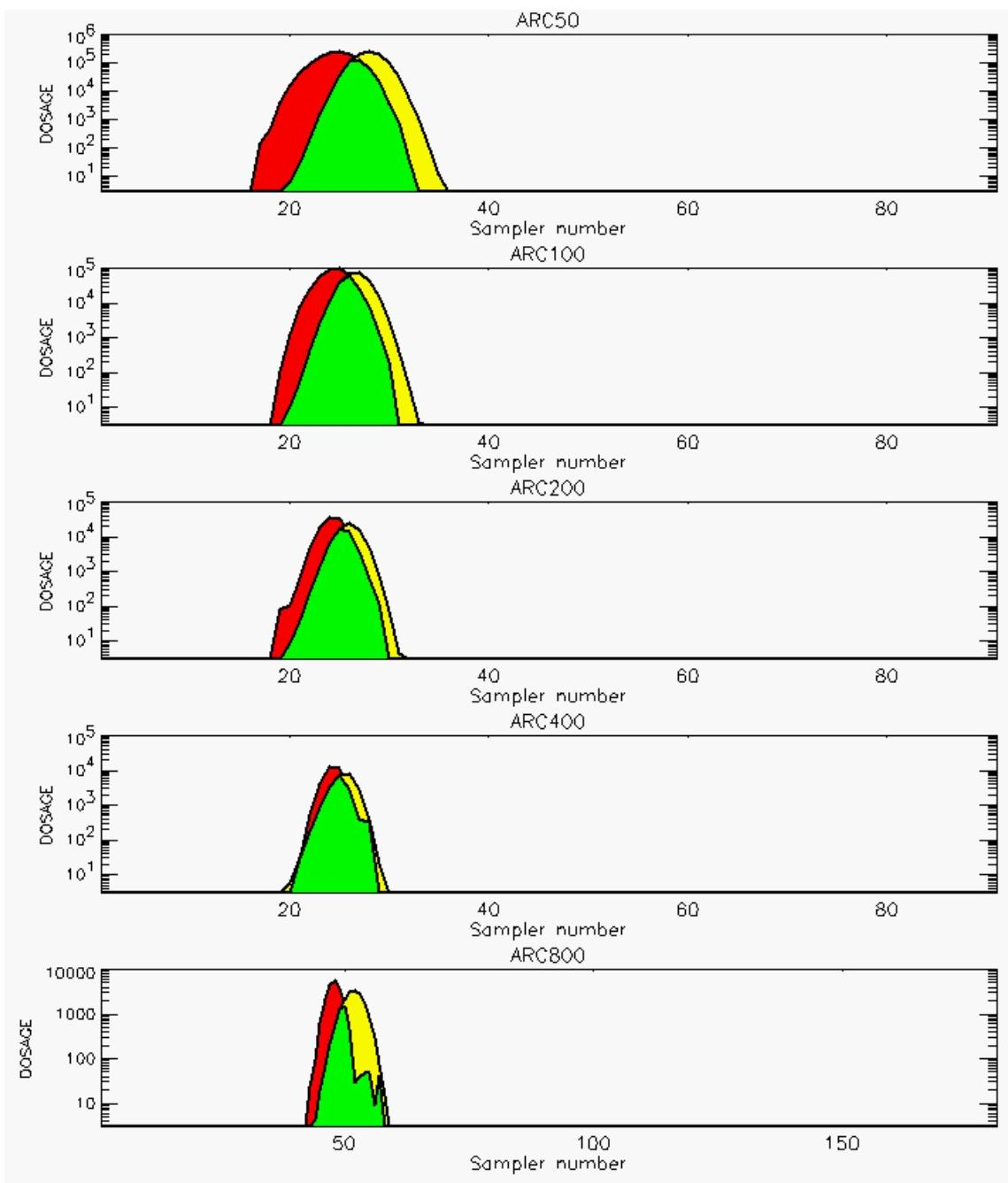


PG Observation to Prediction Comparison

PG Trial File: pr_grass_tracer_Experiment_54.txt

Prediction File: HPAC\nodeposition\pg_54_noxd.out

Figure C-43a. HPAC Prediction to Trial 54 on Linear Scale: Stability Category is 5

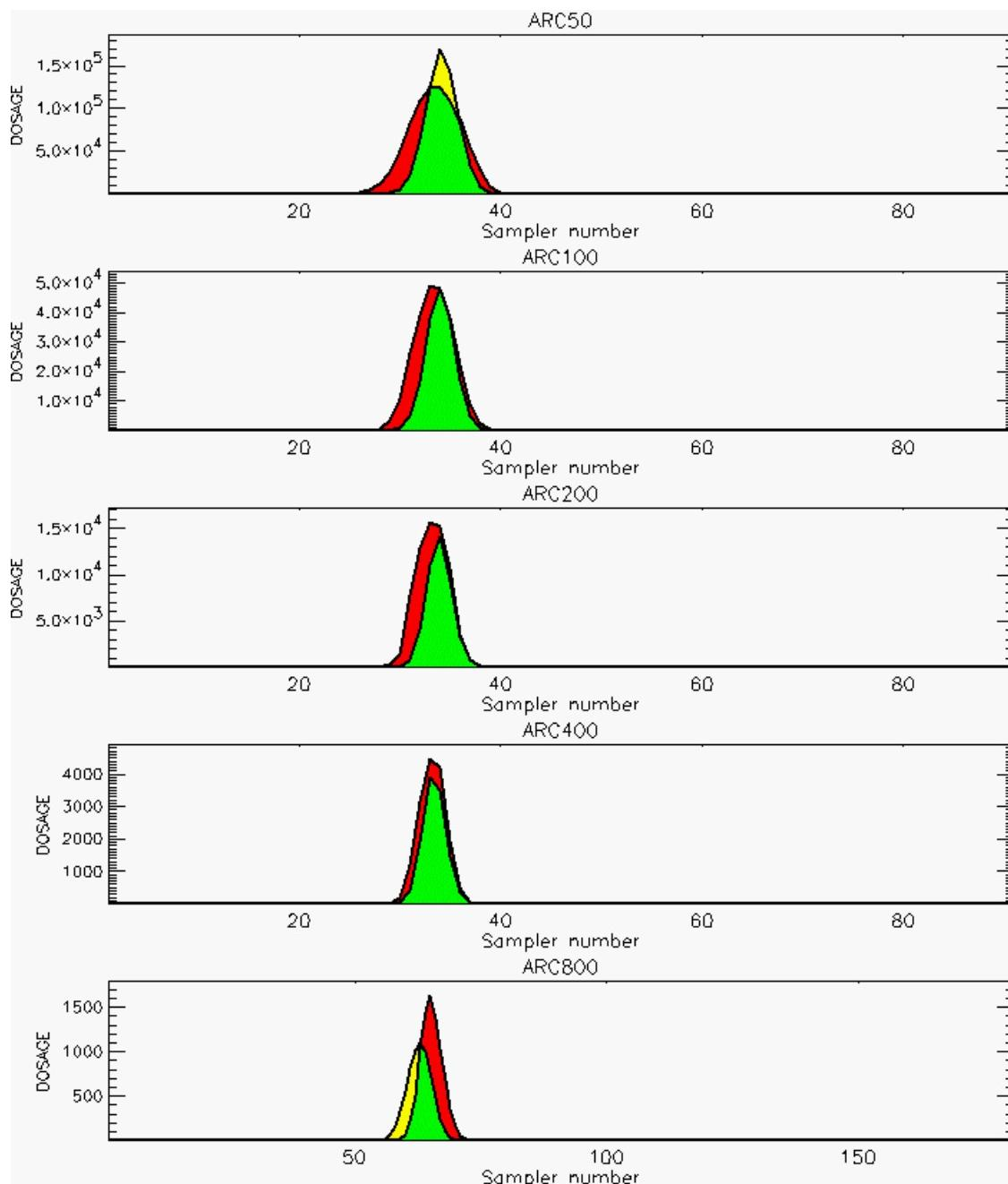


PG Observation to Prediction Comparison

PG Trial File: pr_grass_tracer_Experiment_54.txt

Prediction File: HPAC\nodeposition\pg_54_noxd.out

Figure C-43b. HPAC Prediction to Trial 54 on Logarithmic Scale:
Stability Category is 5

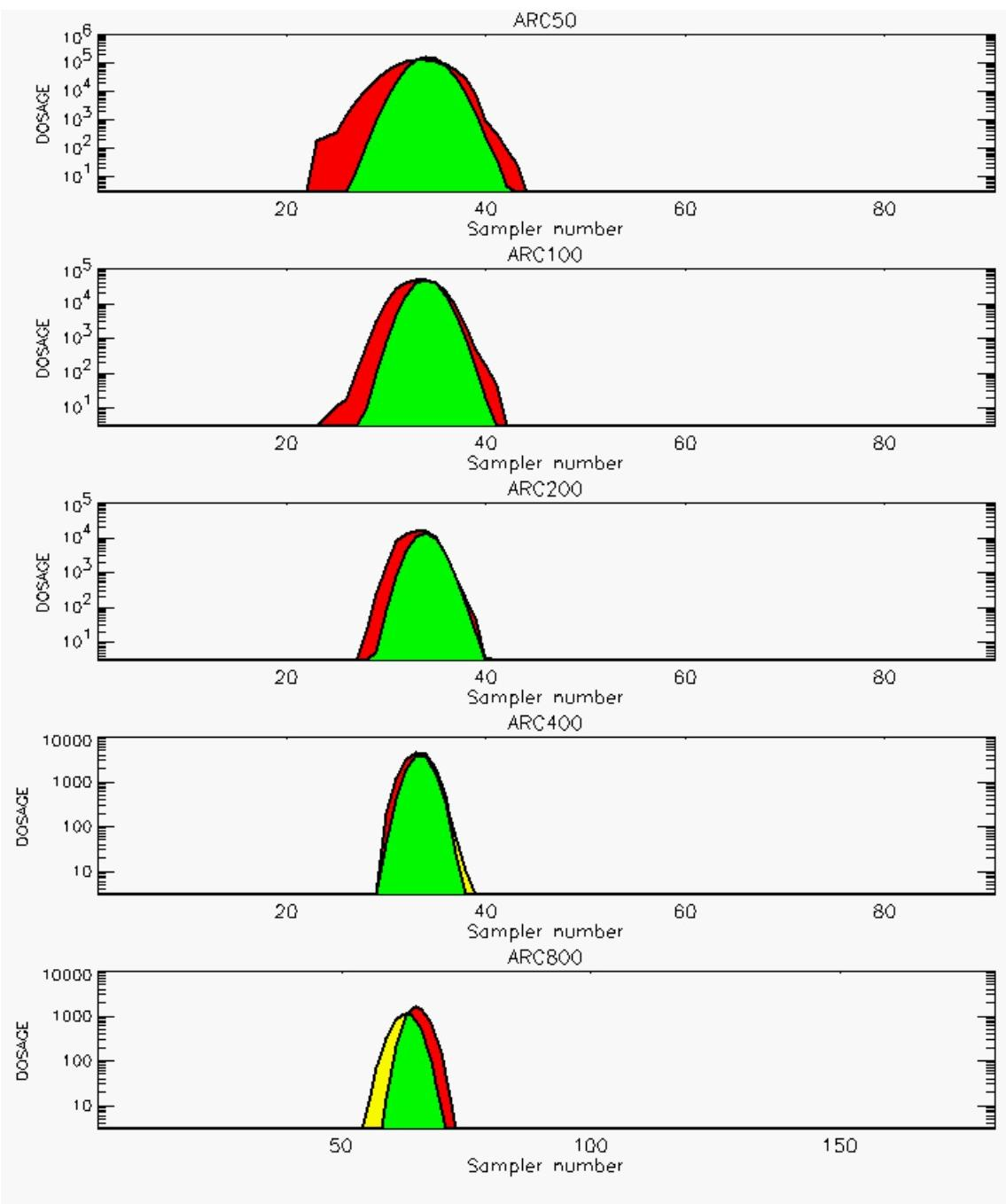


PG Observation to Prediction Comparison

PG Trial File: pr_grass_tracer_Experiment_55.txt

Prediction File: HPAC\nodeposition\pg_55_noxd.out

Figure C-44a. HPAC Prediction to Trial 55 on Linear Scale: Stability Category is 4

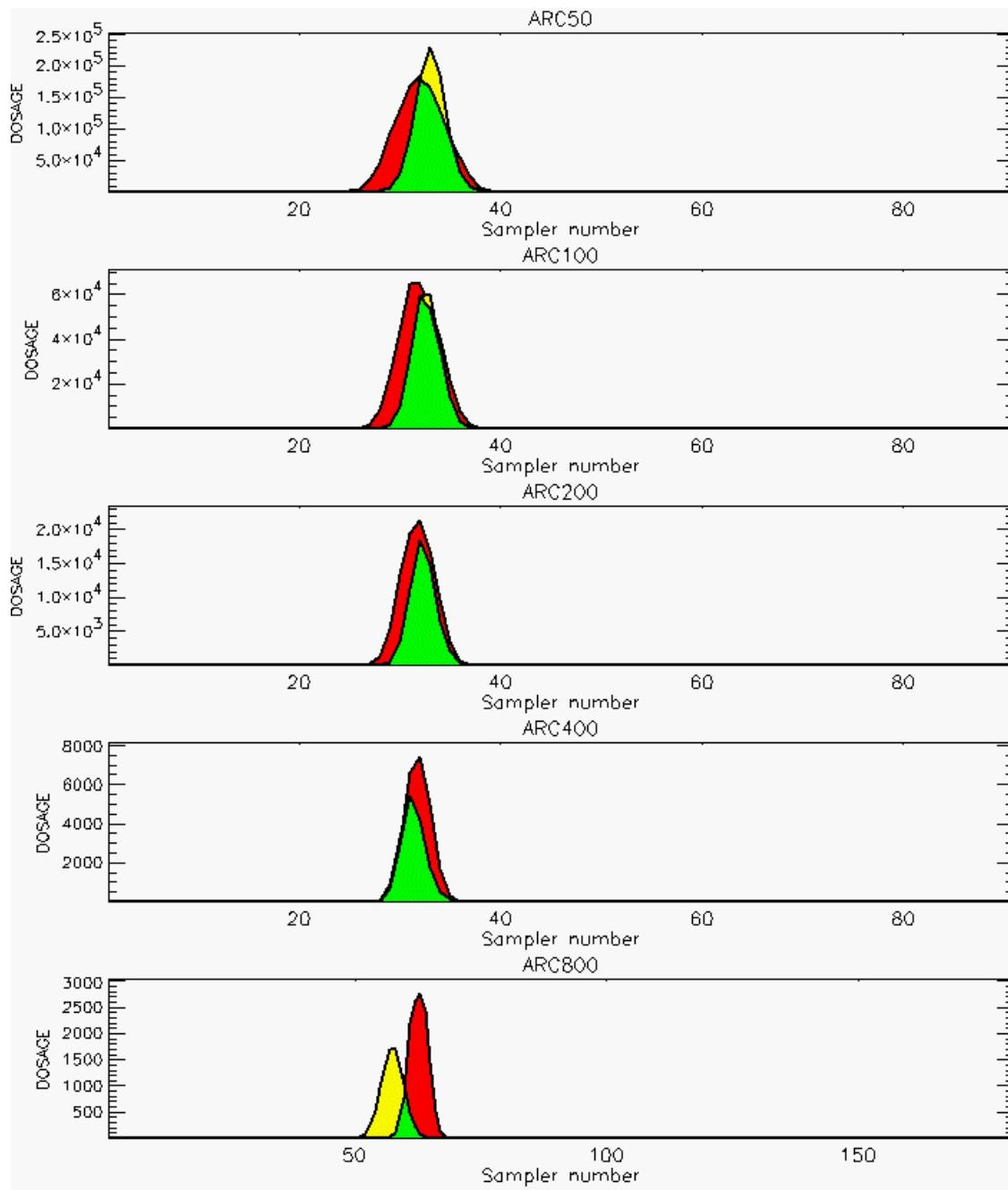


PG Observation to Prediction Comparison

PG Trial File: pr_grass_tracer_Experiment_55.txt

Prediction File: HPAC\nodeposition\pg_55_noxd.out

**Figure C-44b. HPAC Prediction to Trial 55 on Logarithmic Scale:
Stability Category is 4**

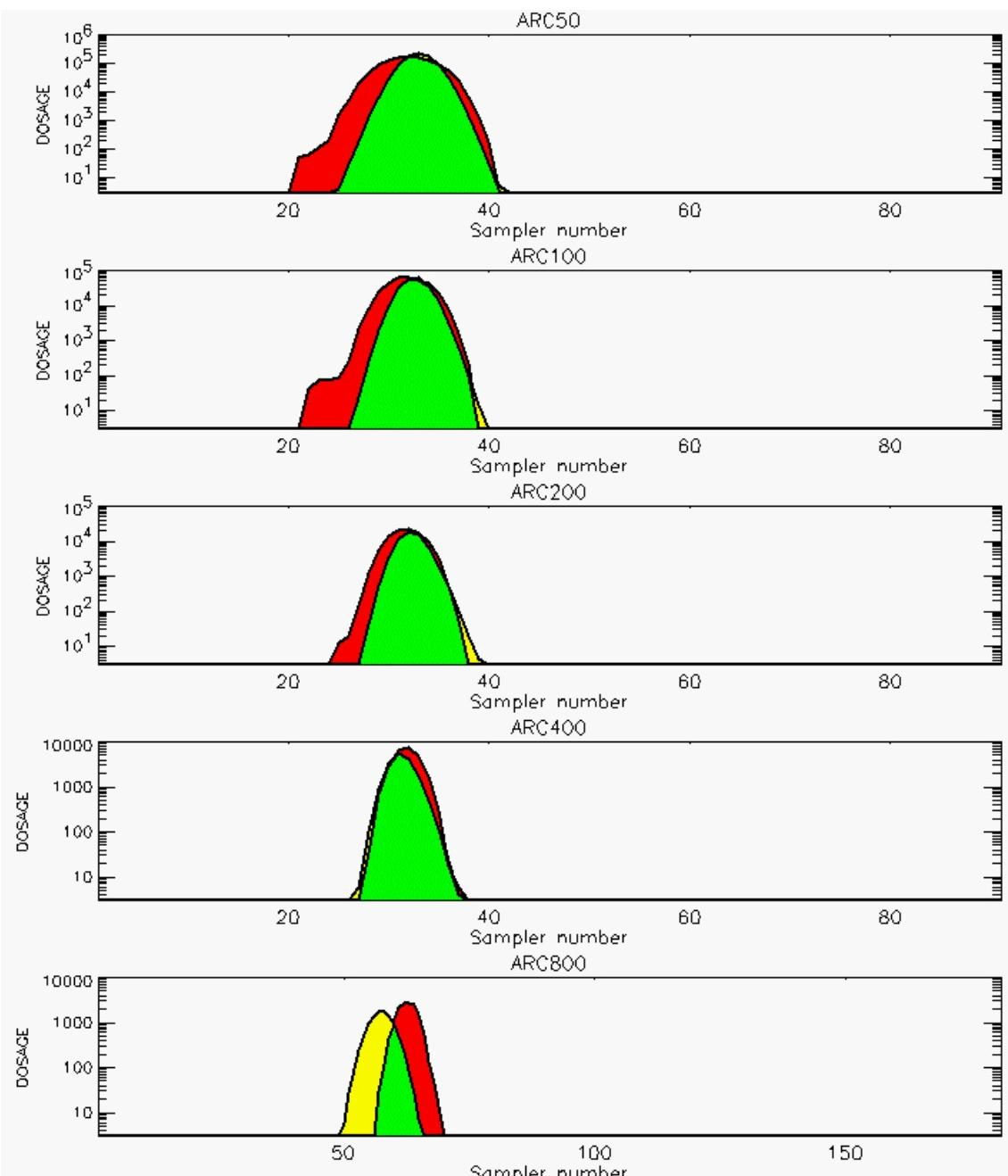


PG Observation to Prediction Comparison

PG Trial File: pr_grass_tracer_Experiment_56.txt

Prediction File: HPAC\nodeposition\pg_56_noxd.out

Figure C-45a. HPAC Prediction to Trial 56 on Linear Scale: Stability Category is 4

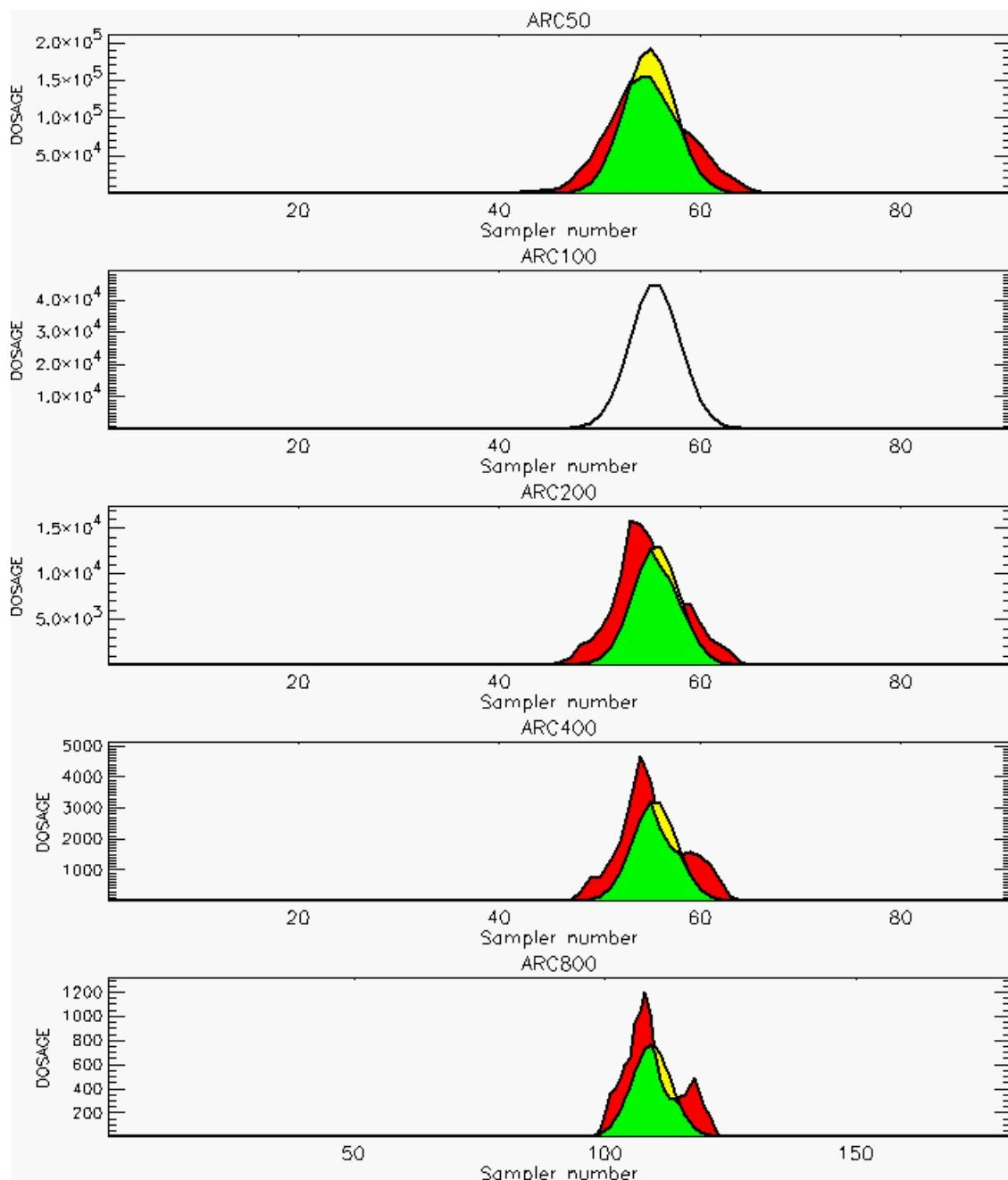


PG Observation to Prediction Comparison

PG Trial File: pr_grass_tracer_Experiment_56.txt

Prediction File: HPAC\nodeposition\pg_56_noxd.out

**Figure C-45b. HPAC Prediction to Trial 56 on Logarithmic Scale:
Stability Category is 4**

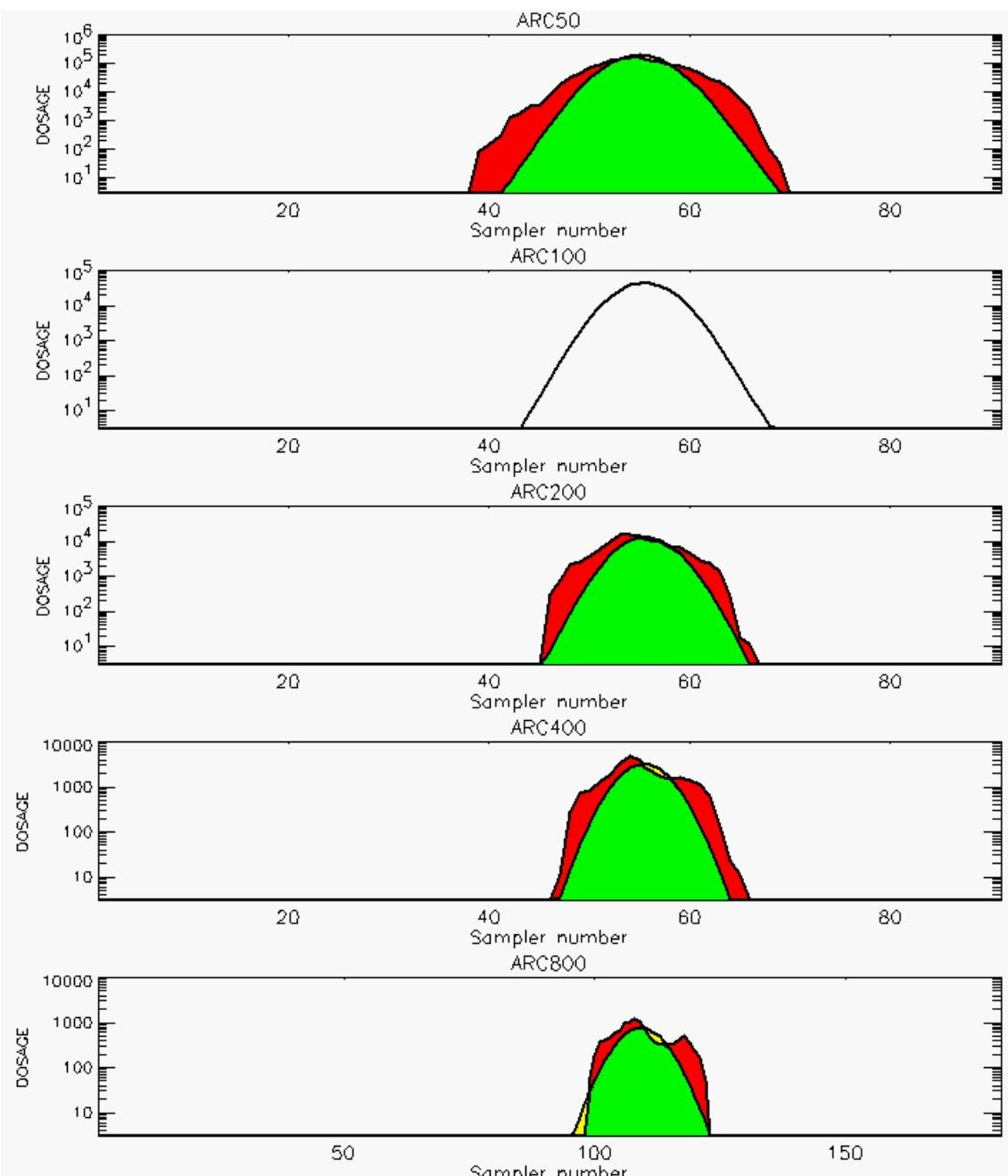


PG Observation to Prediction Comparison

PG Trial File: pr_grass_tracer_Experiment_57.txt

Prediction File: HPAC\nodeposition\pg_57_noxd.out

Figure C-46a. HPAC Prediction to Trial 57 on Linear Scale: Stability Category is 3 (Values for Sampler of 100-Meter Arc are Replaced by Missing Values [Ref. C-2])

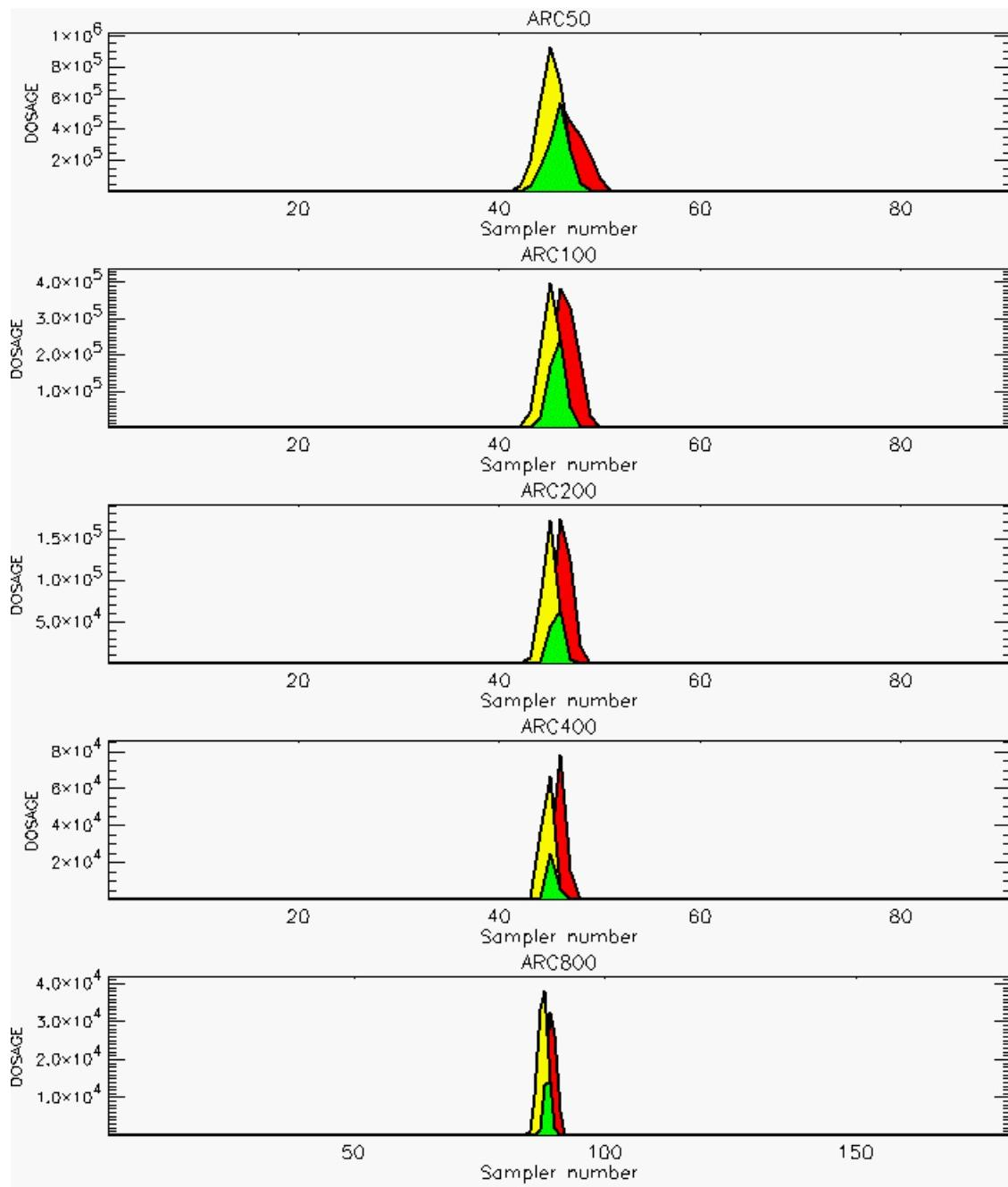


PG Observation to Prediction Comparison

PG Trial File: pr_grass_tracer_Experiment_57.txt

Prediction File: HPAC\nodeposition\pg_57_noxd.out

Figure C-46b. HPAC Prediction to Trial 57 on Logarithmic Scale: Stability Category is 3 (Values for Sampler of 100-Meter Arc are Replaced by Missing Values [Ref. C-2])

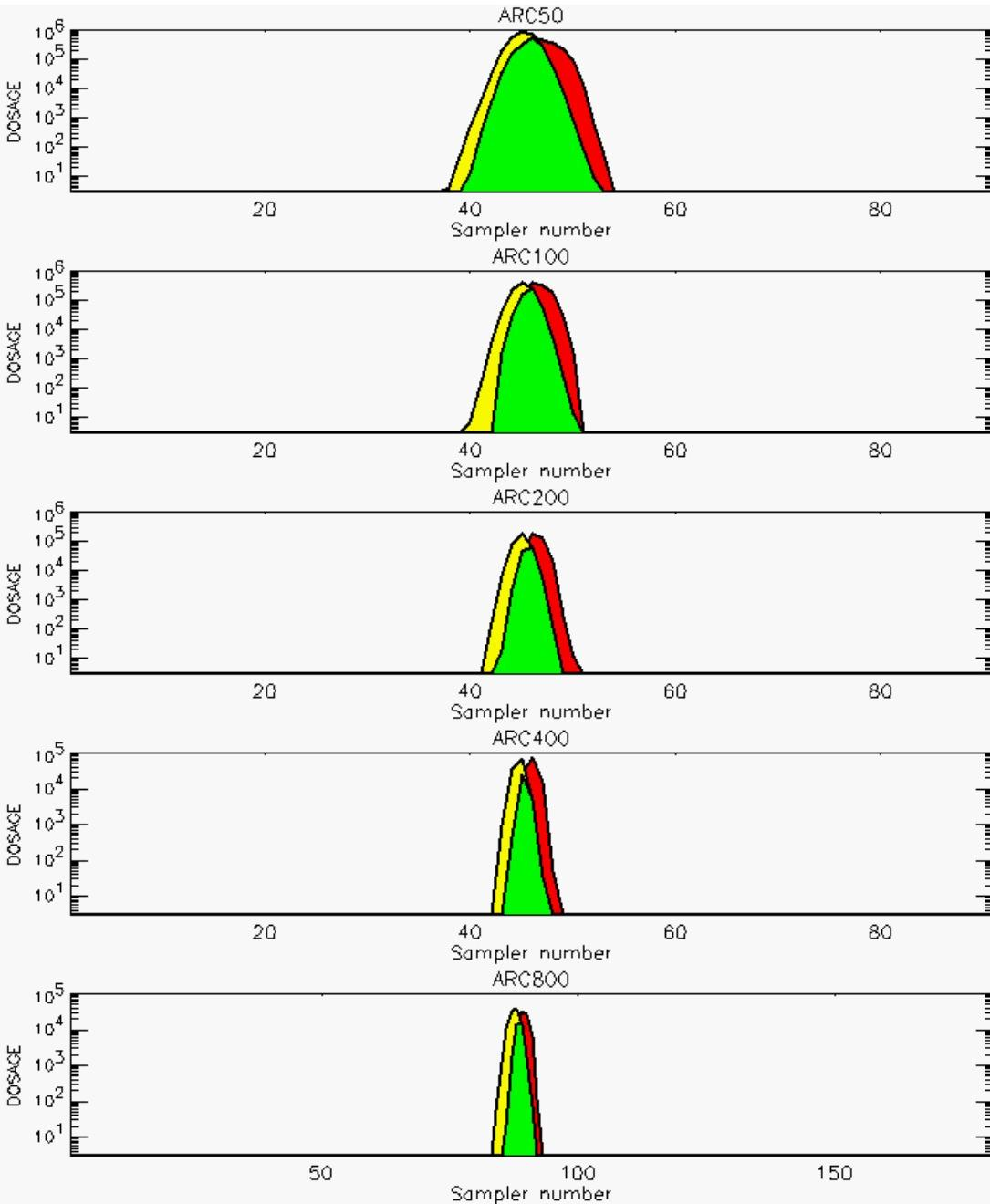


PG Observation to Prediction Comparison

PG Trial File: pr_grass_tracer_Experiment_58.txt

Prediction File: HPAC\nodeposition\pg_58_noxd.out

Figure C-47a. HPAC Prediction to Trial 58 on Linear Scale: Stability Category is 6

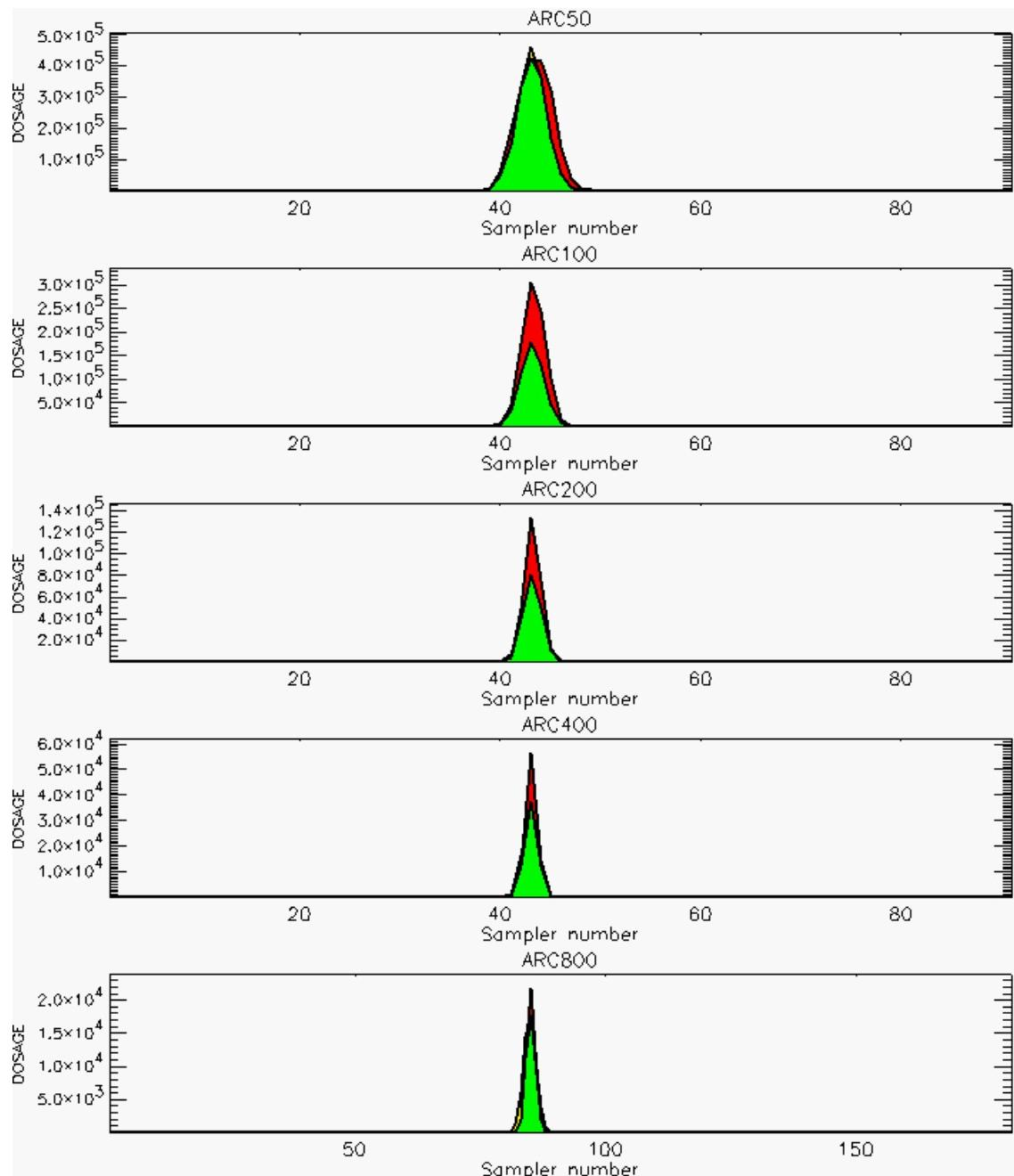


PG Observation to Prediction Comparison

PG Trial File: pr_grass_tracer_Experiment_58.txt

Prediction File: HPAC\nodeposition\pg_58_noxd.out

**Figure C-47b. HPAC Prediction to Trial 58 on Logarithmic Scale:
Stability Category is 6**

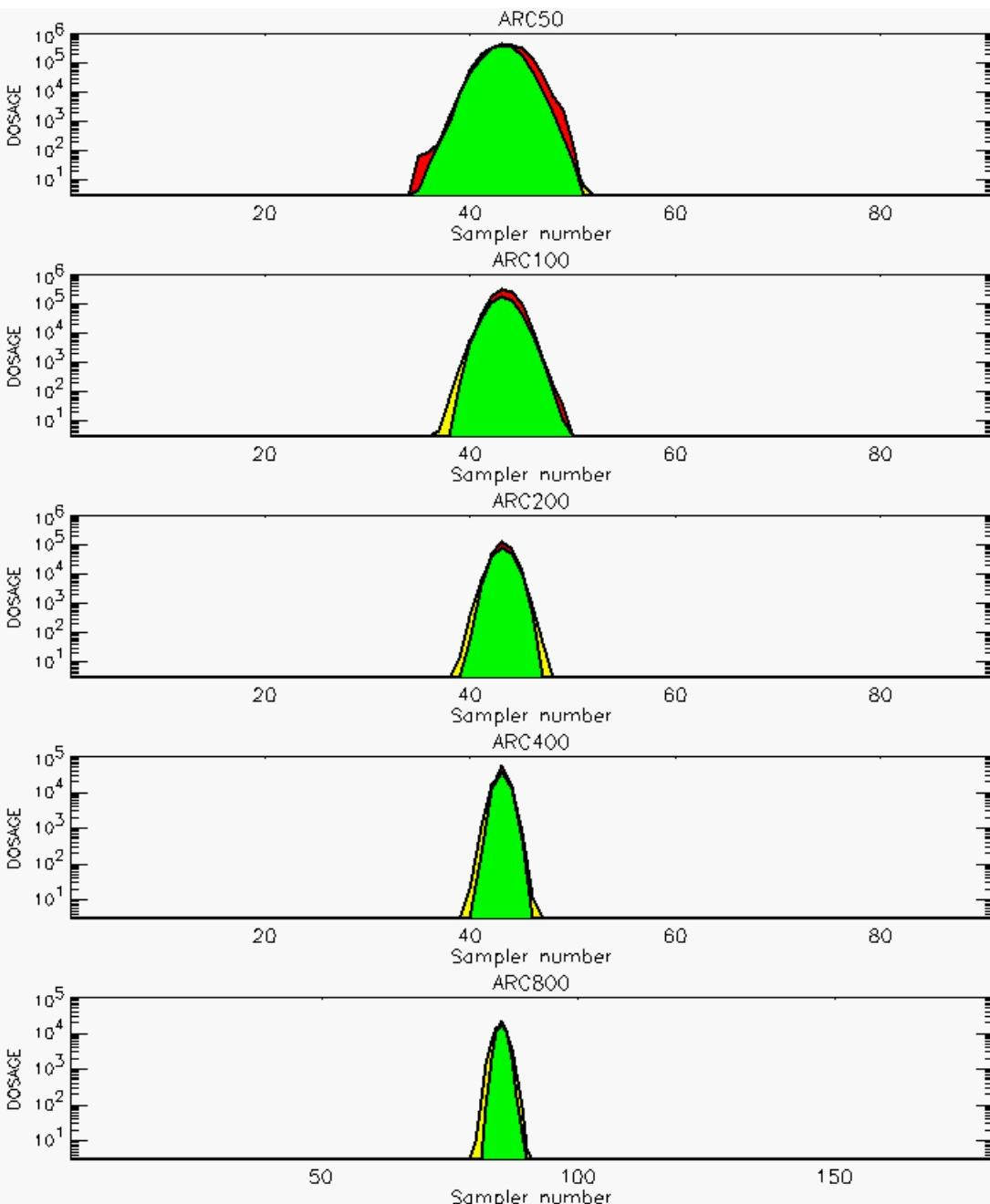


PG Observation to Prediction Comparison

PG Trial File: pr_grass_tracer_Experiment_59.txt

Prediction File: HPAC\nodeposition\pg_59_noxd.out

Figure C-48a. HPAC Prediction to Trial 59 on Linear Scale: Stability Category is 5

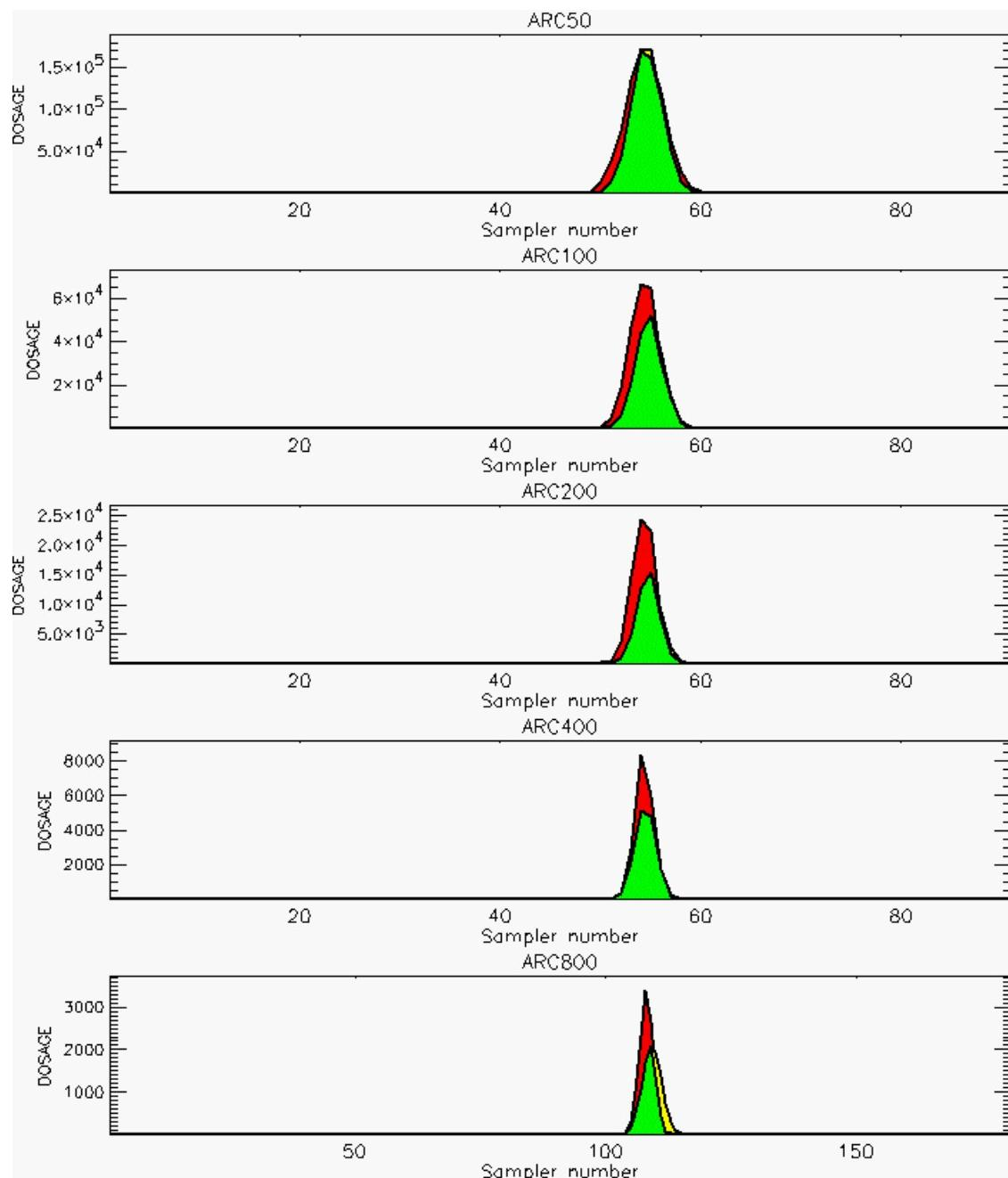


PG Observation to Prediction Comparison

PG Trial File: pr_grass_tracer_Experiment_59.txt

Prediction File: HPAC\nodeposition\pg_59_noxd.out

**Figure C-48b. HPAC Prediction to Trial 59 on Logarithmic Scale:
Stability Category is 5**

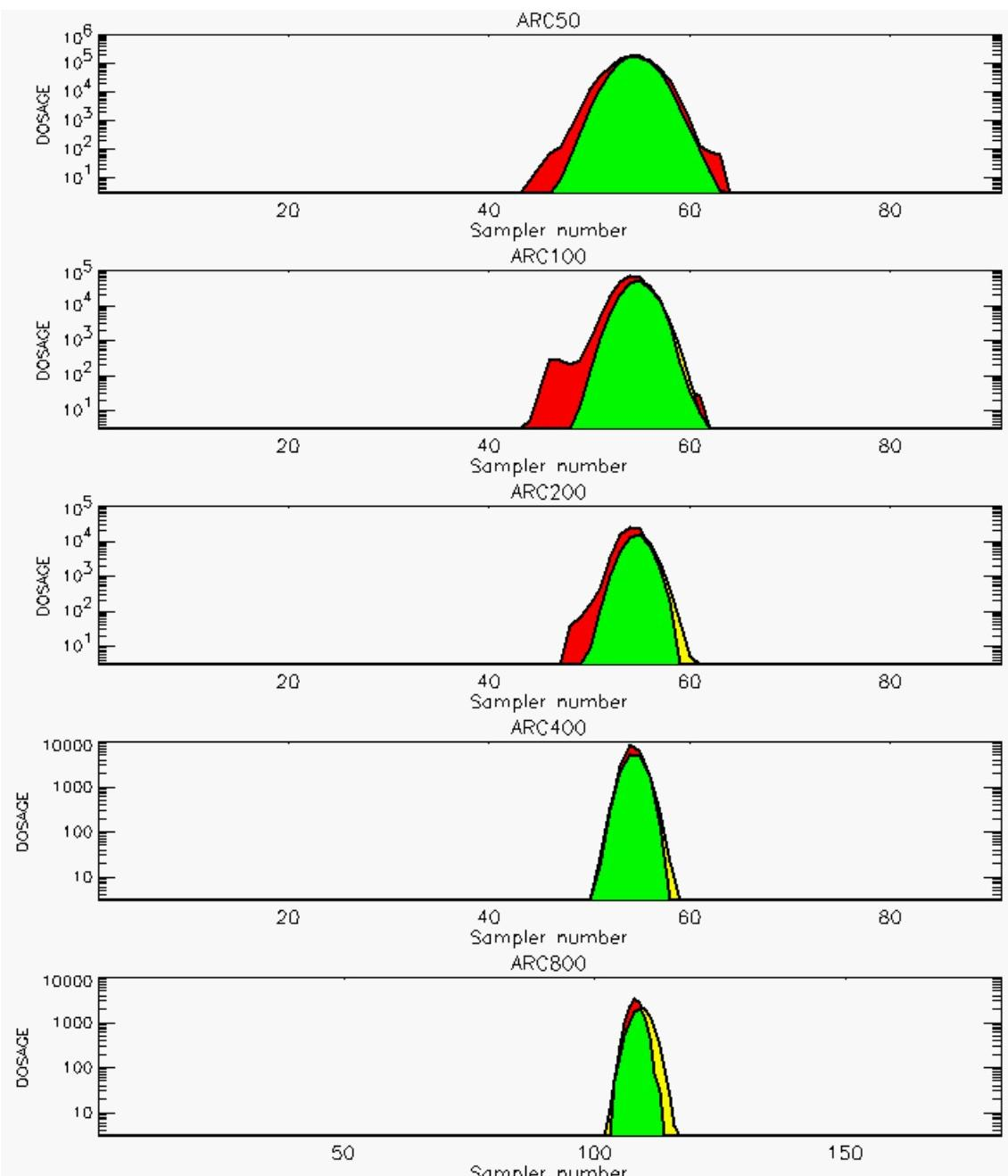


PG Observation to Prediction Comparison

PG Trial File: pr_grass_tracer_Experiment_60.txt

Prediction File: HPAC\nodeposition\pg_60_noxd.out

Figure C-49a. HPAC Prediction to Trial 60 on Linear Scale: Stability Category is 5

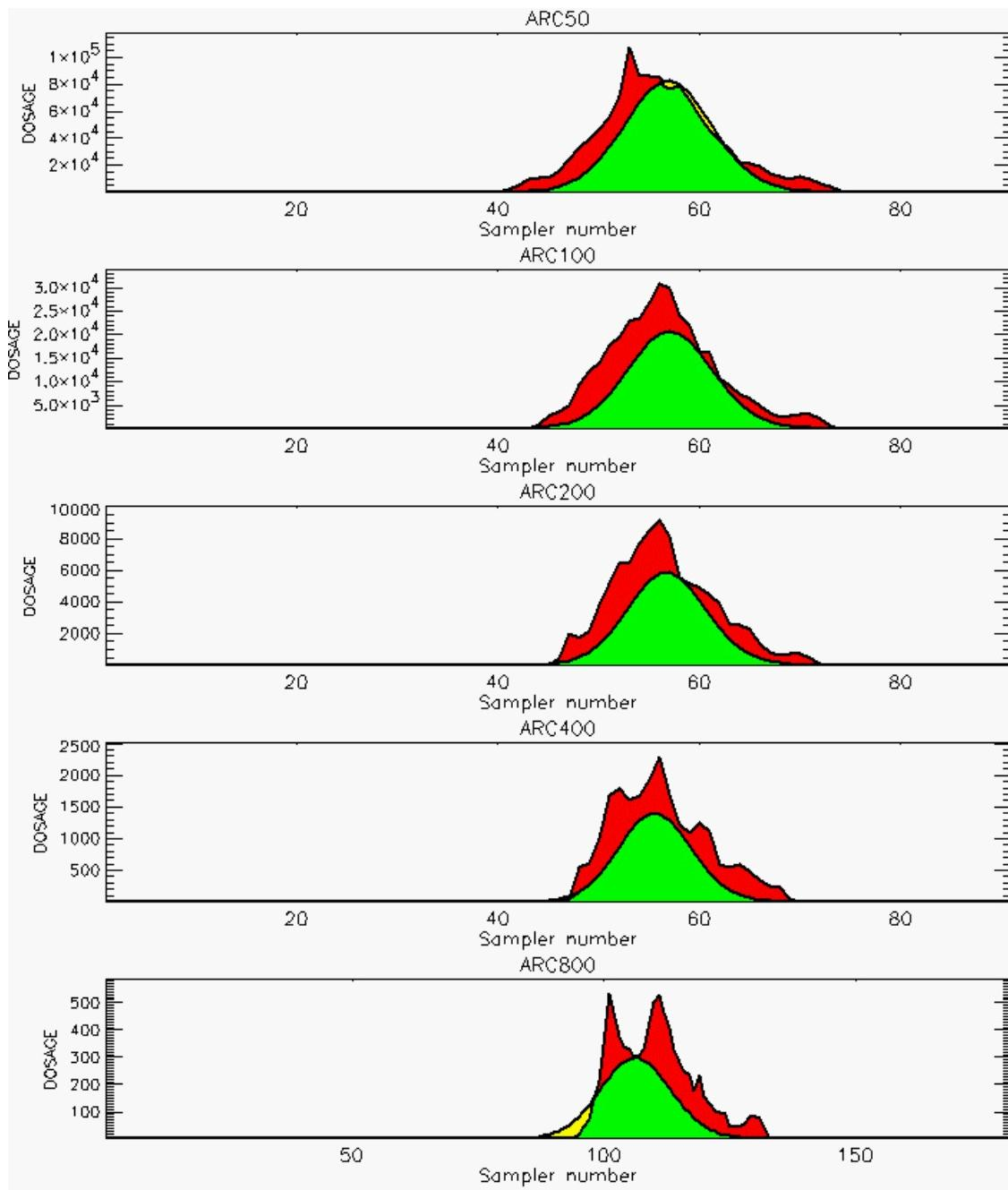


PG Observation to Prediction Comparison

PG Trial File: pr_grass_tracer_Experiment_60.txt

Prediction File: HPAC\nodeposition\pg_60_noxd.out

Figure C-49b. HPAC Prediction to Trial 60 on Logarithmic Scale: Stability Category is 5

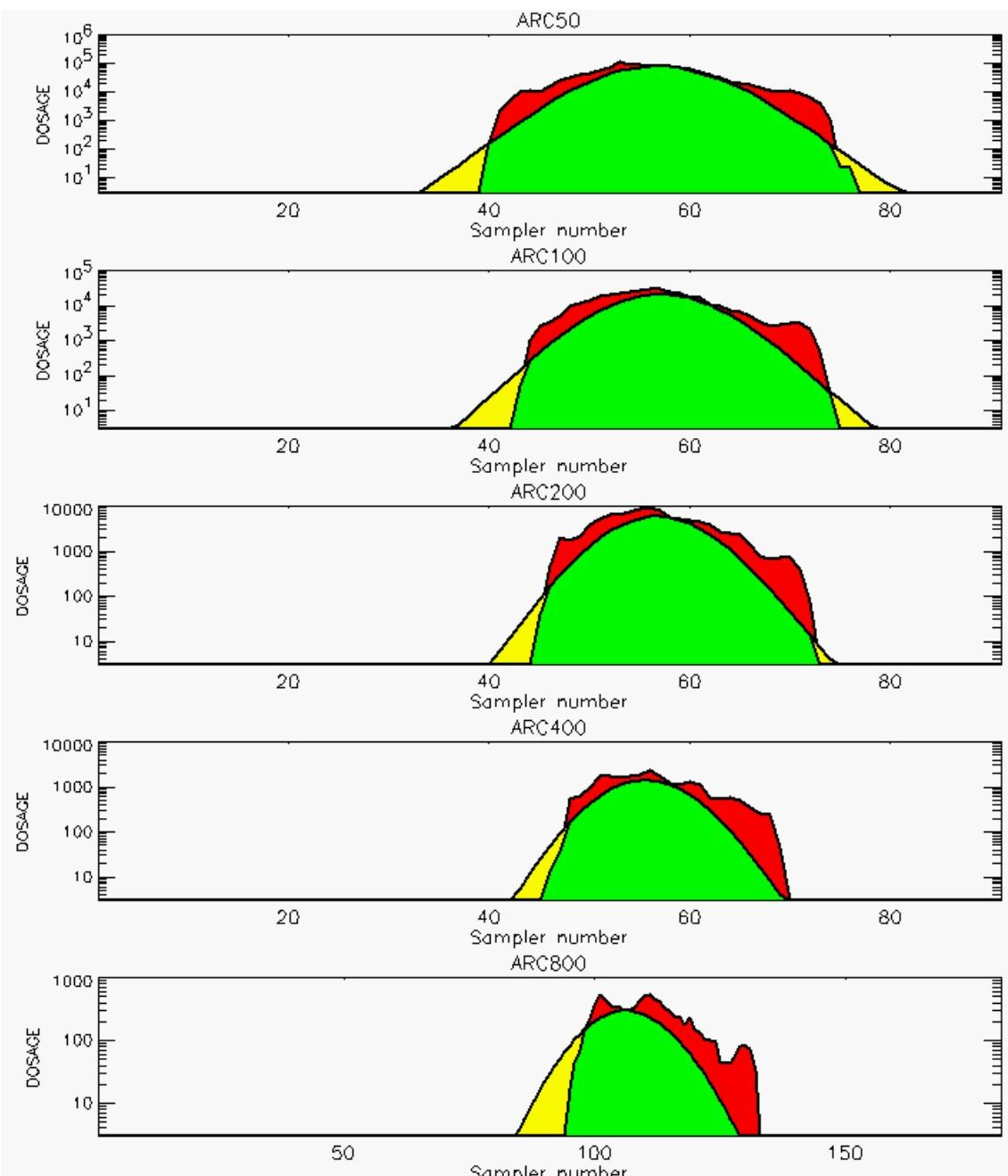


PG Observation to Prediction Comparison

PG Trial File: pr_grass_tracer_Experiment_61.txt

Prediction File: HPAC\nodeposition\pg_61_noxd.out

Figure C-50a. HPAC Prediction to Trial 61 on Linear Scale: Stability Category is 3

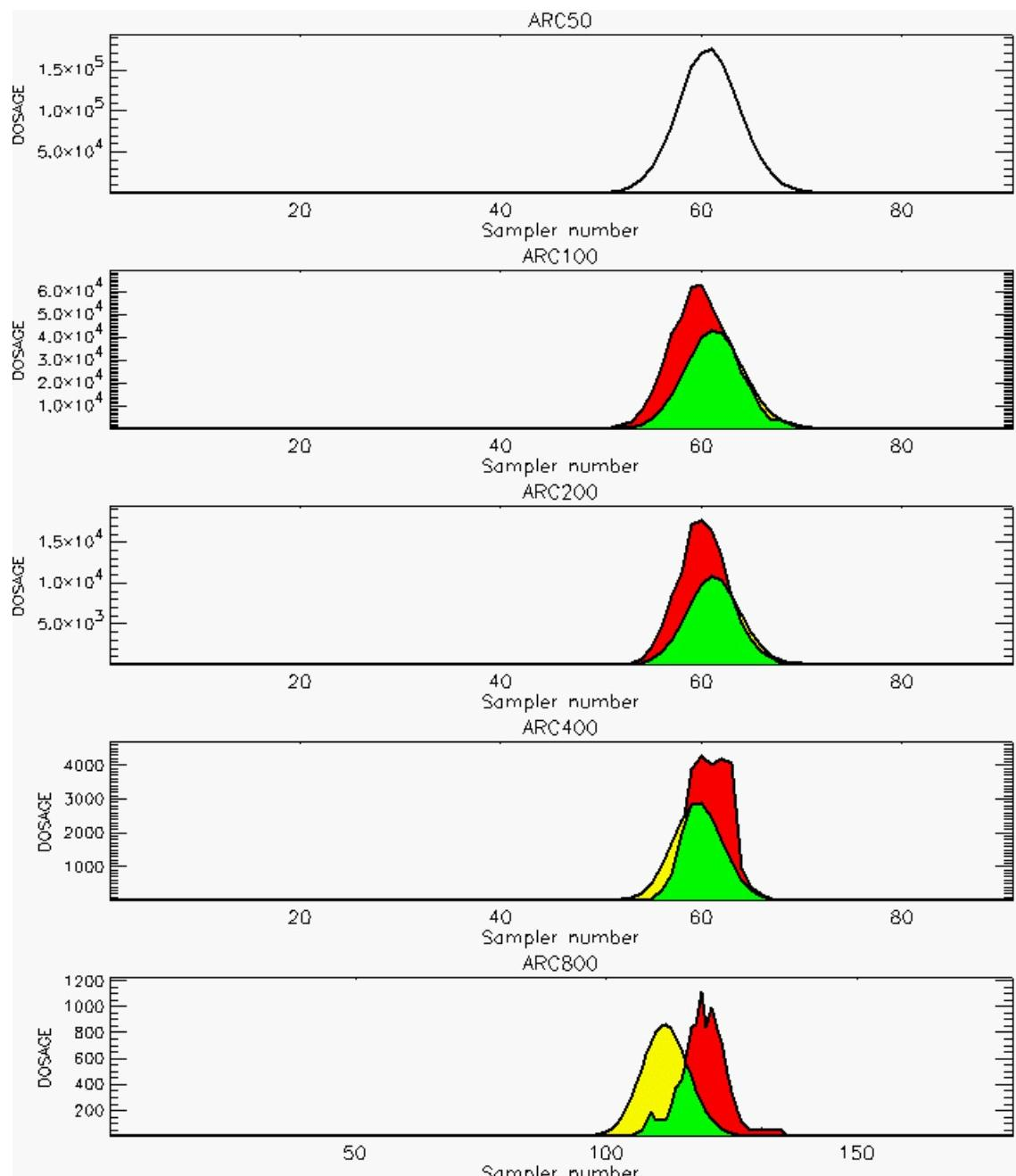


PG Observation to Prediction Comparison

PG Trial File: pr_grass_tracer_Experiment_61.txt

Prediction File: HPAC\nodeposition\pg_61_noxd.out

Figure C-50b. HPAC Prediction to Trial 61 on Logarithmic Scale: Stability Category is 3

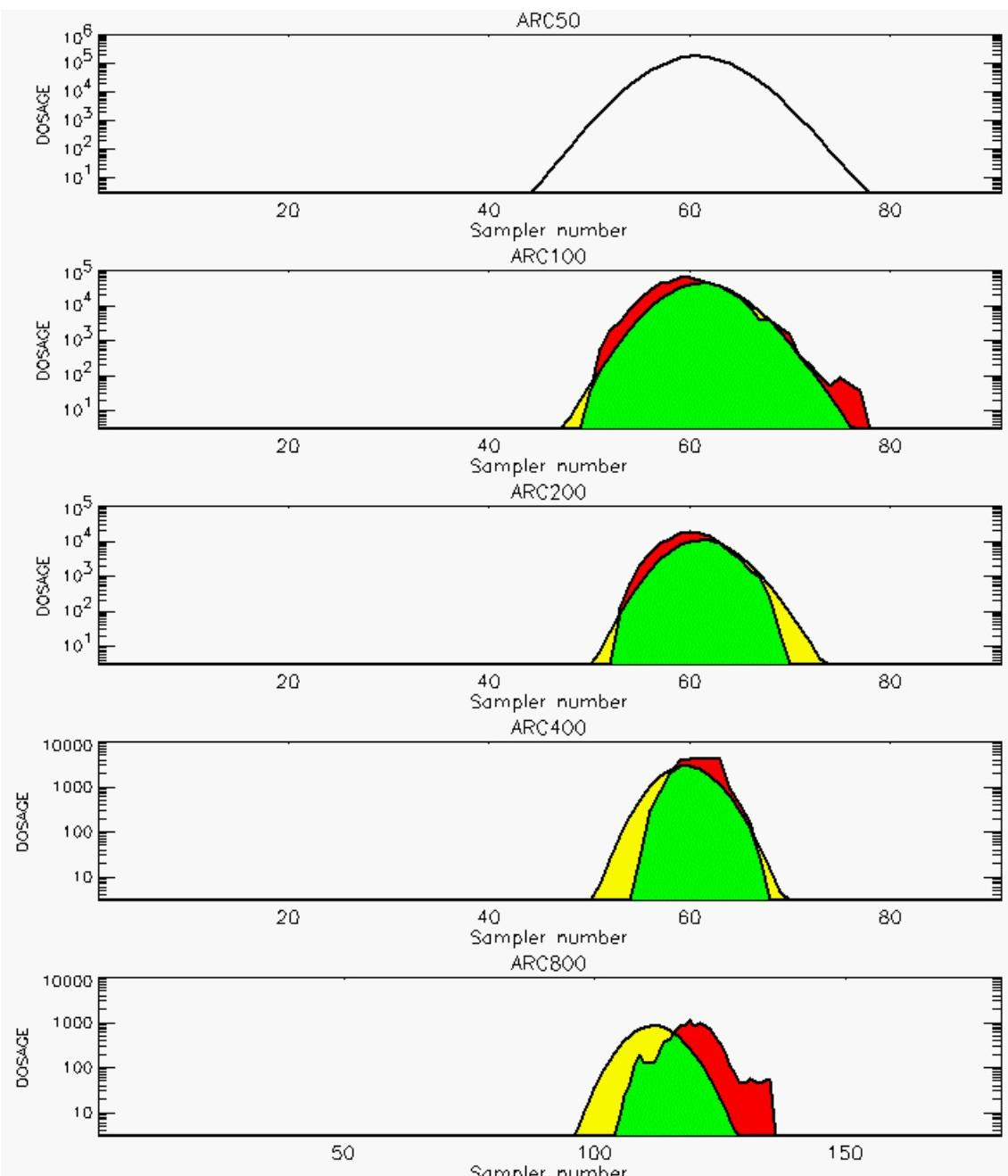


PG Observation to Prediction Comparison

PG Trial File: pr_grass_tracer_Experiment_62.txt

Prediction File: HPAC\nodeposition\pg_62_noxd.out

Figure C-51a. HPAC Prediction to Trial 62 on Linear Scale: Stability Category is 2 (Values for Samplers of 50-Meter Arc are Replaced by Missing Values [Ref. C-2])



PG Observation to Prediction Comparison

PG Trial File: pr_grass_tracer_Experiment_62.txt

Prediction File: HPAC\nodeposition\pg_62_noxd.out

Figure C-51b. HPAC Prediction to Trial 62 on Logarithmic Scale: Stability Category is 2 (Values for Samplers of 50-Meter Arc are Replaced by Missing Values [Ref. C-2])

REFERENCES

- C-1. Barad, M. L. (Editor), *Project Prairie Grass, A Field Program in Diffusion*, Geophysical Research Papers No. 59, Volumes I and II, DTIC #AD-152572/AFCRC-TR-58-235(I), Air Geophysical Laboratory, Hanscom Air Force Base, MA, 1958.
- C-2. Barad, M. L. (Editor), *Project Prairie Grass, a Field Program in Diffusion*, Geophysical Research Papers, No. 59, Volume I, DTIC #AD-152572/AFCRC-TR-58-235(I), pages 79-80, 201, 1958.
- C-3. Irwin, J. S. and Rosu, M-R., *Comments on a Draft Practice for Statistical Evaluation of Atmospheric Dispersion Models*, Proceedings of the 10th Joint Conference on the Applications of Air Pollution Meteorology. American Meteorological Society, Boston, pp. 6-10, 1998.

APPENDIX D
NARAC PREDICTIONS COMPARED TO *PRAIRIE GRASS* TRIALS

APPENDIX D

NARAC PREDICTIONS COMPARED TO *PRAIRIE GRASS* TRIALS

This appendix presents graphical comparison of NARAC predictions with no SO₂ surface deposition to *Prairie Grass* field trials [Ref. D-1]. Vertical plot units are dosage units of mg-sec/m³. Horizontal plot units are sampler numbers as presented in the *Prairie Grass* field trials with sampler number 1 oriented to the west, the middle sampler (45 or 90) oriented to the north, and the last sampler (91 or 181) oriented to the east of the SO₂ gas release source. Only data values greater than the cutoff threshold of 3 mg-sec/m³ (0.005 mg/m³) are presented for both field trial data and NARAC predictions. This cutoff threshold value corresponds to a minimum value reported in *Prairie Grass* field trials.

Comparisons of NARAC predictions and *Prairie Grass* field trial observations are presented on both linear and logarithmic dosage scales. Each graphical comparison consists of five plots (one for each arc) with the top plot depicting the 50-meter arc, the second plot depicting the 100-meter arc, the third plot depicting the 200-meter arc, and so on. The last panel (just above the figure caption) contains information about the data files used to produce these plots. The *Prairie Grass* field trial file name contains a two-digit number corresponding to the trial number. The NARAC prediction file name contains the moniker “nodeposition,” denoting that SO₂ surface deposition was not considered in these predictions, and a one- or two-digit number reflecting the *Prairie Grass* field trial being predicted. Odd-numbered pages contain figures on the linear dosage scale while even-numbered pages contain figures on the logarithmic dosage scale.

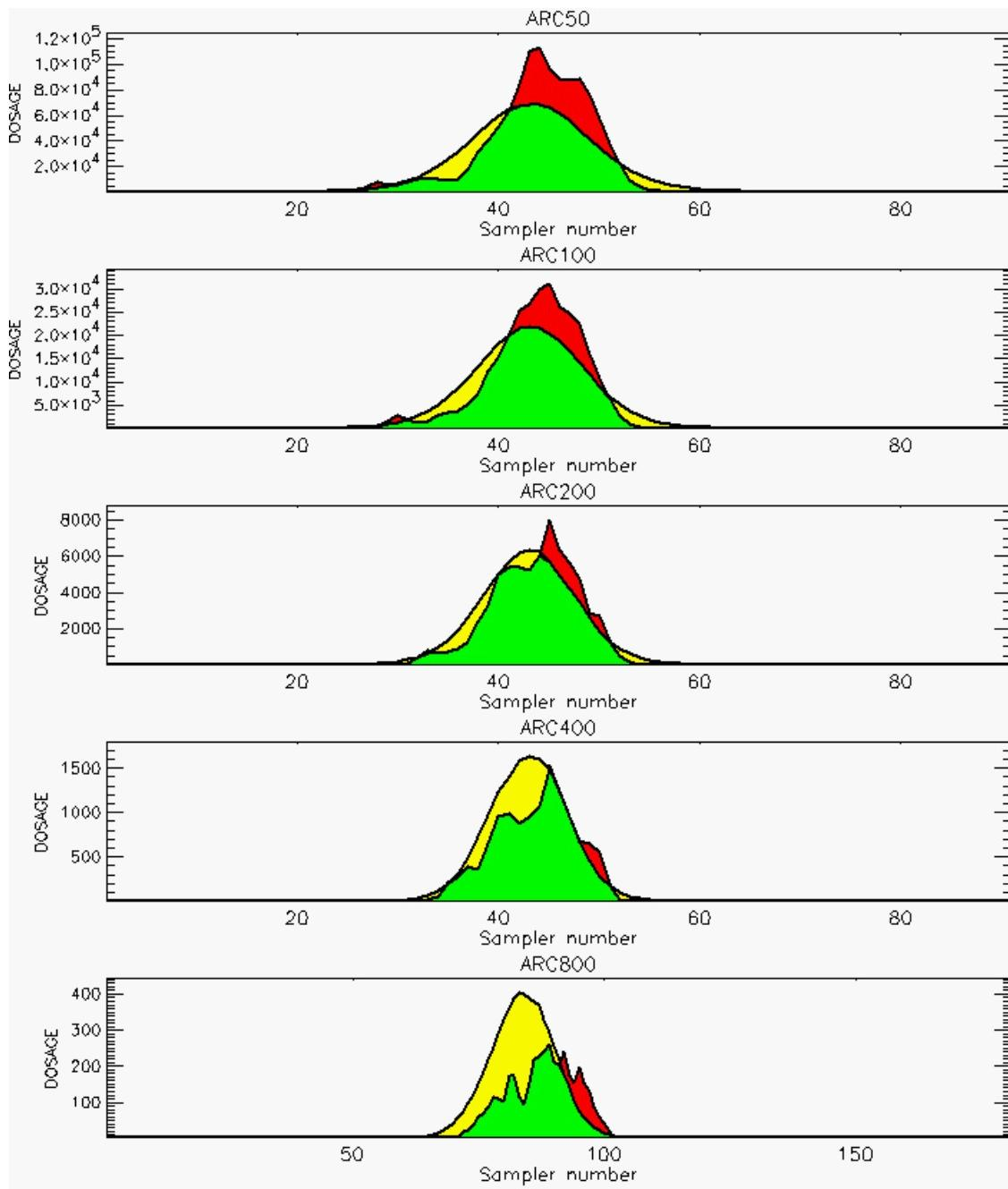
The meanings of the colors used in the plots are described below:

- Red — trial dosages that are higher than the prediction
- Green — trial dosages that overlap with the prediction
- Yellow — prediction dosages that are higher than the trial
- White — trial sampler observation is missing.

These shadings correspond to AE2 as described in Chapter 2.

Samplers with missing values, or spurious maximum that were fixed by moving the decimal point, are noted in the figure captions [Ref. D-2] (see also Appendix K).

Irwin stability categories that were used in our analyses are denoted in the figure captions. These stability category assignments are based on Reference D-3.

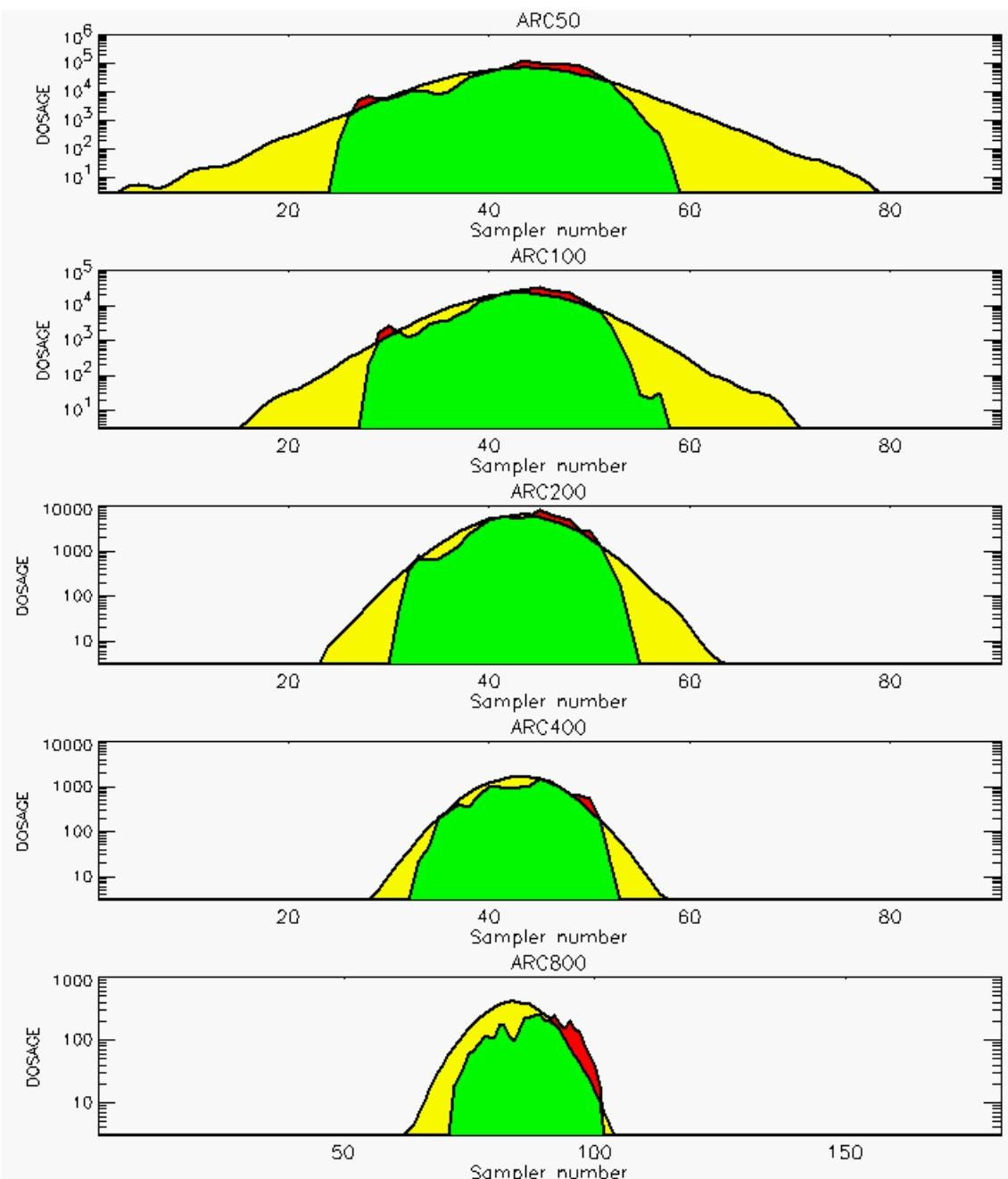


PG Observation to Prediction Comparison

PG Trial File: pr_grass_tracer_Experiment_05.txt

Prediction File: ARAC\nodeposition\pg_5_noxd.arac

Figure D-1a. NARAC Predictions to Trial 5 on Linear Scale: Stability Category is 2

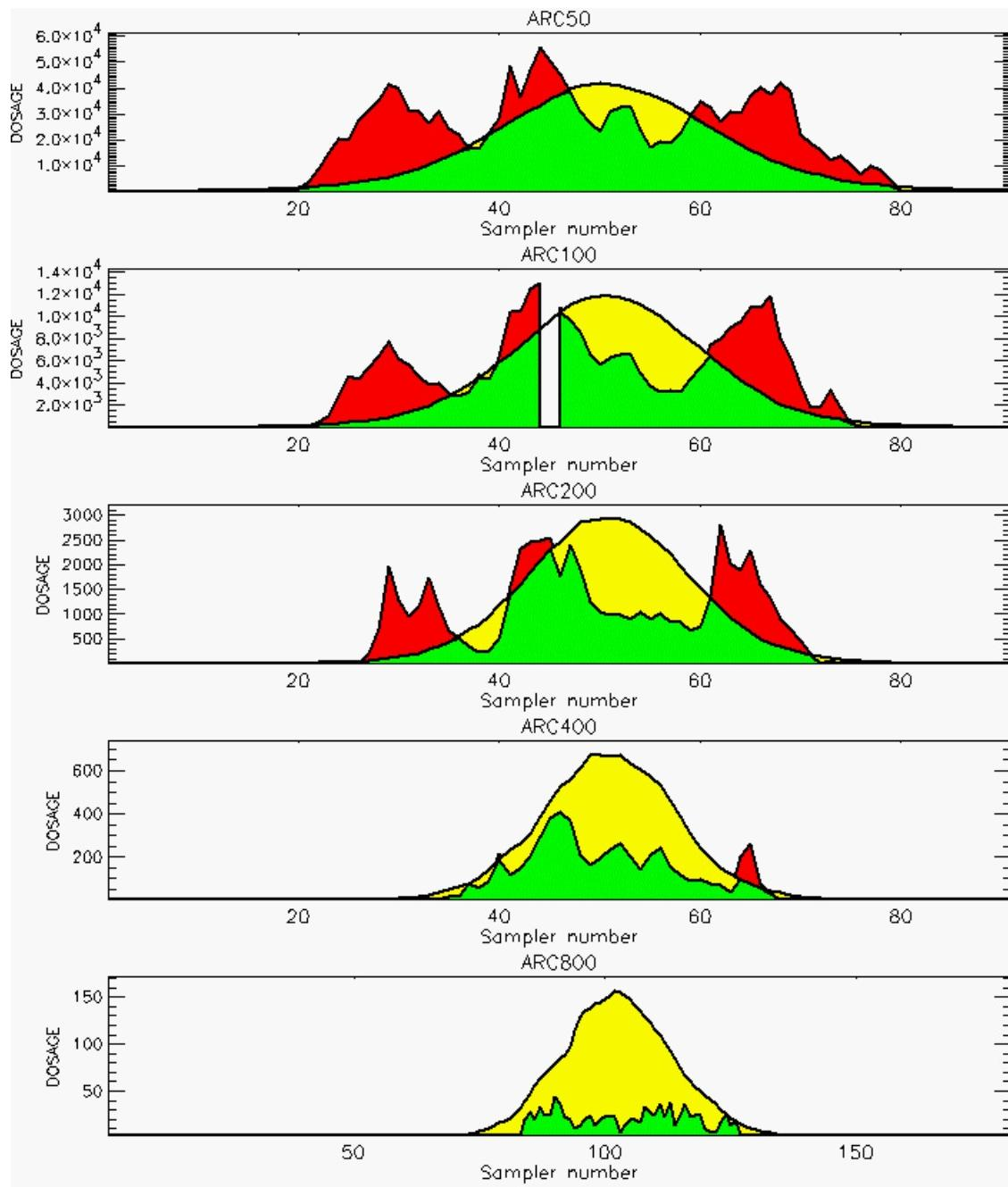


PG Observation to Prediction Comparison

PG Trial File: pr_grass_tracer_Experiment_05.txt

Prediction File: ARAC\nodeposition\pg_5_noxd.arac

Figure D-1b. NARAC Prediction to Trial 5 on Logarithmic Scale: Stability Category is 2

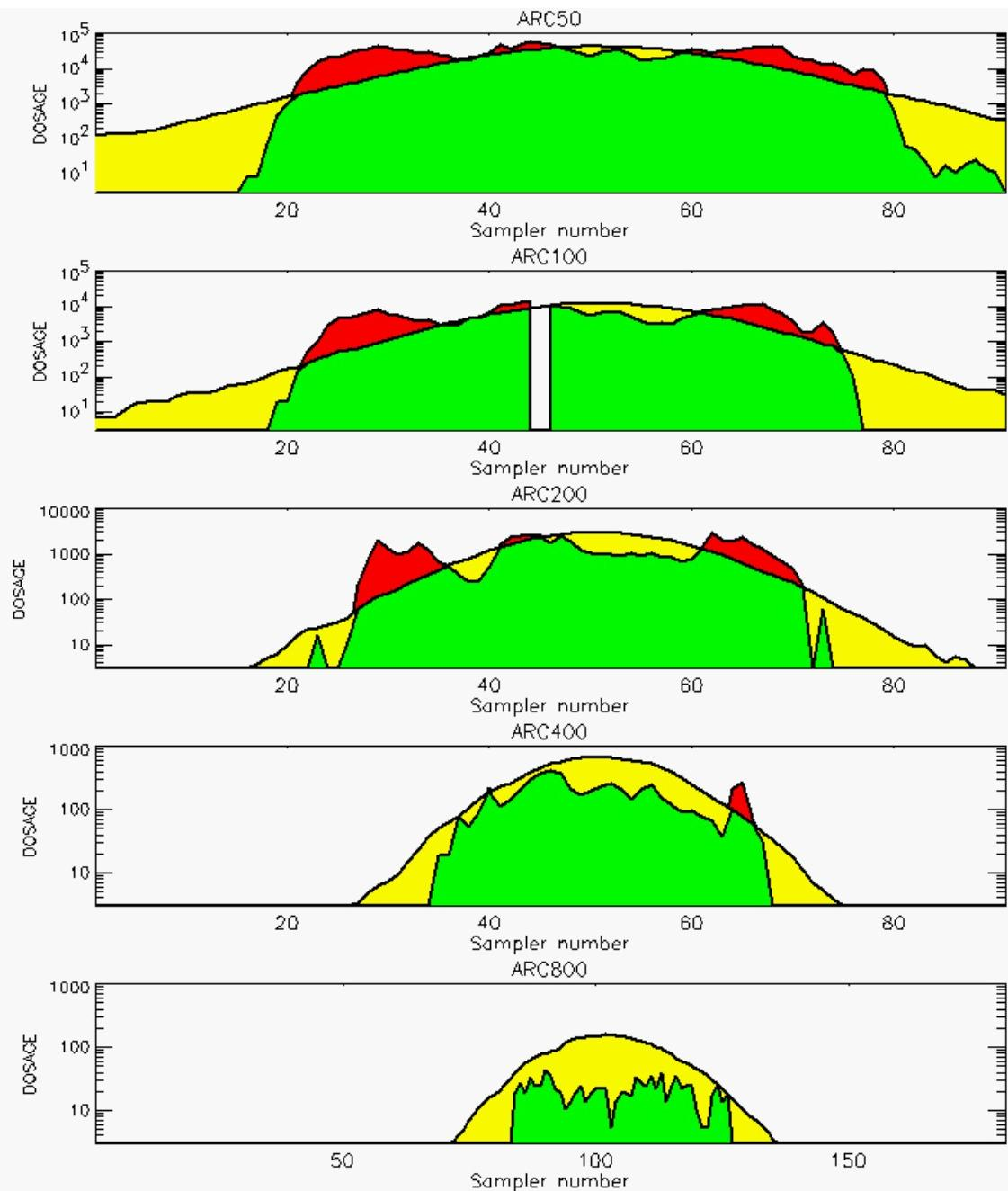


PG Observation to Prediction Comparison

PG Trial File: pr_grass_tracer_Experiment_07.txt

Prediction File: ARAC\nodeposition\pg_7_nozd.arac

**Figure D-2a. NARAC Prediction to Trial 7 on Linear Scale: Stability Category is 1
(Value for Sampler 45 of 100-Meter Arc is Missing)**

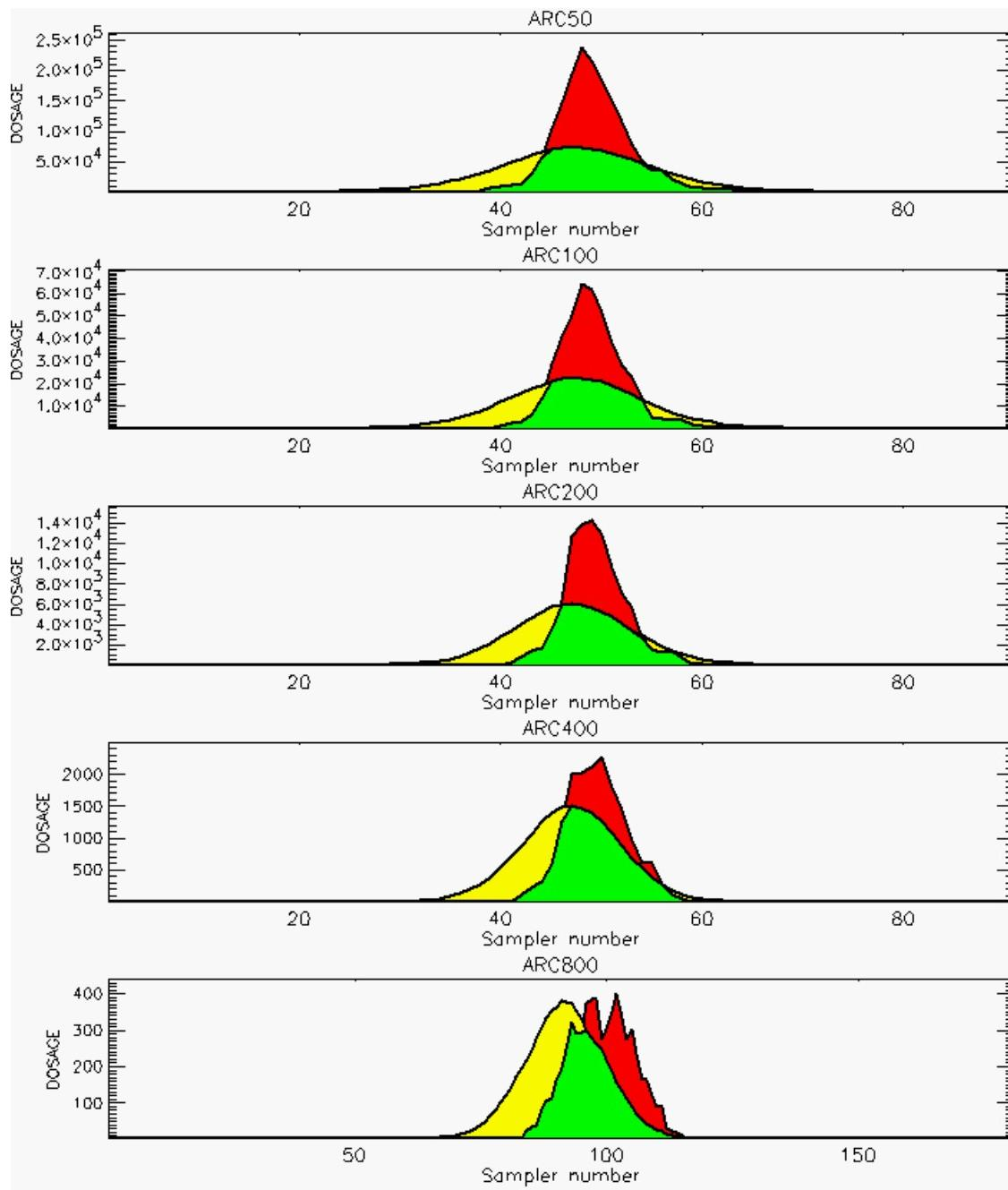


PG Observation to Prediction Comparison

PG Trial File: pr_grass_tracer_Experiment_07.txt

Prediction File: ARAC\nodeposition\pg_7_novd.arc

**Figure D-2b. NARAC Prediction to Trial 7 on Logarithmic Scale: Stability Category is 1
(Value for Sampler 45 of 100-Meter Arc is Missing)**

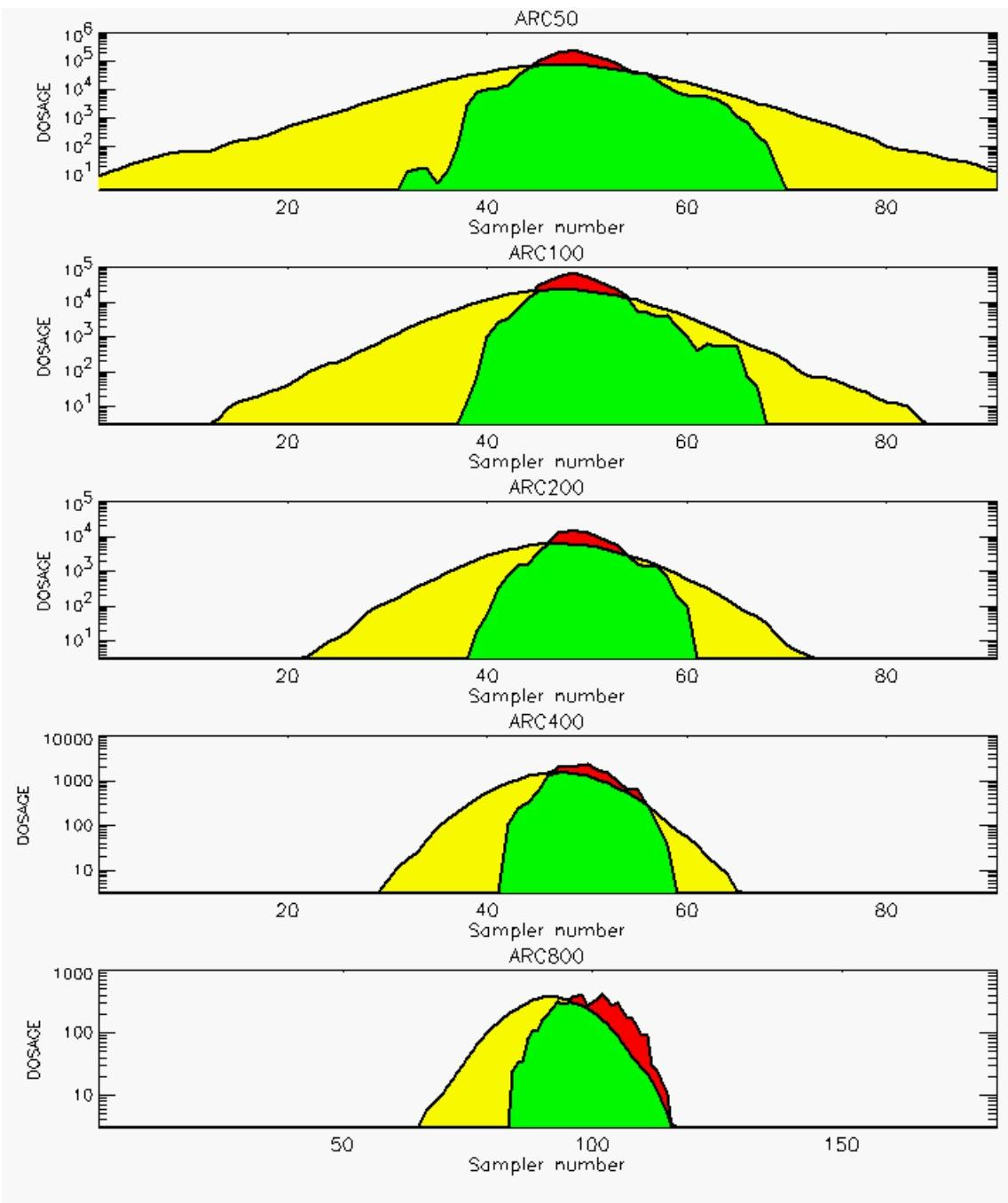


PG Observation to Prediction Comparison

PG Trial File: pr_grass_tracer_Experiment_08.txt

Prediction File: ARAC\nodeposition\pg_8_noxd.arac

Figure D-3a. NARAC Prediction to Trial 8 on Linear Scale: Stability Category is 2

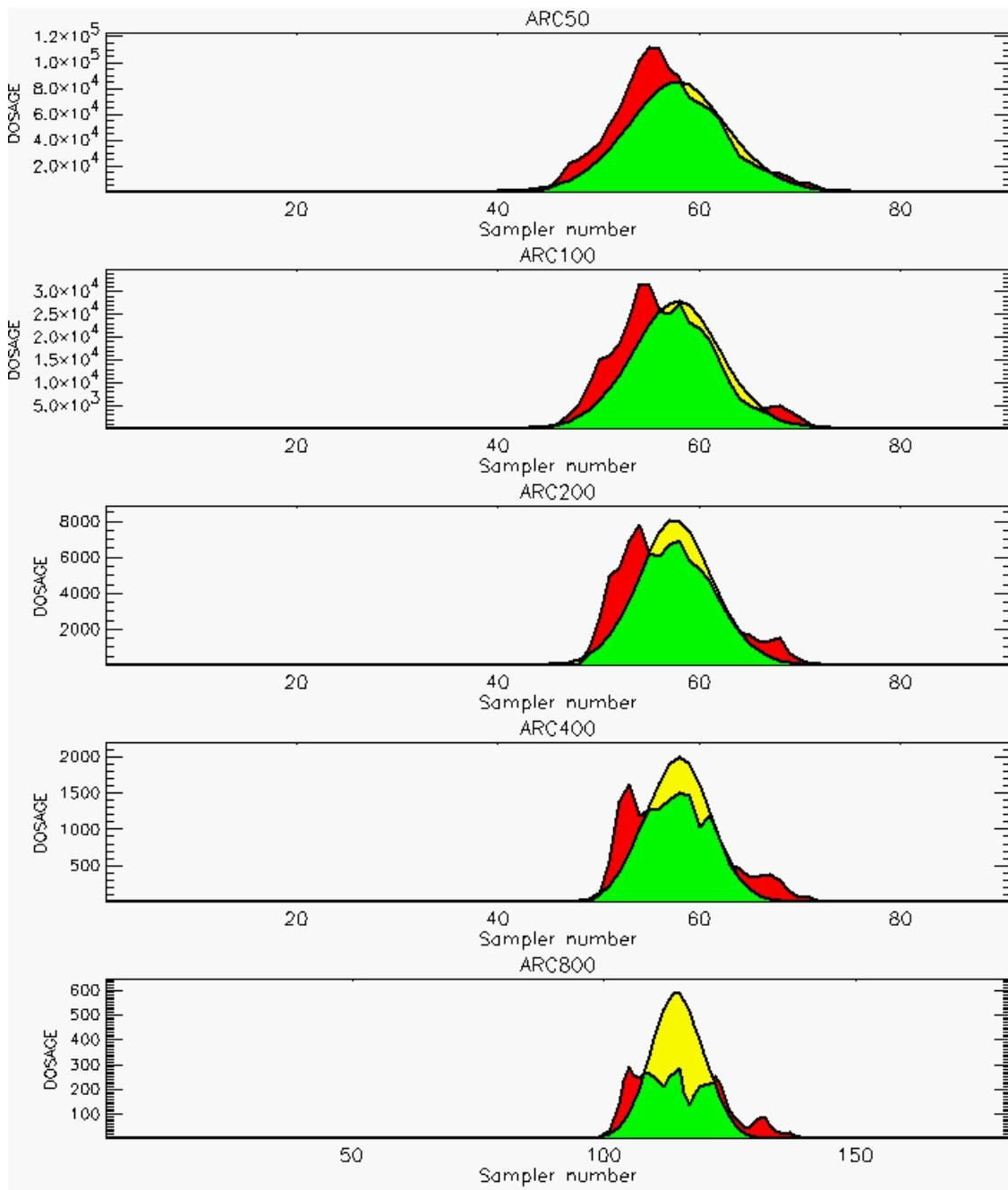


PG Observation to Prediction Comparison

PG Trial File: pr_grass_tracer_Experiment_08.txt

Prediction File: ARAC\nodeposition\pg_8_noxd.arac

Figure D-3b. NARAC Prediction to Trial 8 on Logarithmic Scale: Stability Category is 2

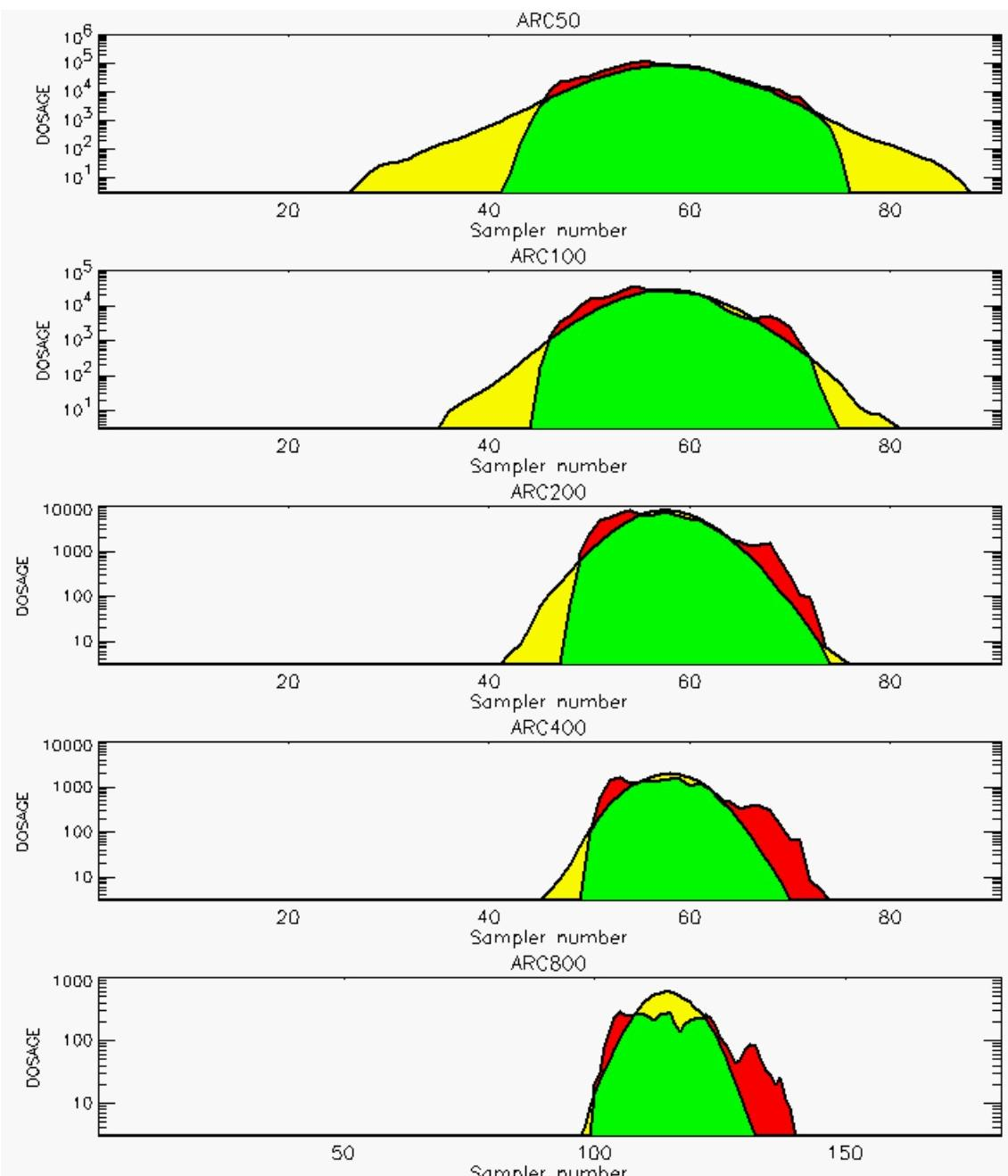


PG Observation to Prediction Comparison

PG Trial File: pr_grass_tracer_Experiment_09.txt

Prediction File: ARAC\nodeposition\pg_9_noxd.arac

Figure D-4a. NARAC Prediction to Trial 9 on Linear Scale: Stability Category is 2

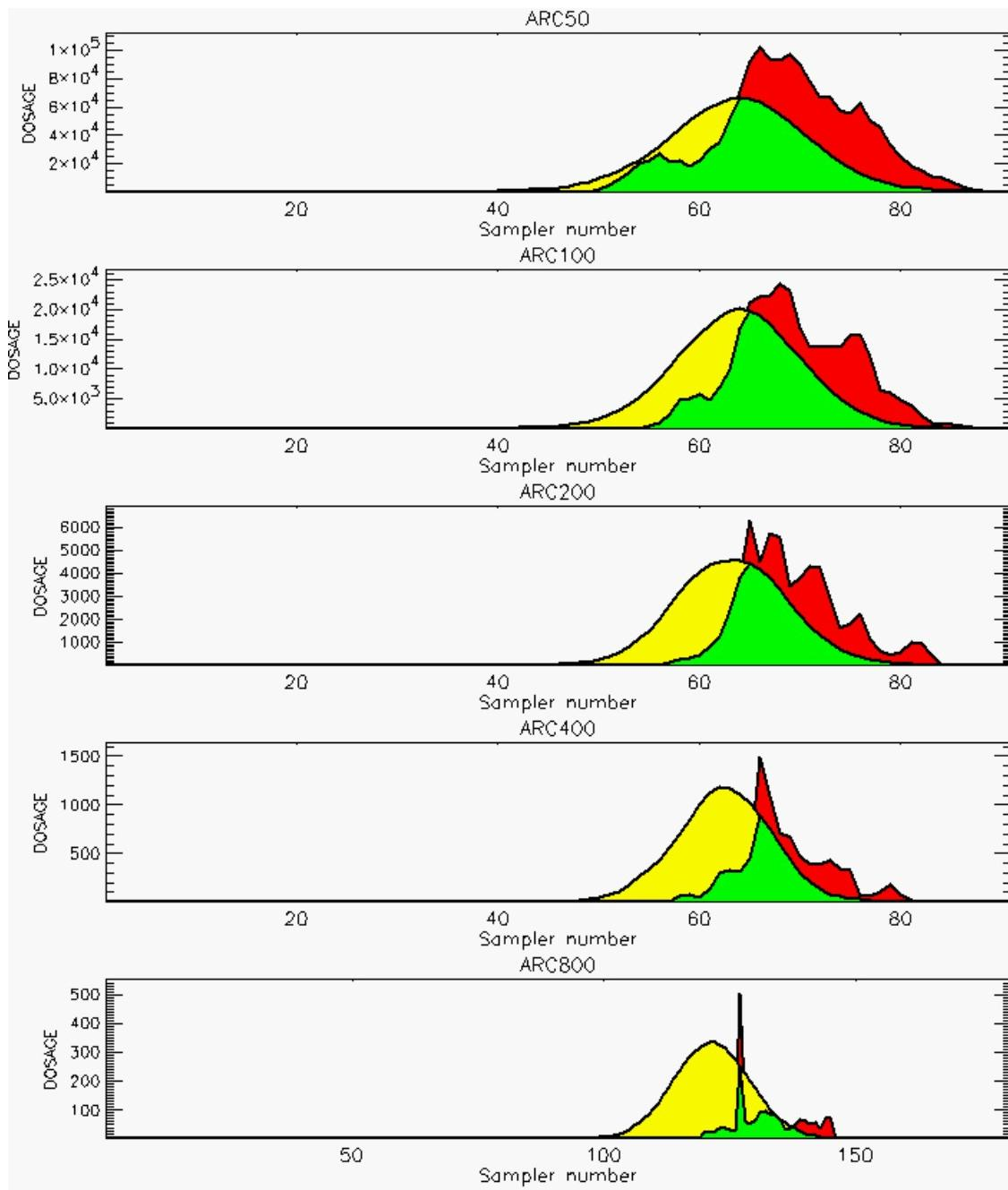


PG Observation to Prediction Comparison

PG Trial File: pr_grass_tracer_Experiment_09.txt

Prediction File: ARAC\nodeposition\pg_9_noxd.arac

Figure D-4b. NARAC Prediction to Trial 9 on Logarithmic Scale: Stability Category is 2

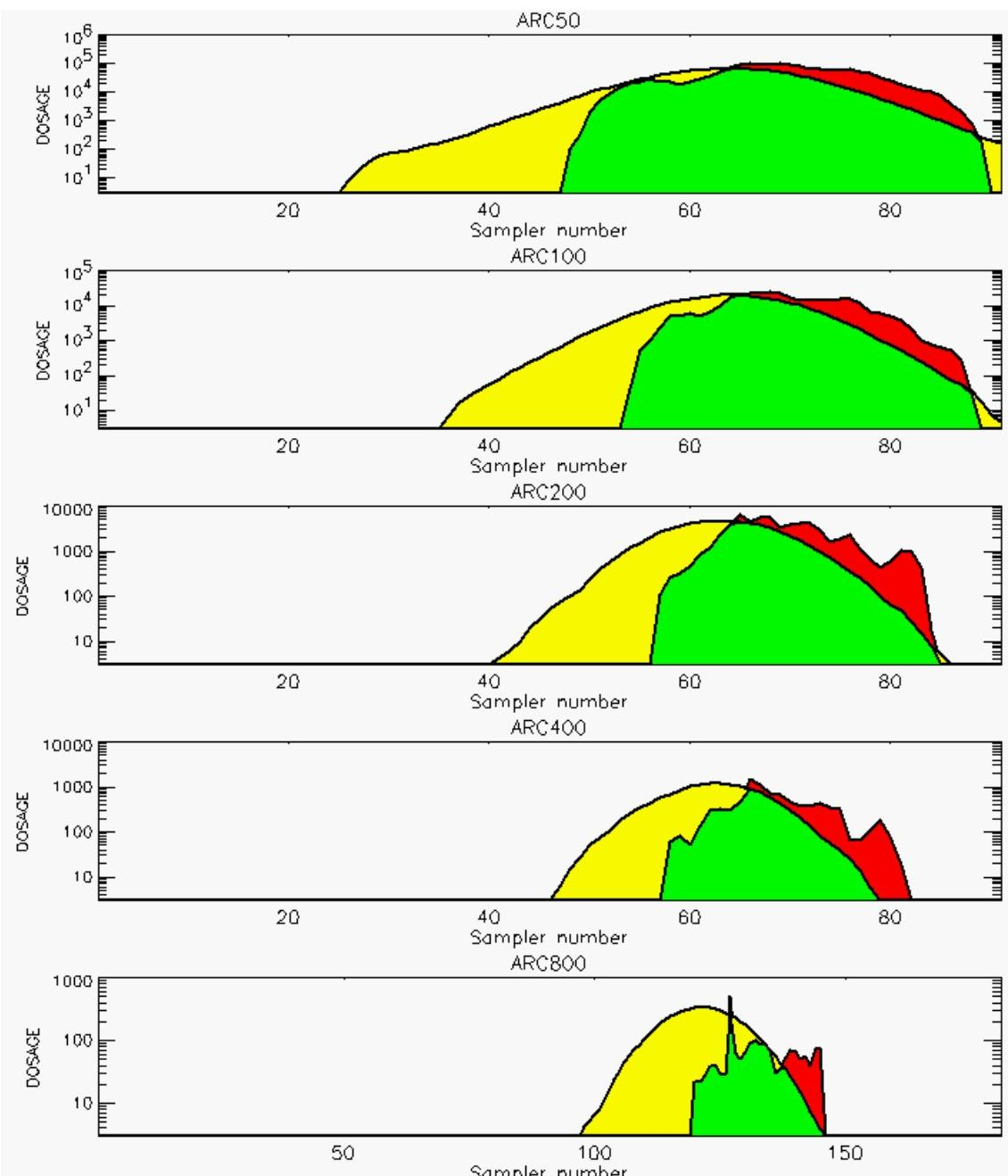


PG Observation to Prediction Comparison

PG Trial File: pr_grass_tracer_Experiment_10.txt

Prediction File: ARAC\nodeposition\pg_10_noxd.arac

Figure D-5a. NARAC Prediction to Trial 10 on Linear Scale: Stability Category is 1

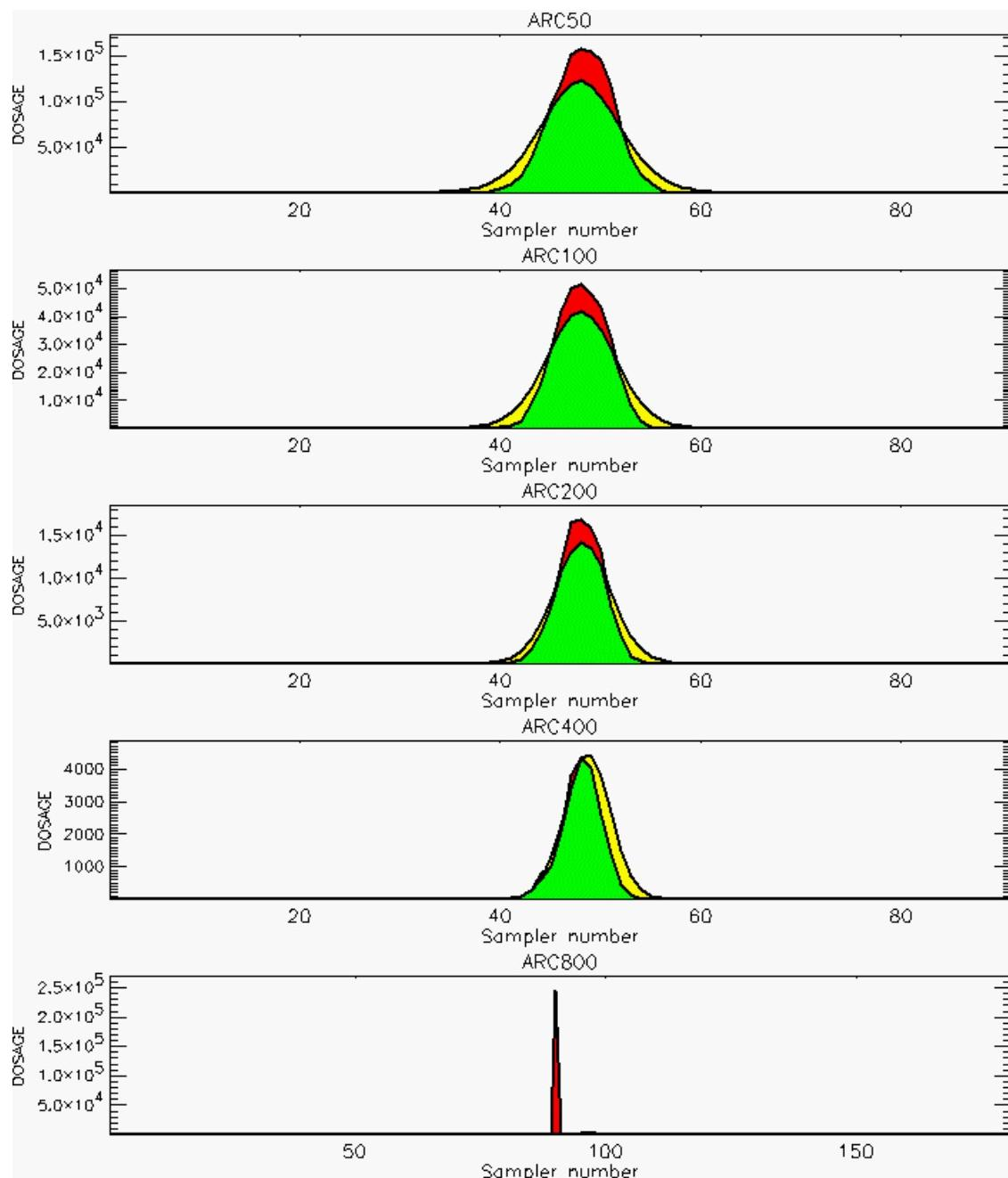


PG Observation to Prediction Comparison

PG Trial File: pr_grass_tracer_Experiment_10.txt

Prediction File: ARAC\nodeposition\pg_10_noxd.arac

Figure D-5b. NARAC Prediction to Trial 10 on Logarithmic Scale: Stability Category is 1

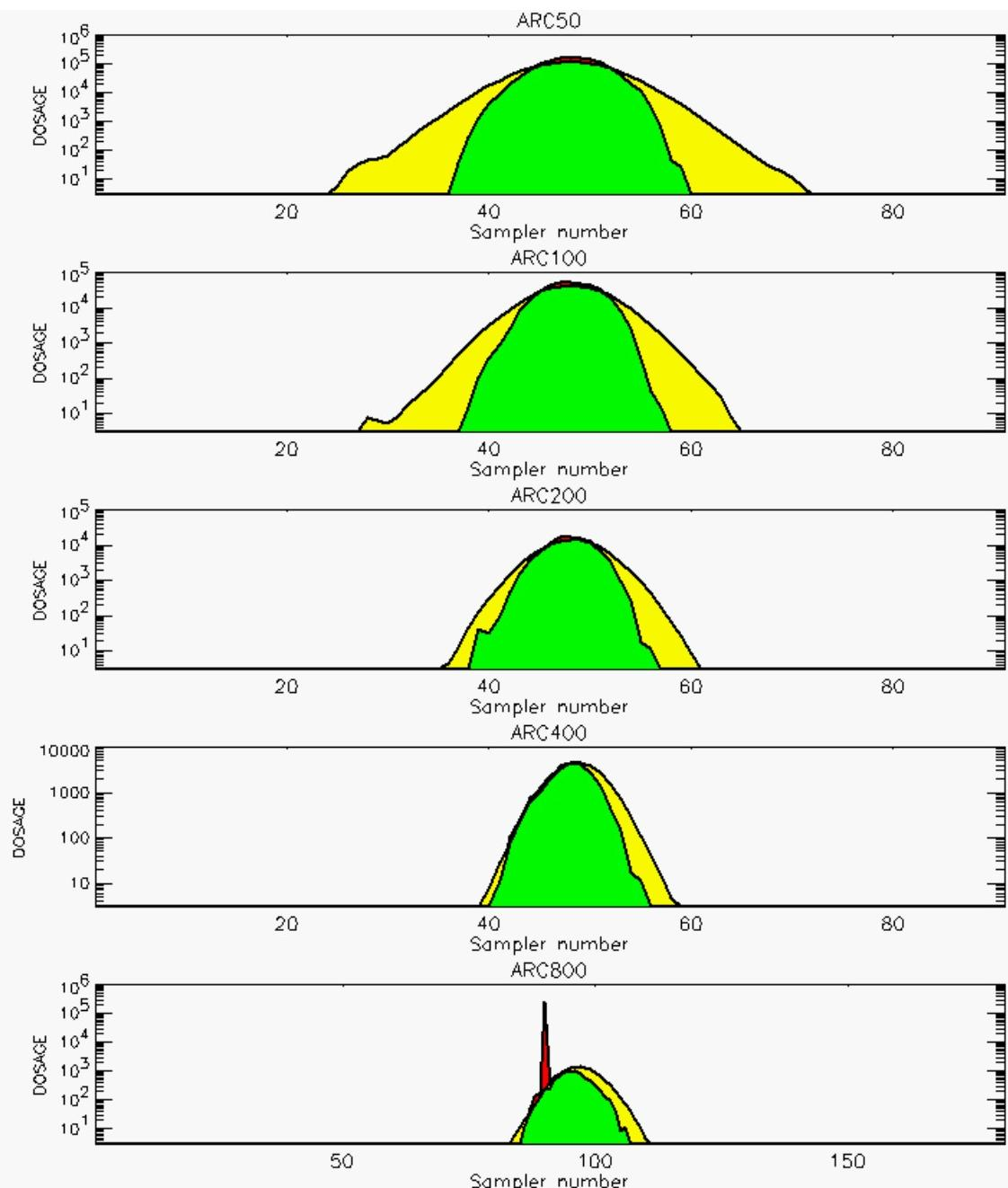


PG Observation to Prediction Comparison

PG Trial File: pr_grass_tracer_Experiment_11.txt

Prediction File: ARAC\nodeposition\pg_11_noxd.arac

**Figure D-6a. NARAC Prediction to Trial 11 on Linear Scale: Stability Category is 3
(Value for Sampler 90 of 800-Meter Arc is Considered “Spurious” and is Fixed by Moving Decimal Point)**

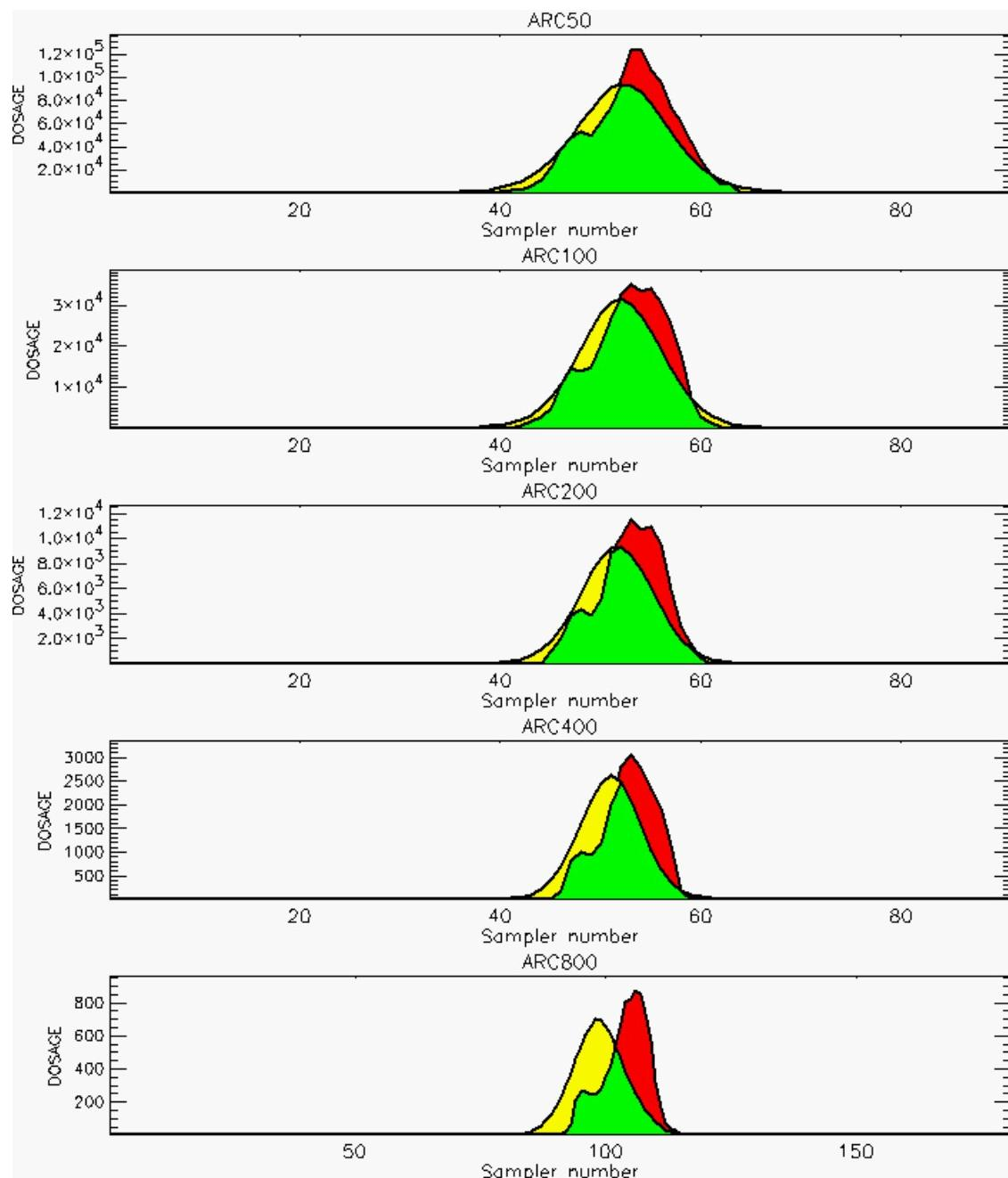


PG Observation to Prediction Comparison

PG Trial File: pr_grass_tracer_Experiment_11.txt

Prediction File: ARAC\nodeposition\pg_11_noxd.arac

Figure D-6b. NARAC Prediction to Trial 11 on Logarithmic Scale: Stability Category is 3 (Value for Sampler 90 of 800-Meter Arc is Considered "Spurious" and is Fixed by Moving Decimal Point)

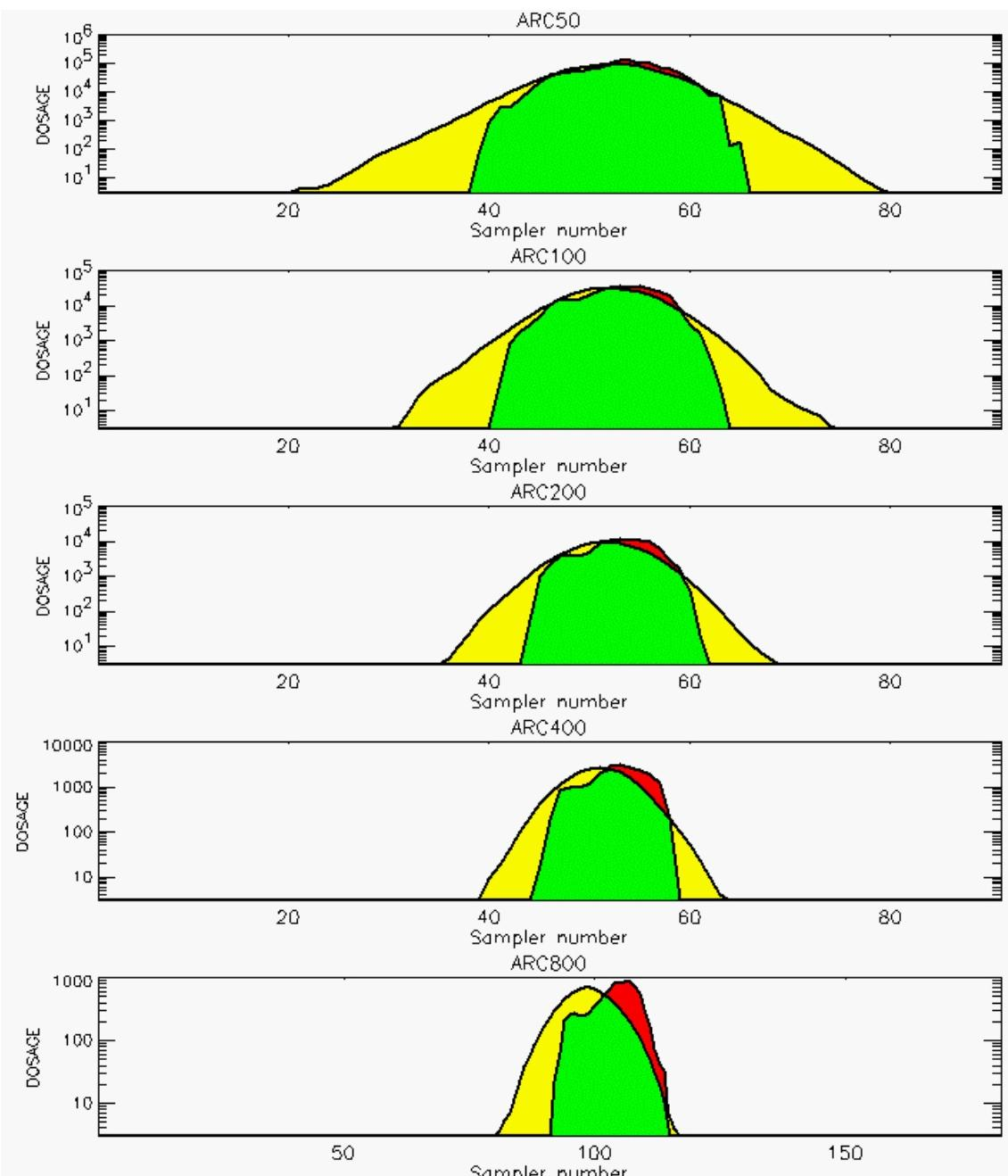


PG Observation to Prediction Comparison

PG Trial File: pr_grass_tracer_Experiment_12.txt

Prediction File: ARAC\nodeposition\pg_12_noxd.arac

Figure D-7a. NARAC Prediction to Trial 12 on Linear Scale: Stability Category is 3

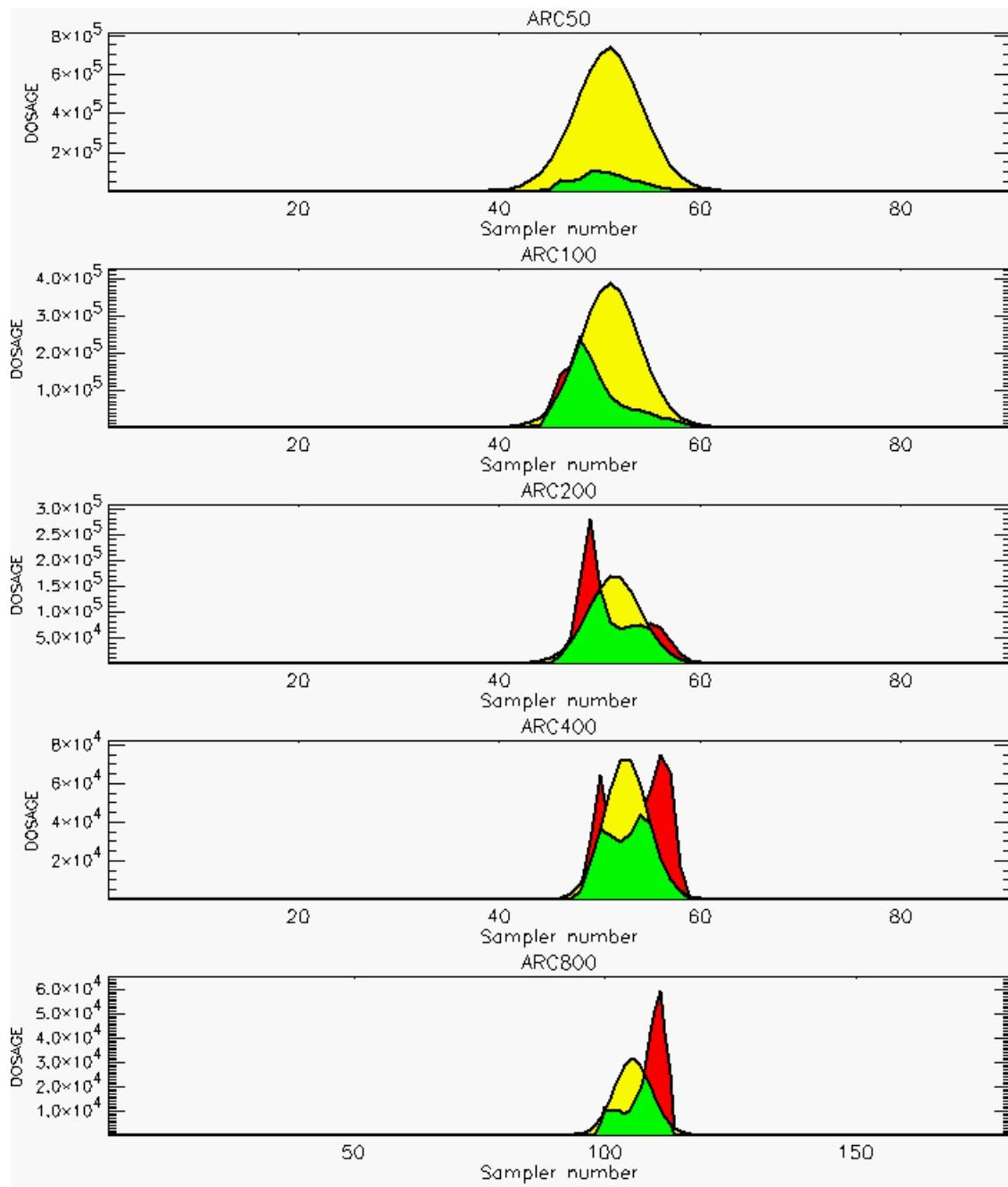


PG Observation to Prediction Comparison

PG Trial File: pr_grass_tracer_Experiment_12.txt

Prediction File: ARAC\nodeposition\pg_12_noxd.arac

Figure D-7b. NARAC Prediction to Trial 12 on Logarithmic Scale: Stability Category is 3

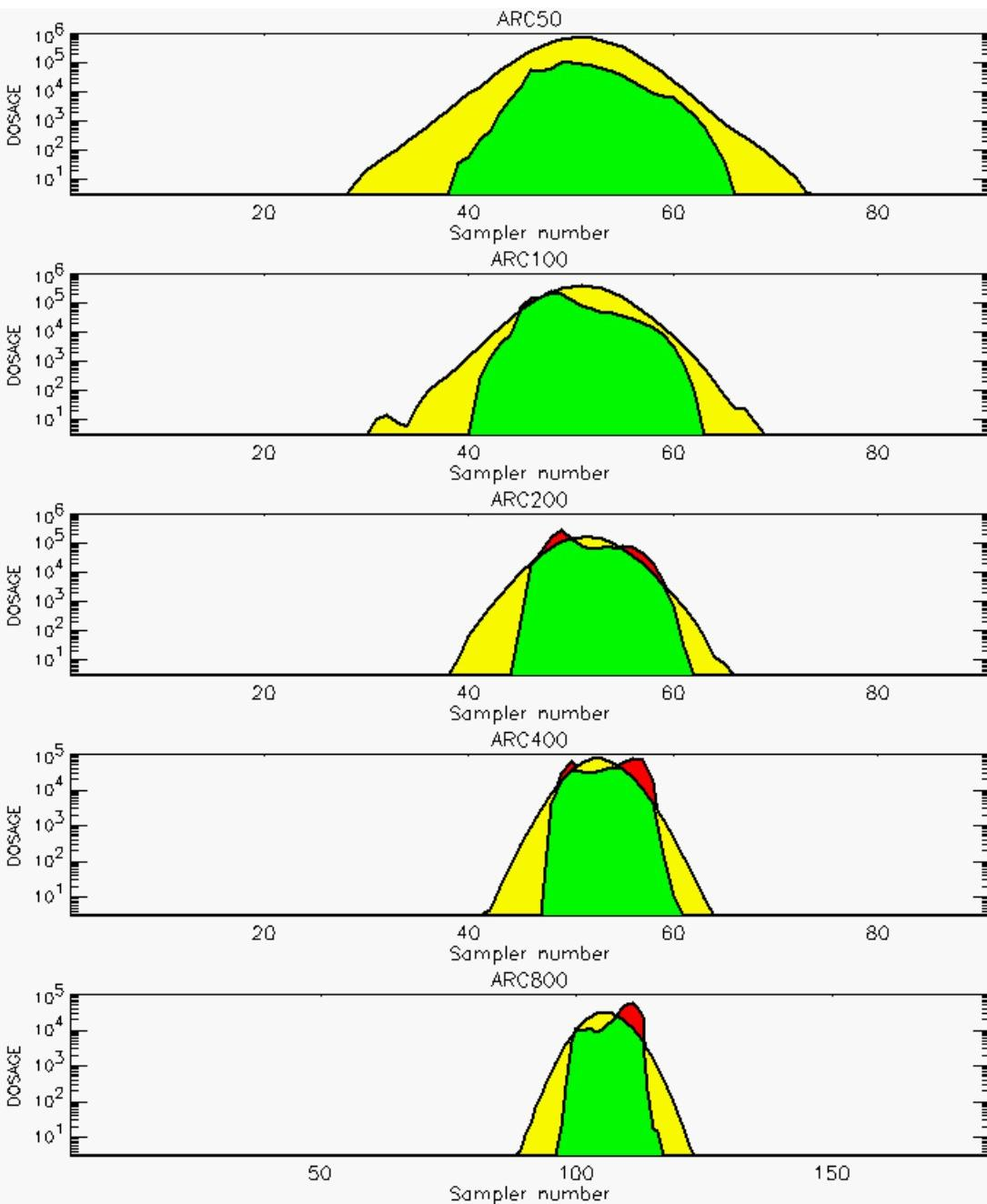


PG Observation to Prediction Comparison

PG Trial File: pr_grass_tracer_Experiment_13.txt

Prediction File: ARAC\nodeposition\pg_13_noxd.arac

Figure D-8a. NARAC Prediction to Trial 13 on Linear Scale: Stability Category is 7

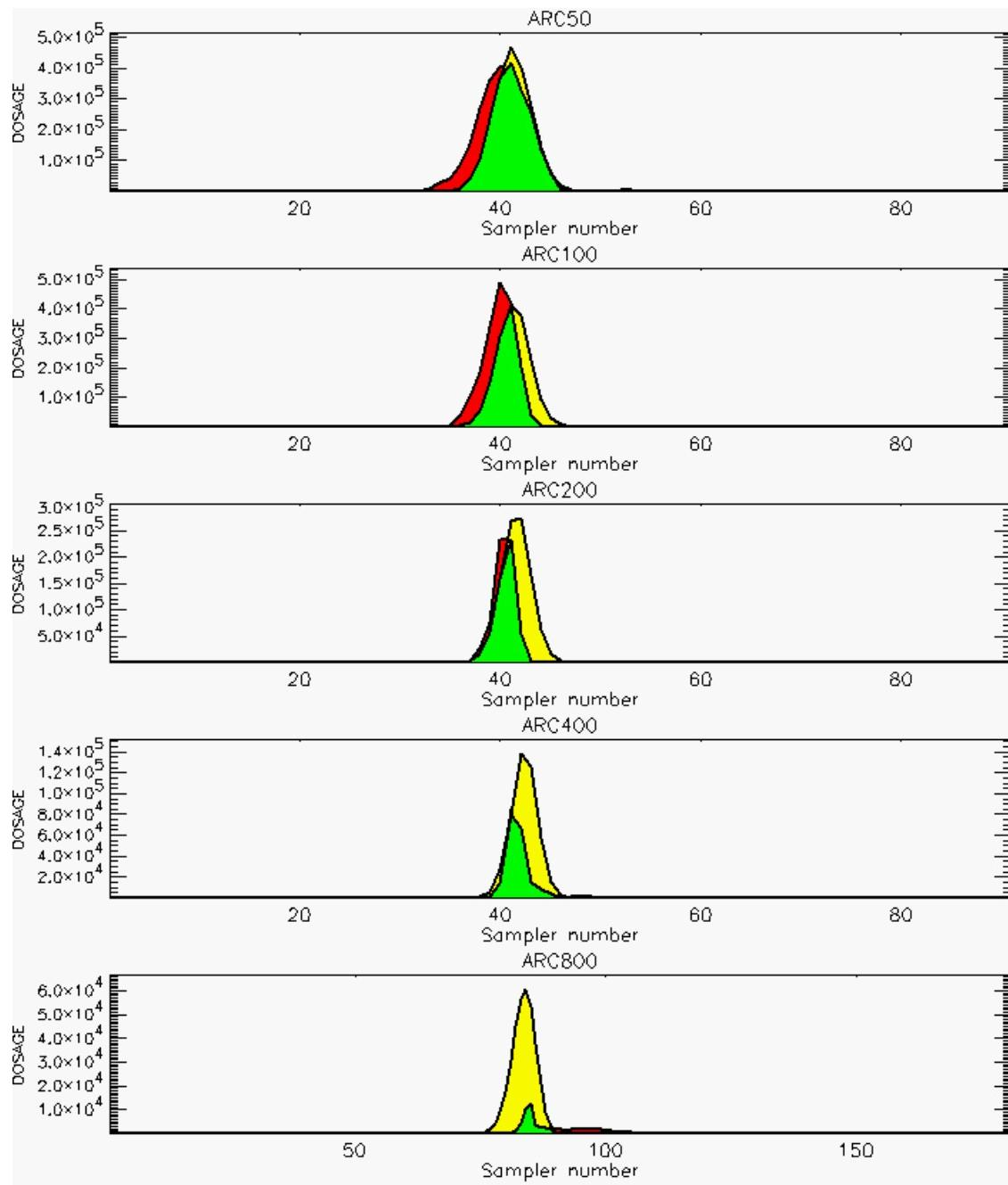


PG Observation to Prediction Comparison

PG Trial File: pr_grass_tracer_Experiment_13.txt

Prediction File: ARAC\nodeposition\pg_13_noxd.arac

Figure D-8b. NARAC Prediction to Trial 13 on Logarithmic Scale: Stability Category is 7

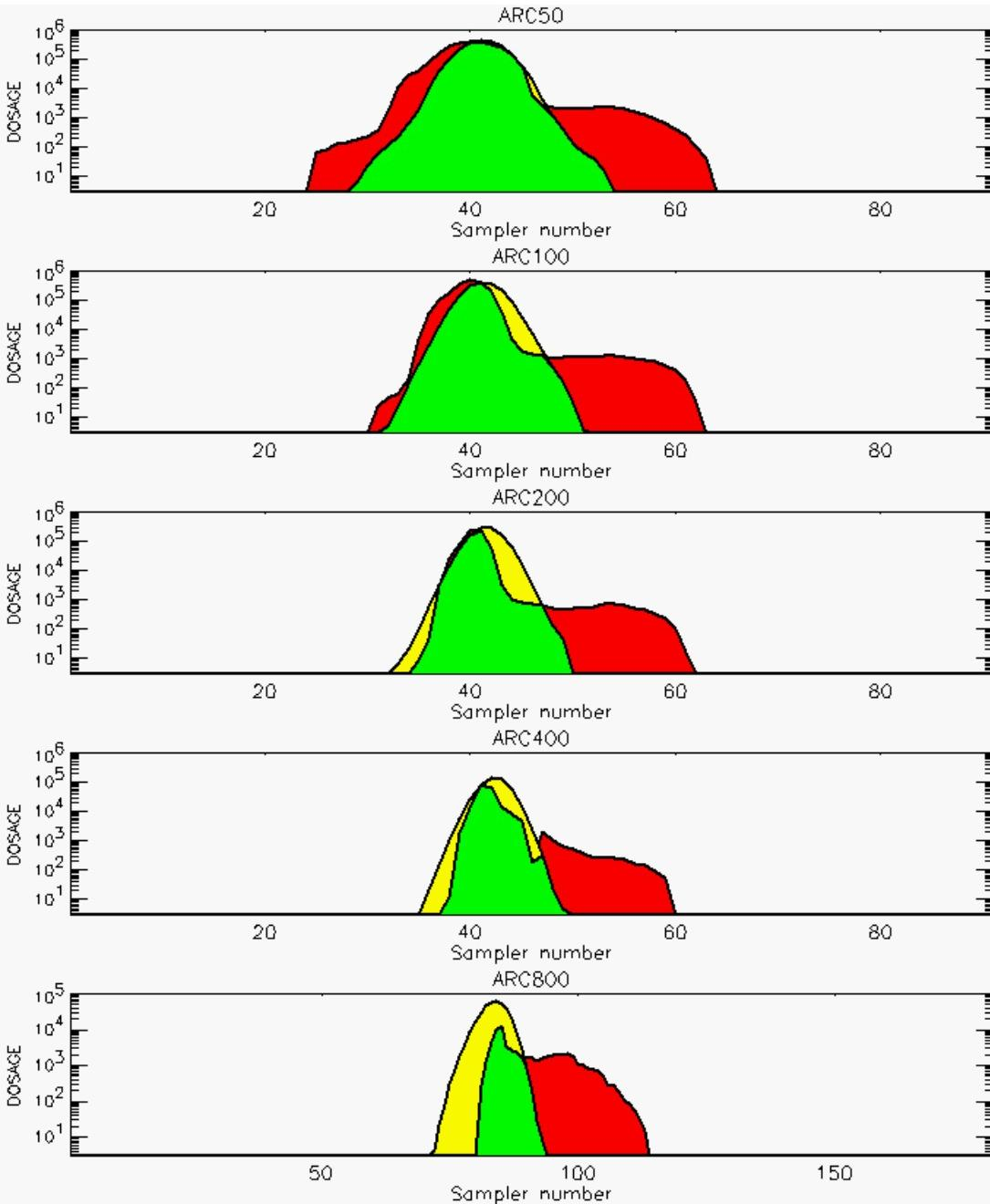


PG Observation to Prediction Comparison

PG Trial File: pr_grass_tracer_Experiment_14.txt

Prediction File: ARAC\nodeposition\pg_14_noxd.arac

Figure D-9a. NARAC Prediction to Trial 14 on Linear Scale: Stability Category is 7

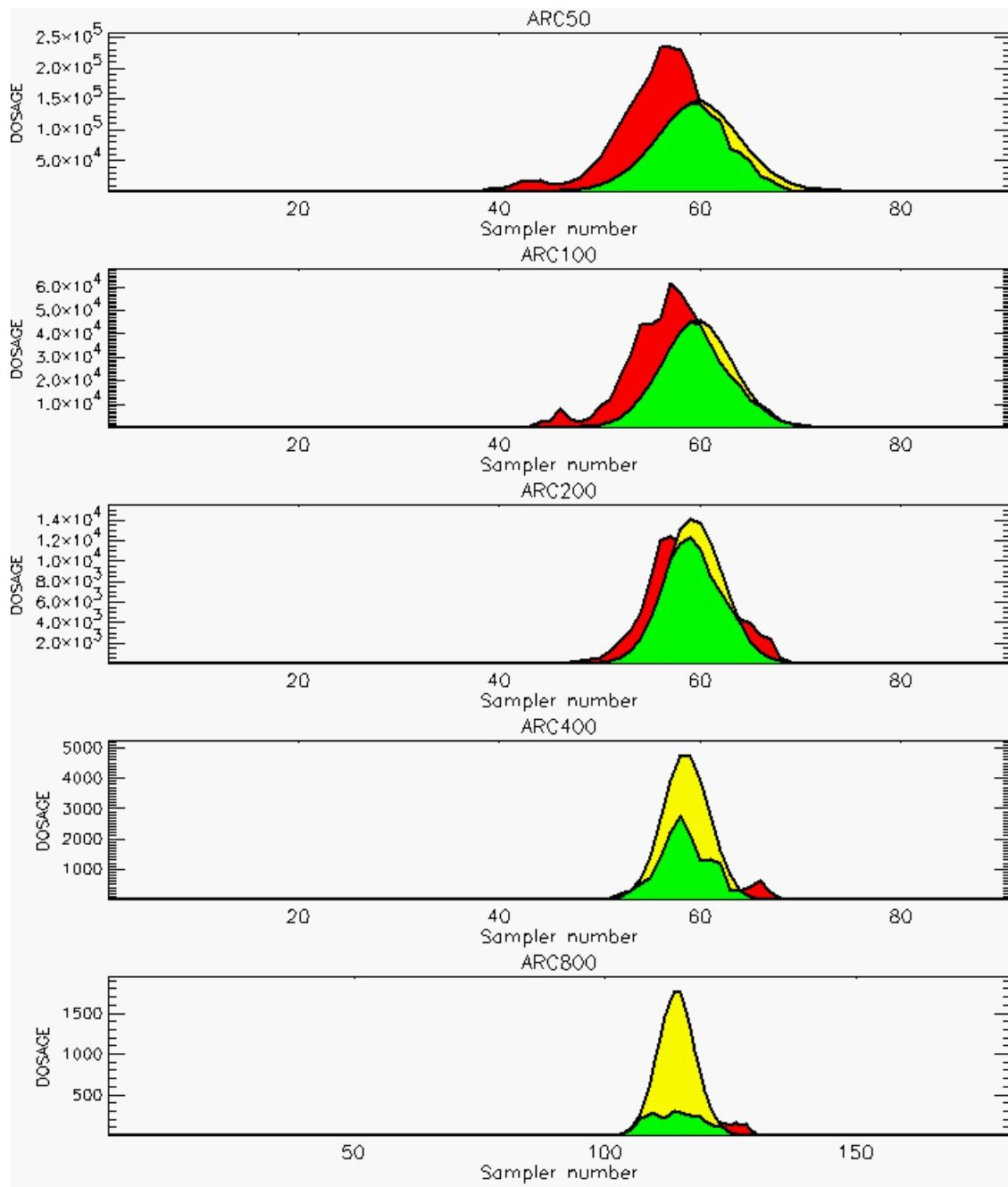


PG Observation to Prediction Comparison

PG Trial File: pr_grass_tracer_Experiment_14.txt

Prediction File: ARAC\nodeposition\pg_14_noxd.arac

Figure D-9b. NARAC Prediction to Trial 14 on Logarithmic Scale: Stability Category is 7

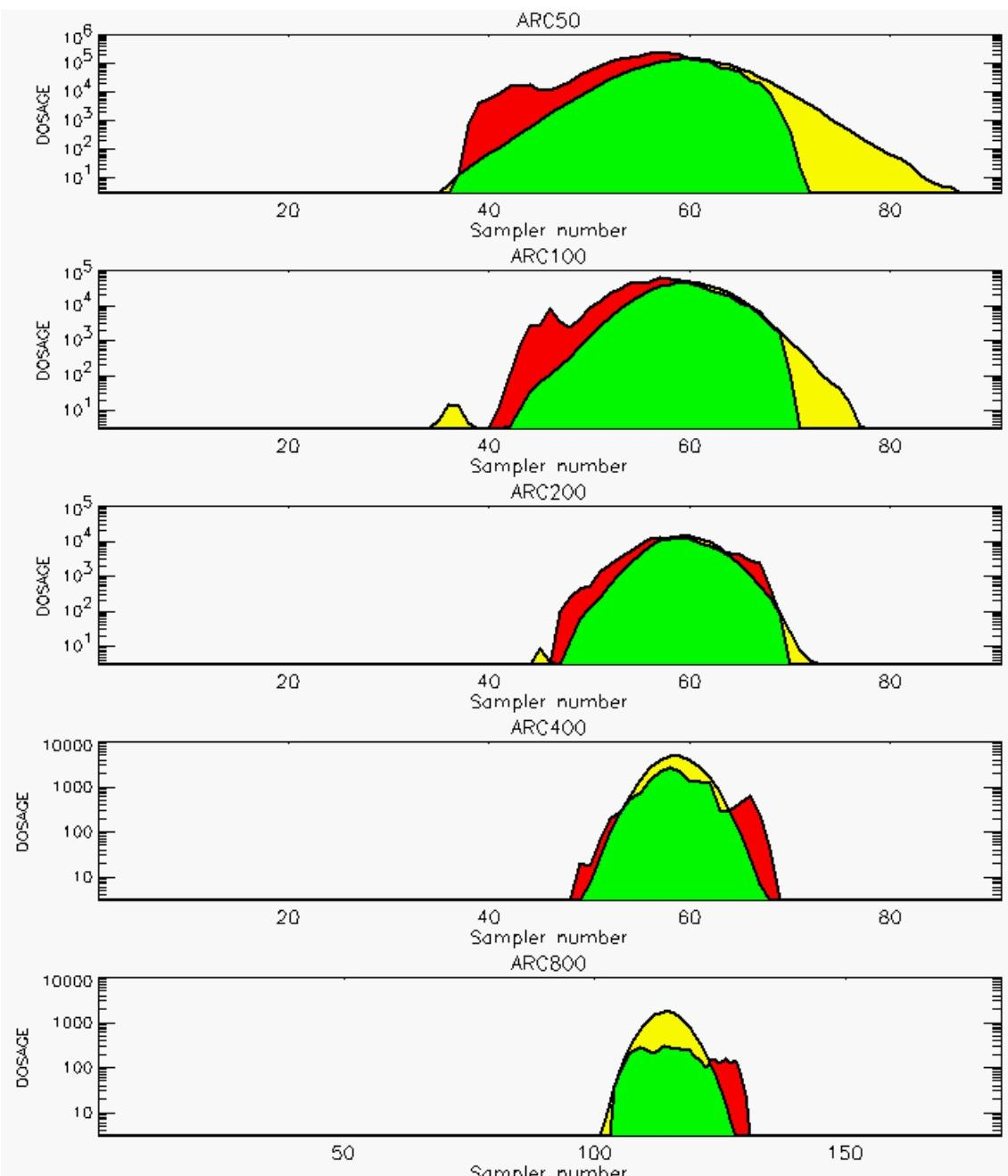


PG Observation to Prediction Comparison

PG Trial File: pr_grass_tracer_Experiment_15.txt

Prediction File: ARAC\nodeposition\pg_15_noxd.arac

Figure D-10a. NARAC Prediction to Trial 15 on Linear Scale: Stability Category is 1

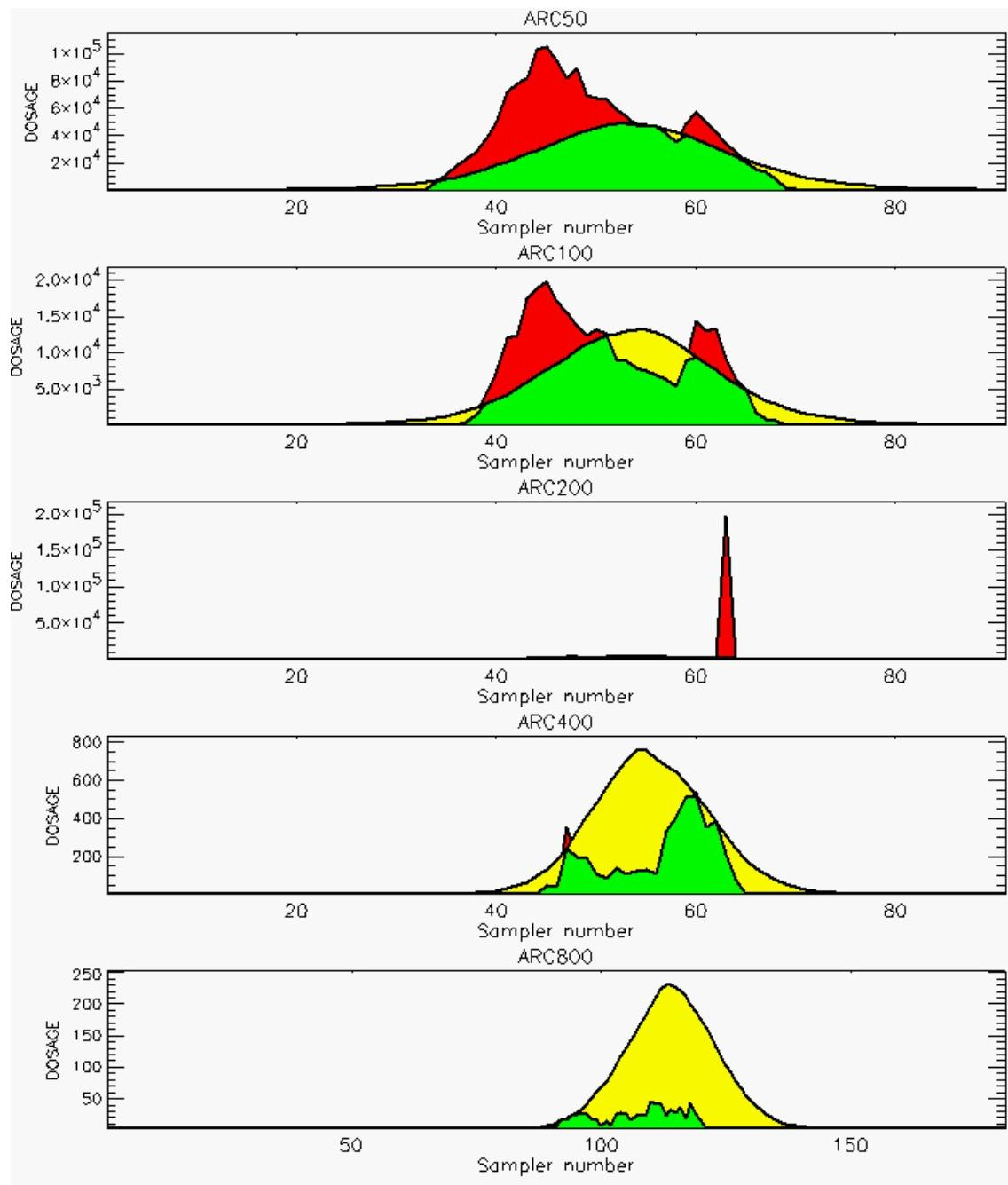


PG Observation to Prediction Comparison

PG Trial File: pr_grass_tracer_Experiment_15.txt

Prediction File: ARAC\nodeposition\pg_15_noxd.arac

Figure D-10b. NARAC Prediction to Trial 15 on Logarithmic Scale: Stability Category is 1

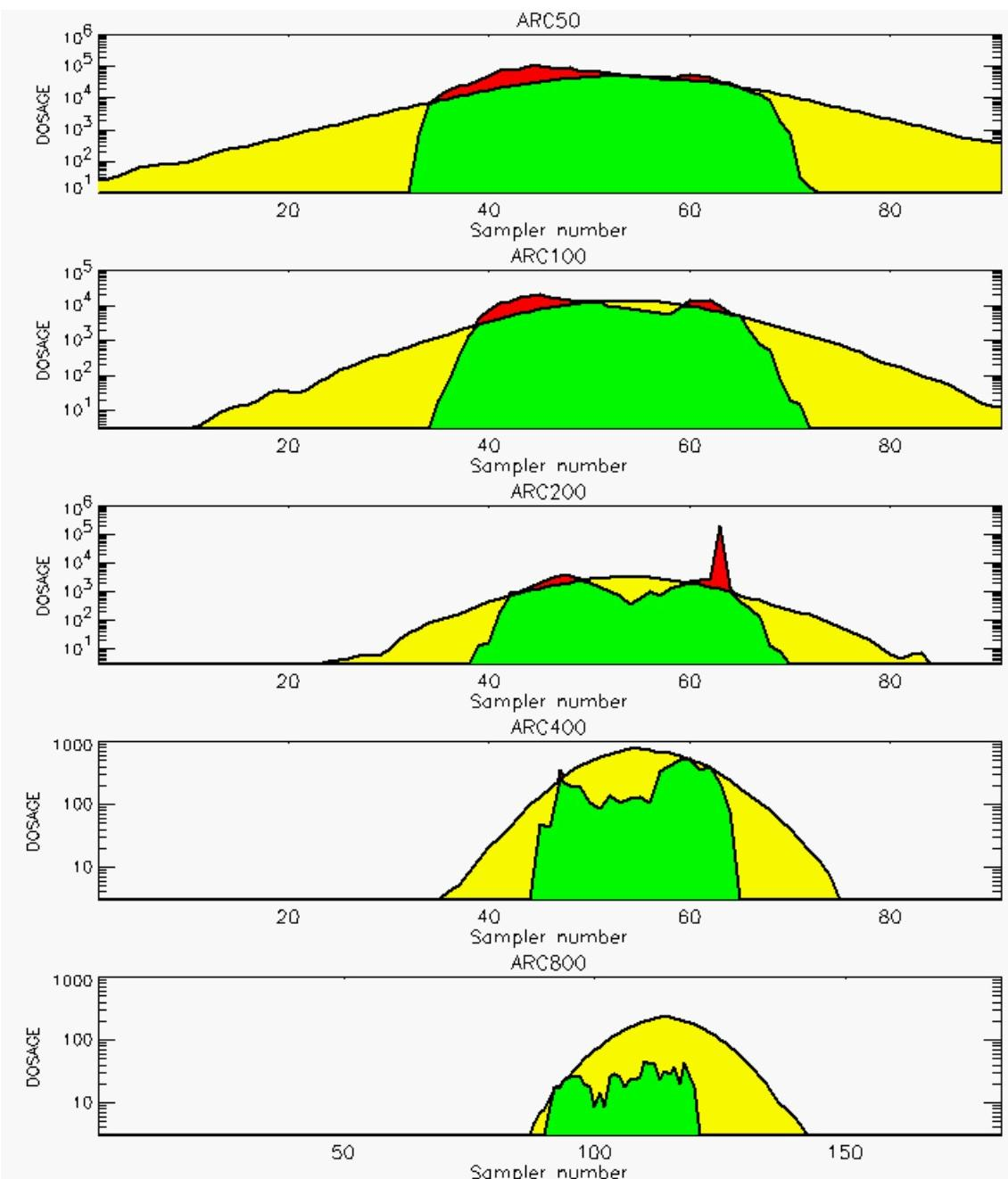


PG Observation to Prediction Comparison

PG Trial File: pr_grass_tracer_Experiment_16.txt

Prediction File: ARAC\nodeposition\pg_16_noxd.arac

Figure D-11a. NARAC Prediction to Trial 16 on Linear Scale: Stability Category is 1 (Value for Sampler 63 of 200-Meter Arc is Considered "Spurious" and is Fixed by Moving Decimal Point)

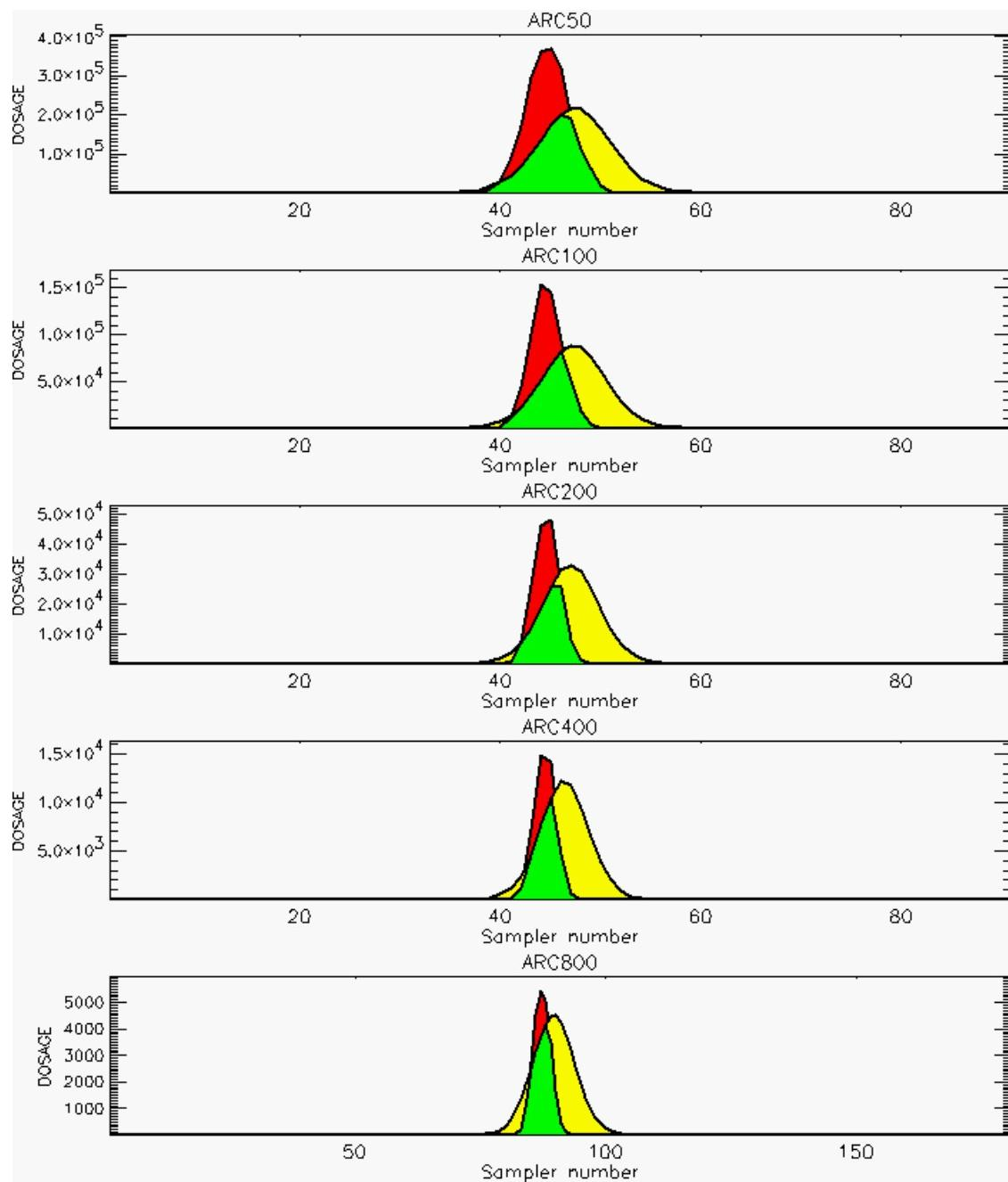


PG Observation to Prediction Comparison

PG Trial File: pr_grass_tracer_Experiment_16.txt

Prediction File: ARAC\nodeposition\pg_16_noxd.arac

Figure D-11b. NARAC Prediction to Trial 16 on Logarithmic Scale: Stability Category is 1 (Value for Sampler 63 of 200-Meter Arc is Considered "Spurious" and is Fixed by Moving Decimal Point)

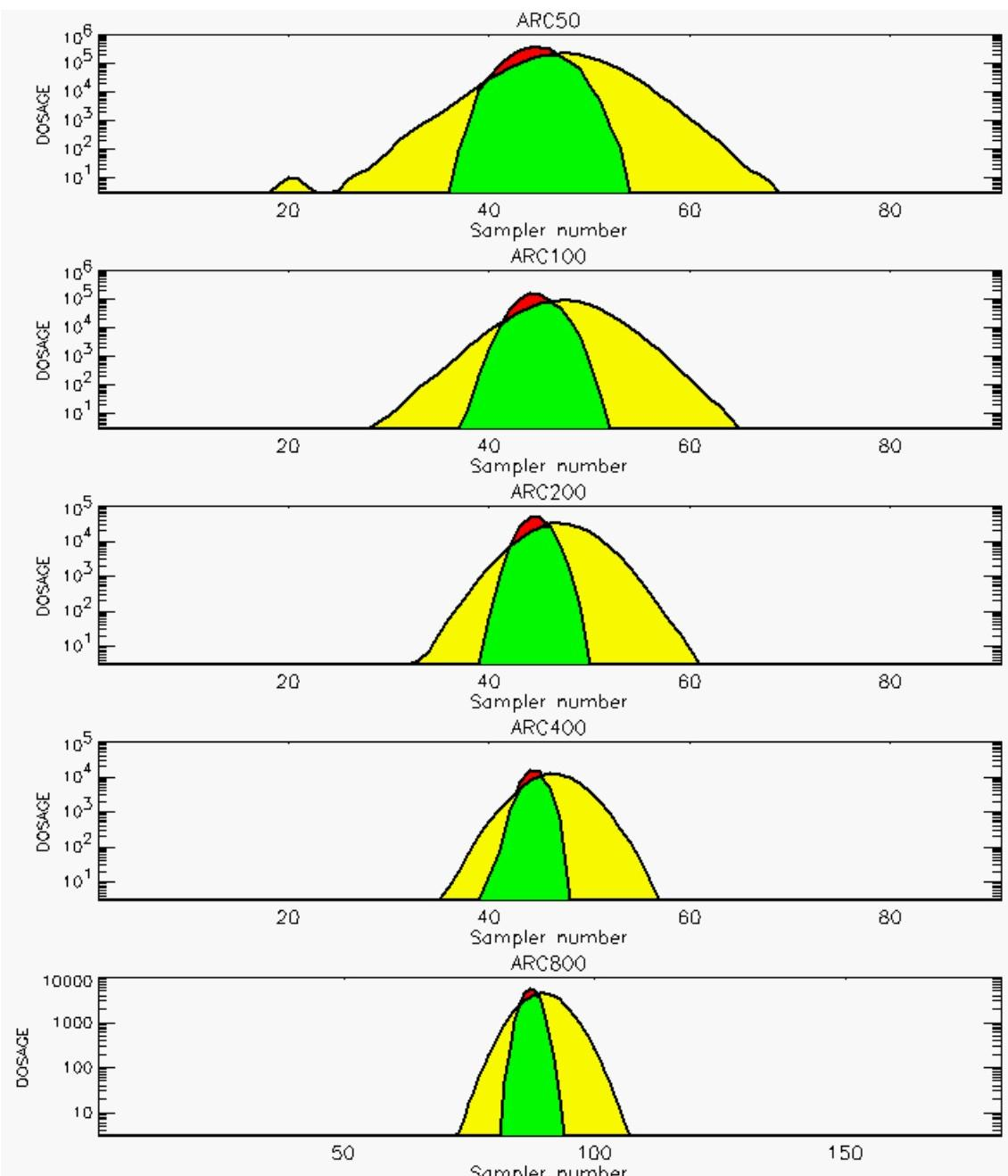


PG Observation to Prediction Comparison

PG Trial File: pr_grass_tracer_Experiment_17.txt

Prediction File: ARAC\nodeposition\pg_17_noxd.arac

Figure D-12a. NARAC Prediction to Trial 17 on Linear Scale: Stability Category is 5

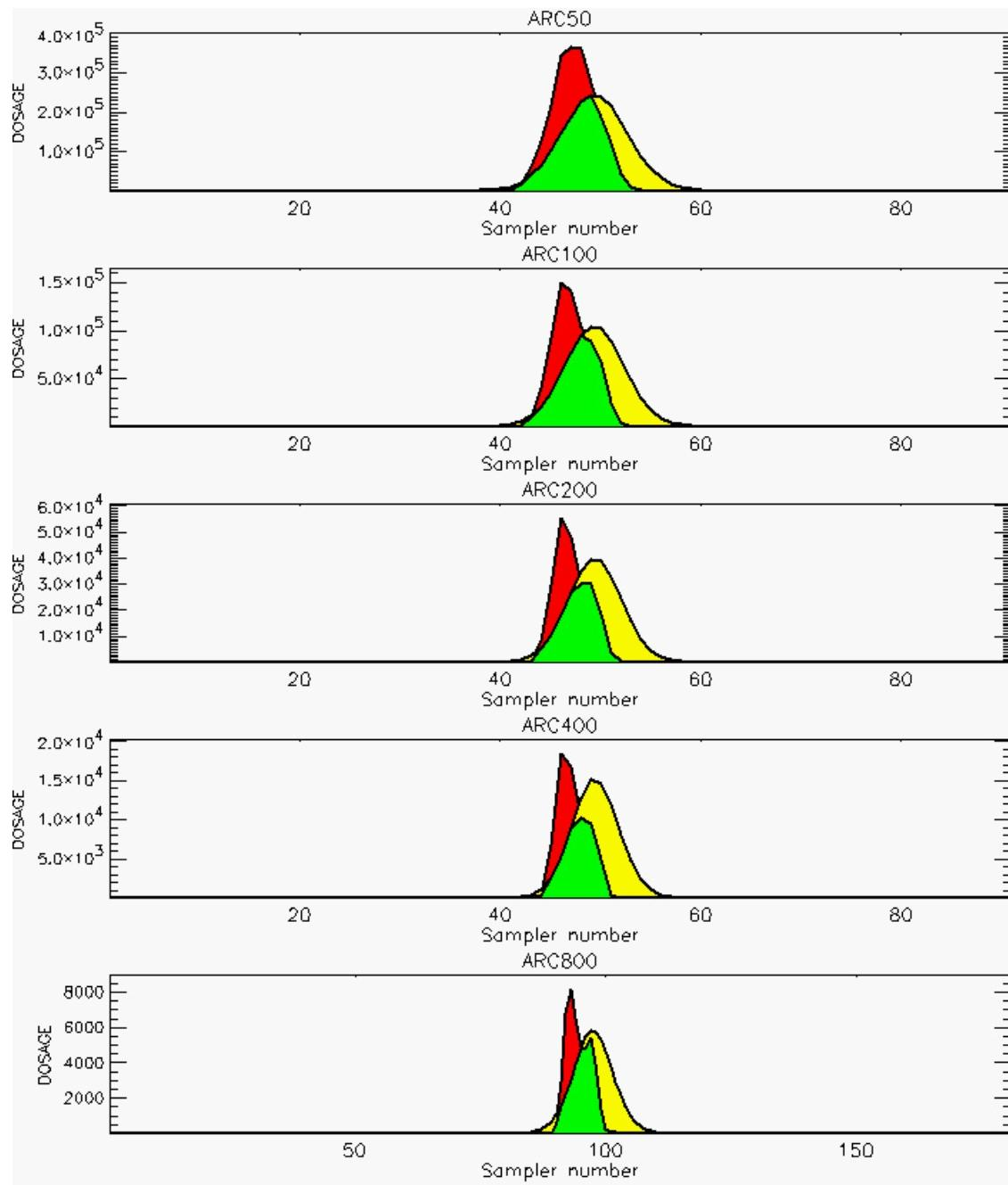


PG Observation to Prediction Comparison

PG Trial File: pr_grass_tracer_Experiment_17.txt

Prediction File: ARAC\nodeposition\pg_17_noxd.arac

Figure D-12b. NARAC Prediction to Trial 17 on Logarithmic Scale: Stability Category is 5

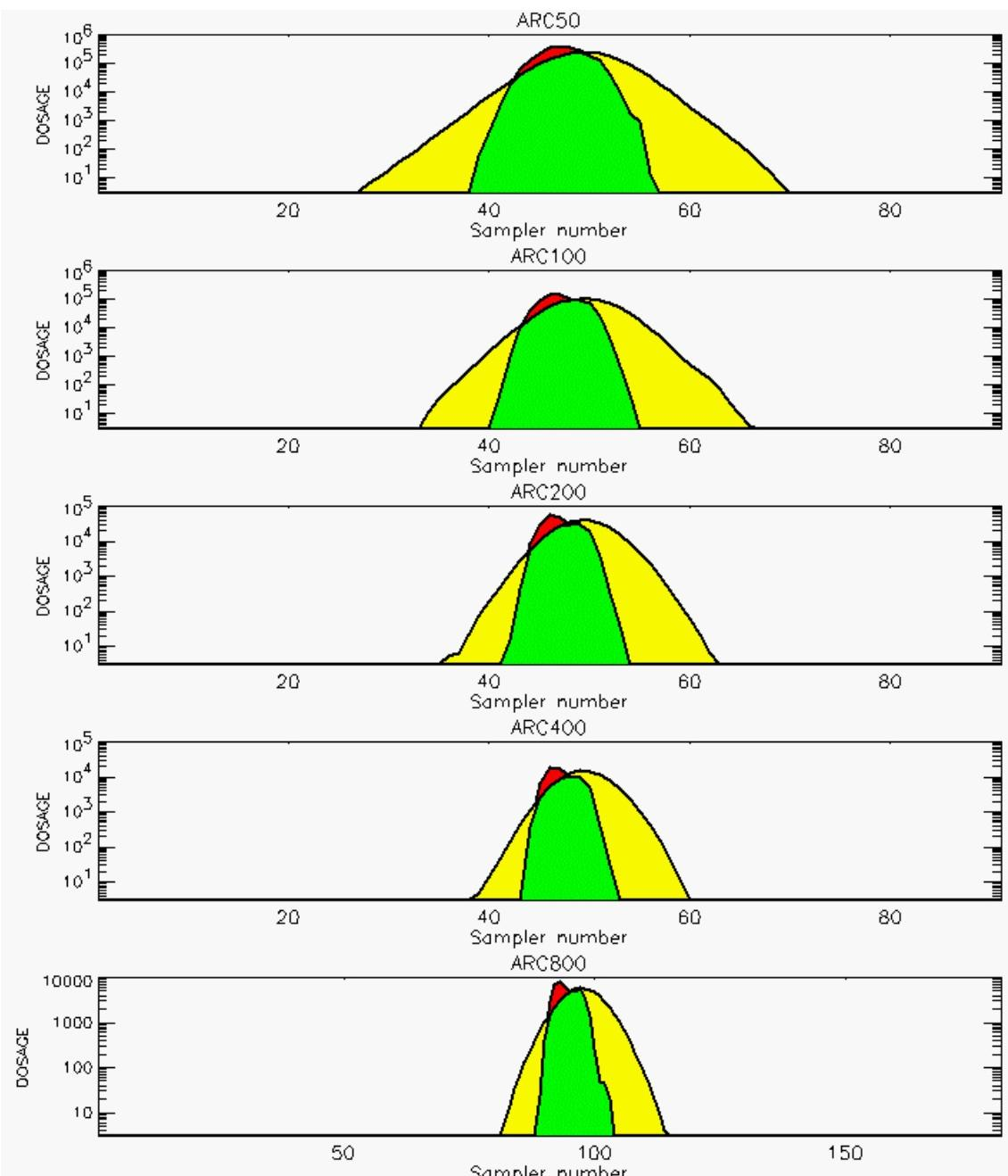


PG Observation to Prediction Comparison

PG Trial File: pr_grass_tracer_Experiment_18.txt

Prediction File: ARAC\nodeposition\pg_18_noxd.arac

Figure D-13a. NARAC Prediction to Trial 18 on Linear Scale: Stability Category is 5

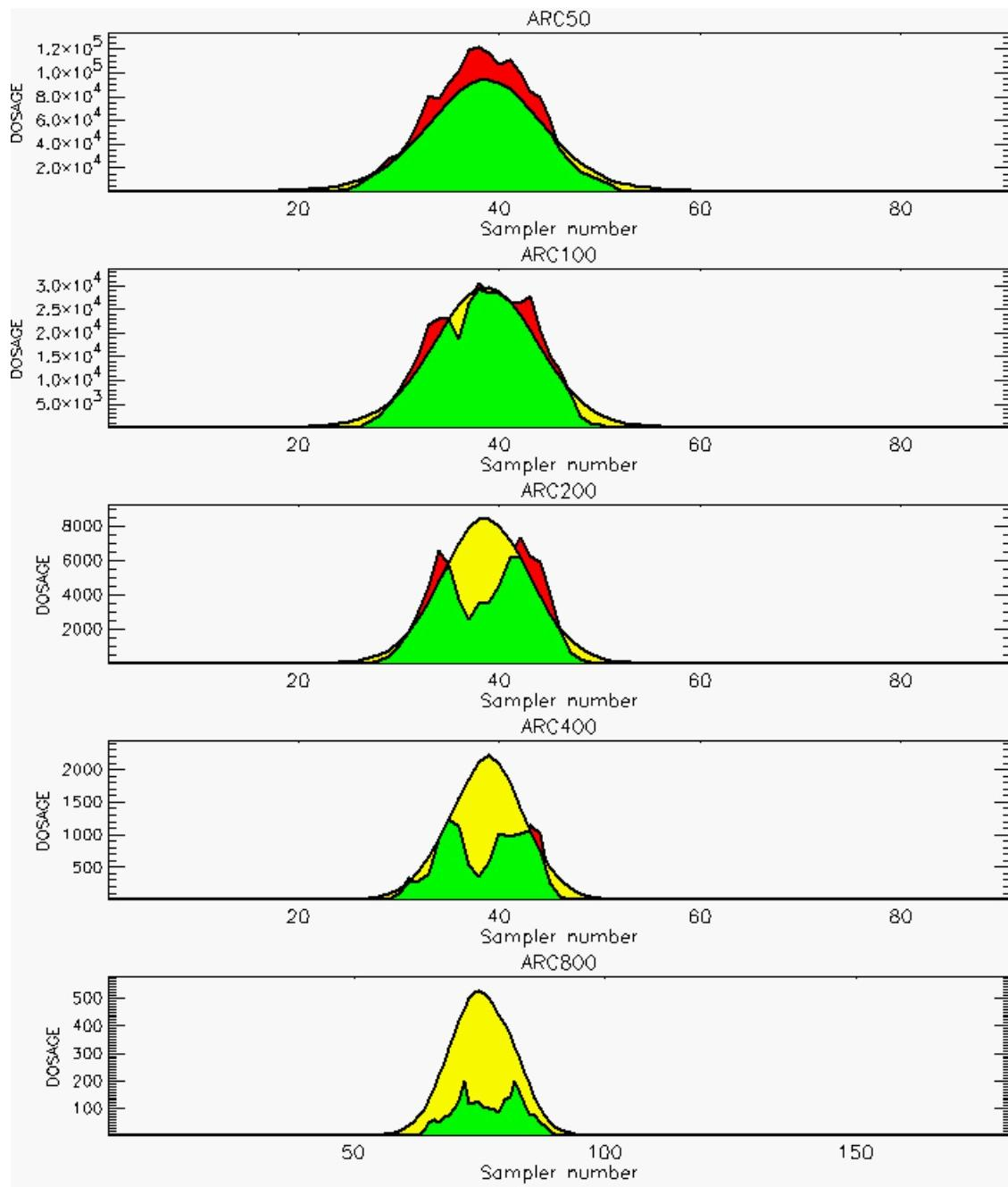


PG Observation to Prediction Comparison

PG Trial File: pr_grass_tracer_Experiment_18.txt

Prediction File: ARAC\nodeposition\pg_18_noxd.arac

Figure D-13b. NARAC Prediction to Trial 18 on Logarithmic Scale: Stability Category is 5

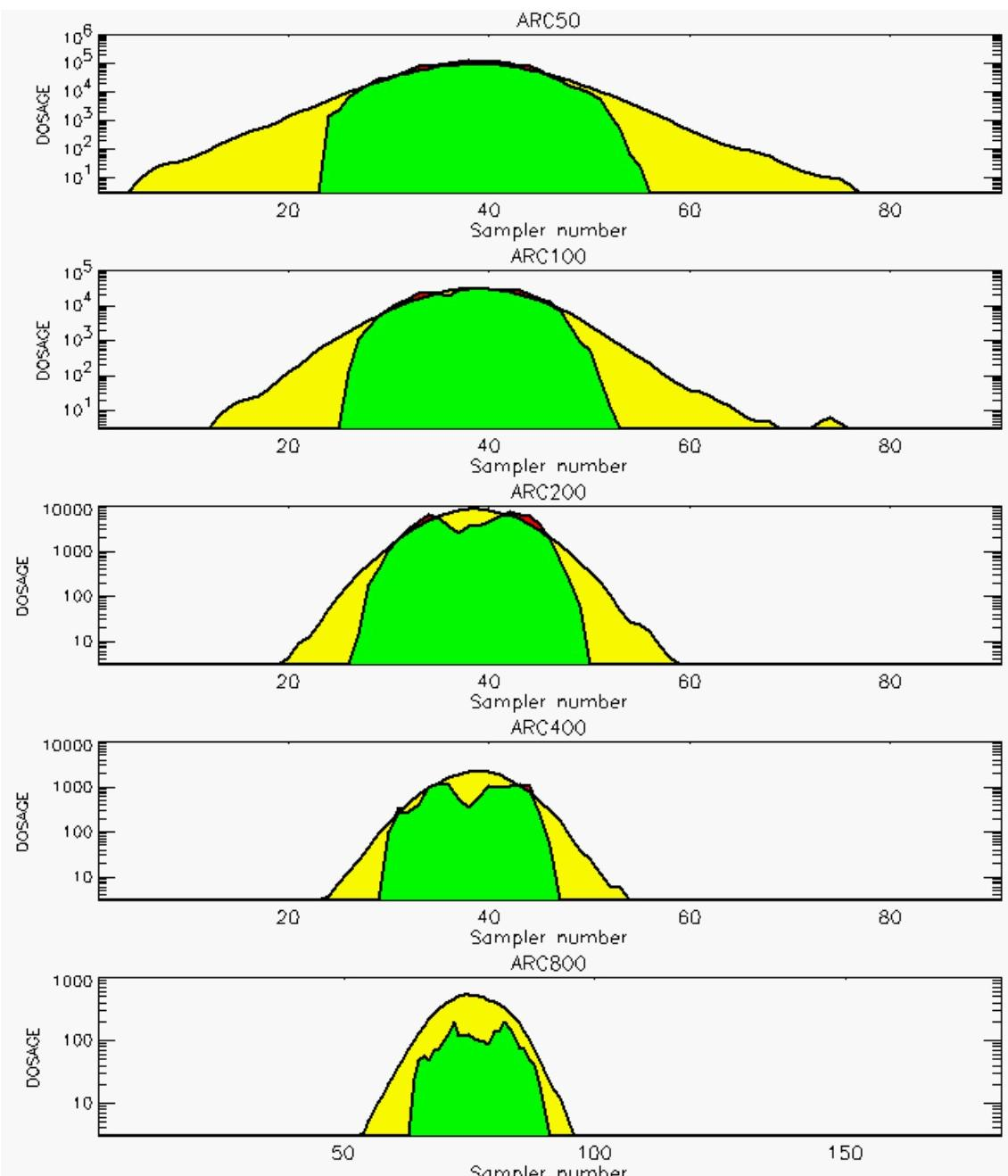


PG Observation to Prediction Comparison

PG Trial File: pr_grass_tracer_Experiment_19.txt

Prediction File: ARAC\nodeposition\pg_19_noxd.arac

Figure D-14a. NARAC Prediction to Trial 19 on Linear Scale: Stability Category is 2

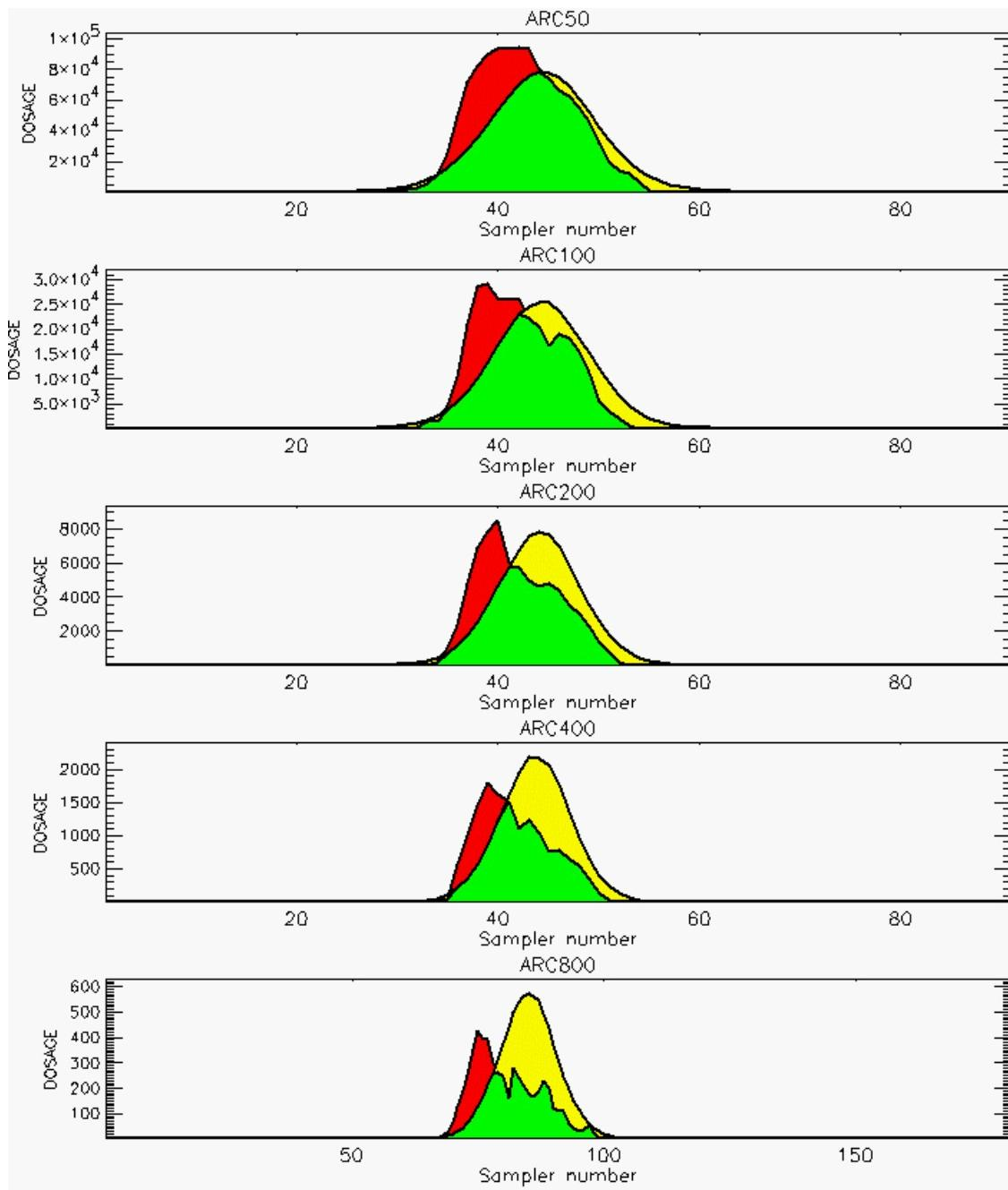


PG Observation to Prediction Comparison

PG Trial File: pr_grass_tracer_Experiment_19.txt

Prediction File: ARAC\nodeposition\pg_19_noxd.arac

Figure D-14b. NARAC Prediction to Trial 19 on Logarithmic Scale: Stability Category is 2

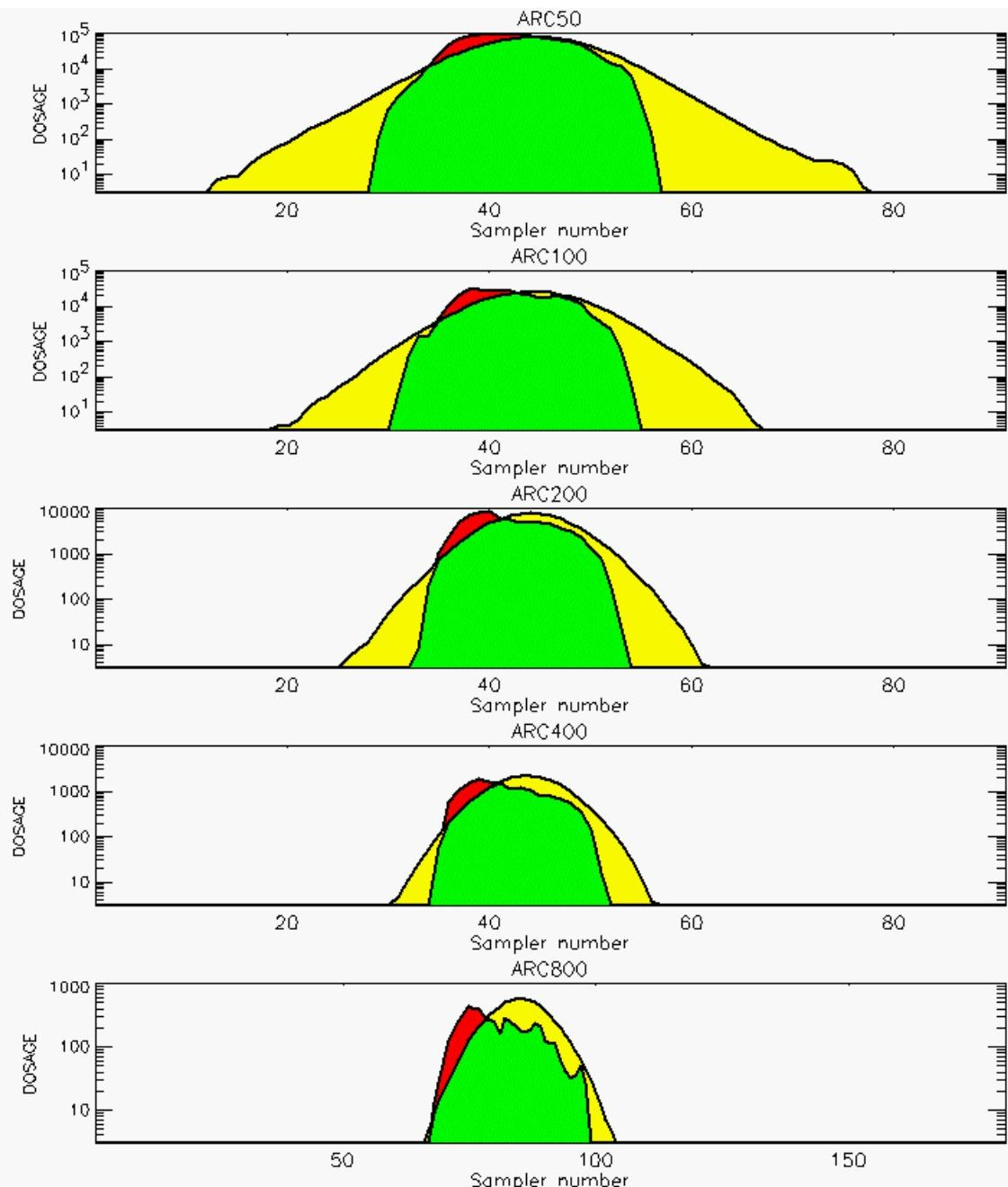


PG Observation to Prediction Comparison

PG Trial File: pr_grass_tracer_Experiment_20.txt

Prediction File: ARAC\nodeposition\pg_20_noxd.arac

Figure D-15a. NARAC Prediction to Trial 20 on Linear Scale: Stability Category is 3

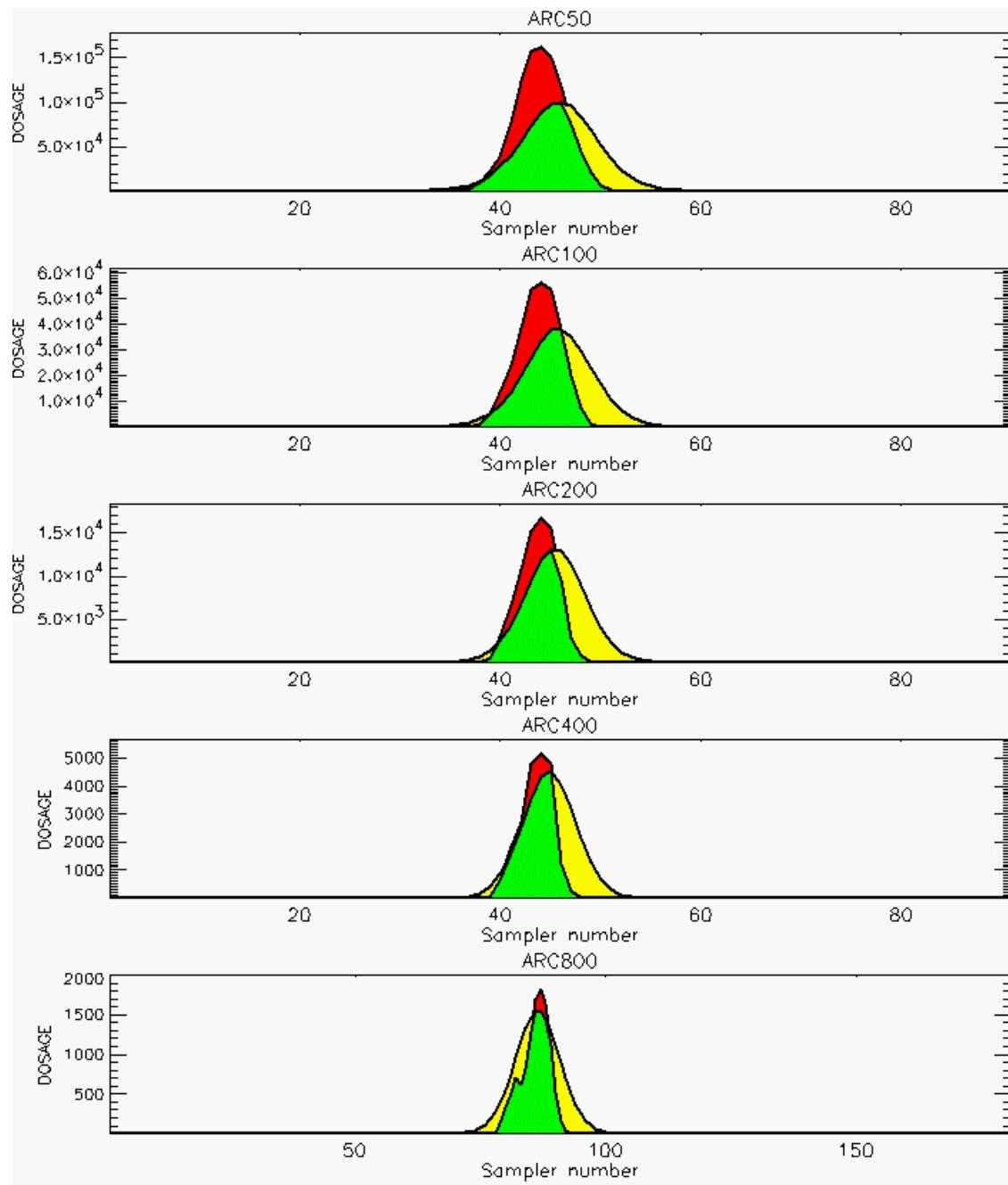


PG Observation to Prediction Comparison

PG Trial File: pr_grass_tracer_Experiment_20.txt

Prediction File: ARAC\nodeposition\pg_20_noxd.arac

Figure D-15b. NARAC Prediction to Trial 20 on Logarithmic Scale: Stability Category is 3

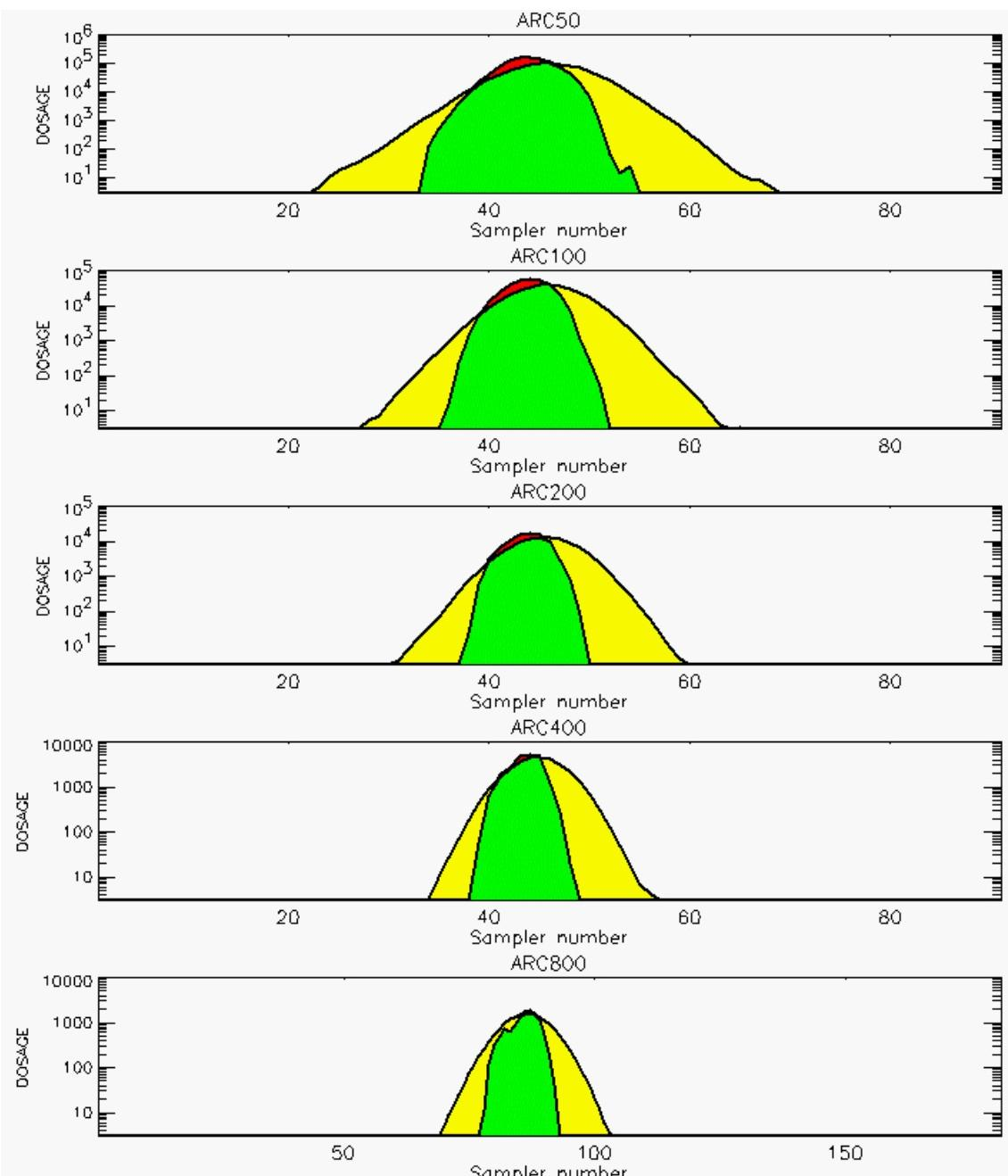


PG Observation to Prediction Comparison

PG Trial File: pr_grass_tracer_Experiment_21.txt

Prediction File: ARAC\nodeposition\pg_21_noxd.arac

Figure D-16a. NARAC Prediction to Trial 21 on Linear Scale: Stability Category is 4

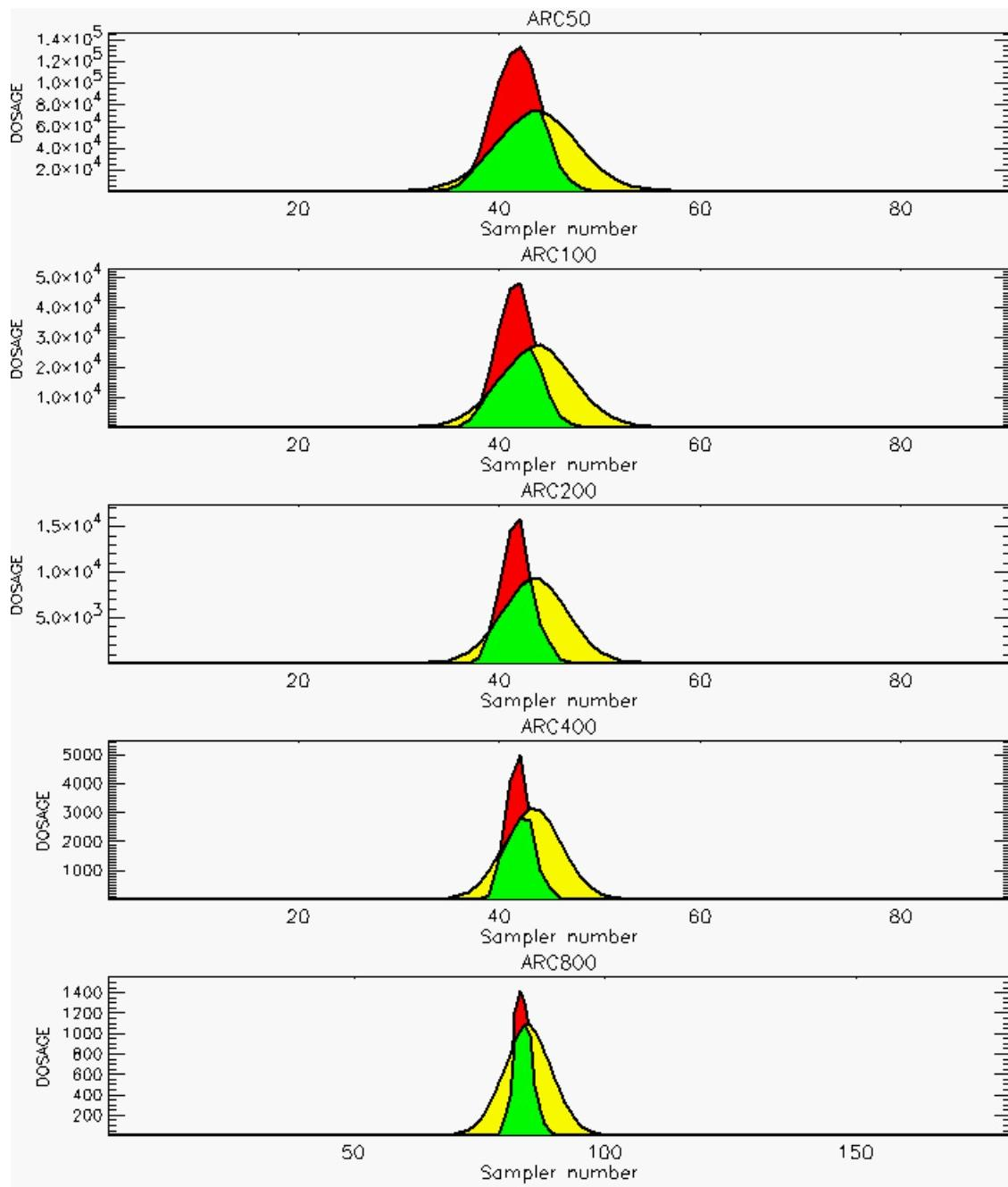


PG Observation to Prediction Comparison

PG Trial File: pr_grass_tracer_Experiment_21.txt

Prediction File: ARAC\nodeposition\pg_21_noxd.arac

Figure D-16b. NARAC Prediction to Trial 21 on Logarithmic Scale: Stability Category is 4

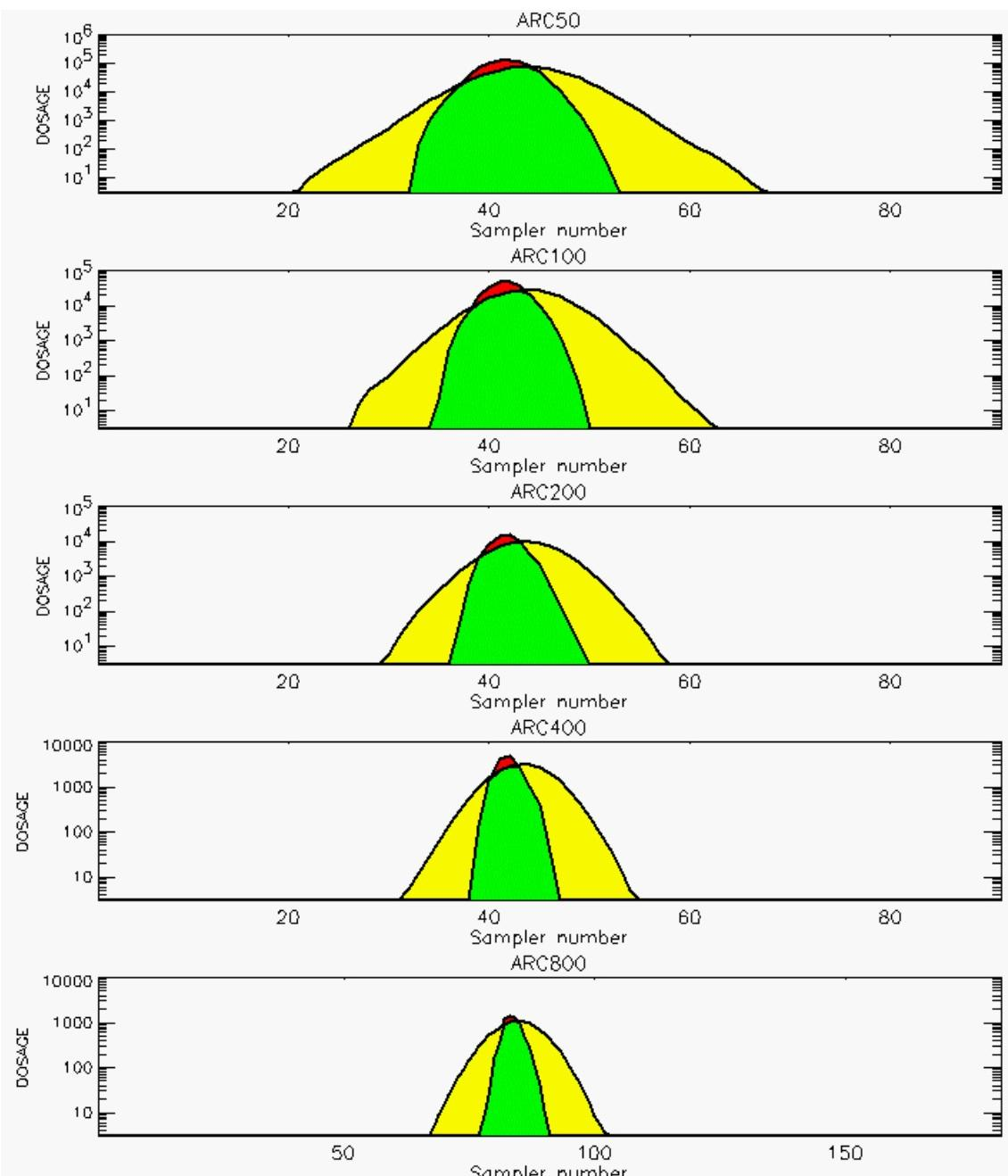


PG Observation to Prediction Comparison

PG Trial File: pr_grass_tracer_Experiment_22.txt

Prediction File: ARAC\nodeposition\pg_22_noxd.arac

Figure D-17a. NARAC Prediction to Trial 22 on Linear Scale: Stability Category is 4

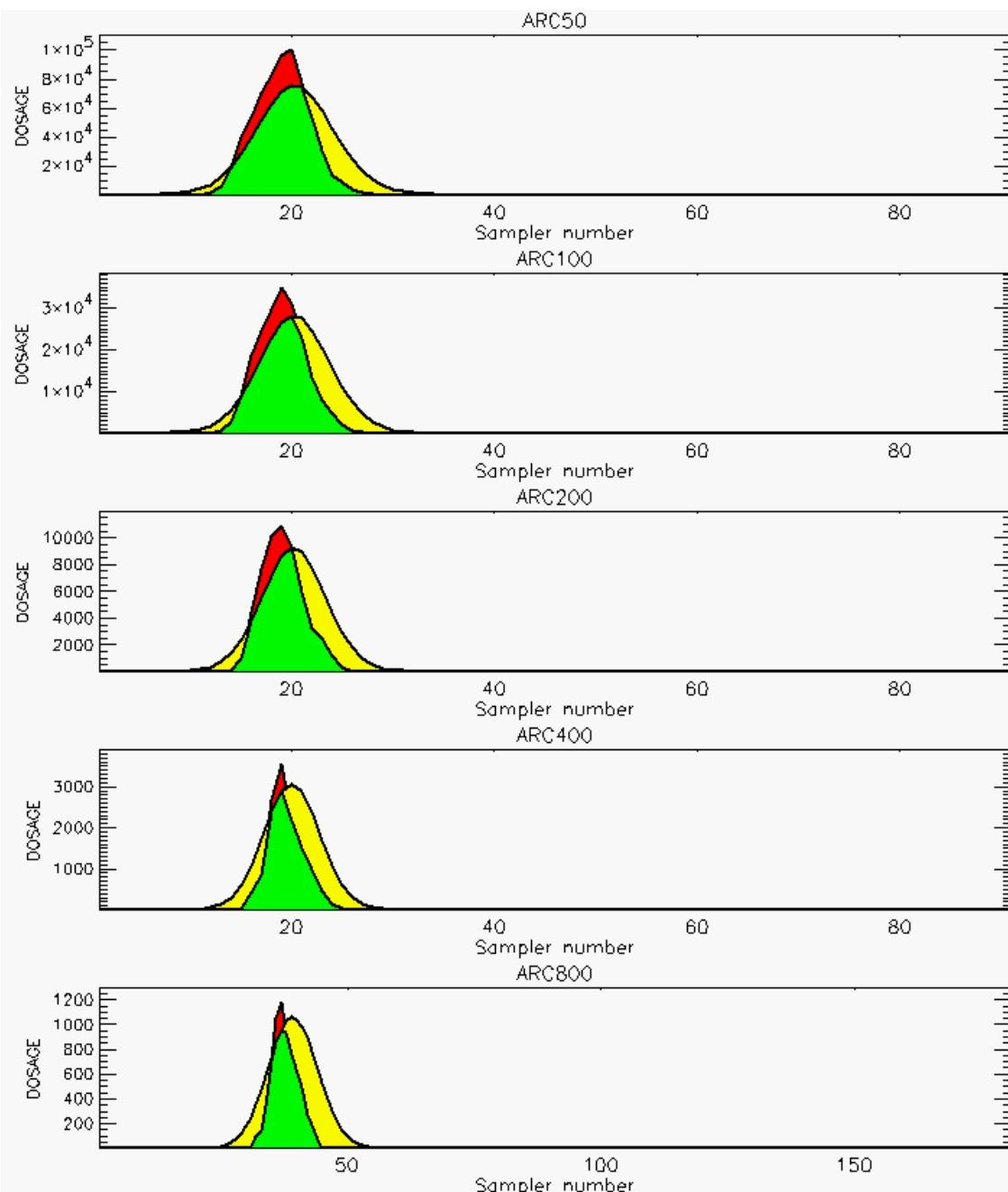


PG Observation to Prediction Comparison

PG Trial File: pr_grass_tracer_Experiment_22.txt

Prediction File: ARAC\nodeposition\pg_22_noxd.arac

Figure D-17b. NARAC Prediction to Trial 22 on Logarithmic Scale: Stability Category is 4

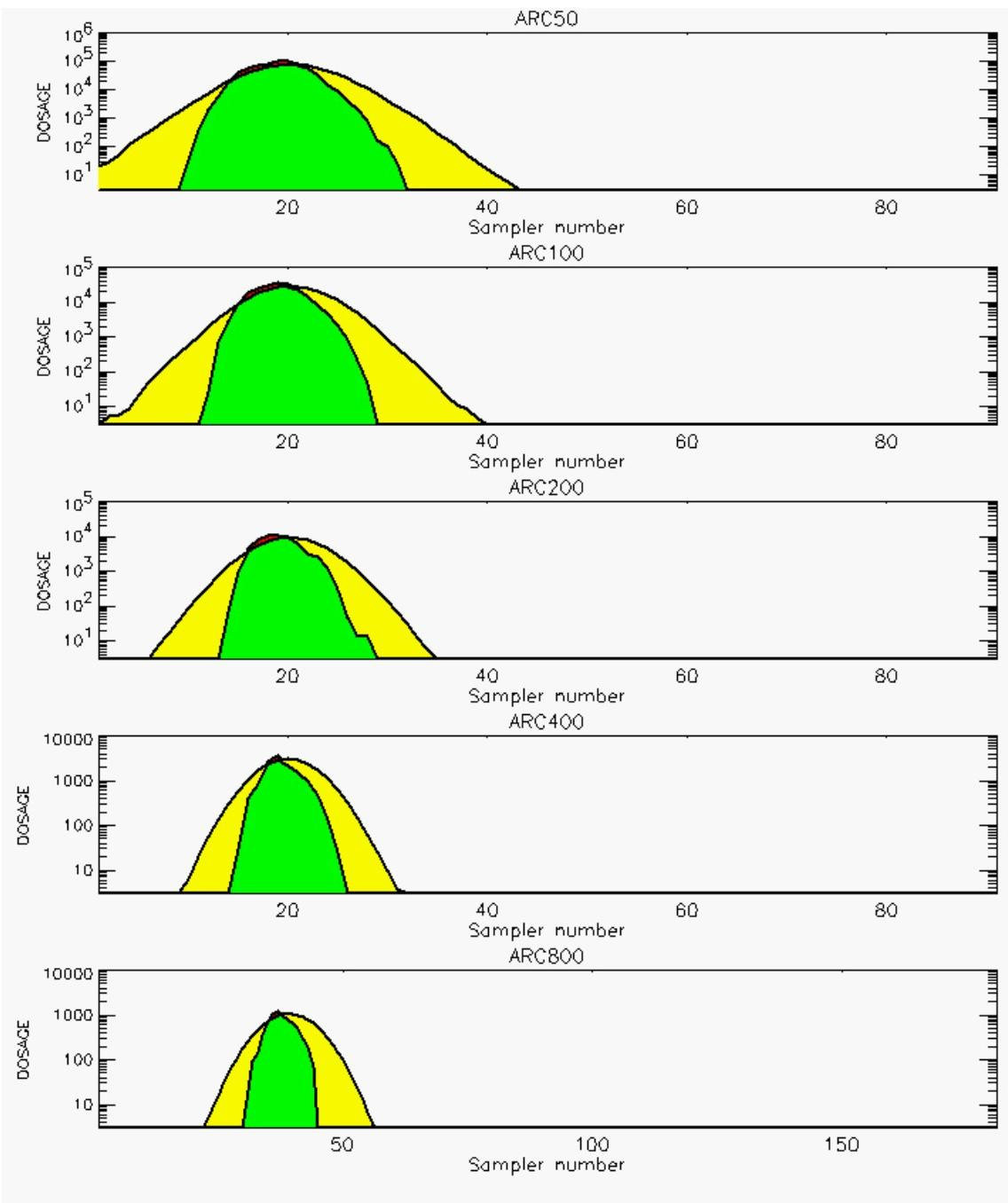


PG Observation to Prediction Comparison

PG Trial File: pr_grass_tracer_Experiment_23.txt

Prediction File: ARAC\nodeposition\pg_23_noxd.arac

Figure D-18a. NARAC Prediction to Trial 23 on Linear Scale: Stability Category is 4

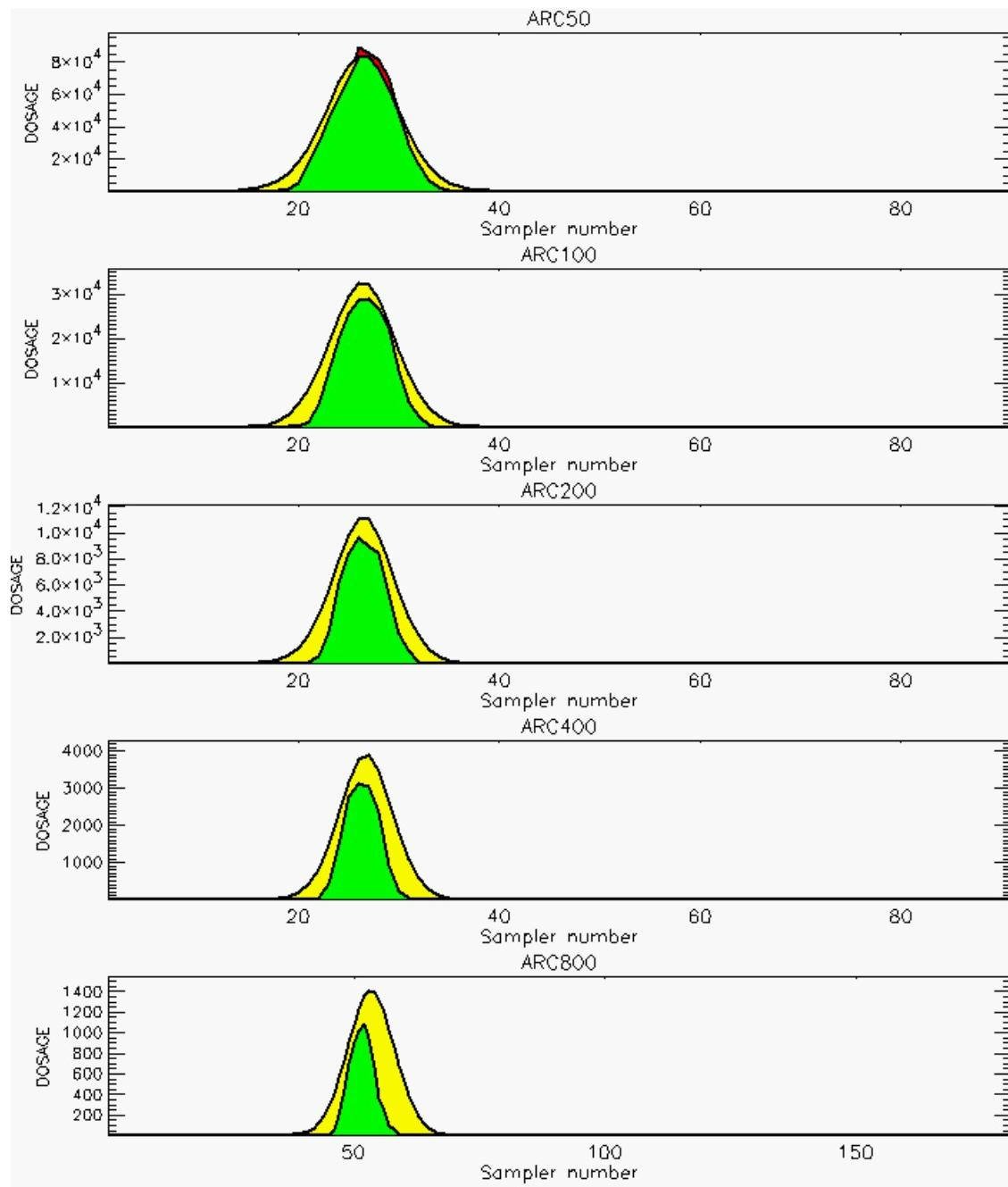


PG Observation to Prediction Comparison

PG Trial File: pr_grass_tracer_Experiment_23.txt

Prediction File: ARAC\nodeposition\pg_23_noxd.arac

Figure D-18b. NARAC Prediction to Trial 23 on Logarithmic Scale: Stability Category is 4

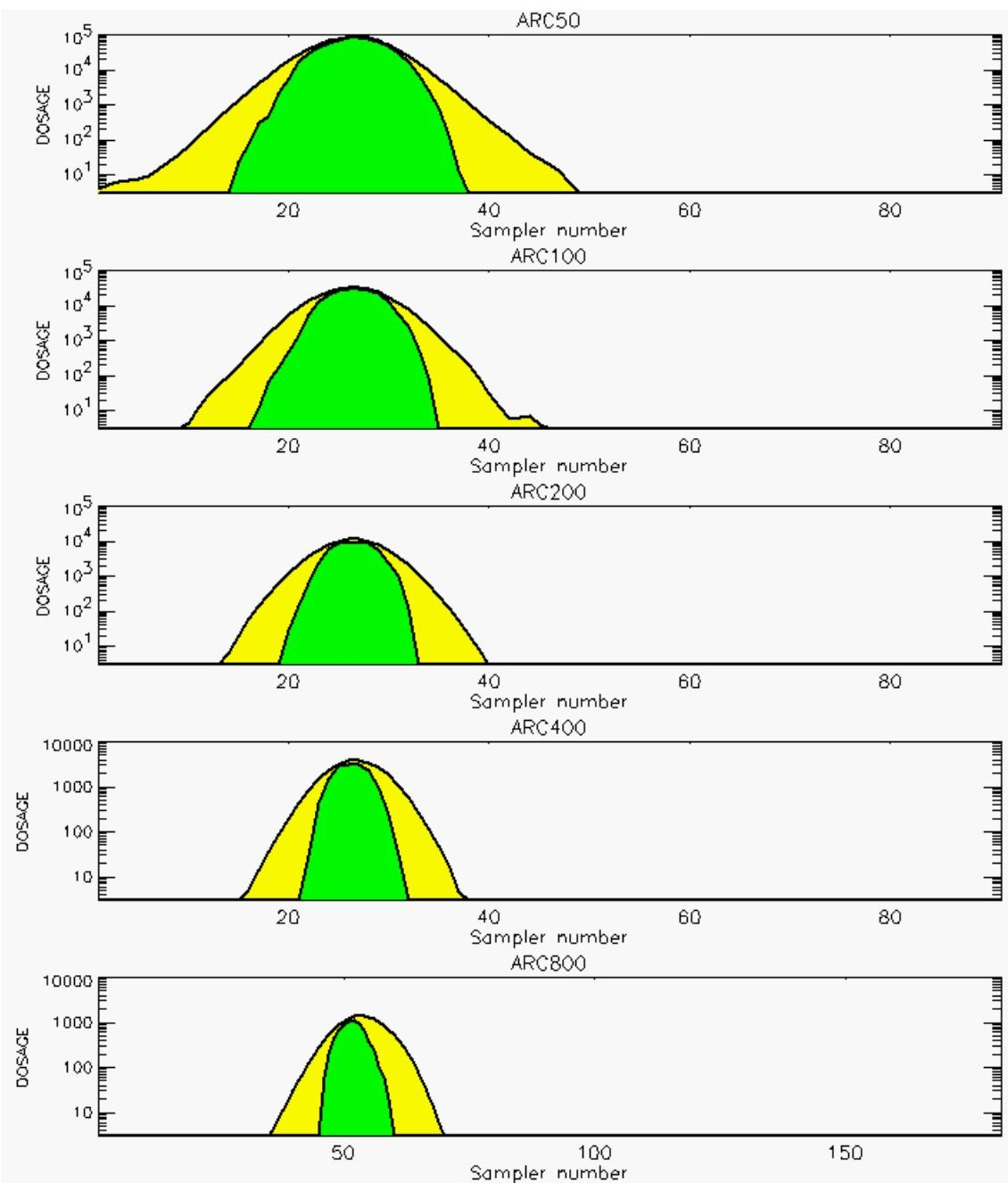


PG Observation to Prediction Comparison

PG Trial File: pr_grass_tracer_Experiment_24.txt

Prediction File: ARAC\nodeposition\pg_24_noxd.arac

Figure D-19a. NARAC Prediction to Trial 24 on Linear Scale: Stability Category is 4

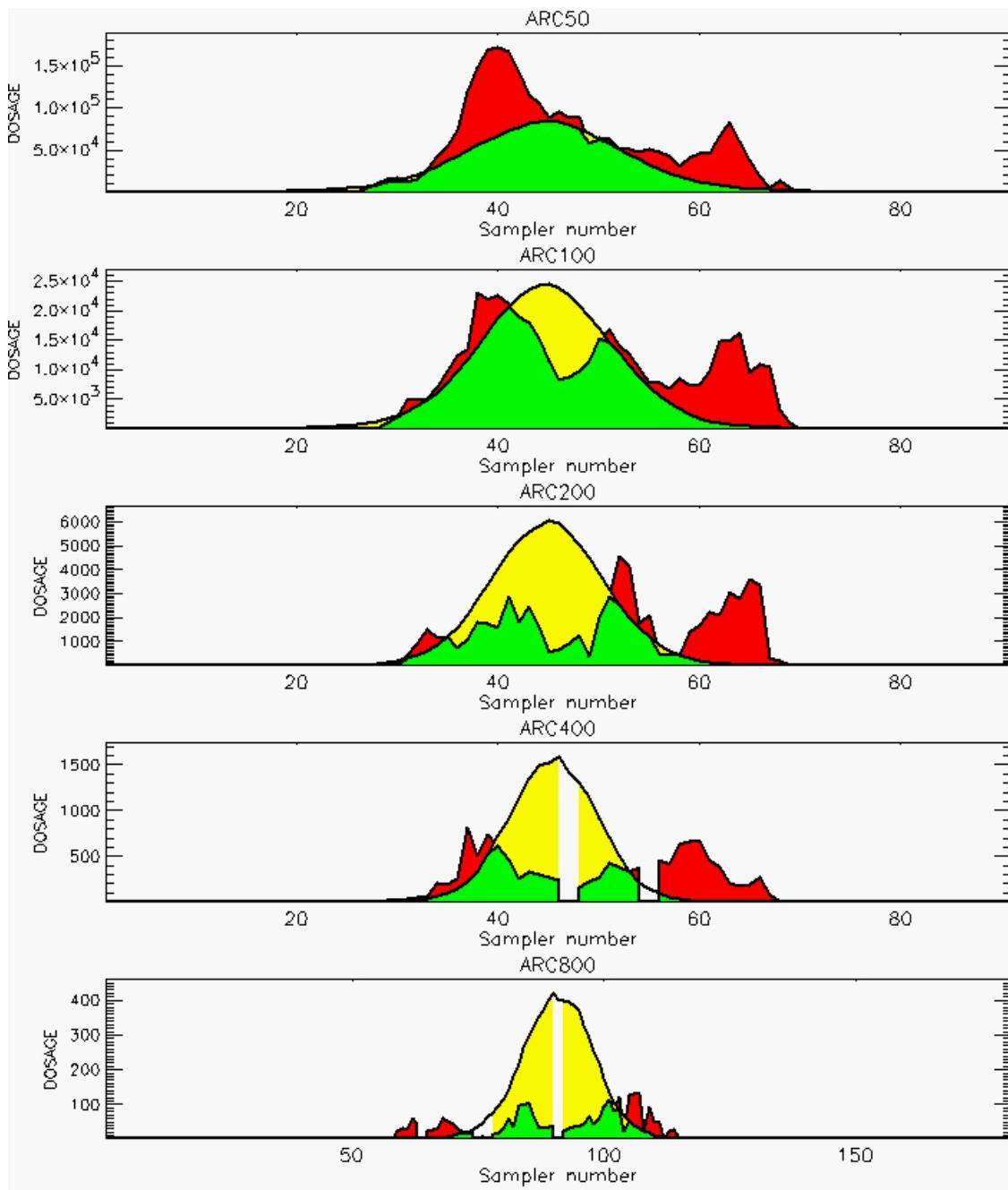


PG Observation to Prediction Comparison

PG Trial File: pr_grass_tracer_Experiment_24.txt

Prediction File: ARAC\nodeposition\pg_24_noxd.arac

Figure D-19b. NARAC Prediction to Trial 24 on Logarithmic Scale: Stability Category is 4

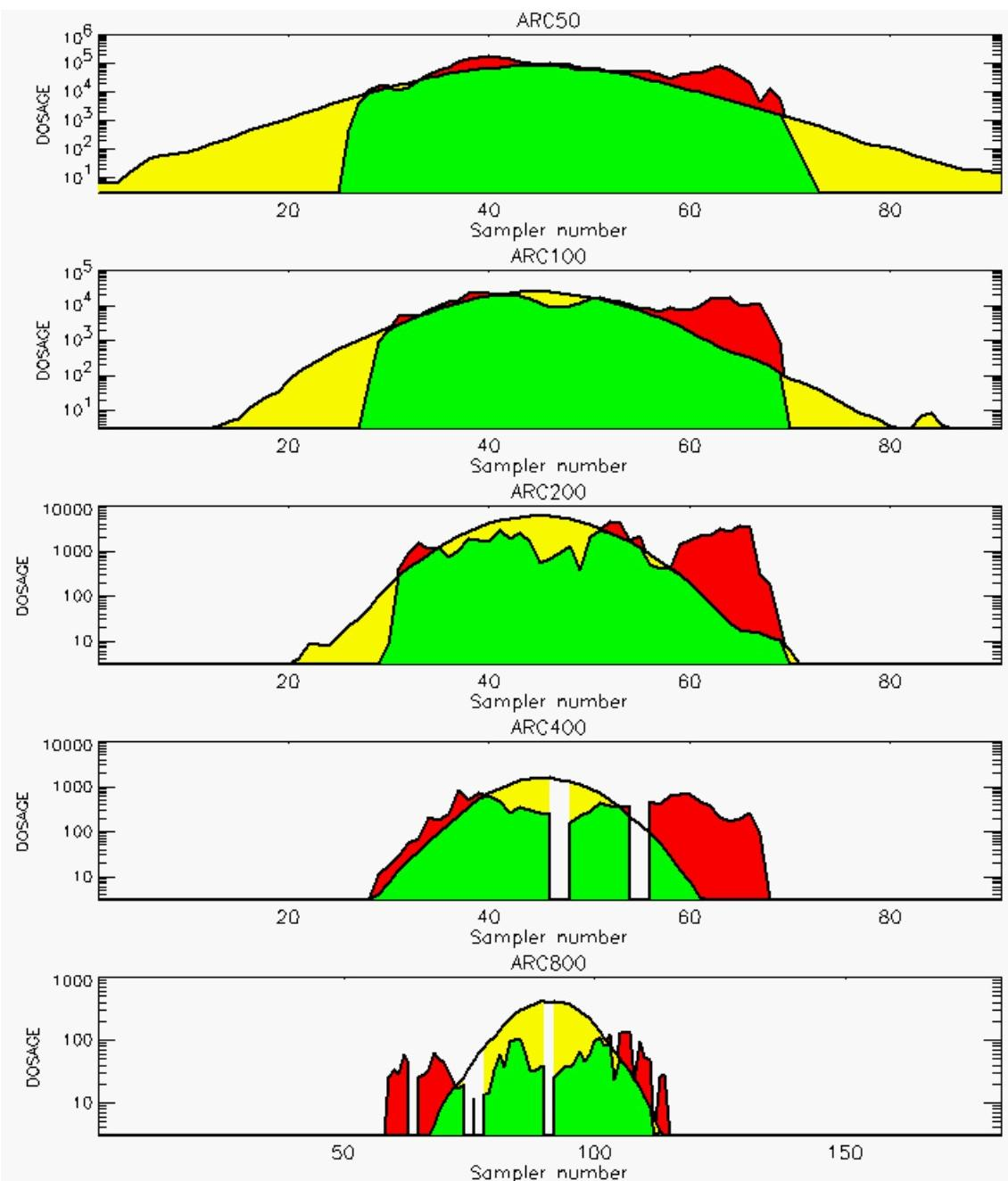


PG Observation to Prediction Comparison

PG Trial File: pr_grass_tracer_Experiment_25.txt

Prediction File: ARAC\nodeposition\pg_25_noxd.arac

Figure D-20a. NARAC Prediction to Trial 25 on Linear Scale: Stability Category is 1 (Values for Samplers 47 55 of 400-Meter Arc and 64, 75, 77, 91 of 800-Meter Arc are Missing)

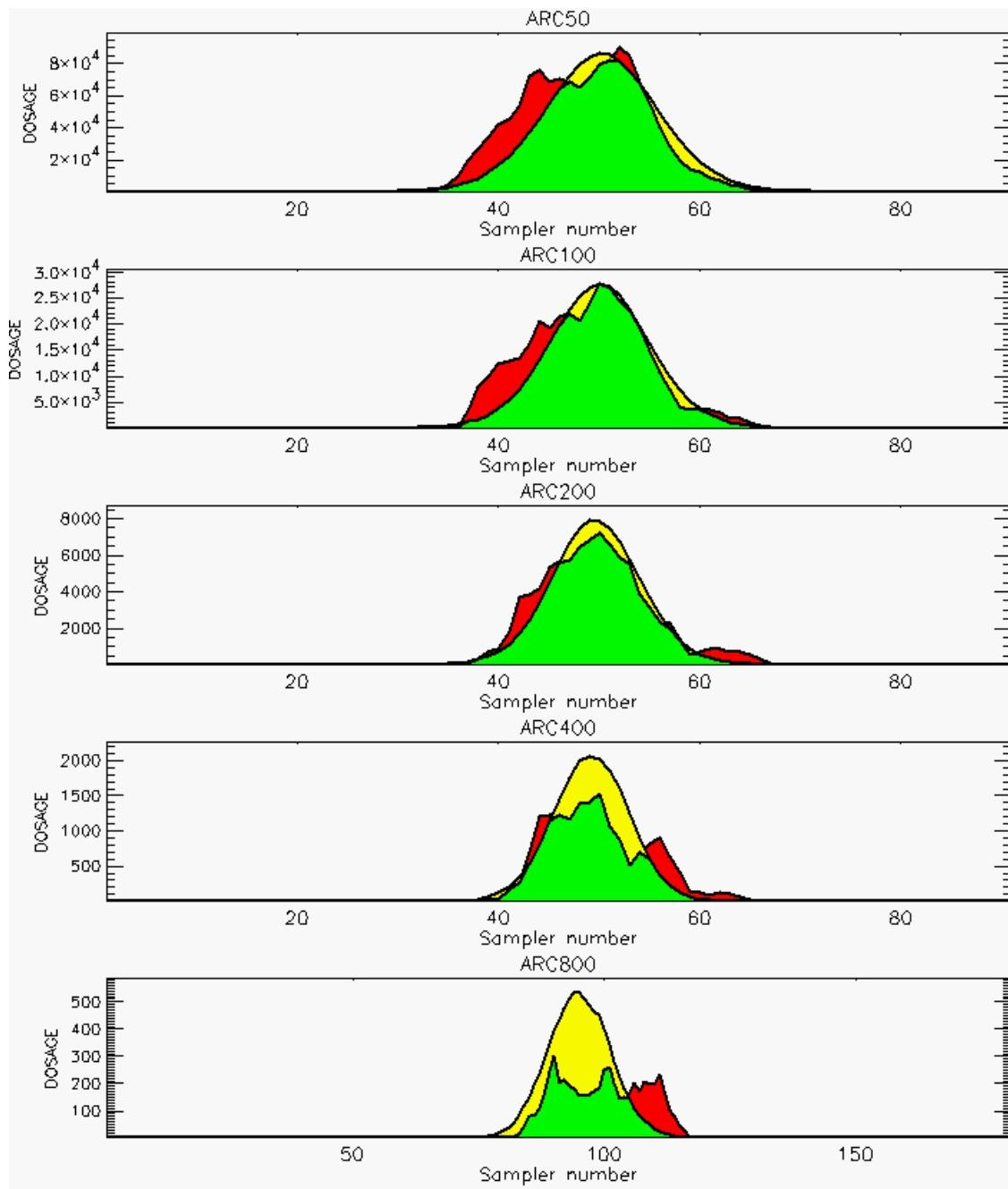


PG Observation to Prediction Comparison

PG Trial File: pr_grass_tracer_Experiment_25.txt

Prediction File: ARAC\nodeposition\pg_25_noxd.arac

**Figure D-20b. NARAC Prediction to Trial 25 on Logarithmic Scale: Stability Category is 1
(Values for Samplers 47 55 of 400-Meter Arc and 64, 75, 77, 91 of 800-Meter Arc are Missing)**

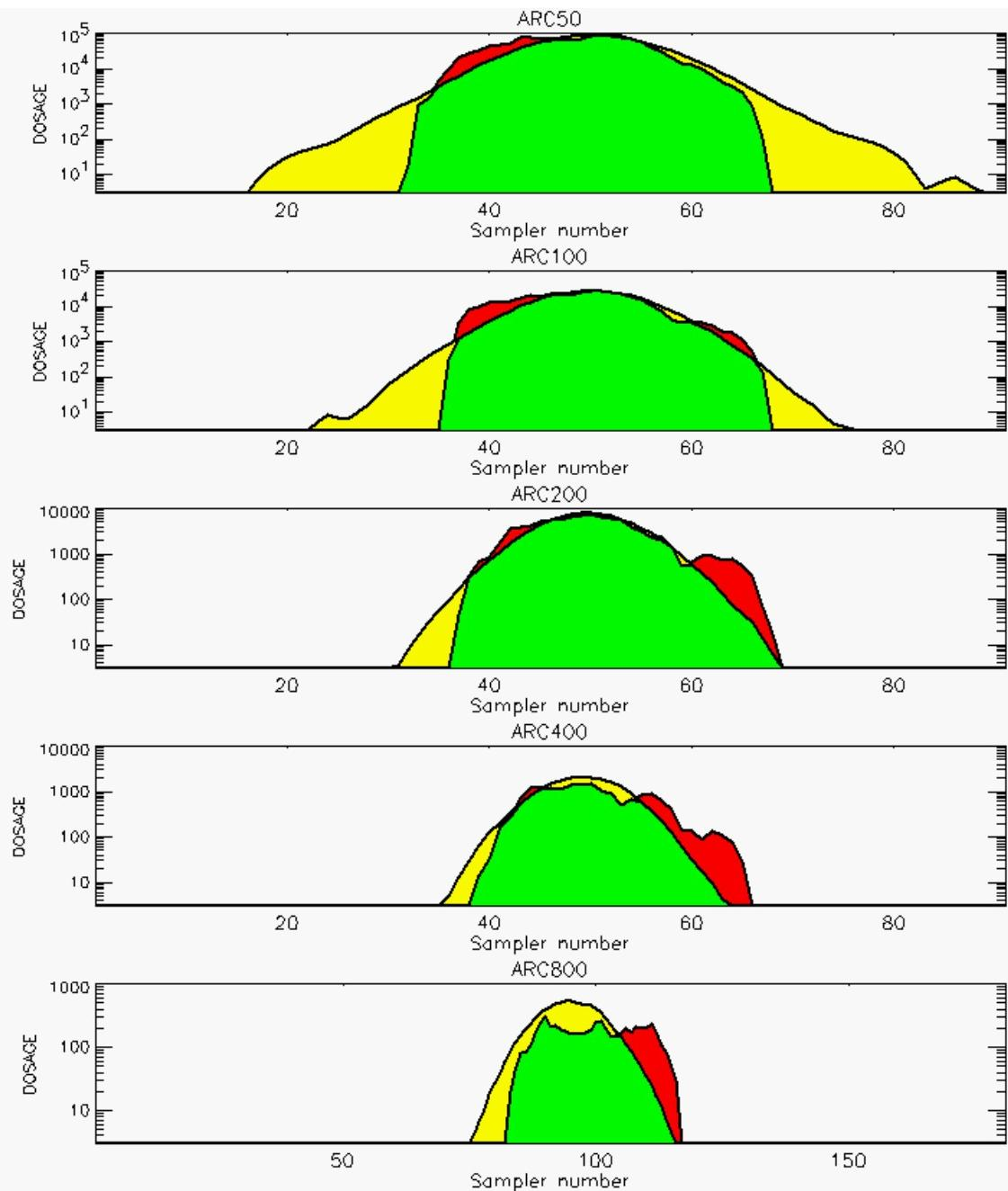


PG Observation to Prediction Comparison

PG Trial File: pr_grass_tracer_Experiment_26.txt

Prediction File: ARAC\nodeposition\pg_26_noxd.arac

Figure D-21a. NARAC Prediction to Trial 26 on Linear Scale: Stability Category is 2

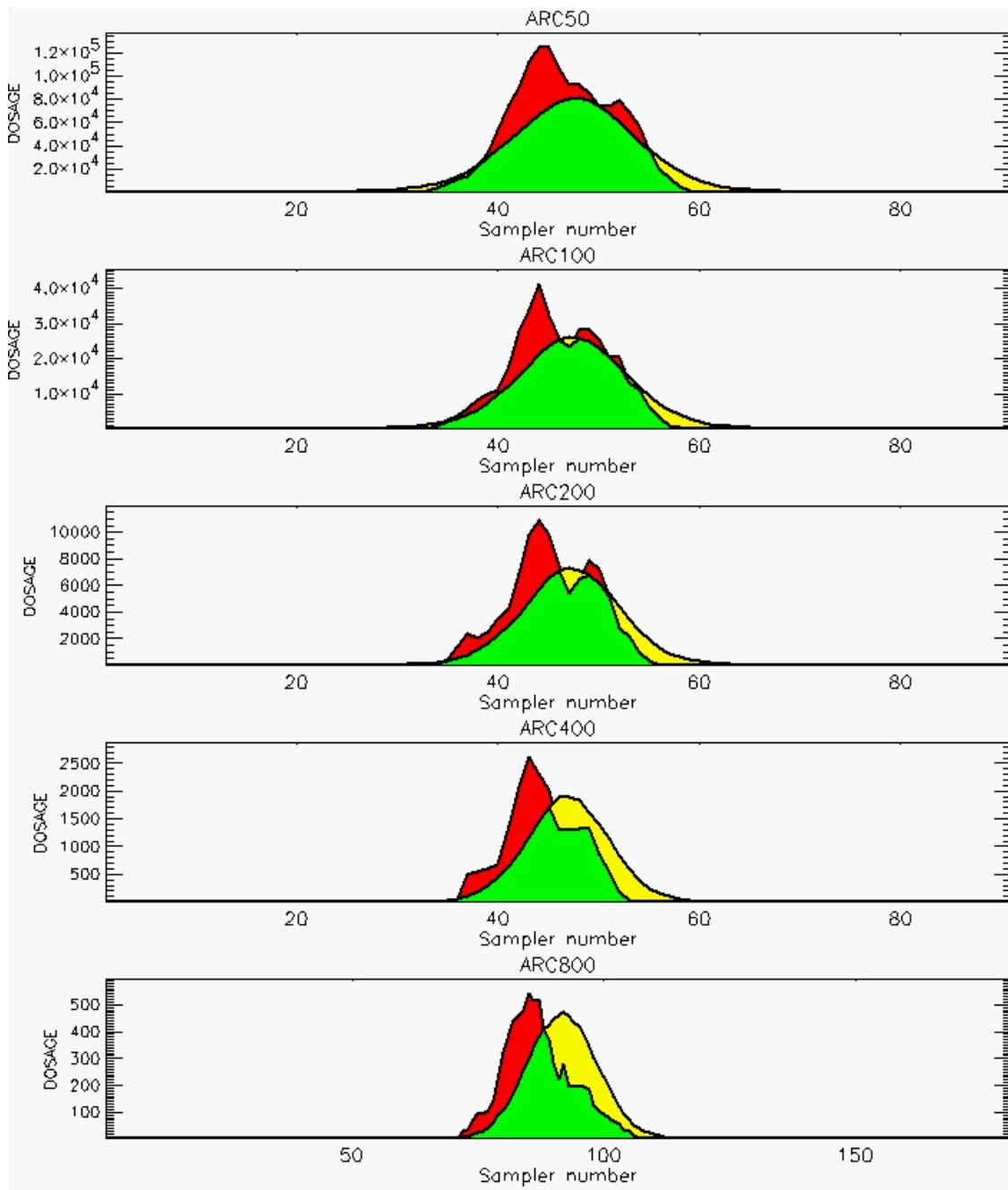


PG Observation to Prediction Comparison

PG Trial File: pr_grass_tracer_Experiment_26.txt

Prediction File: ARAC\nodeposition\pg_26_noxd.arac

Figure D-21b. NARAC Prediction to Trial 26 on Logarithmic Scale: Stability Category is 2

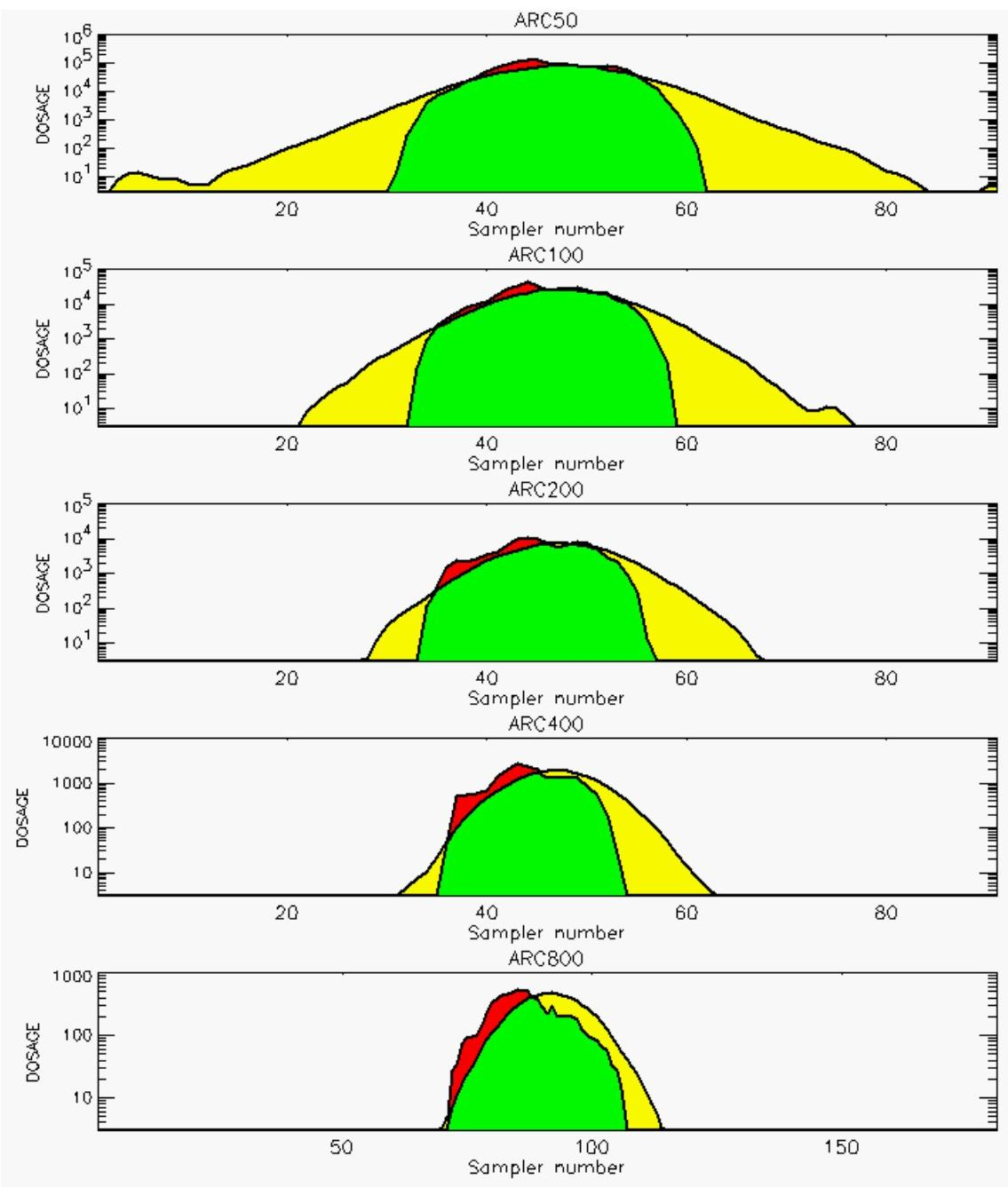


PG Observation to Prediction Comparison

PG Trial File: pr_grass_tracer_Experiment_27.txt

Prediction File: ARAC\nodeposition\pg_27_noxd.arac

Figure D-22a. NARAC Prediction to Trial 27 on Linear Scale: Stability Category is 2

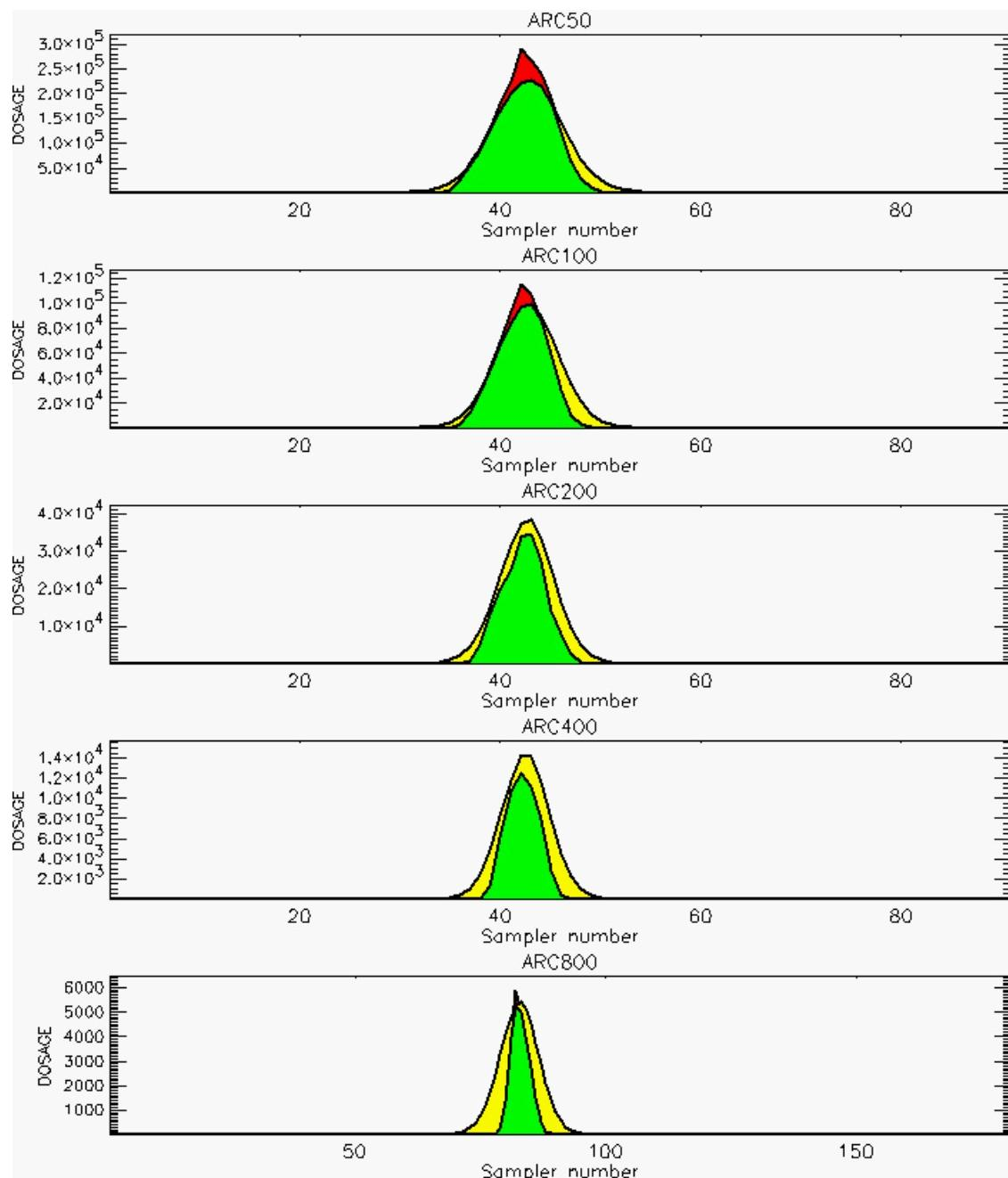


PG Observation to Prediction Comparison

PG Trial File: pr_grass_tracer_Experiment_27.txt

Prediction File: ARAC\nodeposition\pg_27_noxd.arac

Figure D-22b. NARAC Prediction to Trial 27 on Logarithmic Scale: Stability Category is 2

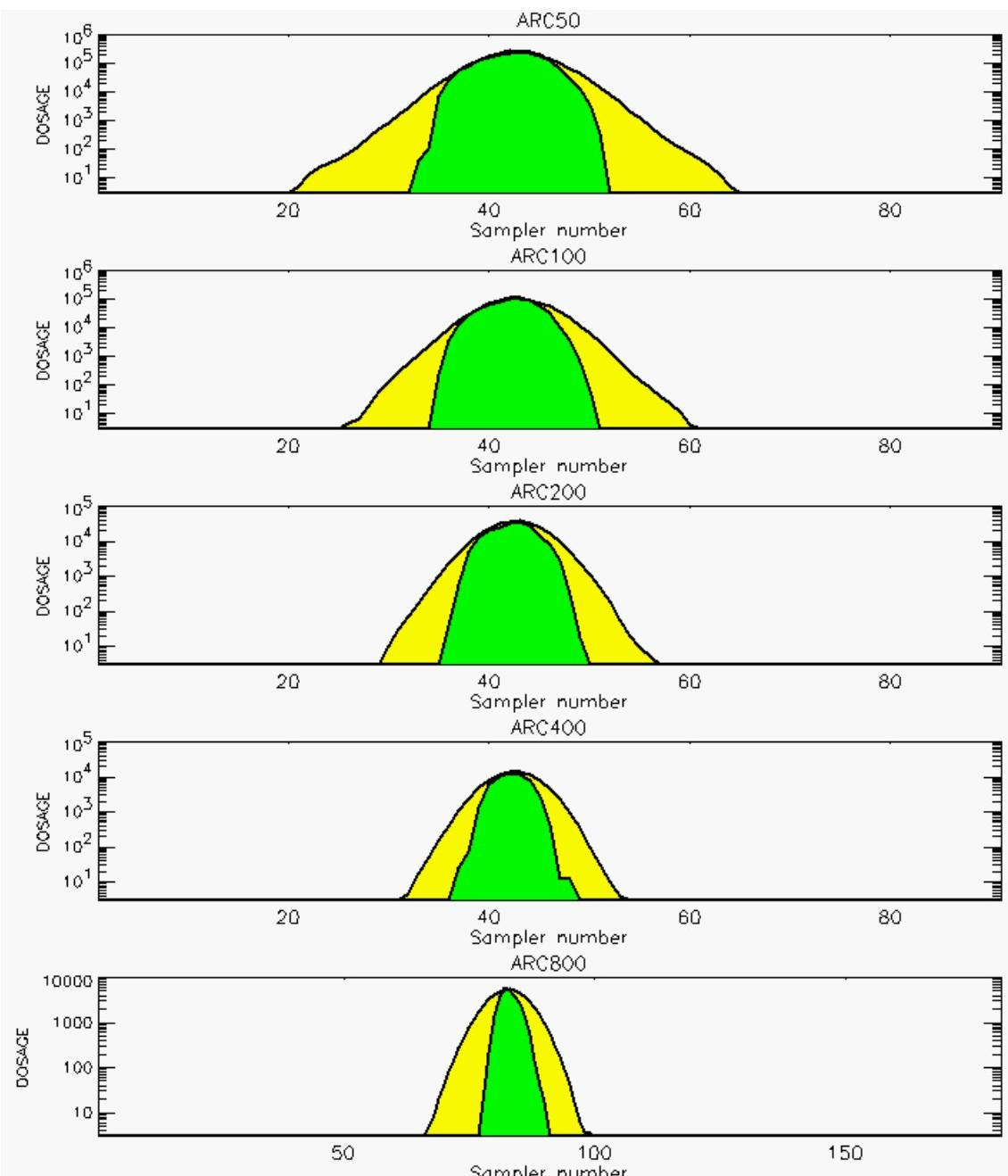


PG Observation to Prediction Comparison

PG Trial File: pr_grass_tracer_Experiment_28.txt

Prediction File: ARAC\nodeposition\pg_28_noxd.arac

Figure D-23a. NARAC Prediction to Trial 28 on Linear Scale: Stability Category is 5

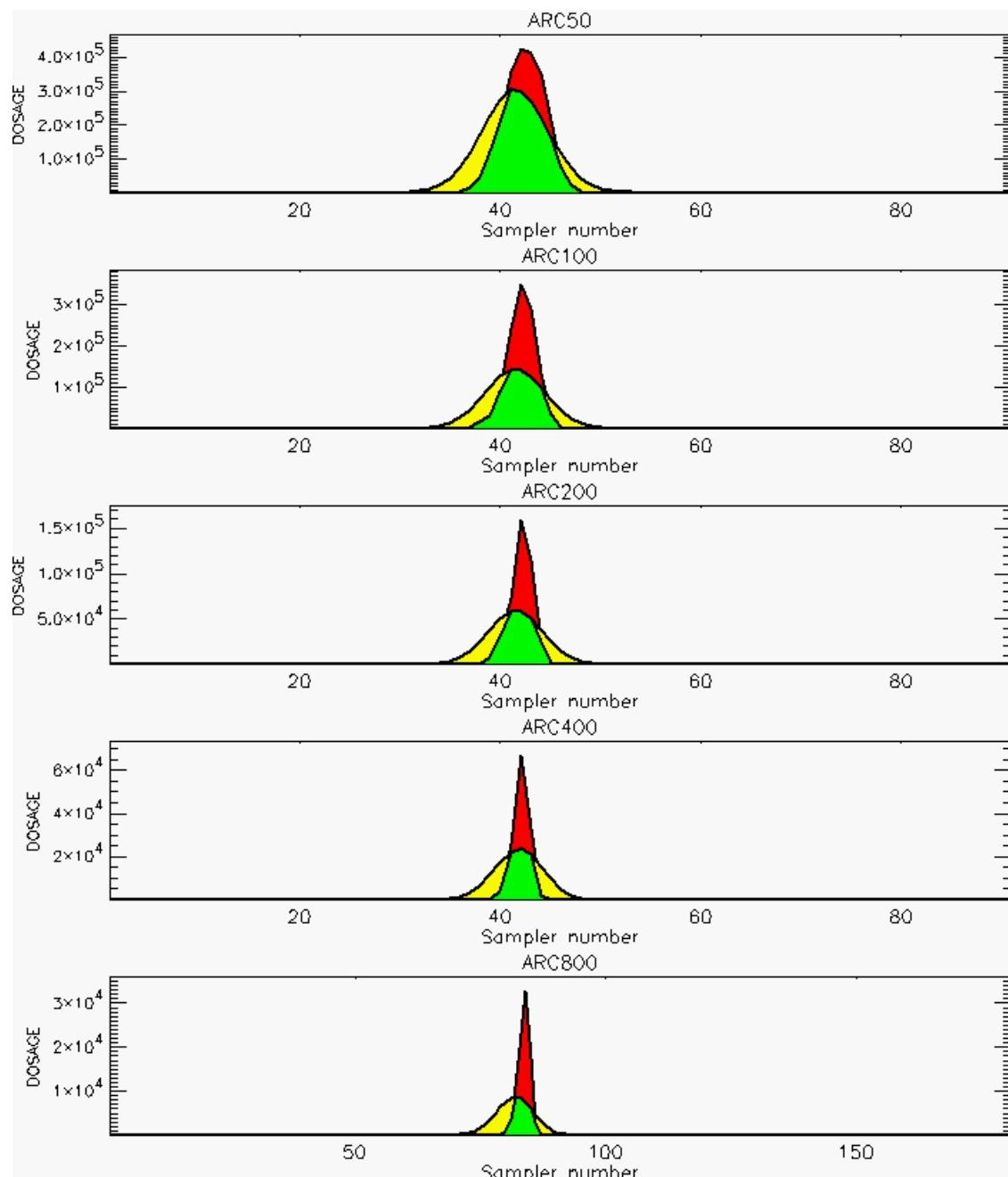


PG Observation to Prediction Comparison

PG Trial File: pr_grass_tracer_Experiment_28.txt

Prediction File: ARAC\nodeposition\pg_28_noxd.arac

Figure D-23b. NARAC Prediction to Trial 28 on Logarithmic Scale: Stability Category is 5

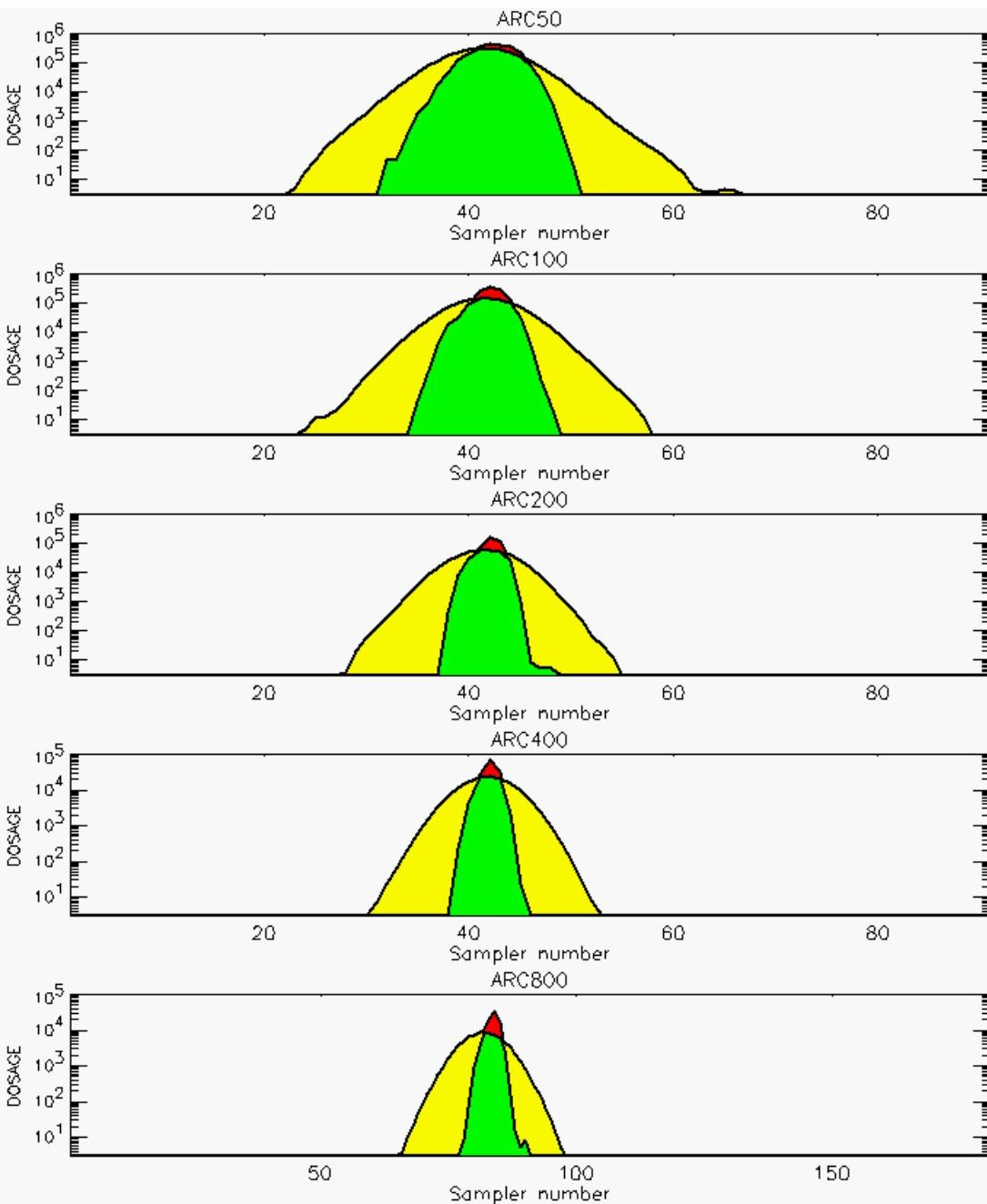


PG Observation to Prediction Comparison

PG Trial File: pr_grass_tracer_Experiment_32.txt

Prediction File: ARAC\nodeposition\pg_32_noxd.arac

Figure D-24a. NARAC Prediction to Trial 32 on Linear Scale: Stability Category is 6

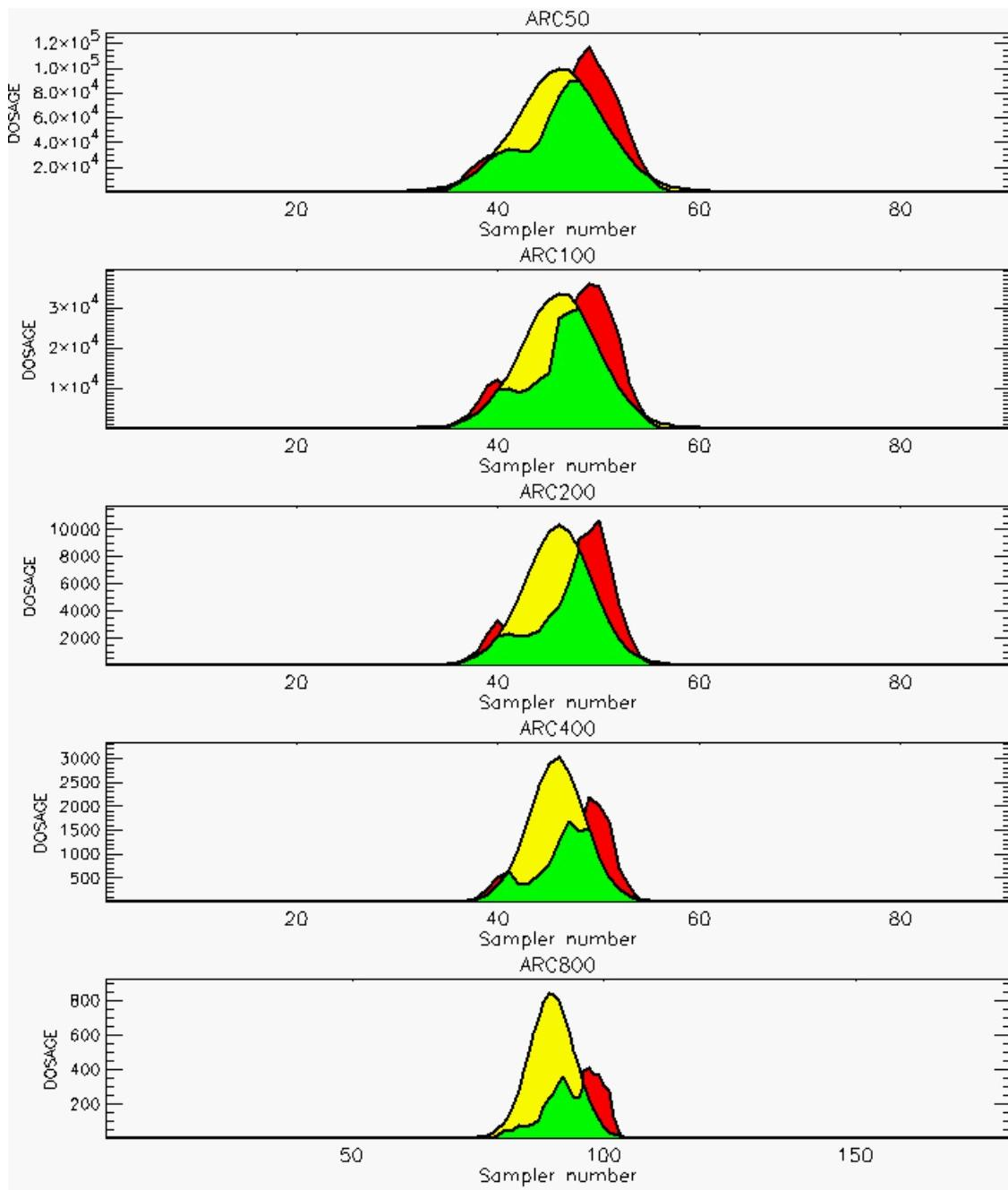


PG Observation to Prediction Comparison

PG Trial File: pr_grass_tracer_Experiment_32.txt

Prediction File: ARAC\nodeposition\pg_32_noxd.arac

Figure D-24b. NARAC Prediction to Trial 32 on Logarithmic Scale: Stability Category is 6



PG Observation to Prediction Comparison

PG Trial File: pr_grass_tracer_Experiment_33.txt

Prediction File: ARAC\nodeposition\pg_33_noxd.arac

Figure D-25a. NARAC Prediction to Trial 33 on Linear Scale: Stability Category is 3

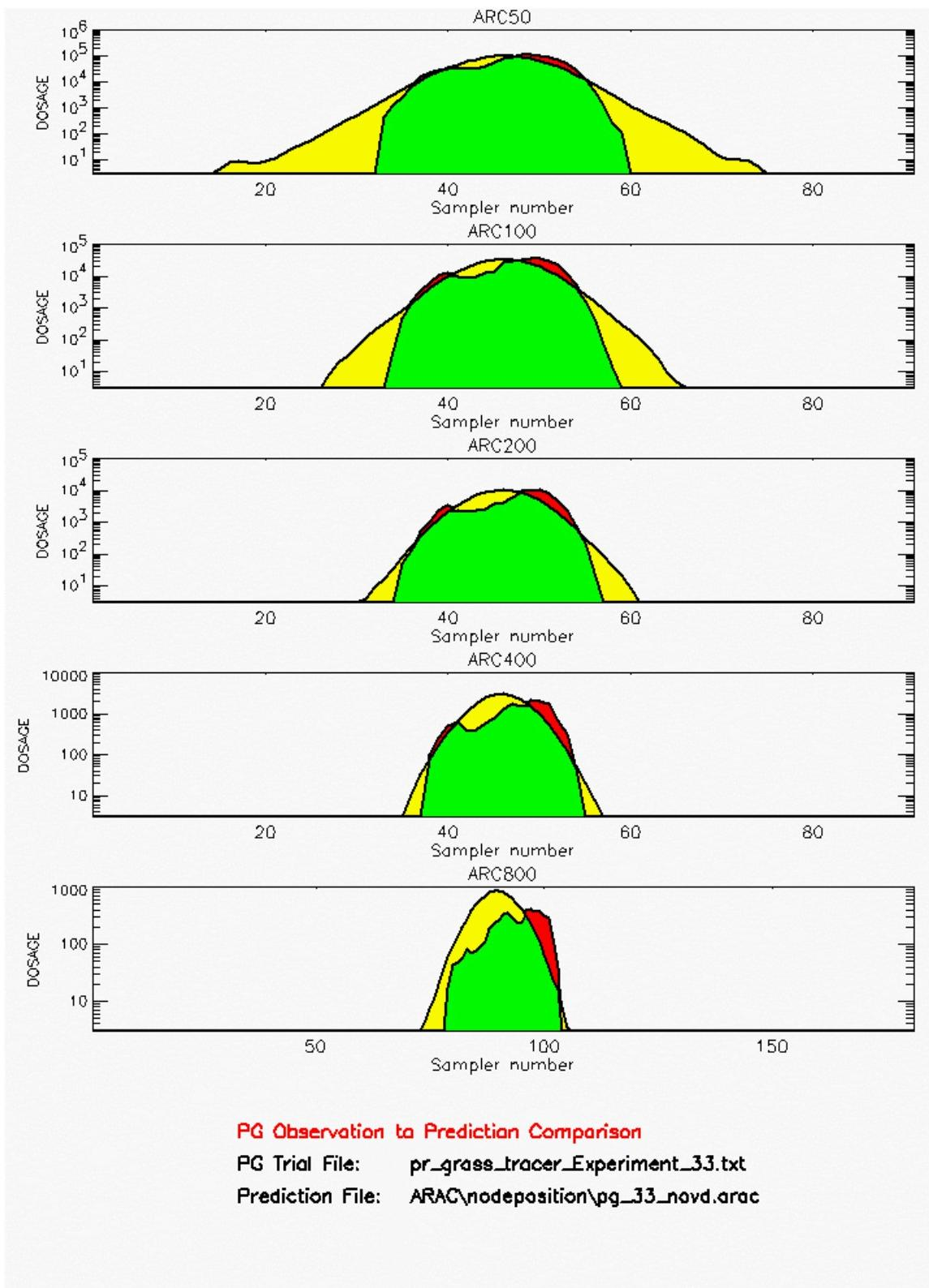
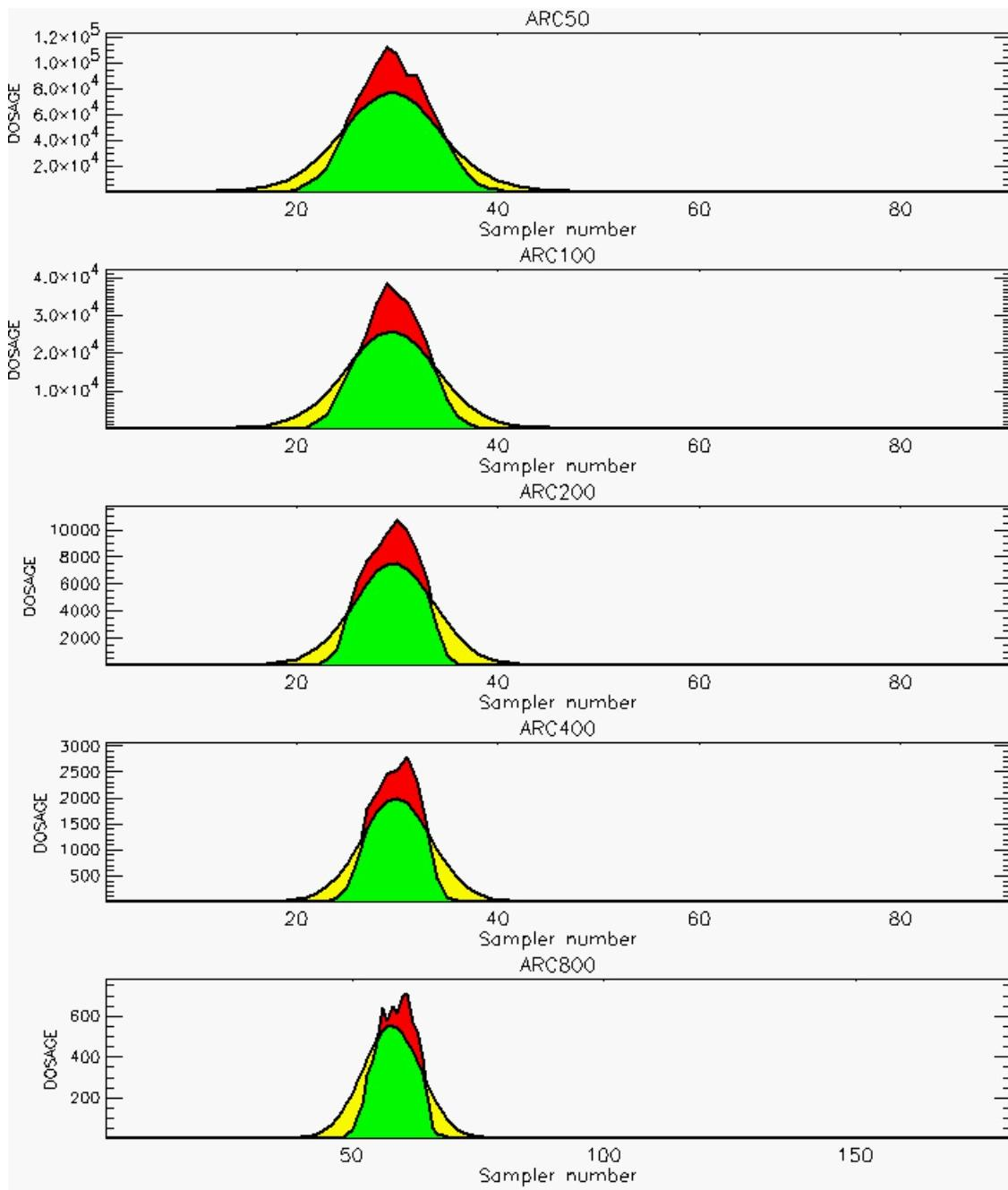


Figure D-25b. NARAC Prediction to Trial 33 on Logarithmic Scale: Stability Category is 3

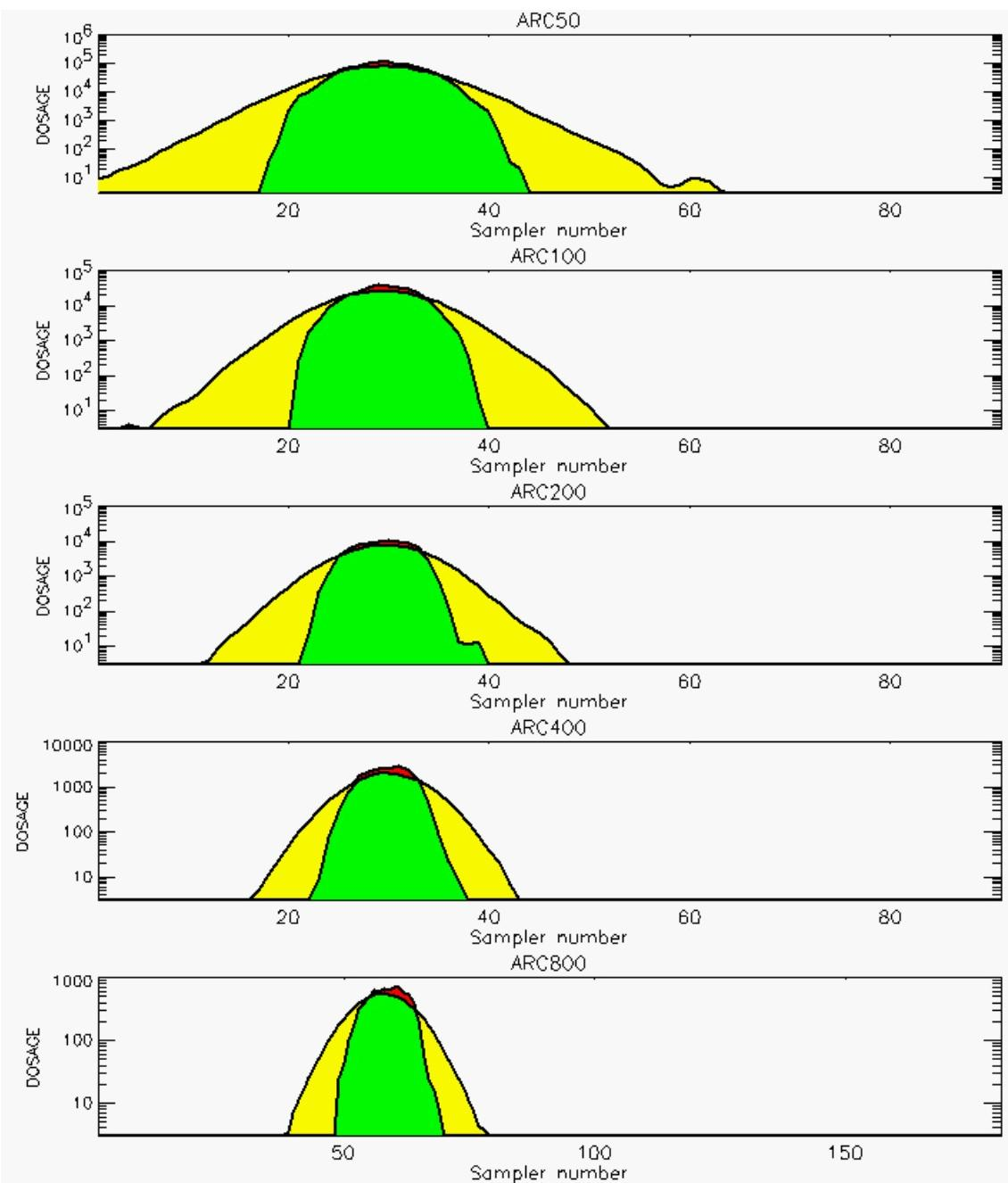


PG Observation to Prediction Comparison

PG Trial File: pr_grass_tracer_Experiment_34.txt

Prediction File: ARAC\nodeposition\pg_34_noxd.arac

Figure D-26a. NARAC Prediction to Trial 34 on Linear Scale: Stability Category is 3

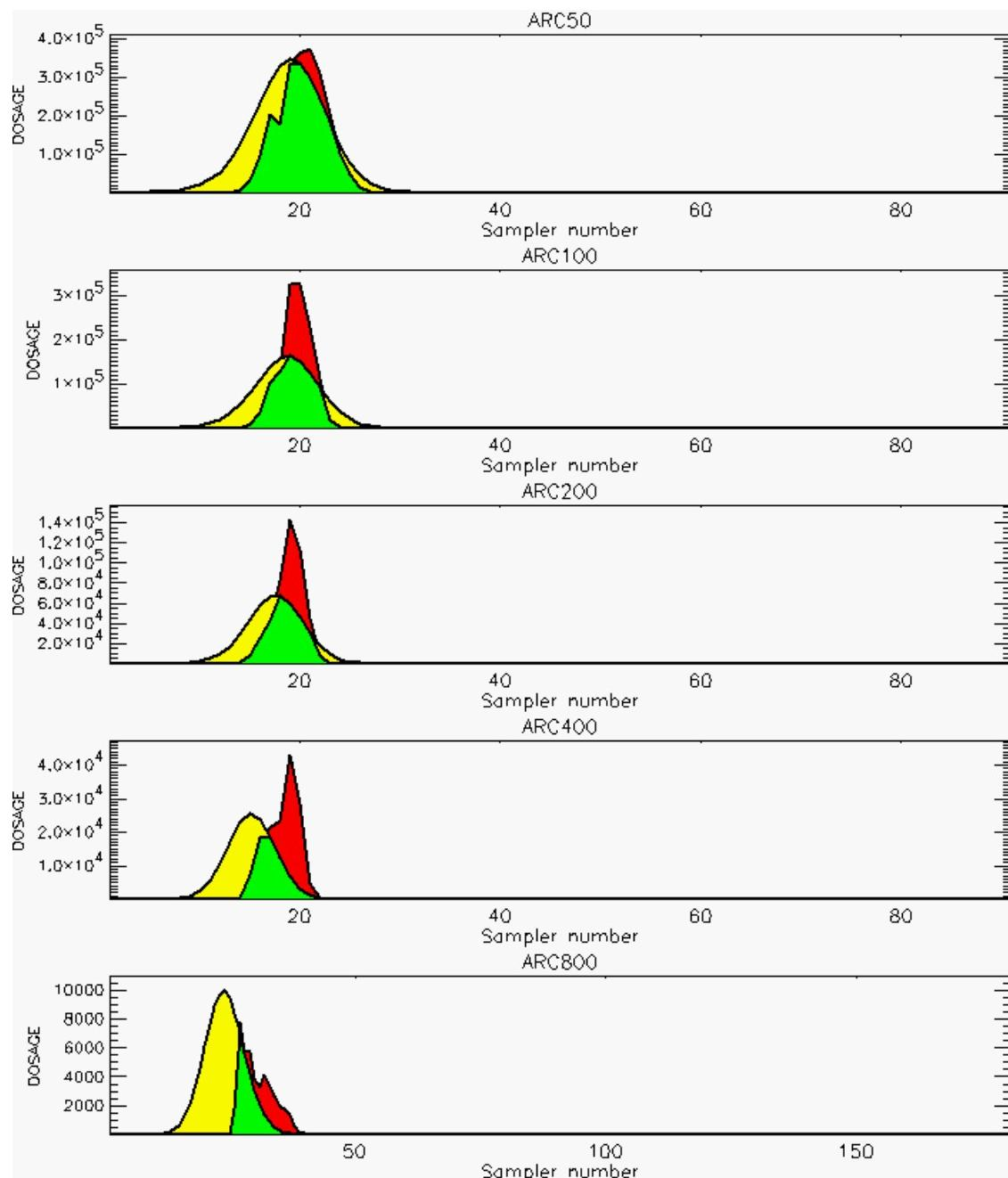


PG Observation to Prediction Comparison

PG Trial File: pr_grass_tracer_Experiment_34.txt

Prediction File: ARAC\nodeposition\pg_34_noxd.arac

Figure D-26b. NARAC Prediction to Trial 34 on Logarithmic Scale: Stability Category is 3

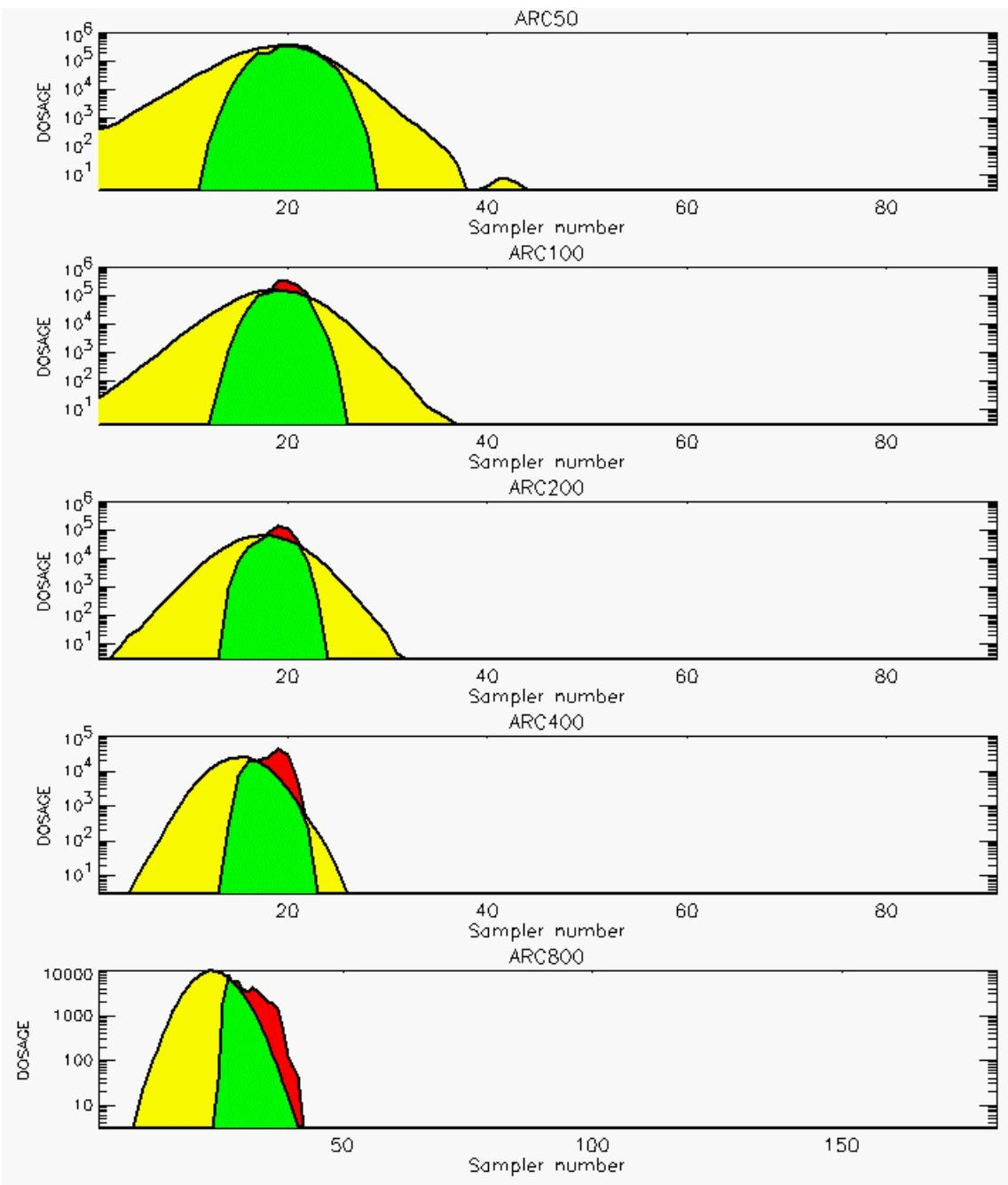


PG Observation to Prediction Comparison

PG Trial File: pr_grass_tracer_Experiment_35.txt

Prediction File: ARAC\nodeposition\pg_35_noxd.arac

Figure D-27a. NARAC Prediction to Trial 35 on Linear Scale: Stability Category is 6

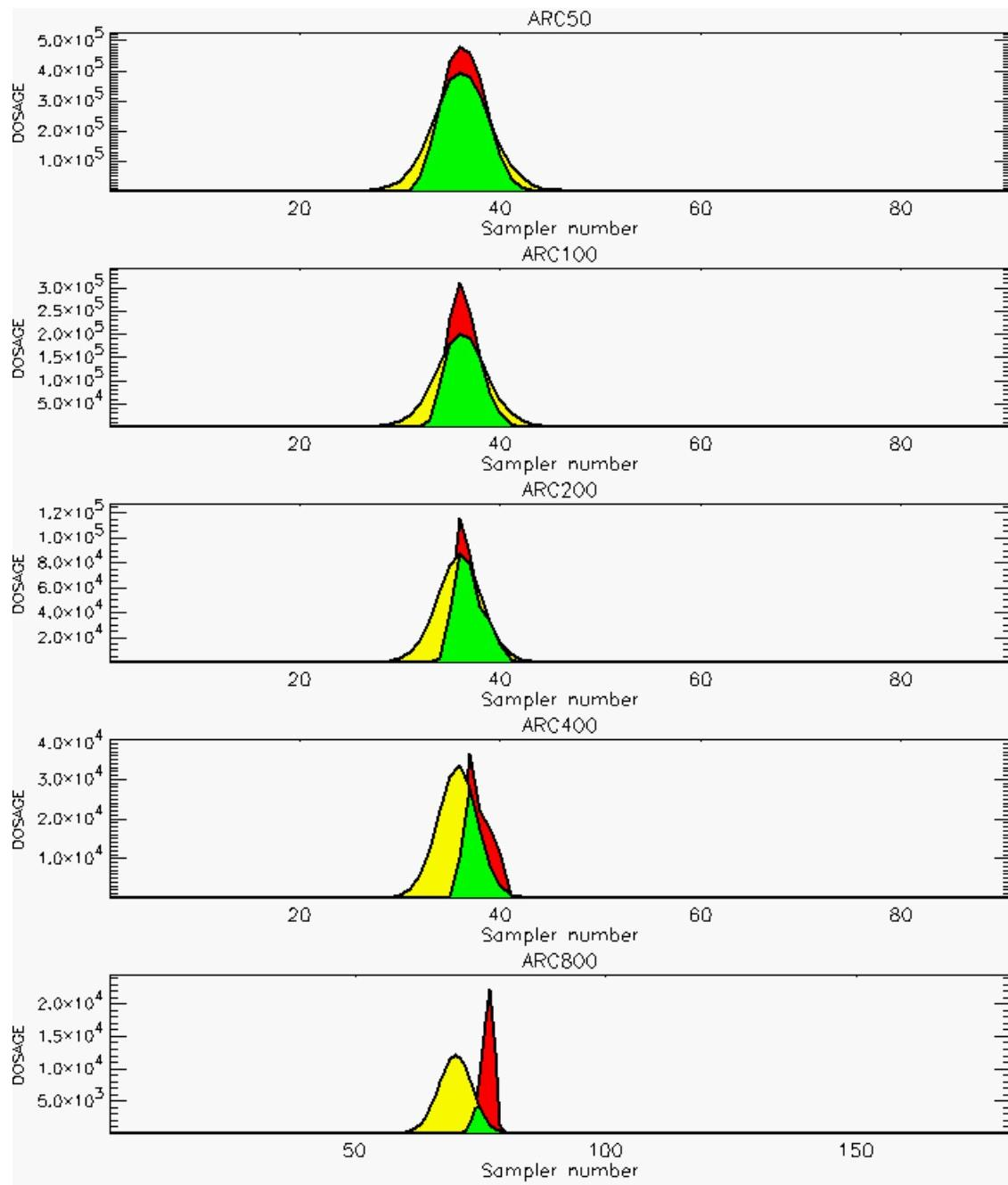


PG Observation to Prediction Comparison

PG Trial File: pr_grass_tracer_Experiment_35.txt

Prediction File: ARAC\nodeposition\pg_35_noxd.arac

Figure D-27b. NARAC Prediction to Trial 35 on Logarithmic Scale: Stability Category is 6

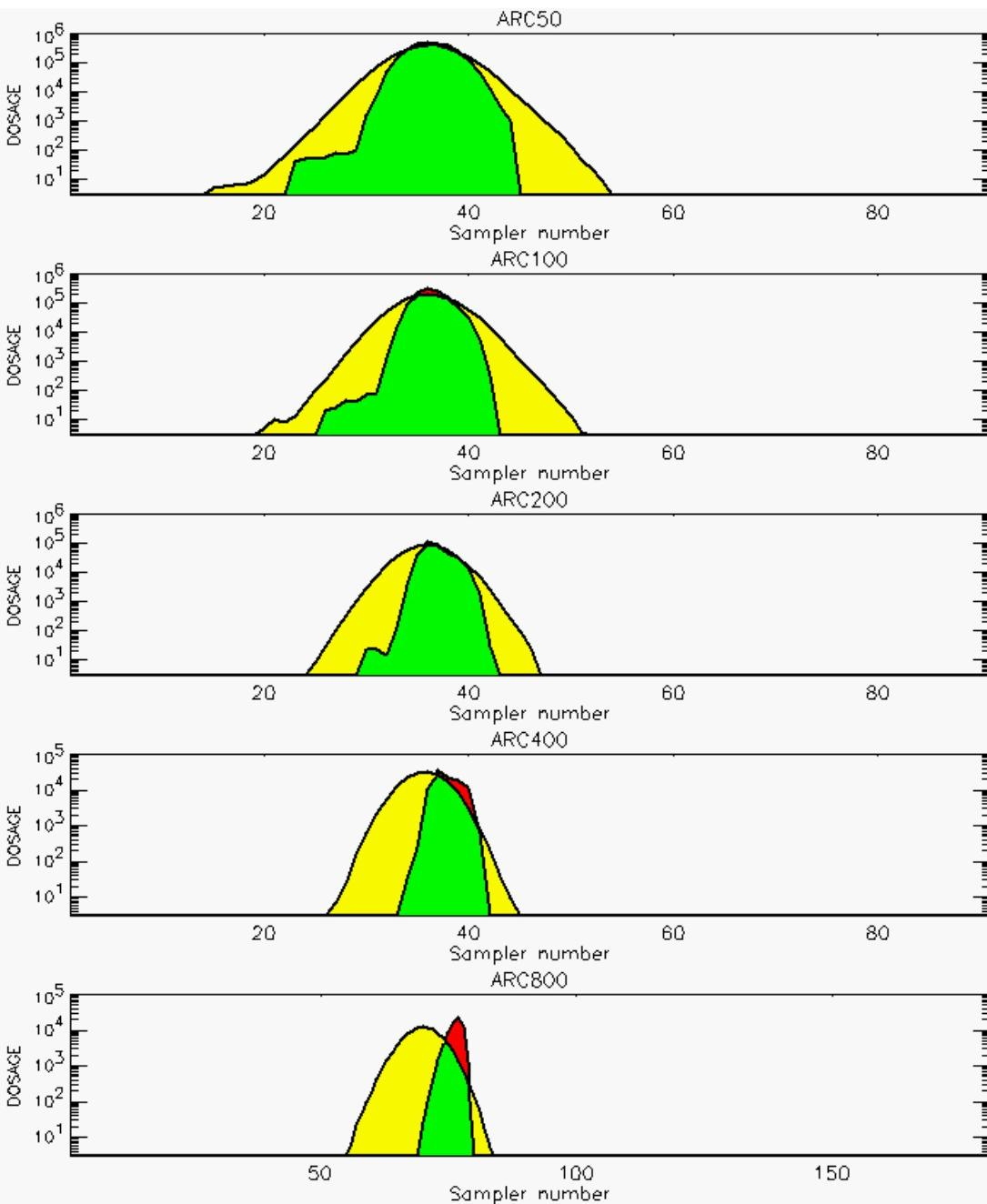


PG Observation to Prediction Comparison

PG Trial File: pr_grass_tracer_Experiment_36.txt

Prediction File: ARAC\nodeposition\pg_36_noxd.arac

Figure D-28a. NARAC Prediction to Trial 36 on Linear Scale: Stability Category is 6

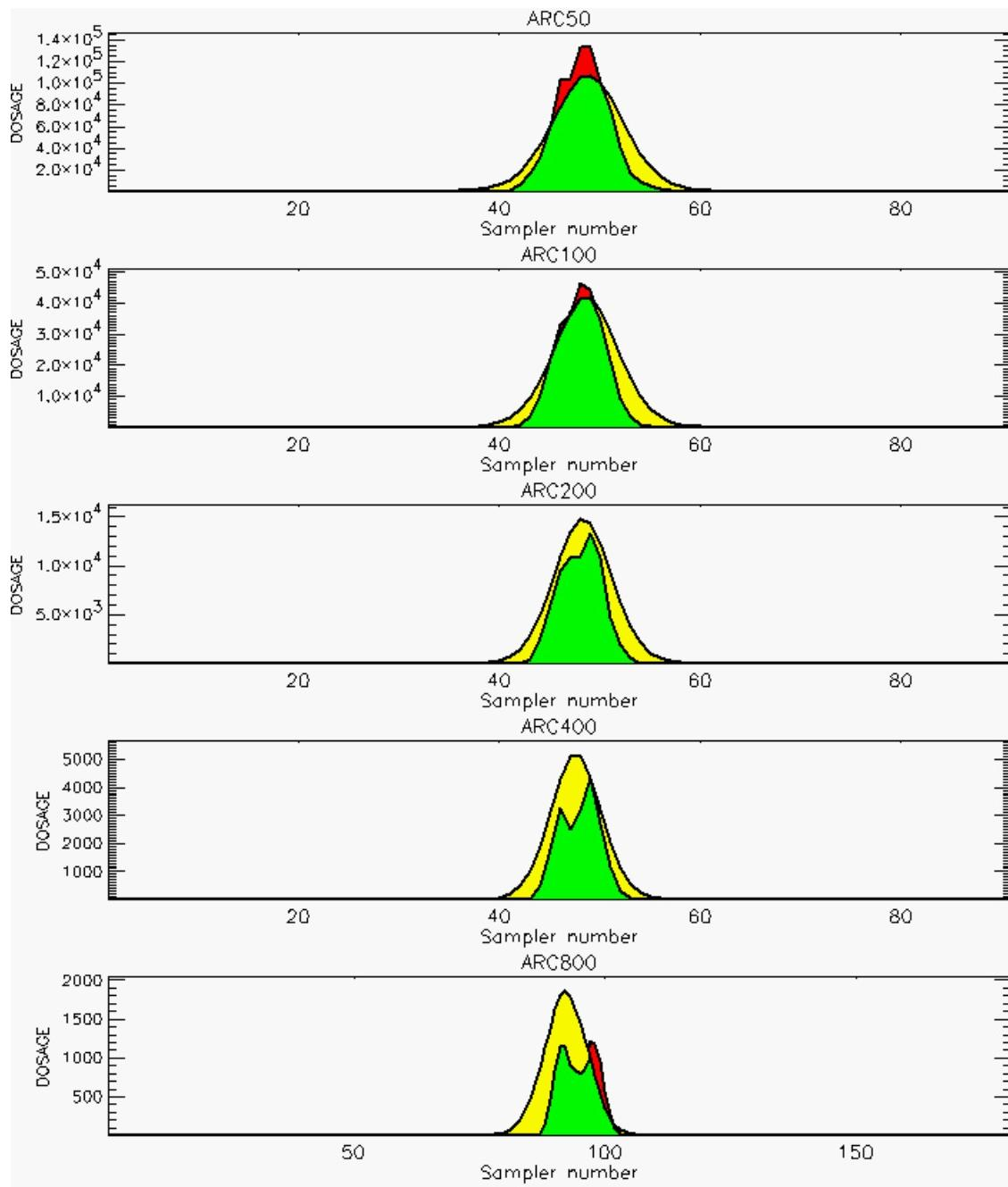


PG Observation to Prediction Comparison

PG Trial File: pr_grass_tracer_Experiment_36.txt

Prediction File: ARAC\nodeposition\pg_36_noxd.arac

Figure D-28b. NARAC Prediction to Trial 36 on Logarithmic Scale: Stability Category is 6

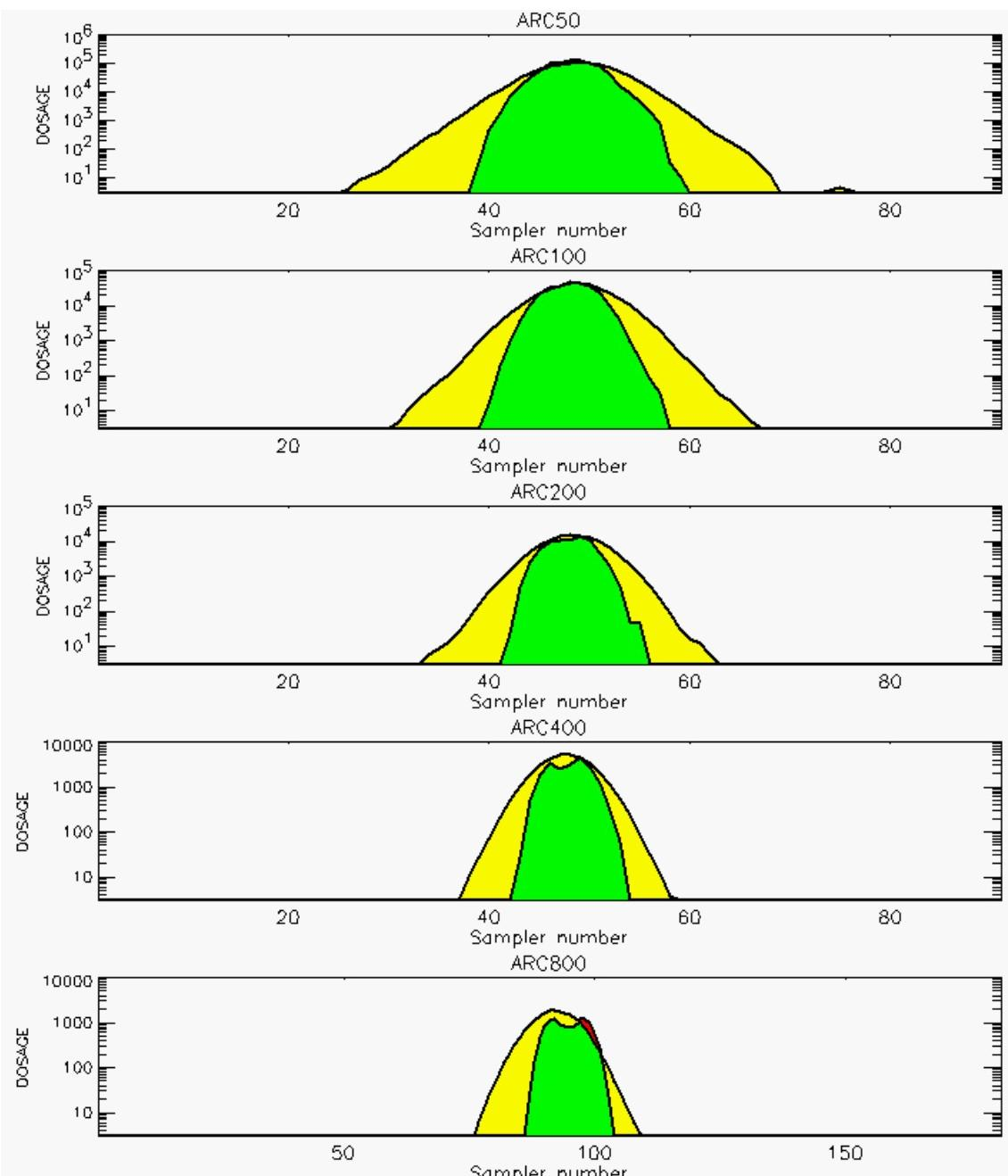


PG Observation to Prediction Comparison

PG Trial File: pr_grass_tracer_Experiment_37.txt

Prediction File: ARAC\nodeposition\pg_37_noxd.arac

Figure D-29a. NARAC Prediction to Trial 37 on Linear Scale: Stability Category is 4

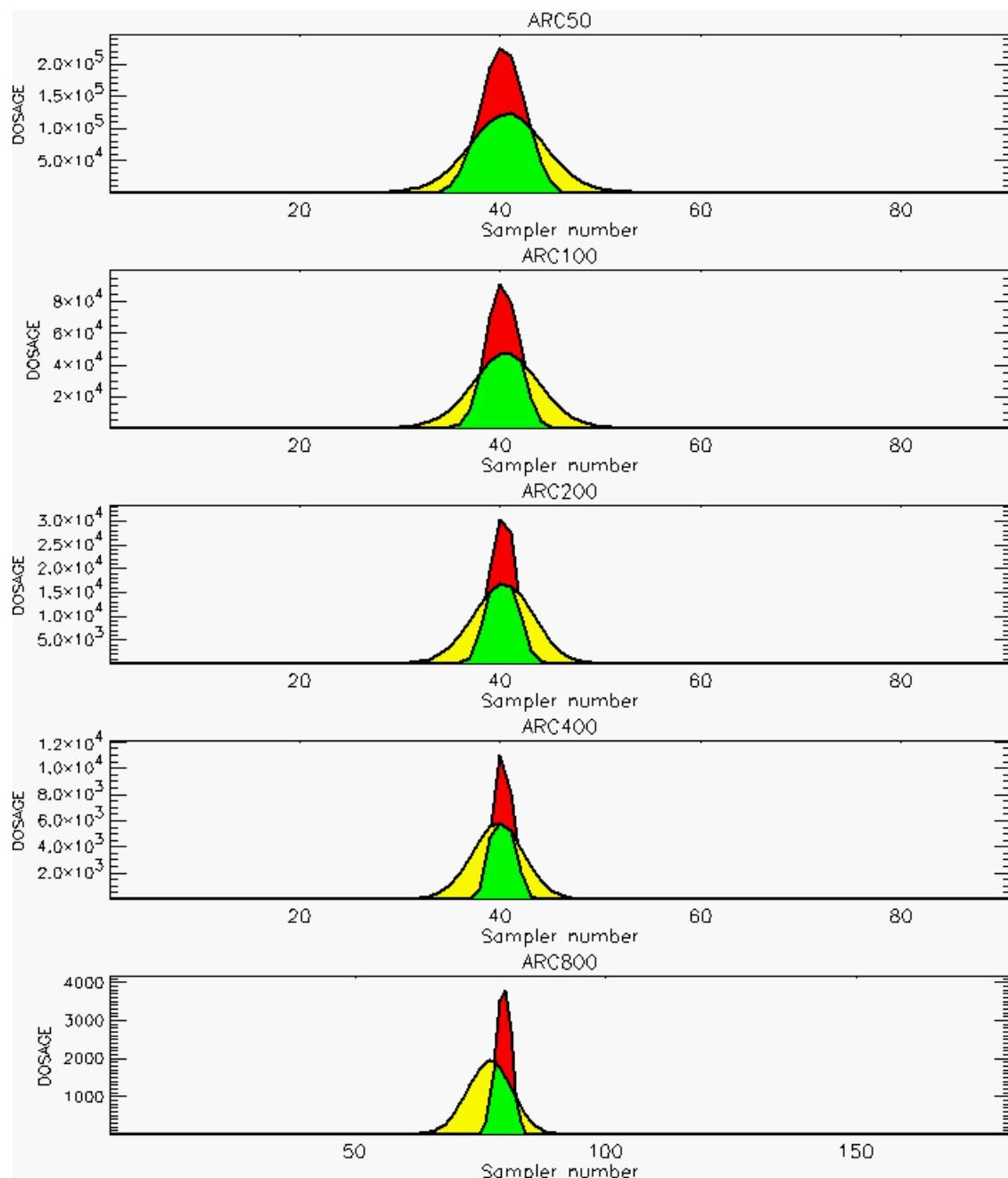


PG Observation to Prediction Comparison

PG Trial File: pr_grass_tracer_Experiment_37.txt

Prediction File: ARAC\nodeposition\pg_37_noxd.arac

Figure D-29b. NARAC Prediction to Trial 37 on Logarithmic Scale: Stability Category is 4

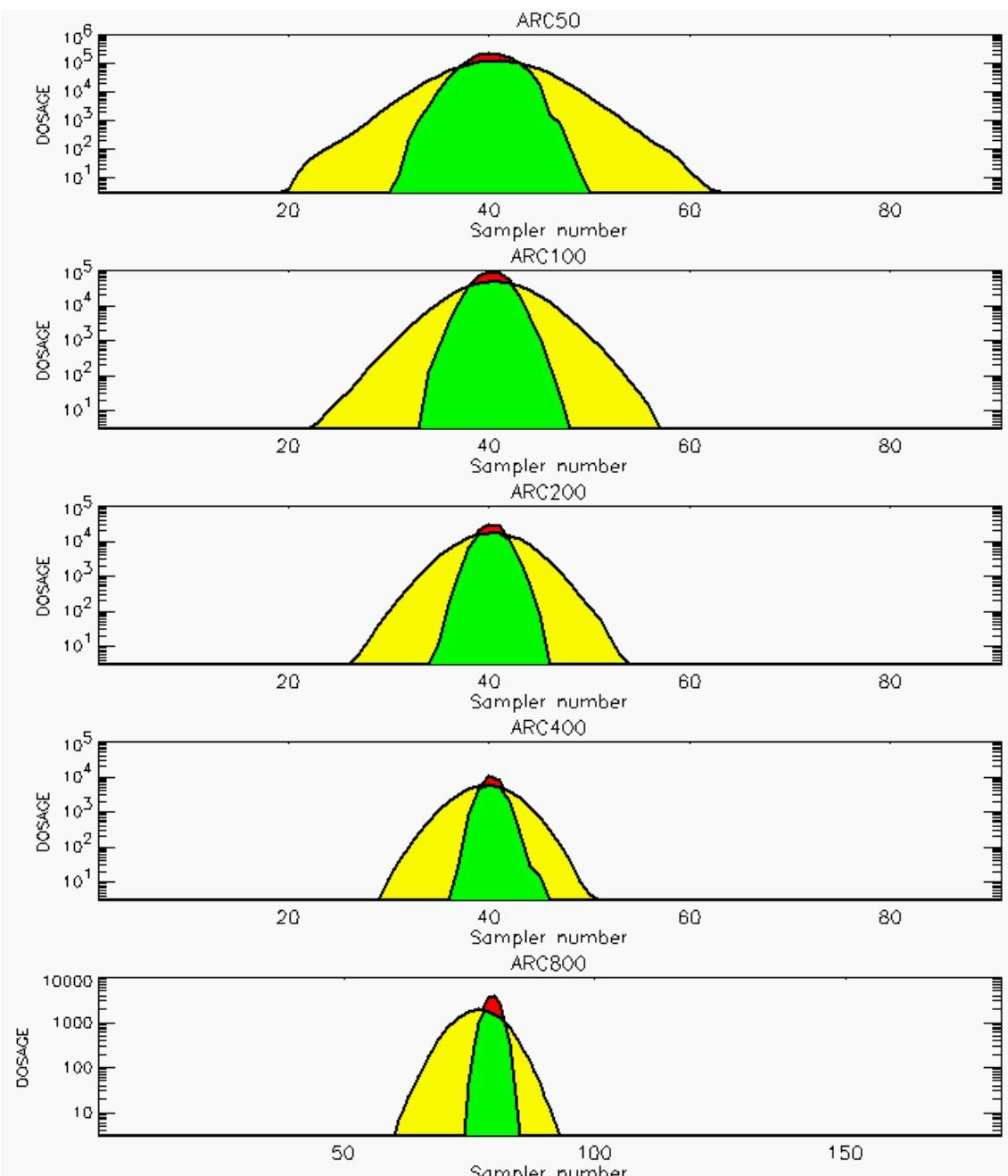


PG Observation to Prediction Comparison

PG Trial File: pr_grass_tracer_Experiment_38.txt

Prediction File: ARAC\nodeposition\pg_38_noxd.arac

Figure D-30a. NARAC Prediction to Trial 38 on Linear Scale: Stability Category is 4

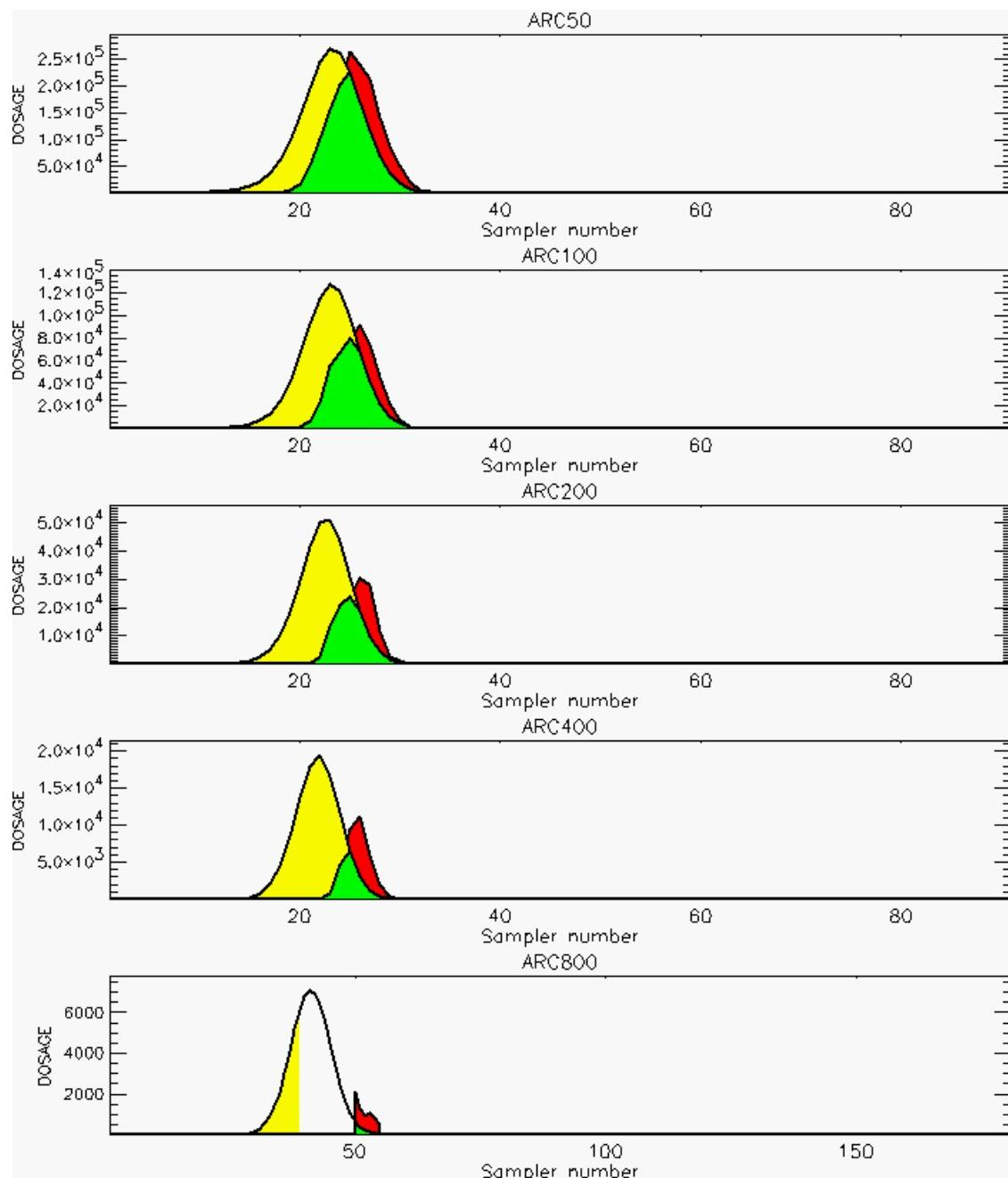


PG Observation to Prediction Comparison

PG Trial File: pr_grass_tracer_Experiment_38.txt

Prediction File: ARAC\nodeposition\pg_38_noxd.arac

Figure D-30b. NARAC Prediction to Trial 38 on Logarithmic Scale: Stability Category is 4



PG Observation to Prediction Comparison

PG Trial File: pr_grass_tracer_Experiment_39.txt

Prediction File: ARAC\nodeposition\pg_39_noxd.arac

**Figure D-31a. NARAC Prediction to Trial 39 on Linear Scale: Stability Category is 6
(Values for Samplers 40-49, 56-58 of 800-Meter Arc are Missing)**

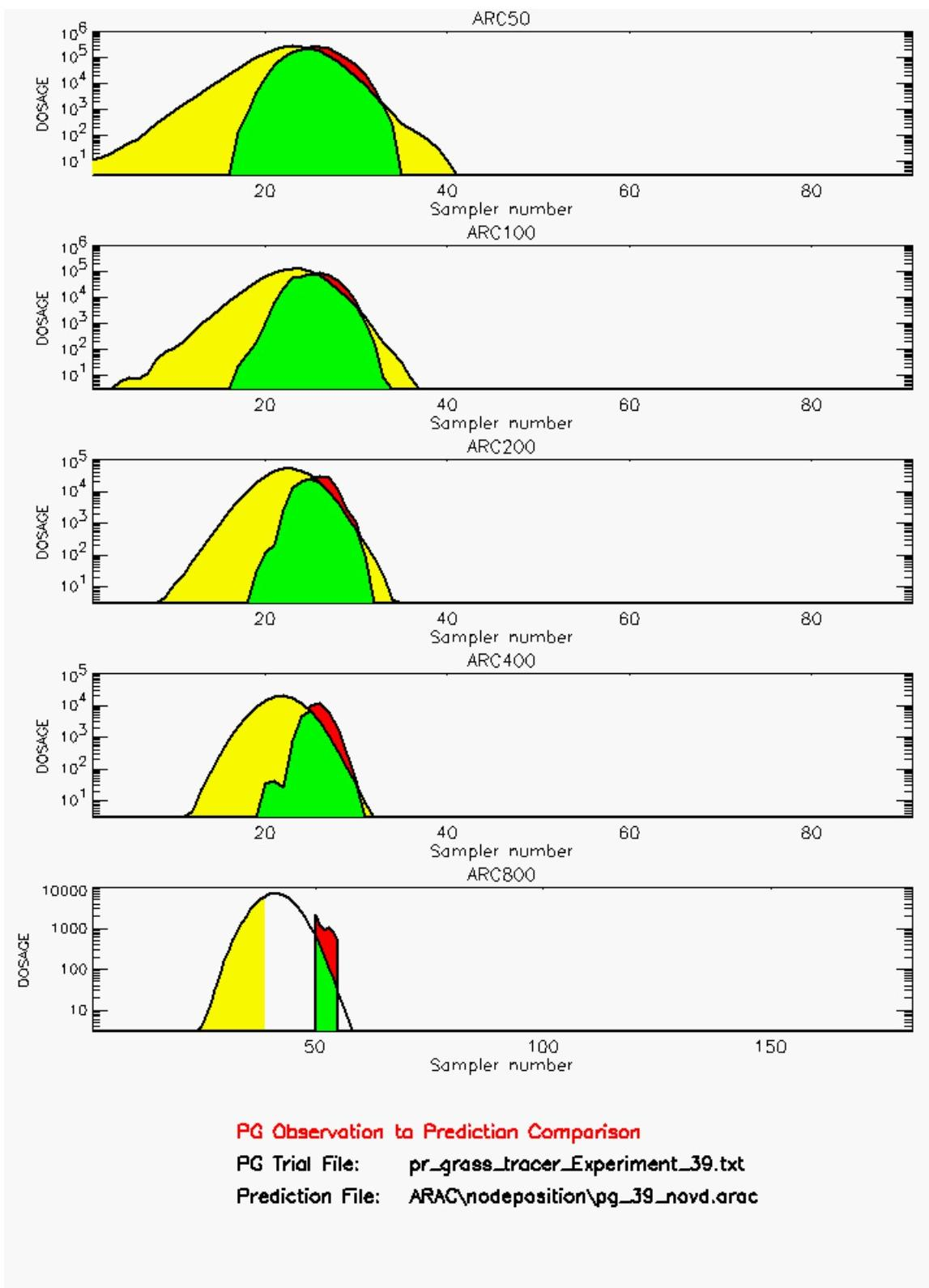
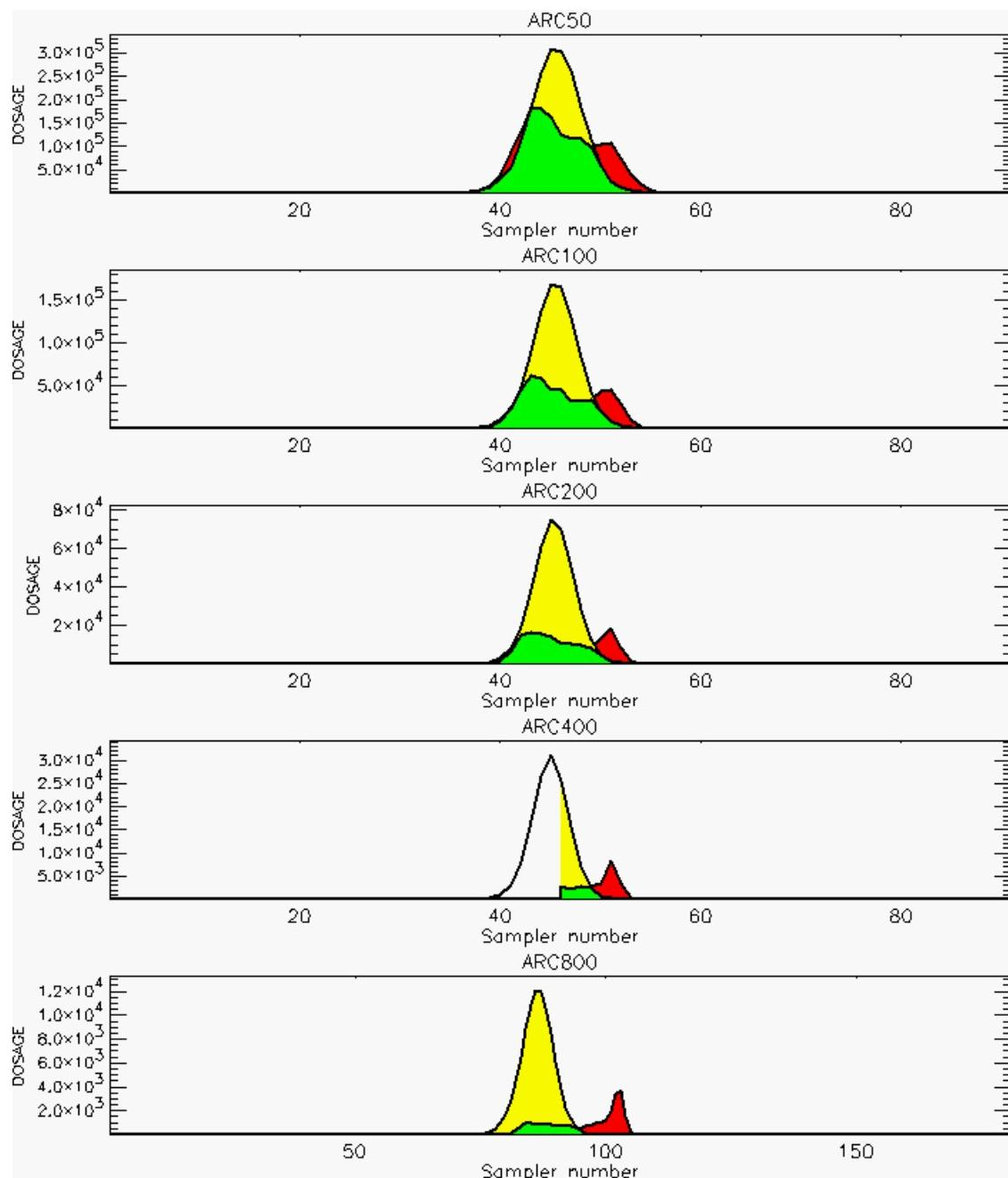


**Figure D-31b. NARAC Prediction to Trial 39 on Logarithmic Scale: Stability Category is 6
(Values for Samplers 40-49, 56-58 of 800-Meter Arc are Missing)**

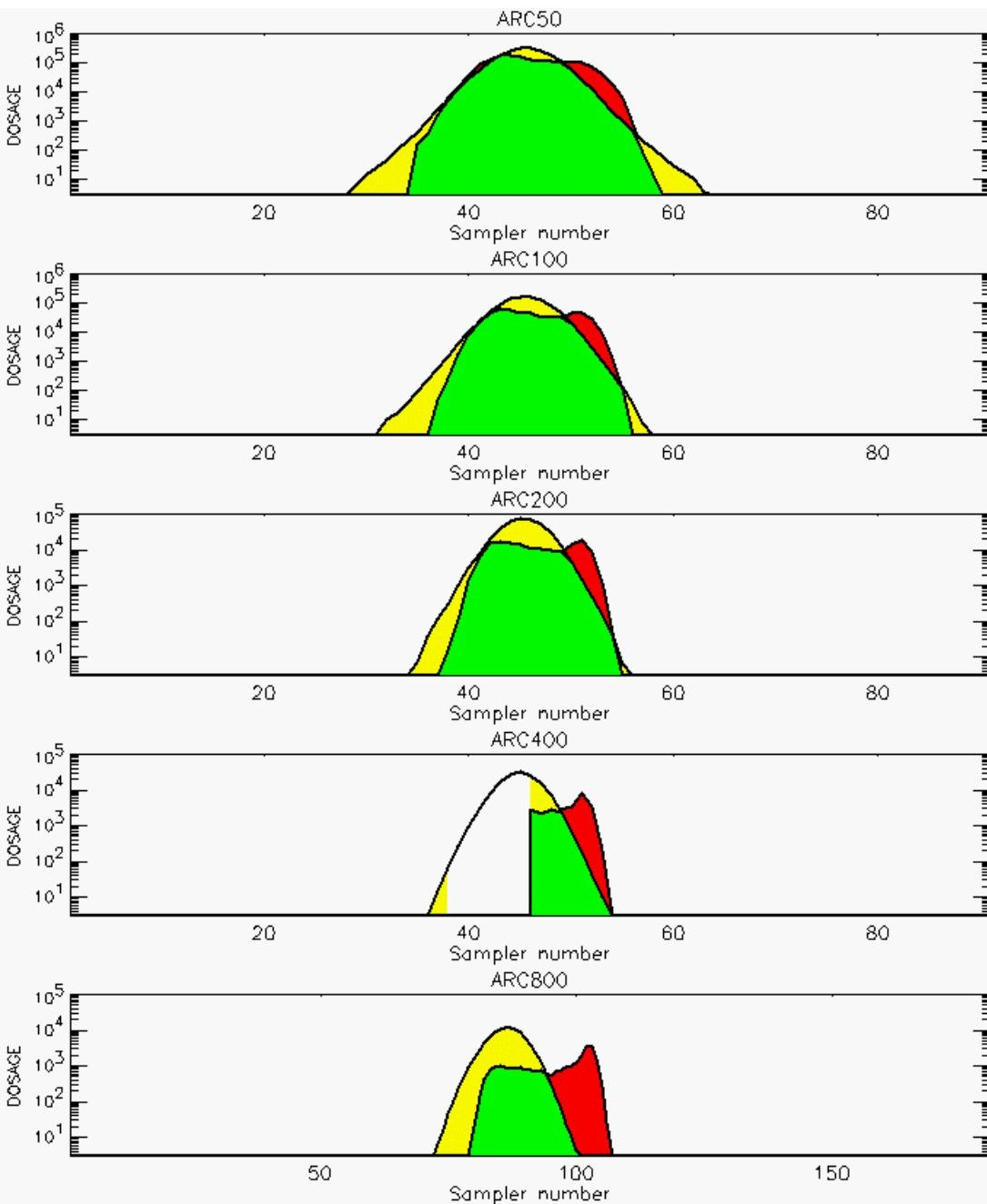


PG Observation to Prediction Comparison

PG Trial File: pr_grass_tracer_Experiment_40.txt

Prediction File: ARAC\nodeposition\pg_40_nozd.arac

**Figure D-32a. NARAC Prediction to Trial 40 on Linear Scale: Stability Category is 6
(Values for Samplers 39-45 of 400-Meter Arc are Missing)**

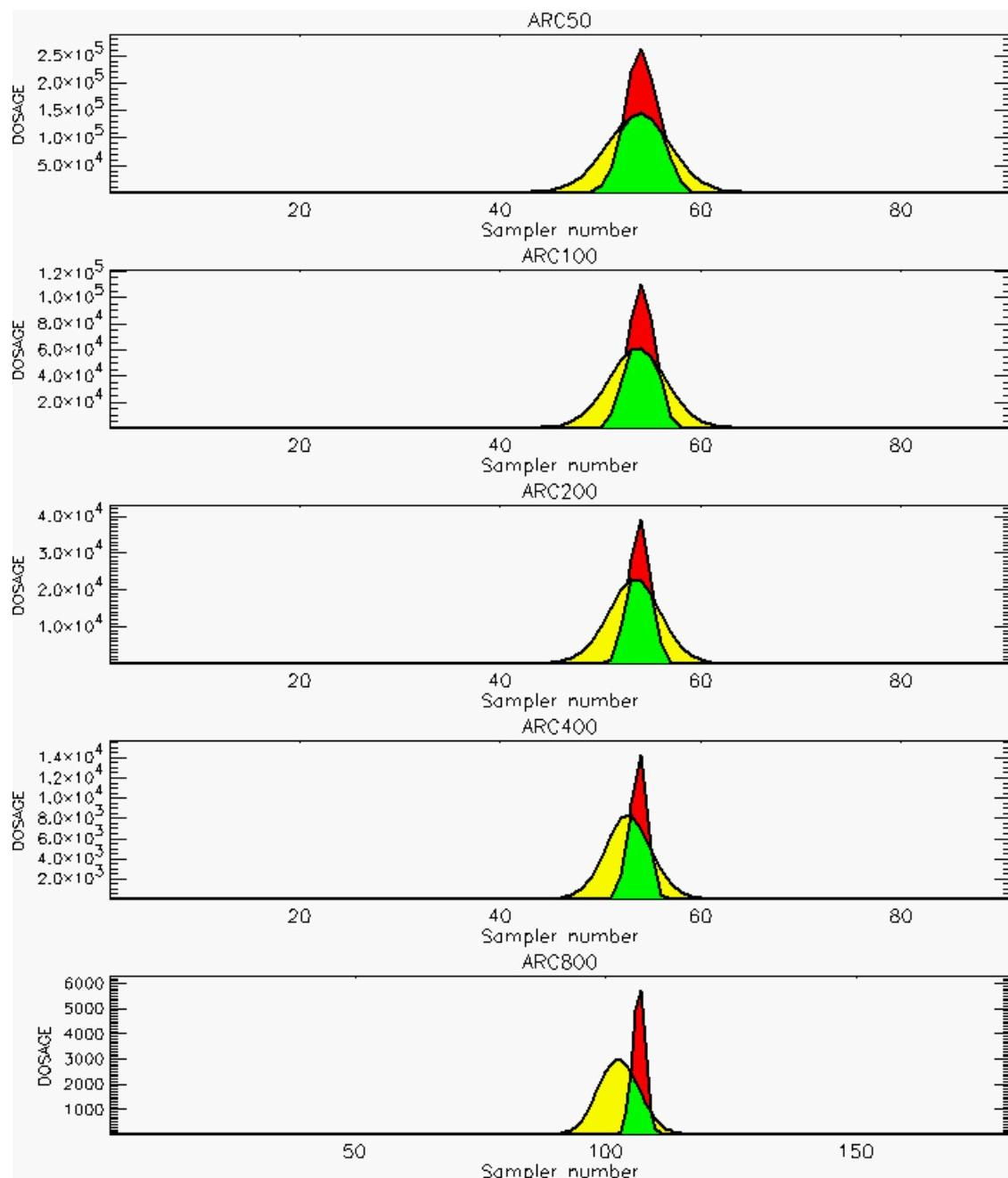


PG Observation to Prediction Comparison

PG Trial File: pr_grass_tracer_Experiment_40.txt

Prediction File: ARAC\nodeposition\pg_40_noxd.arac

**Figure D-32b. NARAC Prediction to Trial 40 on Logarithmic Scale: Stability Category is 6
(Values for Samplers 39-45 of 400-Meter Arc are Missing)**

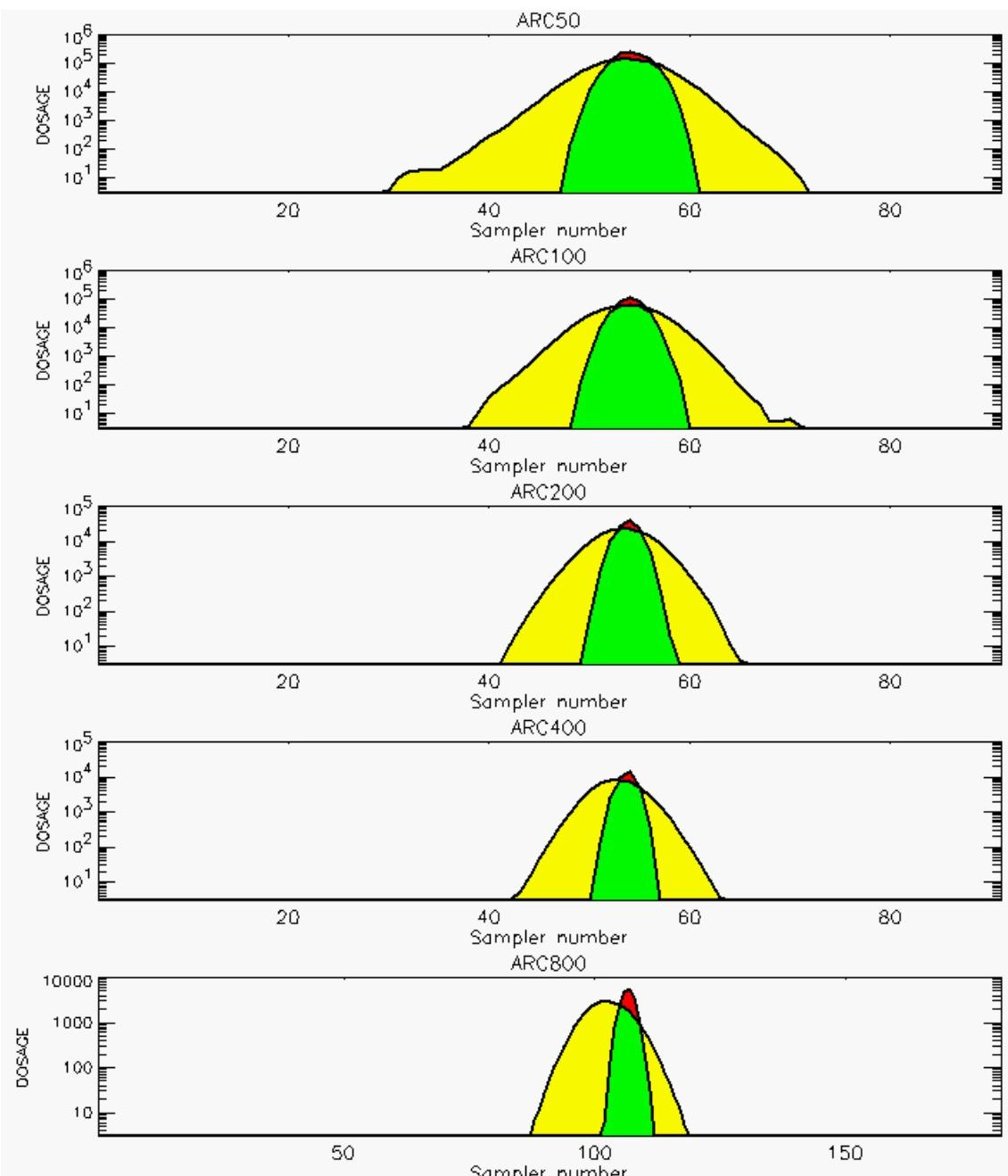


PG Observation to Prediction Comparison

PG Trial File: pr_grass_tracer_Experiment_41.txt

Prediction File: ARAC\nodeposition\pg_41_noxd.arac

Figure D-33a. NARAC Prediction to Trial 41 on Linear Scale: Stability Category is 5

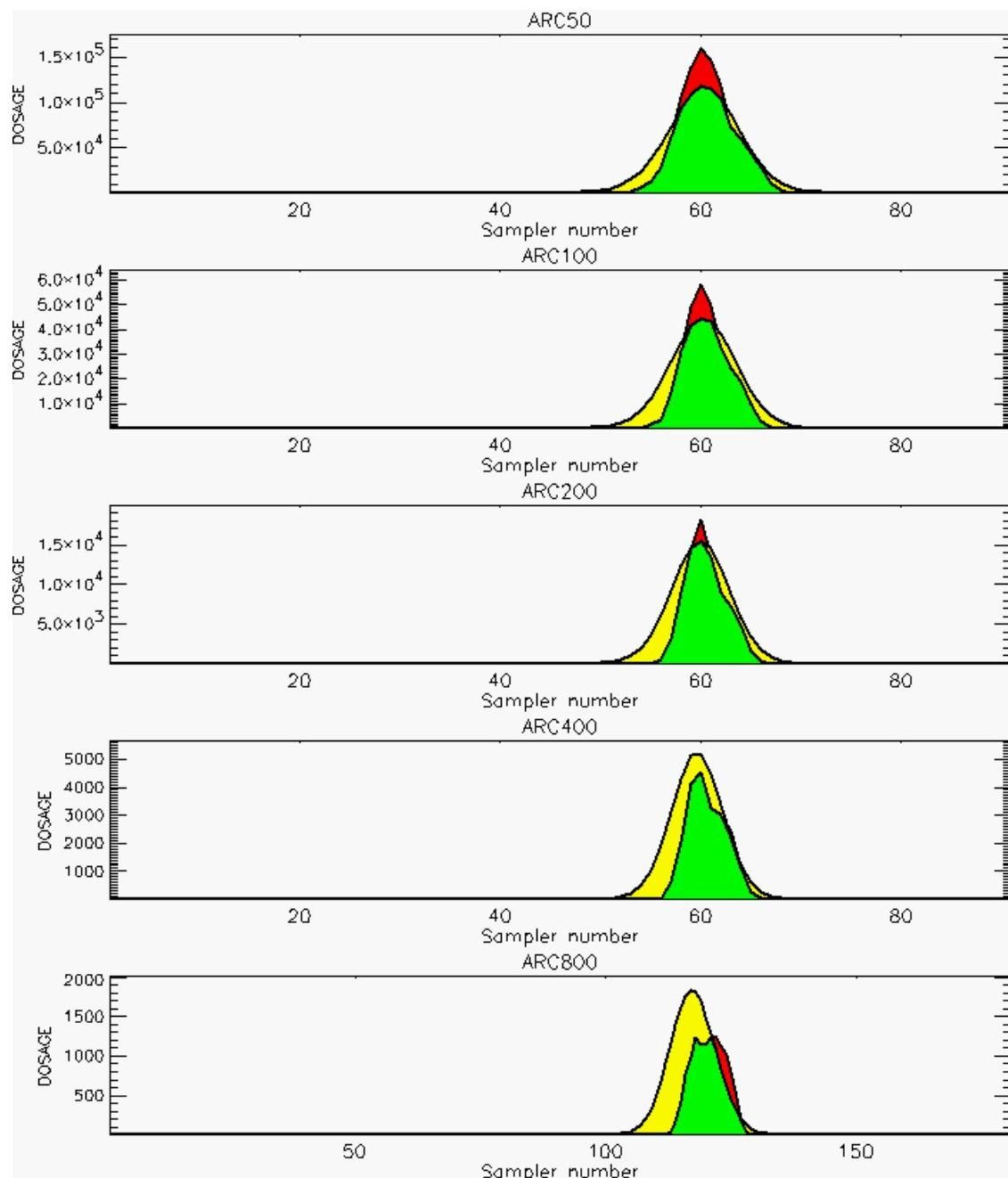


PG Observation to Prediction Comparison

PG Trial File: pr_grass_tracer_Experiment_41.txt

Prediction File: ARAC\nodeposition\pg_41_noxd.arac

Figure D-33b. NARAC Prediction to Trial 41 on Logarithmic Scale: Stability Category is 5

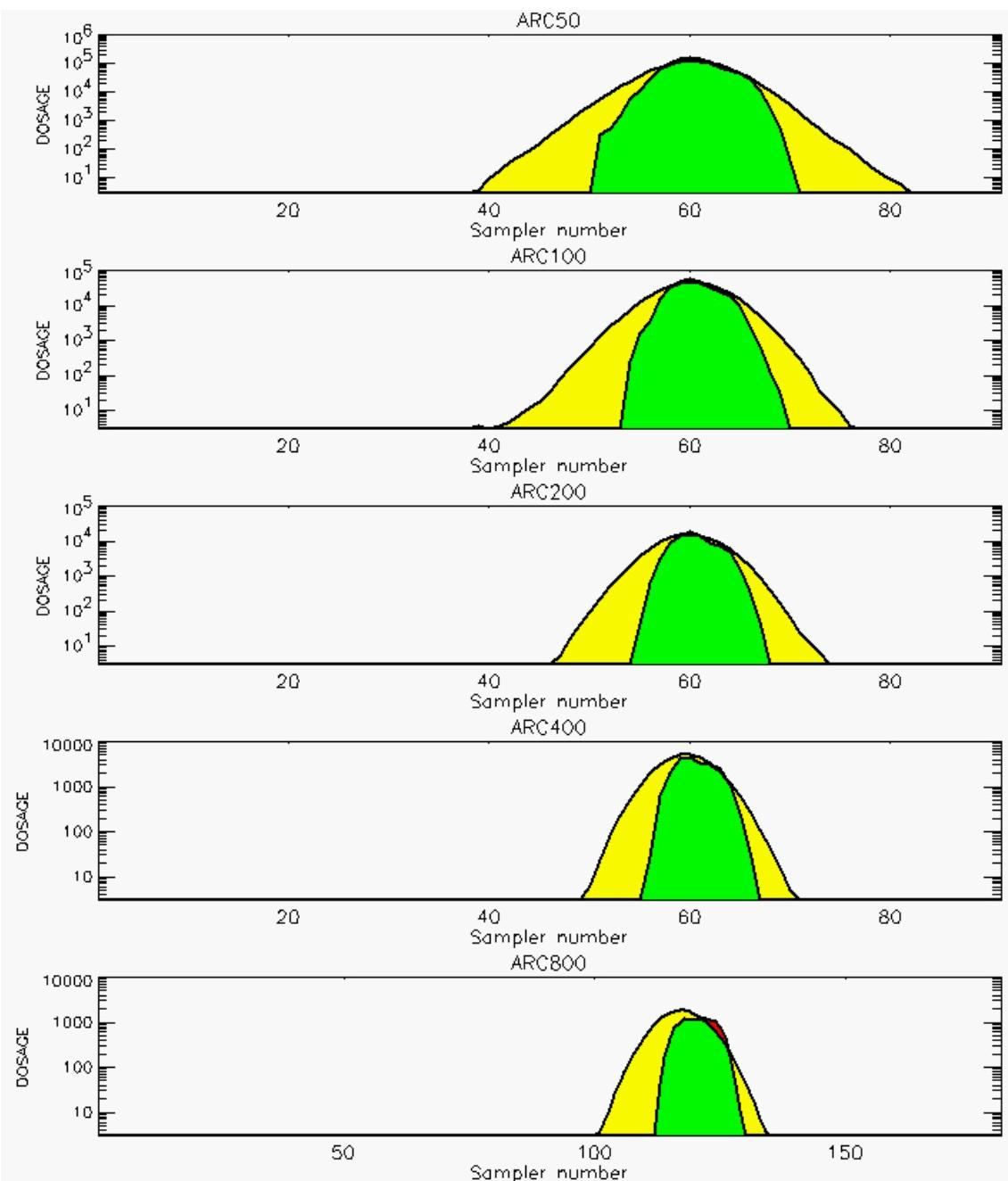


PG Observation to Prediction Comparison

PG Trial File: pr_grass_tracer_Experiment_42.txt

Prediction File: ARAC\nodeposition\pg_42_noxd.arac

Figure D-34a. NARAC Prediction to Trial 42 on Linear Scale: Stability Category is 4

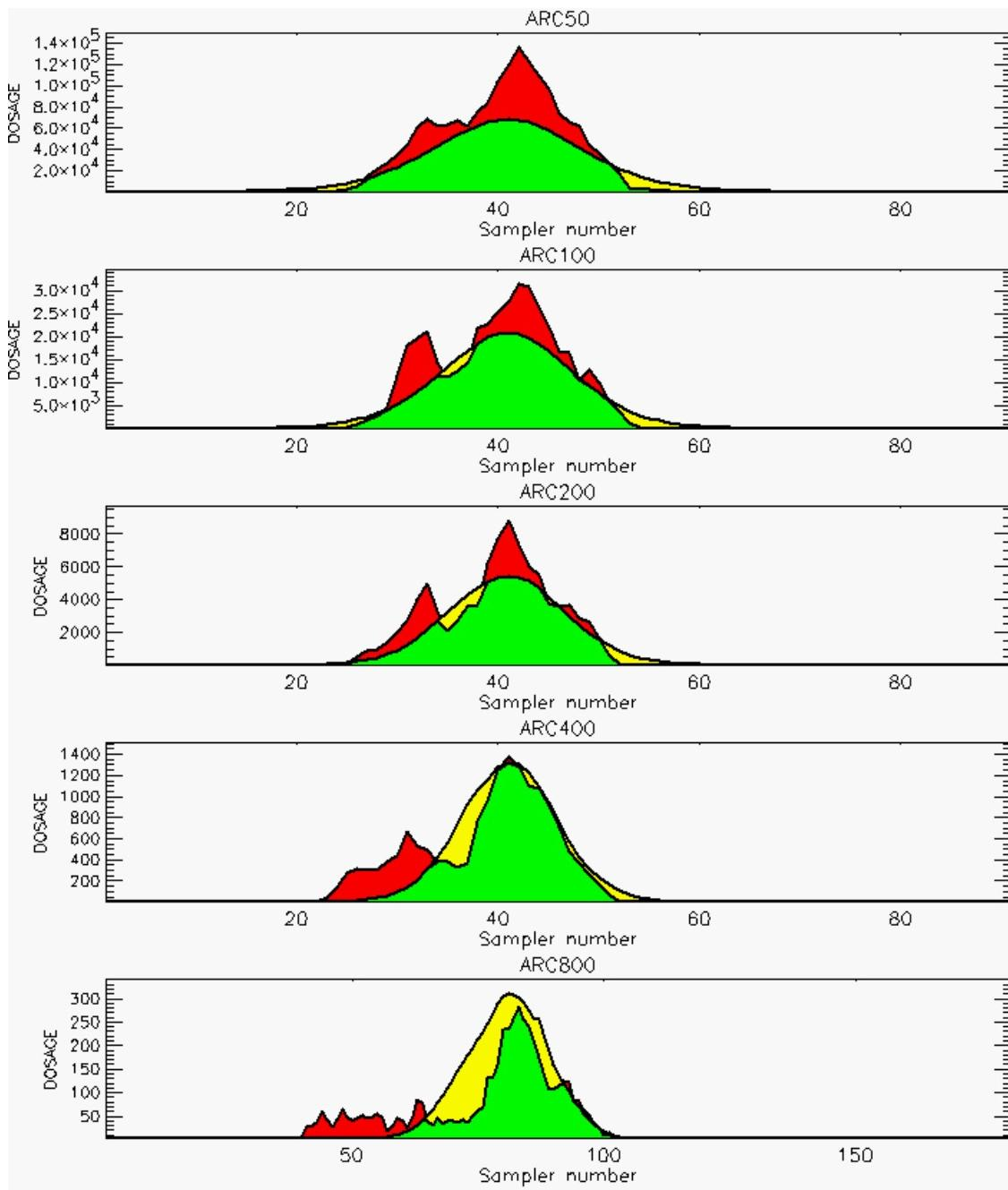


PG Observation to Prediction Comparison

PG Trial File: pr_grass_tracer_Experiment_42.txt

Prediction File: ARAC\nodeposition\pg_42_noxd.arac

Figure D-34b. NARAC Prediction to Trial 42 on Logarithmic Scale: Stability Category is 4

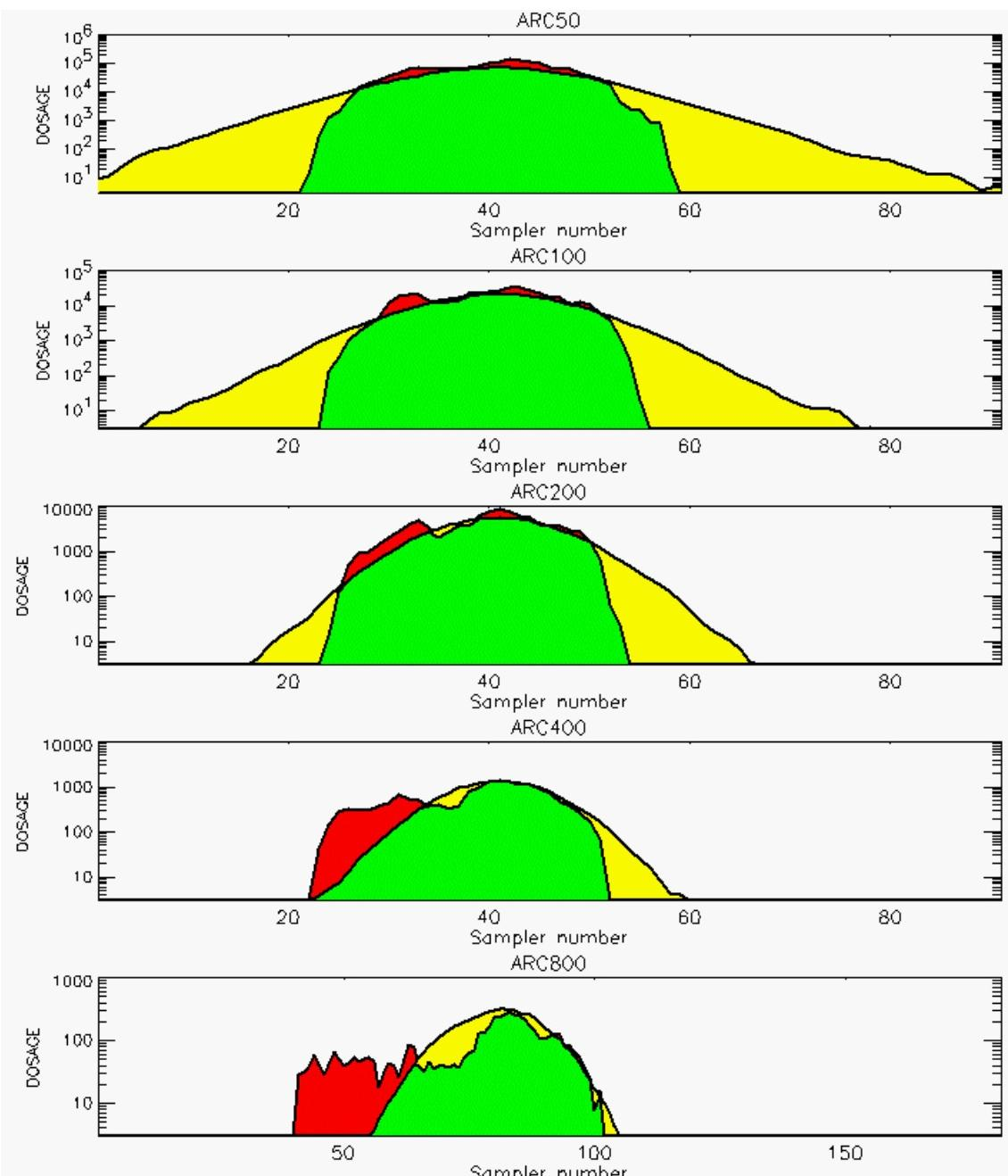


PG Observation to Prediction Comparison

PG Trial File: pr_grass_tracer_Experiment_43.txt

Prediction File: ARAC\nodeposition\pg_43_noxd.arac

Figure D-35a. NARAC Prediction to Trial 43 on Linear Scale: Stability Category is 1

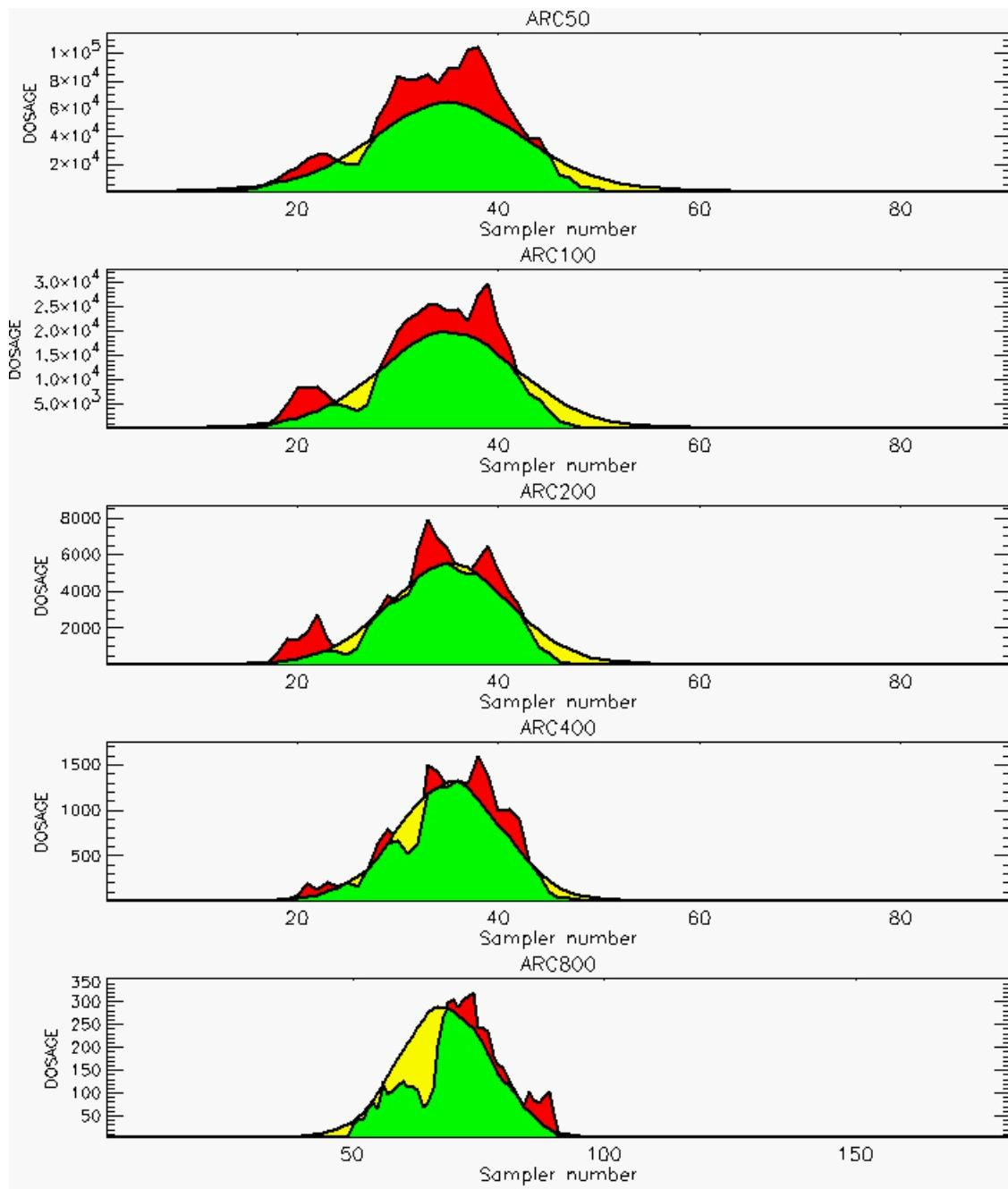


PG Observation to Prediction Comparison

PG Trial File: pr_grass_tracer_Experiment_43.txt

Prediction File: ARAC\nodeposition\pg_43_noxd.arac

Figure D-35b. NARAC Prediction to Trial 43 on Logarithmic Scale: Stability Category is 1



PG Observation to Prediction Comparison

PG Trial File: pr_grass_tracer_Experiment_44.txt

Prediction File: ARAC\nodeposition\pg_44_noxd.arac

Figure D-36a. NARAC Prediction to Trial 44 on Linear Scale: Stability Category is 2

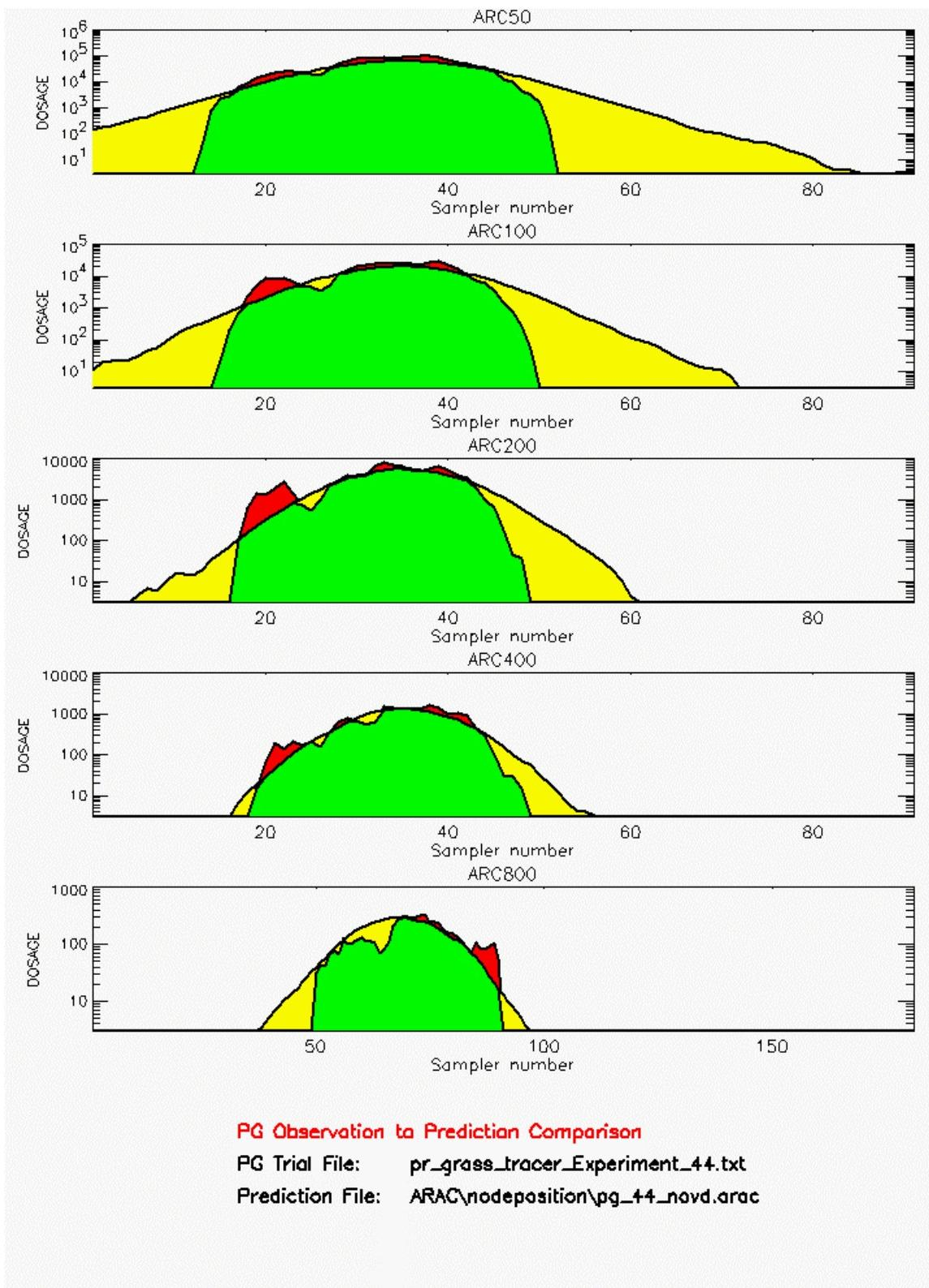
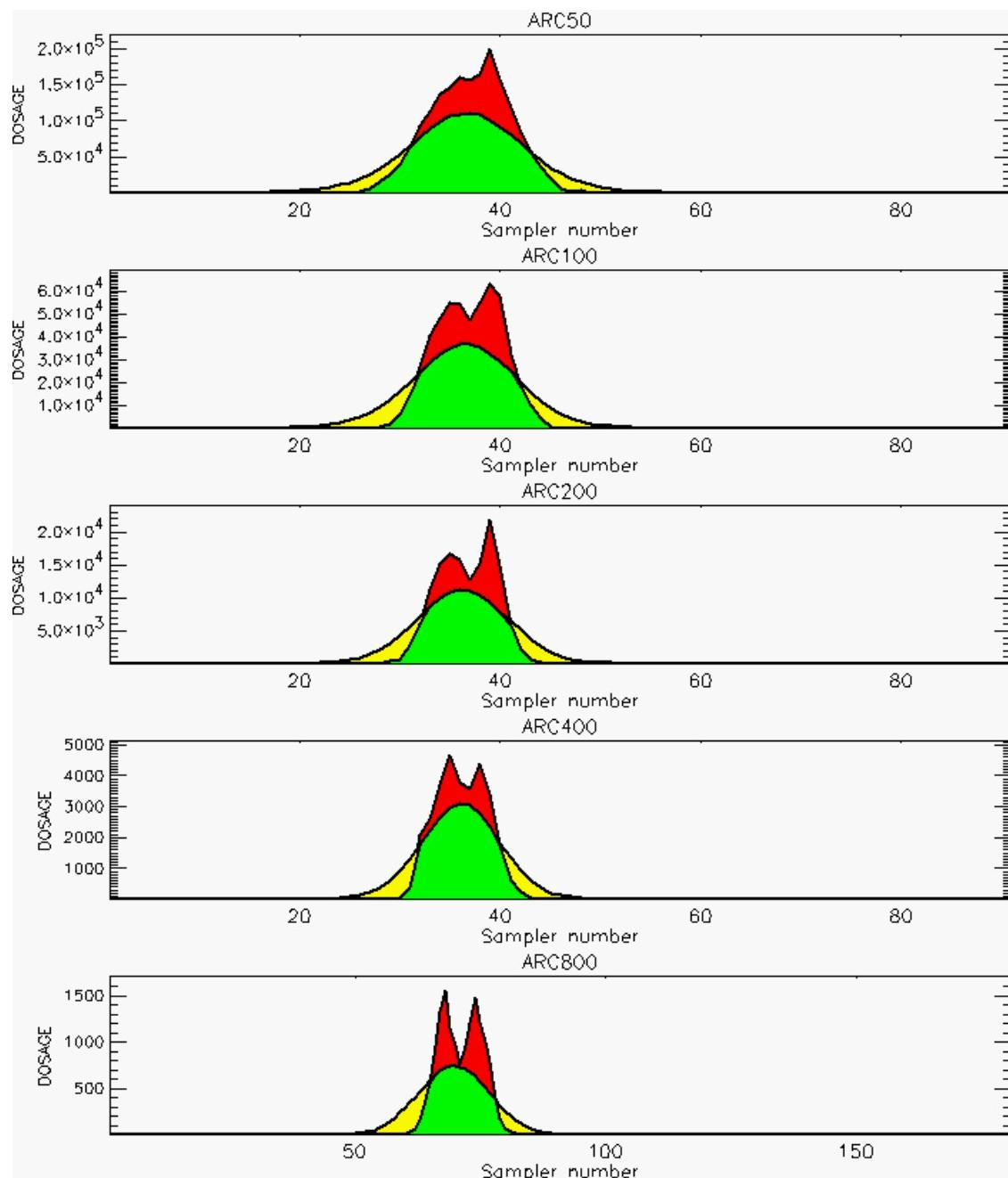


Figure D-36b. NARAC Prediction to Trial 44 on Logarithmic Scale: Stability Category is 2

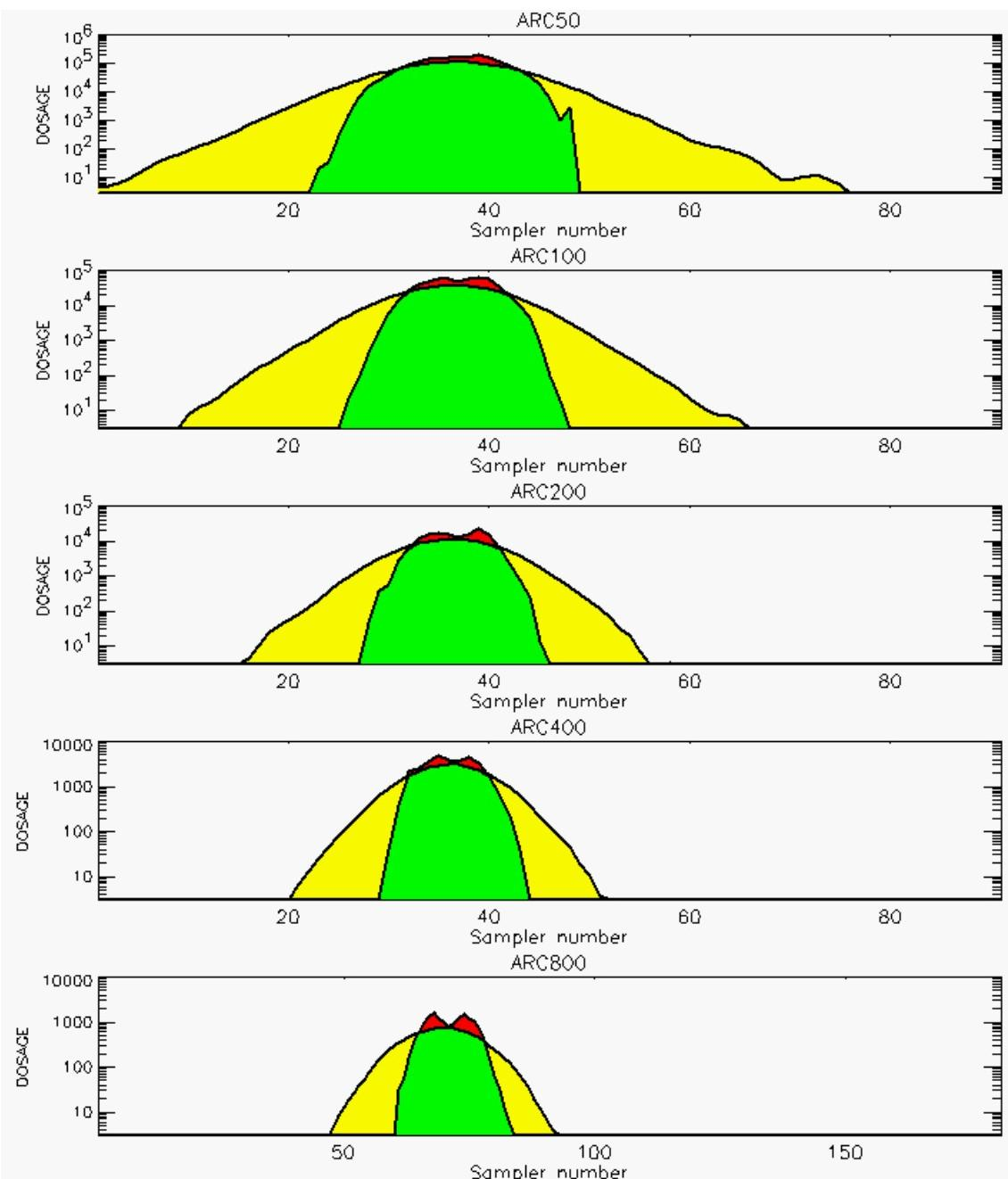


PG Observation to Prediction Comparison

PG Trial File: pr_grass_tracer_Experiment_45.txt

Prediction File: ARAC\nodeposition\pg_45_noxd.arac

Figure D-37a. NARAC Prediction to Trial 45 on Linear Scale: Stability Category is 3

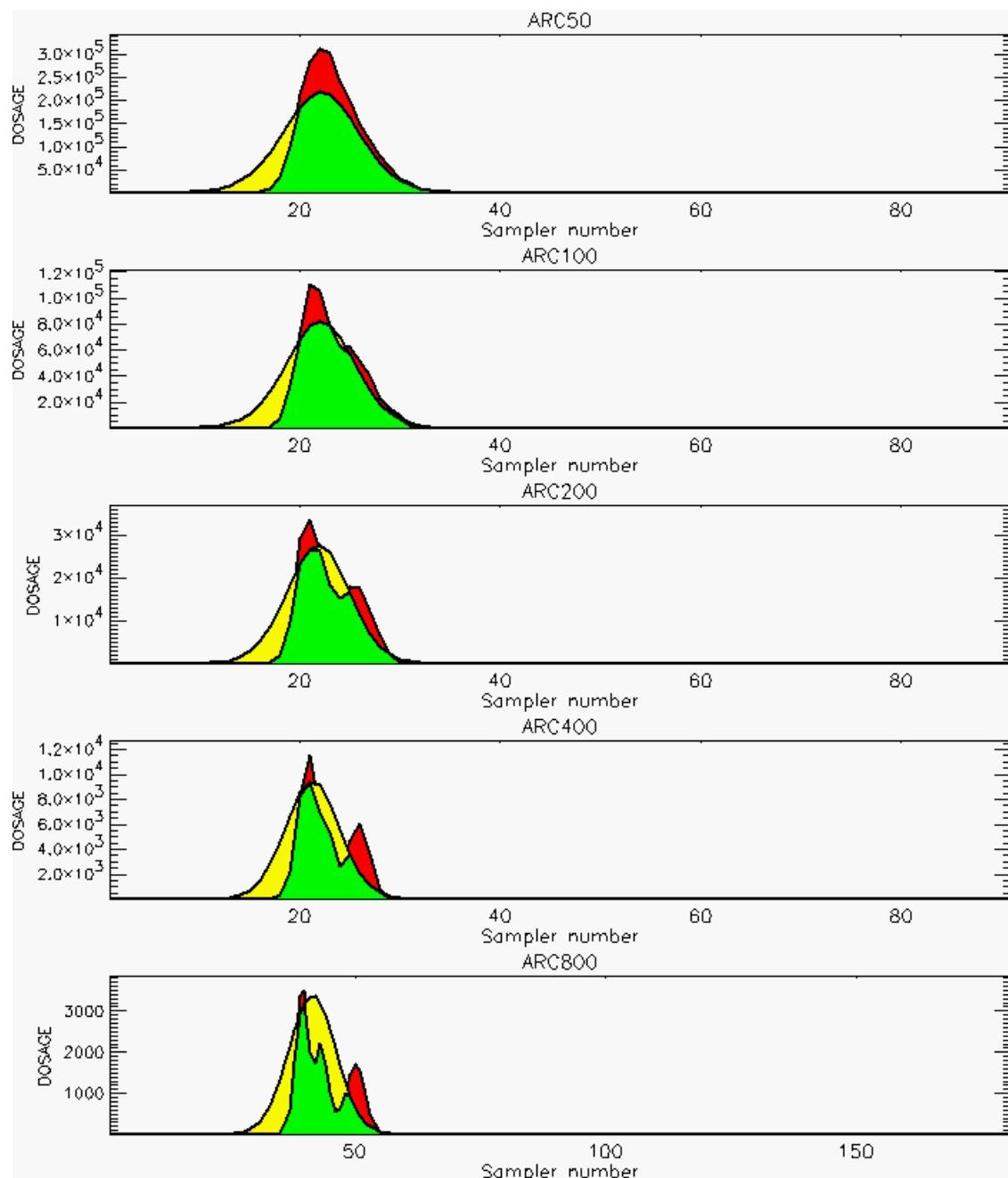


PG Observation to Prediction Comparison

PG Trial File: pr_grass_tracer_Experiment_45.txt

Prediction File: ARAC\nodeposition\pg_45_noxd.arac

Figure D-37b. NARAC Prediction to Trial 45 on Logarithmic Scale: Stability Category is 3



PG Observation to Prediction Comparison

PG Trial File: pr_grass_tracer_Experiment_46.txt

Prediction File: ARAC\nodeposition\pg_46_noxd.arac

Figure D-38a. NARAC Prediction to Trial 46 on Linear Scale: Stability Category is 4

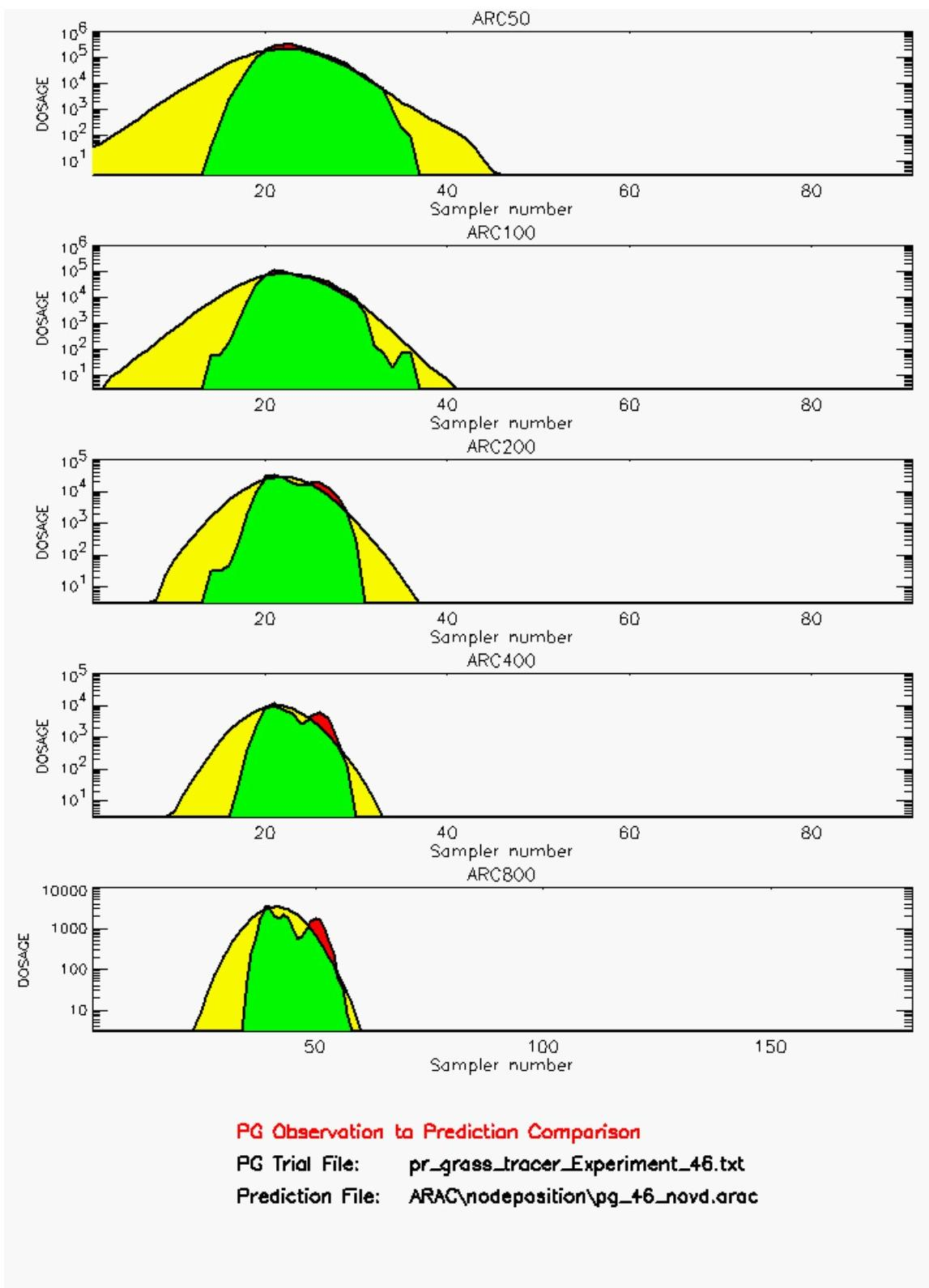
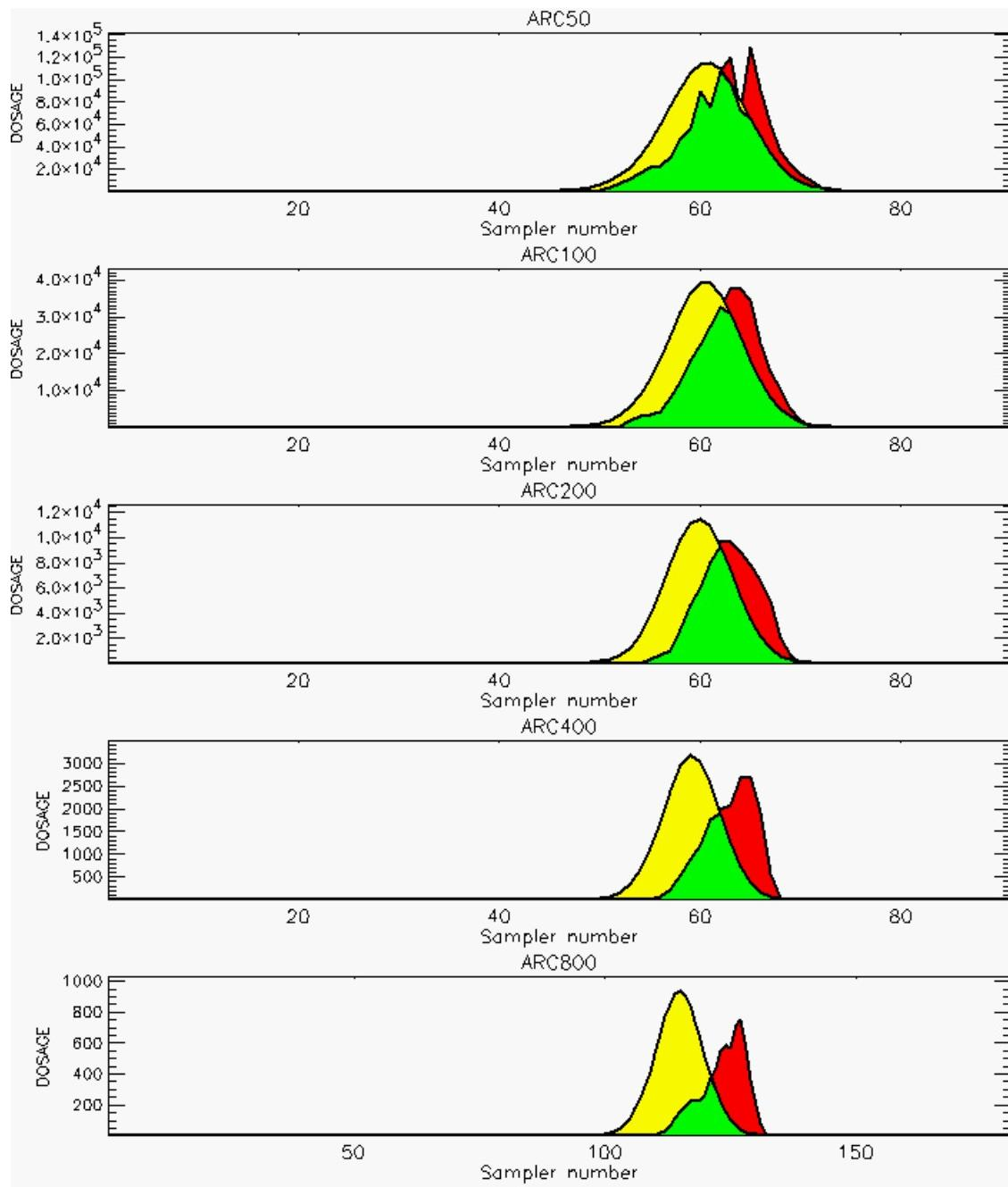


Figure D-38b. NARAC Prediction to Trial 46 on Logarithmic Scale: Stability Category is 4

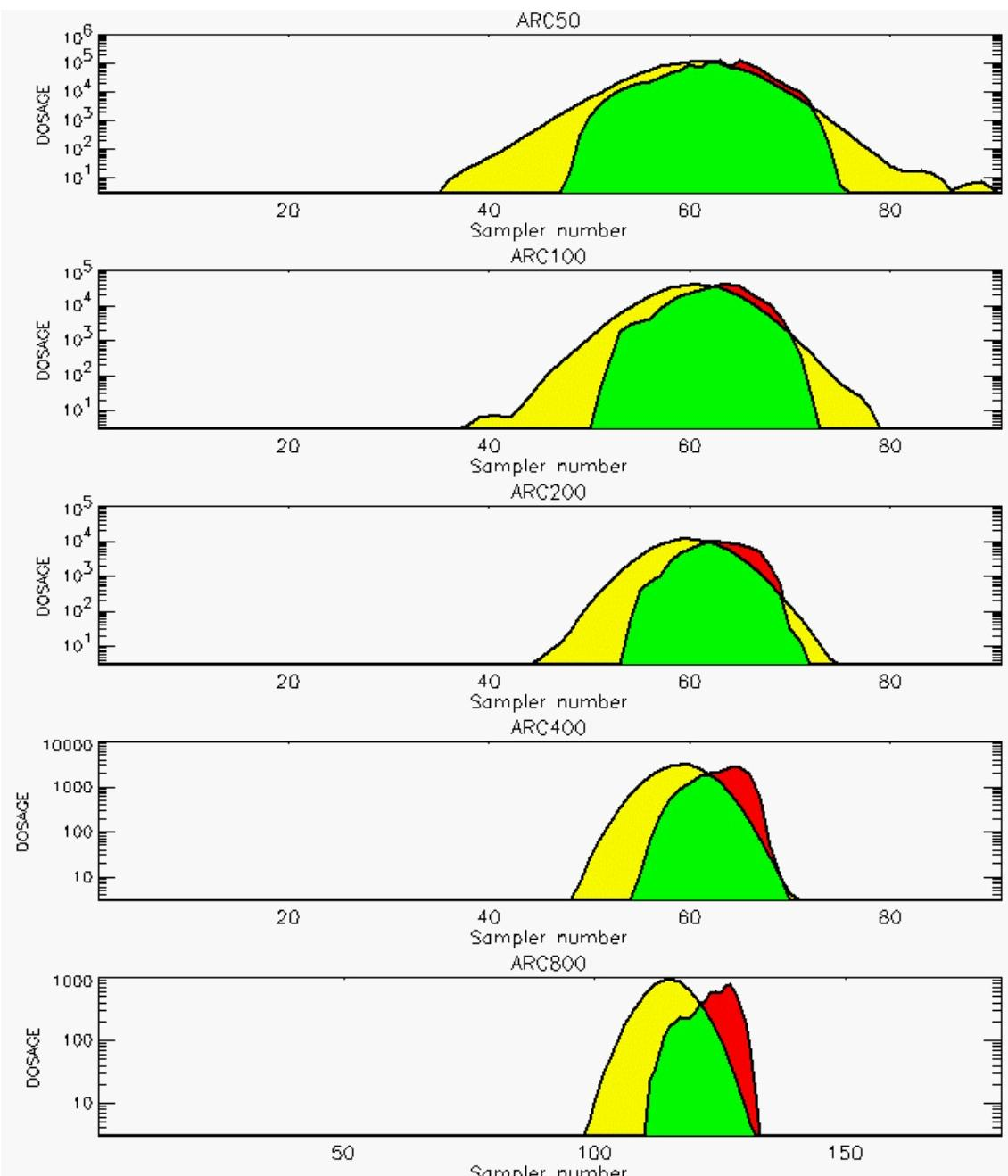


PG Observation to Prediction Comparison

PG Trial File: pr_grass_tracer_Experiment_48.txt

Prediction File: ARAC\nodeposition\pg_48_noxd.arac

Figure D-39a. NARAC Prediction to Trial 48 on Linear Scale: Stability Category is 3

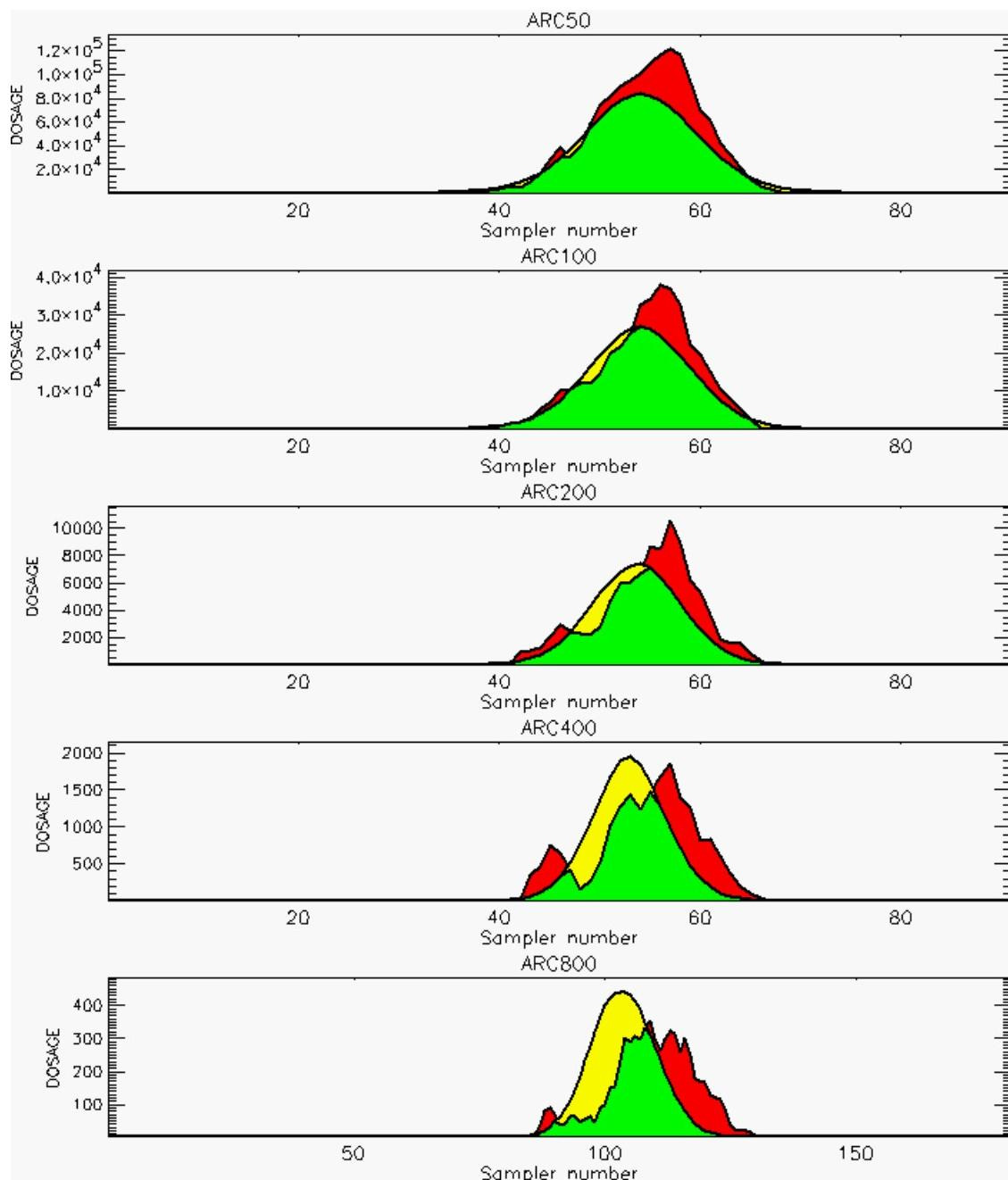


PG Observation to Prediction Comparison

PG Trial File: pr_grass_tracer_Experiment_48.txt

Prediction File: ARAC\nodeposition\pg_48_noxd.arac

Figure D-39b. NARAC Prediction to Trial 48 on Logarithmic Scale: Stability Category is 3

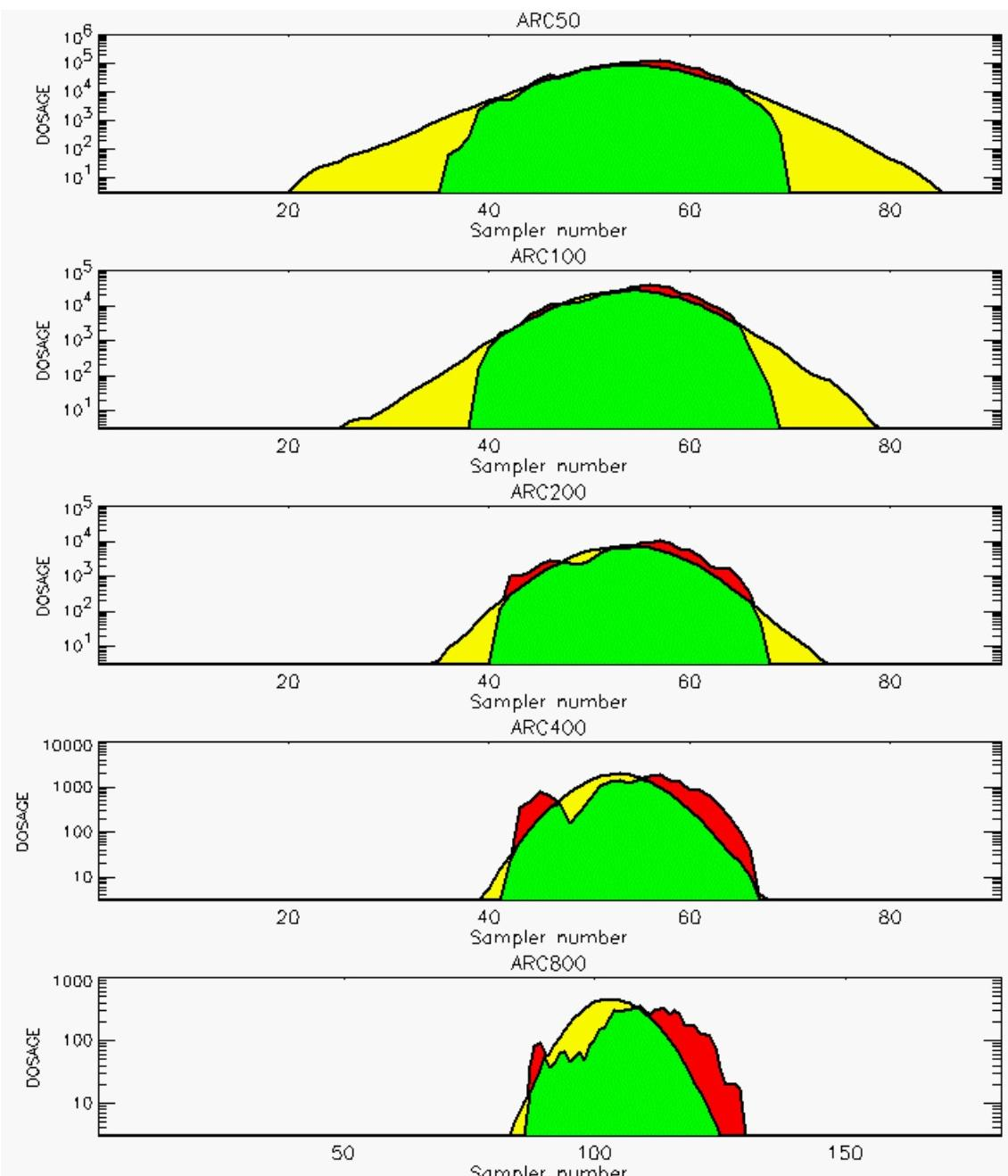


PG Observation to Prediction Comparison

PG Trial File: pr_grass_tracer_Experiment_49.txt

Prediction File: ARAC\nodeposition\pg_49_noxd.arac

Figure D-40a. NARAC Prediction to Trial 49 on Linear Scale: Stability Category is 2

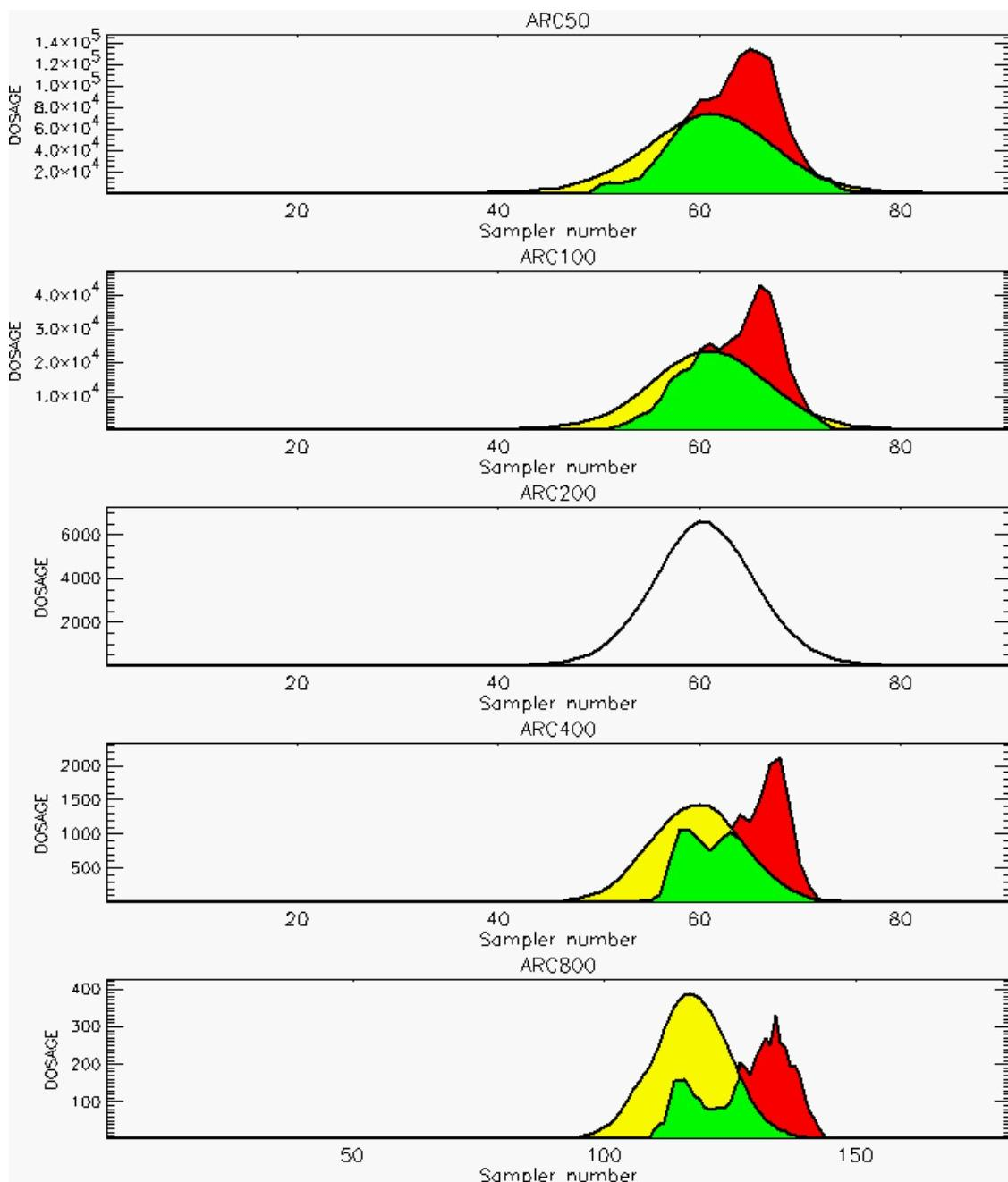


PG Observation to Prediction Comparison

PG Trial File: pr_grass_tracer_Experiment_49.txt

Prediction File: ARAC\nodeposition\pg_49_noxd.arac

Figure D-40b. NARAC Prediction to Trial 49 on Logarithmic Scale: Stability Category is 2

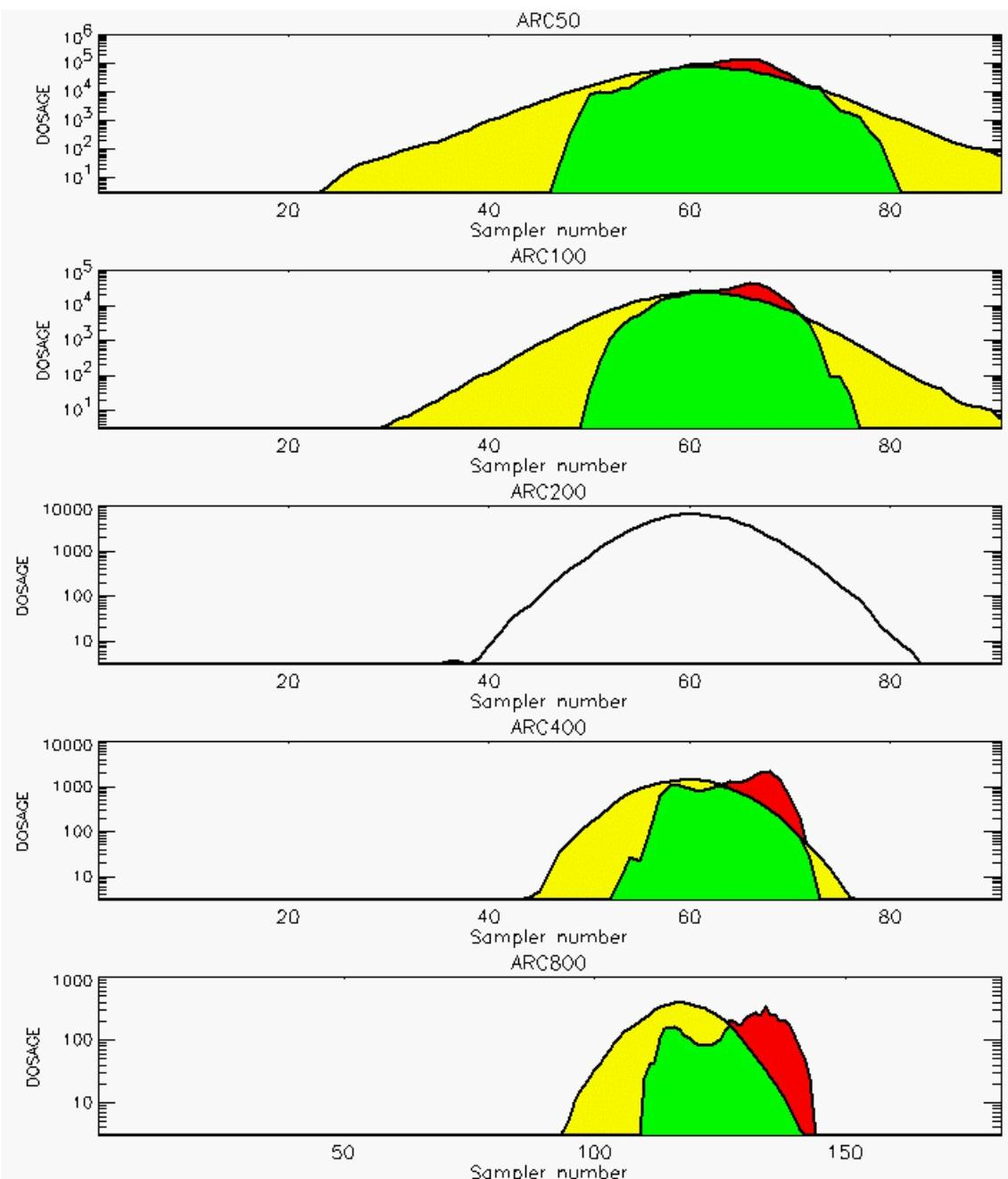


PG Observation to Prediction Comparison

PG Trial File: pr_grass_tracer_Experiment_50.txt

Prediction File: ARAC\nodeposition\pg_50_noxd.arac

Figure D-41a. NARAC Prediction to Trial 50 on Linear Scale: Stability Category is 2 (Values for Samplers of 200-Meter Arc are Replaced by Missing Values [Ref. D-2])

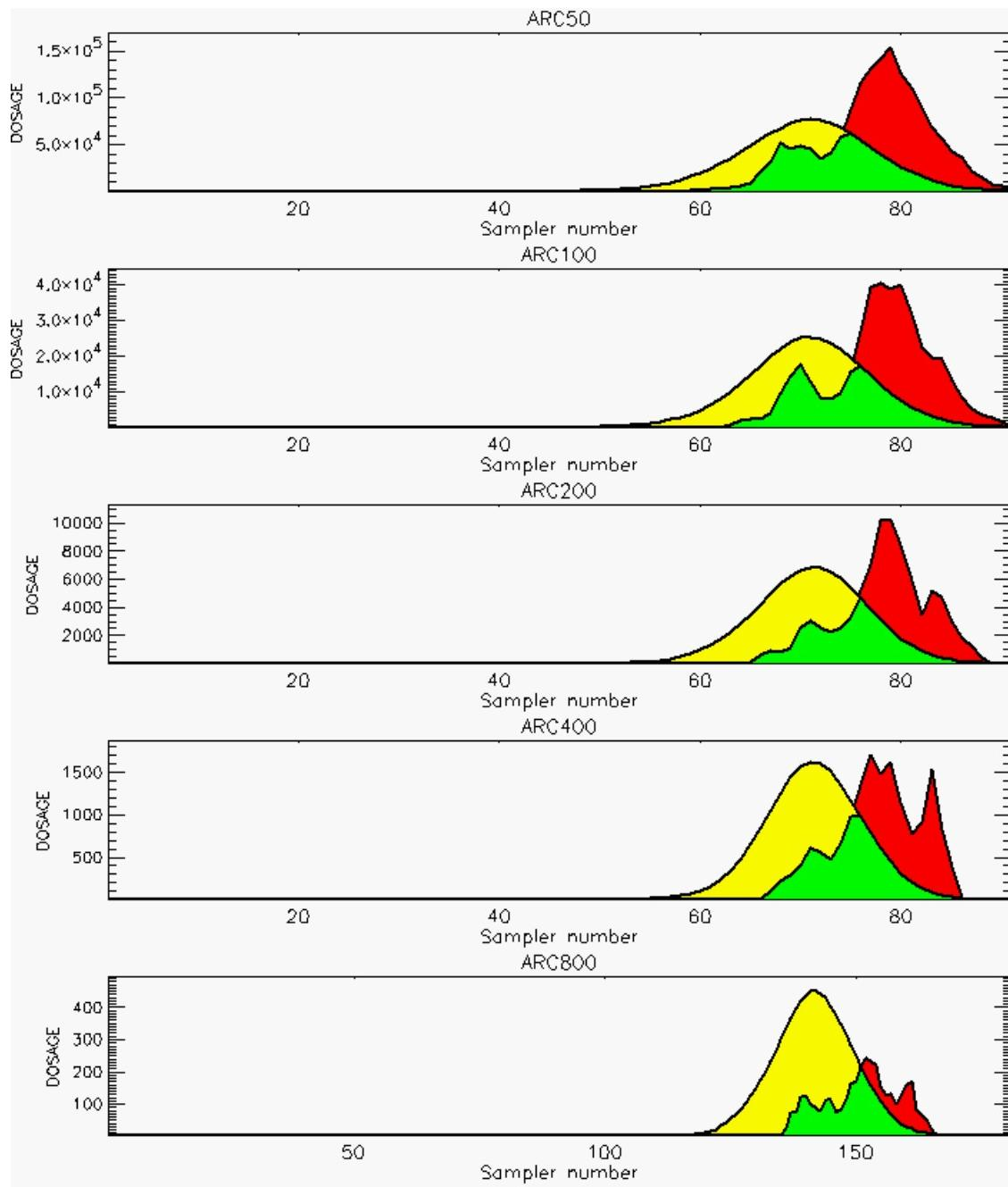


PG Observation to Prediction Comparison

PG Trial File: pr_grass_tracer_Experiment_50.txt

Prediction File: ARAC\nodeposition\pg_50_noxd.arac

Figure D-41b. NARAC Prediction to Trial 50 on Logarithmic Scale: Stability Category is 2 (Values for Samplers of 200-Meter Arc are Replaced by Missing Values [Ref. D-2])

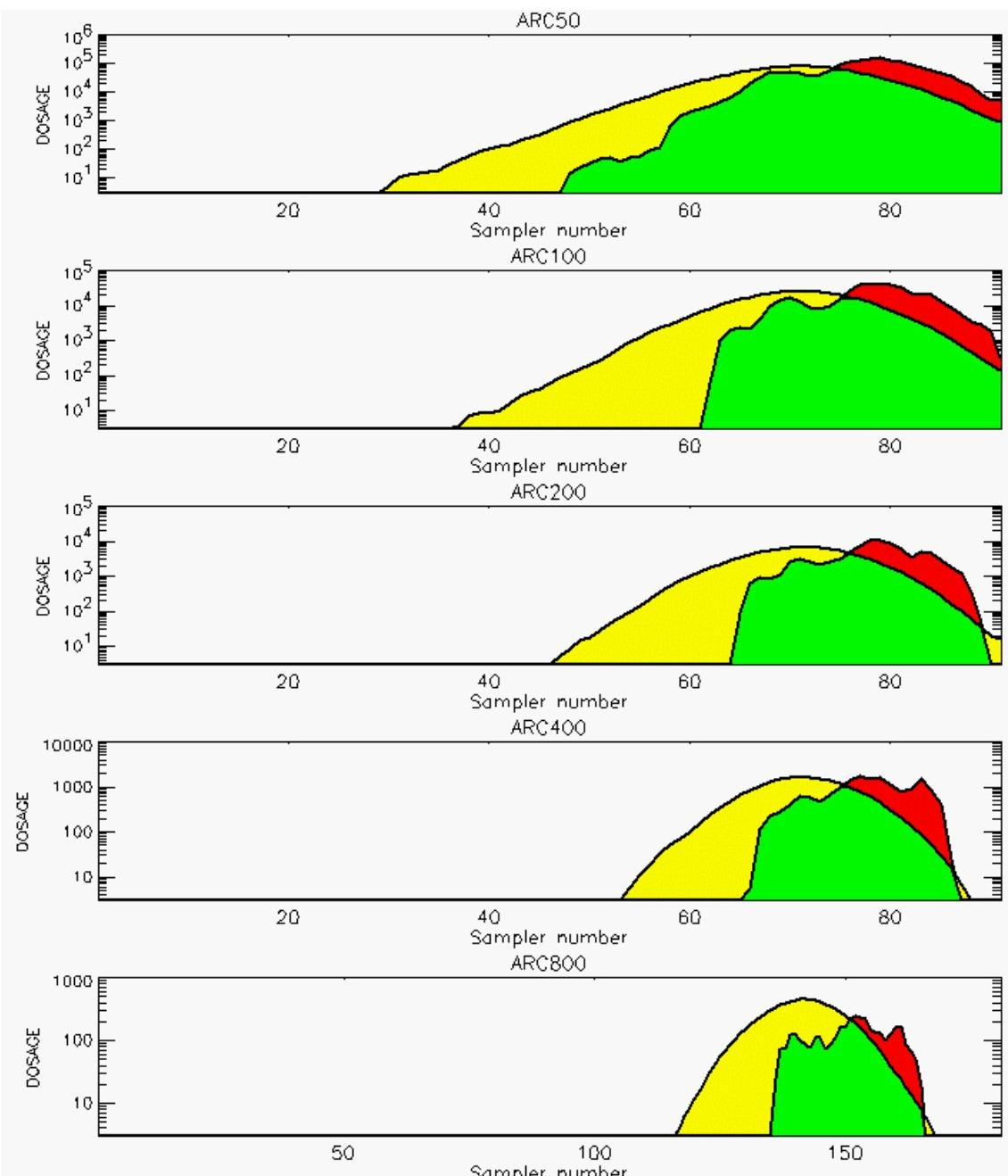


PG Observation to Prediction Comparison

PG Trial File: pr_grass_tracer_Experiment_51.txt

Prediction File: ARAC\nodeposition\pg_51_noxd.arac

Figure D-42a. NARAC Prediction to Trial 51 on Linear Scale: Stability Category is 2

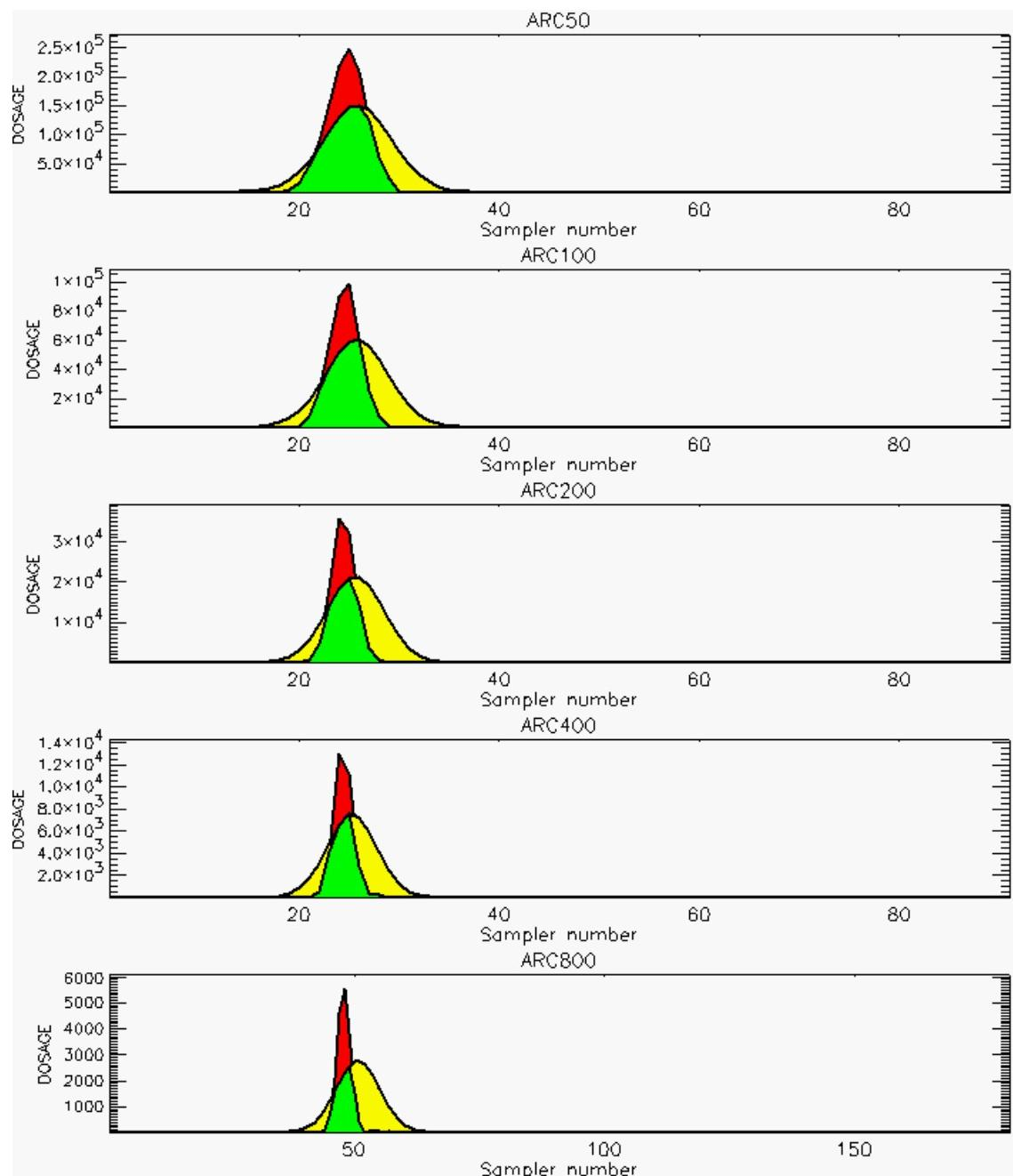


PG Observation to Prediction Comparison

PG Trial File: pr_grass_tracer_Experiment_51.txt

Prediction File: ARAC\nodeposition\pg_51_noxd.arac

Figure D-42b. NARAC Prediction to Trial 51 on Logarithmic Scale: Stability Category is 2

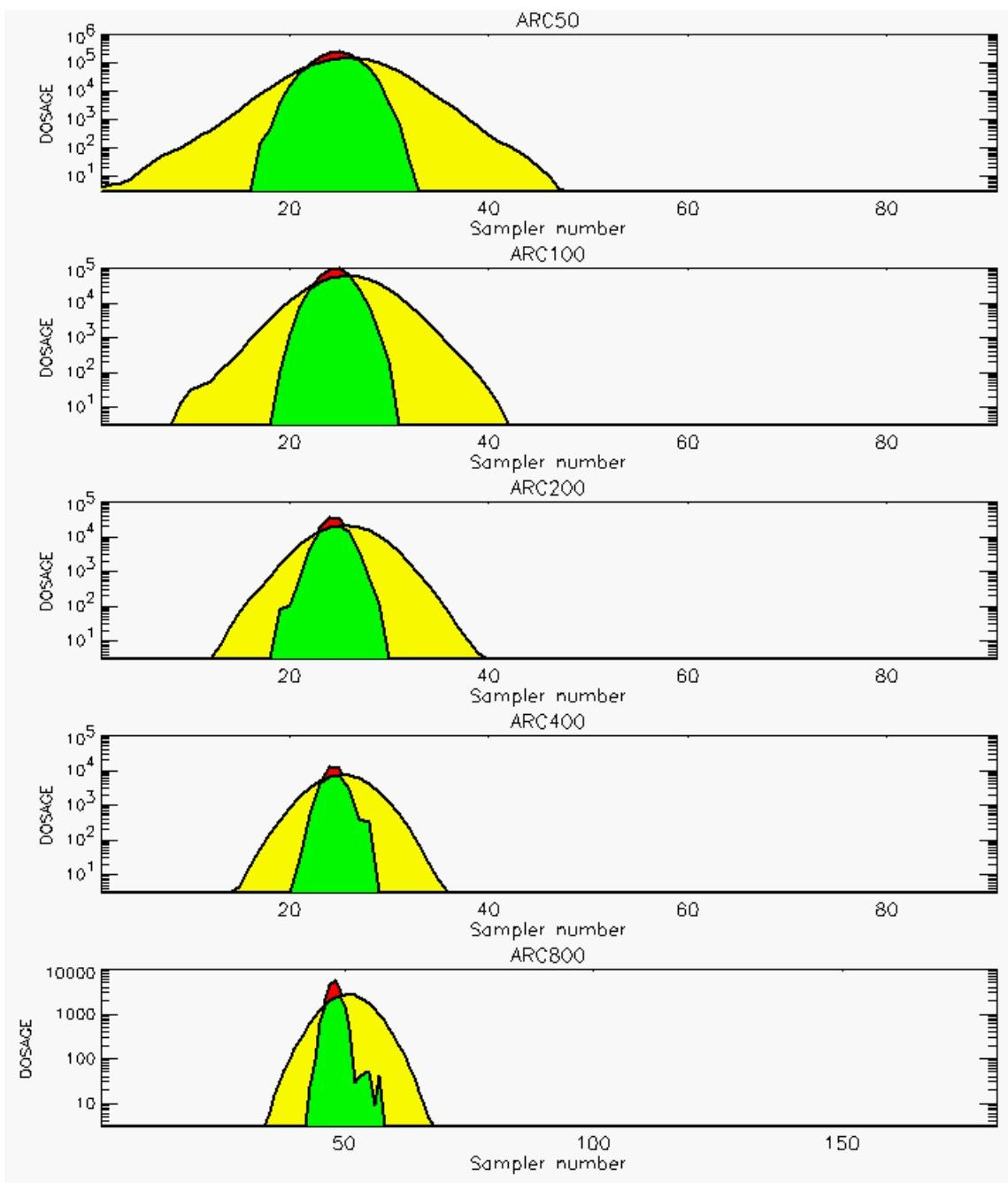


PG Observation to Prediction Comparison

PG Trial File: pr_grass_tracer_Experiment_54.txt

Prediction File: ARAC\nodeposition\pg_54_noxd.arac

Figure D-43a. NARAC Prediction to Trial 54 on Linear Scale: Stability Category is 5

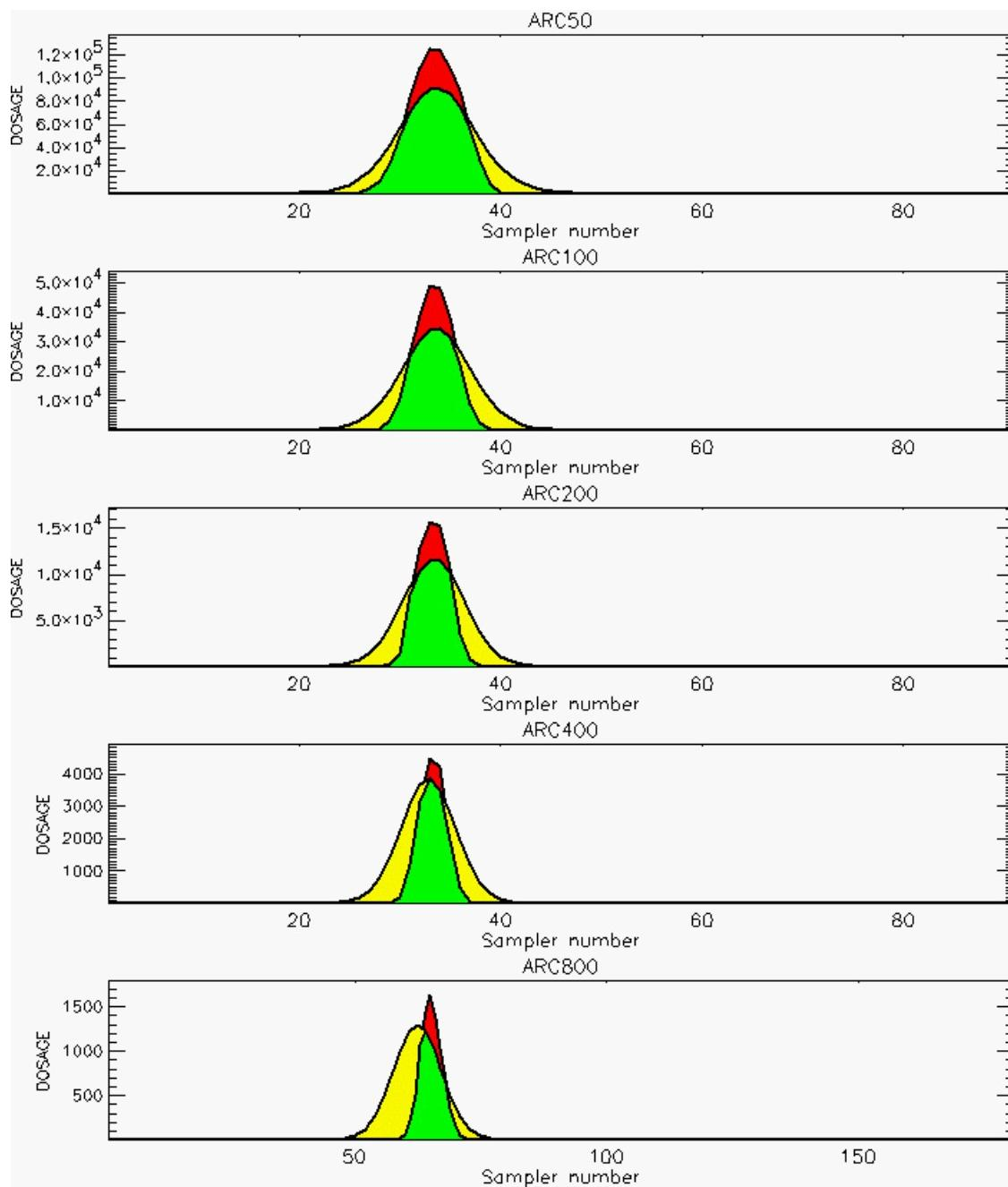


PG Observation to Prediction Comparison

PG Trial File: pr_grass_tracer_Experiment_54.txt

Prediction File: ARAC\nodeposition\pg_54_noxd.arac

Figure D-43b. NARAC Prediction to Trial 54 on Logarithmic Scale: Stability Category is 5

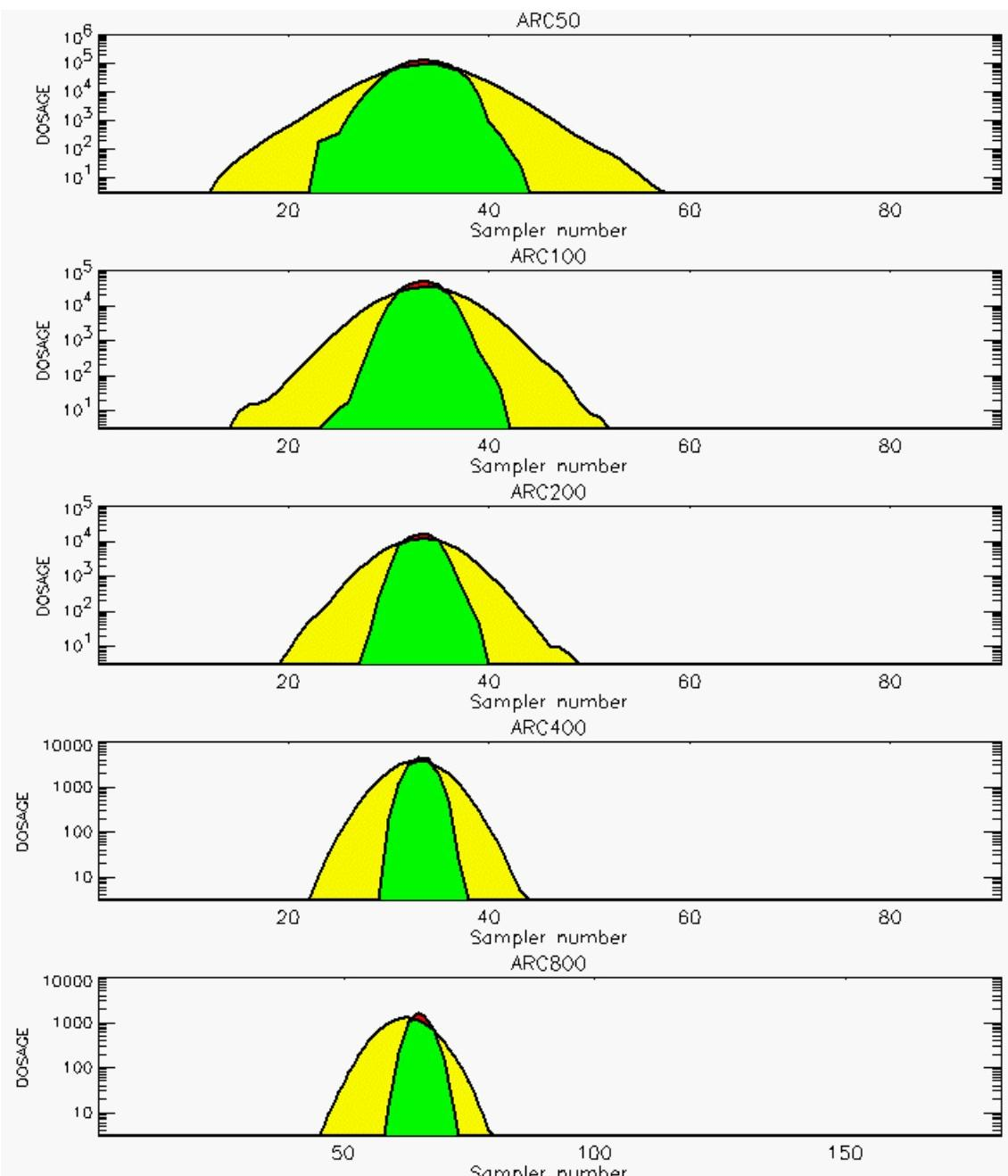


PG Observation to Prediction Comparison

PG Trial File: pr_grass_tracer_Experiment_55.txt

Prediction File: ARAC\nodeposition\pg_55_noxd.arac

Figure D-44a. NARAC Prediction to Trial 55 on Linear Scale: Stability Category is 4

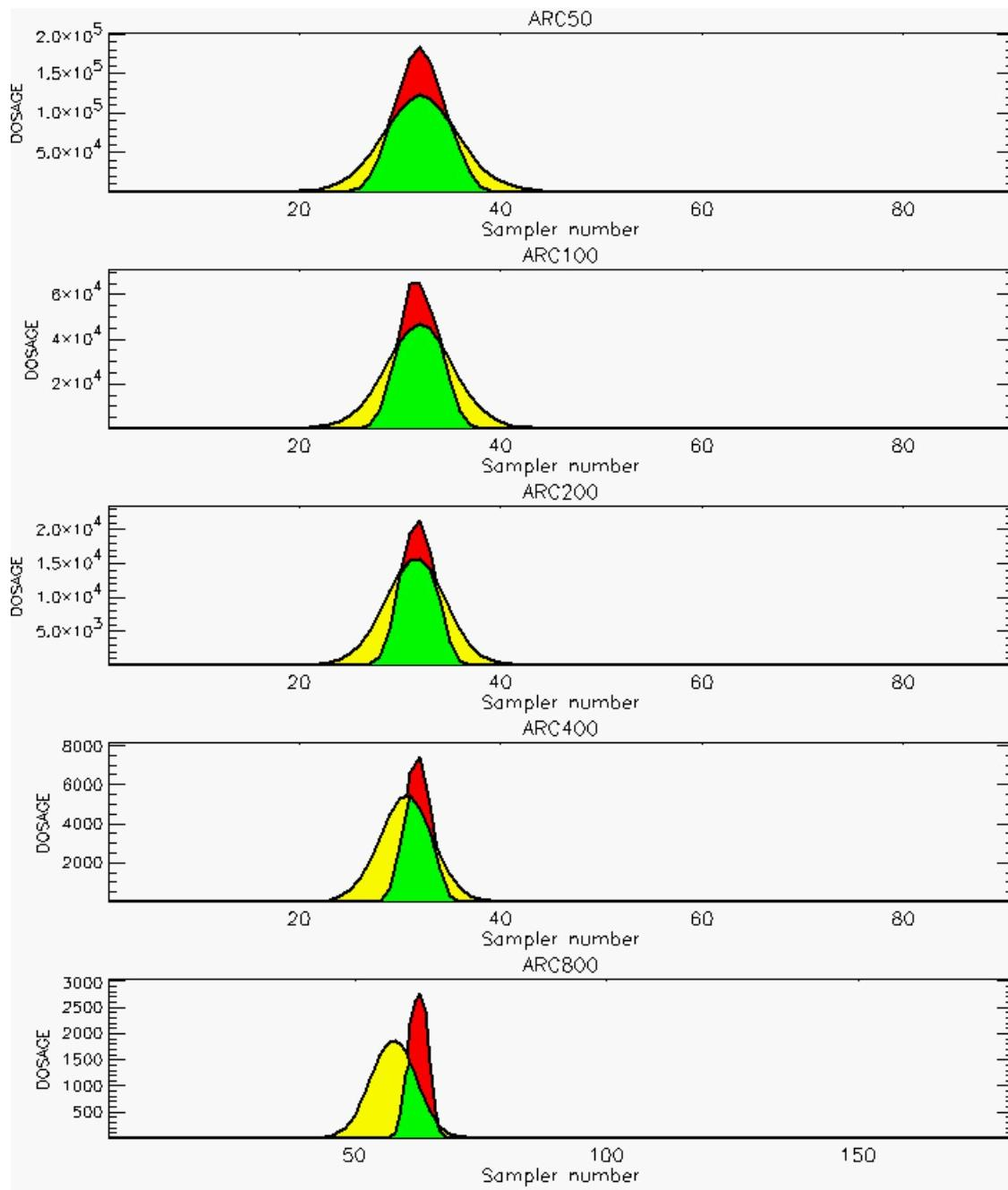


PG Observation to Prediction Comparison

PG Trial File: pr_grass_tracer_Experiment_55.txt

Prediction File: ARAC\nodeposition\pg_55_noxd.arac

Figure D-44b. NARAC Prediction to Trial 55 on Logarithmic Scale: Stability Category is 4

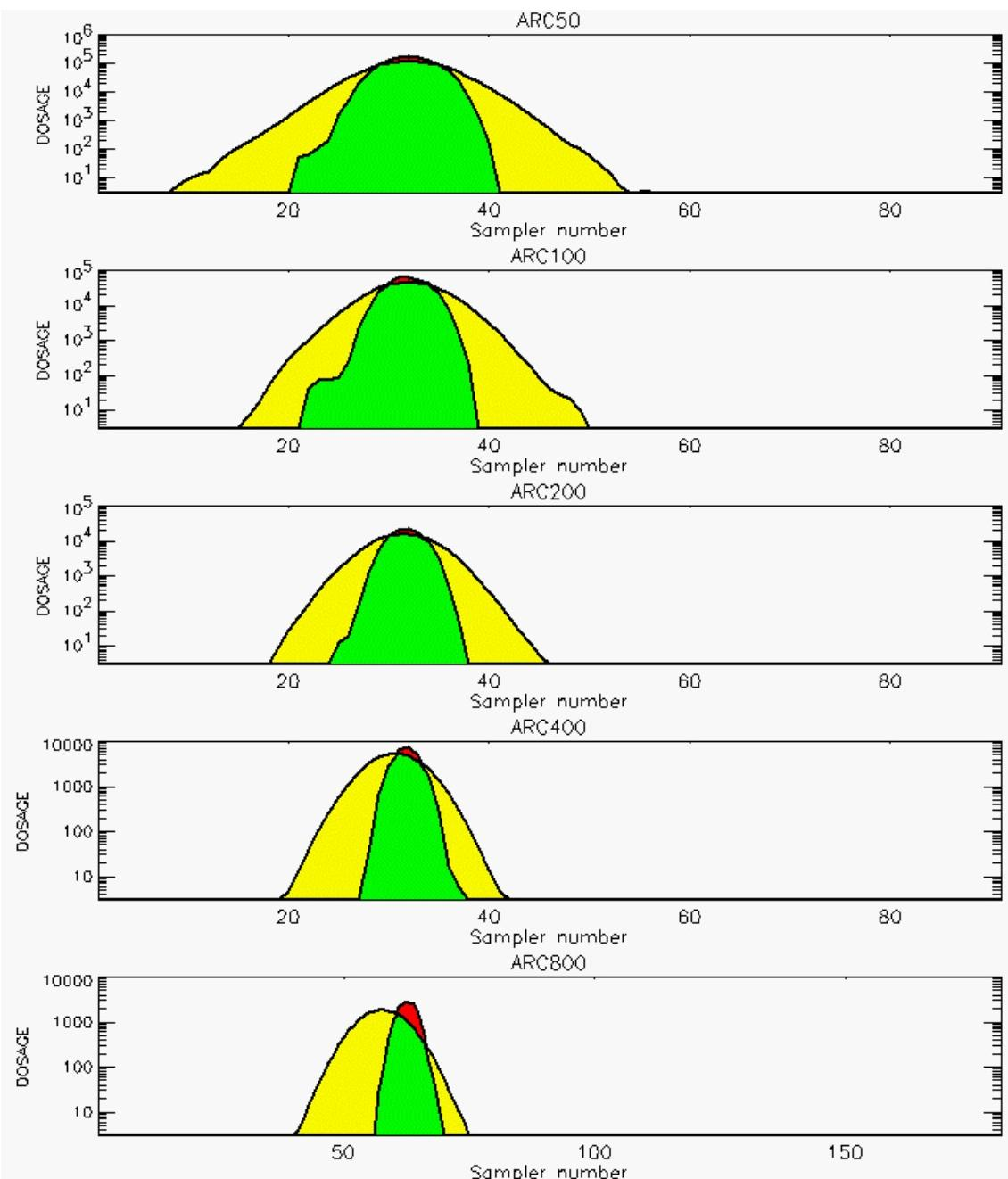


PG Observation to Prediction Comparison

PG Trial File: pr_grass_tracer_Experiment_56.txt

Prediction File: ARAC\nodeposition\pg_56_noxd.arac

Figure D-45a. NARAC Prediction to Trial 56 on Linear Scale: Stability Category is 4

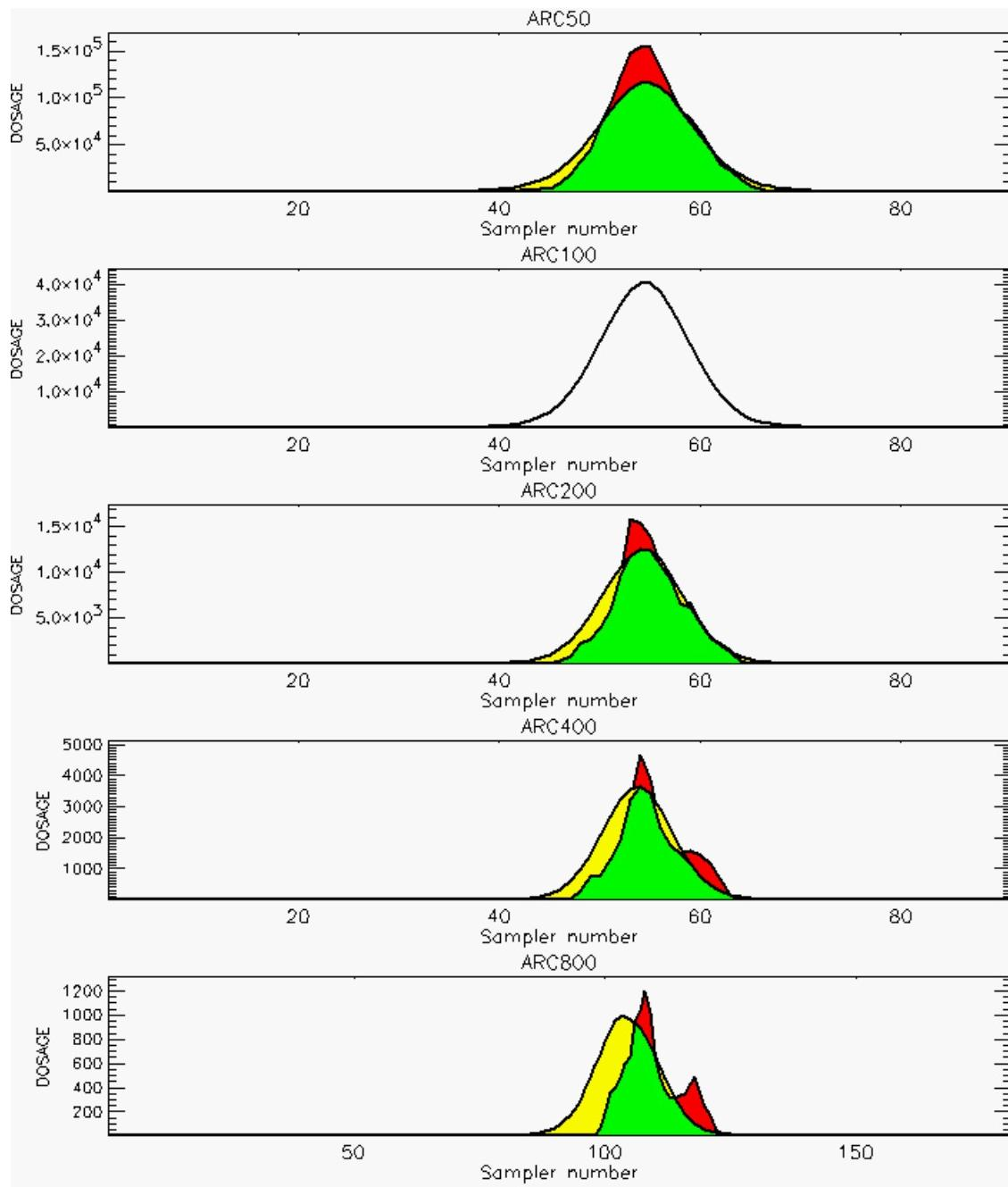


PG Observation to Prediction Comparison

PG Trial File: pr_grass_tracer_Experiment_56.txt

Prediction File: ARAC\nodeposition\pg_56_noxd.arac

Figure D-45b. NARAC Prediction to Trial 56 on Logarithmic Scale: Stability Category is 4

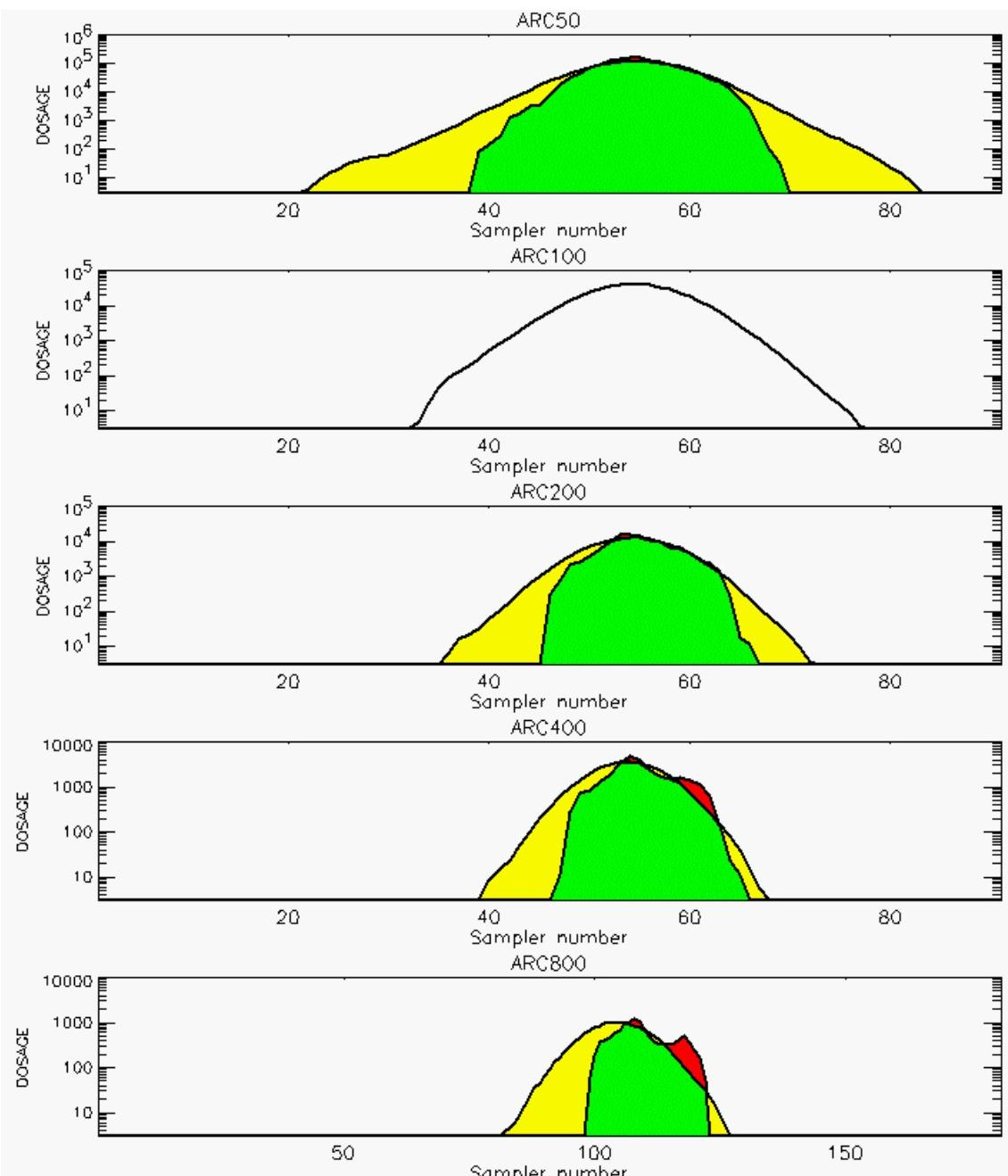


PG Observation to Prediction Comparison

PG Trial File: pr_grass_tracer_Experiment_57.txt

Prediction File: ARAC\nodeposition\pg_57_nozd.arac

**Figure D-46a. NARAC Prediction to Trial 57 on Linear Scale: Stability Category is 3
(Values for Sampler of 100-Meter Arc are Replaced by Missing Values [Ref. D-2])**

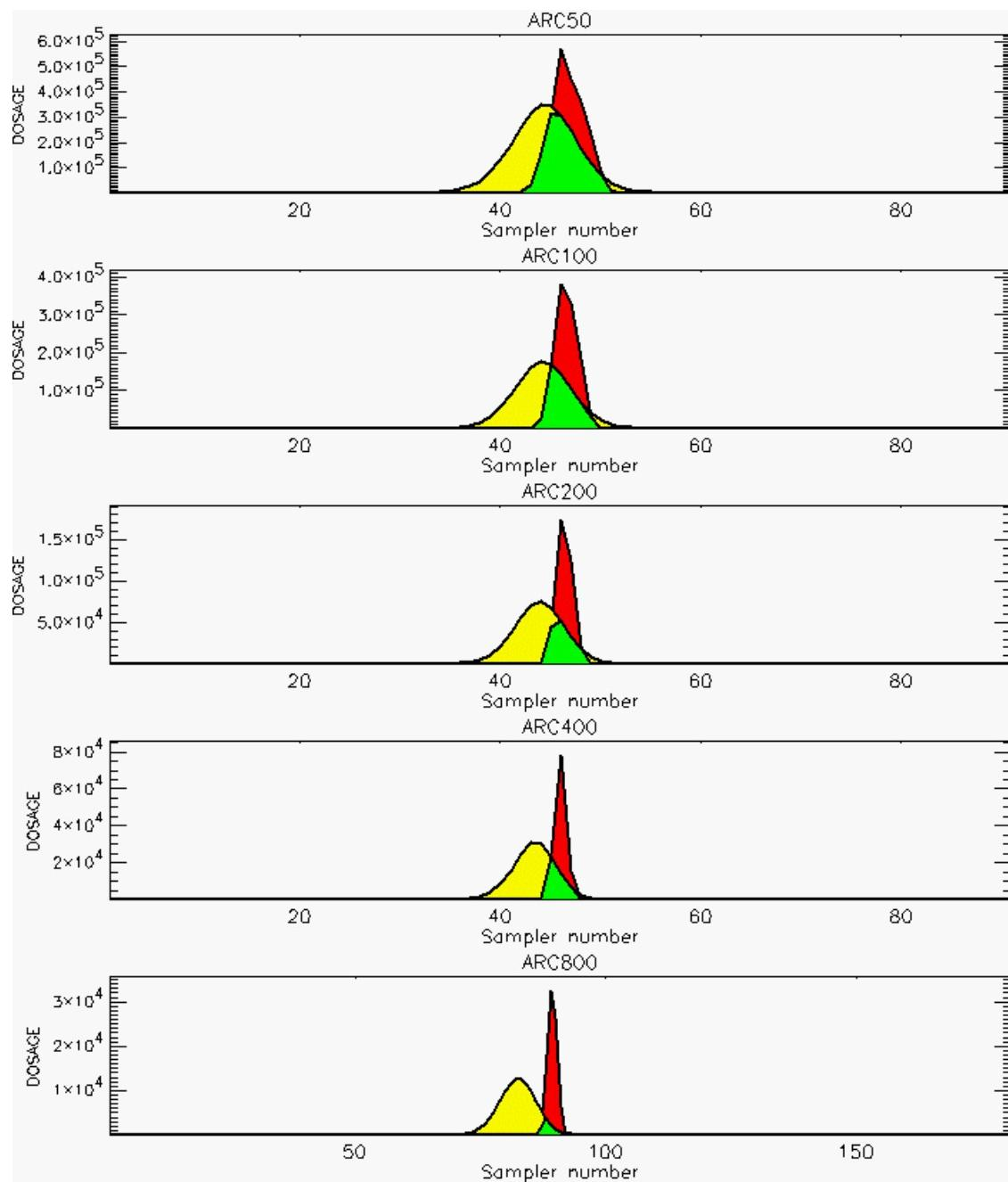


PG Observation to Prediction Comparison

PG Trial File: pr_grass_tracer_Experiment_57.txt

Prediction File: ARAC\nodeposition\pg_57_noxd.arac

**Figure D-46b. NARAC Prediction to Trial 57 on Logarithmic Scale: Stability Category is 3
(Values for Sampler of 100-Meter Arc are Replaced by Missing Values [Ref. D-2])**

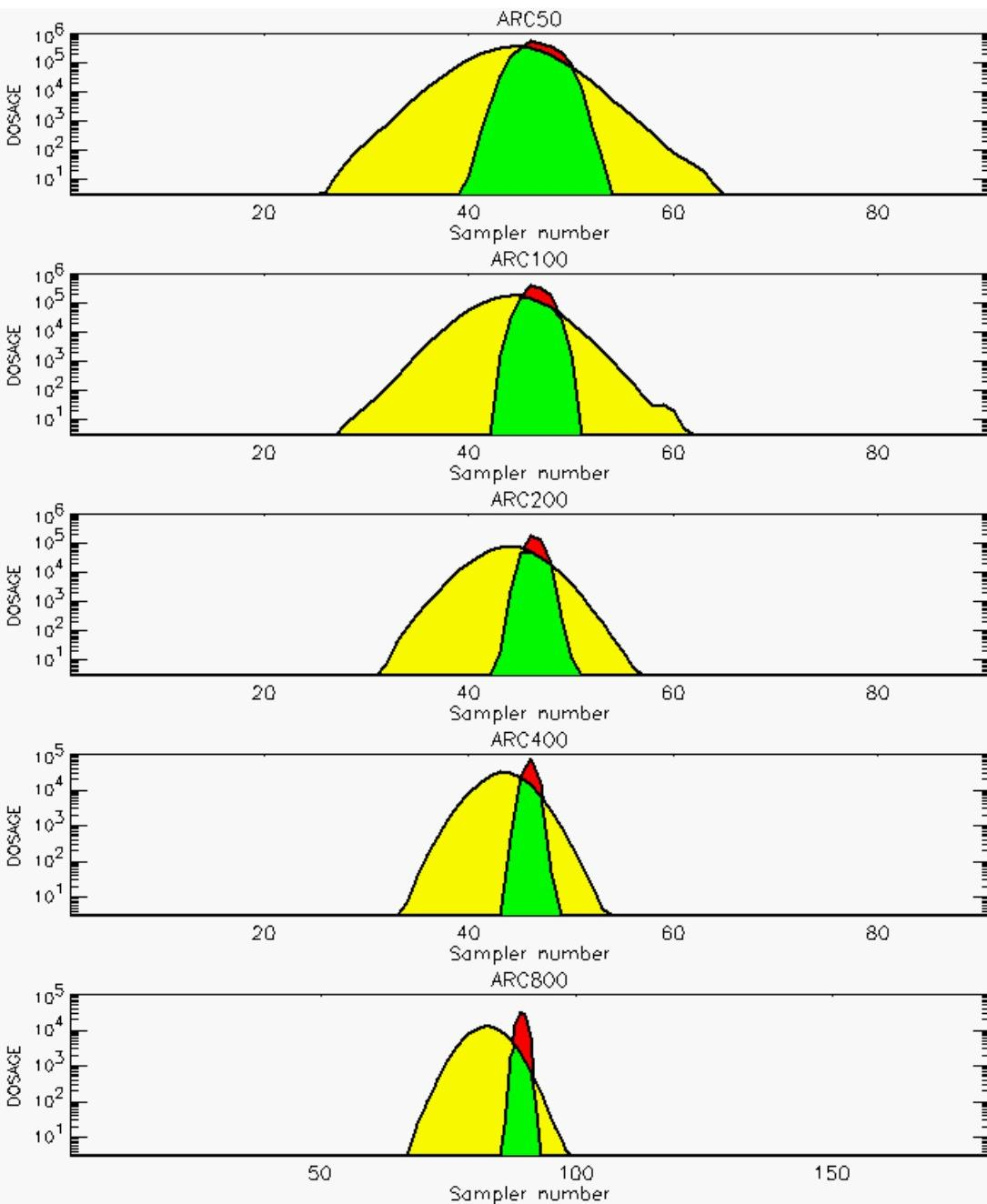


PG Observation to Prediction Comparison

PG Trial File: pr_grass_tracer_Experiment_58.txt

Prediction File: ARAC\nodeposition\pg_58_noxd.arac

Figure D-47a. NARAC Prediction to Trial 58 on Linear Scale: Stability Category is 6

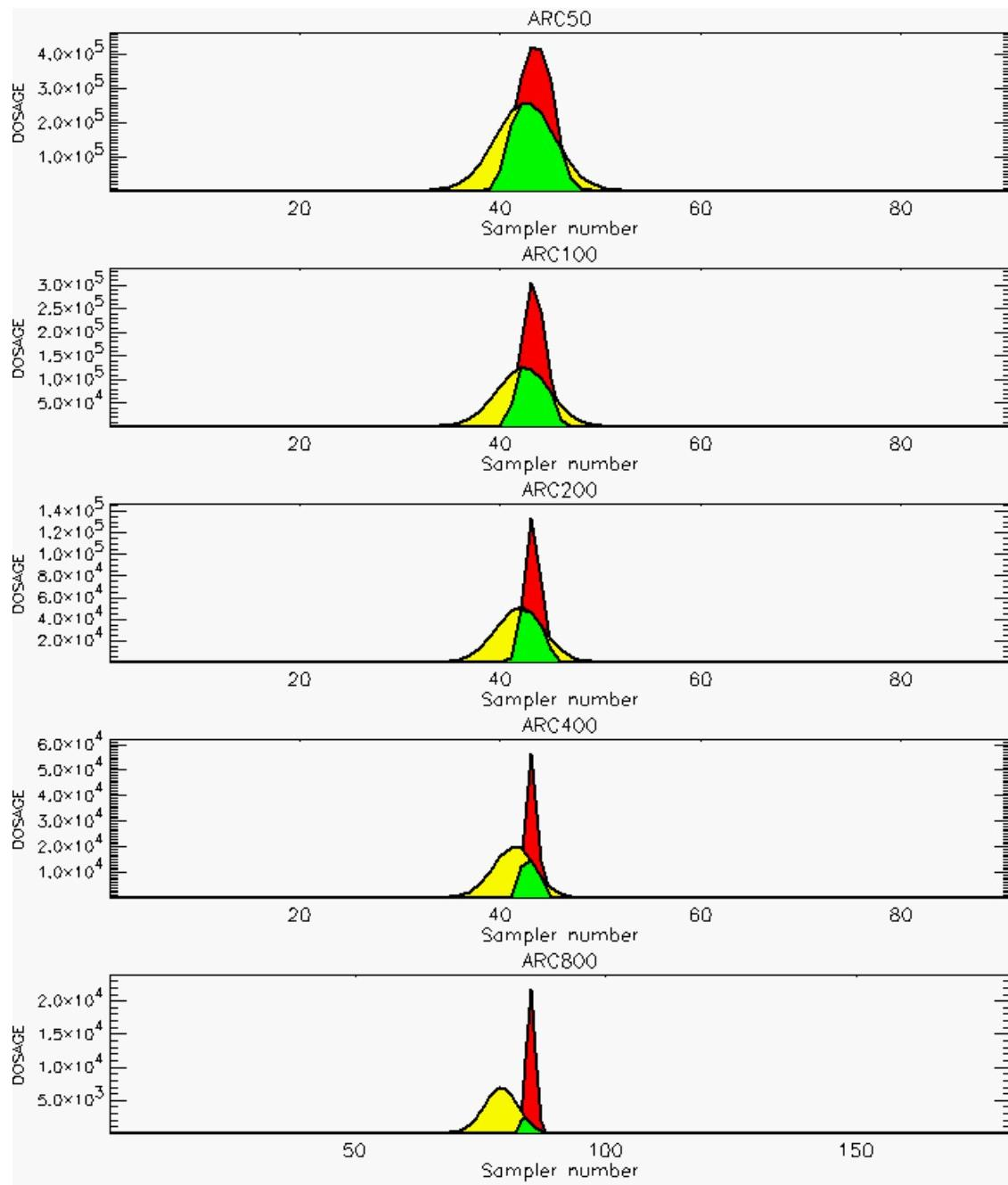


PG Observation to Prediction Comparison

PG Trial File: pr_grass_tracer_Experiment_58.txt

Prediction File: ARAC\nodeposition\pg_58_noxd.arac

Figure D-47b. NARAC Prediction to Trial 58 on Logarithmic Scale: Stability Category is 6

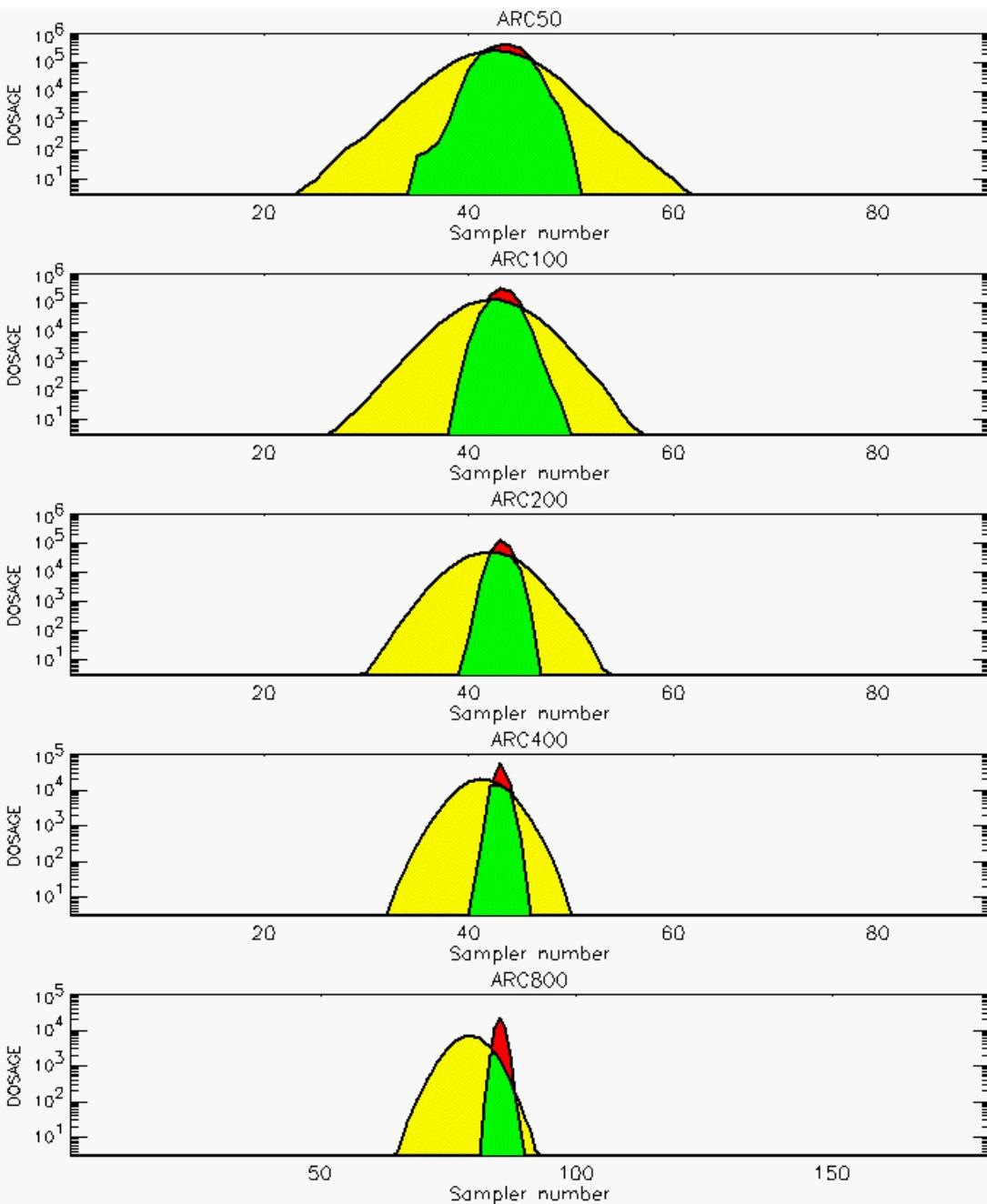


PG Observation to Prediction Comparison

PG Trial File: pr_grass_tracer_Experiment_59.txt

Prediction File: ARAC\nodeposition\pg_59_noxd.arac

Figure D-48a. NARAC Prediction to Trial 59 on Linear Scale: Stability Category is 5

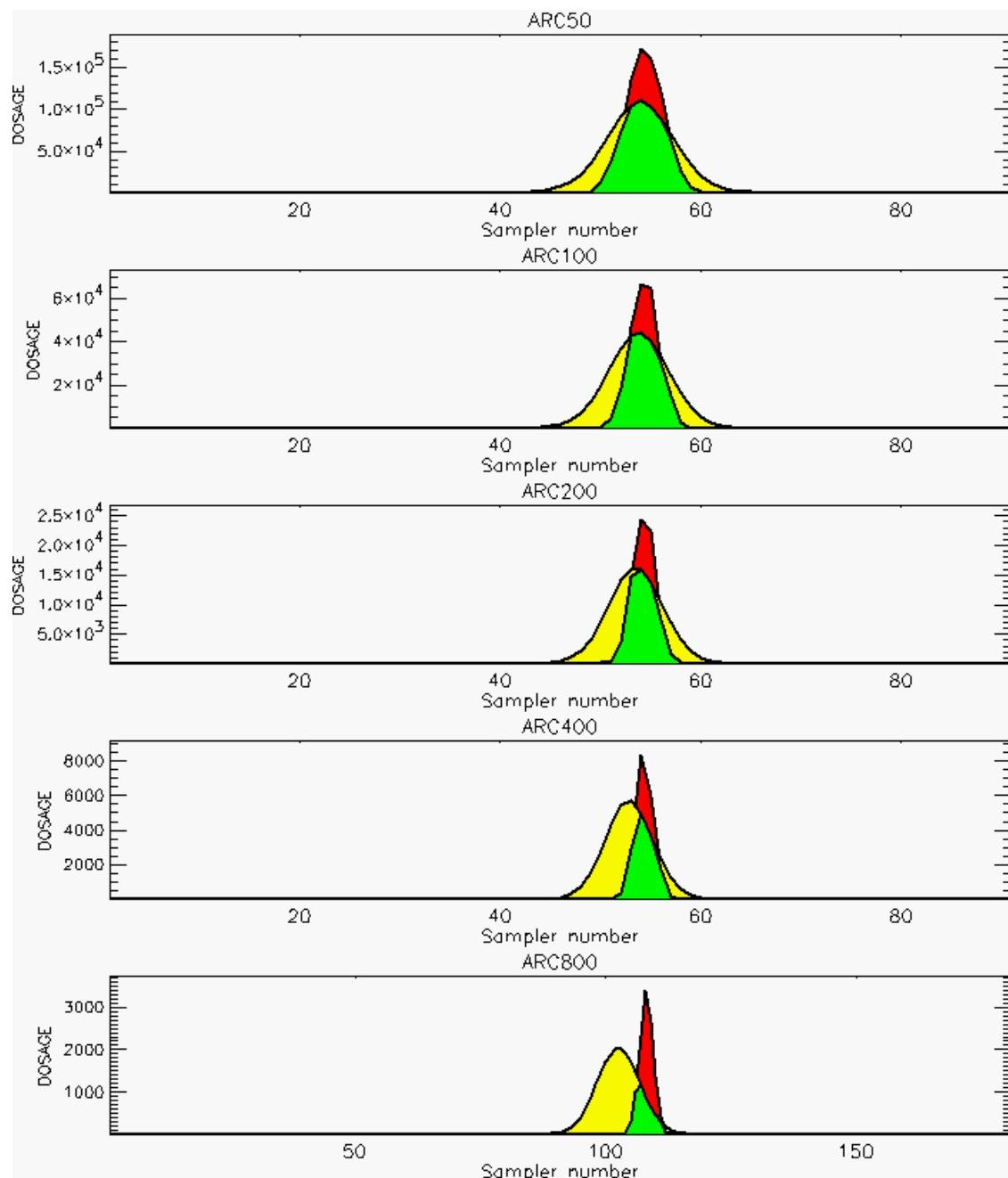


PG Observation to Prediction Comparison

PG Trial File: pr_grass_tracer_Experiment_59.txt

Prediction File: ARAC\nodeposition\pg_59_noxd.arac

Figure D-48b. NARAC Prediction to Trial 59 on Logarithmic Scale: Stability Category is 5

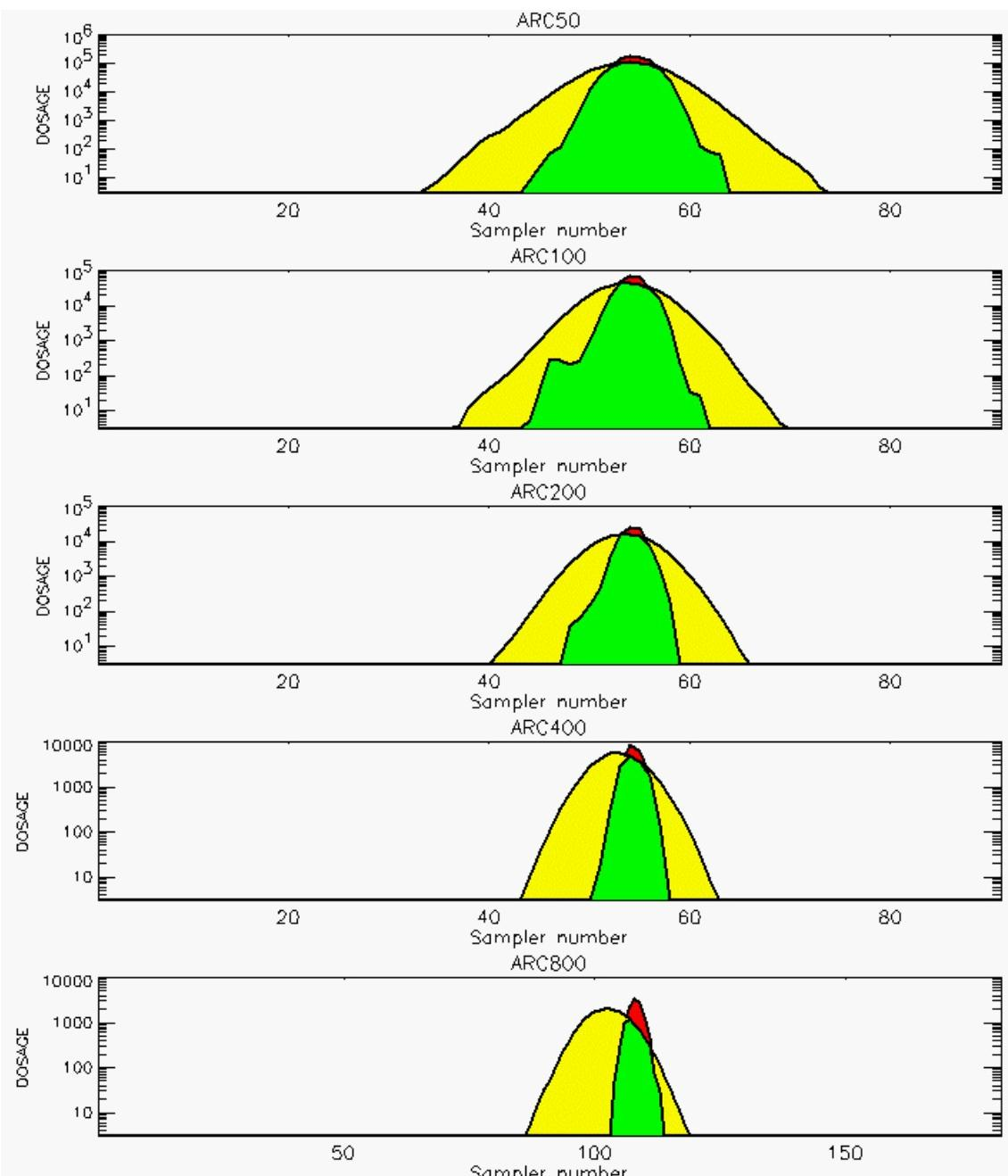


PG Observation to Prediction Comparison

PG Trial File: pr_grass_tracer_Experiment_60.txt

Prediction File: ARAC\nodeposition\pg_60_noxd.arac

Figure D-49a. NARAC Prediction to Trial 60 on Linear Scale: Stability Category is 5

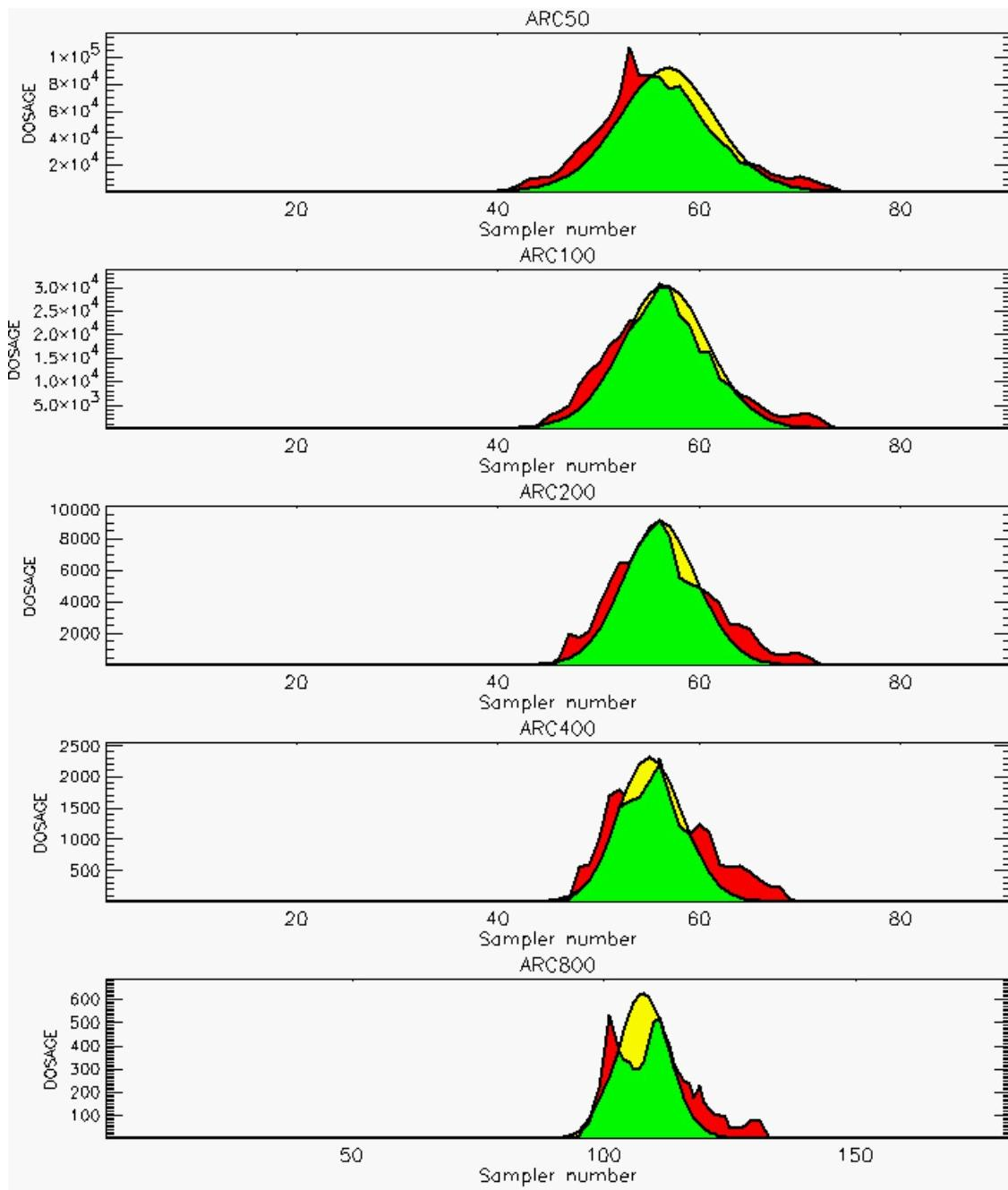


PG Observation to Prediction Comparison

PG Trial File: pr_grass_tracer_Experiment_60.txt

Prediction File: ARAC\nodeposition\pg_60_noxd.arac

Figure D-49b. NARAC Prediction to Trial 60 on Logarithmic Scale: Stability Category is 5

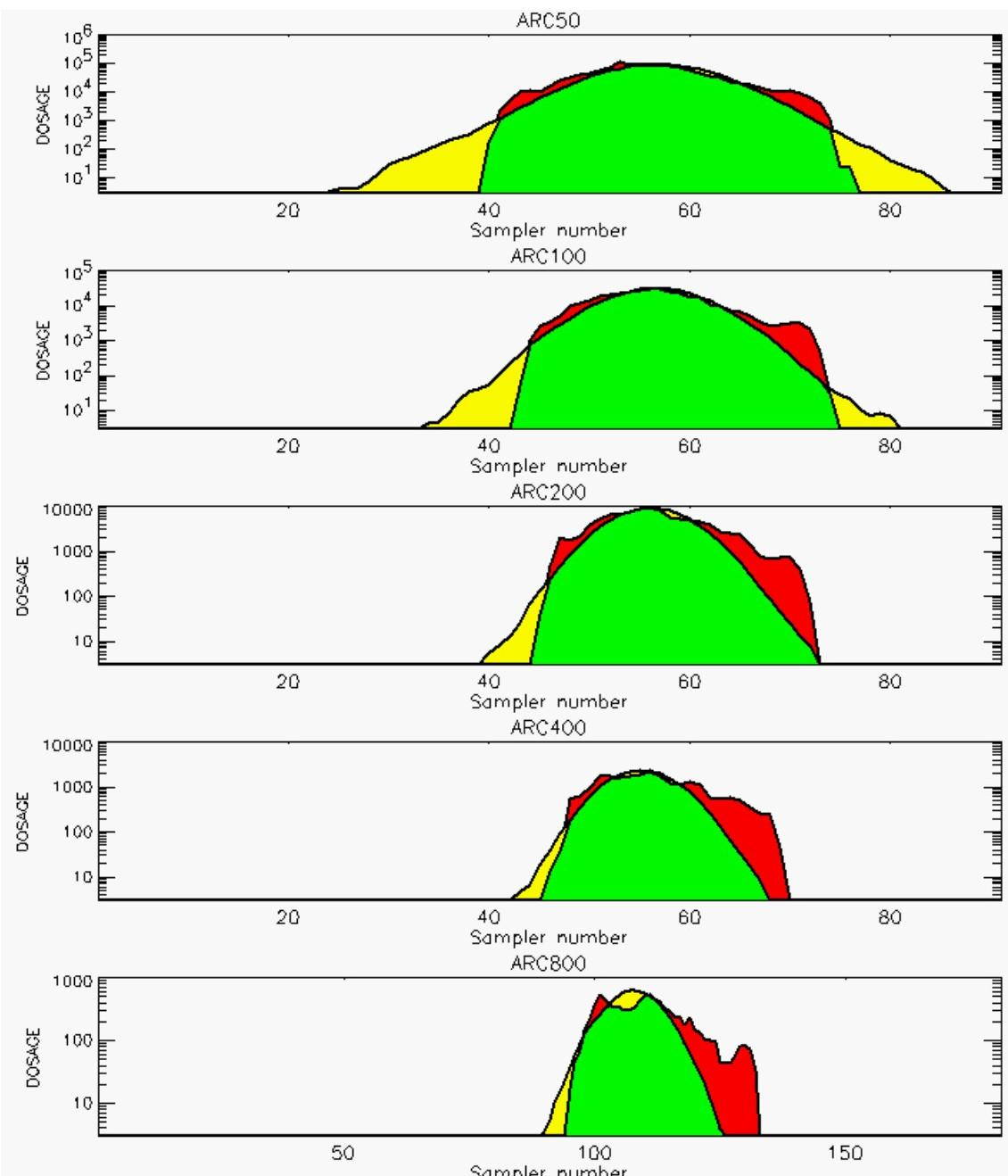


PG Observation to Prediction Comparison

PG Trial File: pr_grass_tracer_Experiment_61.txt

Prediction File: ARAC\nodeposition\pg_61_noxd.arac

Figure D-50a. NARAC Prediction to Trial 61 on Linear Scale: Stability Category is 3

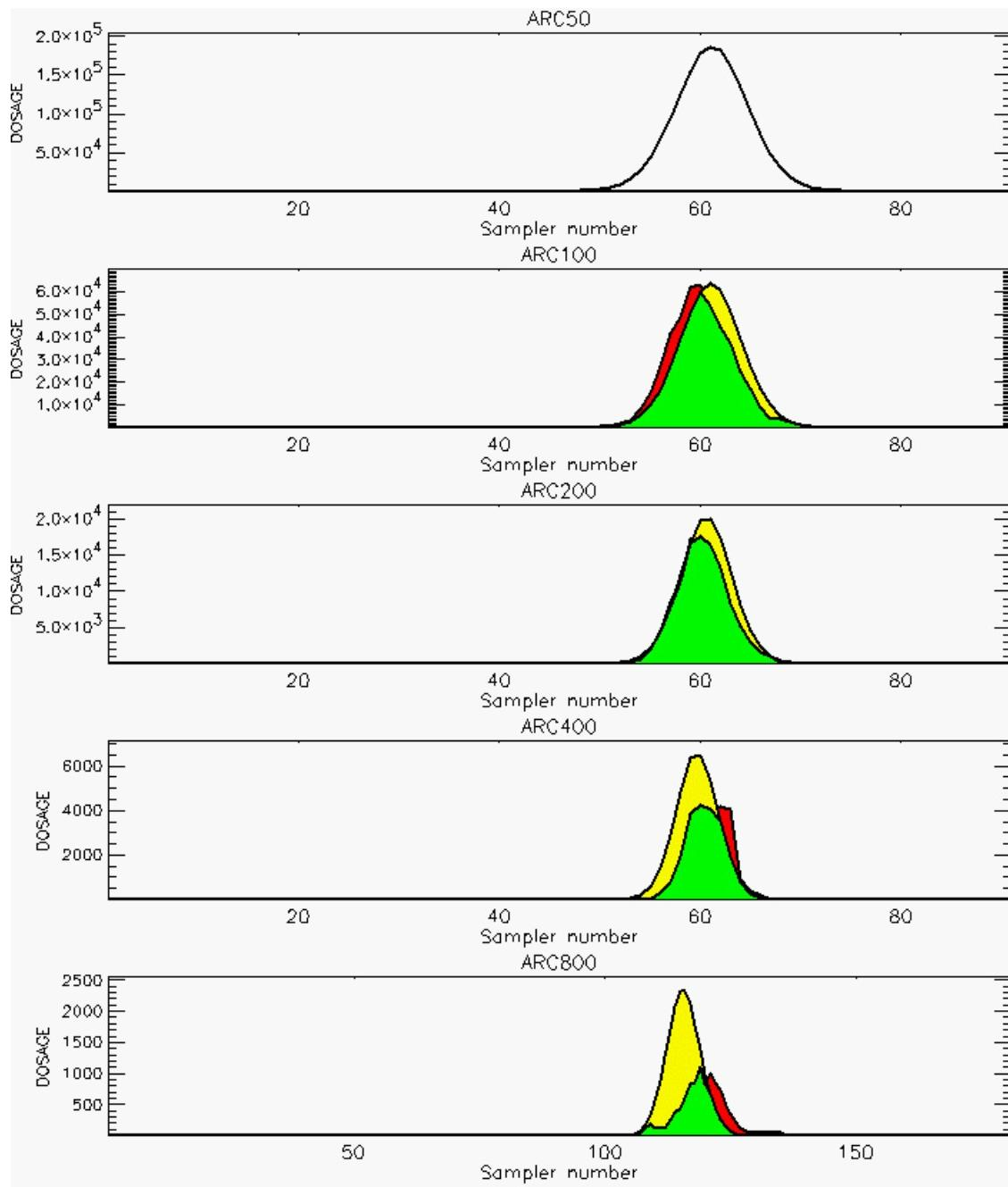


PG Observation to Prediction Comparison

PG Trial File: pr_grass_tracer_Experiment_61.txt

Prediction File: ARAC\nodeposition\pg_61_noxd.arac

Figure D-50b. NARAC Prediction to Trial 61 on Logarithmic Scale: Stability Category is 3

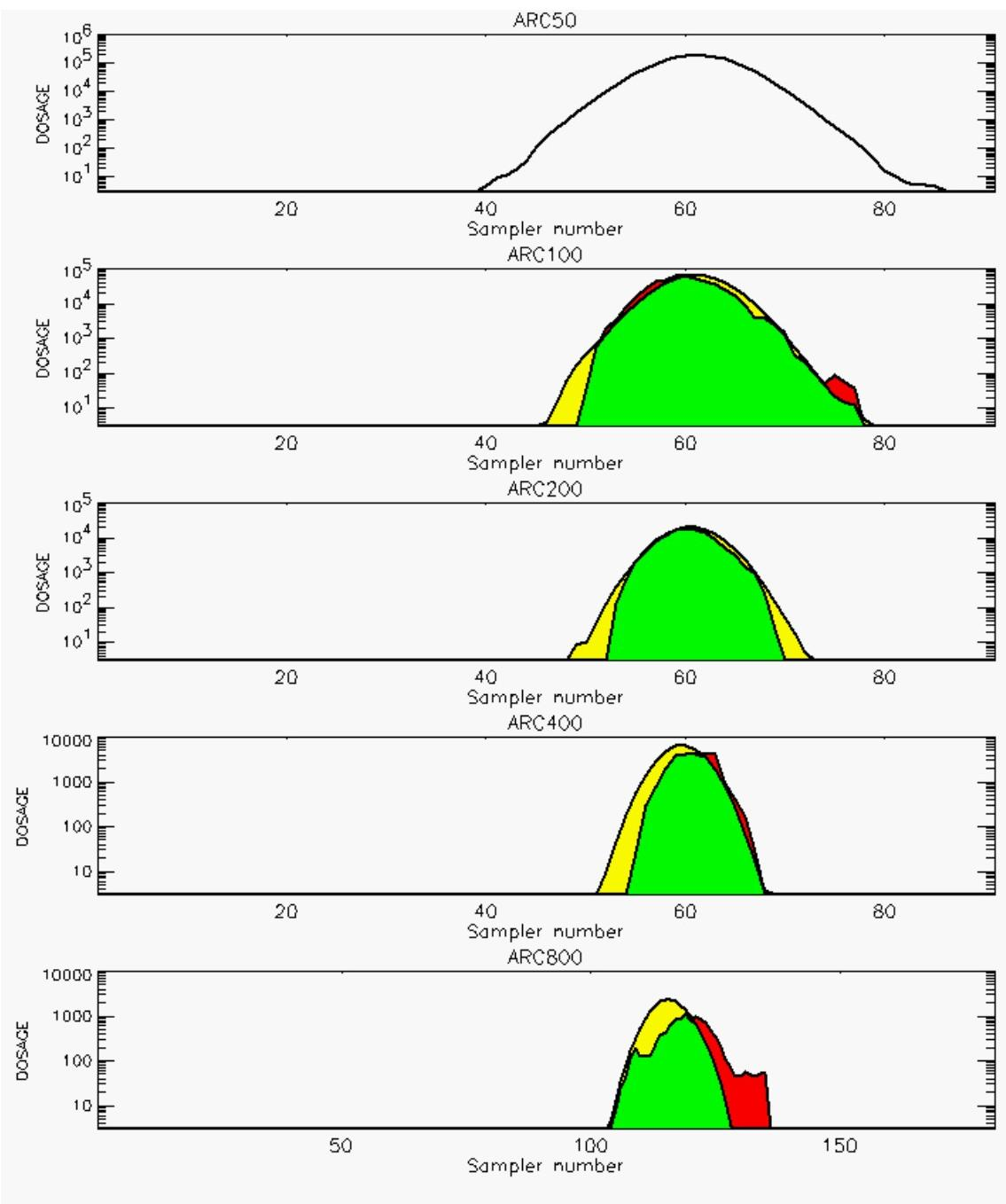


PG Observation to Prediction Comparison

PG Trial File: pr_grass_tracer_Experiment_62.txt

Prediction File: ARAC\nodeposition\pg_62_noxd.arac

**Figure D-51a. NARAC Prediction to Trial 62 on Linear Scale: Stability Category is 2
(Values for Samplers of 50-Meter Arc are Replaced by Missing Values [Ref. D-2])**



PG Observation to Prediction Comparison

PG Trial File: pr_grass_tracer_Experiment_62.txt

Prediction File: ARAC\nodeposition\pg_62_noxd.arac

Figure D-51b. NARAC Prediction to Trial 62 on Logarithmic Scale: Stability Category is 2 (Values for Samplers of 50-Meter Arc are Replaced by Missing Values [Ref. D-2])

REFERENCES

- D-1. Barad, M. L. (Editor), *Project Prairie Grass, A Field Program in Diffusion*, Geophysical Research Papers No. 59, Volumes I and II, DTIC #AD-152572/AFCRC-TR-58-235(I), Air Geophysical Laboratory, Hanscom Air Force Base, MA, 1958.
- D-2. Barad, M. L. (Editor), *Project Prairie Grass, a Field Program in Diffusion*, Geophysical Research Papers, No. 59, Volume I, DTIC #AD-152572/AFCRC-TR-58-235(I), pages 79-80, 201, 1958.
- D-3. Irwin, J. S. and Rosu, M-R., *Comments on a Draft Practice for Statistical Evaluation of Atmospheric Dispersion Models*, Proceedings of the 10th Joint Conference on the Applications of Air Pollution Meteorology. American Meteorological Society, Boston, pp. 6-10, 1998.

APPENDIX E
COMPARISONS OF HPAC AND NARAC PREDICTIONS

APPENDIX E

COMPARISONS OF HPAC AND NARAC PREDICTIONS

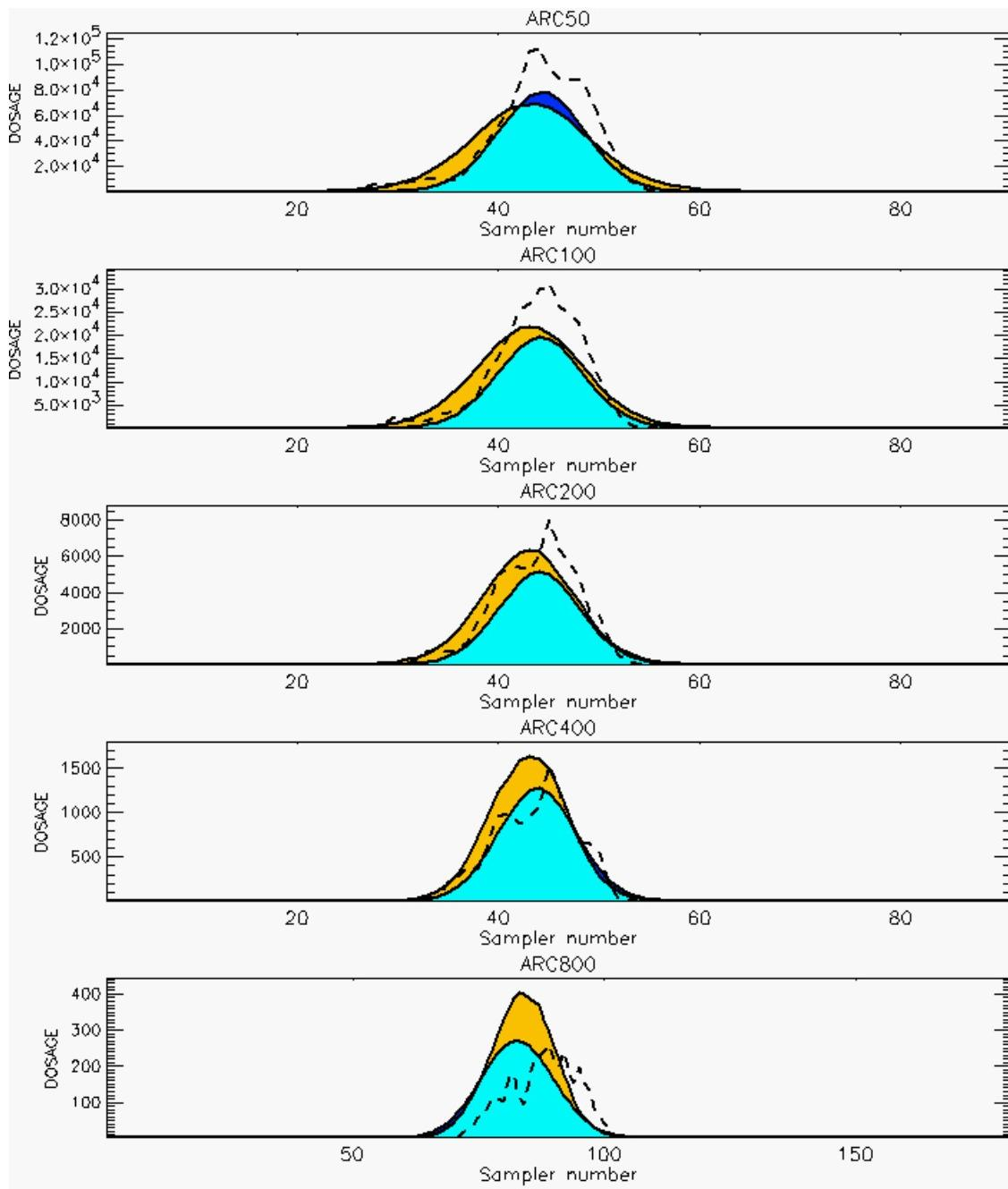
This appendix presents graphical comparison of HPAC and NARAC predictions with no SO₂ surface deposition. Vertical plot units are dosage units of mg-sec/m³. The horizontal plot units are sampler numbers as presented in the *Prairie Grass* field trials [Ref. E-1]. Sampler number 1 is oriented to the west, the middle sampler (45 or 90) is oriented to the north, and the last sampler (91 or 181) is oriented to the east of the SO₂ gas release source. Only data values greater than the cutoff threshold of 3 mg-sec/m³ (0.005 mg/m³) are presented. This cutoff threshold value corresponds to a minimum value reported in *Prairie Grass* field trials.

Comparisons of HPAC and NARAC predictions are presented on both linear and logarithmic dosage scales. Each graphical comparison consists of five plots (one for each arc) with the top plot depicting the 50-meter arc, the second plot depicting the 100-meter arc, the third plot depicting the 200-meter arc, and so on. The last panel (just above the figure caption) contains information about the data files used to produce these plots. The *Prairie Grass* field trial file name contains a two-digit number corresponding to the trial number. Both HPAC and NARAC prediction file names contain the moniker “nodeposition,” denoting that SO₂ surface deposition was not considered in these predictions, and a one- or two-digit number reflecting the *Prairie Grass* field trial being predicted. Even-numbered pages contain figures on the linear dosage scale while odd-numbered pages contain figures on the logarithmic dosage scale.

The meanings of the colors used in the plots are described below:

- Dark Blue — HPAC dosages that are higher than NARAC dosages
- Turquoise — HPAC dosages that overlap with NARAC dosages
- Brown — NARAC dosages that are higher than HPAC dosages.

The dashed lines depict dosage values actually obtained in the field trial. Irwin stability categories that were used in our analyses are denoted in the figure captions. These stability category assignments are based on Reference E-2.



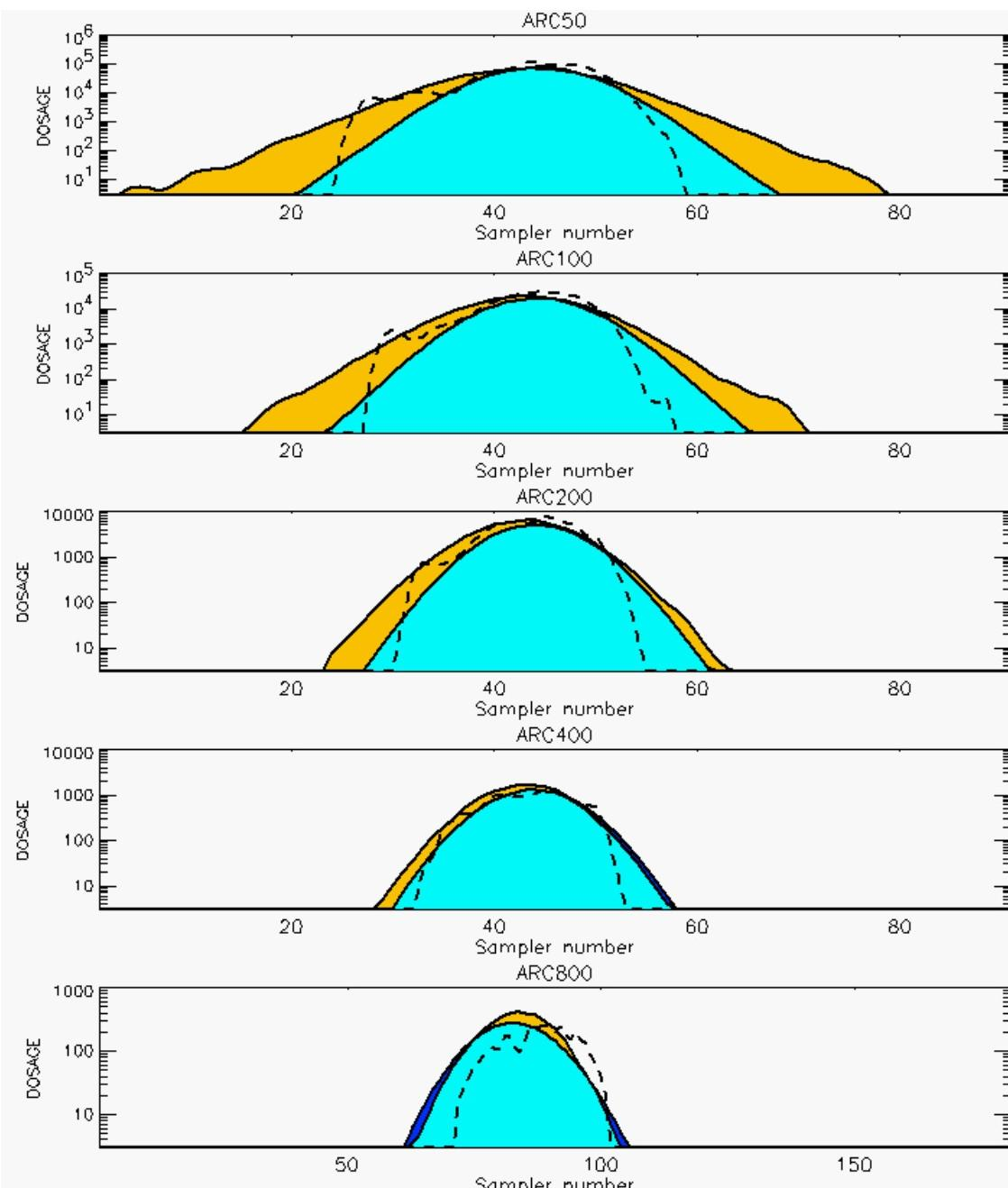
PG Prediction1 to Prediction2 Comparison

PG Trial File: pr_grass_tracer_Experiment_05.txt

PG Prediction File 1: HPAC\nodeposition\pg_5_novd.out

PG Prediction File 2: ARAC\nodeposition\pg_5_novd.arac

**Figure E-1a. HPAC and NARAC Predictions to Trial 5 on Linear Scale:
Stability Category is 2**



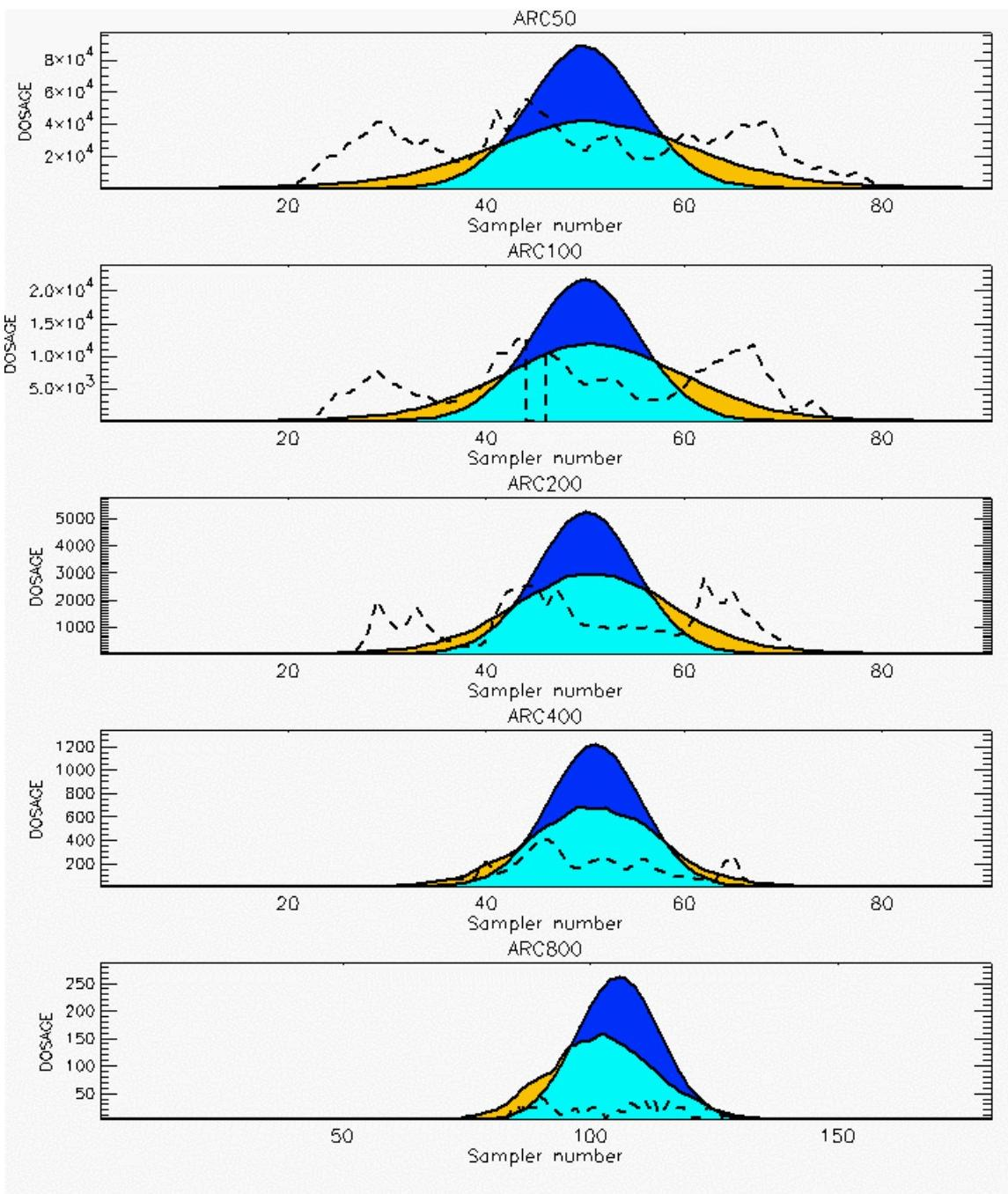
PG Prediction1 to Prediction2 Comparison

PG Trial File: pr_grass_tracer_Experiment_05.txt

PG Prediction File 1: HPAC\nodeposition\pg_5_novd.out

PG Prediction File 2: ARAC\nodeposition\pg_5_novd.arac

**Figure E-1b. HPAC and NARAC Predictions to Trial 5 on Logarithmic Scale:
Stability Category is 2**



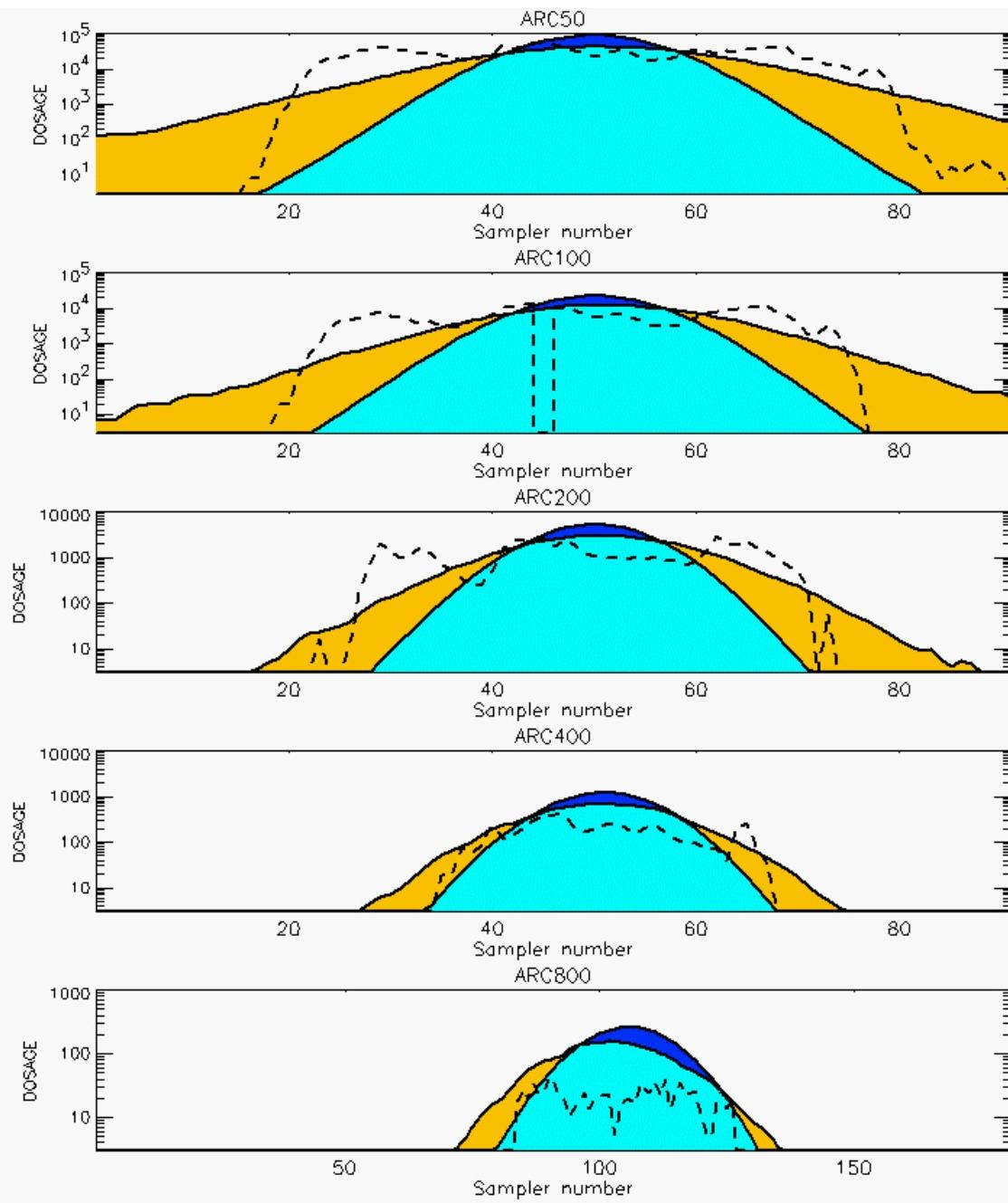
PG Prediction1 to Prediction2 Comparison

PG Trial File: pr_grass_tracer_Experiment_07.txt

PG Prediction File 1: HPAC\nodeposition\pg_7_nozd.out

PG Prediction File 2: ARAC\nodeposition\pg_7_nozd.arac

**Figure E-2a. HPAC and NARAC Predictions to Trial 7 on Linear Scale:
Stability Category is 1**



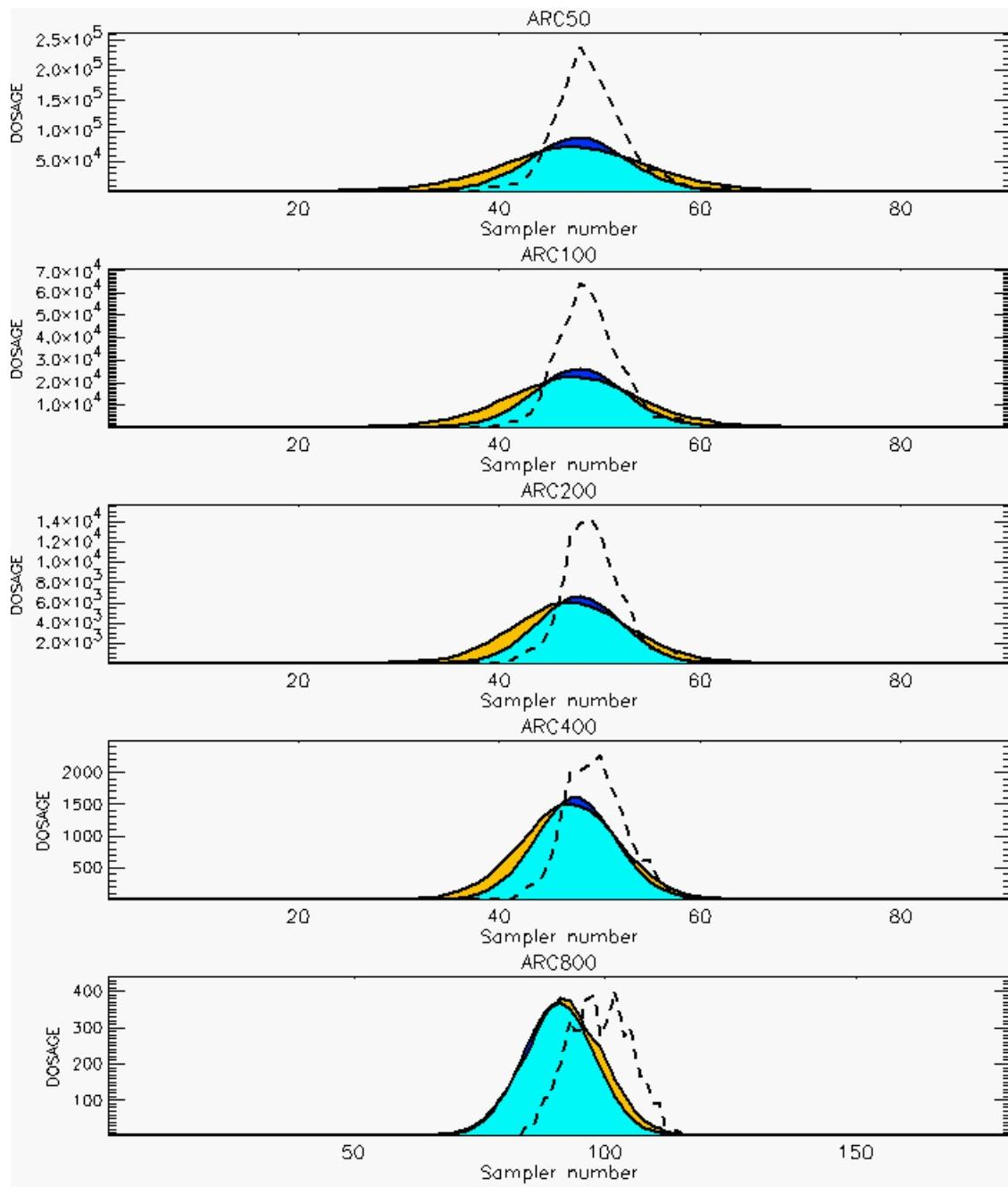
PG Prediction1 to Prediction2 Comparison

PG Trial File: pr_grass_tracer_Experiment_07.txt

PG Prediction File 1: HPAC\nodeposition\pg_7_novd.out

PG Prediction File 2: ARAC\nodeposition\pg_7_novd.arac

**Figure E-2b. HPAC and NARAC Predictions to Trial 7 on Logarithmic Scale:
Stability Category is 1**



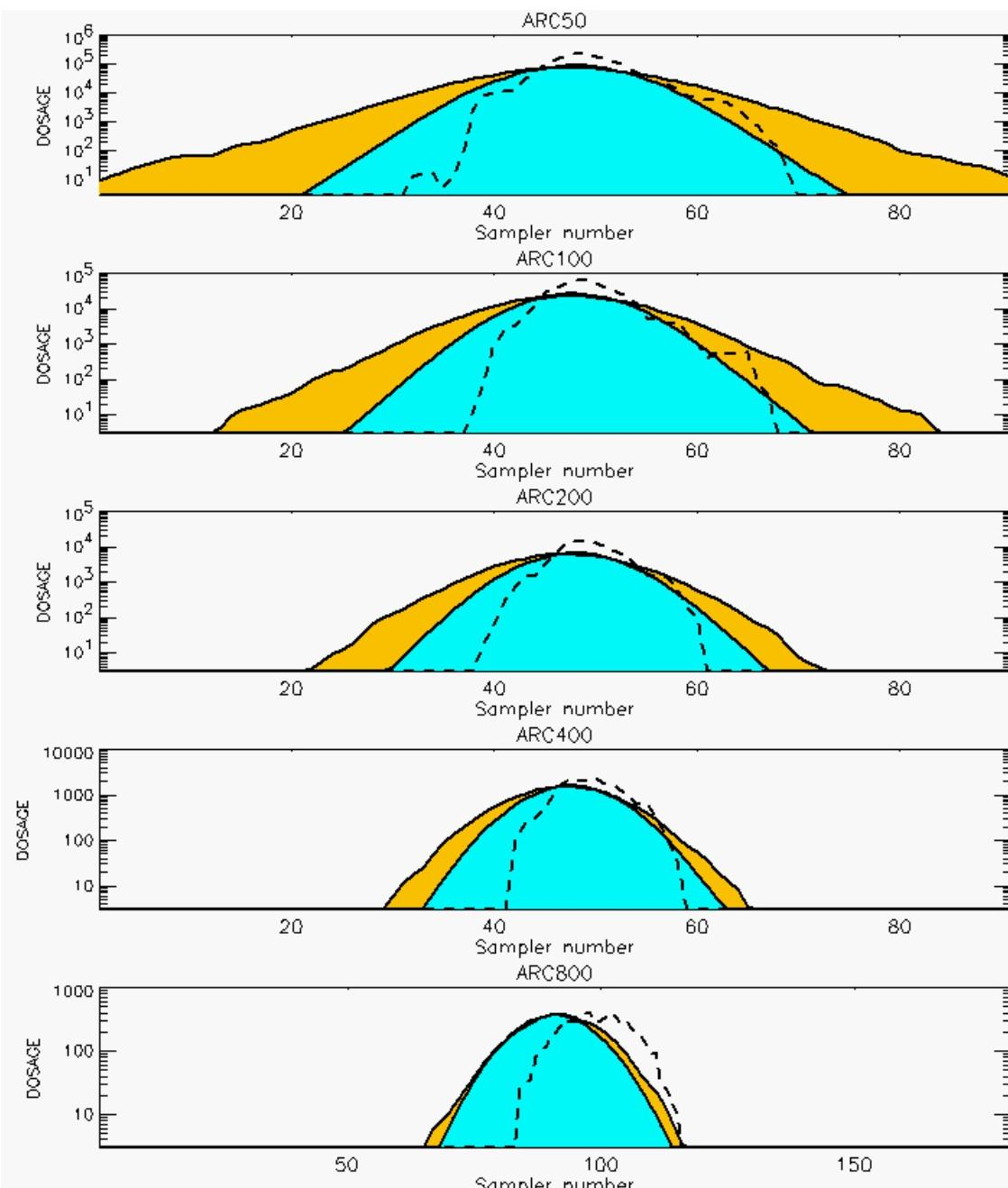
PG Prediction1 to Prediction2 Comparison

PG Trial File: pr_grass_tracer_Experiment_08.txt

PG Prediction File 1: HPAC\nodeposition\pg_8_novd.out

PG Prediction File 2: ARAC\nodeposition\pg_8_novd.arac

**Figure E-3a. HPAC and NARAC Predictions to Trial 8 on Linear Scale:
Stability Category is 2**



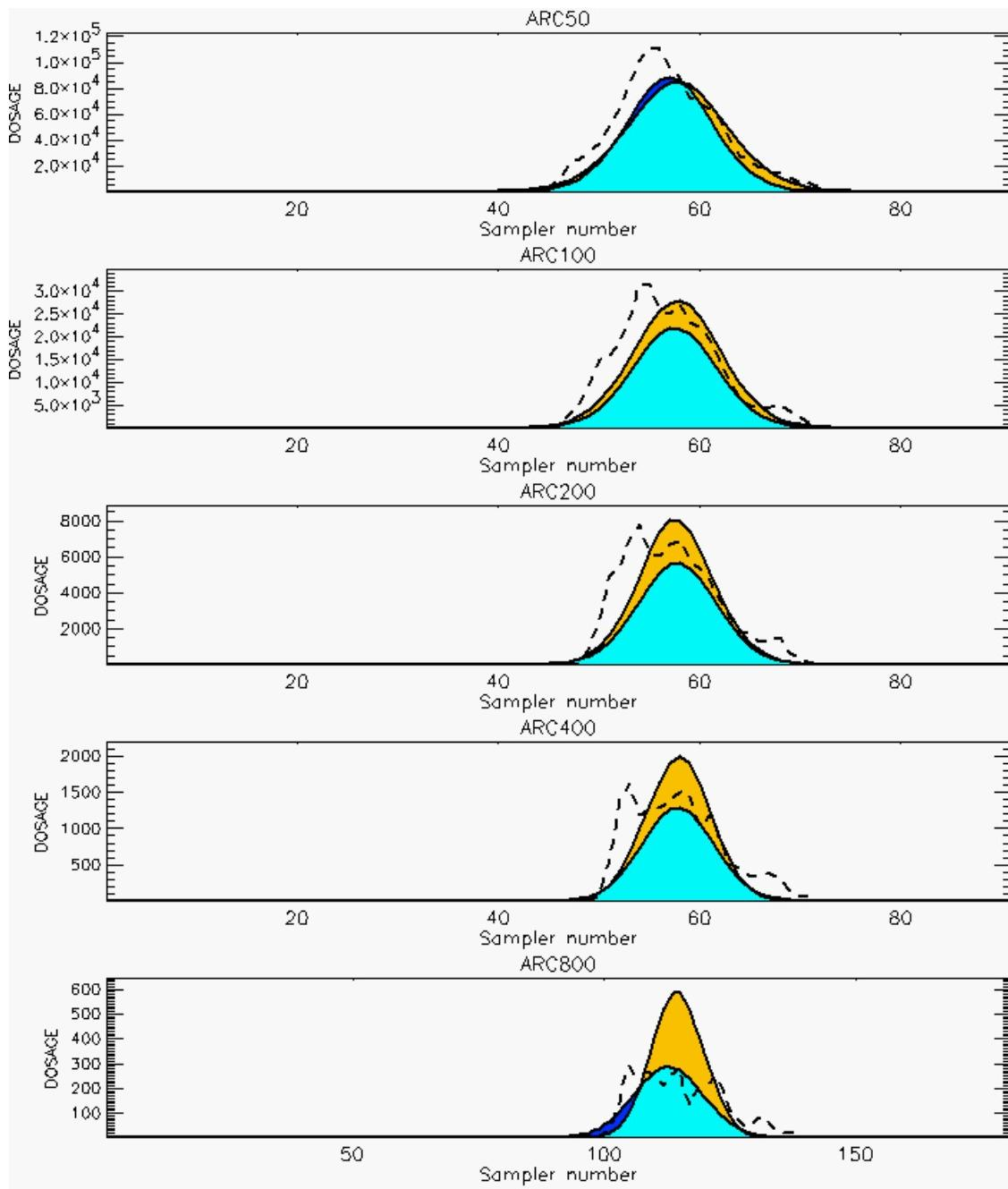
PG Prediction1 to Prediction2 Comparison

PG Trial File: pr_grass_tracer_Experiment_08.txt

PG Prediction File 1: HPAC\nodeposition\pg_8_novd.out

PG Prediction File 2: ARAC\nodeposition\pg_8_novd.arac

**Figure E-3b. HPAC and NARAC Predictions to Trial 8 on Logarithmic Scale:
Stability Category is 2**



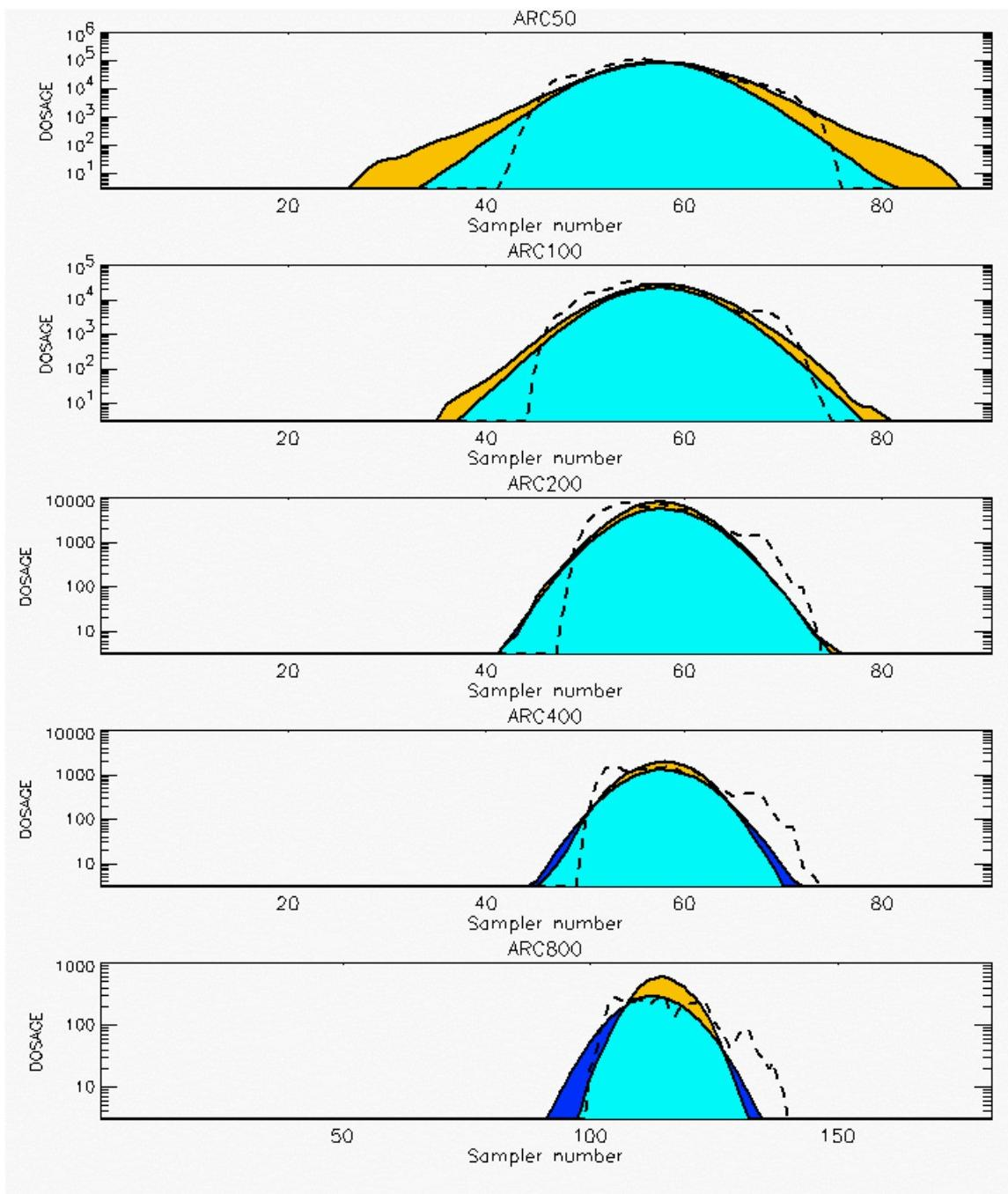
PG Prediction1 to Prediction2 Comparison

PG Trial File: pr_grass_tracer_Experiment_09.txt

PG Prediction File 1: HPAC\nodeposition\pg_9_novd.out

PG Prediction File 2: ARAC\nodeposition\pg_9_novd.arac

**Figure E-4a. HPAC and NARAC Predictions to Trial 9 on Linear Scale:
Stability Category is 2**



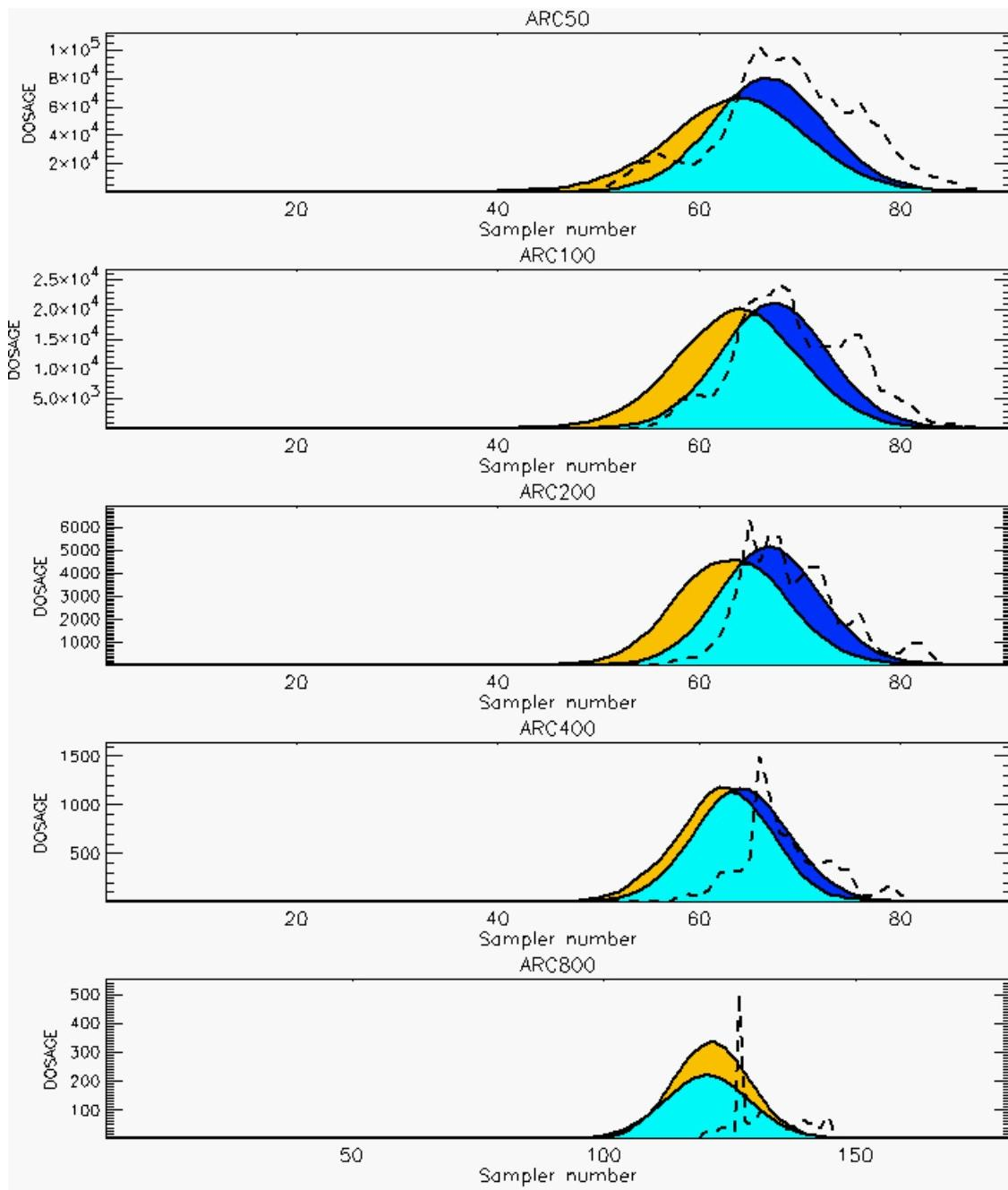
PG Prediction1 to Prediction2 Comparison

PG Trial File: pr_grass_tracer_Experiment_09.txt

PG Prediction File 1: HPAC\nodeposition\pg_9_novd.out

PG Prediction File 2: ARAC\nodeposition\pg_9_novd.arac

**Figure E-4b. HPAC and NARAC Predictions to Trial 9 on Logarithmic Scale:
Stability Category is 2**



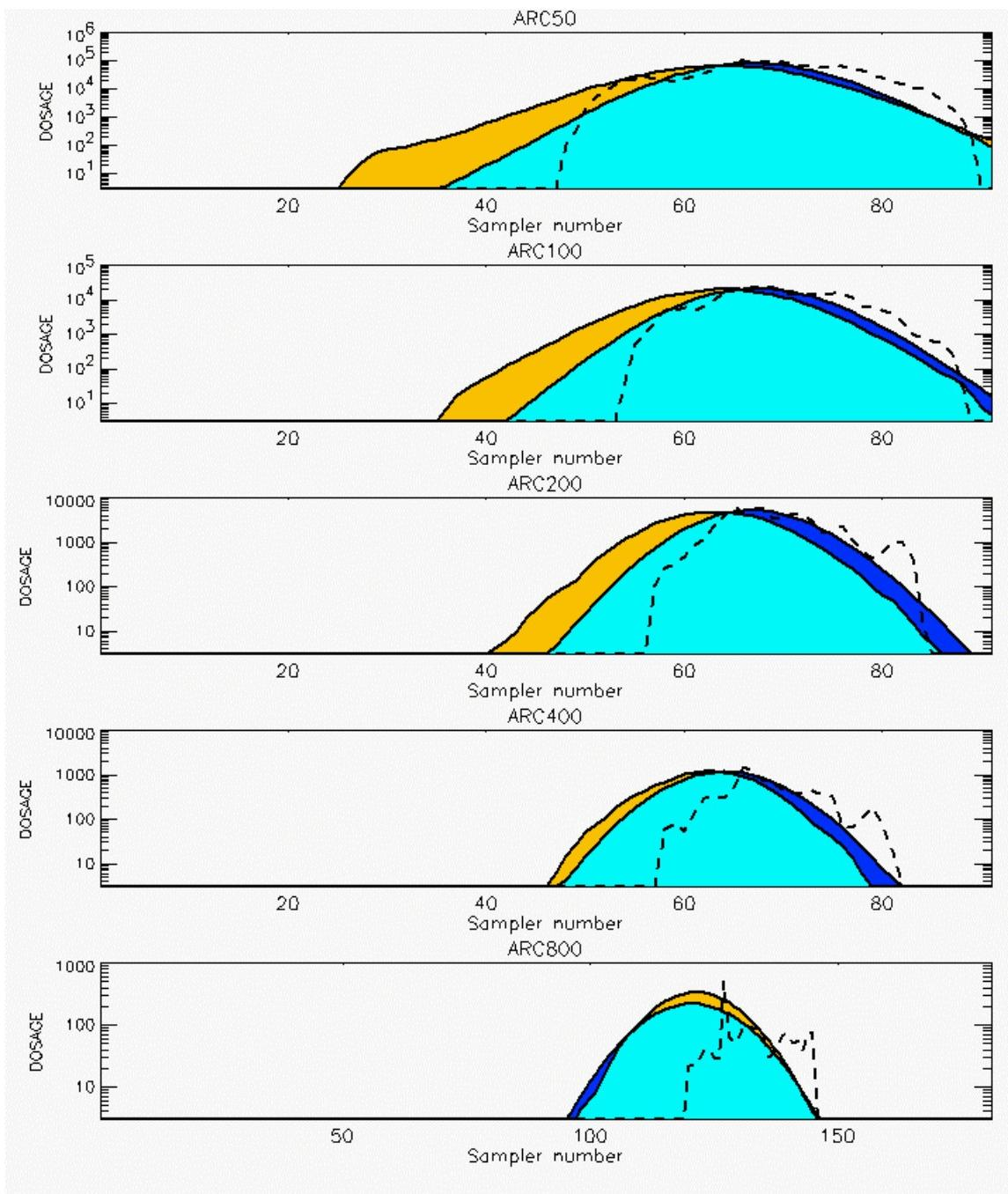
PG Prediction1 to Prediction2 Comparison

PG Trial File: pr_grass_tracer_Experiment_10.txt

PG Prediction File 1: HPAC\nodeposition\pg_10_noxd.out

PG Prediction File 2: ARAC\nodeposition\pg_10_noxd.arac

**Figure E-5a. HPAC and NARAC Predictions to Trial 10 on Linear Scale:
Stability Category is 1**



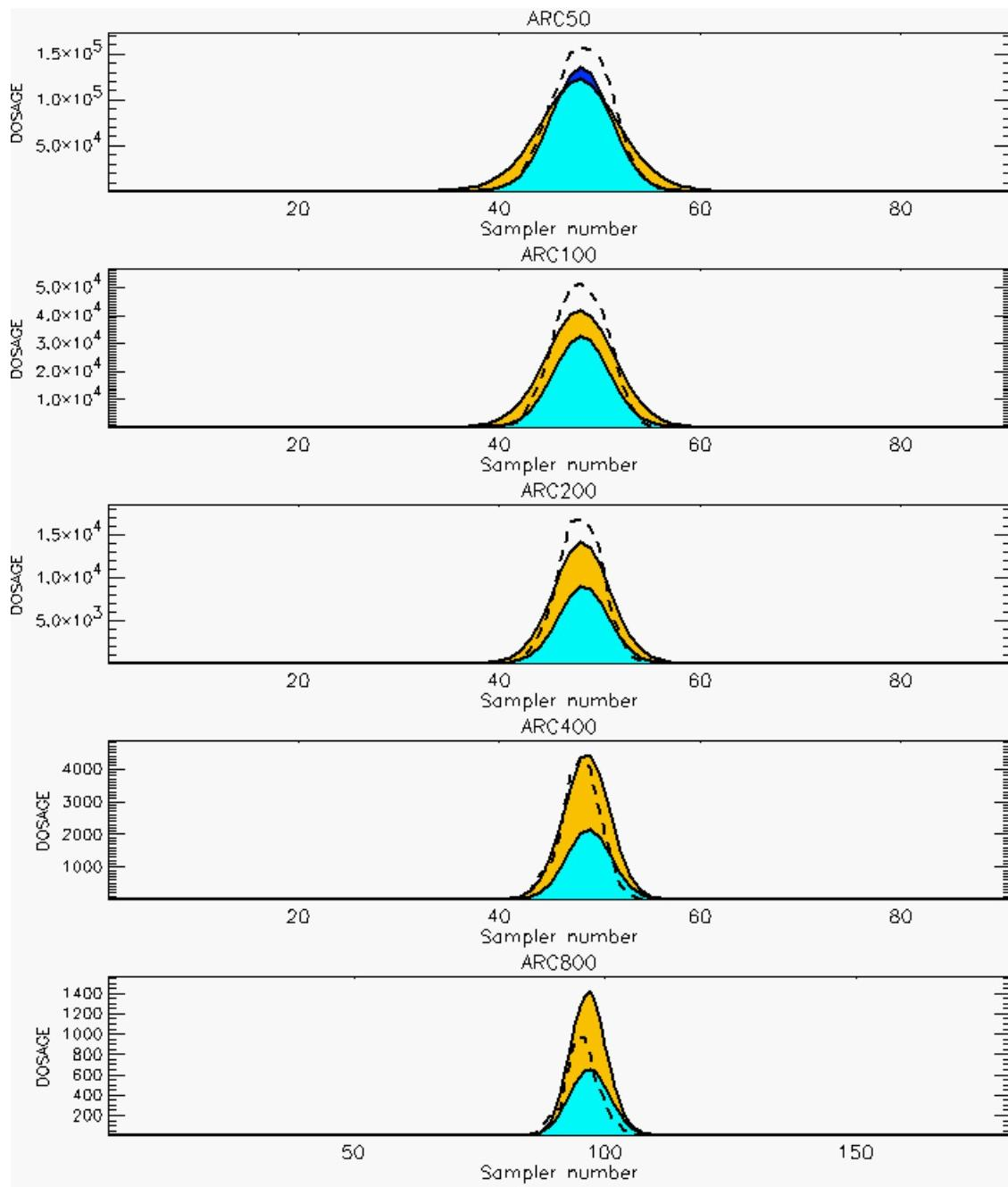
PG Prediction1 to Prediction2 Comparison

PG Trial File: pr_grass_tracer_Experiment_10.txt

PG Prediction File 1: HPAC\nodeposition\pg_10_noxd.out

PG Prediction File 2: ARAC\nodeposition\pg_10_noxd.arac

**Figure E-5b. HPAC and NARAC Predictions to Trial 10 on Logarithmic Scale:
Stability Category is 1**



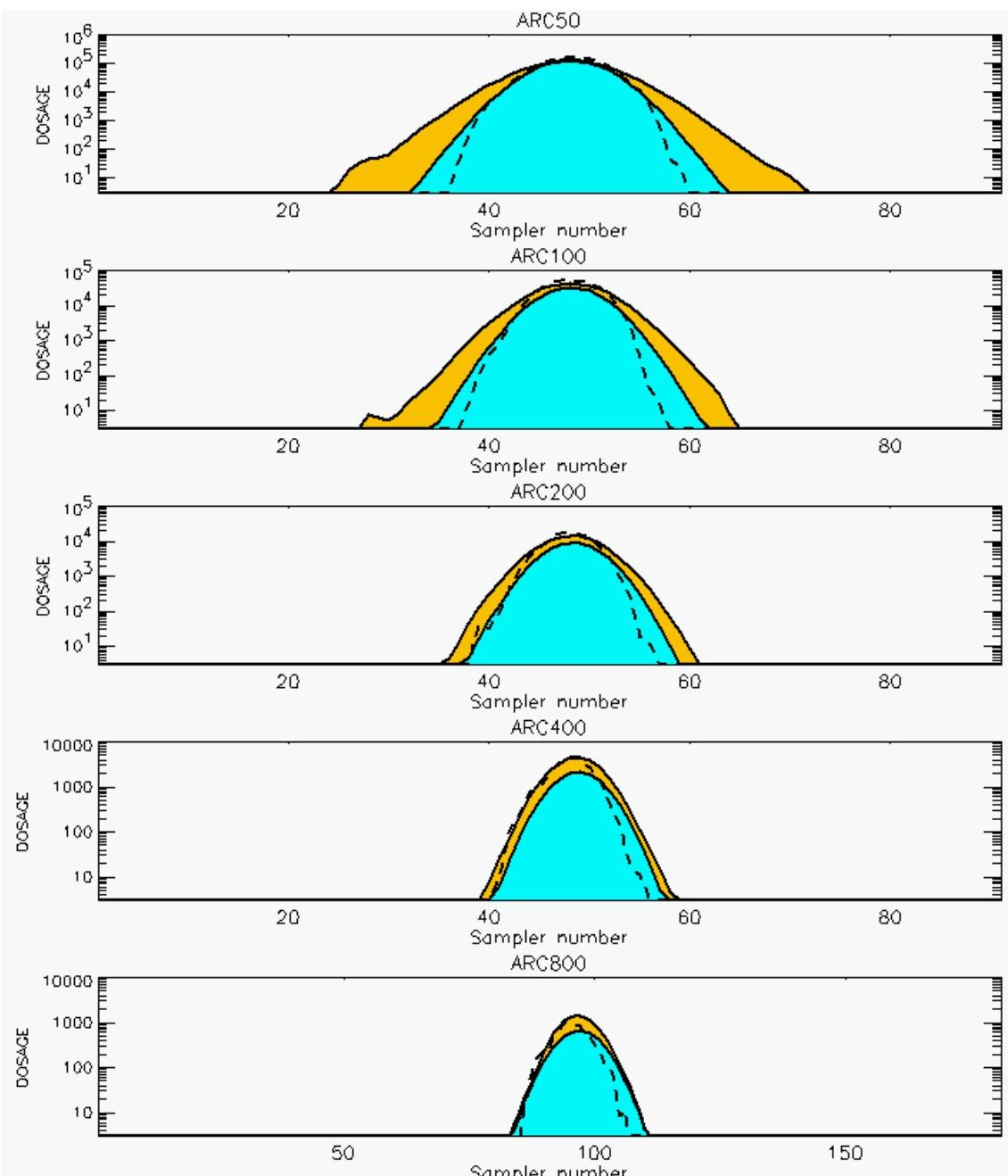
PG Prediction1 to Prediction2 Comparison

PG Trial File: pr_grass_tracer_Experiment_11.txt

PG Prediction File 1: HPAC\nodeposition\pg_11_noxd.out

PG Prediction File 2: ARAC\nodeposition\pg_11_noxd.arac

**Figure E-6a. HPAC and NARAC Predictions to Trial 11 on Linear Scale:
Stability Category is 3**



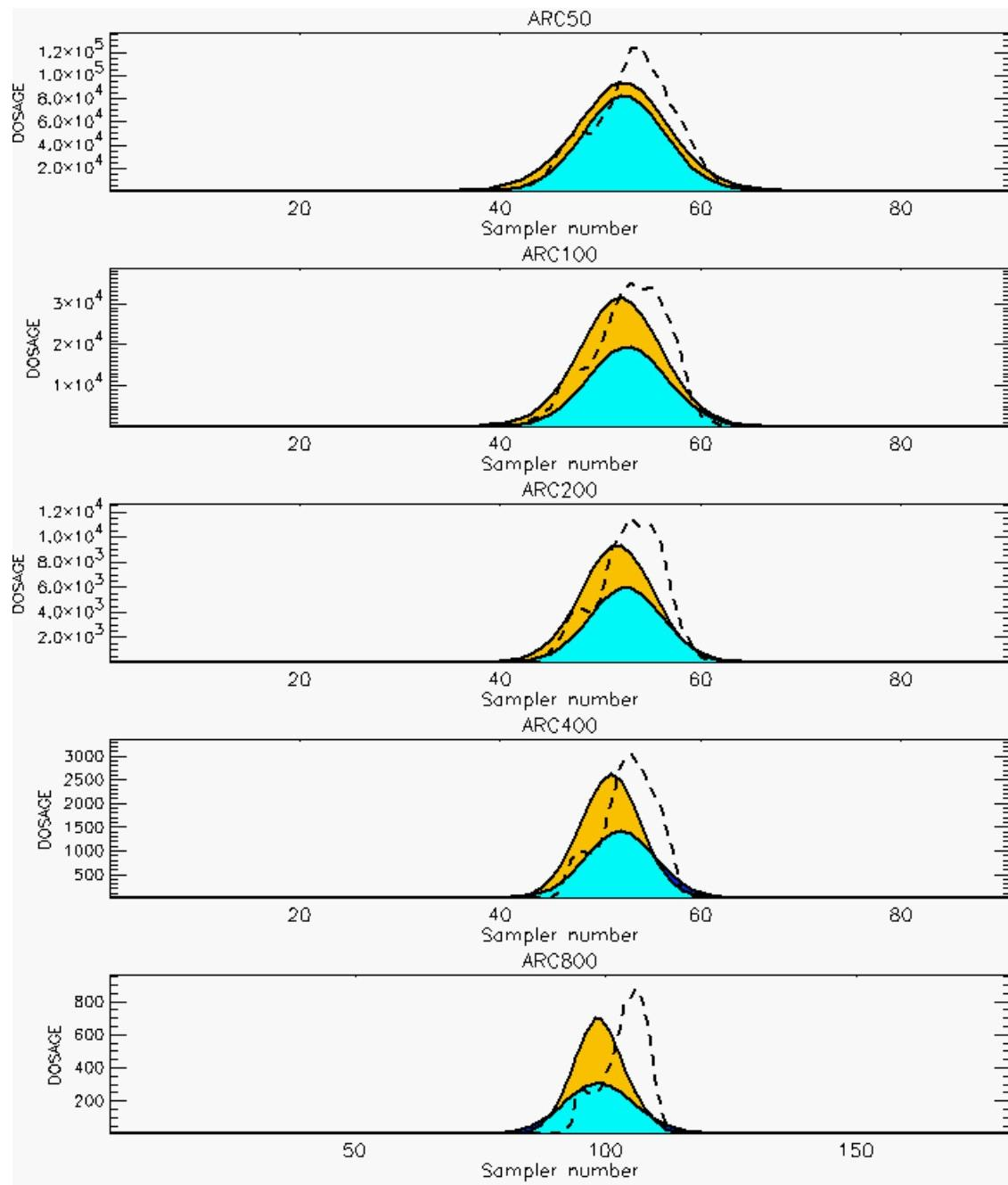
PG Prediction1 to Prediction2 Comparison

PG Trial File: pr_grass_tracer_Experiment_11.txt

PG Prediction File 1: HPAC\nodeposition\pg_11_noxd.out

PG Prediction File 2: ARAC\nodeposition\pg_11_noxd.arac

**Figure E-6b. HPAC and NARAC Predictions to Trial 11 on Logarithmic Scale:
Stability Category is 3**



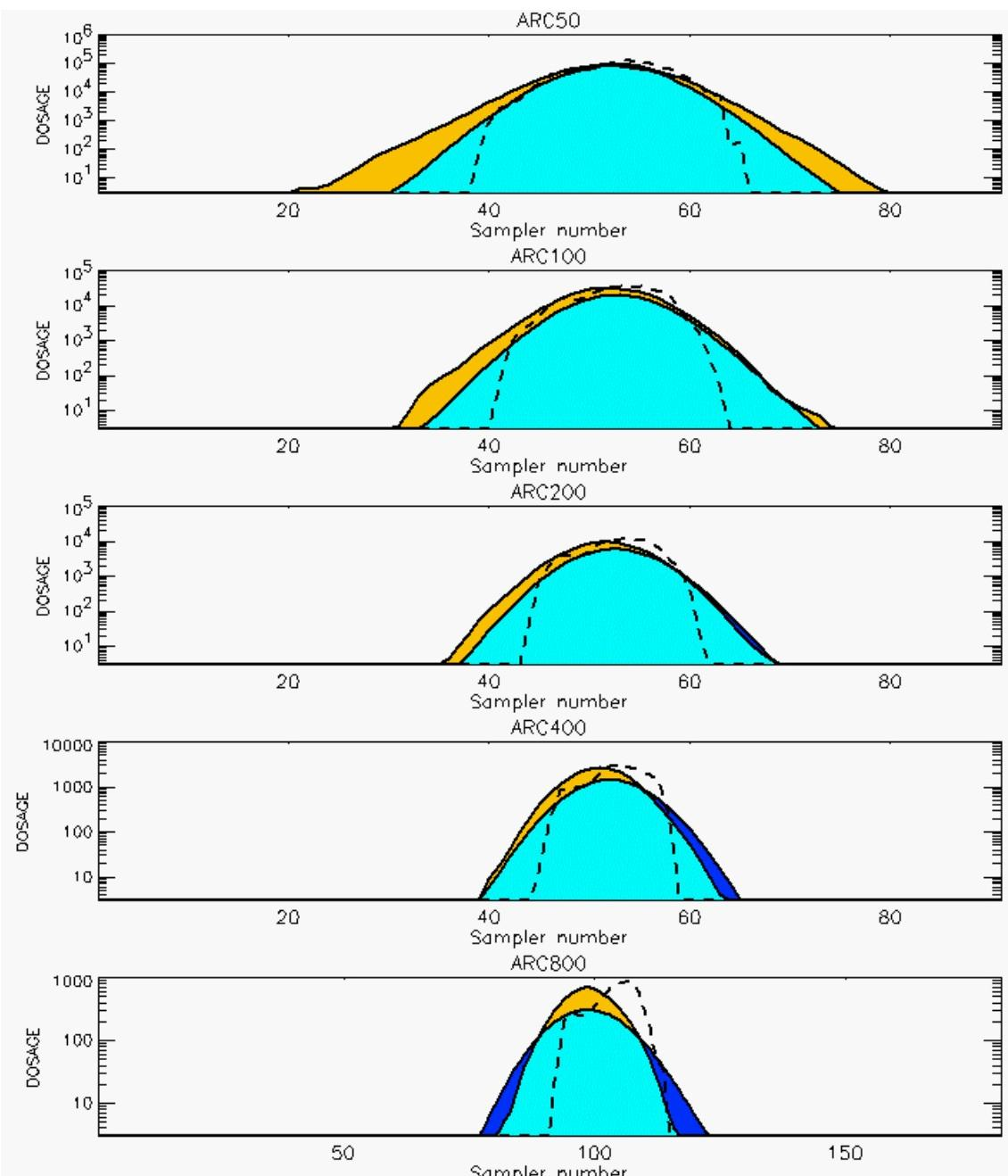
PG Prediction1 to Prediction2 Comparison

PG Trial File: pr_grass_tracer_Experiment_12.txt

PG Prediction File 1: HPAC\nodeposition\pg_12_noxd.out

PG Prediction File 2: ARAC\nodeposition\pg_12_noxd.arac

**Figure E-7a. HPAC and NARAC Predictions to Trial 12 on Linear Scale:
Stability Category is 3**



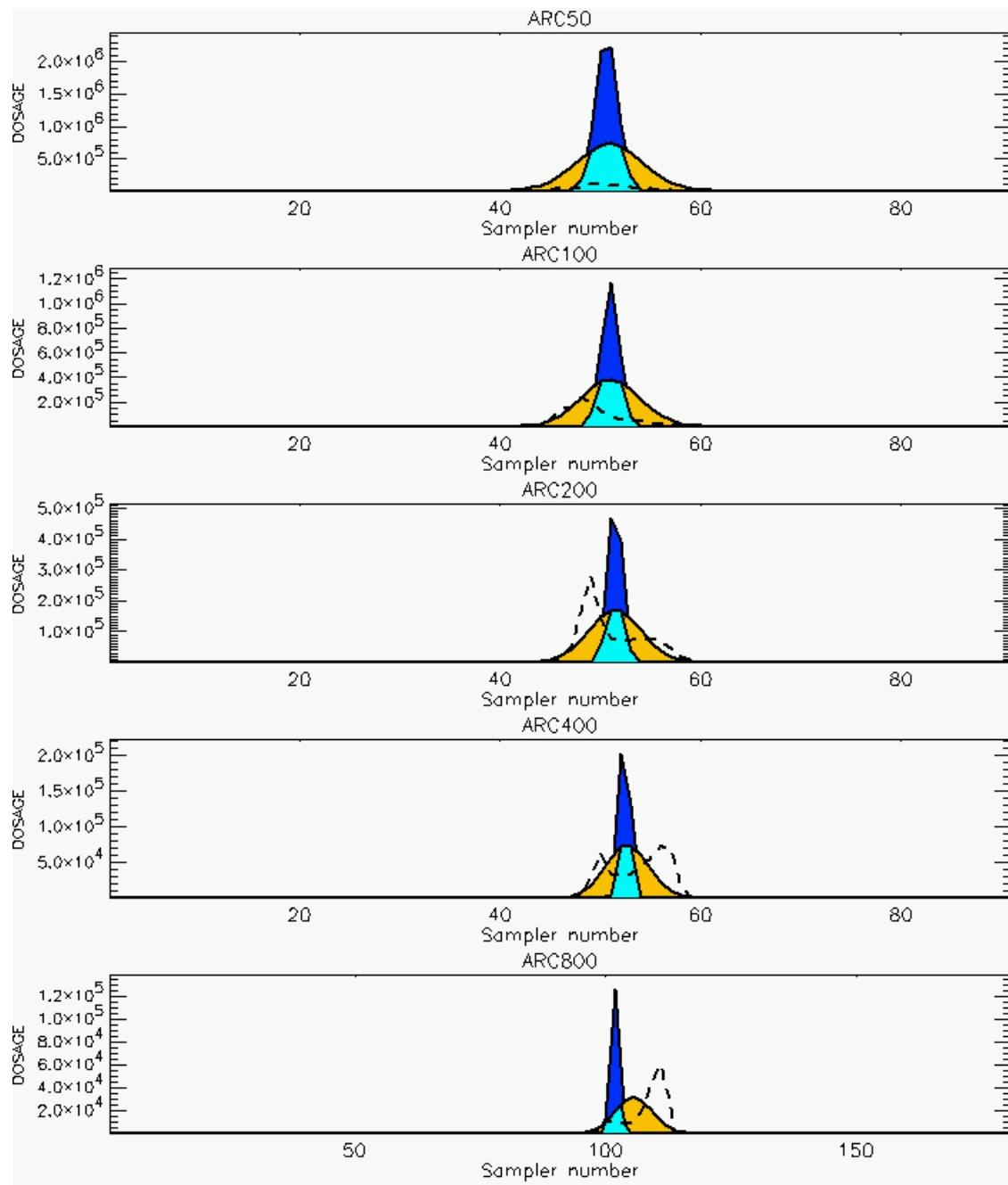
PG Prediction1 to Prediction2 Comparison

PG Trial File: pr_grass_tracer_Experiment_12.txt

PG Prediction File 1: HPAC\nodeposition\pg_12_noxd.out

PG Prediction File 2: ARAC\nodeposition\pg_12_noxd.arac

**Figure E-7b. HPAC and NARAC Predictions to Trial 12 on Logarithmic Scale:
Stability Category is 3**



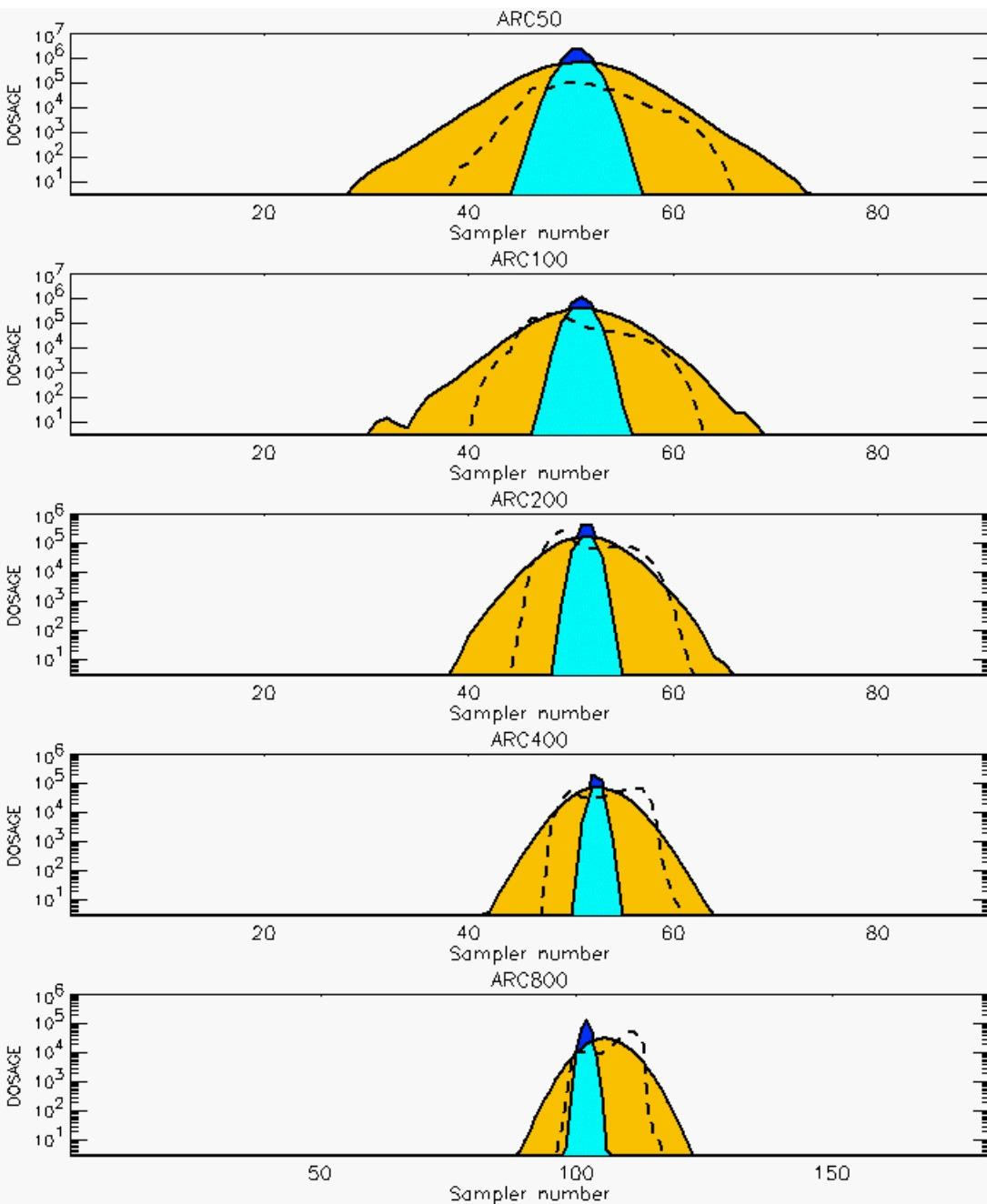
PG Prediction1 to Prediction2 Comparison

PG Trial File: pr_grass_tracer_Experiment_13.txt

PG Prediction File 1: HPAC\nodeposition\pg_13_noxd.out

PG Prediction File 2: ARAC\nodeposition\pg_13_noxd.arac

**Figure E-8a. HPAC and NARAC Predictions to Trial 13 on Linear Scale:
Stability Category is 7**



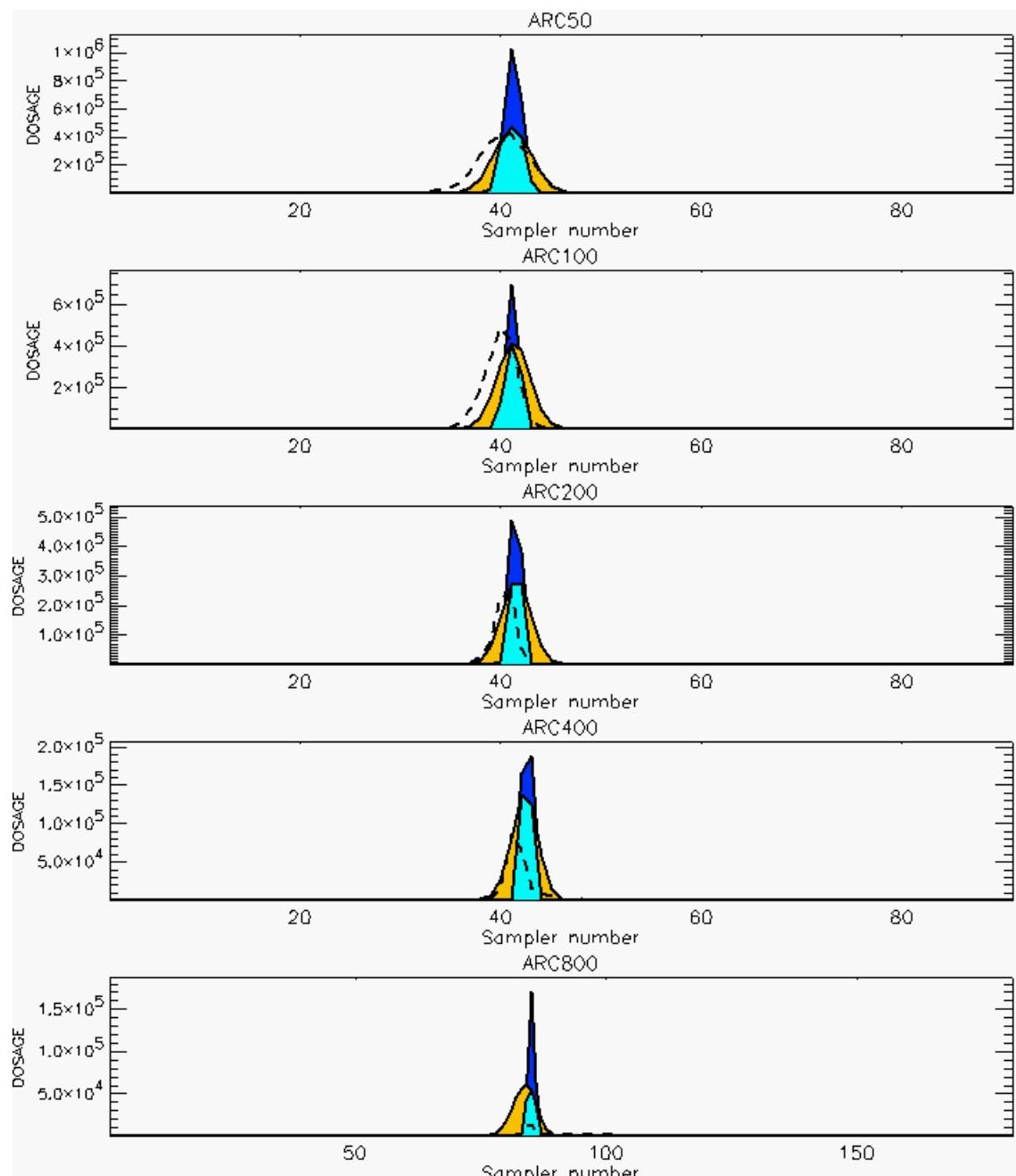
PG Prediction1 to Prediction2 Comparison

PG Trial File: pr_grass_tracer_Experiment_13.txt

PG Prediction File 1: HPAC\nodeposition\pg_13_noxd.out

PG Prediction File 2: ARAC\nodeposition\pg_13_noxd.arac

**Figure E-8b. HPAC and NARAC Predictions to Trial 13 on Logarithmic Scale:
Stability Category is 7**



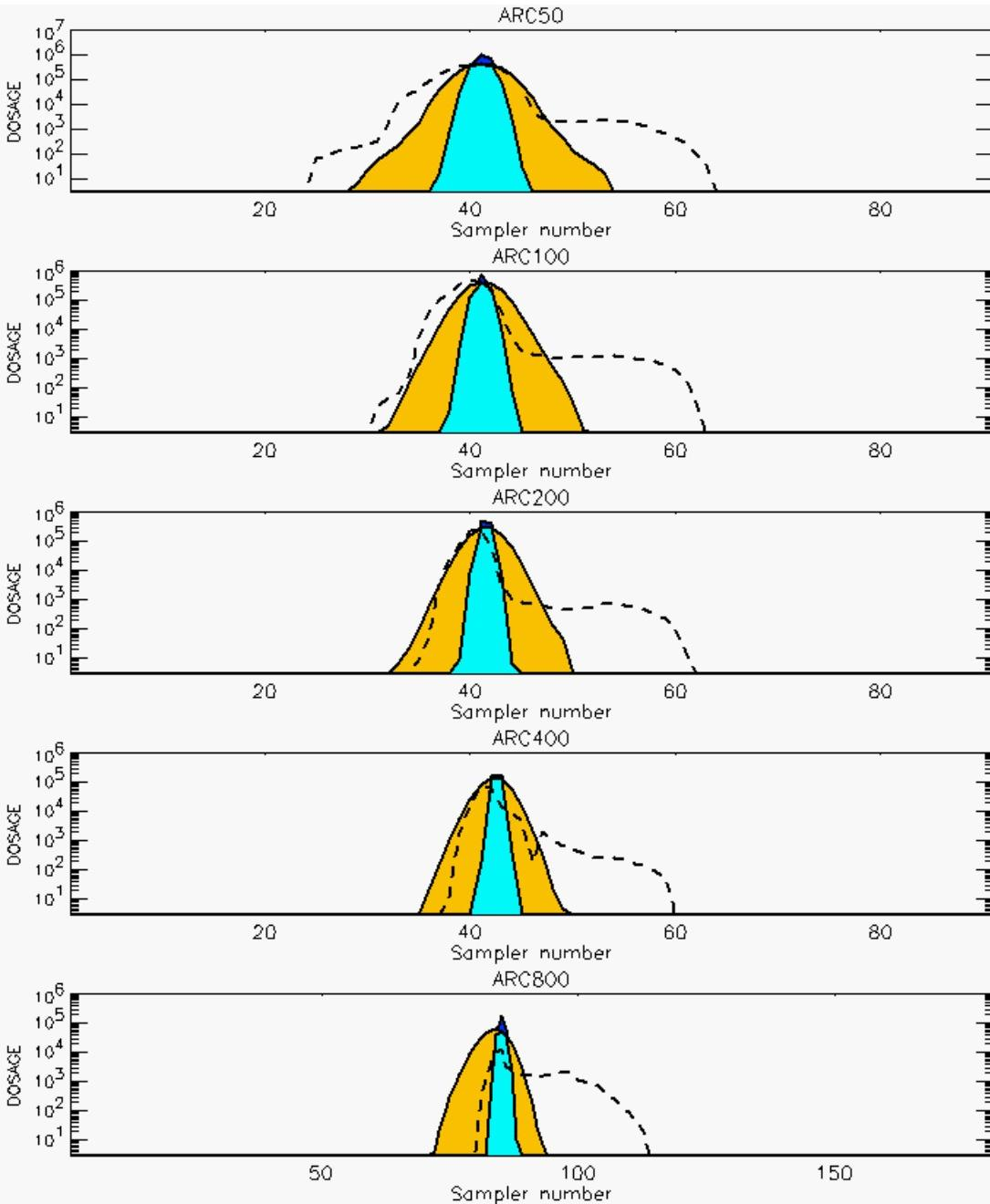
PG Prediction1 to Prediction2 Comparison

PG Trial File: pr_grass_tracer_Experiment_14.txt

PG Prediction File 1: HPAC\nodeposition\pg_14_noxd.out

PG Prediction File 2: ARAC\nodeposition\pg_14_noxd.arac

**Figure E-9a. HPAC and NARAC Predictions to Trial 14 on Linear Scale:
Stability Category is 7**



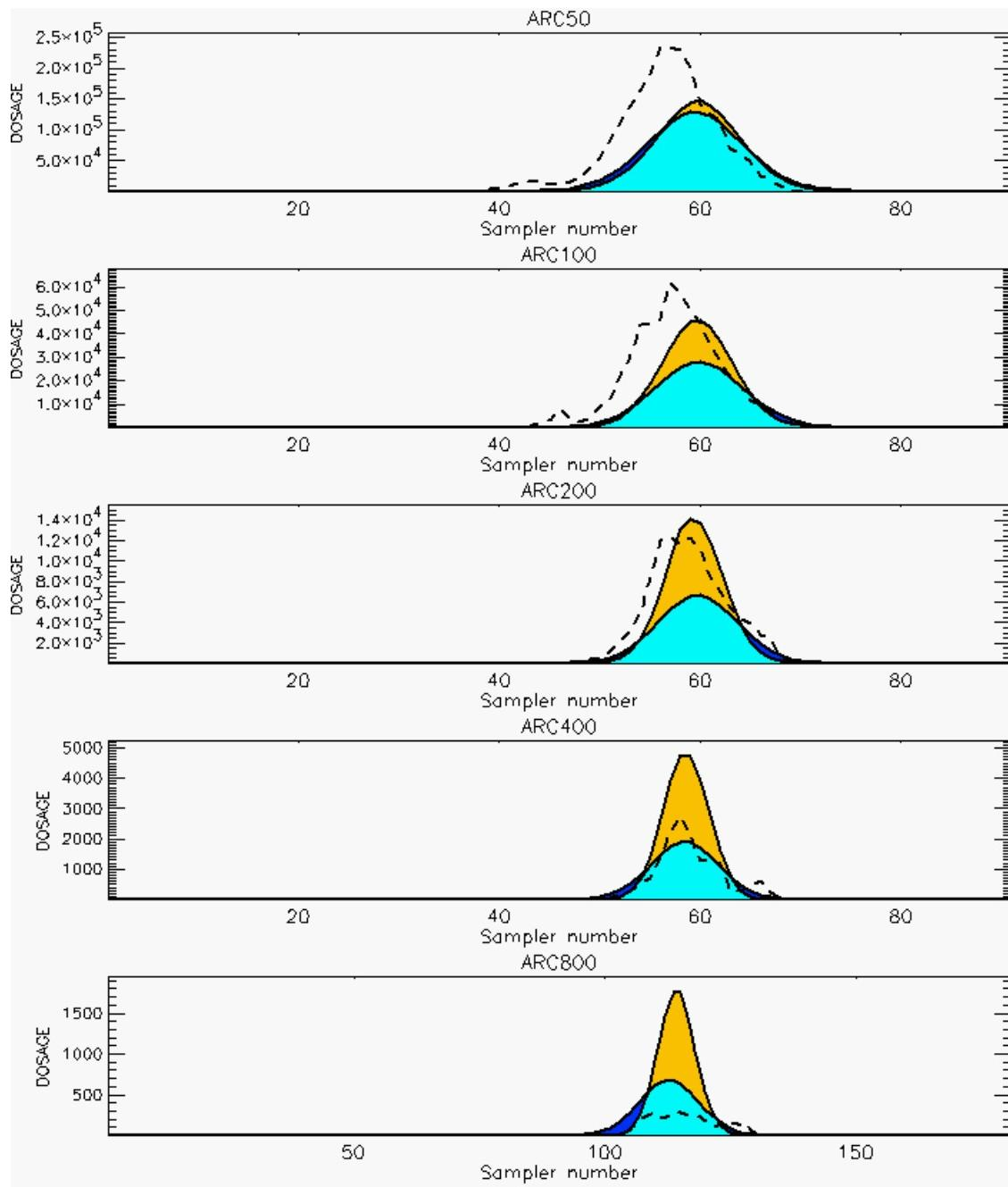
PG Prediction1 to Prediction2 Comparison

PG Trial File: pr_grass_tracer_Experiment_14.txt

PG Prediction File 1: HPAC\nodeposition\pg_14_noxd.out

PG Prediction File 2: ARAC\nodeposition\pg_14_noxd.arac

**Figure E-9b. HPAC and NARAC Predictions to Trial 14 on Logarithmic Scale:
Stability Category is 7**



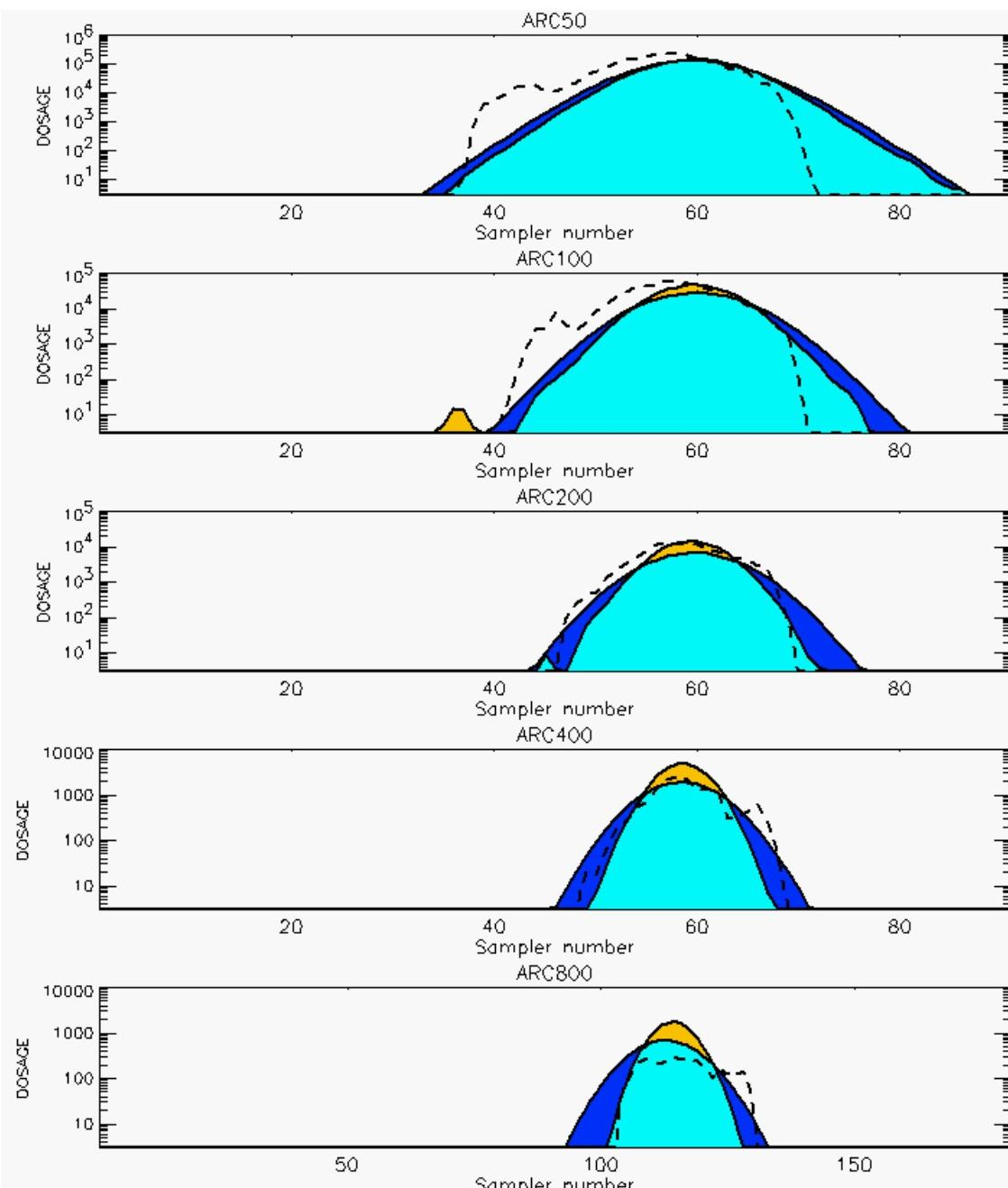
PG Prediction1 to Prediction2 Comparison

PG Trial File: pr_grass_tracer_Experiment_15.txt

PG Prediction File 1: HPAC\nodeposition\pg_15_noxd.out

PG Prediction File 2: ARAC\nodeposition\pg_15_noxd.arac

**Figure E-10a. HPAC and NARAC Predictions to Trial 15 on Linear Scale:
Stability Category is 1**



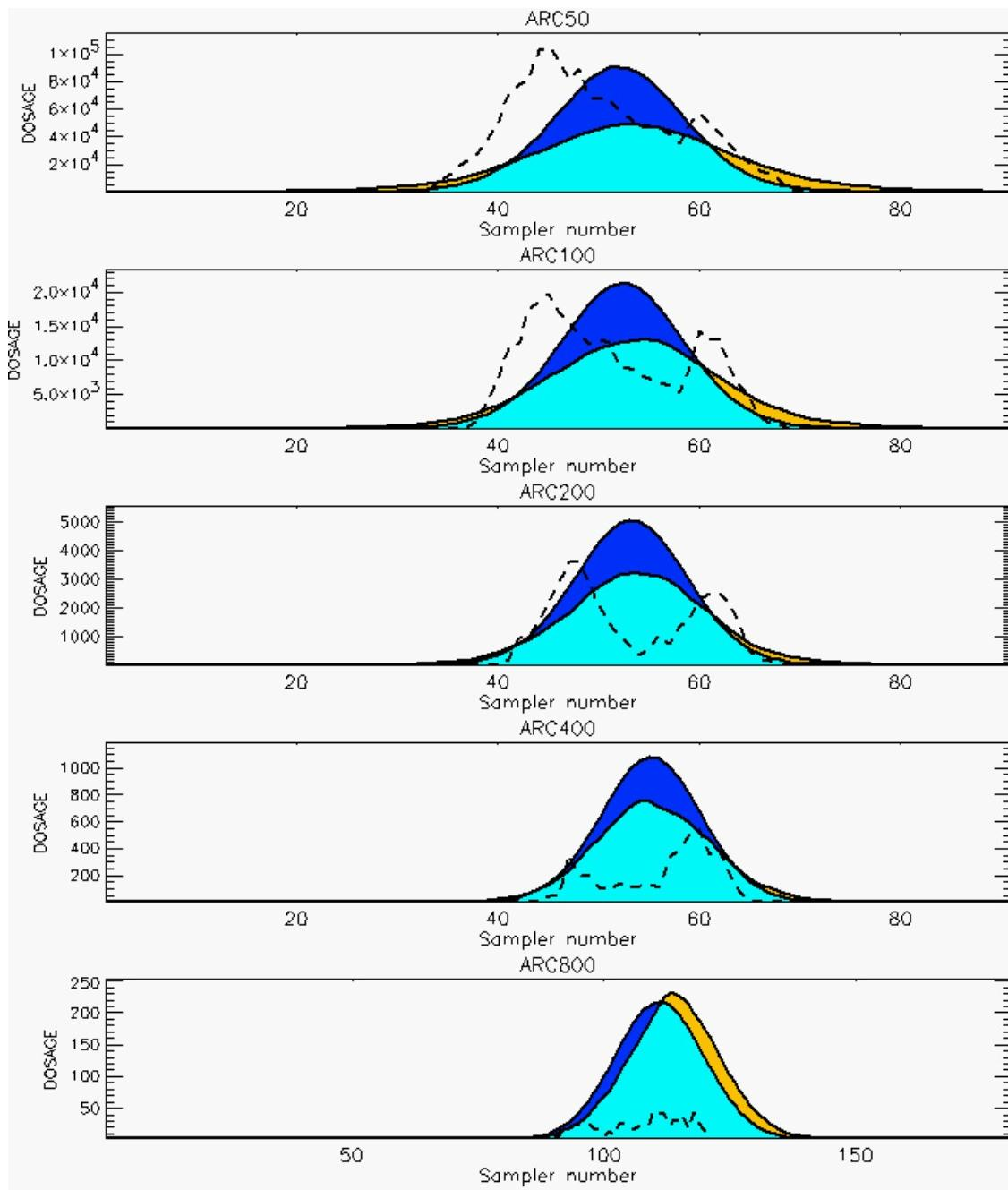
PG Prediction1 to Prediction2 Comparison

PG Trial File: pr_grass_tracer_Experiment_15.txt

PG Prediction File 1: HPAC\nodeposition\pg_15_nozd.out

PG Prediction File 2: ARAC\nodeposition\pg_15_nozd.arac

**Figure E-10b. HPAC and NARAC Predictions to Trial 15 on Logarithmic Scale:
Stability Category is 1**



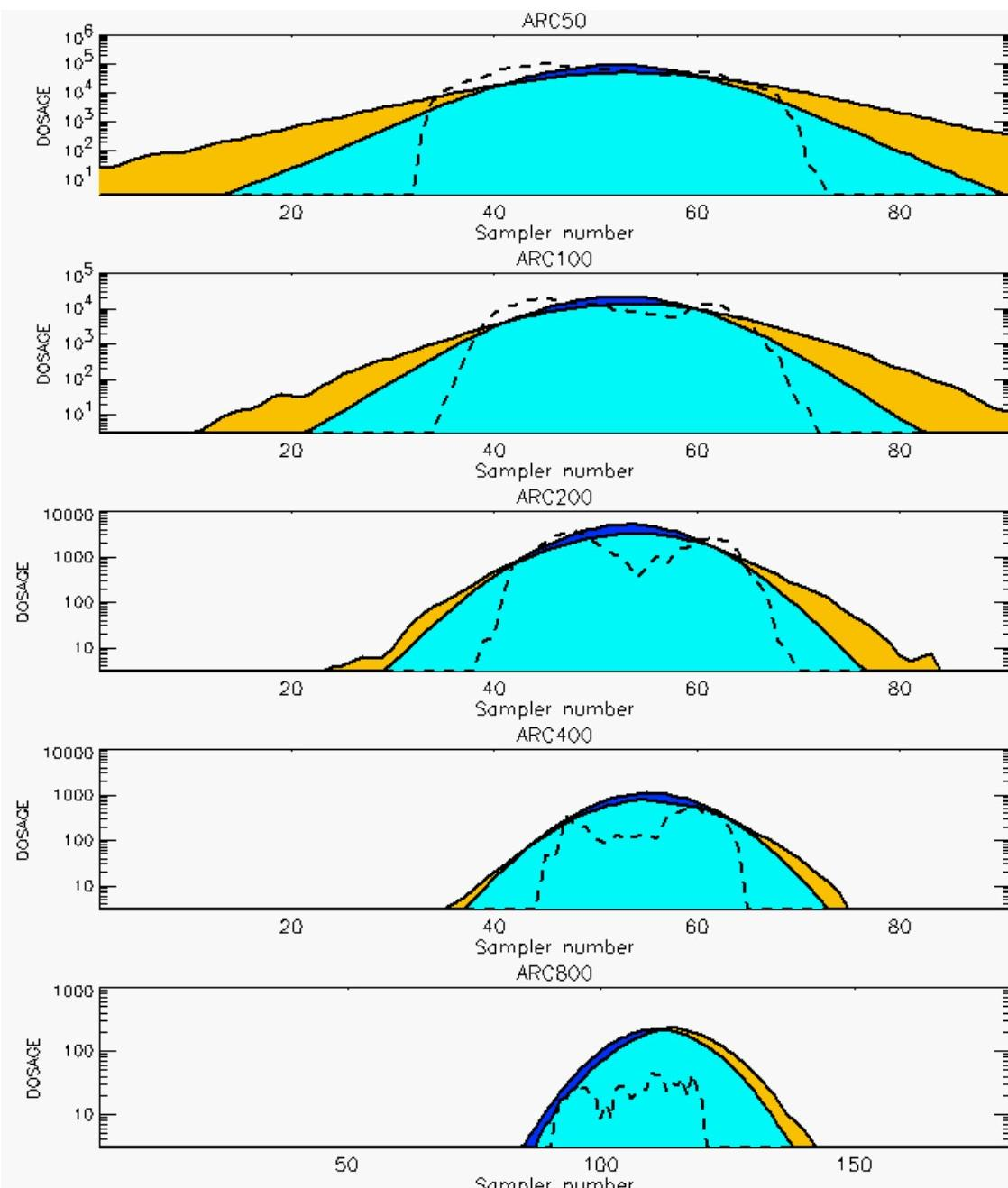
PG Prediction1 to Prediction2 Comparison

PG Trial File: pr_grass_tracer_Experiment_16.txt

PG Prediction File 1: HPAC\nodeposition\pg_16_noxd.out

PG Prediction File 2: ARAC\nodeposition\pg_16_noxd.arac

**Figure E-11a. HPAC and NARAC Predictions to Trial 16 on Linear Scale
Stability Category is 1**



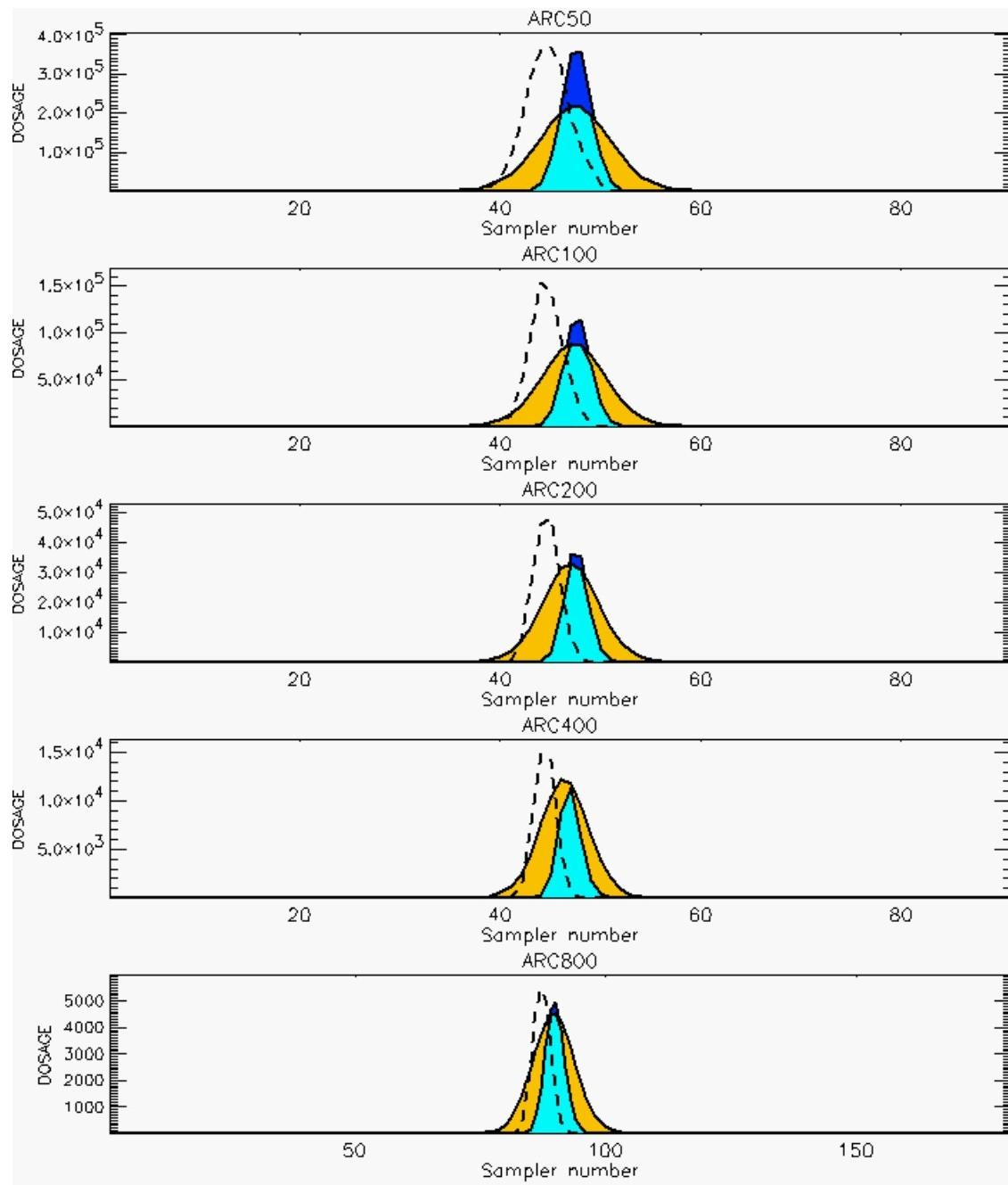
PG Prediction1 to Prediction2 Comparison

PG Trial File: pr_grass_tracer_Experiment_16.txt

PG Prediction File 1: HPAC\nodeposition\pg_16_noxd.out

PG Prediction File 2: ARAC\nodeposition\pg_16_noxd.arac

**Figure E-11b. HPAC and NARAC Predictions to Trial 16 on Logarithmic Scale:
Stability Category is 1**



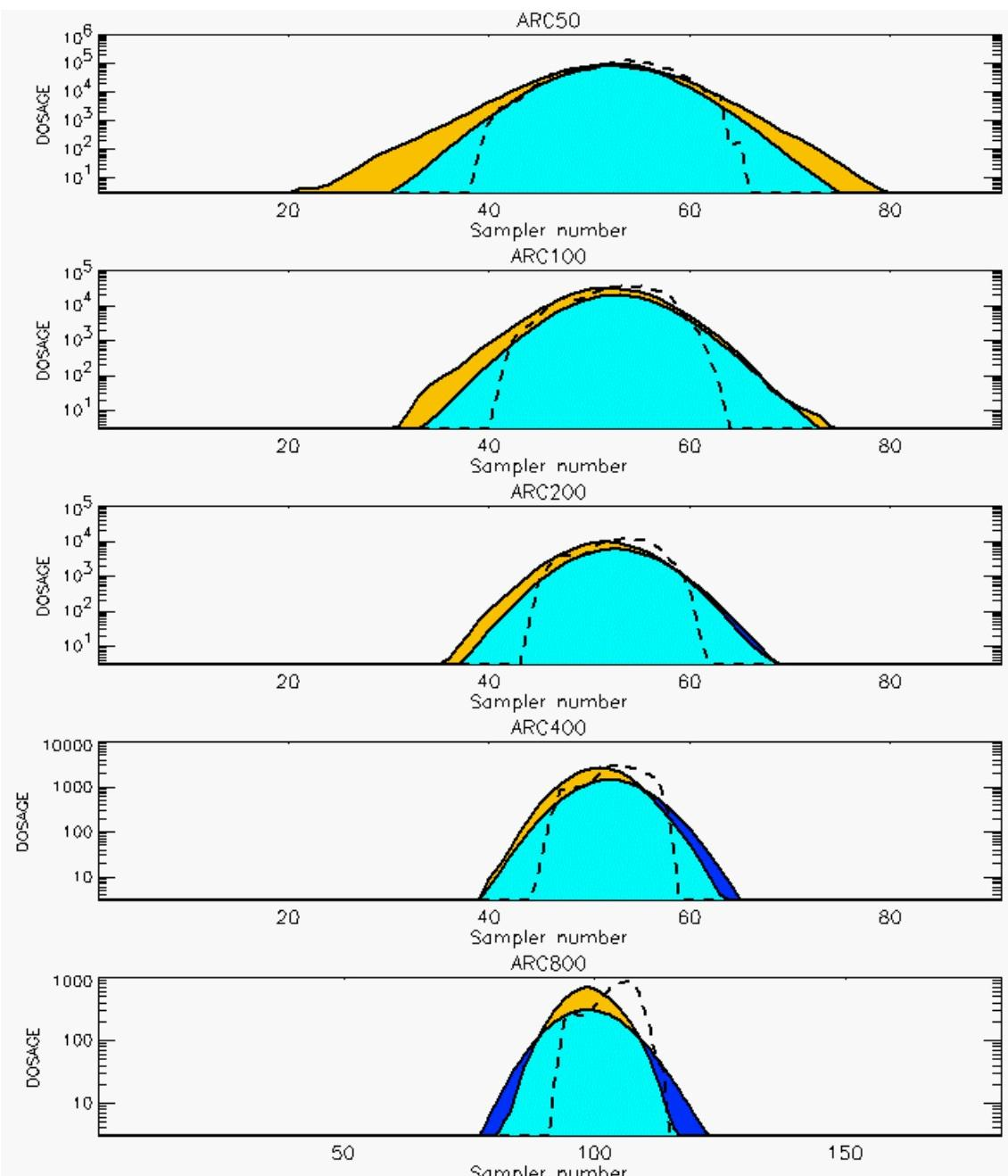
PG Prediction1 to Prediction2 Comparison

PG Trial File: pr_grass_tracer_Experiment_17.txt

PG Prediction File 1: HPAC\nodeposition\pg_17_noxd.out

PG Prediction File 2: ARAC\nodeposition\pg_17_noxd.arac

**Figure E-12a. HPAC and NARAC Predictions to Trial 17 on Linear Scale:
Stability Category is 5**



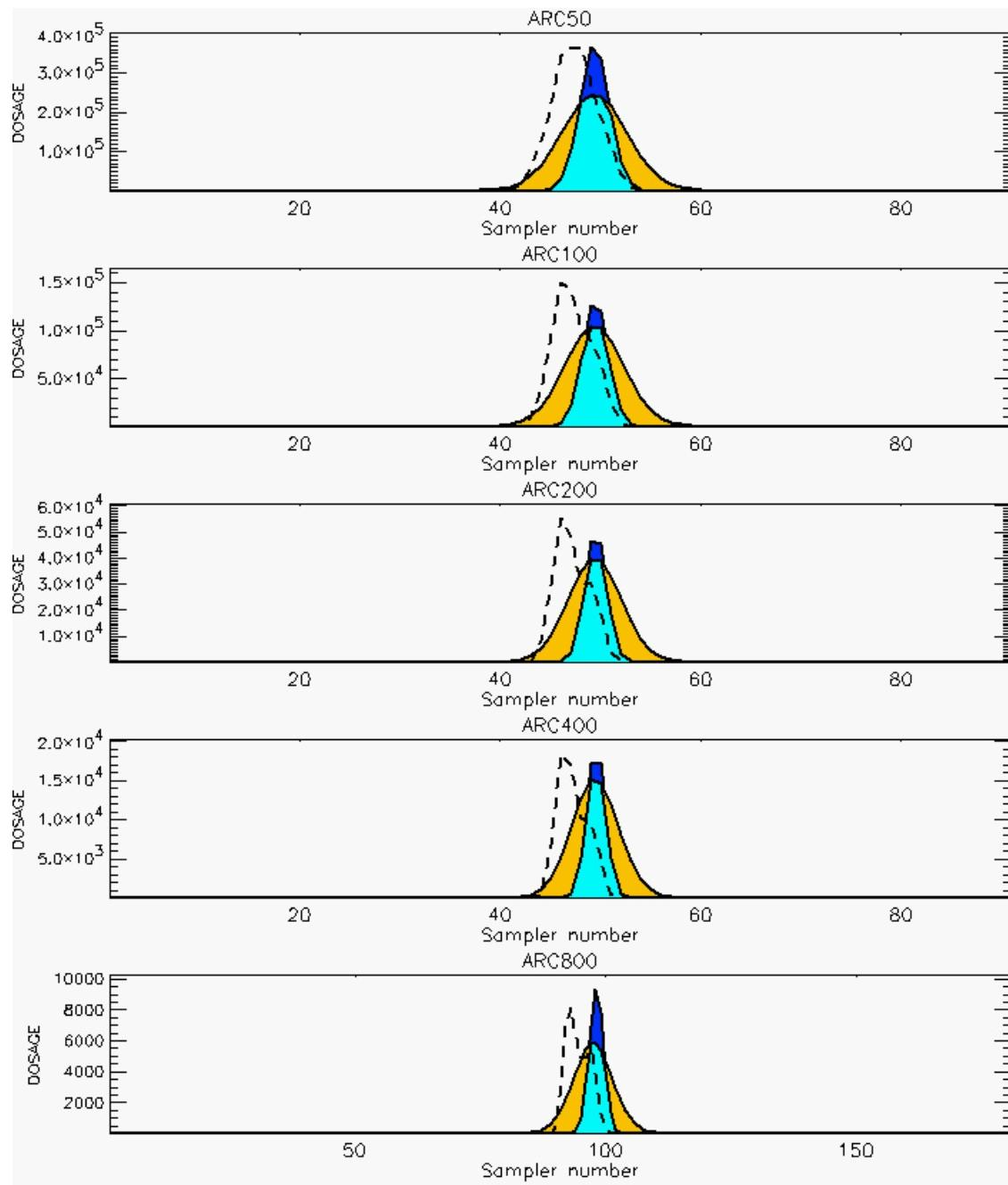
PG Prediction1 to Prediction2 Comparison

PG Trial File: pr_grass_tracer_Experiment_12.txt

PG Prediction File 1: HPAC\nodeposition\pg_12_noxd.out

PG Prediction File 2: ARAC\nodeposition\pg_12_noxd.arac

**Figure E-12b. HPAC and NARAC Predictions to Trial 17 on Logarithmic Scale:
Stability Category is 5**



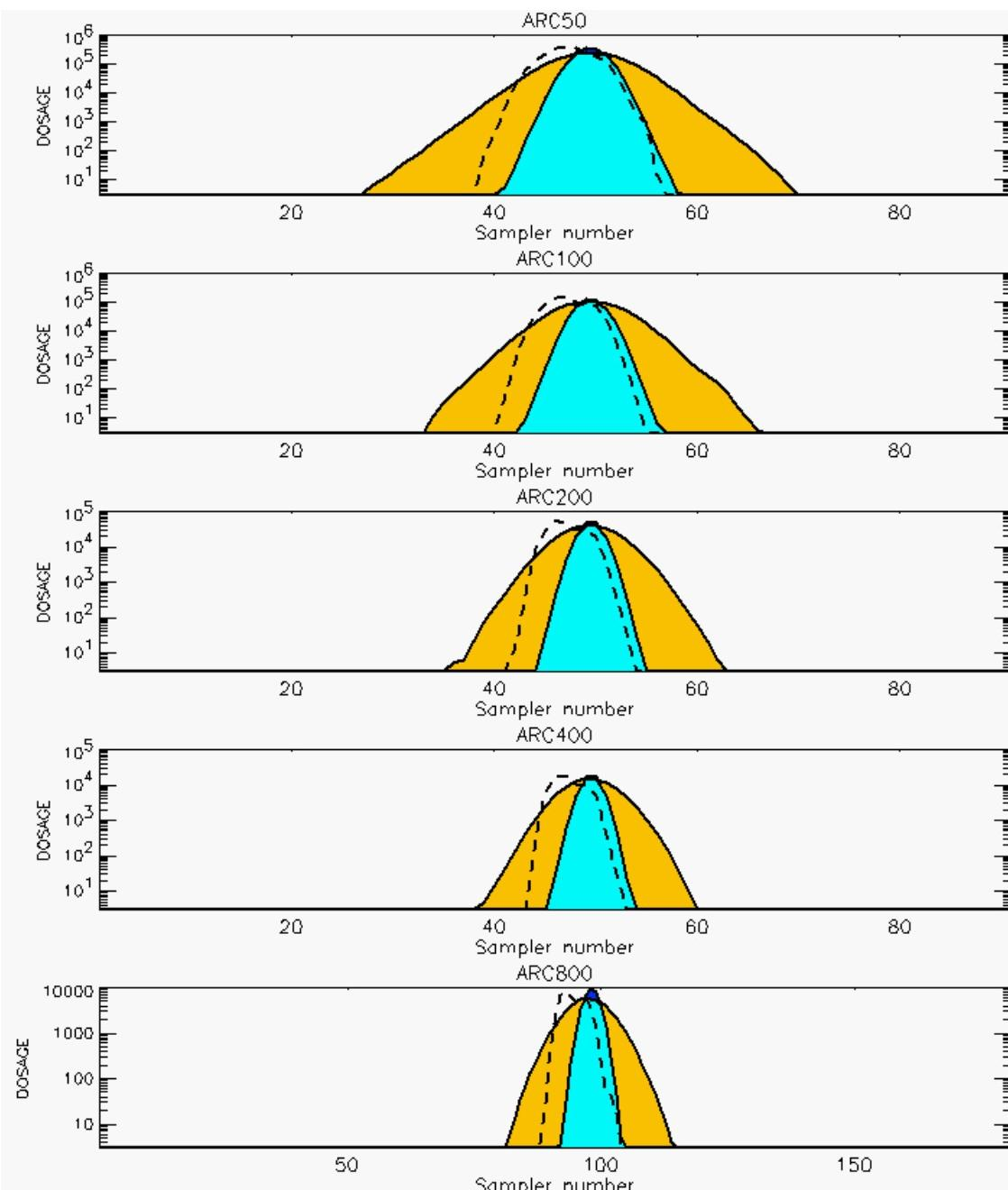
PG Prediction1 to Prediction2 Comparison

PG Trial File: pr_grass_tracer_Experiment_18.txt

PG Prediction File 1: HPAC\nodeposition\pg_18_noxd.out

PG Prediction File 2: ARAC\nodeposition\pg_18_noxd.arac

**Figure E-13a. HPAC and NARAC Predictions to Trial 18 on Linear Scale:
Stability Category is 5**



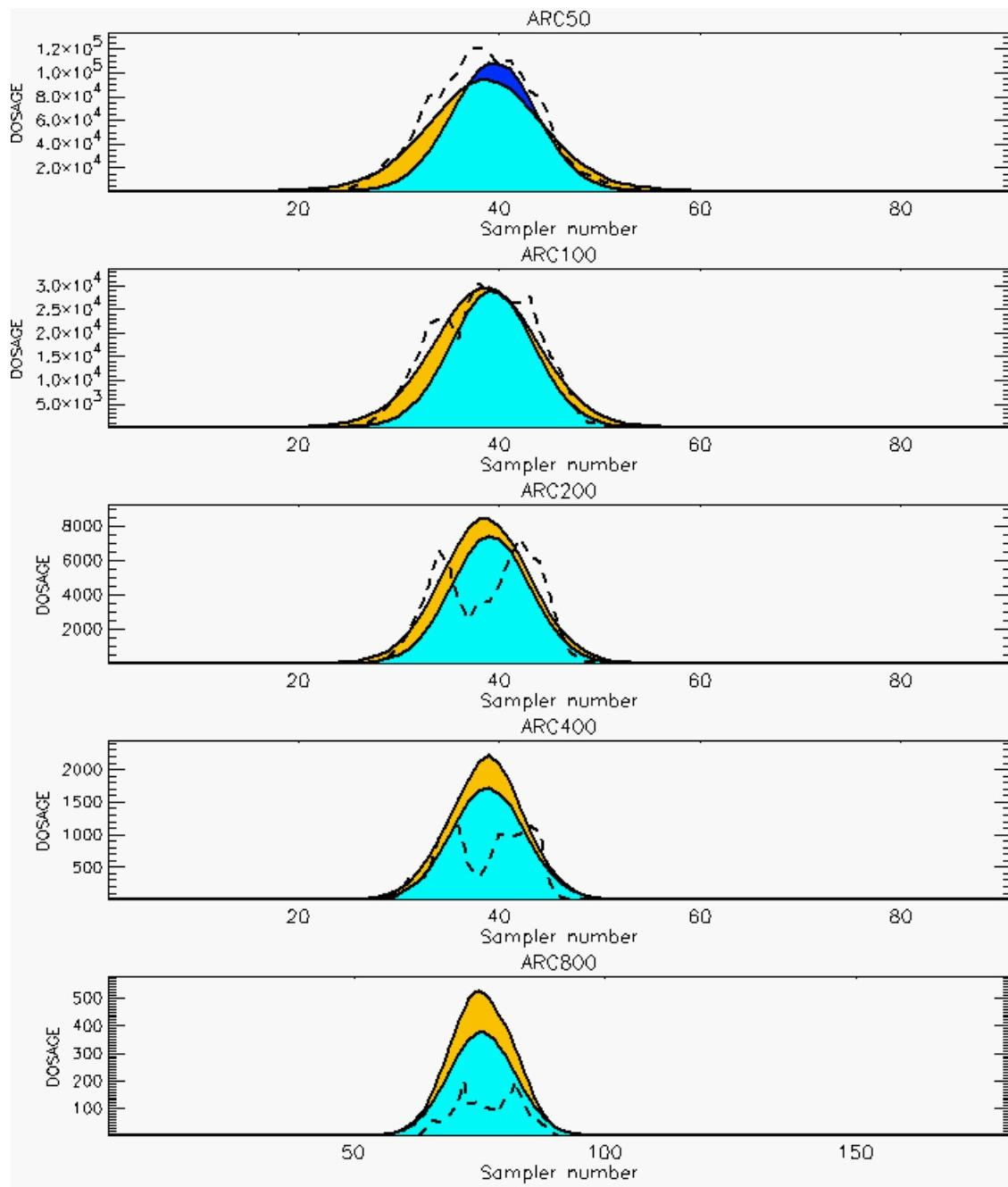
PG Prediction1 to Prediction2 Comparison

PG Trial File: pr_grass_tracer_Experiment_18.txt

PG Prediction File 1: HPAC\nodeposition\pg_18_noxd.out

PG Prediction File 2: ARAC\nodeposition\pg_18_noxd.arac

**Figure E-13b. HPAC and NARAC Predictions to Trial 18 on Logarithmic Scale:
Stability Category is 5**



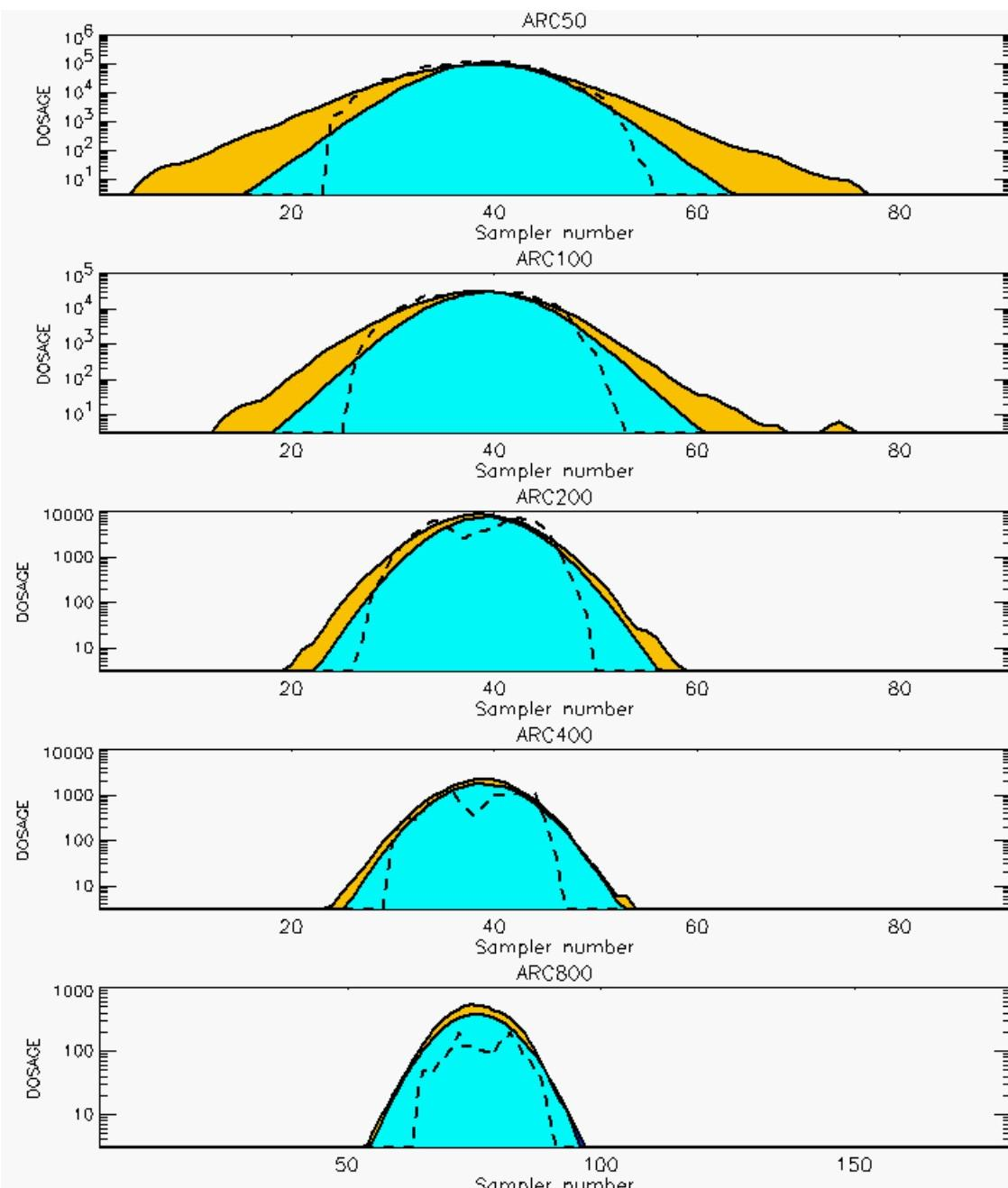
PG Prediction1 to Prediction2 Comparison

PG Trial File: pr_grass_tracer_Experiment_19.txt

PG Prediction File 1: HPAC\nodeposition\pg_19_noxd.out

PG Prediction File 2: ARAC\nodeposition\pg_19_noxd.arac

**Figure E-14a. HPAC and NARAC Predictions to Trial 19 on Linear Scale:
Stability Category is 2**



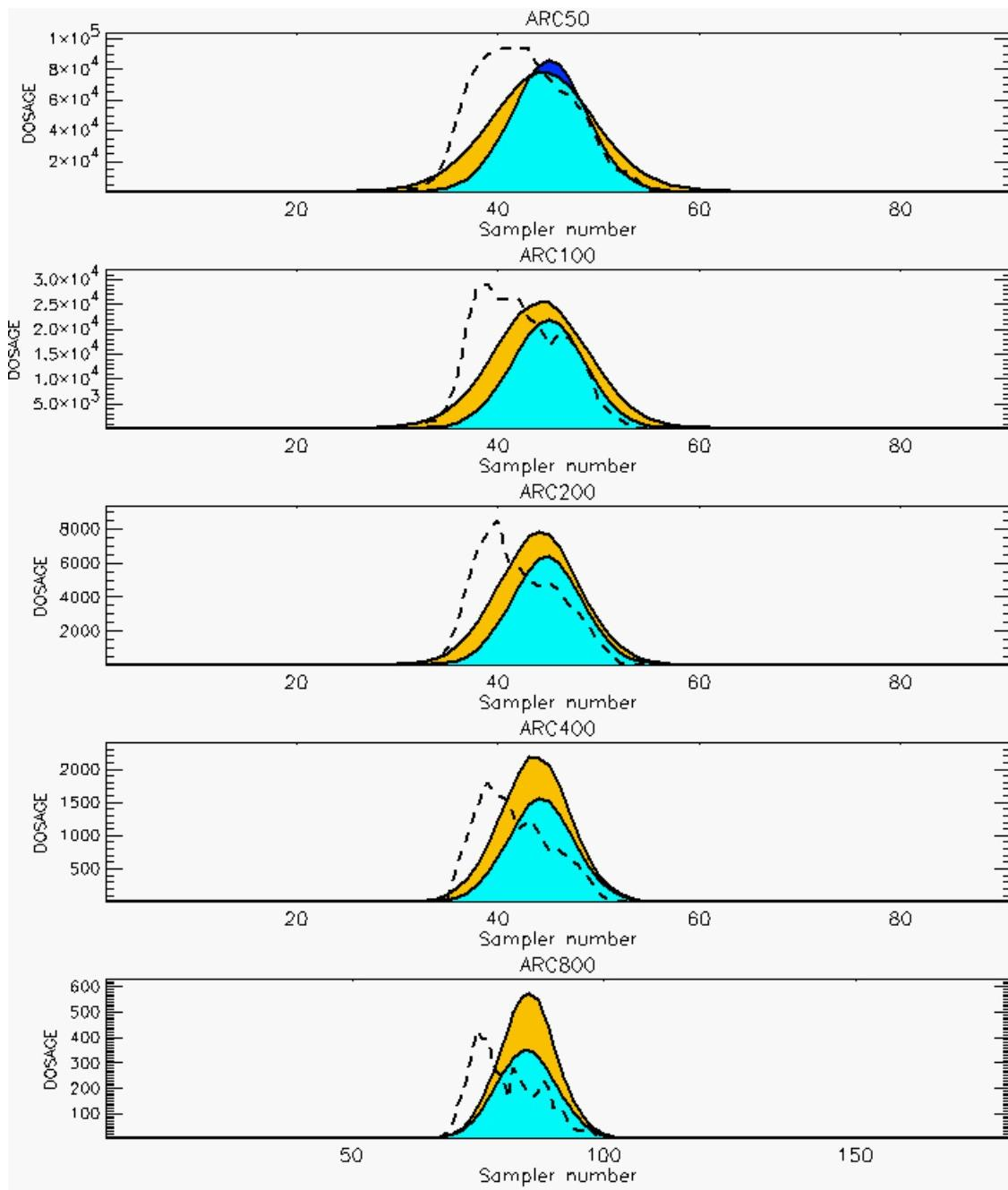
PG Prediction1 to Prediction2 Comparison

PG Trial File: pr_grass_tracer_Experiment_19.txt

PG Prediction File 1: HPAC\nodeposition\pg_19_novd.out

PG Prediction File 2: ARAC\nodeposition\pg_19_novd.arac

**Figure E-14b. HPAC and NARAC Predictions to Trial 19 on Logarithmic Scale:
Stability Category is 2**



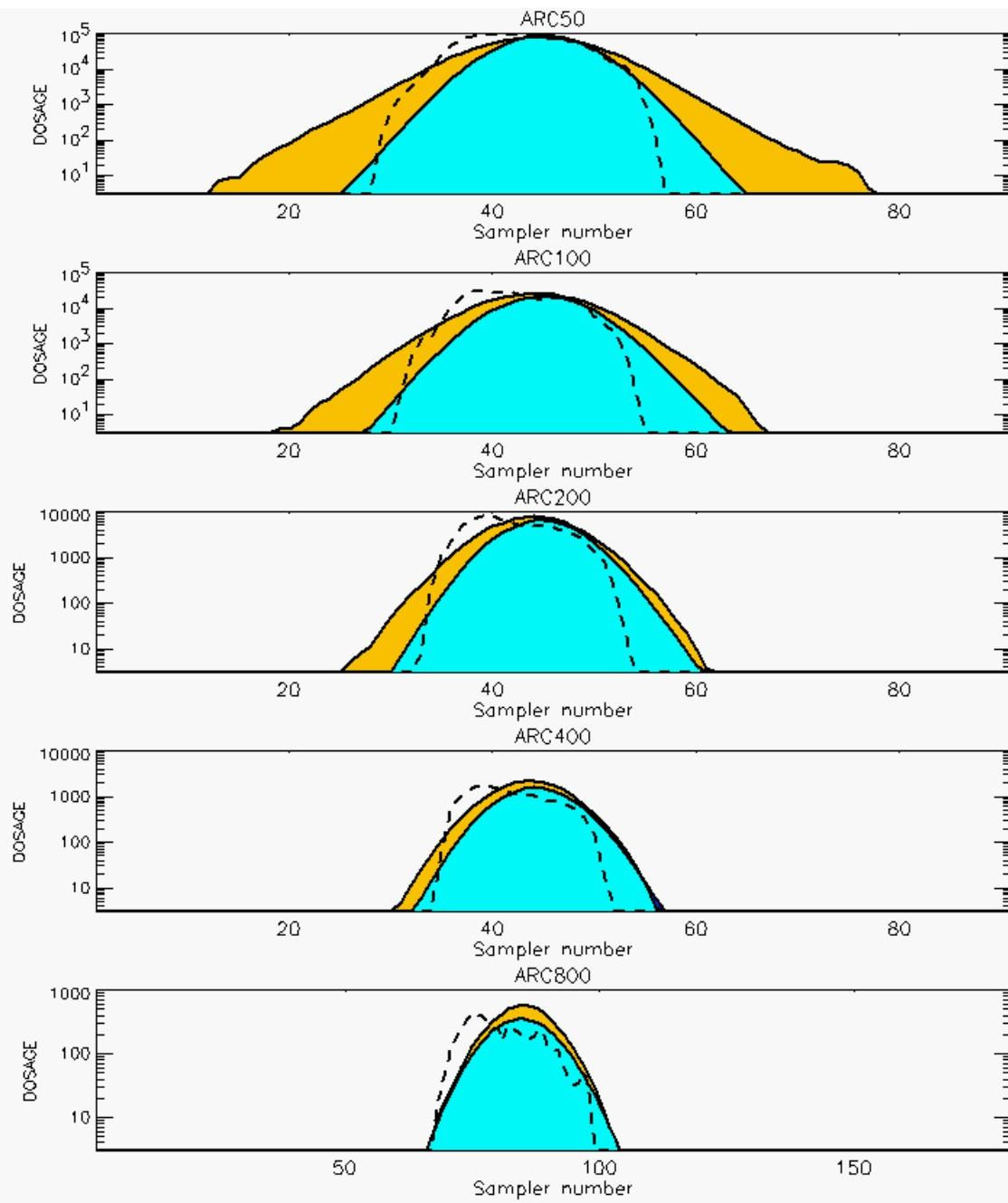
PG Prediction1 to Prediction2 Comparison

PG Trial File: pr_grass_tracer_Experiment_20.txt

PG Prediction File 1: HPAC\nodeposition\pg_20_noxd.out

PG Prediction File 2: ARAC\nodeposition\pg_20_noxd.arac

**Figure E-15a. HPAC and NARAC Predictions to Trial 20 on Linear Scale:
Stability Category is 3**



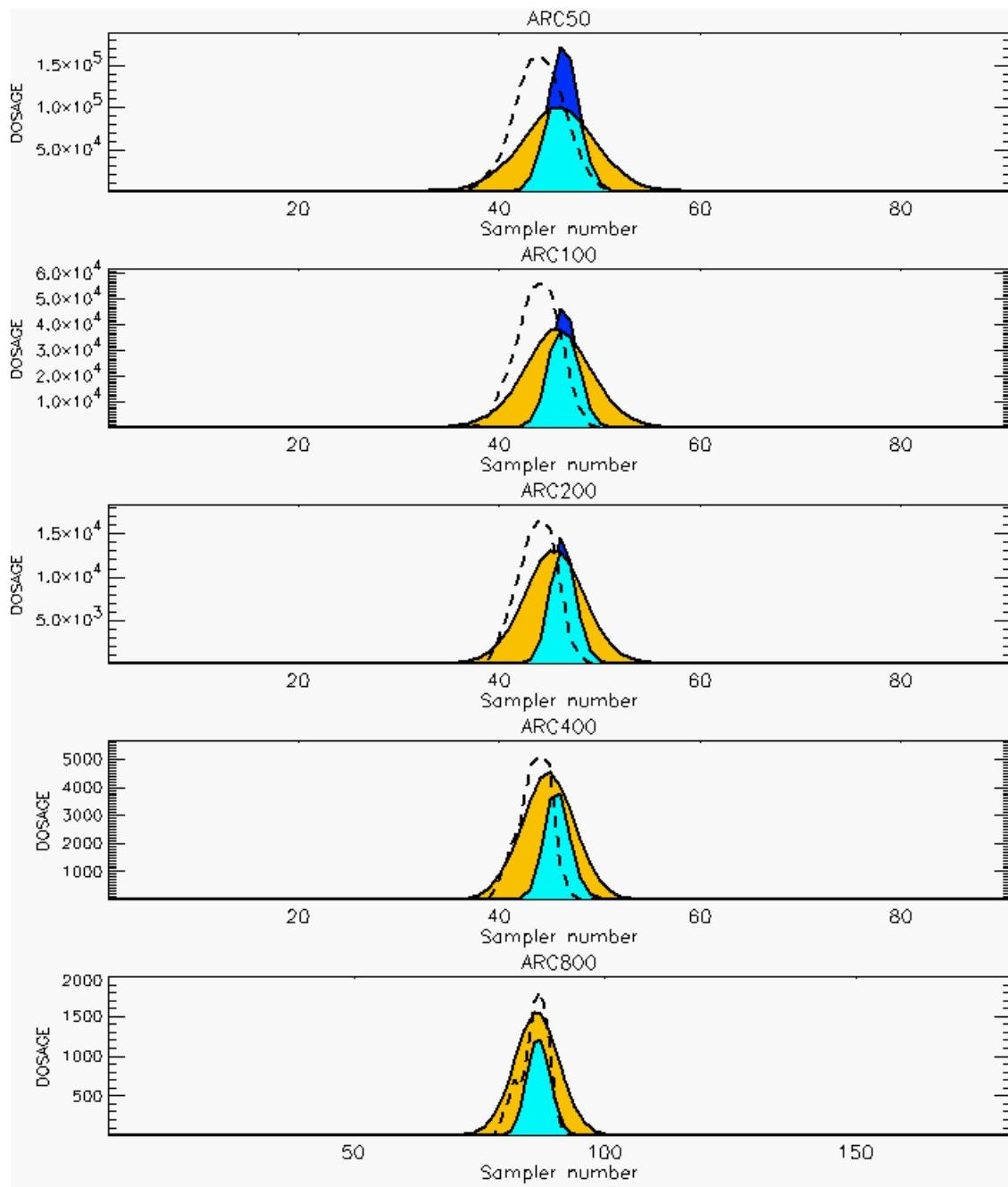
PG Prediction1 to Prediction2 Comparison

PG Trial File: pr_grass_tracer_Experiment_20.txt

PG Prediction File 1: HPAC\nodeposition\pg_20_noxd.out

PG Prediction File 2: ARAC\nodeposition\pg_20_noxd.arac

**Figure E-15b. HPAC and NARAC Predictions to Trial 20 on Logarithmic Scale:
Stability Category is 3**



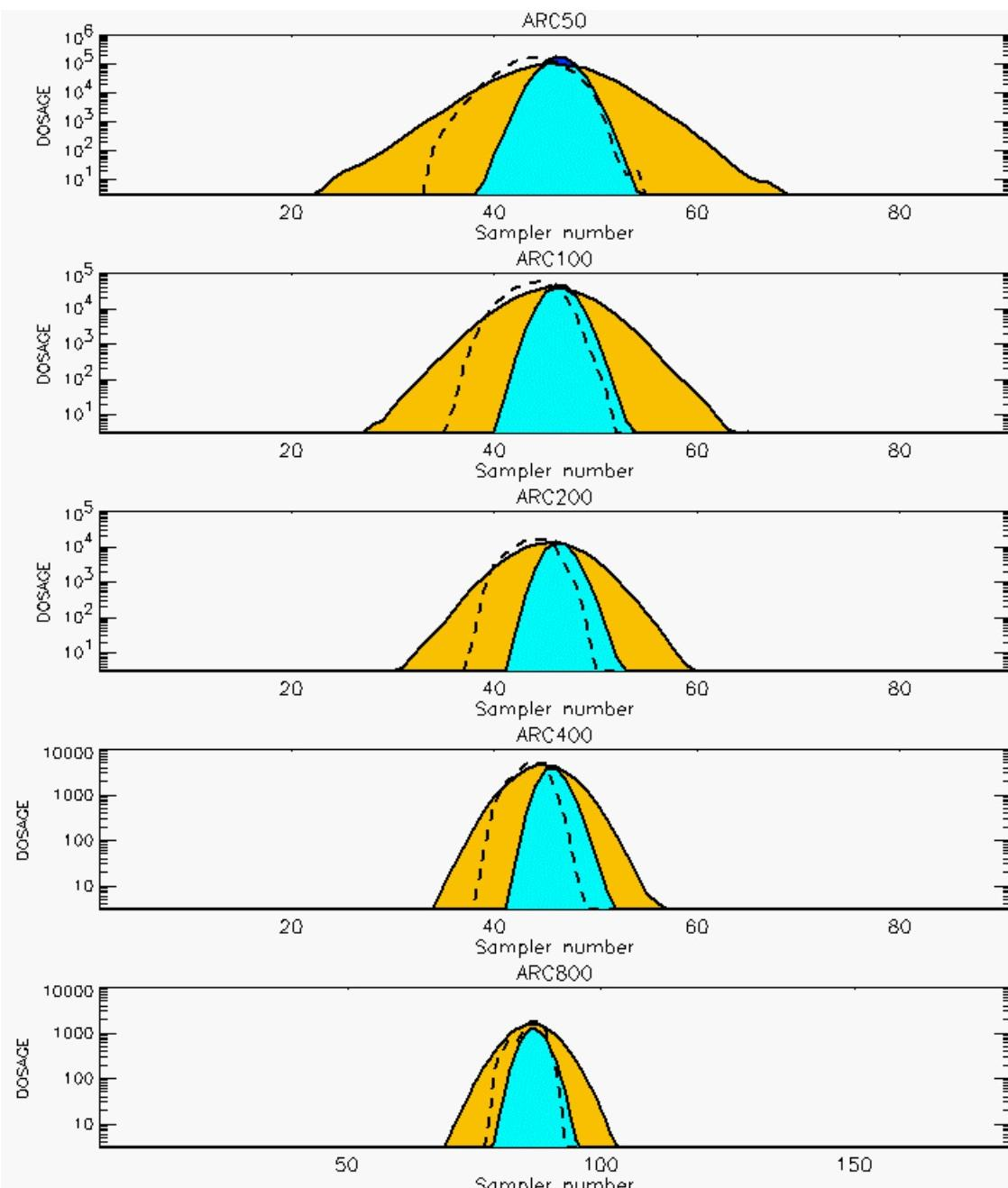
PG Prediction1 to Prediction2 Comparison

PG Trial File: pr_grass_tracer_Experiment_21.txt

PG Prediction File 1: HPAC\nodeposition\pg_21_noxd.out

PG Prediction File 2: ARAC\nodeposition\pg_21_noxd.arac

**Figure E-16a. HPAC and NARAC Predictions to Trial 21 on Linear Scale:
Stability Category is 4**



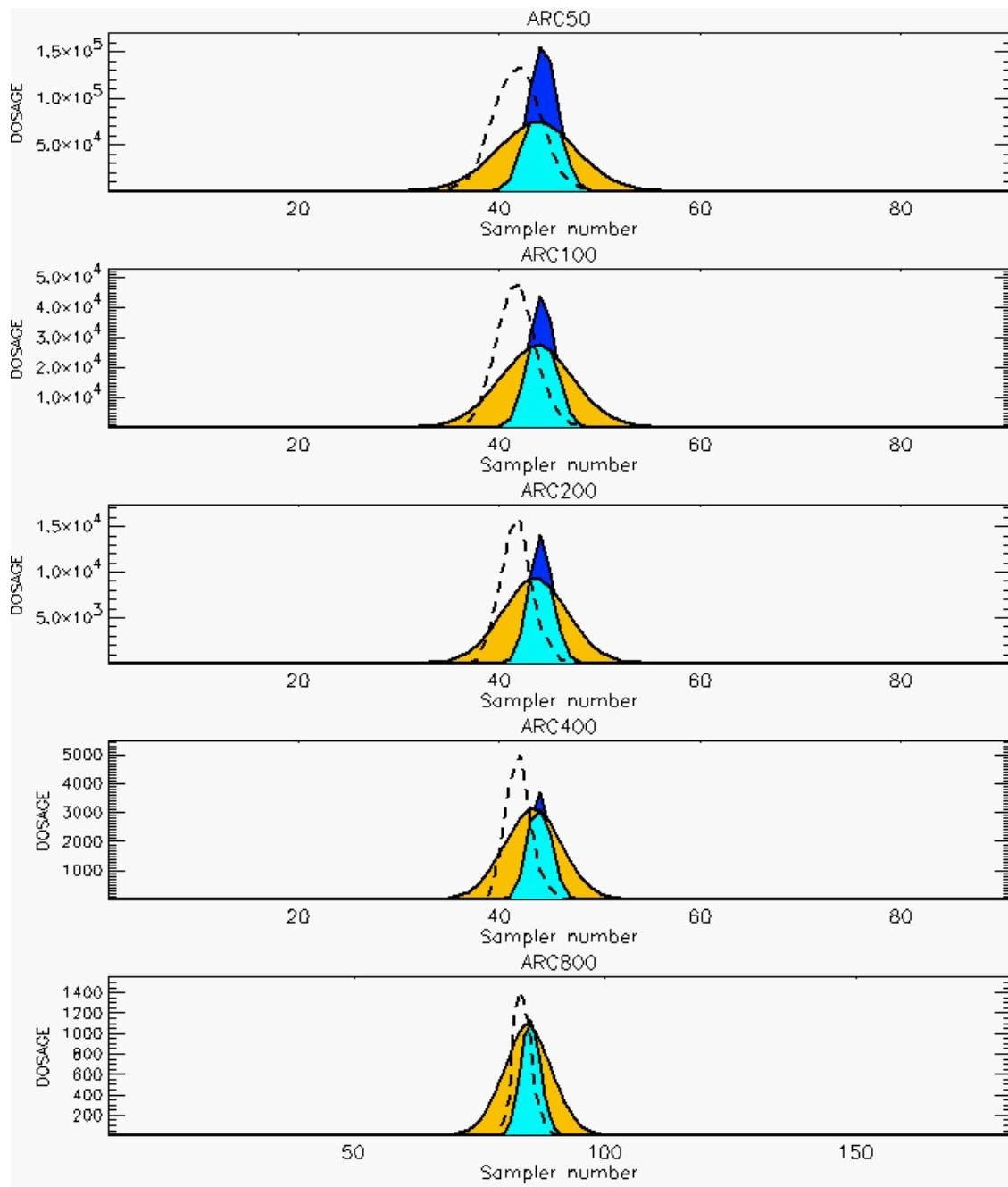
PG Prediction1 to Prediction2 Comparison

PG Trial File: pr_grass_tracer_Experiment_21.txt

PG Prediction File 1: HPAC\nodeposition\pg_21_noxd.out

PG Prediction File 2: ARAC\nodeposition\pg_21_noxd.arac

**Figure E-16b. HPAC and NARAC Predictions to Trial 21 on Logarithmic Scale:
Stability Category is 4**



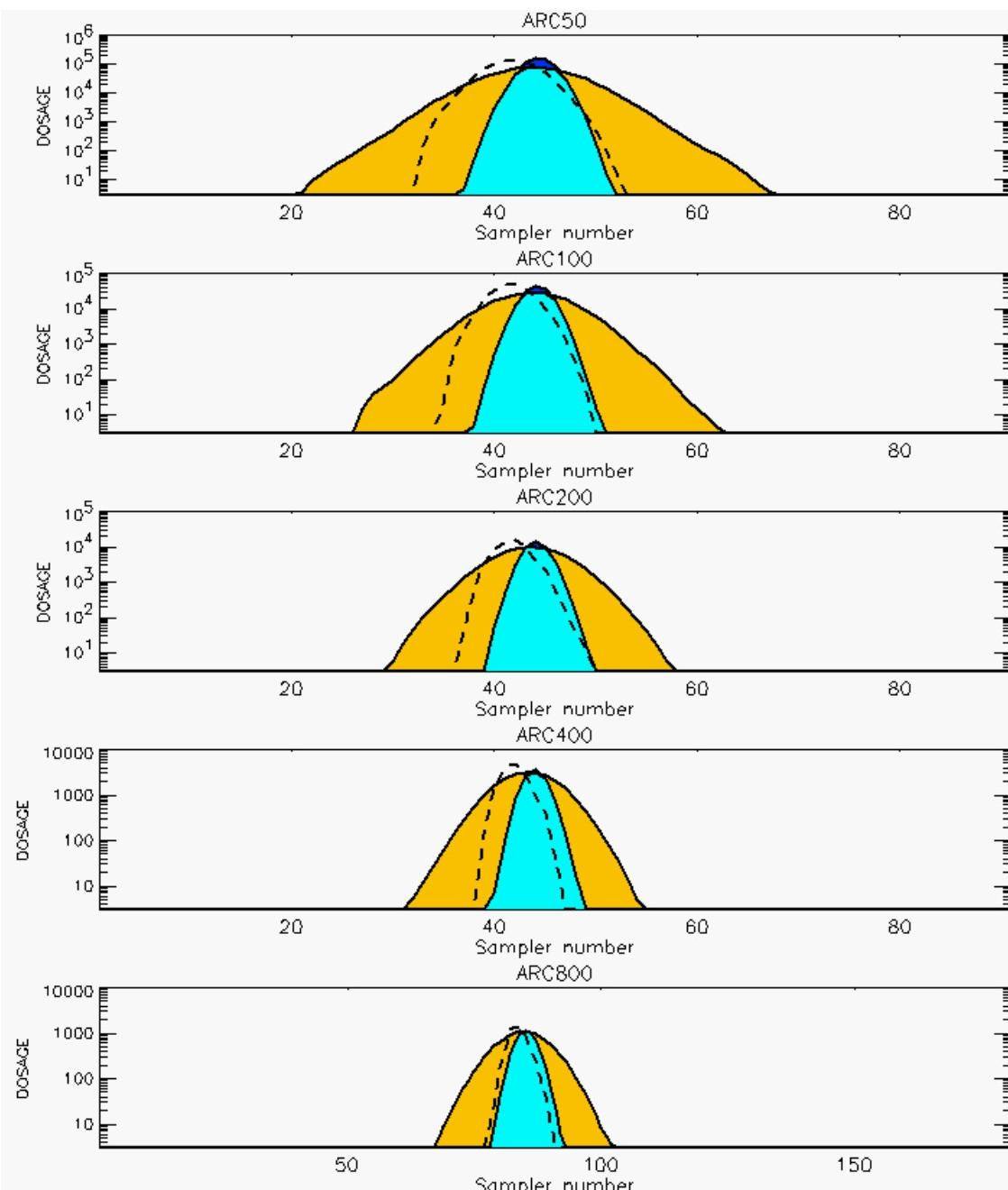
PG Prediction1 to Prediction2 Comparison

PG Trial File: pr_grass_tracer_Experiment_22.txt

PG Prediction File 1: HPAC\nodeposition\pg_22_noxd.out

PG Prediction File 2: ARAC\nodeposition\pg_22_noxd.arac

**Figure E-17a. HPAC and NARAC Predictions to Trial 22 on Linear Scale:
Stability Category is 4**



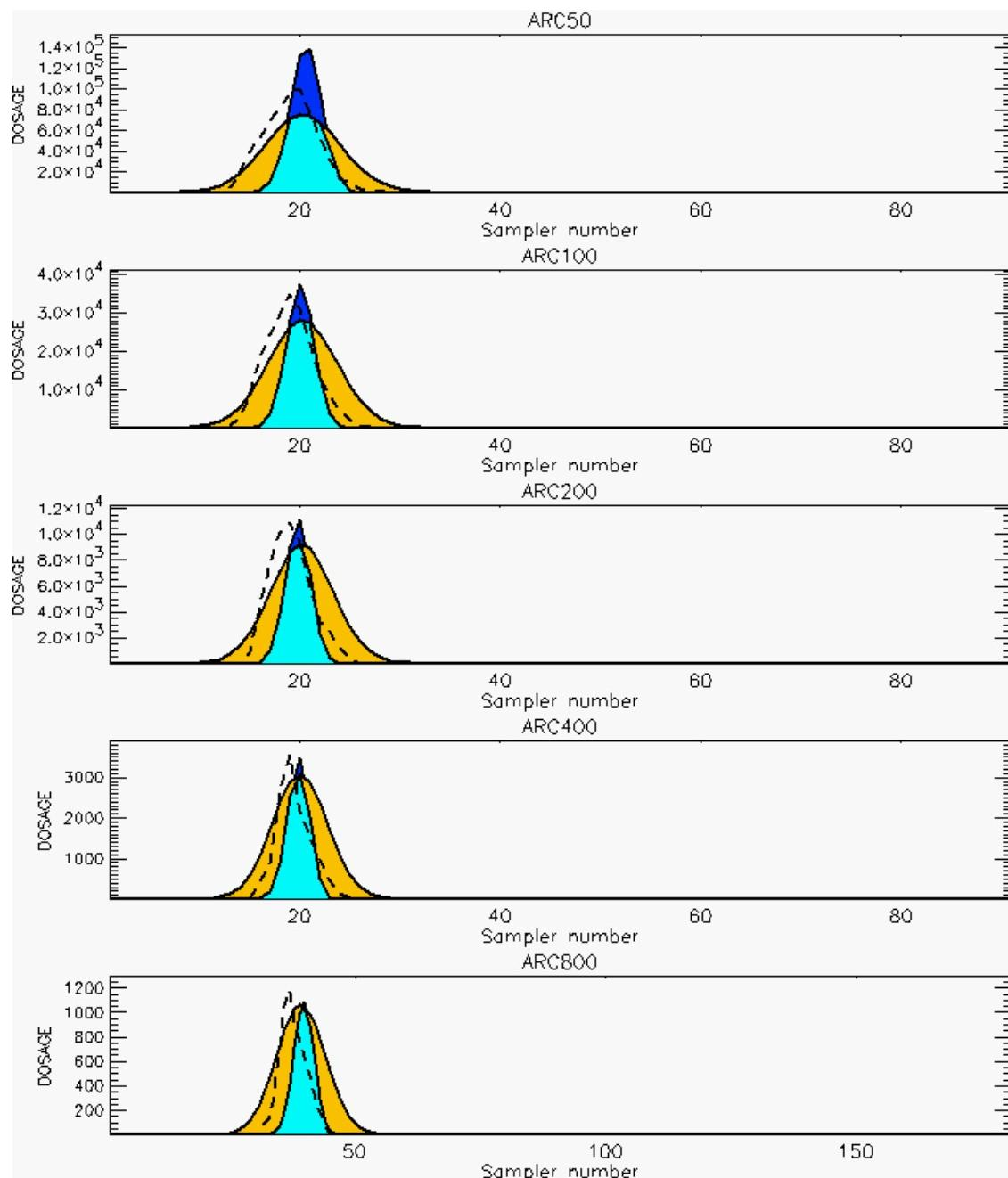
PG Prediction1 to Prediction2 Comparison

PG Trial File: pr_grass_tracer_Experiment_22.txt

PG Prediction File 1: HPAC\nodeposition\pg_22_noxd.out

PG Prediction File 2: ARAC\nodeposition\pg_22_noxd.arac

**Figure E-17b. HPAC and NARAC Predictions to Trial 22 on Logarithmic Scale:
Stability Category is 4**



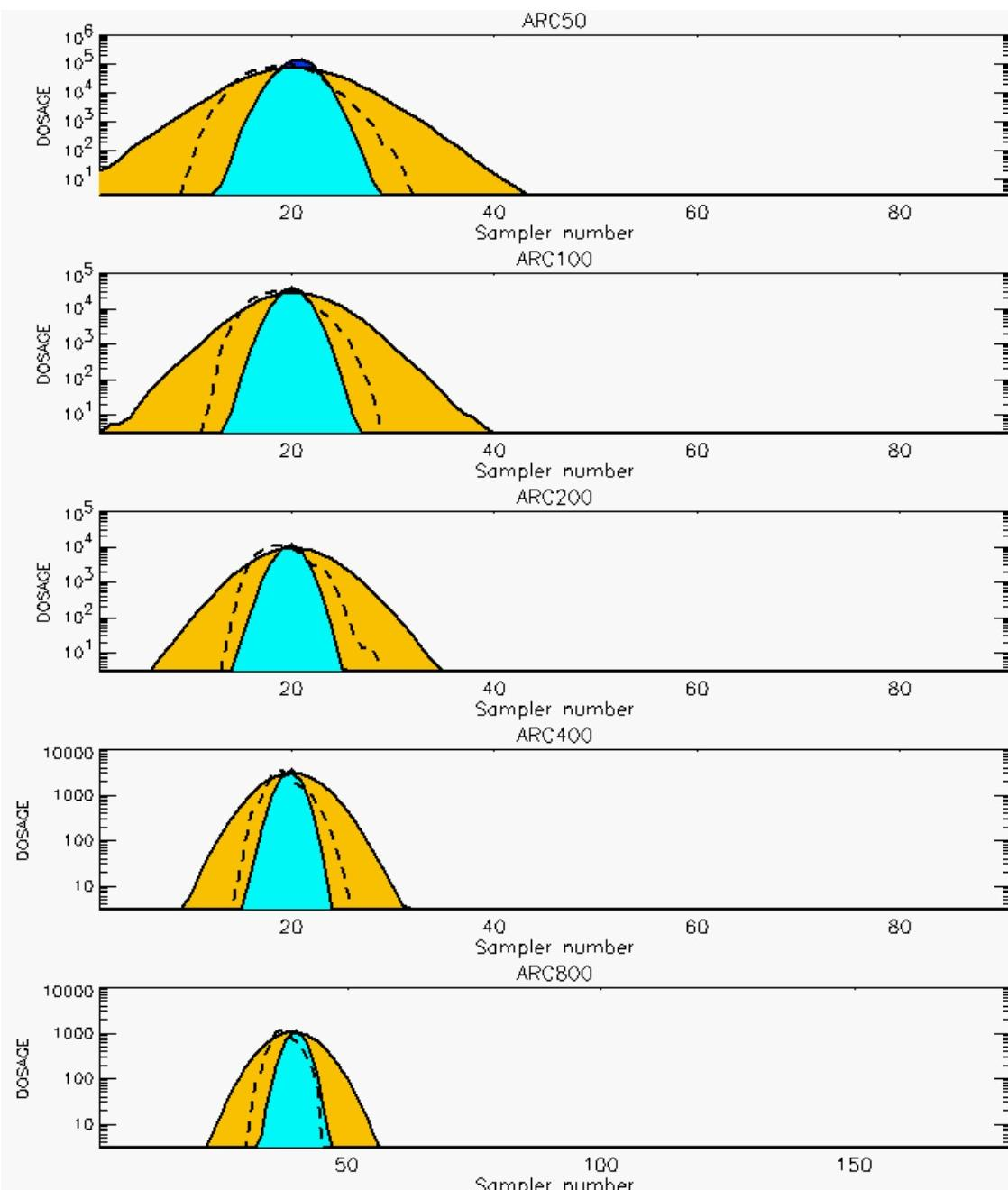
PG Prediction1 to Prediction2 Comparison

PG Trial File: pr_grass_tracer_Experiment_23.txt

PG Prediction File 1: HPAC\nodeposition\pg_23_noxd.out

PG Prediction File 2: ARAC\nodeposition\pg_23_noxd.arac

**Figure E-18a. HPAC and NARAC Predictions to Trial 23 on Linear Scale:
Stability Category is 4**



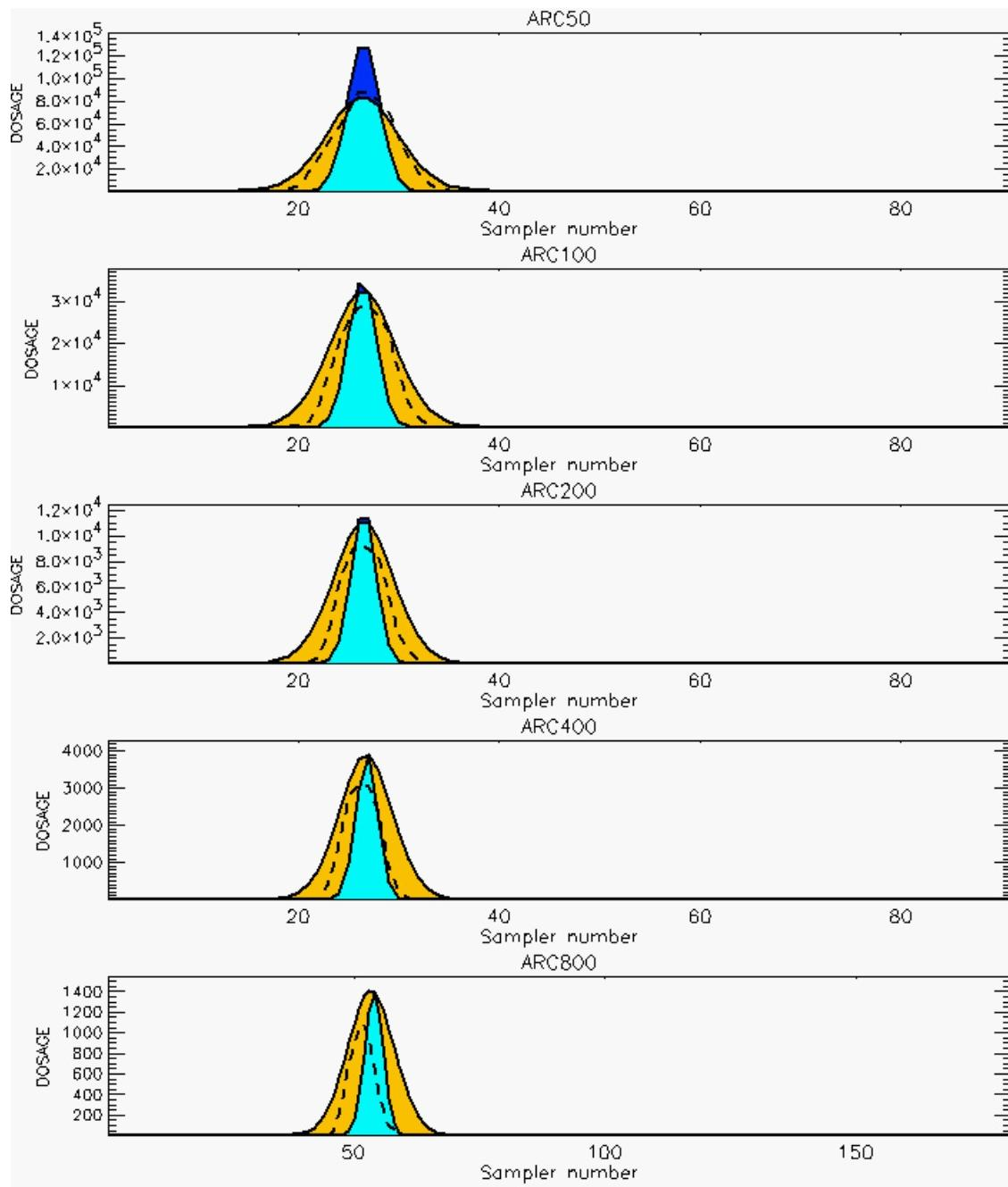
PG Prediction1 to Prediction2 Comparison

PG Trial File: pr_grass_tracer_Experiment_23.txt

PG Prediction File 1: HPAC\nodeposition\pg_23_noxd.out

PG Prediction File 2: ARAC\nodeposition\pg_23_noxd.arac

**Figure E-18b. HPAC and NARAC Predictions to Trial 23 on Logarithmic Scale:
Stability Category is 4**



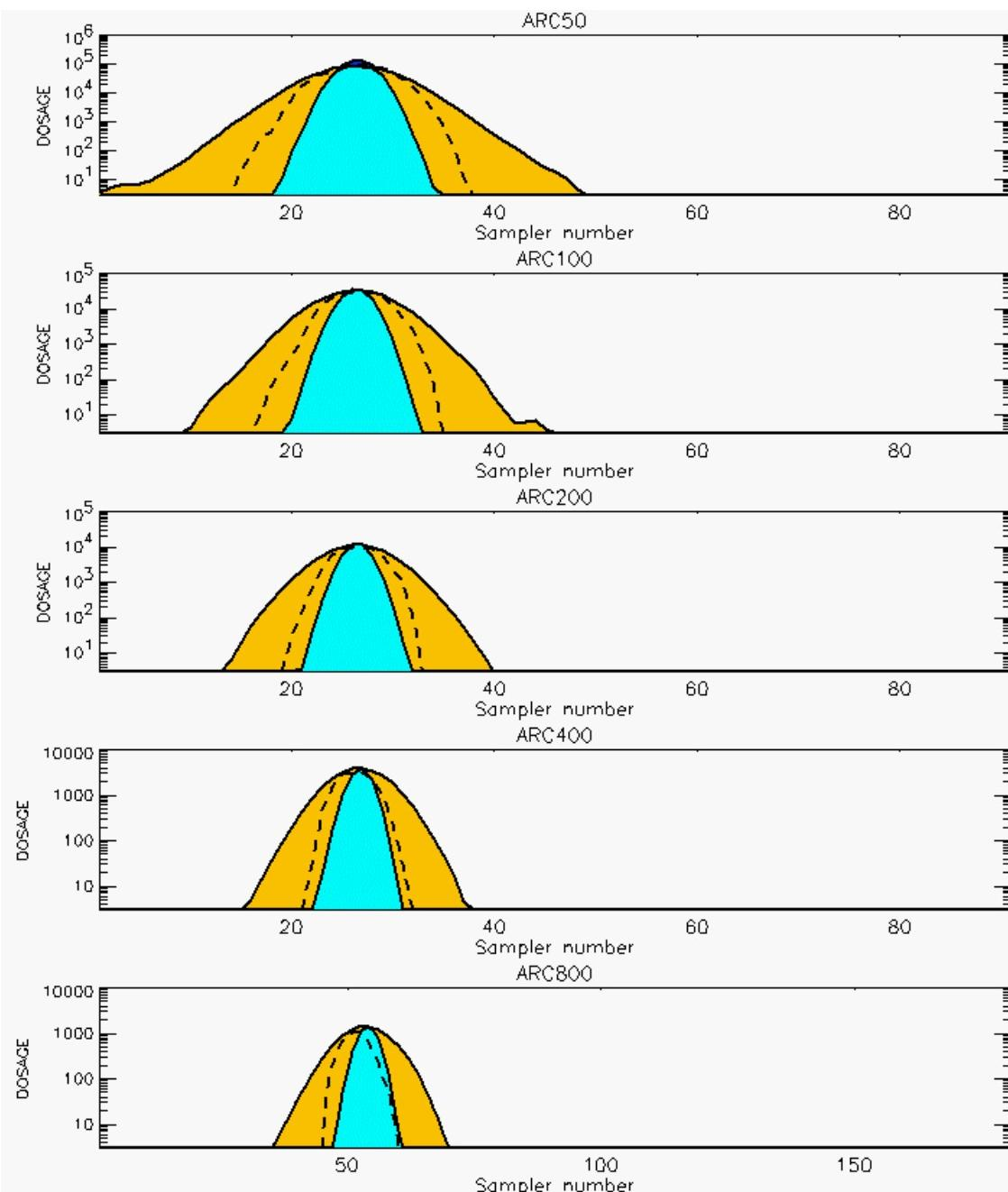
PG Prediction1 to Prediction2 Comparison

PG Trial File: pr_grass_tracer_Experiment_24.txt

PG Prediction File 1: HPAC\nodeposition\pg_24_noxd.out

PG Prediction File 2: ARAC\nodeposition\pg_24_noxd.arac

**Figure E-19a. HPAC and NARAC Predictions to Trial 24 on Linear Scale:
Stability Category is 4**



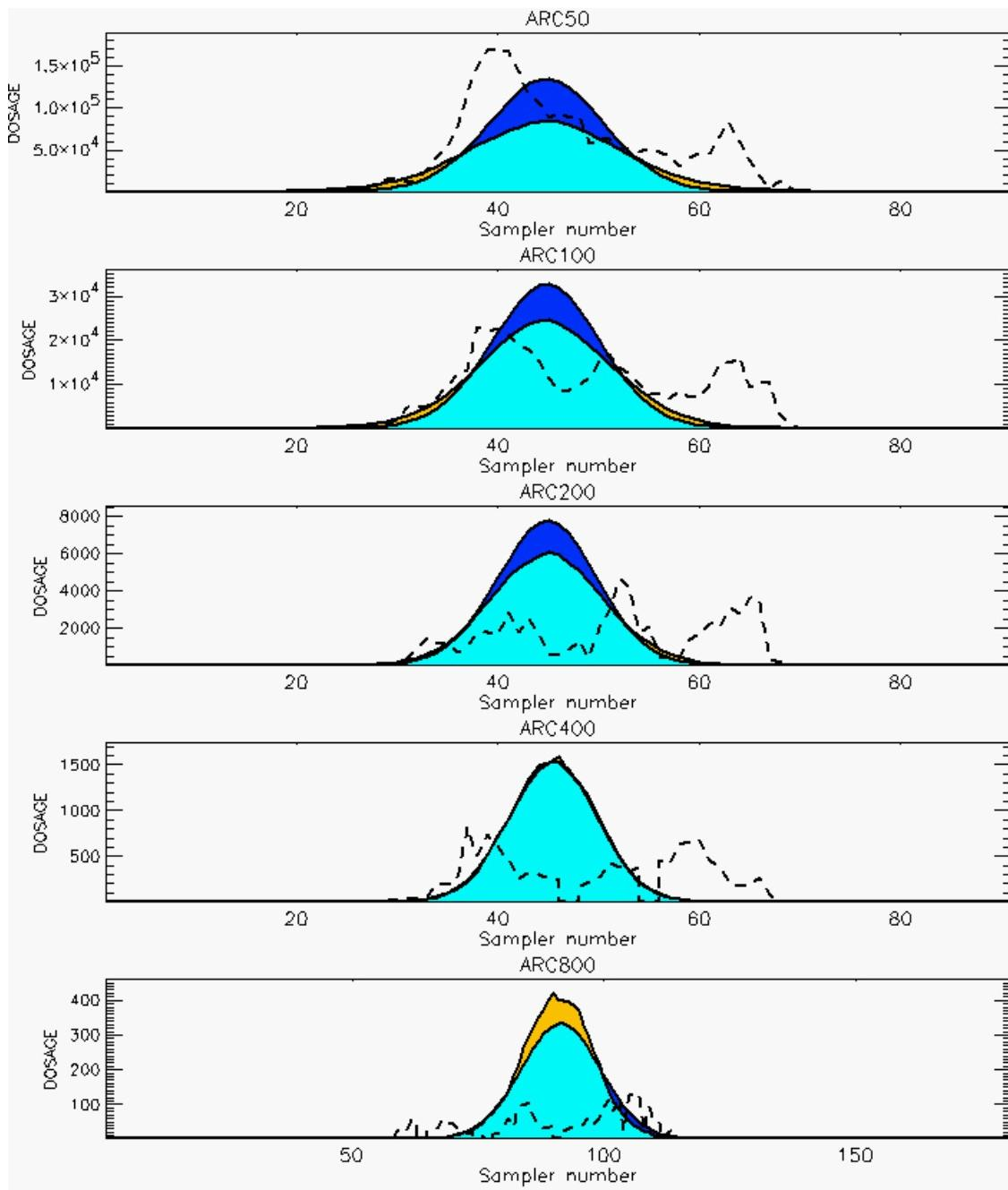
PG Prediction1 to Prediction2 Comparison

PG Trial File: pr_grass_tracer_Experiment_24.txt

PG Prediction File 1: HPAC\nodeposition\pg_24_noxd.out

PG Prediction File 2: ARAC\nodeposition\pg_24_noxd.arac

**Figure E-19b. HPAC and NARAC Predictions to Trial 24 on Logarithmic Scale:
Stability Category is 4**



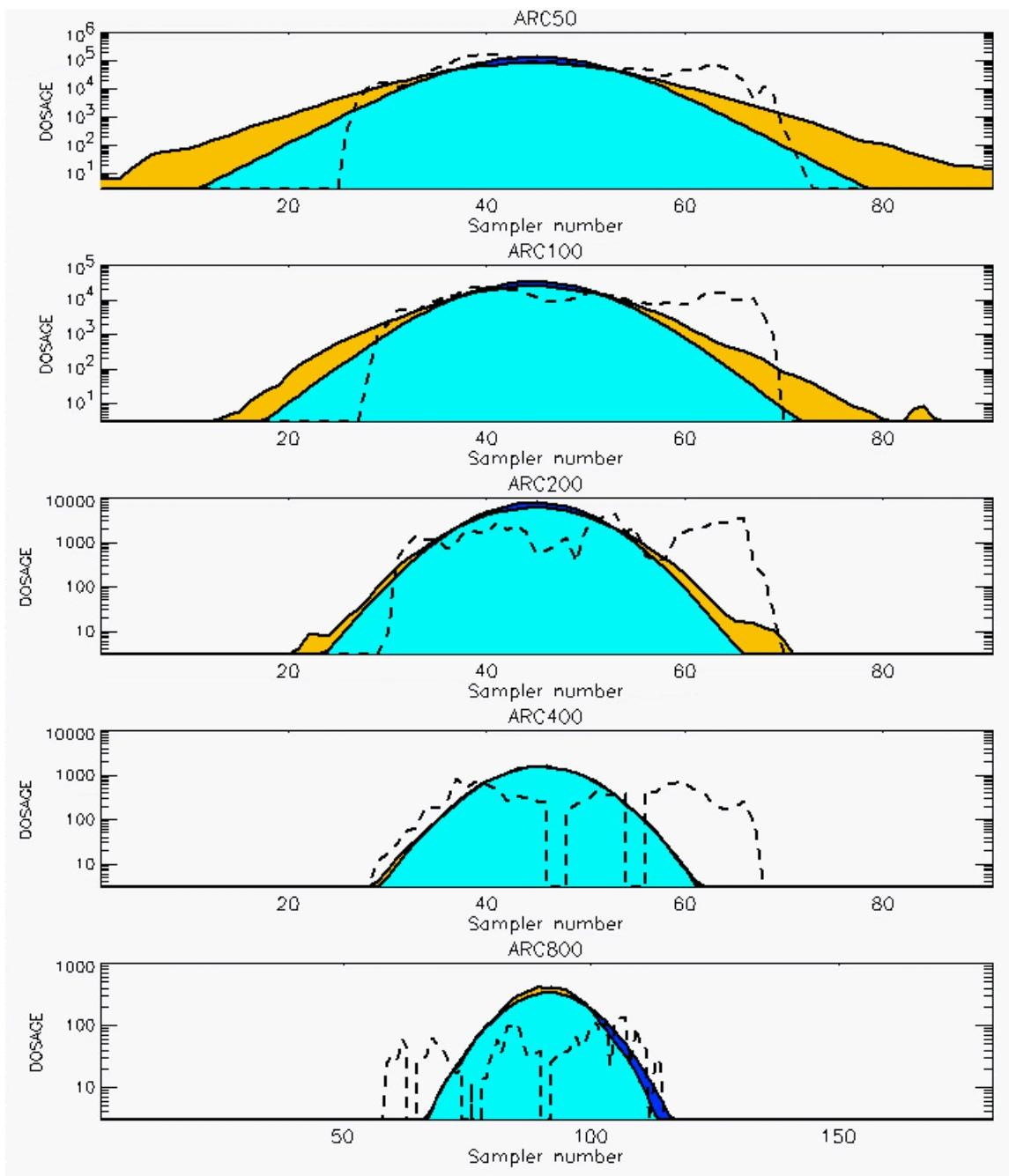
PG Prediction1 to Prediction2 Comparison

PG Trial File: pr_grass_tracer_Experiment_25.txt

PG Prediction File 1: HPAC\nodeposition\pg_25_noxd.out

PG Prediction File 2: ARAC\nodeposition\pg_25_noxd.arac

**Figure E-20a. HPAC and NARAC Predictions to Trial 25 on Linear Scale:
Stability Category is 1**



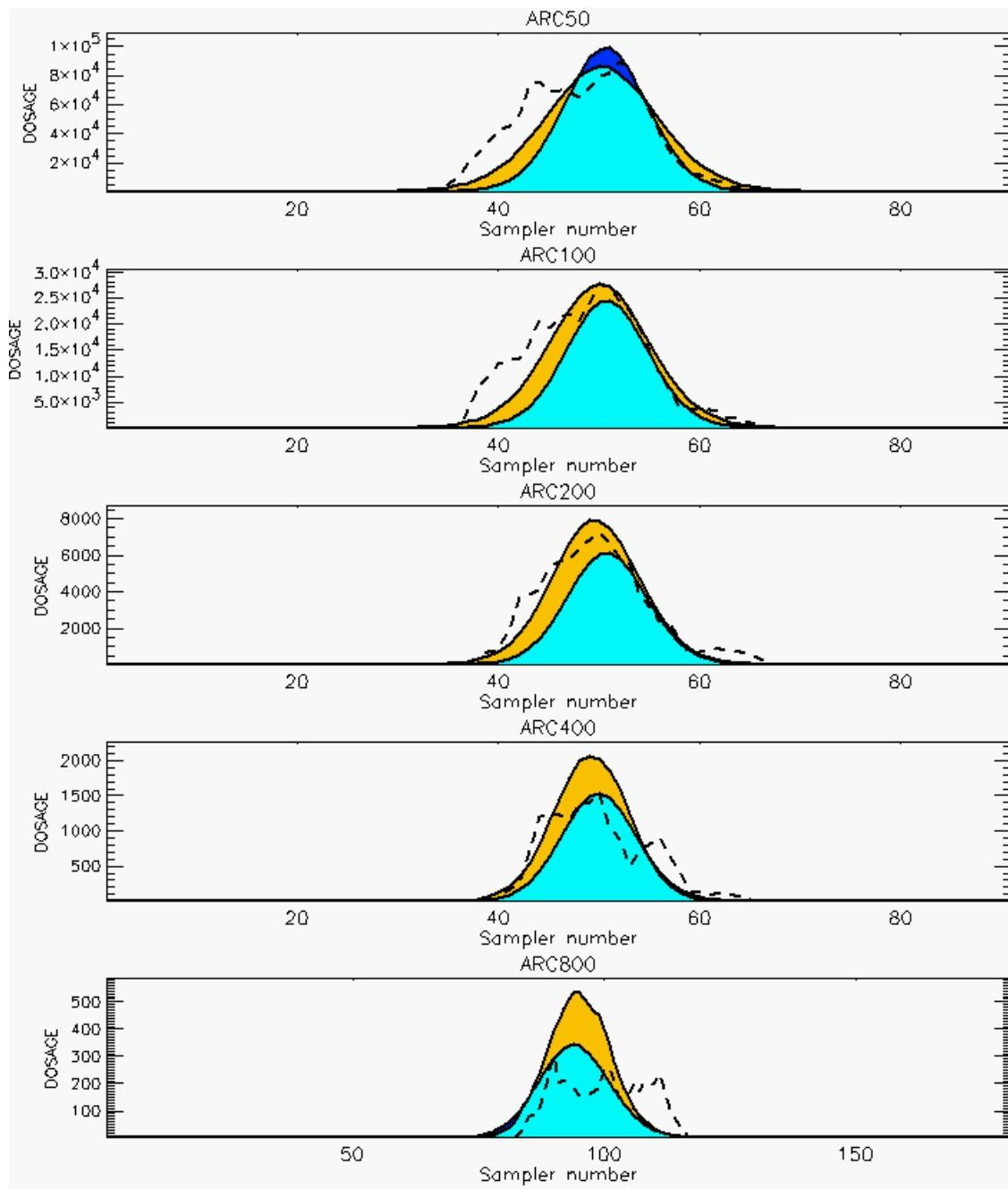
PG Prediction1 to Prediction2 Comparison

PG Trial File: pr_grass_tracer_Experiment_25.txt

PG Prediction File 1: HPAC\nodeposition\pg_25_noxd.out

PG Prediction File 2: ARAC\nodeposition\pg_25_noxd.arac

**Figure E-20b. HPAC and NARAC Predictions to Trial 25 on Logarithmic Scale:
Stability Category is 1**



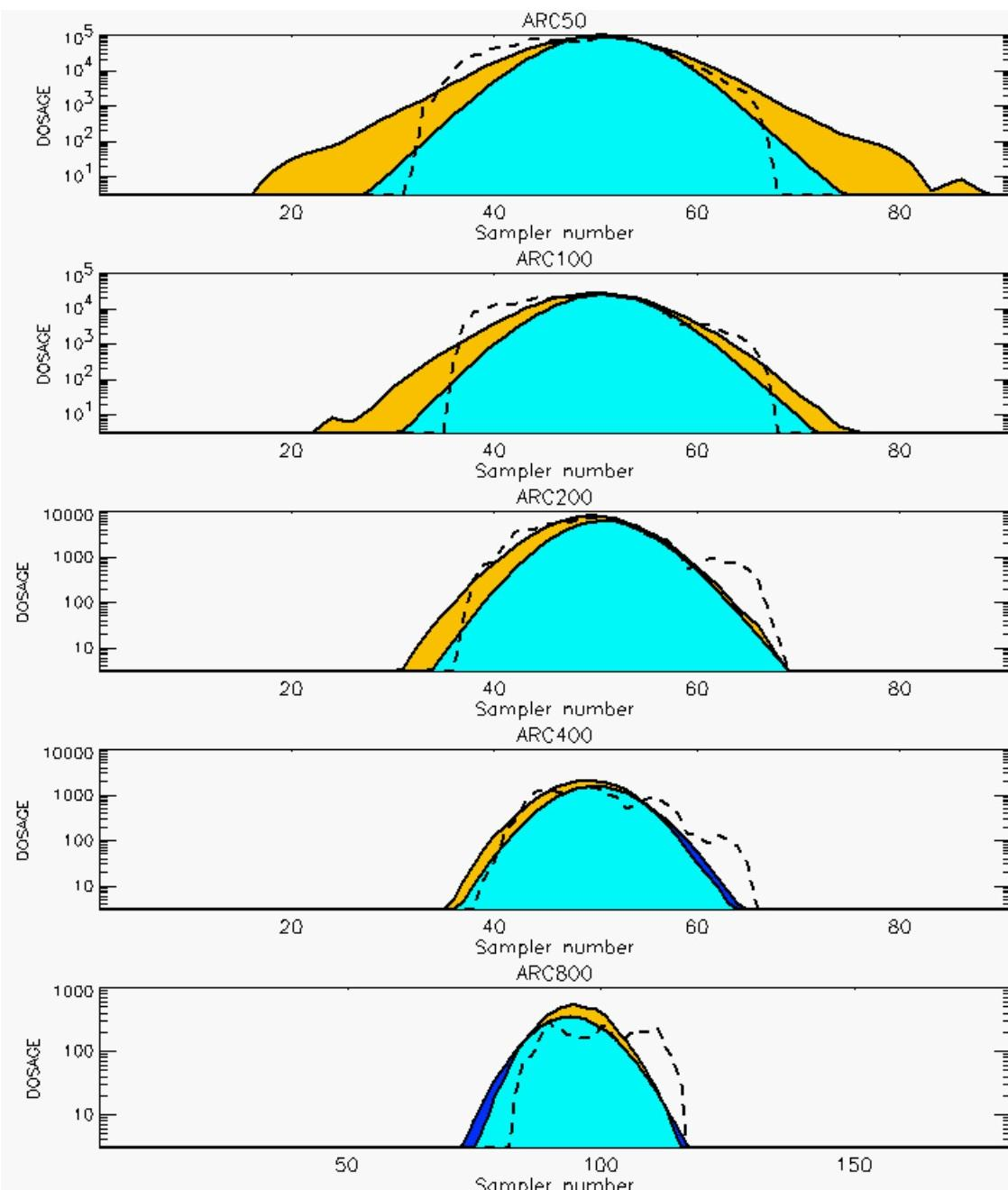
PG Prediction1 to Prediction2 Comparison

PG Trial File: pr_grass_tracer_Experiment_26.txt

PG Prediction File 1: HPAC\nodeposition\pg_26_noxd.out

PG Prediction File 2: ARAC\nodeposition\pg_26_noxd.arac

**Figure E-21a. HPAC and NARAC Predictions to Trial 26 on Linear Scale:
Stability Category is 2**



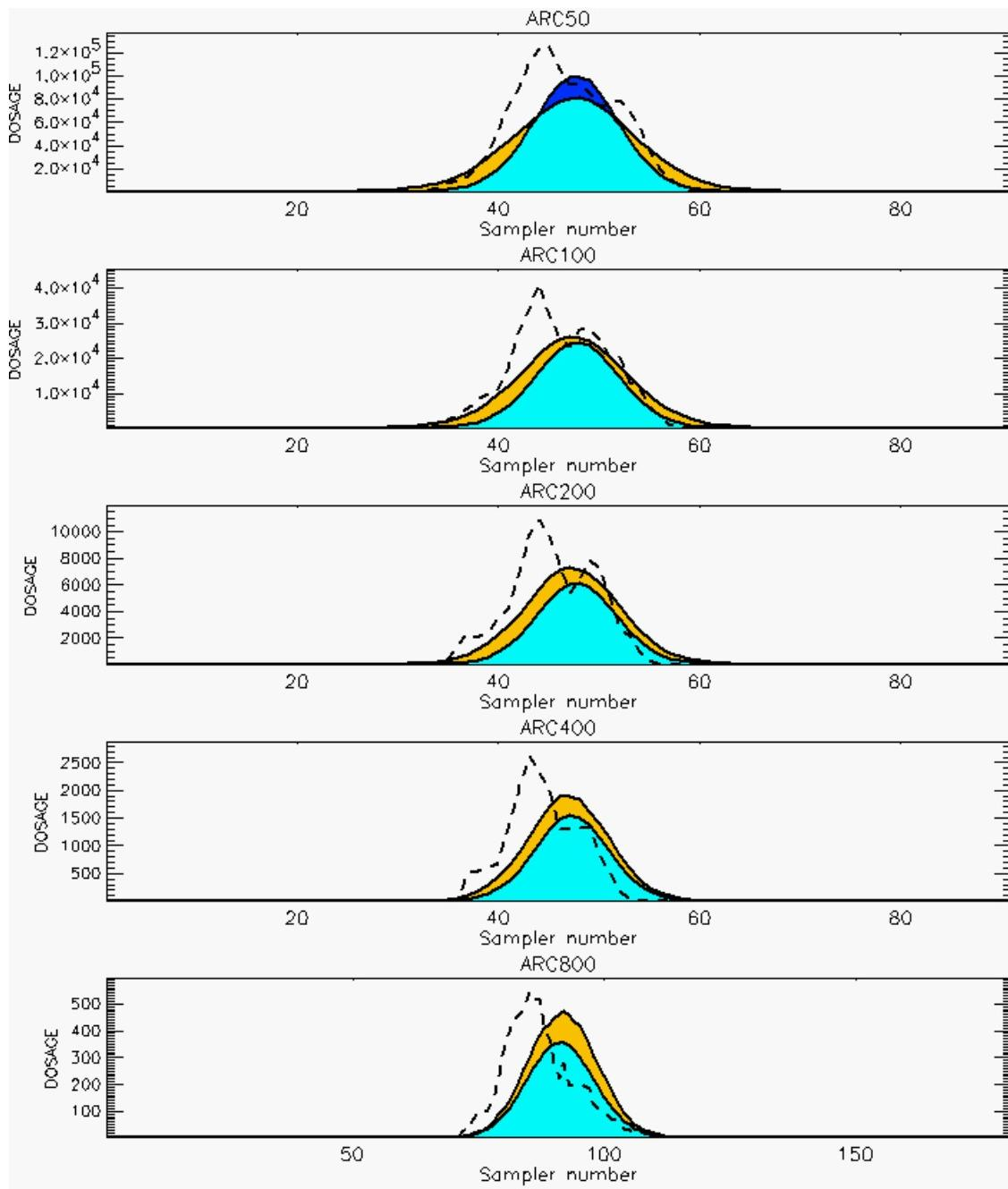
PG Prediction1 to Prediction2 Comparison

PG Trial File: pr_grass_tracer_Experiment_26.txt

PG Prediction File 1: HPAC\nodeposition\pg_26_nozd.out

PG Prediction File 2: ARAC\nodeposition\pg_26_nozd.arac

**Figure E-21b. HPAC and NARAC Predictions to Trial 26 on Logarithmic Scale:
Stability Category is 2**



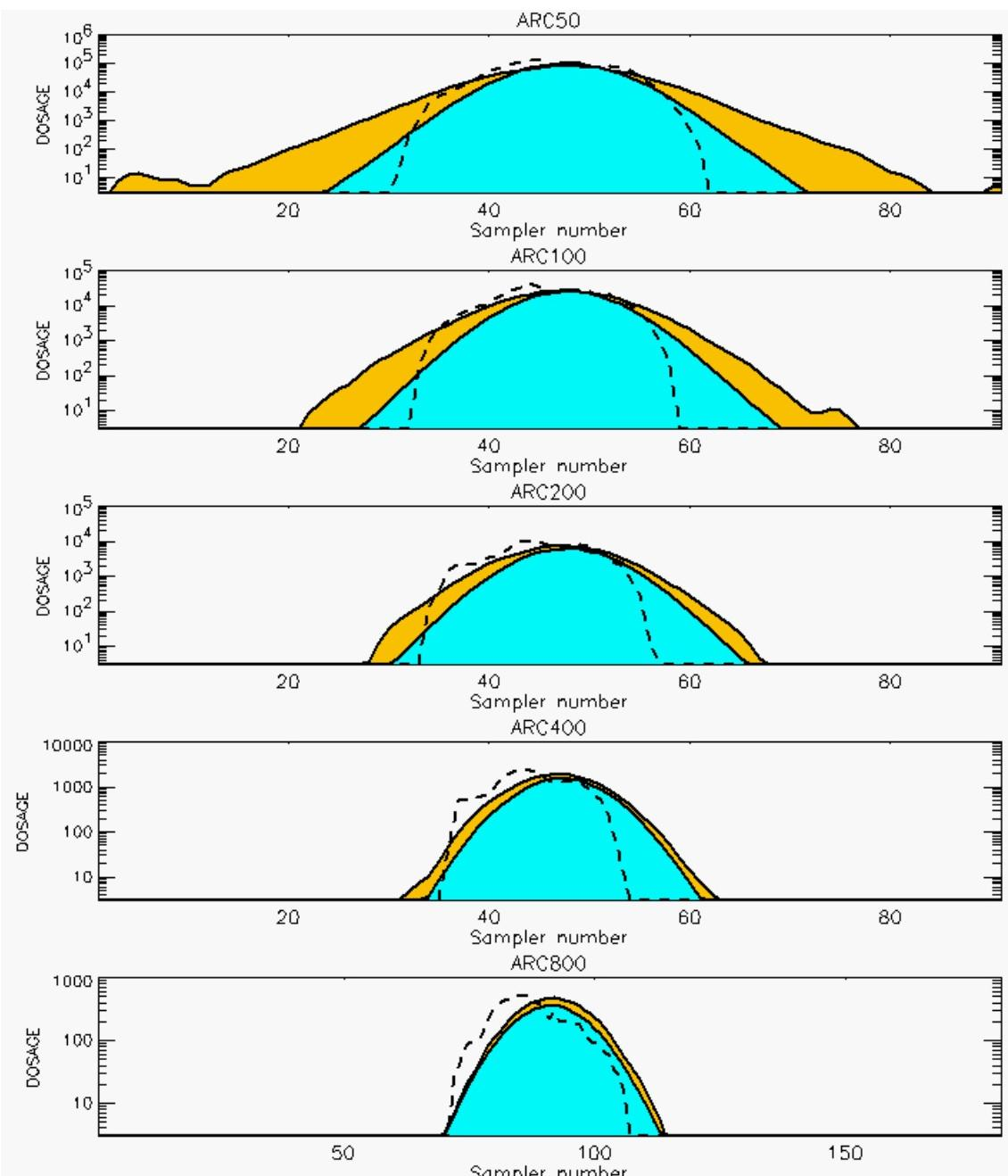
PG Prediction1 to Prediction2 Comparison

PG Trial File: pr_grass_tracer_Experiment_27.txt

PG Prediction File 1: HPAC\nodeposition\pg_27_noxd.out

PG Prediction File 2: ARAC\nodeposition\pg_27_noxd.arac

**Figure E-22a. HPAC and NARAC Predictions to Trial 27 on Linear Scale:
Stability Category is 2**



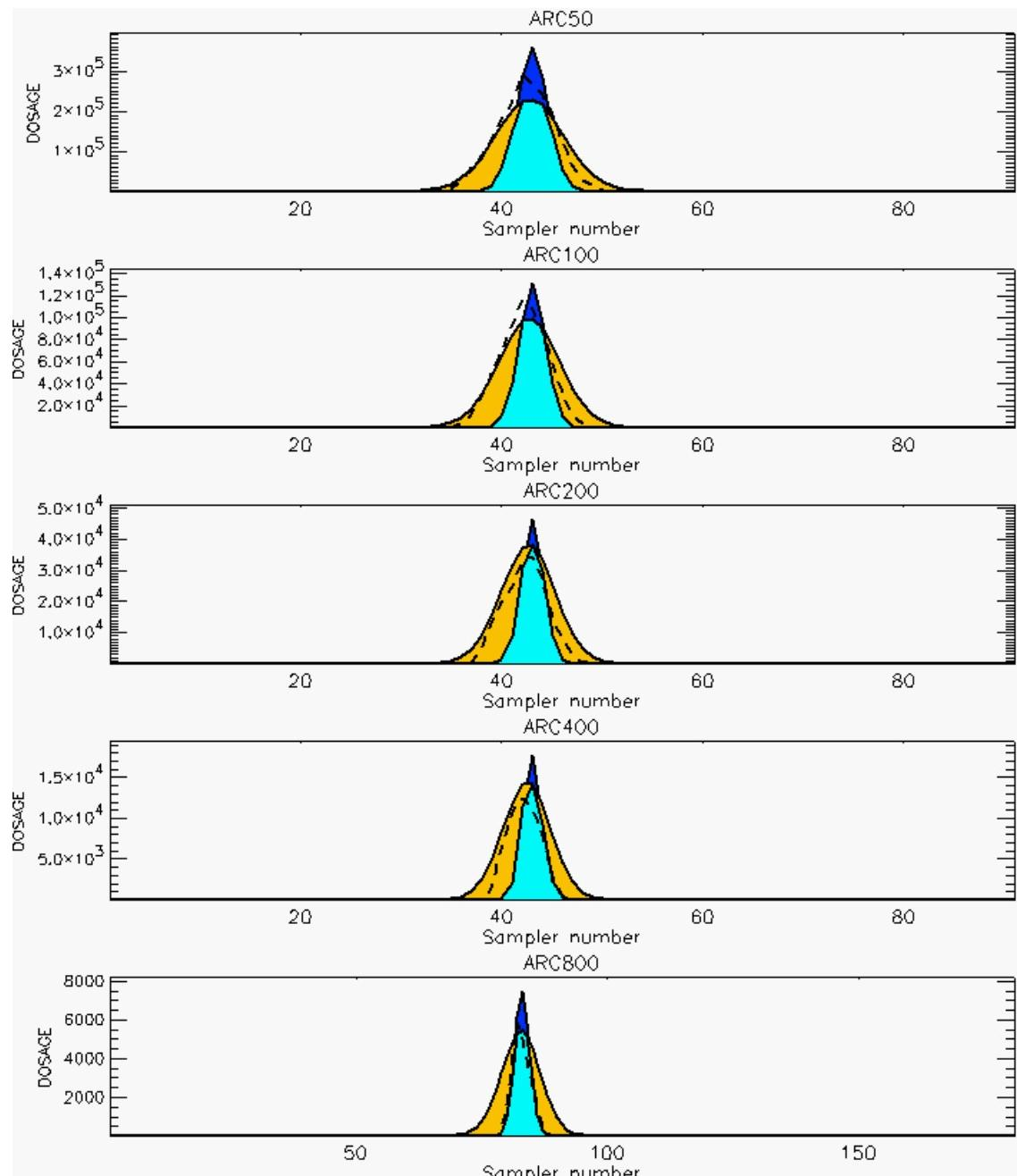
PG Prediction1 to Prediction2 Comparison

PG Trial File: pr_grass_tracer_Experiment_27.txt

PG Prediction File 1: HPAC\nodeposition\pg_27_noxd.out

PG Prediction File 2: ARAC\nodeposition\pg_27_noxd.arac

**Figure E-22b. HPAC and NARAC Predictions to Trial 27 on Logarithmic Scale:
Stability Category is 2**



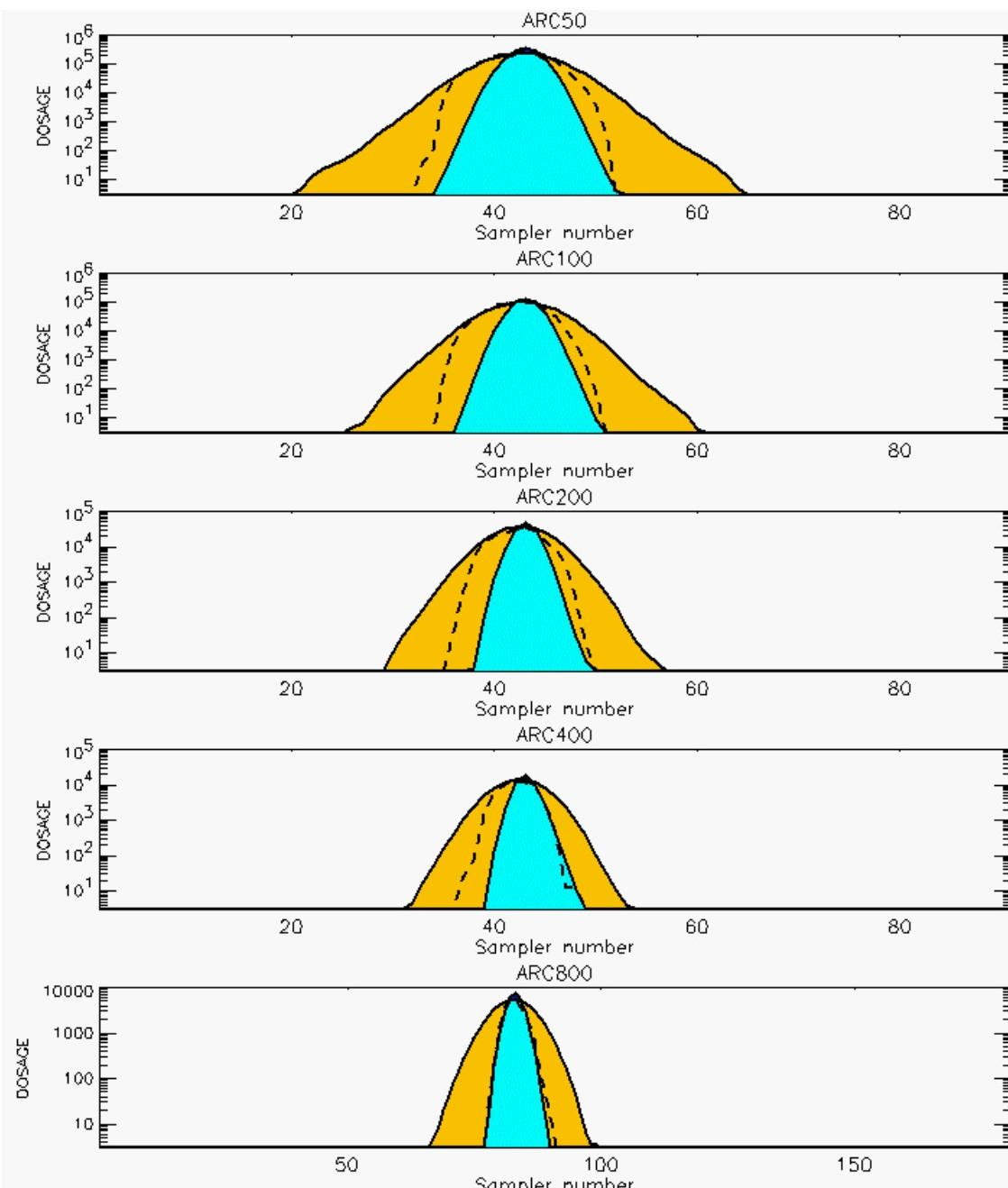
PG Prediction1 to Prediction2 Comparison

PG Trial File: pr_grass_tracer_Experiment_28.txt

PG Prediction File 1: HPAC\nodeposition\pg_28_noxd.out

PG Prediction File 2: ARAC\nodeposition\pg_28_noxd.arac

**Figure E-23a. HPAC and NARAC Predictions to Trial 28 on Linear Scale:
Stability Category is 5**



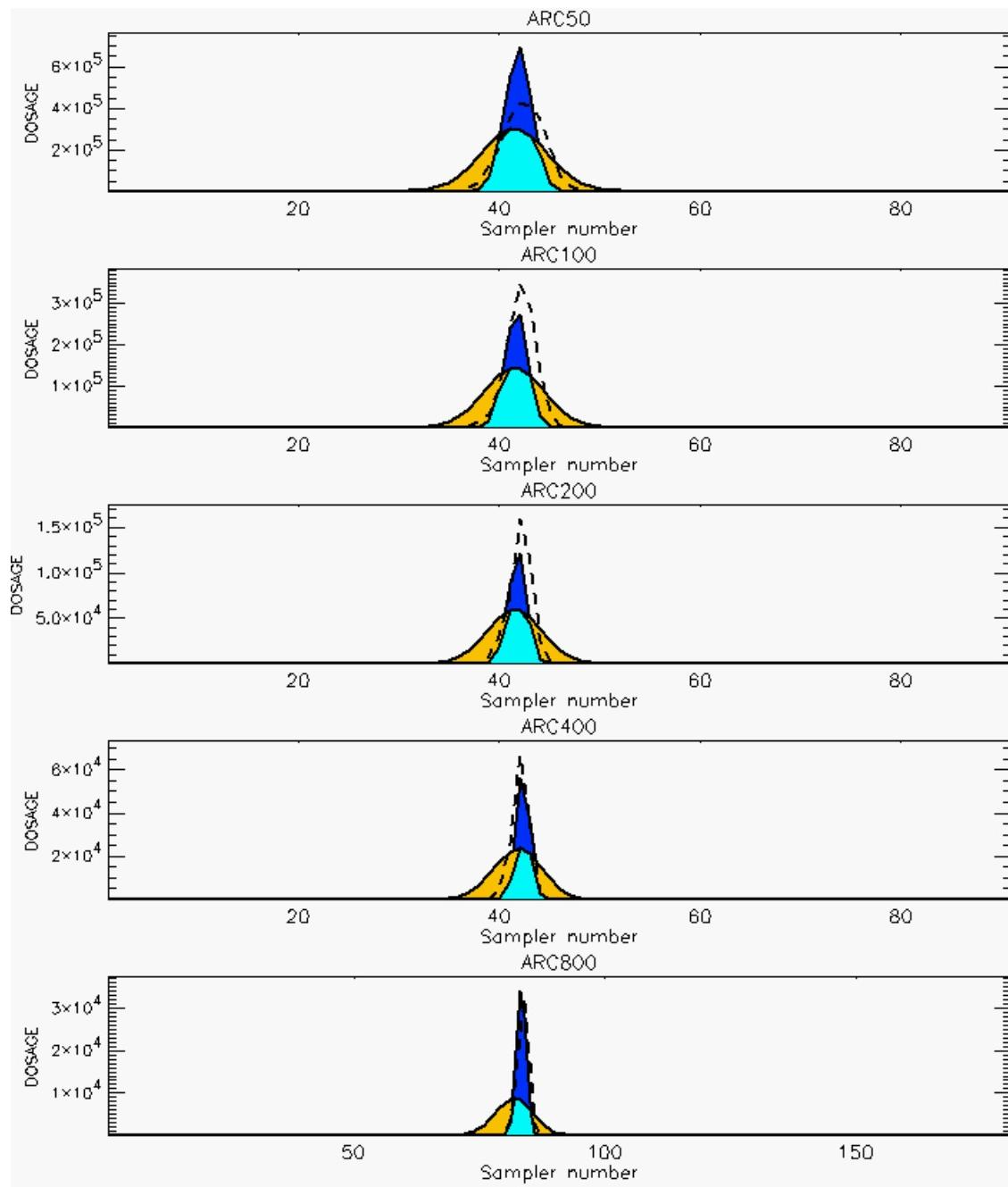
PG Prediction1 to Prediction2 Comparison

PG Trial File: pr_grass_tracer_Experiment_28.txt

PG Prediction File 1: HPAC\nodeposition\pg_28_noxd.out

PG Prediction File 2: ARAC\nodeposition\pg_28_noxd.arac

**Figure E-23b. HPAC and NARAC Predictions to Trial 28 on Logarithmic Scale:
Stability Category is 5**



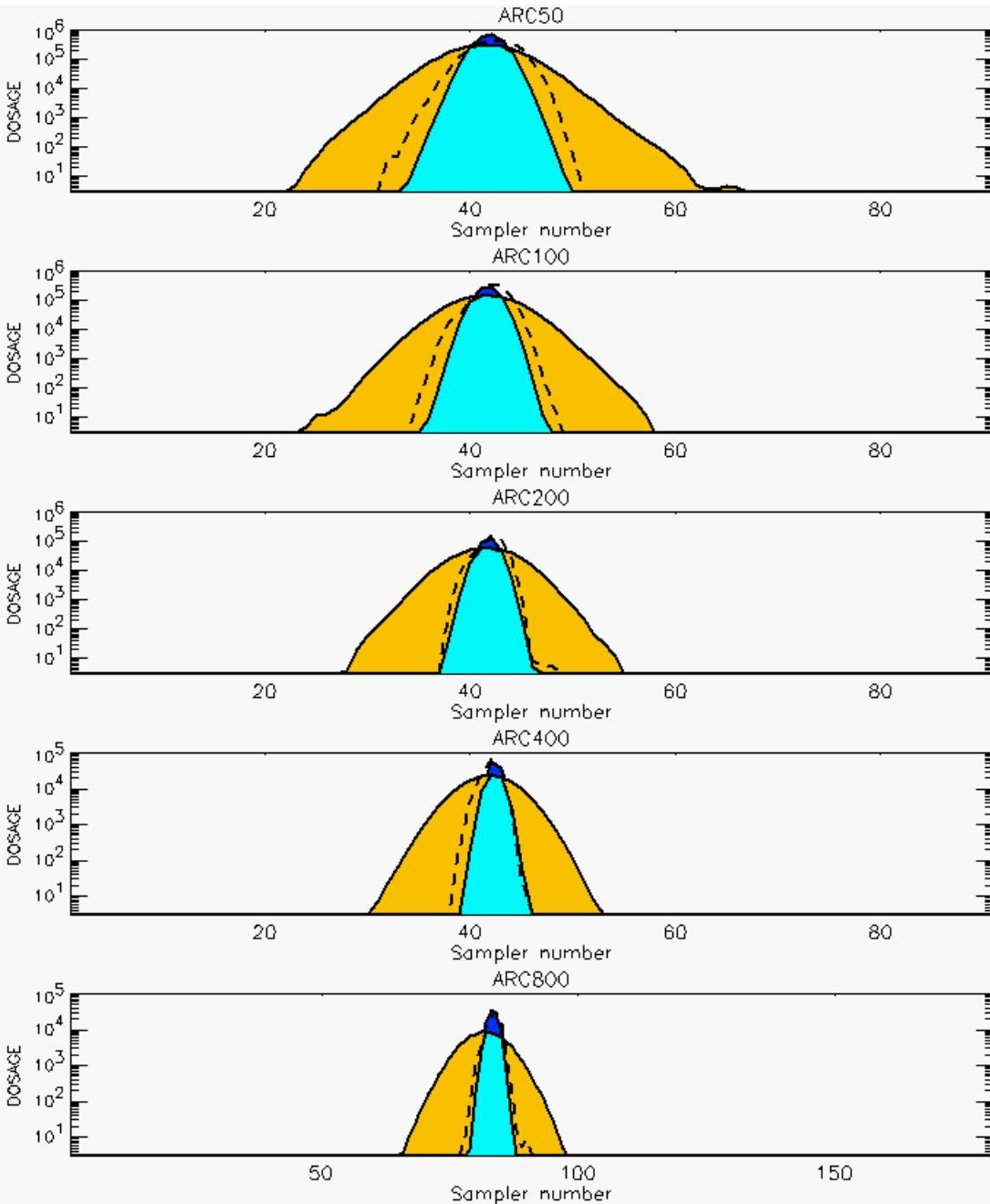
PG Prediction1 to Prediction2 Comparison

PG Trial File: pr_grass_tracer_Experiment_32.txt

PG Prediction File 1: HPAC\nodeposition\pg_32_noxd.out

PG Prediction File 2: ARAC\nodeposition\pg_32_noxd.arac

**Figure E-24a. HPAC and NARAC Predictions to Trial 32 on Linear Scale:
Stability Category is 6**



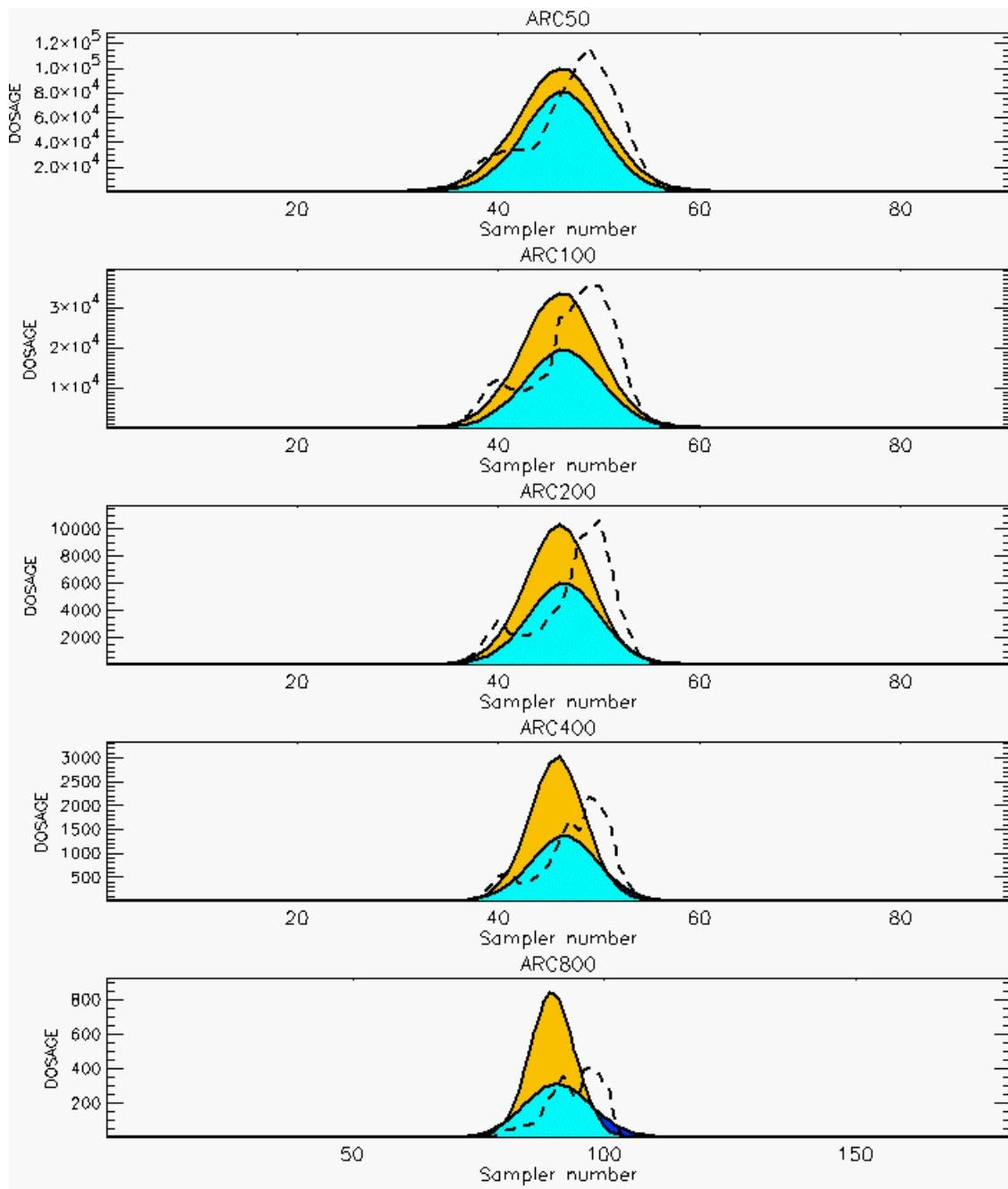
PG Prediction1 to Prediction2 Comparison

PG Trial File: pr_grass_tracer_Experiment_32.txt

PG Prediction File 1: HPAC\nodeposition\pg_32_noxd.out

PG Prediction File 2: ARAC\nodeposition\pg_32_noxd.arac

**Figure E-24b. HPAC and NARAC Predictions to Trial 32 on Logarithmic Scale:
Stability Category is 6**



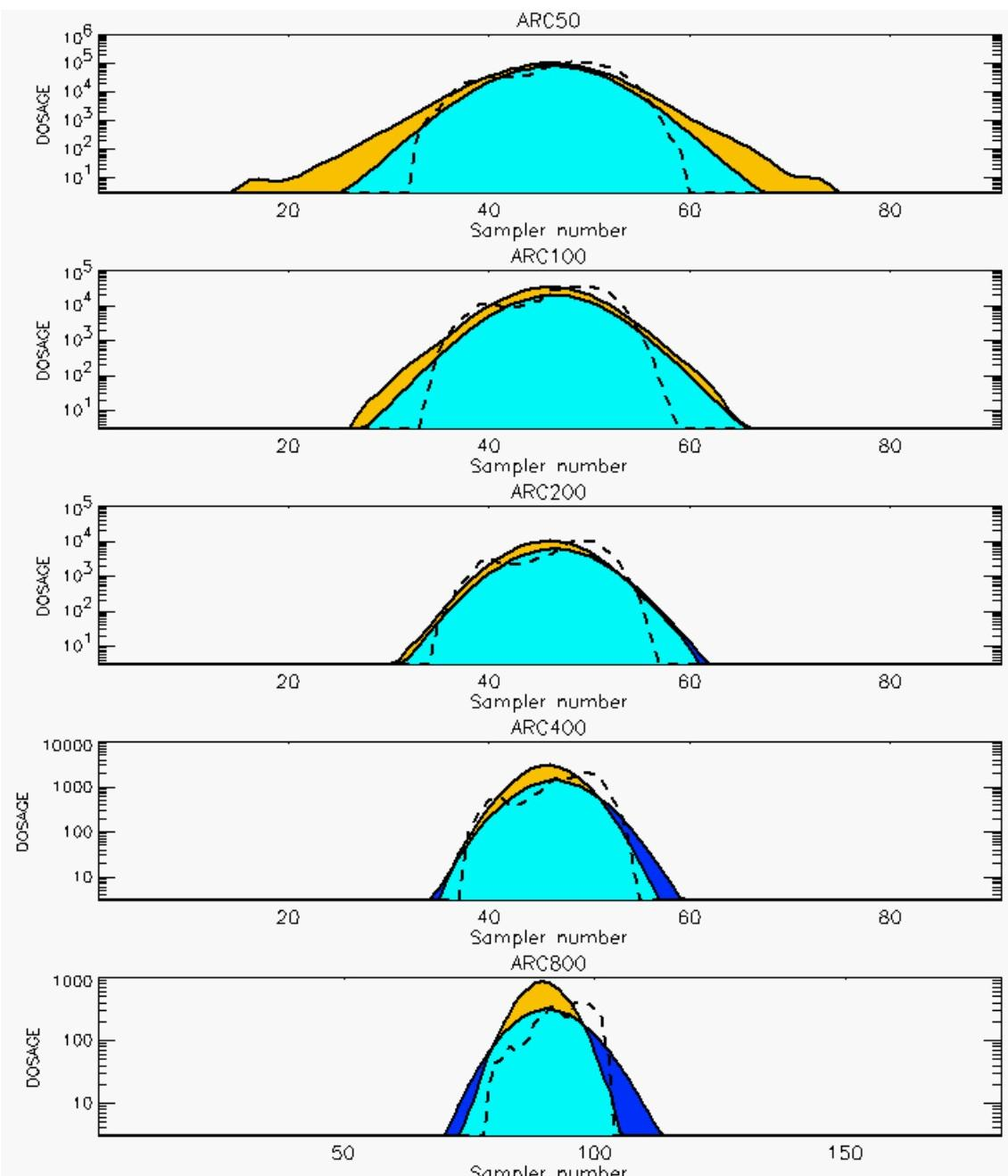
PG Prediction1 to Prediction2 Comparison

PG Trial File: pr_grass_tracer_Experiment_33.txt

PG Prediction File 1: HPAC\nodeposition\pg_33_noxd.out

PG Prediction File 2: ARAC\nodeposition\pg_33_noxd.arac

**Figure E-25a. HPAC and NARAC Predictions to Trial 33 on Linear Scale:
Stability Category is 3**



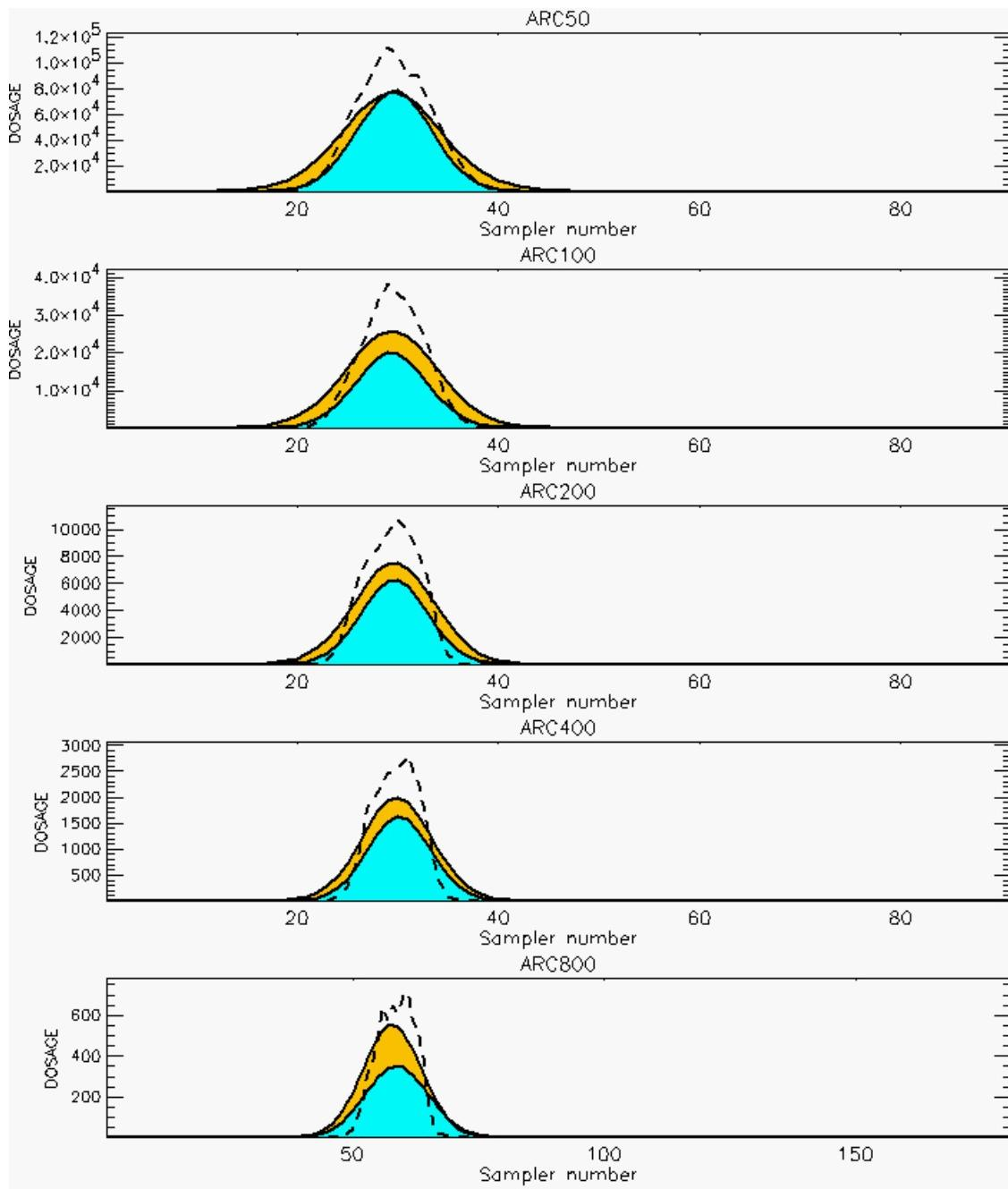
PG Prediction1 to Prediction2 Comparison

PG Trial File: pr_grass_tracer_Experiment_33.txt

PG Prediction File 1: HPAC\nodeposition\pg_33_noxd.out

PG Prediction File 2: ARAC\nodeposition\pg_33_noxd.arac

**Figure E-25b. HPAC and NARAC Predictions to Trial 33 on Logarithmic Scale:
Stability Category is 3**



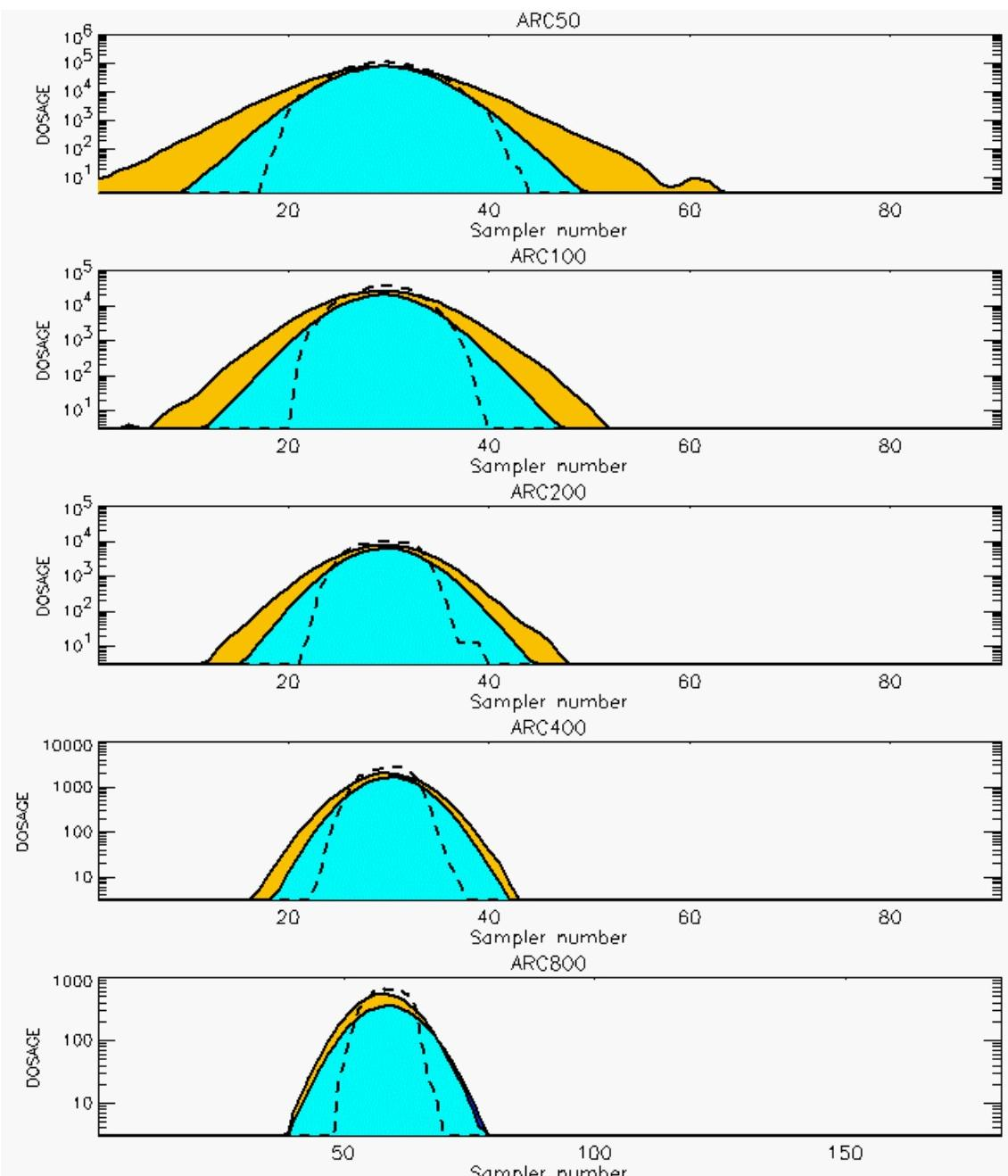
PG Prediction1 to Prediction2 Comparison

PG Trial File: pr_grass_tracer_Experiment_34.txt

PG Prediction File 1: HPAC\nodeposition\pg_34_noxd.out

PG Prediction File 2: ARAC\nodeposition\pg_34_noxd.arac

**Figure E-26a. HPAC and NARAC Predictions to Trial 34 on Linear Scale:
Stability Category is 3**



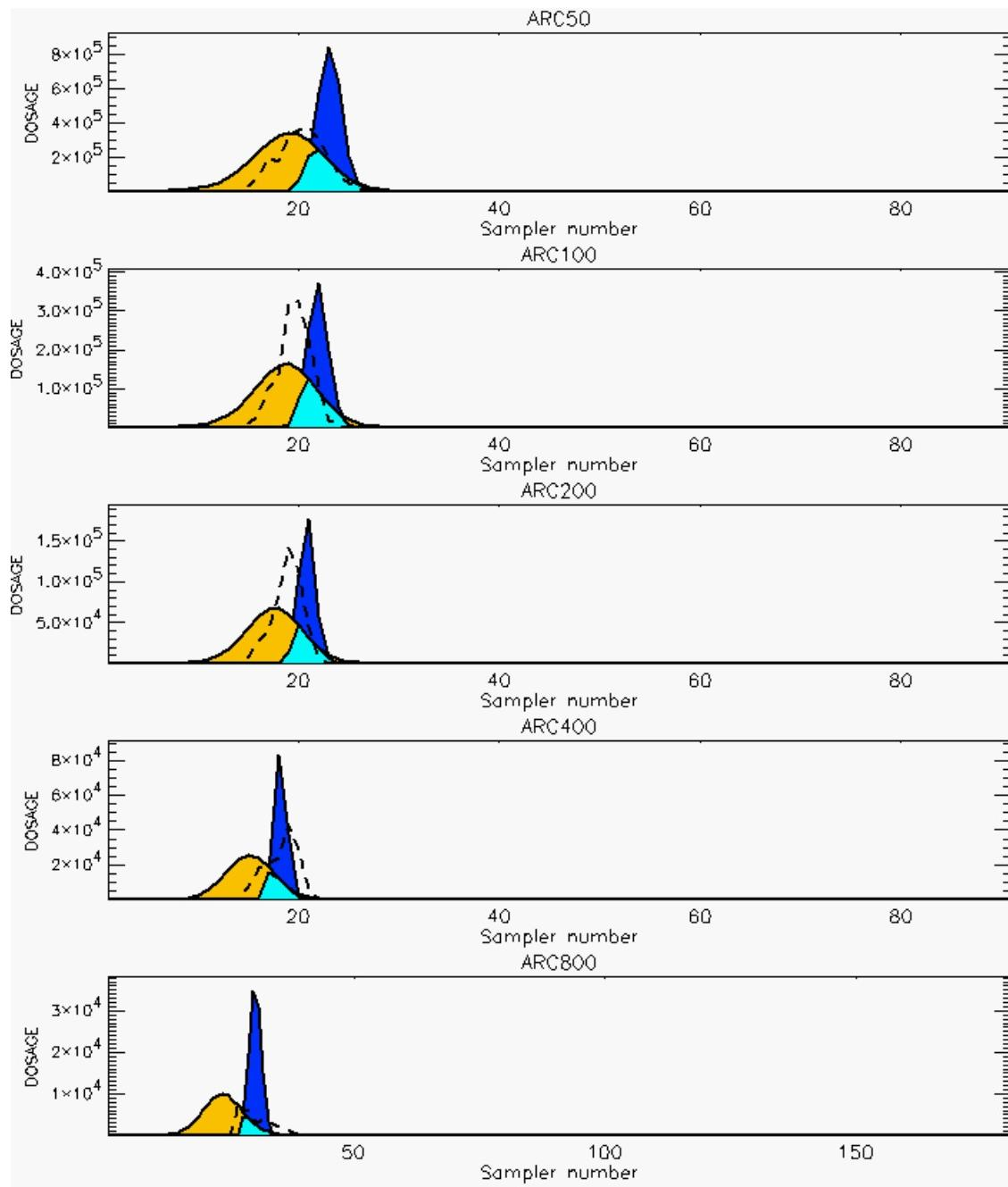
PG Prediction1 to Prediction2 Comparison

PG Trial File: pr_grass_tracer_Experiment_34.txt

PG Prediction File 1: HPAC\nodeposition\pg_34_noxd.out

PG Prediction File 2: ARAC\nodeposition\pg_34_noxd.arac

**Figure E-26b. HPAC and NARAC Predictions to Trial 34 on Logarithmic Scale:
Stability Category is 3**



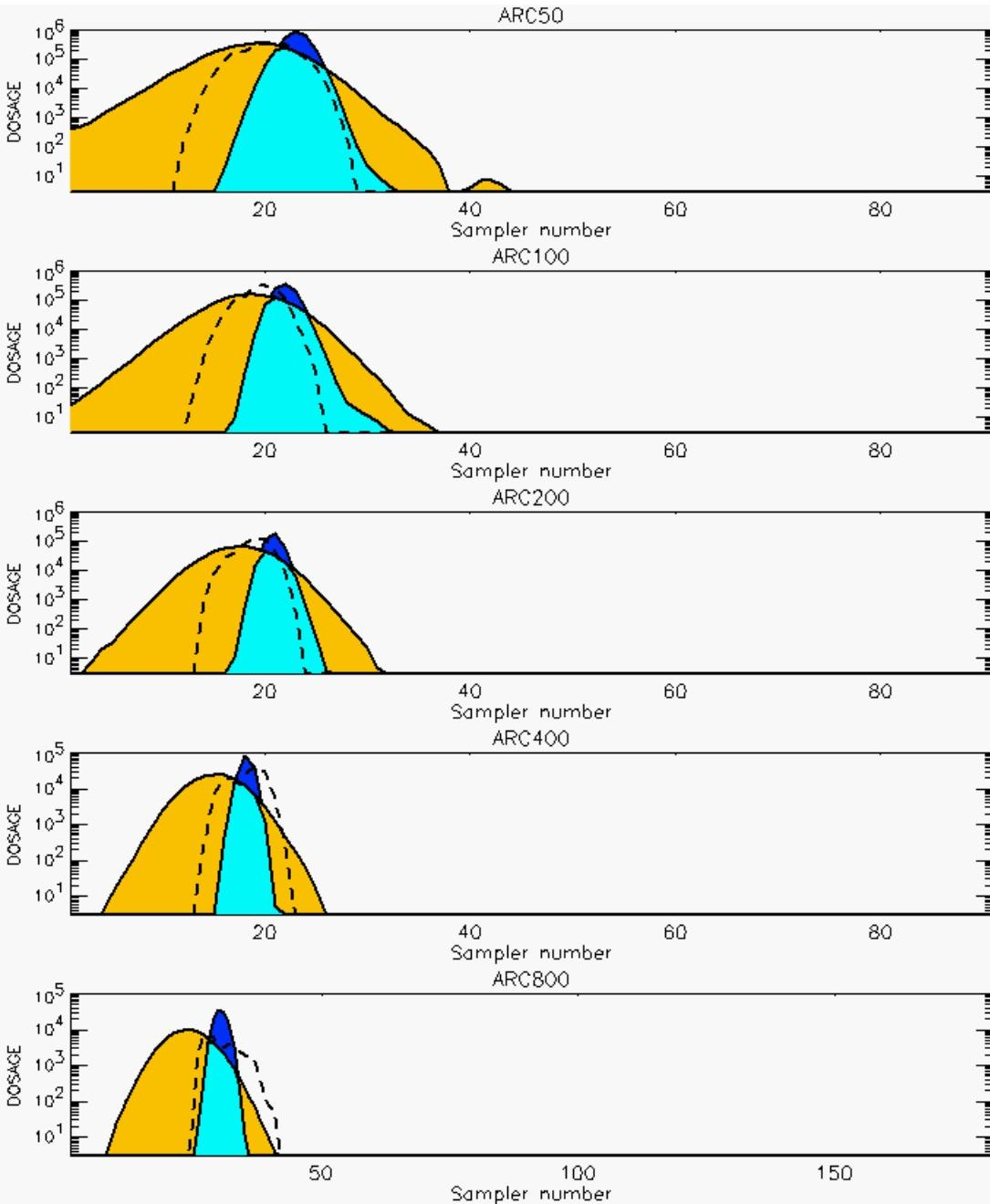
PG Prediction1 to Prediction2 Comparison

PG Trial File: pr_grass_tracer_Experiment_35.txt

PG Prediction File 1: HPAC\nodeposition\pg_35_noxd.out

PG Prediction File 2: ARAC\nodeposition\pg_35_noxd.arac

**Figure E-27a. HPAC and NARAC Predictions to Trial 35 on Linear Scale:
Stability Category is 6**



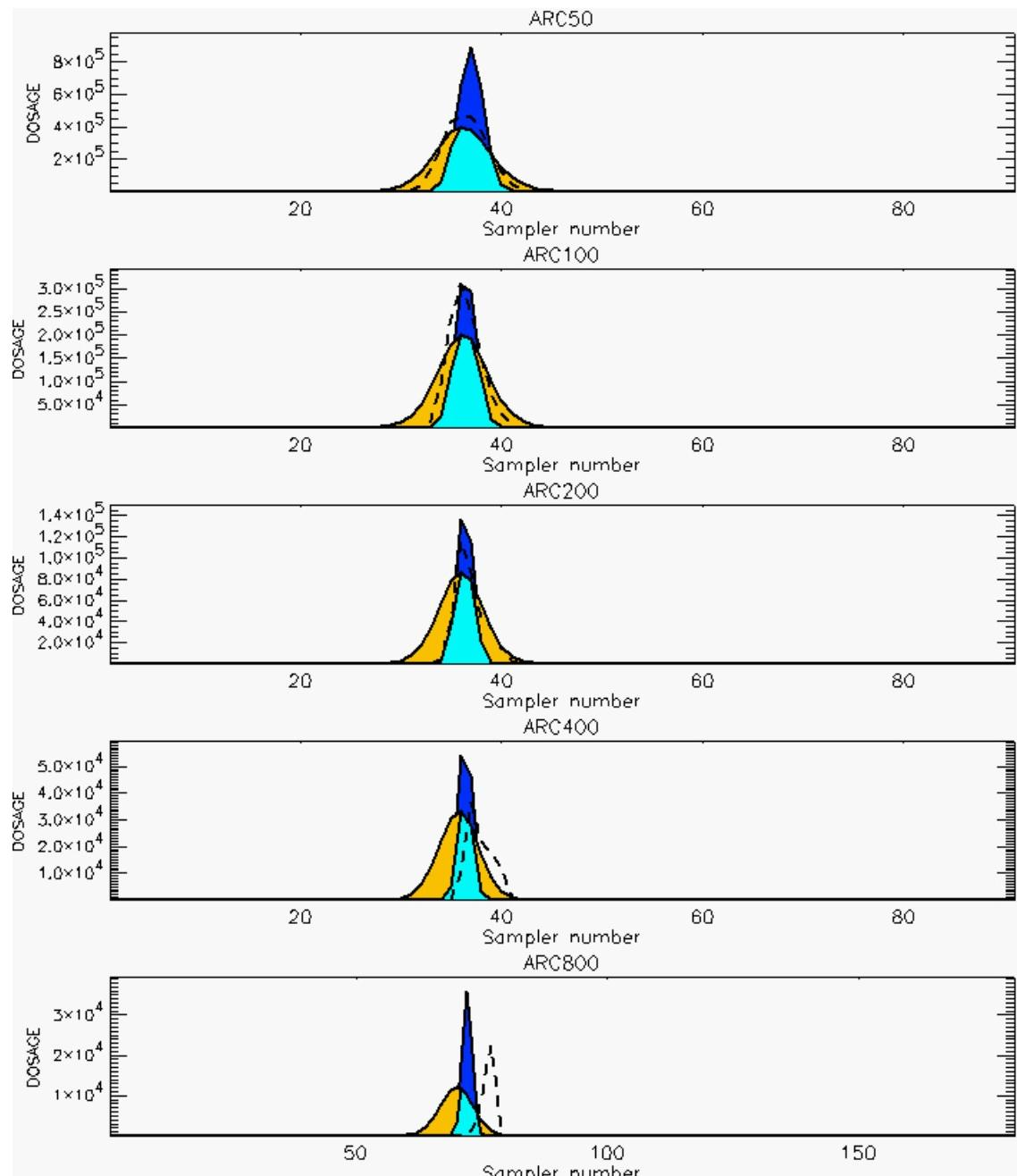
PG Prediction1 to Prediction2 Comparison

PG Trial File: pr_grass_tracer_Experiment_35.txt

PG Prediction File 1: HPAC\nodeposition\pg_35_noxd.out

PG Prediction File 2: ARAC\nodeposition\pg_35_noxd.arac

**Figure E-27b. HPAC and NARAC Predictions to Trial 35 on Logarithmic Scale:
Stability Category is 6**



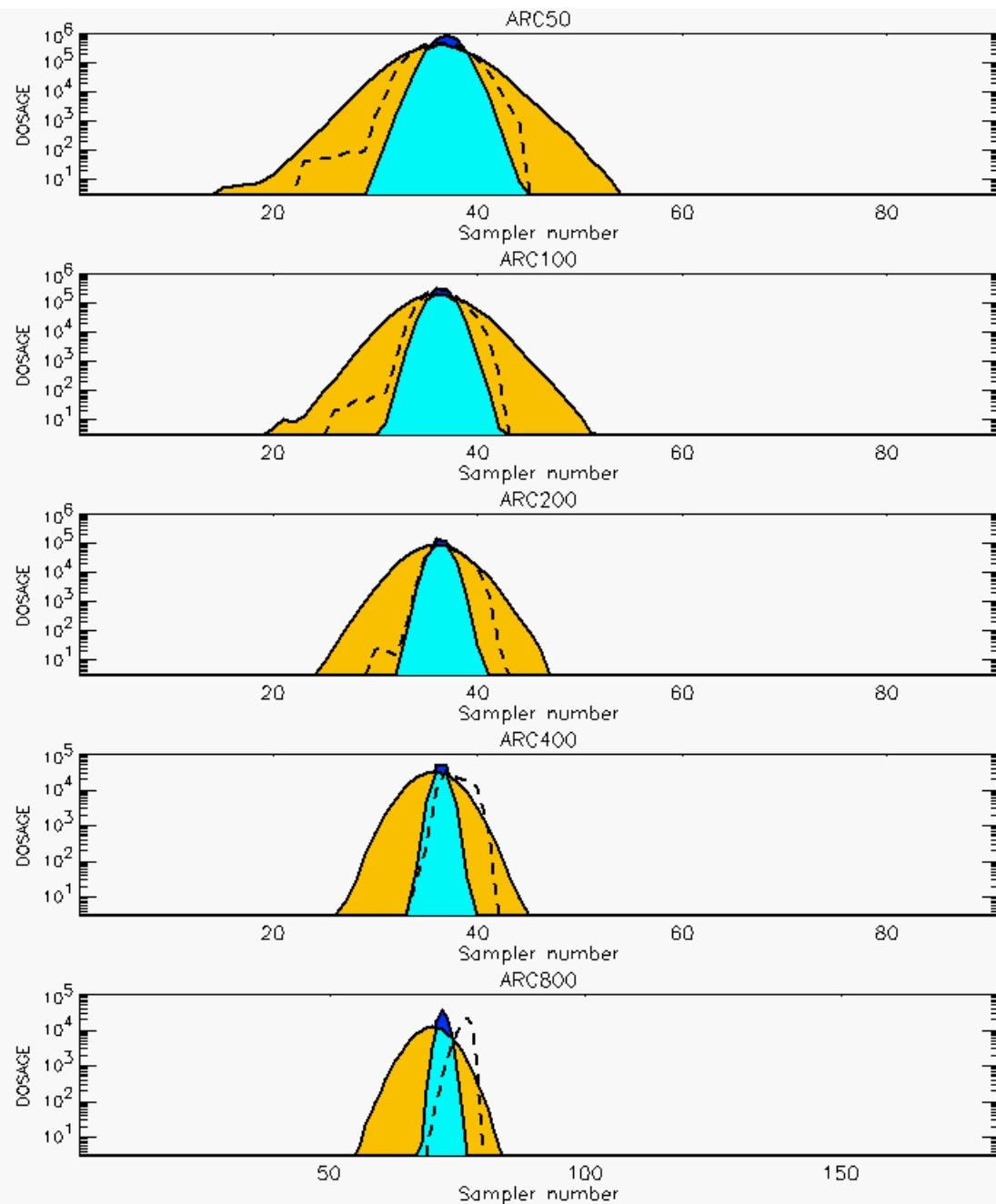
PG Prediction1 to Prediction2 Comparison

PG Trial File: pr_grass_tracer_Experiment_36.txt

PG Prediction File 1: HPAC\nodeposition\pg_36_noxd.out

PG Prediction File 2: ARAC\nodeposition\pg_36_noxd.arac

**Figure E-28a. HPAC and NARAC Predictions to Trial 36 on Linear Scale:
Stability Category is 6**



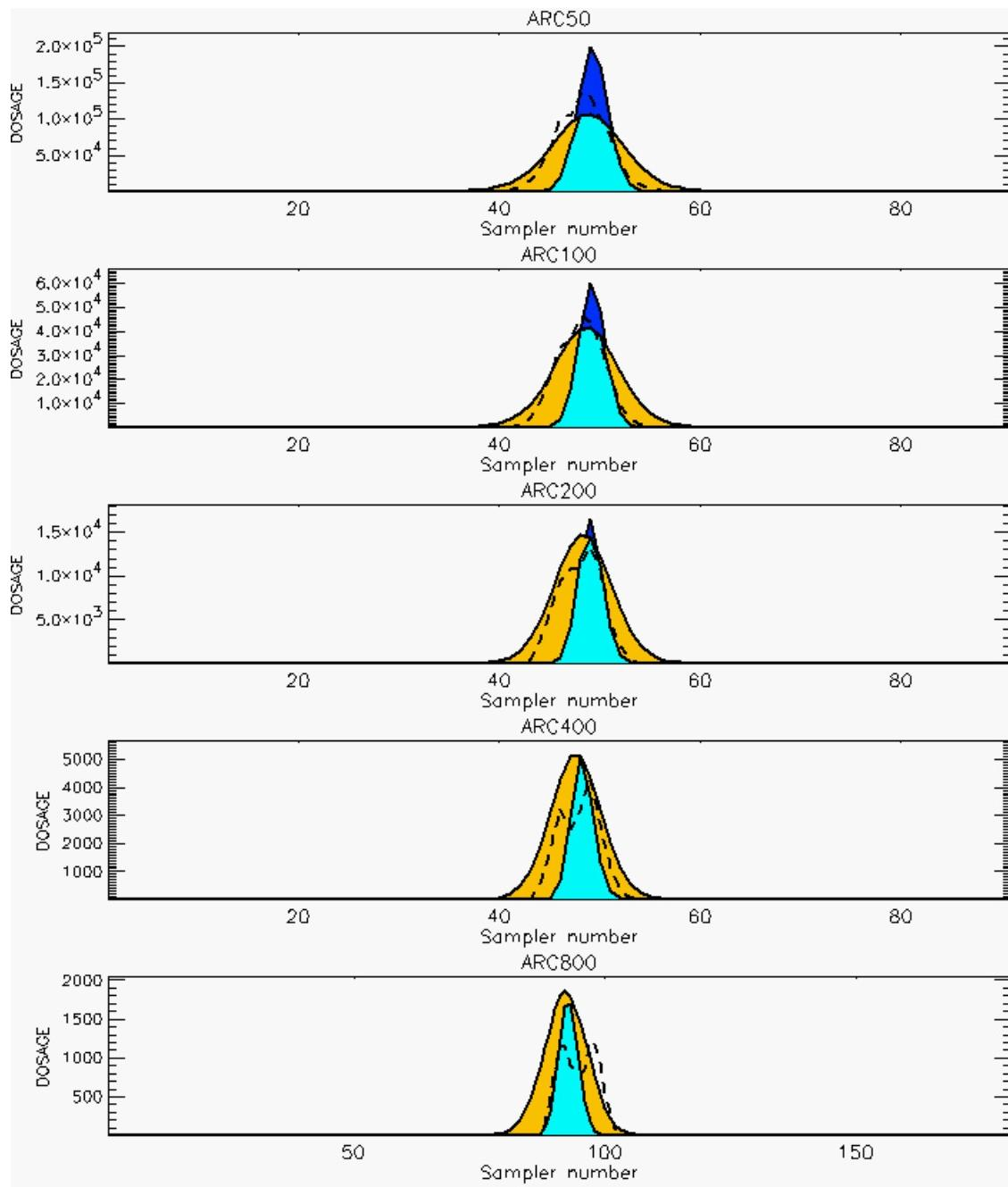
PG Prediction1 to Prediction2 Comparison

PG Trial File: pr_grass_tracer_Experiment_36.txt

PG Prediction File 1: HPAC\nodeposition\pg_36_novd.out

PG Prediction File 2: ARAC\nodeposition\pg_36_novd.arac

**Figure E-28b. HPAC and NARAC Predictions to Trial 36 on Logarithmic Scale:
Stability Category is 6**



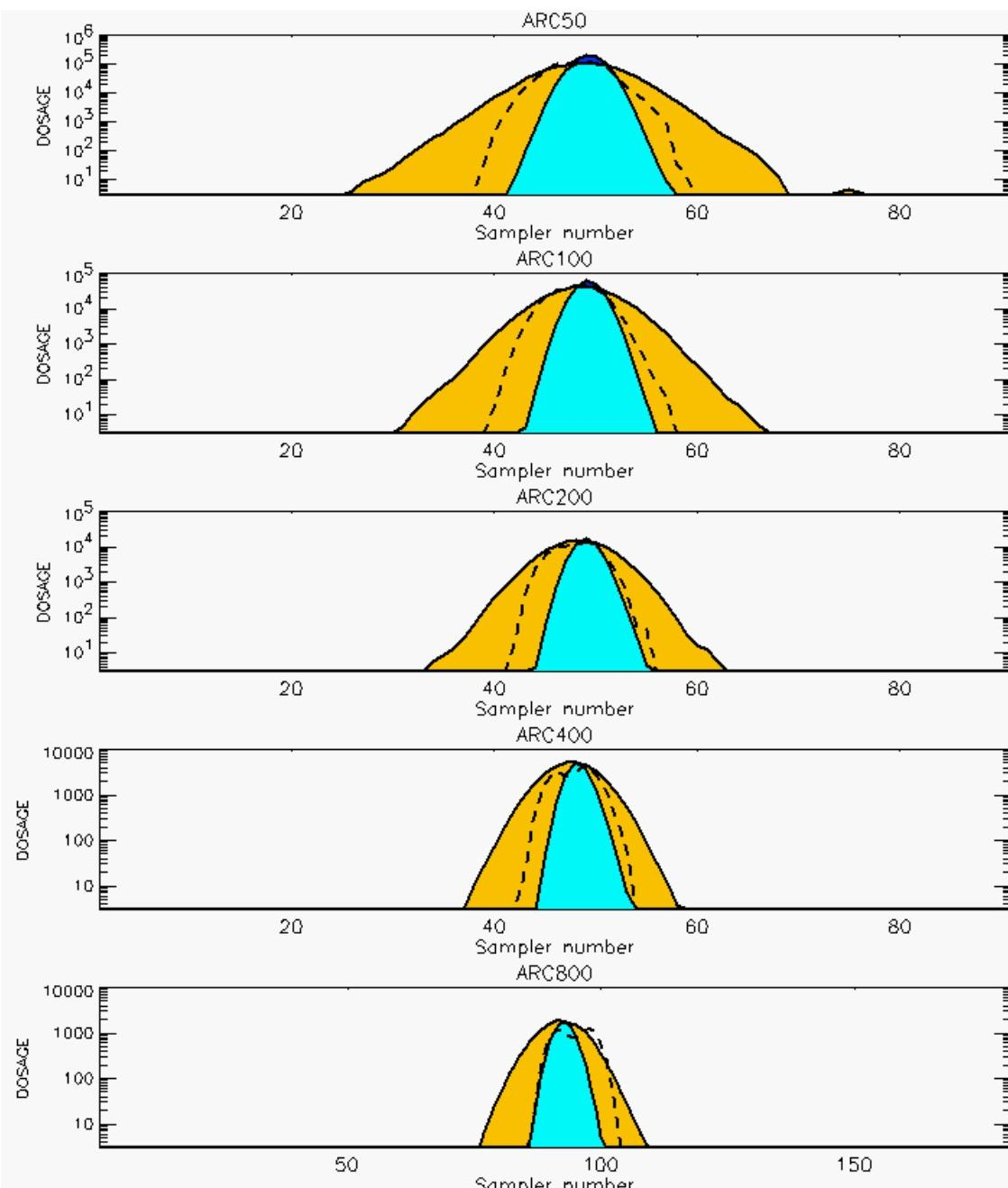
PG Prediction1 to Prediction2 Comparison

PG Trial File: pr_grass_tracer_Experiment_37.txt

PG Prediction File 1: HPAC\nodeposition\pg_37_noxd.out

PG Prediction File 2: ARAC\nodeposition\pg_37_noxd.arac

**Figure E-29a. HPAC and NARAC Predictions to Trial 37 on Linear Scale:
Stability Category is 4**



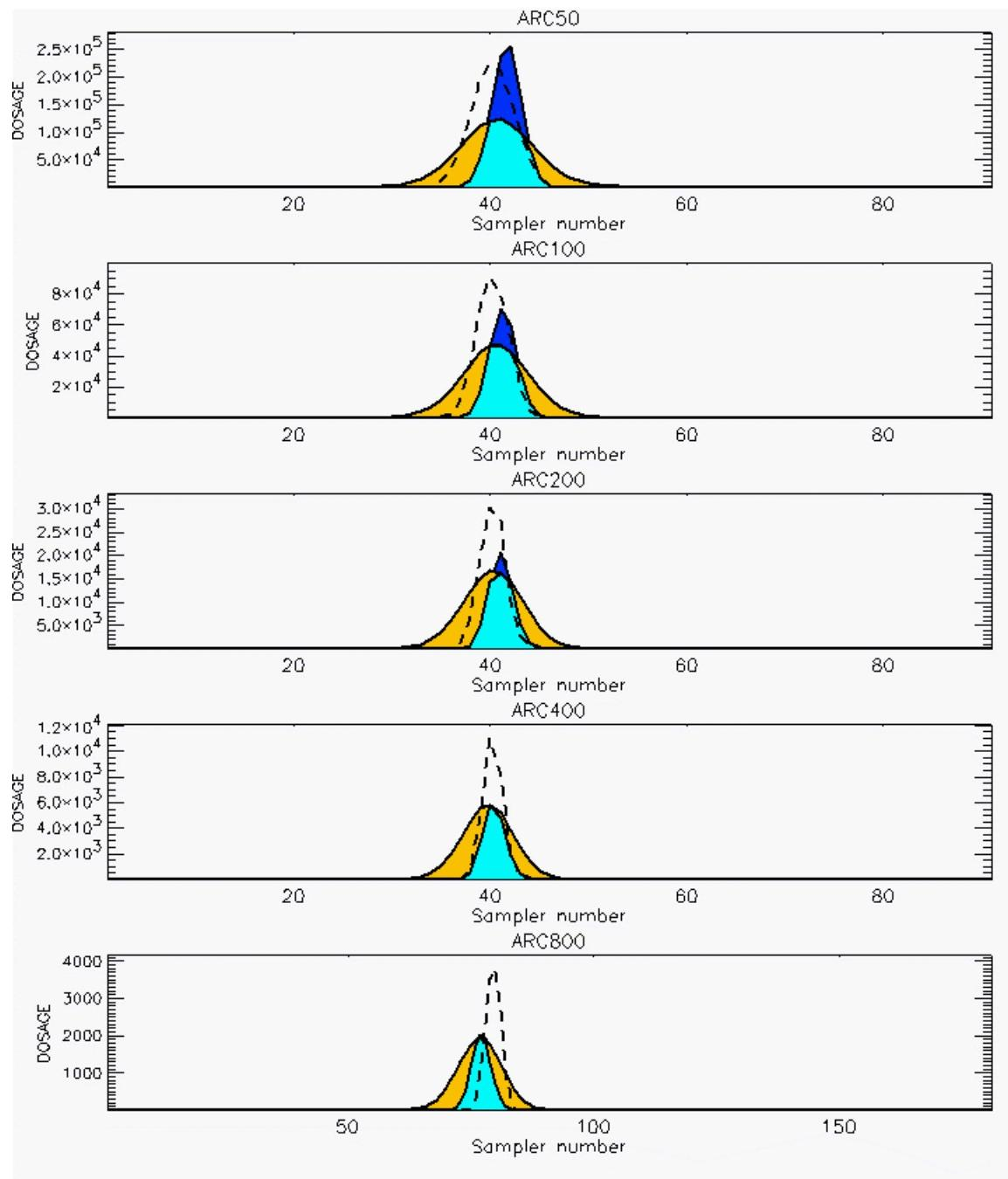
PG Prediction1 to Prediction2 Comparison

PG Trial File: pr_grass_tracer_Experiment_37.txt

PG Prediction File 1: HPAC\nodeposition\pg_37_novd.out

PG Prediction File 2: ARAC\nodeposition\pg_37_novd.arac

**Figure E-29b. HPAC and NARAC Predictions to Trial 37 on Logarithmic Scale:
Stability Category is 4**



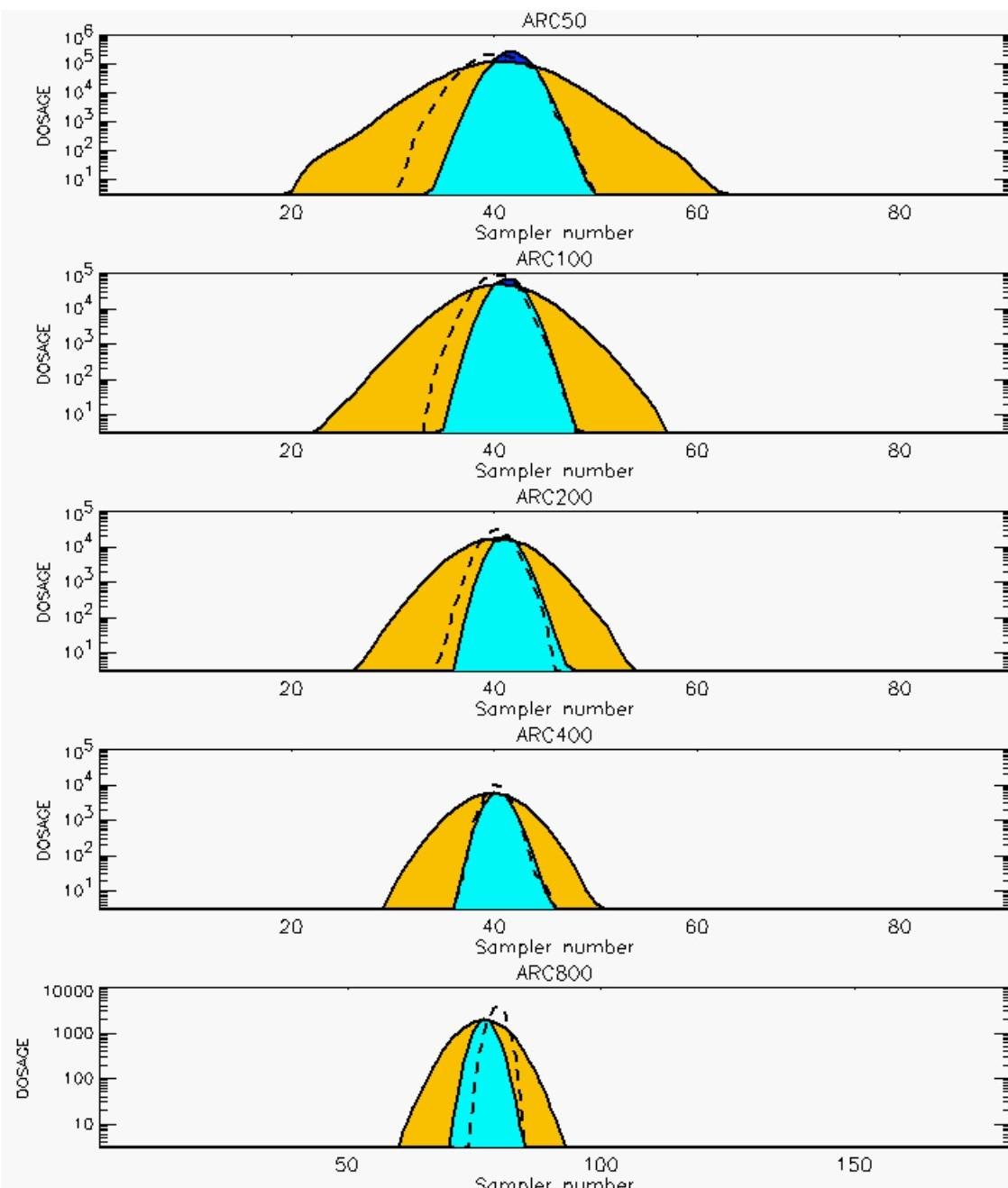
PG Prediction1 to Prediction2 Comparison

PG Trial File: pr_grass_tracer_Experiment_38.txt

PG Prediction File 1: HPAC\nodeposition\pg_38_novd.out

PG Prediction File 2: ARAC\nodeposition\pg_38_novd.arac

**Figure E-30a. HPAC and NARAC Predictions to Trial 38 on Linear Scale:
Stability Category is 4**



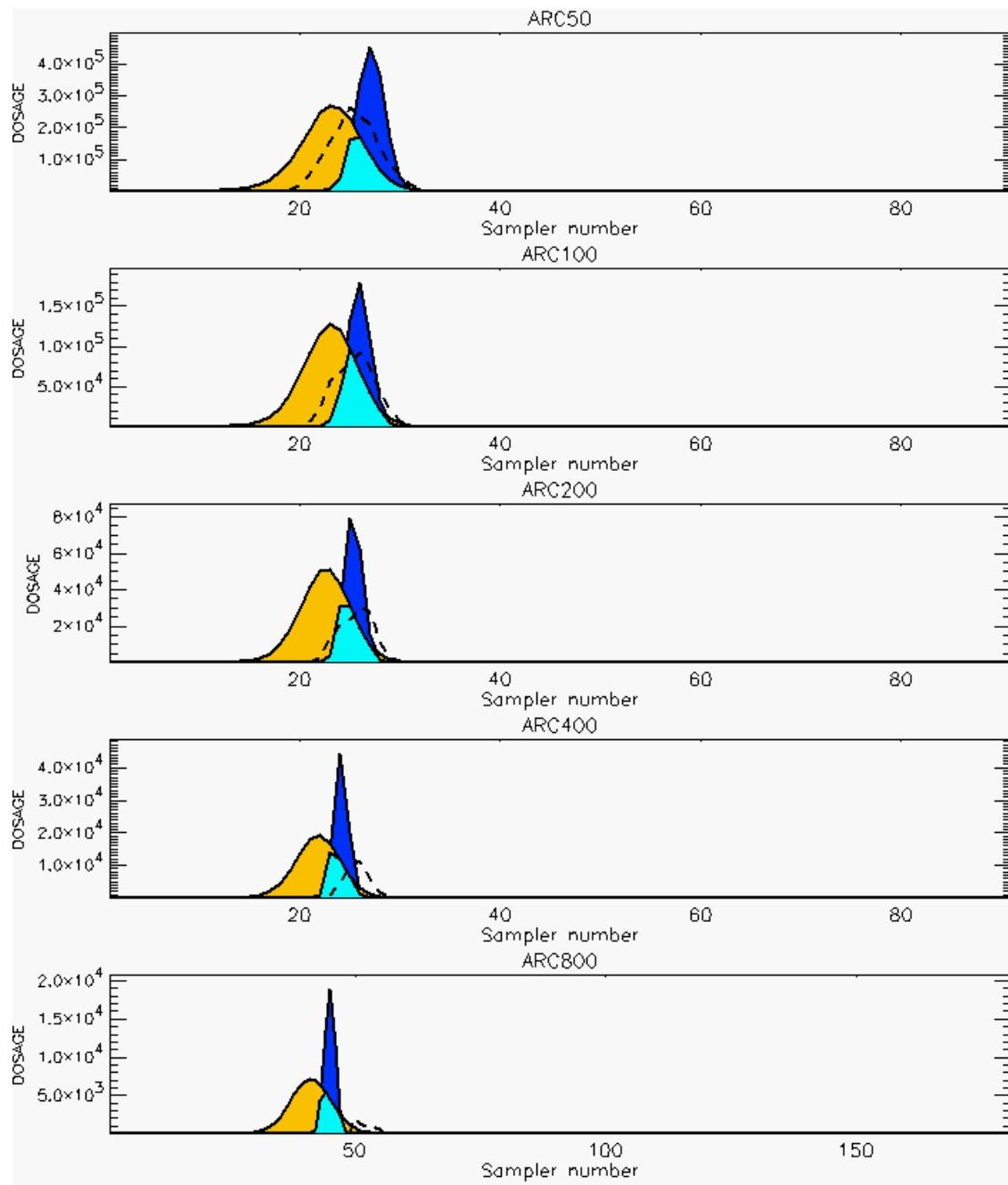
PG Prediction1 to Prediction2 Comparison

PG Trial File: pr_grass_tracer_Experiment_38.txt

PG Prediction File 1: HPAC\nodeposition\pg_38_novd.out

PG Prediction File 2: ARAC\nodeposition\pg_38_novd.arac

**Figure E-30b. HPAC and NARAC Predictions to Trial 38 on Logarithmic Scale:
Stability Category is 4**



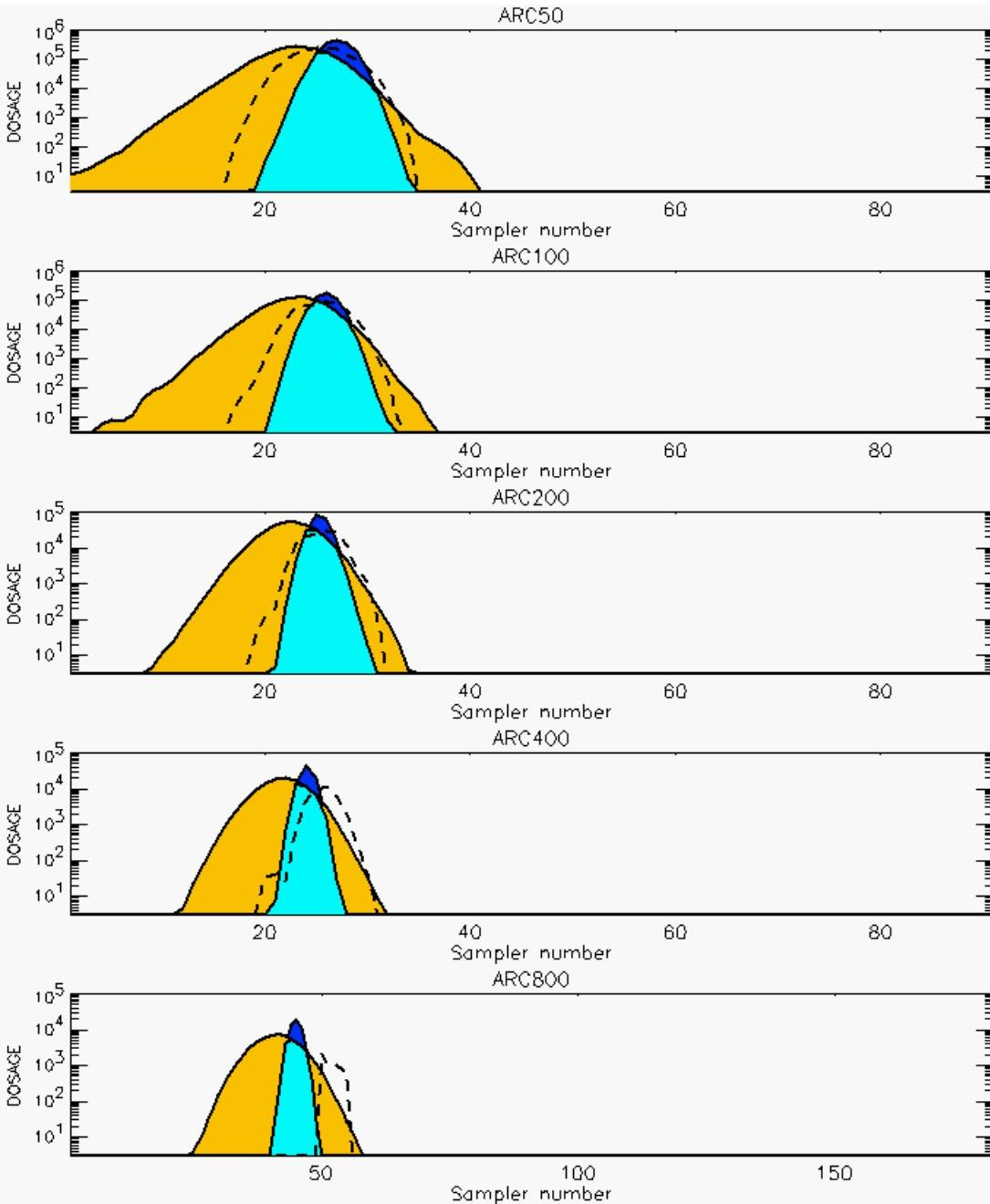
PG Prediction1 to Prediction2 Comparison

PG Trial File: pr_grass_tracer_Experiment_39.txt

PG Prediction File 1: HPAC\nodeposition\pg_39_novd.out

PG Prediction File 2: ARAC\nodeposition\pg_39_novd.arac

**Figure E-31a. HPAC and NARAC Predictions to Trial 39 on Linear Scale:
Stability Category is 6**



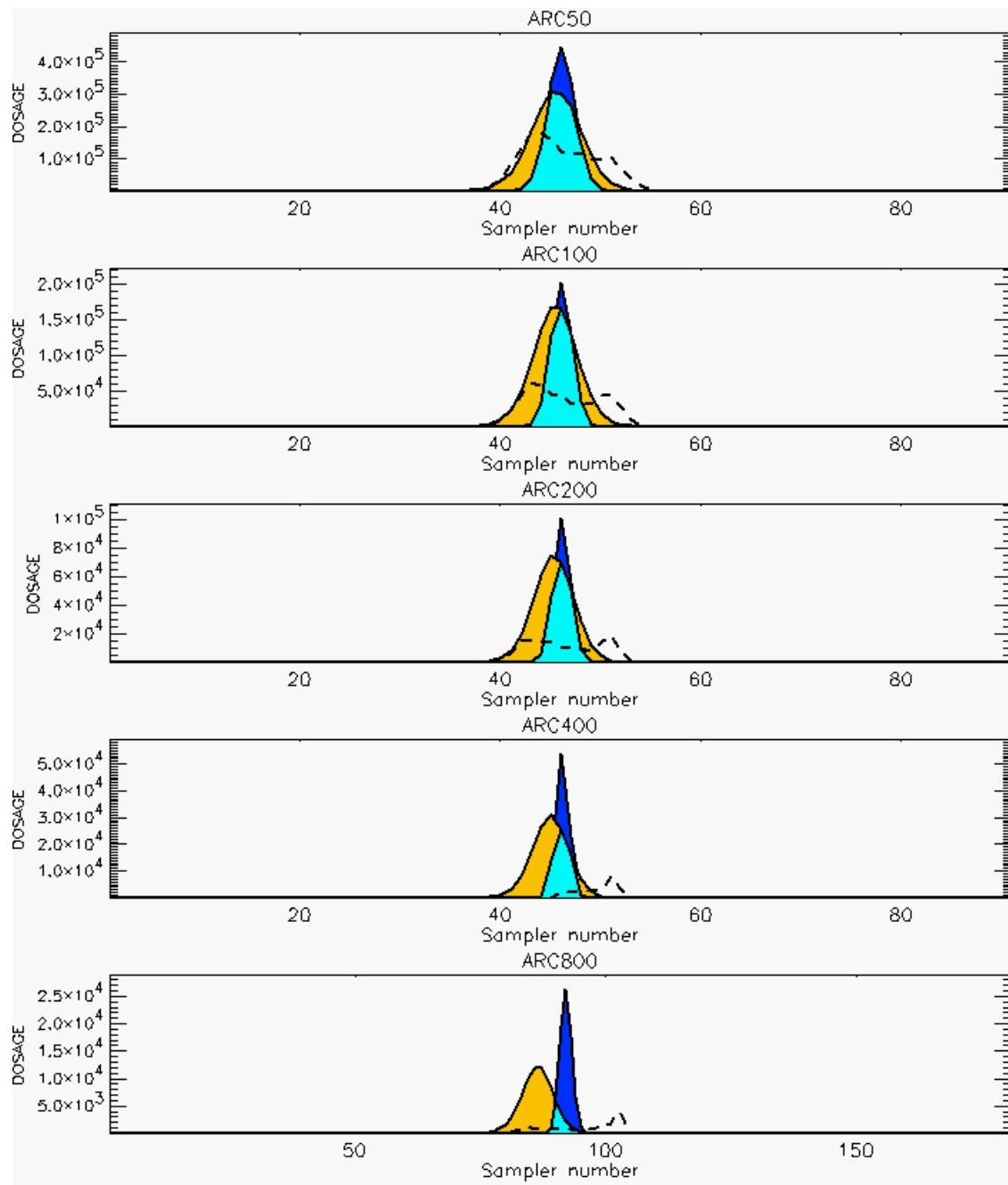
PG Prediction1 to Prediction2 Comparison

PG Trial File: pr_grass_tracer_Experiment_39.txt

PG Prediction File 1: HPAC\nodeposition\pg_39_novd.out

PG Prediction File 2: ARAC\nodeposition\pg_39_novd.arac

**Figure E-31b. HPAC and NARAC Predictions to Trial 39 on Logarithmic Scale:
Stability Category is 6**



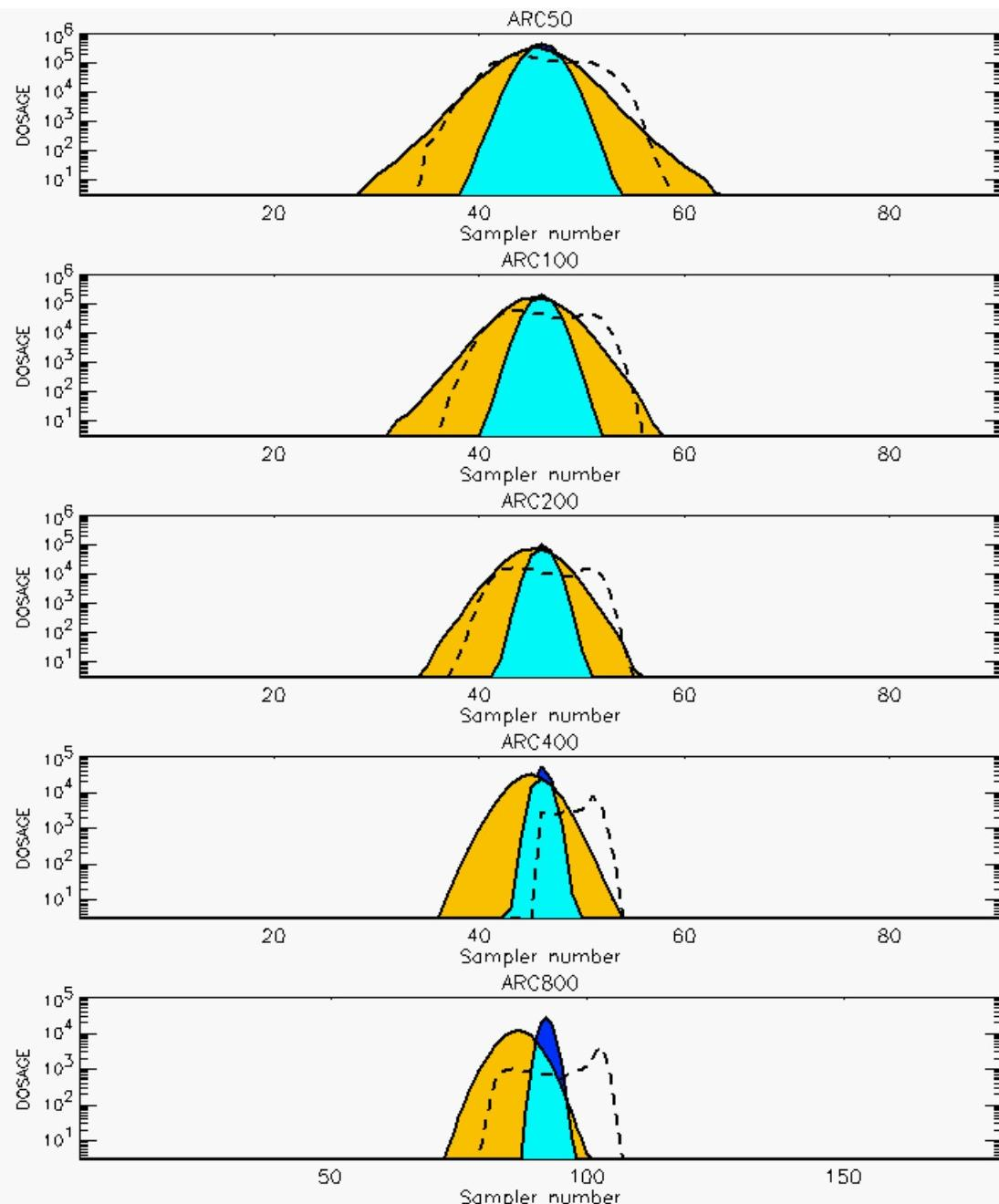
PG Prediction1 to Prediction2 Comparison

PG Trial File: pr_grass_tracer_Experiment_40.txt

PG Prediction File 1: HPAC\nodeposition\pg_40_noxd.out

PG Prediction File 2: ARAC\nodeposition\pg_40_noxd.arac

**Figure E-32a. HPAC and NARAC Predictions to Trial 40 on Linear Scale:
Stability Category is 6**



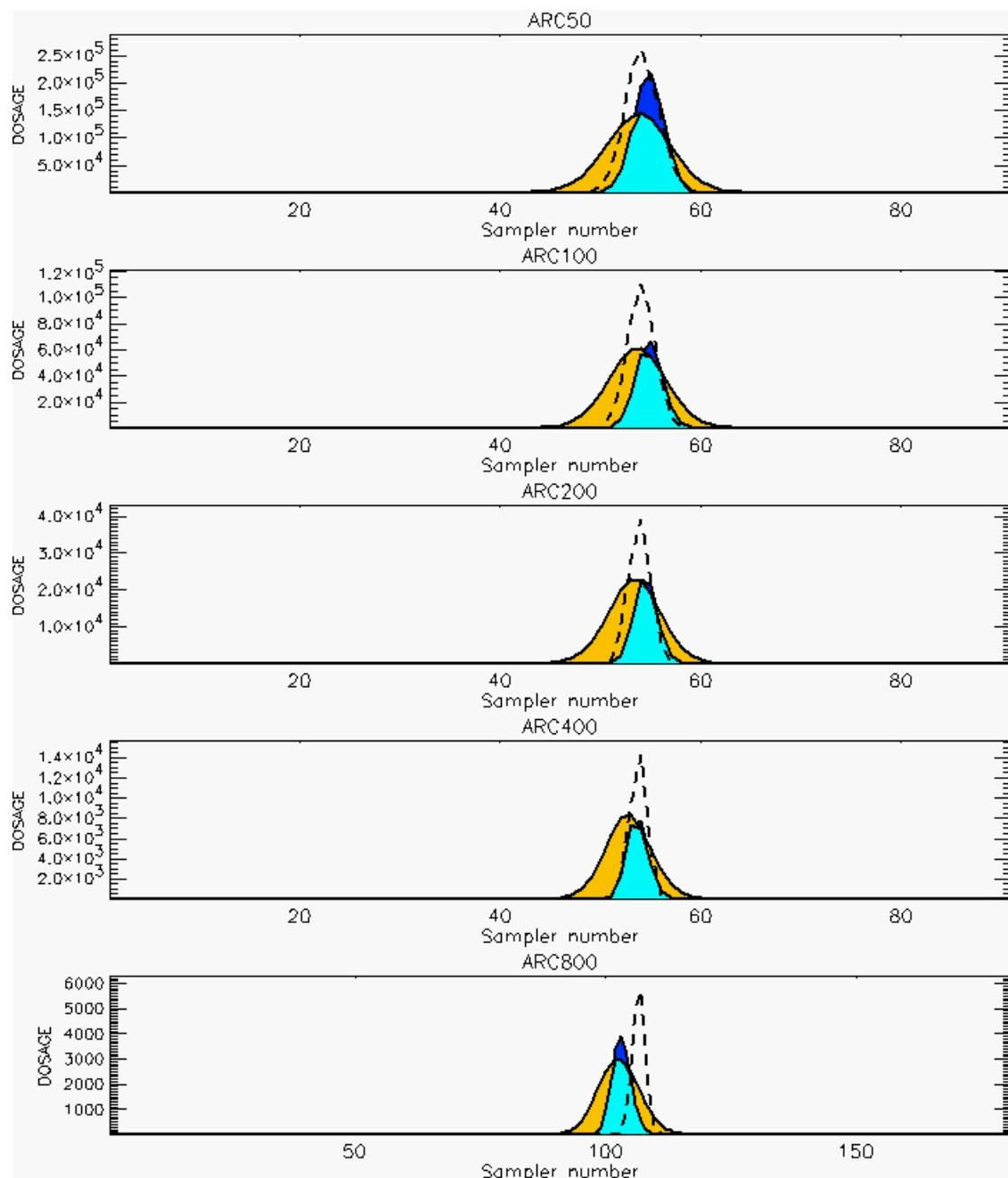
PG Prediction1 to Prediction2 Comparison

PG Trial File: pr_grass_tracer_Experiment_40.txt

PG Prediction File 1: HPAC\nodeposition\pg_40_noxd.out

PG Prediction File 2: ARAC\nodeposition\pg_40_noxd.arac

**Figure E-32b. HPAC and NARAC Predictions to Trial 40 on Logarithmic Scale:
Stability Category is 6**



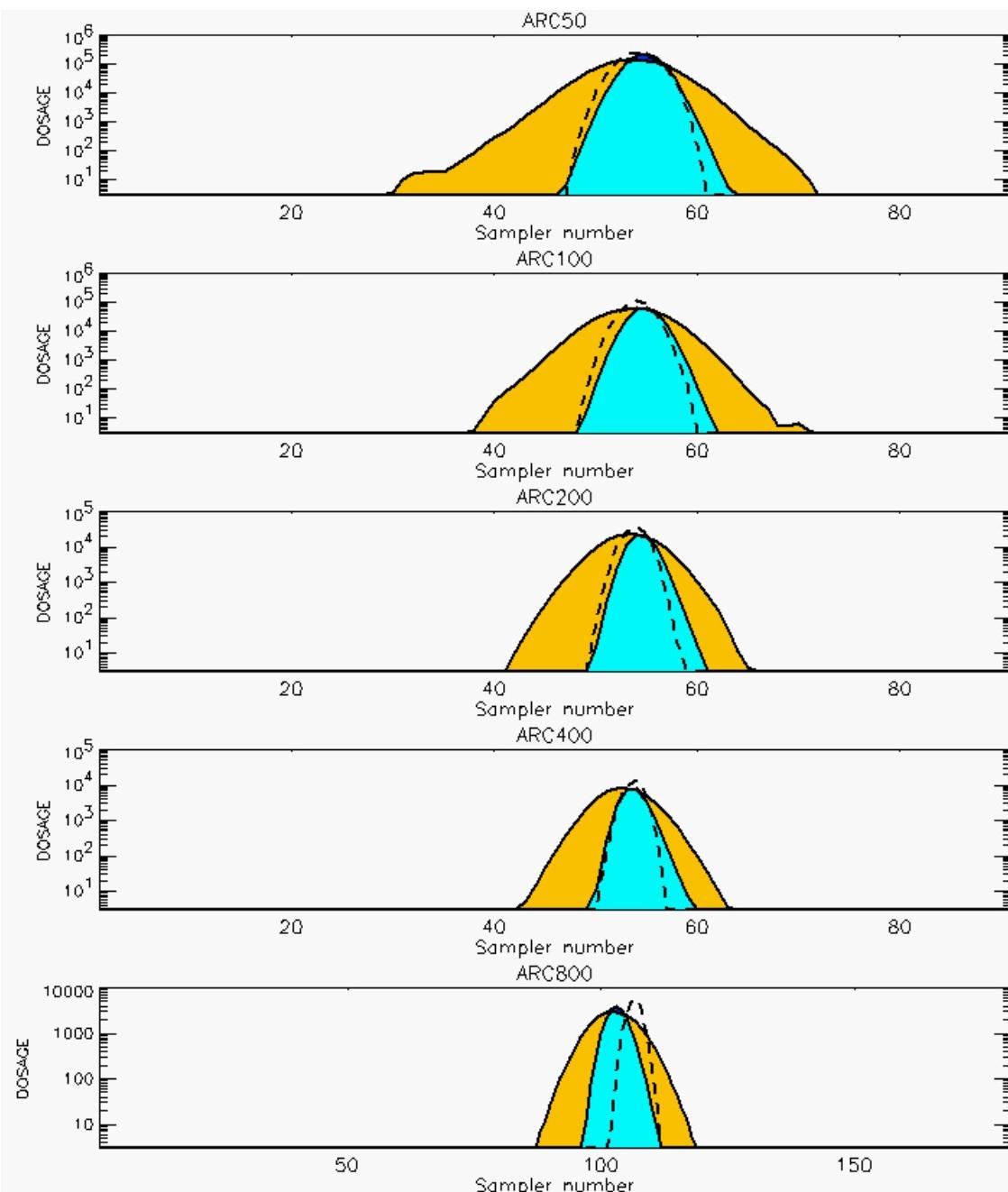
PG Prediction1 to Prediction2 Comparison

PG Trial File: pr_grass_tracer_Experiment_41.txt

PG Prediction File 1: HPAC\nodeposition\pg_41_noxd.out

PG Prediction File 2: ARAC\nodeposition\pg_41_noxd.arac

**Figure E-33a. HPAC and NARAC Predictions to Trial 41 on Linear Scale:
Stability Category is 5**



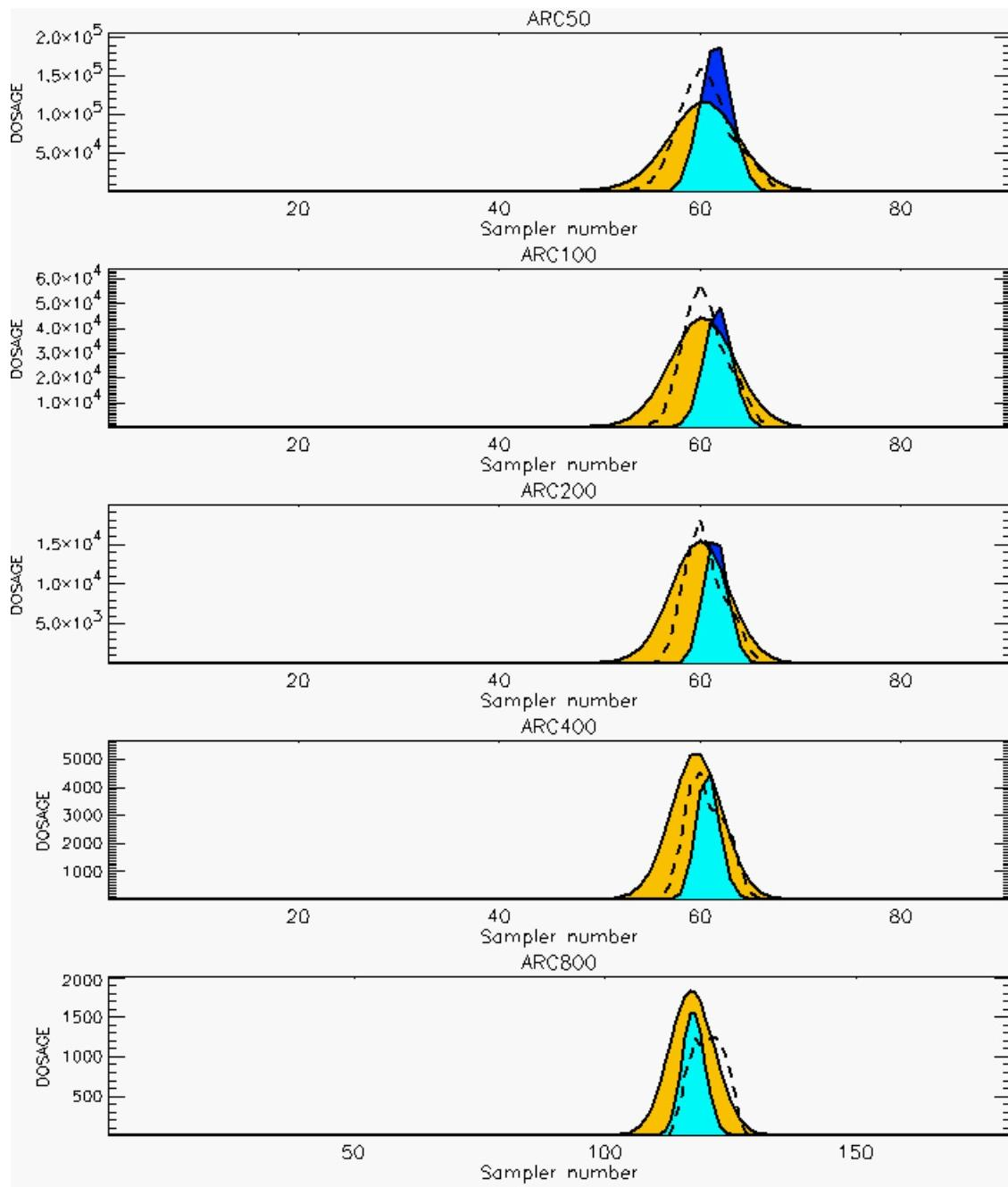
PG Prediction1 to Prediction2 Comparison

PG Trial File: pr_grass_tracer_Experiment_41.txt

PG Prediction File 1: HPAC\nodeposition\pg_41_noxd.out

PG Prediction File 2: ARAC\nodeposition\pg_41_noxd.arac

**Figure E-33b. HPAC and NARAC Predictions to Trial 41 on Logarithmic Scale:
Stability Category is 5**



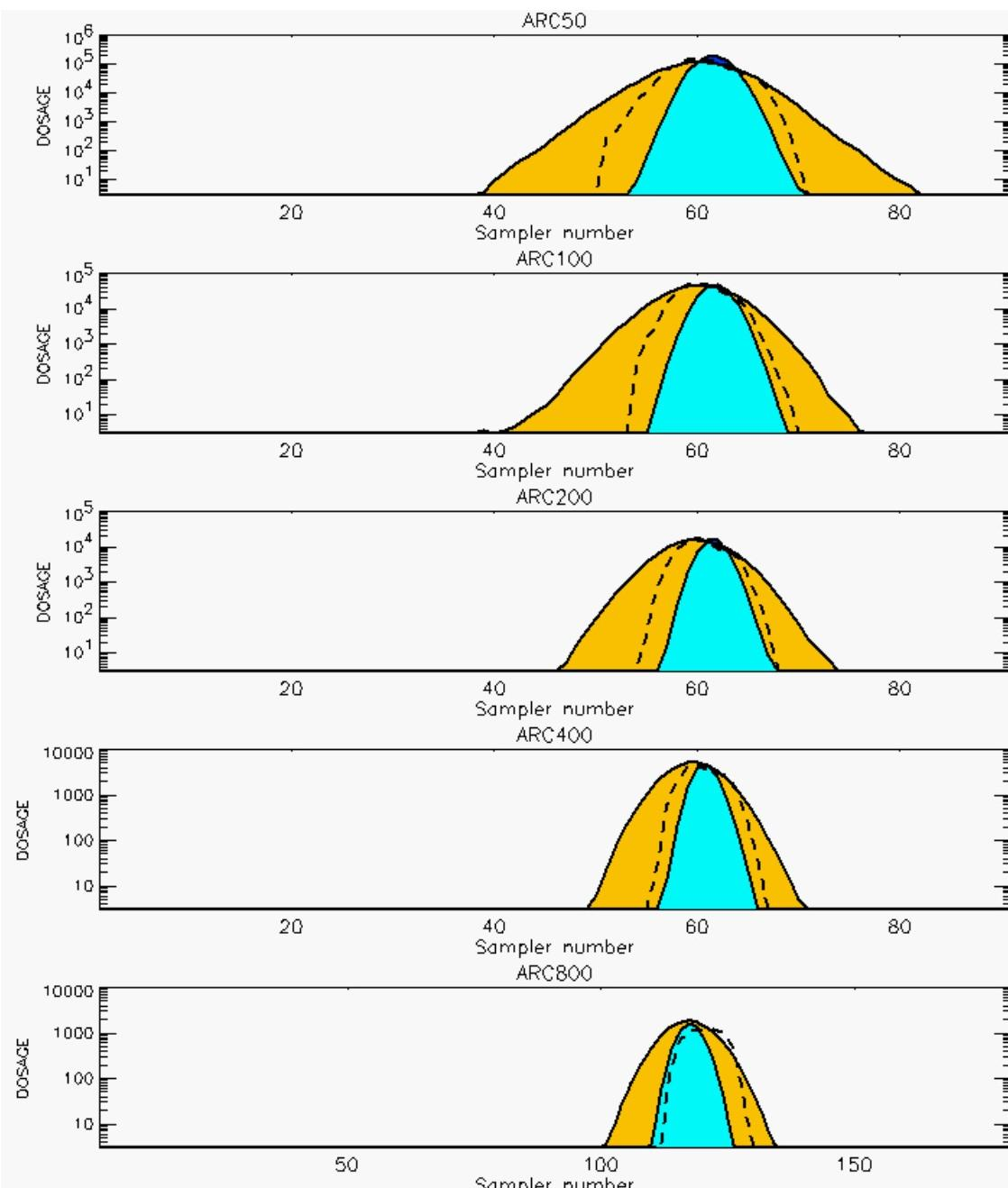
PG Prediction1 to Prediction2 Comparison

PG Trial File: pr_grass_tracer_Experiment_42.txt

PG Prediction File 1: HPAC\nodeposition\pg_42_noxd.out

PG Prediction File 2: ARAC\nodeposition\pg_42_noxd.arac

**Figure E-34a. HPAC and NARAC Predictions to Trial 42 on Linear Scale:
Stability Category is 4**



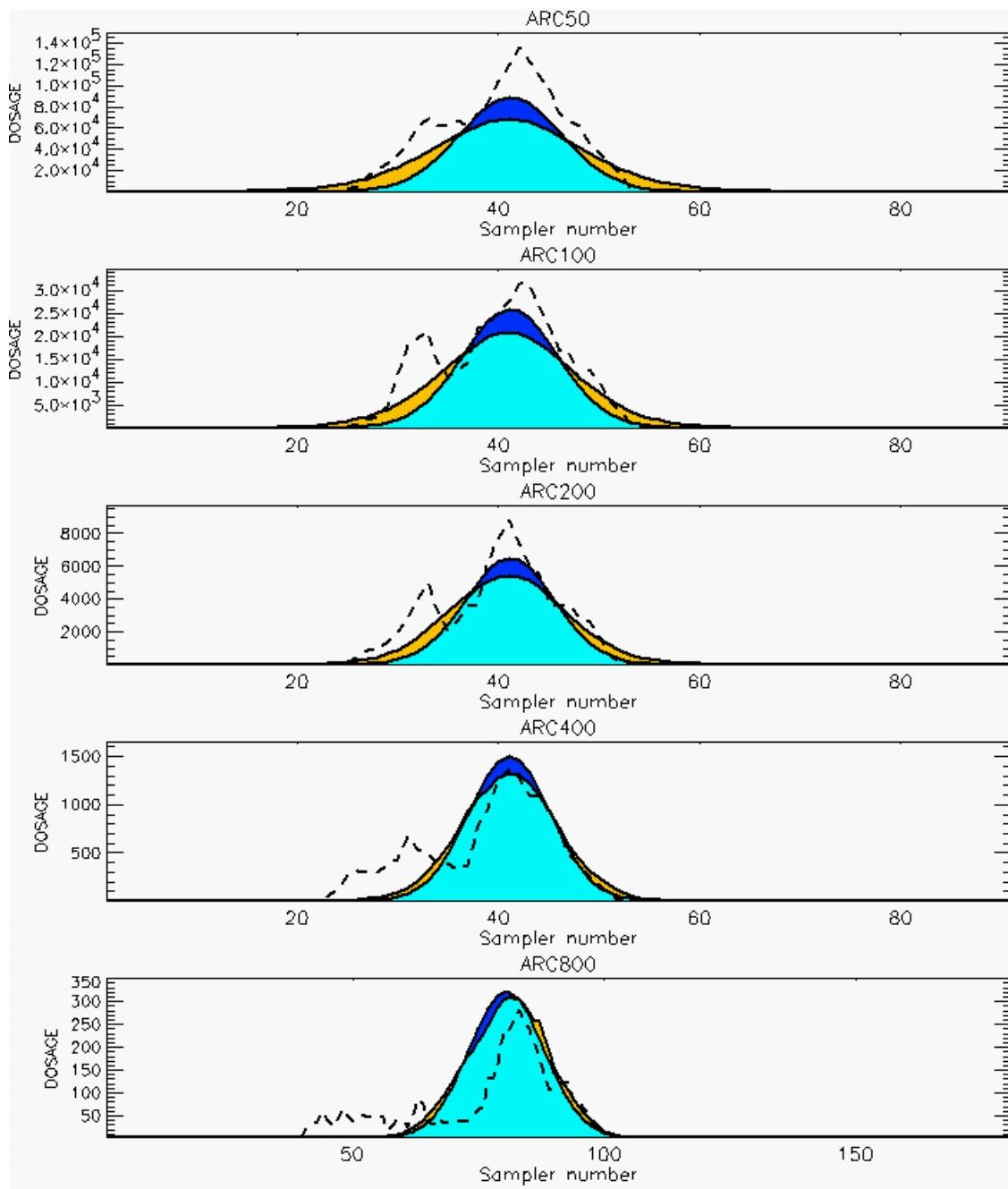
PG Prediction1 to Prediction2 Comparison

PG Trial File: pr_grass_tracer_Experiment_42.txt

PG Prediction File 1: HPAC\nodeposition\pg_42_novd.out

PG Prediction File 2: ARAC\nodeposition\pg_42_novd.arac

**Figure E-34b. HPAC and NARAC Predictions to Trial 42 on Logarithmic Scale:
Stability Category is 4**



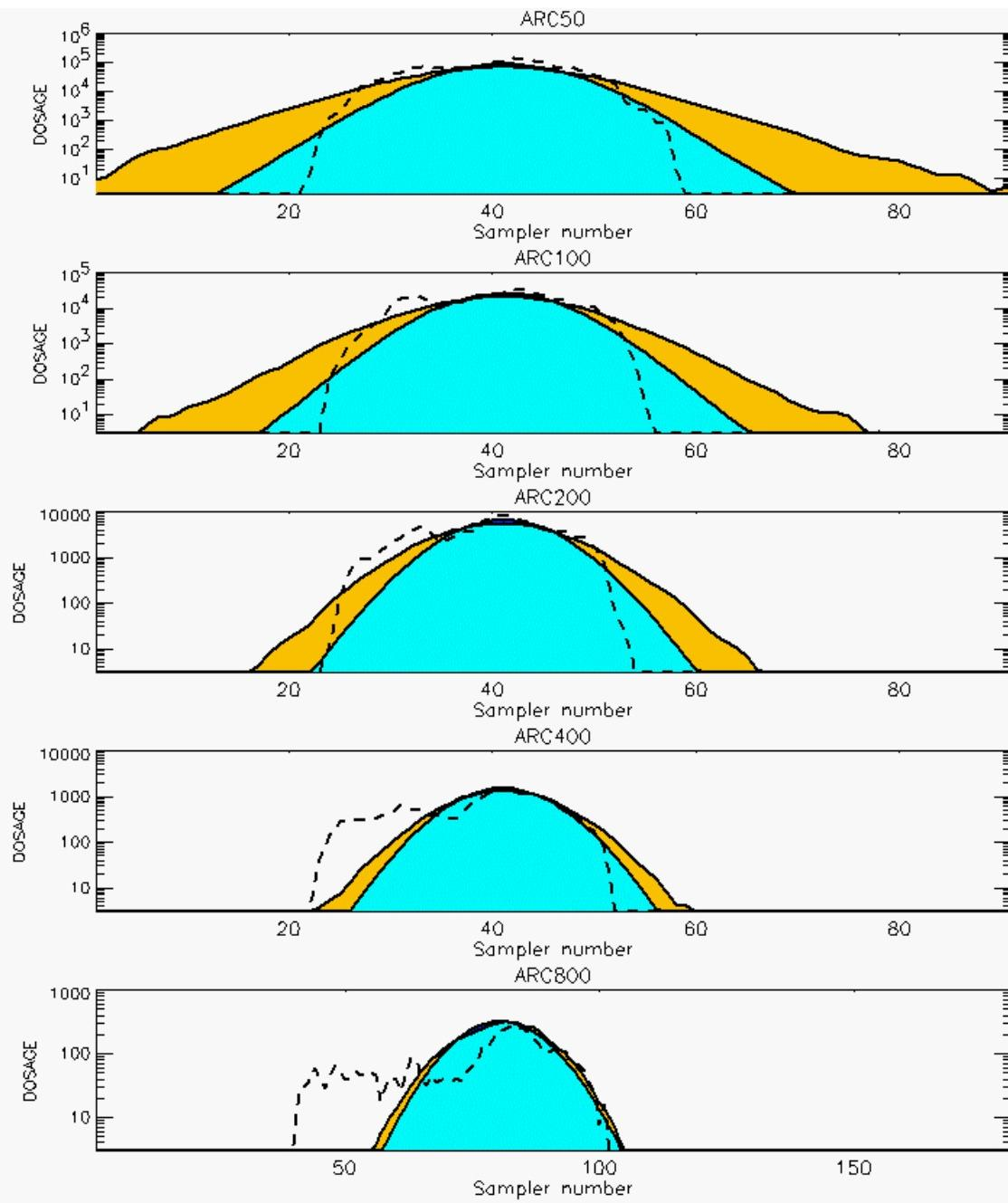
PG Prediction1 to Prediction2 Comparison

PG Trial File: pr_grass_tracer_Experiment_43.txt

PG Prediction File 1: HPAC\nodeposition\pg_43_novd.out

PG Prediction File 2: ARAC\nodeposition\pg_43_novd.arac

**Figure E-35a. HPAC and NARAC Predictions to Trial 43 on Linear Scale:
Stability Category is 1**



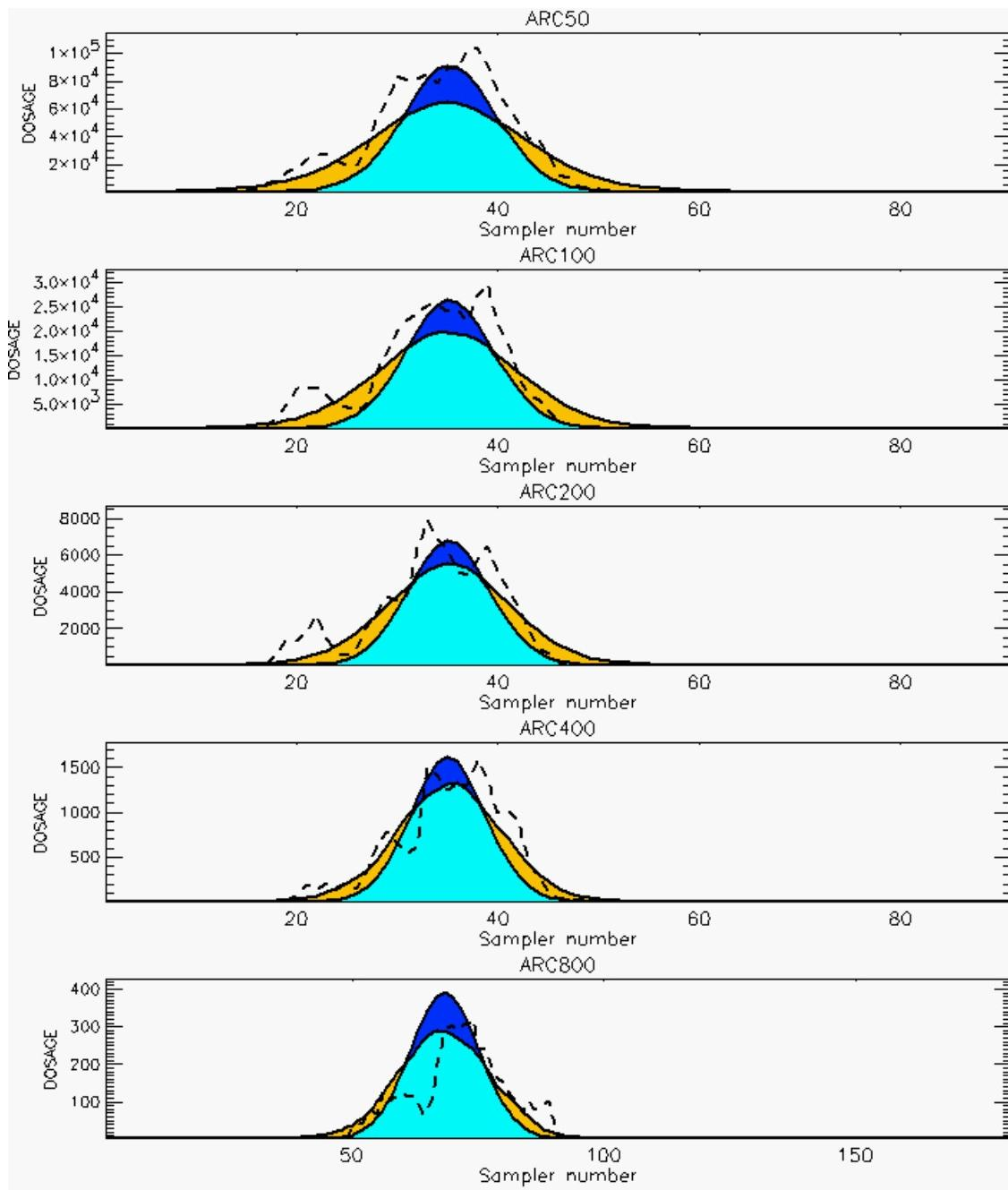
PG Prediction1 to Prediction2 Comparison

PG Trial File: pr_grass_tracer_Experiment_43.txt

PG Prediction File 1: HPAC\nodeposition\pg_43_noxd.out

PG Prediction File 2: ARAC\nodeposition\pg_43_noxd.arac

**Figure E-35b. HPAC and NARAC Predictions to Trial 43 on Logarithmic Scale:
Stability Category is 1**



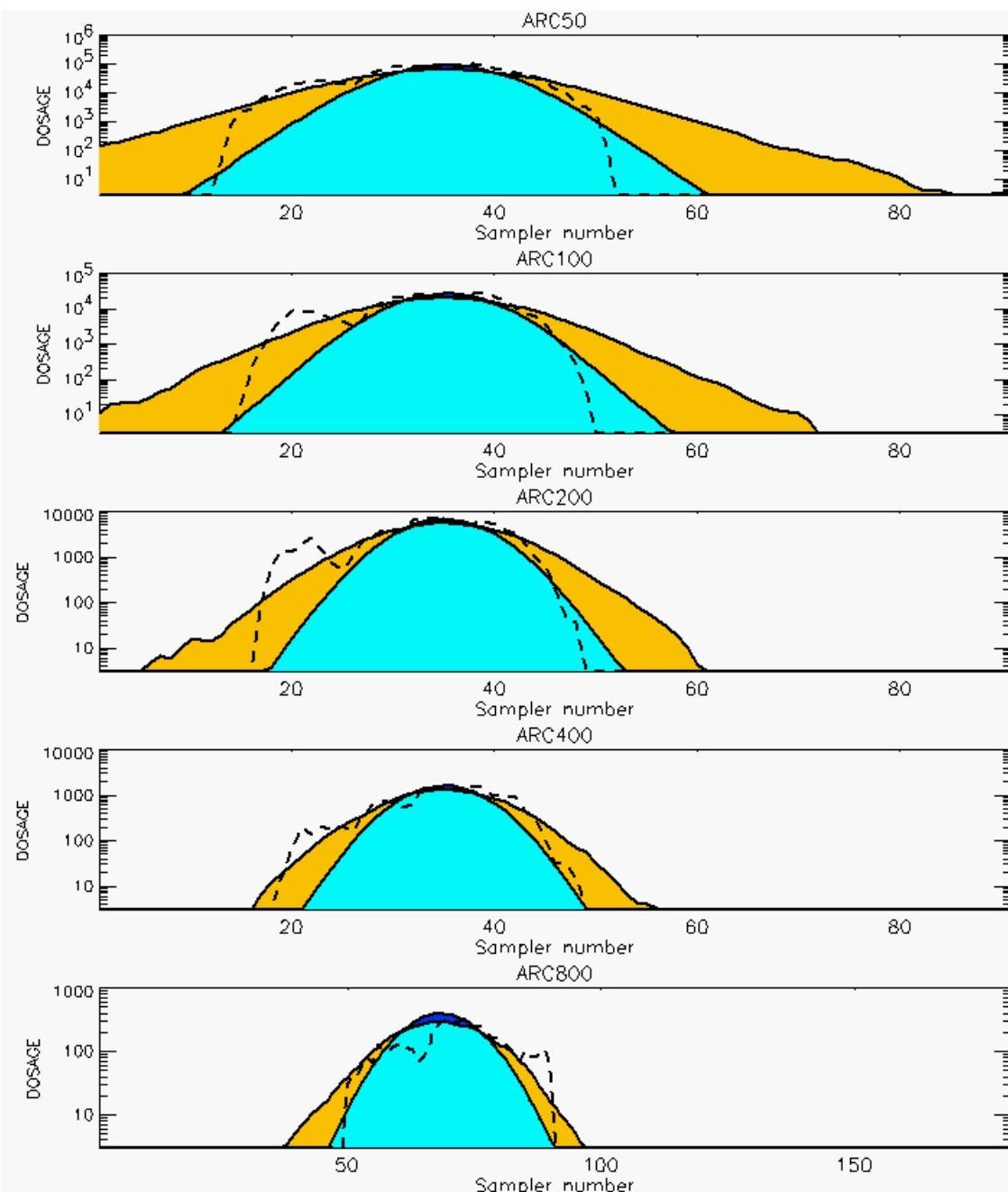
PG Prediction1 to Prediction2 Comparison

PG Trial File: pr_grass_tracer_Experiment_44.txt

PG Prediction File 1: HPAC\nodeposition\pg_44_noxd.out

PG Prediction File 2: ARAC\nodeposition\pg_44_noxd.arac

**Figure E-36a. HPAC and NARAC Predictions to Trial 44 on Linear Scale:
Stability Category is 2**



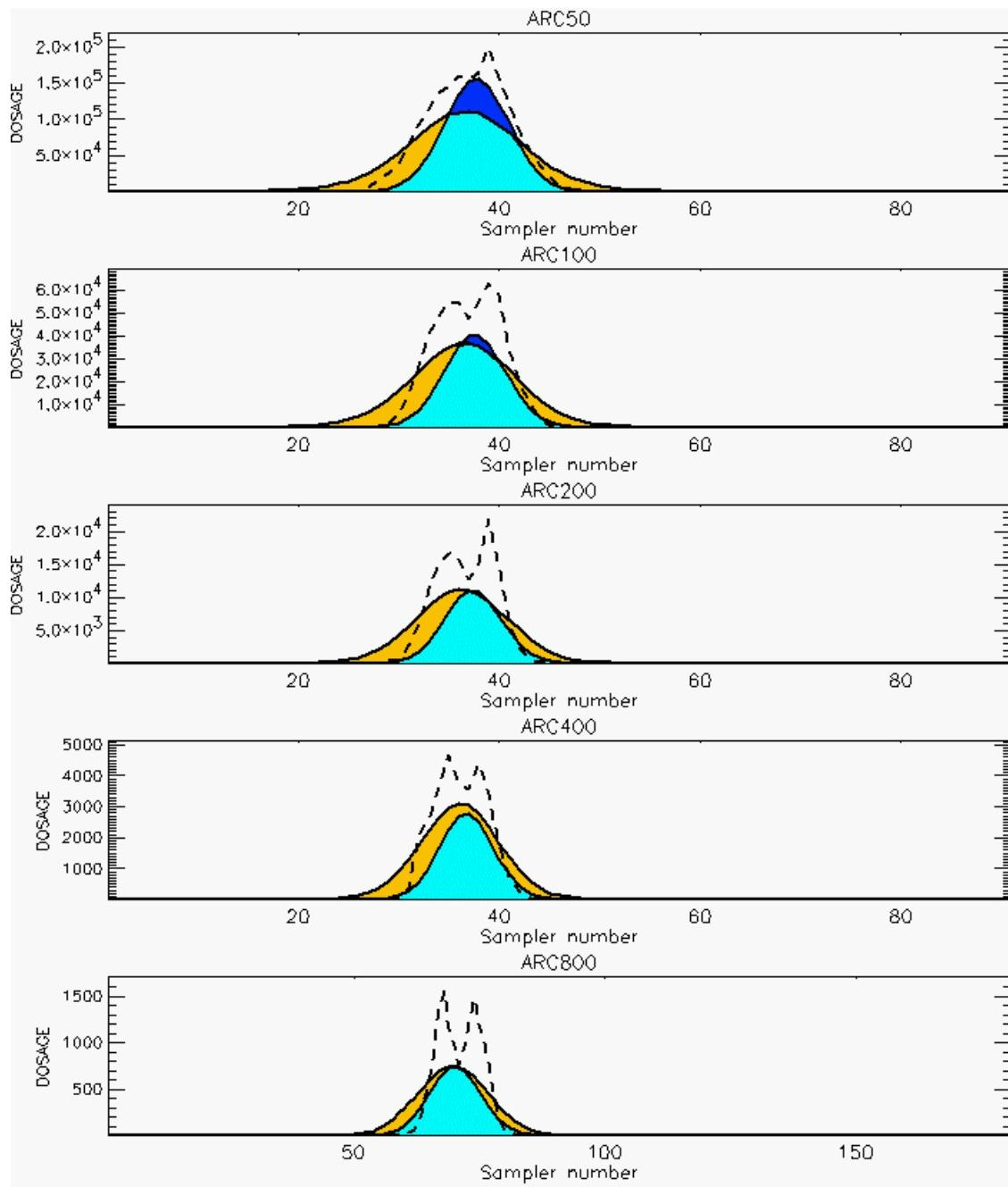
PG Prediction1 to Prediction2 Comparison

PG Trial File: pr_grass_tracer_Experiment_44.txt

PG Prediction File 1: HPAC\nodeposition\pg_44_noxd.out

PG Prediction File 2: ARAC\nodeposition\pg_44_noxd.arac

**Figure E-36b. HPAC and NARAC Predictions to Trial 44 on Logarithmic Scale:
Stability Category is 2**



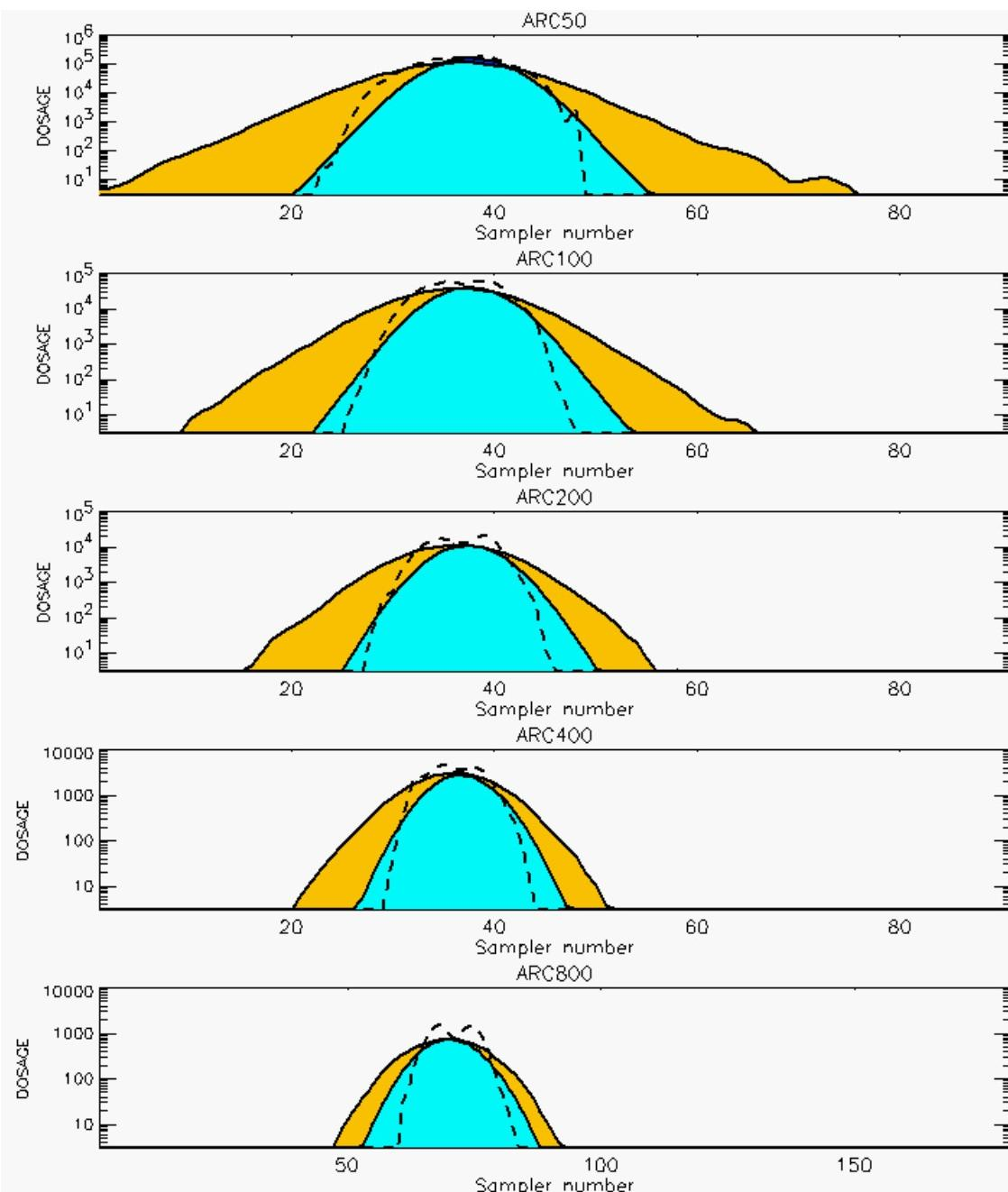
PG Prediction1 to Prediction2 Comparison

PG Trial File: pr_grass_tracer_Experiment_45.txt

PG Prediction File 1: HPAC\nodeposition\pg_45_noxd.out

PG Prediction File 2: ARAC\nodeposition\pg_45_noxd.arac

**Figure E-37a. HPAC and NARAC Predictions to Trial 45 on Linear Scale:
Stability Category is 3**



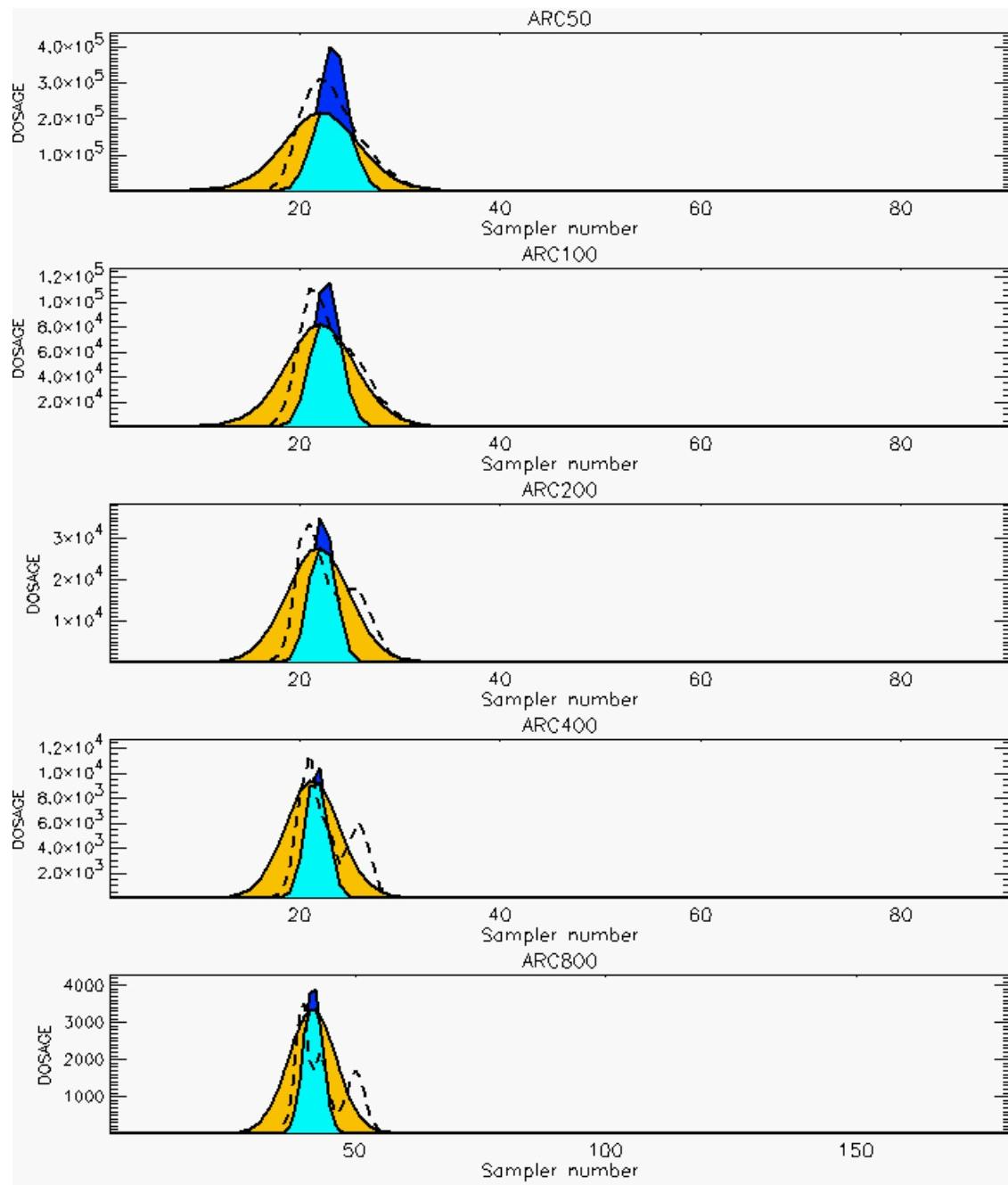
PG Prediction1 to Prediction2 Comparison

PG Trial File: pr_grass_tracer_Experiment_45.txt

PG Prediction File 1: HPAC\nodeposition\pg_45_noxd.out

PG Prediction File 2: ARAC\nodeposition\pg_45_noxd.arac

**Figure E-37b. HPAC and NARAC Predictions to Trial 45 on Logarithmic Scale:
Stability Category is 3**



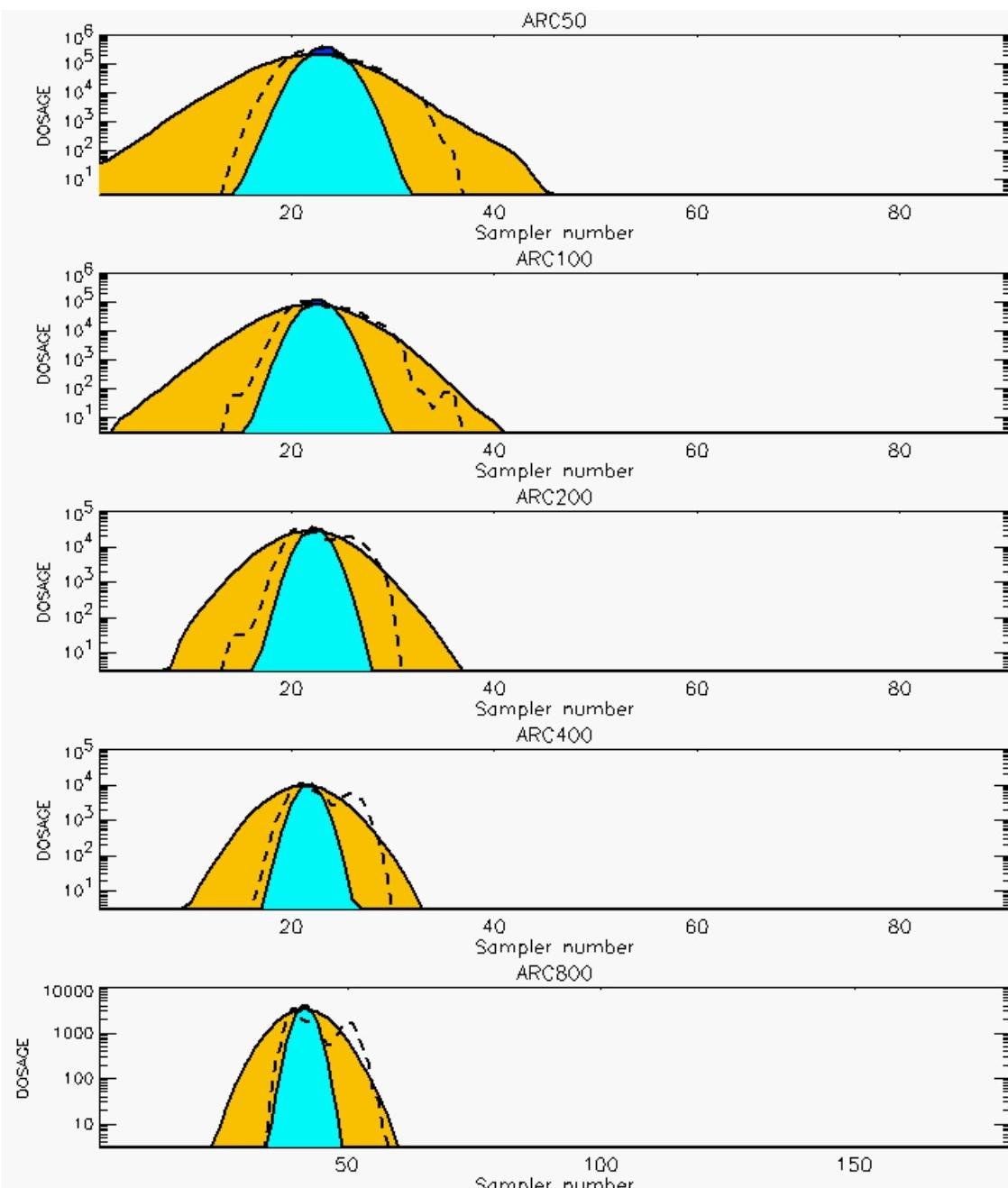
PG Prediction1 to Prediction2 Comparison

PG Trial File: pr_grass_tracer_Experiment_46.txt

PG Prediction File 1: HPAC\nodeposition\pg_46_noxd.out

PG Prediction File 2: ARAC\nodeposition\pg_46_noxd.arac

**Figure E-38a. HPAC and NARAC Predictions to Trial 46 on Linear Scale:
Stability Category is 4**



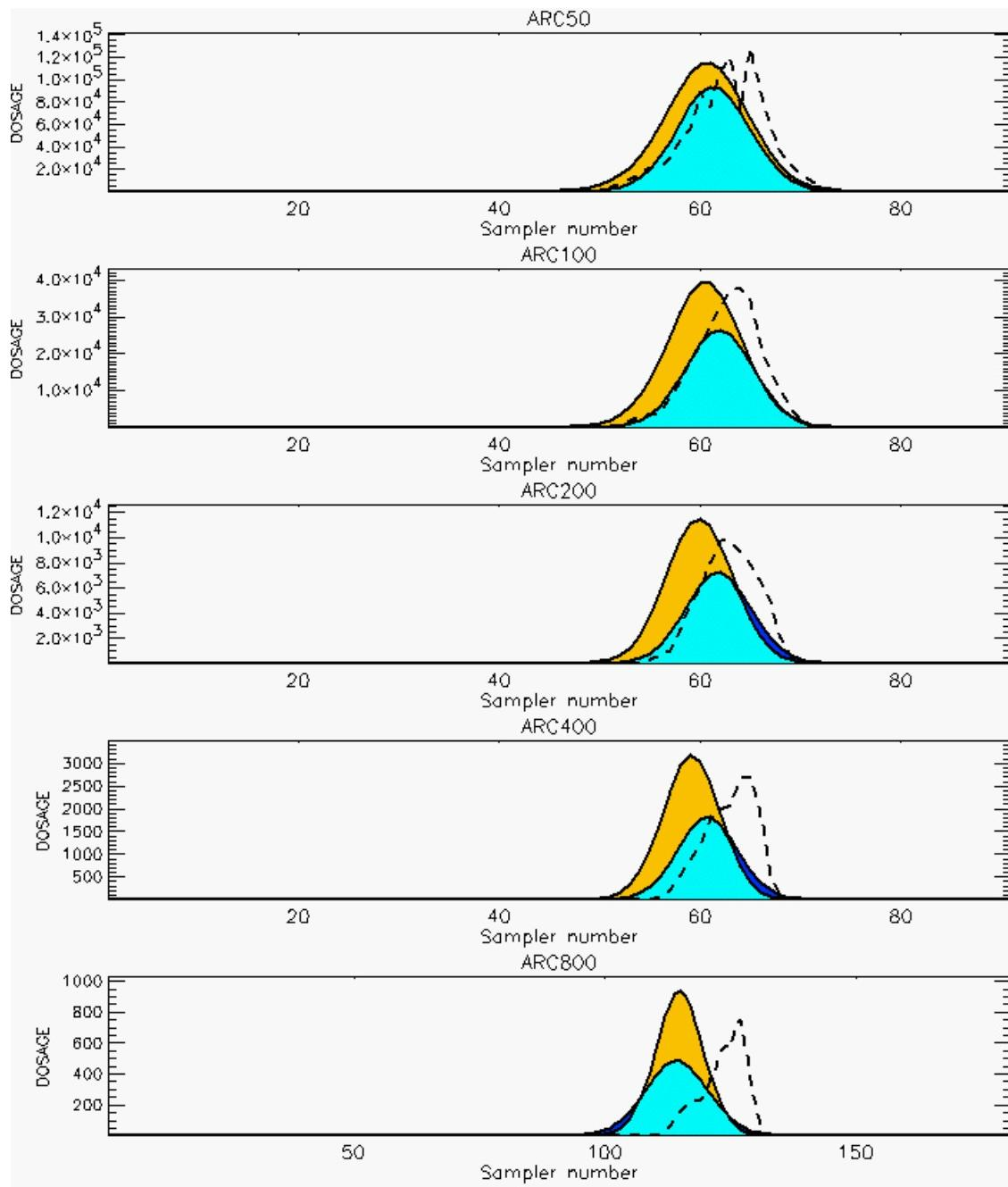
PG Prediction1 to Prediction2 Comparison

PG Trial File: pr_grass_tracer_Experiment_46.txt

PG Prediction File 1: HPAC\nodeposition\pg_46_noxd.out

PG Prediction File 2: ARAC\nodeposition\pg_46_noxd.arac

**Figure E-38b. HPAC and NARAC Predictions to Trial 46 on Logarithmic Scale:
Stability Category is 4**



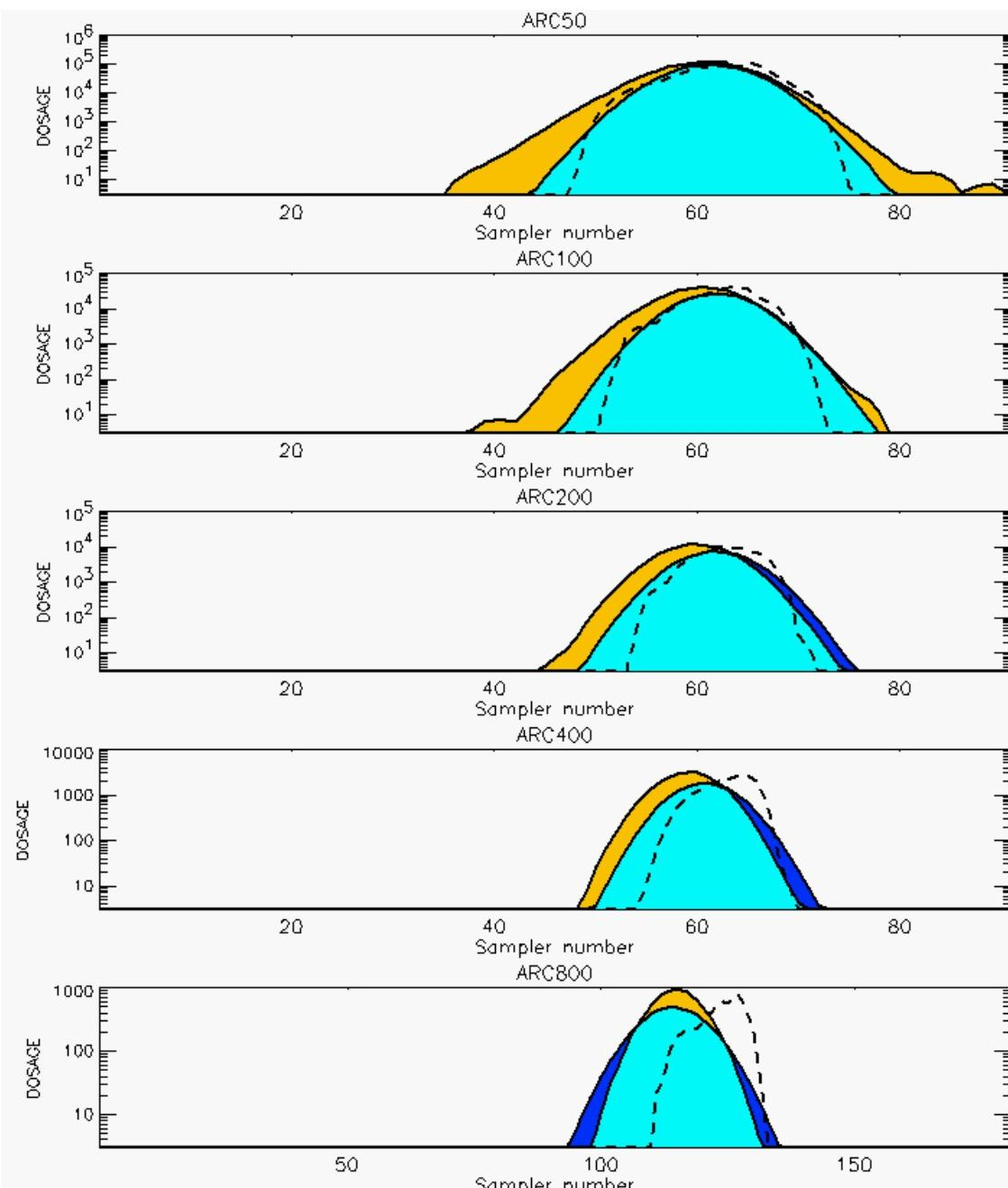
PG Prediction1 to Prediction2 Comparison

PG Trial File: pr_grass_tracer_Experiment_48.txt

PG Prediction File 1: HPAC\nodeposition\pg_48_noxd.out

PG Prediction File 2: ARAC\nodeposition\pg_48_noxd.arac

**Figure E-39a. HPAC and NARAC Predictions to Trial 48 on Linear Scale:
Stability Category is 3**



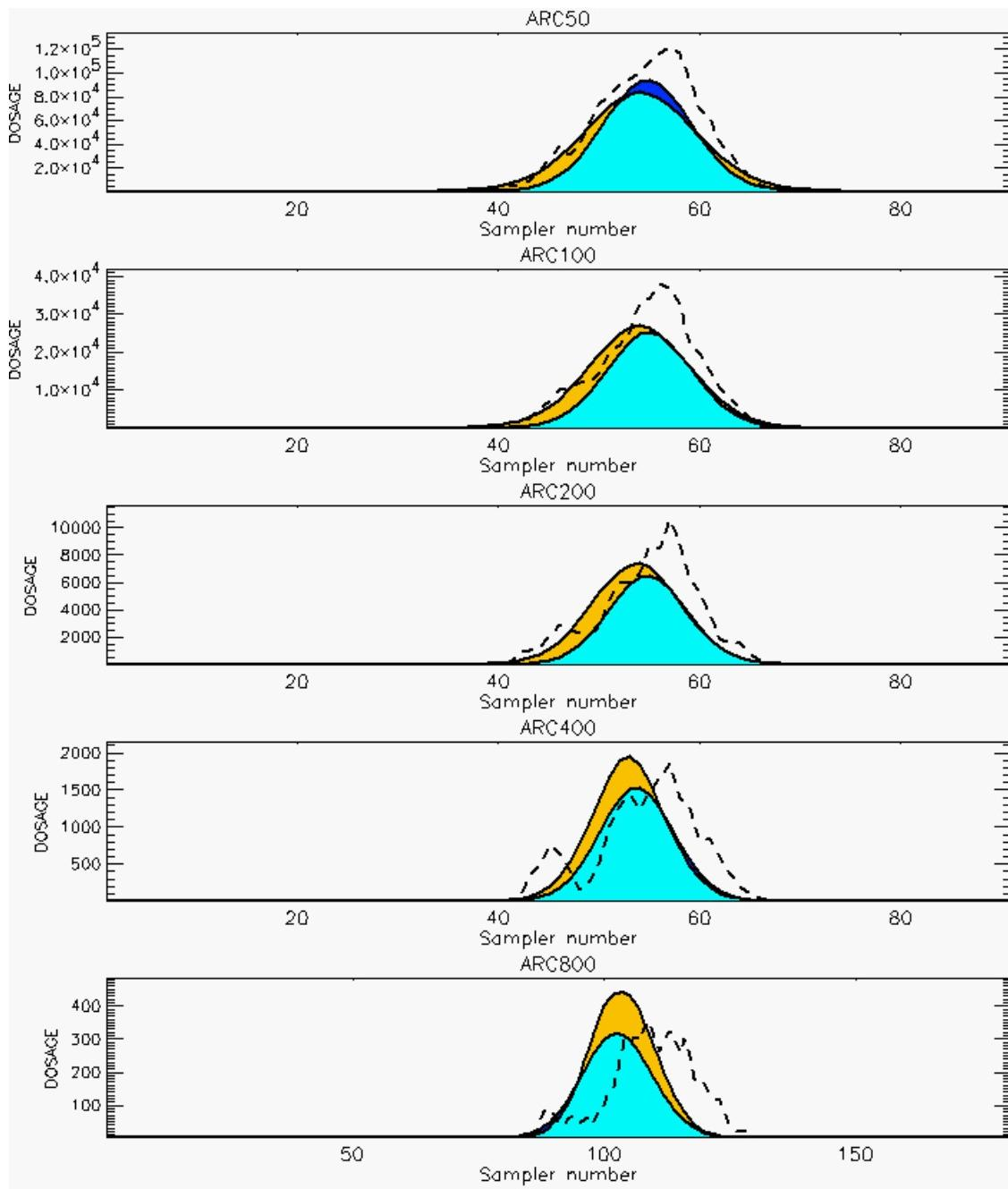
PG Prediction1 to Prediction2 Comparison

PG Trial File: pr_grass_tracer_Experiment_48.txt

PG Prediction File 1: HPAC\nodeposition\pg_48_novd.out

PG Prediction File 2: ARAC\nodeposition\pg_48_novd.arac

**Figure E-39b. HPAC and NARAC Predictions to Trial 48 on Logarithmic Scale:
Stability Category is 3**



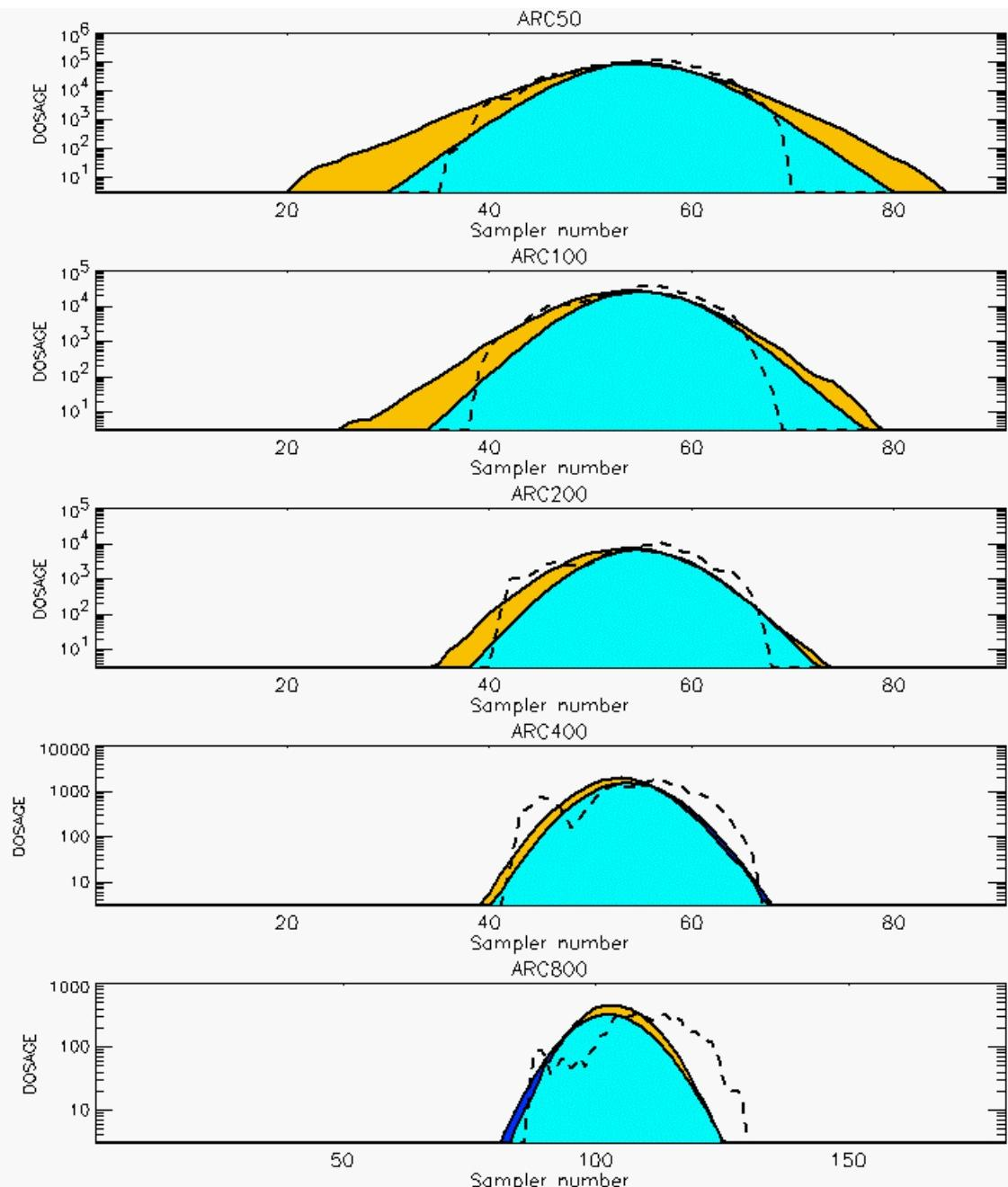
PG Prediction1 to Prediction2 Comparison

PG Trial File: pr_grass_tracer_Experiment_49.txt

PG Prediction File 1: HPAC\nodeposition\pg_49_noxd.out

PG Prediction File 2: ARAC\nodeposition\pg_49_noxd.arac

**Figure E-40a. HPAC and NARAC Predictions to Trial 49 on Linear Scale:
Stability Category is 2**



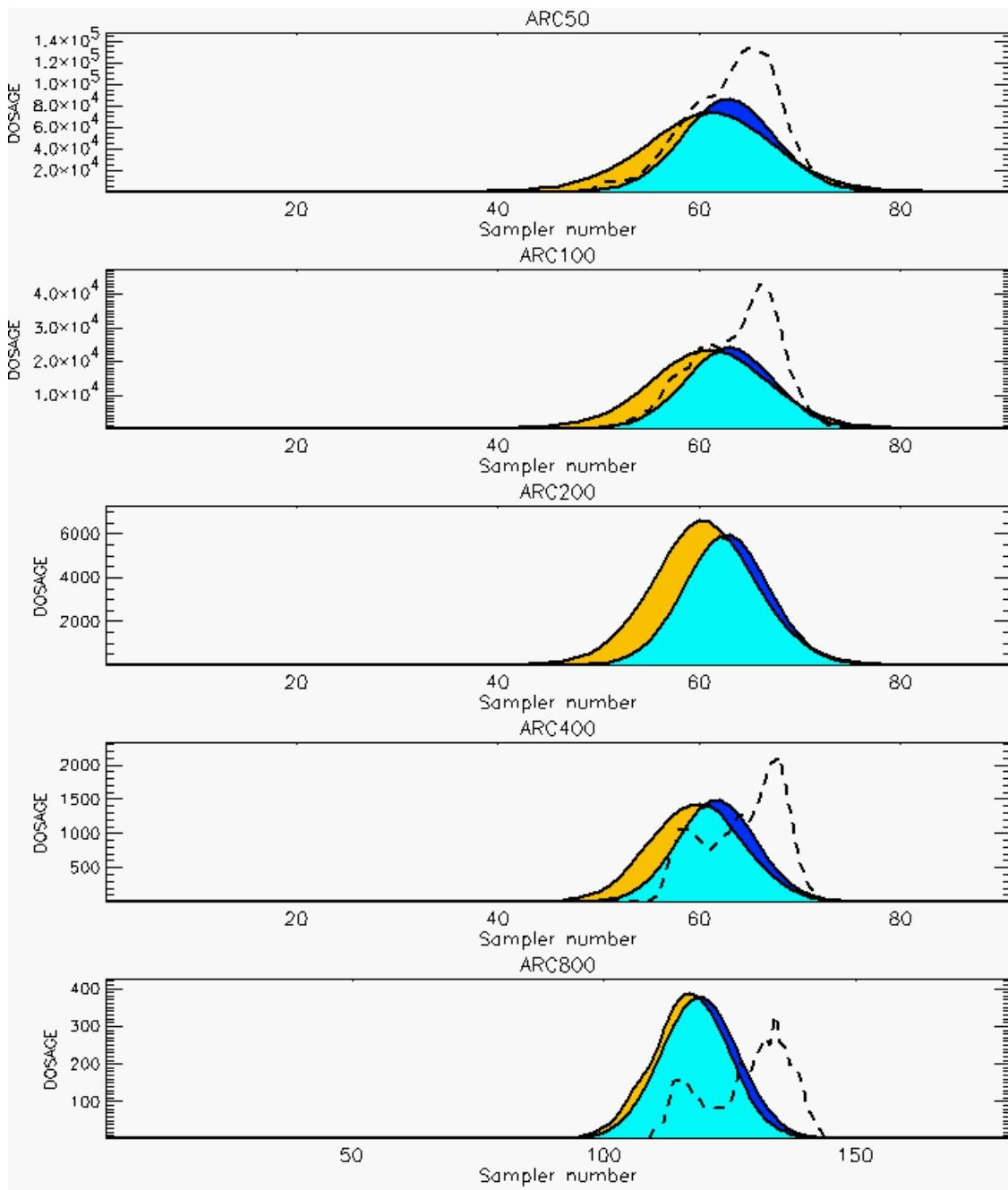
PG Prediction1 to Prediction2 Comparison

PG Trial File: pr_grass_tracer_Experiment_49.txt

PG Prediction File 1: HPAC\nodeposition\pg_49_novd.out

PG Prediction File 2: ARAC\nodeposition\pg_49_novd.arac

**Figure E-40b. HPAC and NARAC Predictions to Trial 49 on Logarithmic Scale:
Stability Category is 2**



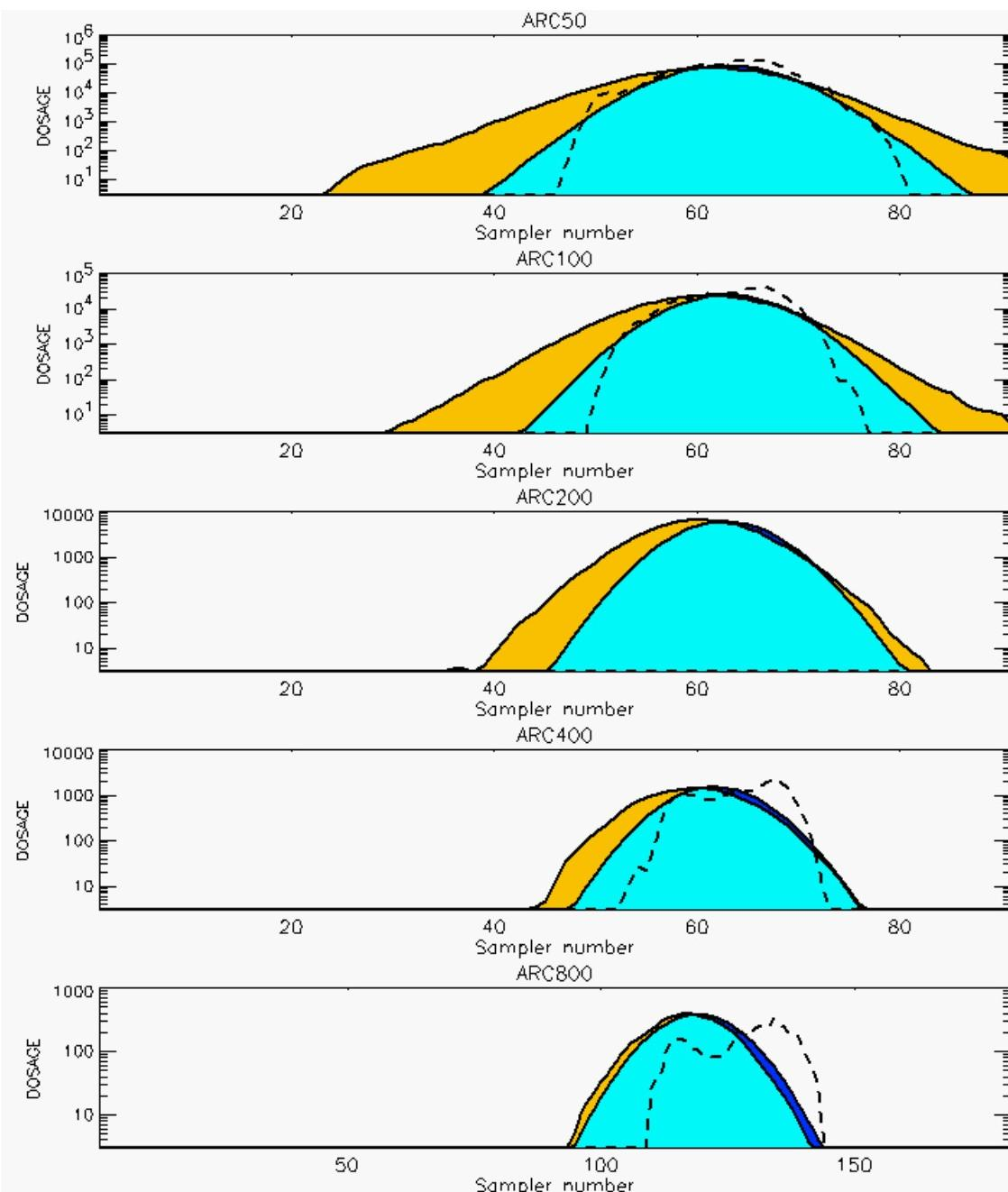
PG Prediction1 to Prediction2 Comparison

PG Trial File: pr_grass_tracer_Experiment_50.txt

PG Prediction File 1: HPAC\nodeposition\pg_50_noxd.out

PG Prediction File 2: ARAC\nodeposition\pg_50_noxd.arac

**Figure E-41a. HPAC and NARAC Predictions to Trial 50 on Linear Scale:
Stability Category is 2**



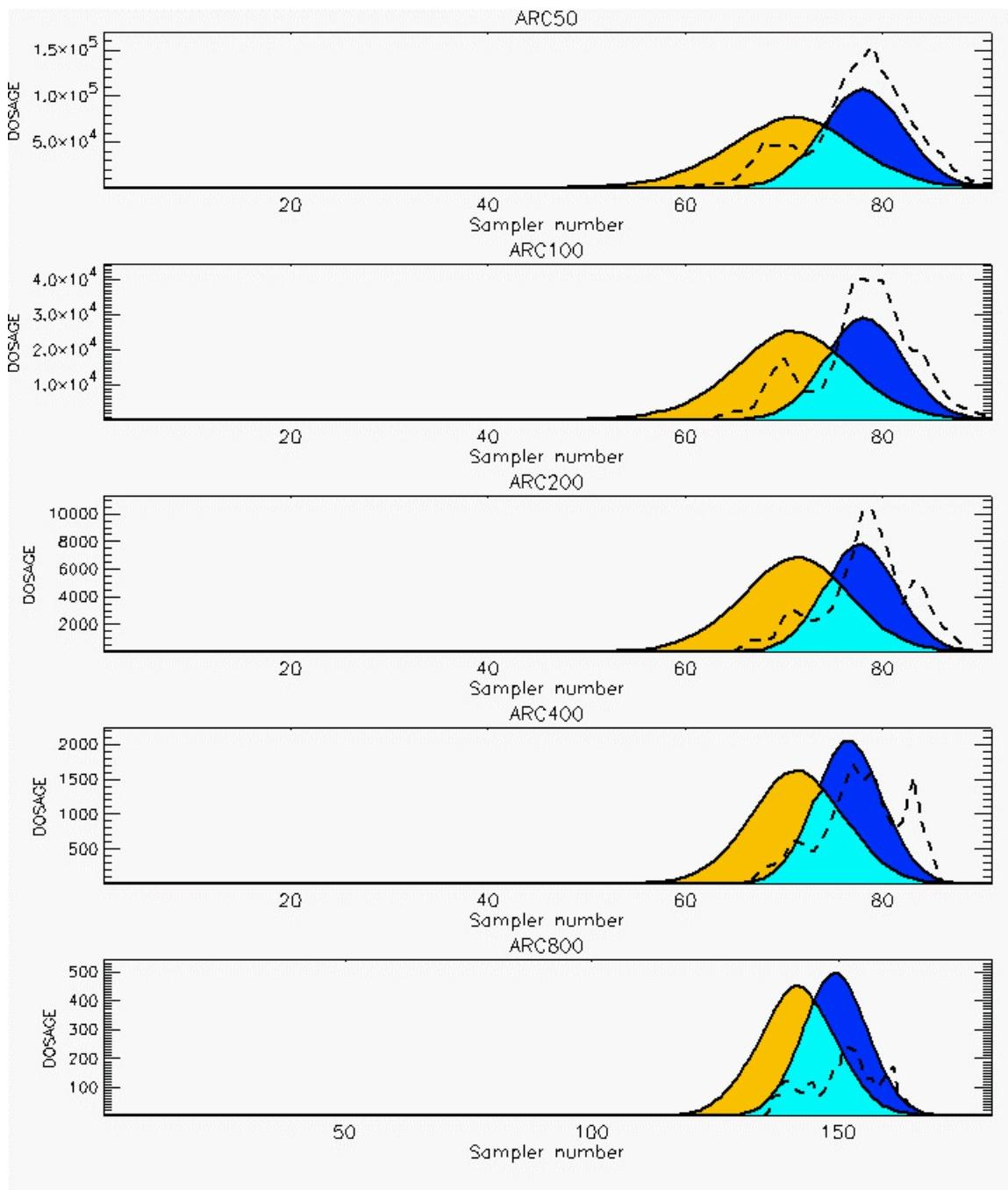
PG Prediction1 to Prediction2 Comparison

PG Trial File: pr_grass_tracer_Experiment_50.txt

PG Prediction File 1: HPAC\nodeposition\pg_50_noxd.out

PG Prediction File 2: ARAC\nodeposition\pg_50_noxd.arac

**Figure E-41b. HPAC and NARAC Predictions to Trial 50 on Logarithmic Scale:
Stability Category is 2**



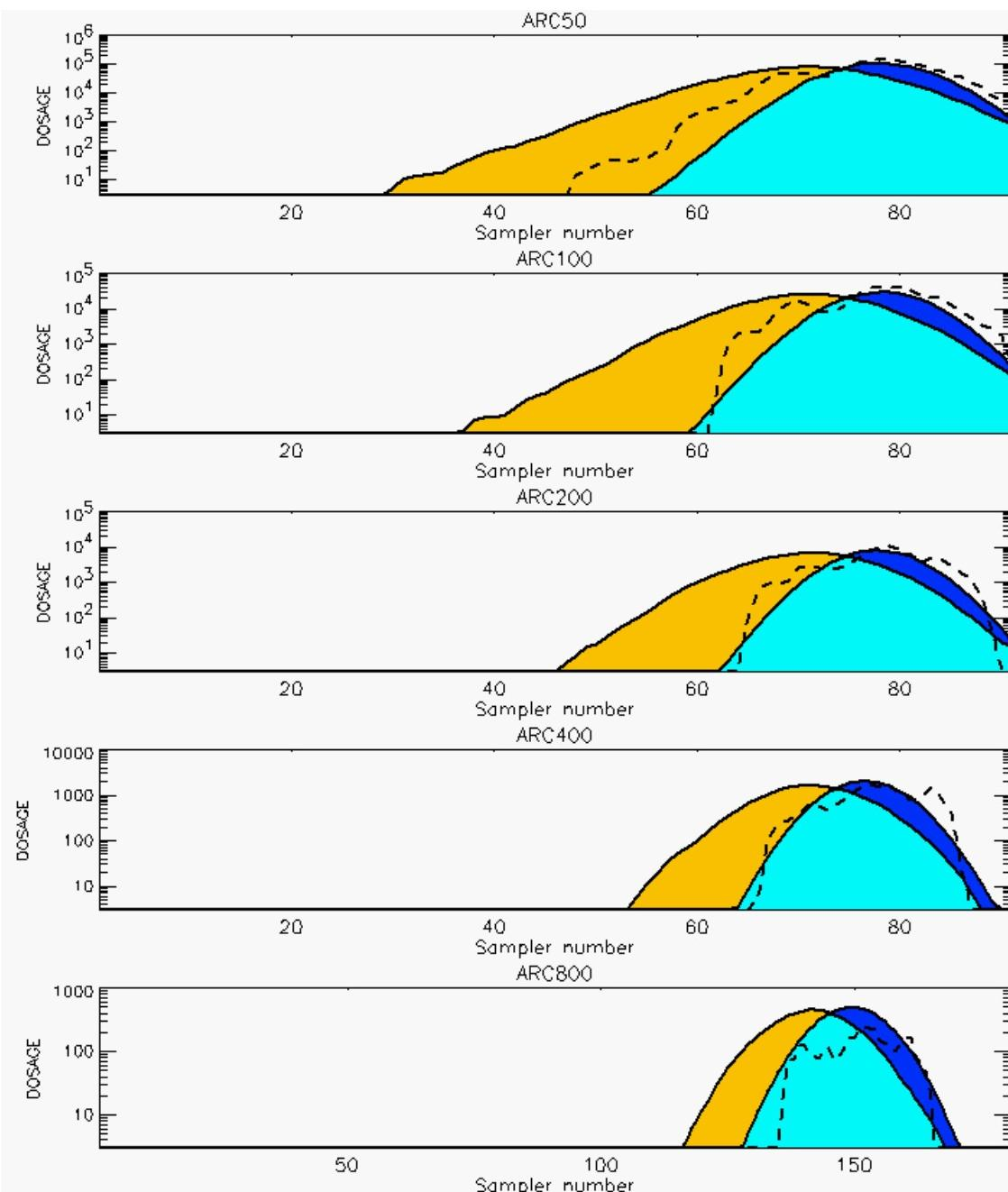
PG Prediction1 to Prediction2 Comparison

PG Trial File: pr_grass_tracer_Experiment_51.txt

PG Prediction File 1: HPAC\nodeposition\pg_51_noxd.out

PG Prediction File 2: ARAC\nodeposition\pg_51_noxd.arac

**Figure E-42a. HPAC and NARAC Predictions to Trial 51 on Linear Scale:
Stability Category is 2**



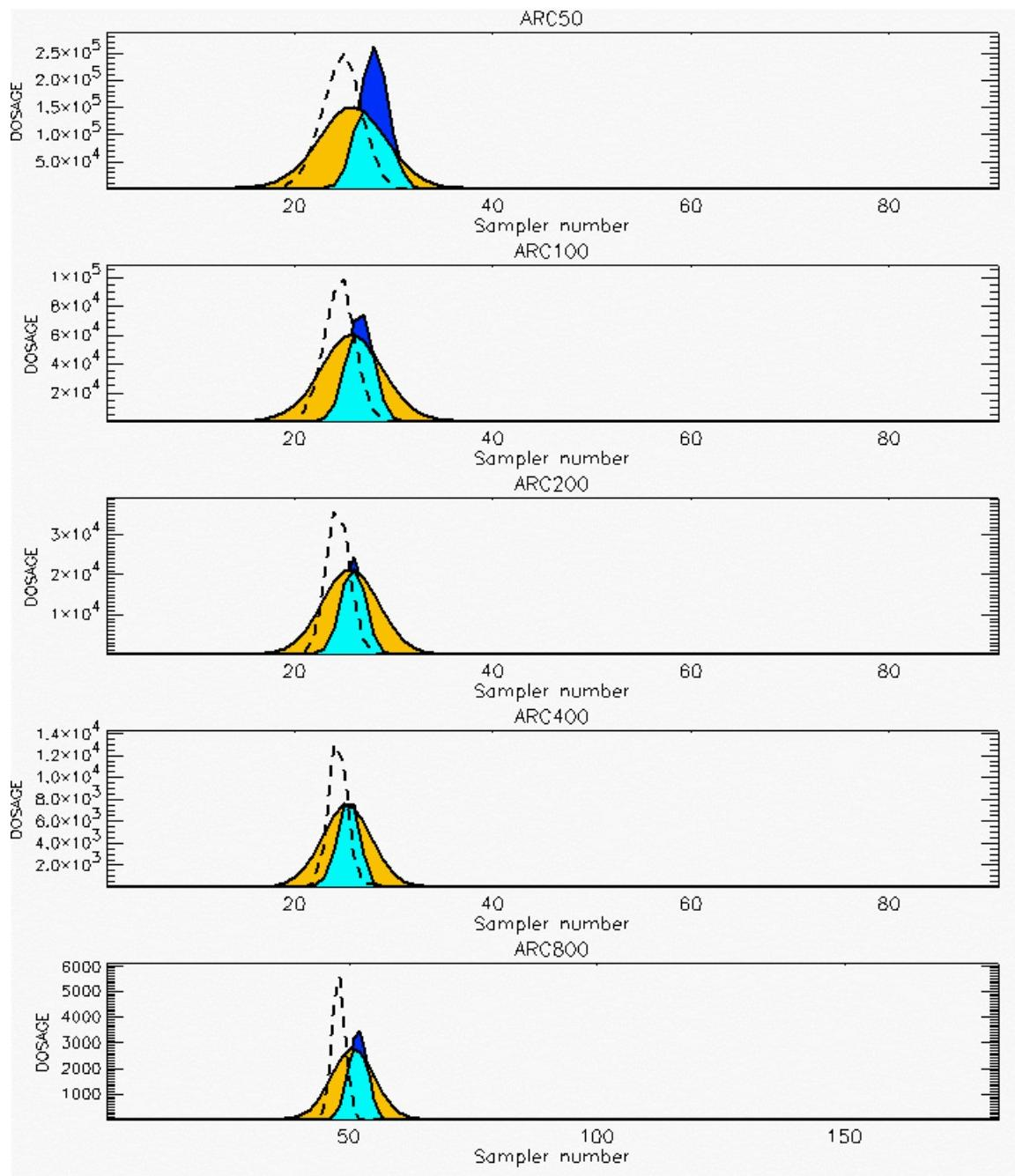
PG Prediction1 to Prediction2 Comparison

PG Trial File: pr_grass_tracer_Experiment_51.txt

PG Prediction File 1: HPAC\nodeposition\pg_51_noxd.out

PG Prediction File 2: ARAC\nodeposition\pg_51_noxd.arac

**Figure E-42b. HPAC and NARAC Predictions to Trial 51 on Logarithmic Scale:
Stability Category is 2**



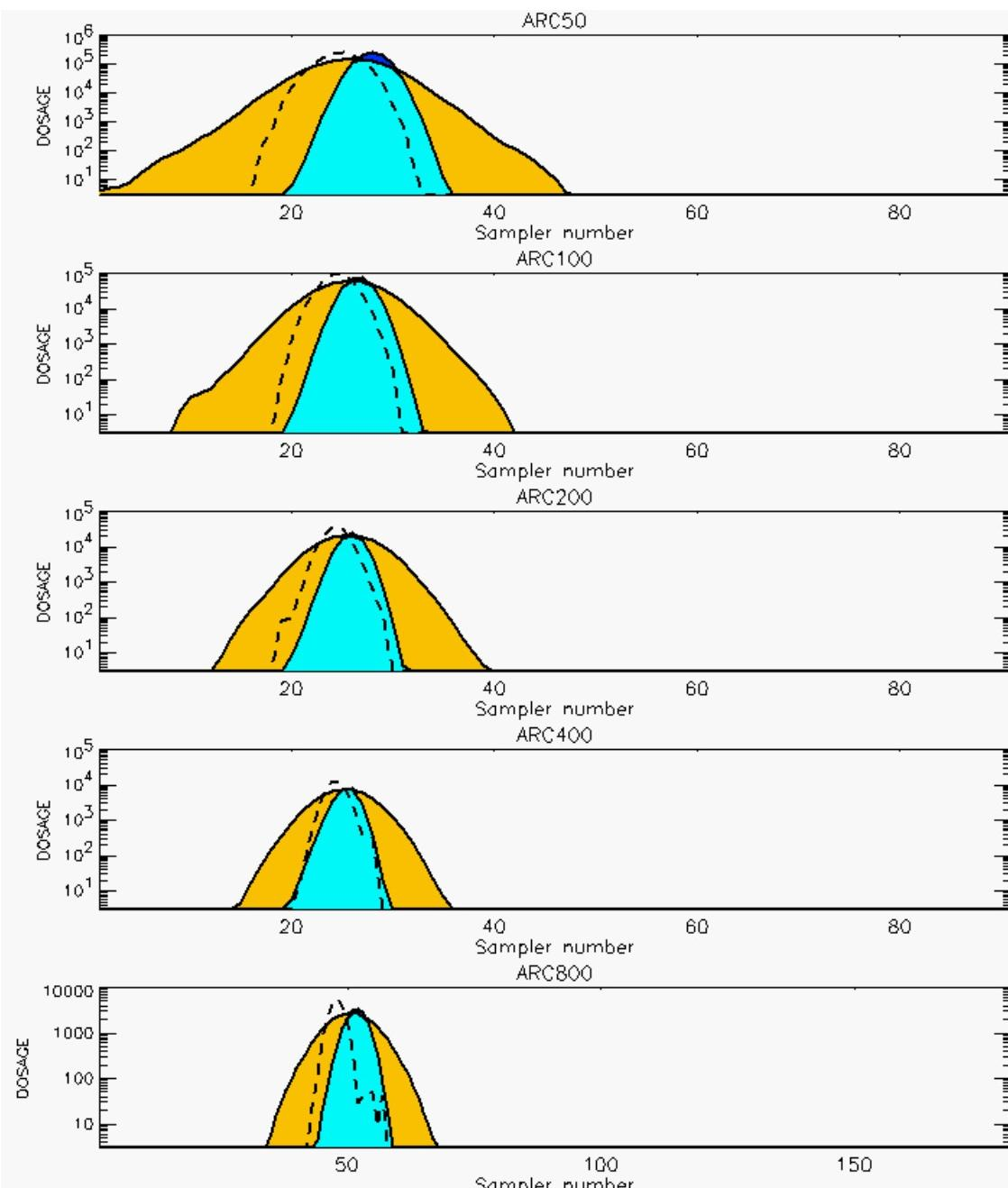
PG Prediction1 to Prediction2 Comparison

PG Trial File: pr_grass_tracer_Experiment_54.txt

PG Prediction File 1: HPAC\nodeposition\pg_54_noxd.out

PG Prediction File 2: ARAC\nodeposition\pg_54_noxd.arac

**Figure E-43a. HPAC and NARAC Predictions to Trial 54 on Linear Scale:
Stability Category is 5**



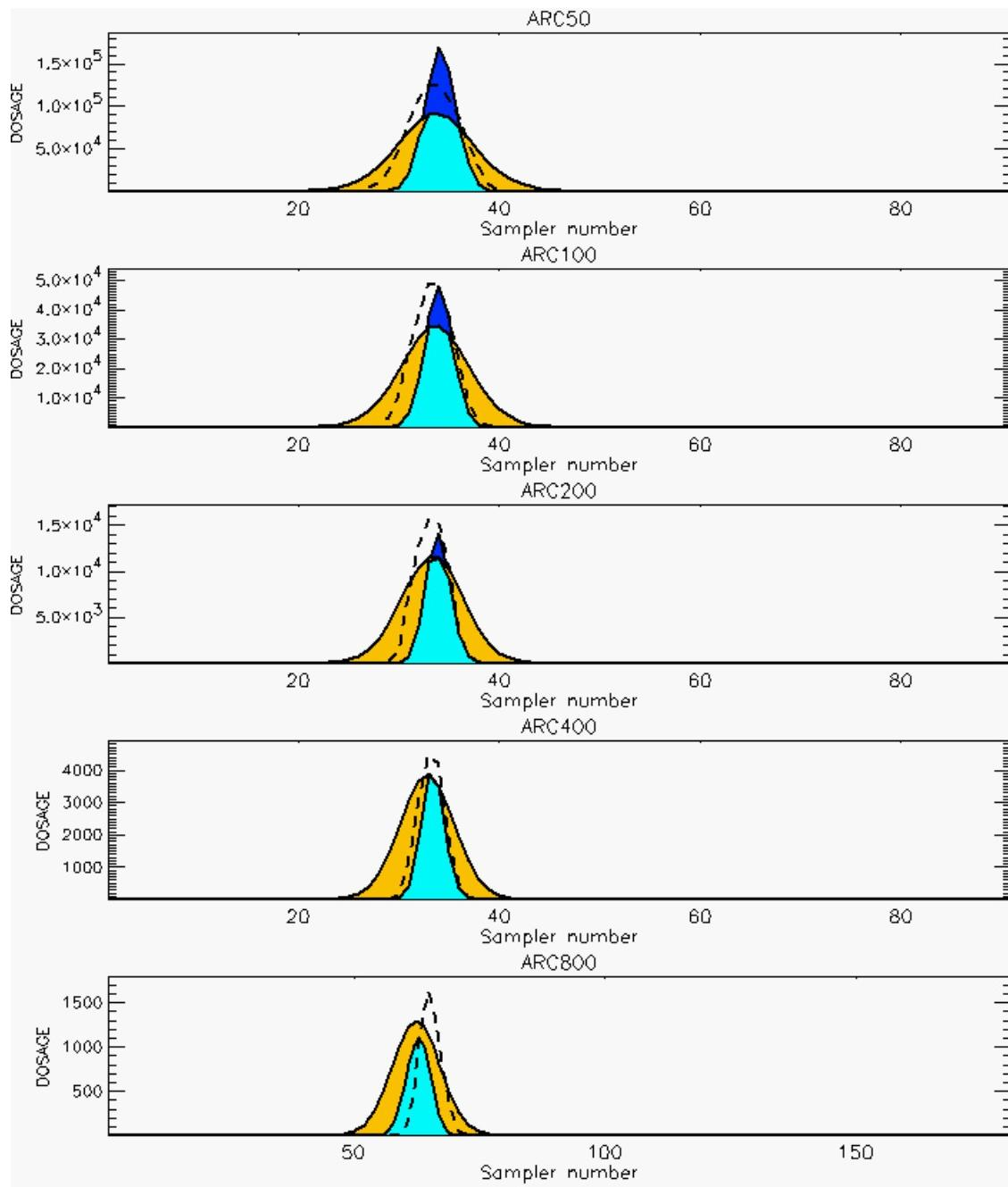
PG Prediction1 to Prediction2 Comparison

PG Trial File: pr_grass_tracer_Experiment_54.txt

PG Prediction File 1: HPAC\nodeposition\pg_54_nozd.out

PG Prediction File 2: ARAC\nodeposition\pg_54_nozd.arac

**Figure E-43b. HPAC and NARAC Predictions to Trial 54 on Logarithmic Scale:
Stability Category is 5**



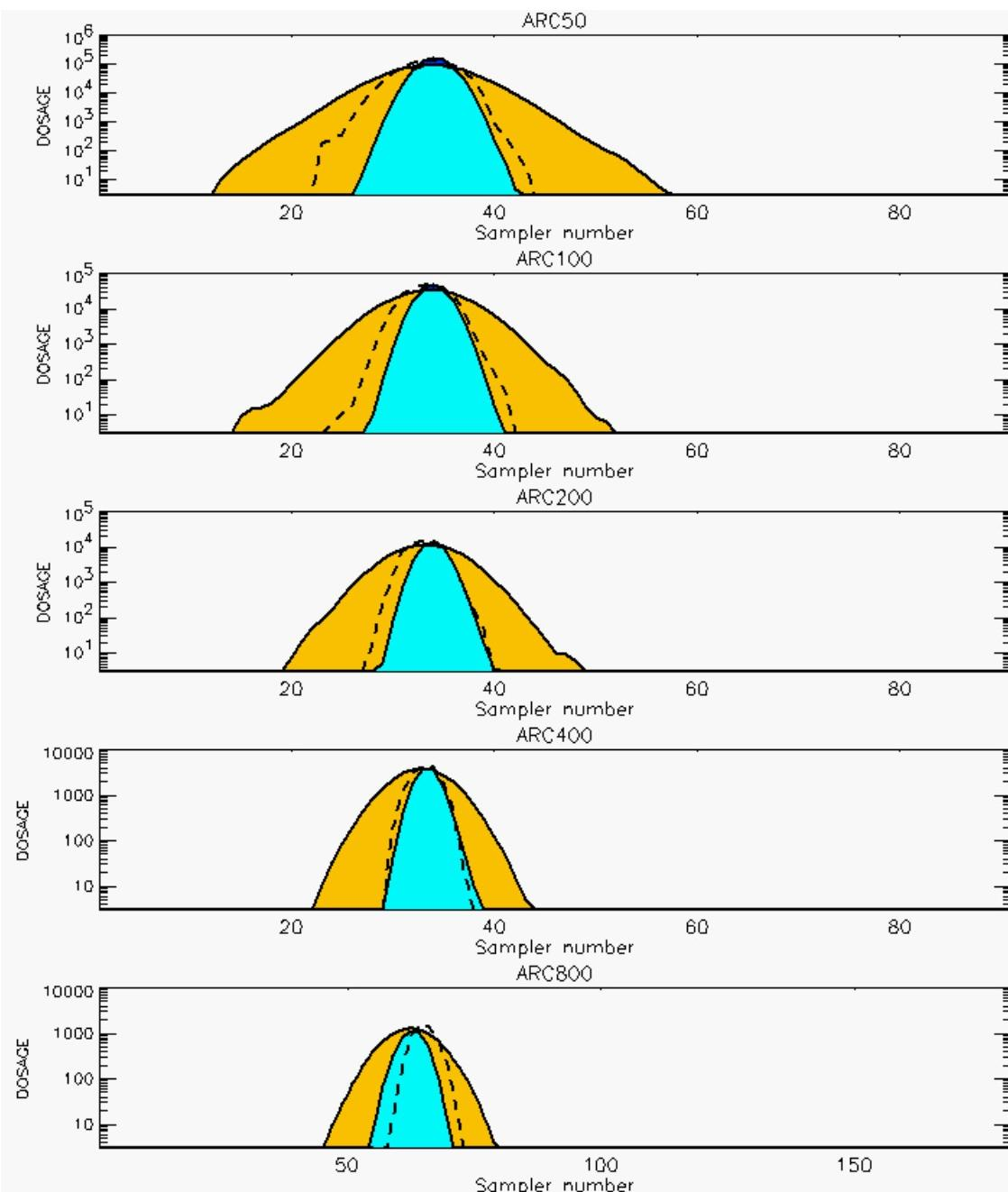
PG Prediction1 to Prediction2 Comparison

PG Trial File: pr_grass_tracer_Experiment_55.txt

PG Prediction File 1: HPAC\nodeposition\pg_55_noxd.out

PG Prediction File 2: ARAC\nodeposition\pg_55_noxd.arac

**Figure E-44a. HPAC and NARAC Predictions to Trial 55 on Linear Scale:
Stability Category is 4**



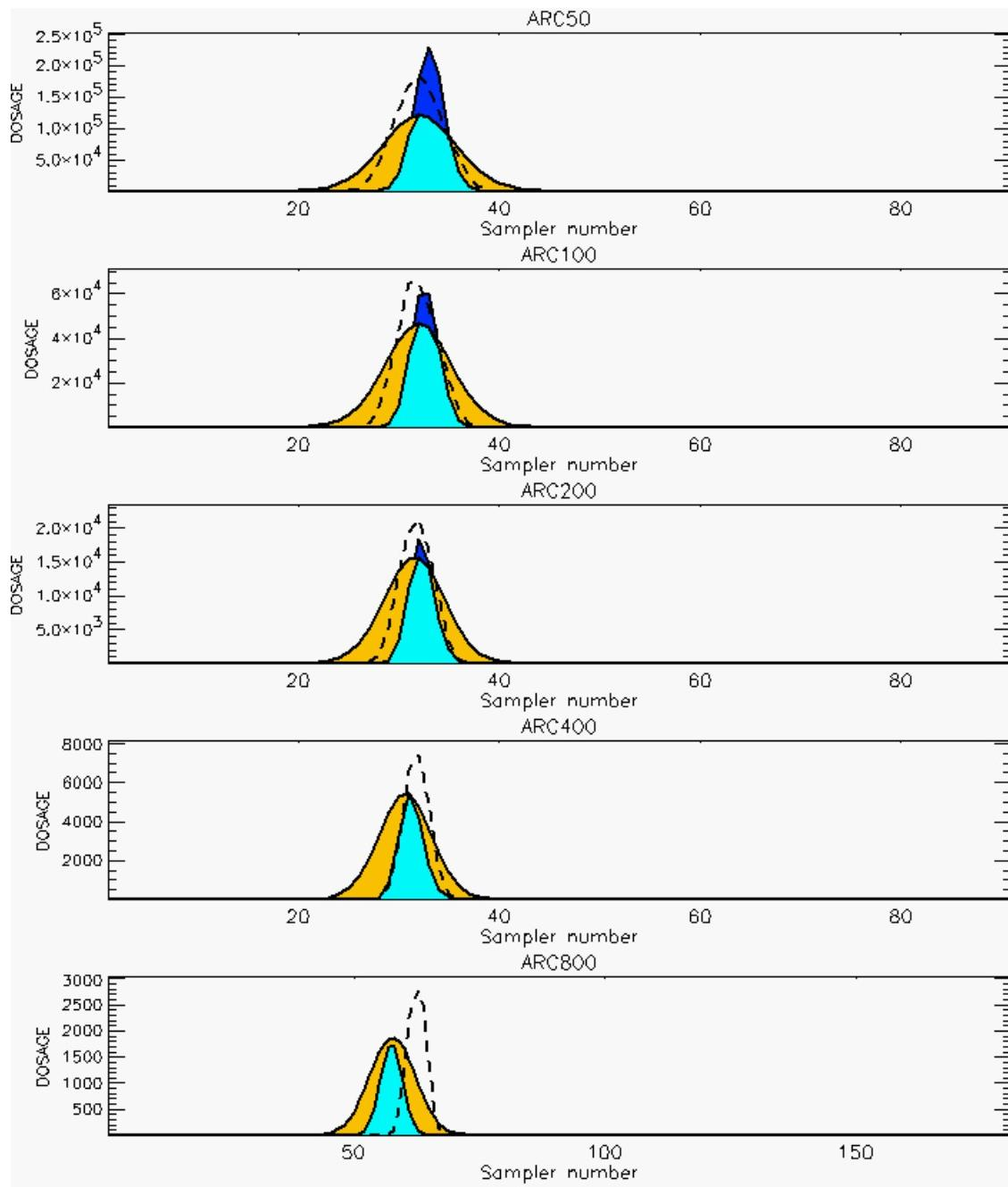
PG Prediction1 to Prediction2 Comparison

PG Trial File: pr_grass_tracer_Experiment_55.txt

PG Prediction File 1: HPAC\nodeposition\pg_55_noxd.out

PG Prediction File 2: ARAC\nodeposition\pg_55_noxd.arac

**Figure E-44b. HPAC and NARAC Predictions to Trial 55 on Logarithmic Scale:
Stability Category is 4**



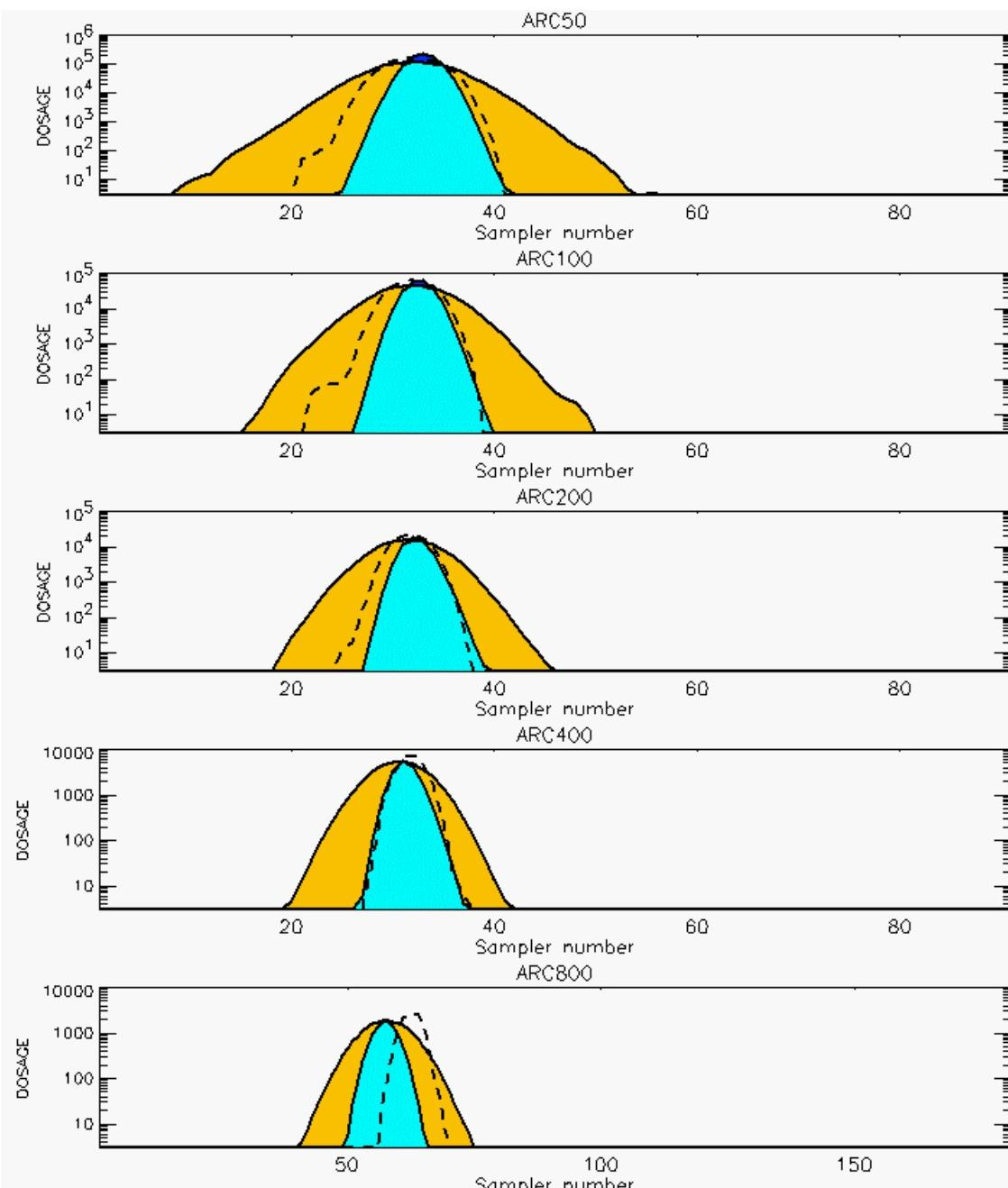
PG Prediction1 to Prediction2 Comparison

PG Trial File: pr_grass_tracer_Experiment_56.txt

PG Prediction File 1: HPAC\nodeposition\pg_56_noxd.out

PG Prediction File 2: ARAC\nodeposition\pg_56_noxd.arac

**Figure E-45a. HPAC and NARAC Predictions to Trial 56 on Linear Scale:
Stability Category is 4**



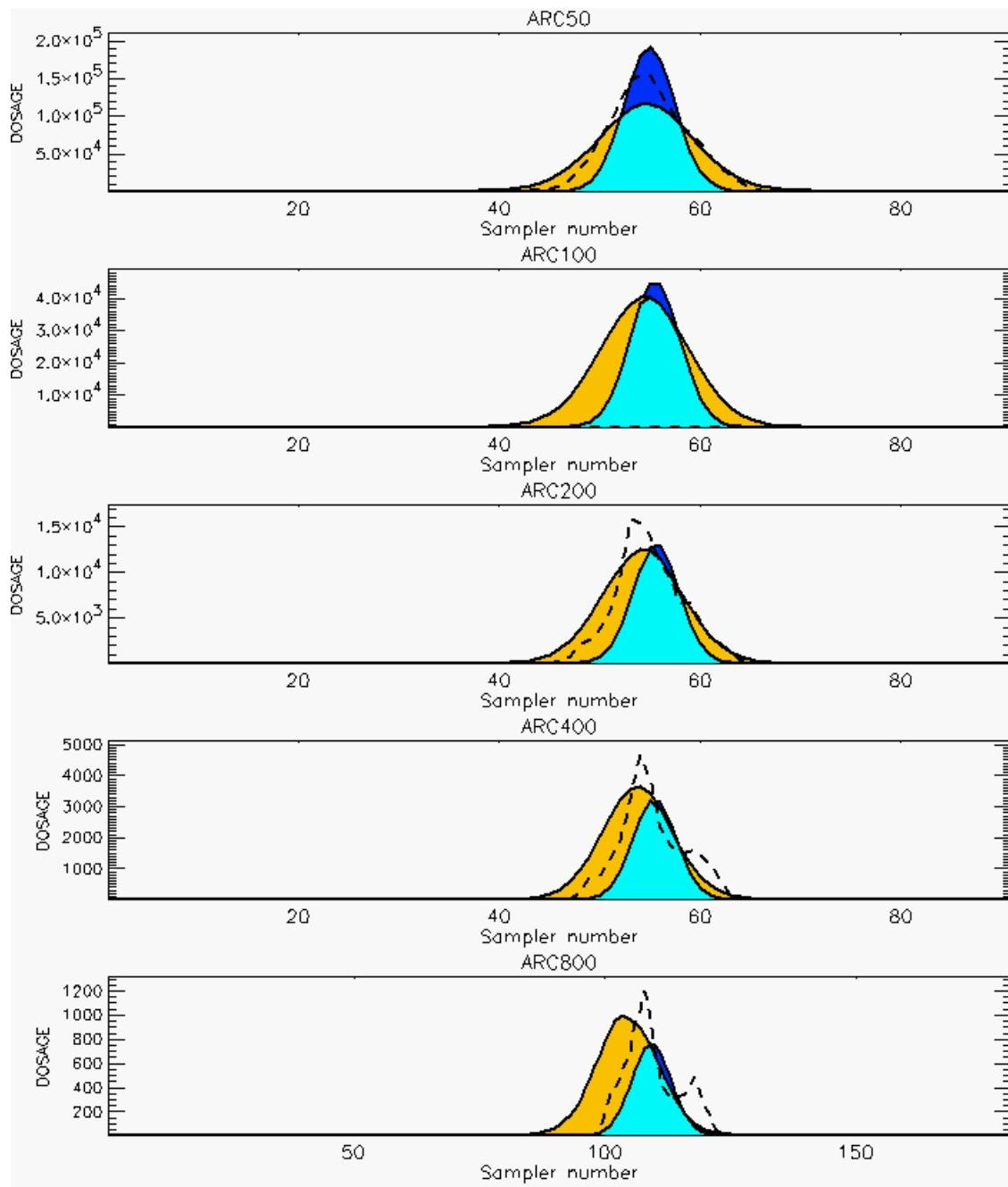
PG Prediction1 to Prediction2 Comparison

PG Trial File: pr_grass_tracer_Experiment_56.txt

PG Prediction File 1: HPAC\nodeposition\pg_56_novd.out

PG Prediction File 2: ARAC\nodeposition\pg_56_novd.arac

**Figure E-45b. HPAC and NARAC Predictions to Trial 56 on Logarithmic Scale:
Stability Category is 4**



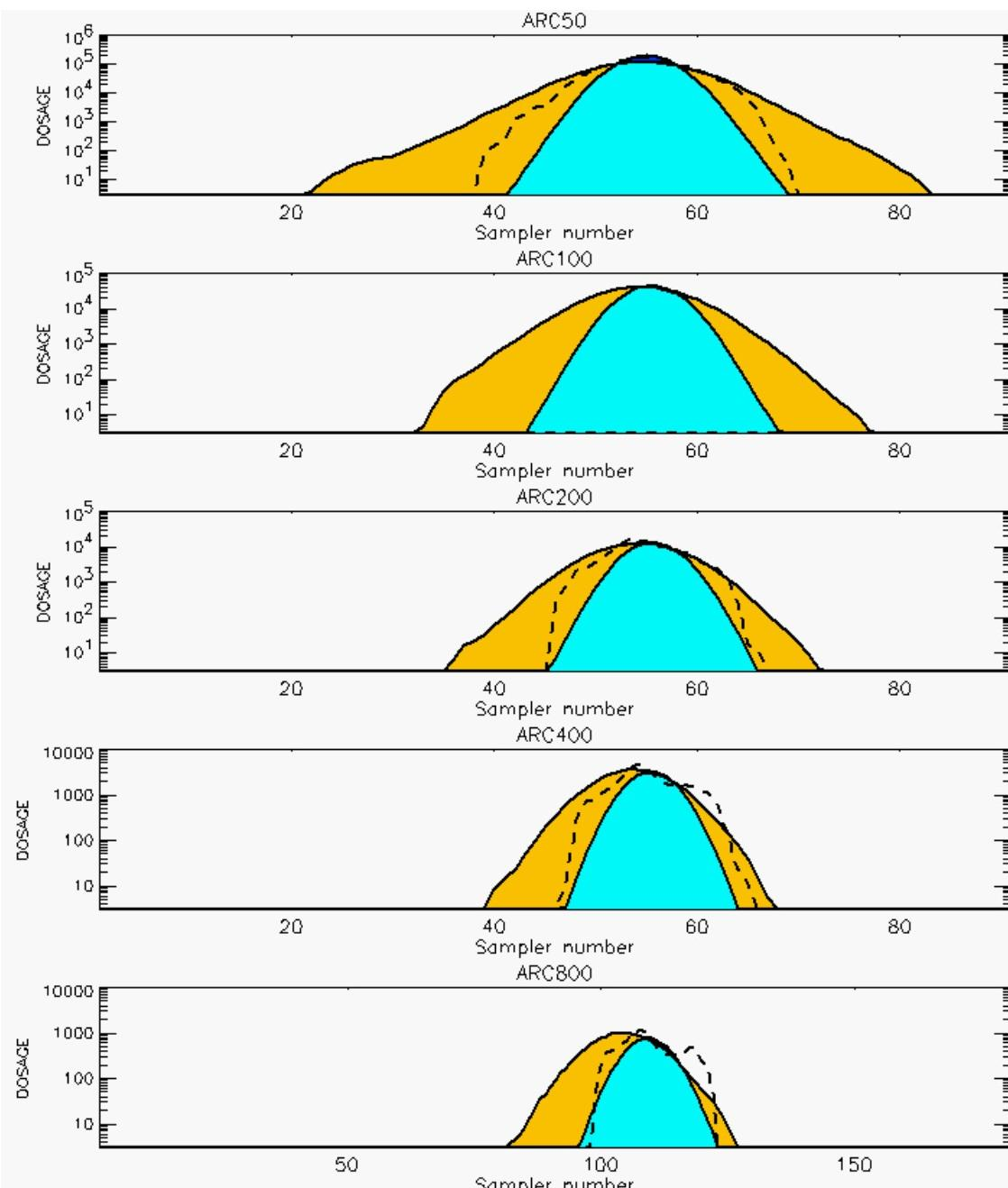
PG Prediction1 to Prediction2 Comparison

PG Trial File: pr_grass_tracer_Experiment_57.txt

PG Prediction File 1: HPAC\nodeposition\pg_57_noxd.out

PG Prediction File 2: ARAC\nodeposition\pg_57_noxd.arac

**Figure E-46a. HPAC and NARAC Predictions to Trial 57 on Linear Scale:
Stability Category is 3**



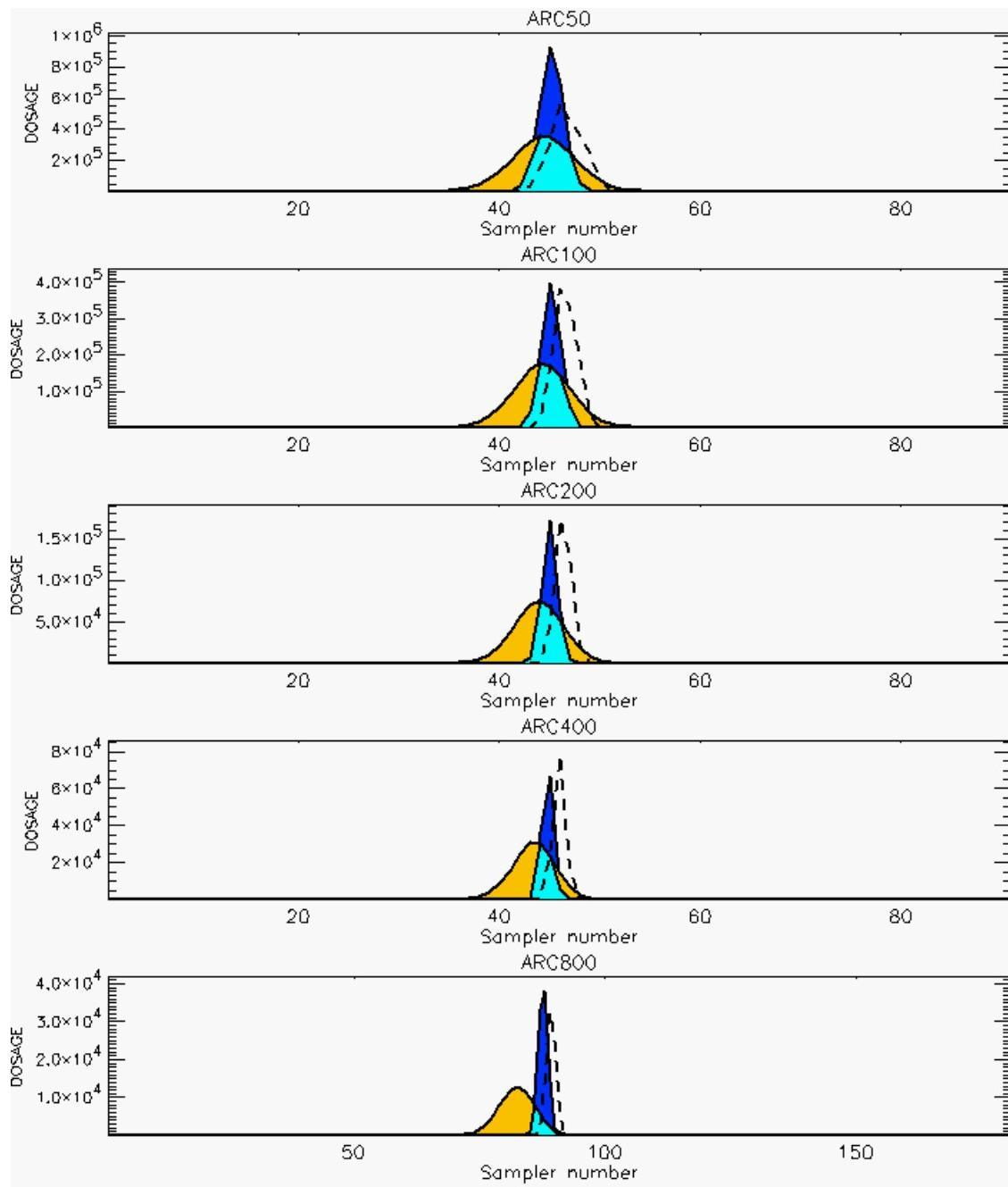
PG Prediction1 to Prediction2 Comparison

PG Trial File: pr_grass_tracer_Experiment_57.txt

PG Prediction File 1: HPAC\nodeposition\pg_57_noxd.out

PG Prediction File 2: ARAC\nodeposition\pg_57_noxd.arac

**Figure E-46b. HPAC and NARAC Predictions to Trial 57 on Logarithmic Scale:
Stability Category is 3**



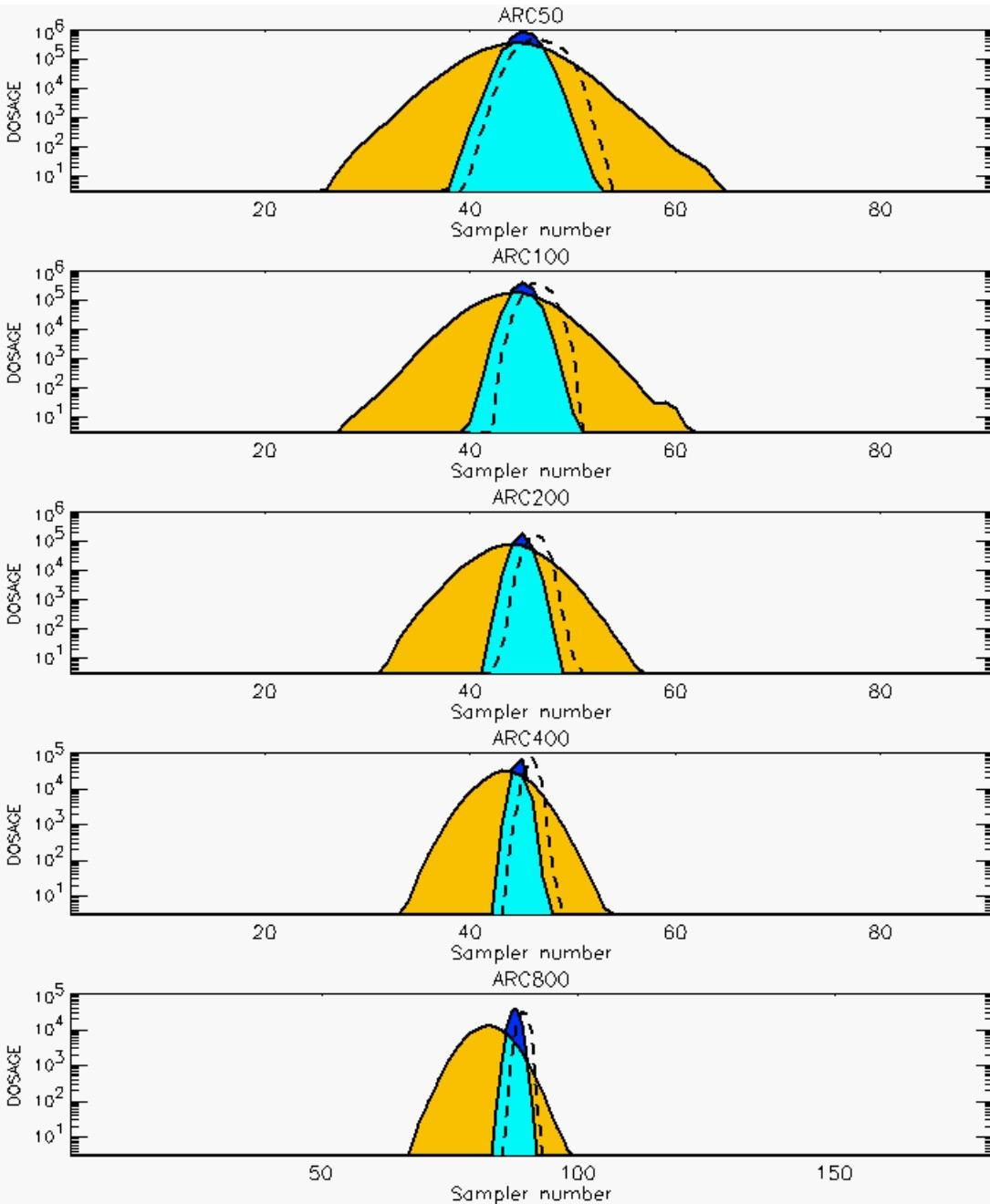
PG Prediction1 to Prediction2 Comparison

PG Trial File: pr_grass_tracer_Experiment_58.txt

PG Prediction File 1: HPAC\nodeposition\pg_58_noxd.out

PG Prediction File 2: ARAC\nodeposition\pg_58_noxd.arac

**Figure E-47a. HPAC and NARAC Predictions to Trial 58 on Linear Scale:
Stability Category is 6**



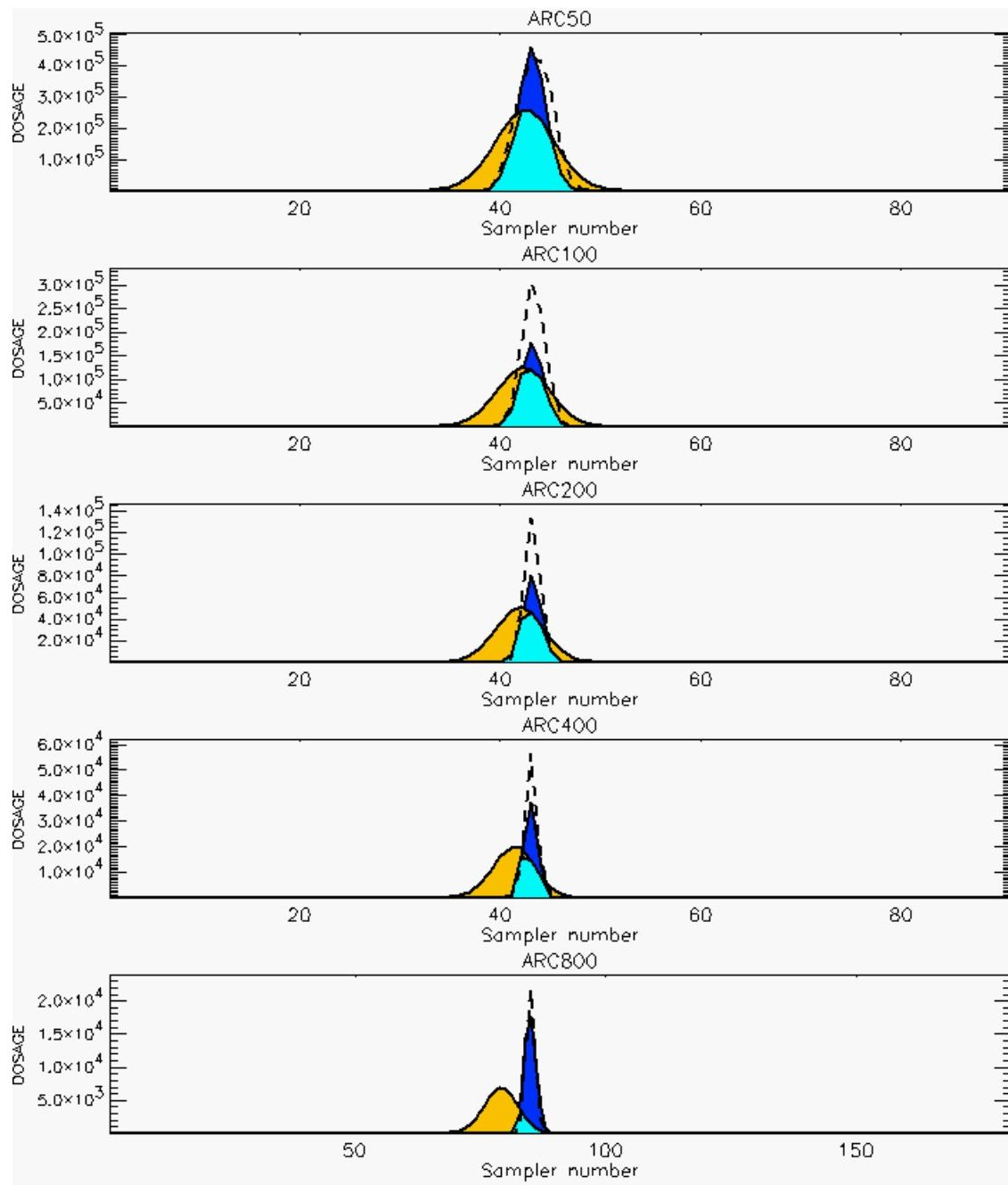
PG Prediction1 to Prediction2 Comparison

PG Trial File: pr_grass_tracer_Experiment_58.txt

PG Prediction File 1: HPAC\nodeposition\pg_58_novd.out

PG Prediction File 2: ARAC\nodeposition\pg_58_novd.arac

**Figure E-47b. HPAC and NARAC Predictions to Trial 58 on Logarithmic Scale:
Stability Category is 6**



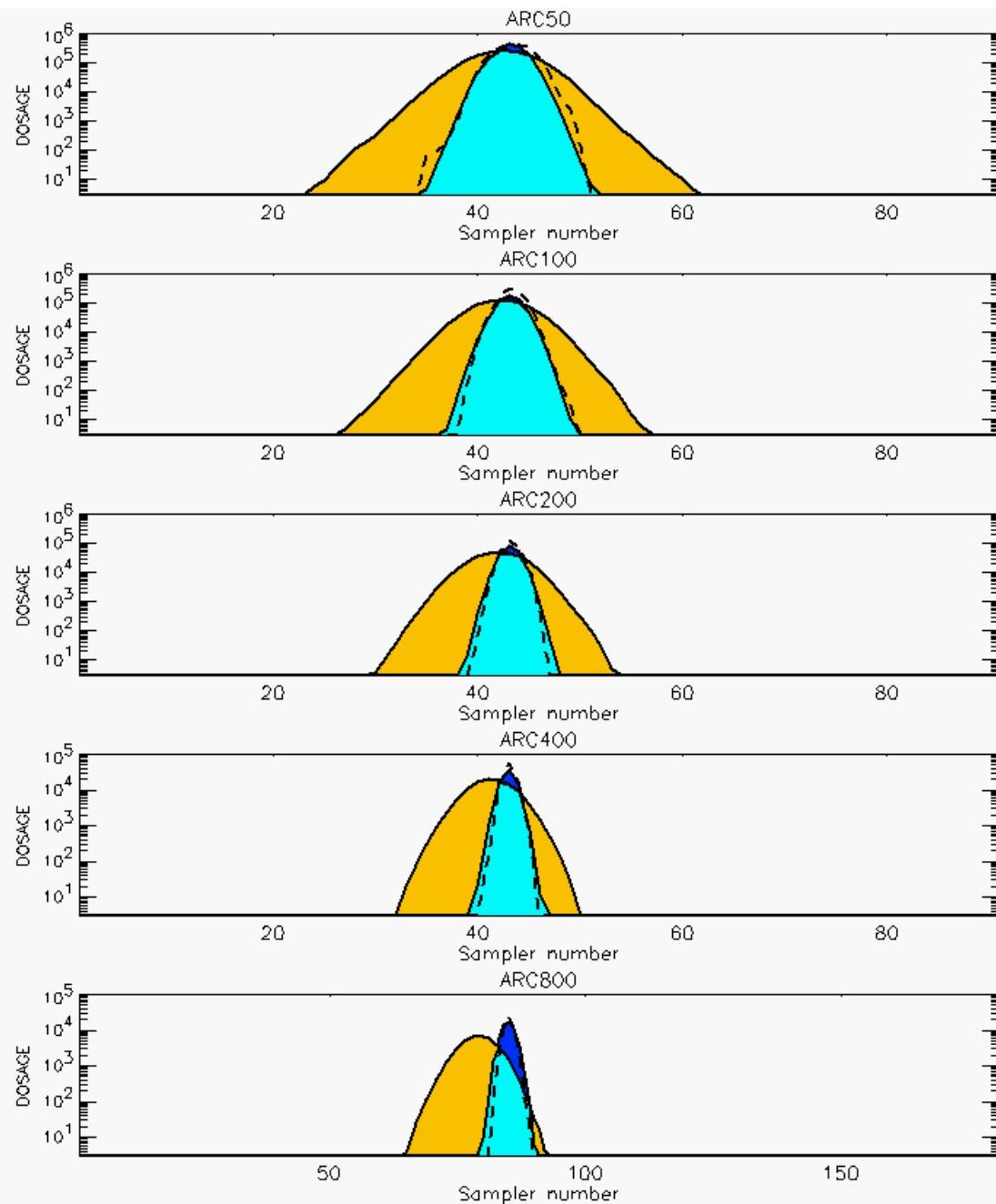
PG Prediction1 to Prediction2 Comparison

PG Trial File: pr_grass_tracer_Experiment_59.txt

PG Prediction File 1: HPAC\nodeposition\pg_59_noxd.out

PG Prediction File 2: ARAC\nodeposition\pg_59_noxd.arac

**Figure E-48a. HPAC and NARAC Predictions to Trial 59 on Linear Scale:
Stability Category is 5**



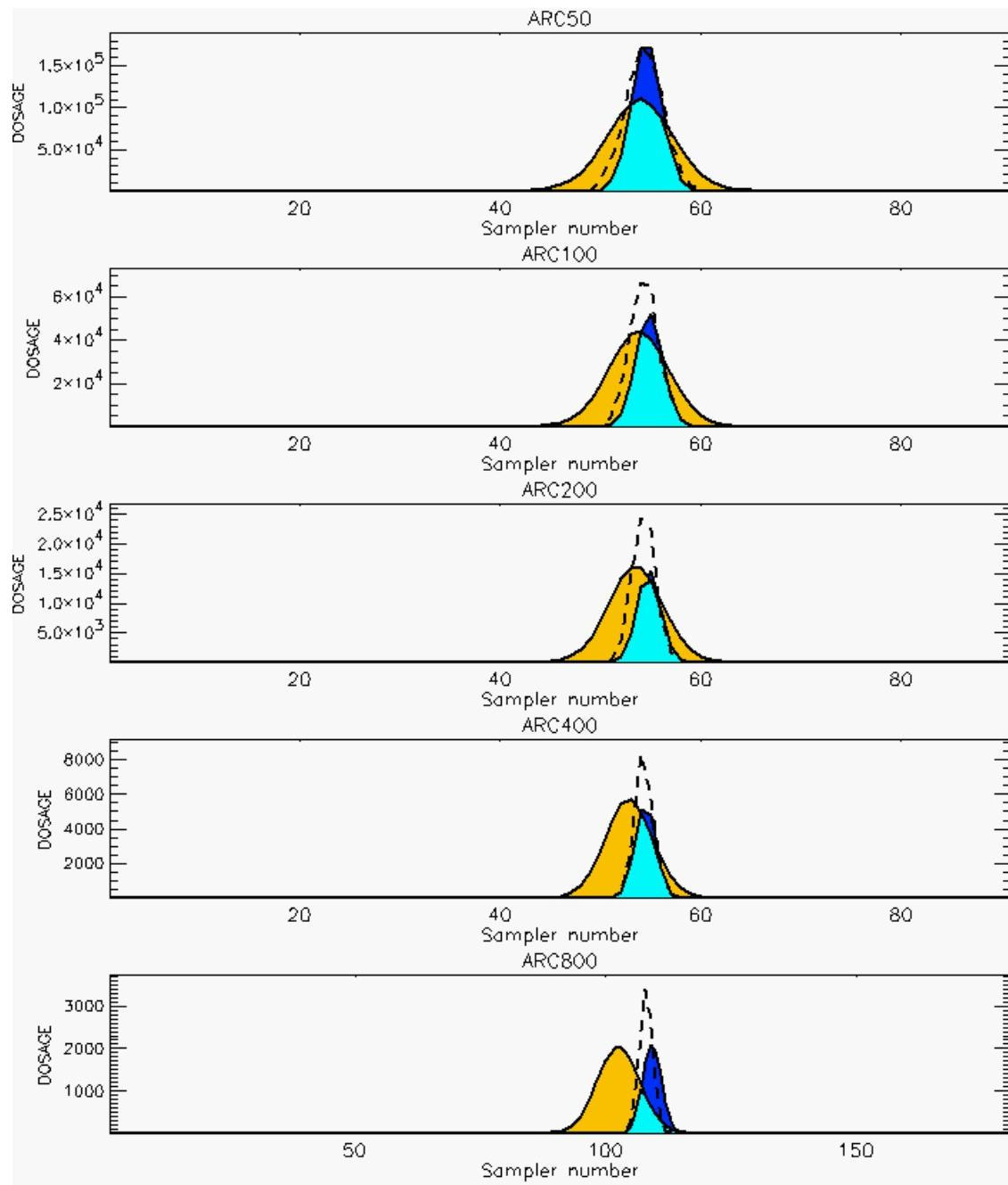
PG Prediction1 to Prediction2 Comparison

PG Trial File: pr_grass_tracer_Experiment_59.txt

PG Prediction File 1: HPAC\nodeposition\pg_59_novd.out

PG Prediction File 2: ARAC\nodeposition\pg_59_novd.arac

**Figure E-48b. HPAC and NARAC Predictions to Trial 59 on Logarithmic Scale:
Stability Category is 5**



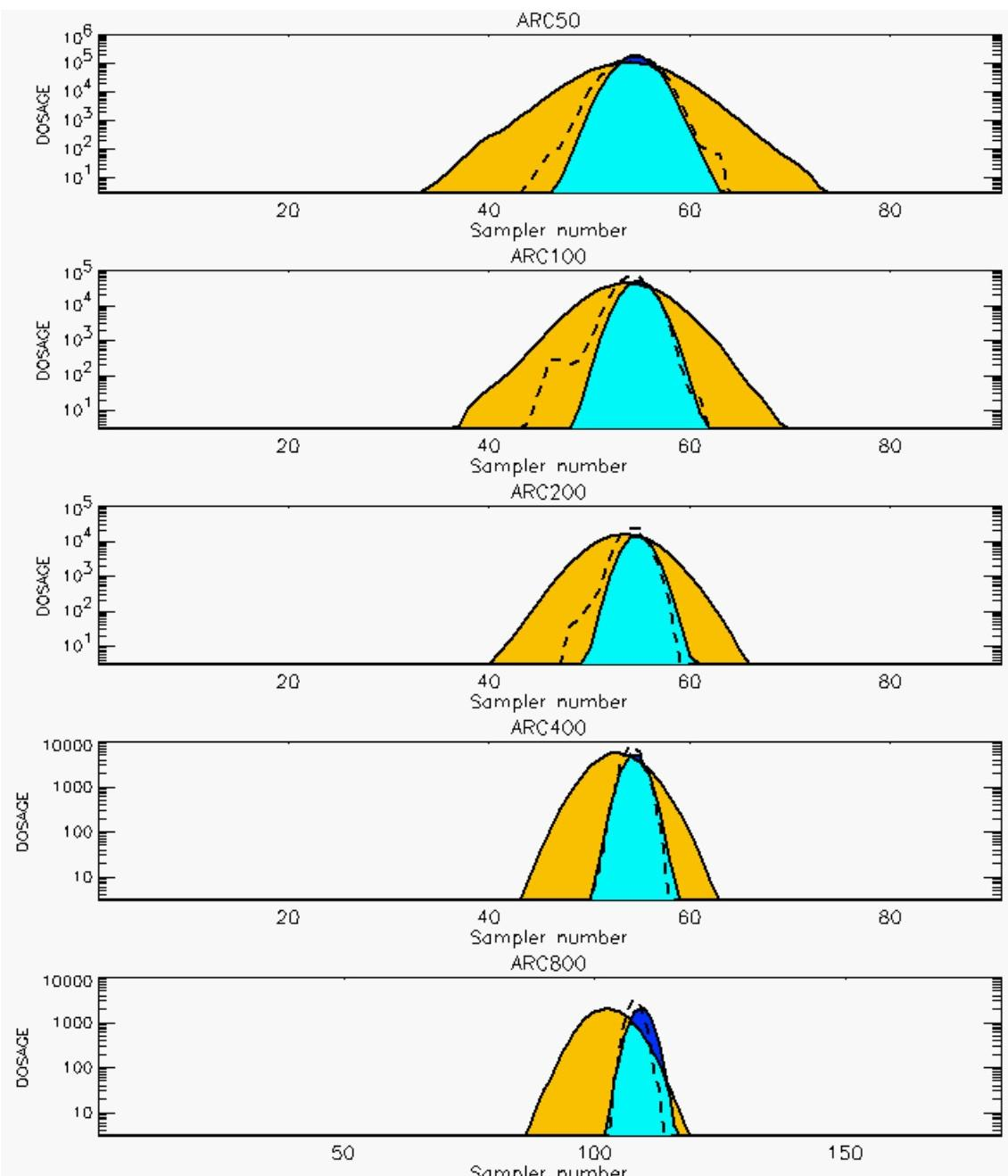
PG Prediction1 to Prediction2 Comparison

PG Trial File: pr_grass_tracer_Experiment_60.txt

PG Prediction File 1: HPAC\nodeposition\pg_60_noxd.out

PG Prediction File 2: ARAC\nodeposition\pg_60_noxd.arac

**Figure E-49a. HPAC and NARAC Predictions to Trial 60 on Linear Scale:
Stability Category is 5**



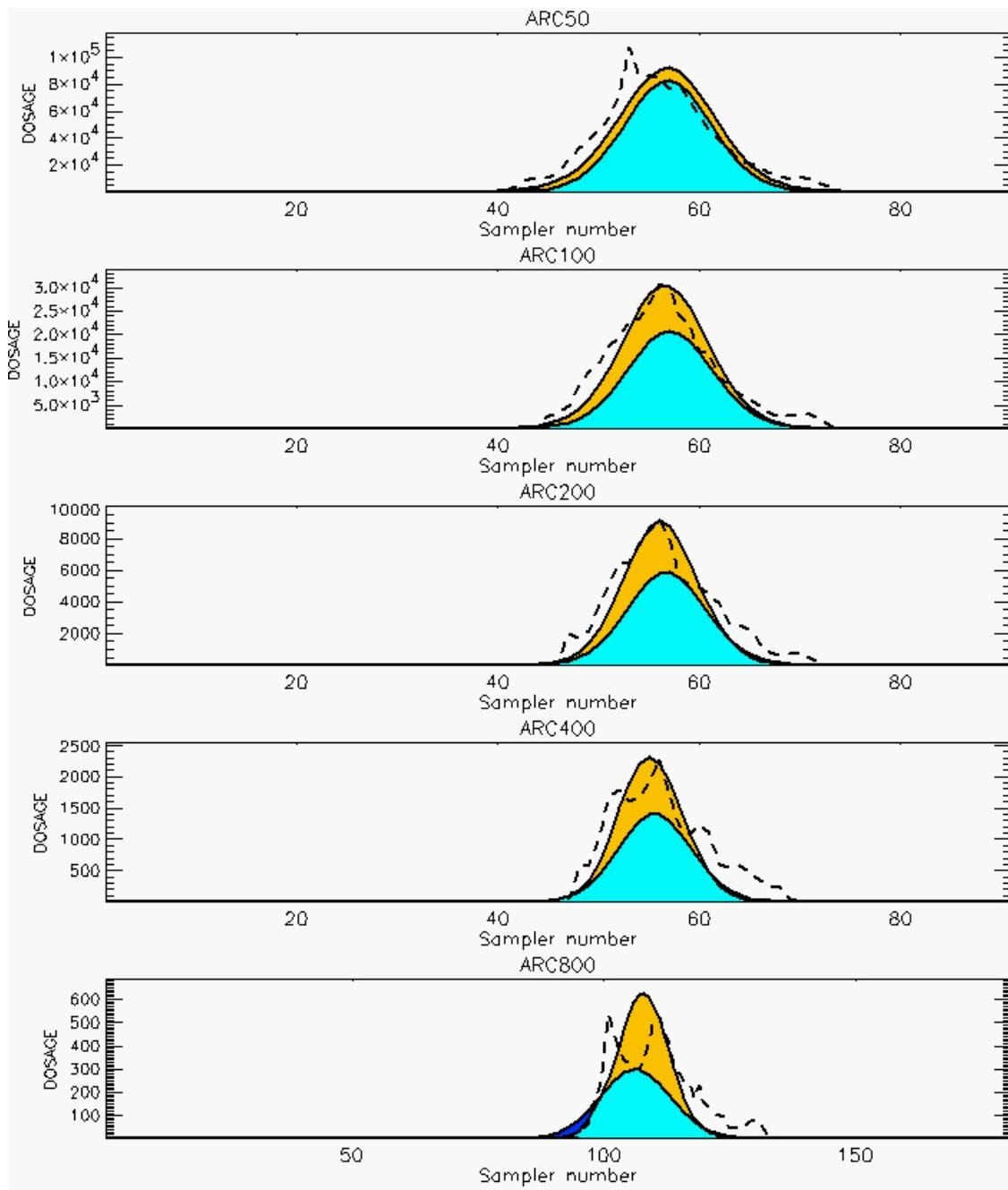
PG Prediction1 to Prediction2 Comparison

PG Trial File: pr_grass_tracer_Experiment_60.txt

PG Prediction File 1: HPAC\nodeposition\pg_60_noxd.out

PG Prediction File 2: ARAC\nodeposition\pg_60_noxd.arac

**Figure E-49b. HPAC and NARAC Predictions to Trial 60 on Logarithmic Scale:
Stability Category is 5**



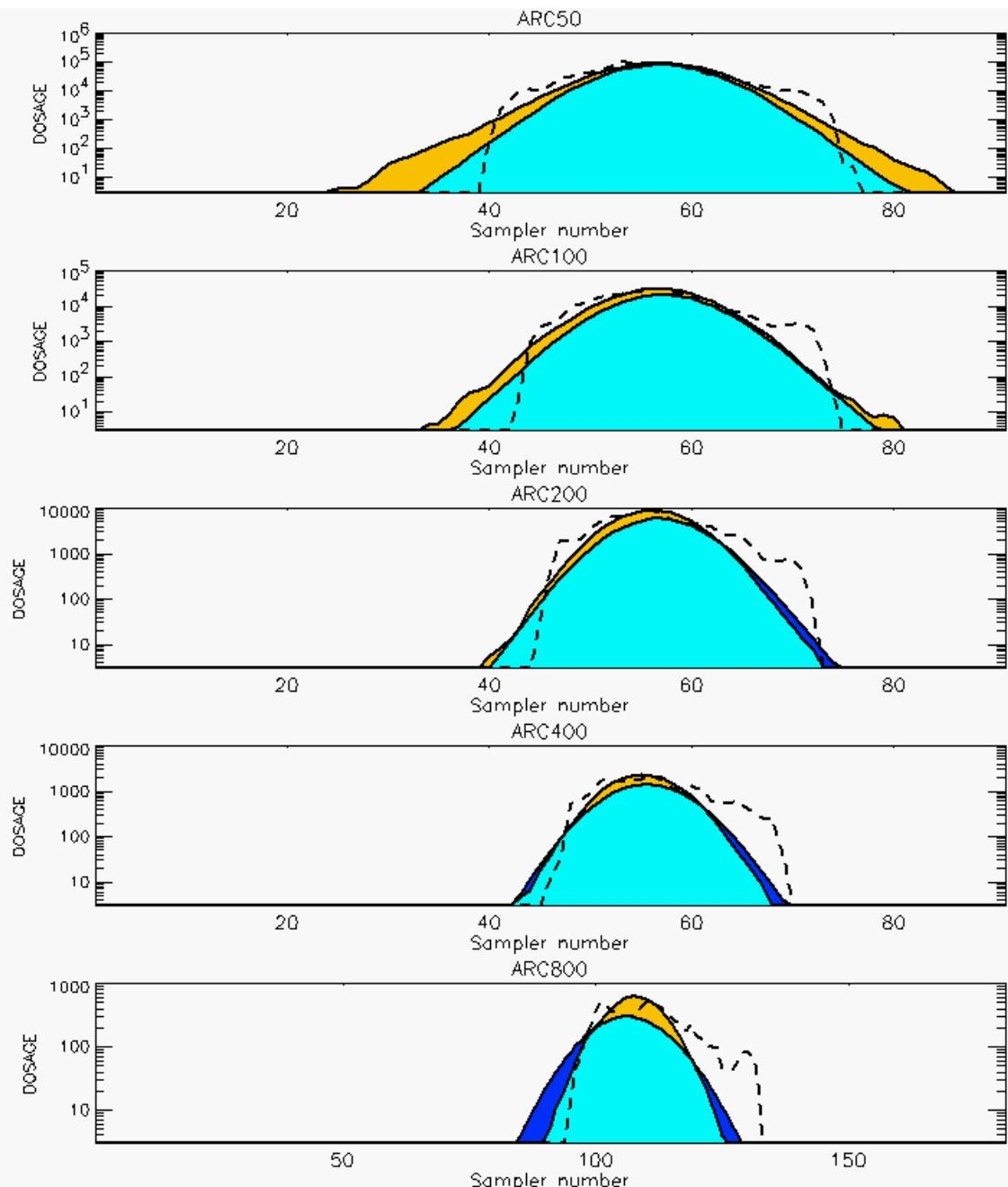
PG Prediction1 to Prediction2 Comparison

PG Trial File: pr_grass_tracer_Experiment_61.txt

PG Prediction File 1: HPAC\nodeposition\pg_61_noxd.out

PG Prediction File 2: ARAC\nodeposition\pg_61_noxd.arac

**Figure E-50a. HPAC and NARAC Predictions to Trial 61 on Linear Scale:
Stability Category is 3**



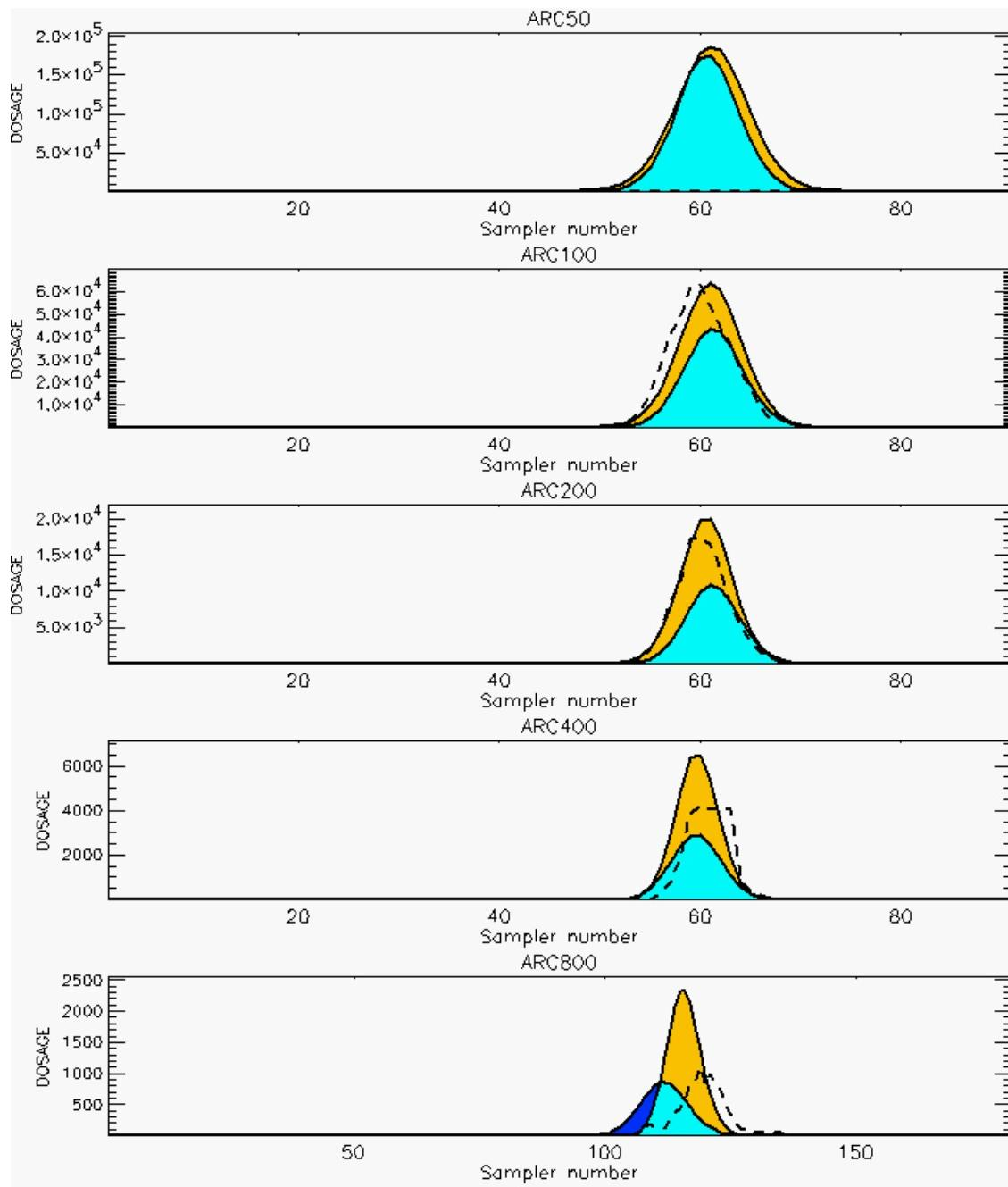
PG Prediction1 to Prediction2 Comparison

PG Trial File: pr_grass_tracer_Experiment_61.txt

PG Prediction File 1: HPAC\nodeposition\pg_61_noxd.out

PG Prediction File 2: ARAC\nodeposition\pg_61_noxd.arac

**Figure E-50b. HPAC and NARAC Predictions to Trial 61 on Logarithmic Scale:
Stability Category is 3**



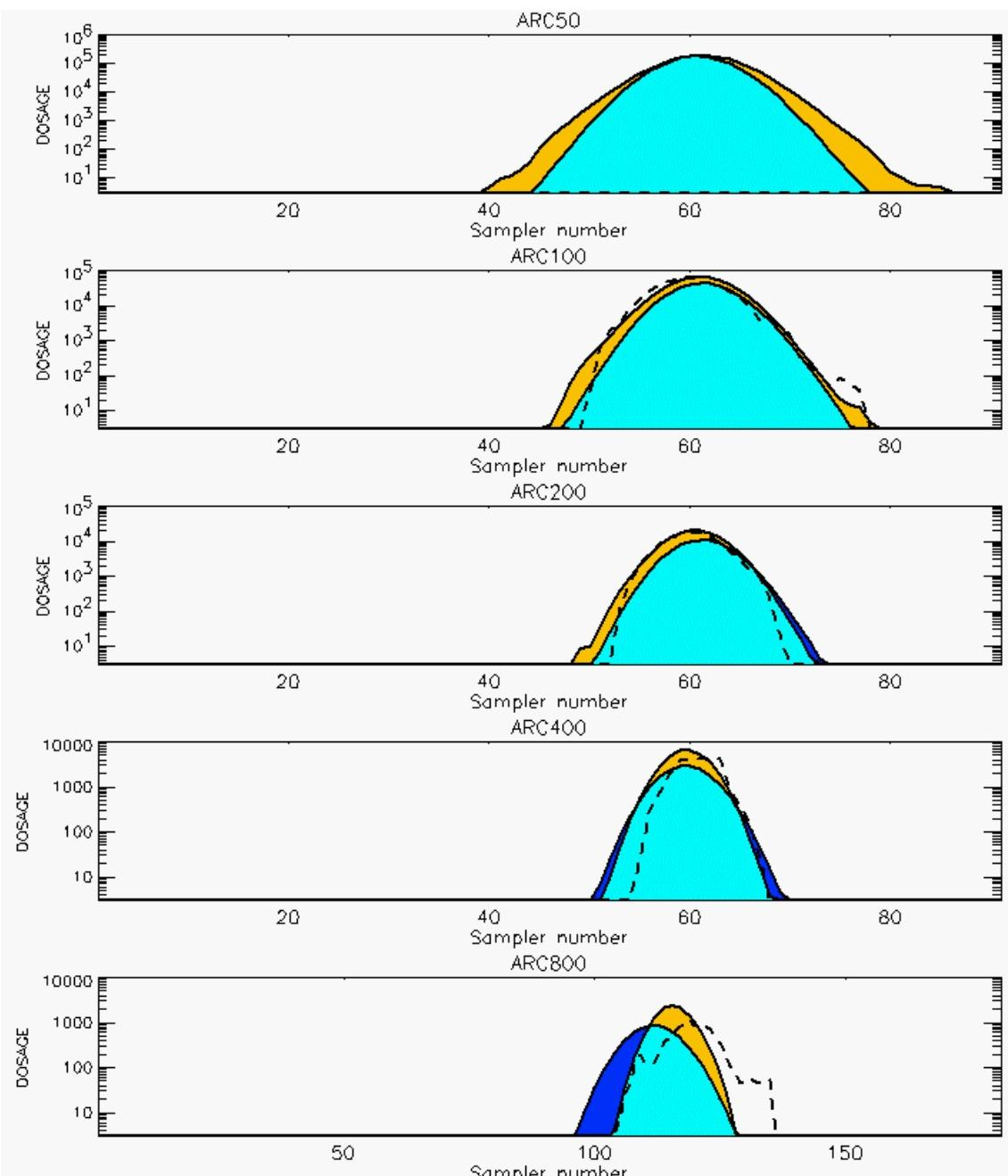
PG Prediction1 to Prediction2 Comparison

PG Trial File: pr_grass_tracer_Experiment_62.txt

PG Prediction File 1: HPAC\nodeposition\pg_62_noxd.out

PG Prediction File 2: ARAC\nodeposition\pg_62_noxd.arac

**Figure E-51a. HPAC and NARAC Predictions to Trial 62 on Linear Scale:
Stability Category is 2**



PG Prediction1 to Prediction2 Comparison

PG Trial File: pr_grass_tracer_Experiment_62.txt

PG Prediction File 1: HPAC\nodeposition\pg_62_noxd.out

PG Prediction File 2: ARAC\nodeposition\pg_62_noxd.arac

**Figure E-51b. HPAC and NARAC Predictions to Trial 62 on Logarithmic Scale:
Stability Category is 2**

REFERENCES

- E-1. Barad, M. L. (Editor), *Project Prairie Grass, A Field Program in Diffusion*, Geophysical Research Papers No. 59, Volumes I and II, DTIC #AD-152572/AFCRC-TR-58-235(I), Air Geophysical Laboratory, Hanscom Air Force Base, MA, 1958.
- E-2. Irwin, J. S. and Rosu, M-R., *Comments on a Draft Practice for Statistical Evaluation of Atmospheric Dispersion Models*, Proceedings of the 10th Joint Conference on the Applications of Air Pollution Meteorology. American Meteorological Society, Boston, pp. 6-10, 1998.

APPENDIX F

**COMPARISONS OF HPAC PREDICTIONS: WITH AND WITHOUT
SURFACE DEPOSITION**

APPENDIX F

COMPARISONS OF HPAC PREDICTIONS: WITH AND WITHOUT SURFACE DEPOSITION

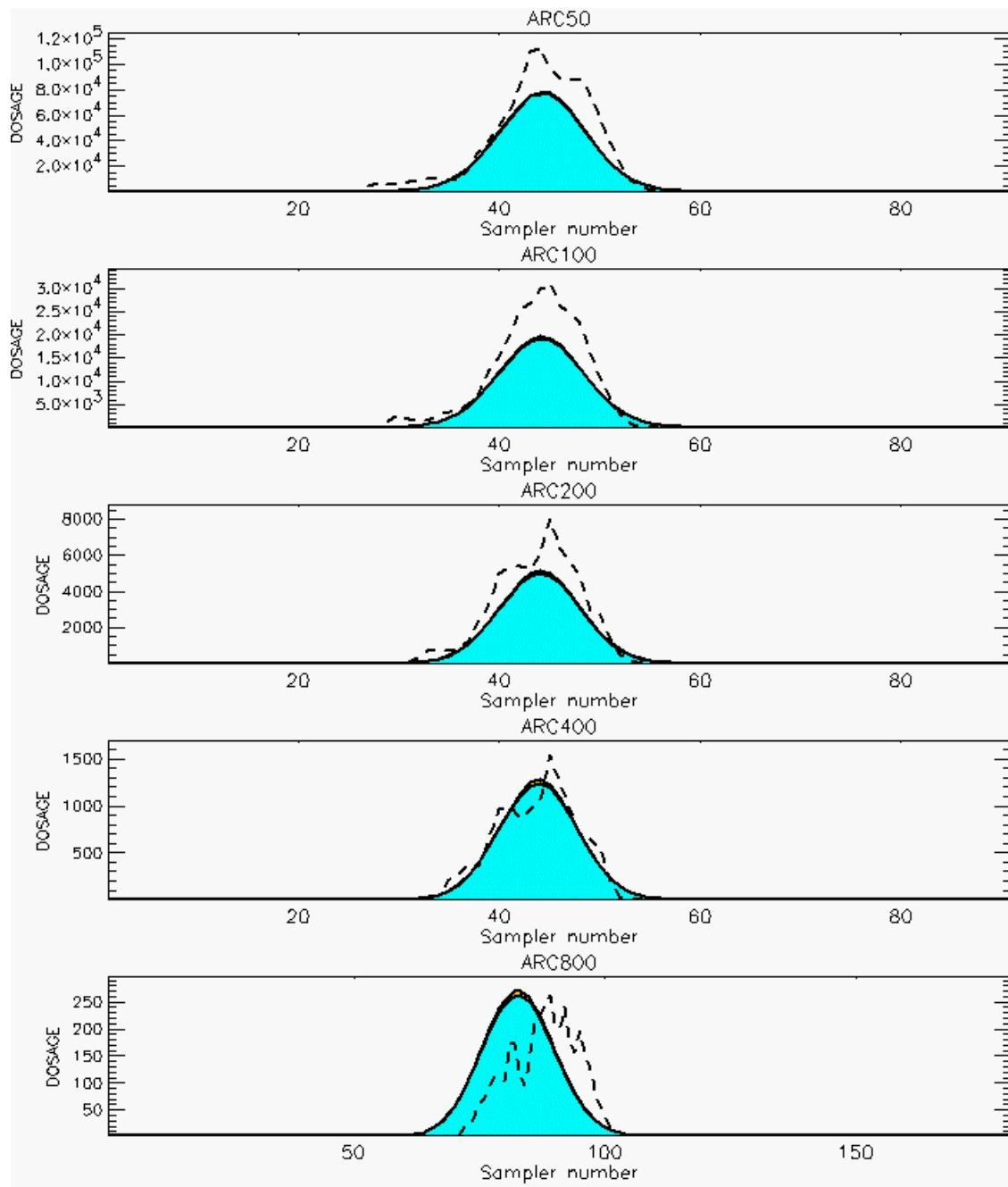
This appendix presents graphical comparisons of HPAC predictions with and without the inclusion of a mechanism for SO₂ surface deposition. Vertical plot units are dosage units of mg-sec/m³. The horizontal plot units are sampler numbers as presented in the *Prairie Grass* field trials [Ref. F-1]. Sampler number 1 is oriented to the west, the middle sampler (45 or 90) is oriented to the north, and the last sampler (91 or 181) is oriented to the east of the SO₂ gas release source. Only data values greater than the cutoff threshold of 3 mg-sec/m³ (0.005 mg/m³) are presented. This cutoff threshold value corresponds to a minimum value reported in *Prairie Grass* field trials.

Comparisons of HPAC predictions with and without SO₂ surface deposition are presented on a linear dosage scale. Each graphical comparison consists of five plots (one for each arc) with the top plot depicting the 50-meter arc, the second plot depicting the 100-meter arc, the third plot depicting the 200-meter arc, and so on. The last panel (just above the figure caption) contains information about the data files used to produce these plots. The *Prairie Grass* field trial file name contains a two-digit number corresponding to the trial number. Prediction file names contain the moniker “nodeposition,” denoting that SO₂ surface deposition was not considered, or the moniker “deposition,” denoting that SO₂ surface deposition was considered, and a one- or two-digit number reflecting the *Prairie Grass* field trial being predicted.

The meanings of the colors used in the plots are described below:

- Turquoise — dosages that overlap for both predictions
- Brown — higher dosages for predictions without SO₂ surface deposition.

The dashed lines depict dosage values actually obtained in the field trial. Irwin stability categories that were used in our analyses are denoted in the figure captions. These stability category assignments are based on Reference F-2.



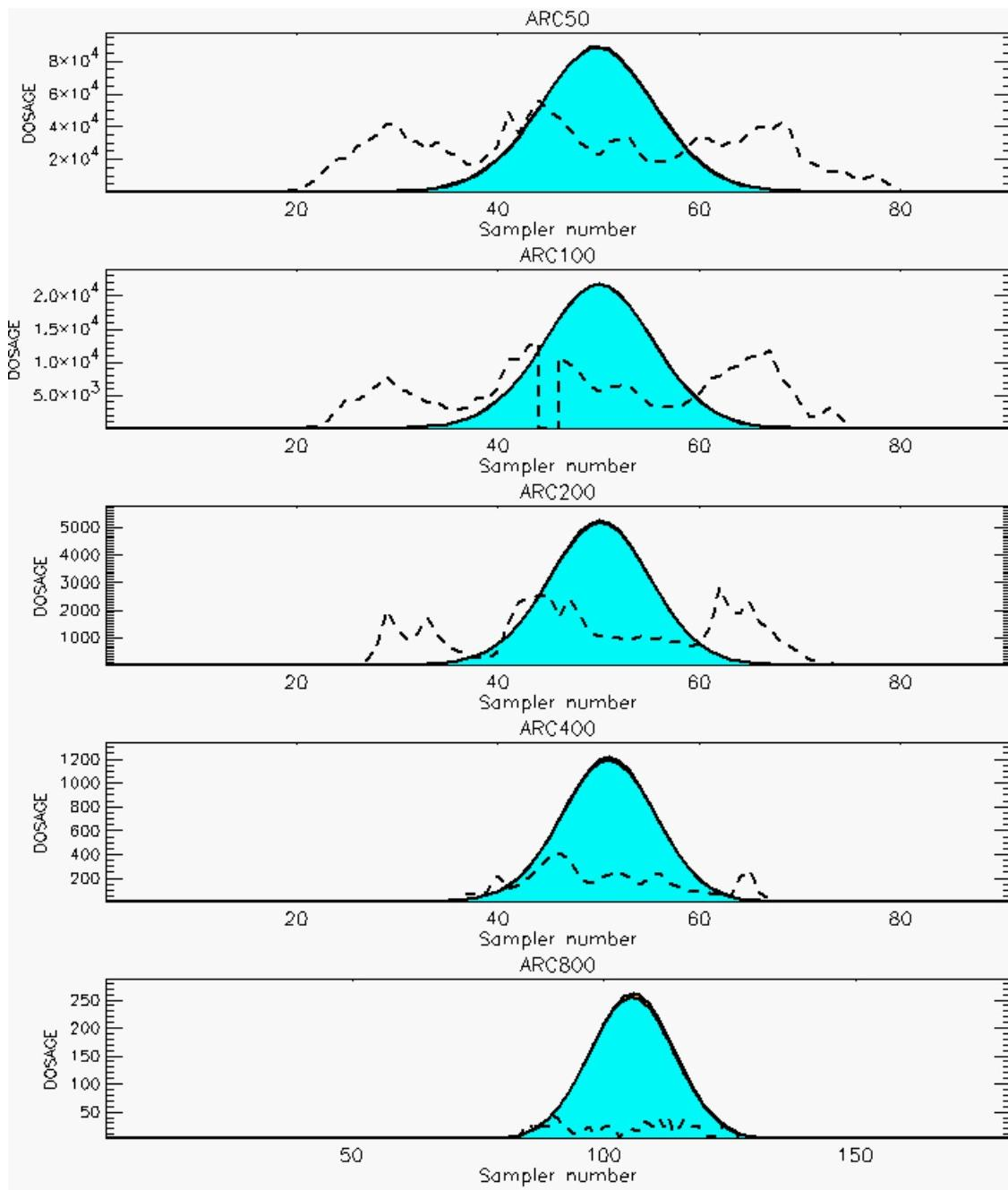
PG Prediction1 to Prediction2 Comparison

PG Trial File: pr_grass_tracer_Experiment_05.txt

PG Prediction File 1: HPAC\deposition\pg_5_vd.out

PG Prediction File 2: HPAC\nodeposition\pg_5_nvd.out

**Figure F-1. HPAC With and Without SO₂ Surface Deposition Predictions to Trial 5:
Stability Category is 2**



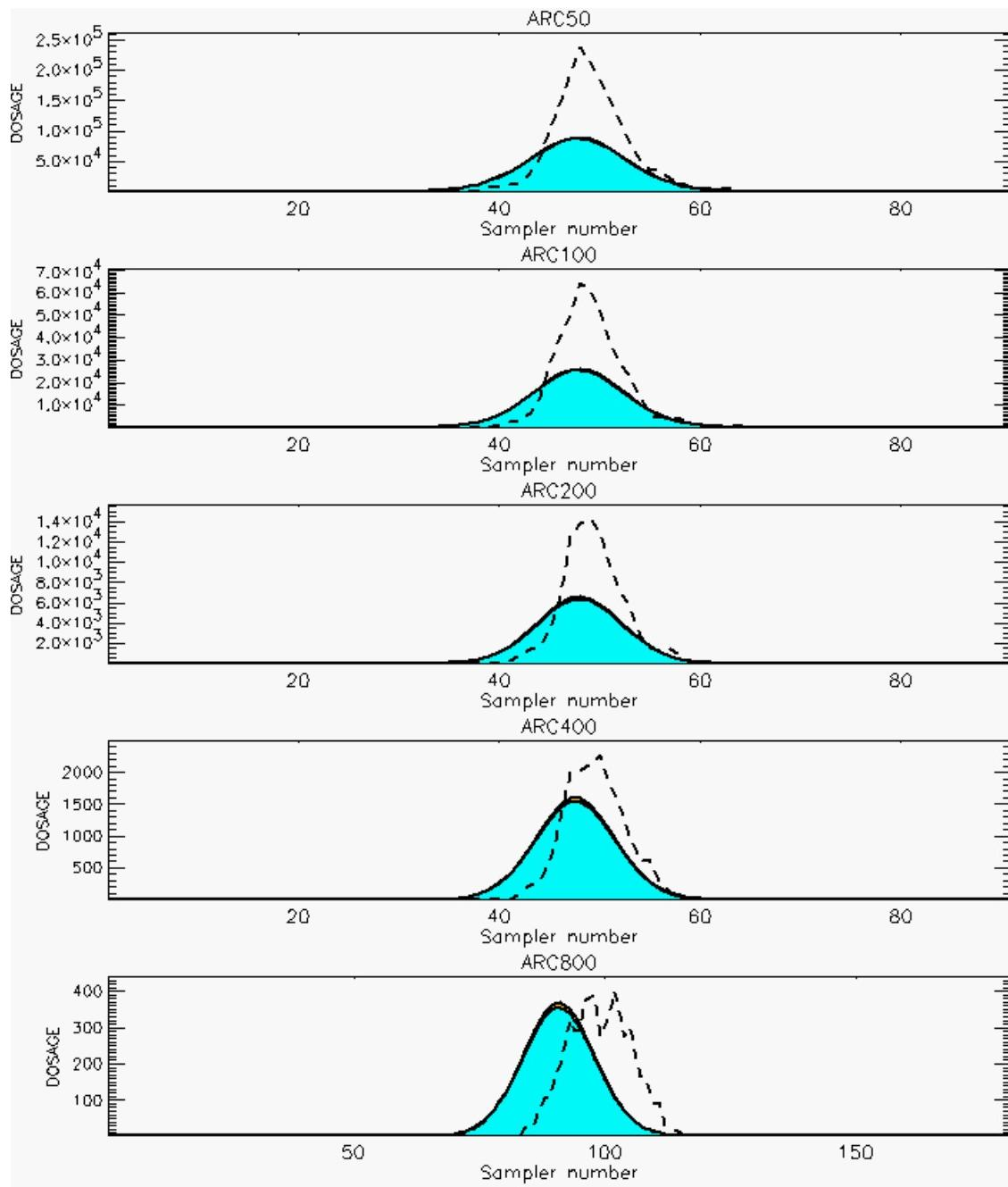
PG Prediction1 to Prediction2 Comparison

PG Trial File: pr_grass_tracer_Experiment_07.txt

PG Prediction File 1: HPAC\deposition\pg_7_vd.out

PG Prediction File 2: HPAC\nodeposition\pg_7_nvd.out

**Figure F-2. HPAC With and Without SO₂ Surface Deposition Predictions to Trial 7:
Stability Category is 1**



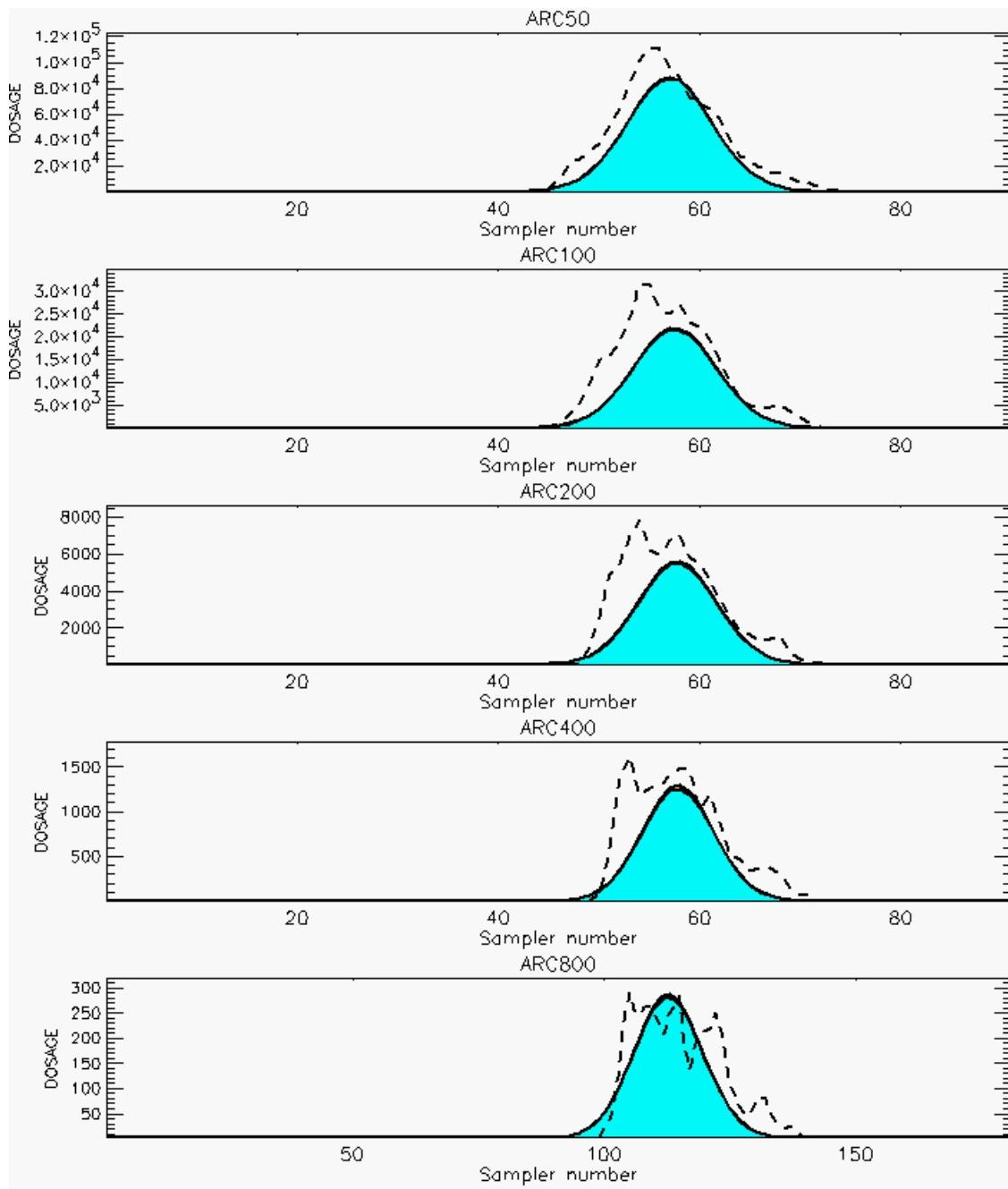
PG Prediction1 to Prediction2 Comparison

PG Trial File: pr_grass_tracer_Experiment_08.txt

PG Prediction File 1: HPAC\deposition\pg_8_vd.out

PG Prediction File 2: HPAC\nodeposition\pg_8_nvd.out

**Figure F-3. HPAC With and Without SO₂ Surface Deposition Predictions to Trial 8:
Stability Category is 2**



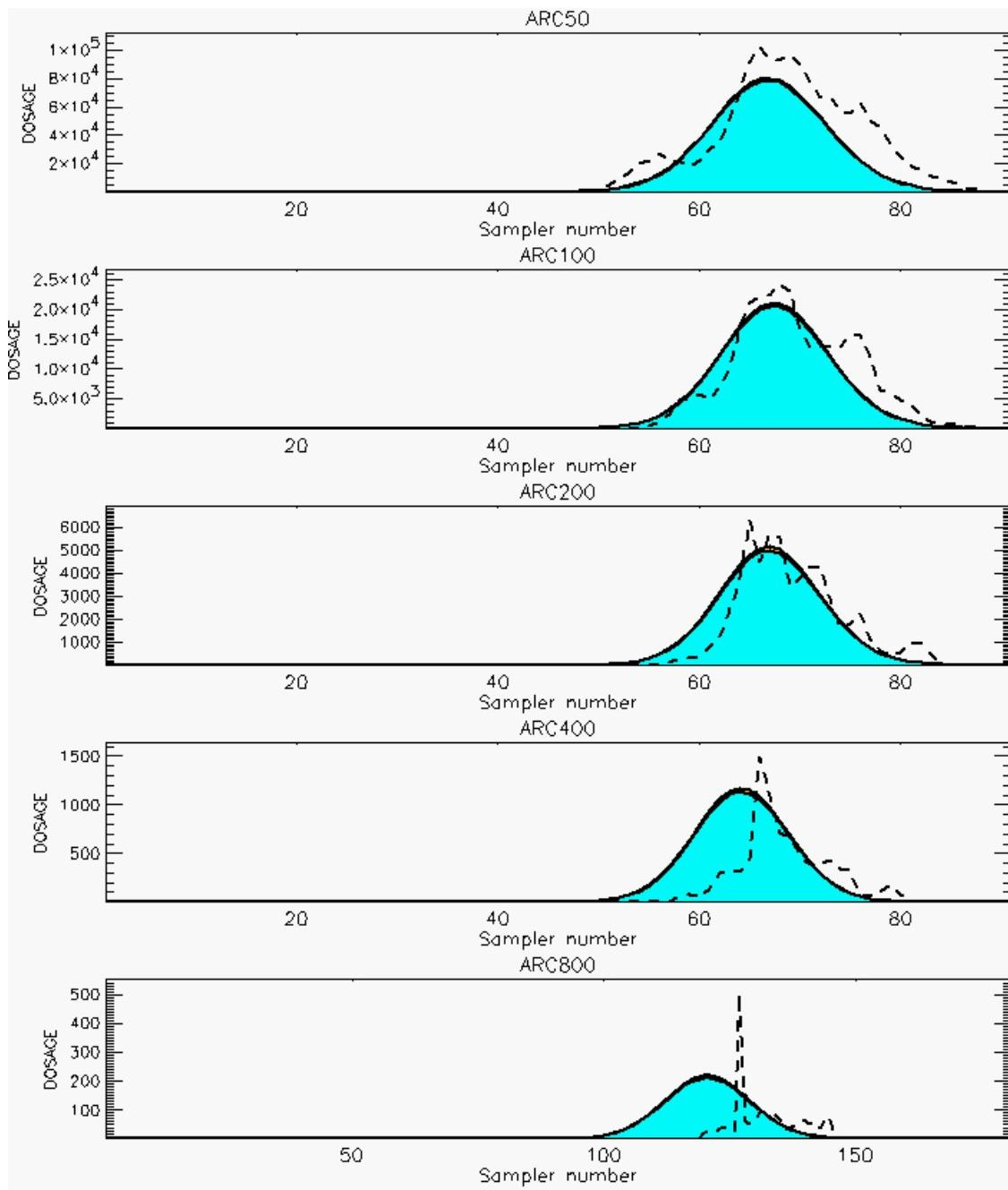
PG Prediction1 to Prediction2 Comparison

PG Trial File: pr_grass_tracer_Experiment_09.txt

PG Prediction File 1: HPAC\deposition\pg_9_vd.out

PG Prediction File 2: HPAC\nodeposition\pg_9_nvd.out

**Figure F-4. HPAC With and Without SO₂ Surface Deposition Predictions to Trial 9:
Stability Category is 2**



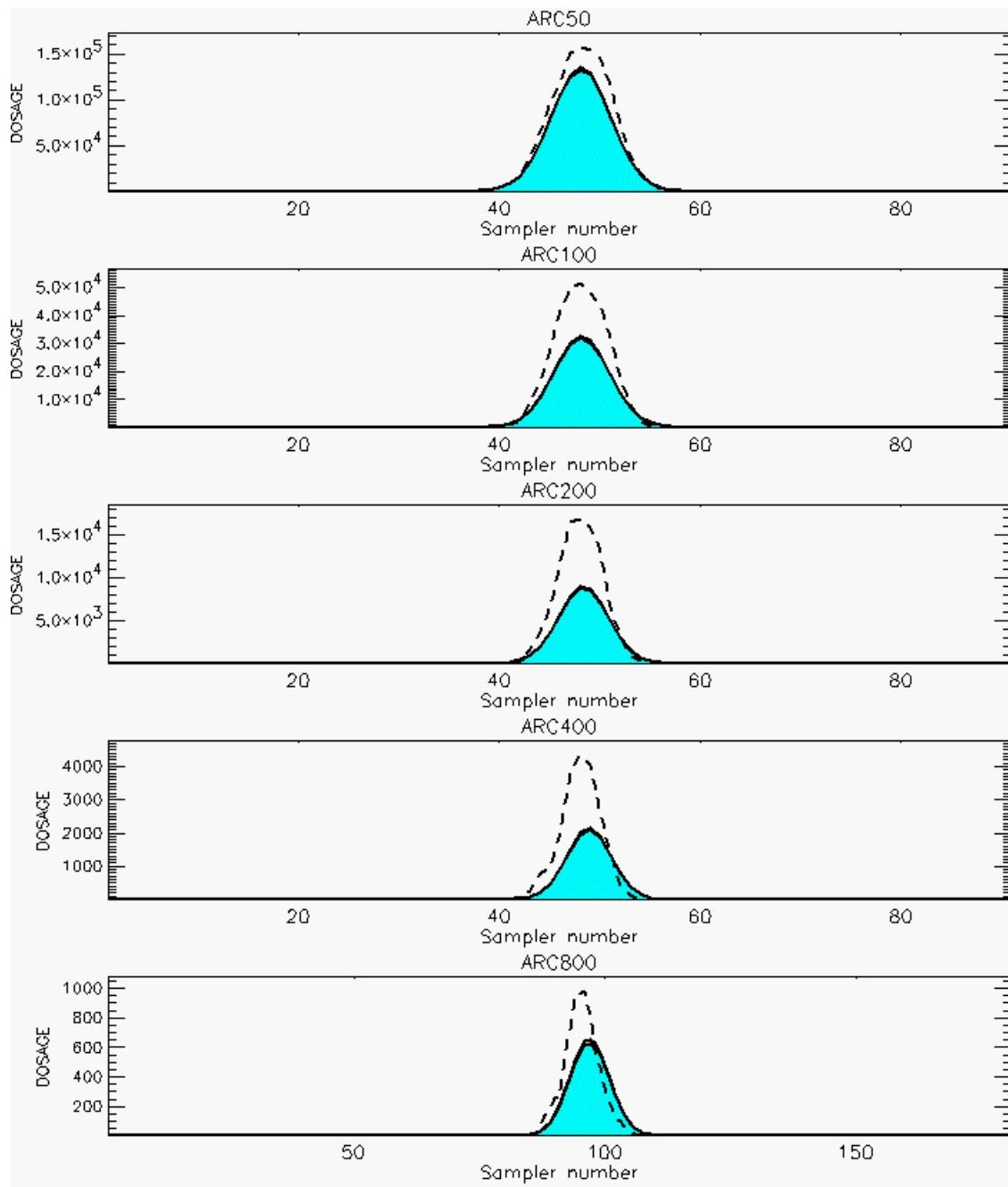
PG Prediction1 to Prediction2 Comparison

PG Trial File: pr_grass_tracer_Experiment_10.txt

PG Prediction File 1: HPAC\deposition\pg_10_vd.out

PG Prediction File 2: HPAC\nodeposition\pg_10_novd.out

**Figure F-5. HPAC With and Without SO₂ Surface Deposition Predictions to Trial 10:
Stability Category is 1**



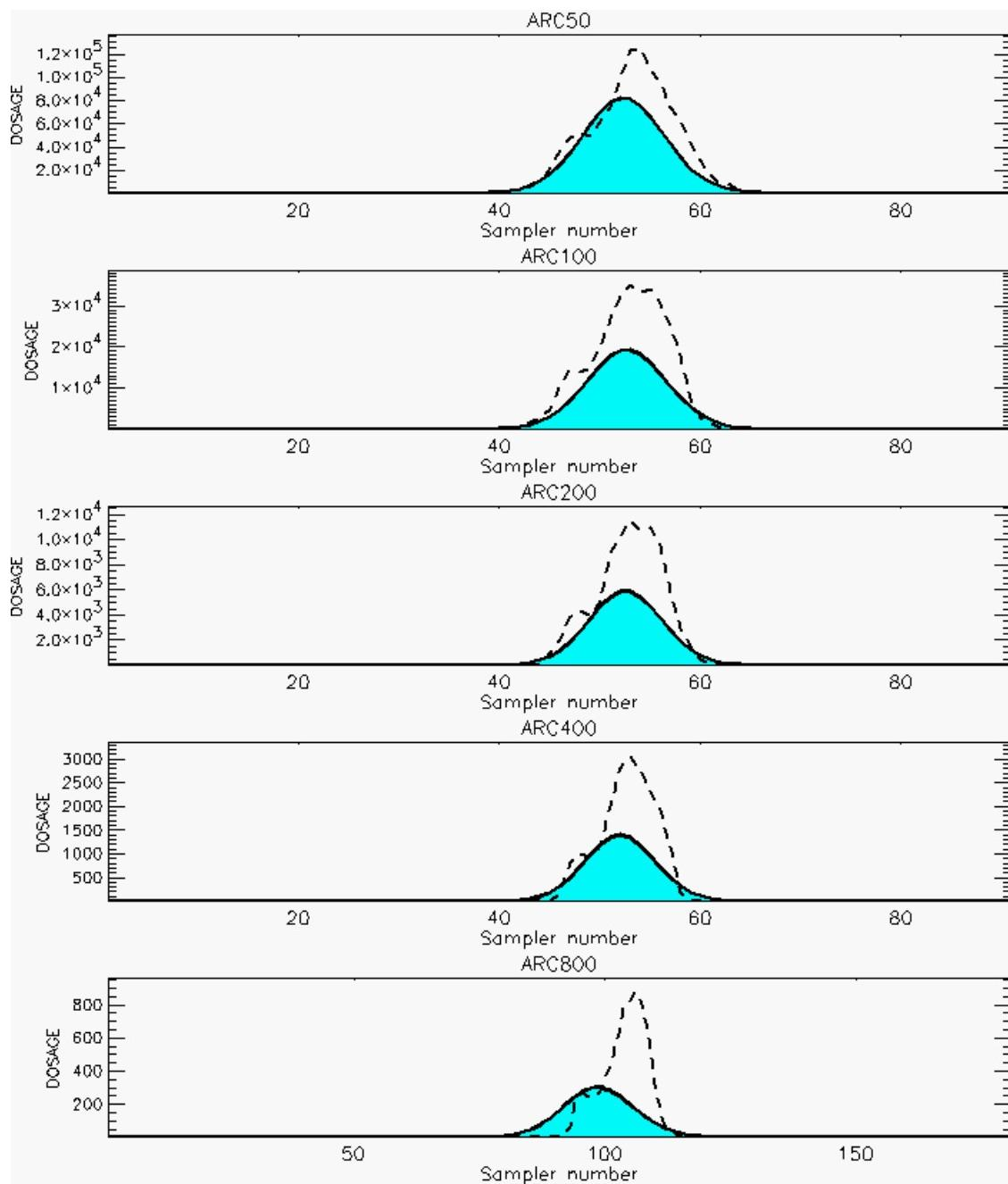
PG Prediction1 to Prediction2 Comparison

PG Trial File: pr_grass_tracer_Experiment_11.txt

PG Prediction File 1: HPAC\deposition\pg_11_vd.out

PG Prediction File 2: HPAC\nodeposition\pg_11_novd.out

**Figure F-6. HPAC With and Without SO₂ Surface Deposition Predictions to Trial 11:
Stability Category is 3**



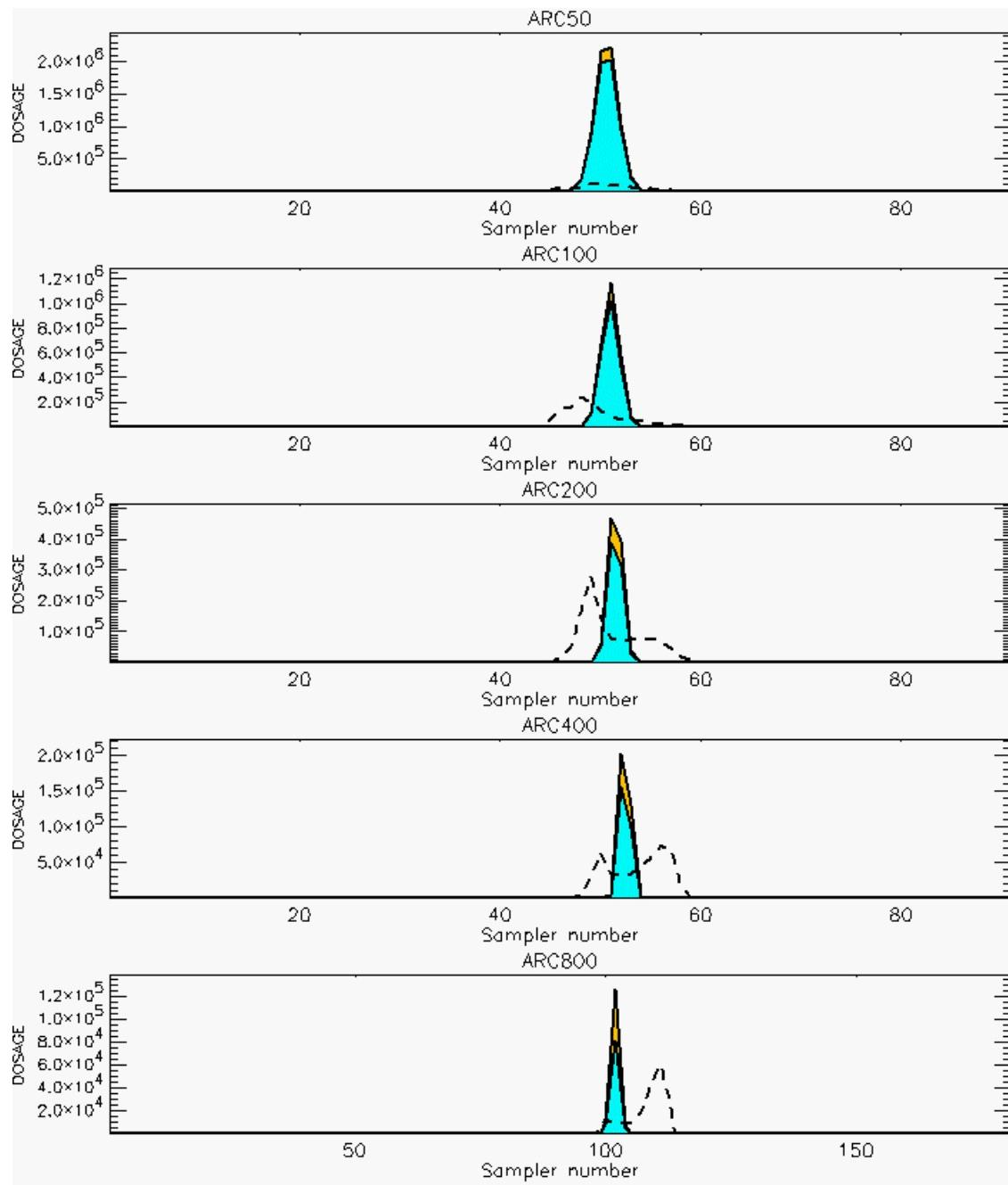
PG Prediction1 to Prediction2 Comparison

PG Trial File: pr_grass_tracer_Experiment_12.txt

PG Prediction File 1: HPAC\deposition\pg_12_vd.out

PG Prediction File 2: HPAC\nodeposition\pg_12_novd.out

**Figure F-7. HPAC With and Without SO₂ Surface Deposition Predictions to Trial 12:
Stability Category is 3**



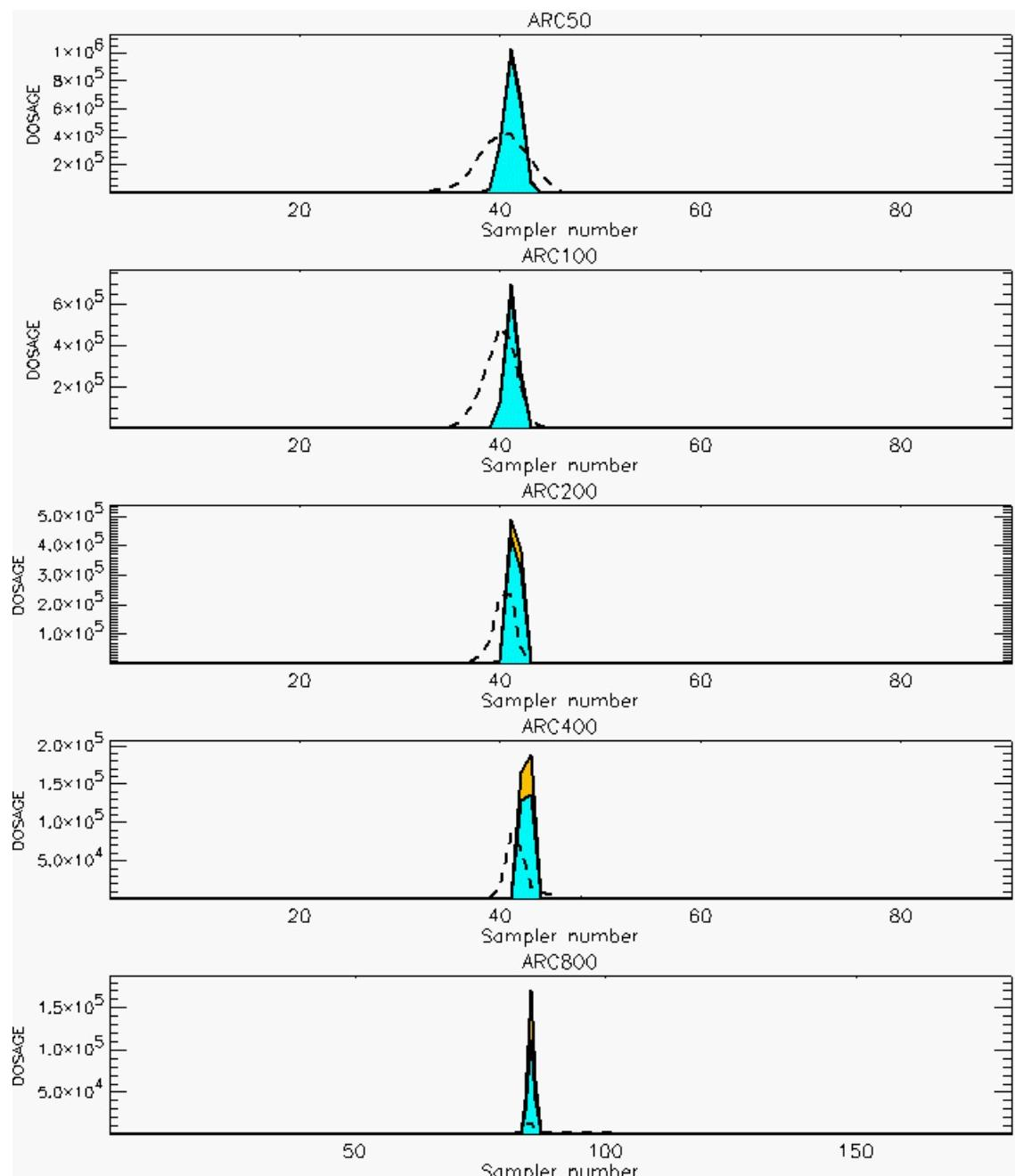
PG Prediction1 to Prediction2 Comparison

PG Trial File: pr_grass_tracer_Experiment_13.txt

PG Prediction File 1: HPAC\deposition\pg_13_vd.out

PG Prediction File 2: HPAC\nodeposition\pg_13_novd.out

**Figure F-8. HPAC With and Without SO₂ Surface Deposition Predictions to Trial 13:
Stability Category is 7**



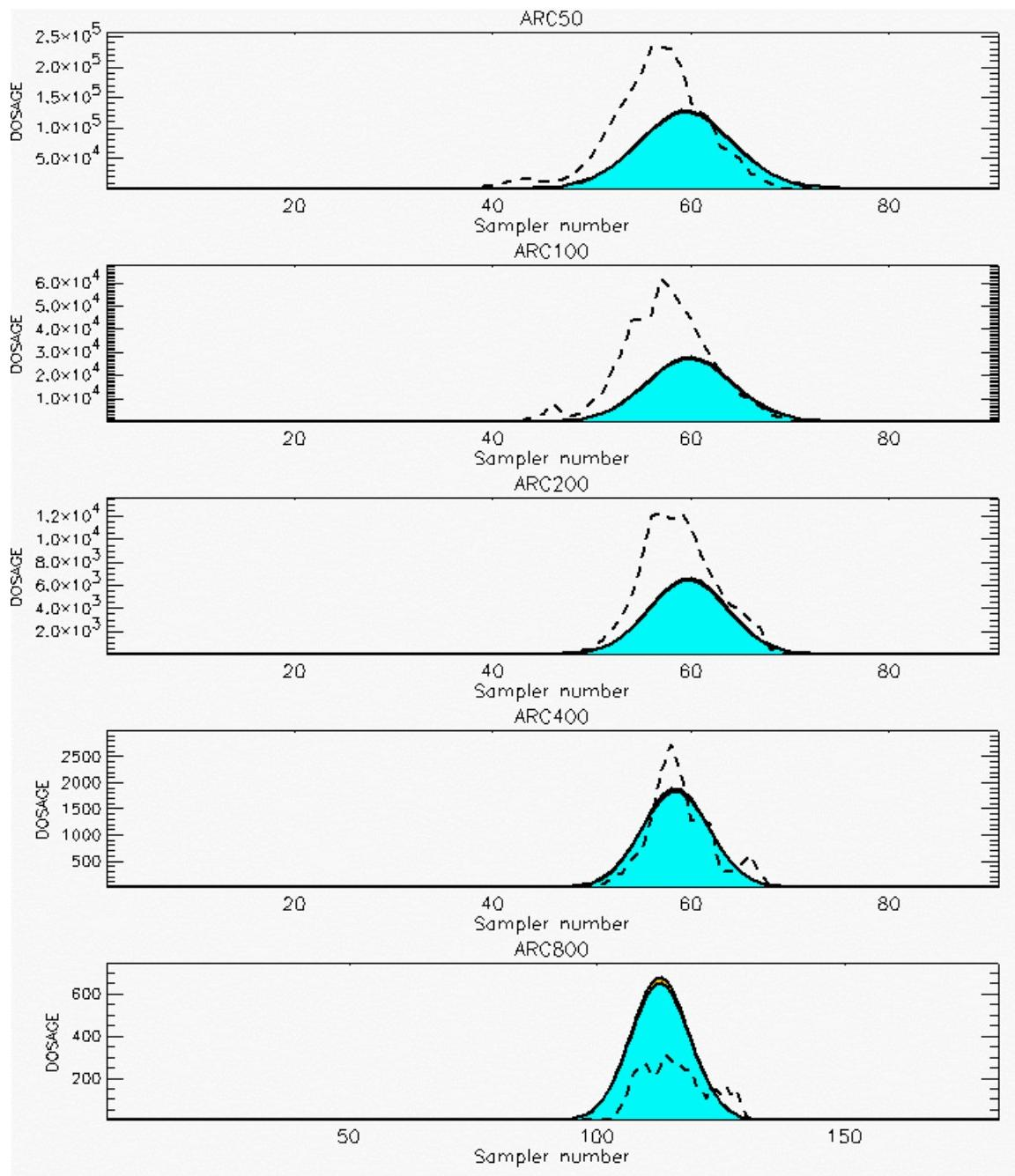
PG Prediction1 to Prediction2 Comparison

PG Trial File: pr_grass_tracer_Experiment_14.txt

PG Prediction File 1: HPAC\deposition\pg_14_vd.out

PG Prediction File 2: HPAC\nodeposition\pg_14_novd.out

**Figure F-9. HPAC With and Without SO₂ Surface Deposition Predictions to Trial 14:
Stability Category is 7**



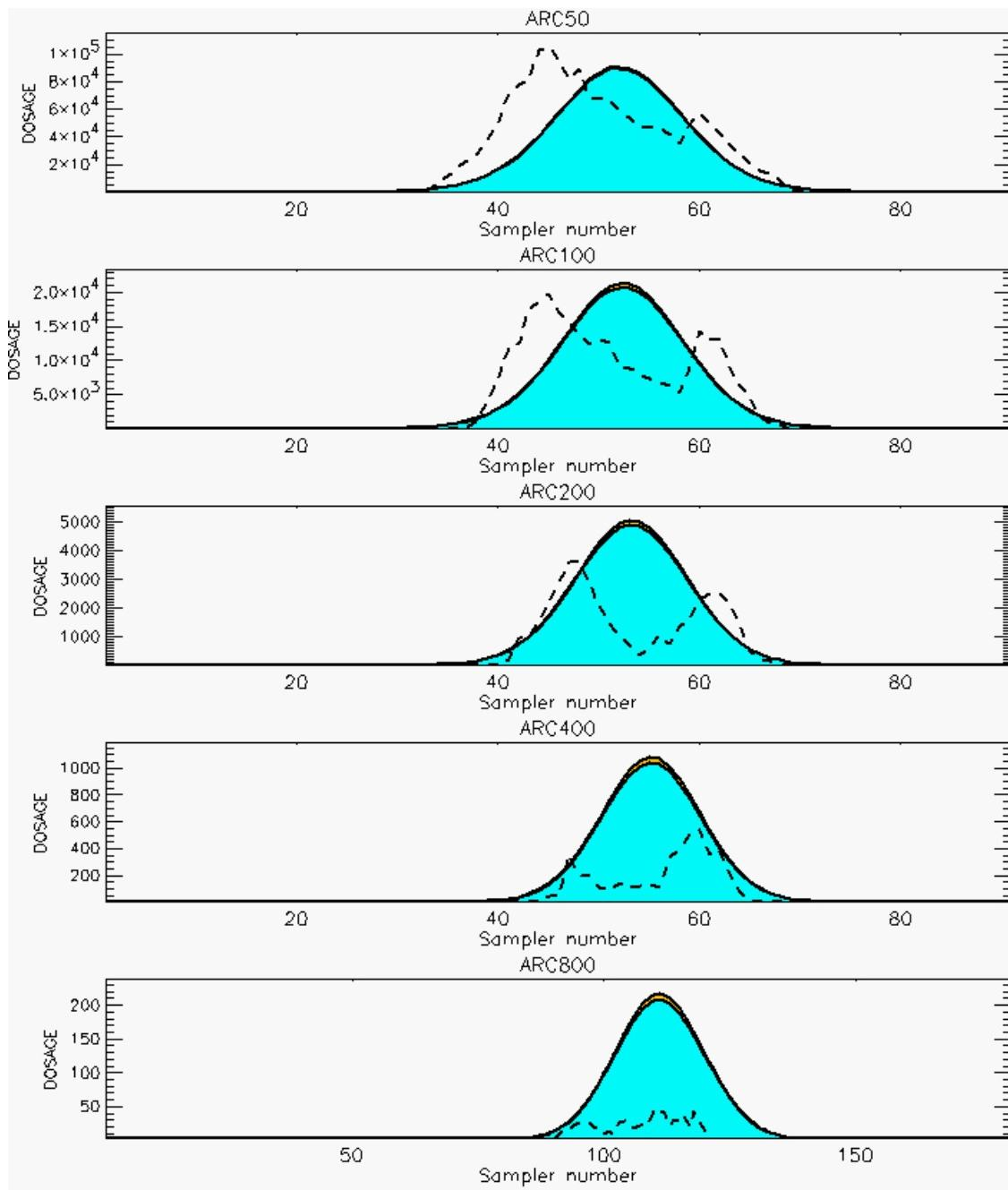
PG Prediction1 to Prediction2 Comparison

PG Trial File: pr_grass_tracer_Experiment_15.txt

PG Prediction File 1: HPAC\deposition\pg_15_vd.out

PG Prediction File 2: HPAC\nodeposition\pg_15_novd.out

**Figure F-10. HPAC With and Without SO₂ Surface Deposition Predictions to Trial 15:
Stability Category is 1**



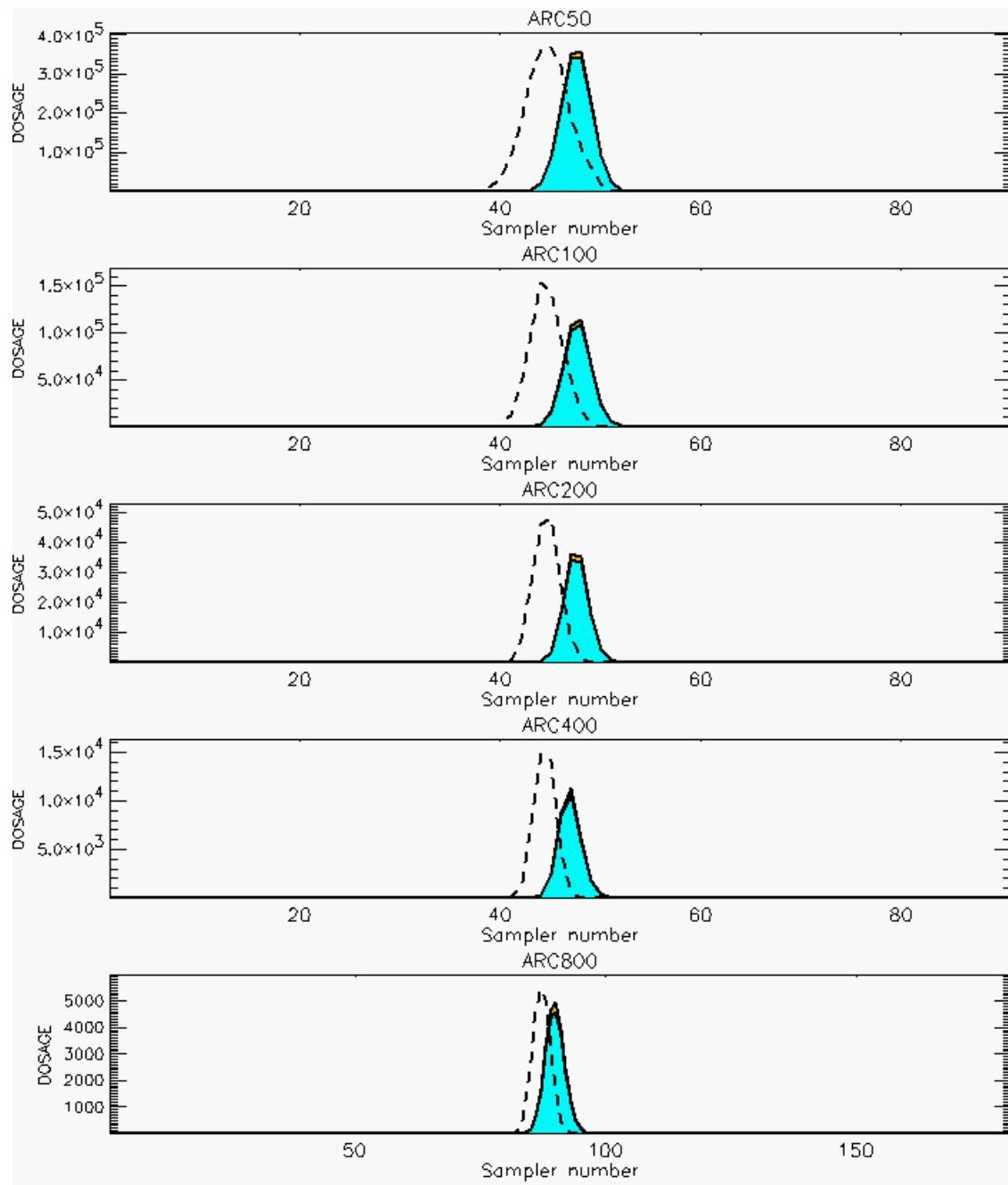
PG Prediction1 to Prediction2 Comparison

PG Trial File: pr_grass_tracer_Experiment_16.txt

PG Prediction File 1: HPAC\deposition\pg_16_vd.out

PG Prediction File 2: HPAC\nodeposition\pg_16_novd.out

**Figure F-11. HPAC With and Without SO₂ Surface Deposition Predictions to Trial 16:
Stability Category is 1**



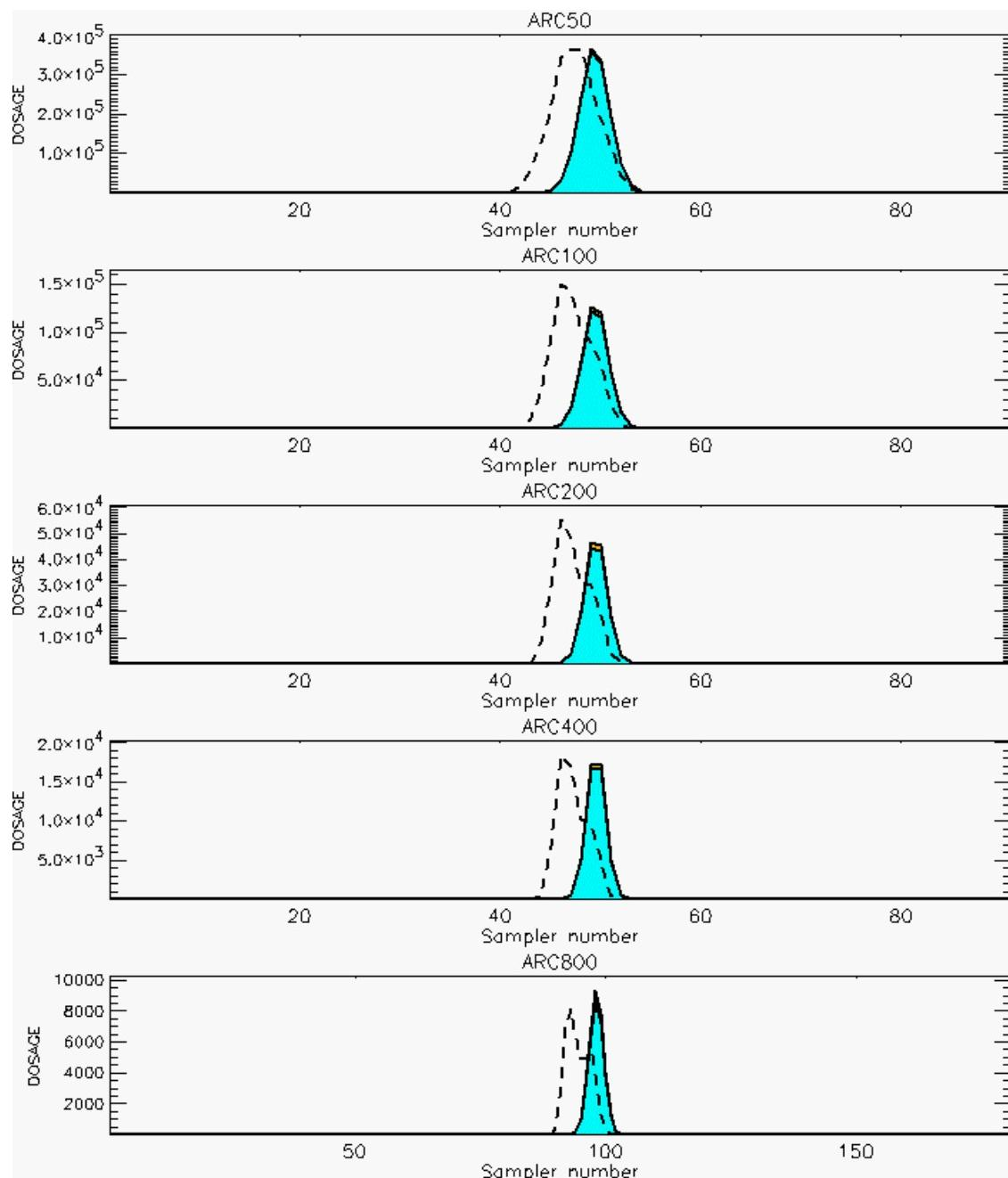
PG Prediction1 to Prediction2 Comparison

PG Trial File: pr_grass_tracer_Experiment_17.txt

PG Prediction File 1: HPAC\deposition\pg_17_vd.out

PG Prediction File 2: HPAC\nodeposition\pg_17_novd.out

**Figure F-12. HPAC With and Without SO₂ Surface Deposition Predictions to Trial 17:
Stability Category is 5**



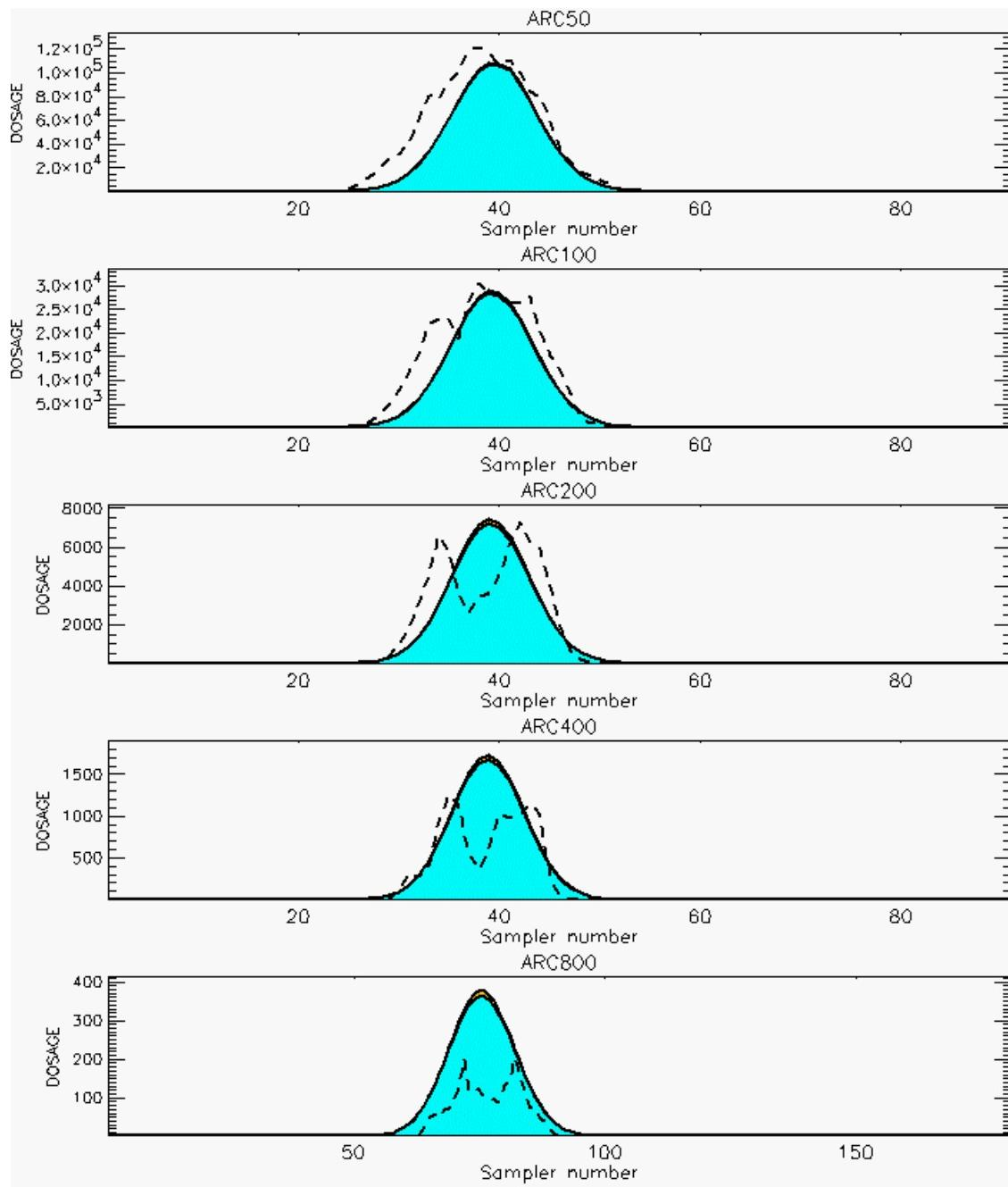
PG Prediction1 to Prediction2 Comparison

PG Trial File: pr_grass_tracer_Experiment_18.txt

PG Prediction File 1: HPAC\deposition\pg_18_vd.out

PG Prediction File 2: HPAC\nodeposition\pg_18_novd.out

**Figure F-13. HPAC With and Without SO₂ Surface Deposition Predictions to Trial 18:
Stability Category is 5**



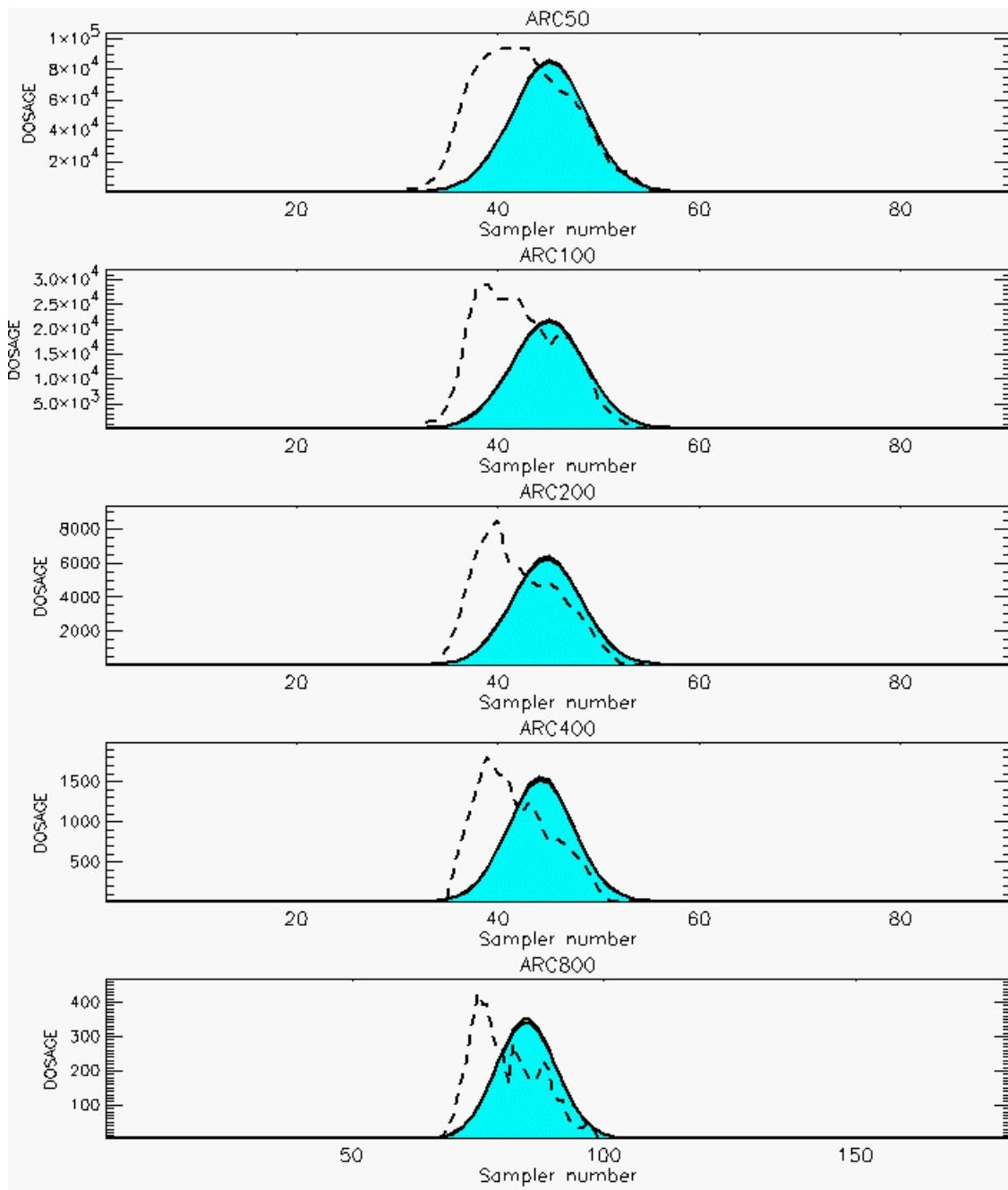
PG Prediction1 to Prediction2 Comparison

PG Trial File: pr_grass_tracer_Experiment_19.txt

PG Prediction File 1: HPAC\deposition\pg_19_vd.out

PG Prediction File 2: HPAC\nodeposition\pg_19_novd.out

**Figure F-14. HPAC With and Without SO₂ Surface Deposition Predictions to Trial 19:
Stability Category is 2**



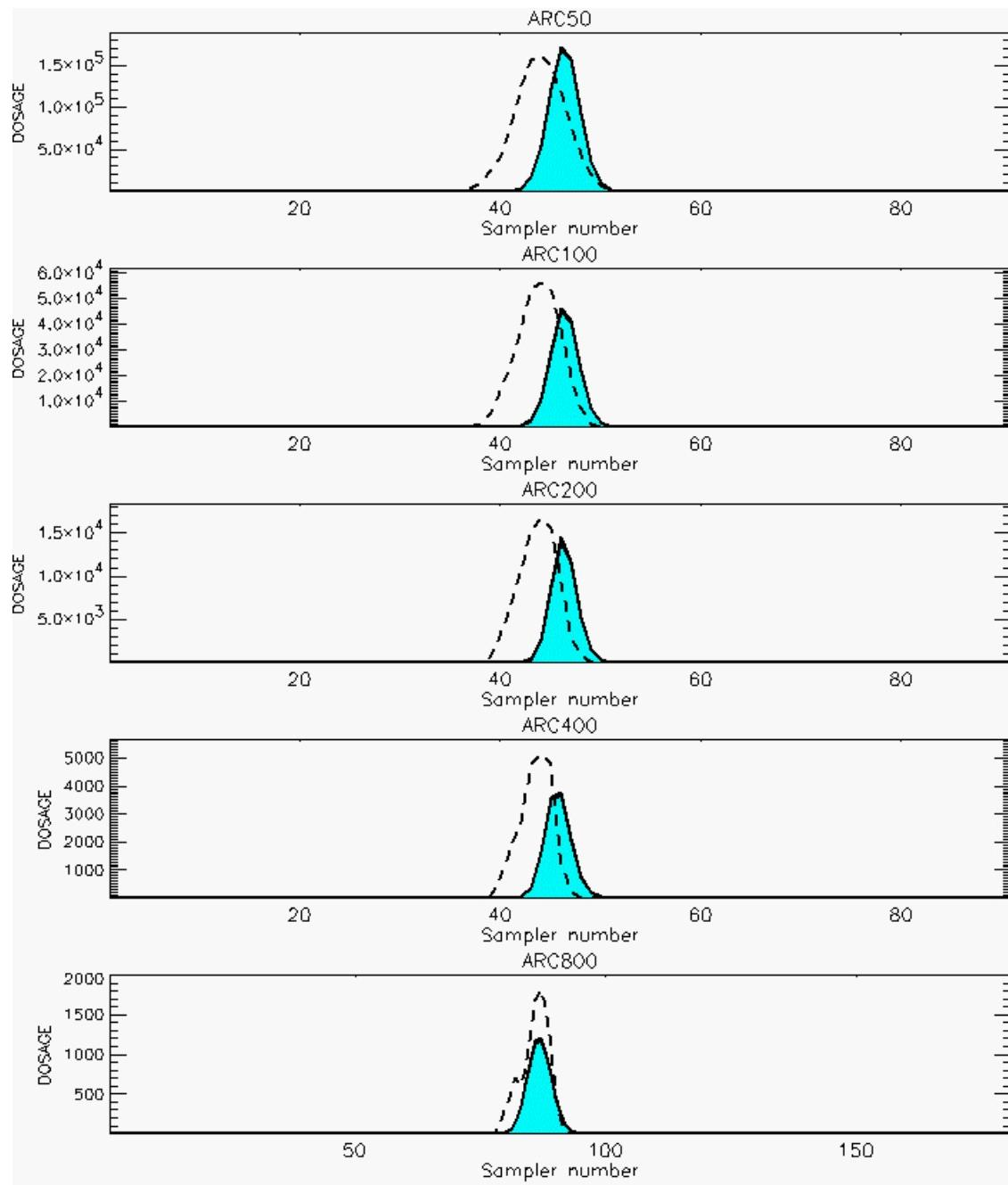
PG Prediction1 to Prediction2 Comparison

PG Trial File: pr_grass_tracer_Experiment_20.txt

PG Prediction File 1: HPAC\deposition\pg_20_vd.out

PG Prediction File 2: HPAC\nodeposition\pg_20_novd.out

**Figure F-15. HPAC With and Without SO₂ Surface Deposition Predictions to Trial 20:
Stability Category is 3**



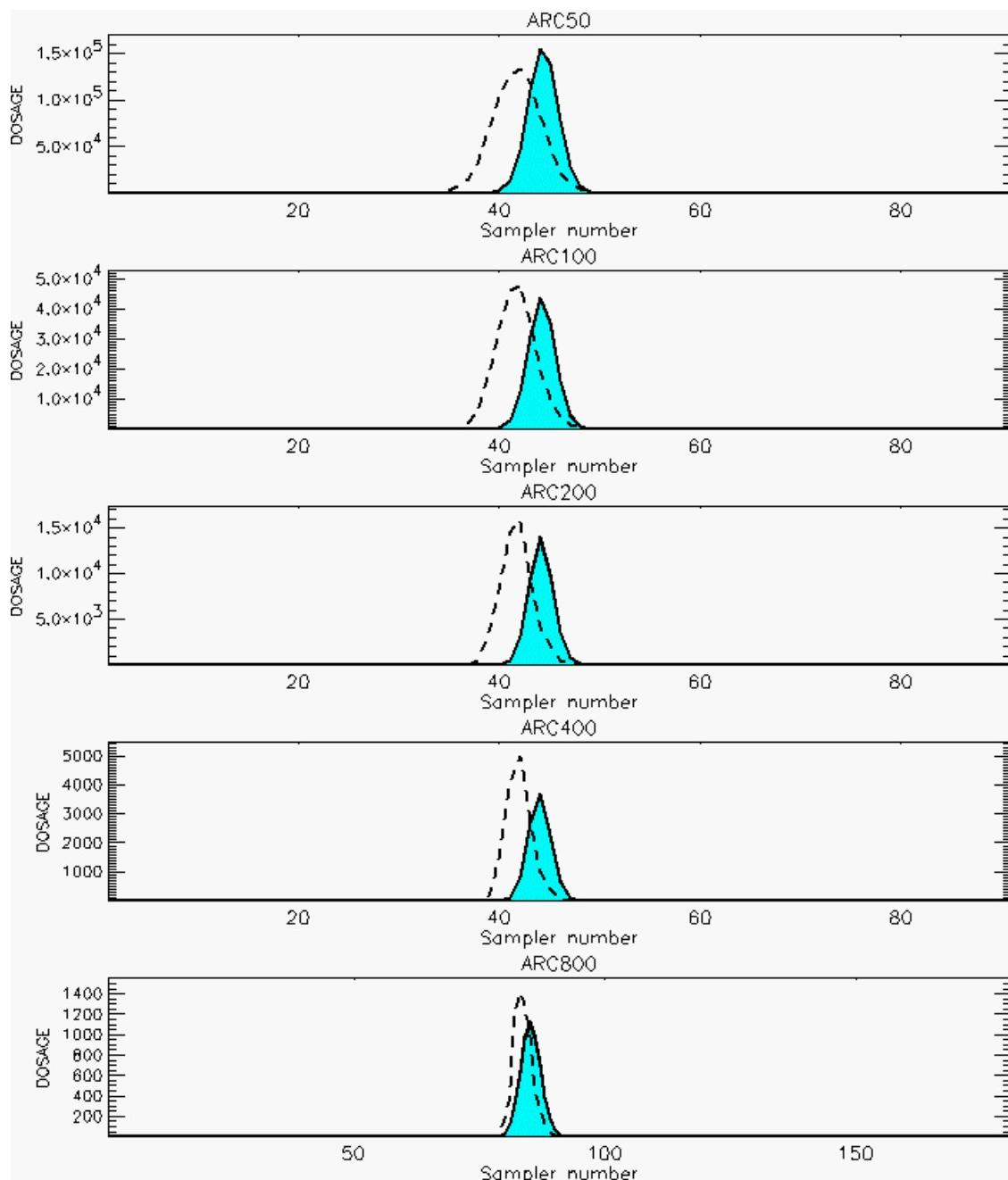
PG Prediction1 to Prediction2 Comparison

PG Trial File: pr_grass_tracer_Experiment_21.txt

PG Prediction File 1: HPAC\deposition\pg_21_vd.out

PG Prediction File 2: HPAC\nodeposition\pg_21_novd.out

**Figure F-16. HPAC With and Without SO₂ Surface Deposition Predictions to Trial 21:
Stability Category is 4**



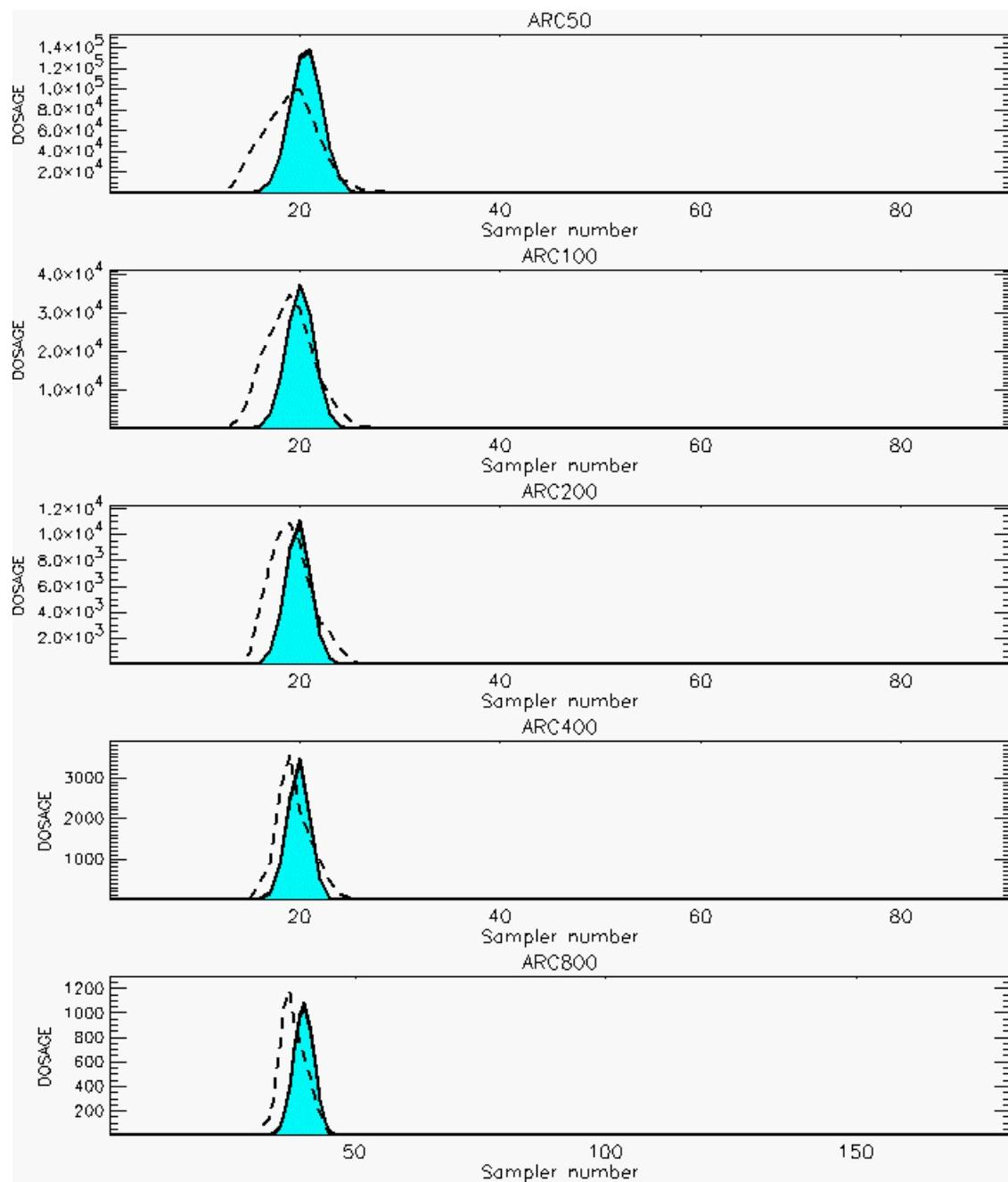
PG Prediction1 to Prediction2 Comparison

PG Trial File: pr_grass_tracer_Experiment_22.txt

PG Prediction File 1: HPAC\deposition\pg_22_vd.out

PG Prediction File 2: HPAC\nodeposition\pg_22_novd.out

**Figure F-17. HPAC With and Without SO_2 Surface Deposition Predictions to Trial 22:
Stability Category is 4**



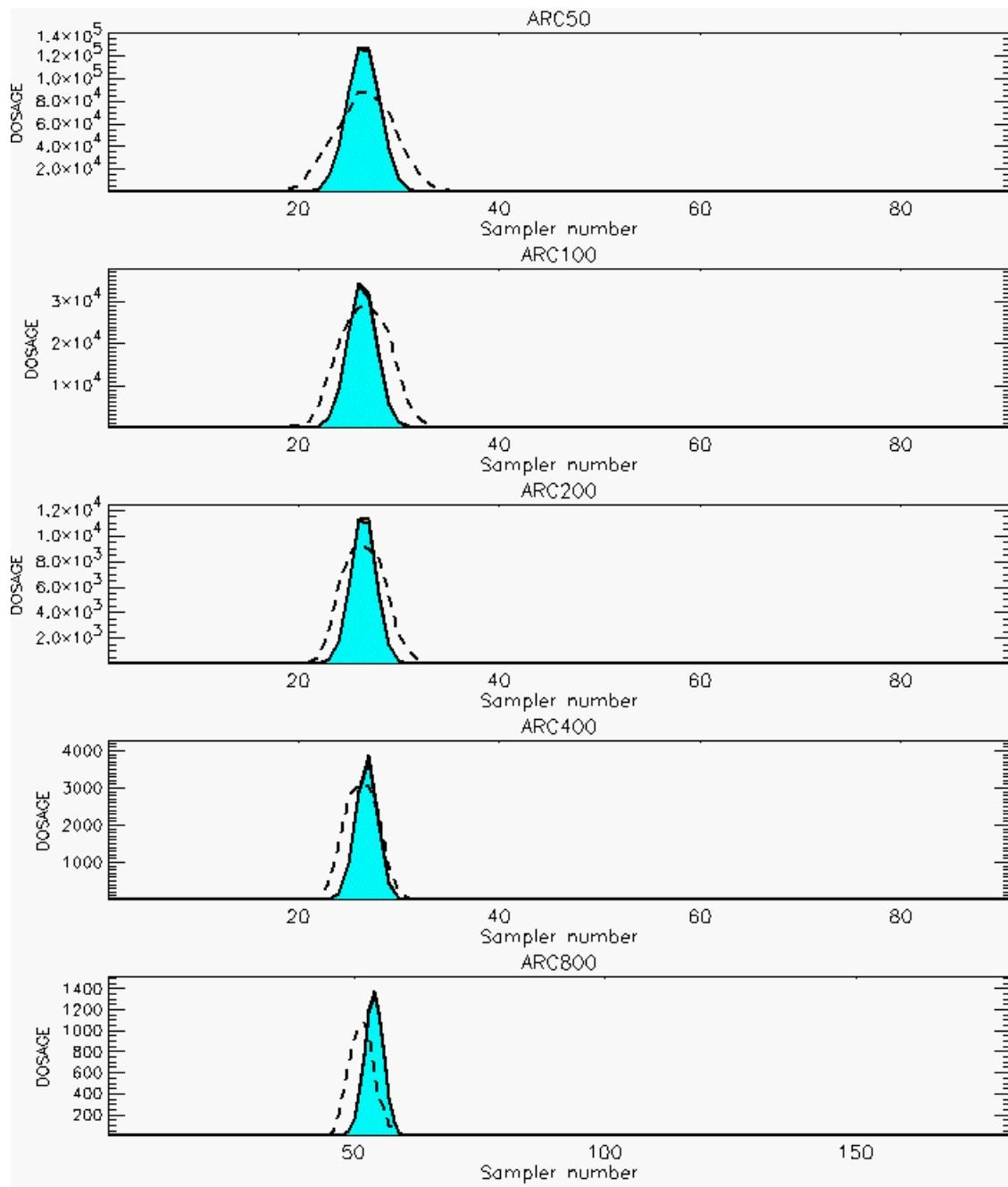
PG Prediction1 to Prediction2 Comparison

PG Trial File: pr_grass_tracer_Experiment_23.txt

PG Prediction File 1: HPAC\deposition\pg_23_vd.out

PG Prediction File 2: HPAC\nodeposition\pg_23_novd.out

**Figure F-18. HPAC With and Without SO₂ Surface Deposition Predictions to Trial 23:
Stability Category is 4**



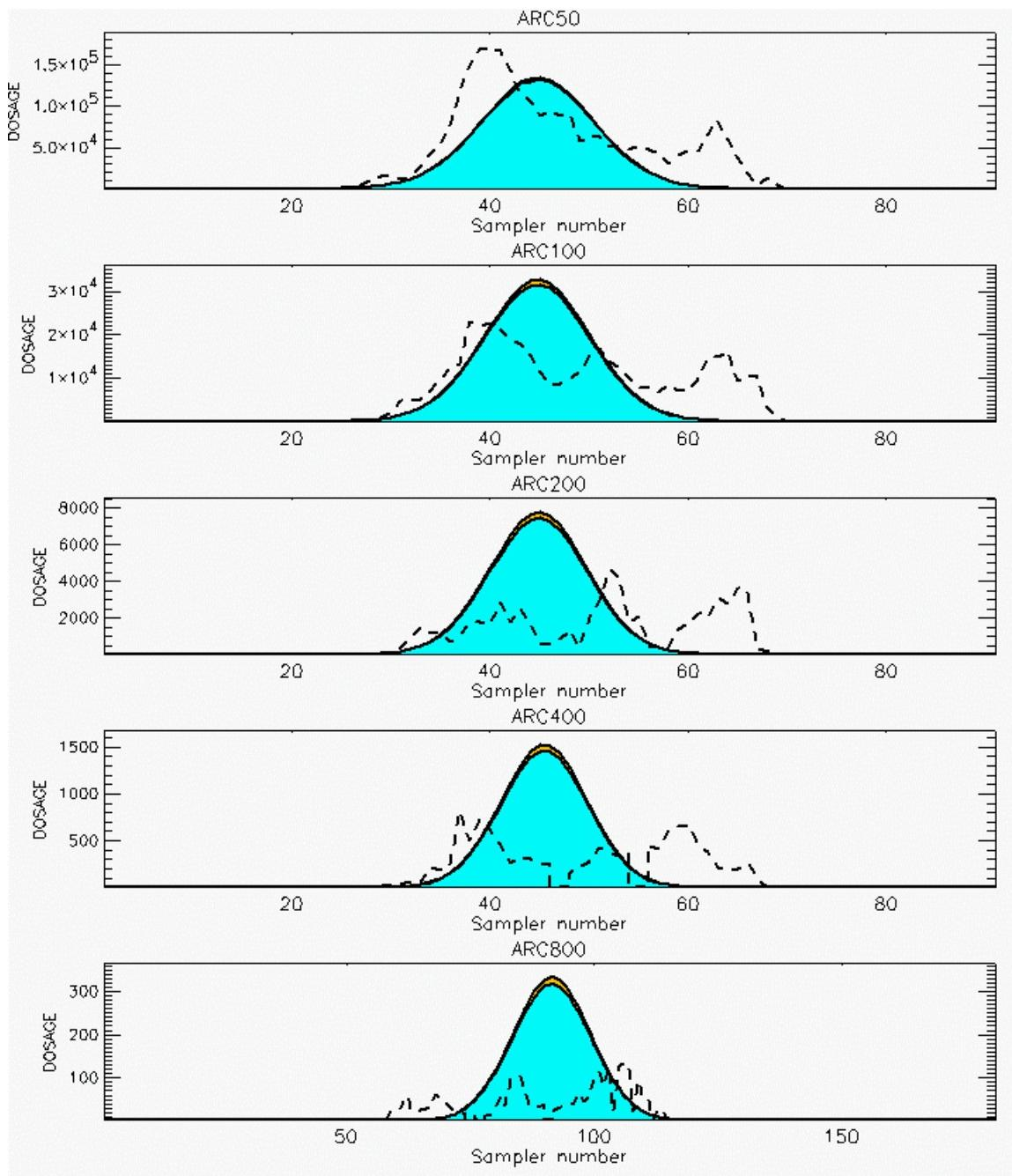
PG Prediction1 to Prediction2 Comparison

PG Trial File: pr_grass_tracer_Experiment_24.txt

PG Prediction File 1: HPAC\deposition\pg_24_vd.out

PG Prediction File 2: HPAC\nodeposition\pg_24_novd.out

**Figure F-19. HPAC With and Without SO₂ Surface Deposition Predictions to Trial 24:
Stability Category is 4**



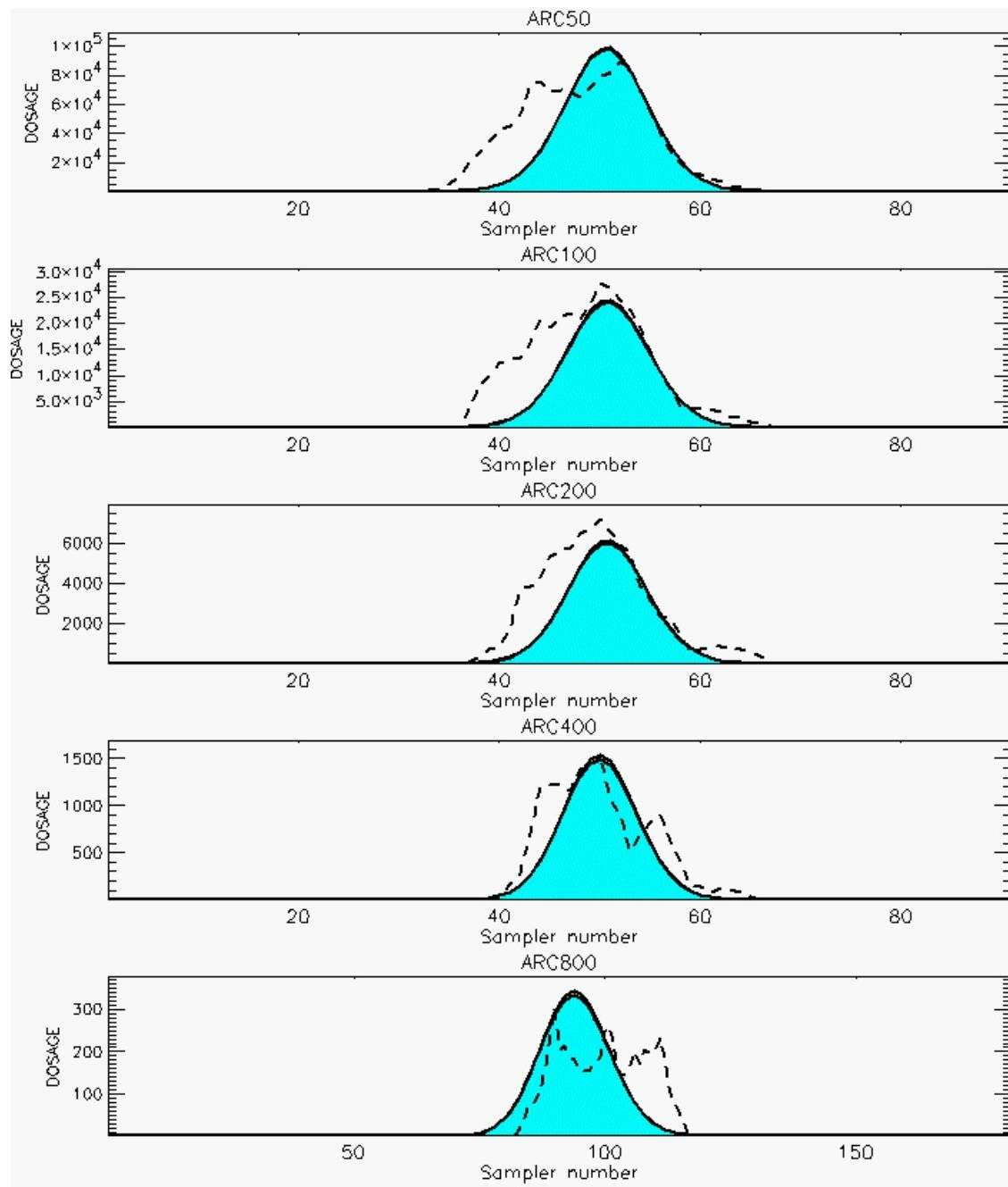
PG Prediction1 to Prediction2 Comparison

PG Trial File: pr_grass_tracer_Experiment_25.txt

PG Prediction File 1: HPAC\deposition\pg_25_vd.out

PG Prediction File 2: HPAC\nodeposition\pg_25_novd.out

**Figure F-20. HPAC With and Without SO₂ Surface Deposition Predictions to Trial 25:
Stability Category is 1**



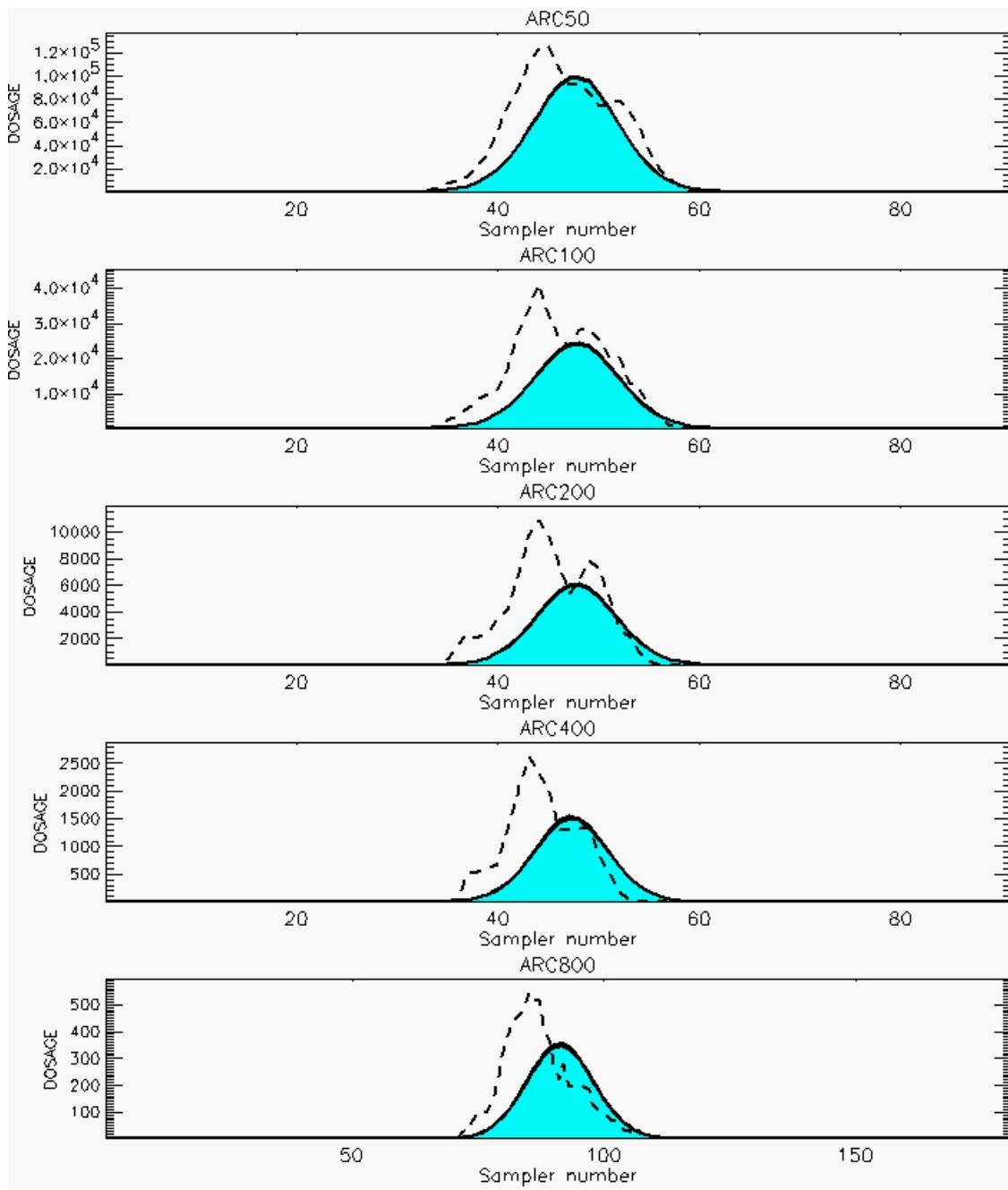
PG Prediction1 to Prediction2 Comparison

PG Trial File: pr_grass_tracer_Experiment_26.txt

PG Prediction File 1: HPAC\deposition\pg_26_vd.out

PG Prediction File 2: HPAC\nodeposition\pg_26_novd.out

**Figure F-21. HPAC With and Without SO₂ Surface Deposition Predictions to Trial 26:
Stability Category is 2**



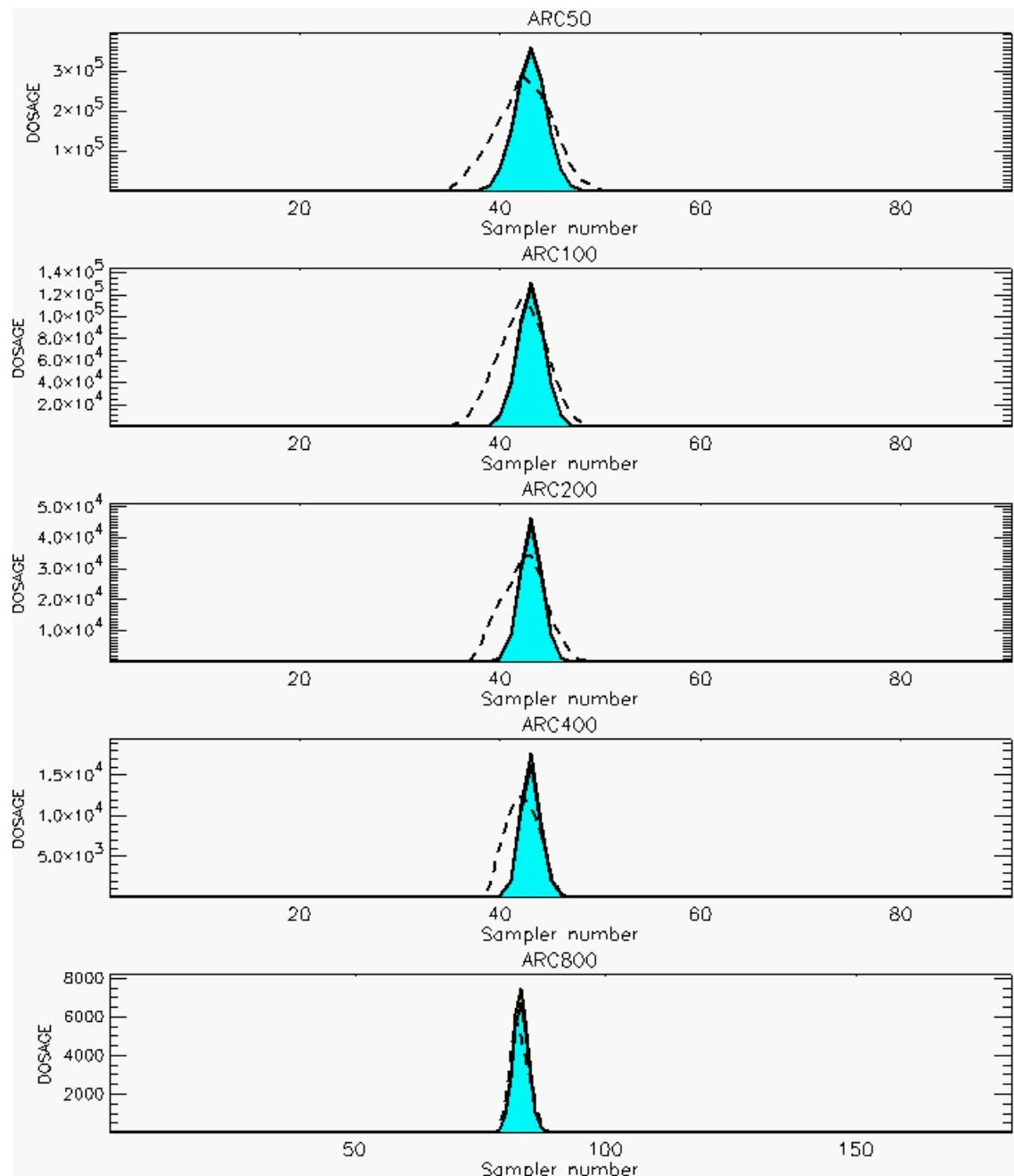
PG Prediction1 to Prediction2 Comparison

PG Trial File: pr_grass_tracer_Experiment_27.txt

PG Prediction File 1: HPAC\deposition\pg_27_vd.out

PG Prediction File 2: HPAC\nodeposition\pg_27_novd.out

**Figure F-22. HPAC With and Without SO₂ Surface Deposition Predictions to Trial 27:
Stability Category is 2**



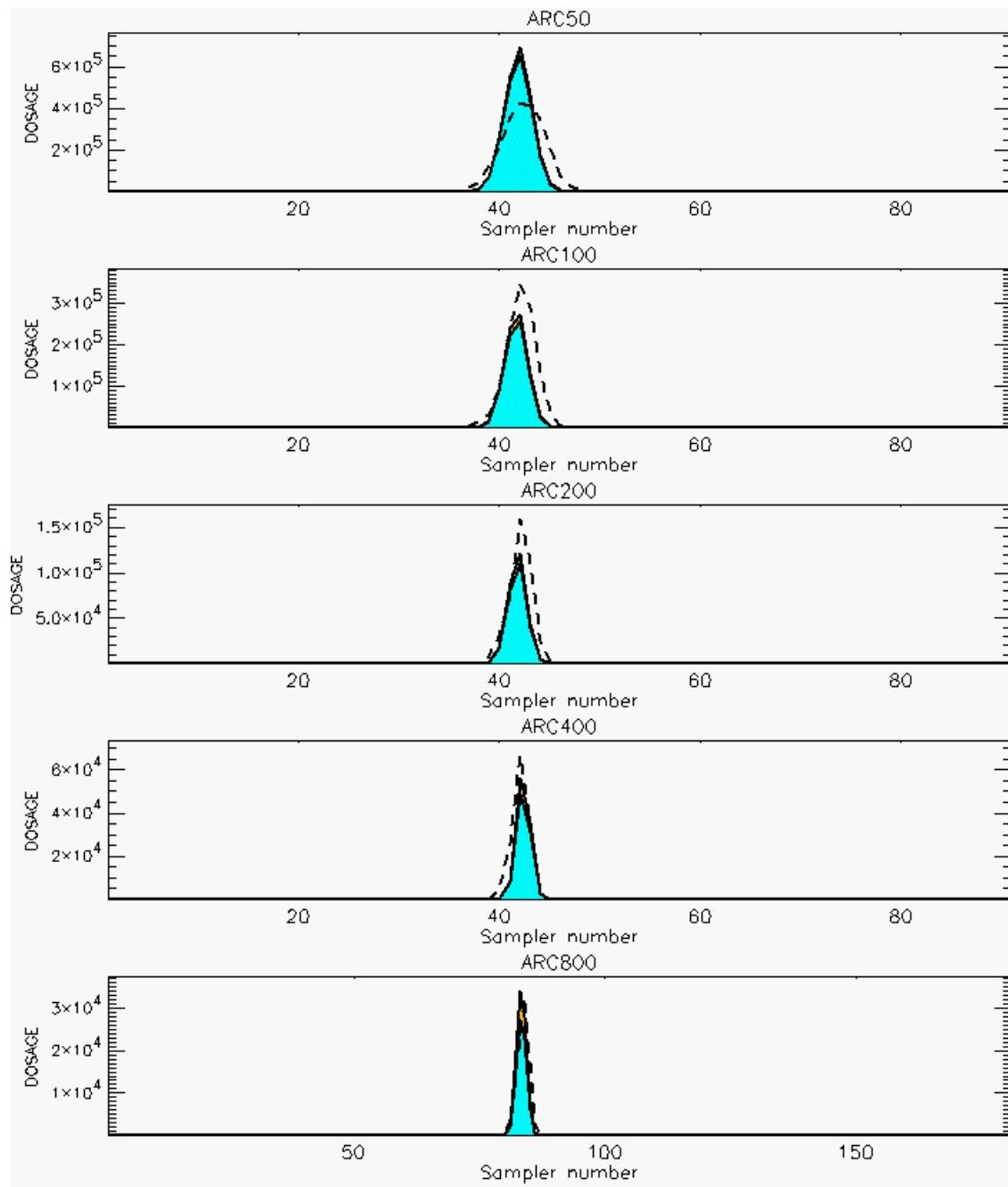
PG Prediction1 to Prediction2 Comparison

PG Trial File: pr_grass_tracer_Experiment_28.txt

PG Prediction File 1: HPAC\deposition\pg_28_vd.out

PG Prediction File 2: HPAC\nodeposition\pg_28_novd.out

**Figure F-23. HPAC With and Without SO₂ Surface Deposition Predictions to Trial 28:
Stability Category is 5**



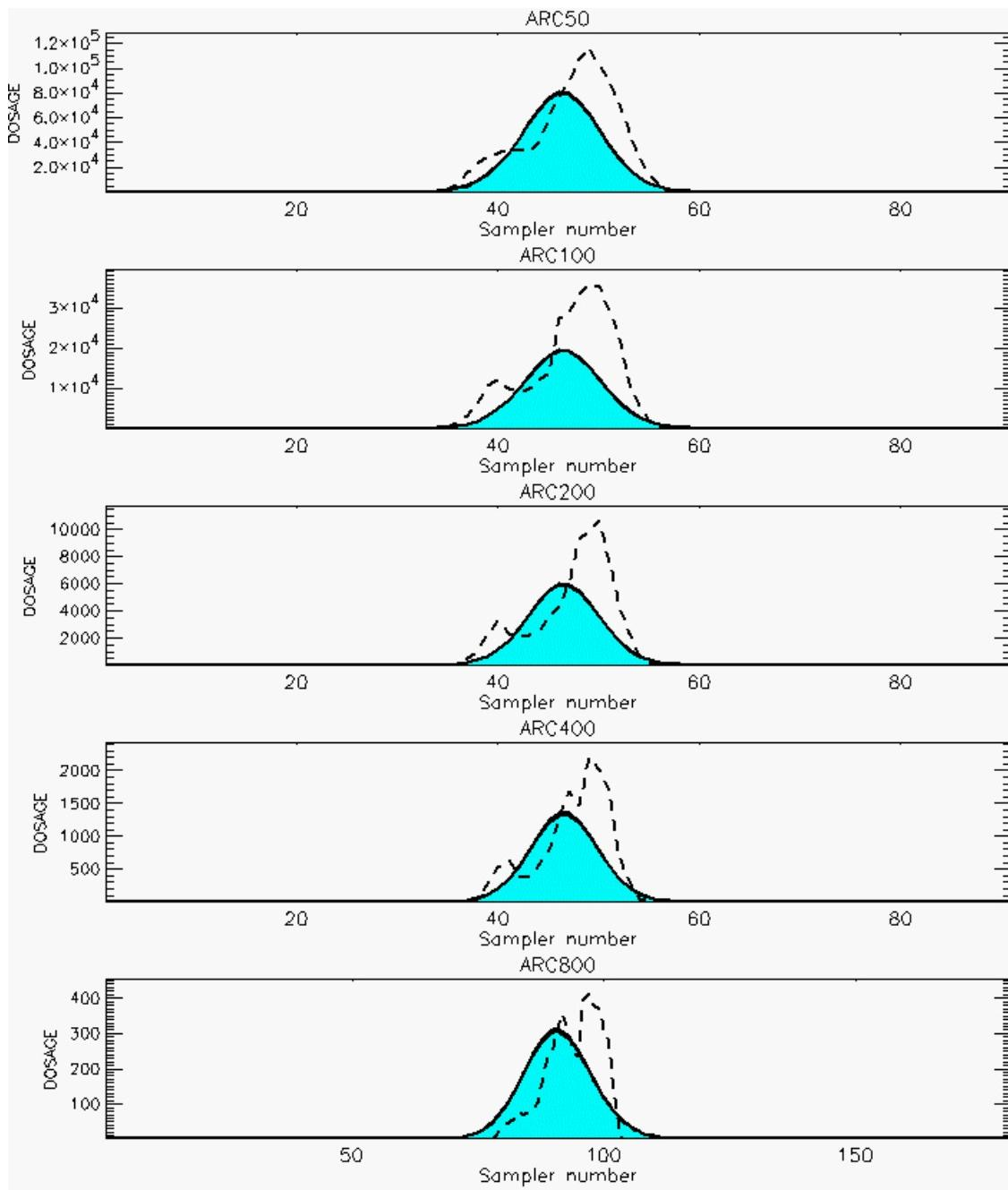
PG Prediction1 to Prediction2 Comparison

PG Trial File: pr_grass_tracer_Experiment_32.txt

PG Prediction File 1: HPAC\deposition\pg_32_vd.out

PG Prediction File 2: HPAC\nodeposition\pg_32_novd.out

**Figure F-24. HPAC With and Without SO₂ Surface Deposition Predictions to Trial 32:
Stability Category is 6**



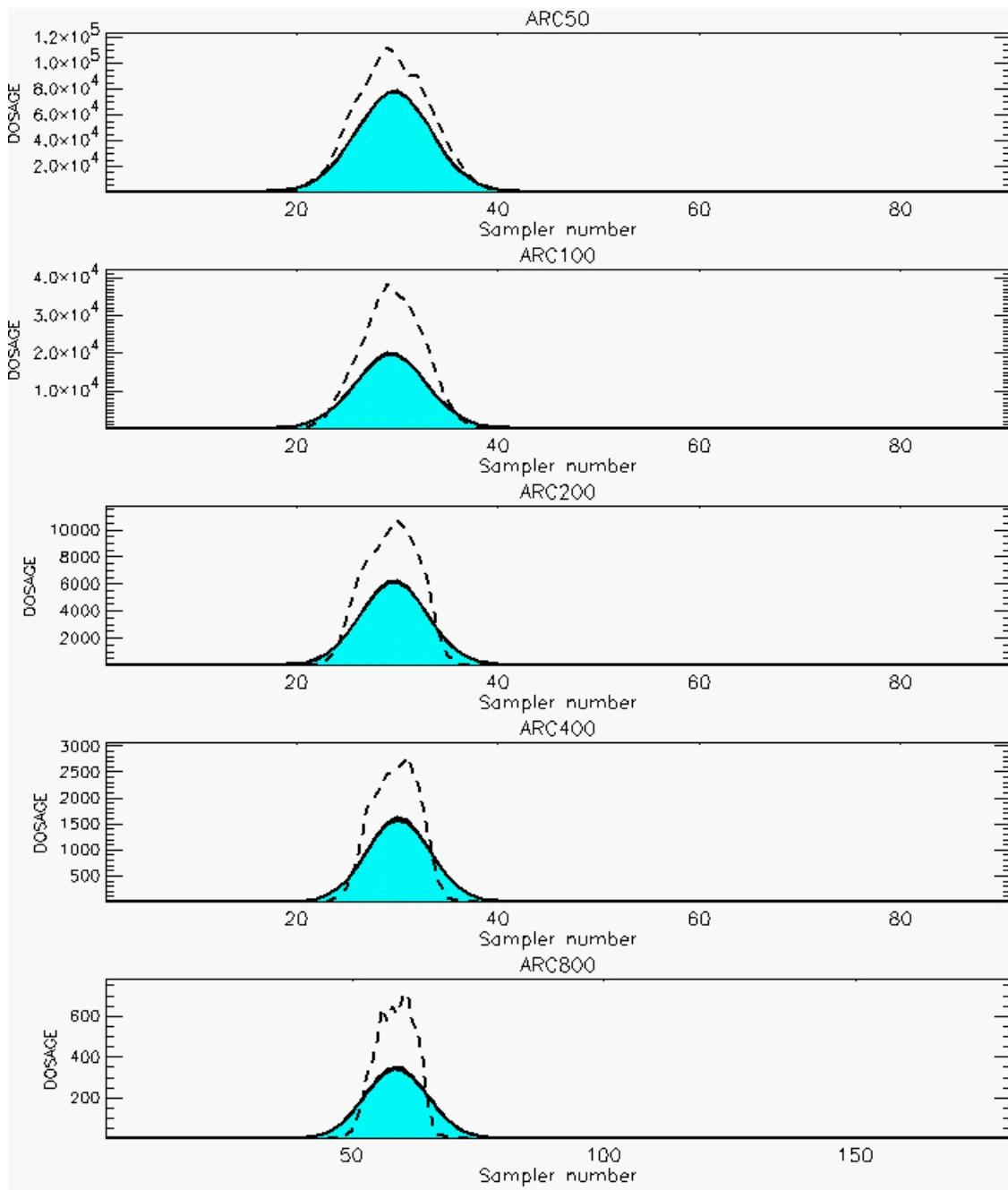
PG Prediction1 to Prediction2 Comparison

PG Trial File: pr_grass_tracer_Experiment_33.txt

PG Prediction File 1: HPAC\deposition\pg_33_vd.out

PG Prediction File 2: HPAC\nodeposition\pg_33_novd.out

**Figure F-25. HPAC With and Without SO₂ Surface Deposition Predictions to Trial 33:
Stability Category is 3**



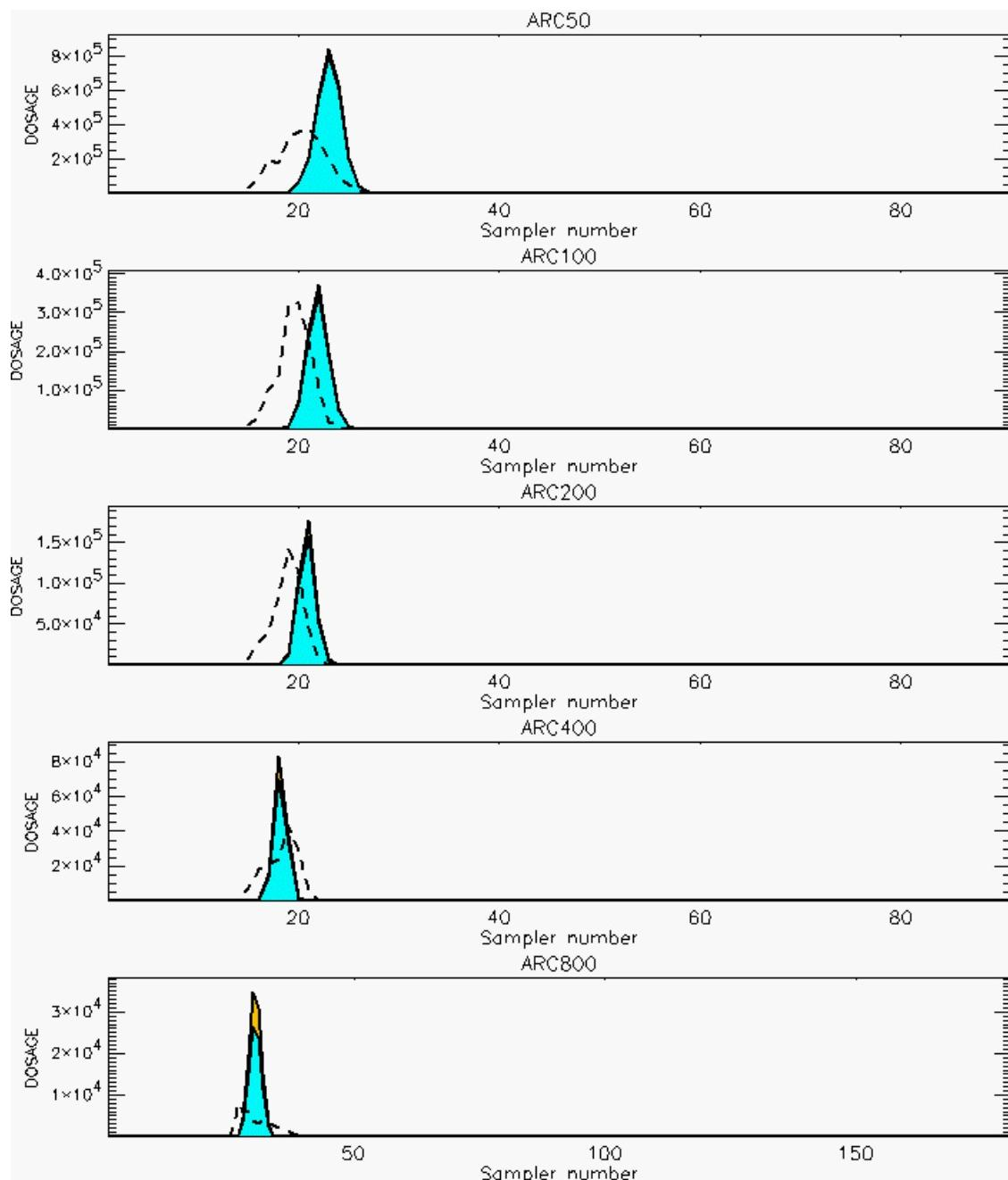
PG Prediction1 to Prediction2 Comparison

PG Trial File: pr_grass_tracer_Experiment_34.txt

PG Prediction File 1: HPAC\deposition\pg_34_vd.out

PG Prediction File 2: HPAC\nodeposition\pg_34_novd.out

**Figure F-26. HPAC With and Without SO_2 Surface Deposition Predictions to Trial 34:
Stability Category is 3**



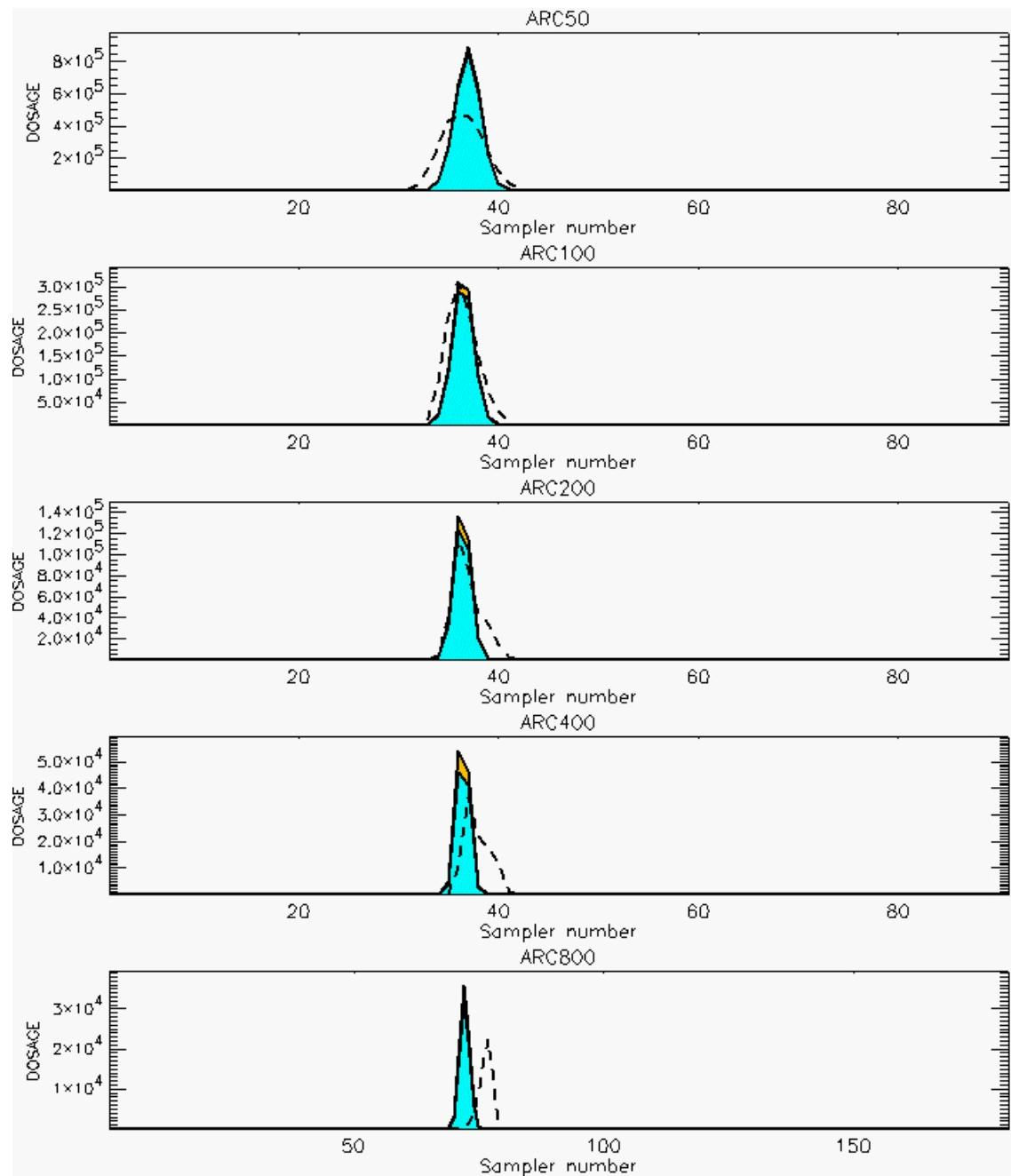
PG Prediction1 to Prediction2 Comparison

PG Trial File: pr_grass_tracer_Experiment_35.txt

PG Prediction File 1: HPAC\deposition\pg_35_vd.out

PG Prediction File 2: HPAC\nodeposition\pg_35_novd.out

**Figure F-27. HPAC With and Without SO₂ Surface Deposition Predictions to Trial 35:
Stability Category is 6**



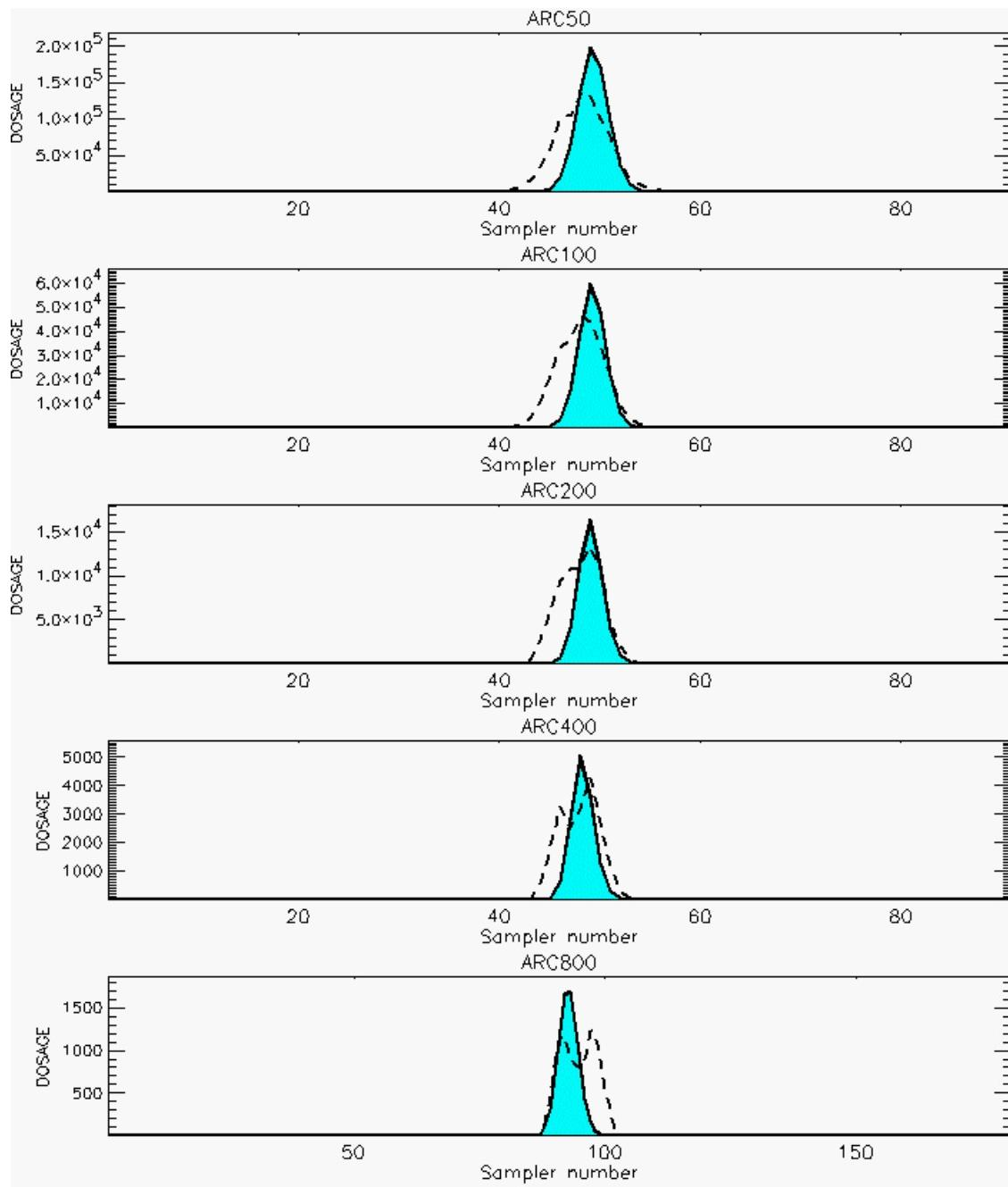
PG Prediction1 to Prediction2 Comparison

PG Trial File: pr_grass_tracer_Experiment_36.txt

PG Prediction File 1: HPAC\deposition\pg_36_vd.out

PG Prediction File 2: HPAC\nodeposition\pg_36_novd.out

**Figure F-28. HPAC With and Without SO₂ Surface Deposition Predictions to Trial 36:
Stability Category is 6**



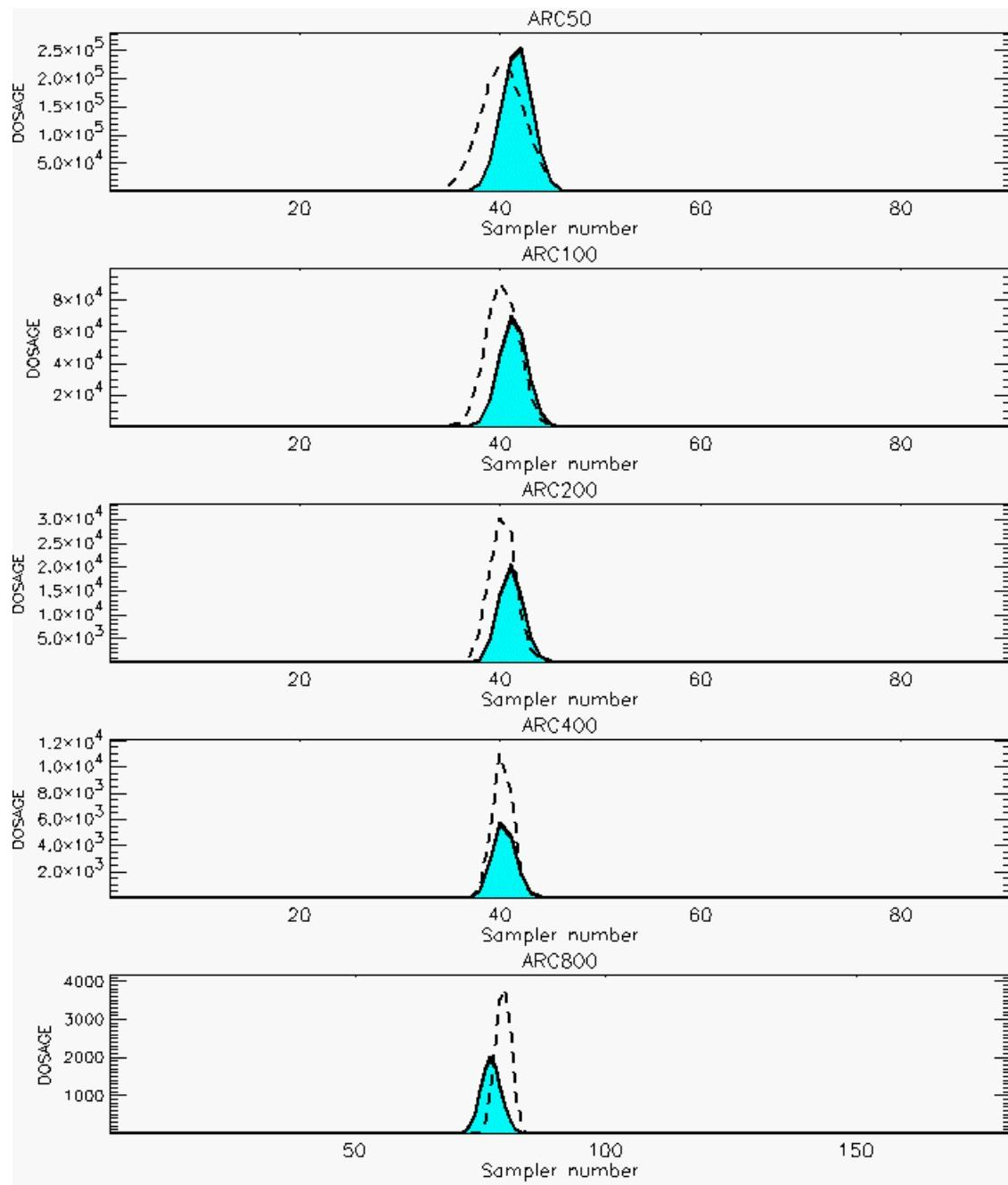
PG Prediction1 to Prediction2 Comparison

PG Trial File: pr_grass_tracer_Experiment_37.txt

PG Prediction File 1: HPAC\deposition\pg_37_vd.out

PG Prediction File 2: HPAC\nodeposition\pg_37_novd.out

**Figure F-29. HPAC With and Without SO₂ Surface Deposition Predictions to Trial 37:
Stability Category is 4**



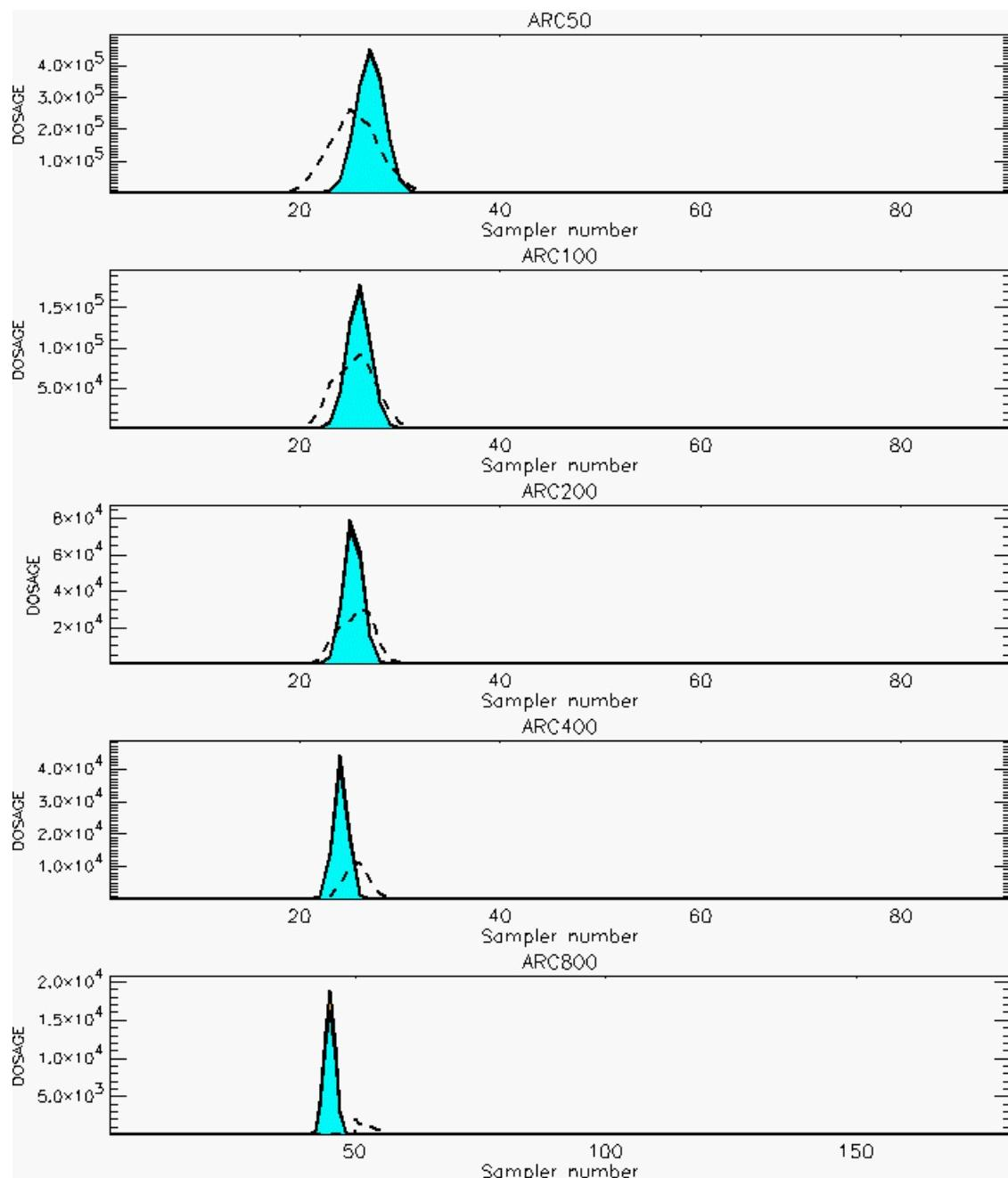
PG Prediction1 to Prediction2 Comparison

PG Trial File: pr_grass_tracer_Experiment_38.txt

PG Prediction File 1: HPAC\deposition\pg_38_vd.out

PG Prediction File 2: HPAC\nodeposition\pg_38_novd.out

**Figure F-30. HPAC With and Without SO₂ Surface Deposition Predictions to Trial 38:
Stability Category is 4**



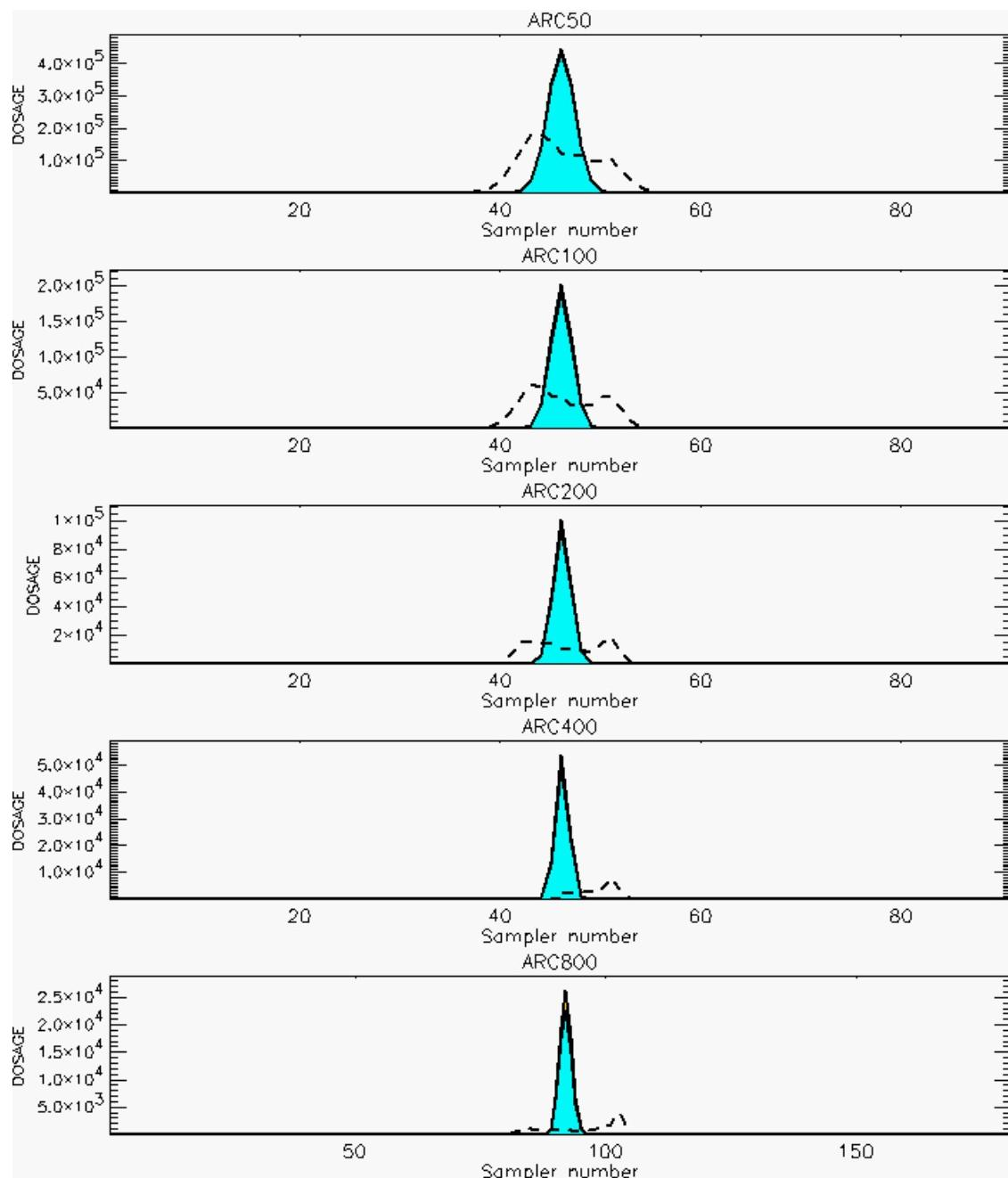
PG Prediction1 to Prediction2 Comparison

PG Trial File: pr_grass_tracer_Experiment_39.txt

PG Prediction File 1: HPAC\deposition\pg_39_vd.out

PG Prediction File 2: HPAC\nodeposition\pg_39_novd.out

**Figure F-31. HPAC With and Without SO₂ Surface Deposition Predictions to Trial 39:
Stability Category is 6**



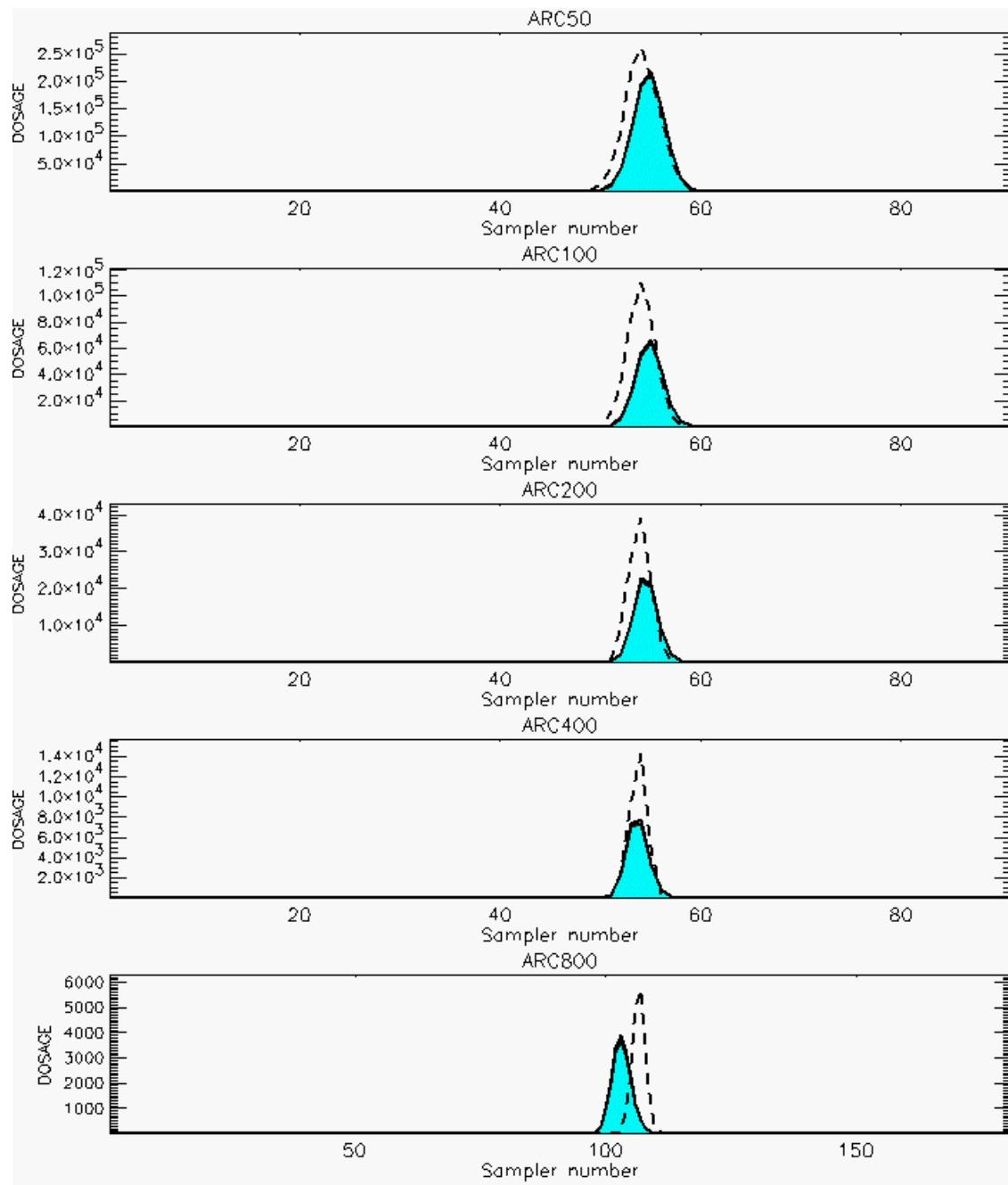
PG Prediction1 to Prediction2 Comparison

PG Trial File: pr_grass_tracer_Experiment_40.txt

PG Prediction File 1: HPAC\deposition\pg_40_vd.out

PG Prediction File 2: HPAC\nodeposition\pg_40_novd.out

**Figure F-32. HPAC With and Without SO₂ Surface Deposition Predictions to Trial 40:
Stability Category is 6**



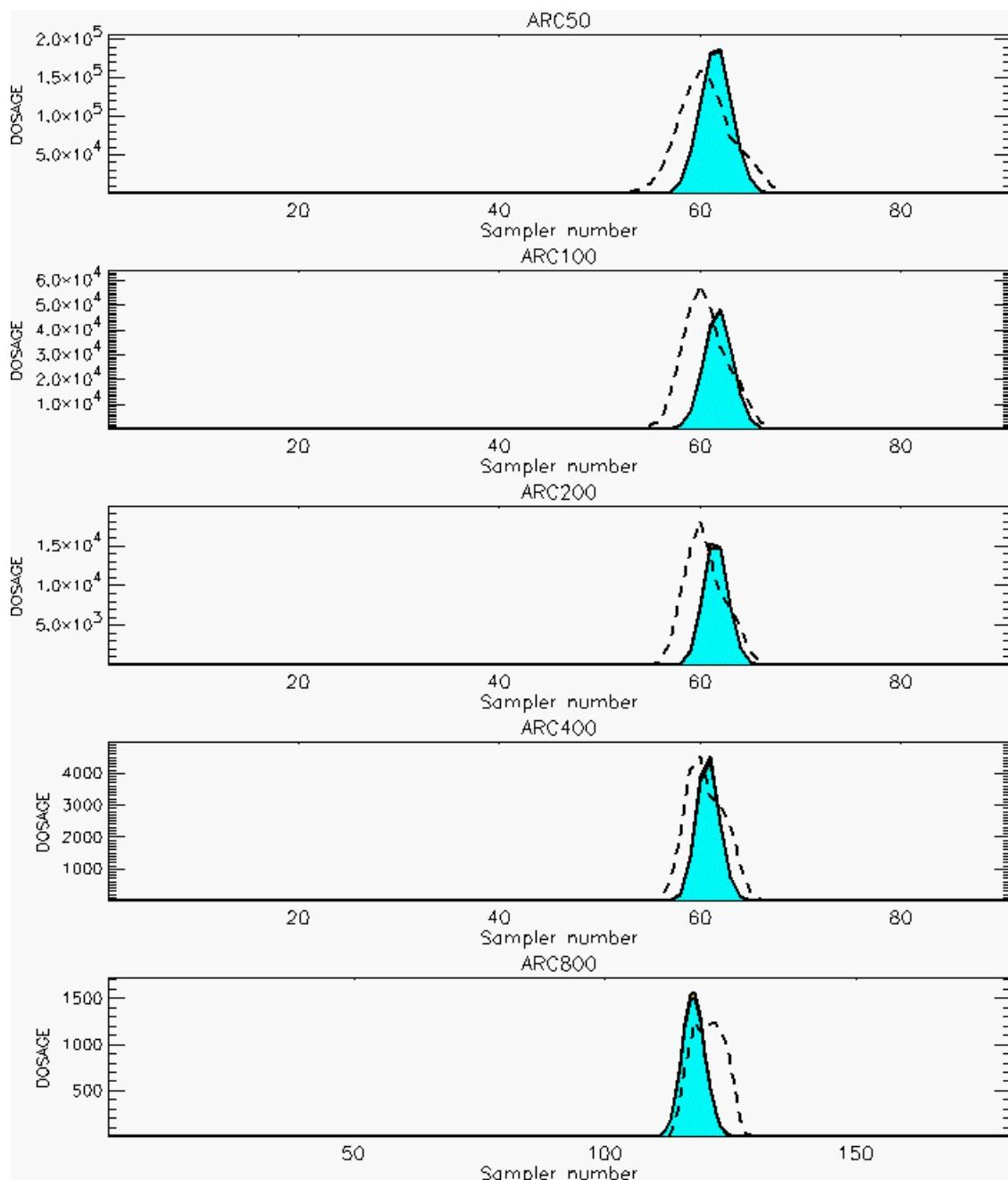
PG Prediction1 to Prediction2 Comparison

PG Trial File: pr_grass_tracer_Experiment_41.txt

PG Prediction File 1: HPAC\deposition\pg_41_vd.out

PG Prediction File 2: HPAC\nodeposition\pg_41_novd.out

Figure F-33. HPAC With and Without SO₂ Surface Deposition Predictions to Trial 41:
Stability Category is 5



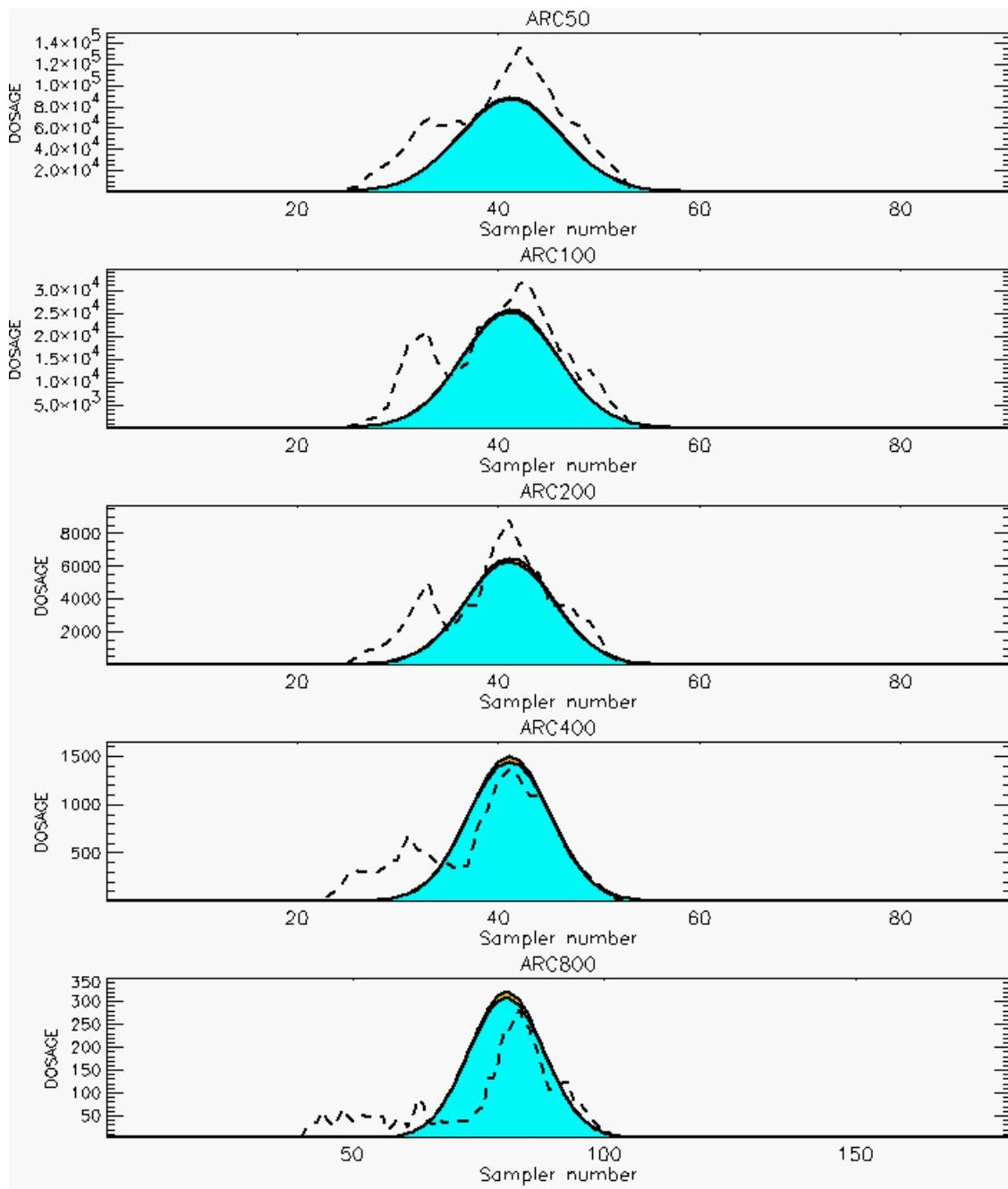
PG Prediction1 to Prediction2 Comparison

PG Trial File: pr_grass_tracer_Experiment_42.txt

PG Prediction File 1: HPAC\deposition\pg_42_vd.out

PG Prediction File 2: HPAC\nodeposition\pg_42_novd.out

**Figure F-34. HPAC With and Without SO_2 Surface Deposition Predictions to Trial 42:
Stability Category is 4**



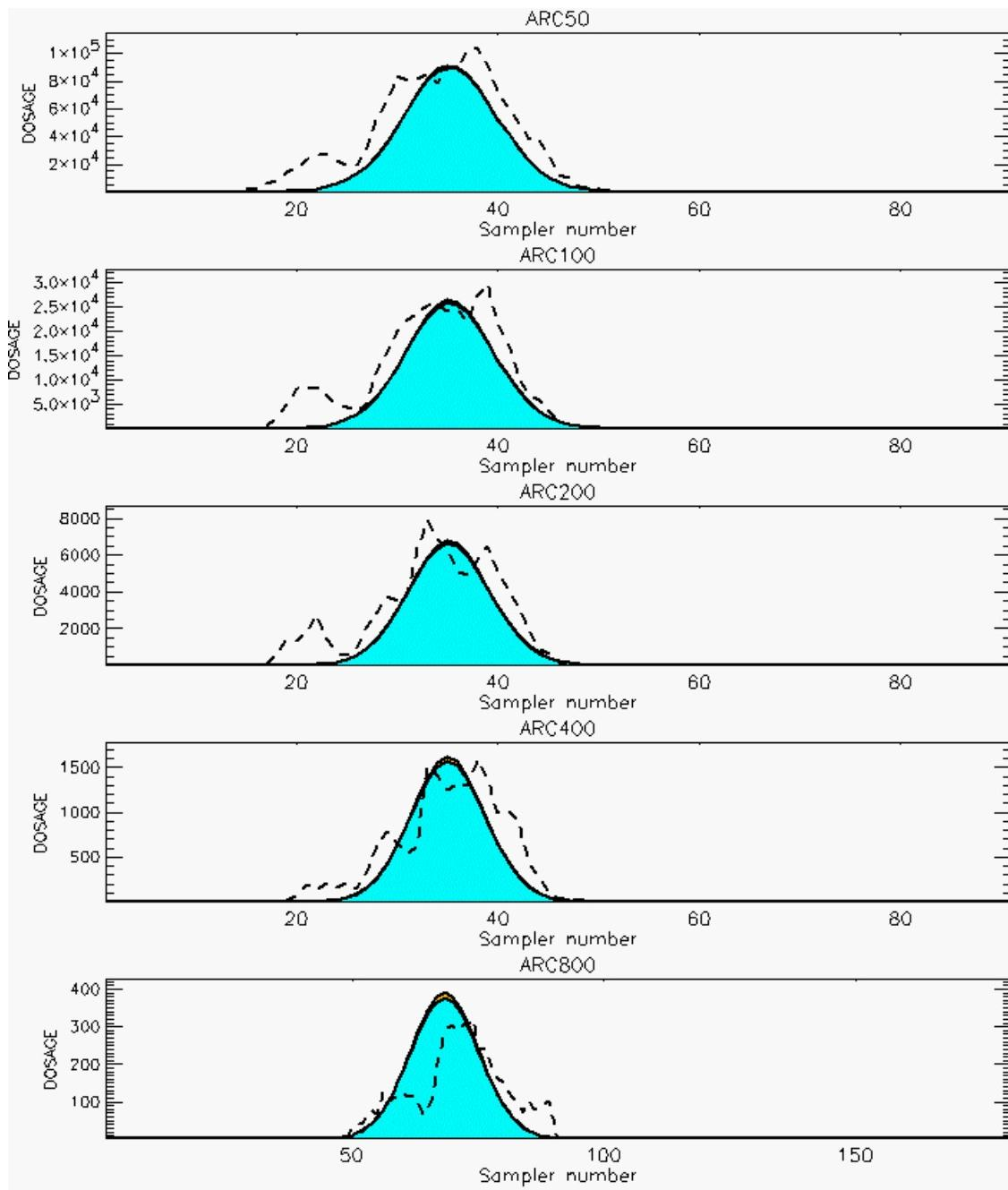
PG Prediction1 to Prediction2 Comparison

PG Trial File: pr_grass_tracer_Experiment_43.txt

PG Prediction File 1: HPAC\deposition\pg_43_vd.out

PG Prediction File 2: HPAC\nodeposition\pg_43_novd.out

Figure F-35. HPAC With and Without SO₂ Surface Deposition Predictions to Trial 43:
Stability Category is 1



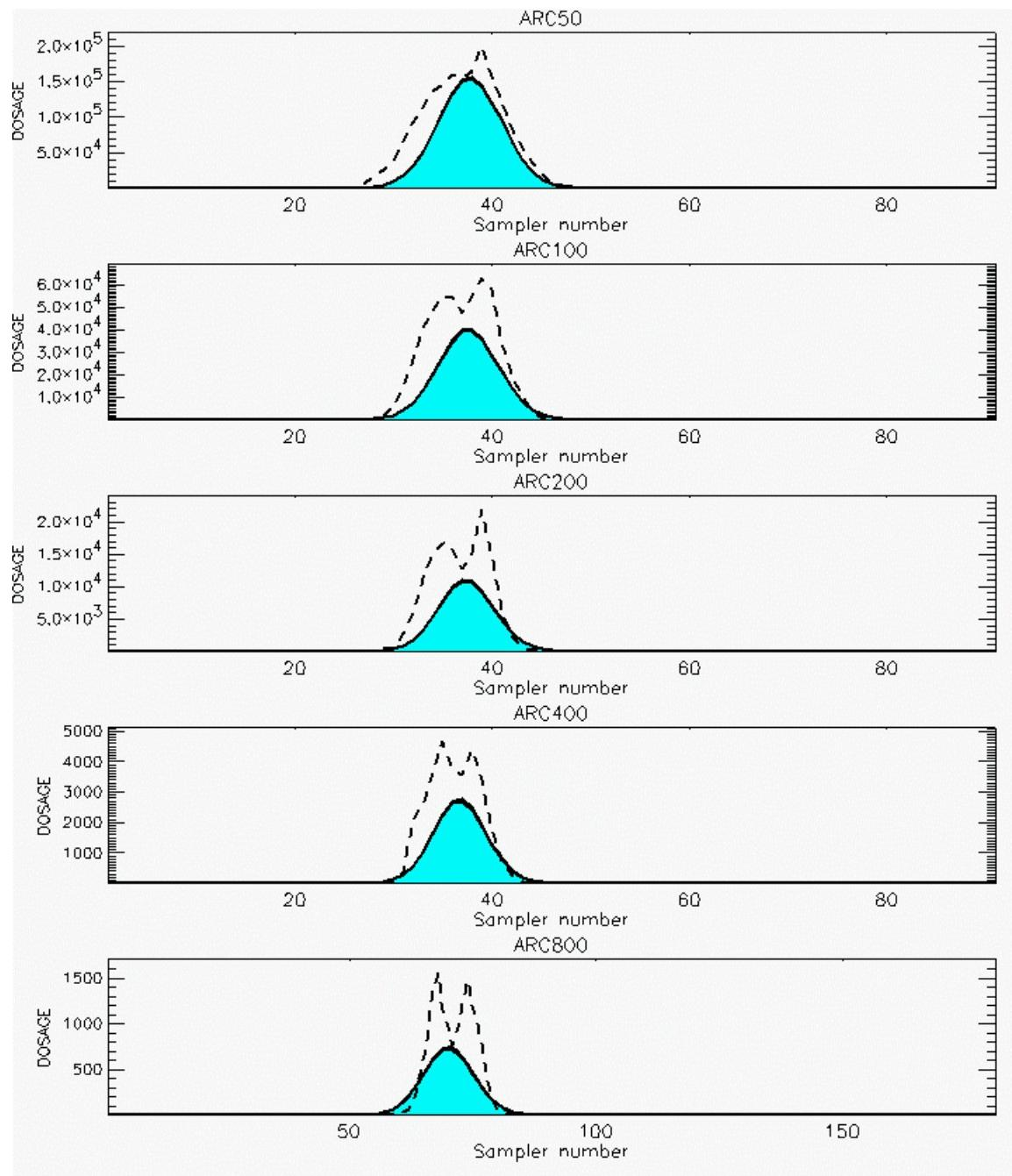
PG Prediction1 to Prediction2 Comparison

PG Trial File: pr_grass_tracer_Experiment_44.txt

PG Prediction File 1: HPAC\deposition\pg_44_vd.out

PG Prediction File 2: HPAC\nodeposition\pg_44_novd.out

**Figure F-36. HPAC With and Without SO₂ Surface Deposition Predictions to Trial 44:
Stability Category is 2**



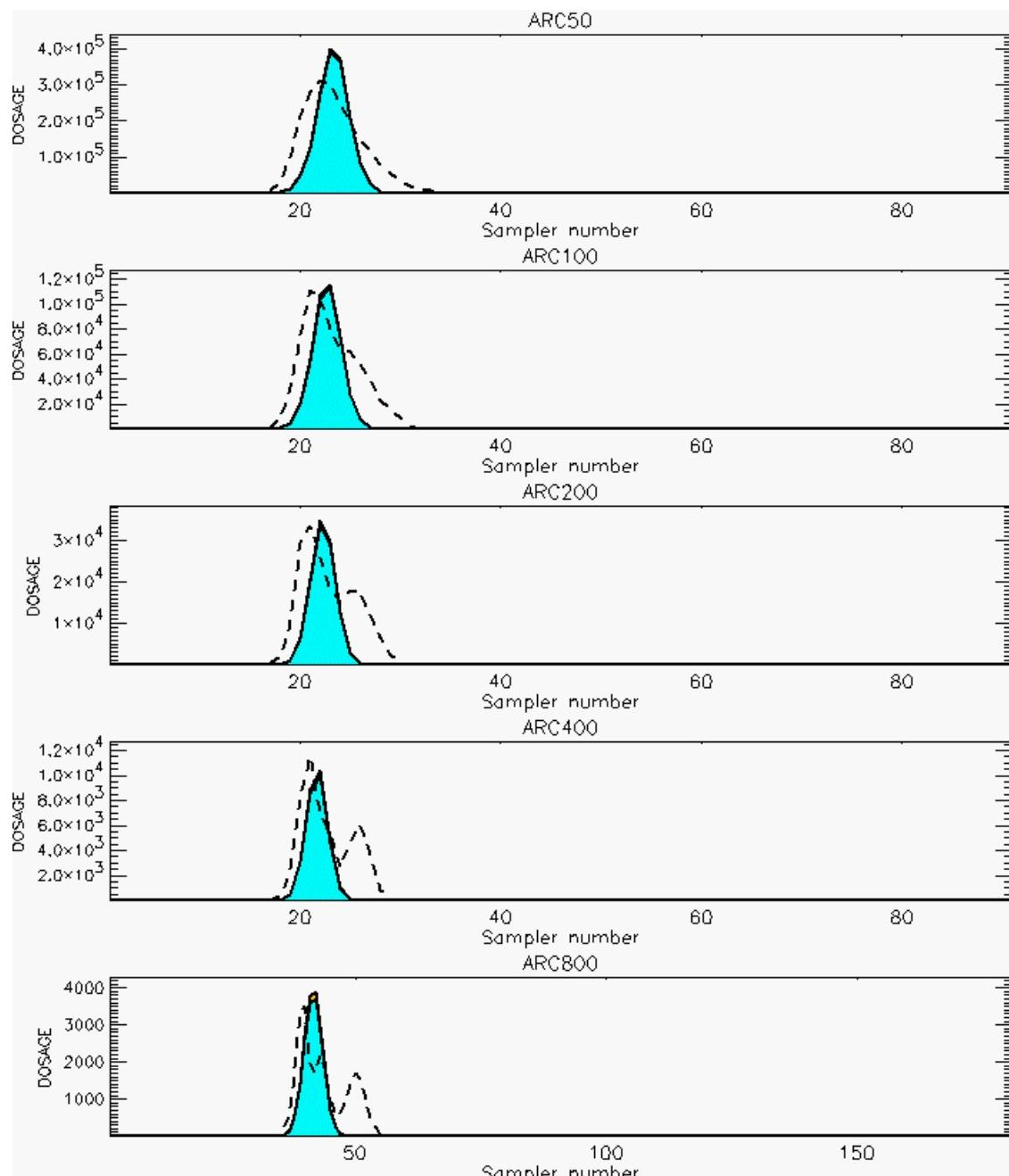
PG Prediction1 to Prediction2 Comparison

PG Trial File: pr_grass_tracer_Experiment_45.txt

PG Prediction File 1: HPAC\deposition\pg_45_vd.out

PG Prediction File 2: HPAC\nodeposition\pg_45_novd.out

**Figure F-37. HPAC With and Without SO_2 Surface Deposition Predictions to Trial 45:
Stability Category is 3**



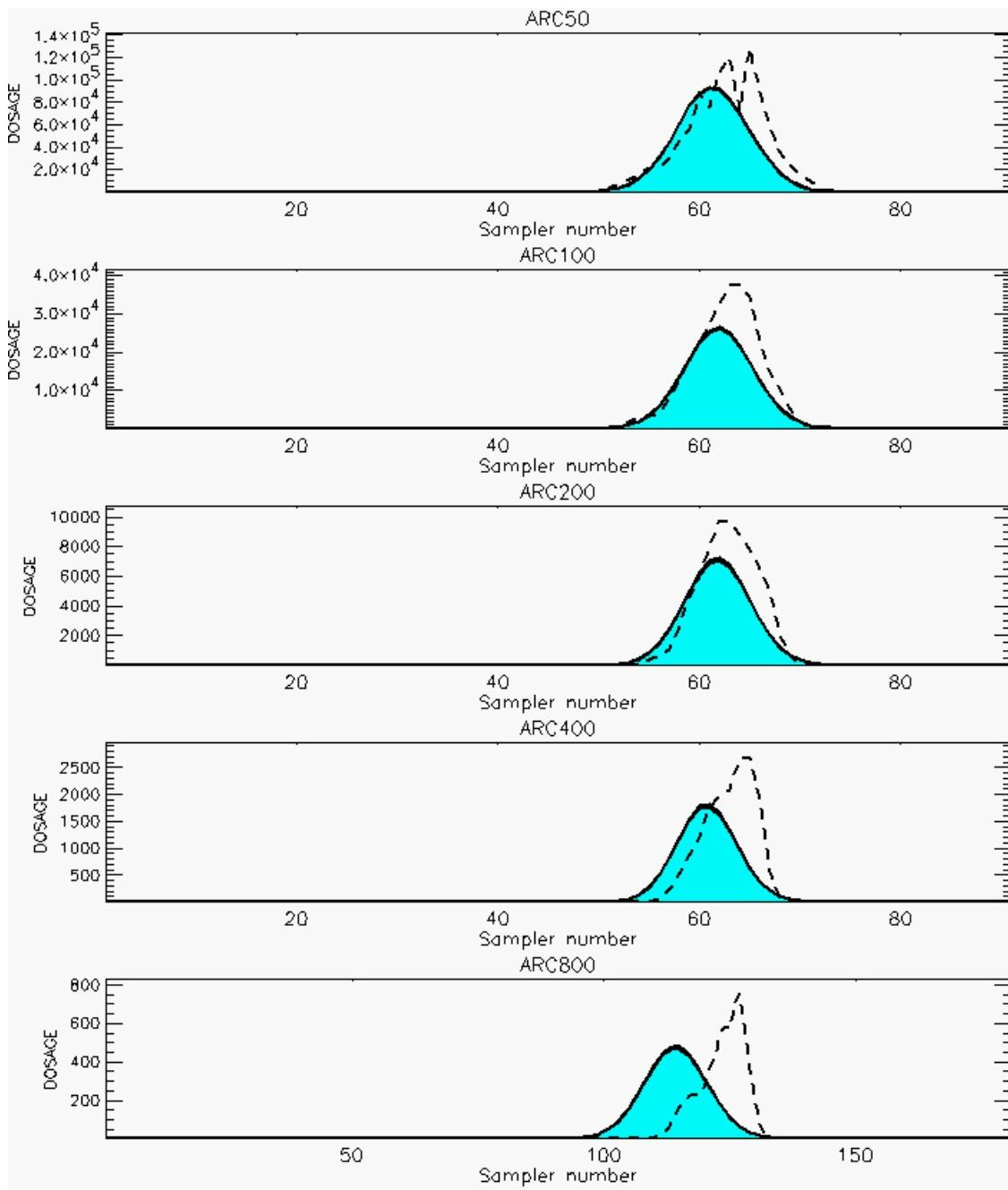
PG Prediction1 to Prediction2 Comparison

PG Trial File: pr_grass_tracer_Experiment_46.txt

PG Prediction File 1: HPAC\deposition\pg_46_vd.out

PG Prediction File 2: HPAC\nodeposition\pg_46_novd.out

**Figure F-38. HPAC With and Without SO_2 Surface Deposition Predictions to Trial 46:
Stability Category is 4**



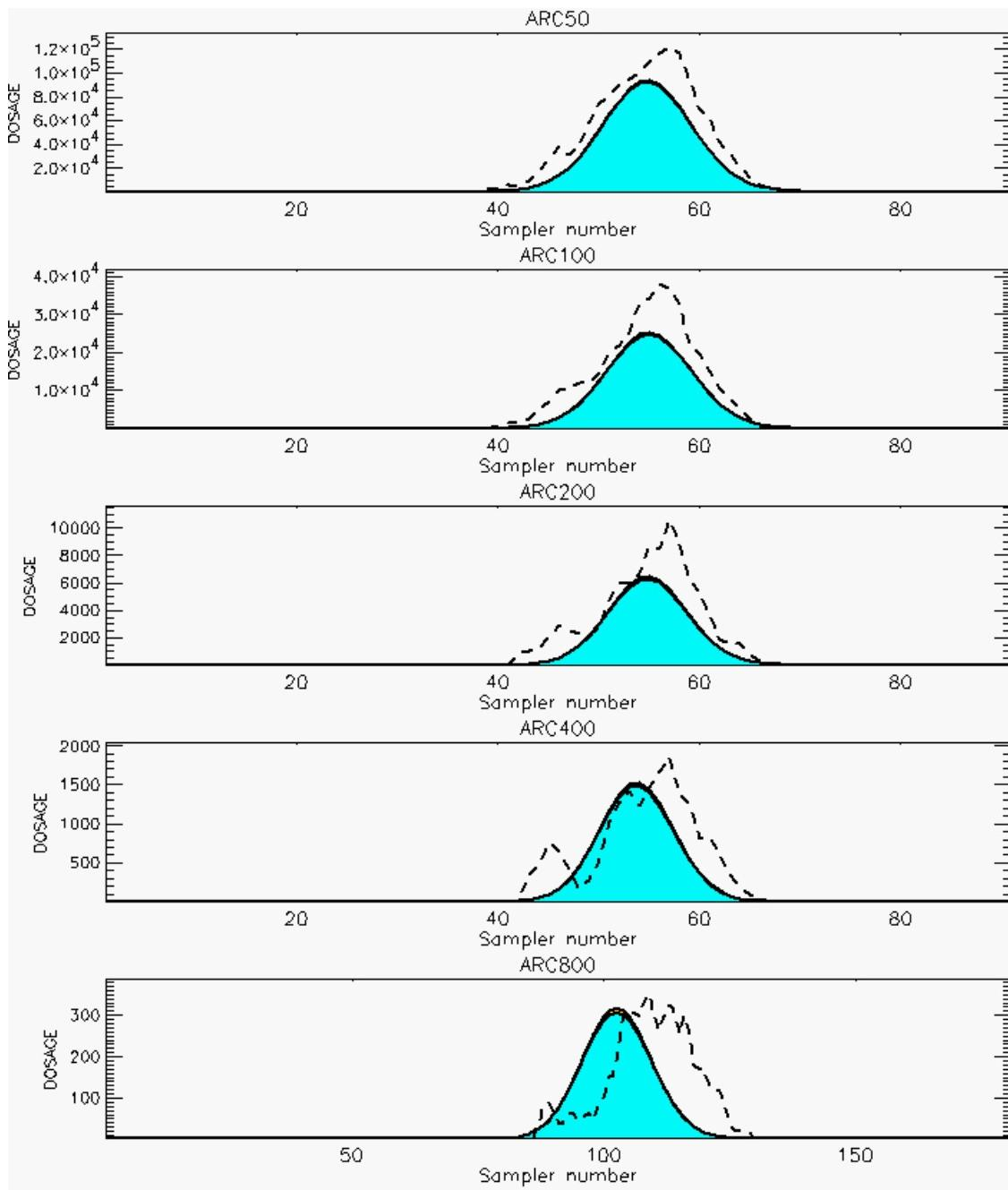
PG Prediction1 to Prediction2 Comparison

PG Trial File: pr_grass_tracer_Experiment_48.txt

PG Prediction File 1: HPAC\deposition\pg_48_vd.out

PG Prediction File 2: HPAC\nodeposition\pg_48_novd.out

**Figure F-39. HPAC With and Without SO_2 Surface Deposition Predictions to Trial 48:
Stability Category is 3**



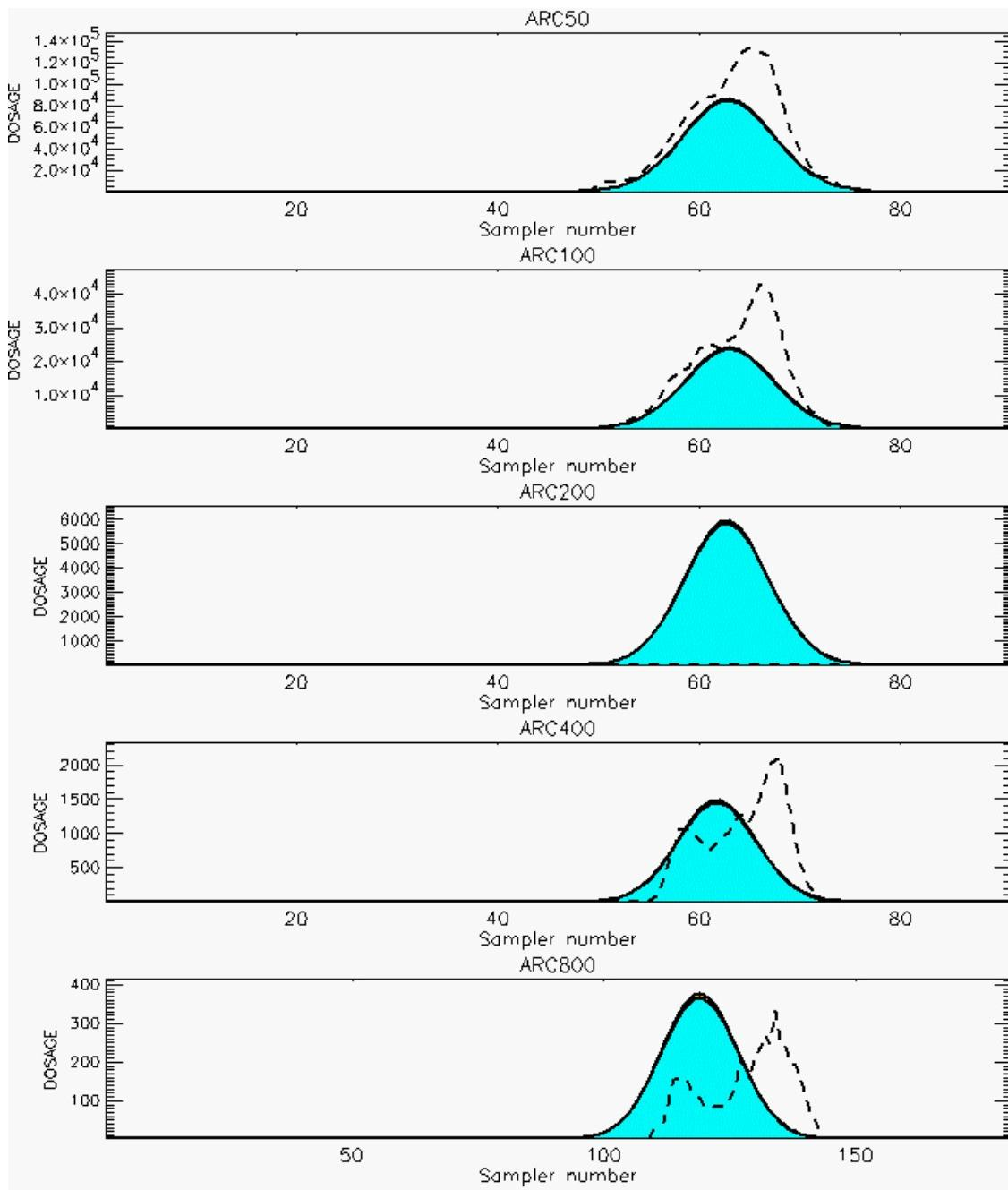
PG Prediction1 to Prediction2 Comparison

PG Trial File: pr_grass_tracer_Experiment_49.txt

PG Prediction File 1: HPAC\deposition\pg_49_vd.out

PG Prediction File 2: HPAC\nodeposition\pg_49_novd.out

**Figure F-40. HPAC With and Without SO₂ Surface Deposition Predictions to Trial 49:
Stability Category is 2**



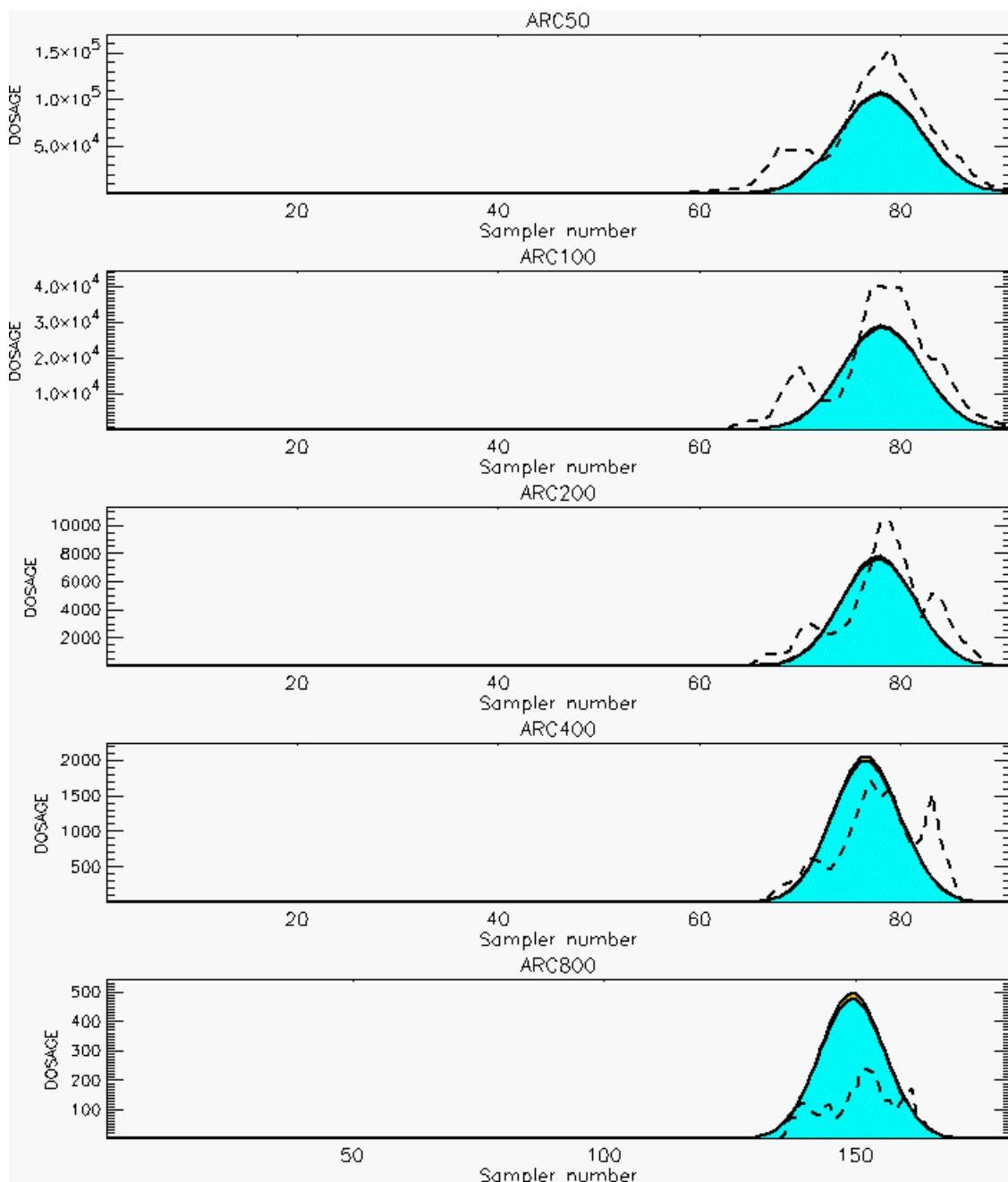
PG Prediction1 to Prediction2 Comparison

PG Trial File: pr_grass_tracer_Experiment_50.txt

PG Prediction File 1: HPAC\deposition\pg_50_vd.out

PG Prediction File 2: HPAC\nodeposition\pg_50_novd.out

**Figure F-41. HPAC With and Without SO₂ Surface Deposition Predictions to Trial 50:
Stability Category is 2**



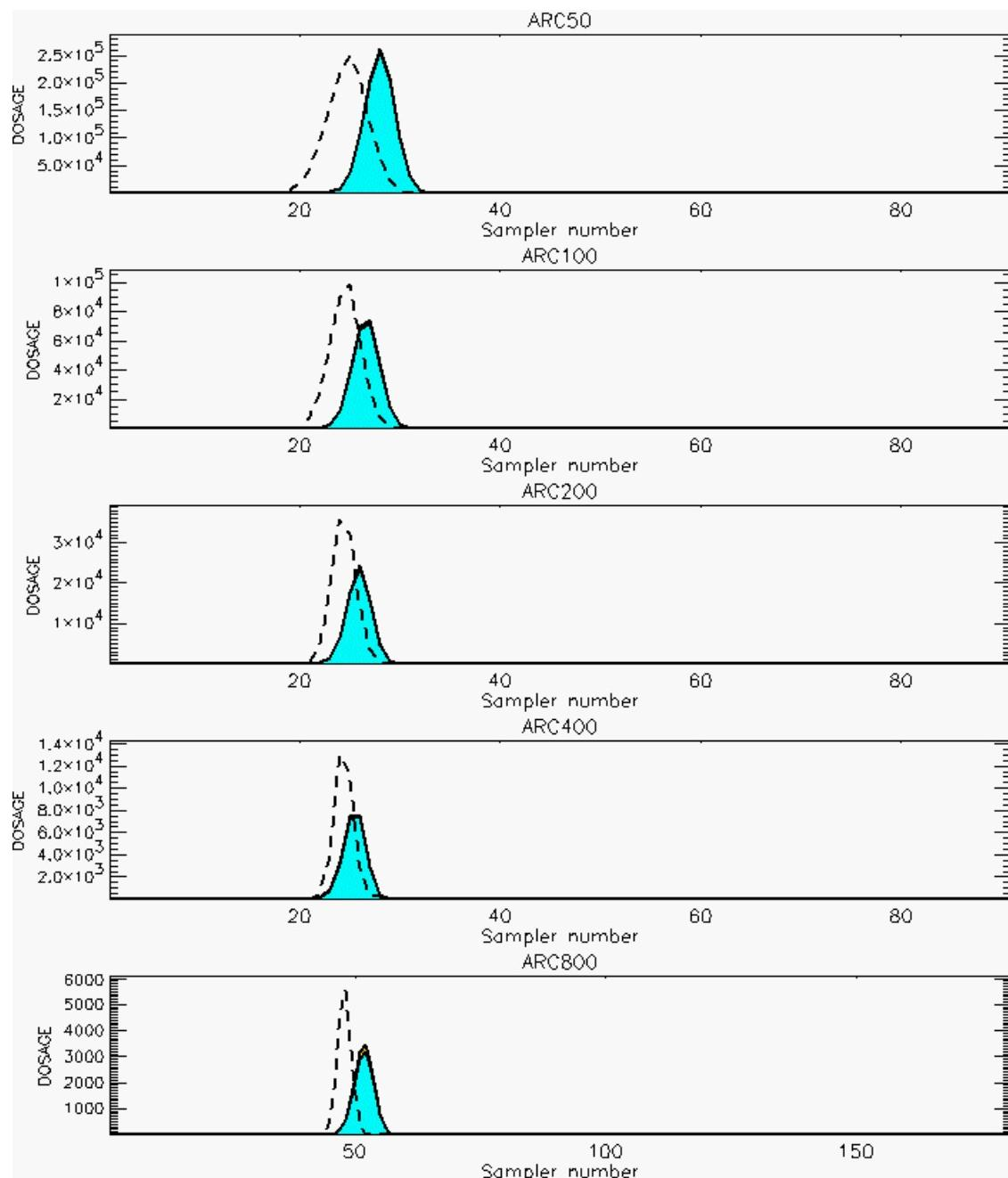
PG Prediction1 to Prediction2 Comparison

PG Trial File: pr_grass_tracer_Experiment_51.txt

PG Prediction File 1: HPAC\deposition\pg_51_vd.out

PG Prediction File 2: HPAC\nodeposition\pg_51_novd.out

**Figure F-42. HPAC With and Without SO₂ Surface Deposition Predictions to Trial 51:
Stability Category is 2**



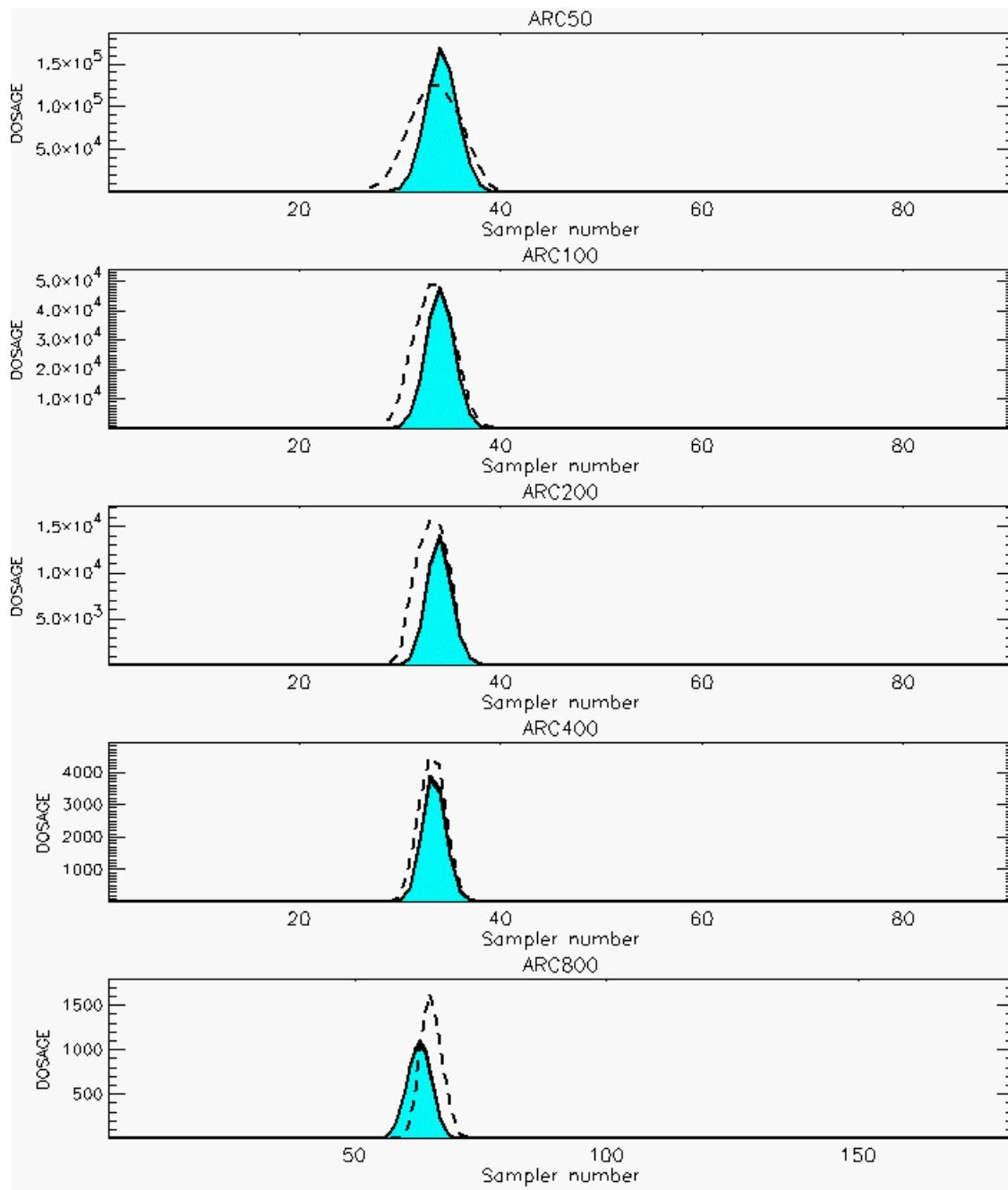
PG Prediction1 to Prediction2 Comparison

PG Trial File: pr_grass_tracer_Experiment_54.txt

PG Prediction File 1: HPAC\deposition\pg_54_vd.out

PG Prediction File 2: HPAC\nodeposition\pg_54_novd.out

**Figure F-43. HPAC With and Without SO₂ Surface Deposition Predictions to Trial 54:
Stability Category is 5**



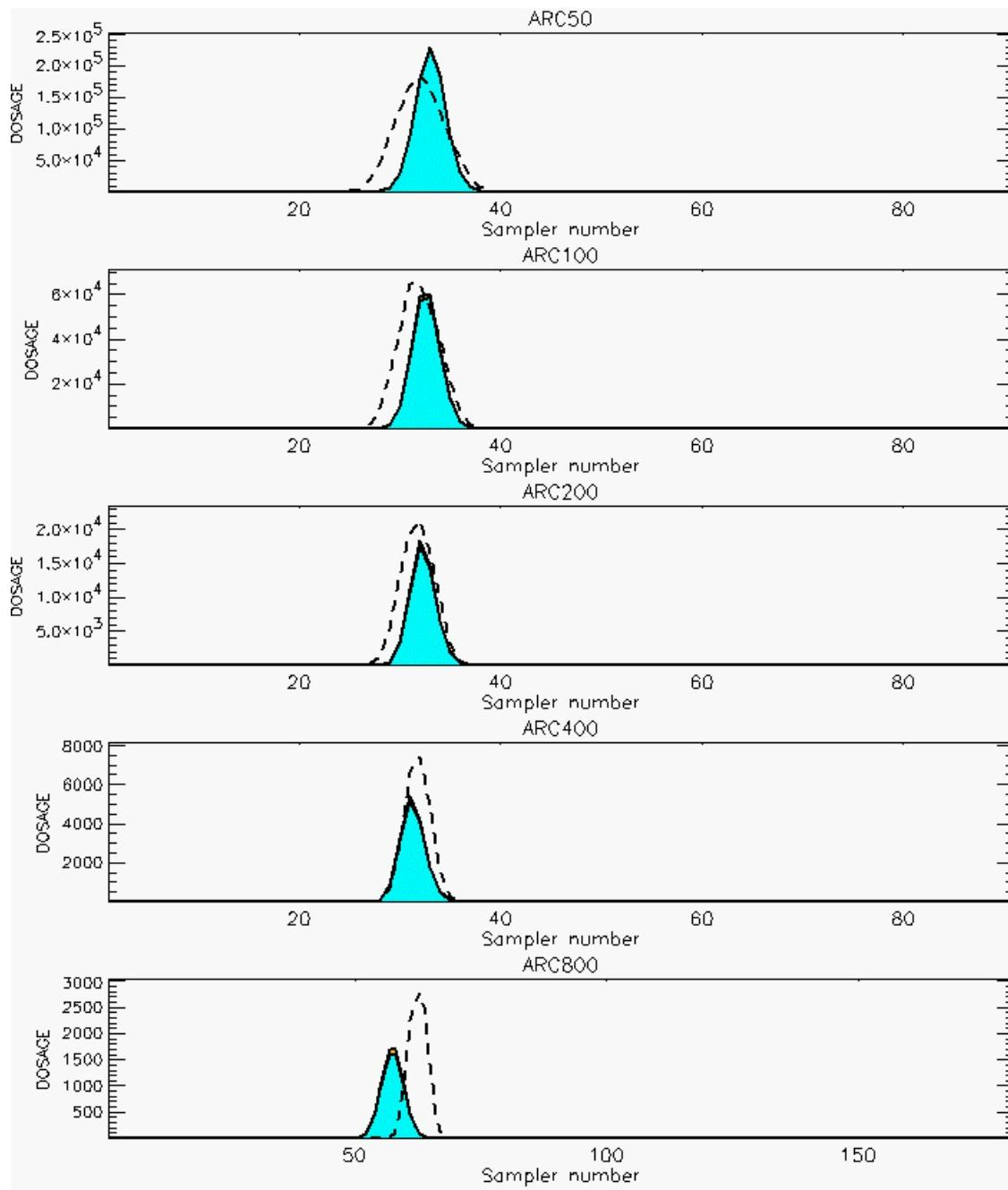
PG Prediction1 to Prediction2 Comparison

PG Trial File: pr_grass_tracer_Experiment_55.txt

PG Prediction File 1: HPAC\deposition\pg_55_vd.out

PG Prediction File 2: HPAC\nodeposition\pg_55_novd.out

**Figure F-44. HPAC With and Without SO₂ Surface Deposition Predictions to Trial 55:
Stability Category is 4**



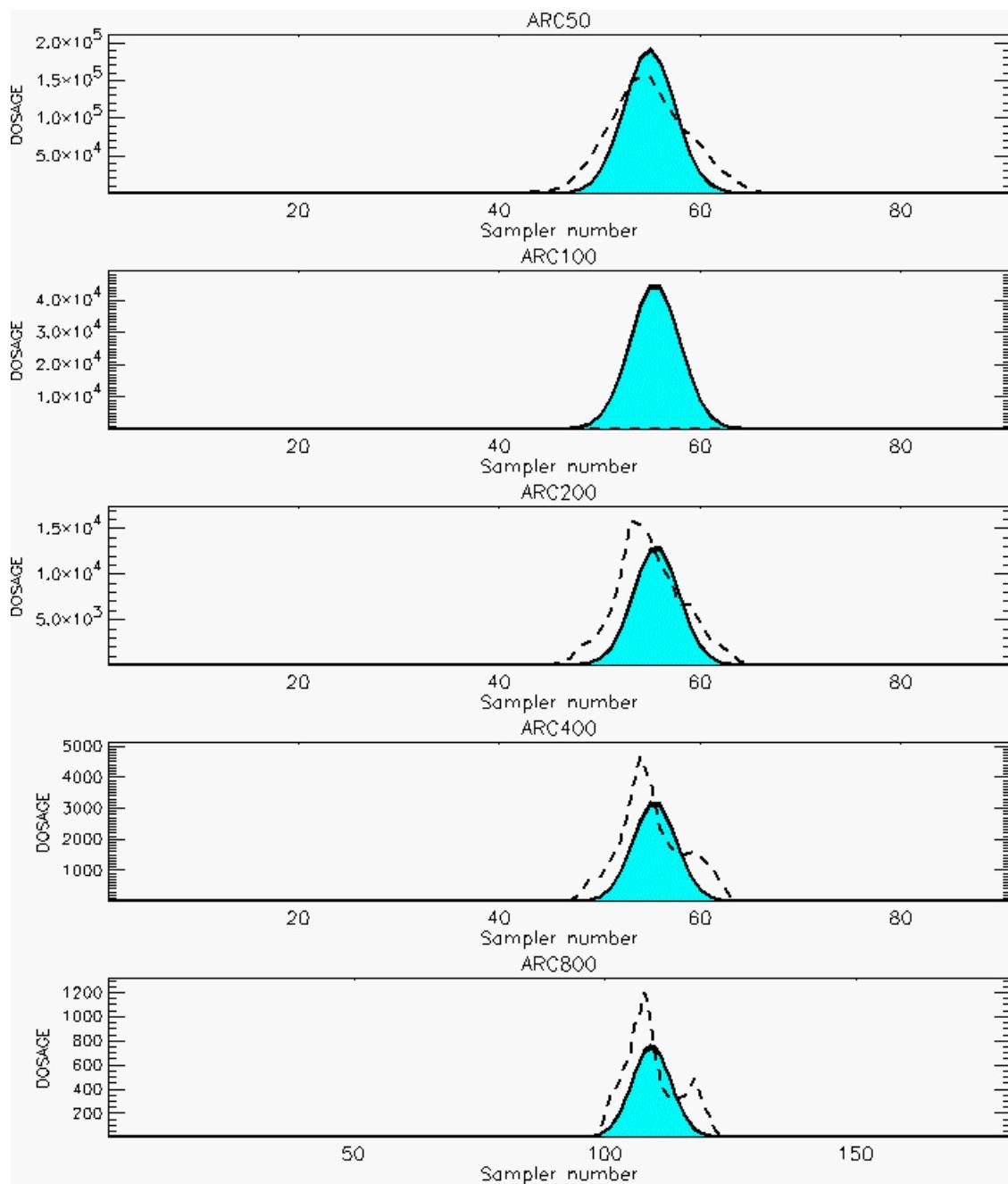
PG Prediction1 to Prediction2 Comparison

PG Trial File: pr_grass_tracer_Experiment_56.txt

PG Prediction File 1: HPAC\deposition\pg_56_vd.out

PG Prediction File 2: HPAC\nodeposition\pg_56_novd.out

**Figure F-45. HPAC With and Without SO_2 Surface Deposition Predictions to Trial 56:
Stability Category is 4**



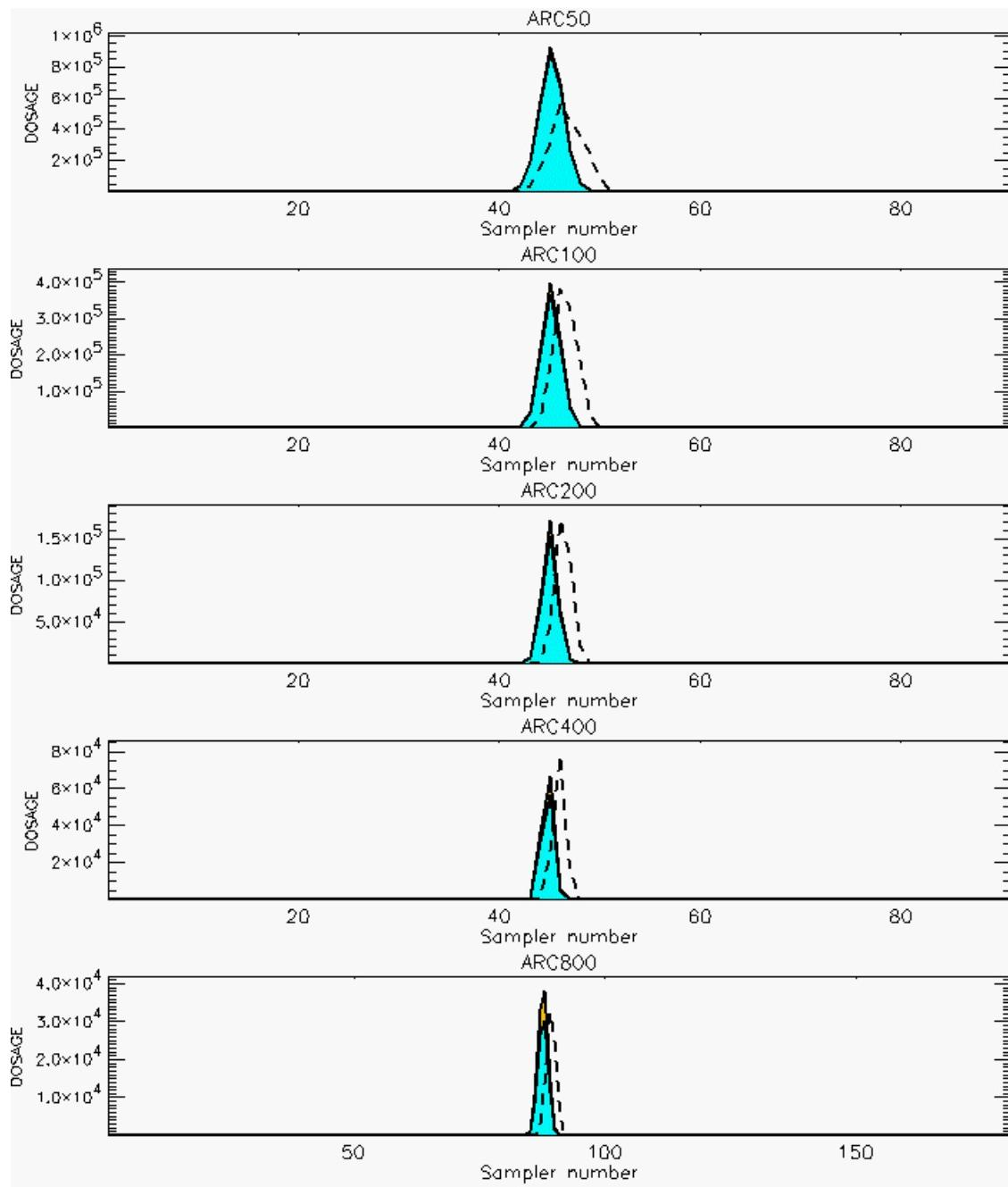
PG Prediction1 to Prediction2 Comparison

PG Trial File: pr_grass_tracer_Experiment_57.txt

PG Prediction File 1: HPAC\deposition\pg_57_vd.out

PG Prediction File 2: HPAC\nodeposition\pg_57_novd.out

**Figure F-46. HPAC With and Without SO₂ Surface Deposition Predictions to Trial 57:
Stability Category is 3**



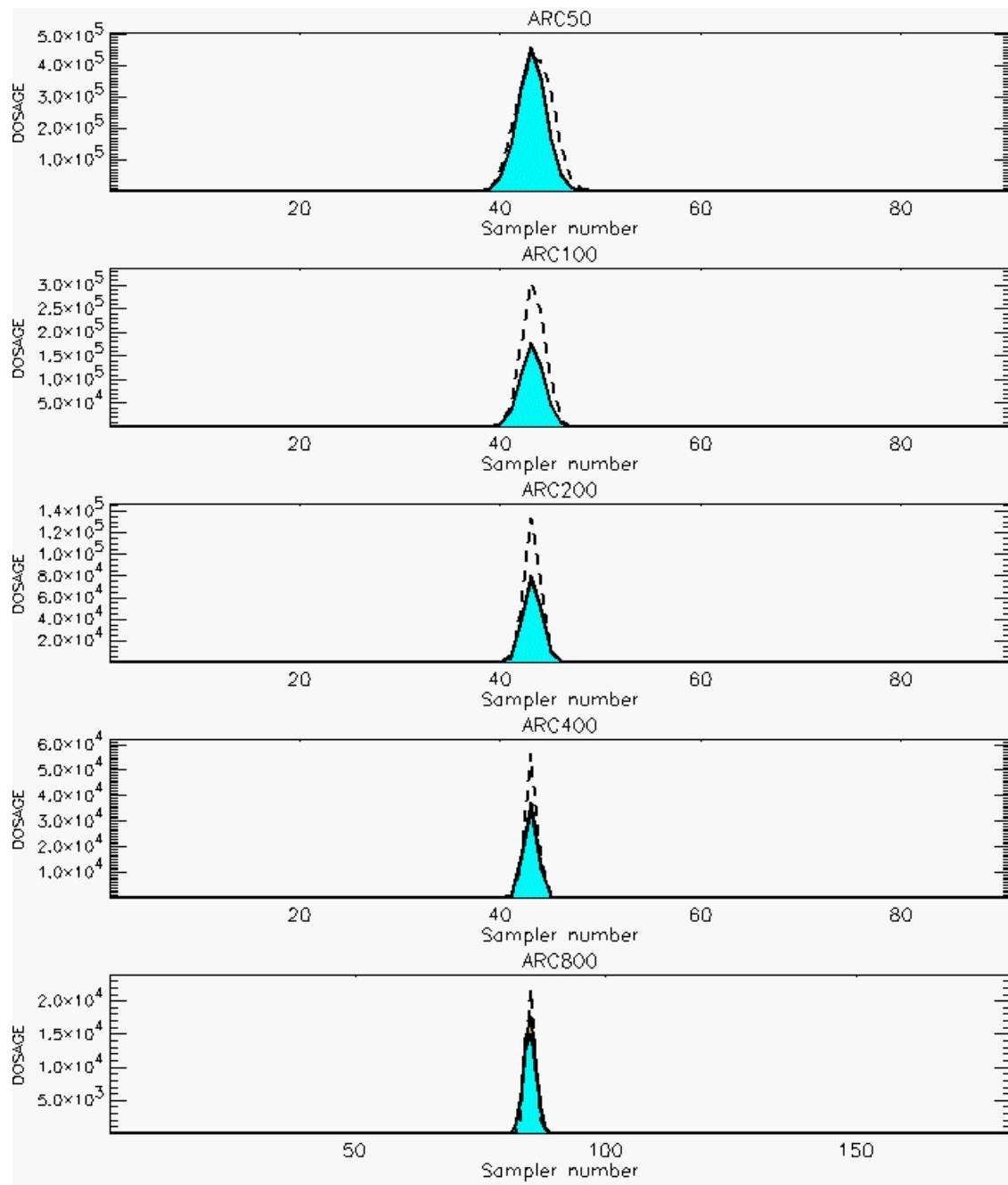
PG Prediction1 to Prediction2 Comparison

PG Trial File: pr_grass_tracer_Experiment_58.txt

PG Prediction File 1: HPAC\deposition\pg_58_vd.out

PG Prediction File 2: HPAC\nodeposition\pg_58_novd.out

**Figure F-47. HPAC With and Without SO₂ Surface Deposition Predictions to Trial 58:
Stability Category is 6**



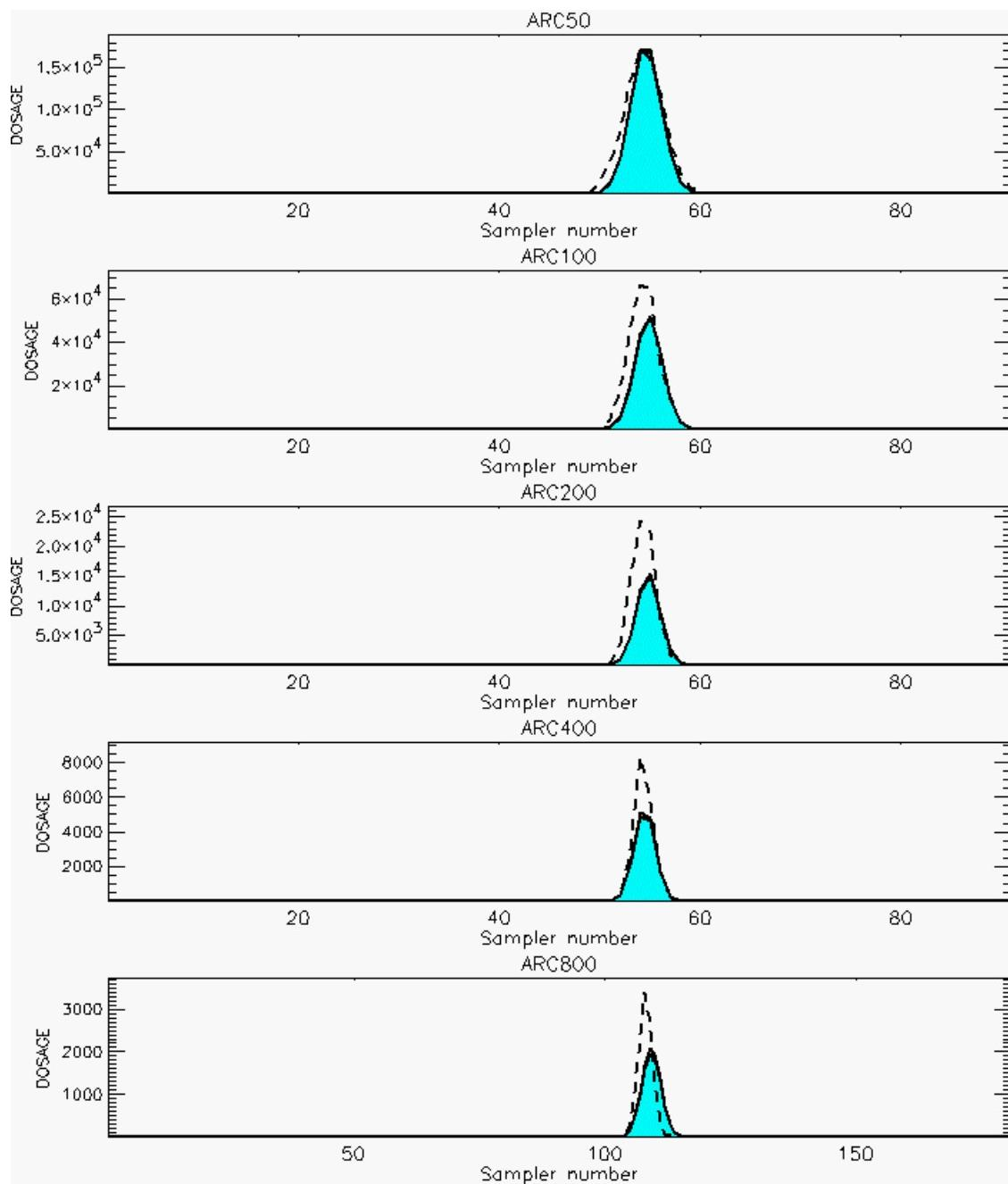
PG Prediction1 to Prediction2 Comparison

PG Trial File: pr_grass_tracer_Experiment_59.txt

PG Prediction File 1: HPAC\deposition\pg_59_vd.out

PG Prediction File 2: HPAC\nodeposition\pg_59_novd.out

**Figure F-48. HPAC With and Without SO₂ Surface Deposition Predictions to Trial 59:
Stability Category is 5**



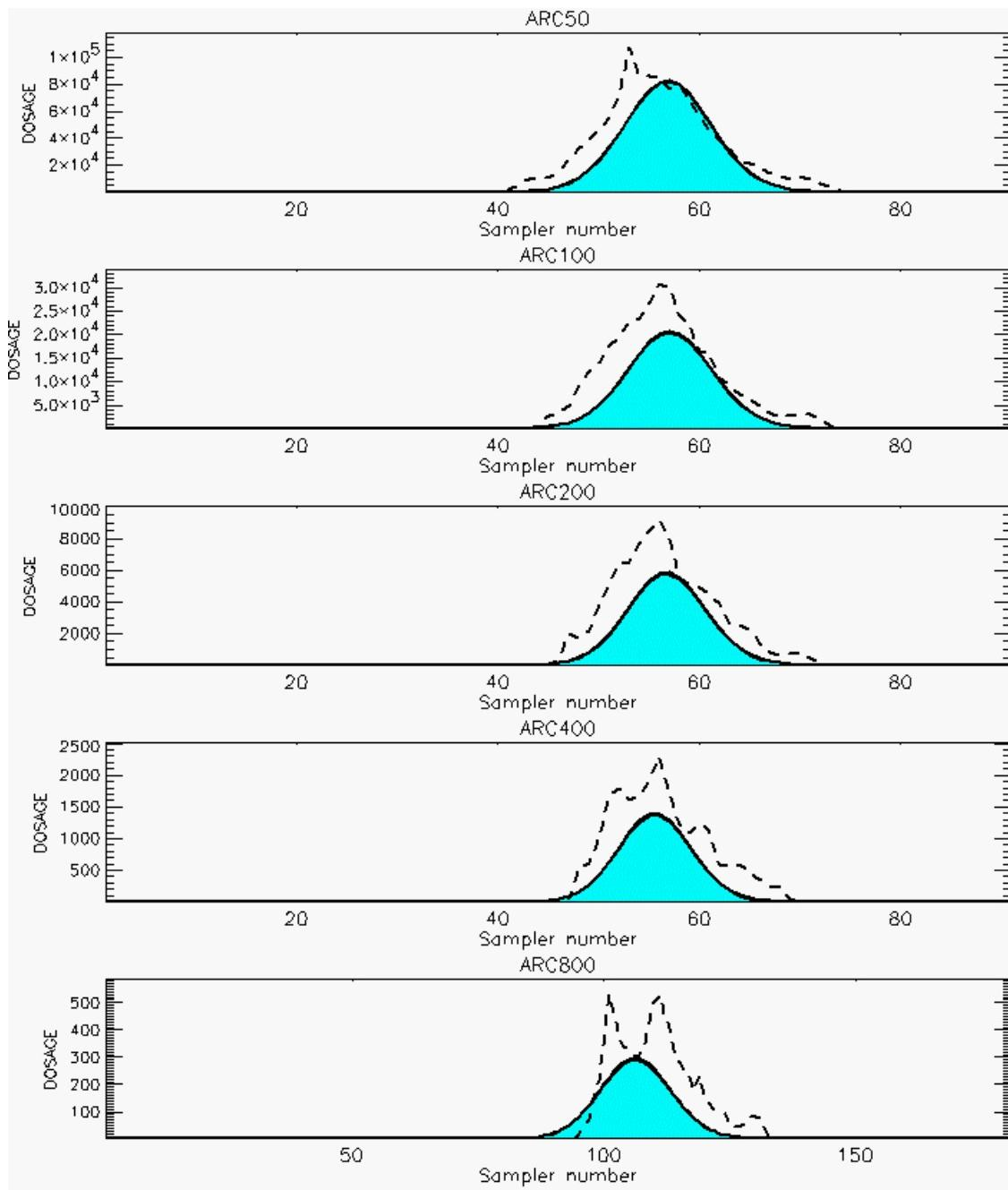
PG Prediction1 to Prediction2 Comparison

PG Trial File: pr_grass_tracer_Experiment_60.txt

PG Prediction File 1: HPAC\deposition\pg_60_vd.out

PG Prediction File 2: HPAC\nodeposition\pg_60_novd.out

**Figure F-49. HPAC With and Without SO₂ Surface Deposition Predictions to Trial 60:
Stability Category is 5**



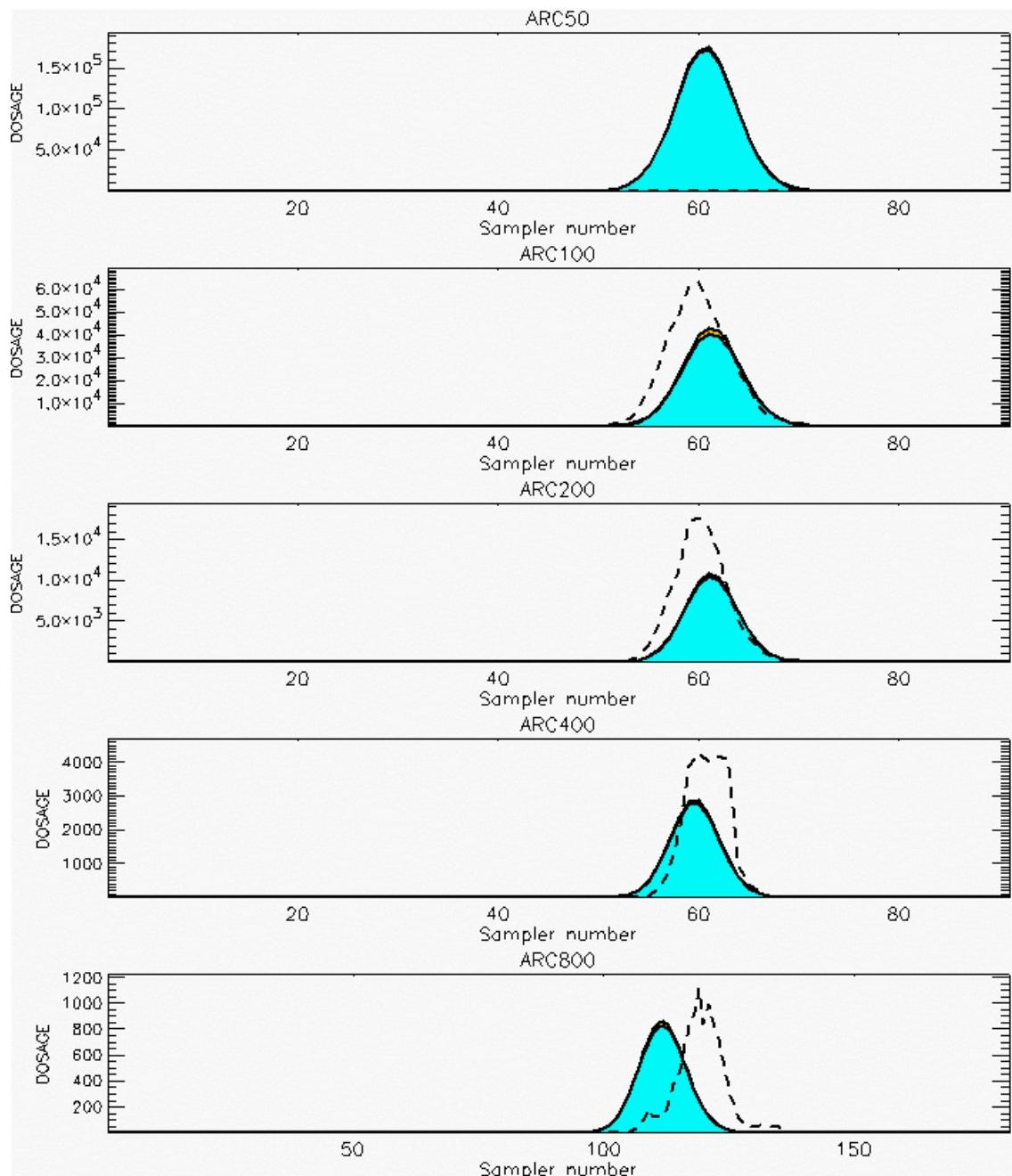
PG Prediction1 to Prediction2 Comparison

PG Trial File: pr_grass_tracer_Experiment_61.txt

PG Prediction File 1: HPAC\deposition\pg_61_vd.out

PG Prediction File 2: HPAC\nodeposition\pg_61_novd.out

**Figure F-50. HPAC With and Without SO_2 Surface Deposition Predictions to Trial 61:
Stability Category is 3**



PG Prediction1 to Prediction2 Comparison

PG Trial File: pr_grass_tracer_Experiment_62.txt

PG Prediction File 1: HPAC\deposition\pg_62_vd.out

PG Prediction File 2: HPAC\nodeposition\pg_62_novd.out

**Figure F-51. HPAC With and Without SO₂ Surface Deposition Predictions to Trial 62:
Stability Category is 2**

REFERENCES

- F-1. Barad, M. L. (Editor), *Project Prairie Grass, A Field Program in Diffusion*, Geophysical Research Papers No. 59, Volumes I and II, DTIC #AD-152572/AFCRC-TR-58-235(I), Air Geophysical Laboratory, Hanscom Air Force Base, MA, 1958.
- F-2. Irwin, J. S. and Rosu, M-R., *Comments on a Draft Practice for Statistical Evaluation of Atmospheric Dispersion Models*, Proceedings of the 10th Joint Conference on the Applications of Air Pollution Meteorology. American Meteorological Society, Boston, pp. 6-10, 1998.

APPENDIX G

**COMPARISONS OF HPAC PREDICTIONS: WITH DIFFERENT
VALUES OF DISPERSION DURING THE LIGHTEST WIND
CONDITIONS**

APPENDIX G

COMPARISONS OF HPAC PREDICTIONS: WITH DIFFERENT VALUES OF DISPERSION DURING THE LIGHTEST WIND CONDITIONS

This appendix presents graphical comparisons of HPAC predictions completed with the dispersion parameter $uu(\text{calm})$ left at the default value of 0.25 and with $uu(\text{calm})$ set to zero. Vertical plot units are dosage units of $\text{mg}\cdot\text{sec}/\text{m}^3$. Horizontal plot units are sampler numbers as presented in the *Prairie Grass* field trials [Ref. G-1]. Sampler number 1 is oriented to the west, the middle sampler (45 or 90) is oriented to the north, and the last sampler (91 or 181) is oriented to the east of the SO_2 gas release source. Only data values greater than the cutoff threshold of $3 \text{ mg}\cdot\text{sec}/\text{m}^3$ ($0.005 \text{ mg}/\text{m}^3$) are presented. This cutoff threshold value corresponds to a minimum value reported in *Prairie Grass* field trials.

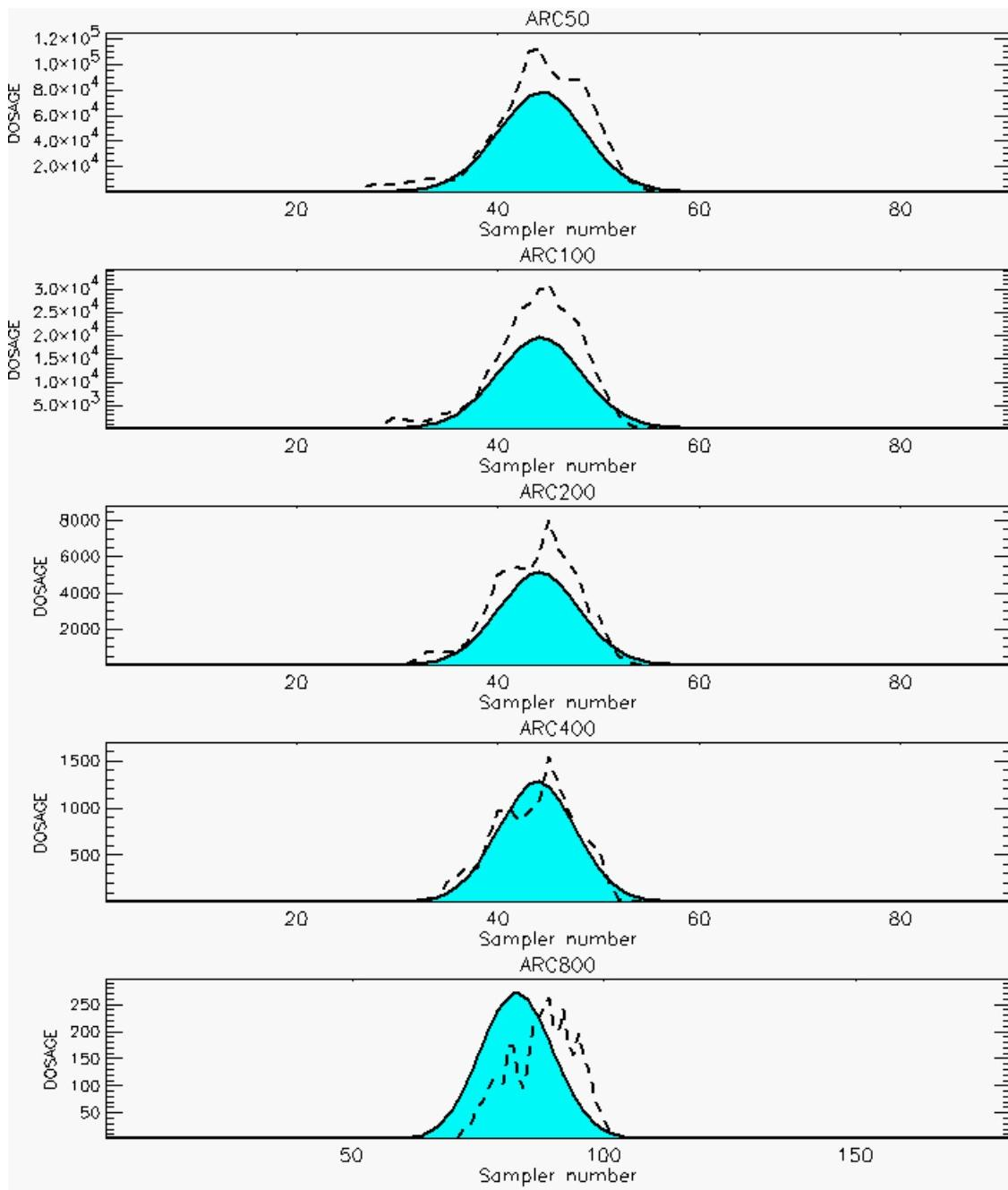
Comparisons of these predictions are presented on a linear dosage scale. Each graphical comparison consists of five plots (one for each arc) with the top plot depicting the 50-meter arc, the second plot depicting the 100-meter arc, the third plot depicting the 200-meter arc, and so on. The last panel (just above the figure caption) contains information about the data files used to produce these plots. The *Prairie Grass* field trial file name contains a two-digit number corresponding to the trial number. The prediction file name contains the moniker “nodeposition,” denoting that SO_2 surface deposition was not considered *and* that $uu(\text{calm})$ was set to zero. The prediction file name containing the moniker “novd_uucalm_0250” implies that $uu(\text{calm})$ was set to 0.250 (HPAC default value) and that surface deposition was not considered. The one- or two-digit number in the file name reflects the *Prairie Grass* field trial being predicted.

The meanings of the colors used in the plots are described below:

- Dark Blue — HPAC predictions with dosages based on $uu(\text{calm})$ set to zero that are higher than HPAC dosages with $uu(\text{calm})$ set to 0.25
- Turquoise — HPAC dosages that overlap

- Brown — HPAC predictions with dosages based on uu(calm) set to 0.250 that are higher than HPAC dosages with uu(calm) set to 0.0.

The dashed lines depict dosage values actually obtained in the field trial. Irwin stability categories that were used in our analyses are denoted in the figure captions. These stability category assignments are based on Reference G-2.



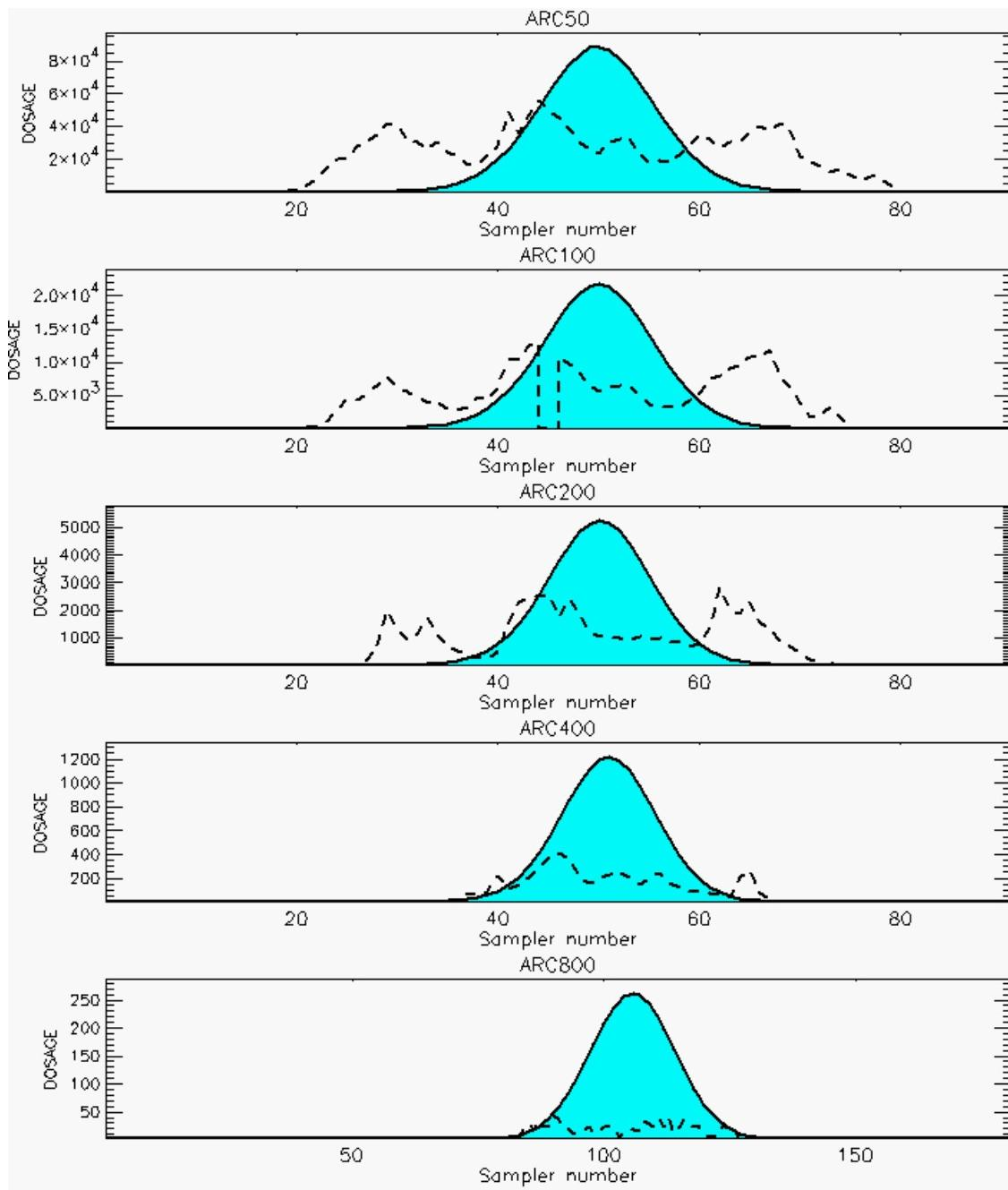
PG Prediction1 to Prediction2 Comparison

PG Trial File: pr_grass_tracer_Experiment_05.txt

PG Prediction File 1: HPAC\nodeposition\pg_5_novd.out

PG Prediction File 2: HPAC\novd_uu(calm_0250\pg_5_novd.out

**Figure G-1. HPAC With uu(calm) Set to 0.0 or 0.250 Predictions to Trial 5:
Stability Category is 2**



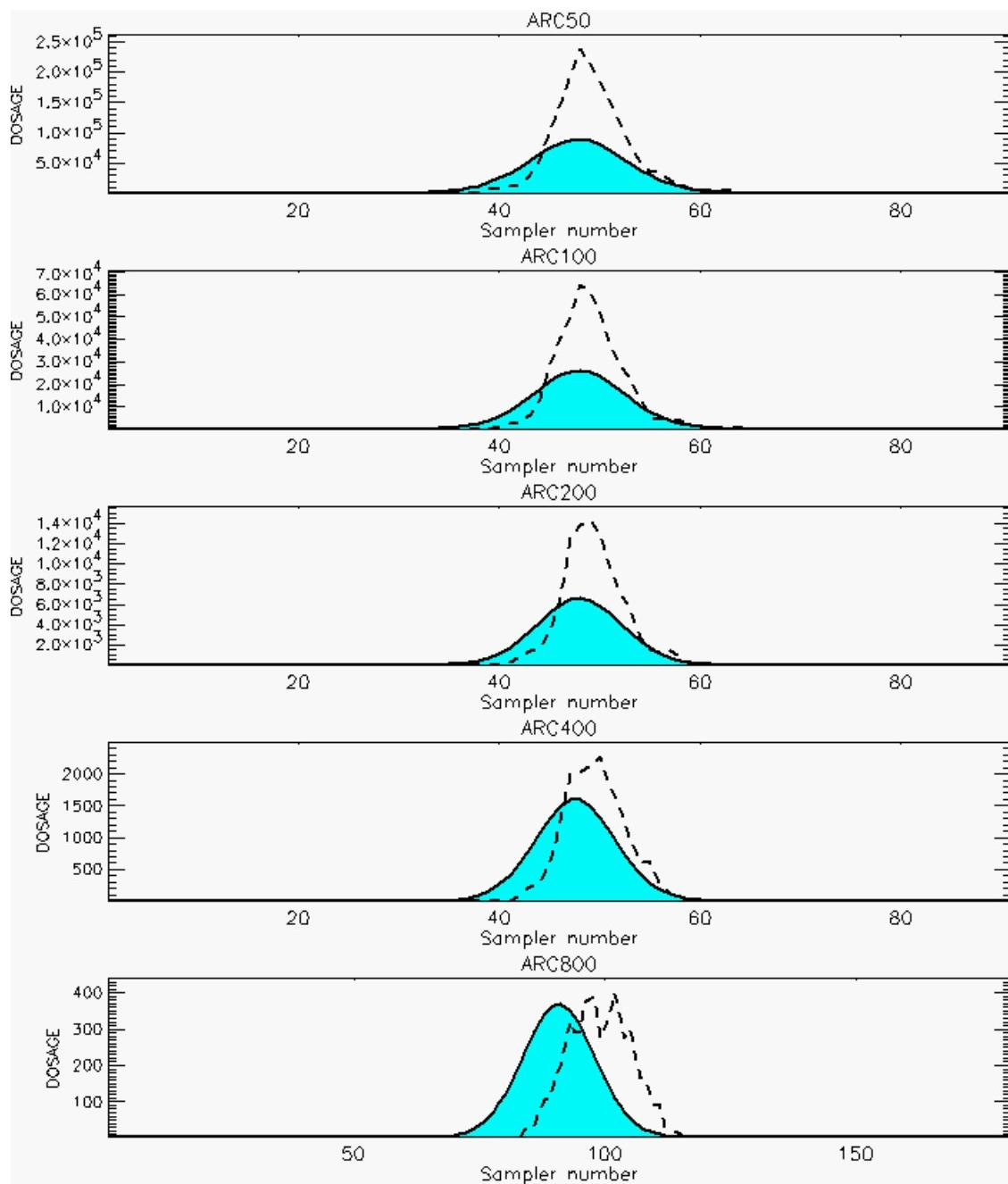
PG Prediction1 to Prediction2 Comparison

PG Trial File: pr_grass_tracer_Experiment_07.txt

PG Prediction File 1: HPAC\nodeposition\pg_7_novd.out

PG Prediction File 2: HPAC\novd_uu calm_0250\pg_7_novd.out

**Figure G-2. HPAC With uu(calm) Set to 0.0 or 0.250 Predictions to Trial 7:
Stability Category is 1**



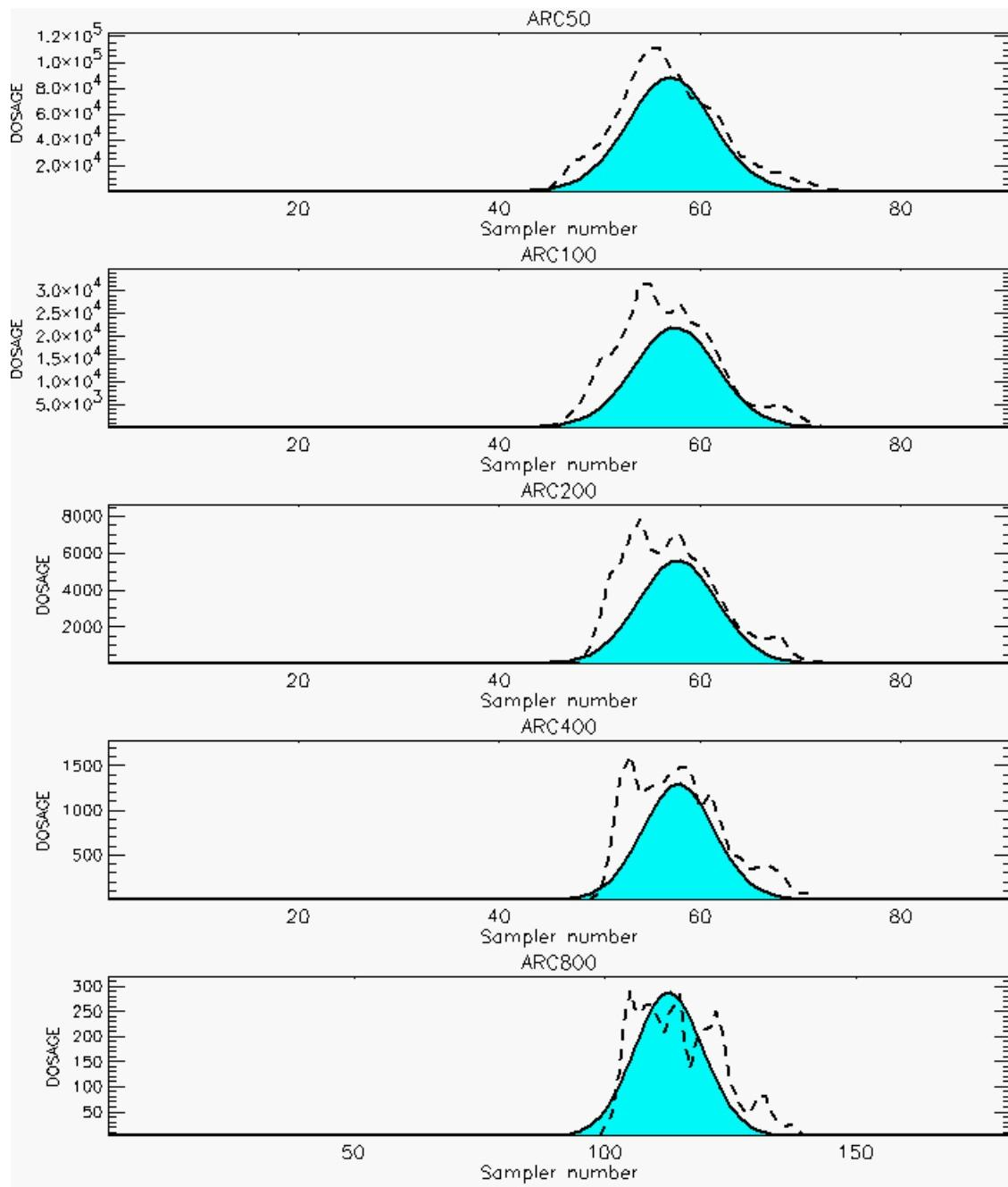
PG Prediction1 to Prediction2 Comparison

PG Trial File: pr_grass_tracer_Experiment_08.txt

PG Prediction File 1: HPAC\nodeposition\pg_8_novd.out

PG Prediction File 2: HPAC\novd_uu calm_0250\pg_8_novd.out

**Figure G-3. HPAC With uu(calm) Set to 0.0 or 0.250 Predictions to Trial 8:
Stability Category is 2**



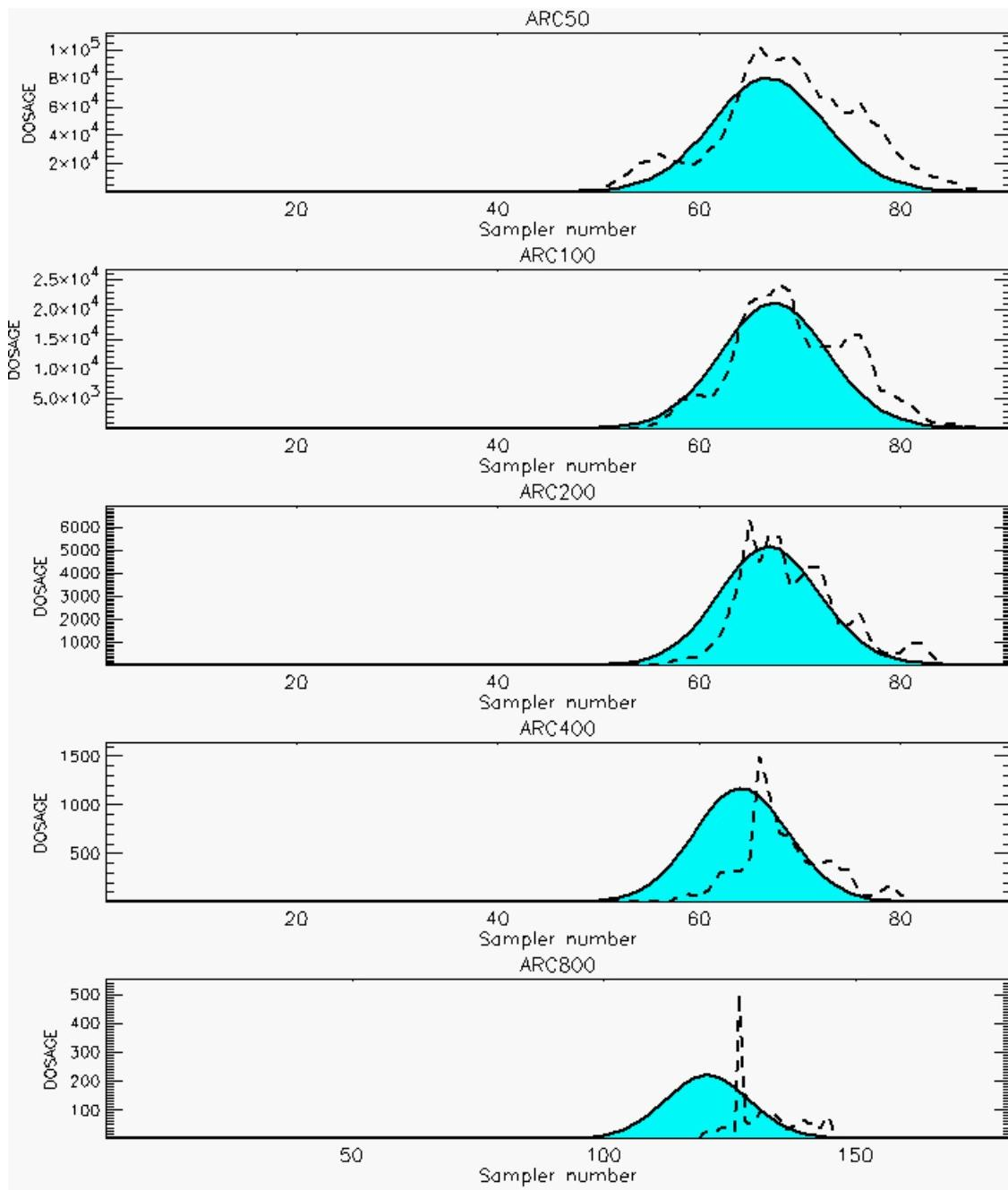
PG Prediction1 to Prediction2 Comparison

PG Trial File: pr_grass_tracer_Experiment_09.txt

PG Prediction File 1: HPAC\nodeposition\pg_9_novd.out

PG Prediction File 2: HPAC\novd_uu calm_0250\pg_9_novd.out

**Figure G-4. HPAC With uu(calm) Set to 0.0 or 0.250 Predictions to Trial 9:
Stability Category is 2**



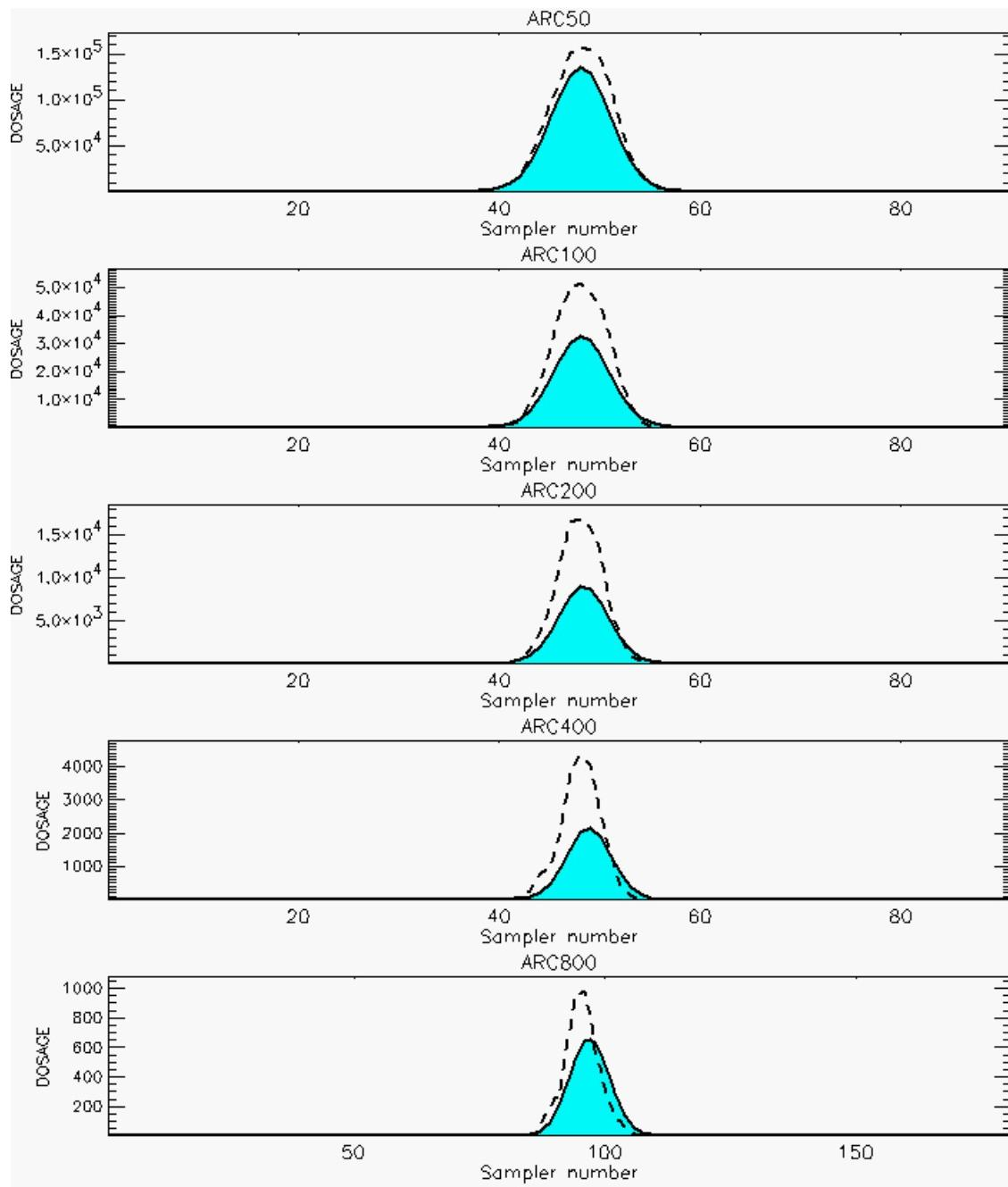
PG Prediction1 to Prediction2 Comparison

PG Trial File: pr_grass_tracer_Experiment_10.txt

PG Prediction File 1: HPAC\nodeposition\pg_10_noxd.out

PG Prediction File 2: HPAC\noxd_uu(calm)_0250\pg_10_noxd.out

**Figure G-5. HPAC With uu(calm) Set to 0.0 or 0.250 Predictions to Trial 10:
Stability Category is 1**



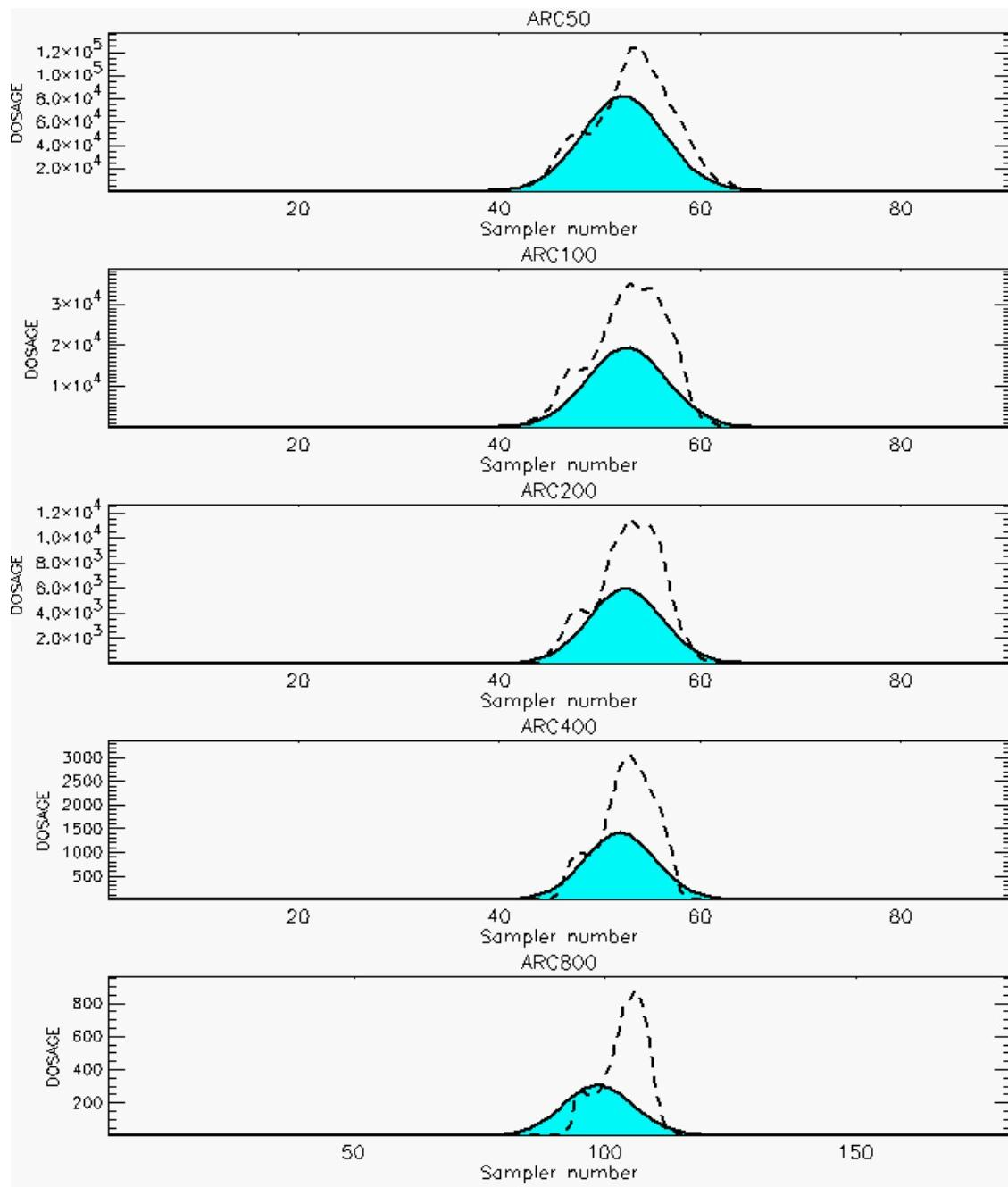
PG Prediction1 to Prediction2 Comparison

PG Trial File: pr_grass_tracer_Experiment_11.txt

PG Prediction File 1: HPAC\nodeposition\pg_11_noxd.out

PG Prediction File 2: HPAC\noxd_uu(calm)_0250\pg_11_noxd.out

**Figure G-6. HPAC With uu(calm) Set to 0.0 or 0.250 Predictions to Trial 11:
Stability Category is 3**



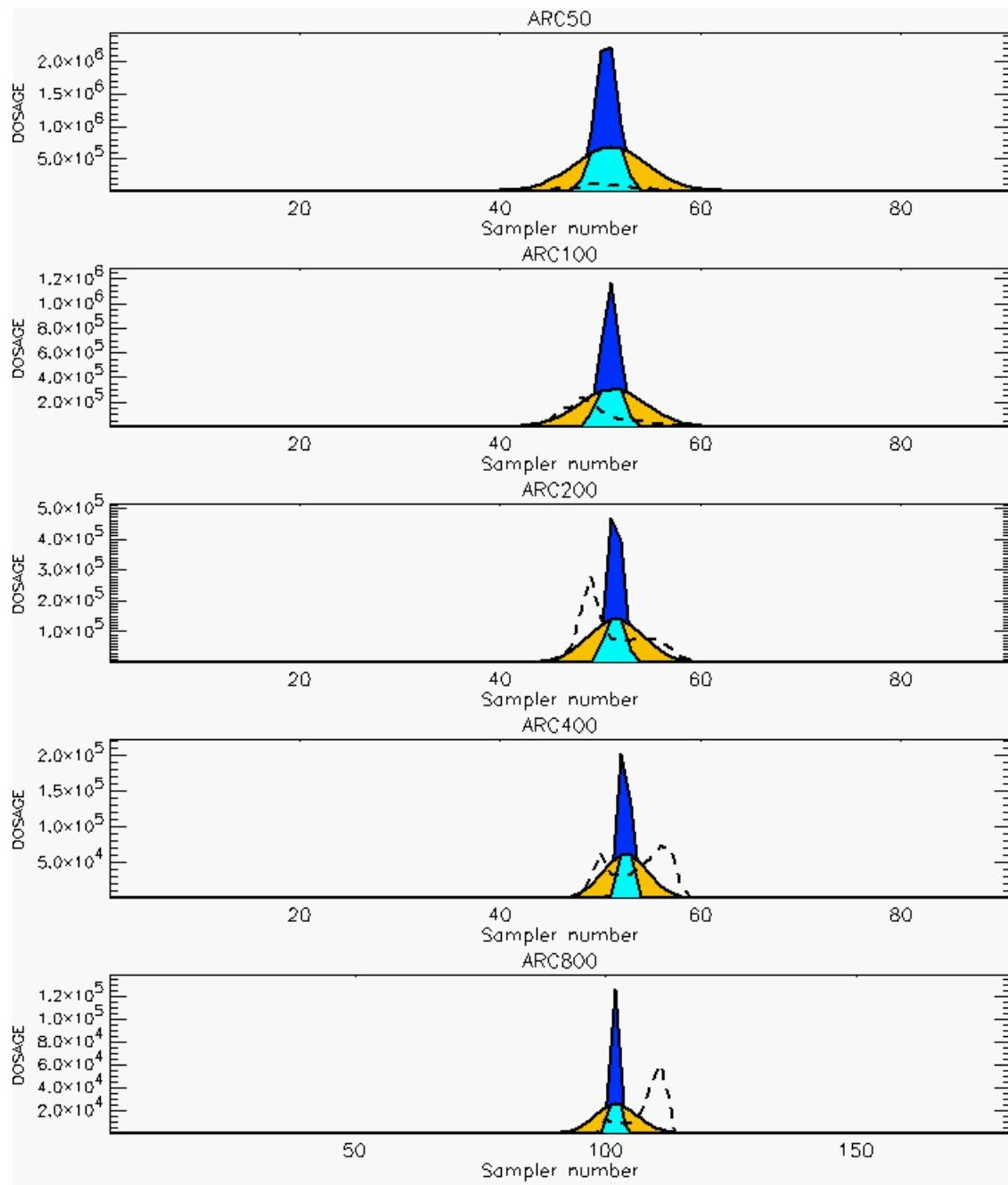
PG Prediction1 to Prediction2 Comparison

PG Trial File: pr_grass_tracer_Experiment_12.txt

PG Prediction File 1: HPAC\nodeposition\pg_12_noxd.out

PG Prediction File 2: HPAC\noxd_uu(calm)_0250\pg_12_noxd.out

**Figure G-7. HPAC With uu(calm) Set to 0.0 or 0.250 Predictions to Trial 12:
Stability Category is 3**



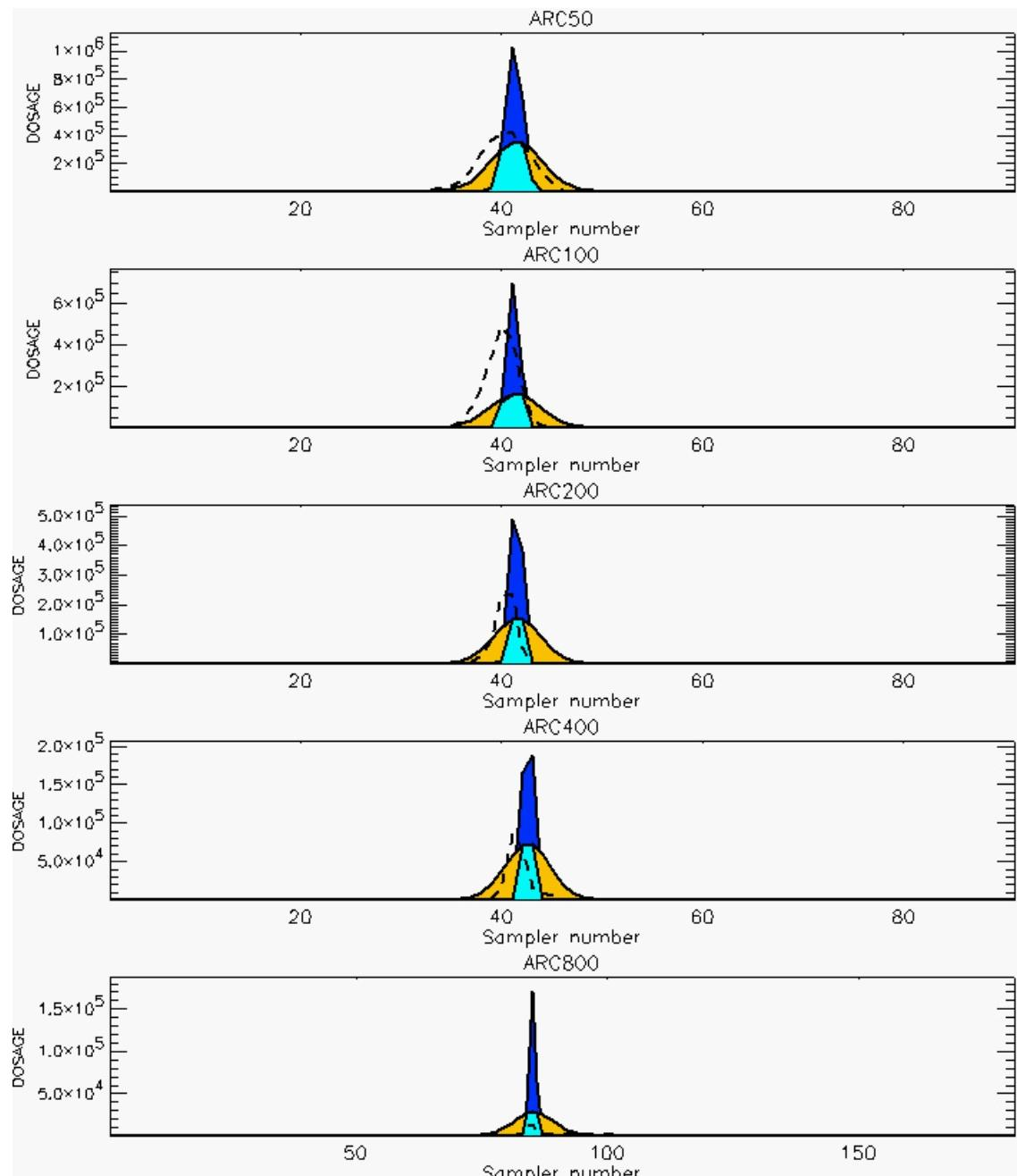
PG Prediction1 to Prediction2 Comparison

PG Trial File: pr_grass_tracer_Experiment_13.txt

PG Prediction File 1: HPAC\nodeposition\pg_13_noxd.out

PG Prediction File 2: HPAC\noxd_uu(calm)_0250\pg_13_noxd.out

**Figure G-8. HPAC With uu(calm) Set to 0.0 or 0.250 Predictions to Trial 13:
Stability Category is 7**



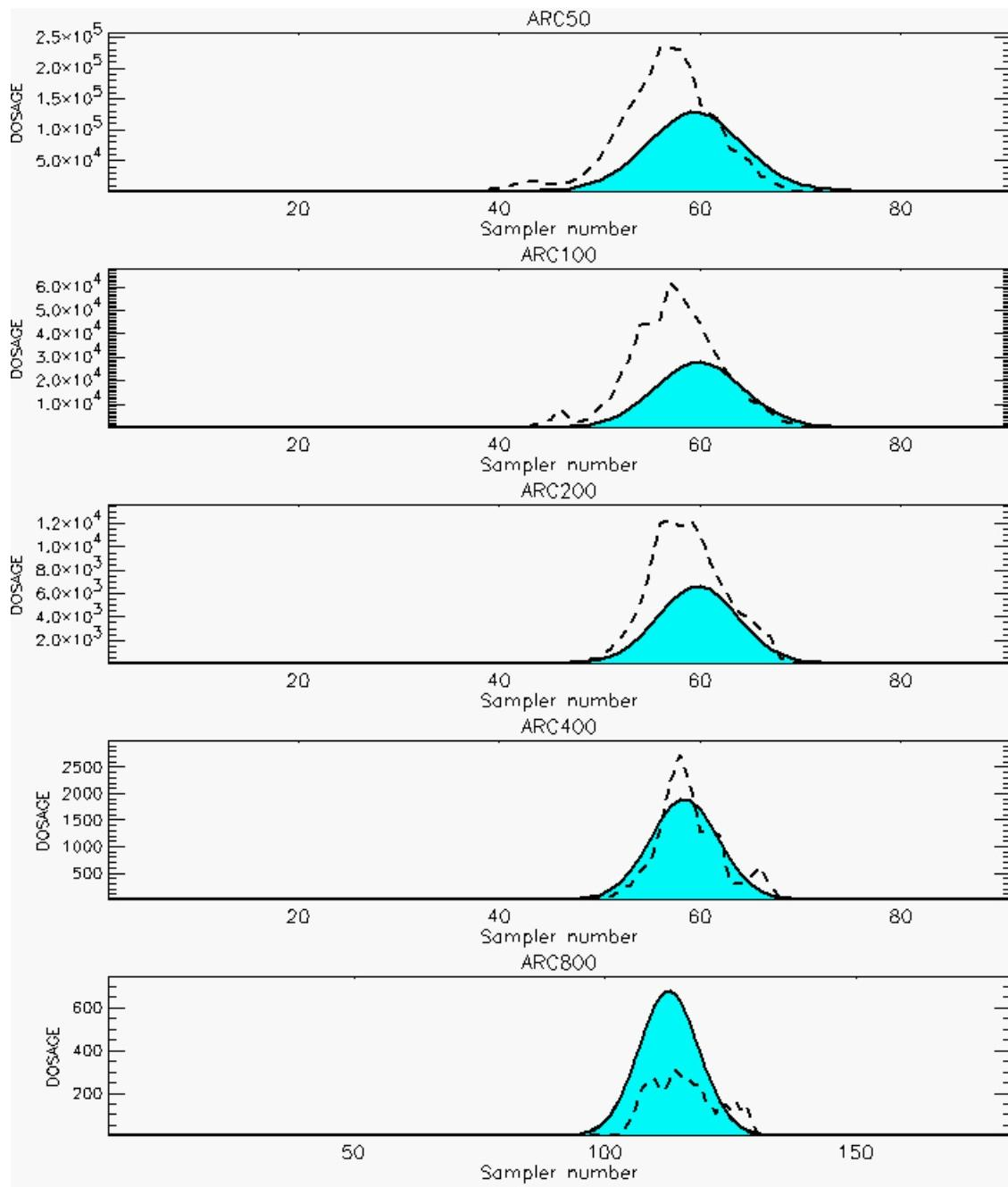
PG Prediction1 to Prediction2 Comparison

PG Trial File: pr_grass_tracer_Experiment_14.txt

PG Prediction File 1: HPAC\nodeposition\pg_14_nozd.out

PG Prediction File 2: HPAC\nozd_uu(calm)_0250\pg_14_nozd.out

**Figure G-9. HPAC With uu(calm) Set to 0.0 or 0.250 Predictions to Trial 14:
Stability Category is 7**



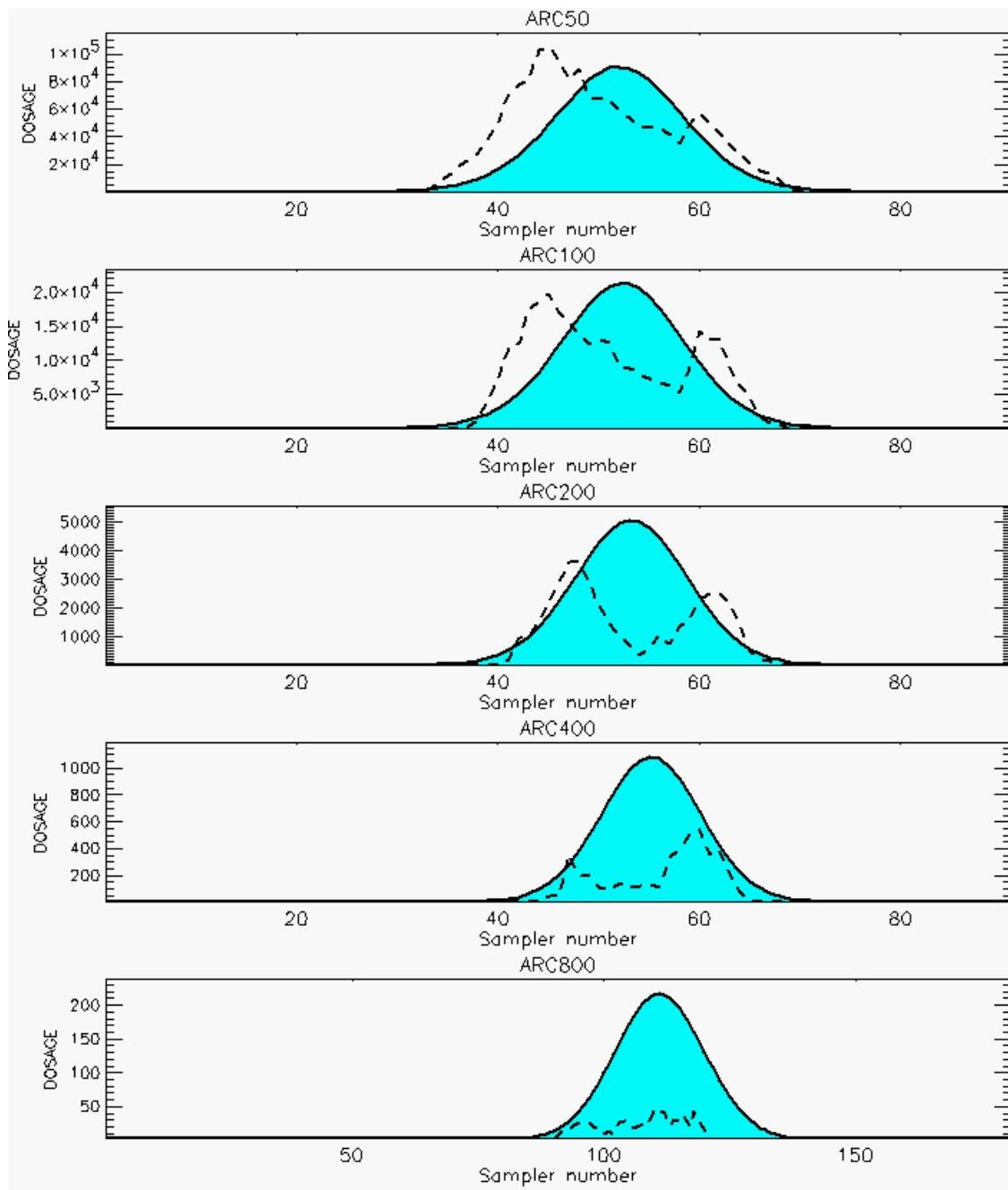
PG Prediction1 to Prediction2 Comparison

PG Trial File: pr_grass_tracer_Experiment_15.txt

PG Prediction File 1: HPAC\nodeposition\pg_15_noxd.out

PG Prediction File 2: HPAC\noxd_uu calm_0250\pg_15_noxd.out

**Figure G-10. HPAC With uu(calm) Set to 0.0 or 0.250 Predictions to Trial 15:
Stability Category is 1**



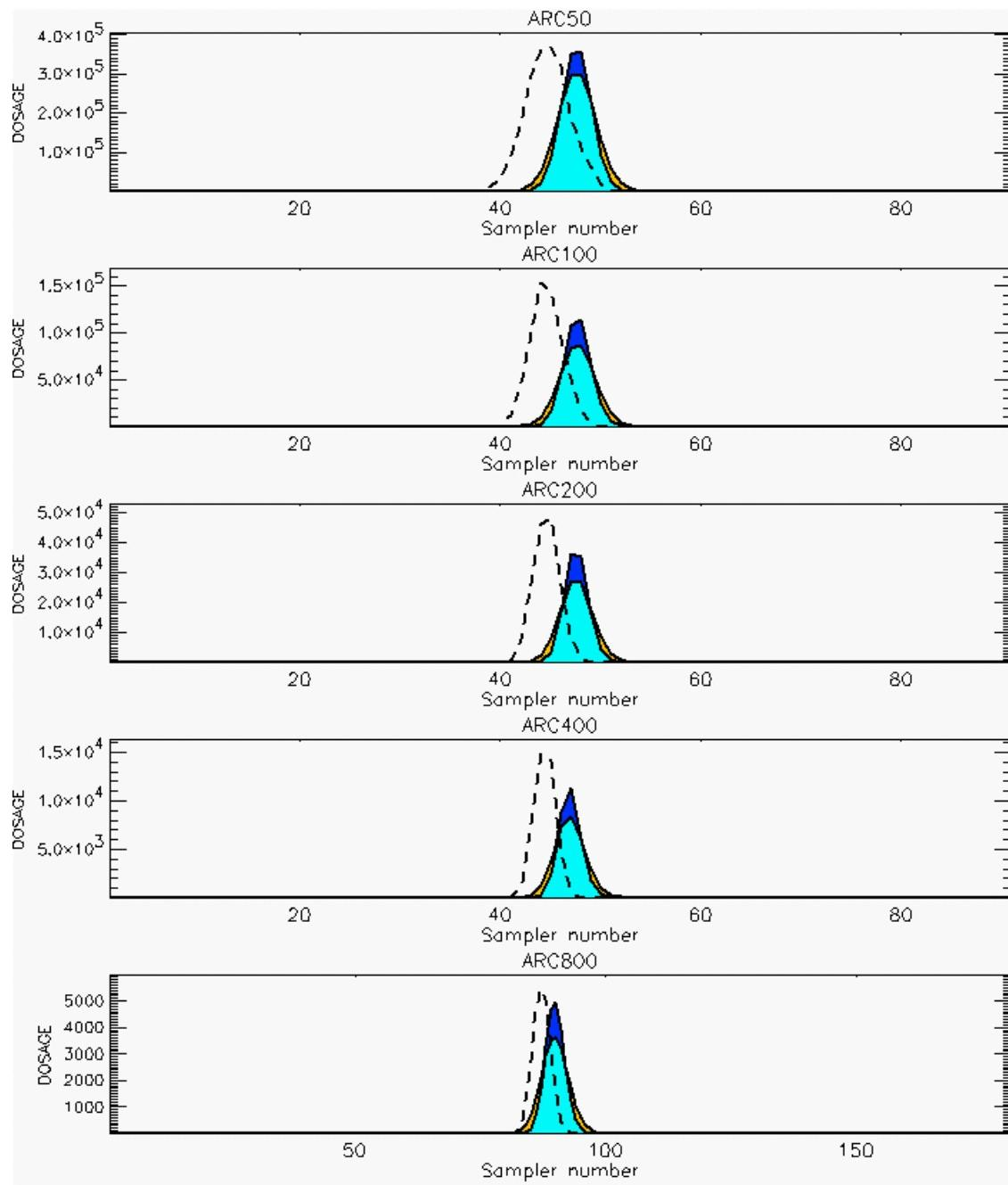
PG Prediction1 to Prediction2 Comparison

PG Trial File: pr_grass_tracer_Experiment_16.txt

PG Prediction File 1: HPAC\nodeposition\pg_16_noxd.out

PG Prediction File 2: HPAC\noxd_uu(calm)_0250\pg_16_noxd.out

**Figure G-11. HPAC With uu(calm) Set to 0.0 or 0.250 Predictions to Trial 16:
Stability Category is 1**



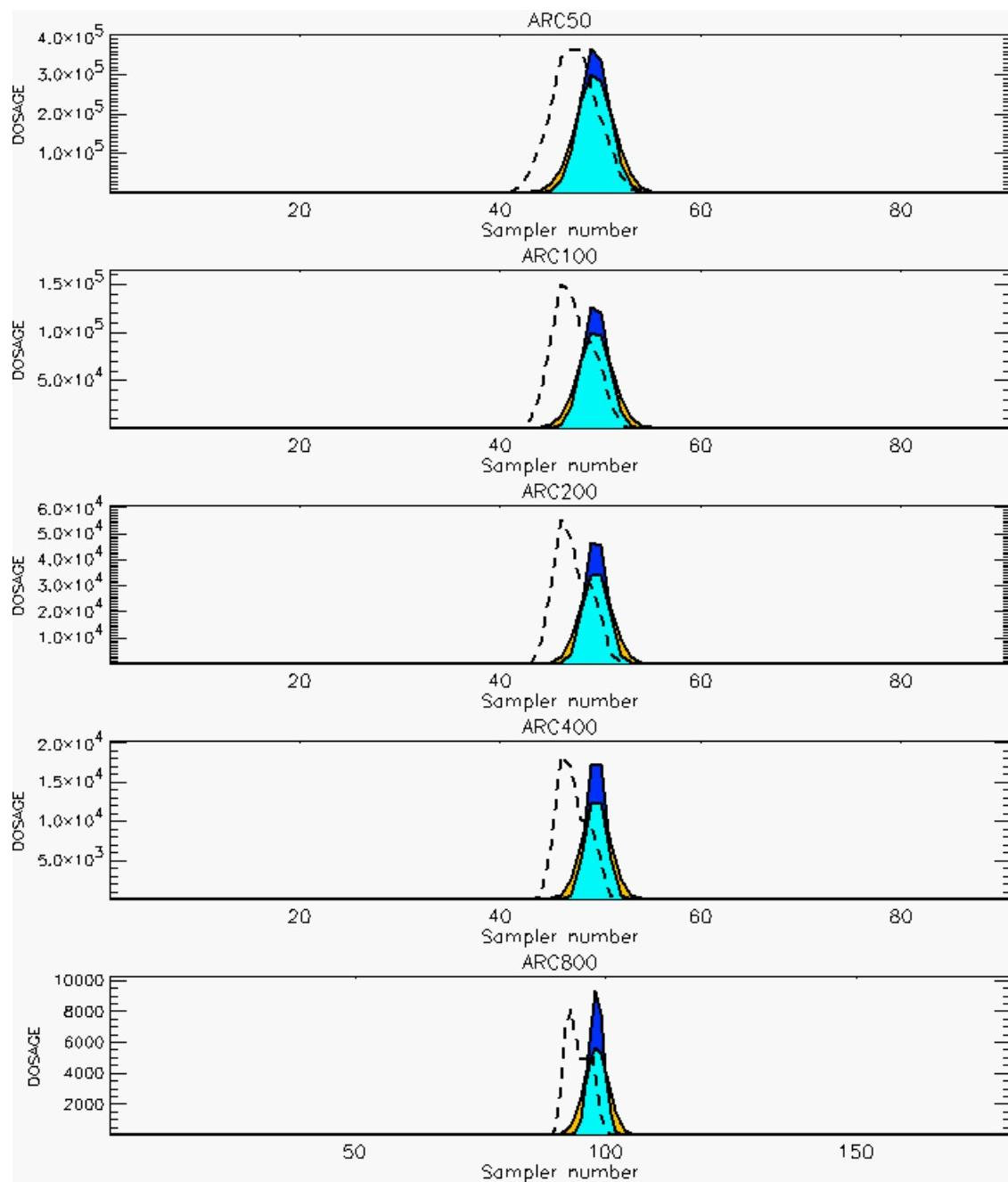
PG Prediction1 to Prediction2 Comparison

PG Trial File: pr_grass_tracer_Experiment_17.txt

PG Prediction File 1: HPAC\nodeposition\pg_17_noxd.out

PG Prediction File 2: HPAC\noxd_uu calm_0250\pg_17_noxd.out

**Figure G-12. HPAC With uu(calm) Set to 0.0 or 0.250 Predictions to Trial 17:
Stability Category is 5**



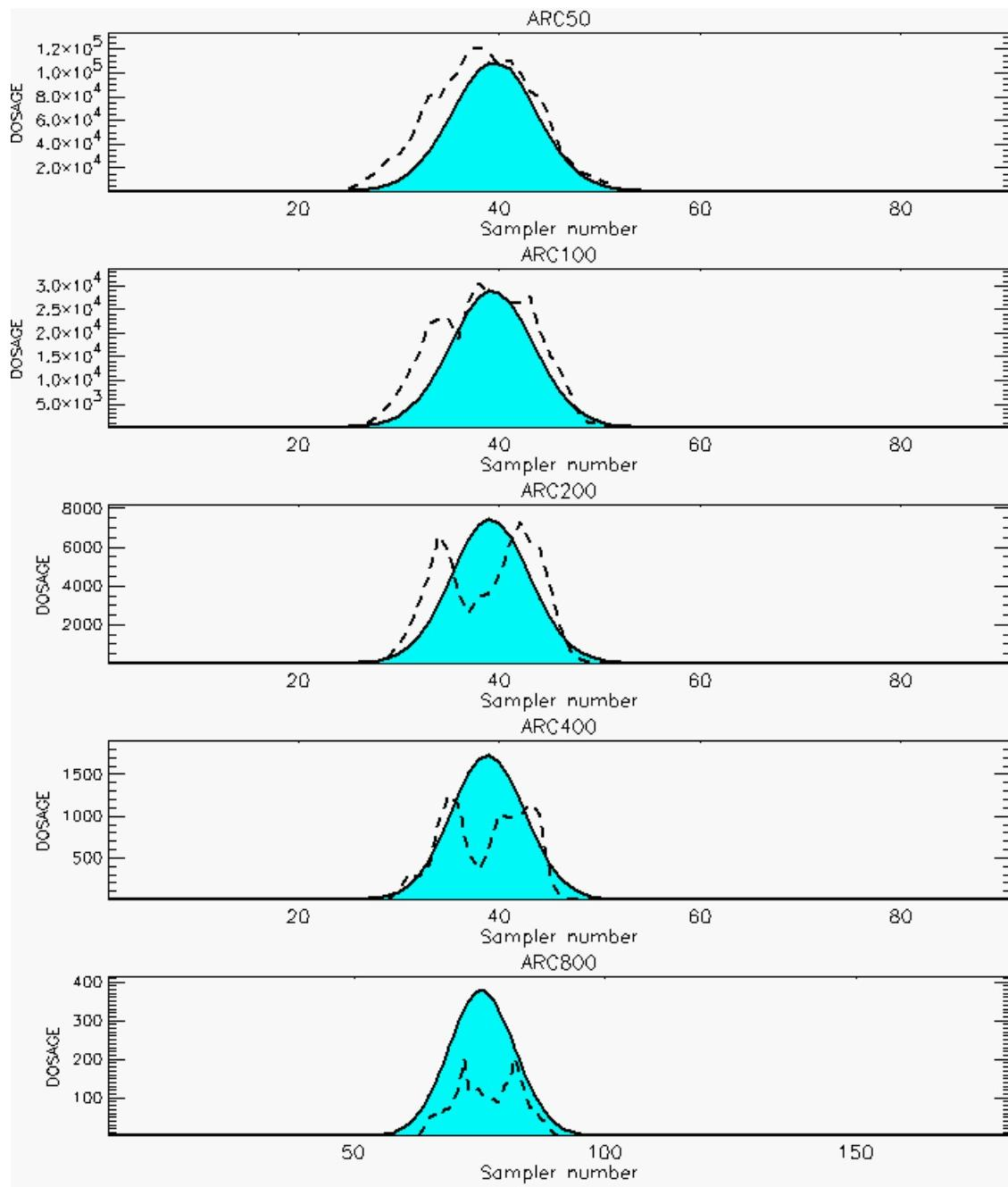
PG Prediction1 to Prediction2 Comparison

PG Trial File: pr_grass_tracer_Experiment_18.txt

PG Prediction File 1: HPAC\nodeposition\pg_18_noxd.out

PG Prediction File 2: HPAC\noxd_uu_calm_0250\pg_18_noxd.out

**Figure G-13. HPAC With uu(calm) Set to 0.0 or 0.250 Predictions to Trial 18:
Stability Category is 5**



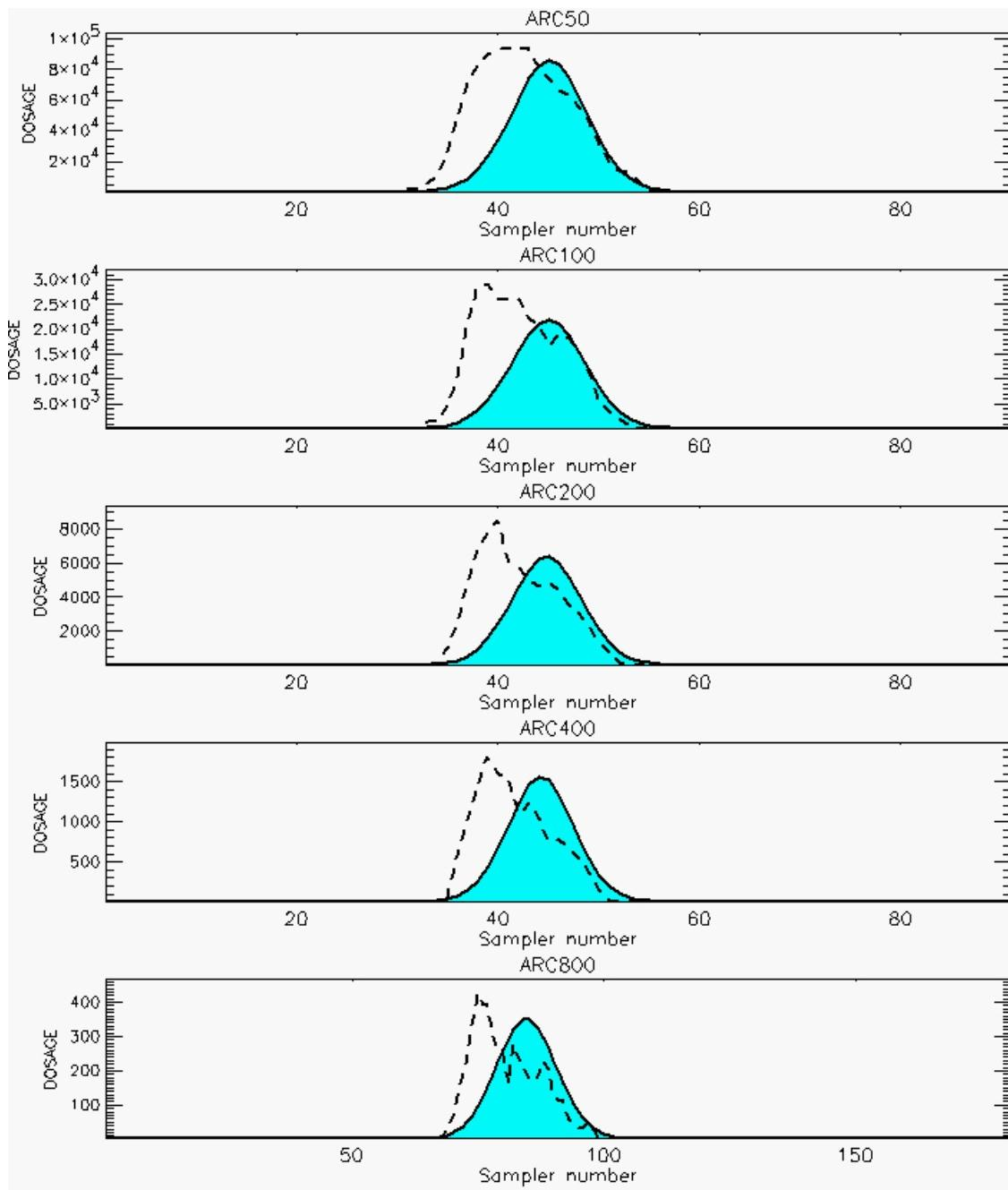
PG Prediction1 to Prediction2 Comparison

PG Trial File: pr_grass_tracer_Experiment_19.txt

PG Prediction File 1: HPAC\nodeposition\pg_19_nozd.out

PG Prediction File 2: HPAC\nozd_uu_calm_0250\pg_19_nozd.out

**Figure G-14. HPAC With uu(calm) Set to 0.0 or 0.250 Predictions to Trial 19:
Stability Category is 2**



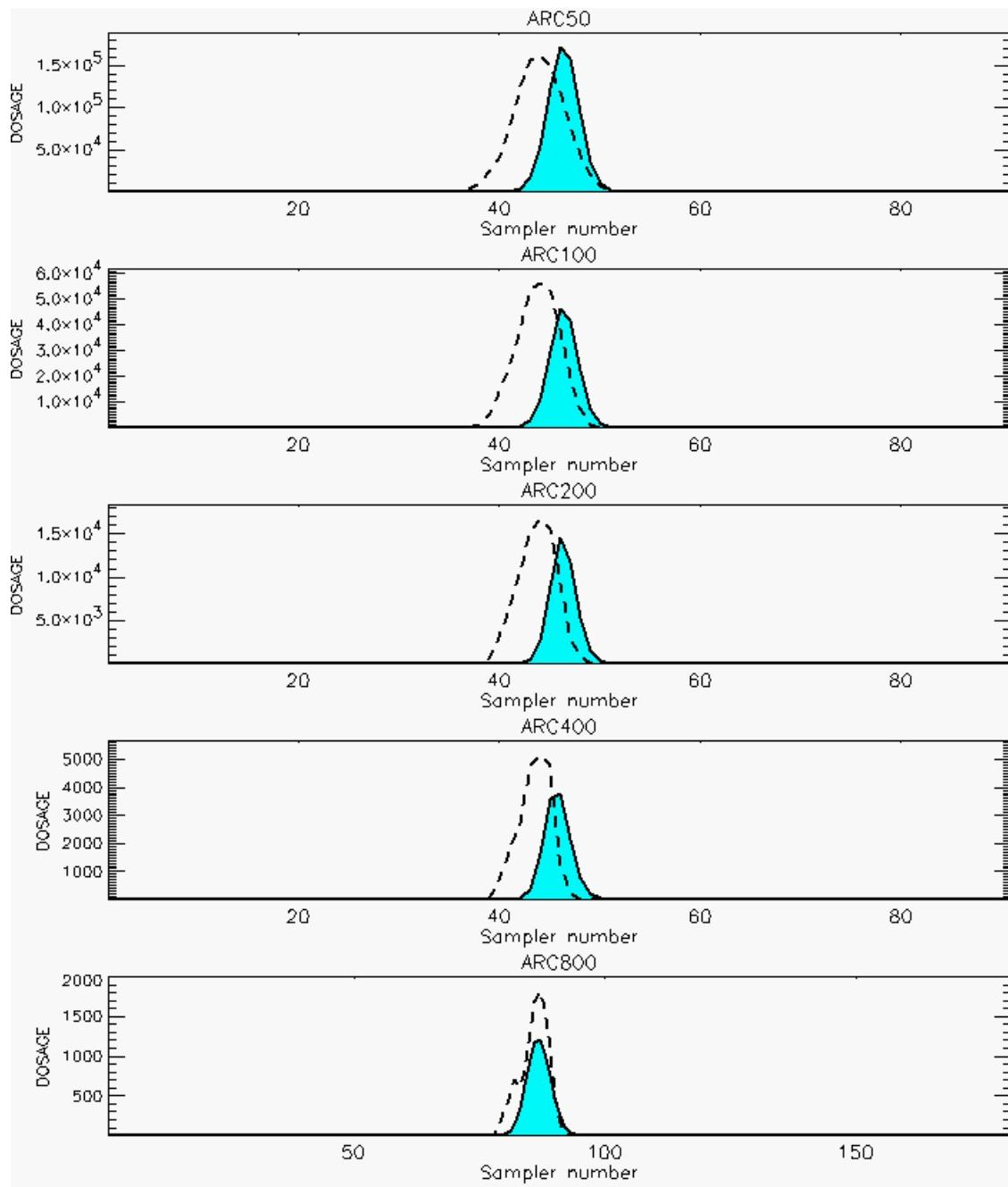
PG Prediction1 to Prediction2 Comparison

PG Trial File: pr_grass_tracer_Experiment_20.txt

PG Prediction File 1: HPAC\nodeposition\pg_20_noxd.out

PG Prediction File 2: HPAC\noxd_uu(calm)_0250\pg_20_noxd.out

**Figure G-15. HPAC With uu(calm) Set to 0.0 or 0.250 Predictions to Trial 20:
Stability Category is 3**



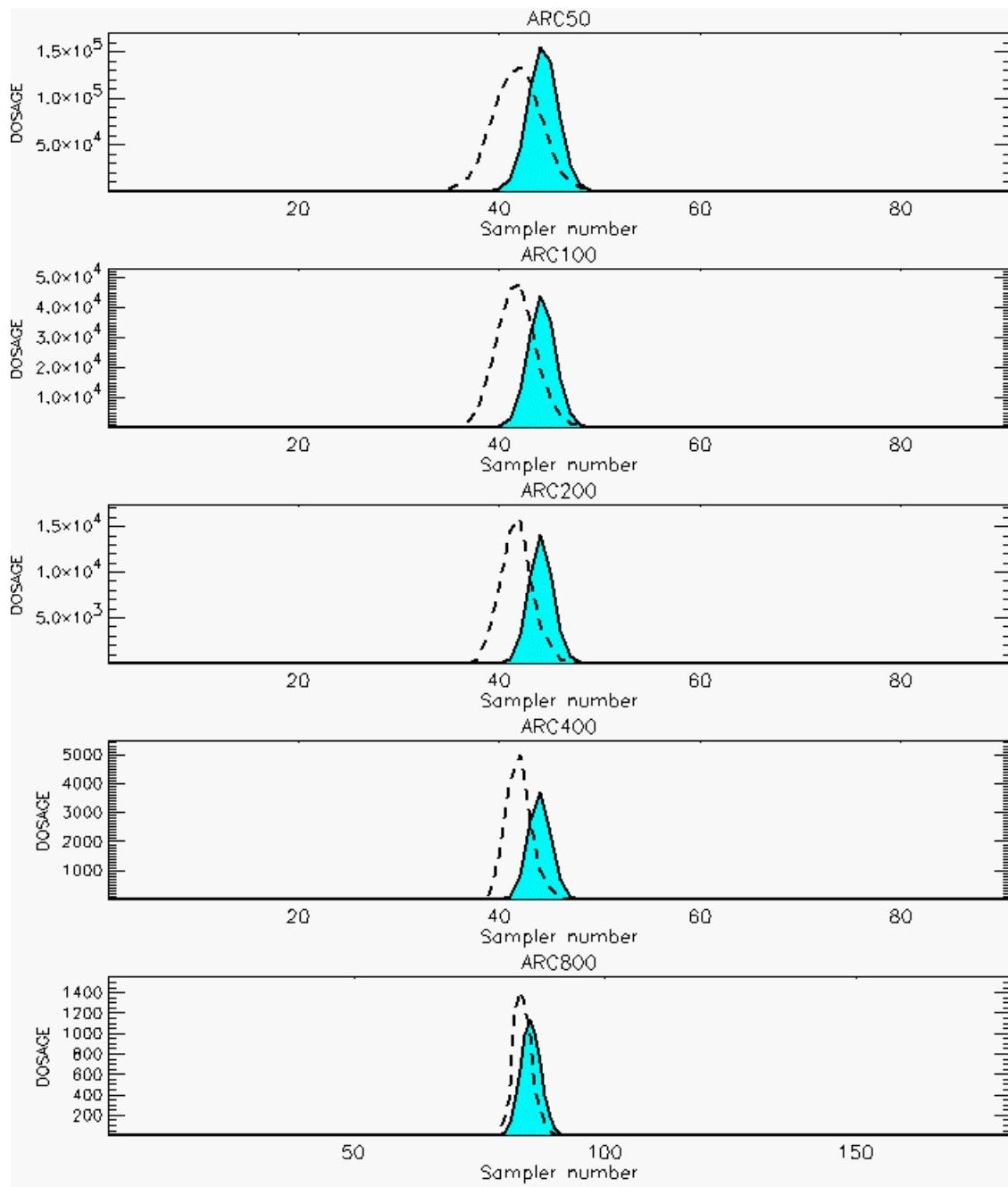
PG Prediction1 to Prediction2 Comparison

PG Trial File: pr_grass_tracer_Experiment_21.txt

PG Prediction File 1: HPAC\nodeposition\pg_21_nozd.out

PG Prediction File 2: HPAC\nozd_uu_calm_0250\pg_21_nozd.out

**Figure G-16. HPAC With uu(calm) Set to 0.0 or 0.250 Predictions to Trial 21:
Stability Category is 4**



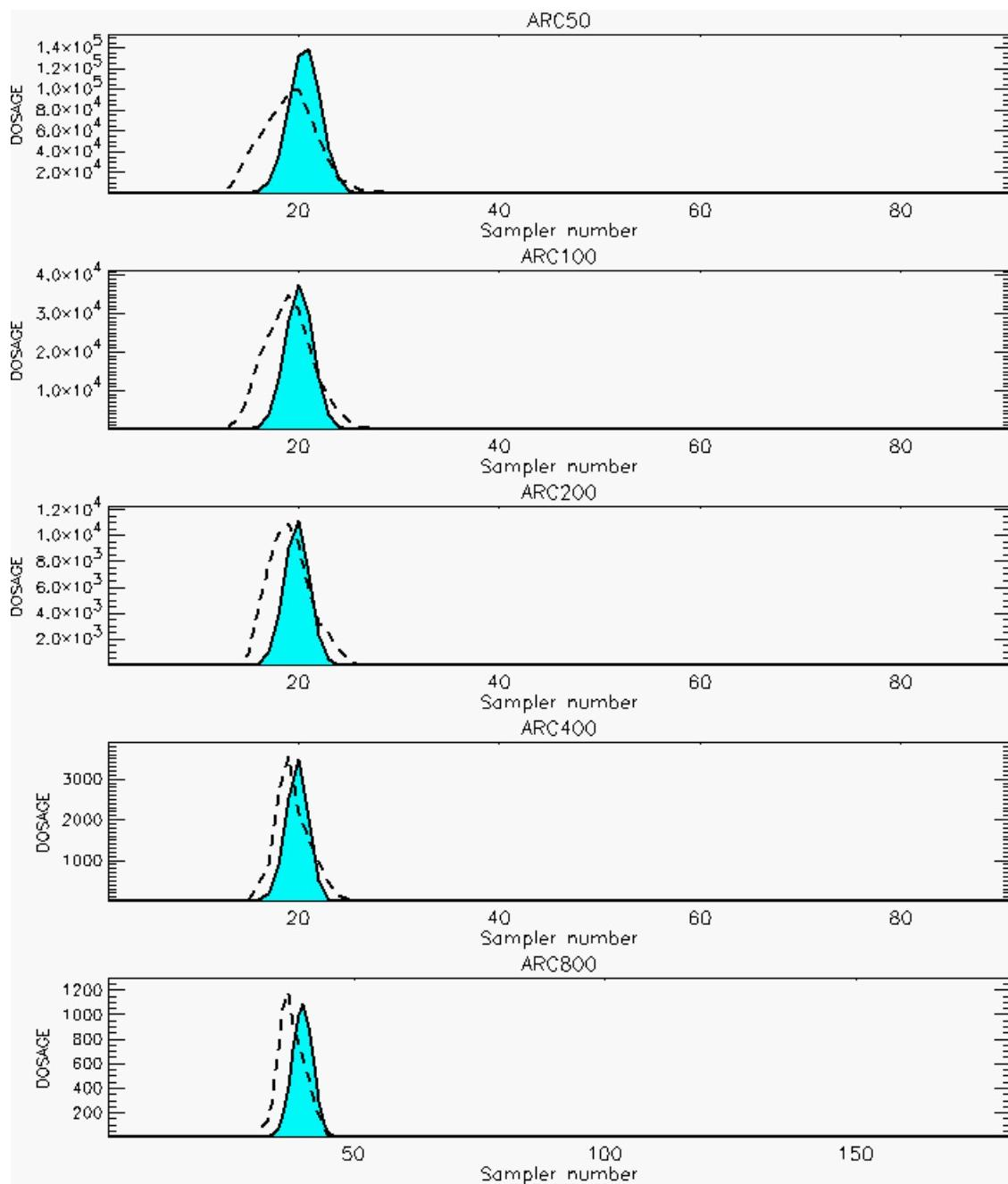
PG Prediction1 to Prediction2 Comparison

PG Trial File: pr_grass_tracer_Experiment_22.txt

PG Prediction File 1: HPAC\nodeposition\pg_22_nozd.out

PG Prediction File 2: HPAC\nozd_uu calm_0250\pg_22_nozd.out

**Figure G-17. HPAC With uu(calm) Set to 0.0 or 0.250 Predictions to Trial 22:
Stability Category is 4**



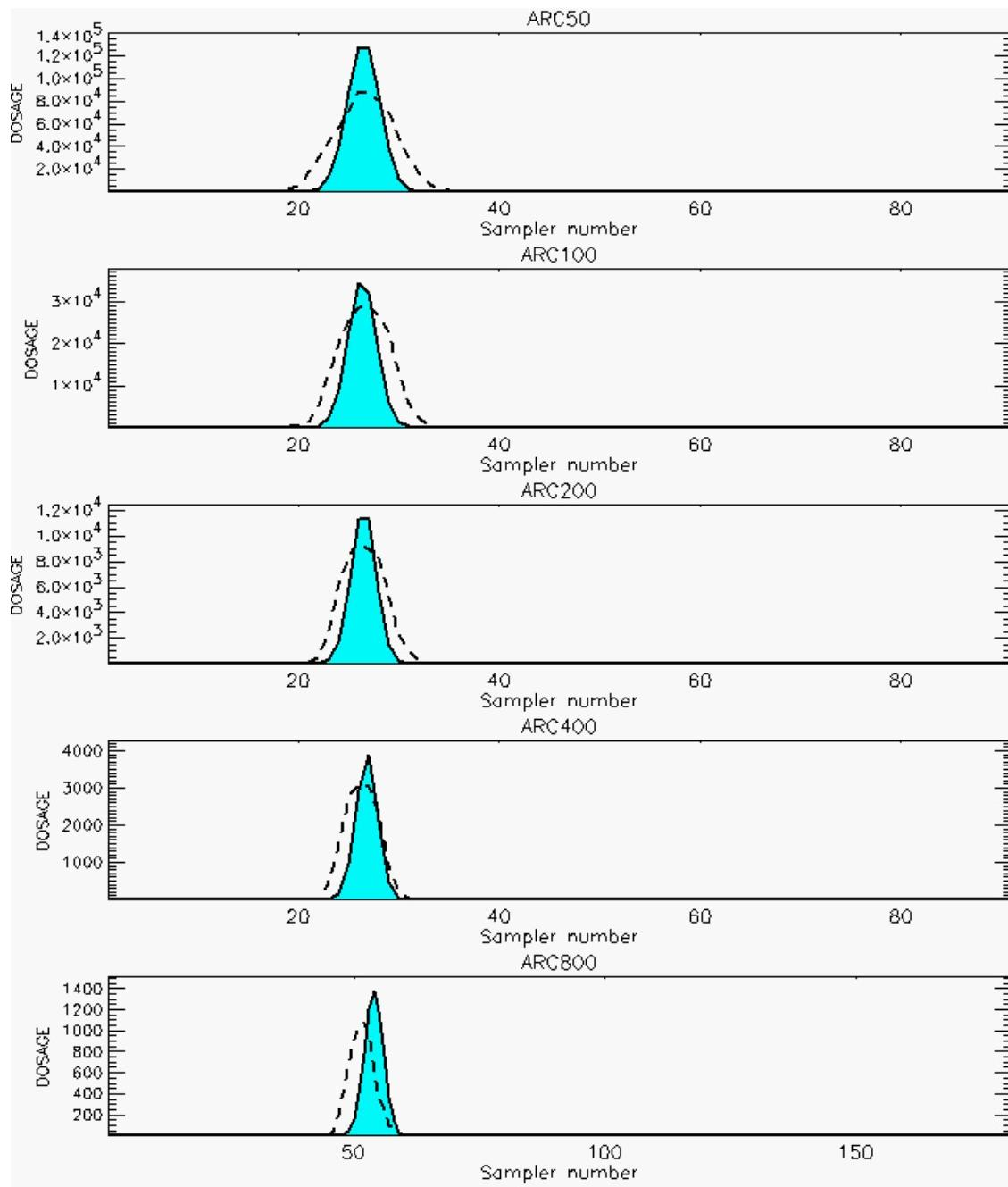
PG Prediction1 to Prediction2 Comparison

PG Trial File: pr_grass_tracer_Experiment_23.txt

PG Prediction File 1: HPAC\nodeposition\pg_23_novd.out

PG Prediction File 2: HPAC\novd_uu(calm)_0250\pg_23_novd.out

**Figure G-18. HPAC With uu(calm) Set to 0.0 or 0.250 Predictions to Trial 23:
Stability Category is 4**



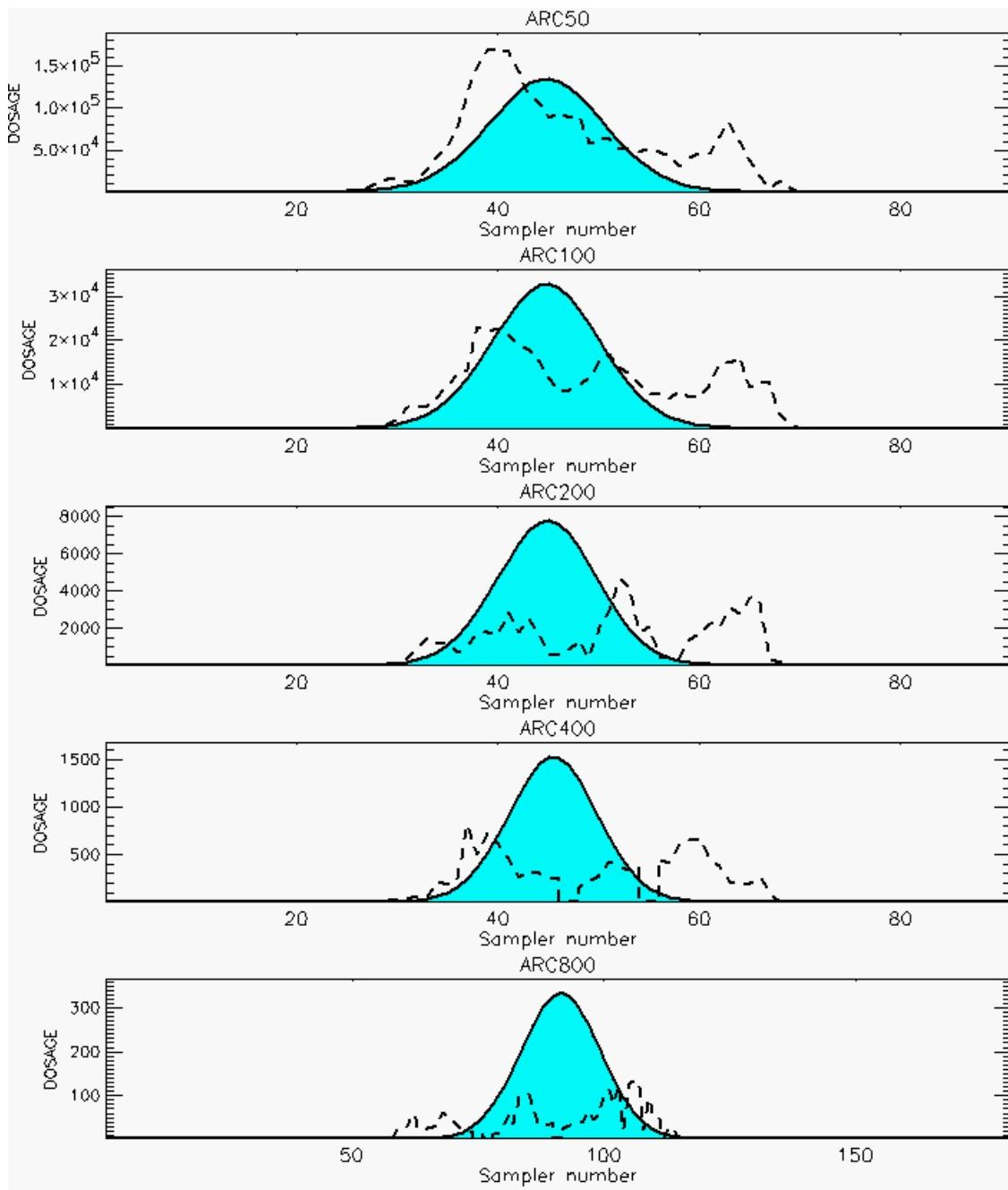
PG Prediction1 to Prediction2 Comparison

PG Trial File: pr_grass_tracer_Experiment_24.txt

PG Prediction File 1: HPAC\nodeposition\pg_24_noxd.out

PG Prediction File 2: HPAC\noxd_uu(calm)_0250\pg_24_noxd.out

**Figure G-19. HPAC With uu(calm) Set to 0.0 or 0.250 Predictions to Trial 24:
Stability Category is 4**



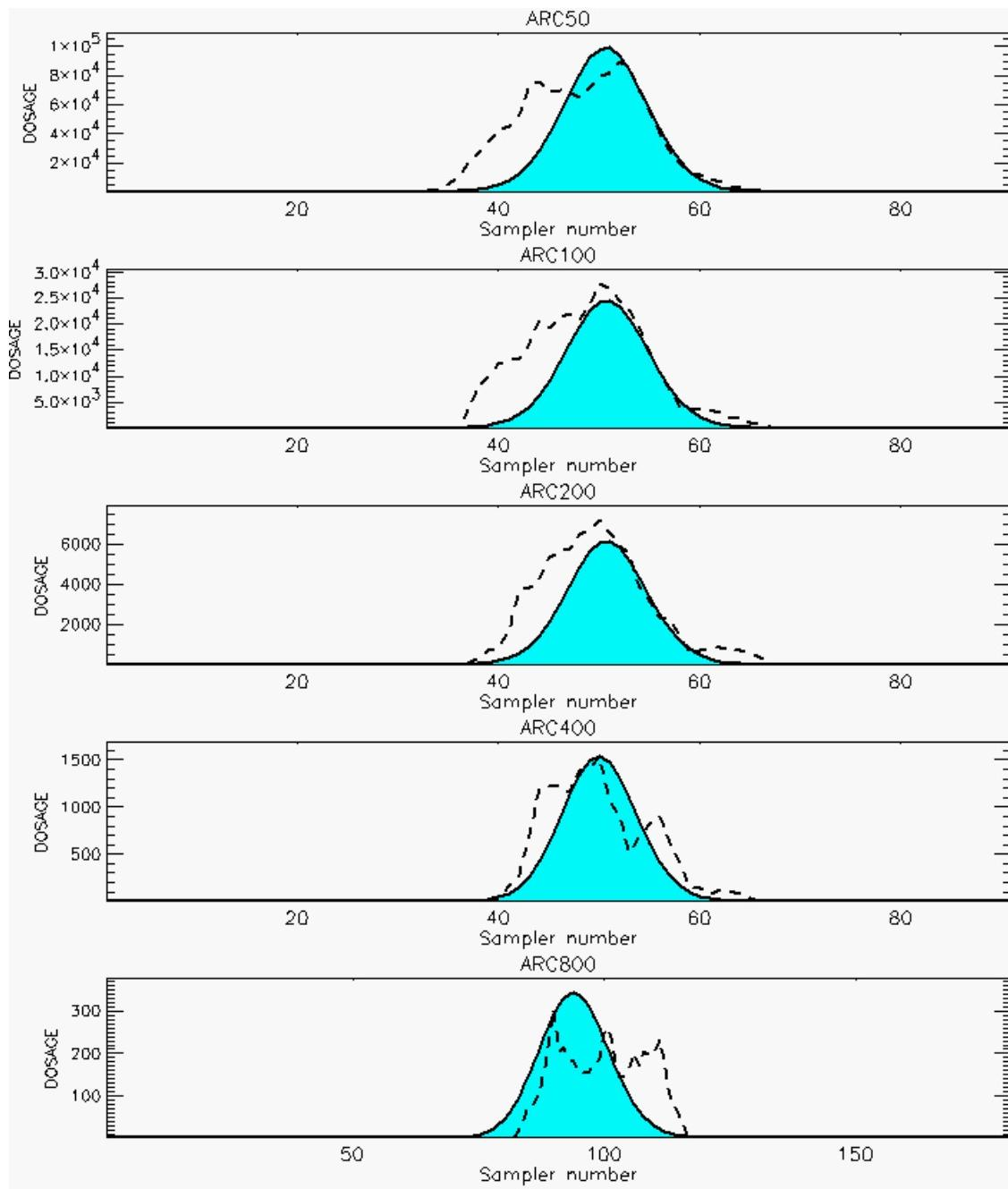
PG Prediction1 to Prediction2 Comparison

PG Trial File: pr_grass_tracer_Experiment_25.txt

PG Prediction File 1: HPAC\nodeposition\pg_25_nozd.out

PG Prediction File 2: HPAC\nozd_uu(calm_0250\pg_25_nozd.out

**Figure G-20. HPAC With uu(calm) Set to 0.0 or 0.250 Predictions to Trial 25:
Stability Category is 1**



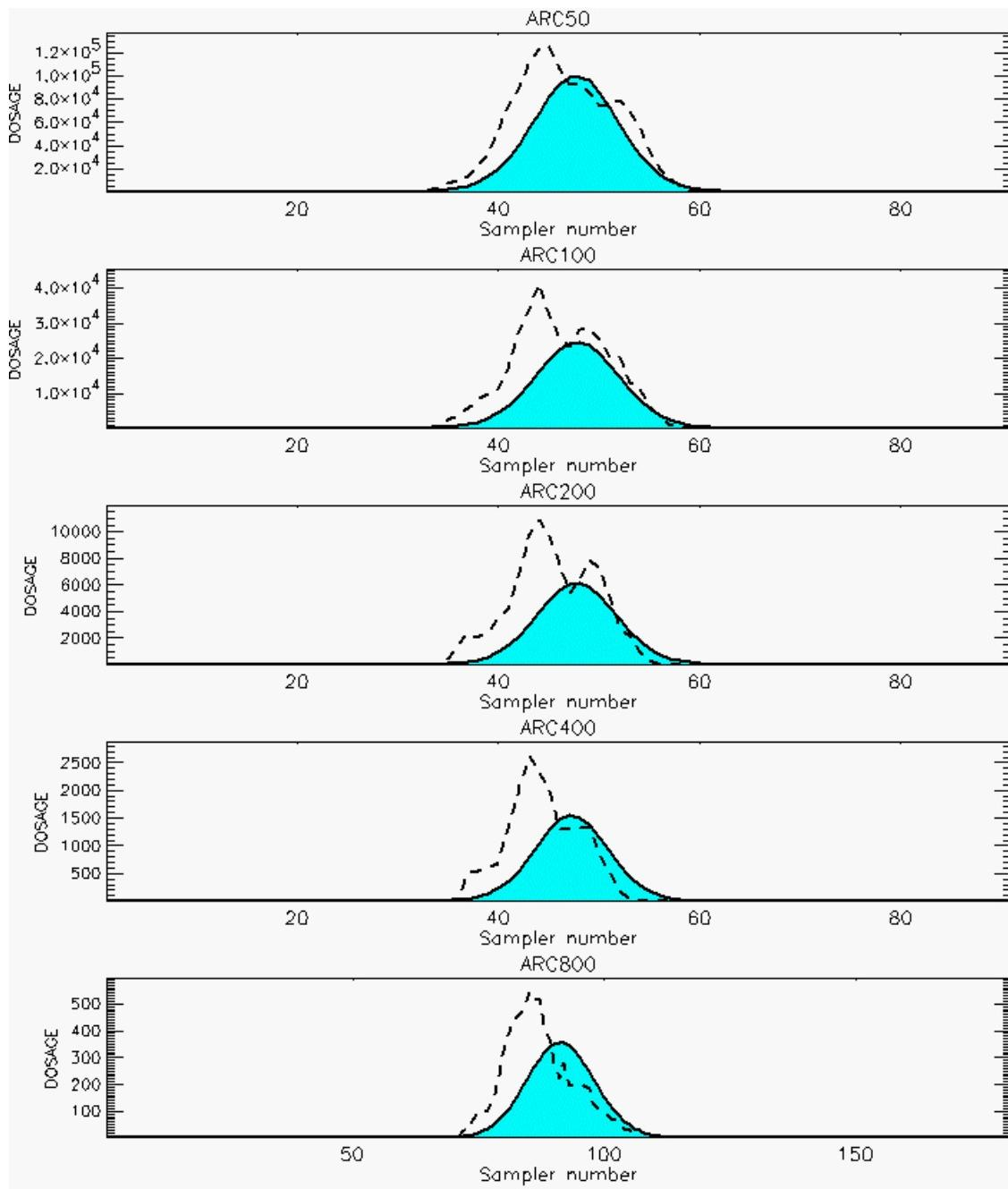
PG Prediction1 to Prediction2 Comparison

PG Trial File: pr_grass_tracer_Experiment_26.txt

PG Prediction File 1: HPAC\nodeposition\pg_26_nozd.out

PG Prediction File 2: HPAC\nozd_uu(calm_0250\pg_26_nozd.out

**Figure G-21. HPAC With uu(calm) Set to 0.0 or 0.250 Predictions to Trial 26:
Stability Category is 2**



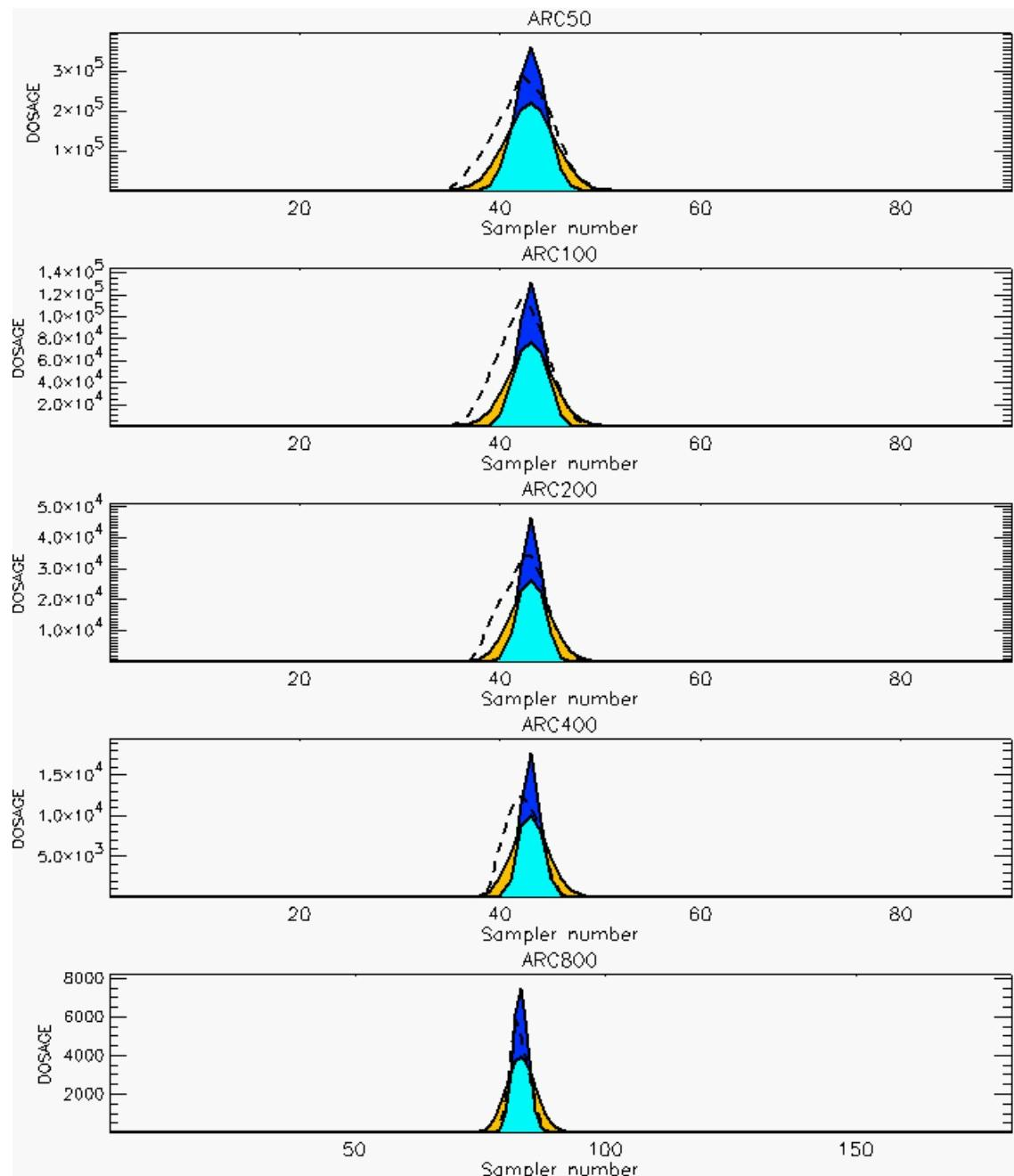
PG Prediction1 to Prediction2 Comparison

PG Trial File: pr_grass_tracer_Experiment_27.txt

PG Prediction File 1: HPAC\nodeposition\pg_27_noxd.out

PG Prediction File 2: HPAC\noxd_uu calm_0250\pg_27_noxd.out

**Figure G-22. HPAC With uu(calm) Set to 0.0 or 0.250 Predictions to Trial 27:
Stability Category is 2**



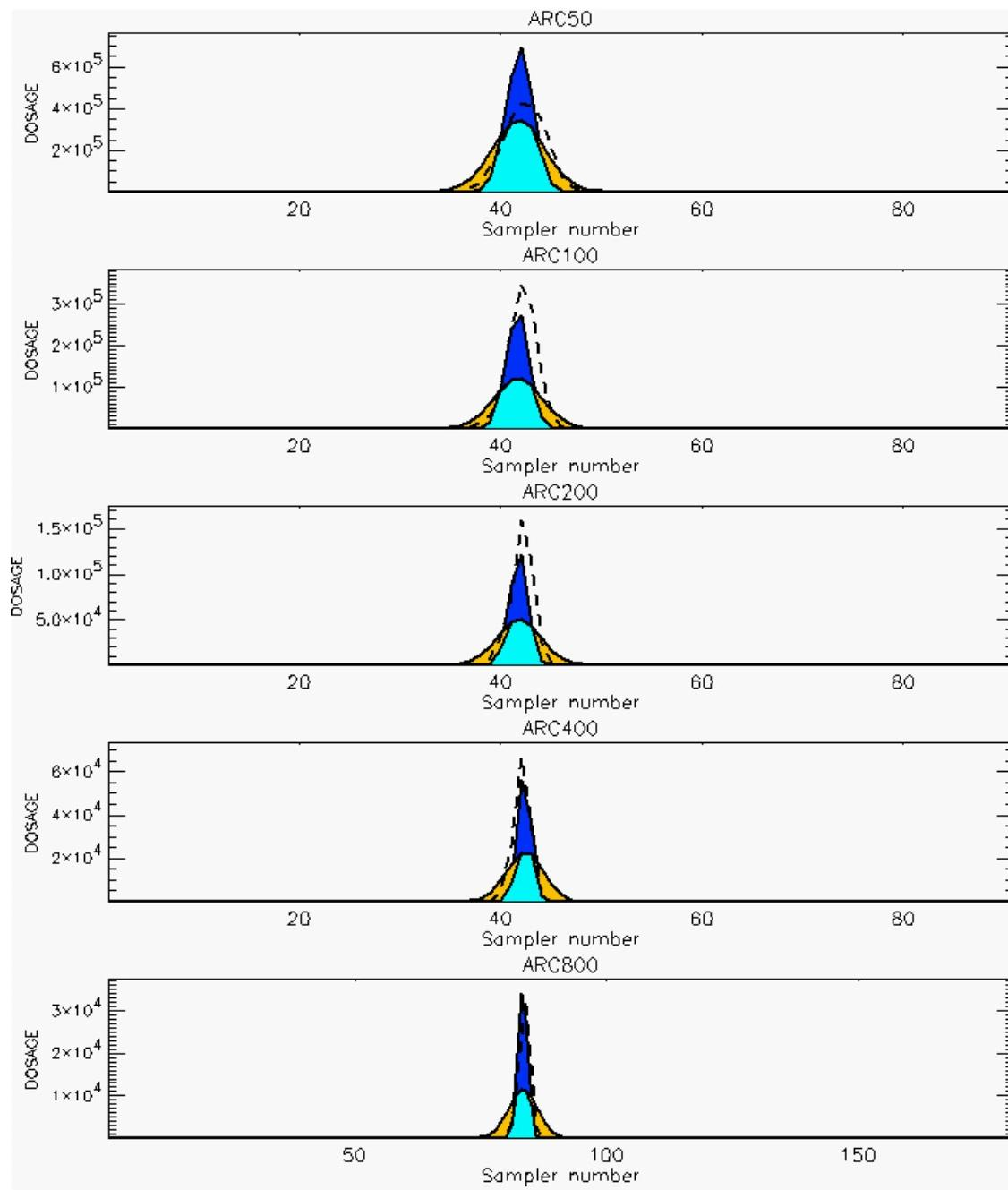
PG Prediction1 to Prediction2 Comparison

PG Trial File: pr_grass_tracer_Experiment_28.txt

PG Prediction File 1: HPAC\nodeposition\pg_28_novd.out

PG Prediction File 2: HPAC\novd_uu calm_0250\pg_28_novd.out

**Figure G-23. HPAC With uu(calm) Set to 0.0 or 0.250 Predictions to Trial 28:
Stability Category is 5**



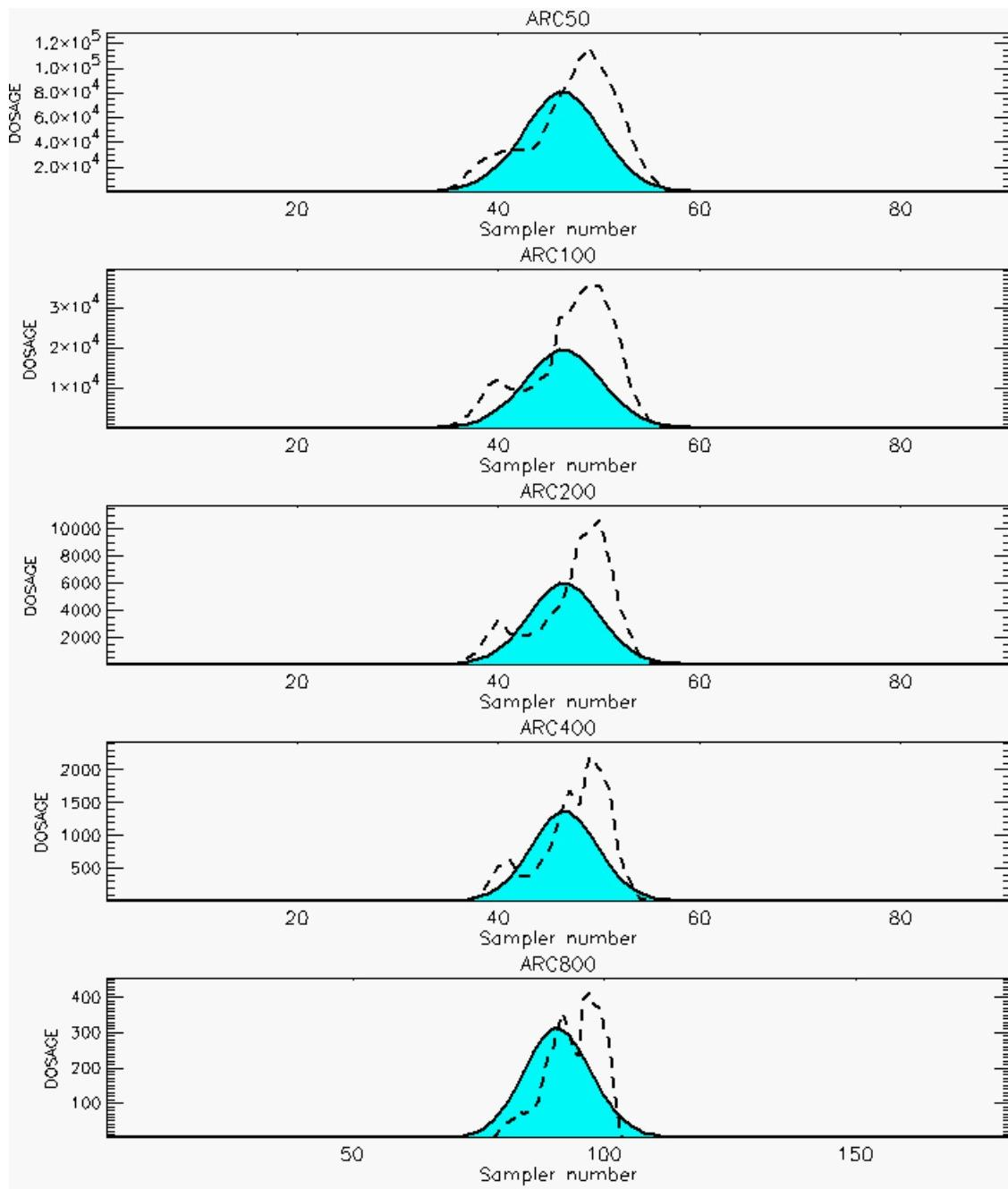
PG Prediction1 to Prediction2 Comparison

PG Trial File: pr_grass_tracer_Experiment_32.txt

PG Prediction File 1: HPAC\nodeposition\pg_32_novd.out

PG Prediction File 2: HPAC\novd_uu calm_0250\pg_32_novd.out

**Figure G-24. HPAC With uu(calm) Set to 0.0 or 0.250 Predictions to Trial 32:
Stability Category is 6**



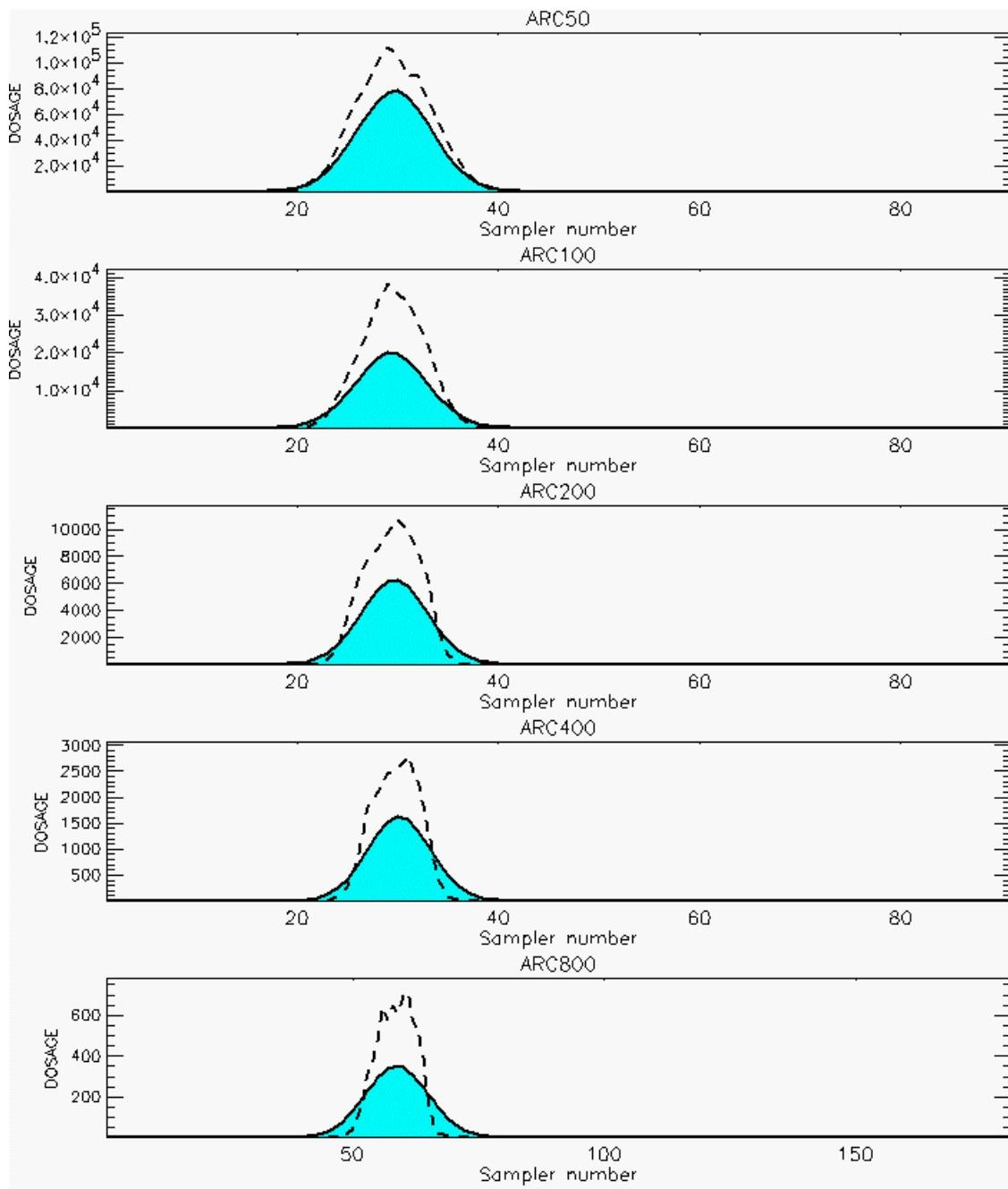
PG Prediction1 to Prediction2 Comparison

PG Trial File: pr_grass_tracer_Experiment_33.txt

PG Prediction File 1: HPAC\nodeposition\pg_33_novd.out

PG Prediction File 2: HPAC\novd_uu(calm)_0250\pg_33_novd.out

**Figure G-25. HPAC With uu(calm) Set to 0.0 or 0.250 Predictions to Trial 33:
Stability Category is 3**



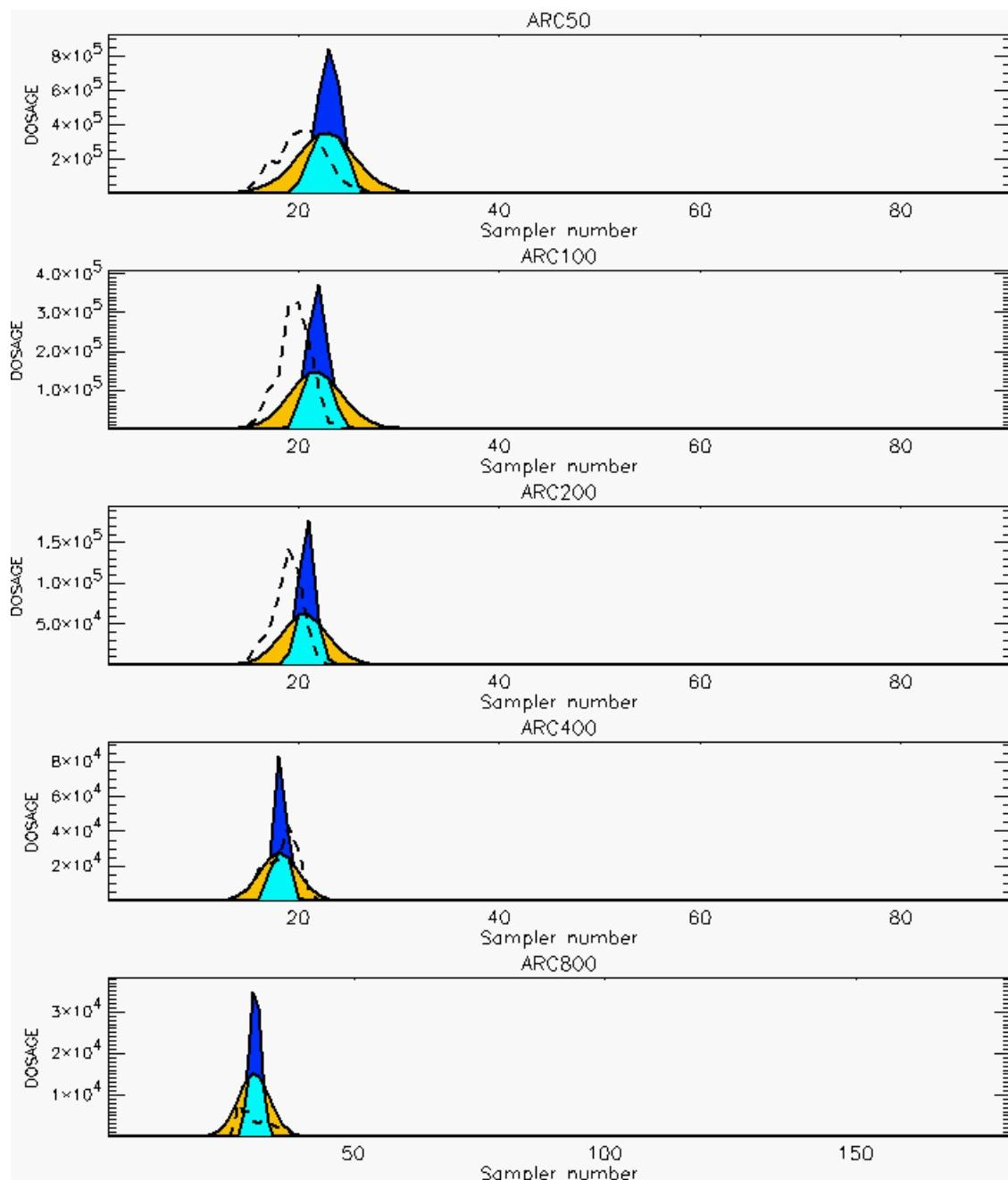
PG Prediction1 to Prediction2 Comparison

PG Trial File: pr_grass_tracer_Experiment_34.txt

PG Prediction File 1: HPAC\nodeposition\pg_34_novd.out

PG Prediction File 2: HPAC\novd_uu calm_0250\pg_34_novd.out

**Figure G-26. HPAC With uu(calm) Set to 0.0 or 0.250 Predictions to Trial 34:
Stability Category is 3**



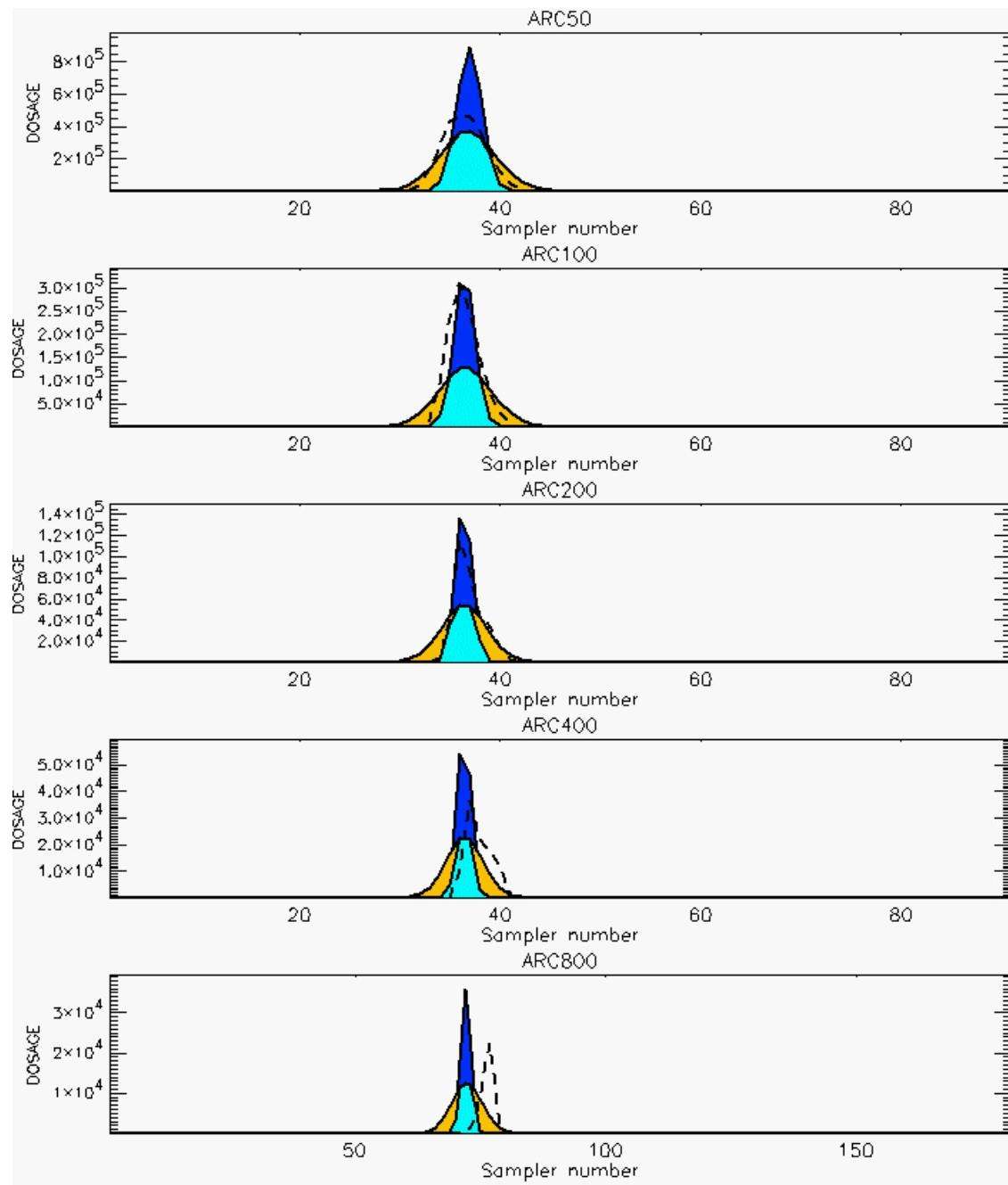
PG Prediction1 to Prediction2 Comparison

PG Trial File: pr_grass_tracer_Experiment_35.txt

PG Prediction File 1: HPAC\nodeposition\pg_35_novd.out

PG Prediction File 2: HPAC\novd_uu calm_0250\pg_35_novd.out

**Figure G-27. HPAC With uu(calm) Set to 0.0 or 0.250 Predictions to Trial 35:
Stability Category is 6**



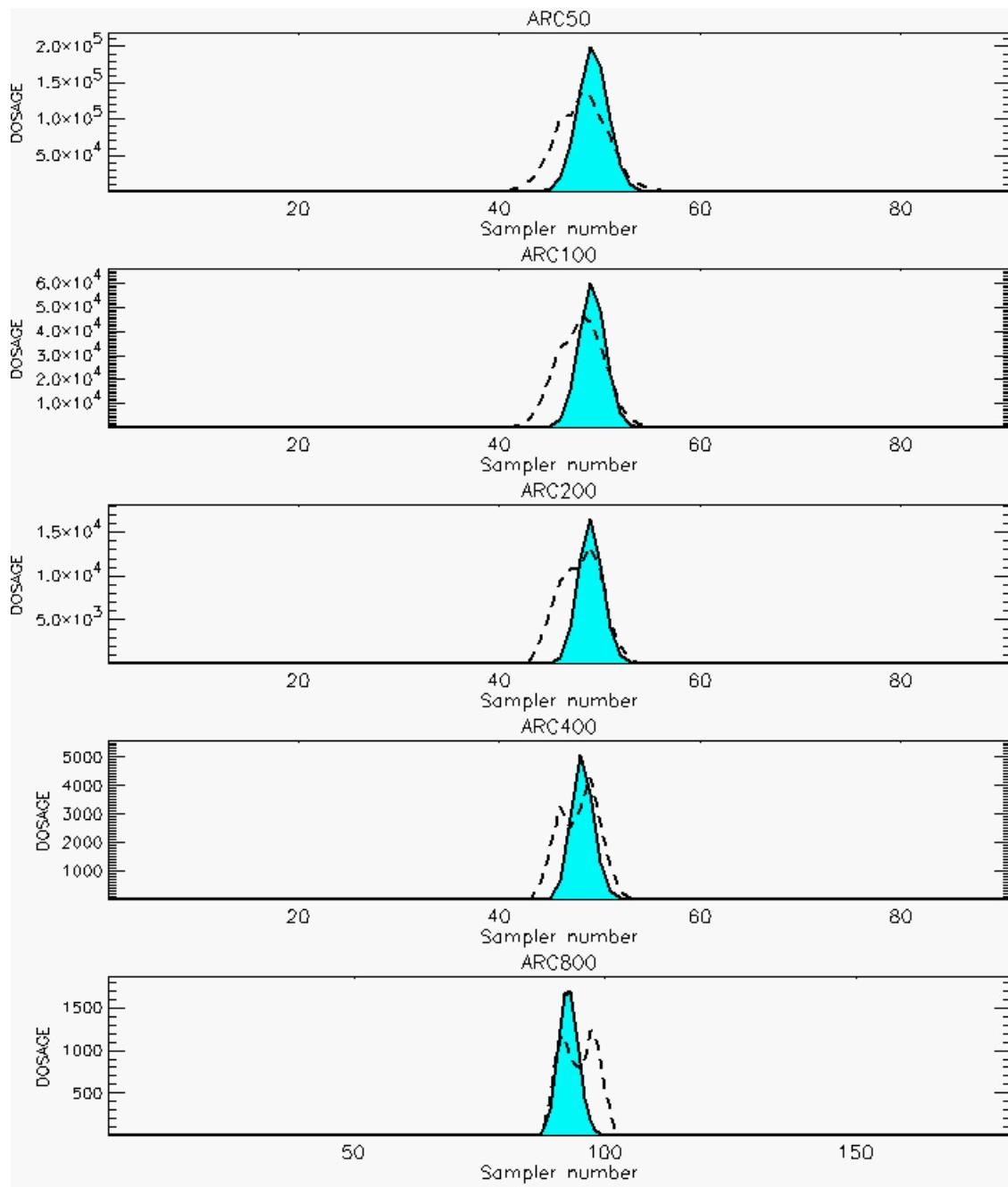
PG Prediction1 to Prediction2 Comparison

PG Trial File: pr_grass_tracer_Experiment_36.txt

PG Prediction File 1: HPAC\nodeposition\pg_36_noxd.out

PG Prediction File 2: HPAC\noxd_uu calm_0250\pg_36_noxd.out

**Figure G-28. HPAC With uu(calm) Set to 0.0 or 0.250 Predictions to Trial 36:
Stability Category is 6**



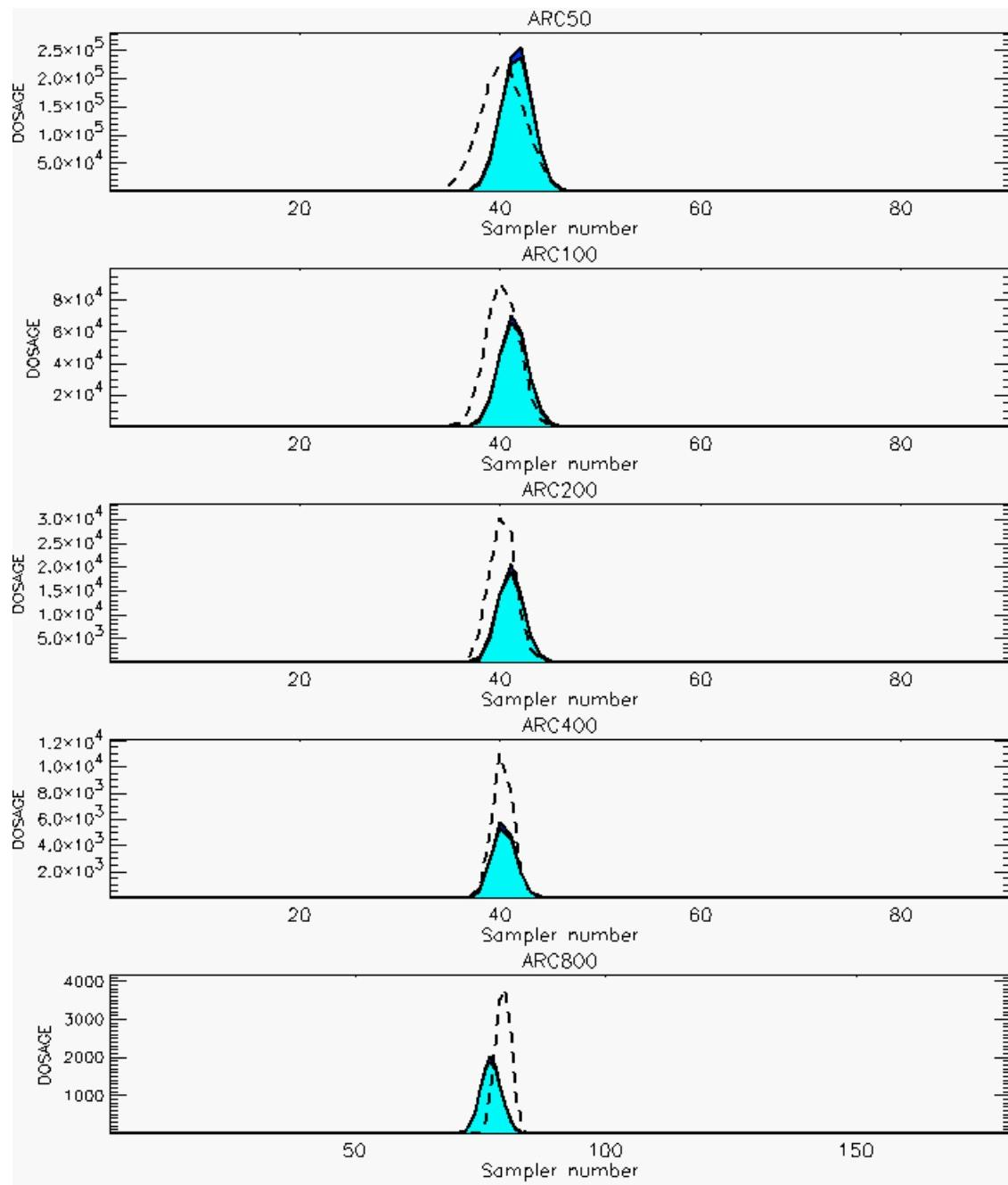
PG Prediction1 to Prediction2 Comparison

PG Trial File: pr_grass_tracer_Experiment_37.txt

PG Prediction File 1: HPAC\nodeposition\pg_37_novd.out

PG Prediction File 2: HPAC\novd_uu calm_0250\pg_37_novd.out

**Figure G-29. HPAC With uu(calm) Set to 0.0 or 0.250 Predictions to Trial 37:
Stability Category is 4**



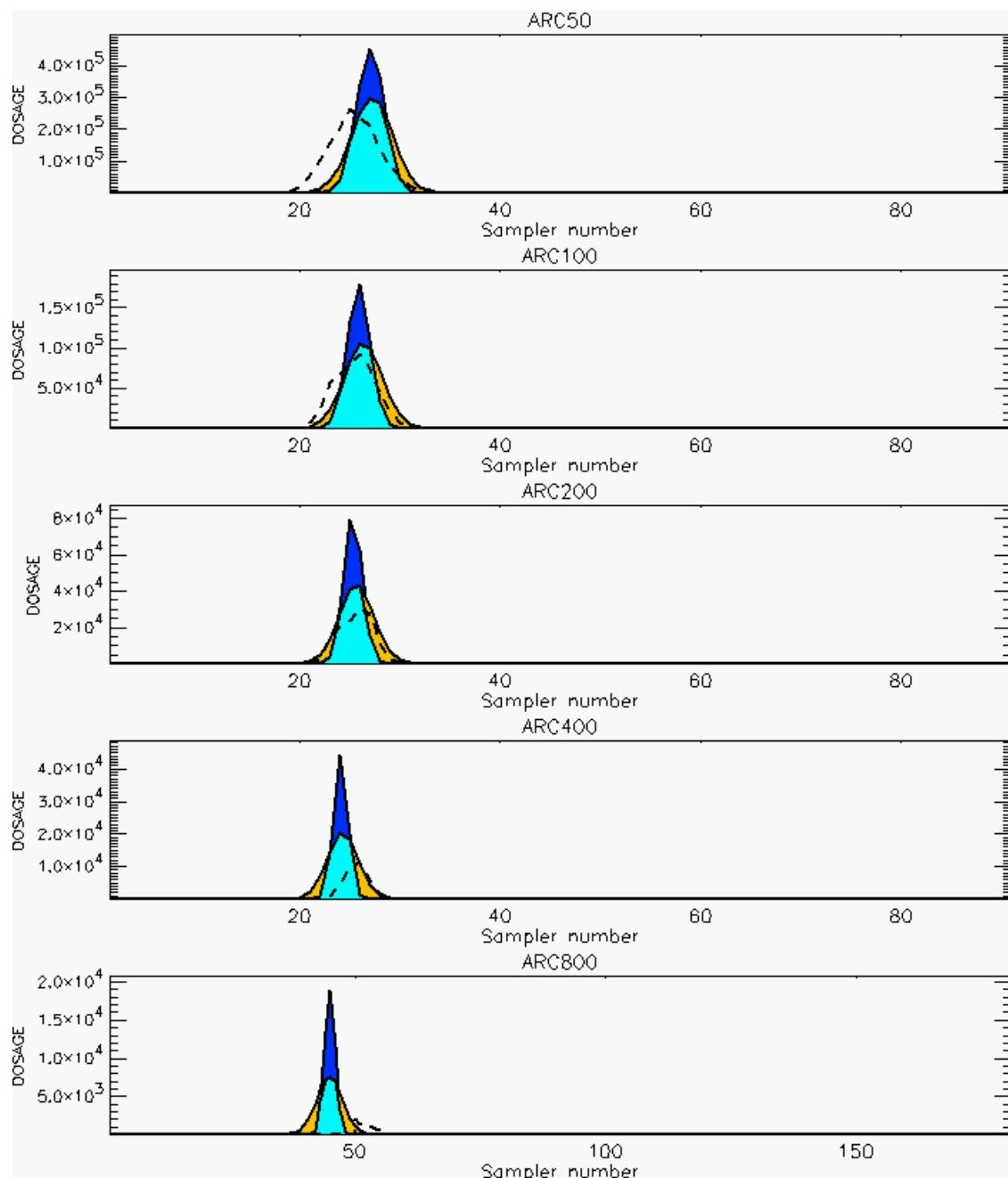
PG Prediction1 to Prediction2 Comparison

PG Trial File: pr_grass_tracer_Experiment_38.txt

PG Prediction File 1: HPAC\nodeposition\pg_38_novd.out

PG Prediction File 2: HPAC\novd_uu calm_0250\pg_38_novd.out

**Figure G-30. HPAC With uu(calm) Set to 0.0 or 0.250 Predictions to Trial 38:
Stability Category is 4**



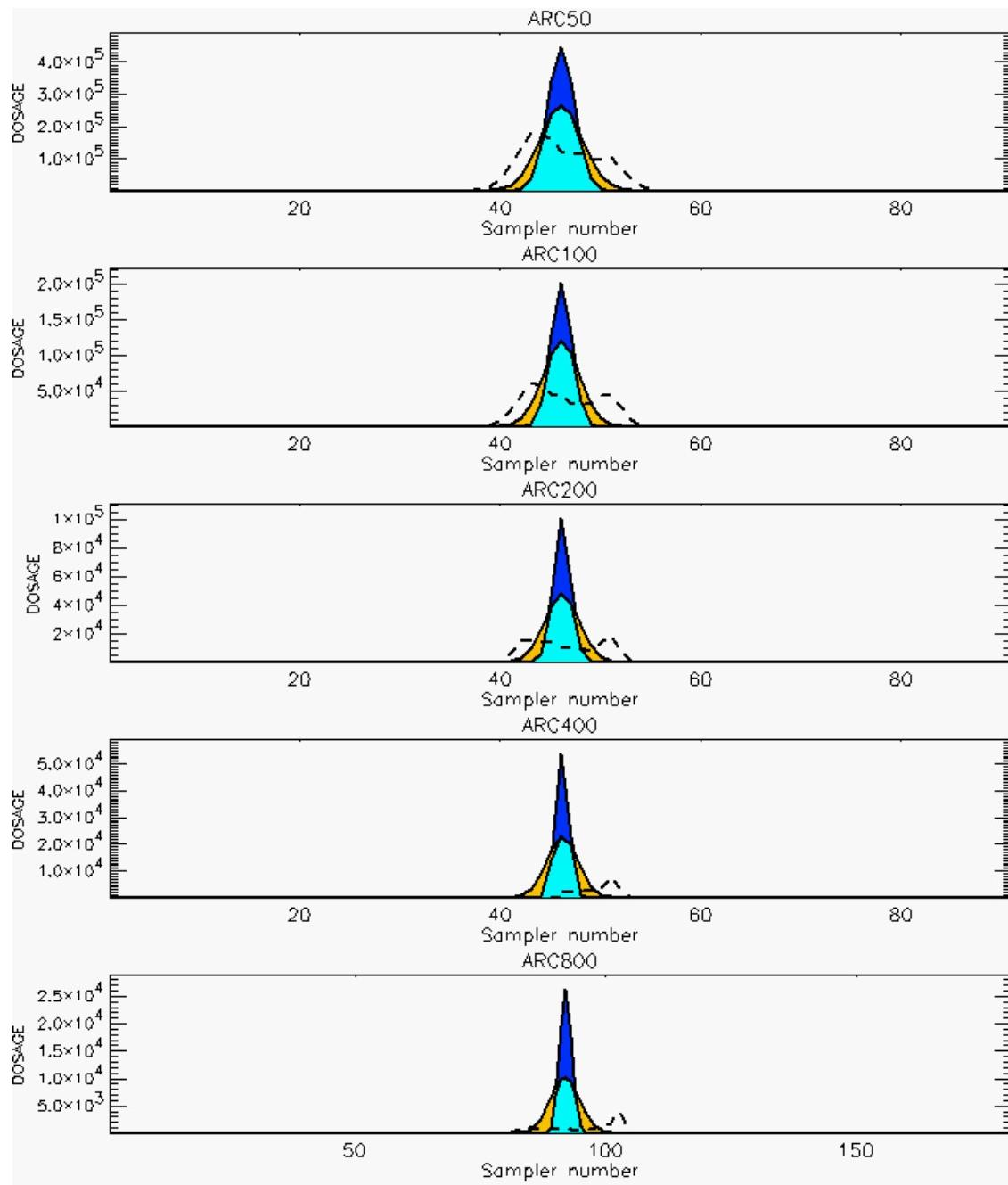
PG Prediction1 to Prediction2 Comparison

PG Trial File: pr_grass_tracer_Experiment_39.txt

PG Prediction File 1: HPAC\nodeposition\pg_39_novd.out

PG Prediction File 2: HPAC\novd_uu calm_0250\pg_39_novd.out

**Figure G-31. HPAC With uu(calm) Set to 0.0 or 0.250 Predictions to Trial 39:
Stability Category is 6**



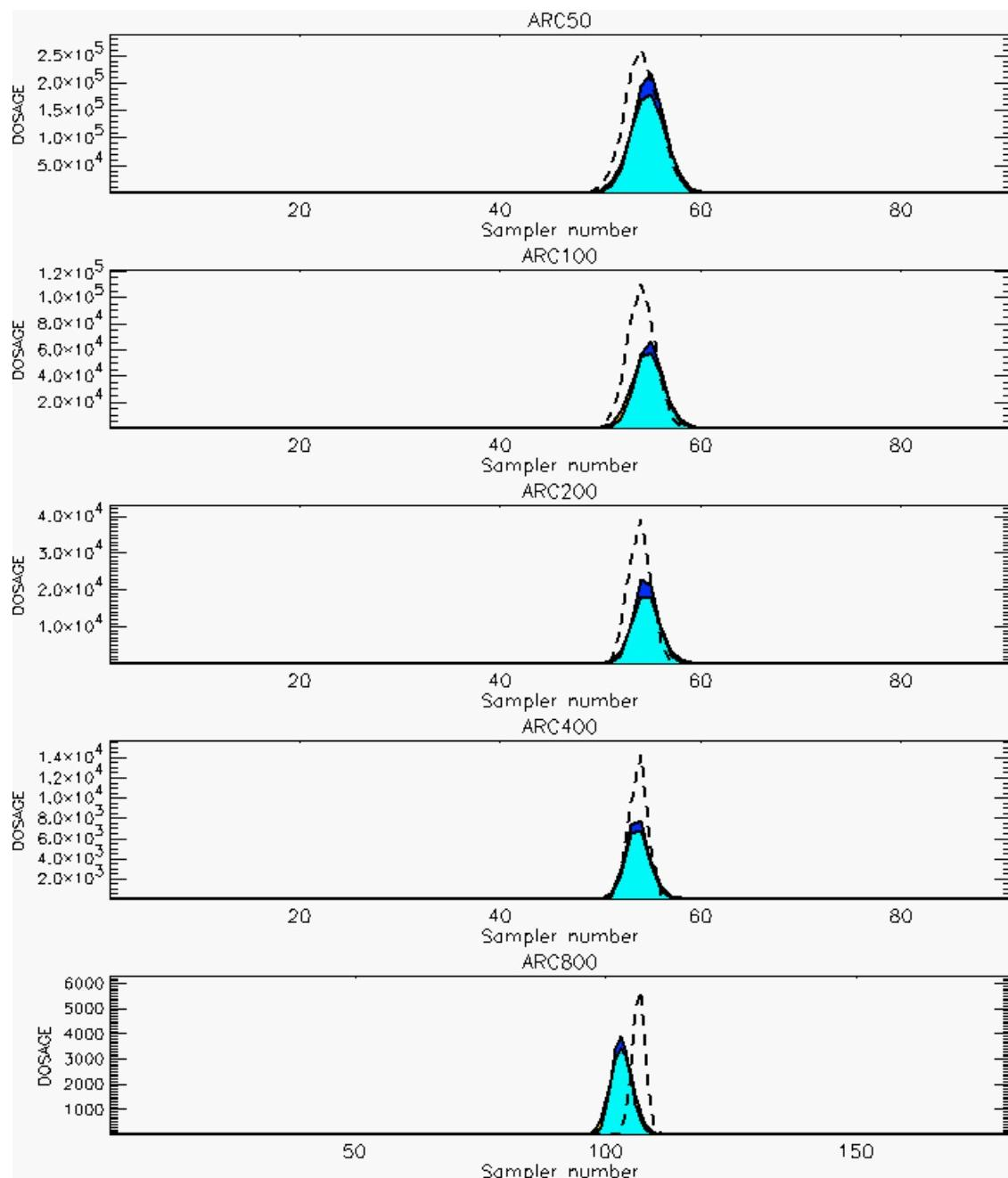
PG Prediction1 to Prediction2 Comparison

PG Trial File: pr_grass_tracer_Experiment_40.txt

PG Prediction File 1: HPAC\nodeposition\pg_40_novd.out

PG Prediction File 2: HPAC\novd_uu calm_0250\pg_40_novd.out

**Figure G-32. HPAC With uu(calm) Set to 0.0 or 0.250 Predictions to Trial 40:
Stability Category is 6**



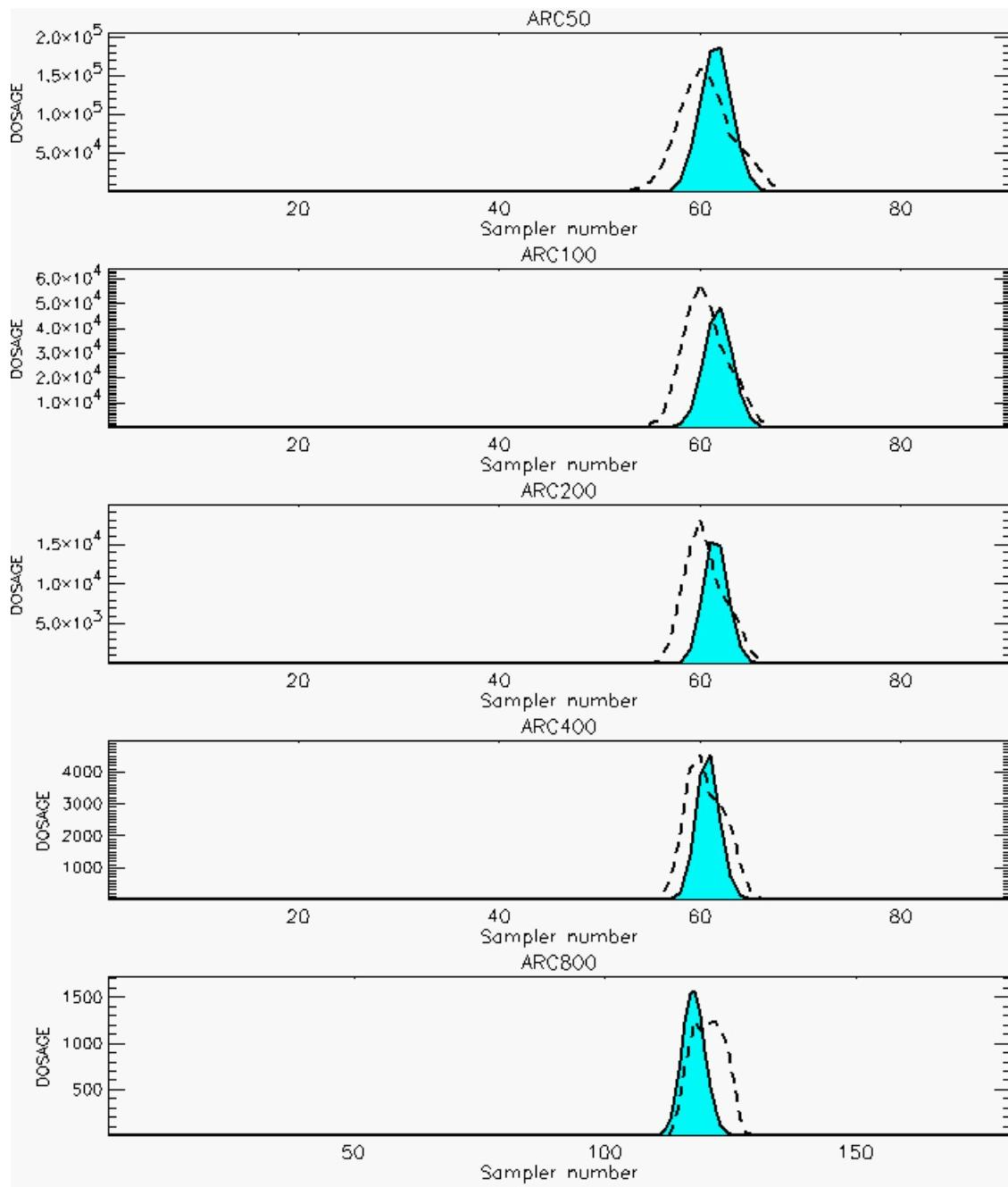
PG Prediction1 to Prediction2 Comparison

PG Trial File: pr_grass_tracer_Experiment_41.txt

PG Prediction File 1: HPAC\nodeposition\pg_41_noxd.out

PG Prediction File 2: HPAC\noxd_uu calm_0250\pg_41_noxd.out

**Figure G-33. HPAC With uu(calm) Set to 0.0 or 0.250 Predictions to Trial 41:
Stability Category is 5**



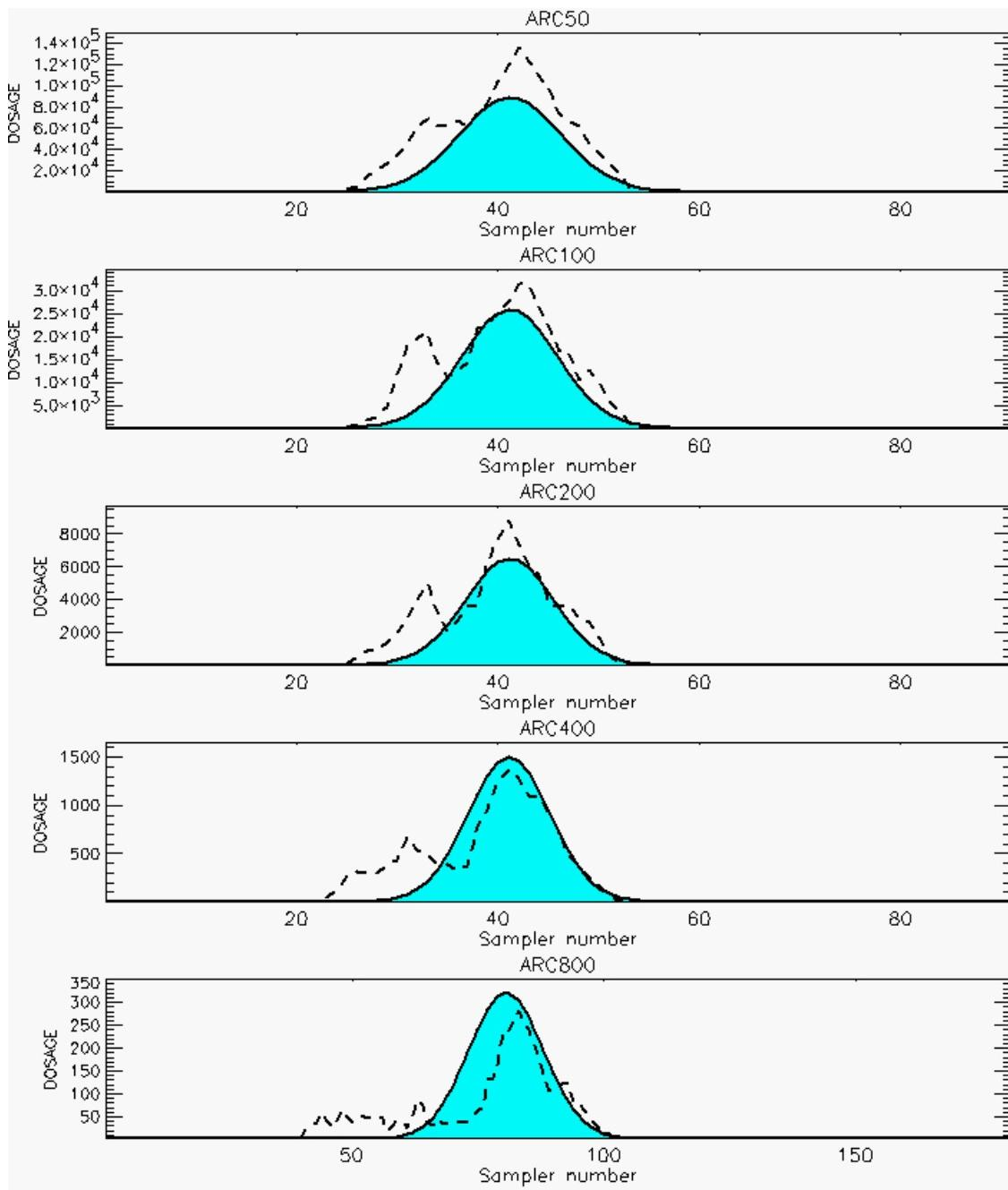
PG Prediction1 to Prediction2 Comparison

PG Trial File: pr_grass_tracer_Experiment_42.txt

PG Prediction File 1: HPAC\nodeposition\pg_42_novd.out

PG Prediction File 2: HPAC\novd_uu(calm)_0250\pg_42_novd.out

**Figure G-34. HPAC With uu(calm) Set to 0.0 or 0.250 Predictions to Trial 42:
Stability Category is 4**



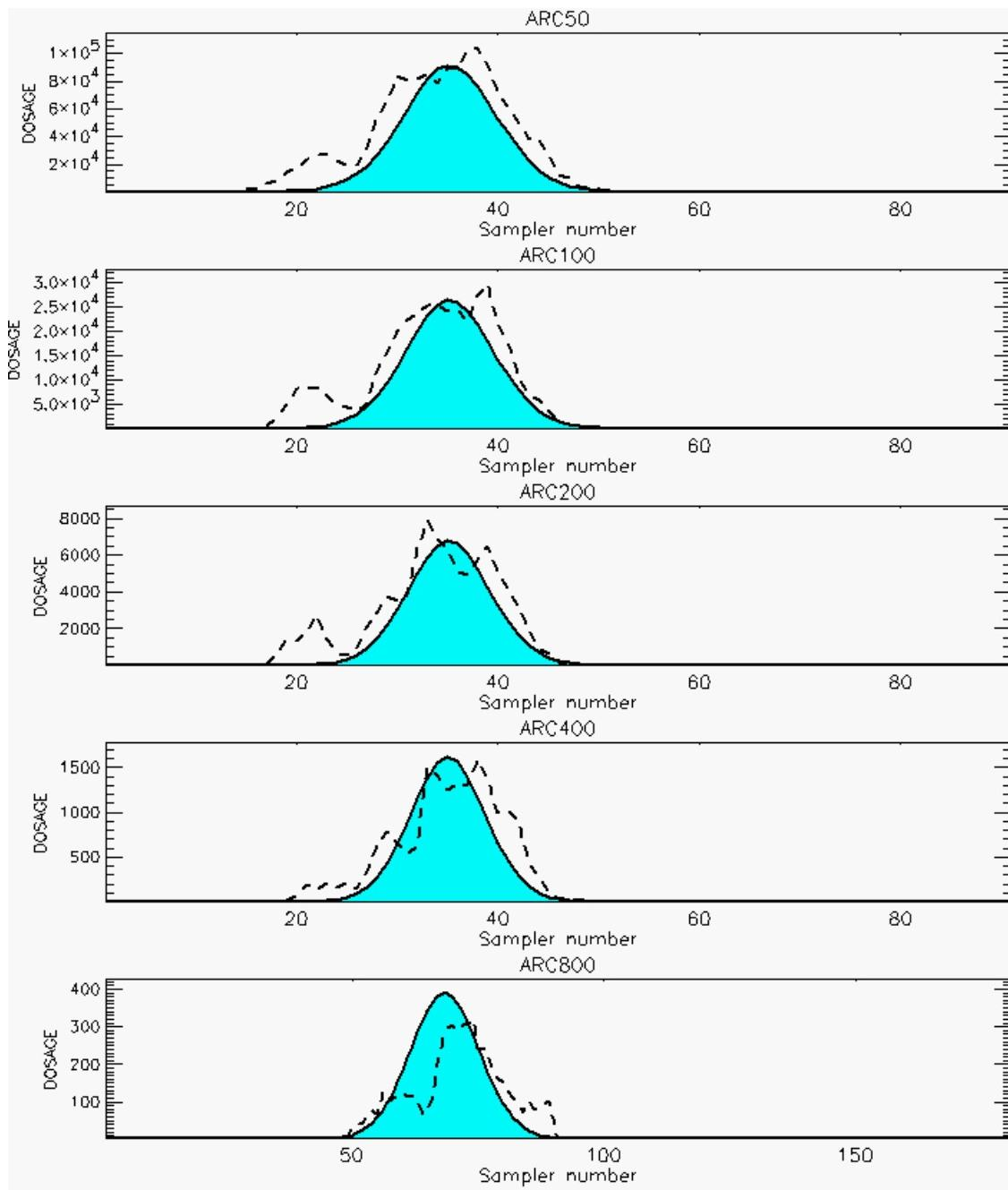
PG Prediction1 to Prediction2 Comparison

PG Trial File: pr_grass_tracer_Experiment_43.txt

PG Prediction File 1: HPAC\nodeposition\pg_43_novd.out

PG Prediction File 2: HPAC\novd_uu(calm_0250\pg_43_novd.out

**Figure G-35. HPAC With uu(calm) Set to 0.0 or 0.250 Predictions to Trial 43:
Stability Category is 1**



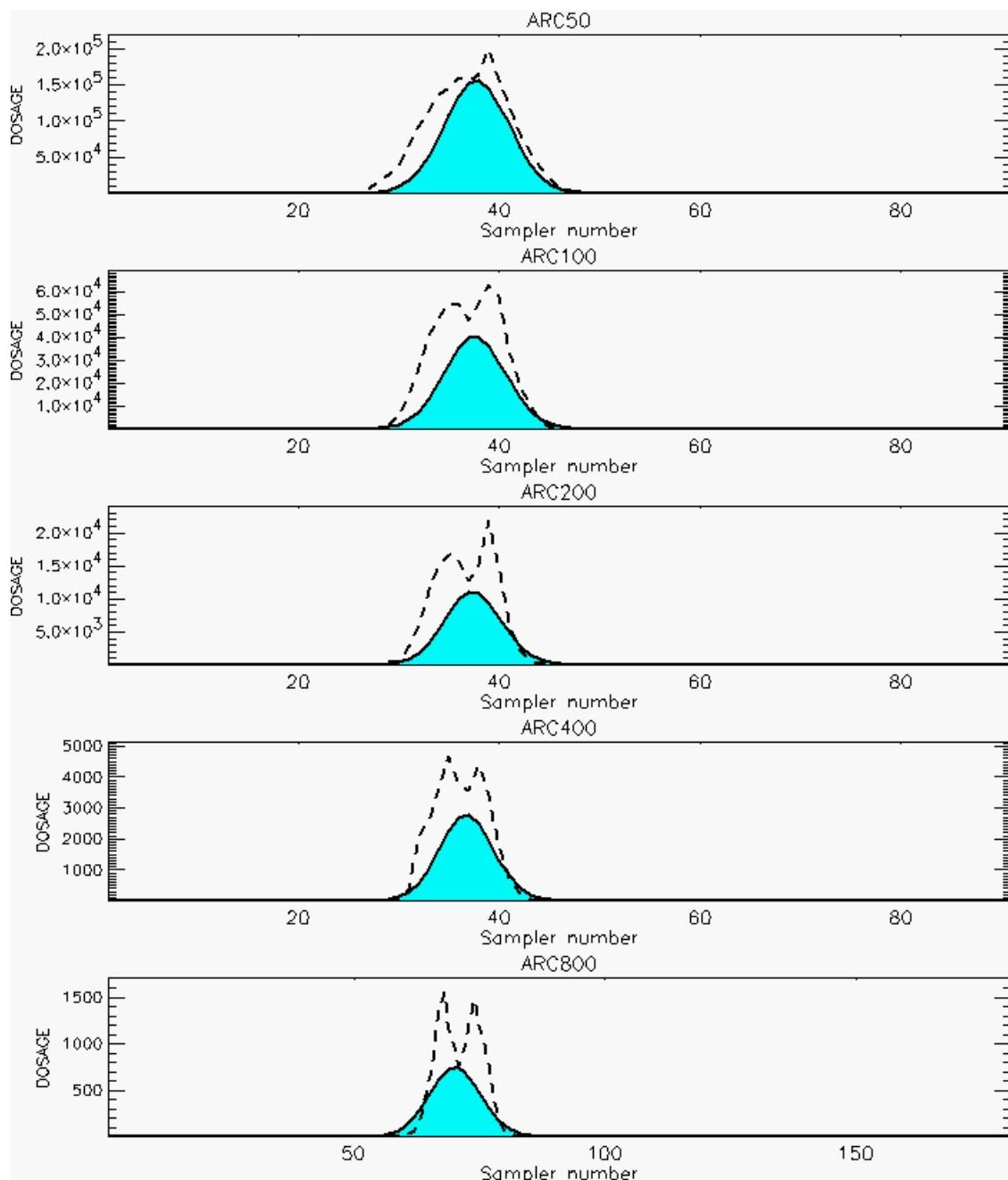
PG Prediction1 to Prediction2 Comparison

PG Trial File: pr_grass_tracer_Experiment_44.txt

PG Prediction File 1: HPAC\nodeposition\pg_44_nozd.out

PG Prediction File 2: HPAC\nozd_uu calm_0250\pg_44_nozd.out

**Figure G-36. HPAC With uu(calm) Set to 0.0 or 0.250 Predictions to Trial 44:
Stability Category is 2**



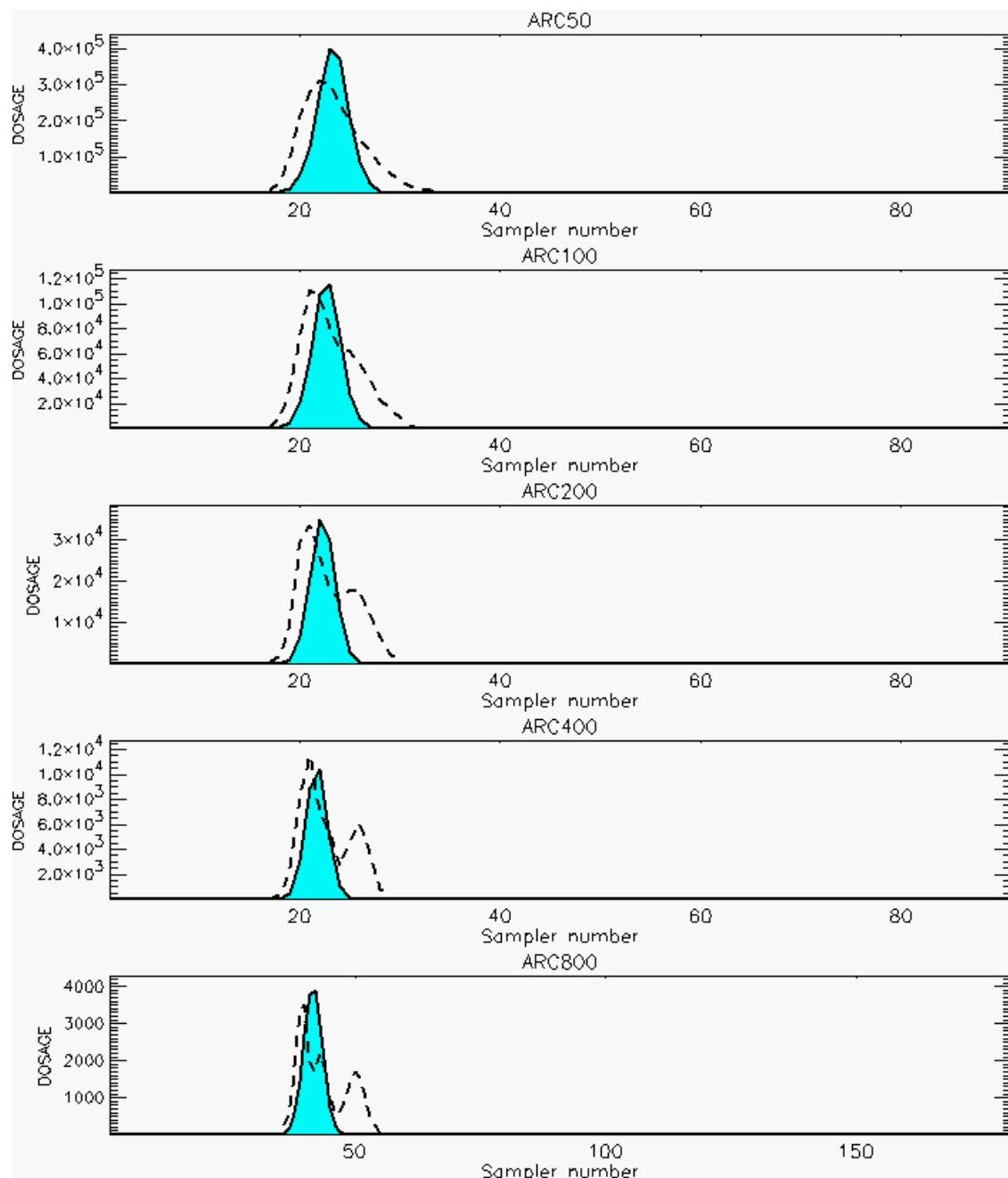
PG Prediction1 to Prediction2 Comparison

PG Trial File: pr_grass_tracer_Experiment_45.txt

PG Prediction File 1: HPAC\nodeposition\pg_45_noxd.out

PG Prediction File 2: HPAC\noxd_uu calm_0250\pg_45_noxd.out

**Figure G-37. HPAC With uu(calm) Set to 0.0 or 0.250 Predictions to Trial 45:
Stability Category is 3**



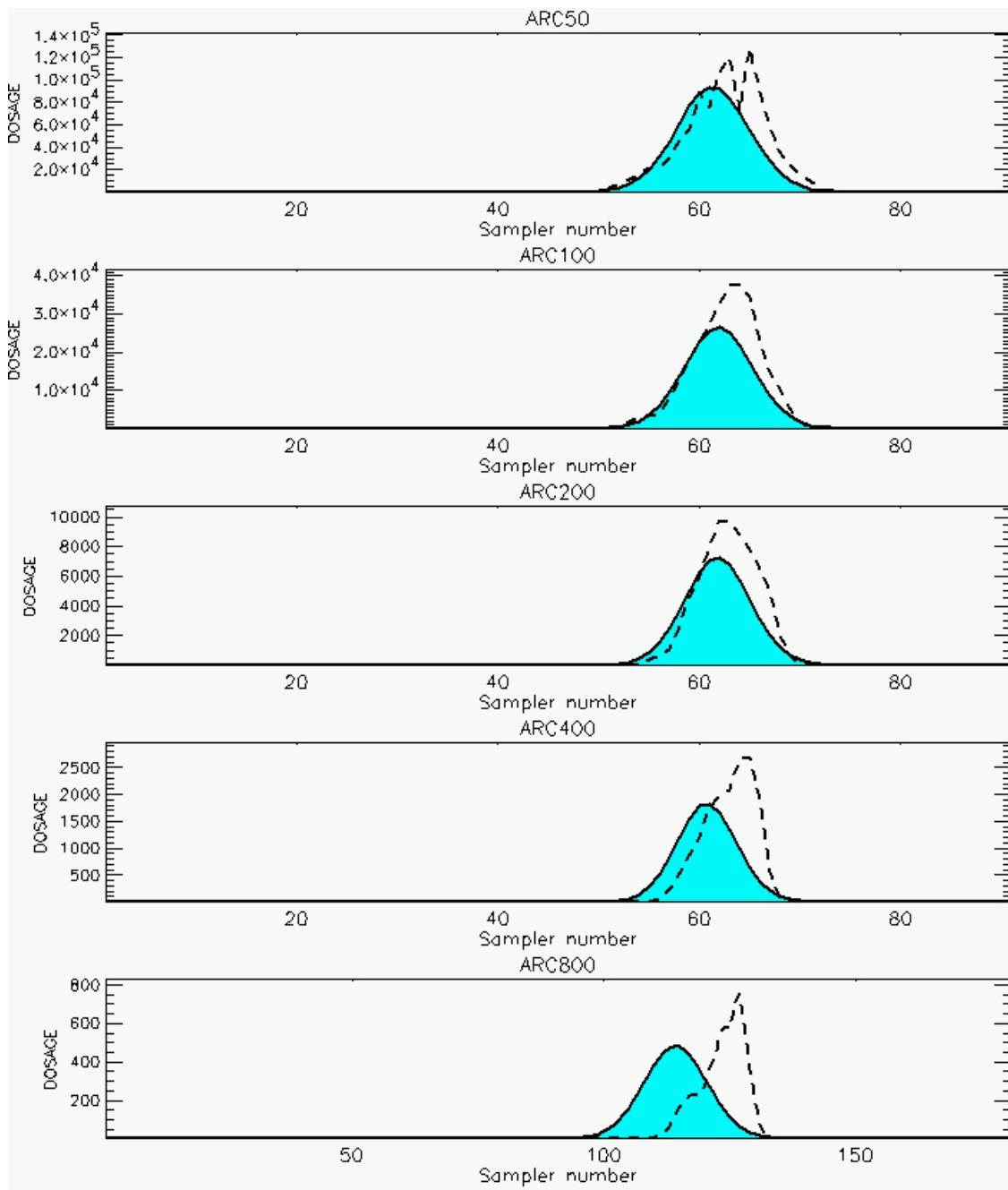
PG Prediction1 to Prediction2 Comparison

PG Trial File: pr_grass_tracer_Experiment_46.txt

PG Prediction File 1: HPAC\nodeposition\pg_46_noxd.out

PG Prediction File 2: HPAC\noxd_uu(calm)_0250\pg_46_noxd.out

**Figure G-38. HPAC With uu(calm) Set to 0.0 or 0.250 Predictions to Trial 46:
Stability Category is 4**



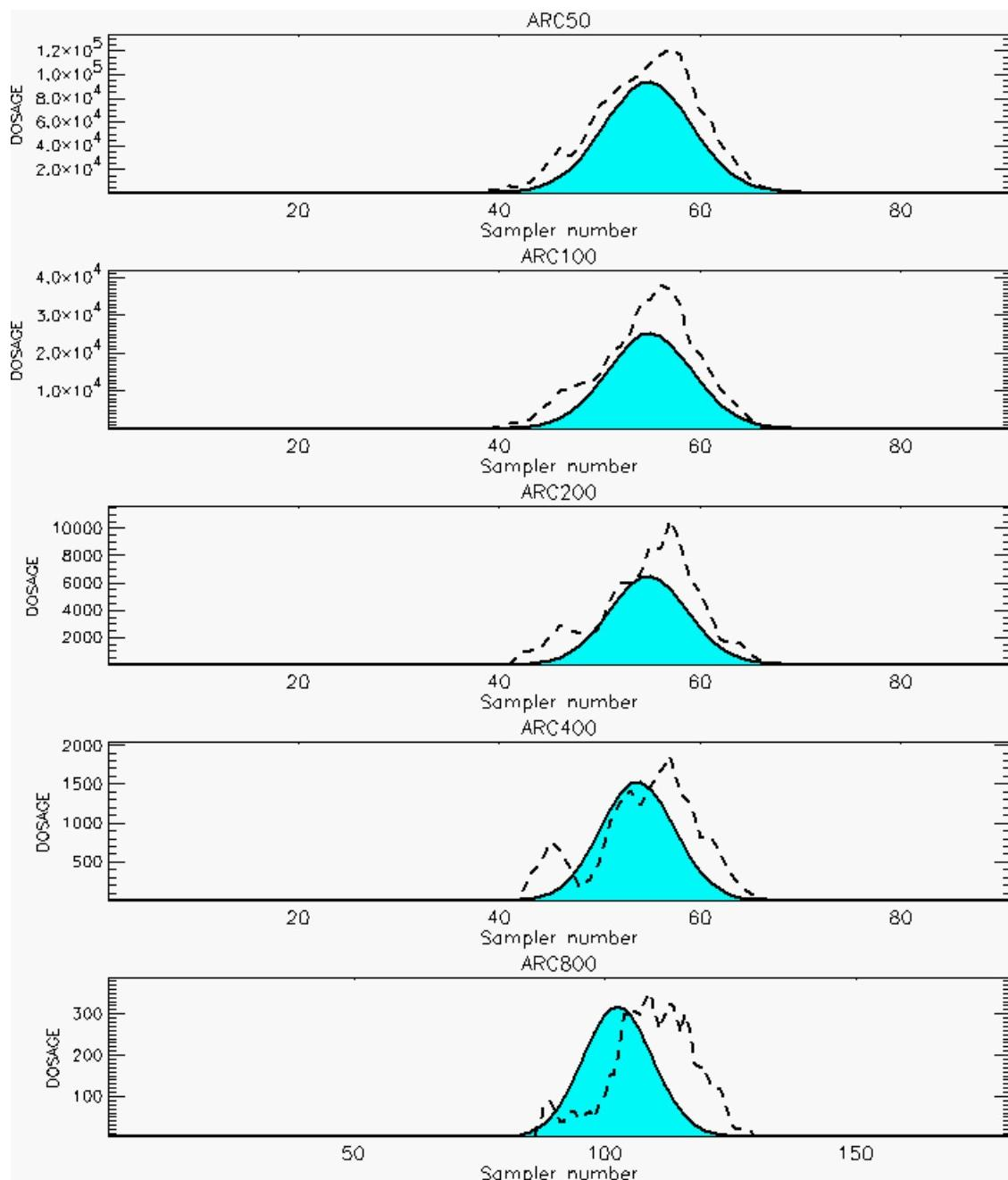
PG Prediction1 to Prediction2 Comparison

PG Trial File: pr_grass_tracer_Experiment_48.txt

PG Prediction File 1: HPAC\nodeposition\pg_48_novd.out

PG Prediction File 2: HPAC\novd_uu(calm)_0250\pg_48_novd.out

**Figure G-39. HPAC With uu(calm) Set to 0.0 or 0.250 Predictions to Trial 48:
Stability Category is 3**



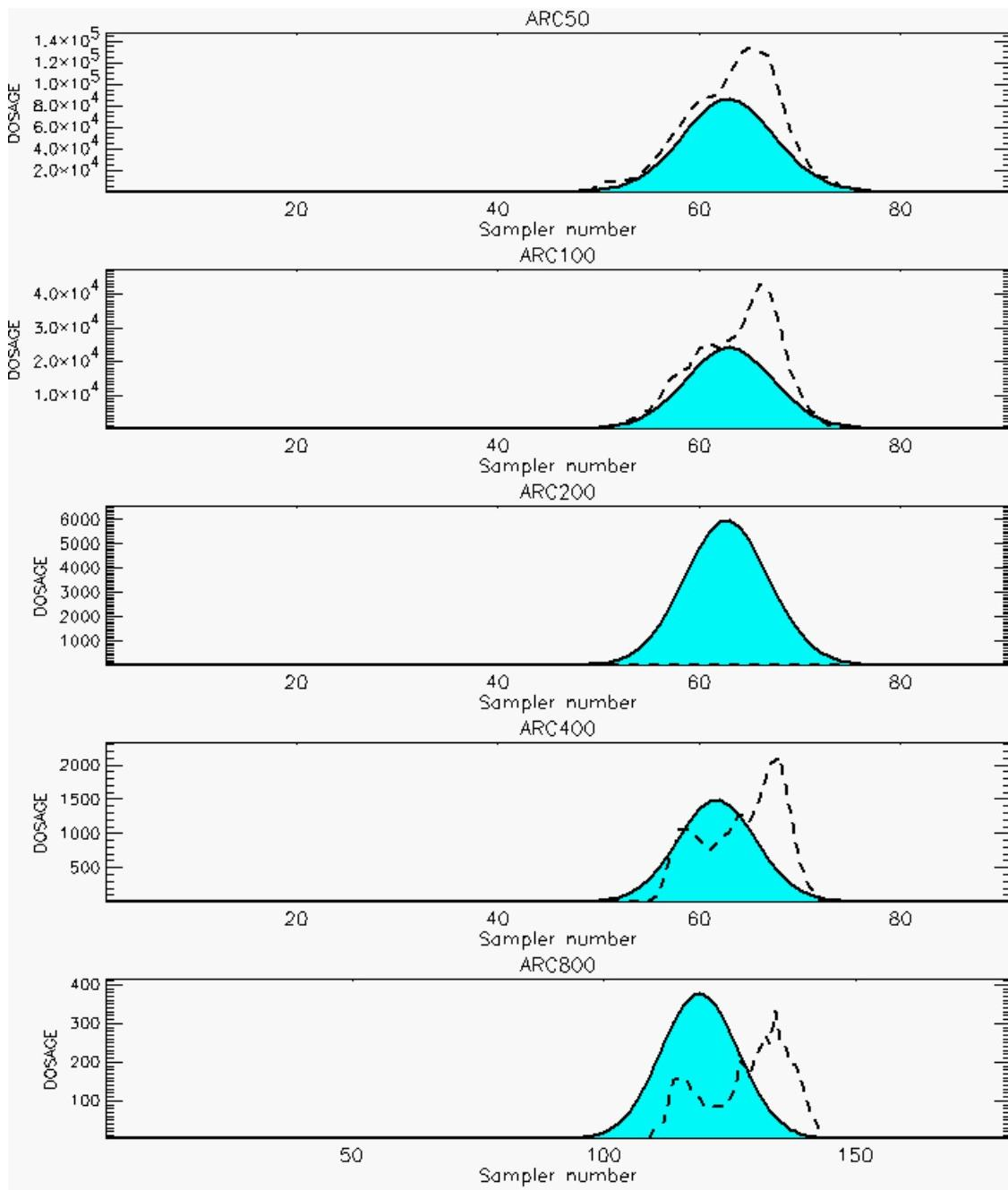
PG Prediction1 to Prediction2 Comparison

PG Trial File: pr_grass_tracer_Experiment_49.txt

PG Prediction File 1: HPAC\nodeposition\pg_49_novd.out

PG Prediction File 2: HPAC\novd_uu calm_0250\pg_49_novd.out

**Figure G-40. HPAC With uu(calm) Set to 0.0 or 0.250 Predictions to Trial 49:
Stability Category is 2**



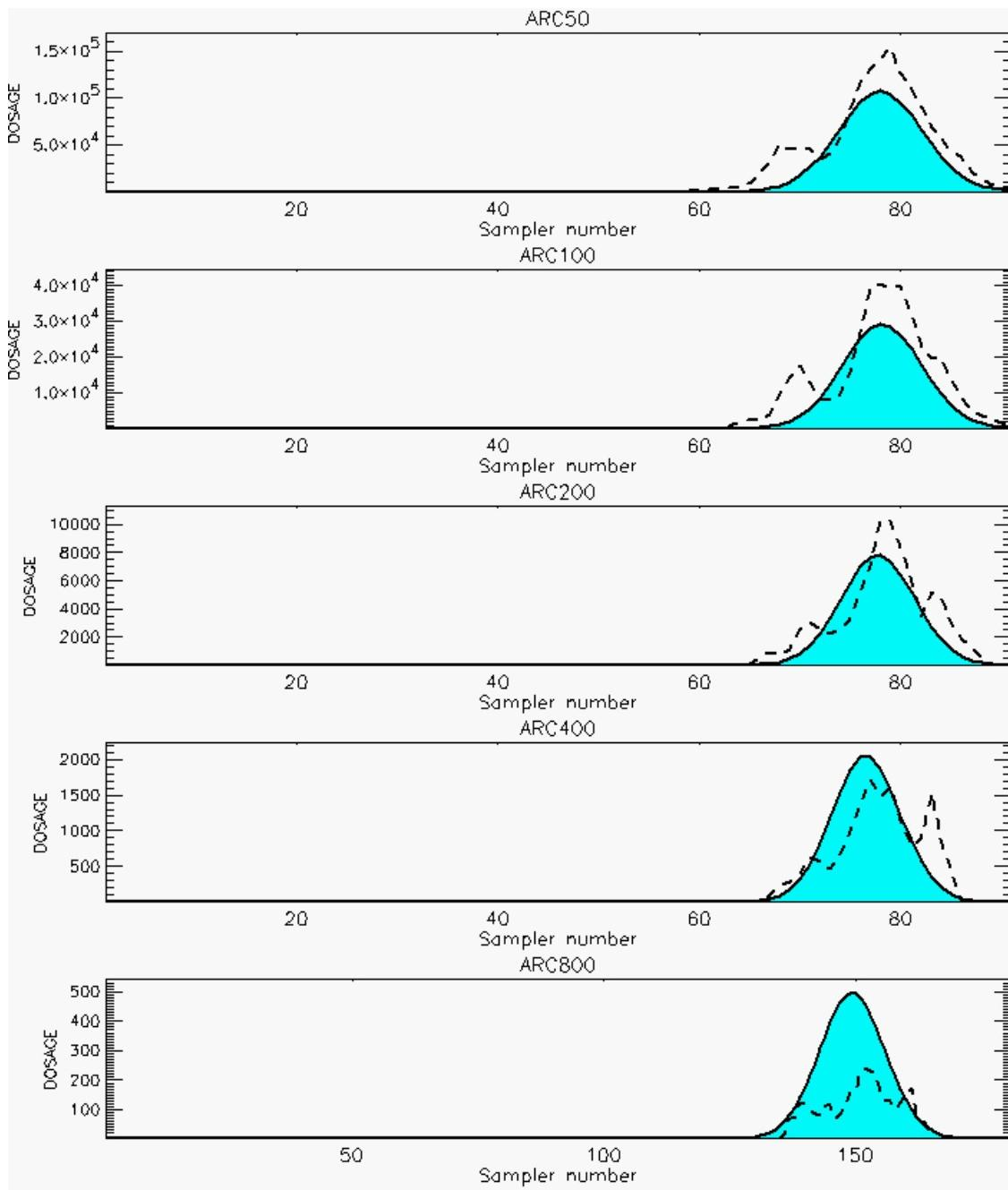
PG Prediction1 to Prediction2 Comparison

PG Trial File: pr_grass_tracer_Experiment_50.txt

PG Prediction File 1: HPAC\nodeposition\pg_50_novd.out

PG Prediction File 2: HPAC\novd_uu(calm)_0250\pg_50_novd.out

**Figure G-41. HPAC With uu(calm) Set to 0.0 or 0.250 Predictions to Trial 50:
Stability Category is 2**



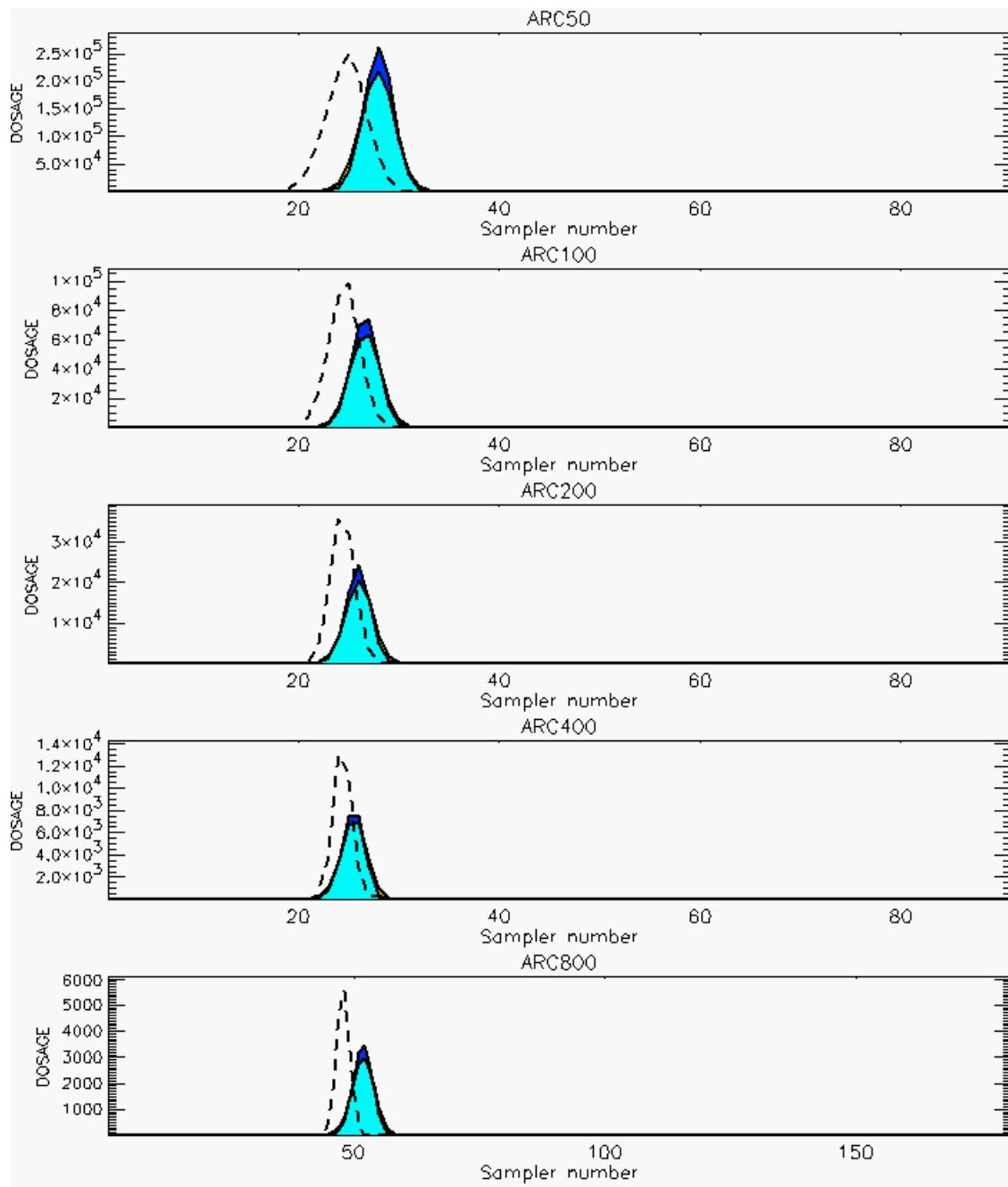
PG Prediction1 to Prediction2 Comparison

PG Trial File: pr_grass_tracer_Experiment_51.txt

PG Prediction File 1: HPAC\nodeposition\pg_51_nozd.out

PG Prediction File 2: HPAC\nozd_uu(calm)_0250\pg_51_nozd.out

**Figure G-42. HPAC With uu(calm) Set to 0.0 or 0.250 Predictions to Trial 51:
Stability Category is 2**



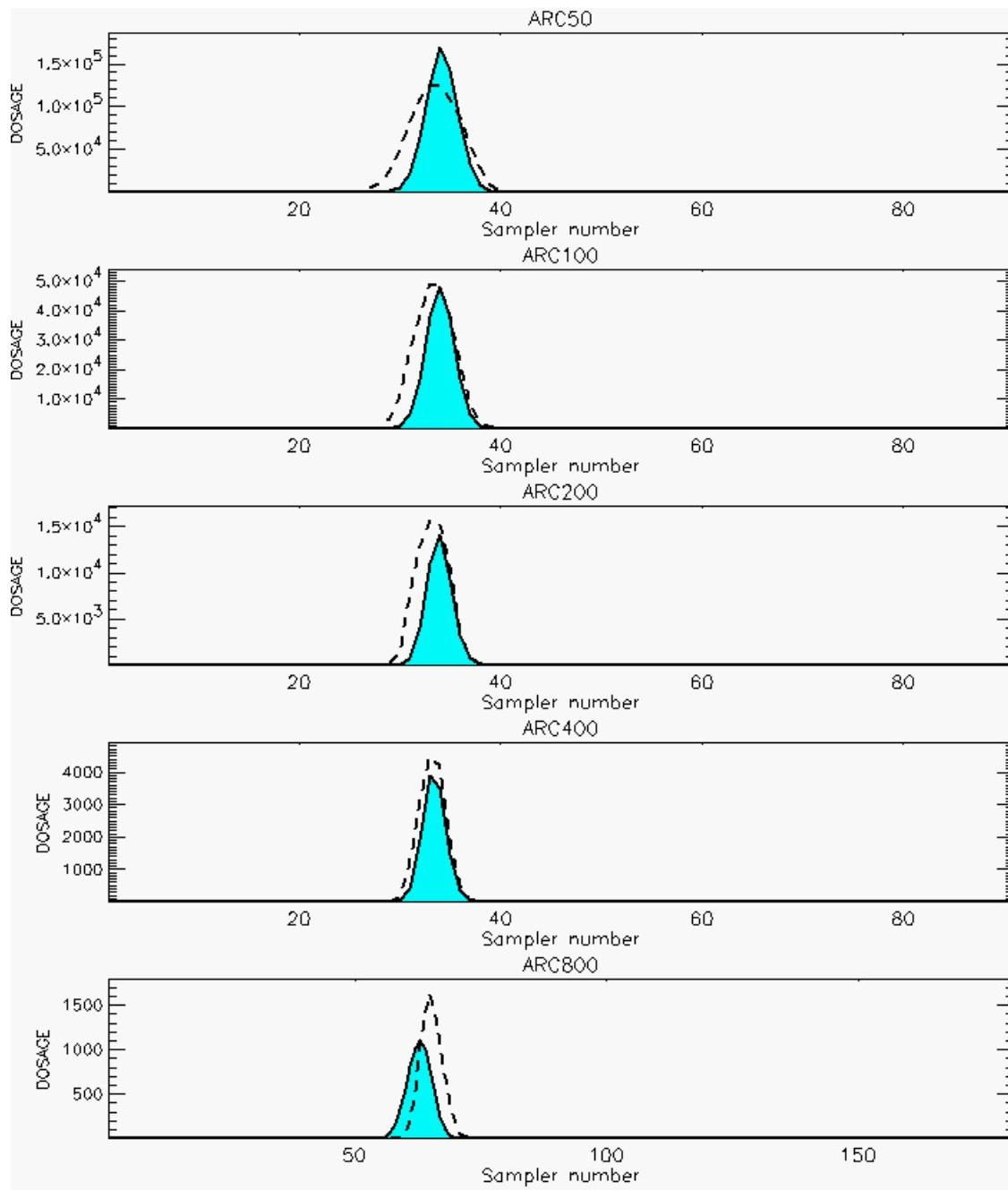
PG Prediction1 to Prediction2 Comparison

PG Trial File: pr_grass_tracer_Experiment_54.txt

PG Prediction File 1: HPAC\nodeposition\pg_54_novd.out

PG Prediction File 2: HPAC\novd_uu_calm_0250\pg_54_novd.out

**Figure G-43. HPAC With uu(calm) Set to 0.0 or 0.250 Predictions to Trial 54:
Stability Category is 5**



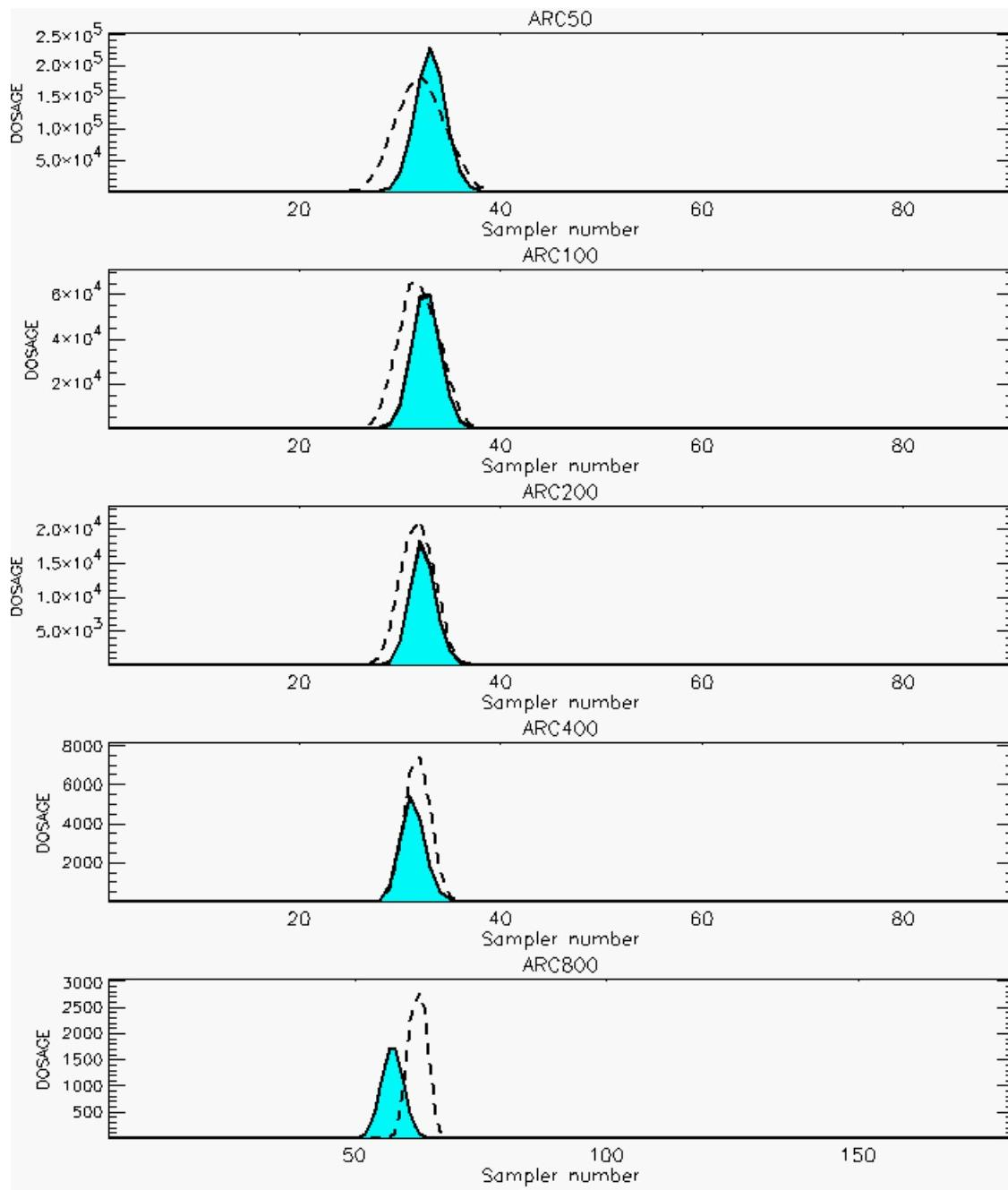
PG Prediction1 to Prediction2 Comparison

PG Trial File: pr_grass_tracer_Experiment_55.txt

PG Prediction File 1: HPAC\nodeposition\pg_55_nozd.out

PG Prediction File 2: HPAC\nozd_uu(calm_0250\pg_55_nozd.out

**Figure G-44. HPAC With uu(calm) Set to 0.0 or 0.250 Predictions to Trial 55:
Stability Category is 4**



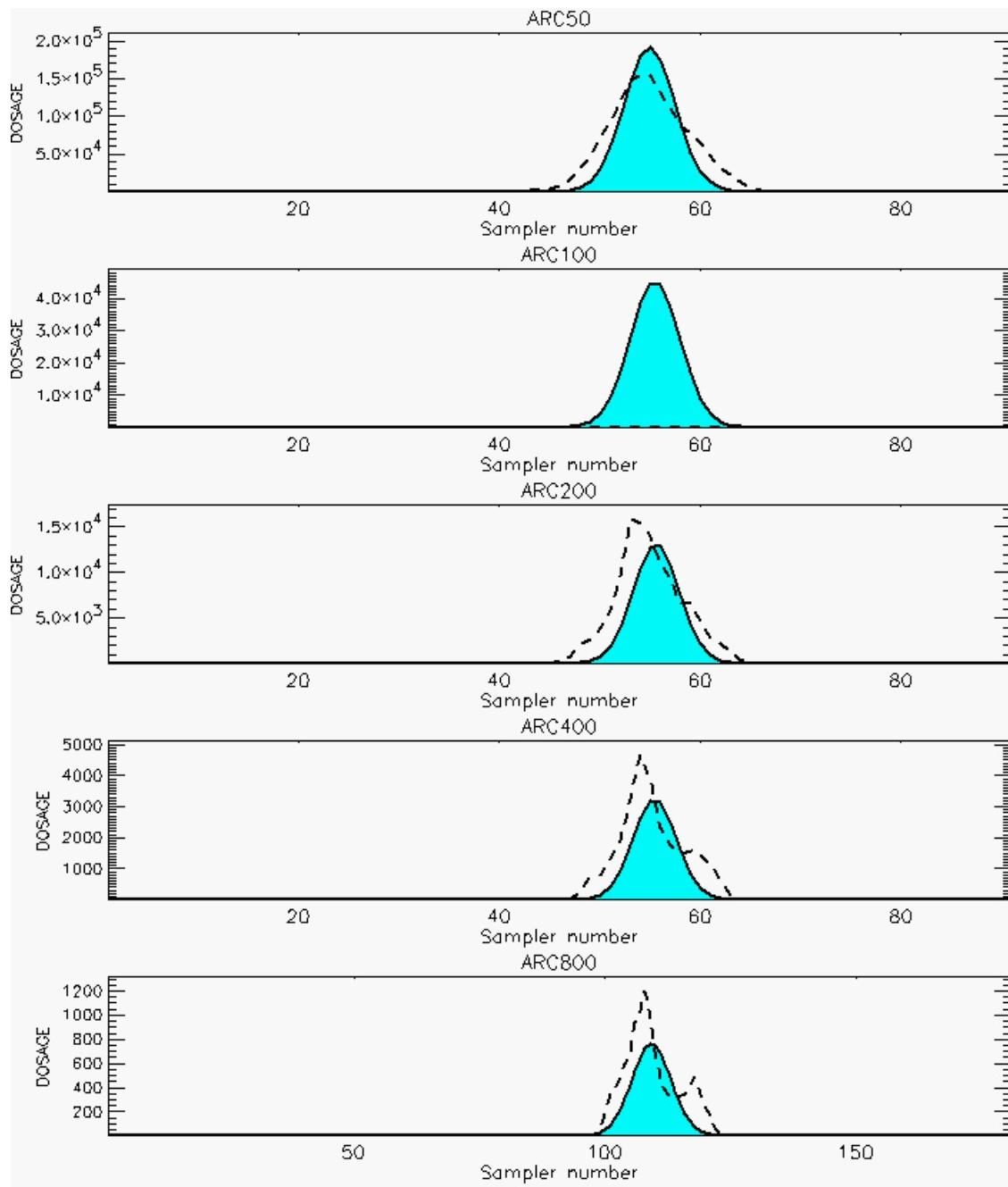
PG Prediction1 to Prediction2 Comparison

PG Trial File: pr_grass_tracer_Experiment_56.txt

PG Prediction File 1: HPAC\nodeposition\pg_56_novd.out

PG Prediction File 2: HPAC\novd_uu_calm_0250\pg_56_novd.out

**Figure G-45. HPAC With uu(calm) Set to 0.0 or 0.250 Predictions to Trial 56:
Stability Category is 4**



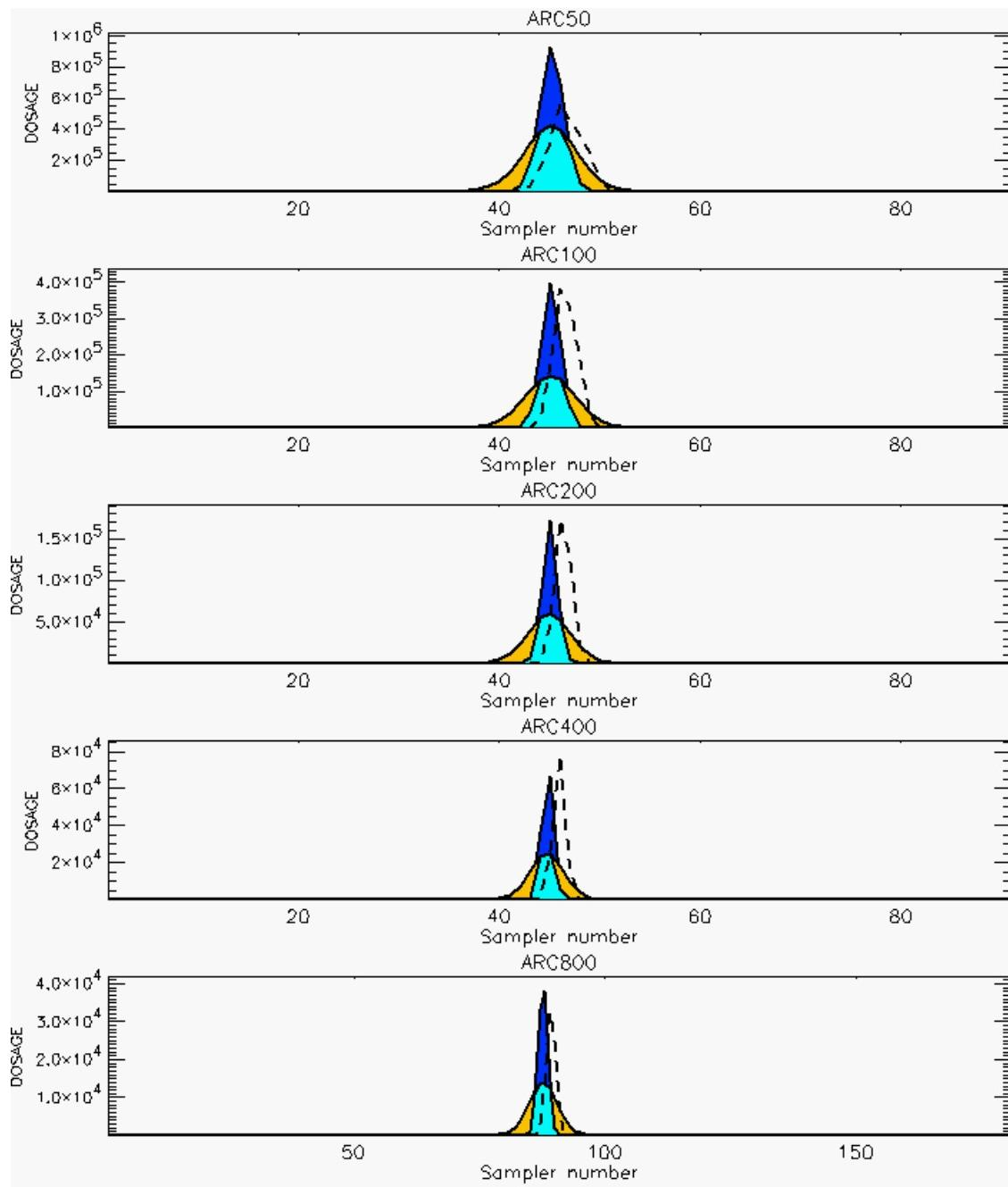
PG Prediction1 to Prediction2 Comparison

PG Trial File: pr_grass_tracer_Experiment_57.txt

PG Prediction File 1: HPAC\nodeposition\pg_57_novd.out

PG Prediction File 2: HPAC\novd_uu(calm)_0250\pg_57_novd.out

**Figure G-46. HPAC With uu(calm) Set to 0.0 or 0.250 Predictions to Trial 57:
Stability Category is 3**



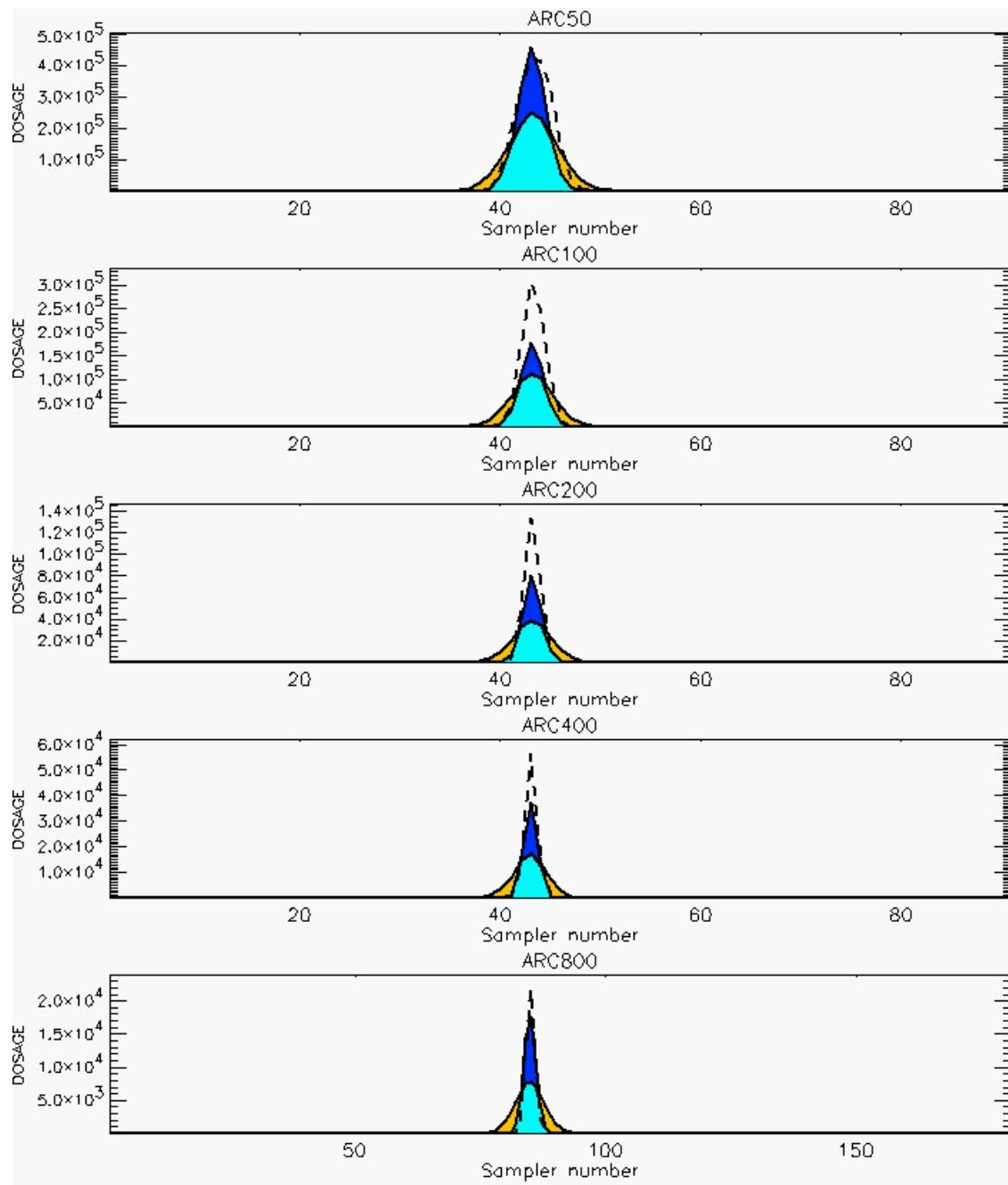
PG Prediction1 to Prediction2 Comparison

PG Trial File: pr_grass_tracer_Experiment_58.txt

PG Prediction File 1: HPAC\nodeposition\pg_58_novd.out

PG Prediction File 2: HPAC\novd_uu calm_0250\pg_58_novd.out

**Figure G-47. HPAC With uu(calm) Set to 0.0 or 0.250 Predictions to Trial 58:
Stability Category is 6**



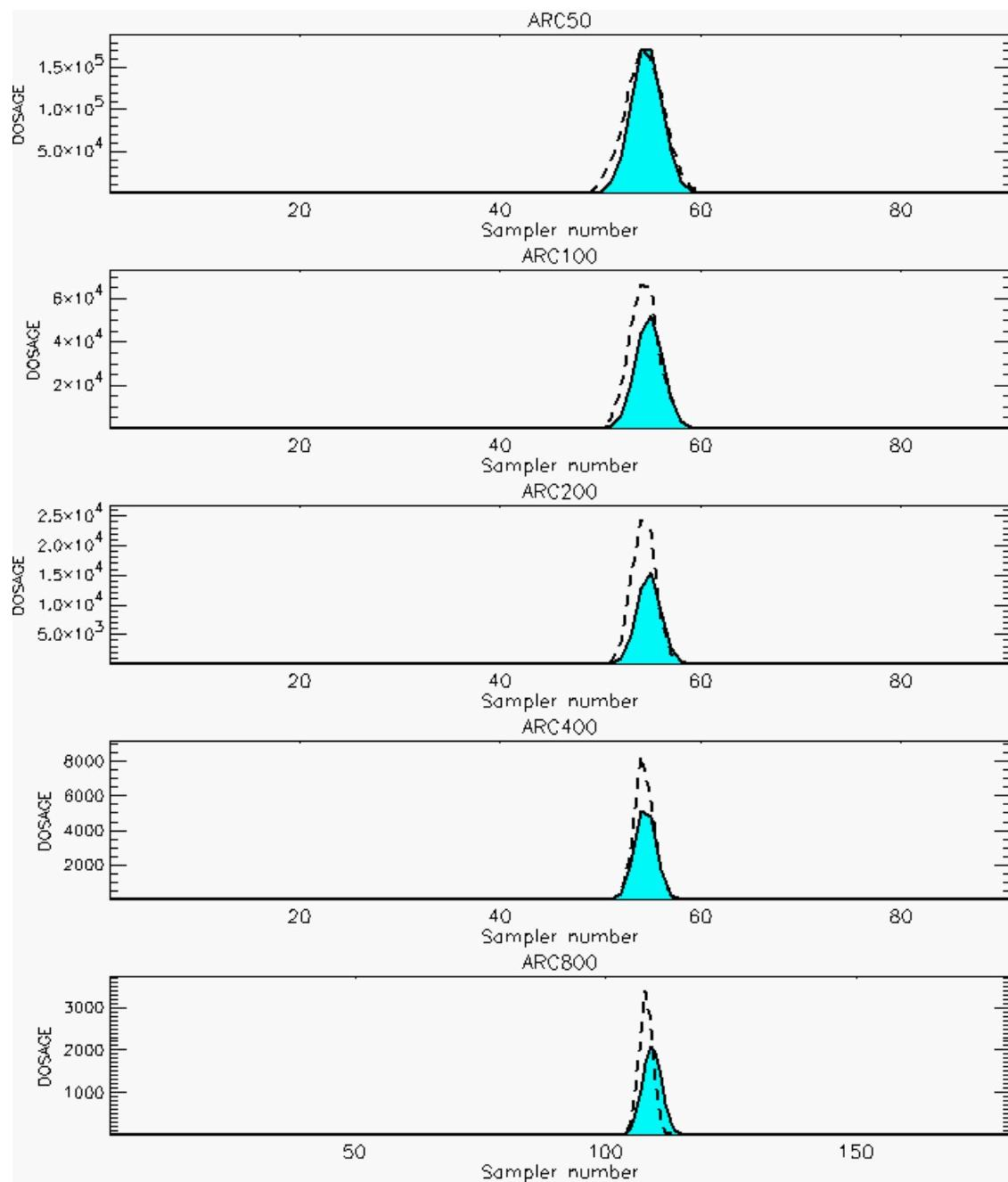
PG Prediction1 to Prediction2 Comparison

PG Trial File: pr_grass_tracer_Experiment_59.txt

PG Prediction File 1: HPAC\nodeposition\pg_59_novd.out

PG Prediction File 2: HPAC\novd_uu_calm_0250\pg_59_novd.out

**Figure G-48. HPAC With uu(calm) Set to 0.0 or 0.250 Predictions to Trial 59:
Stability Category is 5**



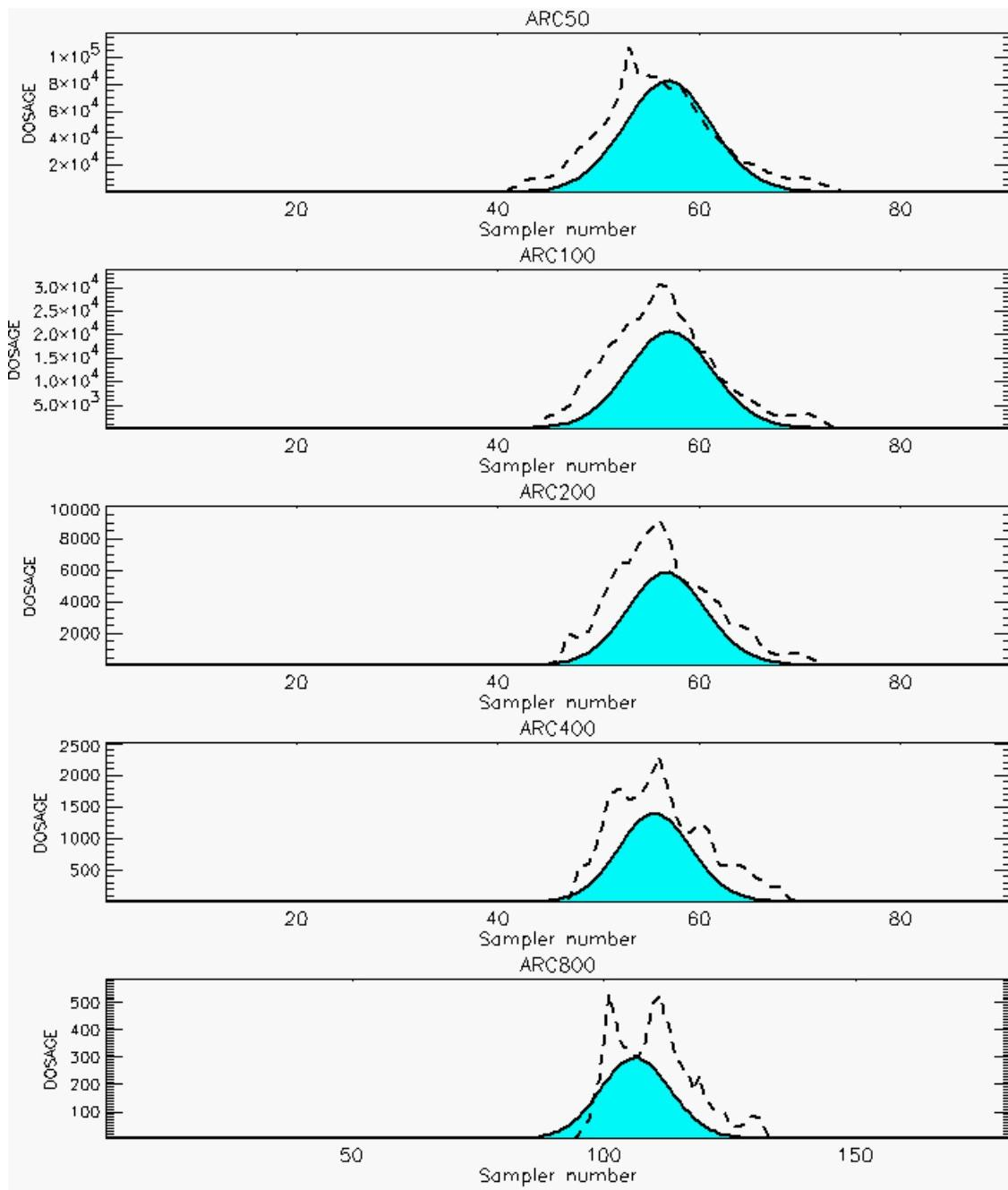
PG Prediction1 to Prediction2 Comparison

PG Trial File: pr_grass_tracer_Experiment_60.txt

PG Prediction File 1: HPAC\nodeposition\pg_60_nozd.out

PG Prediction File 2: HPAC\nozd_uu(calm)_0250\pg_60_nozd.out

**Figure G-49. HPAC With uu(calm) Set to 0.0 or 0.250 Predictions to Trial 60:
Stability Category is 5**



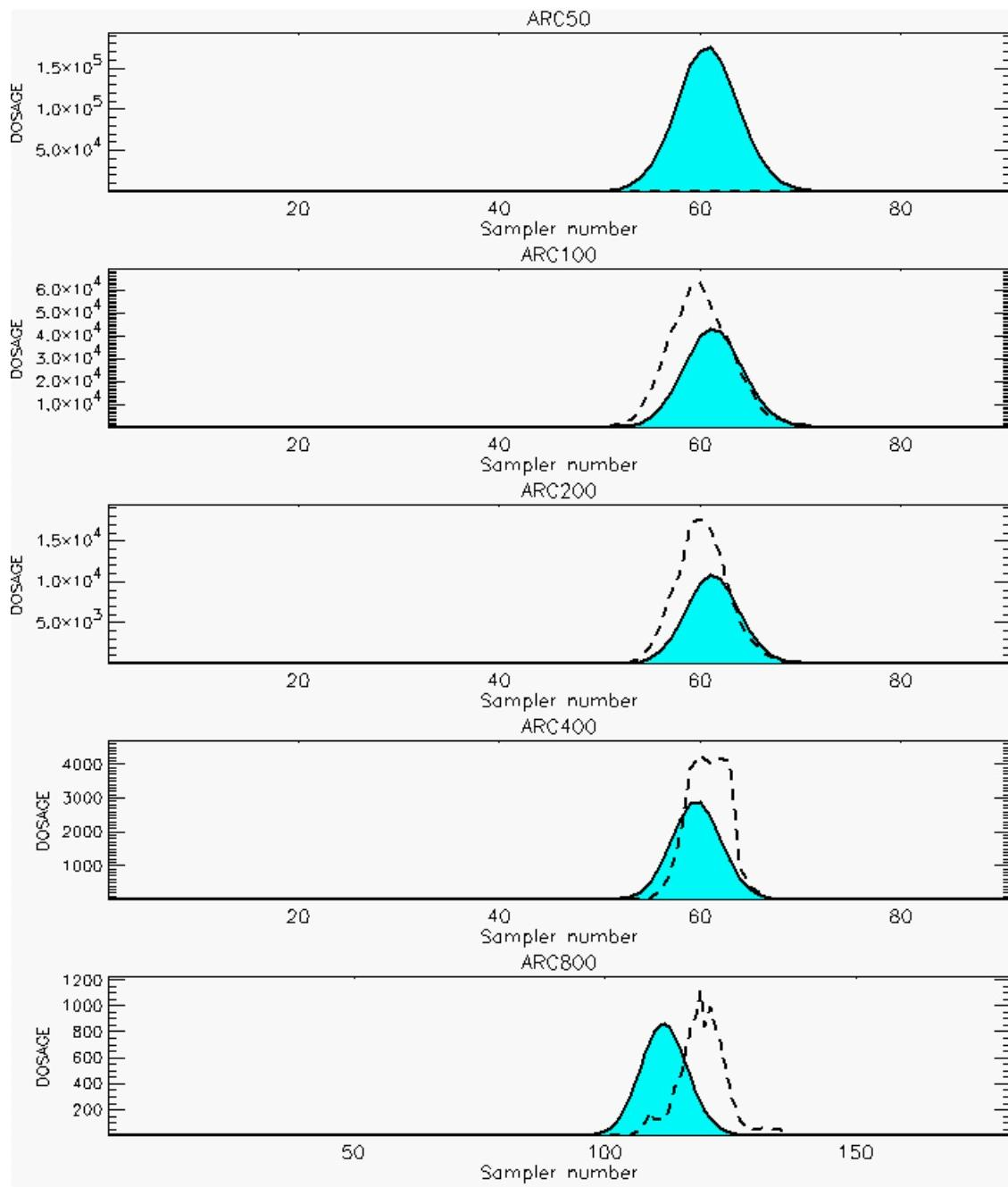
PG Prediction1 to Prediction2 Comparison

PG Trial File: pr_grass_tracer_Experiment_61.txt

PG Prediction File 1: HPAC\nodeposition\pg_61_noxd.out

PG Prediction File 2: HPAC\noxd_uu calm_0250\pg_61_noxd.out

**Figure G-50. HPAC With uu(calm) Set to 0.0 or 0.250 Predictions to Trial 61:
Stability Category is 3**



PG Prediction1 to Prediction2 Comparison

PG Trial File: pr_grass_tracer_Experiment_62.txt

PG Prediction File 1: HPAC\nodeposition\pg_62_novd.out

PG Prediction File 2: HPAC\novd_uu calm_0250\pg_62_novd.out

**Figure G-51. HPAC With uu(calm) Set to 0.0 or 0.250 Predictions to Trial 62:
Stability Category is 2**

REFERENCES

- G-1. Barad, M. L. (Editor), *Project Prairie Grass, A Field Program in Diffusion*, Geophysical Research Papers No. 59, Volumes I and II, DTIC #AD-152572/AFCRC-TR-58-235(I), Air Geophysical Laboratory, Hanscom Air Force Base, MA, 1958.
- G-2. Irwin, J. S. and Rosu, M-R., *Comments on a Draft Practice for Statistical Evaluation of Atmospheric Dispersion Models*, Proceedings of the 10th Joint Conference on the Applications of Air Pollution Meteorology. American Meteorological Society, Boston, pp. 6-10, 1998.

APPENDIX H
RESULTS AND ANALYSES:
SUPPLEMENTAL FIGURES FOR MOEs

APPENDIX H

RESULTS AND ANALYSES:

SUPPLEMENTAL FIGURES FOR MOEs

This appendix contains some of the MOE comparisons that were done for HPAC and NARAC. The first four figures (H-1 through H-4) present MOE 1 comparisons for $C_{FN} = C_{FP} = 1$. The next four figures (H-5 through H-8) present MOE 1 comparisons for $C_{FN} = 5$ and $C_{FP} = 0.5$. MOEs based on AE1 and AE2 are presented, and comparisons based on arc range and stability category grouping (SCG) are shown. The figures shown are based on the nominal linear comparisons of predictions and observations. Although not deposited here, we also computed all MOE 1 values based the logarithms of the compared predictions and observations (see the figures labeled with the “b” in Appendices C and D).

The next eight figures (H-9 through H-16) present MOE 1 (for $C_{FN} = C_{FP} = 1$ and $C_{FN} = 5$, $C_{FP} = 0.5$) results based on using two probit curves as a lethality/effects filter. We computed these MOEs for the LD₅₀ values and probit slopes shown in Table H-1. The example lethality/effects filter figures shown in this appendix are for LD₅₀ values of 100 and 5,000 mg·sec/m³.

Table H-1. LD₅₀ Values and Probit Slopes Used for Lethality/Effects Filter Calculations

LD ₅₀ Value (mg·sec/m ³)	Slope
3	2
10	2
100	6
1,000	6
2,000	12
5,000	12
10,000	12
50,000	6

The comparisons shown in this appendix are based on a threshold dosage value of 60 mg-sec/m³ as described in Chapter 2. We also completed a set of HPAC and NARAC comparisons to *Prairie Grass* trials at a dosage threshold of 3 mg-sec/m³. The results and conclusions based on the two different threshold dosage values are substantially similar. A few of the results at the lower threshold level are briefly described in Chapter 3.

The next eight figures present the comparative results for MOE 2, the 2D MOE. The first four (H-17 through H-20) figures present the results for HPAC and NARAC comparisons using AE1 and AE2. Comparisons as a function of range and stability category grouping are provided. The figures shown are based on the nominal linear comparisons of predictions and observations. Although not deposited here, we also computed all MOE 2 values based the logarithms of the compared predictions and observations (see the figures labeled with the “b” in Appendices C and D).

The final four figures (H-21 through H-24) present MOE 2 results based on the usage of the lethality/effects filter methodology – in this case, a probit curve. As was true for MOE 1, the example lethality/effects filter figures shown in this appendix are for LD₅₀ values of 100 and 5,000 mg-sec/m³. However, we computed MOE 2 for all of the probit curves described in Figure H-1.

All of the MOE calculations (with threshold = 60 mg-sec/m³) discussed in this appendix were also completed for comparisons of HPAC predictions with and without surface deposition and with two settings of the uu(calm) feature (0.0 and 0.25).¹ Similarly, MOEs were computed for NARAC predictions with and without surface deposition and included using an experimental sigma-v value. The figures associated with the HPAC and NARAC excursion comparisons are available, but, other than a few used directly in the discussions of Chapter 3, they have not been included in this report.

¹ See Appendices F, G, L, and M for additional information and individual trial comparisons under these conditions.

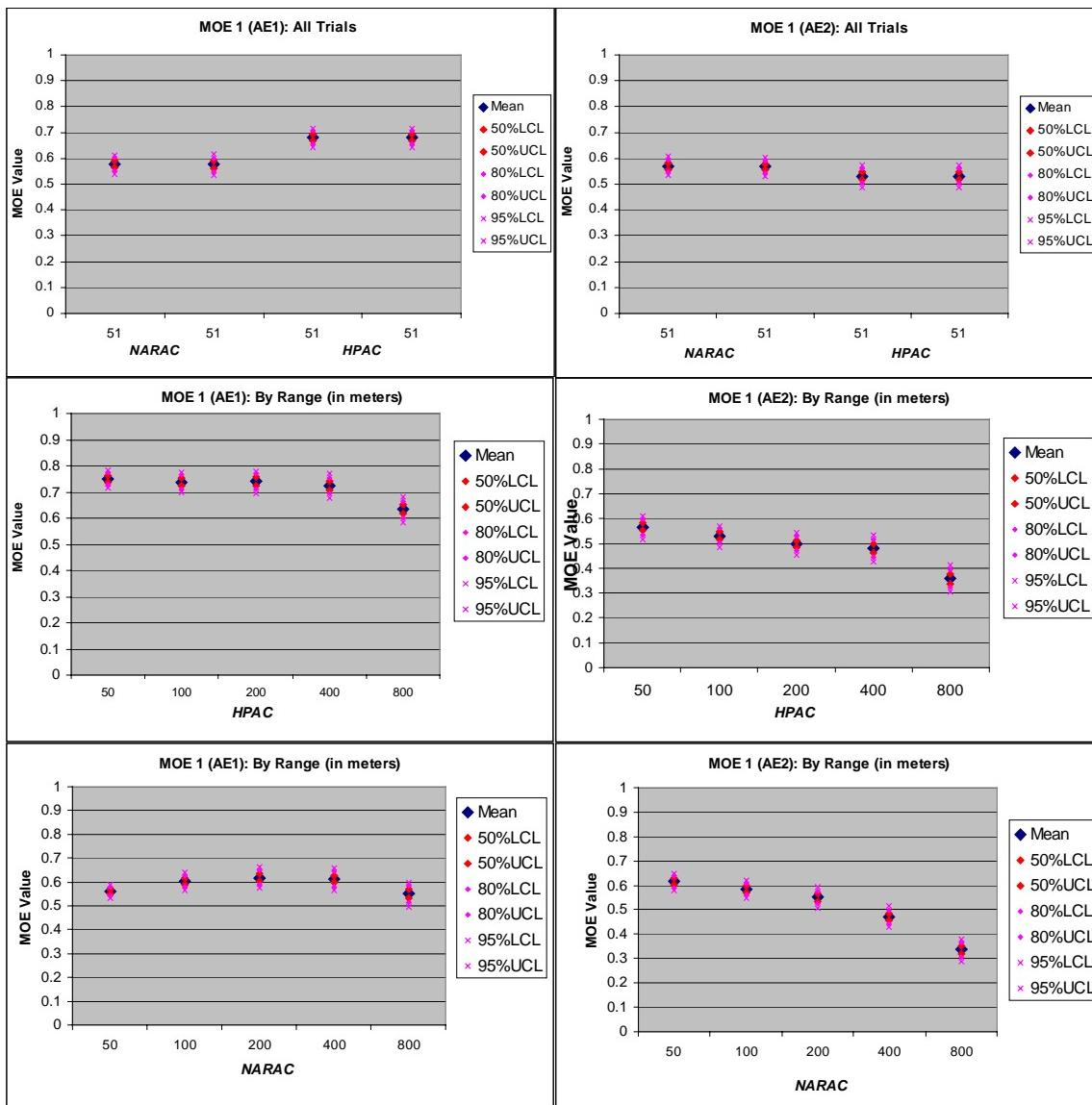
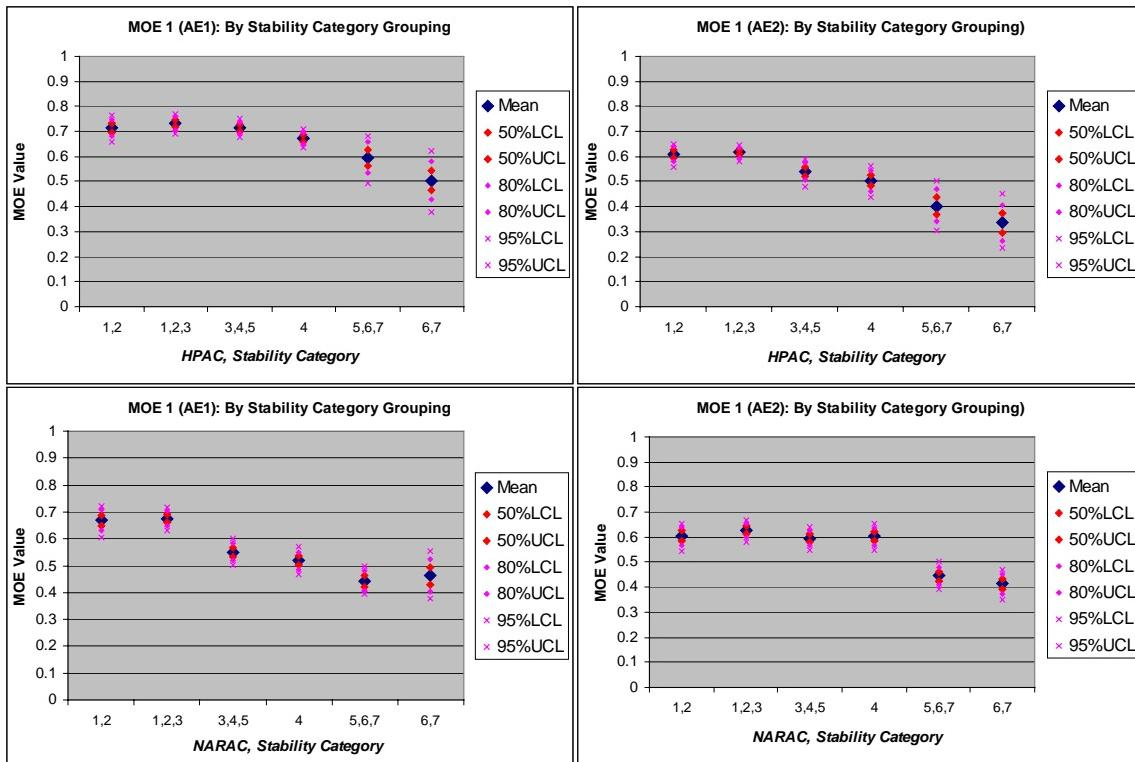
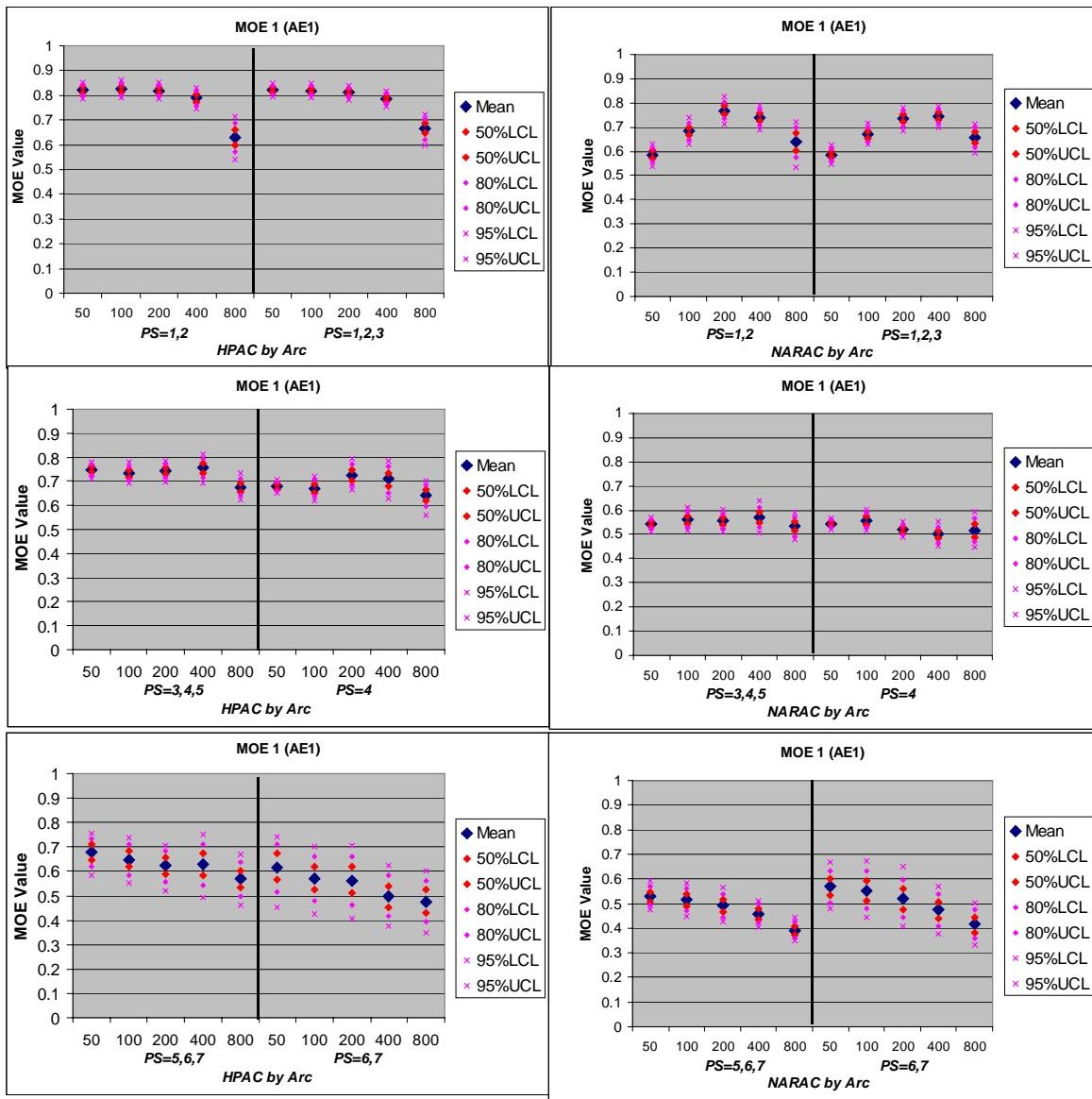


Figure H-1. MOE 1 ($C_{FN} = C_{FP} = 1.0$): HPAC and NARAC Comparisons to Prairie Grass Trials {All Trials and By Range for AE1 and AE2}²

-
- 2 The “All Trials” comparisons show two estimates of the uncertainty for each model. This redundancy allows one to assess the relative amount of variance due to the choice of bootstrap sample size, 1,000. The “51” label on the x-axis refers to the number of Prairie Grass trials considered in the comparison.



**Figure H-2. MOE 1 ($C_{FN} = C_{FP} = 1.0$): HPAC and NARAC Comparisons to Prairie Grass Trials
{By Stability Category Grouping (SCG) for AE1 and AE2}**



**Figure H-3. MOE 1 ($C_{FN} = C_{FP} = 1.0$): HPAC and NARAC Comparisons to Prairie Grass Trials
(SCG × Range for AE1)**

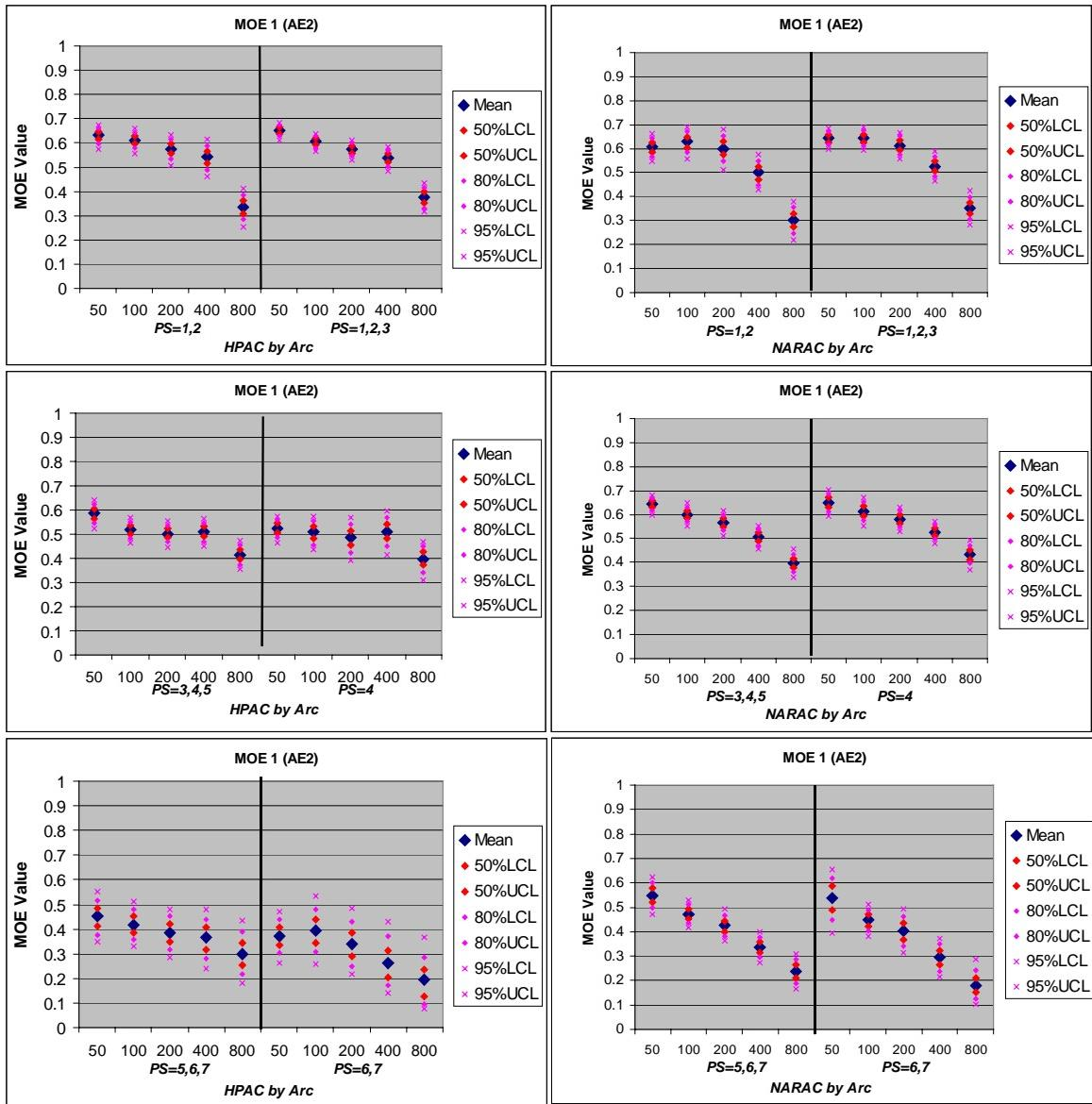


Figure H-4. MOE 1 ($C_{FN} = C_{FP} = 1.0$): HPAC and NARAC Comparisons to Prairie Grass Trials {SCG \times Range for AE2}

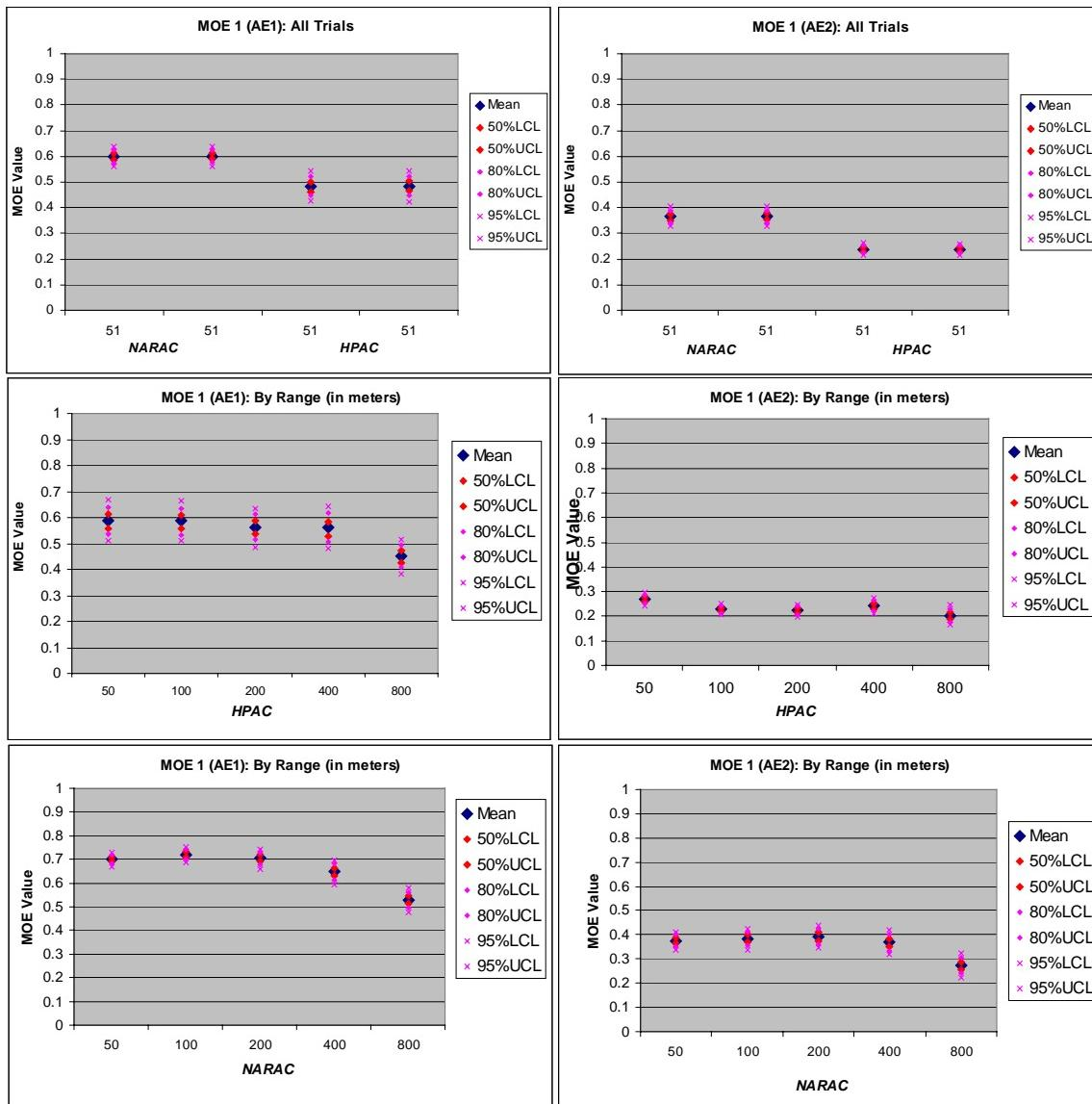


Figure H-5. MOE 1 ($C_{FN} = 5$, $C_{FP} = 0.5$): HPAC and NARAC Comparisons to Prairie Grass Trials {All Trials and By Range for AE1 and AE2}³

³ The “All Trials” comparisons show two estimates of the uncertainty for each model. This allows one to assess the relative amount of variance due to the choice of bootstrap sample size, 1,000.

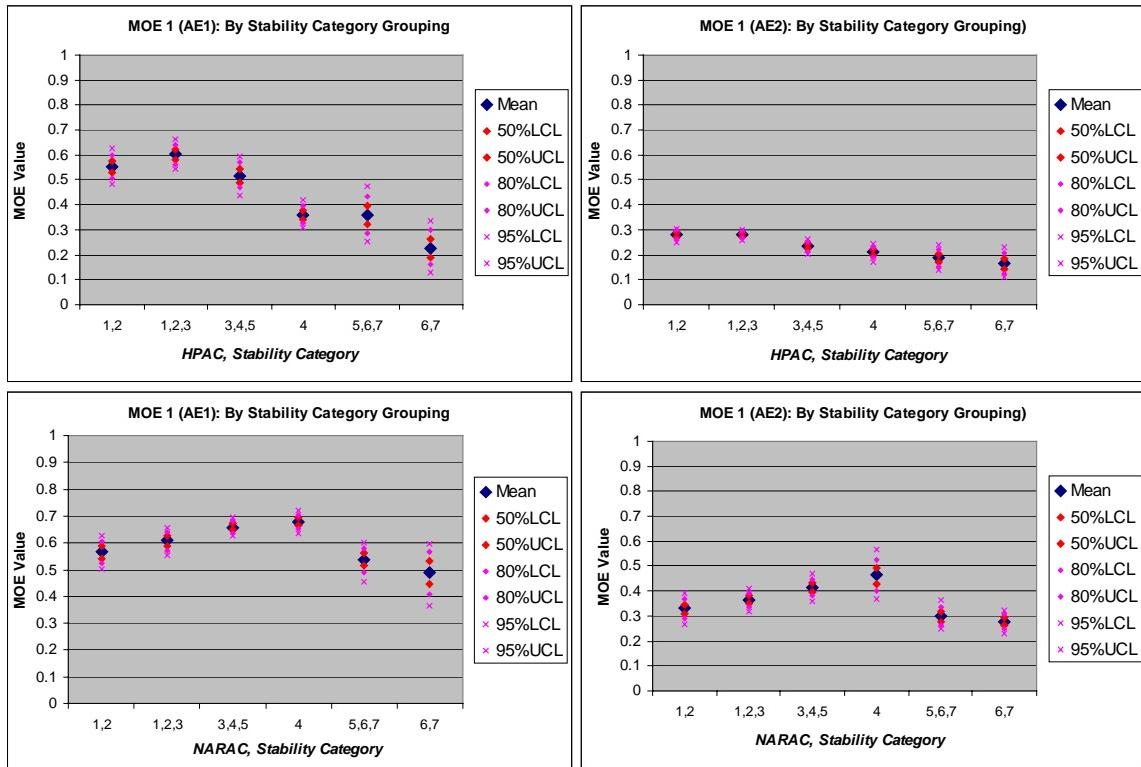


Figure H-6. MOE 1 ($C_{FN} = 5$, $C_{FP} = 0.5$): HPAC and NARAC Comparisons to Prairie Grass Trials {By Stability Category Grouping (SCG) for AE1 and AE2}

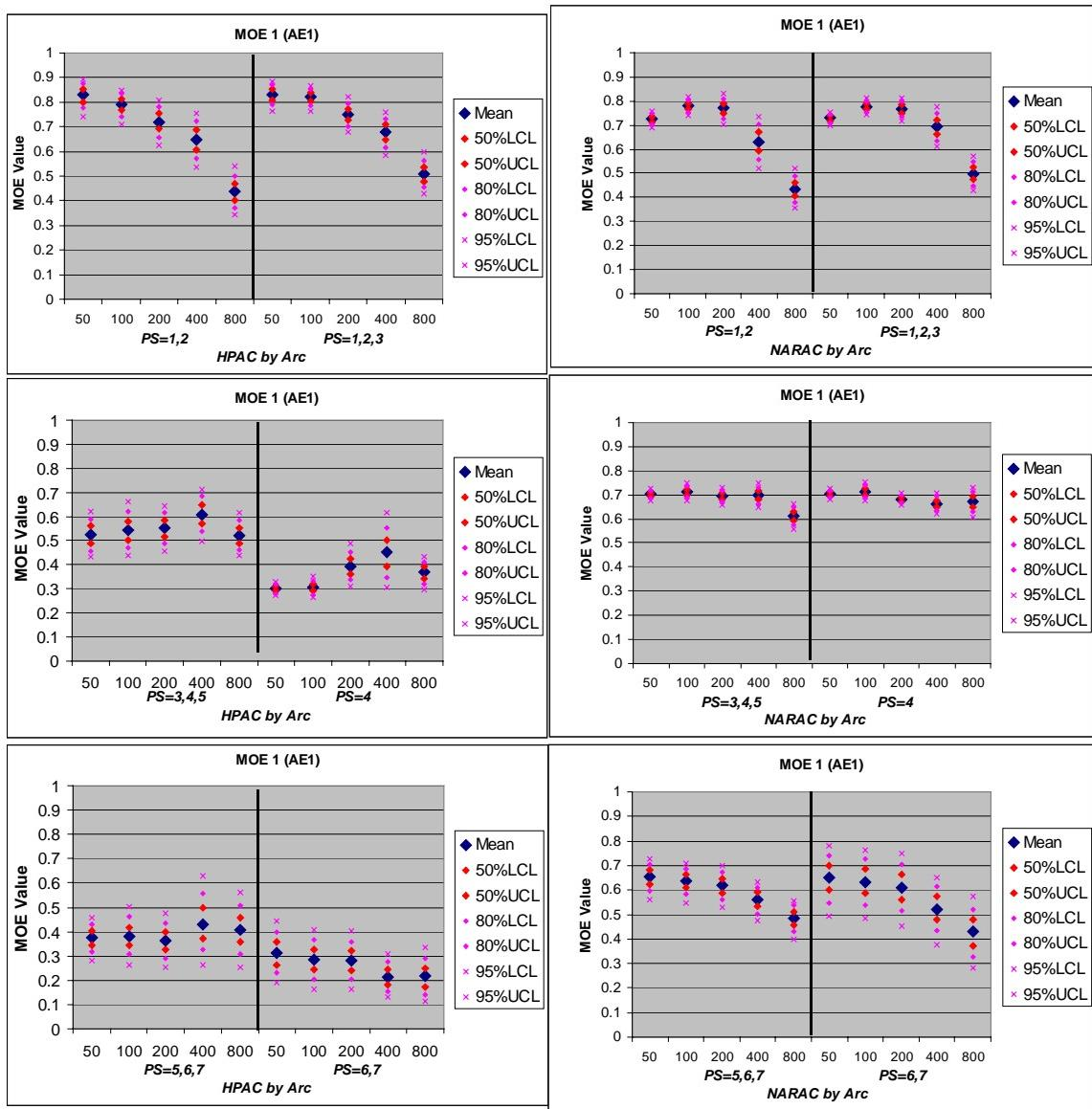


Figure H-7. MOE 1 ($C_{FN} = 5$, $C_{FP} = 0.5$): HPAC and NARAC Comparisons to Prairie Grass Trials {SCG \times Range for AE1}

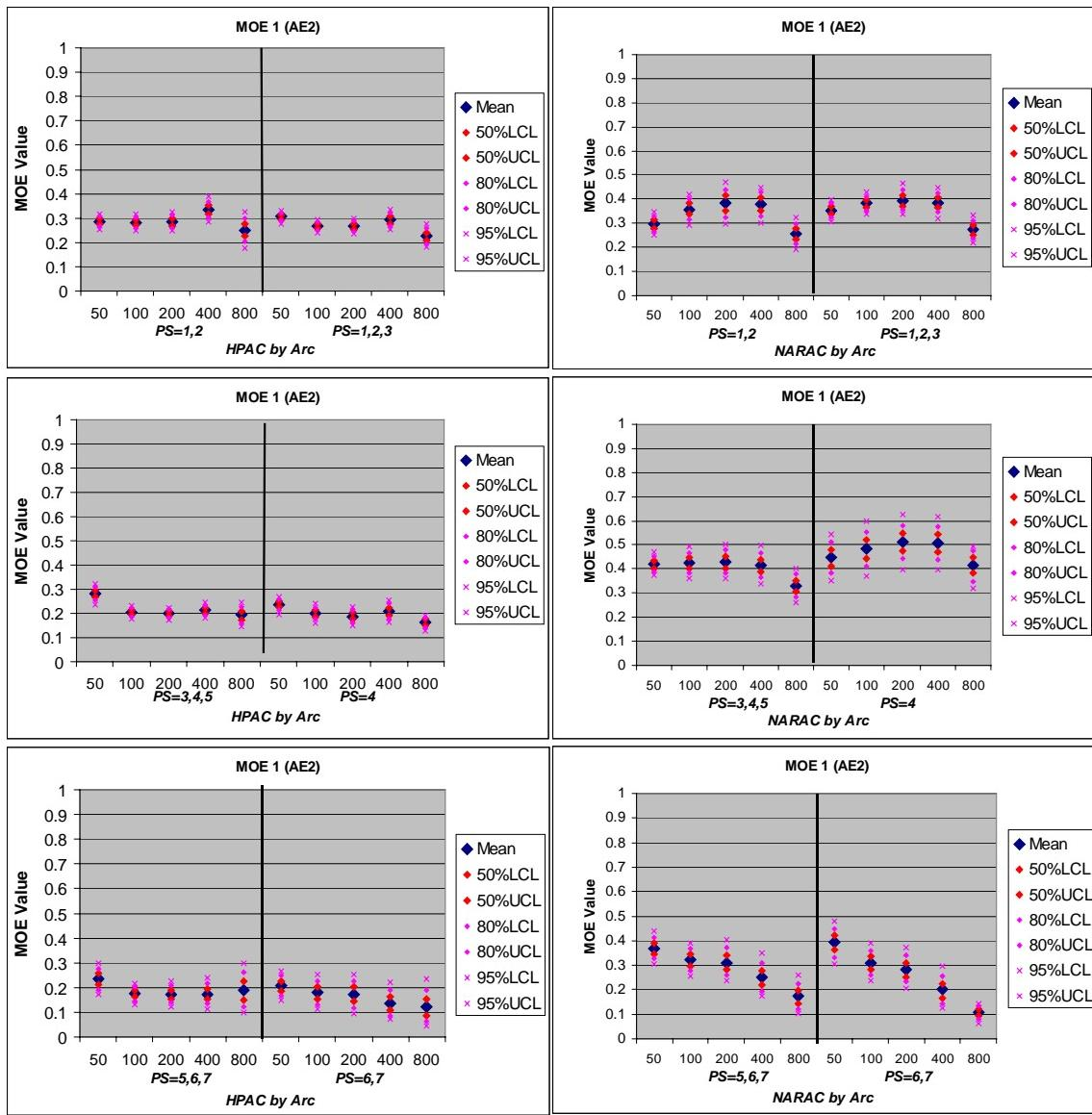


Figure H-8. MOE 1 ($C_{FN} = 5$, $C_{FP} = 0.5$): HPAC and NARAC Comparisons to Prairie Grass Trials {SCG \times Range for AE2}

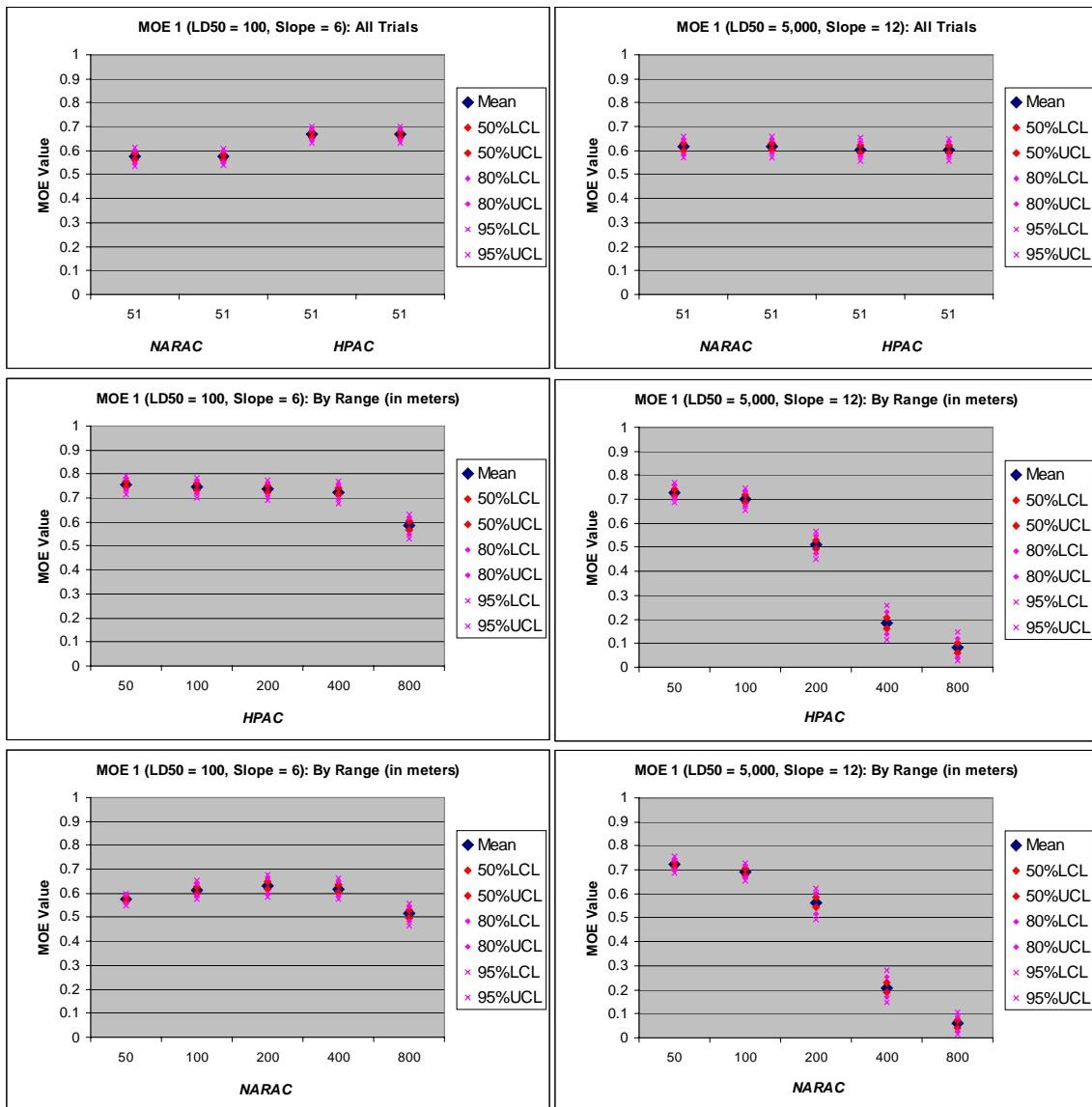


Figure H-9. MOE 1 ($C_{FN} = C_{FP} = 1.0$): HPAC and NARAC Comparisons to Prairie Grass Trials {All Trials and By Range for Two Probit Curves}⁴

⁴ The “All Trials” comparisons show two estimates of the uncertainty for each model. This allows one to assess the relative amount of variance due to the choice of bootstrap sample size, 1,000.

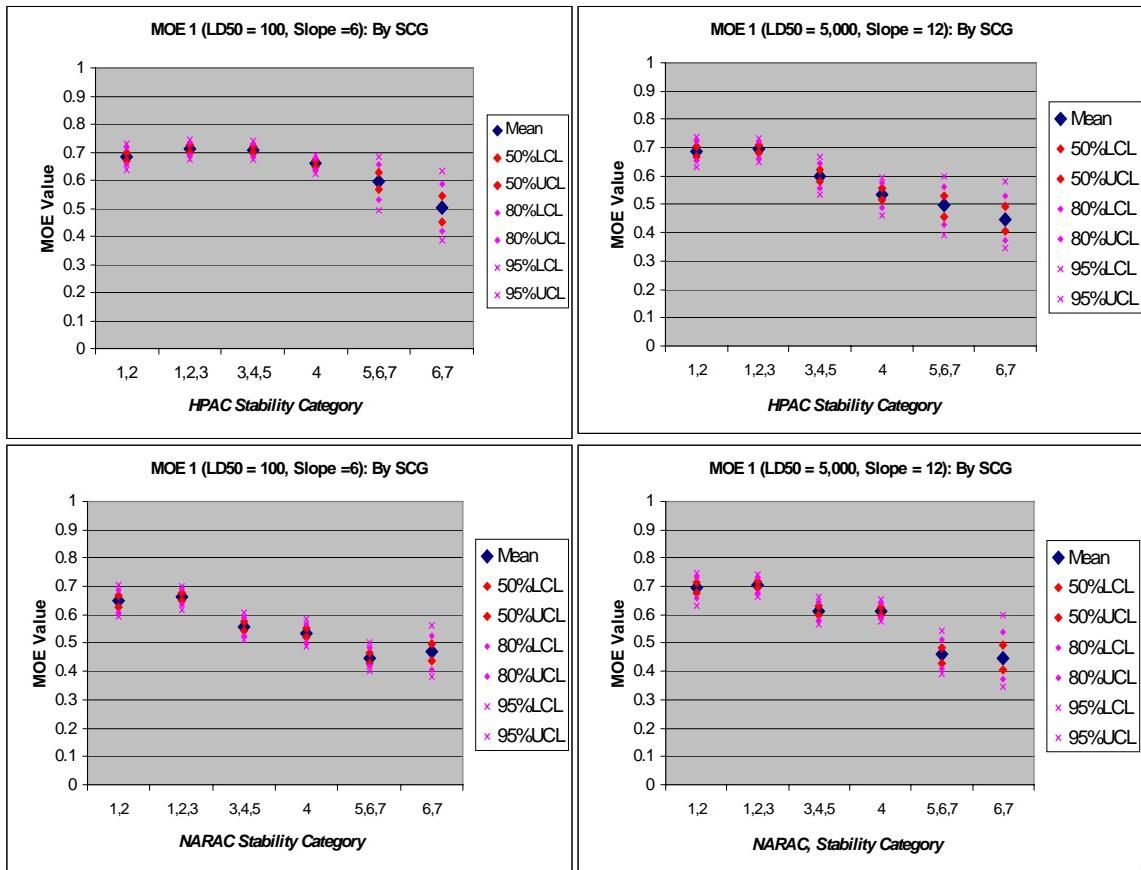


Figure H-10. MOE 1 ($C_{FN} = C_{FP} = 1.0$): HPAC and NARAC Comparisons to Prairie Grass Trials {By Stability Category Grouping (SCG) for Two Probit Curves}

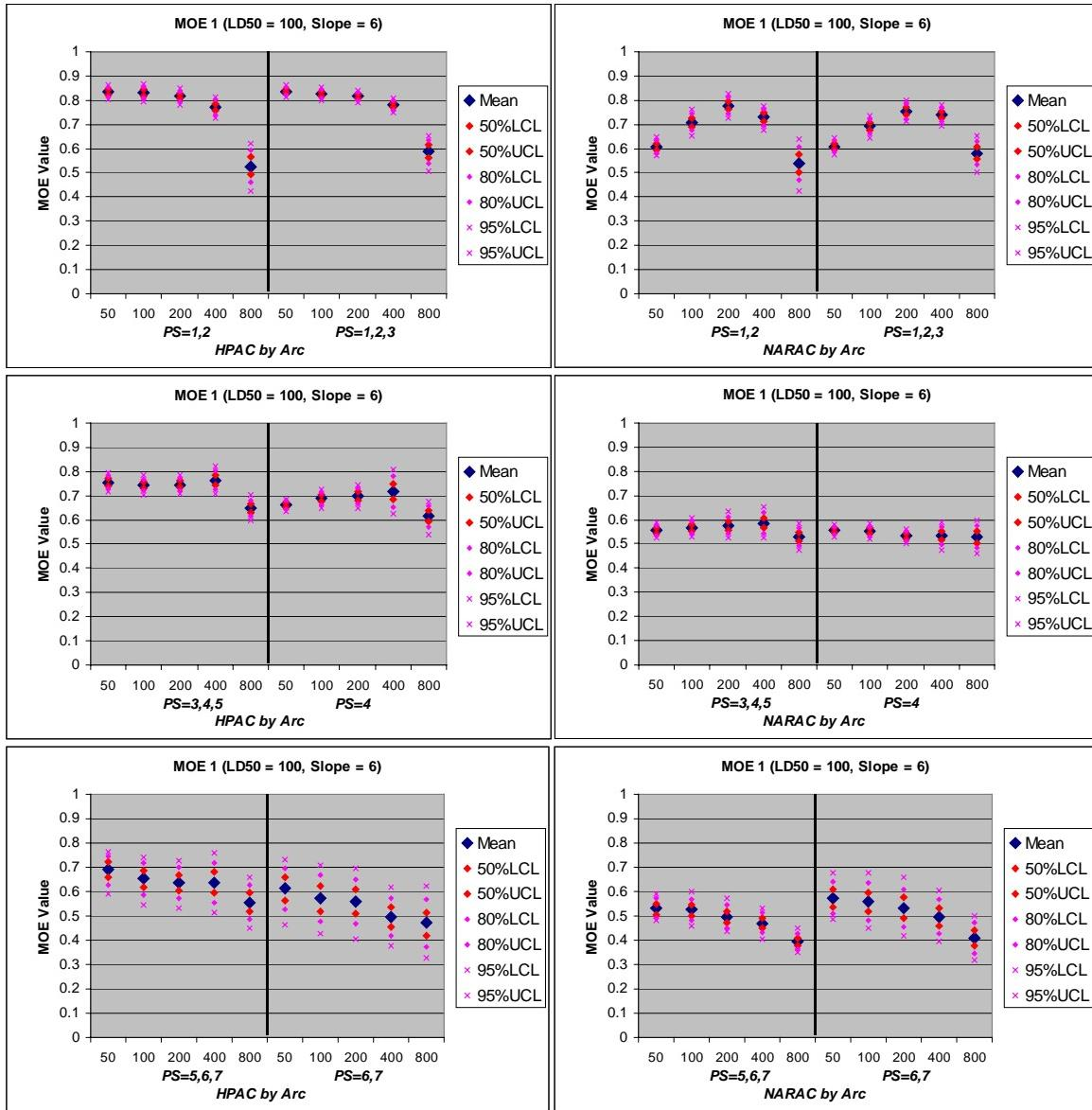


Figure H-11. MOE 1 ($C_{FN} = C_{FP} = 1.0$): HPAC and NARAC Comparisons to Prairie Grass Trials {SCG \times Range for $LD_{50} = 100$, Probit Slope = 6}

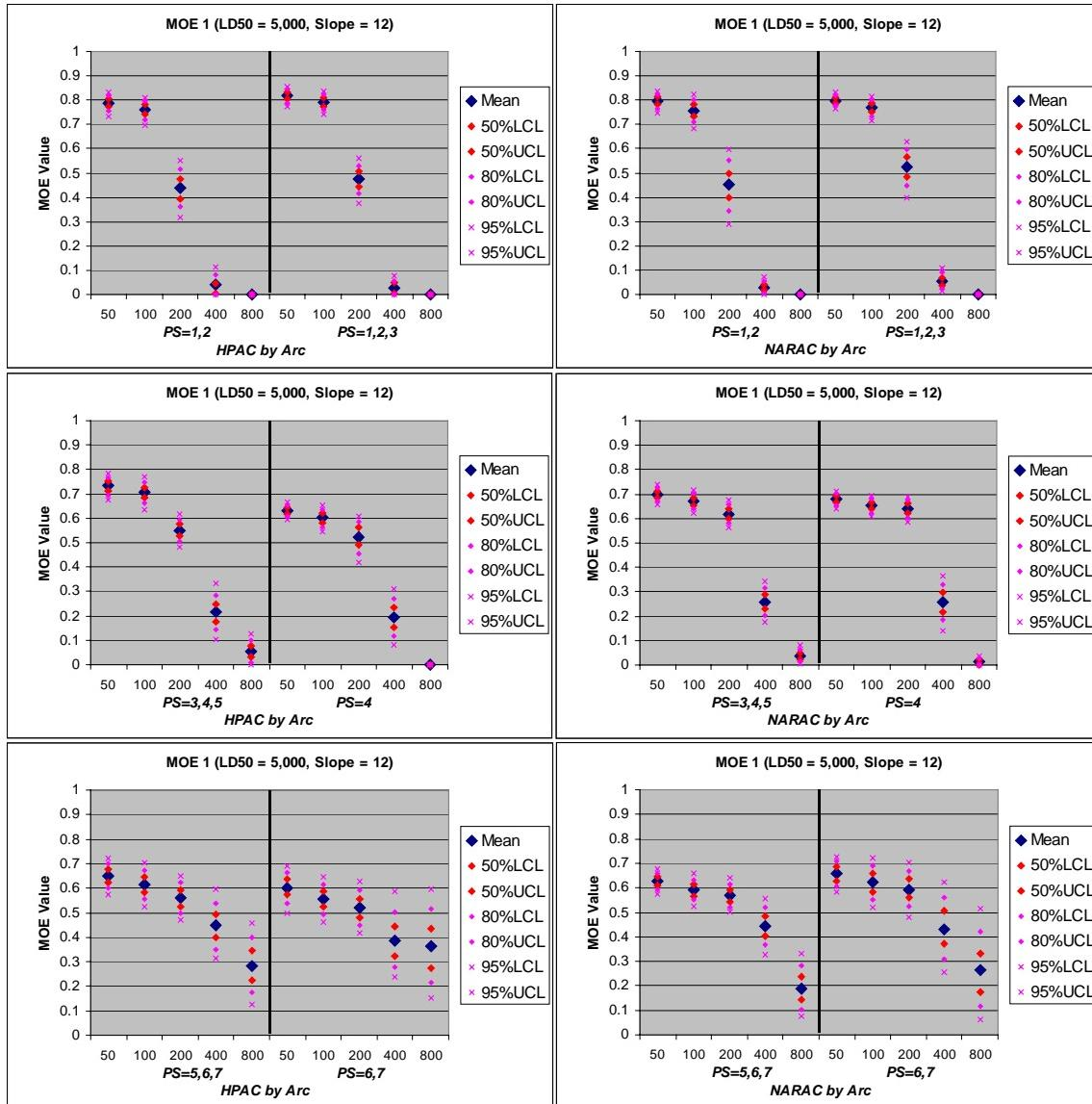


Figure H-12. MOE 1 ($C_{FN} = C_{FP} = 1.0$): HPAC and NARAC Comparisons to Prairie Grass Trials {SCG \times Range for LD₅₀ = 5,000, Probit Slope = 12}

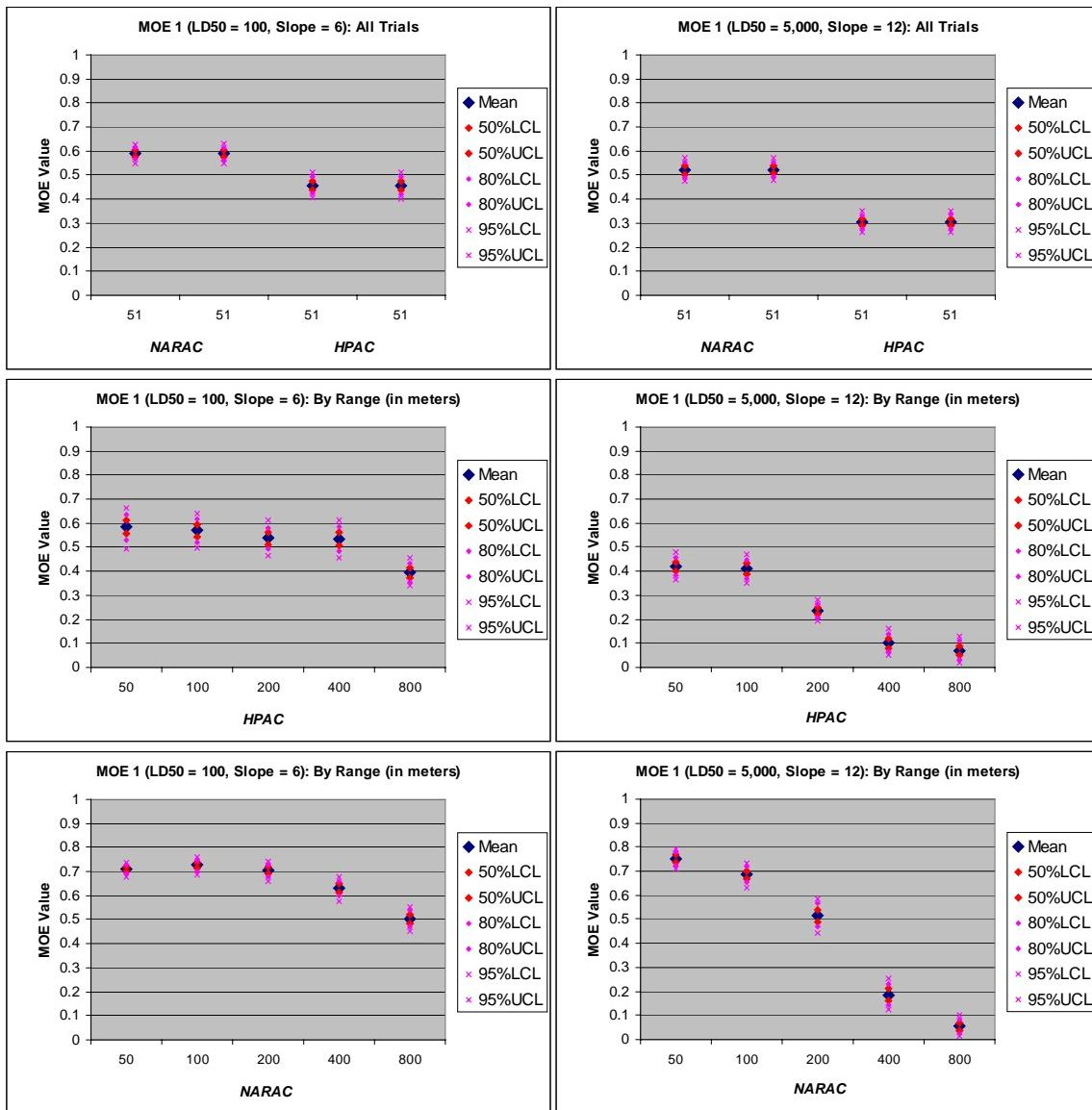


Figure H-13. MOE 1 ($C_{FN} = 5$, $C_{FP} = 0.5$): HPAC and NARAC Comparisons to Prairie Grass Trials {All Trials and By Range for Two Probit Curves}⁵

⁵ The “All Trials” comparisons show two estimates of the uncertainty for each model. This allows one to assess the relative amount of variance due to the choice of bootstrap sample size, 1,000.

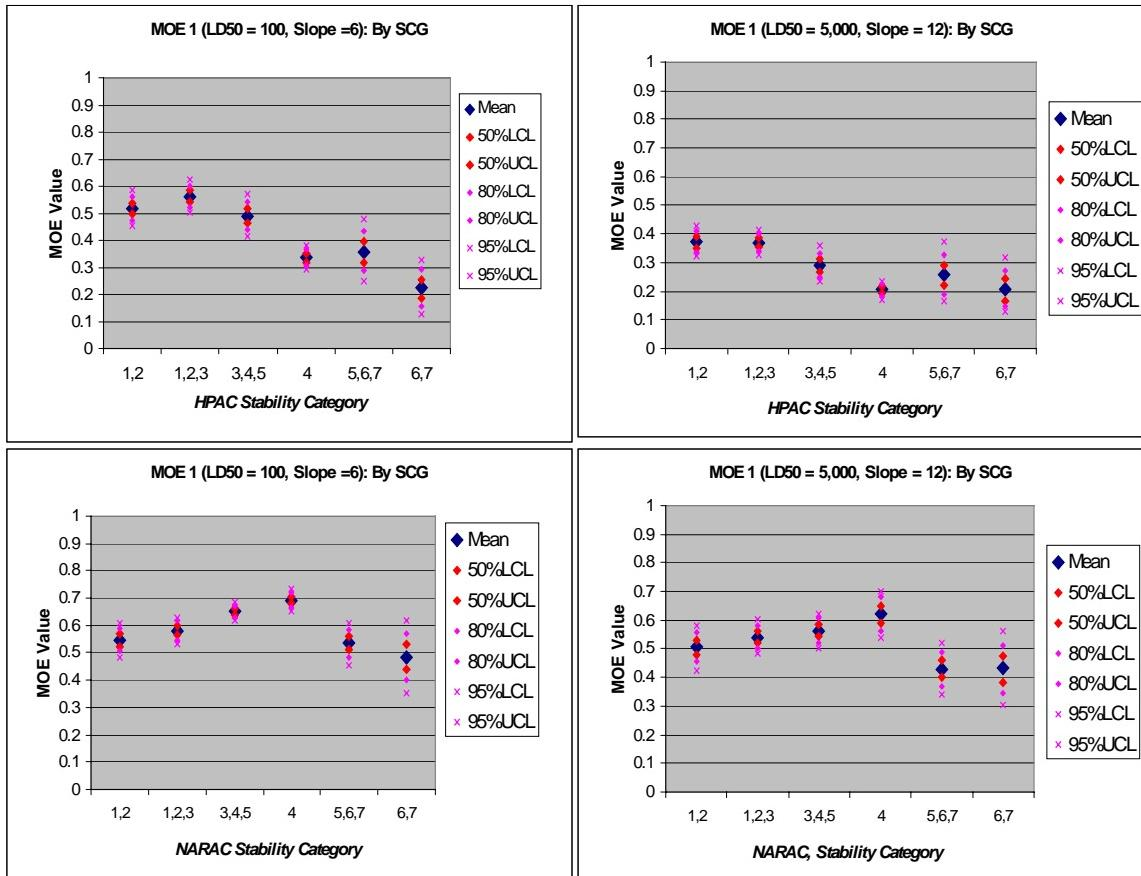


Figure H-14. MOE 1 ($C_{FN} = 5$, $C_{FP} = 0.5$): HPAC and NARAC Comparisons to Prairie Grass Trials {By Stability Category Grouping (SCG) for Two Probit Curves}

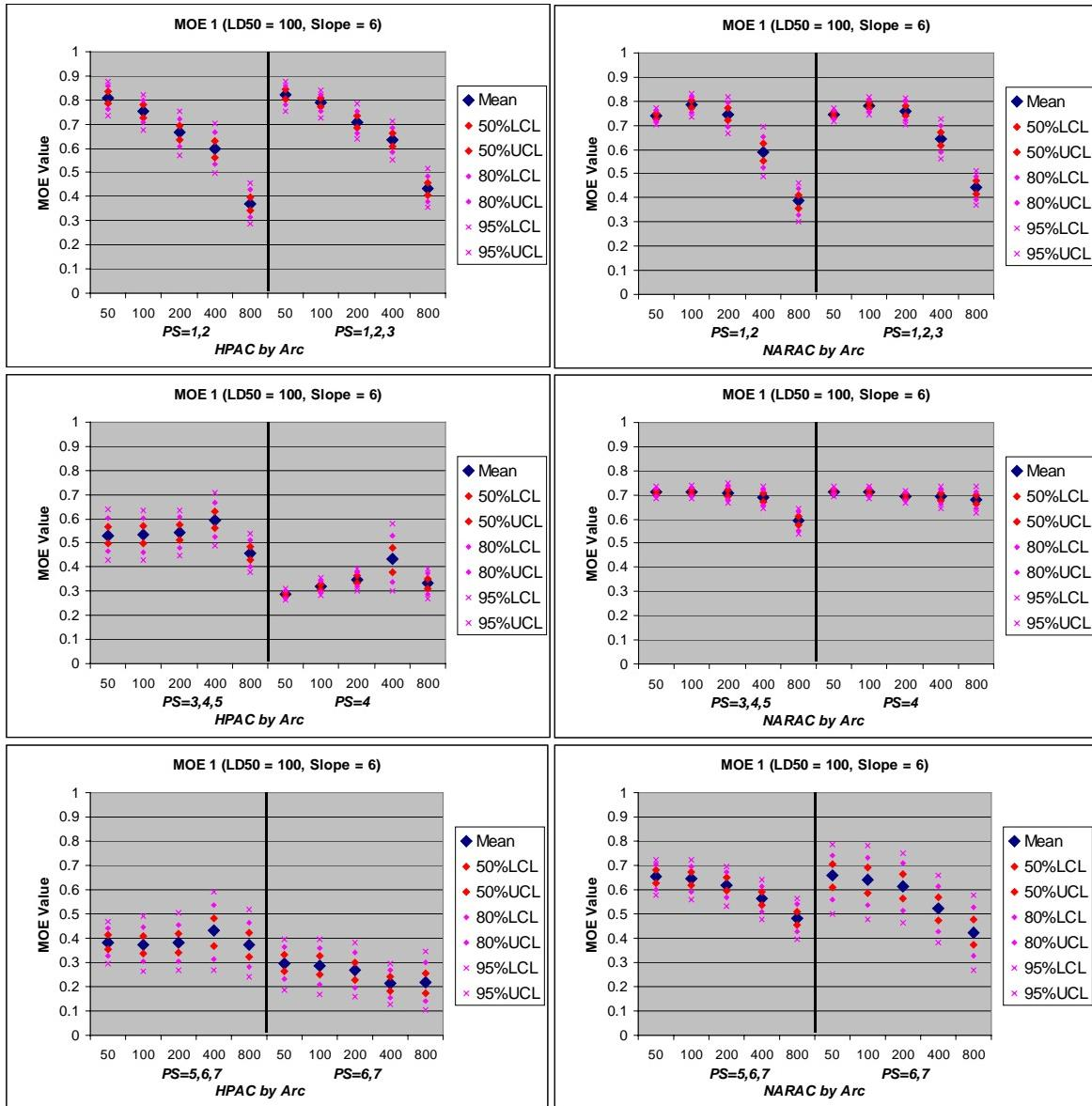


Figure H-15. MOE 1 ($C_{FN} = 5$, $C_{FP} = 0.5$): HPAC and NARAC Comparisons to Prairie Grass Trials {SCG × Range for $LD_{50} = 100$, Probit Slope = 6}

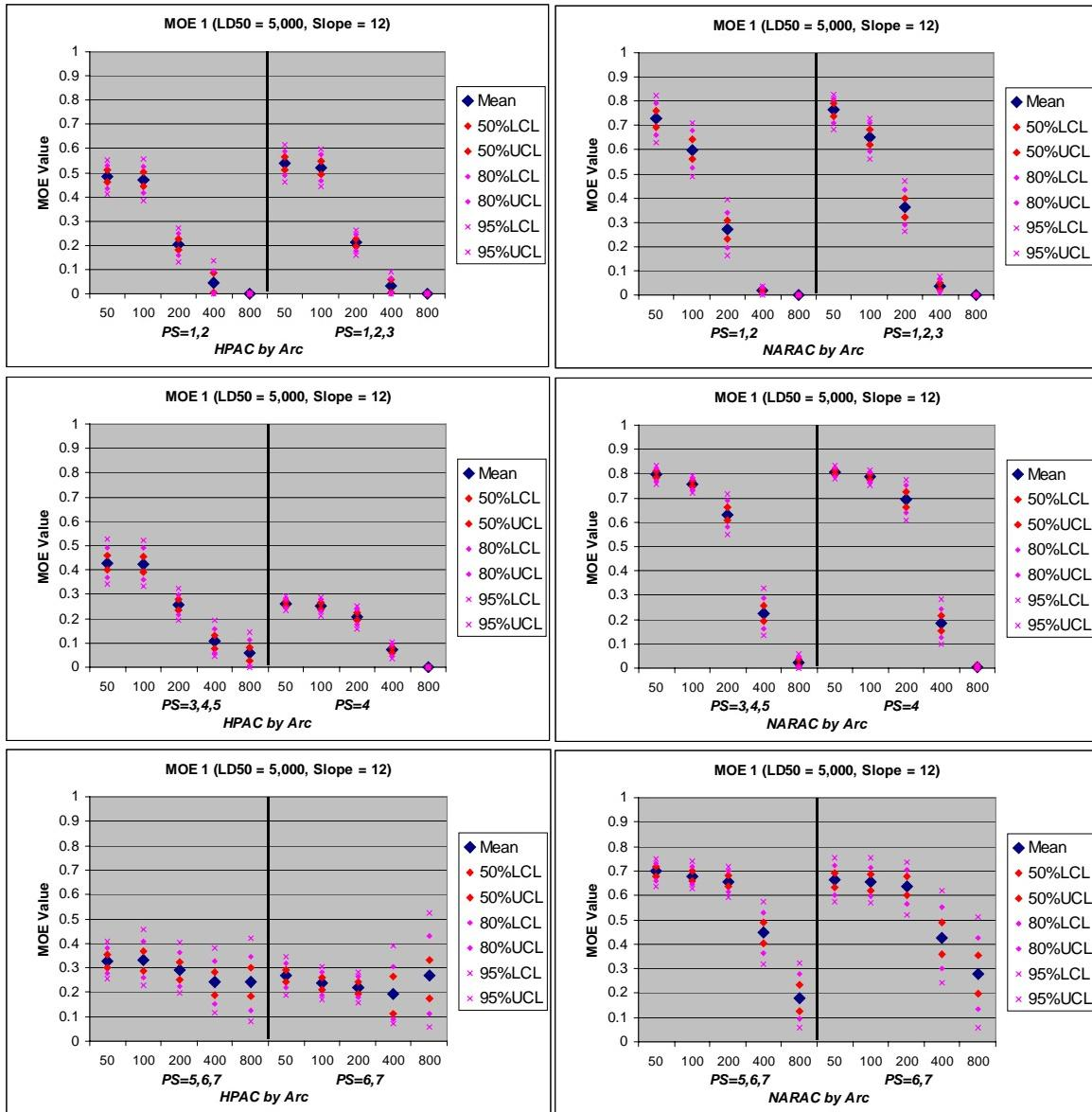


Figure H-16. MOE 1 ($C_{FN} = 5$, $C_{FP} = 0.5$): HPAC and NARAC Comparisons to Prairie Grass Trials {SCG \times Range for $LD_{50} = 5,000$, Probit Slope = 12}

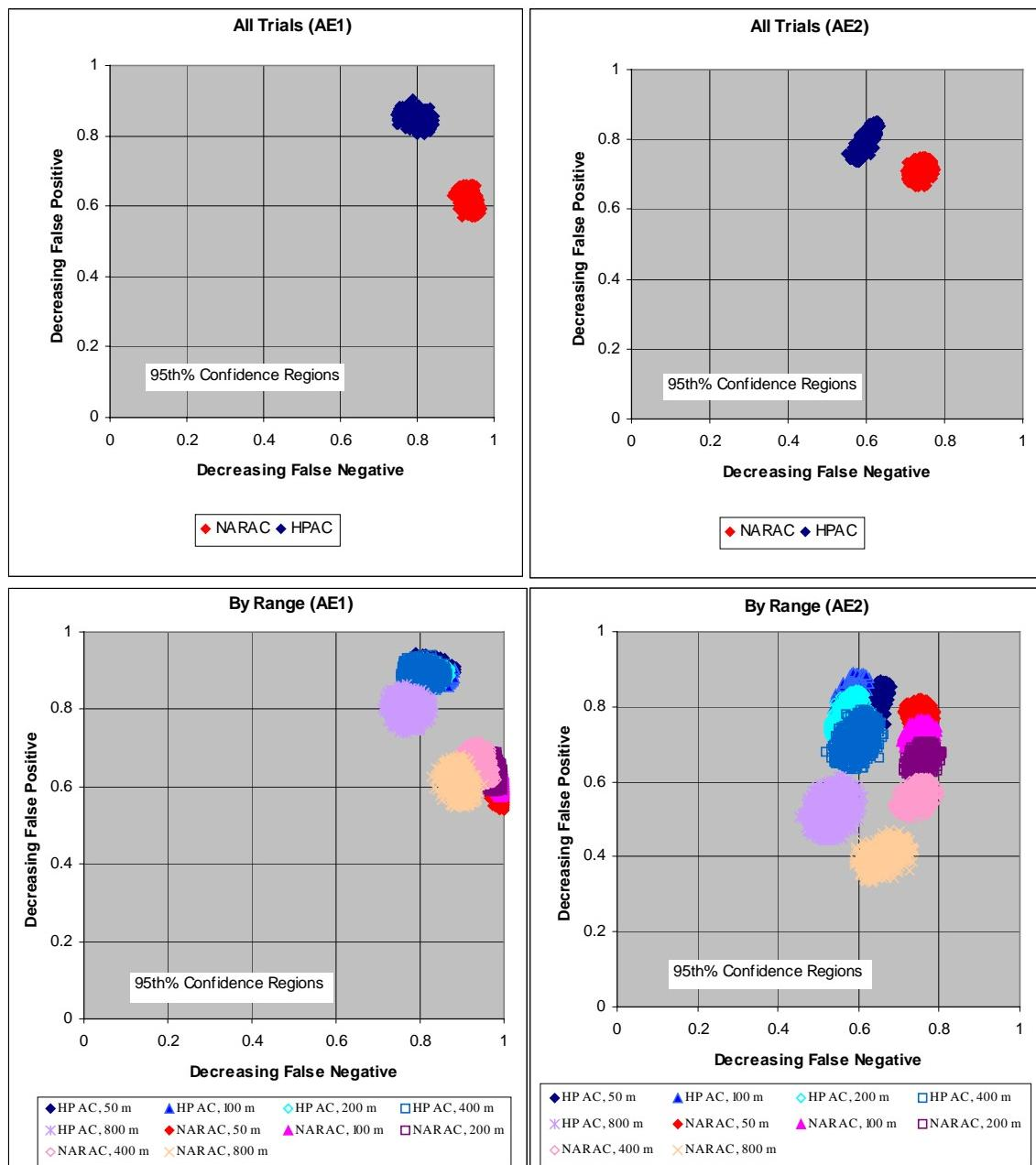


Figure H-17. MOE 2: HPAC and NARAC Comparisons to Prairie Grass Trials {All Trials and By Range for AE1 and AE2}⁶

⁶ The points shown in the above plots correspond to the approximate 95th percent confidence regions associated with the MOE 2 point estimates. These confidence regions were obtained via bootstrap techniques. The actual point estimates lie at approximately the center of these confidence regions.

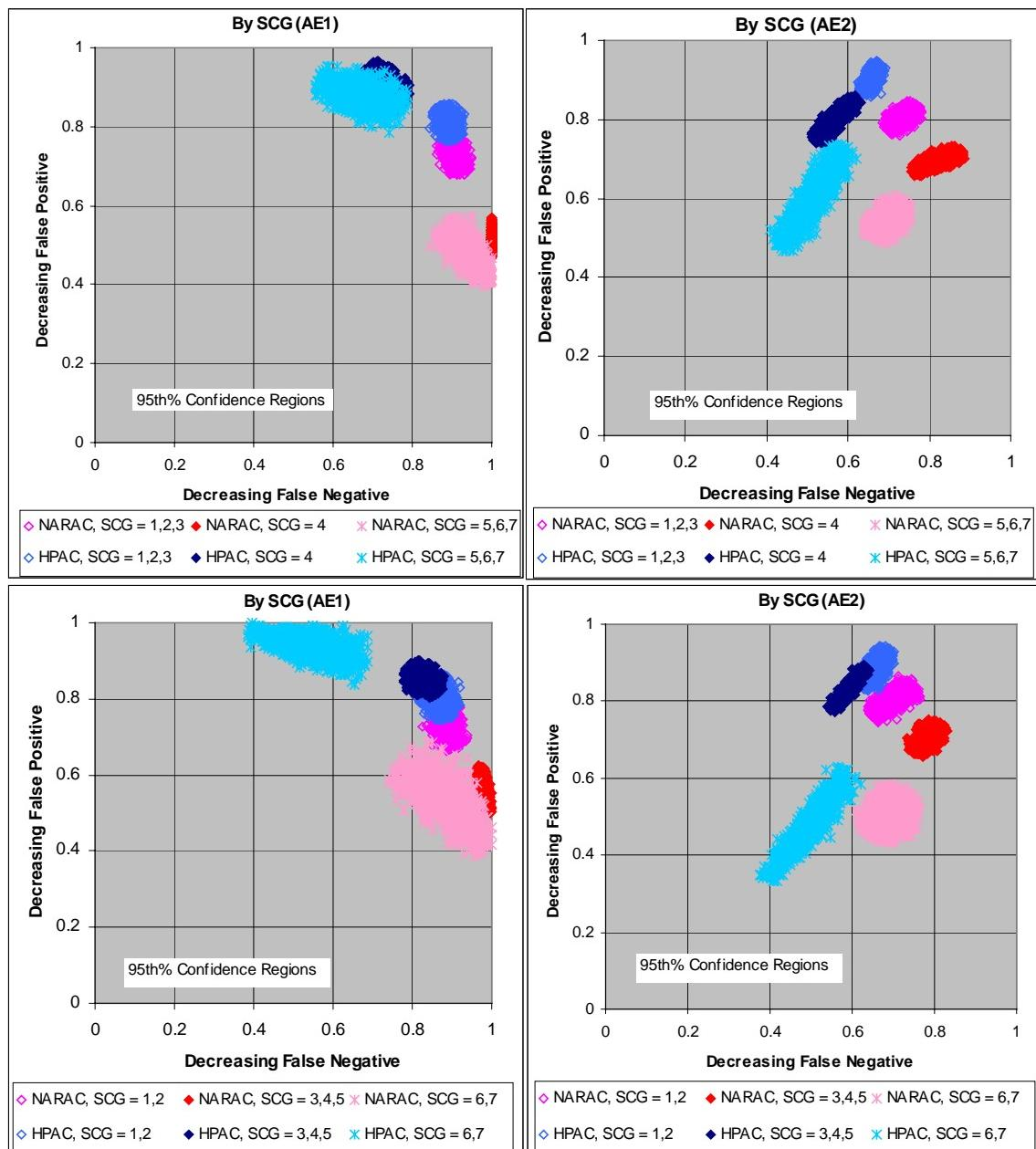


Figure H-18. MOE 2: HPAC and NARAC Comparisons to Prairie Grass Trials {By SCG for AE1 and AE2}⁷

7 Two different independent combinations of stability category groupings are shown above – 1,2; 3,4,5; 6,7 and 1,2,3; 4; 5,6,7. The points shown in the above plots correspond to the approximate 95th percent confidence regions associated with the MOE 2 point estimates. These confidence regions were obtained via bootstrap techniques. The actual point estimates lie at approximately the center of these confidence regions.

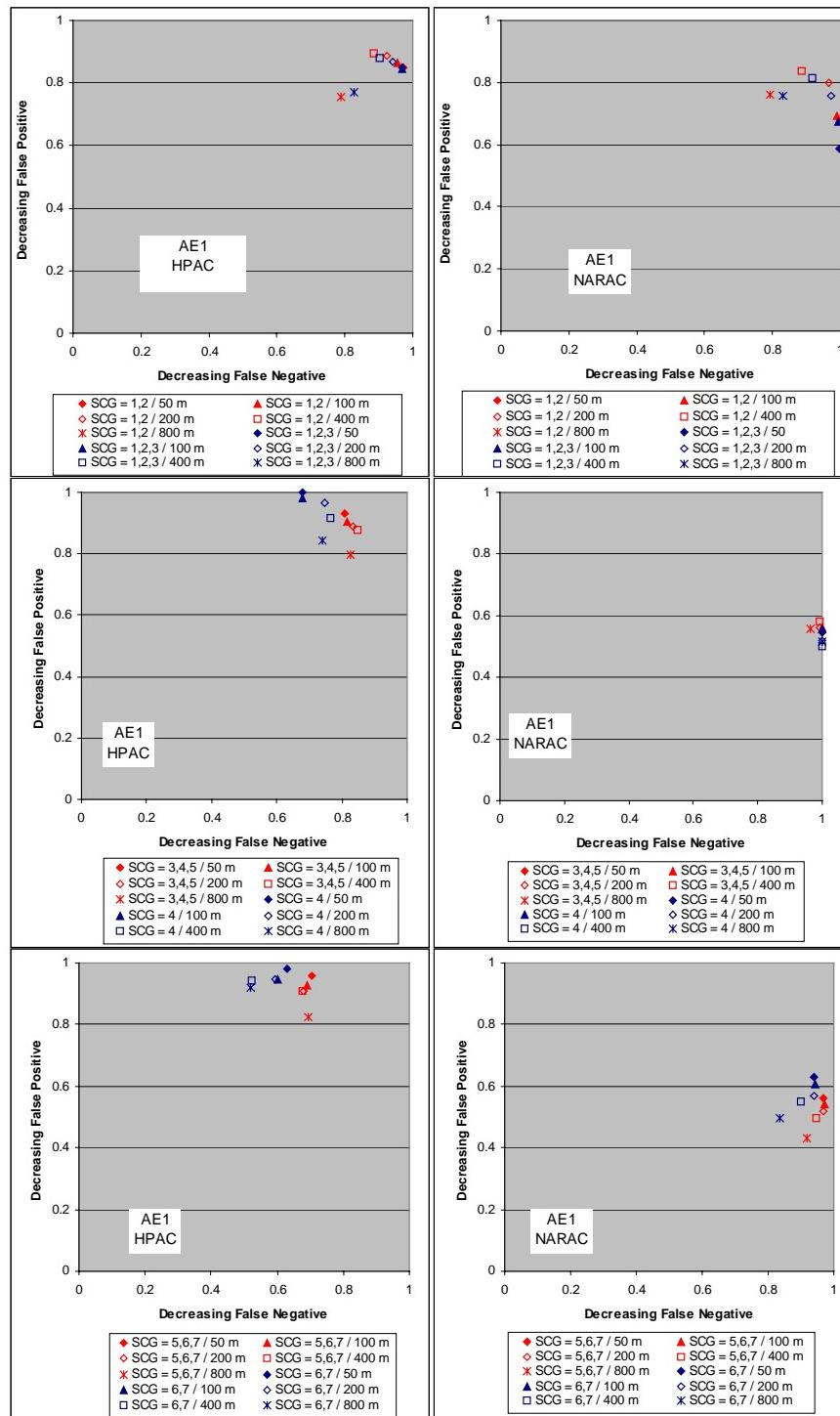


Figure H-19. MOE 2 Point Estimates Only: HPAC and NARAC Comparisons to Prairie Grass Trials {SCG × Range for AE1}⁸

8 Two different independent combinations of stability category groupings are shown above – 1,2; 3,4,5; 6,7 and 1,2,3; 4; 5,6,7.

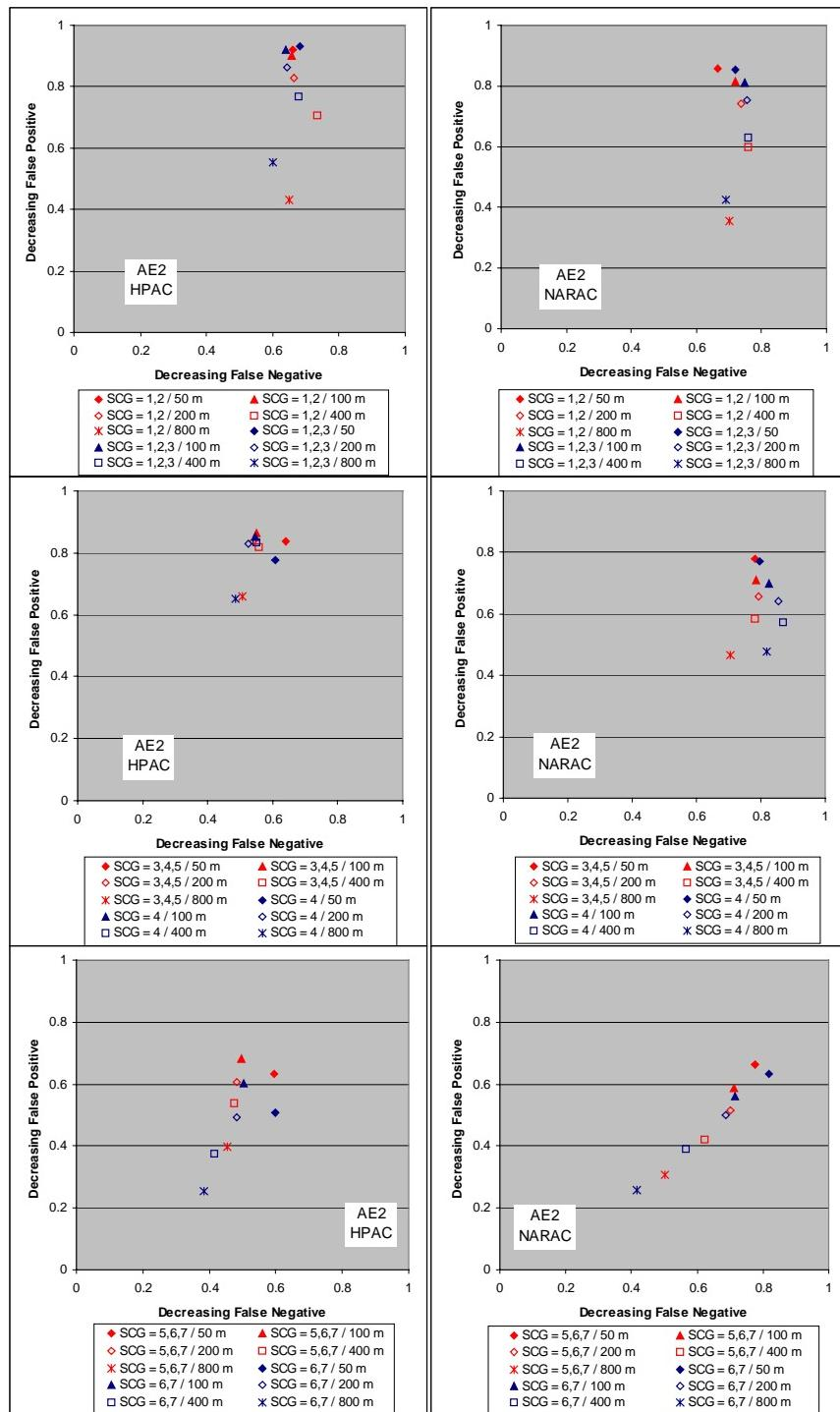


Figure H-20. MOE 2 Point Estimates Only: HPAC and NARAC Comparisons to Prairie Grass Trials {SCG × Range for AE2}⁹

⁹ Two different independent combinations of stability category groupings are shown above – 1,2; 3,4,5; 6,7 and 1,2,3; 4; 5,6,7.

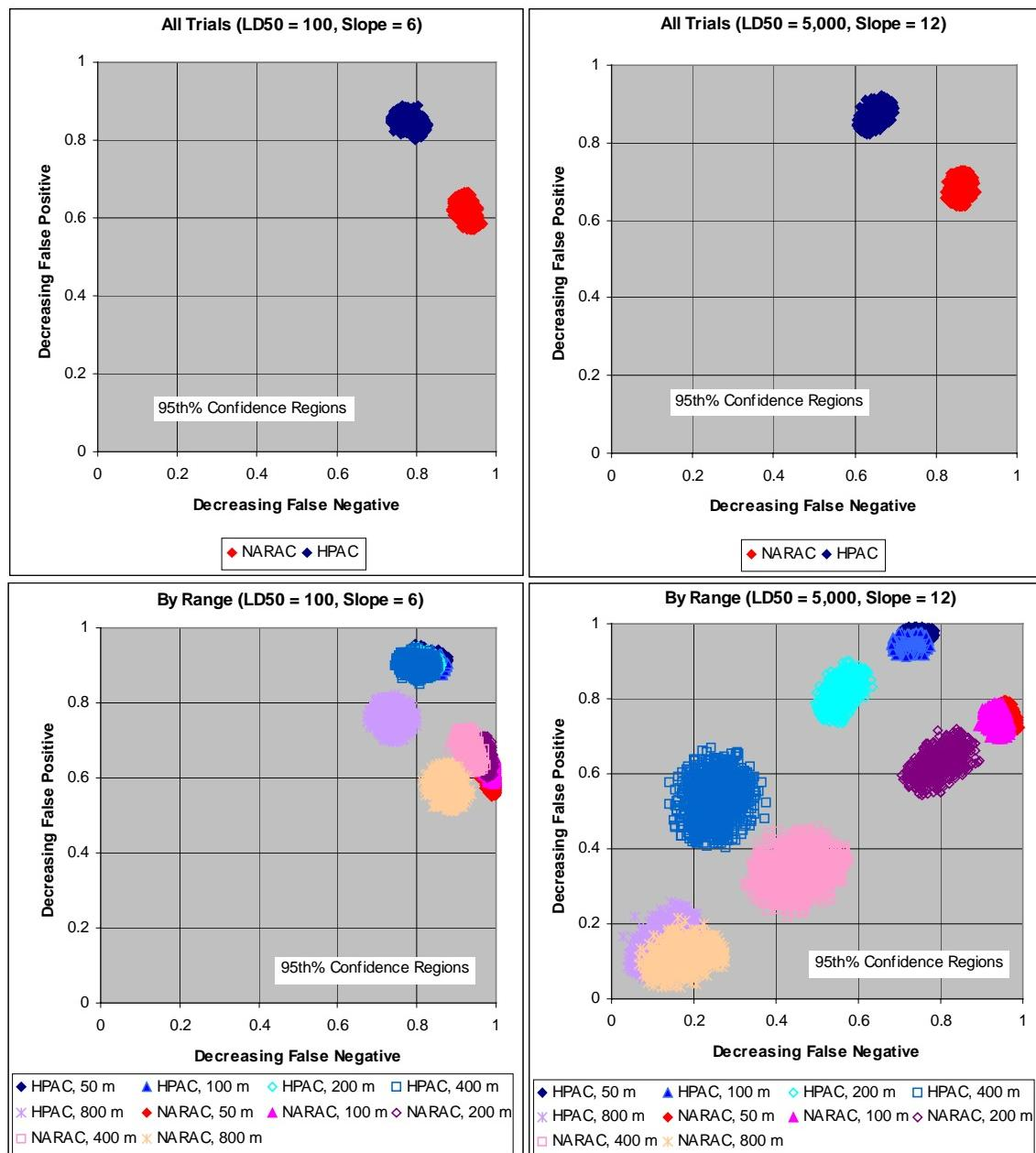


Figure H-21. MOE 2: HPAC and NARAC Comparisons to Prairie Grass Trials {All Trials and By Range for Two Probit Curves}¹⁰

10 The points shown in the above plots correspond to the approximate 95th percent confidence regions associated with the MOE 2 point estimates. These regions were obtained via bootstrap techniques. The actual point estimates lie at approximately the center of these confidence regions.

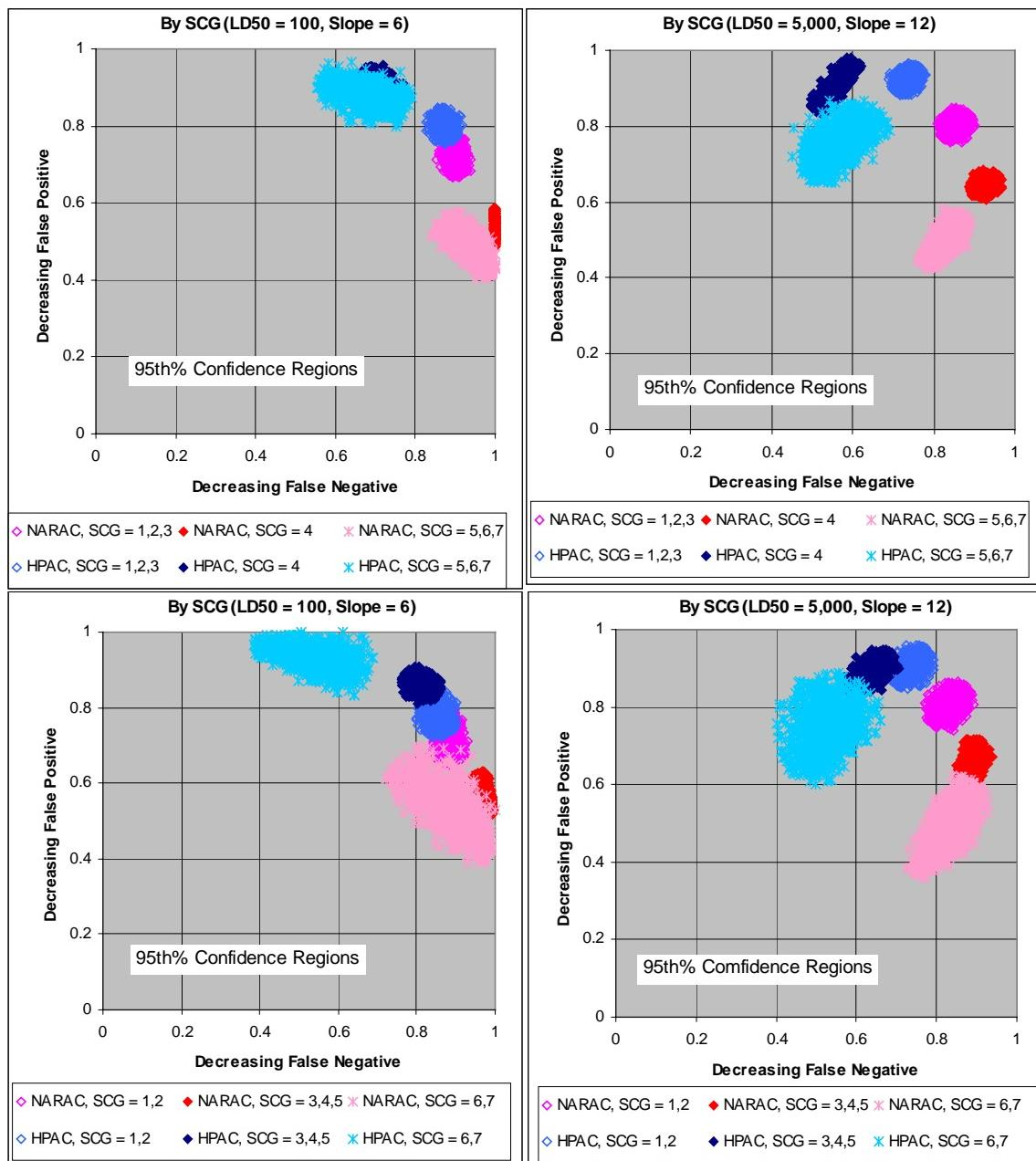


Figure H-22. MOE 2: HPAC and NARAC Comparisons to Prairie Grass Trials {By SCG for Two Probit Curves}¹¹

¹¹ Two different independent combinations of stability category groupings are shown above – 1,2; 3,4,5; 6,7 and 1,2,3; 4; 5,6,7. The points shown in the above plots correspond to the approximate 95th percent confidence regions associated with the MOE 2 point estimates. These confidence regions were obtained via bootstrap techniques. The actual point estimates lie at approximately the center of these confidence regions.

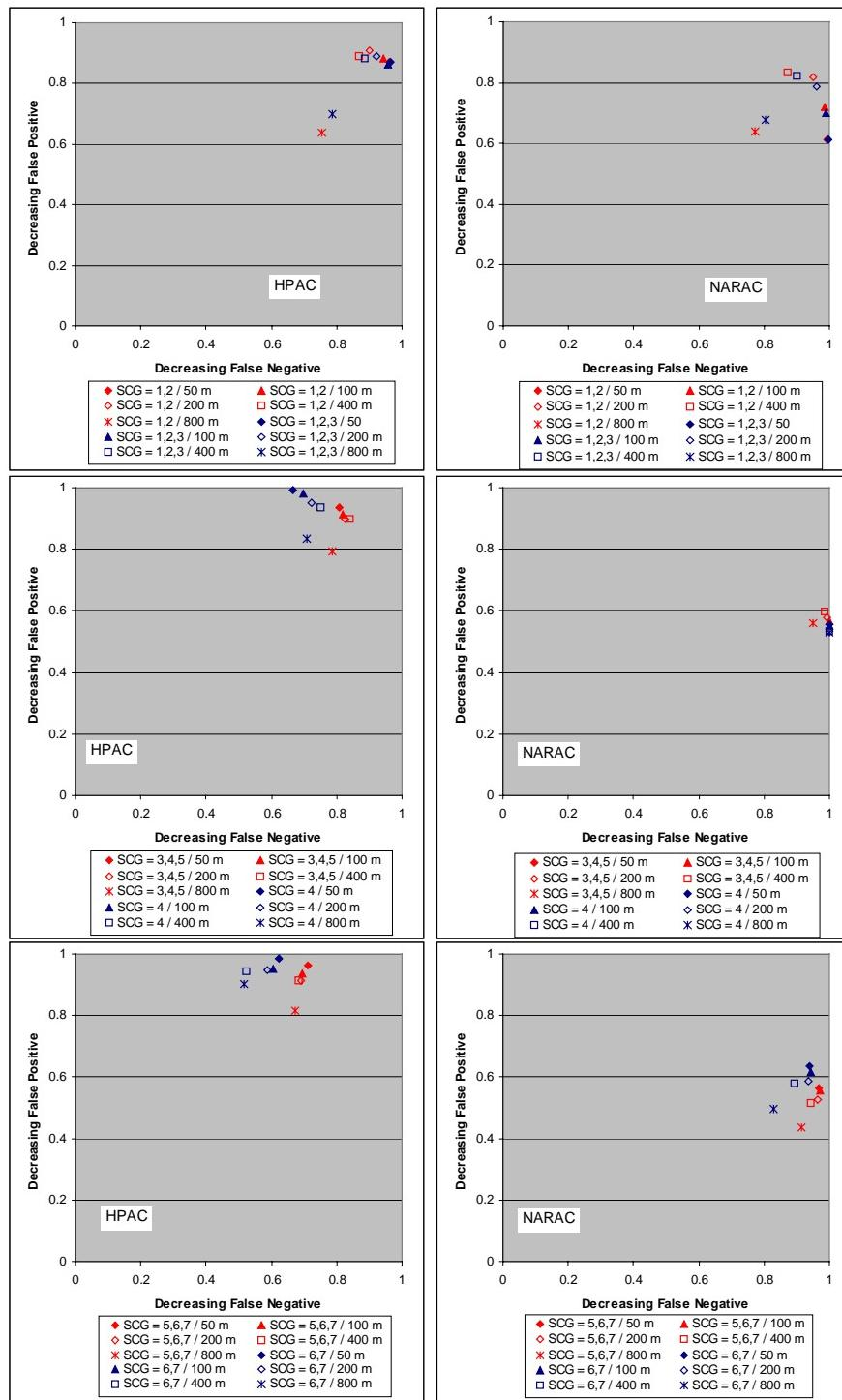


Figure H-23. MOE 2 Point Estimates Only: HPAC and NARAC Comparisons to Prairie Grass Trials {SCG × Range for $LD_{50} = 100$, Probit Slope = 6}¹²

12 Two different independent combinations of stability category groupings are shown above – 1,2; 3,4,5; 6,7 and 1,2,3; 4; 5,6,7.

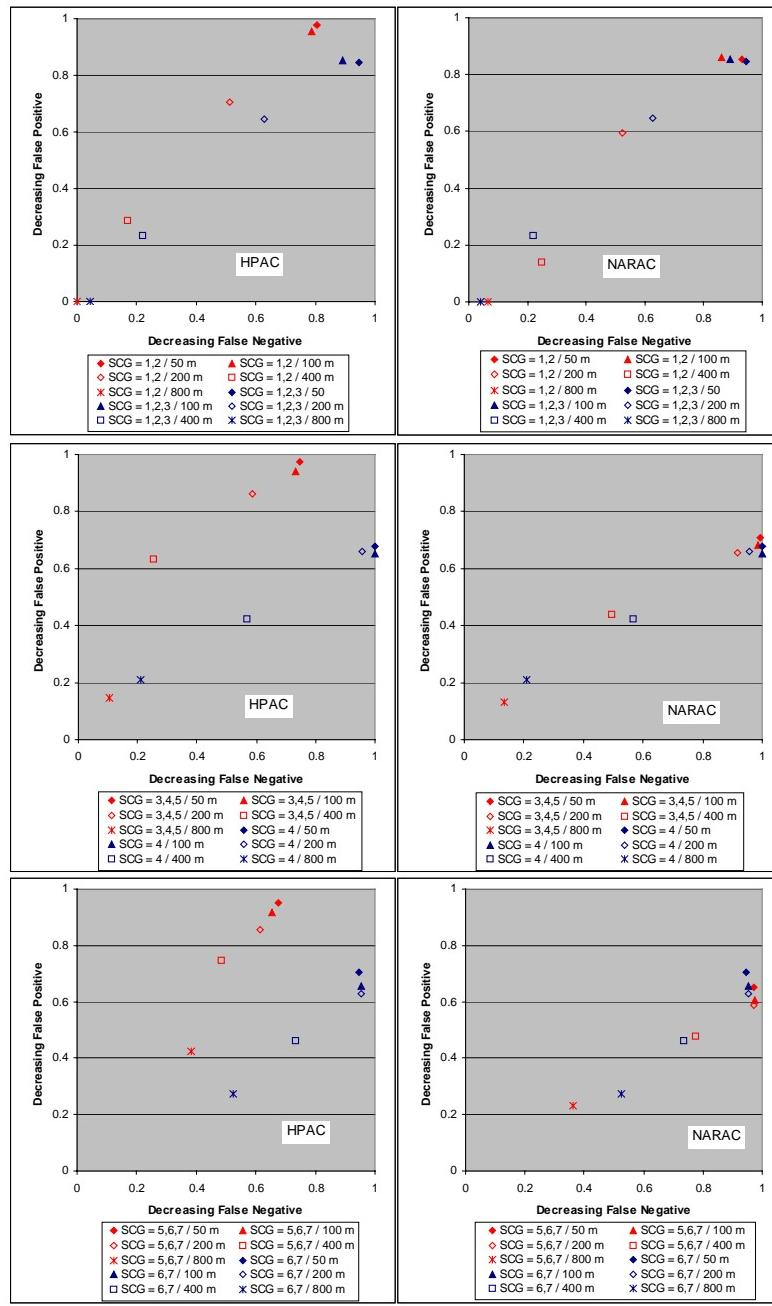


Figure H-24. MOE 2 Point Estimates Only: HPAC and NARAC Comparisons to Prairie Grass Trials {SCG × Range for $LD_{50} = 5,000$, Probit Slope = 12}¹³

¹³ Two different independent combinations of stability category groupings are shown above – 1,2; 3,4,5; 6,7 and 1,2,3; 4; 5,6,7.

APPENDIX I

**RESULTS AND ANALYSES: SUPPLEMENTAL FIGURES AND
TABLES FOR STANDARD STATISTICAL MEASURES**

APPENDIX I

RESULTS AND ANALYSES: SUPPLEMENTAL FIGURES AND TABLES FOR STANDARD STATISTICAL MEASURES

This appendix provides figures and tables that describe comparisons of HPAC and NARAC¹ predictions of *Prairie Grass* trials based on standard statistical measures. The statistical measures included in this appendix are fractional bias (FB), normalized mean square error (NMSE), geometric mean bias (MG), geometric mean variance (VG), correlation coefficient (R), fraction of predictions within a factor of 2 (FAC2), fraction of predictions within a factor of 5 (FAC5), and fraction of predictions within a factor of 10 (FAC10).

The first six figures (I-1 through I-6) present the results for computations involving the ArcMax. Charts that display FB, NMSE, VG, and MG are provided for all trials and as a function of range and SCG. The next six figures (I-7 through I-12) provide the results obtained for crosswind integrated (CWI) dosage. Since NMSE and VG for a model can be due to mean bias and random error, there are minimum values of NMSE and VG for a given FB and MG, respectively. The limiting curves described on some of the charts represent the minimum possible values of NMSE and VG and were computed in the following way:

$$NMSE = \frac{4FB}{4 - FB^2} \quad (I-1)$$

$$\ln VG = (\ln MG)^2 \quad (I-2)^2$$

Figures I-13 through I-15 provide tables that describe the values obtained for FAC2, FAC5, and FAC10 for ArcMax and CWI dosage. In several of the figures and tables, “U,” “N,” and “S” refer to stability category groupings unstable, neutral, and stable, respectively.

¹ NARAC is also referred to as ARAC in the figures of this appendix.

² See Chapter 2, Reference 2-9.

The next three figures (I-16 through I-18) present FB and NMSE values for the plume width parameter computed via the equal cuts-off-the-sides method (W_{ec}). See Appendix J for additional details associated with this novel parameter.

The final three figures (I-19 through I-21) provide results for the parameter CentDir. The statistical measures root mean square error (RMSE) and bias were computed for this parameter. See Appendix J for additional discussion.

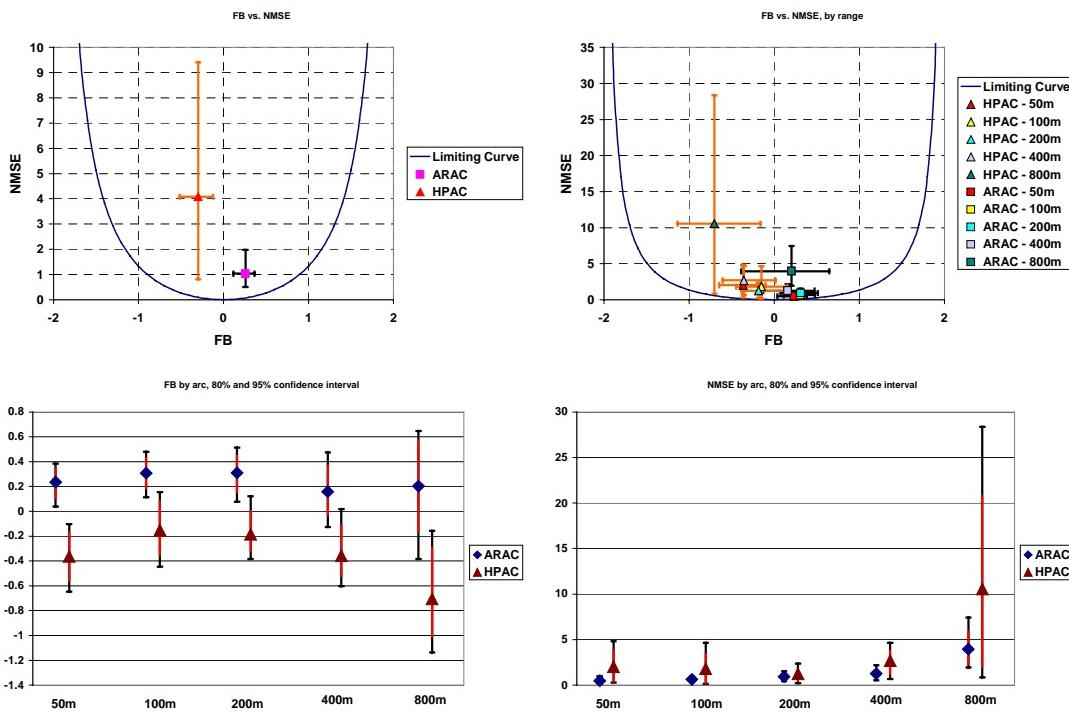


Figure I-1. FB and NMSE: HPAC and NARAC ArcMax Comparisons to Prairie Grass Trials {All Trials and By Range}

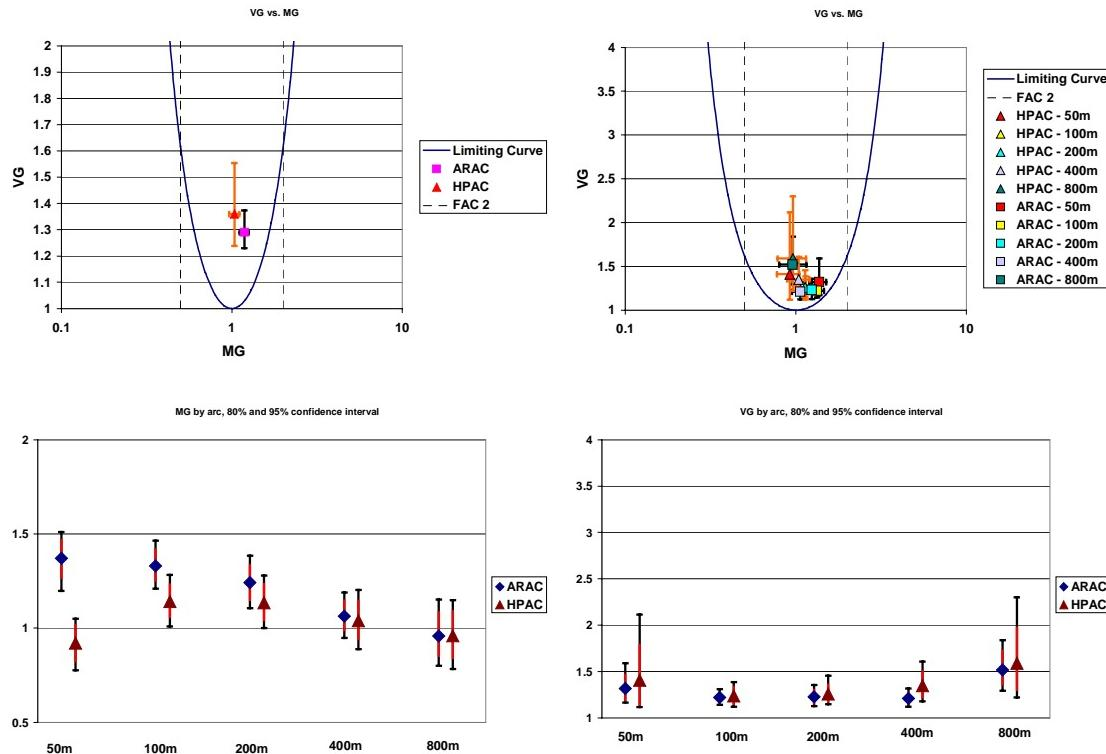


Figure I-2. MG and VG: HPAC and NARAC ArcMax Comparisons to Prairie Grass Trials {All Trials and By Range}

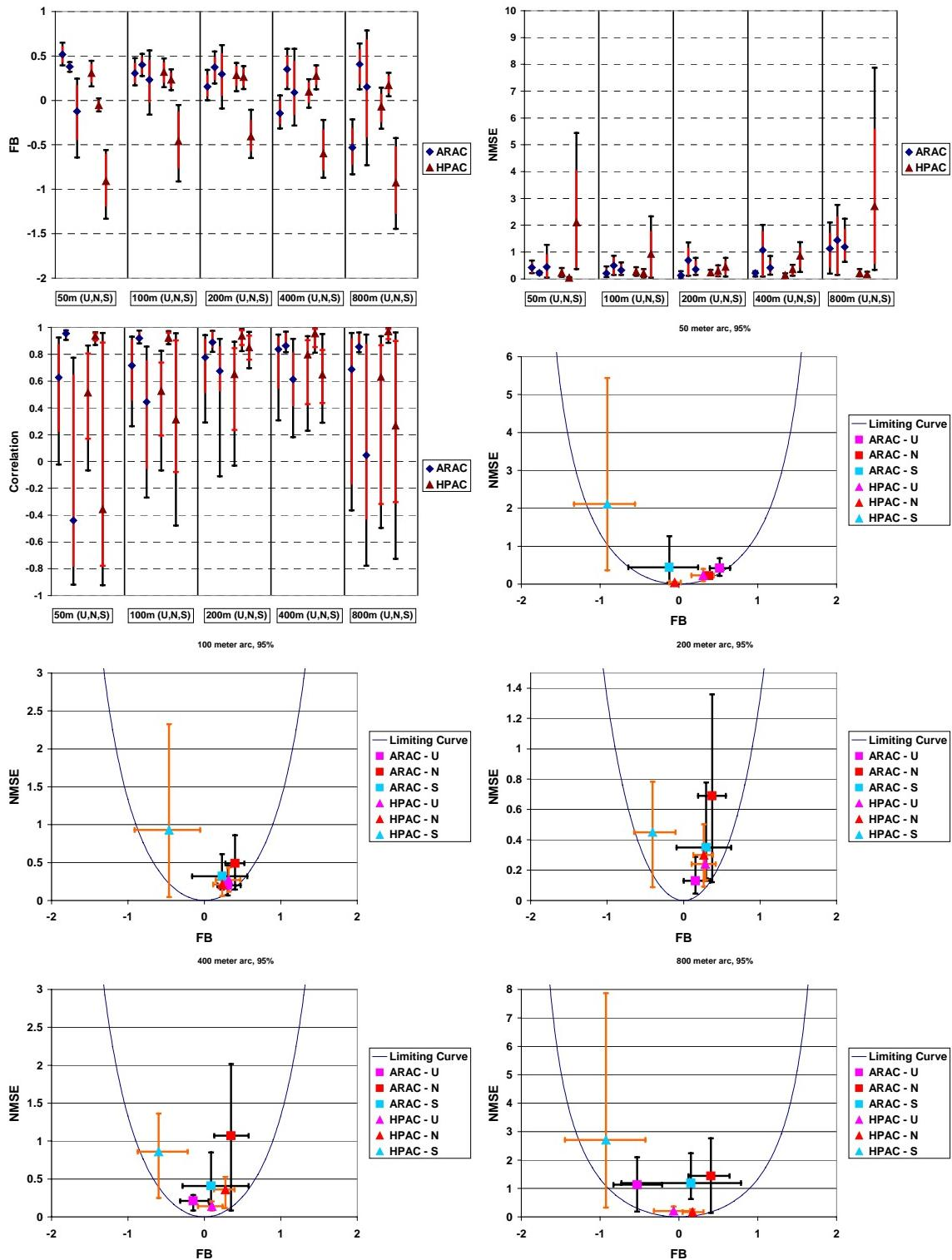
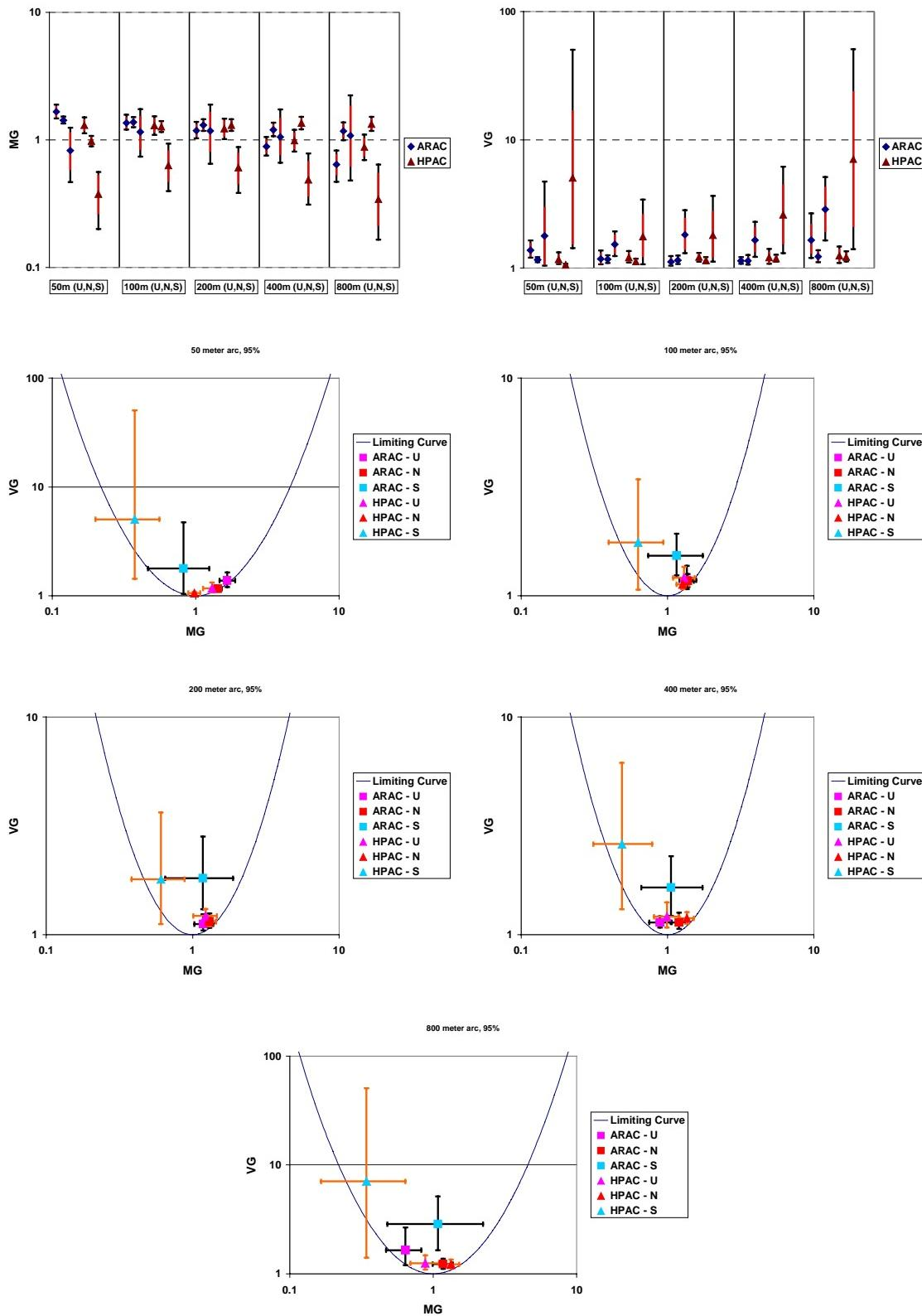
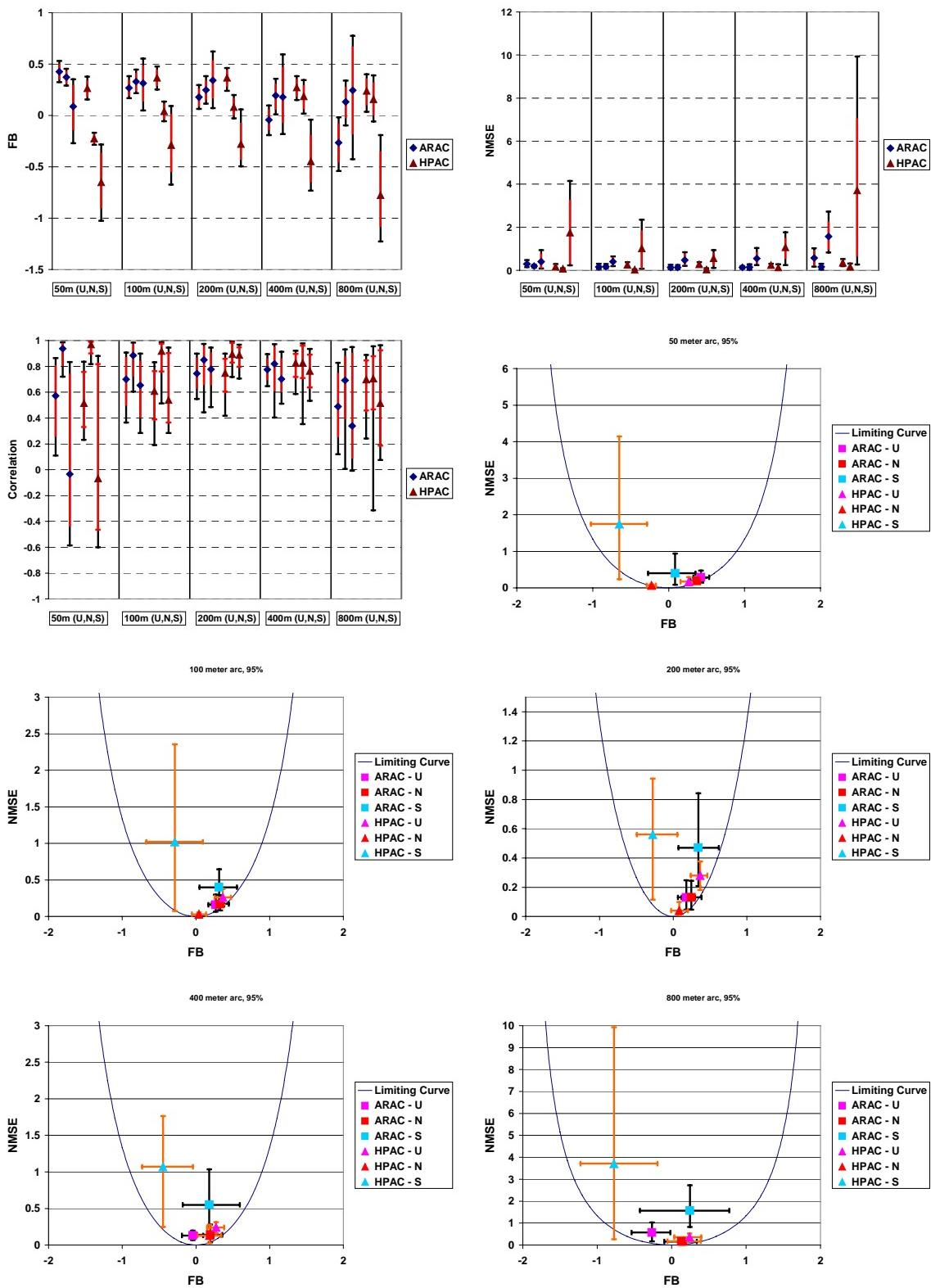


Figure I-3. FB, NMSE, and R: HPAC and NARAC ArcMax Comparisons to Prairie Grass Trials {By SCG – U = 1,2; N = 3,4,5; and S = 6,7}



**Figure I-4. MG and VG: HPAC and NARAC ArcMax Comparisons to Prairie Grass Trials
{By SCG – U = 1,2; N = 3,4,5; and S = 6,7}**



**Figure I-5. FB, NMSE, R: HPAC and NARAC ArcMax Comparisons to Prairie Grass Trials
{By SCG – U = 1,2,3; N = 4,; and S = 5,6,7}**

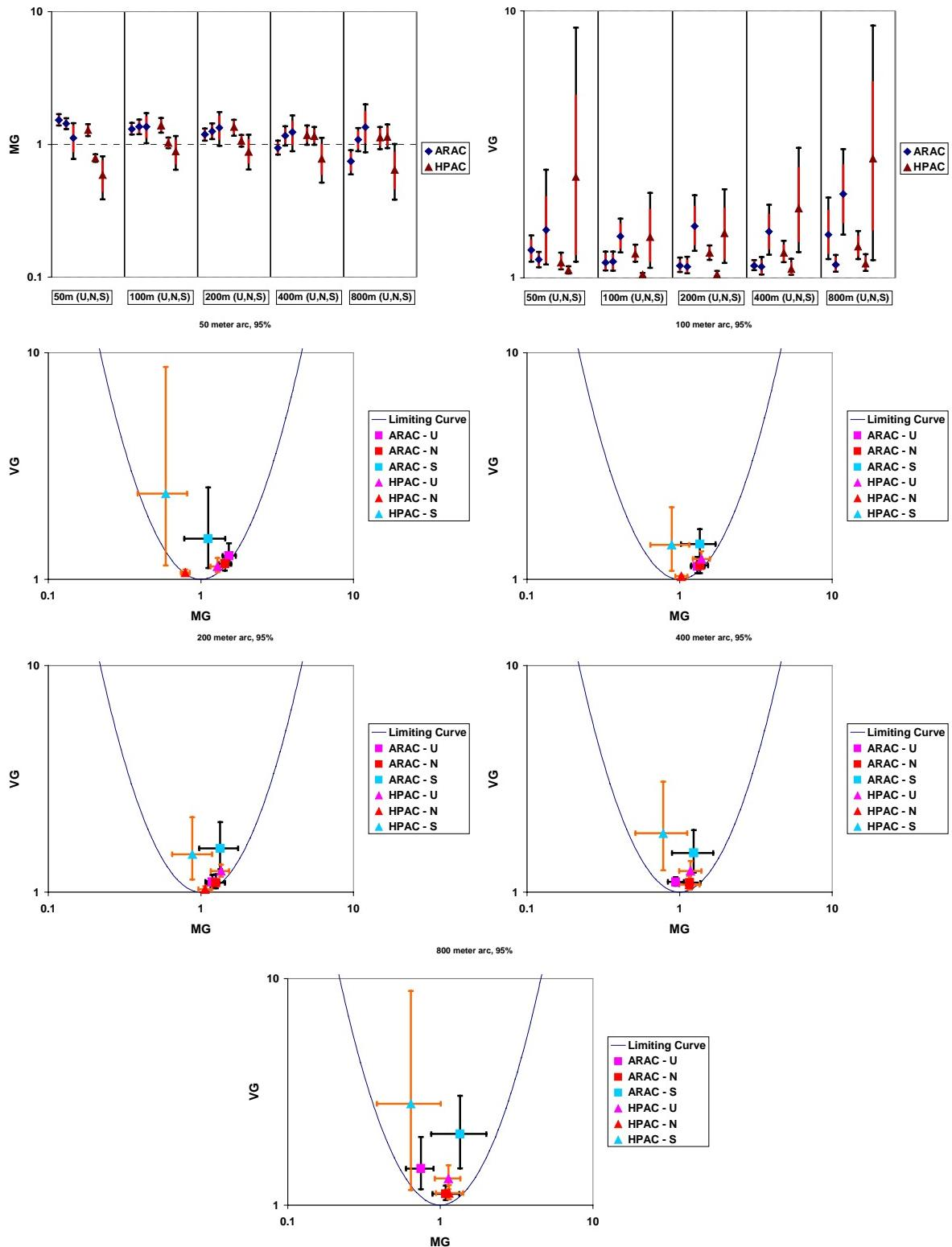


**Figure I-6. MG and VG: HPAC and NARAC ArcMax Comparisons to Prairie Grass Trials
{By SCG – U = 1,2,3; N = 4,; and S = 5,6,7}**

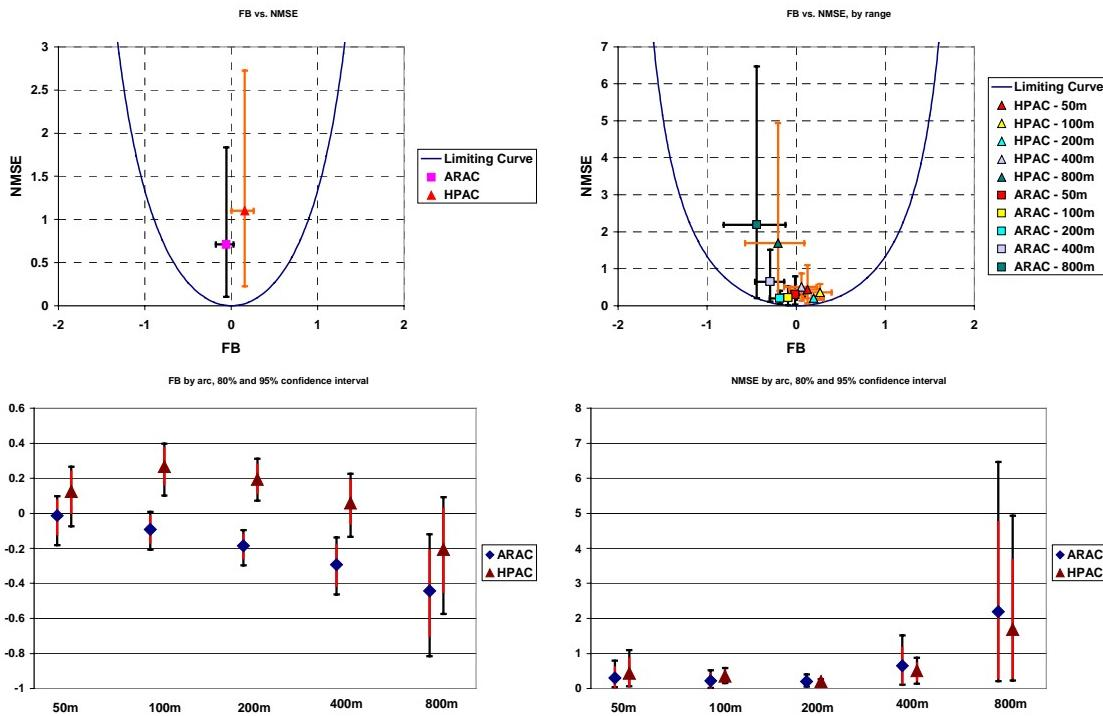


Figure I-7. FB and NMSE: HPAC and NARAC CWI Dosage Comparisons to Prairie Grass Trials {All Trials and By Range}

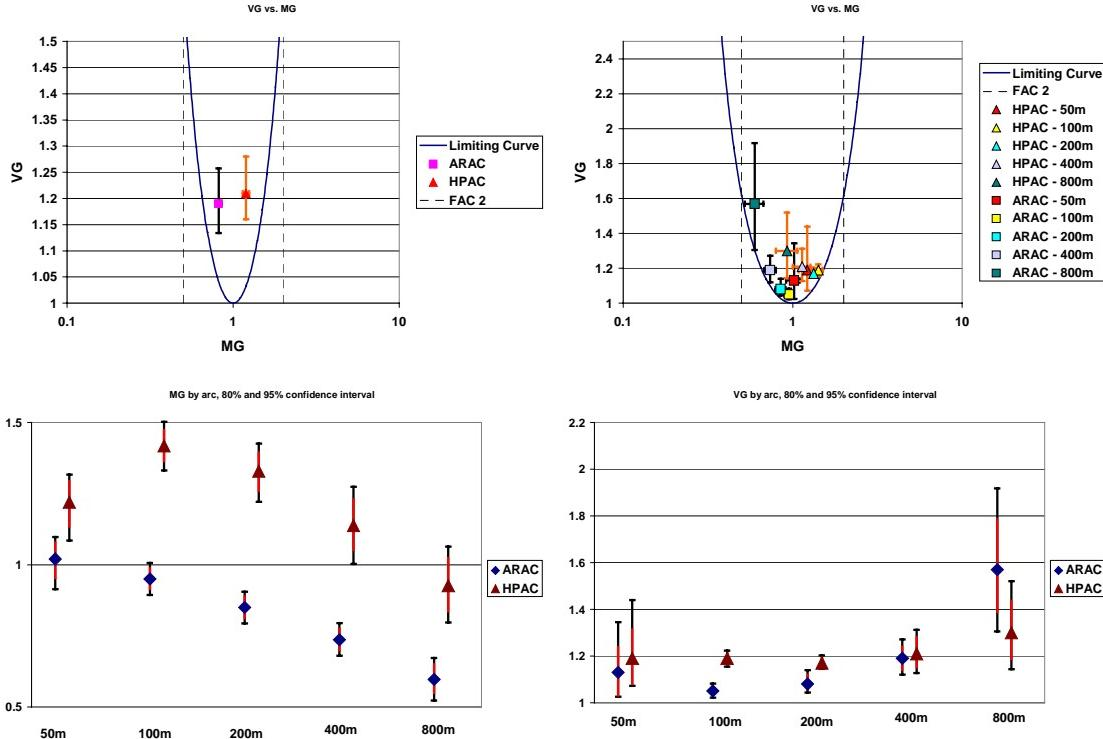


Figure I-8. MG and VG: HPAC and NARAC CWI Dosage Comparisons to Prairie Grass Trials {All Trials and By Range}

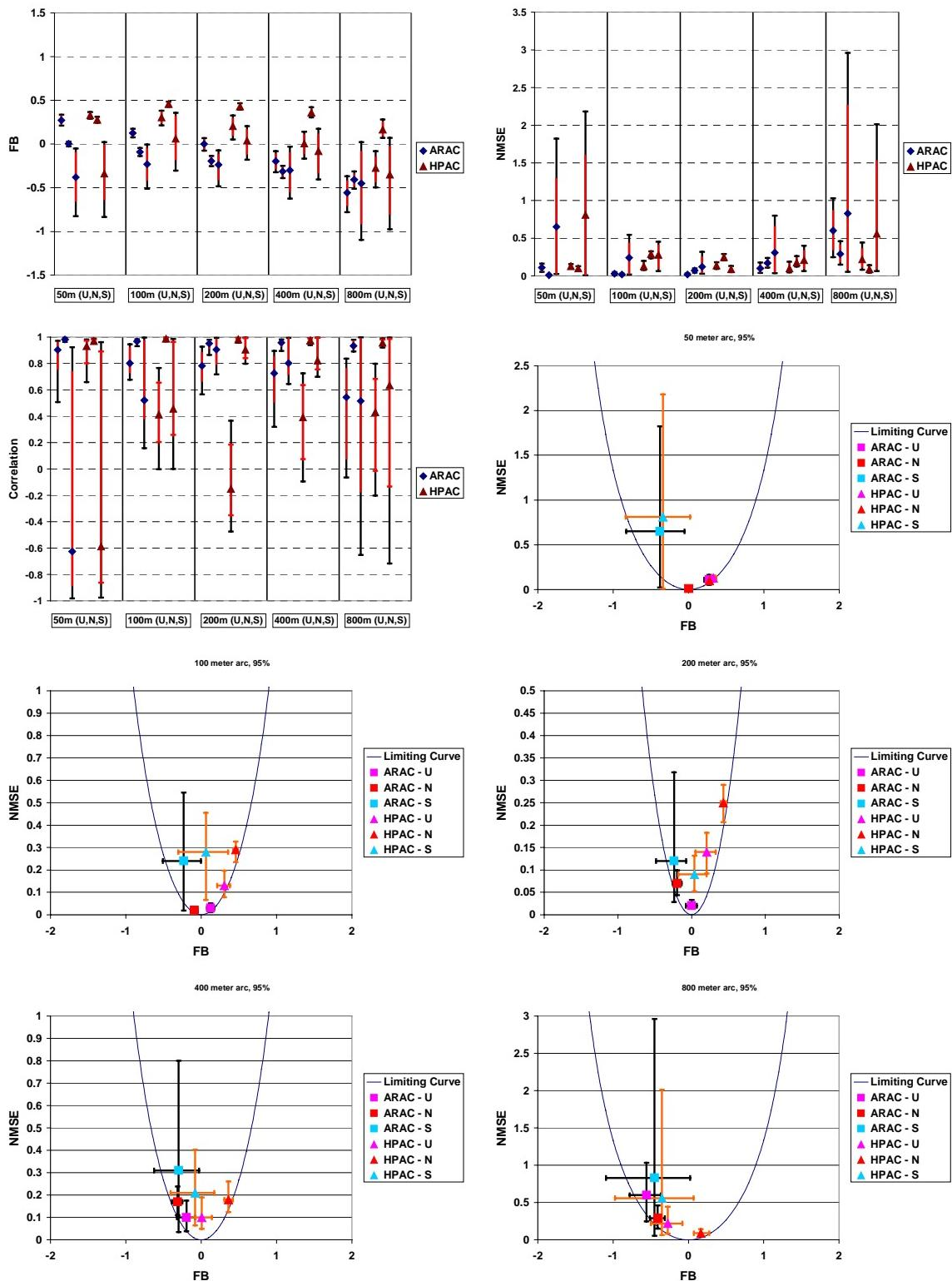


Figure I-9. FB, NMSE, and R: HPAC and NARAC CWI Dosage Comparisons to Prairie Grass Trials {By SCG – U = 1,2; N = 3,4,5; and S = 6,7}

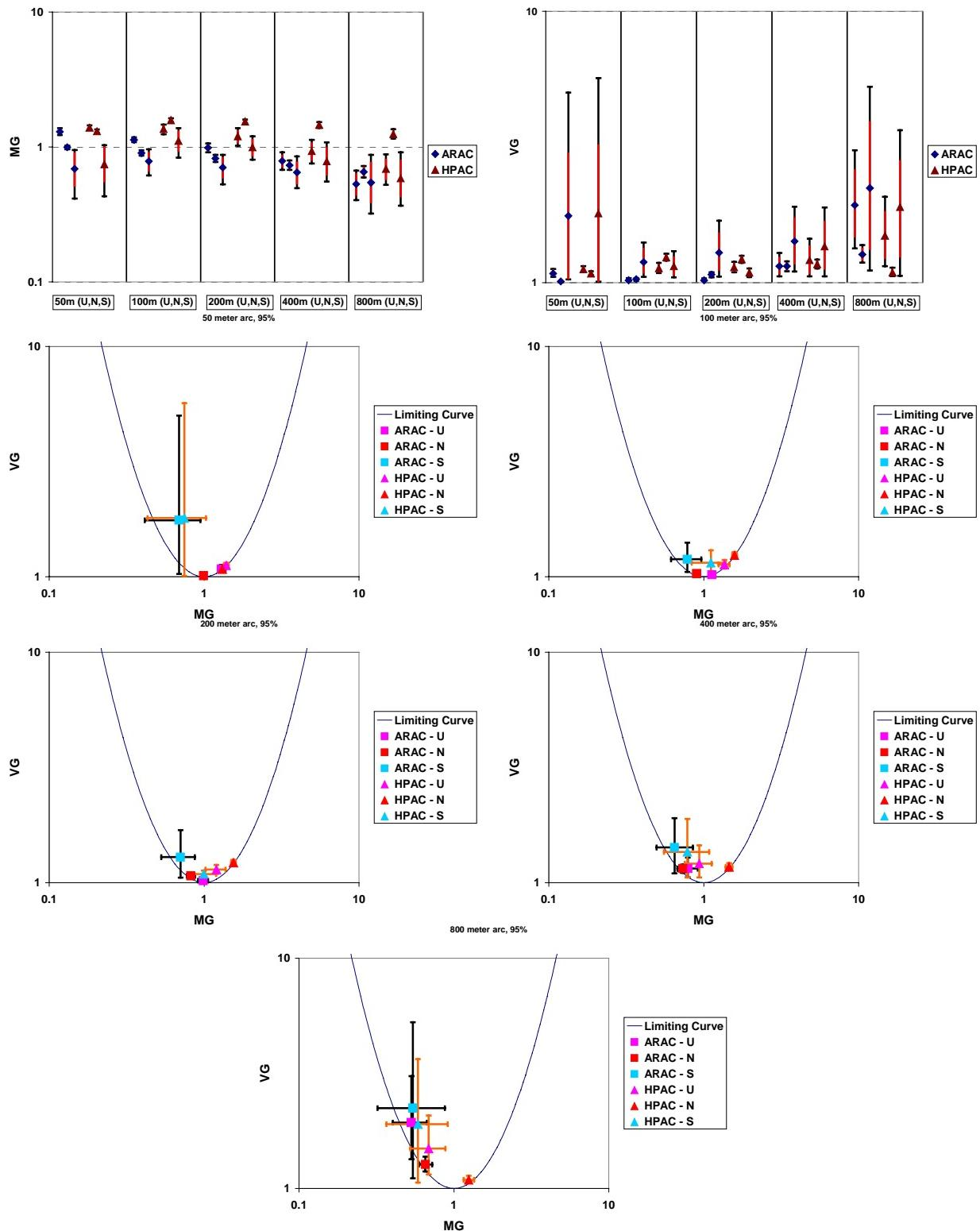


Figure I-10. MG and VG: HPAC and NARAC CWI Dosage Comparisons to Prairie Grass Trials {By SCG – U = 1,2; N = 3,4,5; and S = 6,7}

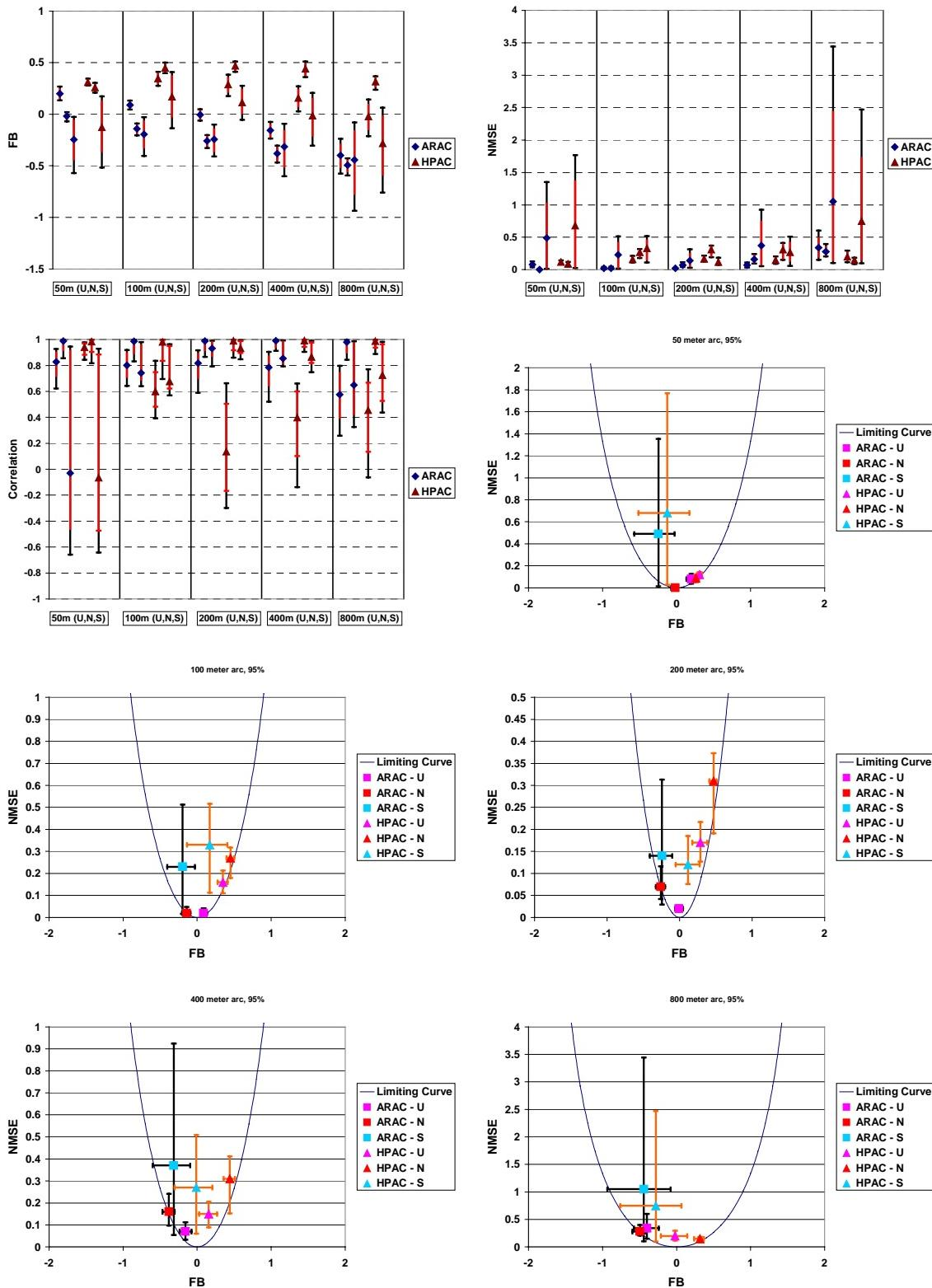


Figure I-11. FB, NMSE, and R: HPAC and NARAC CWI Dosage Comparisons to Prairie Grass Trials {By SCG – U = 1,2,3; N = 4,; and S = 5,6,7}

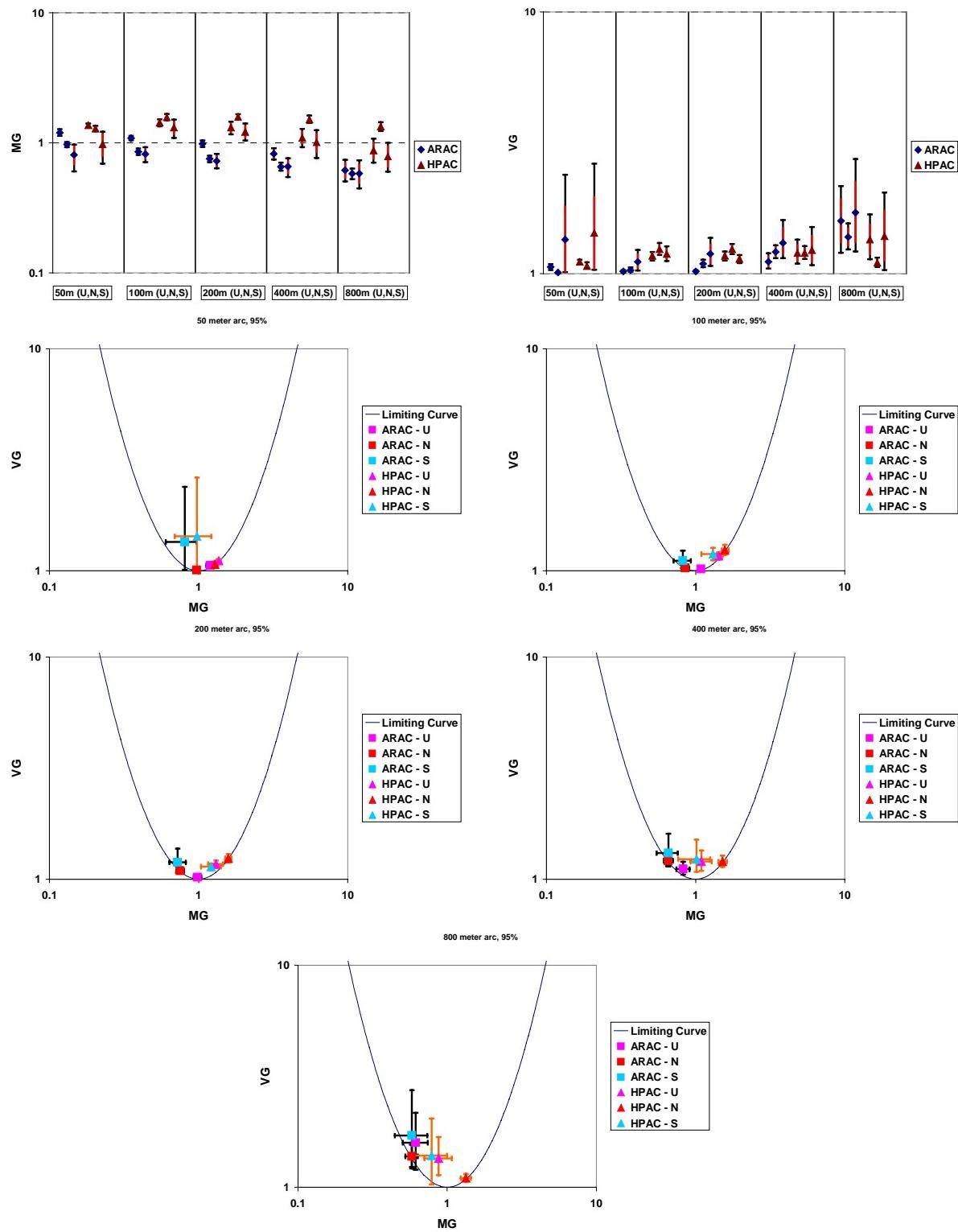


Figure I-12. MG and VG: HPAC and NARAC CWI Dosage Comparisons to Prairie Grass Trials {By SCG – U = 1,2,3; N = 4,; and S = 5,6,7}

Cross Wind Integrated						
ARAC				HPAC		
Factors	2	5	10	Factors	2	5
all	92%	99%	100%	all	94%	100%
50m	98%	98%	100%	50m	98%	98%
100m	98%	100%	100%	100m	98%	100%
200m	96%	100%	100%	200m	100%	100%
400m	90%	100%	100%	400m	92%	100%
800m	77%	98%	100%	800m	83%	100%

Arc Maxima						
ARAC				HPAC		
Factors	2	5	10	Factors	2	5
all	87%	99%	100%	all	87%	98%
50m	92%	98%	100%	50m	90%	98%
100m	90%	100%	100%	100m	92%	100%
200m	88%	100%	100%	200m	92%	98%
400m	92%	100%	100%	400m	84%	98%
800m	73%	98%	100%	800m	77%	96%

Figure I-13. **FAC2, FAC5, and FAC10 Tables:** HPAC and NARAC Comparisons to Prairie Grass Trials {All Trials and By Range}

Cross Wind Integrated						
ARAC				HPAC		
Factors	2	5	10	Factors	2	5
all	92%	99%	100%	all	94%	100%
50m (U)	100%	100%	100%	50m (U)	100%	100%
50m (N)	100%	100%	100%	50m (N)	100%	100%
50m (S)	88%	88%	100%	50m (S)	88%	88%
100m (U)	100%	100%	100%	100m (U)	100%	100%
100m (N)	100%	100%	100%	100m (N)	100%	100%
100m (S)	88%	100%	100%	100m (S)	88%	100%
200m (U)	100%	100%	100%	200m (U)	100%	100%
200m (N)	100%	100%	100%	200m (N)	100%	100%
200m (S)	75%	100%	100%	200m (S)	100%	100%
400m (U)	88%	100%	100%	400m (U)	88%	100%
400m (N)	100%	100%	100%	400m (N)	100%	100%
400m (S)	63%	100%	100%	400m (S)	75%	100%
800m (U)	60%	100%	100%	800m (U)	67%	100%
800m (N)	92%	100%	100%	800m (N)	100%	100%
800m (S)	57%	86%	100%	800m (S)	57%	100%

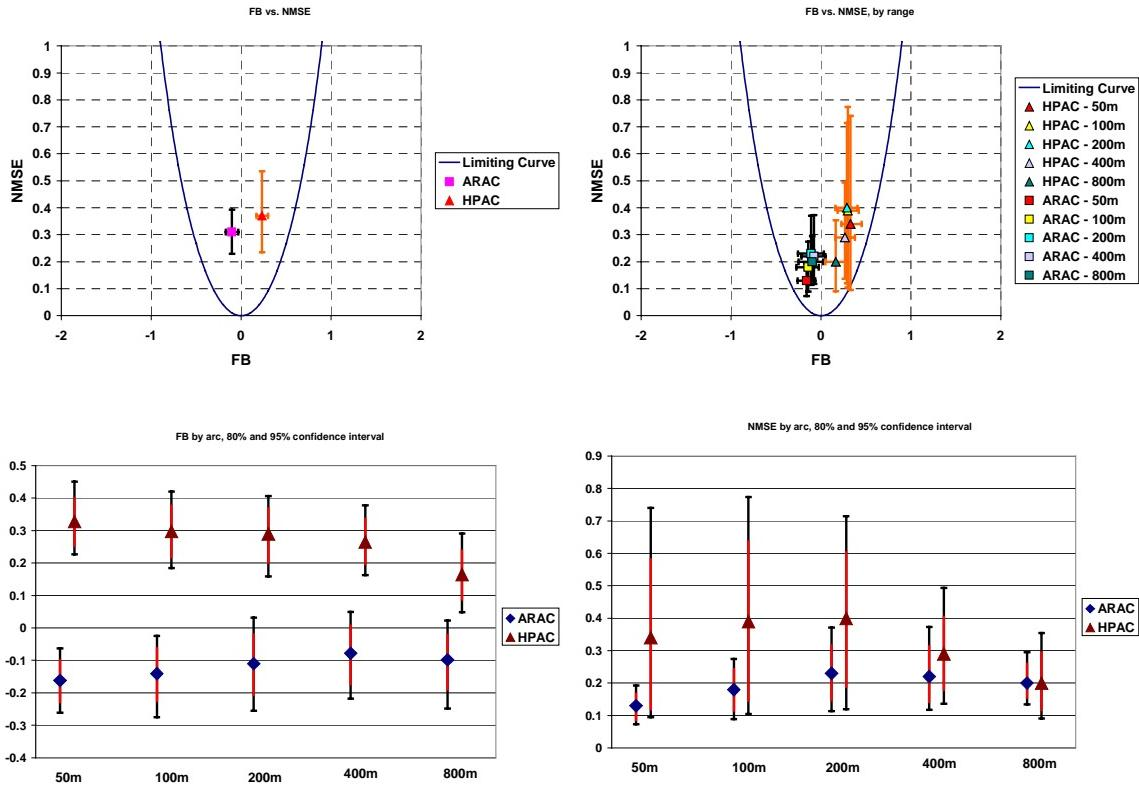
Arc Maxima						
ARAC				HPAC		
Factors	2	5	10	Factors	2	5
all	87%	99%	100%	all	87%	98%
50m (U)	81%	100%	100%	50m (U)	94%	100%
50m (N)	100%	100%	100%	50m (N)	100%	100%
50m (S)	88%	88%	100%	50m (S)	50%	88%
100m (U)	94%	100%	100%	100m (U)	88%	100%
100m (N)	96%	100%	100%	100m (N)	100%	100%
100m (S)	63%	100%	100%	100m (S)	75%	100%
200m (U)	94%	100%	100%	200m (U)	94%	100%
200m (N)	96%	100%	100%	200m (N)	100%	100%
200m (S)	50%	100%	100%	200m (S)	63%	88%
400m (U)	100%	100%	100%	400m (U)	88%	100%
400m (N)	96%	100%	100%	400m (N)	92%	100%
400m (S)	63%	100%	100%	400m (S)	50%	88%
800m (U)	67%	93%	100%	800m (U)	73%	100%
800m (N)	85%	100%	100%	800m (N)	89%	100%
800m (S)	43%	100%	100%	800m (S)	43%	71%

Figure I-14. **FAC2, FAC5, and FAC10 Tables:** HPAC and NARAC Comparisons to Prairie Grass Trials {By SCGs – U = 1,2; N = 3,4,5; and S = 6,7}

Cross Wind Integrated						
ARAC				HPAC		
Factors	2	5	10	Factors	2	5
all	92%	99%	100%	all	94%	100%
50m (U)	100%	100%	100%	50m (U)	100%	100%
50m (N)	100%	100%	100%	50m (N)	100%	100%
50m (S)	93%	93%	100%	50m (S)	93%	93%
100m (U)	100%	100%	100%	100m (U)	100%	100%
100m (N)	100%	100%	100%	100m (N)	100%	100%
100m (S)	93%	100%	100%	100m (S)	93%	100%
200m (U)	100%	100%	100%	200m (U)	100%	100%
200m (N)	100%	100%	100%	200m (N)	100%	100%
200m (S)	87%	100%	100%	200m (S)	100%	100%
400m (U)	92%	100%	100%	400m (U)	92%	100%
400m (N)	100%	100%	100%	400m (N)	100%	100%
400m (S)	80%	100%	100%	400m (S)	87%	100%
800m (U)	75%	100%	100%	800m (U)	79%	100%
800m (N)	90%	100%	100%	800m (N)	100%	100%
800m (S)	71%	93%	100%	800m (S)	79%	100%

Arc Maxima						
ARAC				HPAC		
Factors	2	5	10	Factors	2	5
all	87%	99%	100%	all	87%	98%
50m (U)	88%	100%	100%	50m (U)	96%	100%
50m (N)	100%	100%	100%	50m (N)	100%	100%
50m (S)	93%	93%	100%	50m (S)	73%	93%
100m (U)	96%	100%	100%	100m (U)	92%	100%
100m (N)	100%	100%	100%	100m (N)	100%	100%
100m (S)	73%	100%	100%	100m (S)	87%	100%
200m (U)	96%	100%	100%	200m (U)	96%	100%
200m (N)	100%	100%	100%	200m (N)	100%	100%
200m (S)	67%	100%	100%	200m (S)	80%	93%
400m (U)	100%	100%	100%	400m (U)	85%	100%
400m (N)	100%	100%	100%	400m (N)	100%	100%
400m (S)	73%	100%	100%	400m (S)	73%	93%
800m (U)	71%	96%	100%	800m (U)	71%	100%
800m (N)	100%	100%	100%	800m (N)	100%	100%
800m (S)	57%	100%	100%	800m (S)	71%	86%

Figure I-15. **FAC2, FAC5, and FAC10 Tables:** HPAC and NARAC Comparisons to Prairie Grass Trials {By SCGs – U = 1,2,3; N = 4,; and S = 5,6,7}



**Figure I-16. FB and NMSE: HPAC and NARAC W_{ec} Comparisons to Prairie Grass Trials
(All Trials and By Range)**

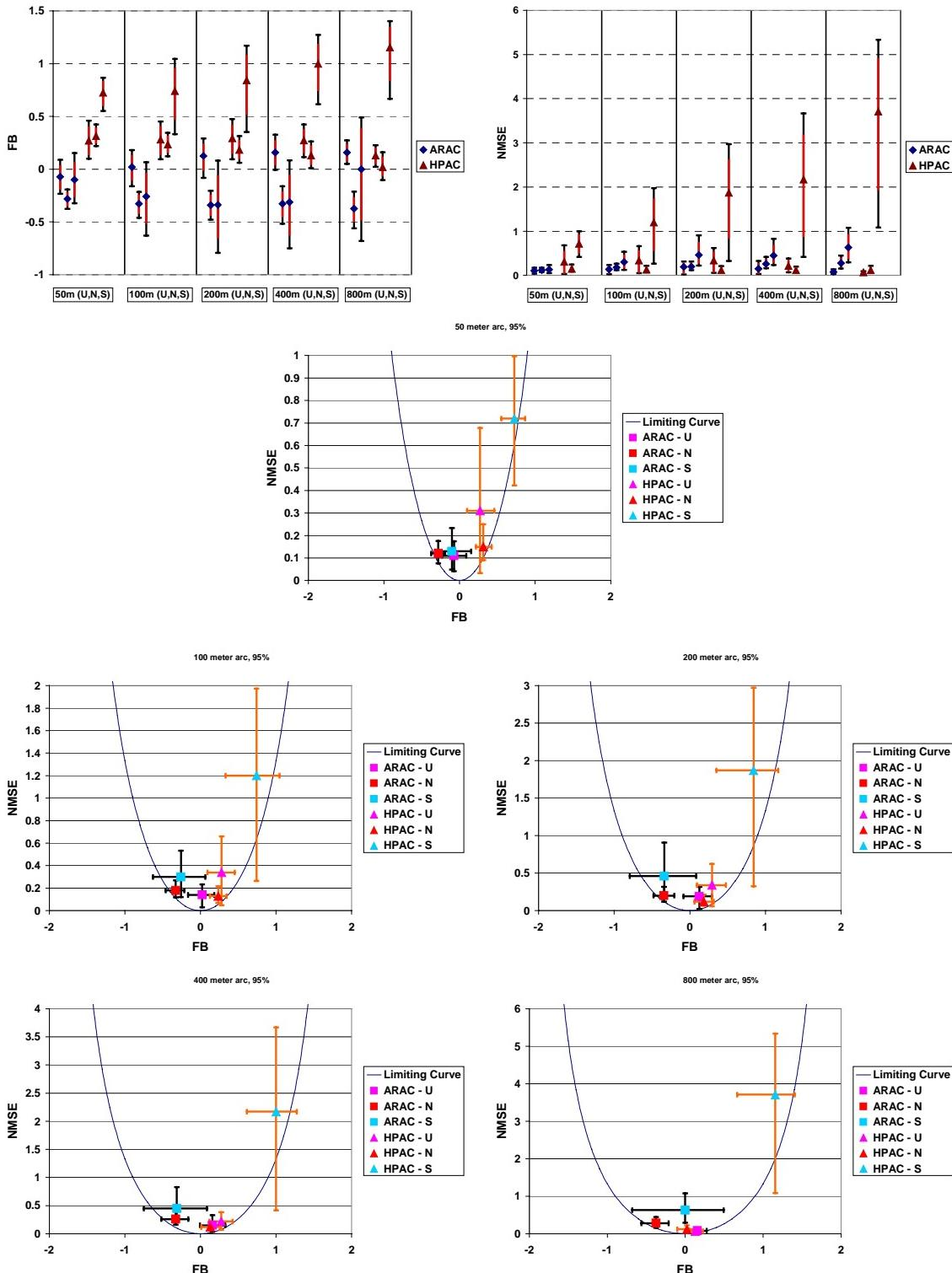


**Figure I-17. FB, NMSE, and R: HPAC and NARAC W_{ec} Comparisons to Prairie Grass Trials
(By SCG – U = 1,2; N = 3,4,5; and S = 6,7)**

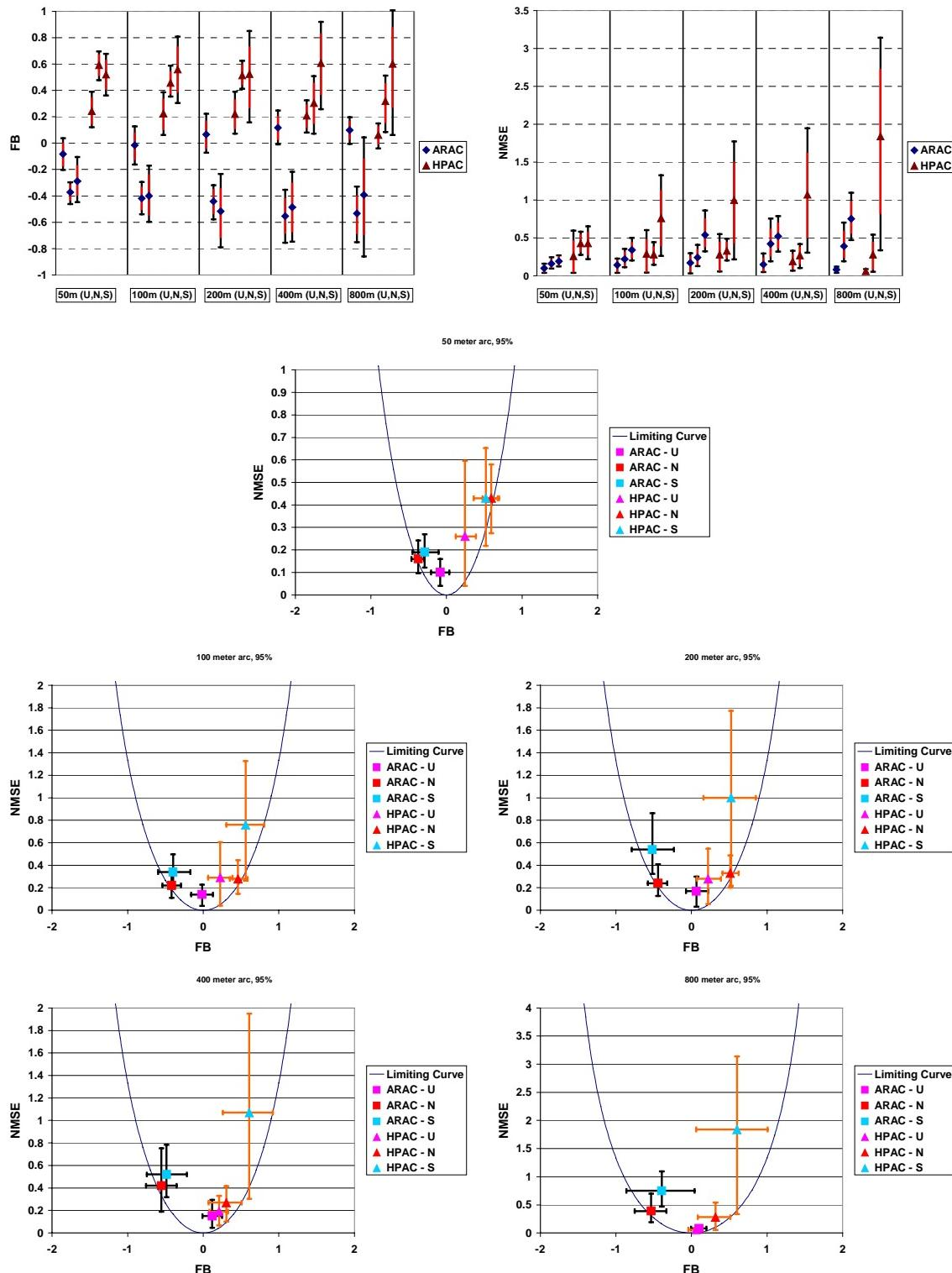


Figure I-18. FB, NMSE, and R: HPAC and NARAC W_{ec} Comparisons to Prairie Grass Trials {By SCG – U = 1,2,3; N = 4,; and S = 5,6,7}

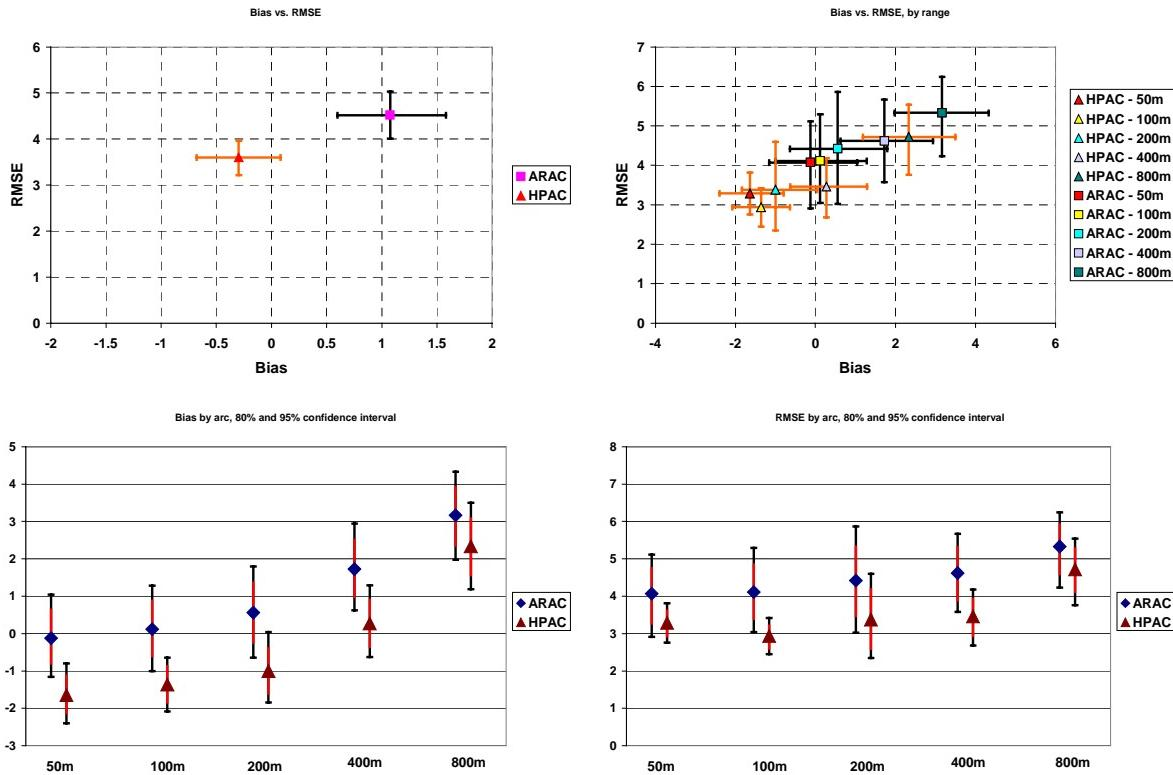


Figure I-19. Bias and RMSE: HPAC and NARAC CentDir Comparisons to Prairie Grass Trials {All Trials and By Range}

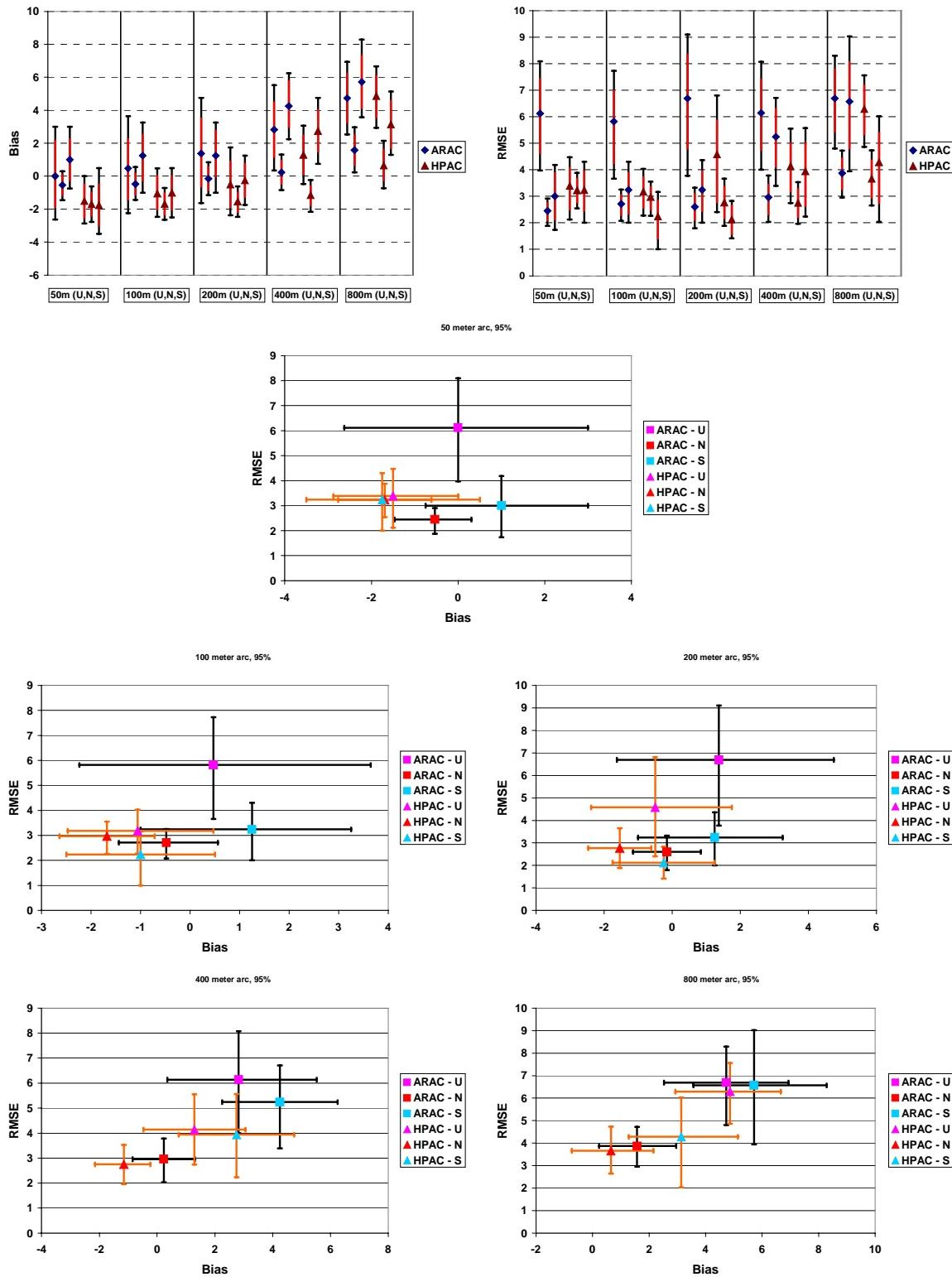


Figure I-20. Bias and RMSE: HPAC and NARAC CentDir Comparisons to Prairie Grass Trials {By SCG – U = 1,2; N = 3,4,5; and S = 6,7}

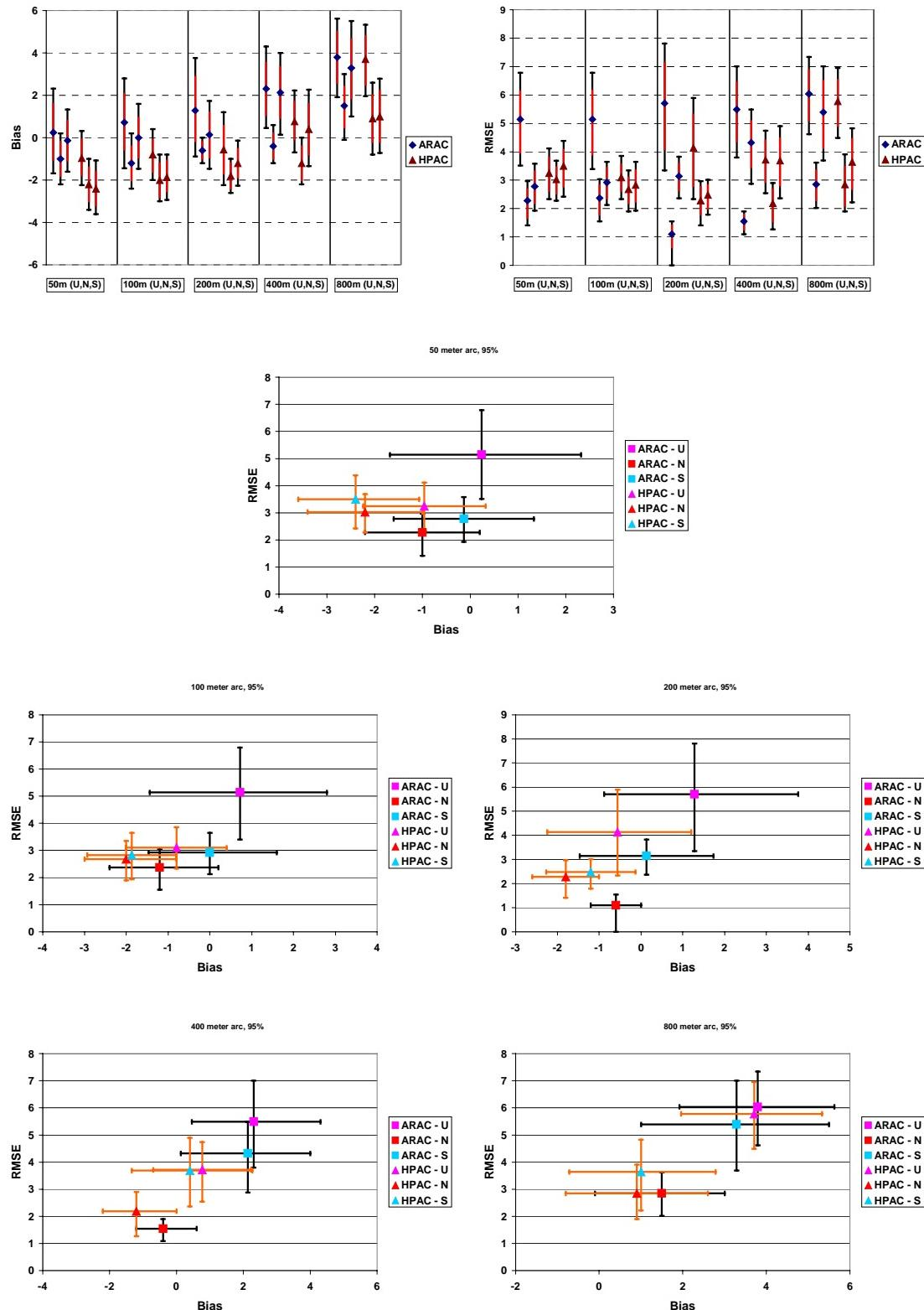


Figure I-21. Bias and RMSE: HPAC and NARAC CentDir Comparisons to Prairie Grass Trials {By SCG – U = 1,2,3; N = 4,; and S = 5,6,7}

APPENDIX J
SOME COMMENTS ON THE ESTIMATION OF PLUME WIDTH
AND DIRECTION

APPENDIX J

SOME COMMENTS ON THE ESTIMATION OF PLUME WIDTH AND DIRECTION

There are several ways that one might define the centerline direction (CentDir) and width for the observed dosages along a given *Prairie Grass* field trial arc. We considered two methods of defining the centerline or direction (with corresponding definitions for the widths), plus a separate method of determining the “width” of the observation that does not involve the direction of the plume. Here, we define the plume in terms of dosage, not concentration. Therefore, the plume widths are defined in terms of crosswind integrated dosage.

1. METHOD I (CENTER OF MASS)

This method describes the centerline of the plume, based on the center of mass (COM).¹ We define the centerline of the plume at any given arc by:

$$COM = \frac{\sum_{i=1}^N iD_i}{\sum_{i=1}^N D_i}, \quad (J-1)$$

where D_i is a dosage collected at sampler i .

Then, given a particular fraction of the crosswind integrated dosage that we want to capture inside the plume (e.g., 0.75), we find the smallest offset k , such that:

$$k_{half-width} = \min \left\{ k \mid 0.75 \sum_i D_i \leq \sum_{i=COM-k}^{COM+k} D_i \right\}. \quad (J-2)$$

Then the width of the plume is $2k_{half-width}$.

¹ Reference J-1 uses this definition, with the exception that the center of mass of the plume *concentration* is considered.

2. METHOD II (MEDIAN OF MASS)

This method is based on defining the centerline as a point that divides the plume into two equally weighted plumes (i.e., this is a median-based calculation). We define the median of mass (MOM) centerline of the plume for any given arc by finding the sampler with index, MOM, such that:

$$MOM = \min \left\{ k \mid \sum_{i=1}^k D_i > 0.5 \sum_{i=1}^N D_i \right\}, \quad (J-3)$$

where D_i is a dosage collected at sampler i .

Then, given a particular fraction of crosswind integrated dosage that we want to capture inside the plume (e.g., 0.75), we find the smallest offset k such that:

$$k_{half-width} = \min \left\{ k \mid 0.75 \sum_i D_i \leq \sum_{i=MOM-k}^{MOM+k} D_i \right\}. \quad (J-4)$$

Then the width of the plume is $2k_{half-width}$.

3. METHOD III (EQUAL CUTS OFF THE SIDES):

This method defines the width of the plume independent of the centerline (or plume direction). For this method, one “cuts” equal crosswind integrated dosages from the sides of the plume. Given a particular fraction of the crosswind integrated dosage that we want to capture inside the plume (e.g., 0.75), we can find the maximal index k_{left} , and minimal index k_{right} (from the left and right, respectively) such that:

$$\begin{aligned} k_{left} &= \max \left\{ k \mid \sum_{i=1}^k D_i \leq \frac{1-0.75}{2} = 0.125 \right\} \\ k_{right} &= \min \left\{ k \mid \sum_{i=k}^N D_i \leq \frac{1-0.75}{2} = 0.125 \right\} \end{aligned} \quad (J-5)$$

Then, we define width for this equal-cuts-off-the-sides method (W_{ec}) as:

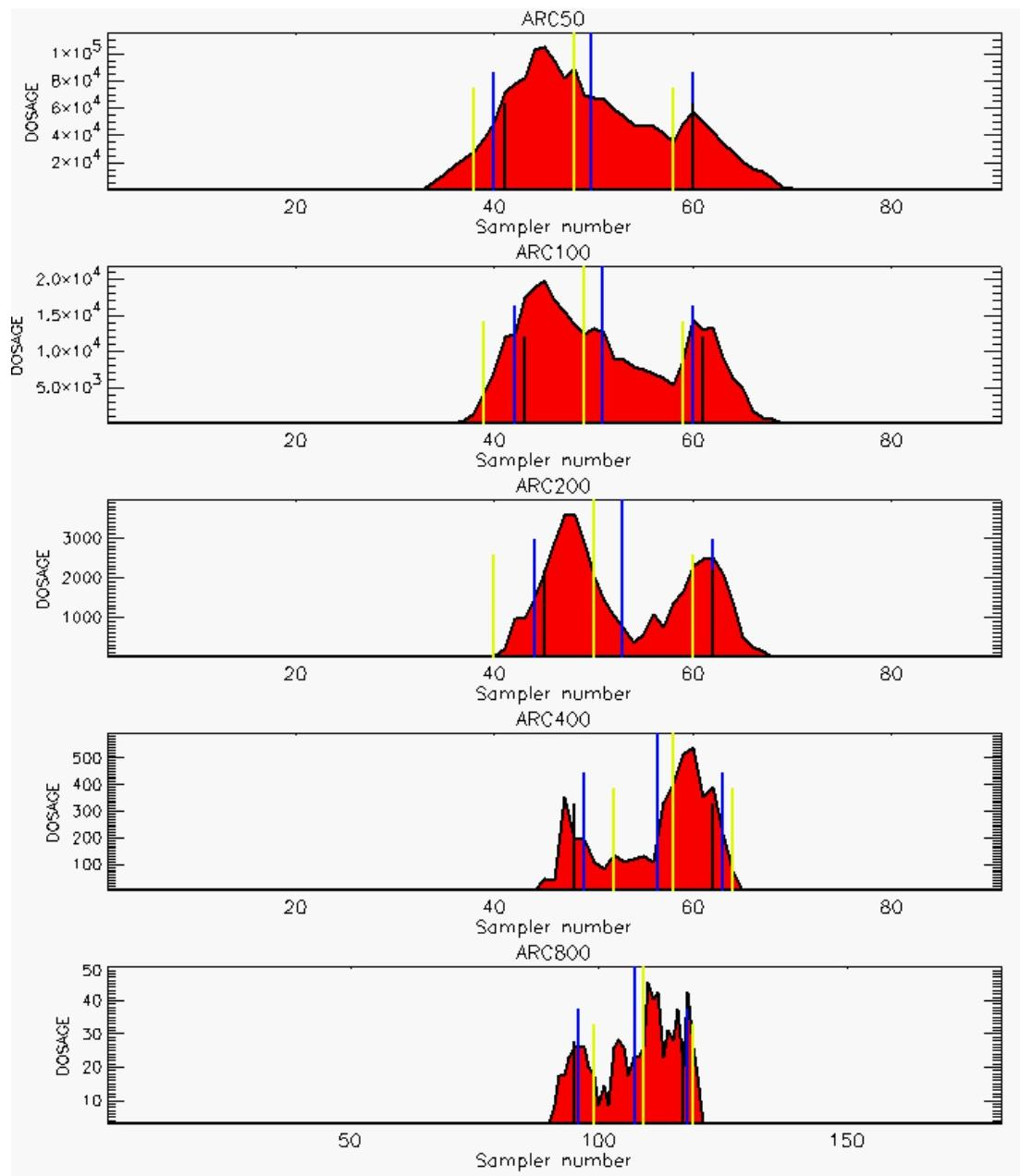
$$W_{ec} = r\theta \times (k_{right} - k_{left}) \quad (J-6)$$

where r is the distance in meters to the arc and θ is the angular separation (in radians) between the samplers. W_{ec} is estimated in units of meters.

Figures J-1 and J-2 demonstrate the above definitions for two *Prairie Gras* field trials. The blue lines denote calculations based on the COM method, the yellow lines denote calculations based on the MOM method, and the black lines denote calculations

based on the “equal-cuts-off-the-sides” method. For the majority of the *Prairie Grass* trials, these different definitions produced very similar results.

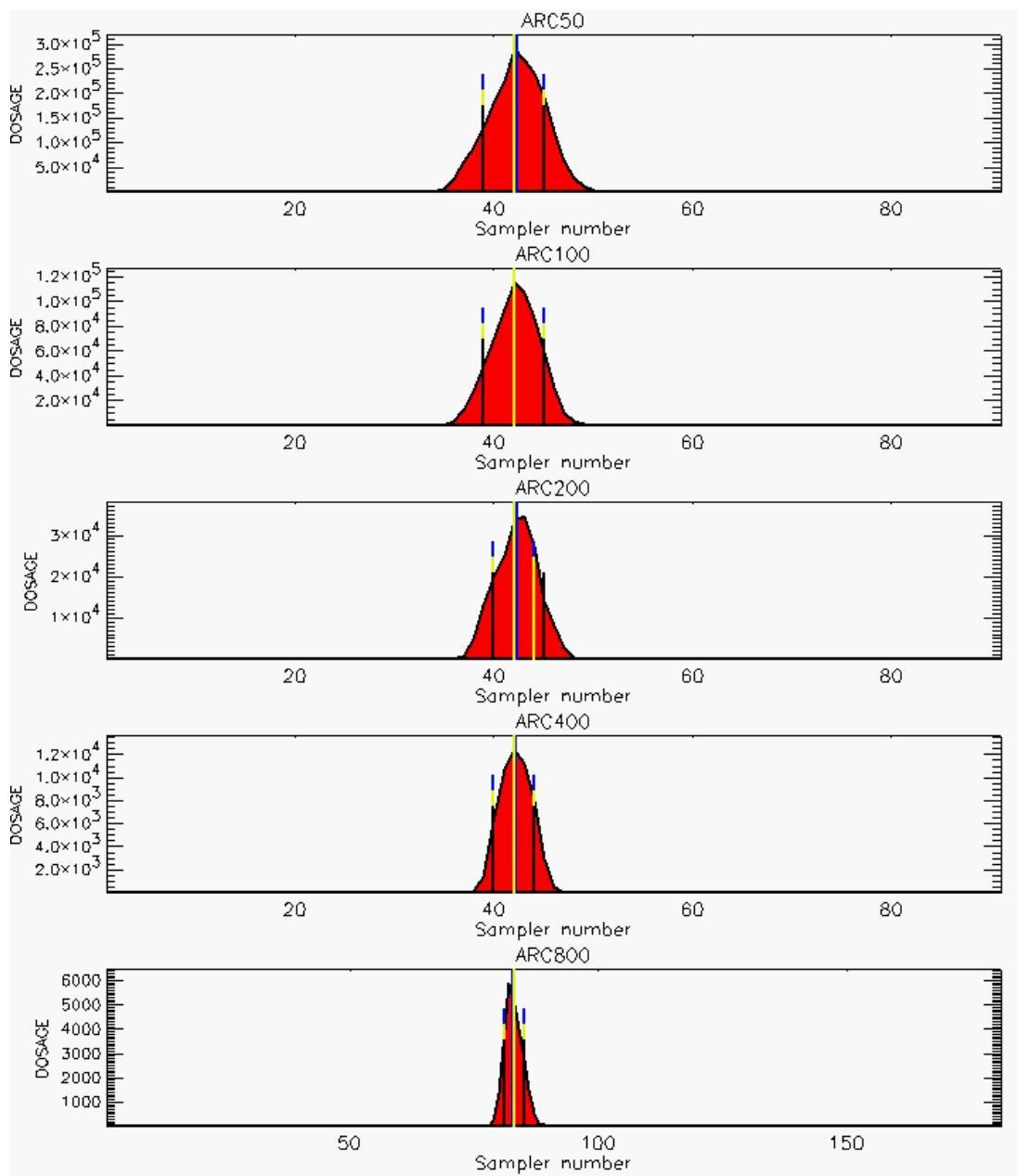
Figure J-1 corresponds to a case where there is a discernible disagreement between the methodologies. It can be seen that the observations associated with this field trial were not particularly Gaussian-like (nor were they even symmetric). Figure J-2 corresponds to a case somewhat more typical of the *Prairie Grass* field trials. In this case, there is very good agreement among the different methodologies. *The results presented in this appendix and in Chapter 3 are based on the MOM method to compute the plume centerline direction (CentDir) and the equal-cuts-off-the-sides method to estimate the plume’s width (W_{ec}).*



PG Observation

PG Trial File: pr_grass_tracer_Experiment_16.txt

**Figure J-1. Centerline and Width Estimation, “Worst Case”:
Blue – COM-Based, Yellow – MOM-Based, Black – Equal Areas Cut Off the Sides-Based**



PG Observation

PG Trial File: pr_grass_tracer_Experiment_28.txt

**Figure J-1. Centerline and Width Estimation, “Best Case”:
Blue – COM-Based, Yellow – MOM-Based, Black – Equal Areas Cut Off the Sides-Based**

REFERENCES

- J-1. Irwin, J. S. and Rosu, M-R., "Comments on a Draft Practice for Statistical Evaluation of Atmospheric Dispersion Models," *Proceedings of the 10th Joint Conference on the Applications of Air Pollution Meteorology*, American Meteorological Society, Boston, pp. 6-10, 1998.

APPENDIX K
PRAIRIE GRASS FIELD TRIAL DATA ANOMALIES
THAT WERE CORRECTED

APPENDIX K

PRAIRIE GRASS FIELD TRIAL DATA ANOMALIES THAT WERE CORRECTED

A computer-ready version of *Prairie Grass* field trial observations was provided by Lawrence Livermore National Laboratory [Ref. K-1]. Later, we discovered that hardcopy of the field trial data were presented in the original *Prairie Grass* report [Ref. K-2]. During our analysis of the *Prairie Grass* field trial data, we encountered two types of data anomalies: “spurious” peaks reported at some samplers¹ and apparent data transcription mistakes that occurred when data were copied from the hardcopy of the report into the computer file. Examination of the field trial data revealed that “spurious” peaks most likely corresponded to misplacement of the decimal point by the authors of the *Prairie Grass* report [Ref. K-2]. After consultation with a researcher who has previously used *Prairie Grass* field trial data [Ref. K-3], we decided to correct the “spurious” peaks by fixing the decimal point misplacements (using our processing software).

The majority of computer data transcription errors occurred as a result of incorrect placement of the decimal point. Only field trials that were used in the “official” HPAC/NARAC comparison were scanned for data transcription mistakes. At present, no tower sampler data were checked since they were not used in our HPAC/NARAC comparisons.

Tables K-1, K-2, and K-3, that follow, provide additional details.

¹ We somewhat arbitrarily define a data peak to be spurious if it is more than an order of magnitude larger than the next largest value in the arc under consideration.

Table K-1. List of Prairie Grass Trials That Were Scanned for Transcription Errors

{5, 7, 8, 9, 10, 11, 12, 13, 14, 15, 16, 17, 18, 19, 20, 21, 22, 23, 24, 25, 26, 27, 28, 32, 33, 34, 35, 36, 37, 38, 39, 40, 41, 42, 43, 44, 45, 46, 48, 49, 50, 51, 54, 55, 56, 57, 58, 59, 60, 61, 62}
--

Table K-2. Prairie Grass Trials That Were Modified as a Result of Decimal Point and Missing Value Data Transcription Errors

Trial #, arc, sampler #	Old value	New Value	Comments
T7, 800m, S102	0.004	0.037	factor of 10
T7, 800m, S103	0.092	0.009	
T8, 50m, S44	949.400	94.940	factor of 0.1
T11, 800m, S90	missing	408.500	"spurious" peak added
T13, 50m, S65	0.728	0.073	factor of 0.1
T21, 400m, S40	0.105	1.055	factor of 10
T23, 50m, S22	899.70	89.965	factor of 0.1
T45, 800m, S77	0.132	1.320	factor of 10
T51, 100m, S67	missing	6.717	appears valid
T51, 50m, S80	missing	210.24	appears valid

Table K-3. Prairie Grass Trials That Have "Spurious" Peaks Replaced by Fixing Decimal Point Position (Done in Software Only)

Trial #, arc, sampler #	Old Value	New Values	Comments
T11, 800m, S90	408.500	0.408	factor of 250 greater than next largest value
T16, 200m, S63	329.000	3.29	factor of 55 greater than next largest value

REFERENCES

- K-1. The sampler data in the arcs were obtained from Doug Murray of TRC, while 100-meter arc tower data were transcribed by LLNL (private communication, July 2000).
- K-2. Barad, M. L. (Editor), *Project Prairie Grass, A Field Program in Diffusion*, Geophysical Research Papers, No. 59, Volumes I and II, Table 5.2, p. 79-192 DTIC #AD-152572/AFCRC-TR-58-235(I), 1958.
- K-3. Irwin, J. S., *PGINPUT.BAK* file of Eval(6).zip package available at authors ftp site <ftp://ftp.epa.gov/AMD/asmd/irwin/>, and private e-mail communications concerning replacement of “spurious” peaks, September 2000.

APPENDIX L
COMPARISONS OF NARAC PREDICTIONS: WITH AND
WITHOUT SURFACE DEPOSITION

APPENDIX L

COMPARISONS OF NARAC PREDICTIONS: WITH AND WITHOUT SURFACE DEPOSITION

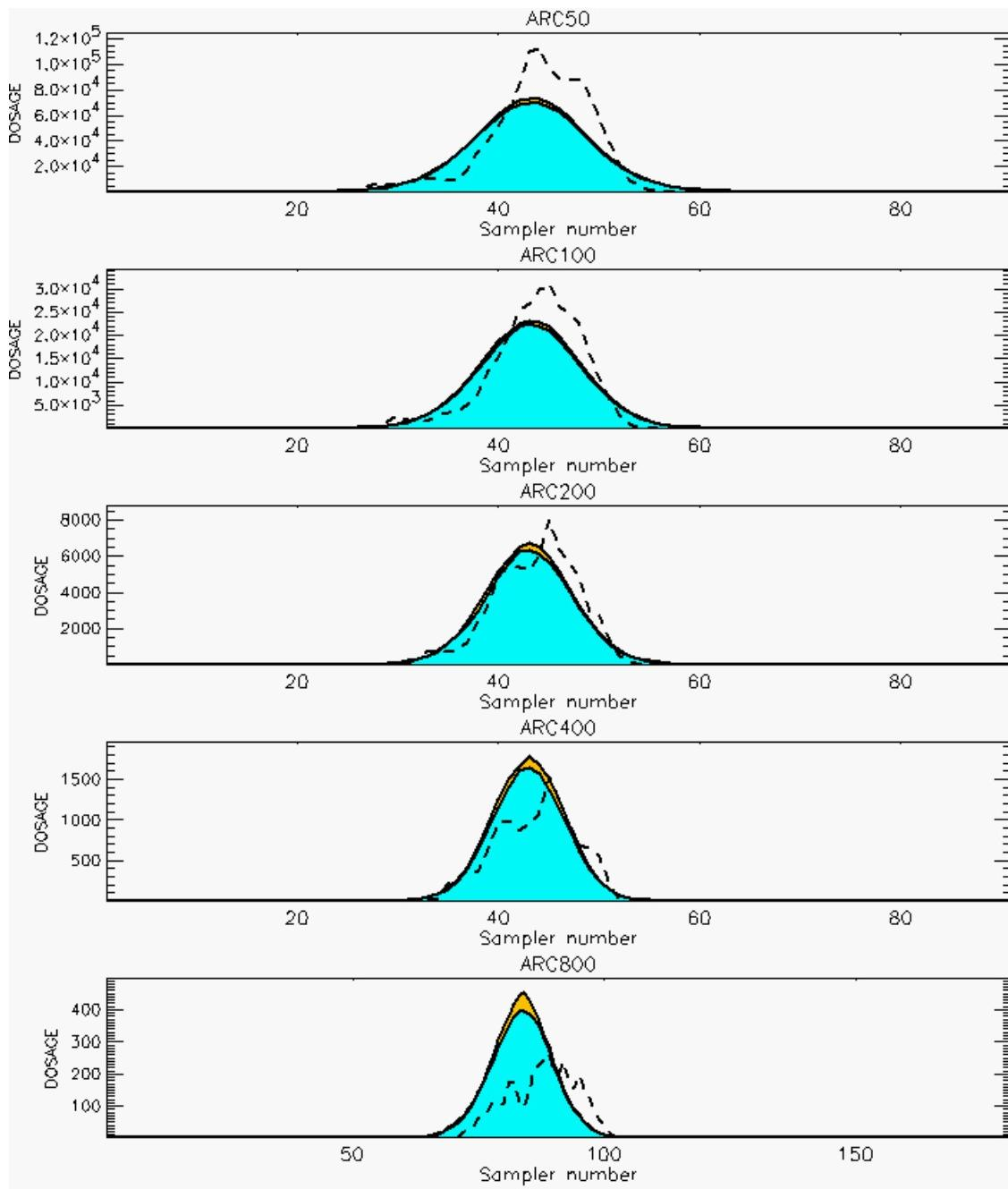
This appendix presents graphical comparisons of NARAC predictions with and without the inclusion of a mechanism for SO₂ surface deposition. Vertical plot units are dosage units of mg-sec/m³. The horizontal plot units are sampler numbers as presented in the *Prairie Grass* field trials [Ref. L-1]. Sampler number 1 oriented to the west, the middle sampler (45 or 90) oriented to the north, and the last sampler (91 or 181) is oriented to the east of the SO₂ gas release source. Only data values greater than the cutoff threshold of 3 mg-sec/m³ (0.005 mg/m³) are presented. This cutoff threshold value corresponds to a minimum value reported in *Prairie Grass* field trials.

Comparisons of NARAC predictions with and without SO₂ surface deposition are presented on linear and log dosage scales. Each graphical comparison consists of five plots (one for each arc) with the top plot depicting the 50-meter arc, the second plot depicting the 100-meter arc, the third plot depicting the 200-meter arc, and so on. The last panel (just above the figure caption) contains information about the data files used to produce these plots. The *Prairie Grass* field trial file name contains a two-digit number corresponding to the trial number. Prediction file names contain the moniker “novd” denoting that SO₂ surface deposition was not considered, or the moniker “vd” denoting that SO₂ surface deposition was considered; and a one- or two-digit number reflecting the *Prairie Grass* field trial being predicted. Even-numbered pages contain figures on the linear dosage scale while odd-numbered pages contain figures on the logarithmic dosage scale.

The meanings of the colors used in the plots are described in the below legend:

- Dark Blue — higher dosages for predictions with SO₂ surface deposition
- Turquoise — dosages that agree for both predictions.
- Brown — higher dosages for predictions without SO₂ deposition.

The dashed lines depict dosage values actually obtained in the field trial. Irwin stability categories that were used in our analyses are denoted in the figure captions. These stability category assignments are based on Reference L-2.



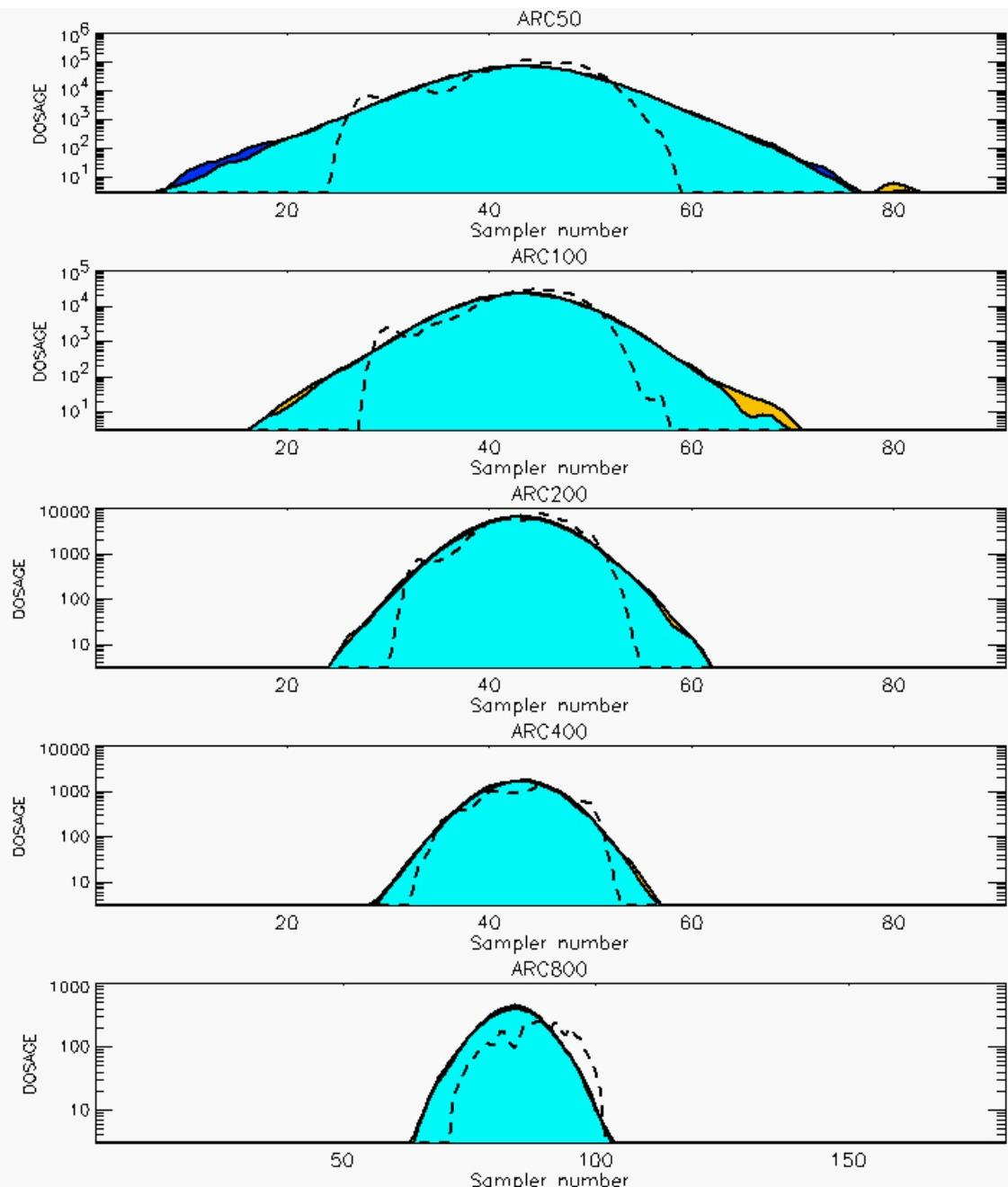
PG Prediction1 to Prediction2 Comparison

PG Trial File: pr_grass_tracer_Experiment_05.txt

PG Prediction File 1: ARAC\sv_vd\pg_5_sv_vd.arac

PG Prediction File 2: ARAC\sv_nvd\pg_5_sv_nvd.arac

Figure L-1a. NARAC With and Without SO₂ Surface Deposition Predictions to Trial 5 on Linear Scale: Stability Category is 2



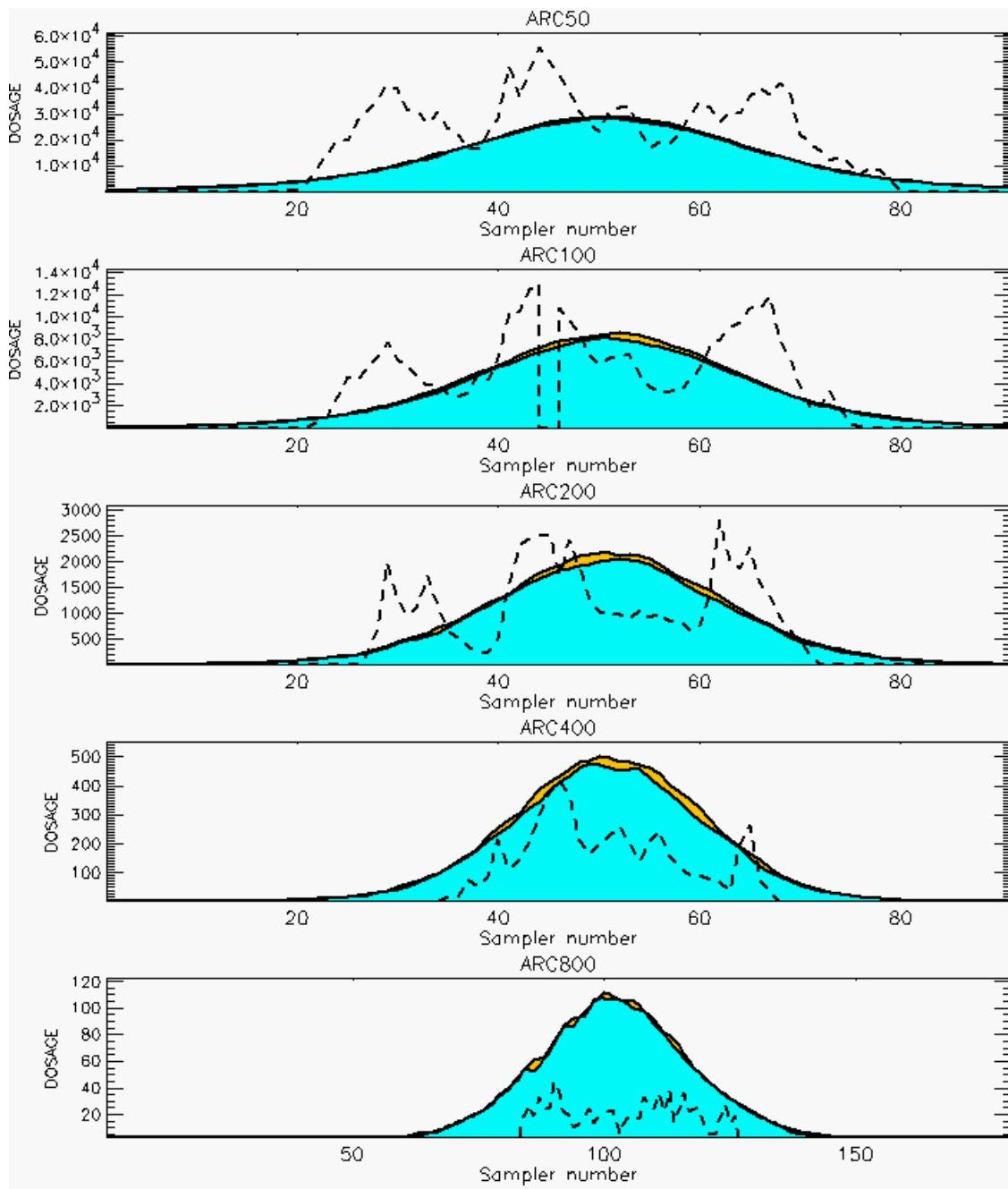
PG Prediction1 to Prediction2 Comparison

PG Trial File: pr_grass_tracer_Experiment_05.txt

PG Prediction File 1: ARAC\sv_vd\pg_5_sv_vd.arac

PG Prediction File 2: ARAC\sv_nvd\pg_5_sv_nvd.arac

Figure L-1b. NARAC With and Without SO₂ Surface Deposition Predictions to Trial 5 on Logarithmic Scale: Stability Category is 2



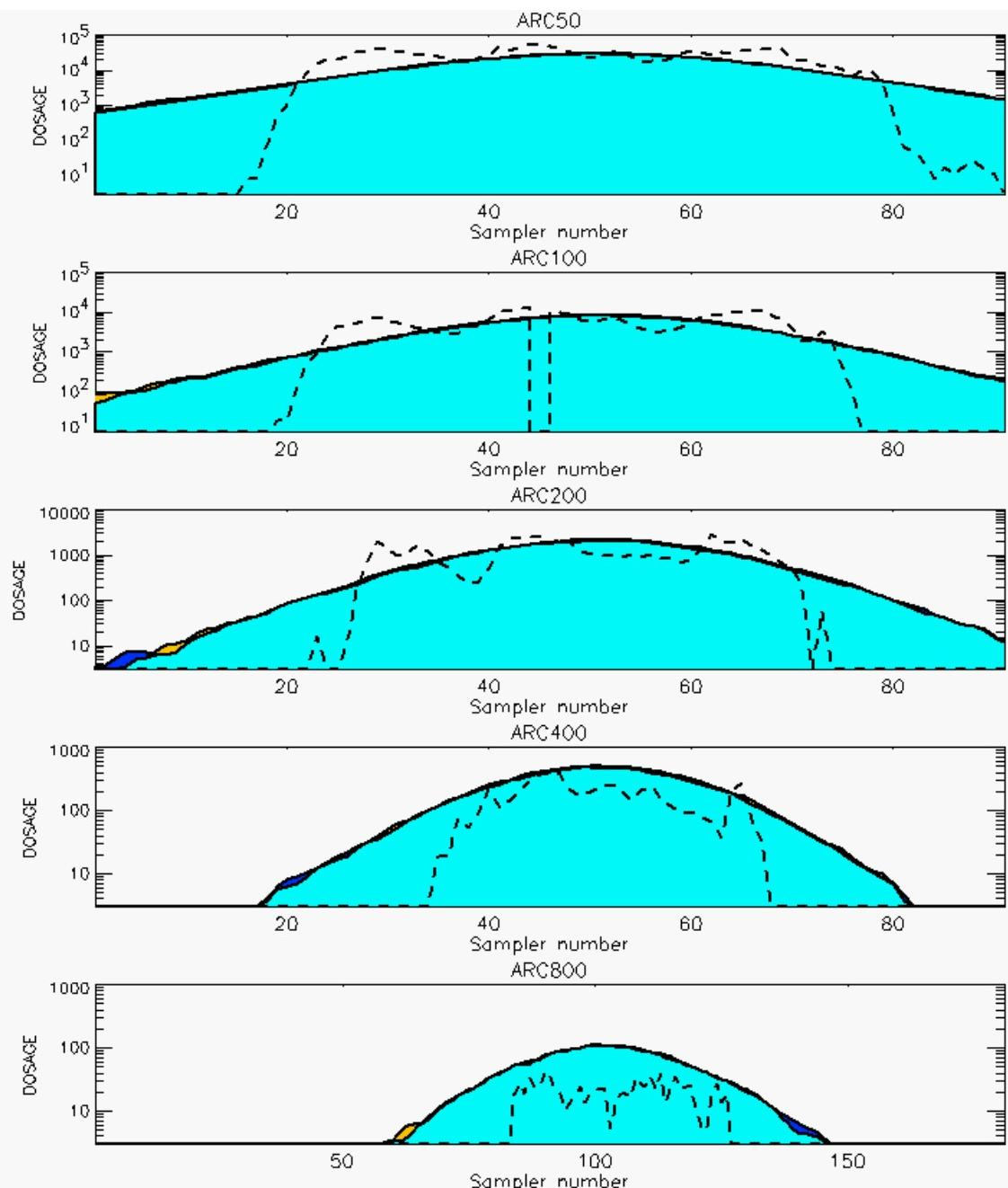
PG Prediction1 to Prediction2 Comparison

PG Trial File: pr_grass_tracer_Experiment_07.txt

PG Prediction File 1: ARAC\sv_vd\pg_7_sv_vd.arac

PG Prediction File 2: ARAC\sv_nvd\pg_7_sv_nvd.arac

Figure L-2a. NARAC With and Without SO₂ Surface Deposition Predictions to Trial 7 on Linear Scale: Stability Category is 1



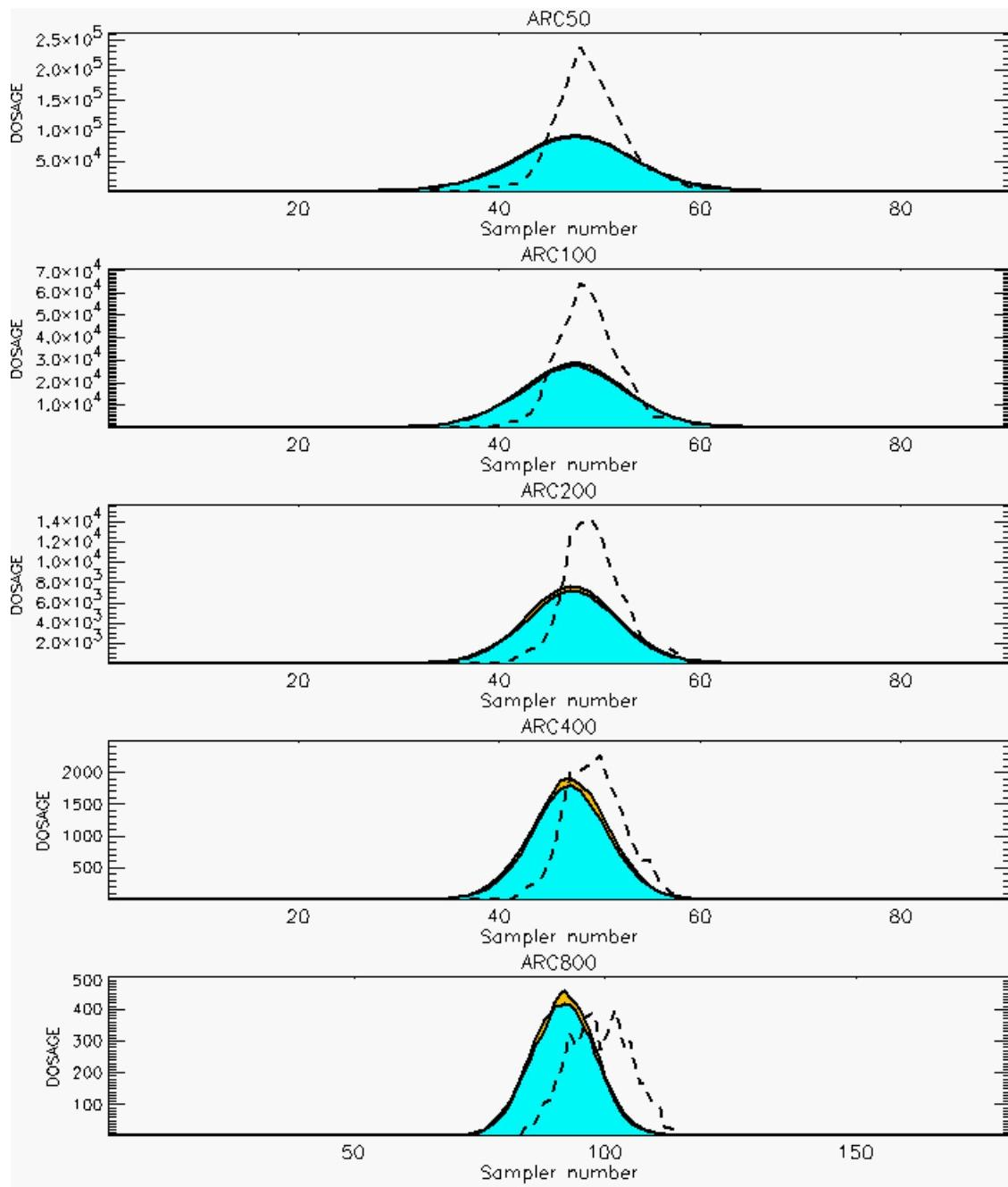
PG Prediction1 to Prediction2 Comparison

PG Trial File: pr_grass_tracer_Experiment_07.txt

PG Prediction File 1: ARAC\sv_vd\pg_7_sv_vd.arac

PG Prediction File 2: ARAC\sv_nvd\pg_7_sv_nvd.arac

Figure L-2b. NARAC With and Without SO₂ Surface Deposition Predictions to Trial 7 on Logarithmic Scale: Stability Category is 1



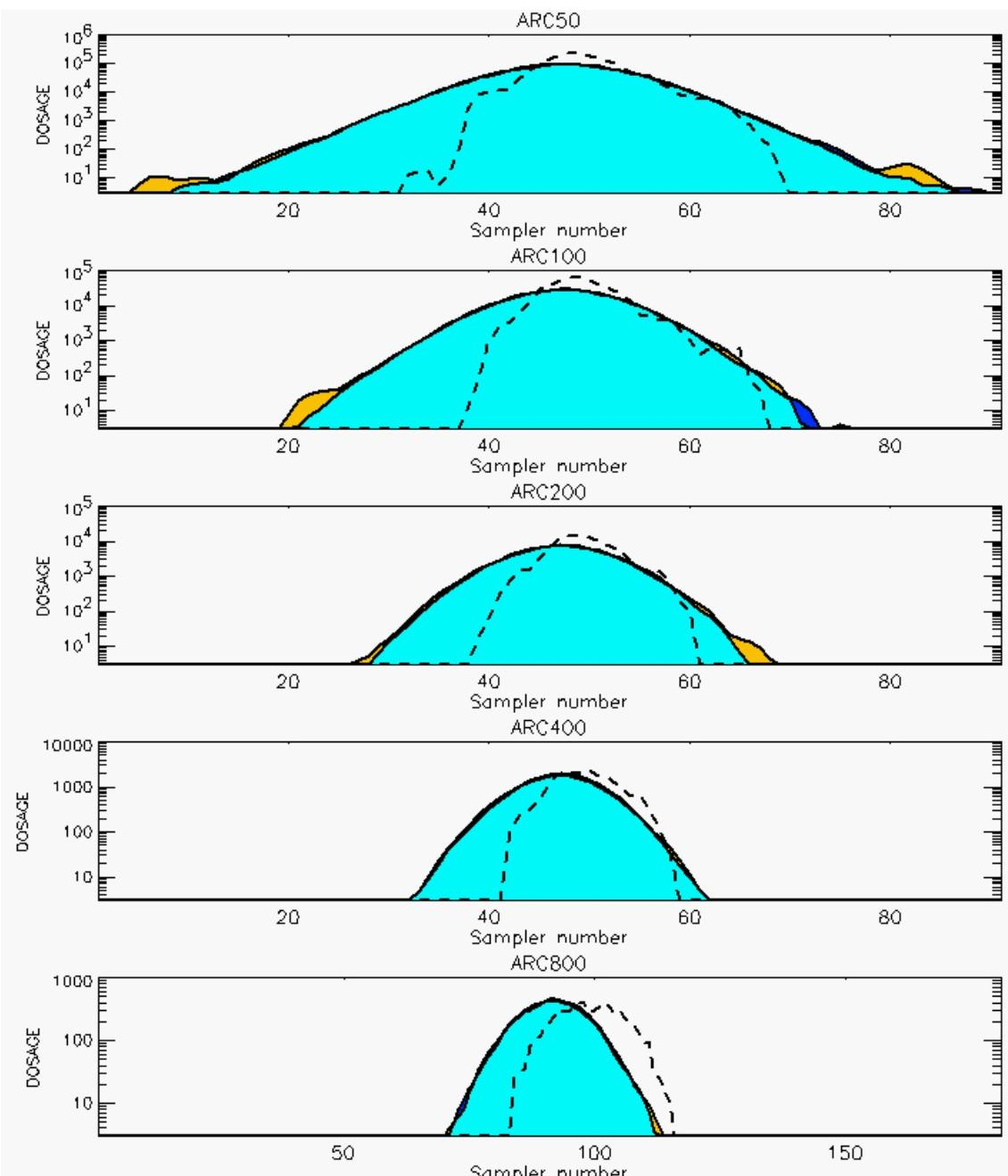
PG Prediction1 to Prediction2 Comparison

PG Trial File: pr_grass_tracer_Experiment_08.txt

PG Prediction File 1: ARAC\sv_vd\pg_8_sv_vd.arac

PG Prediction File 2: ARAC\sv_nvd\pg_8_sv_nvd.arac

Figure L-3a. NARAC With and Without SO₂ Surface Deposition Predictions to Trial 8 on Linear Scale: Stability Category is 2



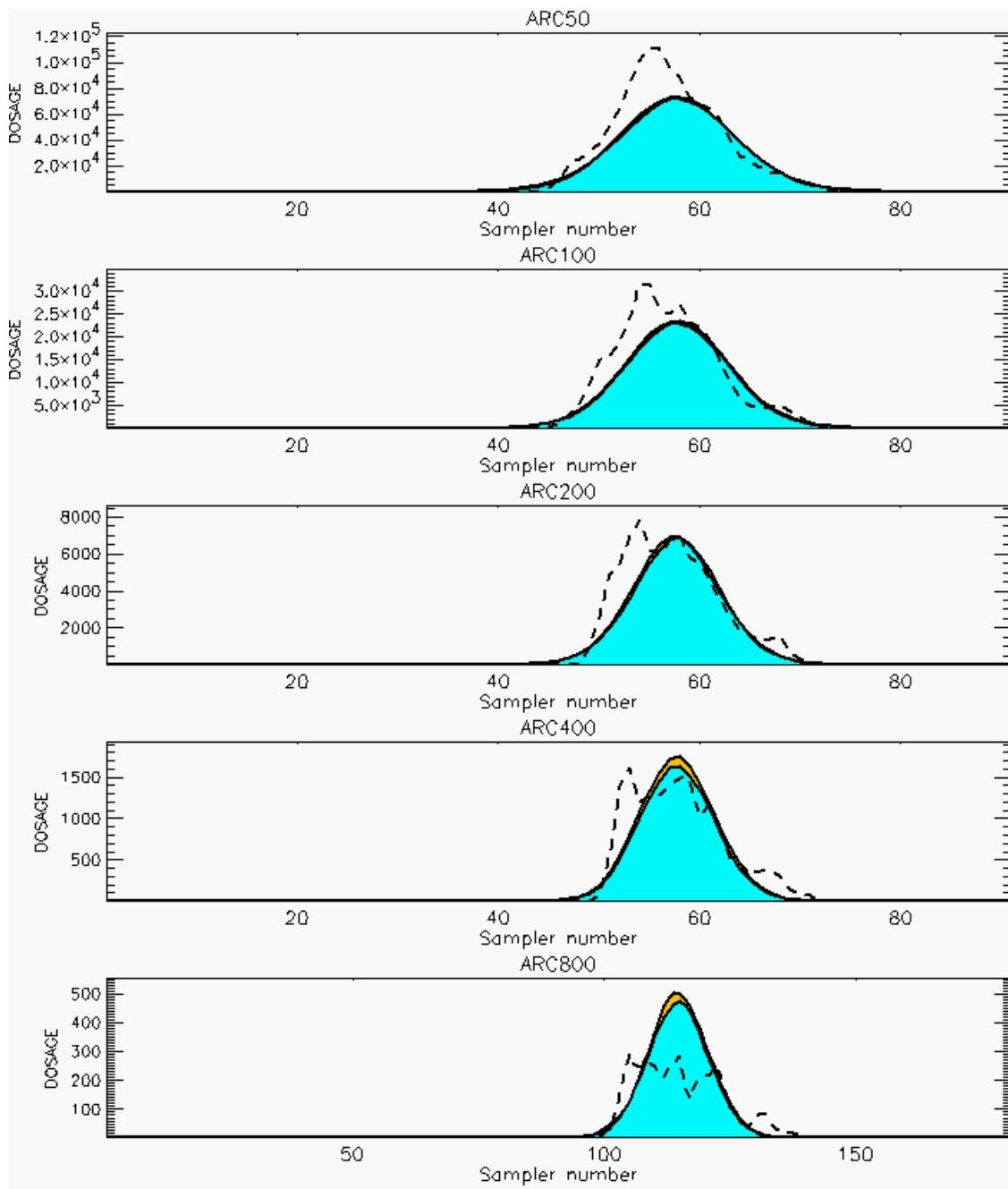
PG Prediction1 to Prediction2 Comparison

PG Trial File: pr_grass_tracer_Experiment_08.txt

PG Prediction File 1: ARAC\sv_vd\pg_8_sv_vd.arac

PG Prediction File 2: ARAC\sv_nvd\pg_8_sv_nvd.arac

Figure L-3b. NARAC With and Without SO₂ Surface Deposition Predictions to Trial 8 on Logarithmic Scale: Stability Category is 2



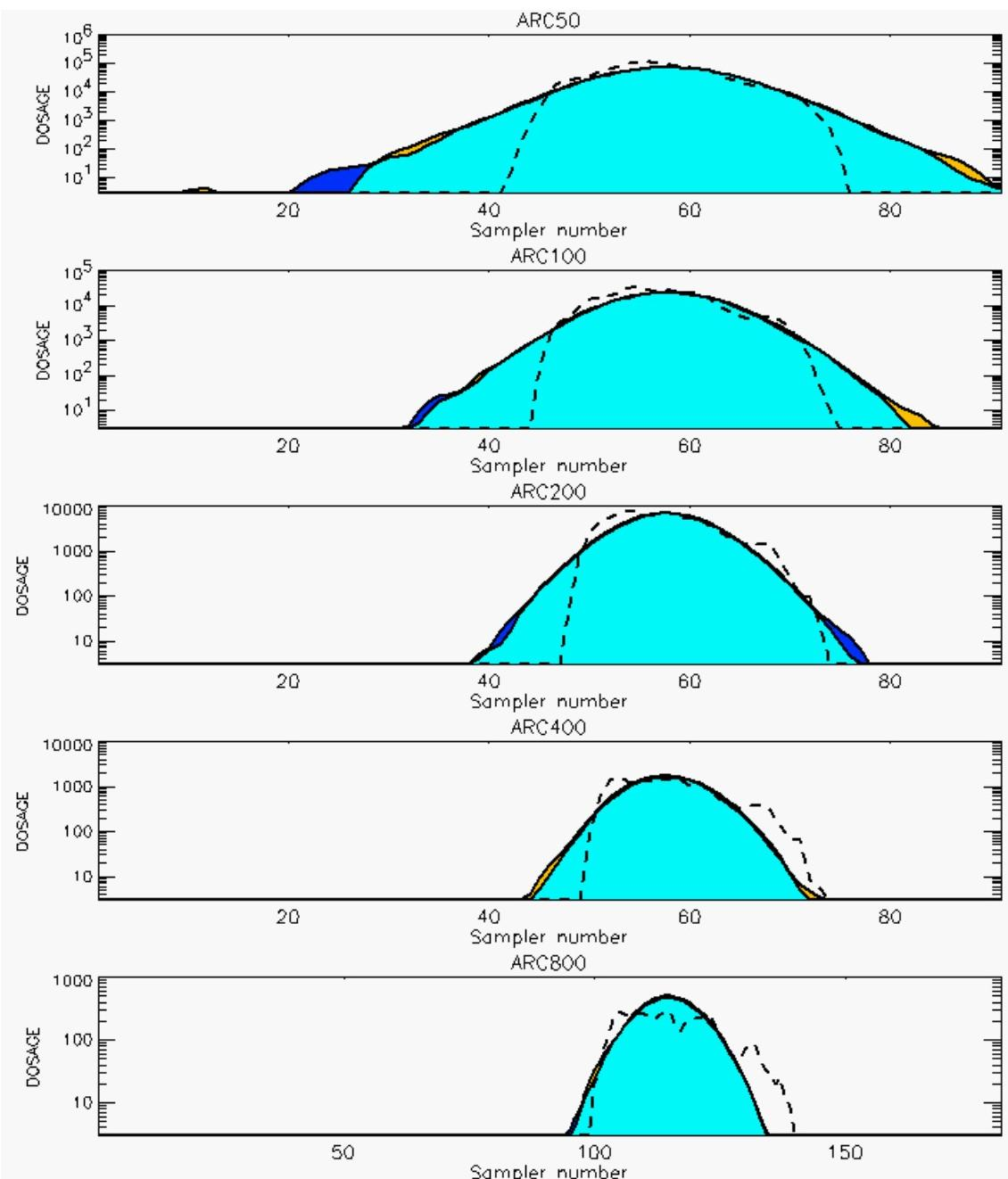
PG Prediction1 to Prediction2 Comparison

PG Trial File: pr_grass_tracer_Experiment_09.txt

PG Prediction File 1: ARAC\sv_vd\pg_9_sv_vd.arac

PG Prediction File 2: ARAC\sv_nadv\pg_9_sv_nadv.arac

Figure L-4a. NARAC With and Without SO₂ Surface Deposition Predictions to Trial 9 on Linear Scale: Stability Category is 2



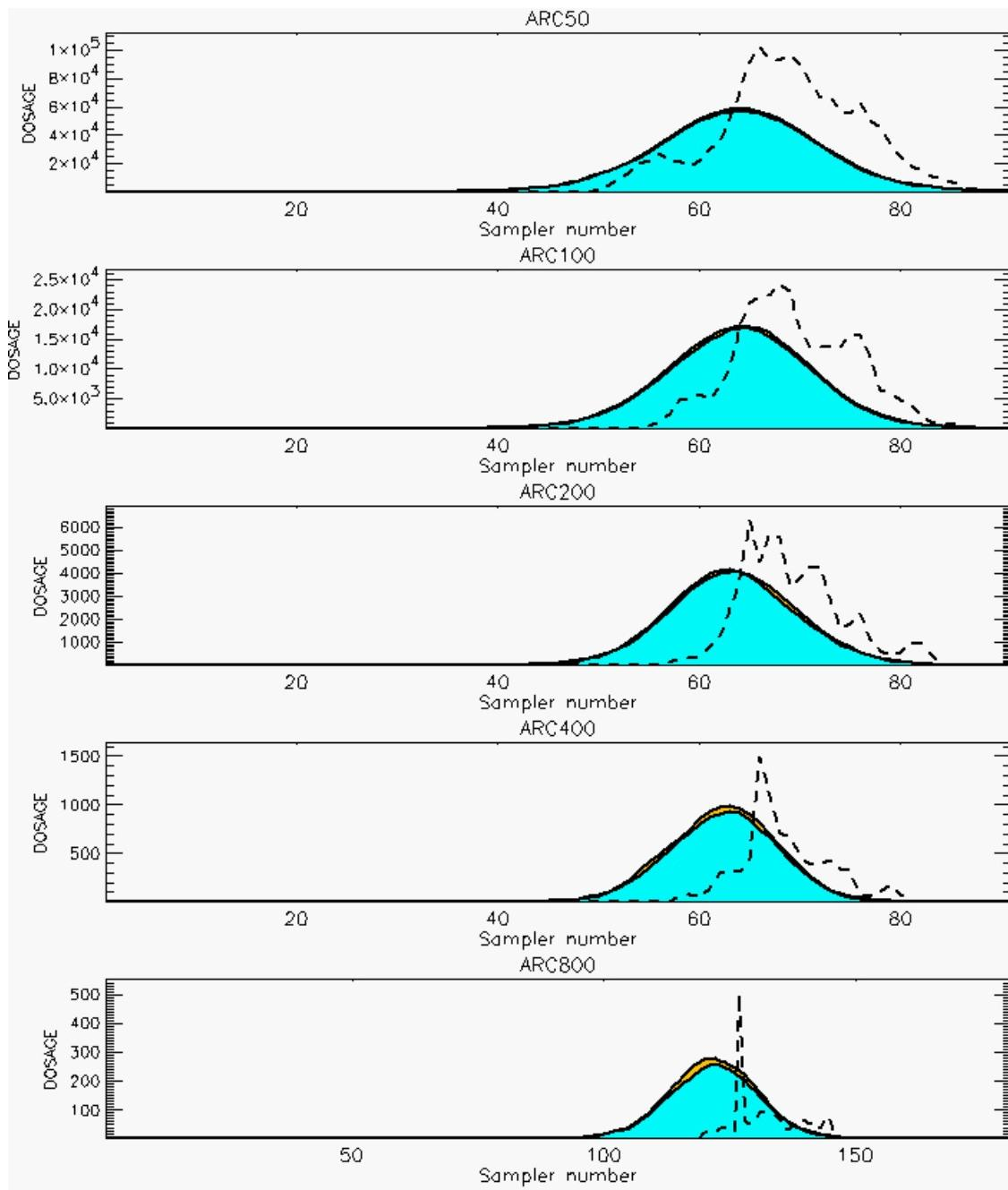
PG Prediction1 to Prediction2 Comparison

PG Trial File: pr_grass_tracer_Experiment_09.txt

PG Prediction File 1: ARAC\sv_vd\pg_9_sv_vd.arac

PG Prediction File 2: ARAC\sv_nvd\pg_9_sv_nvd.arac

Figure L-4b. NARAC With and Without SO₂ Surface Deposition Predictions to Trial 9 on Logarithmic Scale: Stability Category is 2



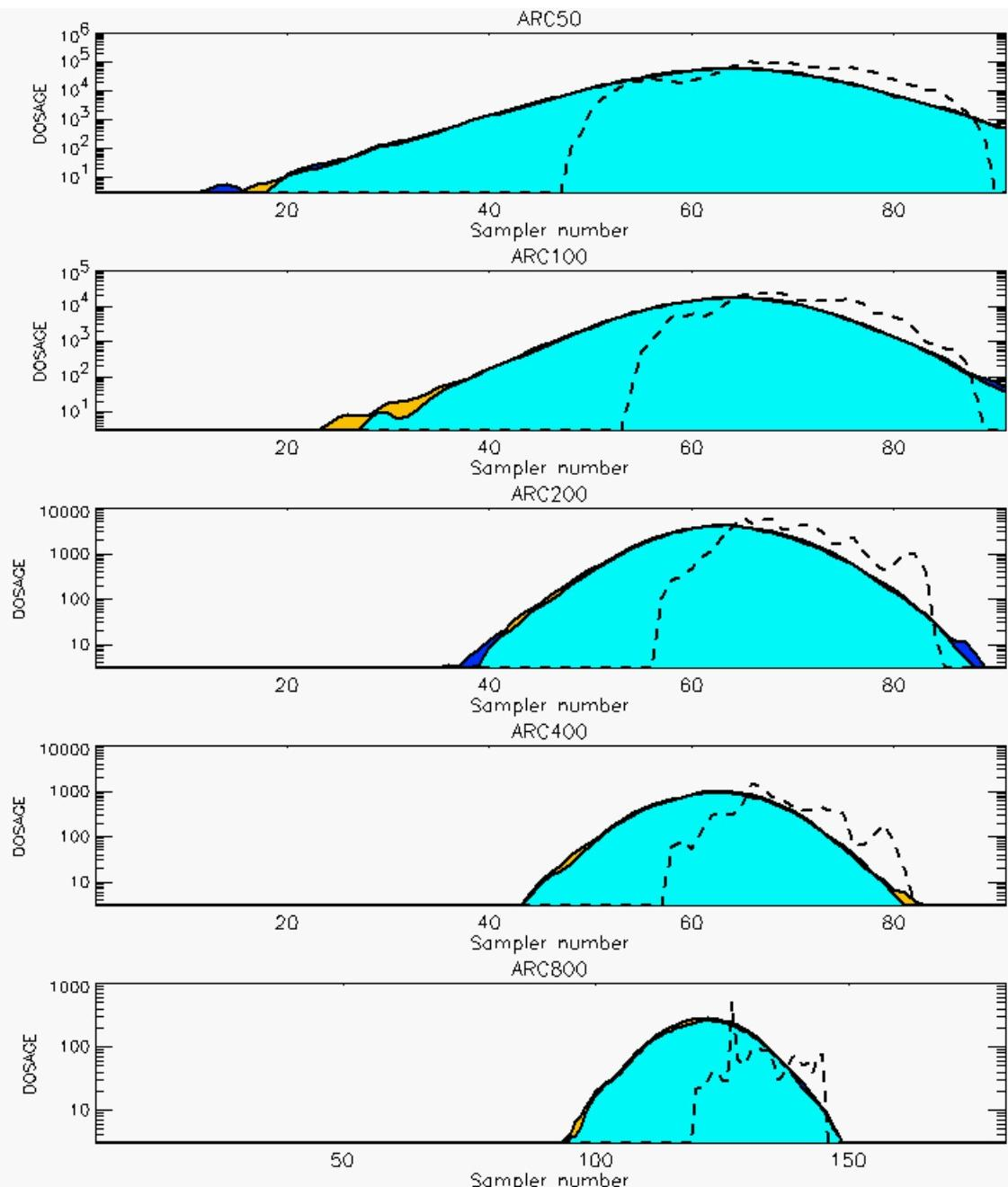
PG Prediction1 to Prediction2 Comparison

PG Trial File: pr_grass_tracer_Experiment_10.txt

PG Prediction File 1: ARAC\sv_vd\pg_10_sv_vd.arac

PG Prediction File 2: ARAC\sv_novd\pg_10_sv_novd.arac

Figure L-5a. NARAC With and Without SO_2 Surface Deposition Predictions to Trial 10 on Linear Scale: Stability Category is 1



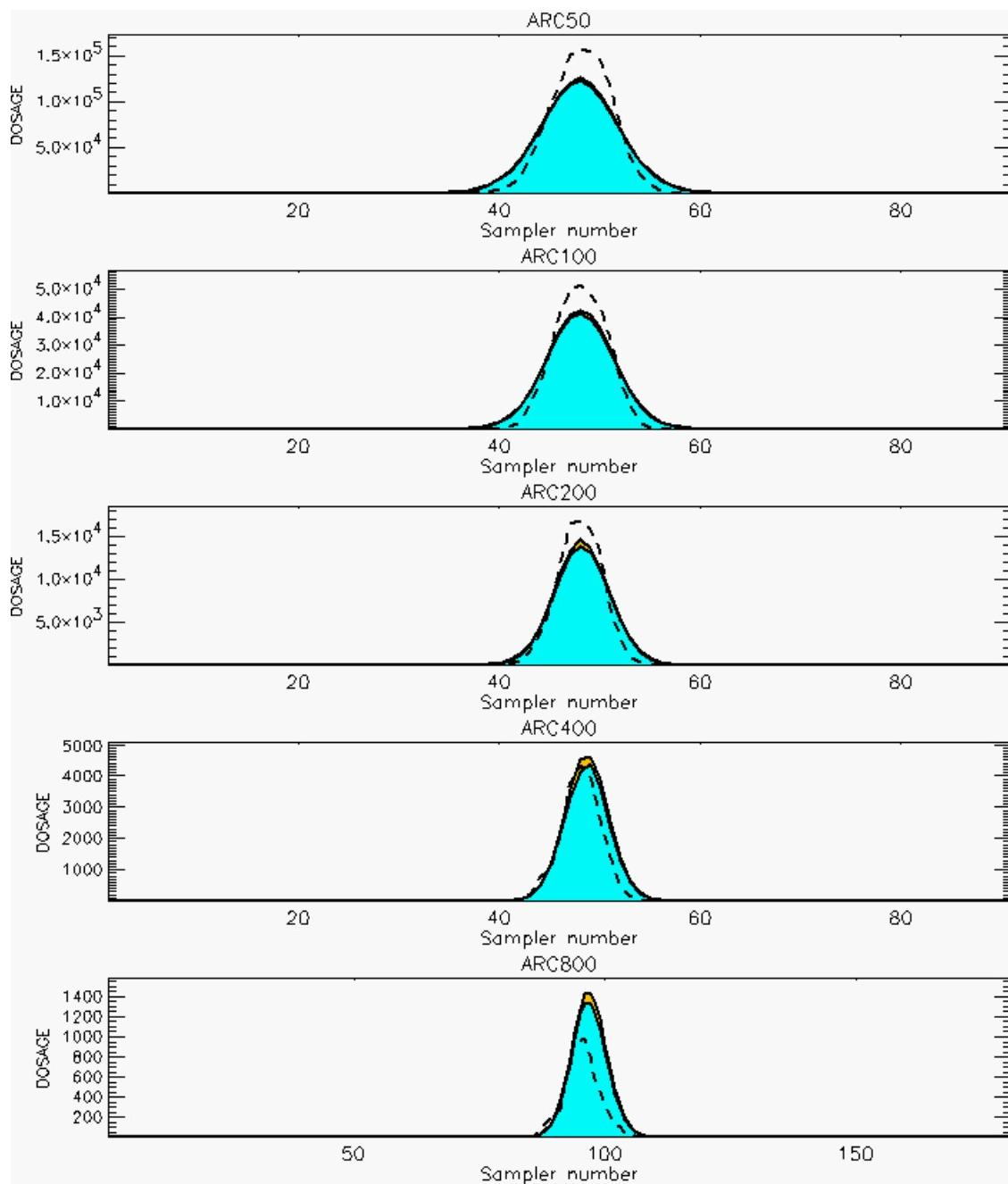
PG Prediction1 to Prediction2 Comparison

PG Trial File: pr_grass_tracer_Experiment_10.txt

PG Prediction File 1: ARAC\sv_vd\pg_10_sv_vd.arac

PG Prediction File 2: ARAC\sv_novd\pg_10_sv_novd.arac

Figure L-5b. NARAC With and Without SO₂ Surface Deposition Predictions to Trial 10 on Logarithmic Scale: Stability Category is 1



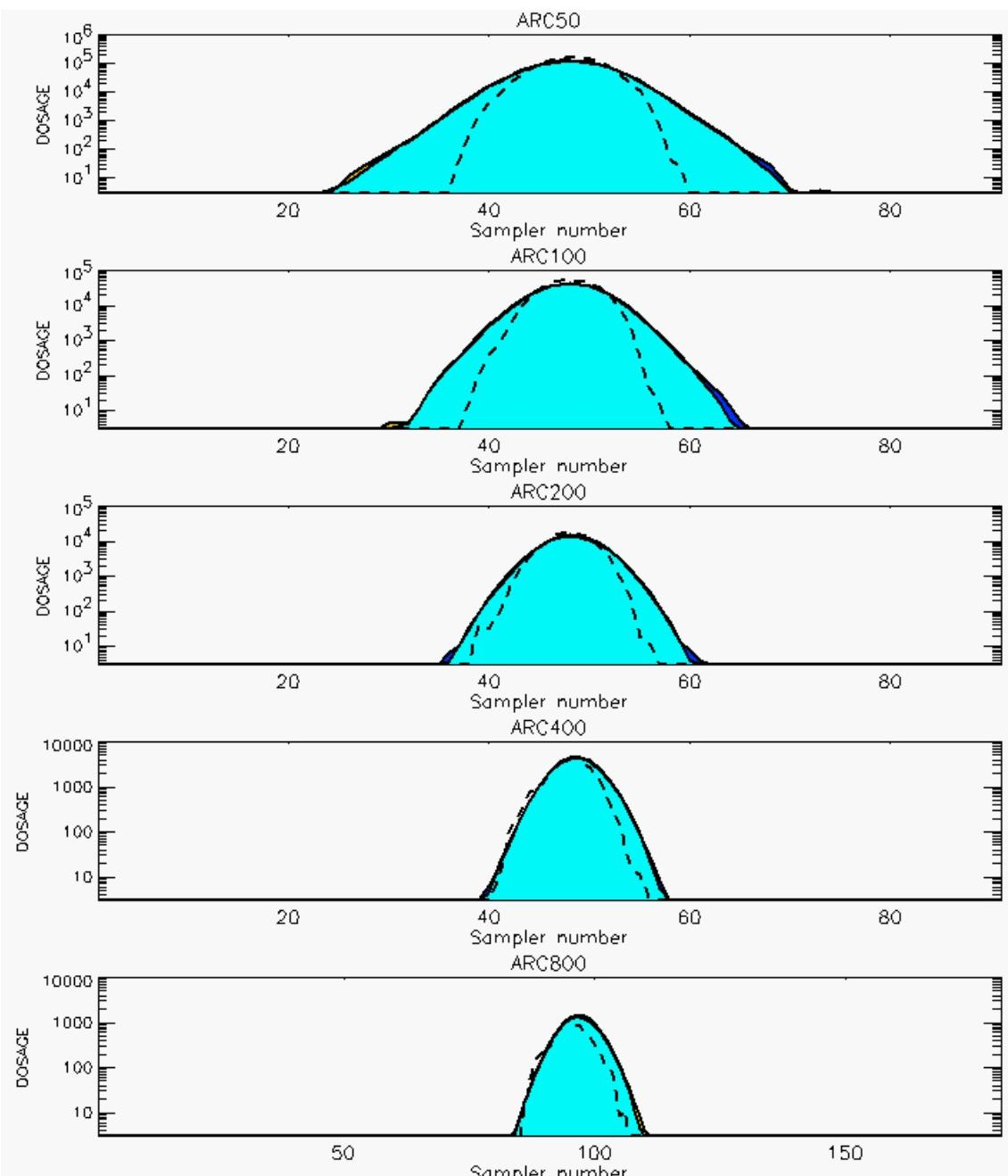
PG Prediction1 to Prediction2 Comparison

PG Trial File: pr_grass_tracer_Experiment_11.txt

PG Prediction File 1: ARAC\sv_vd\pg_11_sv_vd.arac

PG Prediction File 2: ARAC\sv_novd\pg_11_sv_novd.arac

Figure L-6a. NARAC With and Without SO₂ Surface Deposition Predictions to Trial 11 on Linear Scale: Stability Category is 3



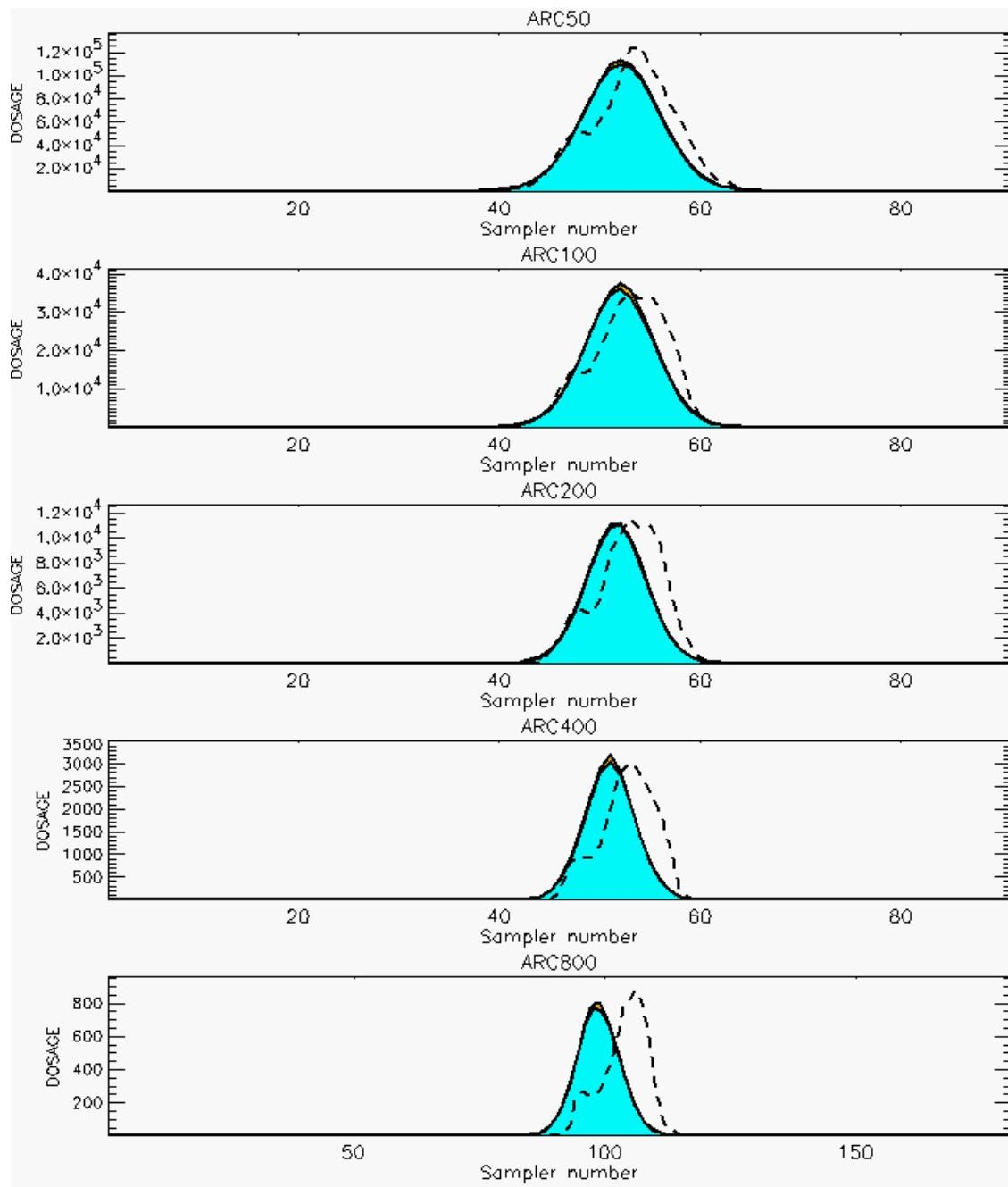
PG Prediction1 to Prediction2 Comparison

PG Trial File: pr_grass_tracer_Experiment_11.txt

PG Prediction File 1: ARAC\sv_vd\pg_11_sv_vd.arac

PG Prediction File 2: ARAC\sv_novd\pg_11_sv_novd.arac

Figure L-6b. NARAC With and Without SO₂ Surface Deposition Predictions to Trial 11 on Logarithmic Scale: Stability Category is 3



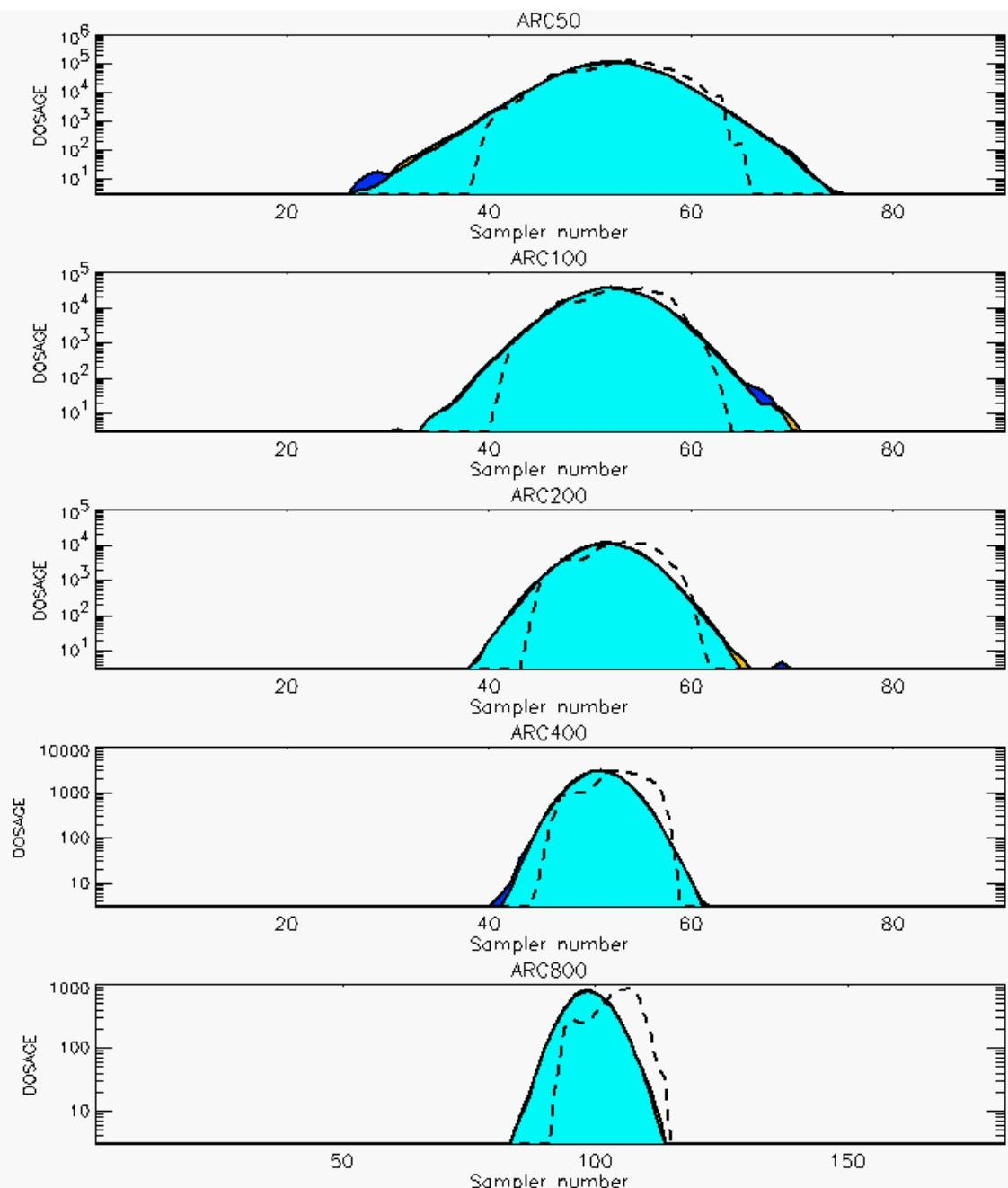
PG Prediction1 to Prediction2 Comparison

PG Trial File: pr_grass_tracer_Experiment_12.txt

PG Prediction File 1: ARAC\sv_vd\pg_12_sv_vd.arac

PG Prediction File 2: ARAC\sv_novd\pg_12_sv_novd.arac

Figure L-7a. NARAC With and Without SO₂ Surface Deposition Predictions to Trial 12 on Linear Scale: Stability Category is 3



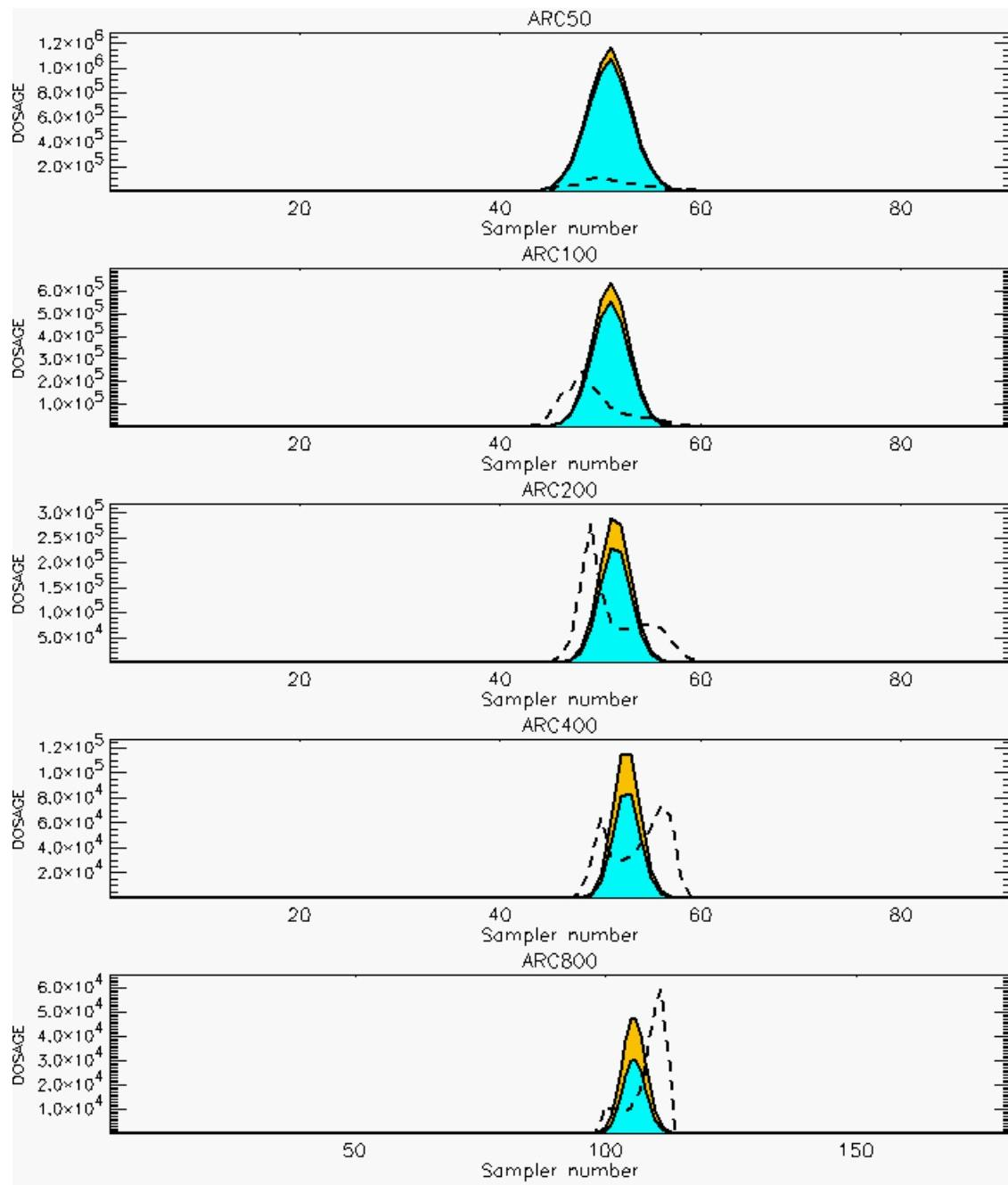
PG Prediction1 to Prediction2 Comparison

PG Trial File: pr_grass_tracer_Experiment_12.txt

PG Prediction File 1: ARAC\sv_vd\pg_12_sv_vd.arac

PG Prediction File 2: ARAC\sv_novd\pg_12_sv_novd.arac

Figure L-7b. NARAC With and Without SO₂ Surface Deposition Predictions to Trial 12 on Logarithmic Scale: Stability Category is 3



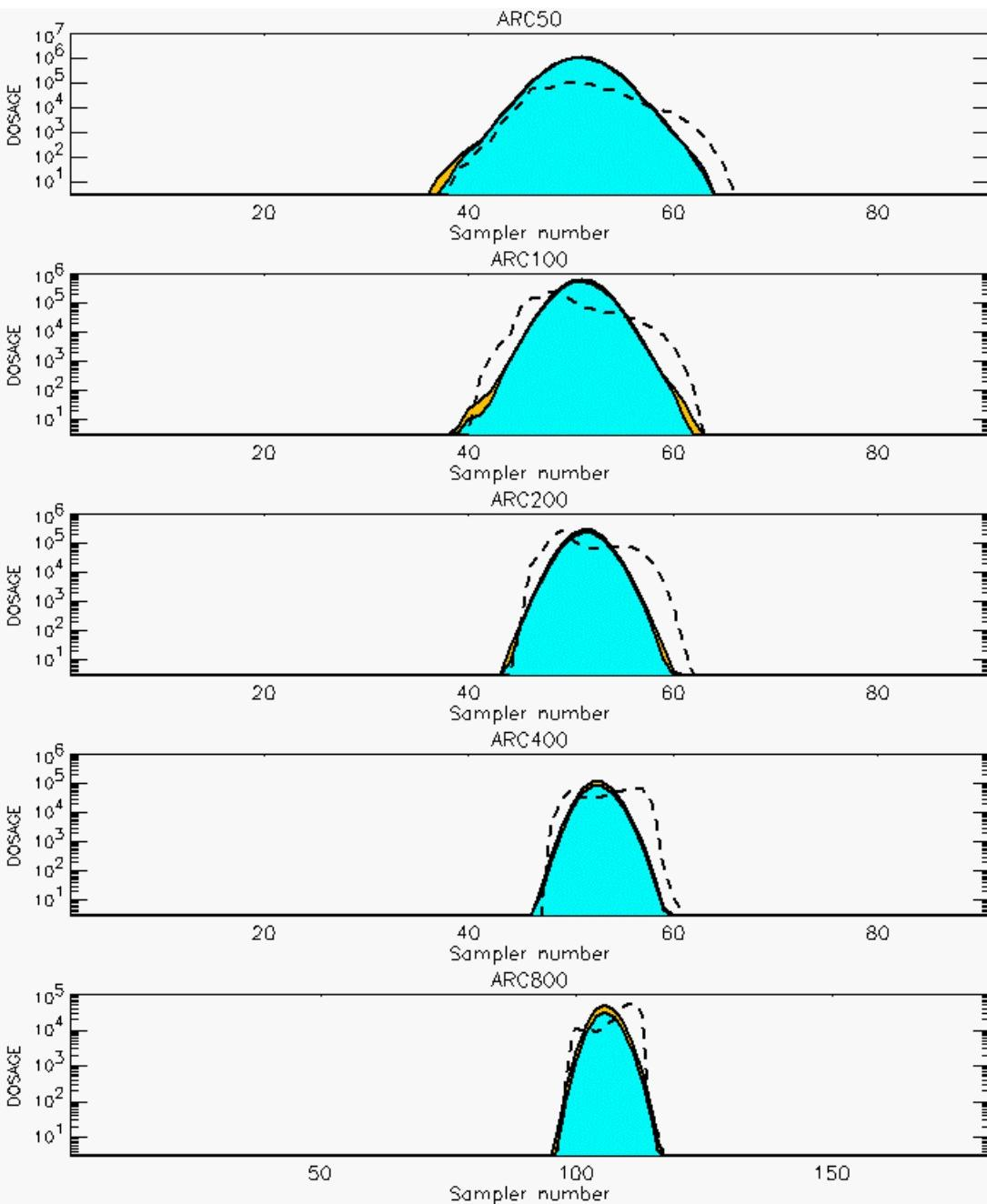
PG Prediction1 to Prediction2 Comparison

PG Trial File: pr_grass_tracer_Experiment_13.txt

PG Prediction File 1: ARAC\sv_vd\pg_13_sv_vd.arac

PG Prediction File 2: ARAC\sv_novd\pg_13_sv_novd.arac

Figure L-8a. NARAC With and Without SO₂ Surface Deposition Predictions to Trial 13 on Linear Scale: Stability Category is 7



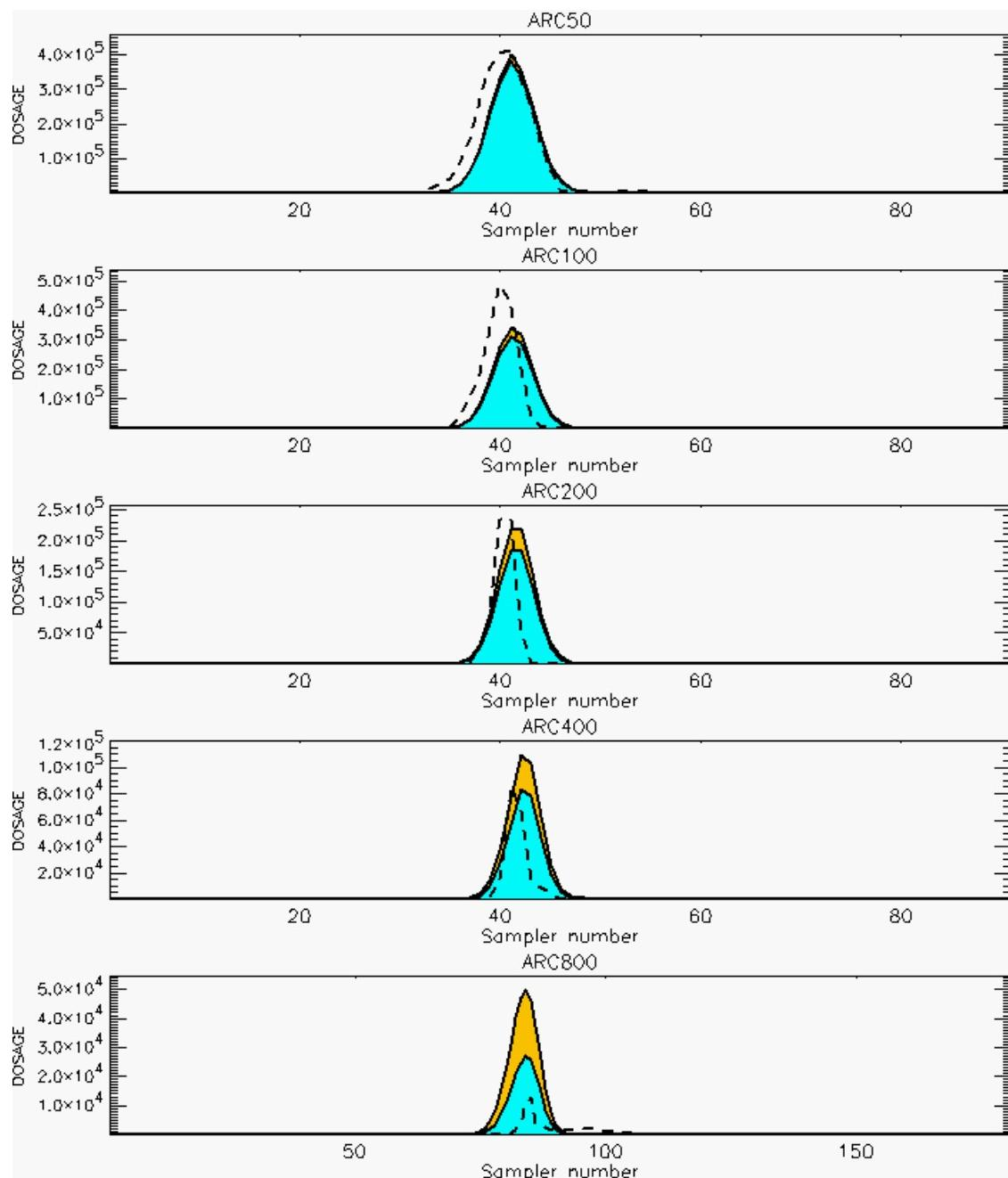
PG Prediction1 to Prediction2 Comparison

PG Trial File: pr_grass_tracer_Experiment_13.txt

PG Prediction File 1: ARAC\sv_vd\pg_13_sv_vd.arac

PG Prediction File 2: ARAC\sv_novd\pg_13_sv_novd.arac

Figure L-8b. NARAC With and Without SO_2 Surface Deposition Predictions to Trial 13 on Logarithmic Scale: Stability Category is 7



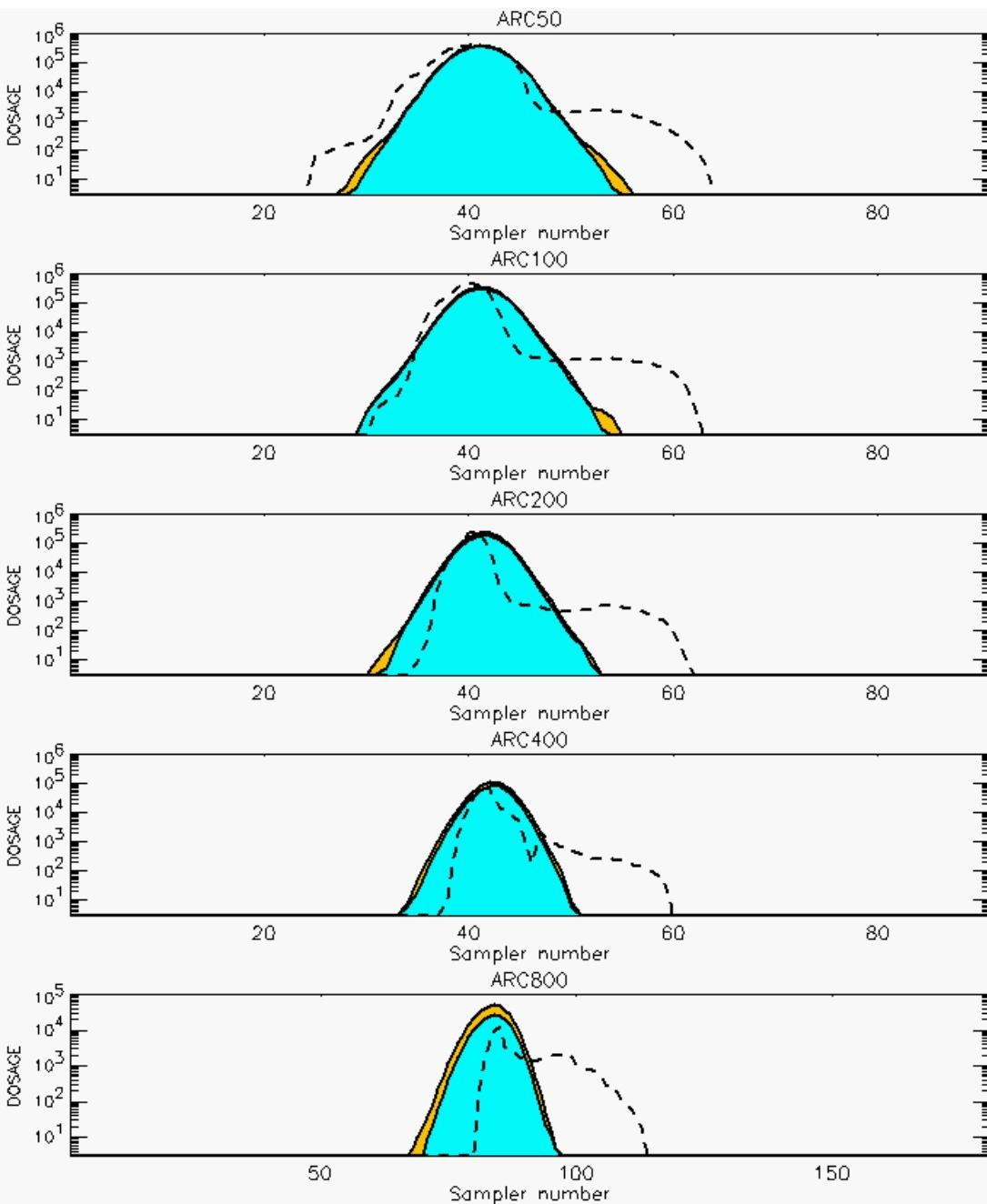
PG Prediction1 to Prediction2 Comparison

PG Trial File: pr_grass_tracer_Experiment_14.txt

PG Prediction File 1: ARAC\sv_vd\pg_14_sv_vd.arac

PG Prediction File 2: ARAC\sv_novd\pg_14_sv_novd.arac

Figure L-9a. NARAC With and Without SO_2 Surface Deposition Predictions to Trial 14 on Linear Scale: Stability Category is 7



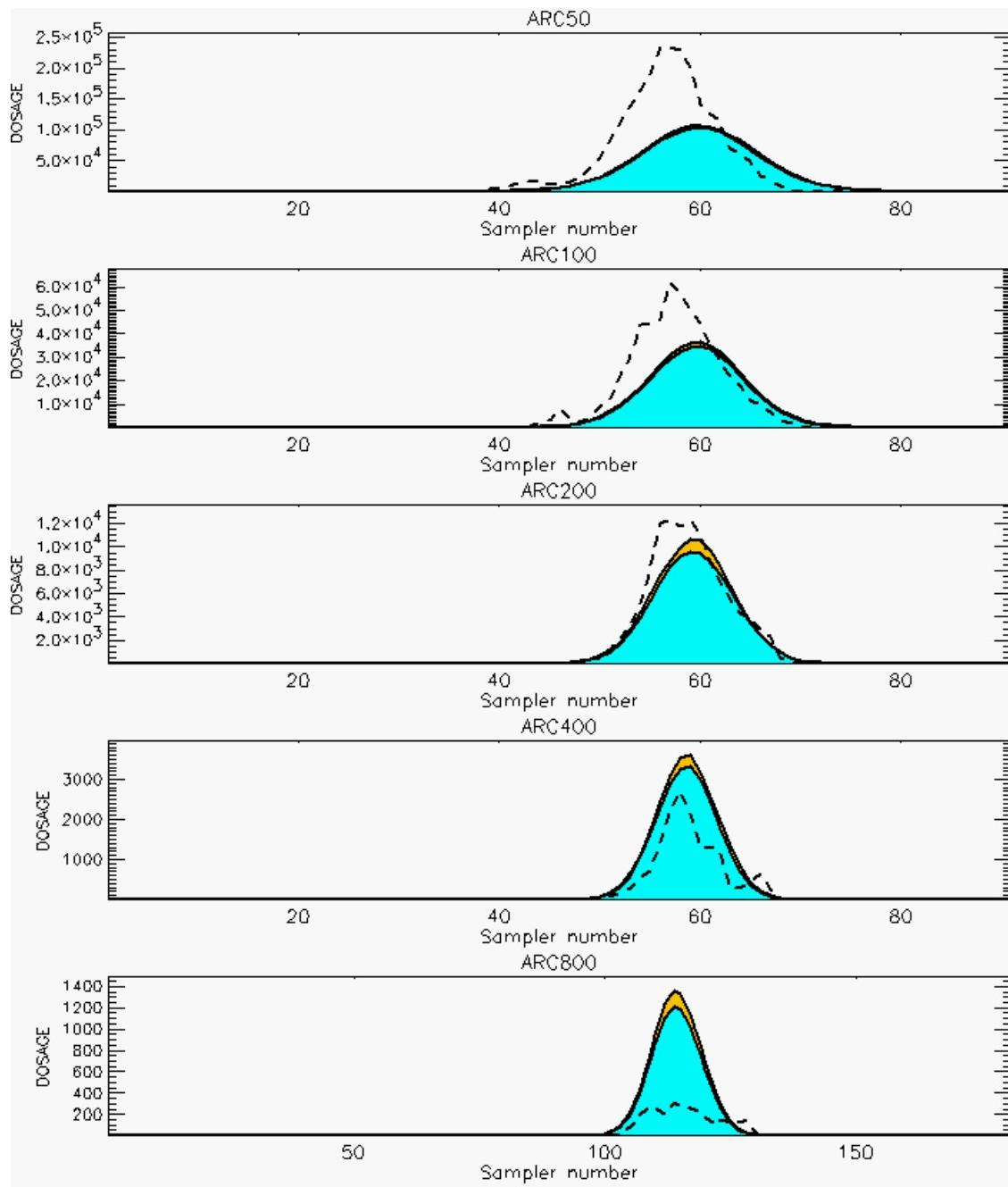
PG Prediction1 to Prediction2 Comparison

PG Trial File: pr_grass_tracer_Experiment_14.txt

PG Prediction File 1: ARAC\sv_vd\pg_14_sv_vd.arac

PG Prediction File 2: ARAC\sv_novd\pg_14_sv_novd.arac

Figure L-9b. NARAC With and Without SO₂ Surface Deposition Predictions to Trial 14 on Logarithmic Scale: Stability Category is 7



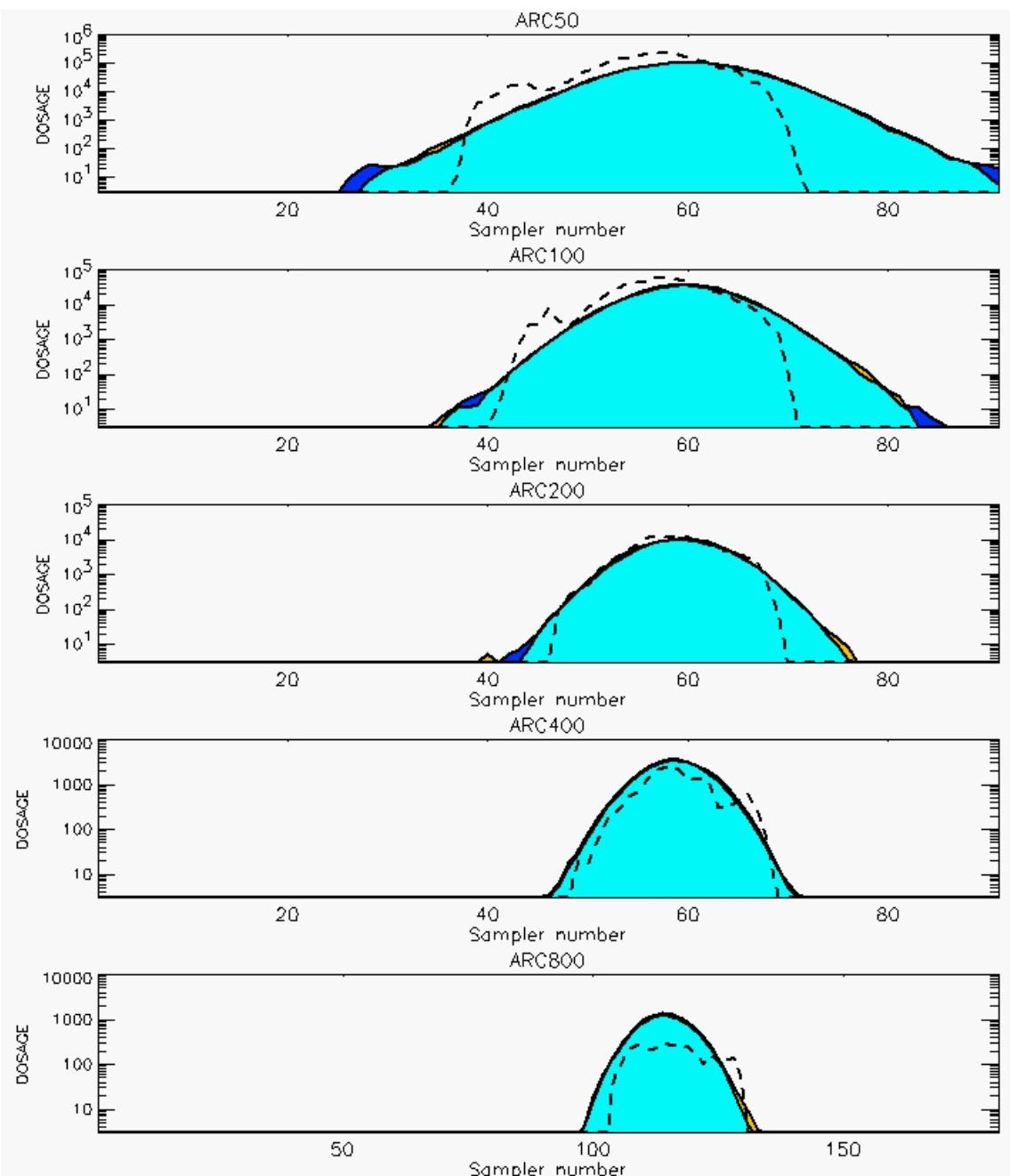
PG Prediction1 to Prediction2 Comparison

PG Trial File: pr_grass_tracer_Experiment_15.txt

PG Prediction File 1: ARAC\sv_vd\pg_15_sv_vd.arac

PG Prediction File 2: ARAC\sv_novd\pg_15_sv_novd.arac

Figure L-10a. NARAC With and Without SO₂ Surface Deposition Predictions to Trial 15 on Linear Scale: Stability Category is 1



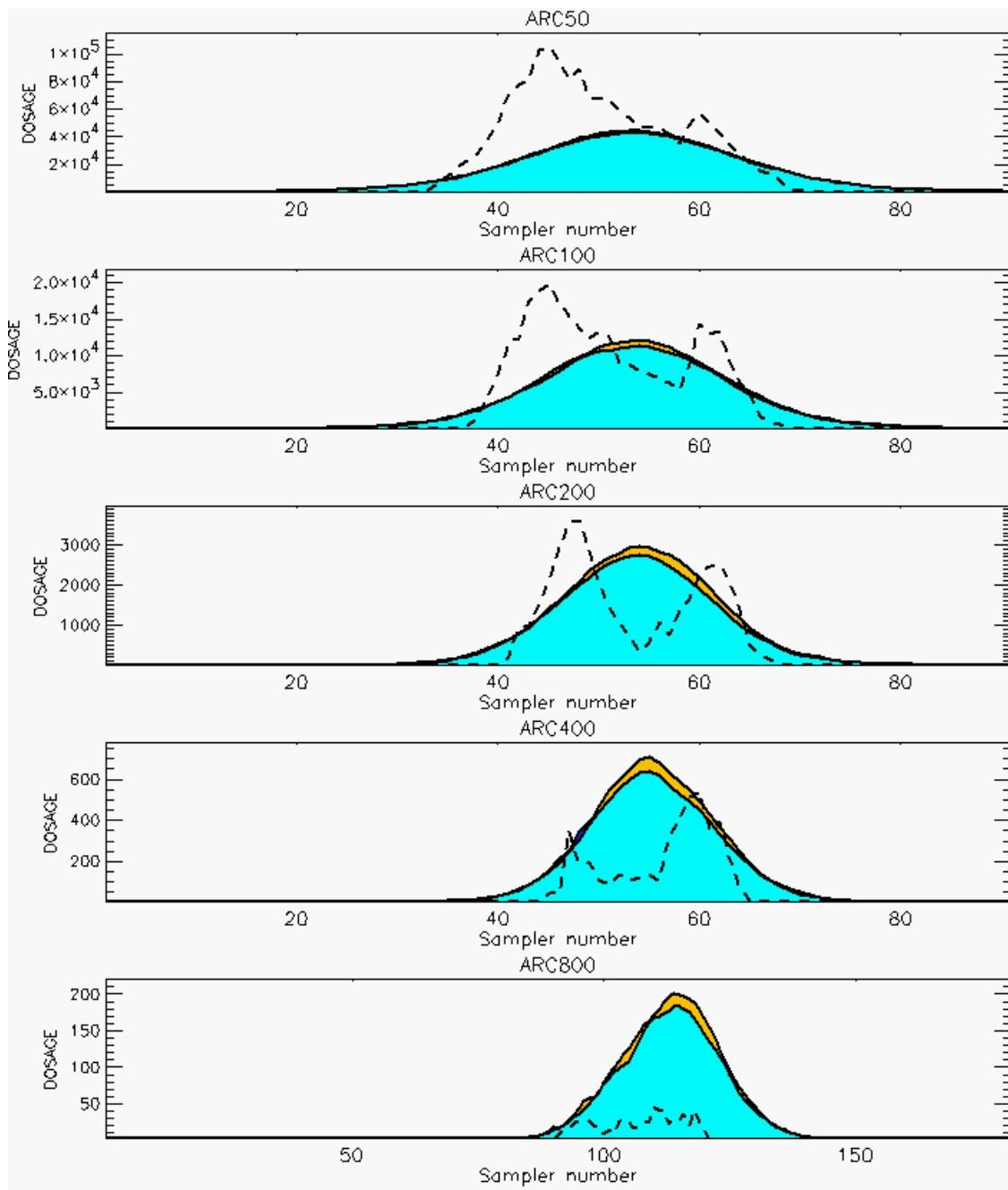
PG Prediction1 to Prediction2 Comparison

PG Trial File: pr_grass_tracer_Experiment_15.txt

PG Prediction File 1: ARAC\sv_vd\pg_15_sv_vd.arac

PG Prediction File 2: ARAC\sv_novd\pg_15_sv_novd.arac

Figure L-10b. NARAC With and Without SO₂ Surface Deposition Predictions to Trial 15 on Logarithmic Scale: Stability Category is 1



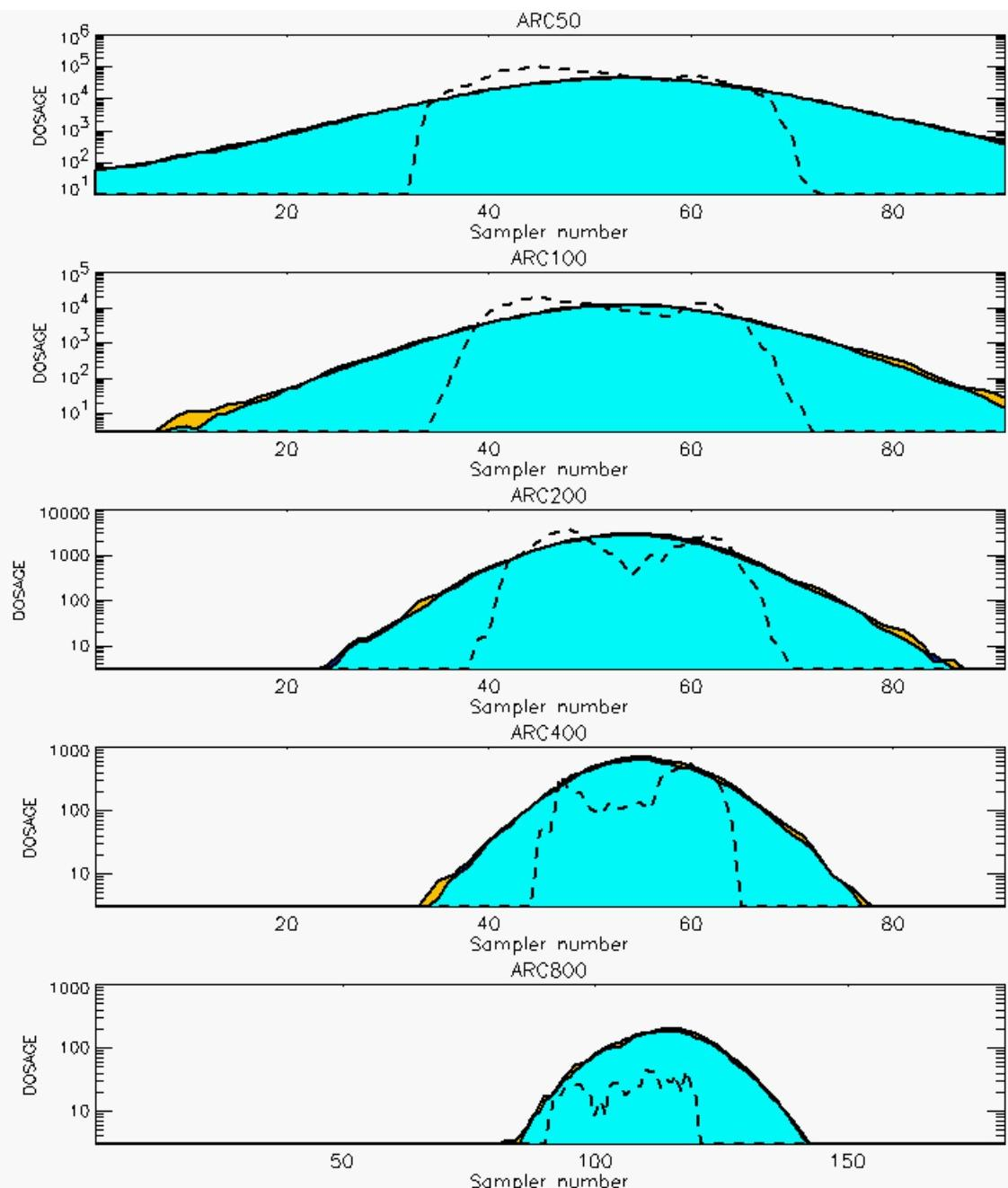
PG Prediction1 to Prediction2 Comparison

PG Trial File: pr_grass_tracer_Experiment_16.txt

PG Prediction File 1: ARAC\sv_vd\pg_16_sv_vd.arac

PG Prediction File 2: ARAC\sv_novd\pg_16_sv_novd.arac

Figure L-11a. NARAC With and Without SO₂ Surface Deposition Predictions to Trial 16 on Linear Scale: Stability Category is 1



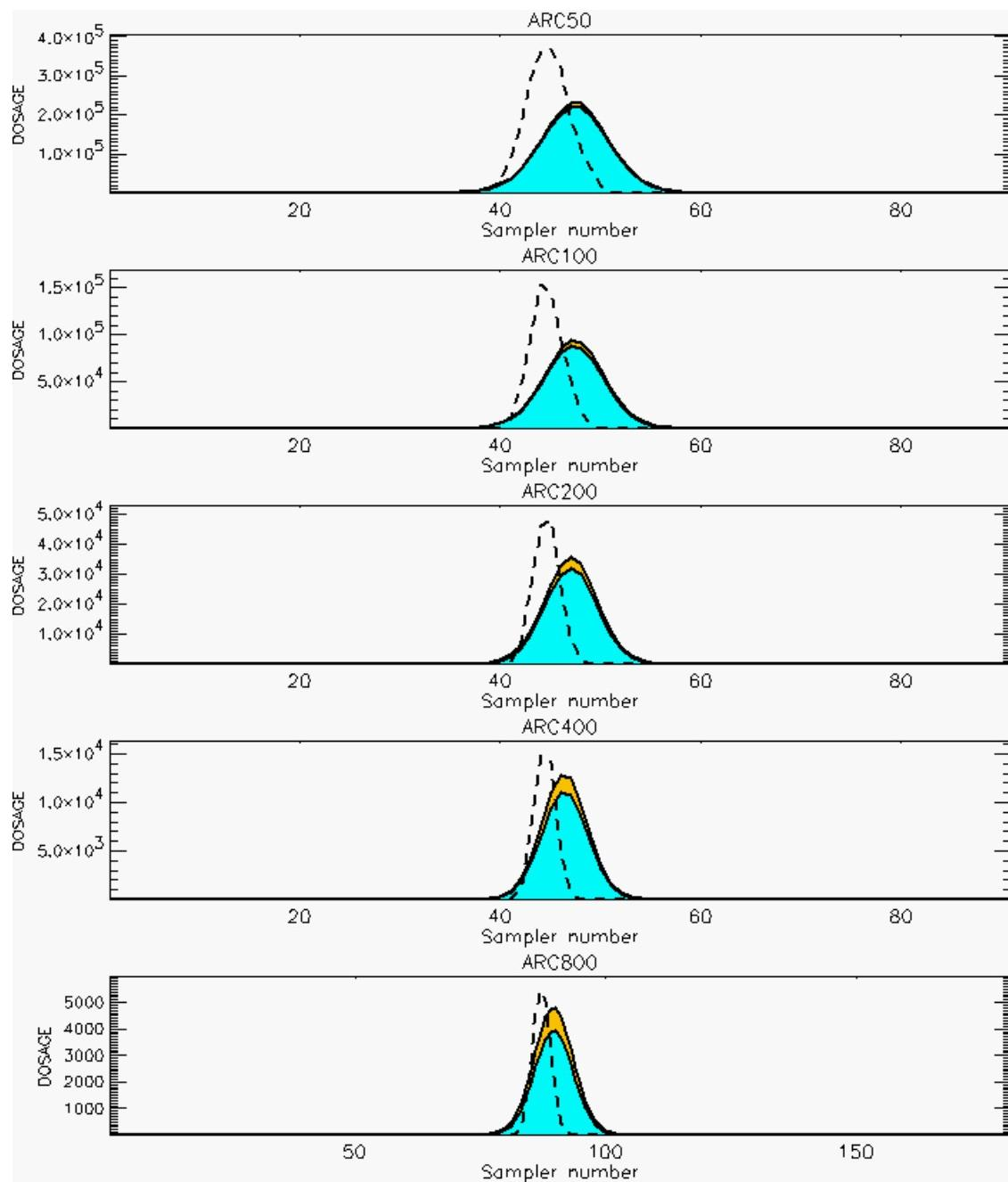
PG Prediction1 to Prediction2 Comparison

PG Trial File: pr_grass_tracer_Experiment_16.txt

PG Prediction File 1: ARAC\sv_vd\pg_16_sv_vd.arac

PG Prediction File 2: ARAC\sv_novd\pg_16_sv_novd.arac

Figure L-11b. NARAC With and Without SO₂ Surface Deposition Predictions to Trial 16 on Logarithmic Scale: Stability Category is 1



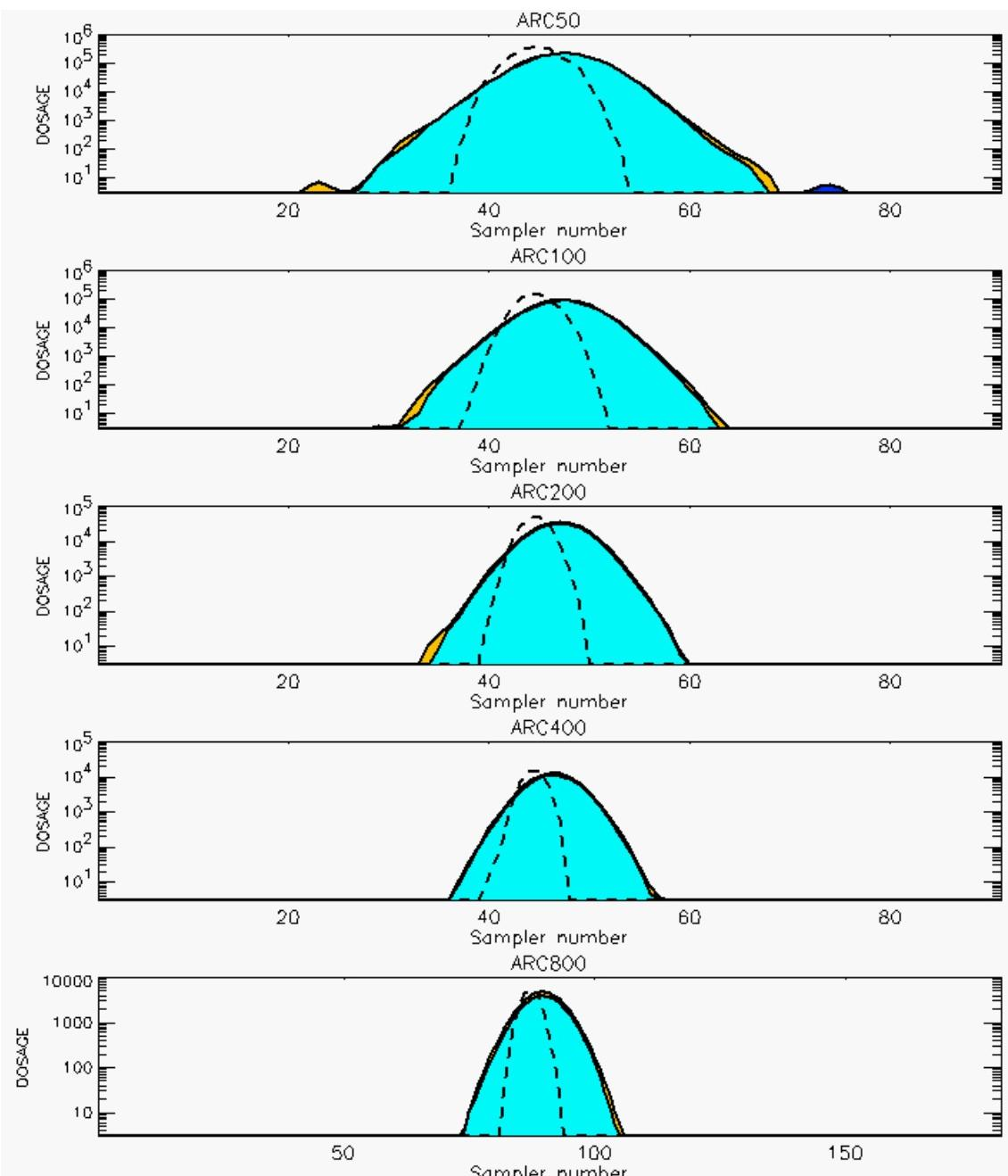
PG Prediction1 to Prediction2 Comparison

PG Trial File: pr_grass_tracer_Experiment_17.txt

PG Prediction File 1: ARAC\sv_vd\pg_17_sv_vd.arac

PG Prediction File 2: ARAC\sv_novd\pg_17_sv_novd.arac

Figure L-12a. NARAC With and Without SO₂ Surface Deposition Predictions to Trial 17 on Linear Scale: Stability Category is 5



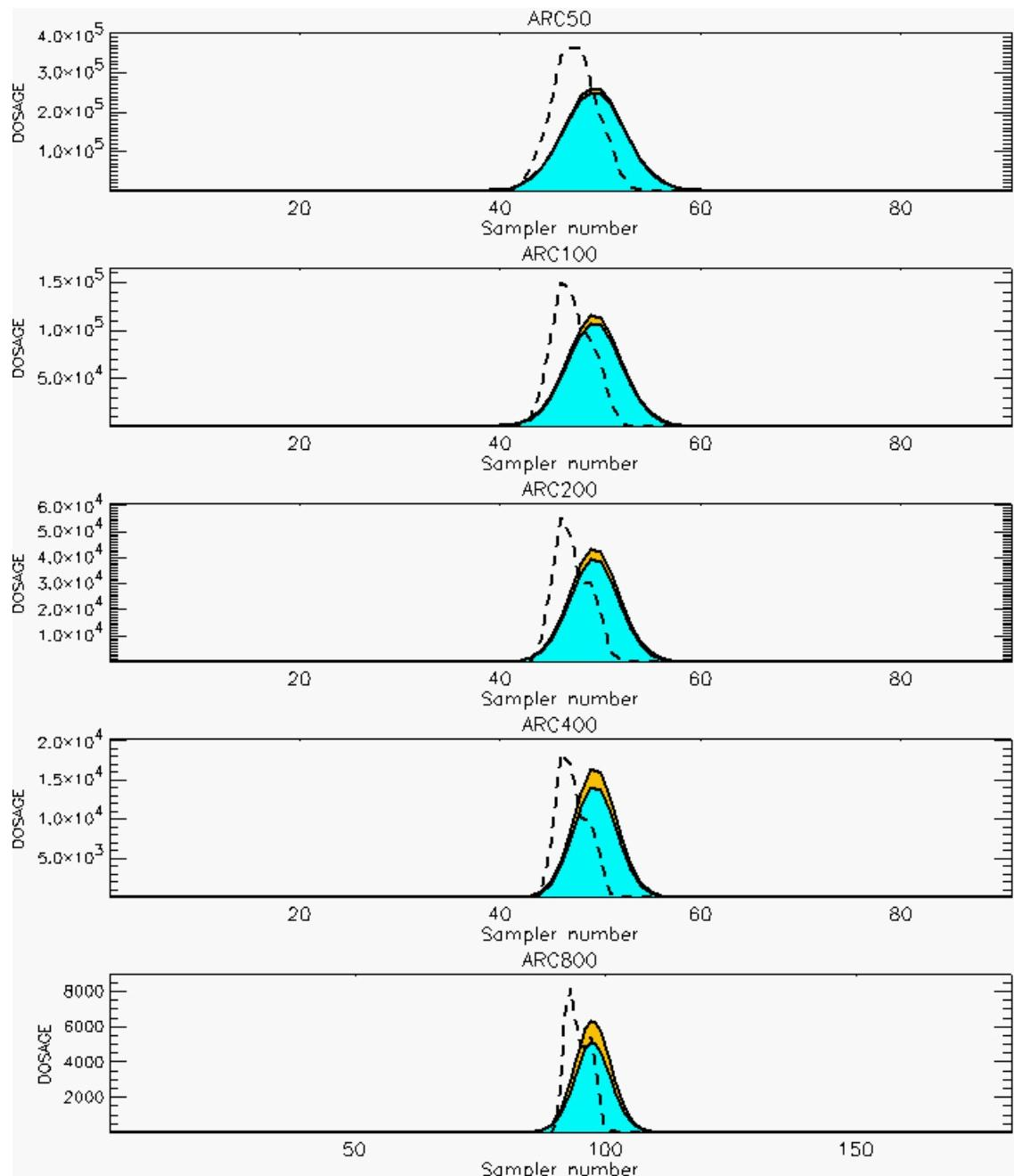
PG Prediction1 to Prediction2 Comparison

PG Trial File: pr_grass_tracer_Experiment_17.txt

PG Prediction File 1: ARAC\sv_vd\pg_17_sv_vd.arac

PG Prediction File 2: ARAC\sv_novd\pg_17_sv_novd.arac

Figure L-12b. NARAC With and Without SO₂ Surface Deposition Predictions to Trial 17 on Logarithmic Scale: Stability Category is 5



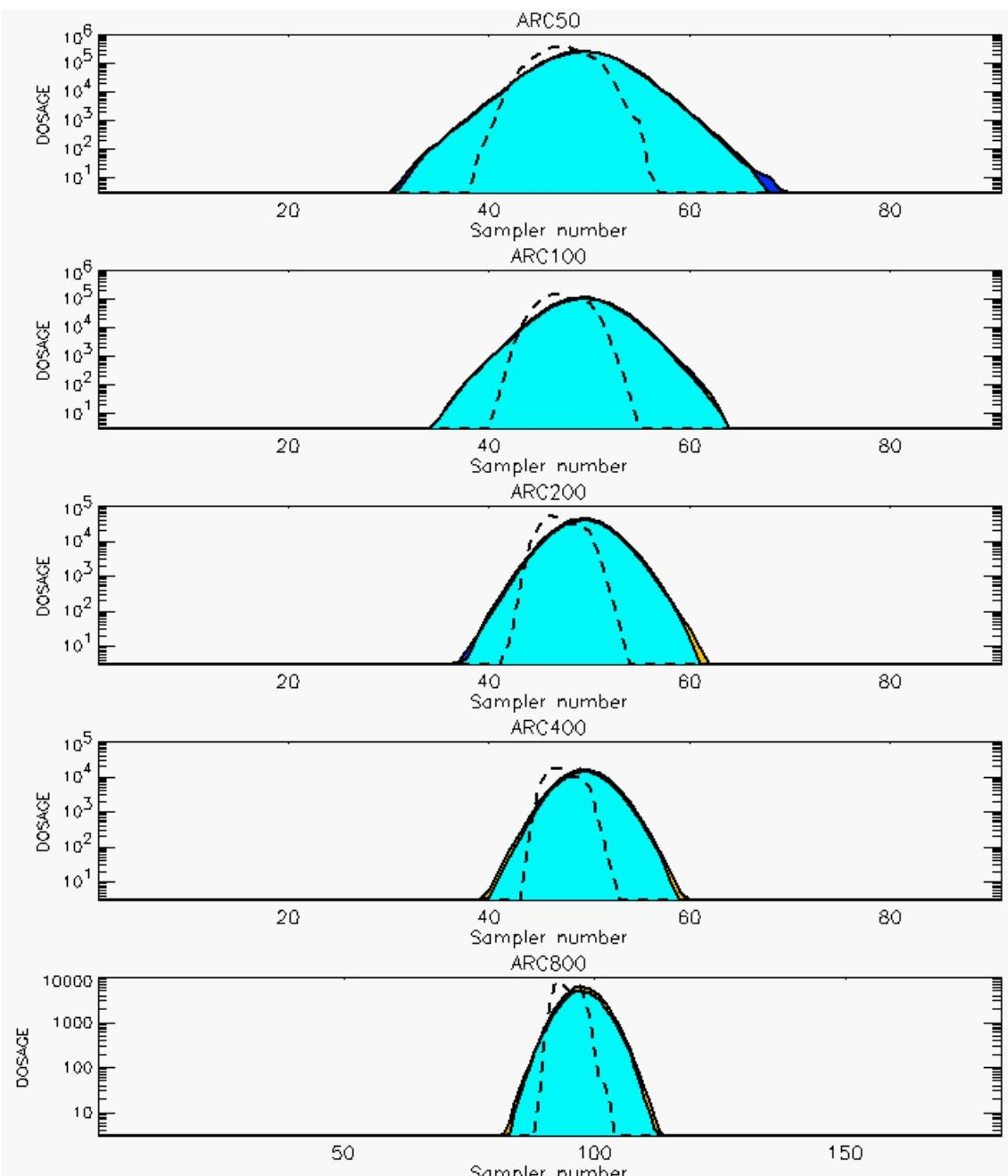
PG Prediction1 to Prediction2 Comparison

PG Trial File: pr_grass_tracer_Experiment_18.txt

PG Prediction File 1: ARAC\sv_vd\pg_18_sv_vd.arac

PG Prediction File 2: ARAC\sv_novd\pg_18_sv_novd.arac

Figure L-13a. NARAC With and Without SO₂ Surface Deposition Predictions to Trial 18 on Linear Scale: Stability Category is 5



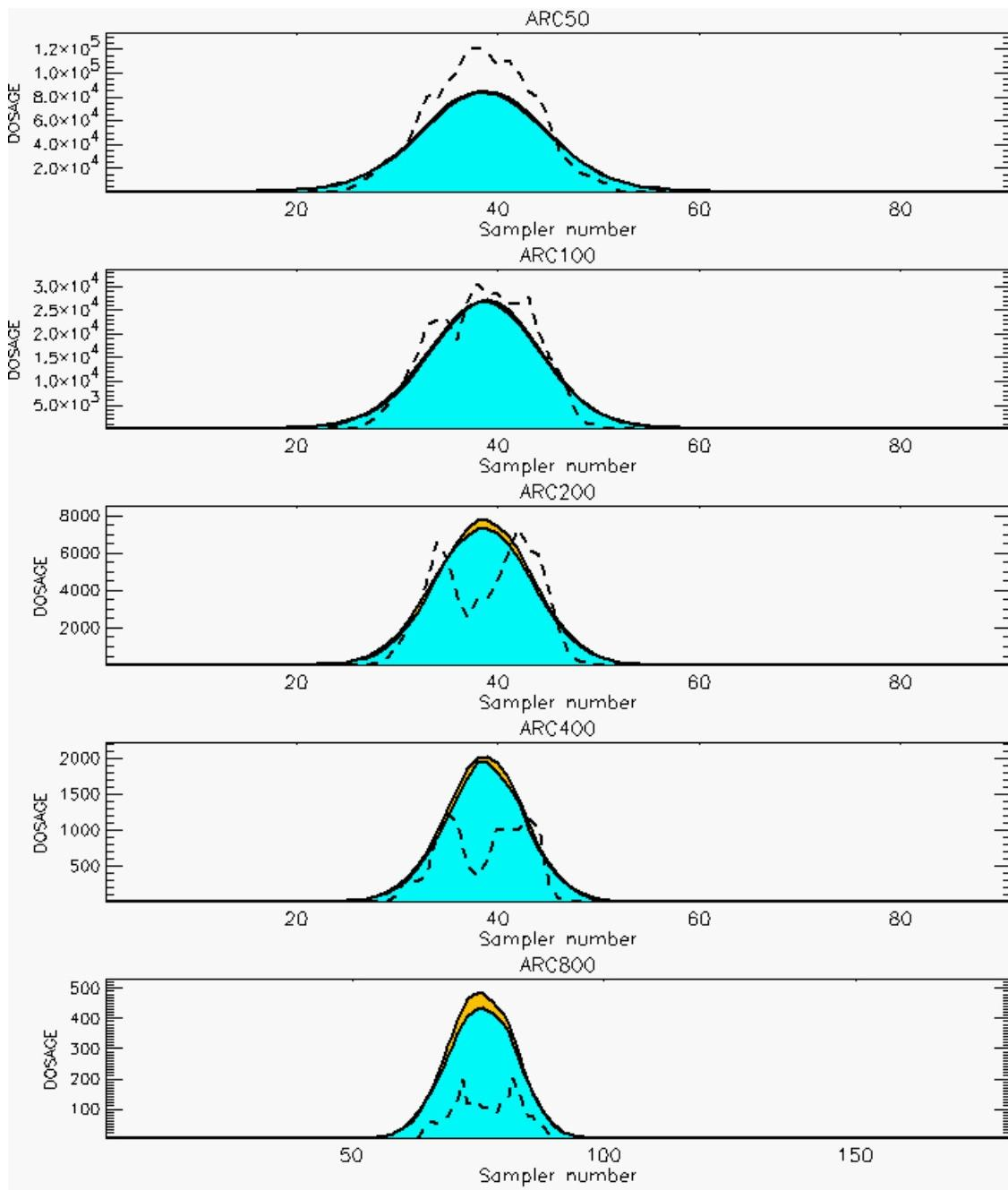
PG Prediction1 to Prediction2 Comparison

PG Trial File: pr_grass_tracer_Experiment_18.txt

PG Prediction File 1: ARAC\sv_vd\pg_18_sv_vd.arac

PG Prediction File 2: ARAC\sv_novd\pg_18_sv_novd.arac

Figure L-13b. NARAC With and Without SO₂ Surface Deposition Predictions to Trial 18 on Logarithmic Scale: Stability Category is 5



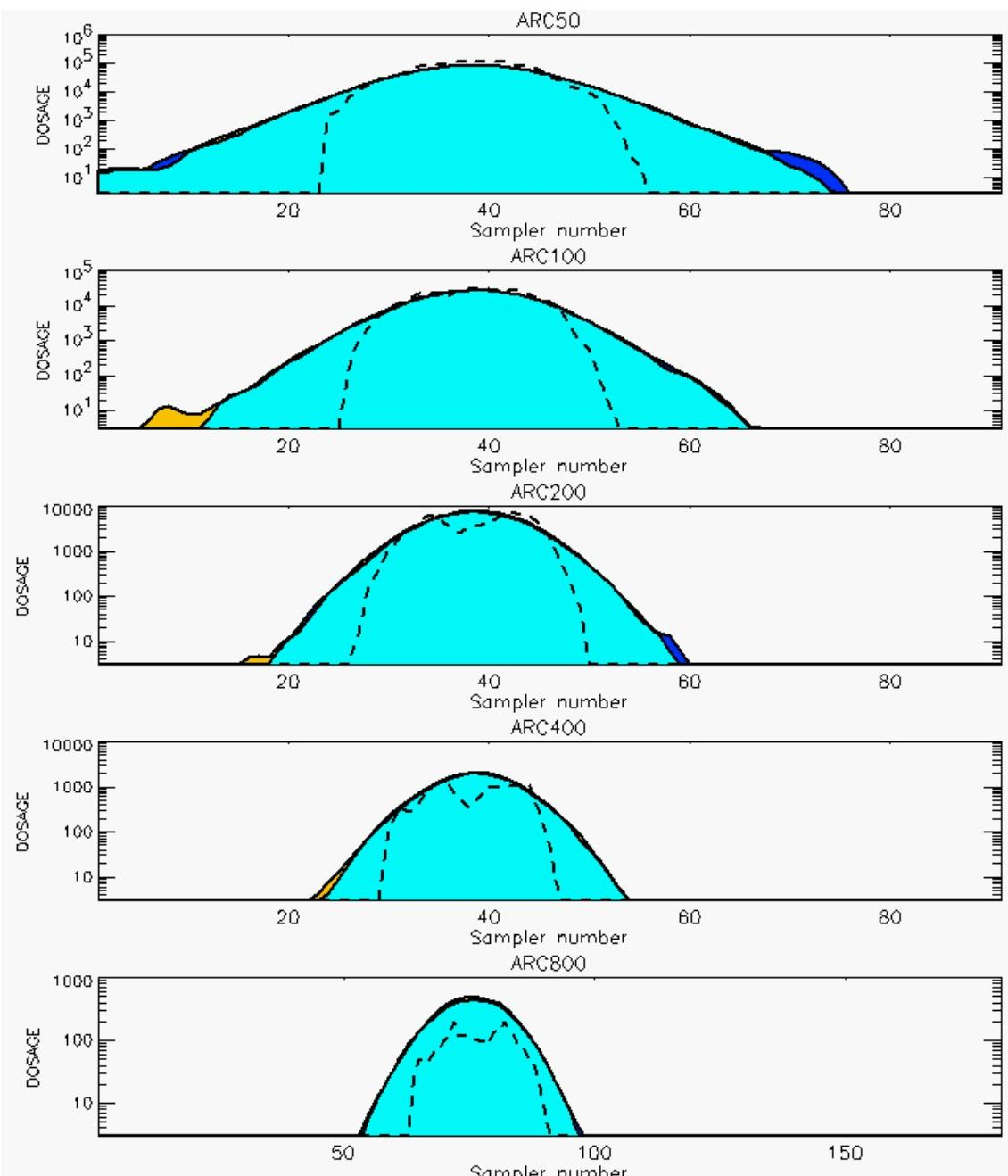
PG Prediction1 to Prediction2 Comparison

PG Trial File: pr_grass_tracer_Experiment_19.txt

PG Prediction File 1: ARAC\sv_vd\pg_19_sv_vd.arac

PG Prediction File 2: ARAC\sv_novd\pg_19_sv_novd.arac

Figure L-14a. NARAC With and Without SO₂ Surface Deposition Predictions to Trial 19 on Linear Scale: Stability Category is 2



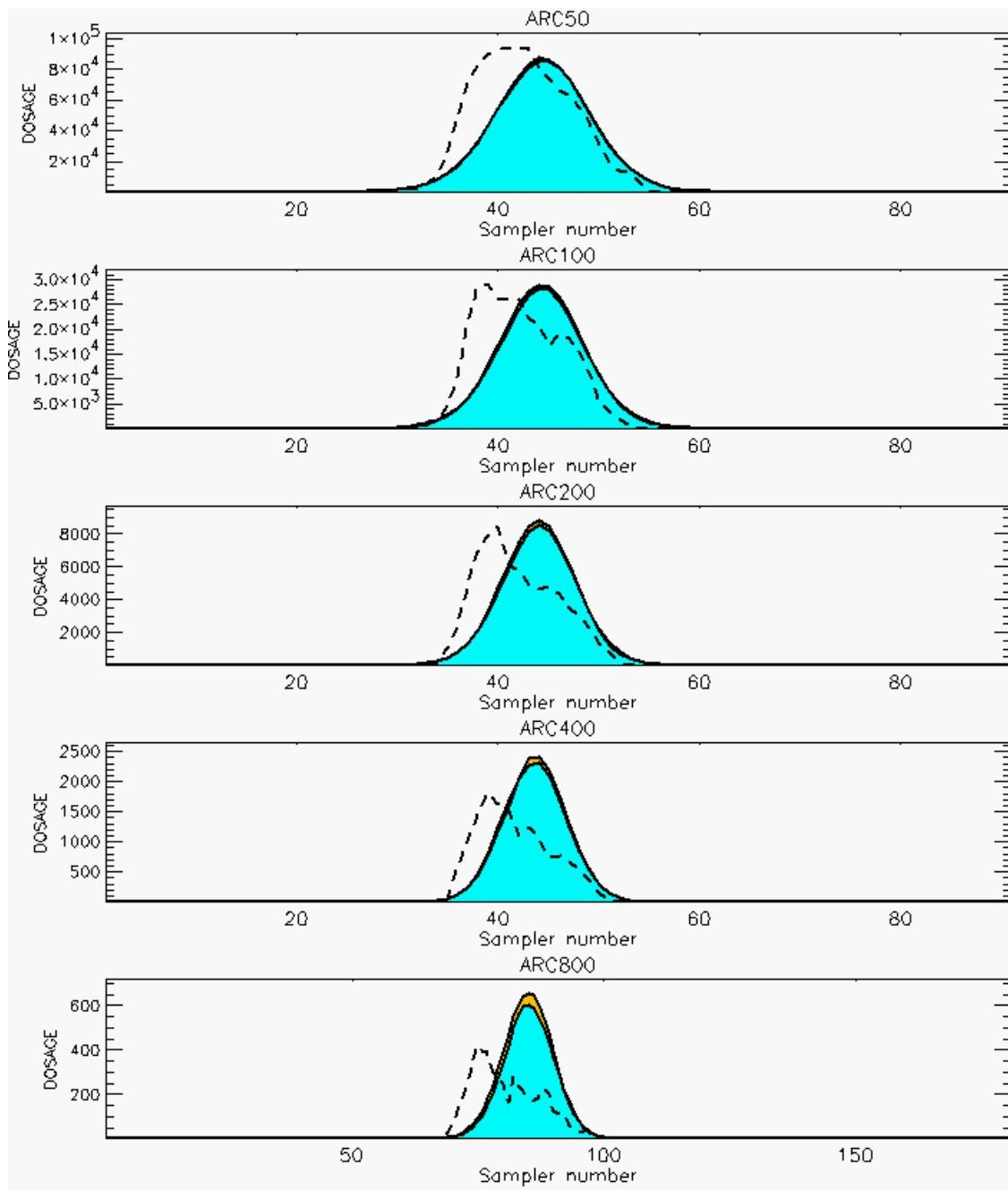
PG Prediction1 to Prediction2 Comparison

PG Trial File: pr_grass_tracer_Experiment_19.txt

PG Prediction File 1: ARAC\sv_vd\pg_19_sv_vd.arac

PG Prediction File 2: ARAC\sv_novd\pg_19_sv_novd.arac

Figure L-14b. NARAC With and Without SO₂ Surface Deposition Predictions to Trial 19 on Logarithmic Scale: Stability Category is 2



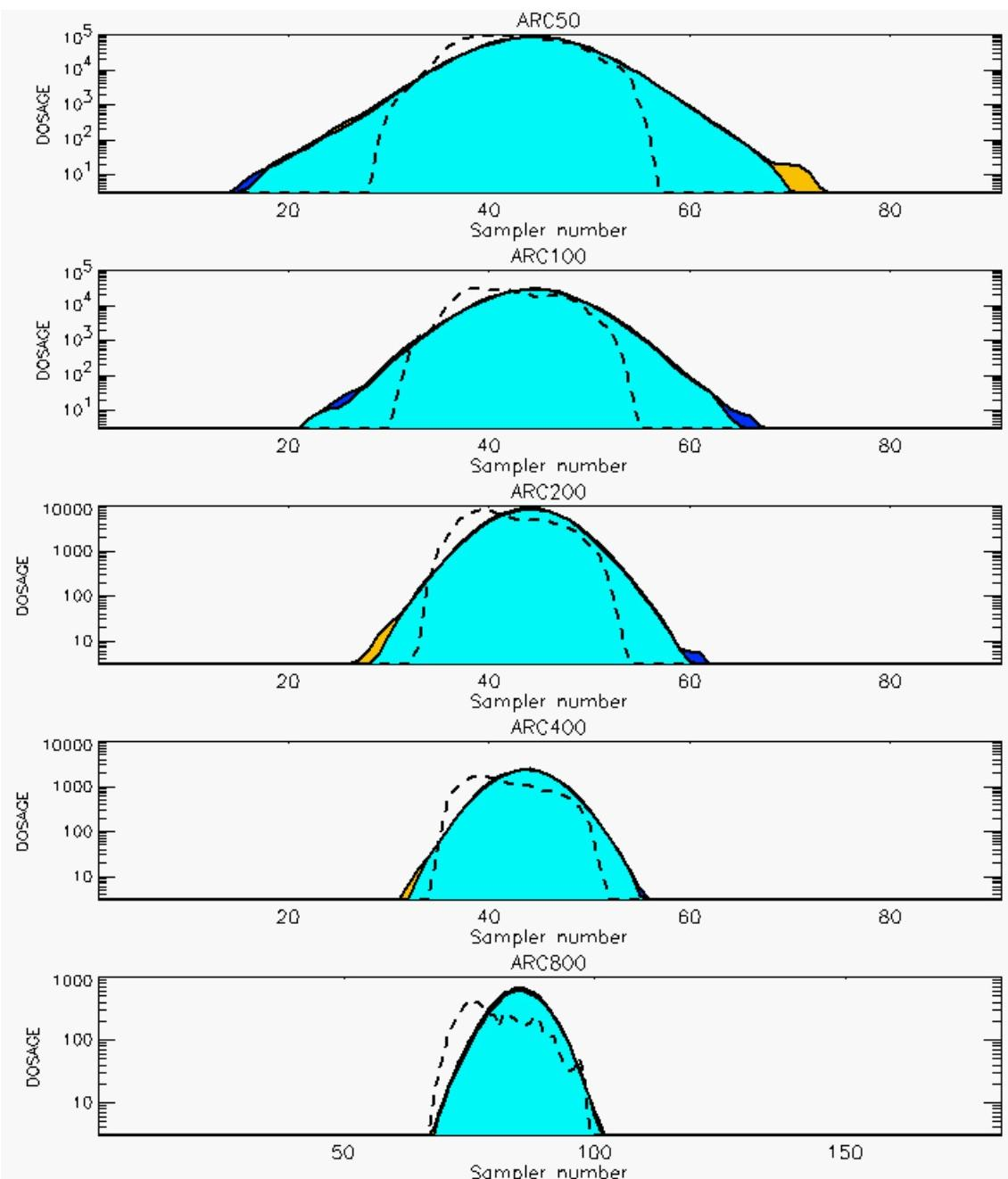
PG Prediction1 to Prediction2 Comparison

PG Trial File: pr_grass_tracer_Experiment_20.txt

PG Prediction File 1: ARAC\sv_vd\pg_20_sv_vd.arac

PG Prediction File 2: ARAC\sv_novd\pg_20_sv_novd.arac

Figure L-15a. NARAC With and Without SO₂ Surface Deposition Predictions to Trial 20 on Linear Scale: Stability Category is 3



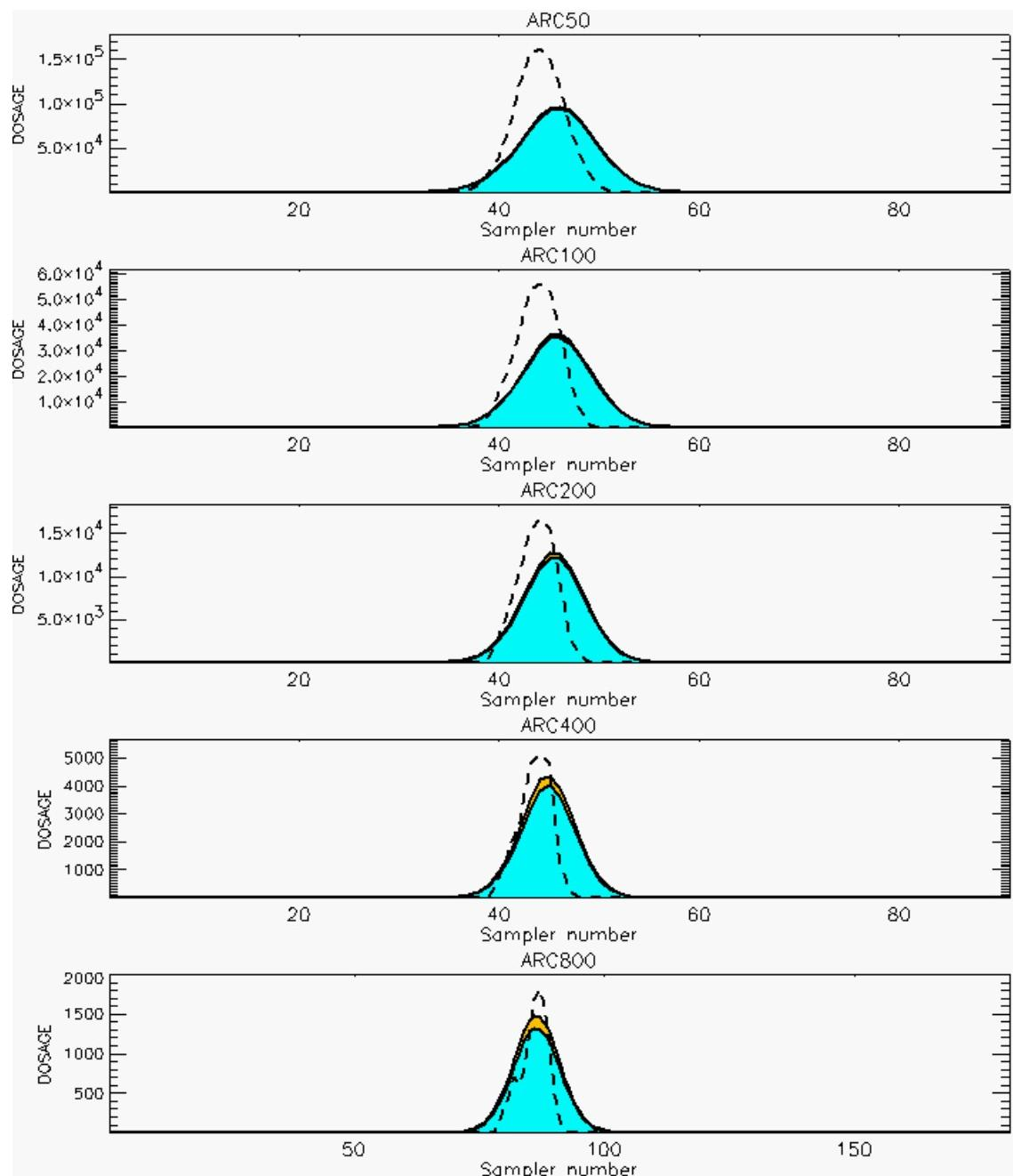
PG Prediction1 to Prediction2 Comparison

PG Trial File: pr_grass_tracer_Experiment_20.txt

PG Prediction File 1: ARAC\sv_vd\pg_20_sv_vd.arac

PG Prediction File 2: ARAC\sv_novd\pg_20_sv_novd.arac

Figure L-15b. NARAC With and Without SO₂ Surface Deposition Predictions to Trial 20 on Logarithmic Scale: Stability Category is 3



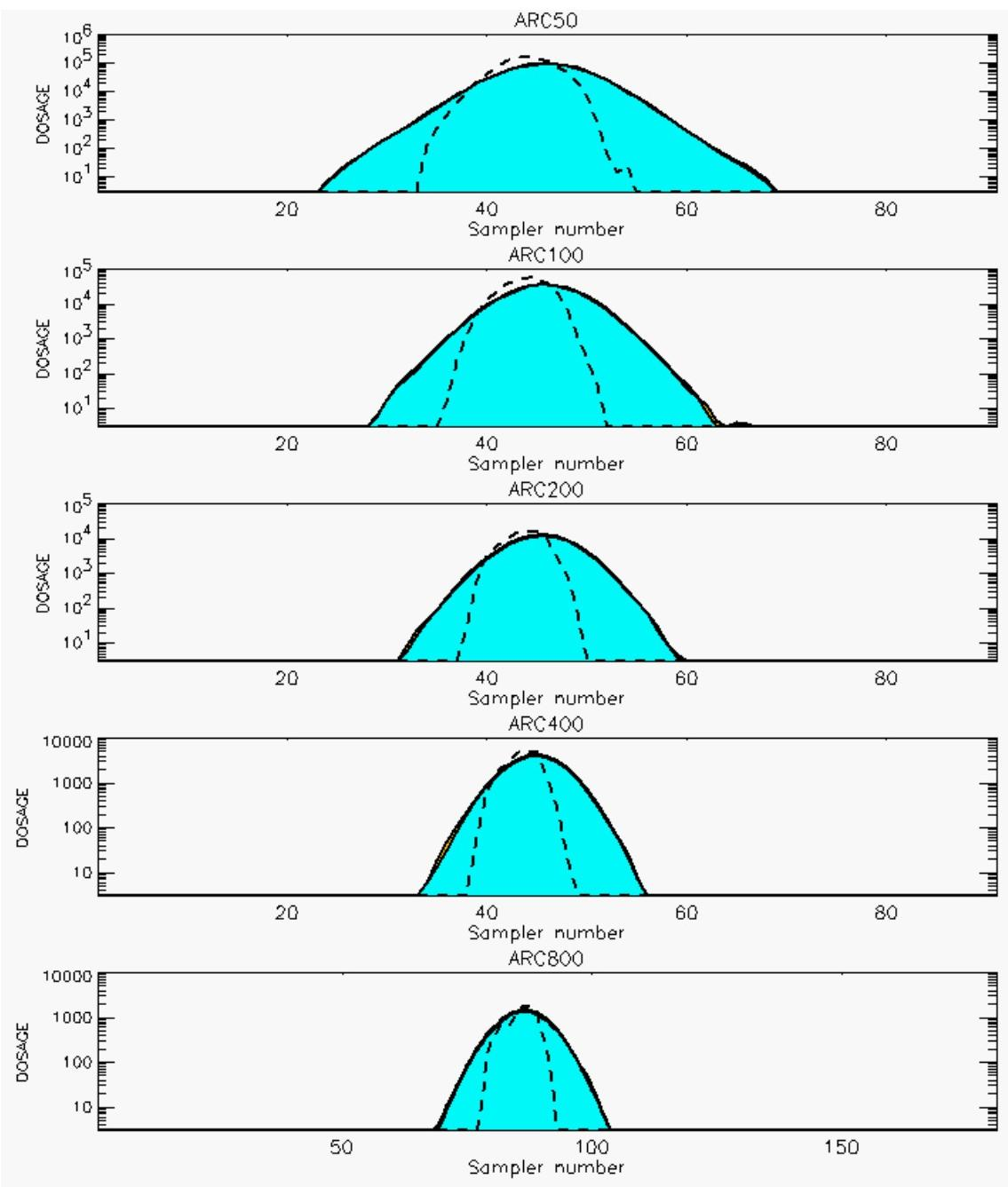
PG Prediction1 to Prediction2 Comparison

PG Trial File: pr_grass_tracer_Experiment_21.txt

PG Prediction File 1: ARAC\sv_vd\pg_21_sv_vd.arac

PG Prediction File 2: ARAC\sv_novd\pg_21_sv_novd.arac

Figure L-16a. NARAC With and Without SO₂ Surface Deposition Predictions to Trial 21 on Linear Scale: Stability Category is 4



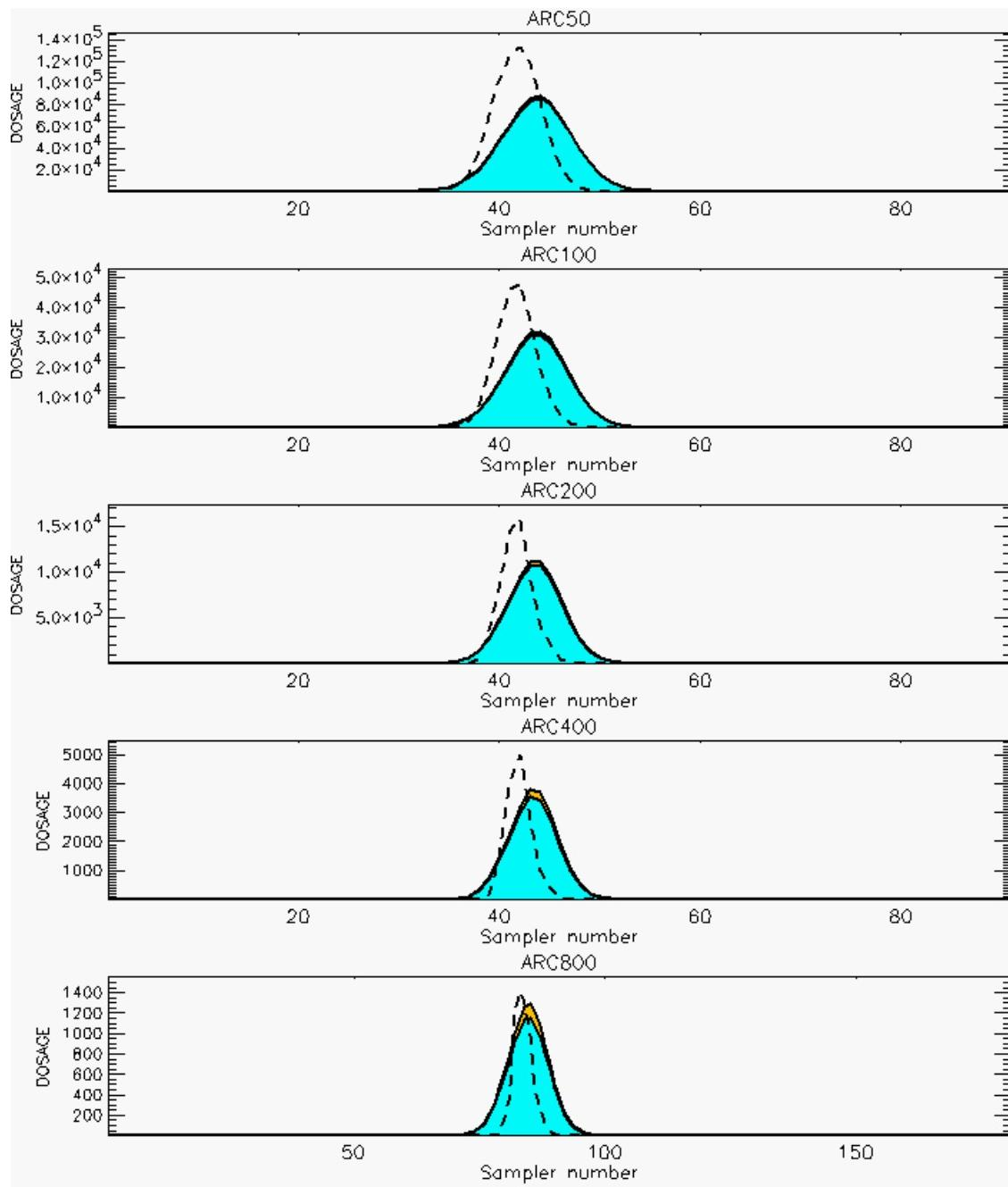
PG Prediction1 to Prediction2 Comparison

PG Trial File: pr_grass_tracer_Experiment_21.txt

PG Prediction File 1: ARAC\sv_vd\pg_21_sv_vd.arac

PG Prediction File 2: ARAC\sv_novd\pg_21_sv_novd.arac

Figure L-16b. NARAC With and Without SO_2 Surface Deposition Predictions to Trial 21 on Logarithmic Scale: Stability Category is 4



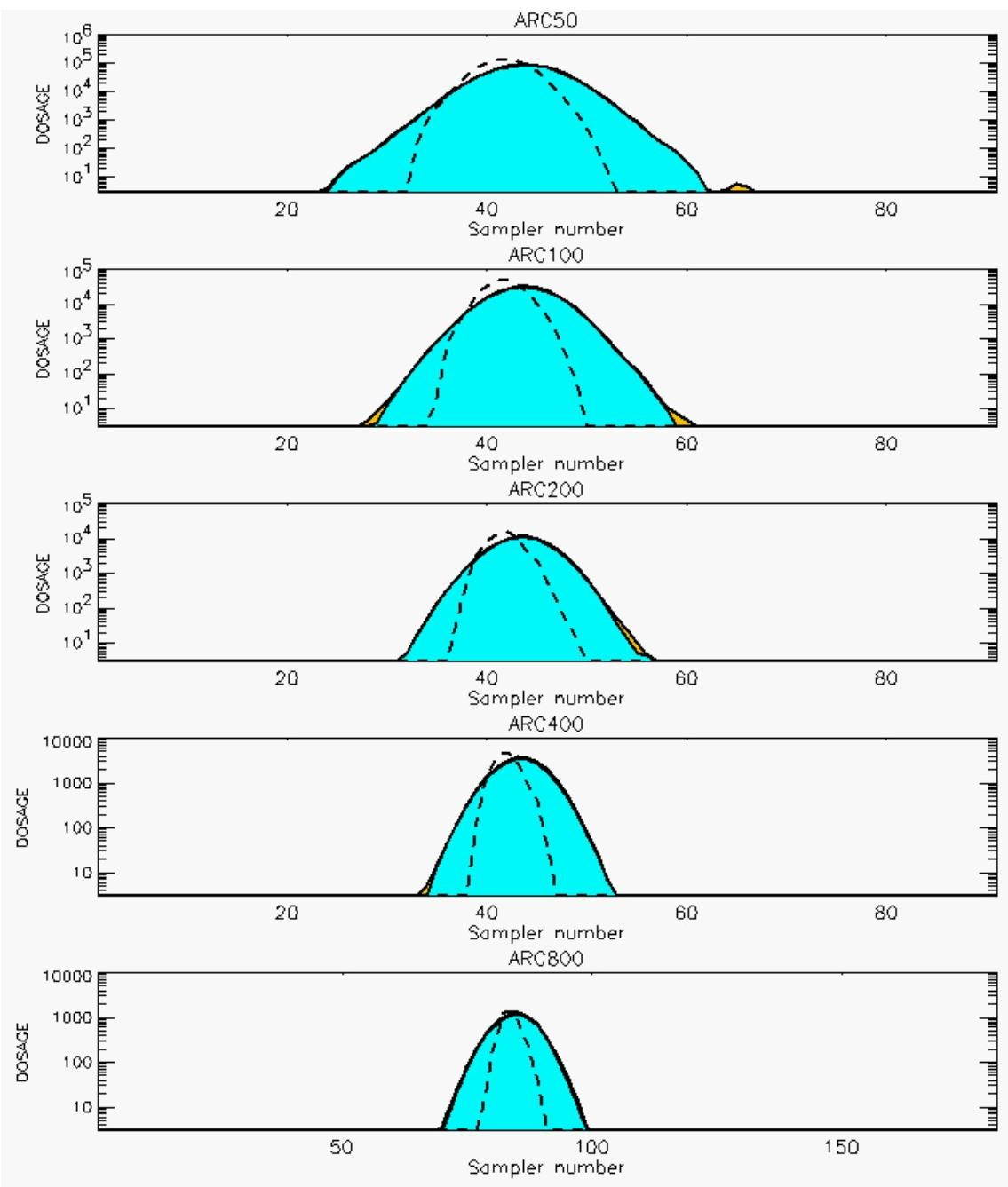
PG Prediction1 to Prediction2 Comparison

PG Trial File: pr_grass_tracer_Experiment_22.txt

PG Prediction File 1: ARAC\sv_vd\pg_22_sv_vd.arac

PG Prediction File 2: ARAC\sv_novd\pg_22_sv_novd.arac

Figure L-17a. NARAC With and Without SO₂ Surface Deposition Predictions to Trial 22 on Linear Scale: Stability Category is 4



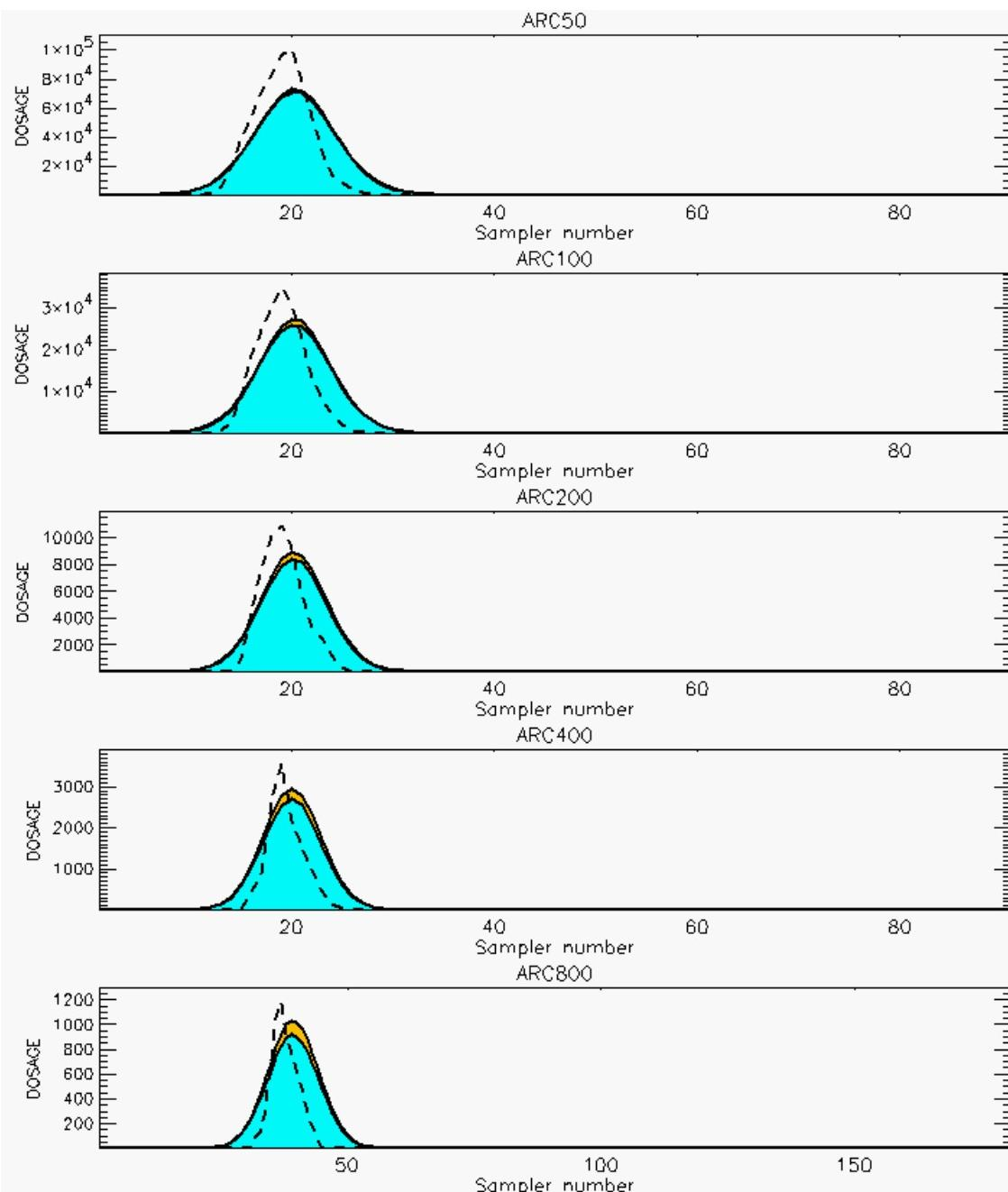
PG Prediction1 to Prediction2 Comparison

PG Trial File: pr_grass_tracer_Experiment_22.txt

PG Prediction File 1: ARAC\sv_vd\pg_22_sv_vd.arac

PG Prediction File 2: ARAC\sv_novd\pg_22_sv_novd.arac

Figure L-17b. NARAC With and Without SO₂ Surface Deposition Predictions to Trial 22 on Logarithmic Scale: Stability Category is 4



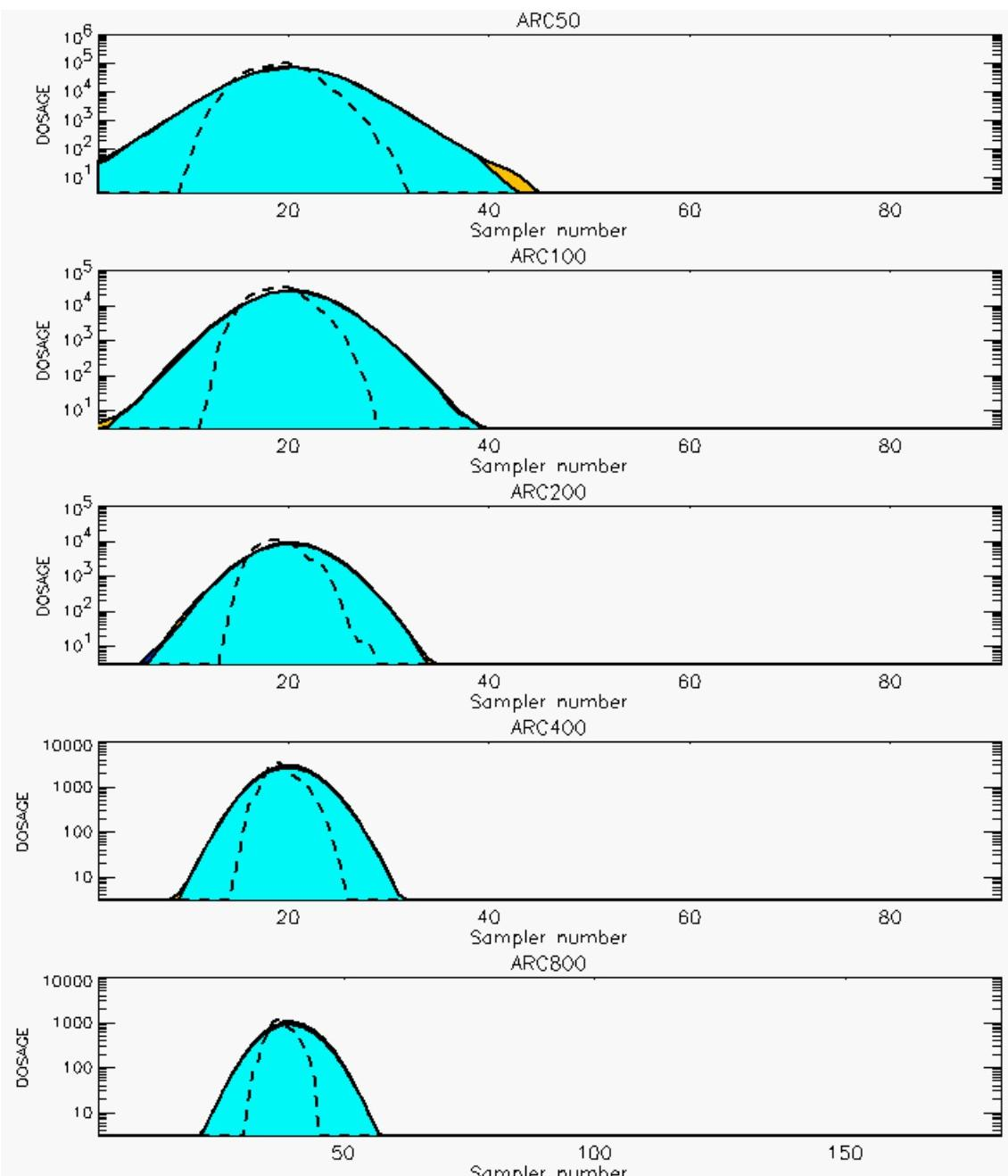
PG Prediction1 to Prediction2 Comparison

PG Trial File: pr_grass_tracer_Experiment_23.txt

PG Prediction File 1: ARAC\sv_vd\pg_23_sv_vd.arac

PG Prediction File 2: ARAC\sv_novd\pg_23_sv_novd.arac

Figure L-18a. NARAC With and Without SO_2 Surface Deposition Predictions to Trial 23 on Linear Scale: Stability Category is 4



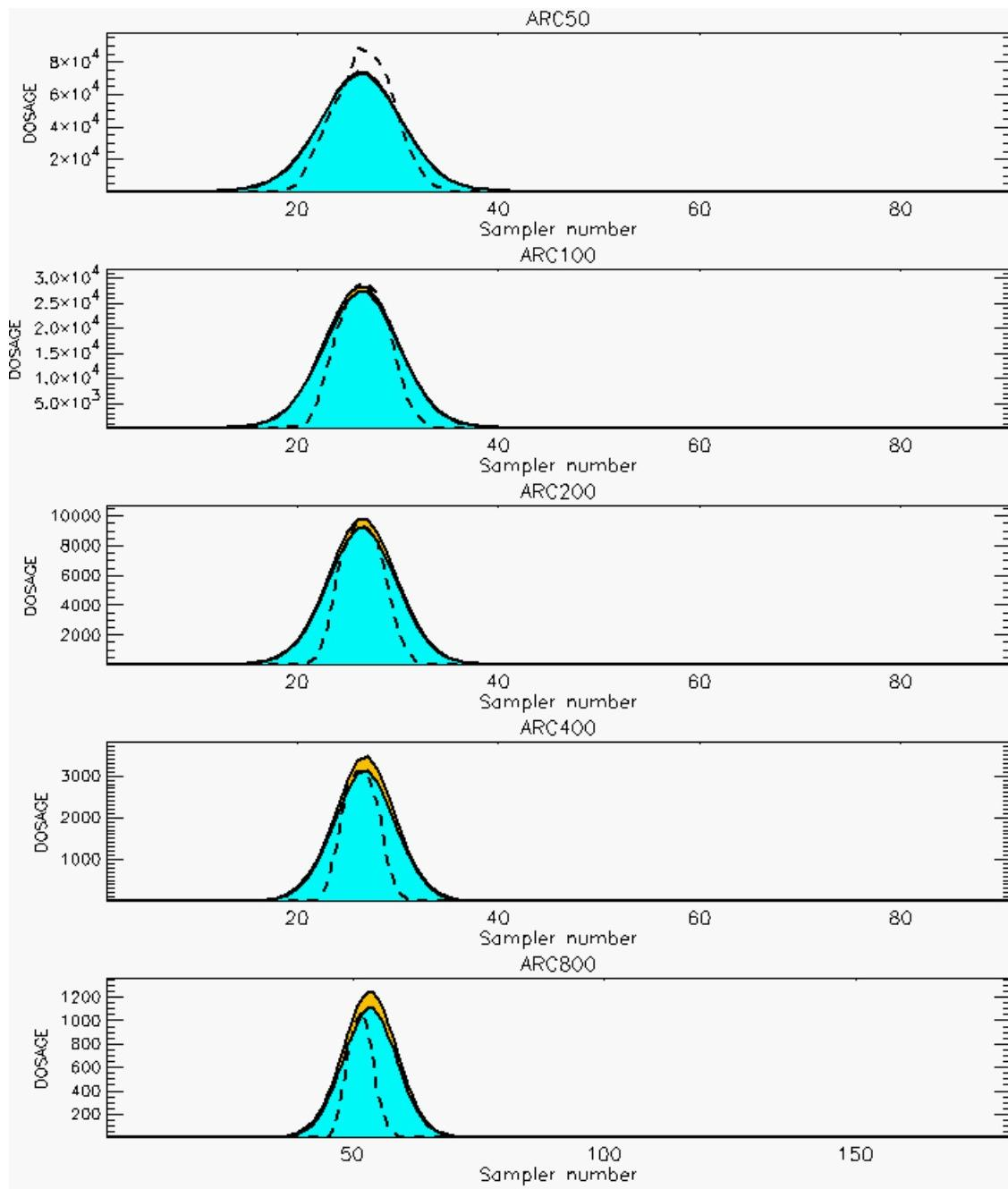
PG Prediction1 to Prediction2 Comparison

PG Trial File: pr_grass_tracer_Experiment_23.txt

PG Prediction File 1: ARAC\sv_vd\pg_23_sv_vd.arac

PG Prediction File 2: ARAC\sv_novd\pg_23_sv_novd.arac

Figure L-18b. NARAC With and Without SO_2 Surface Deposition Predictions to Trial 23 on Logarithmic Scale: Stability Category is 4



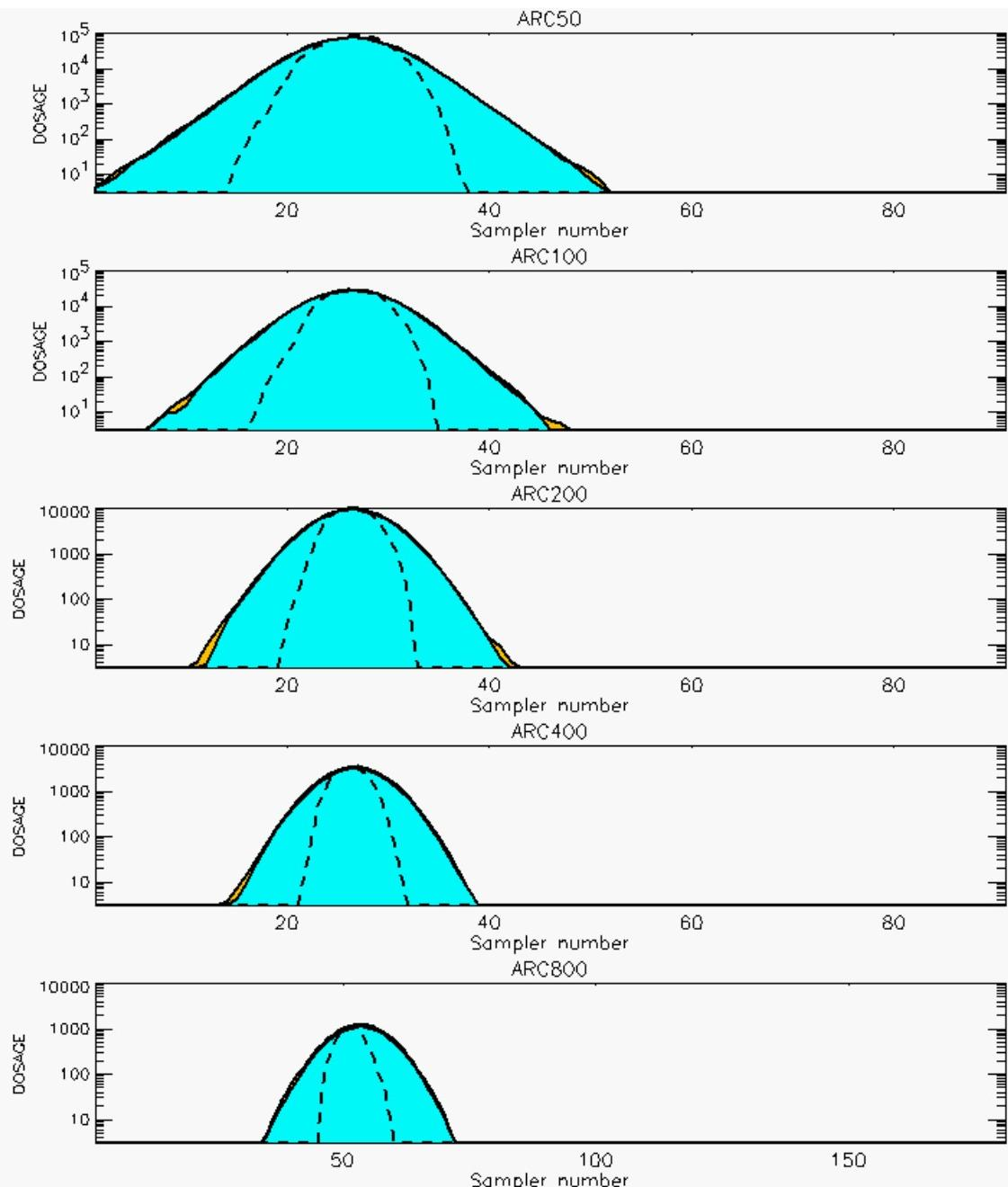
PG Prediction1 to Prediction2 Comparison

PG Trial File: pr_grass_tracer_Experiment_24.txt

PG Prediction File 1: ARAC\sv_vd\pg_24_sv_vd.arac

PG Prediction File 2: ARAC\sv_novd\pg_24_sv_novd.arac

Figure L-19a. NARAC With and Without SO₂ Surface Deposition Predictions to Trial 24 on Linear Scale: Stability Category is 4



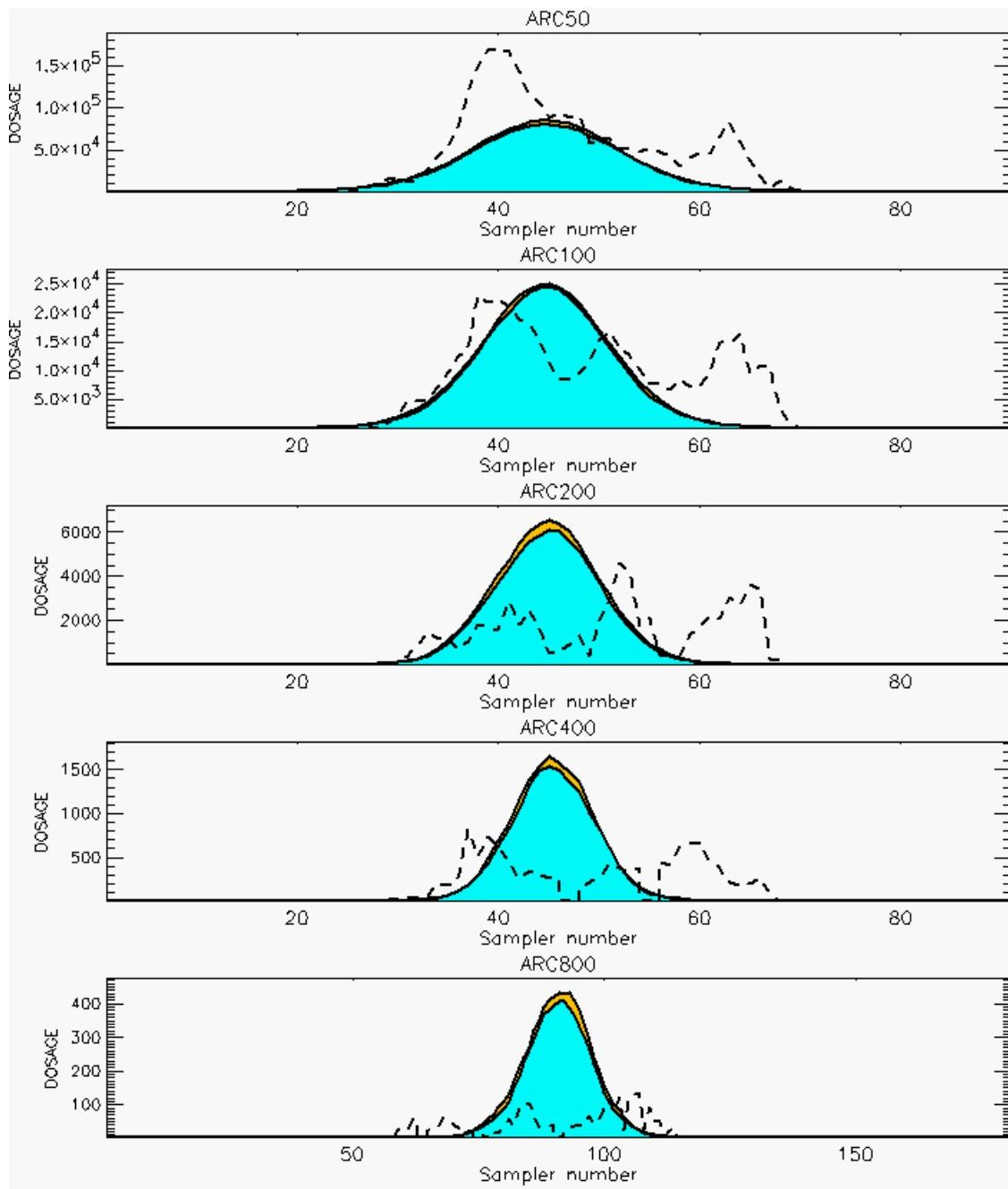
PG Prediction1 to Prediction2 Comparison

PG Trial File: pr_grass_tracer_Experiment_24.txt

PG Prediction File 1: ARAC\sv_vd\pg_24_sv_vd.arac

PG Prediction File 2: ARAC\sv_novd\pg_24_sv_novd.arac

Figure L-19b. NARAC With and Without SO₂ Surface Deposition Predictions to Trial 24 on Logarithmic Scale: Stability Category is 4



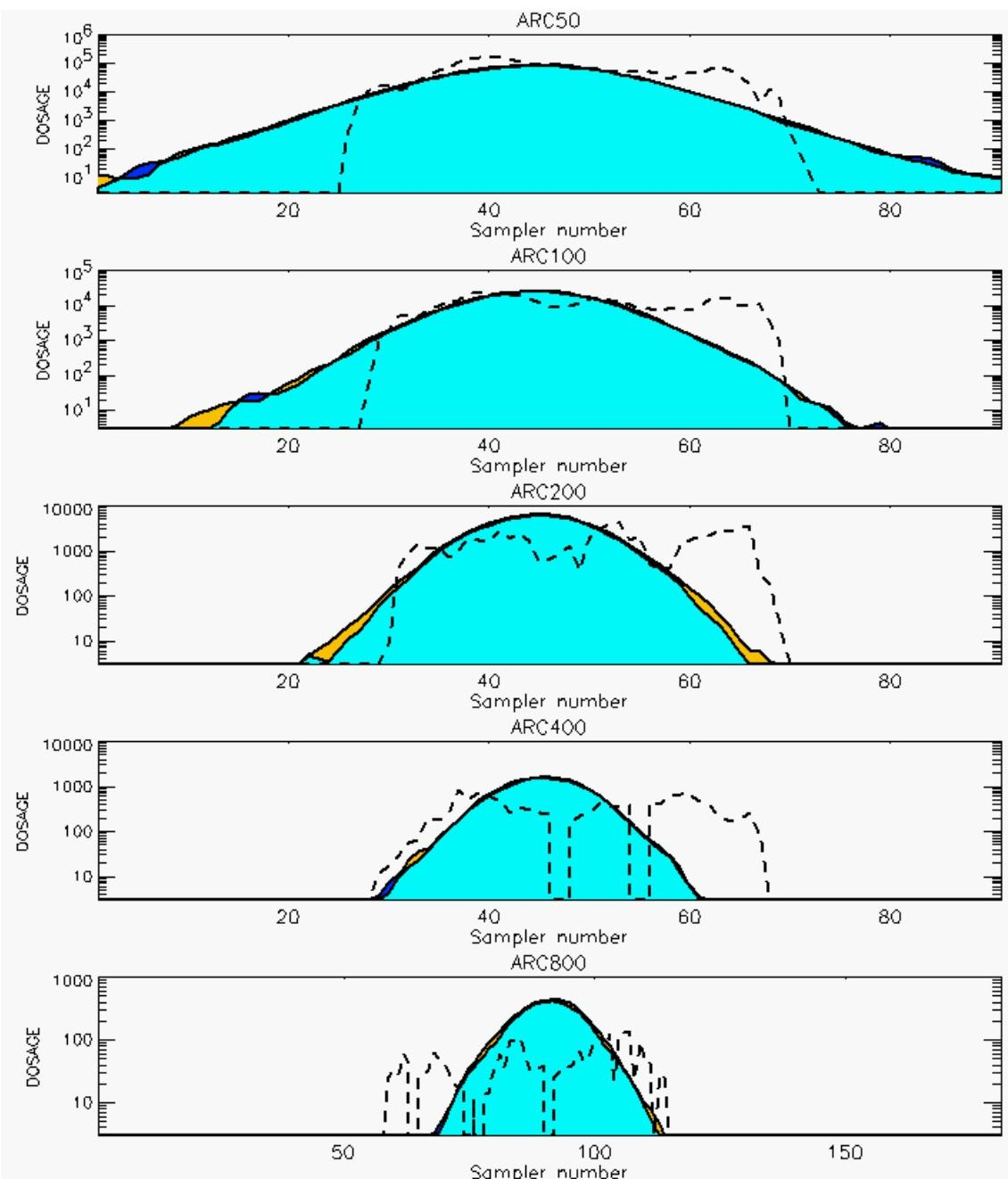
PG Prediction1 to Prediction2 Comparison

PG Trial File: pr_grass_tracer_Experiment_25.txt

PG Prediction File 1: ARAC\sv_vd\pg_25_sv_vd.arac

PG Prediction File 2: ARAC\sv_novd\pg_25_sv_novd.arac

Figure L-20a. NARAC With and Without SO₂ Surface Deposition Predictions to Trial 25 on Linear Scale: Stability Category is 1



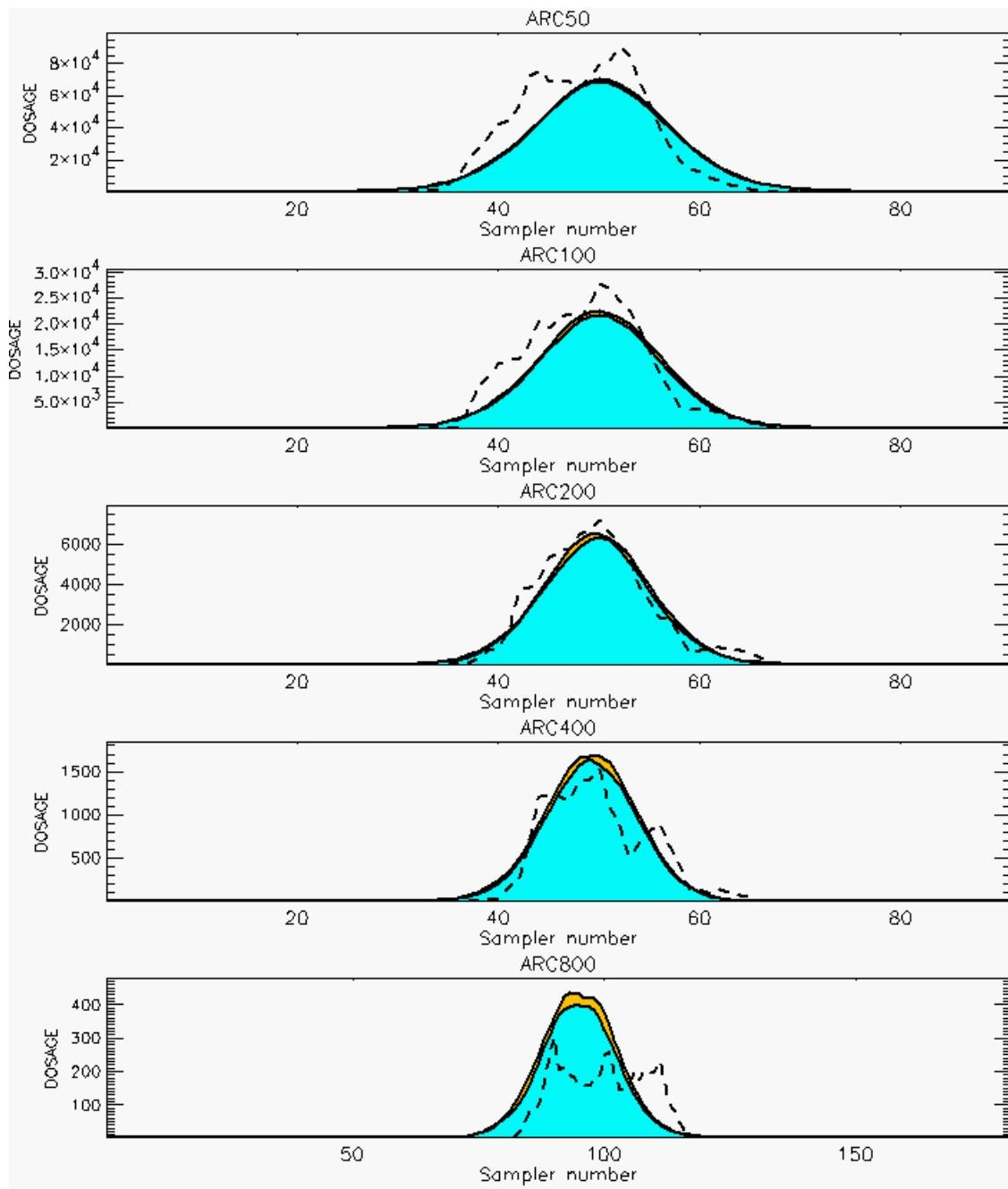
PG Prediction1 to Prediction2 Comparison

PG Trial File: pr_grass_tracer_Experiment_25.txt

PG Prediction File 1: ARAC\sv_vd\pg_25_sv_vd.arac

PG Prediction File 2: ARAC\sv_novd\pg_25_sv_novd.arac

Figure L-20b. NARAC With and Without SO₂ Surface Deposition Predictions to Trial 25 on Logarithmic Scale: Stability Category is 1



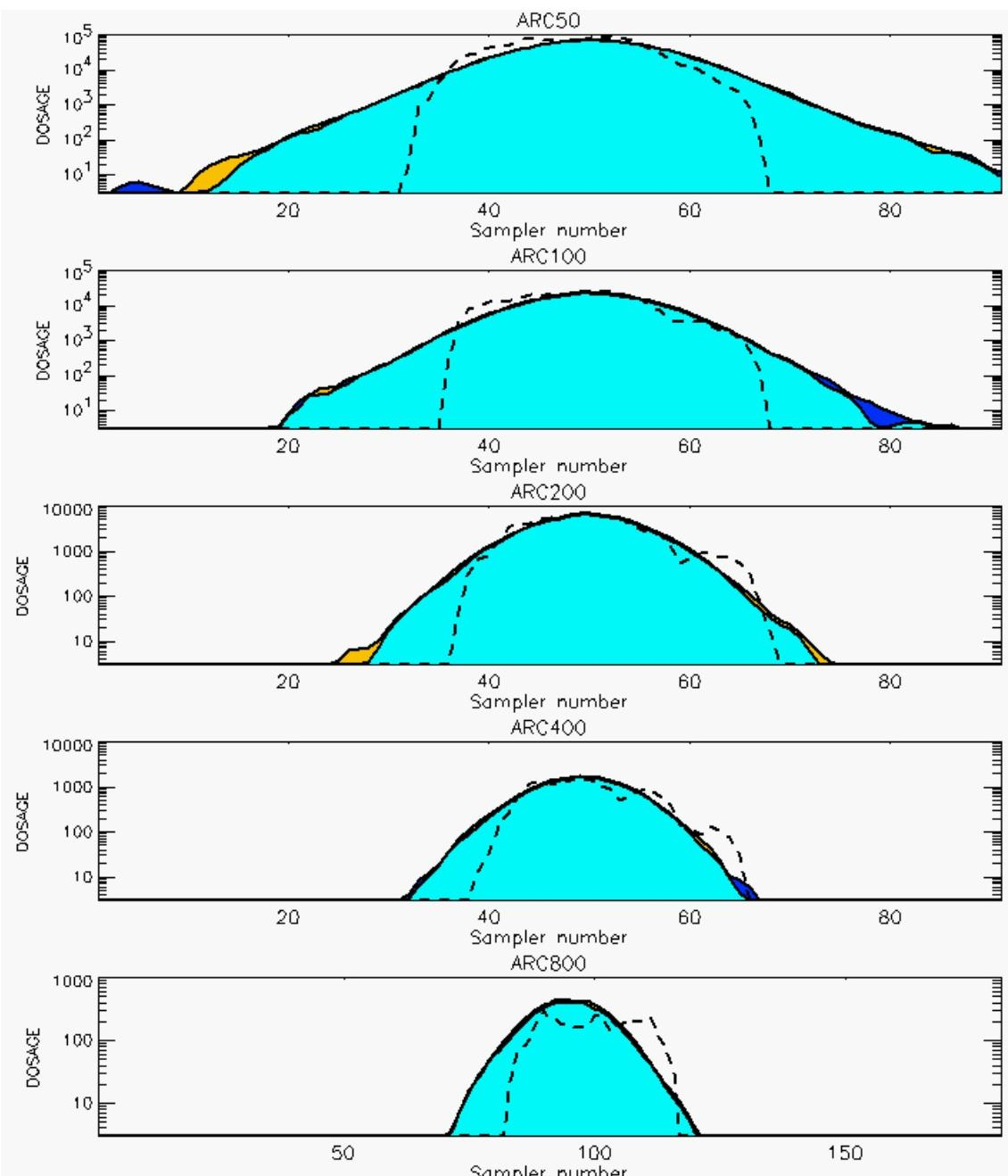
PG Prediction1 to Prediction2 Comparison

PG Trial File: pr_grass_tracer_Experiment_26.txt

PG Prediction File 1: ARAC\sv_vd\pg_26_sv_vd.arac

PG Prediction File 2: ARAC\sv_novd\pg_26_sv_novd.arac

Figure L-21a. NARAC With and Without SO₂ Surface Deposition Predictions to Trial 26 on Linear Scale: Stability Category is 2



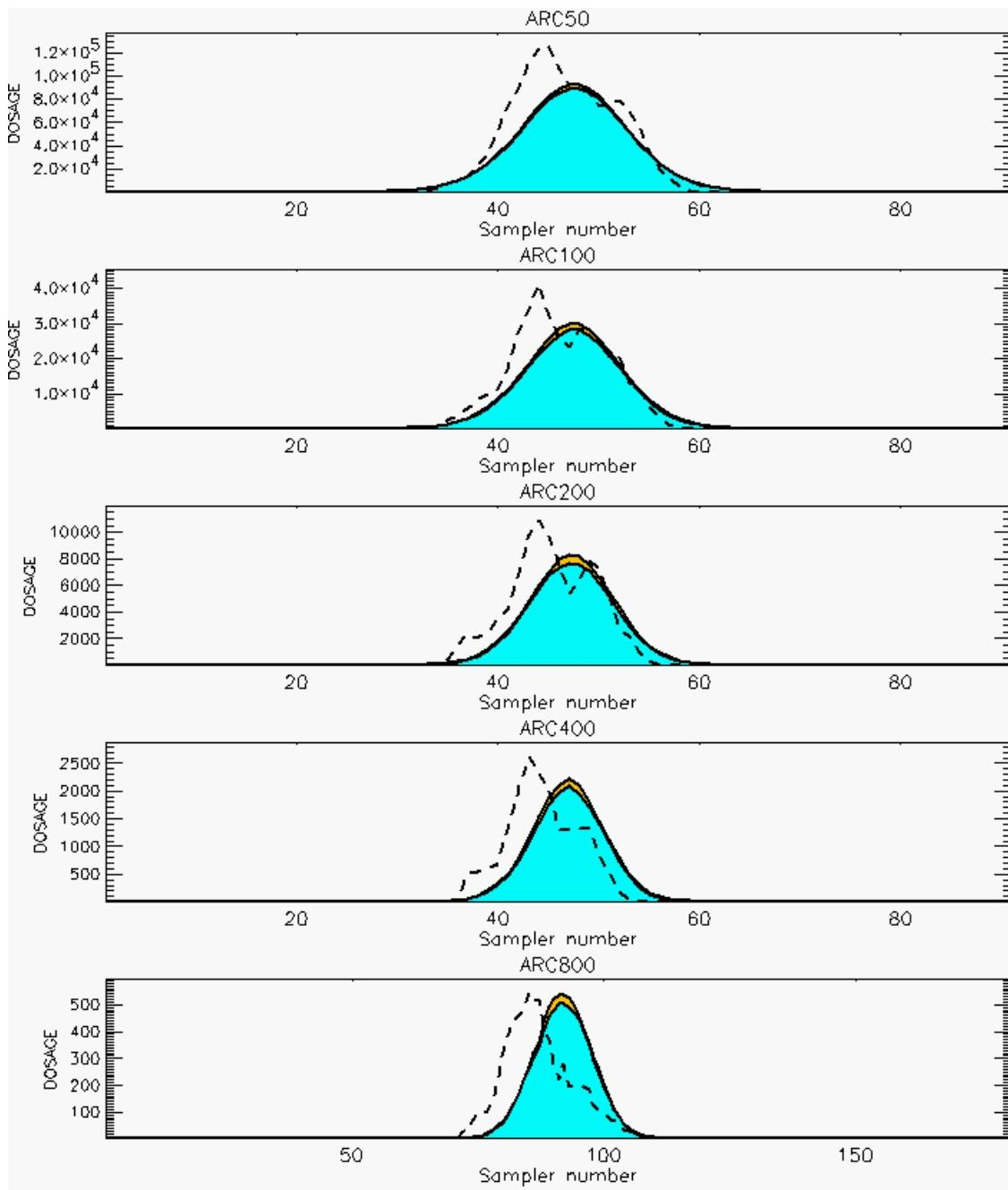
PG Prediction1 to Prediction2 Comparison

PG Trial File: pr_grass_tracer_Experiment_26.txt

PG Prediction File 1: ARAC\sv_vd\pg_26_sv_vd.arac

PG Prediction File 2: ARAC\sv_novd\pg_26_sv_novd.arac

Figure L-21b. NARAC With and Without SO₂ Surface Deposition Predictions to Trial 26 on Logarithmic Scale: Stability Category is 2



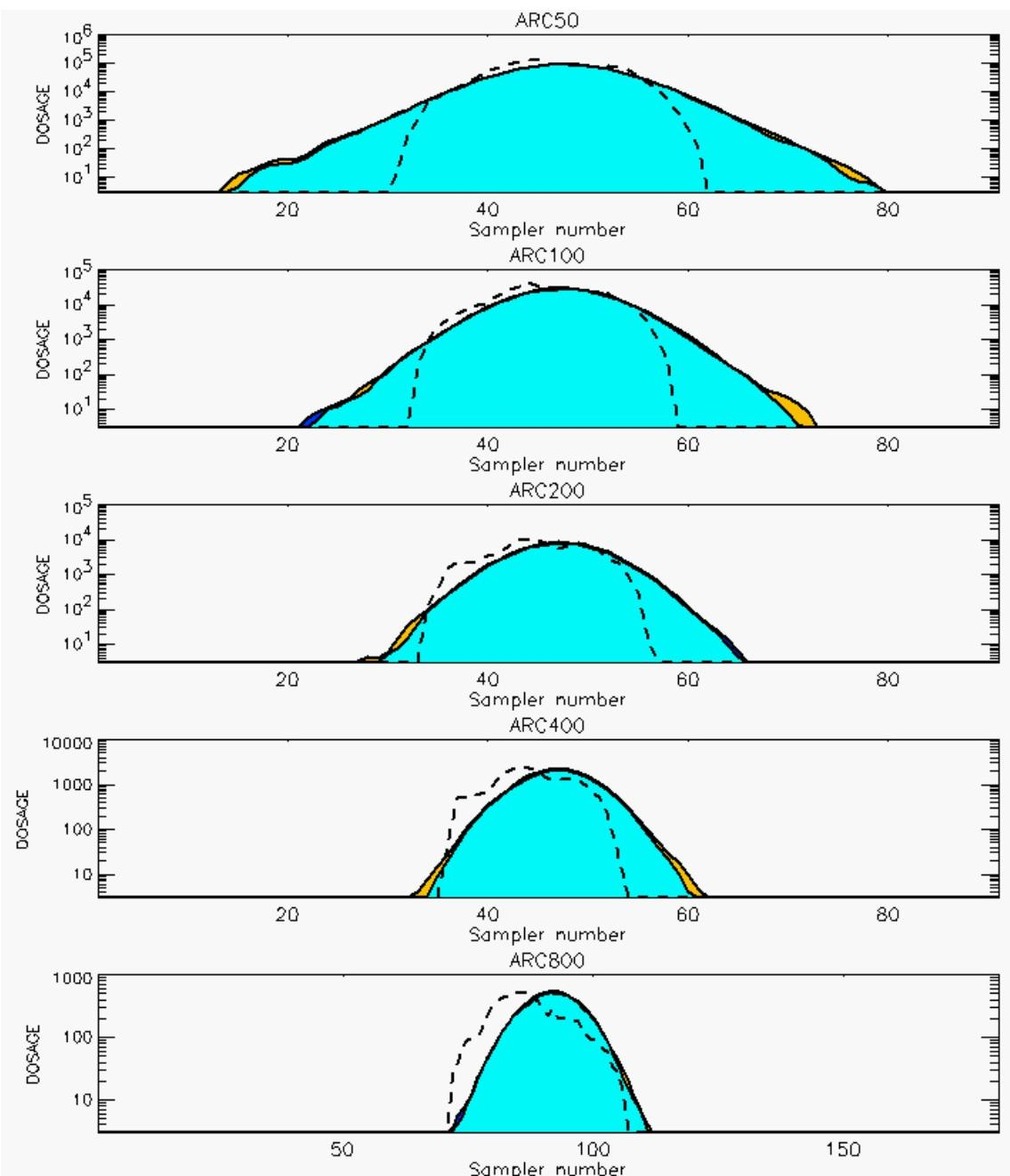
PG Prediction1 to Prediction2 Comparison

PG Trial File: pr_grass_tracer_Experiment_27.txt

PG Prediction File 1: ARAC\sv_vd\pg_27_sv_vd.arac

PG Prediction File 2: ARAC\sv_novd\pg_27_sv_novd.arac

Figure L-22a. NARAC With and Without SO₂ Surface Deposition Predictions to Trial 27 on Linear Scale: Stability Category is 2



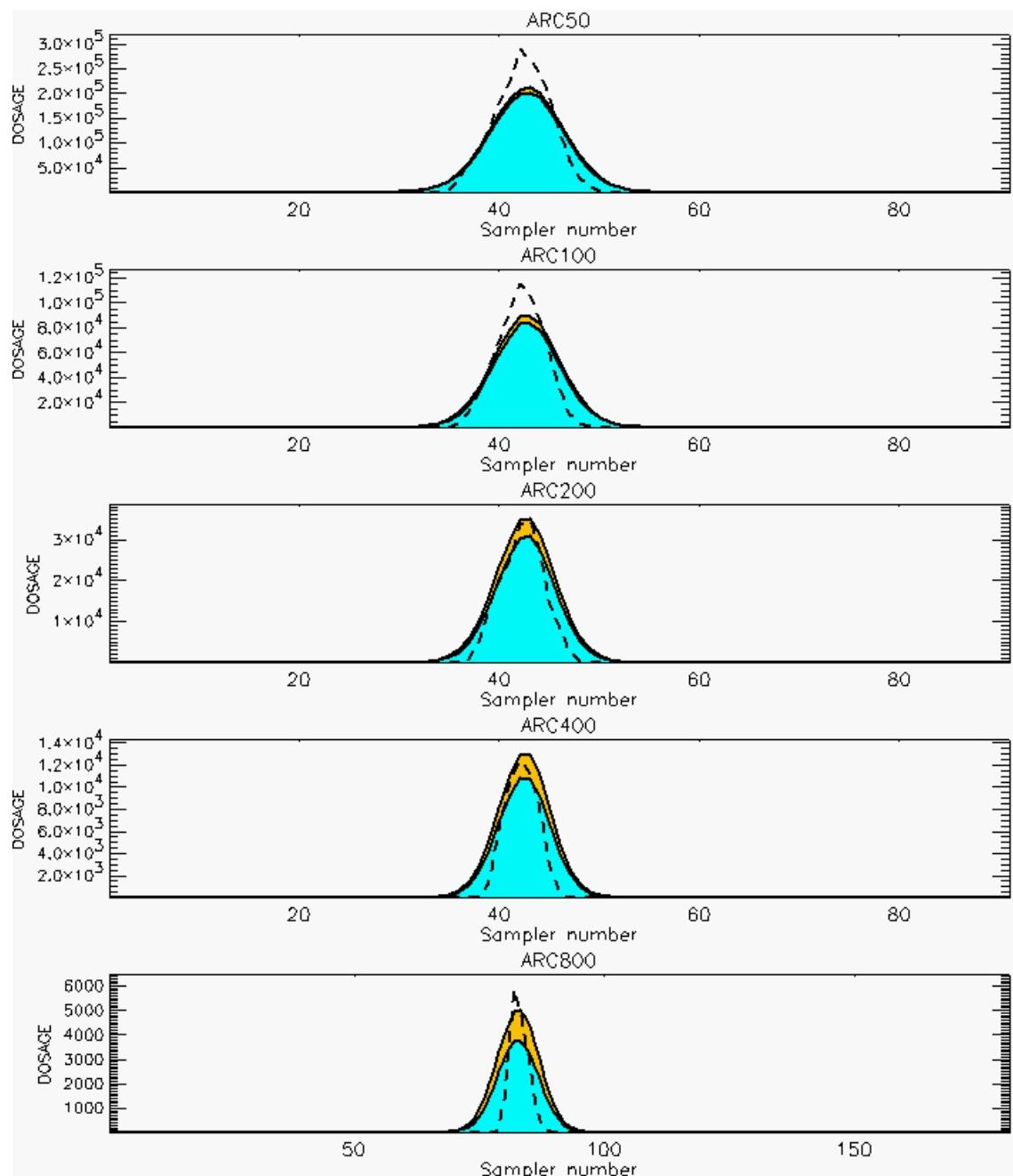
PG Prediction1 to Prediction2 Comparison

PG Trial File: pr_grass_tracer_Experiment_27.txt

PG Prediction File 1: ARAC\sv_vd\pg_27_sv_vd.arac

PG Prediction File 2: ARAC\sv_novd\pg_27_sv_novd.arac

Figure L-22b. NARAC With and Without SO₂ Surface Deposition Predictions to Trial 27 on Logarithmic Scale: Stability Category is 2



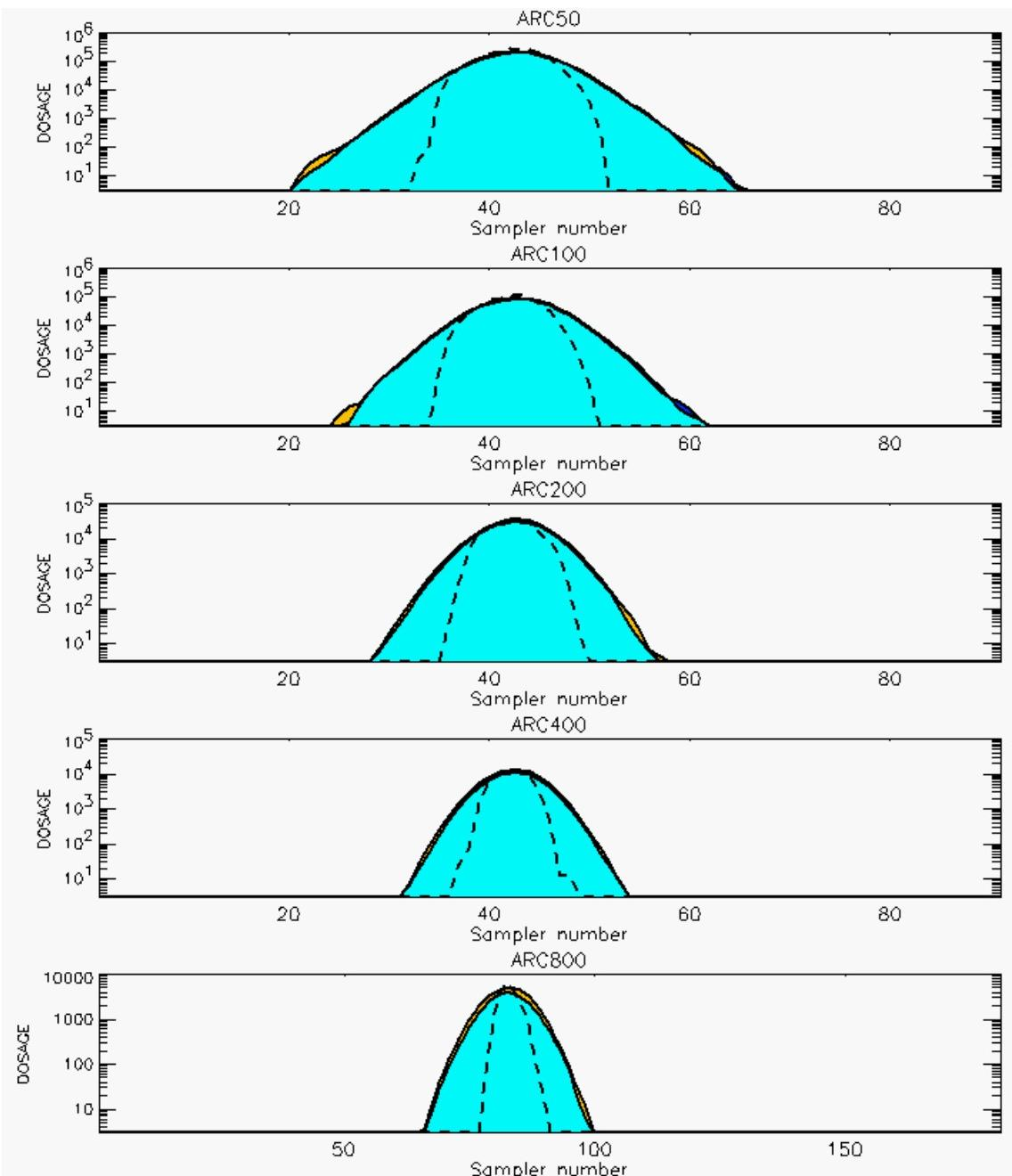
PG Prediction1 to Prediction2 Comparison

PG Trial File: pr_grass_tracer_Experiment_28.txt

PG Prediction File 1: ARAC\sv_vd\pg_28_sv_vd.arac

PG Prediction File 2: ARAC\sv_novd\pg_28_sv_novd.arac

Figure L-23a. NARAC With and Without SO₂ Surface Deposition Predictions to Trial 28 on Linear Scale: Stability Category is 5



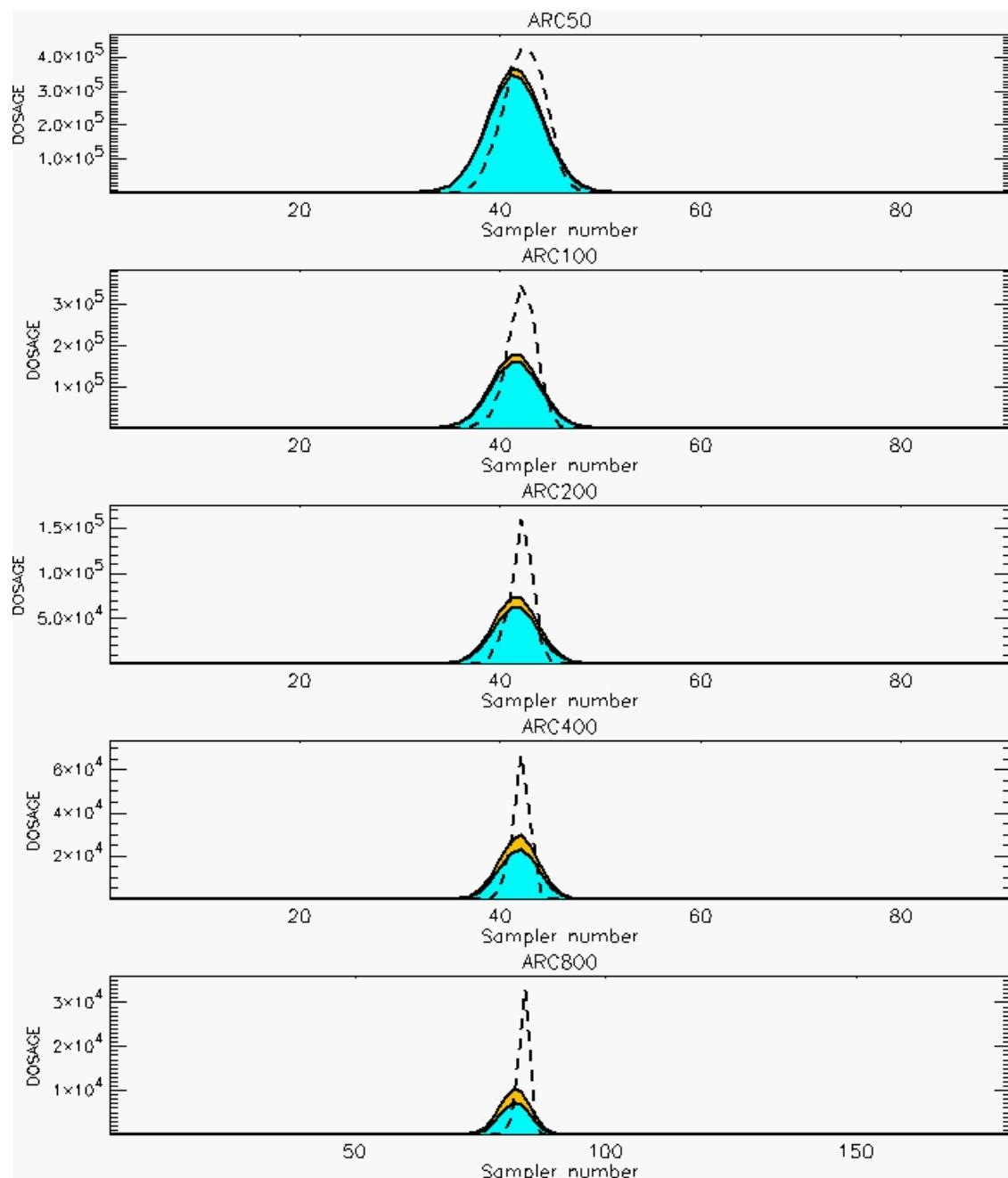
PG Prediction1 to Prediction2 Comparison

PG Trial File: pr_grass_tracer_Experiment_28.txt

PG Prediction File 1: ARAC\sv_vd\pg_28_sv_vd.arac

PG Prediction File 2: ARAC\sv_novd\pg_28_sv_novd.arac

Figure L-23b. NARAC With and Without SO₂ Surface Deposition Predictions to Trial 28 on Logarithmic Scale: Stability Category is 5



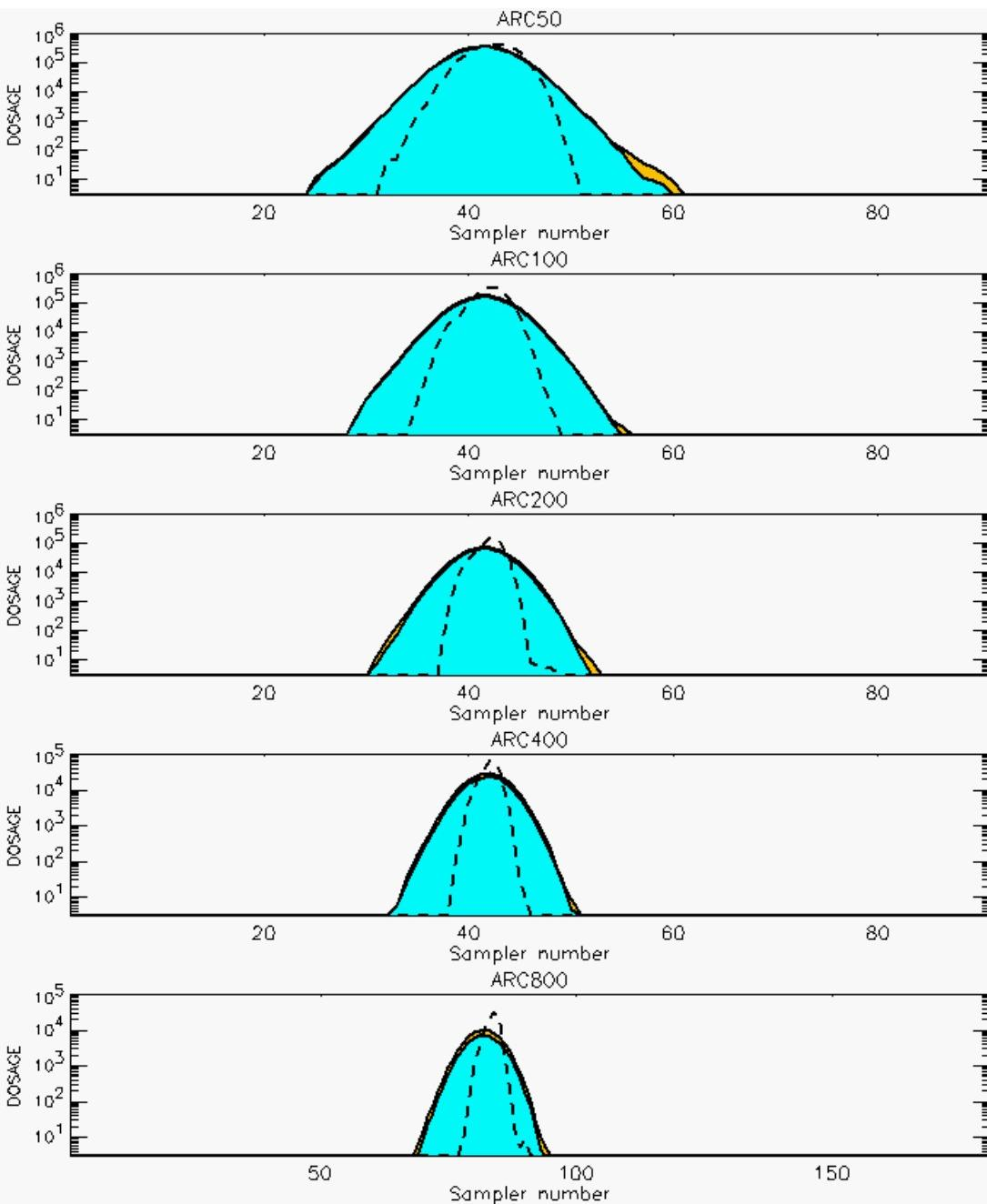
PG Prediction1 to Prediction2 Comparison

PG Trial File: pr_grass_tracer_Experiment_32.txt

PG Prediction File 1: ARAC\sv_vd\pg_32_sv_vd.arac

PG Prediction File 2: ARAC\sv_novd\pg_32_sv_novd.arac

Figure L-24a. NARAC With and Without SO₂ Surface Deposition Predictions to Trial 32 on Linear Scale: Stability Category is 6



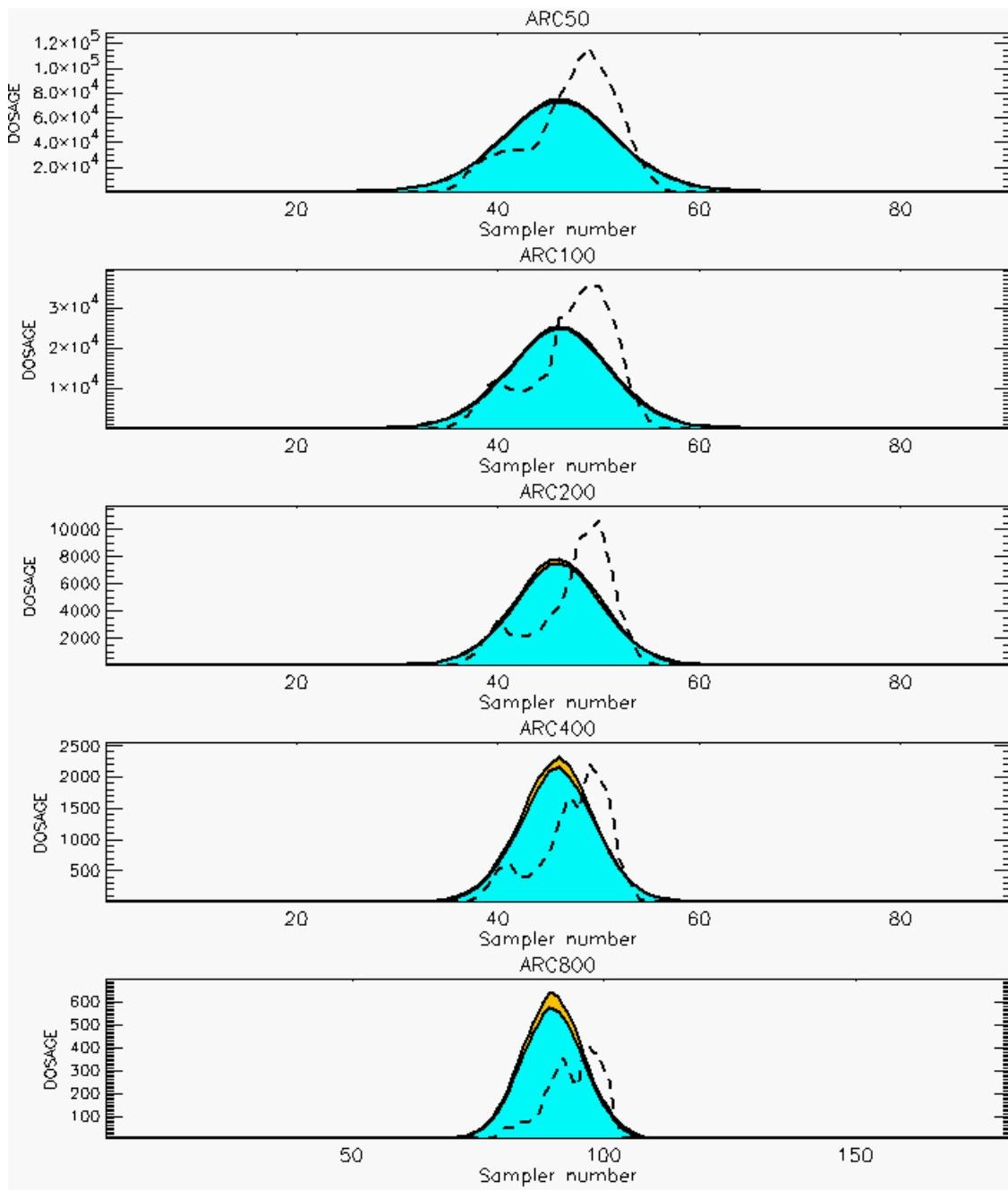
PG Prediction1 to Prediction2 Comparison

PG Trial File: pr_grass_tracer_Experiment_32.txt

PG Prediction File 1: ARAC\sv_vd\pg_32_sv_vd.arac

PG Prediction File 2: ARAC\sv_novd\pg_32_sv_novd.arac

Figure L-24b. NARAC With and Without SO_2 Surface Deposition Predictions to Trial 32 on Logarithmic Scale: Stability Category is 6



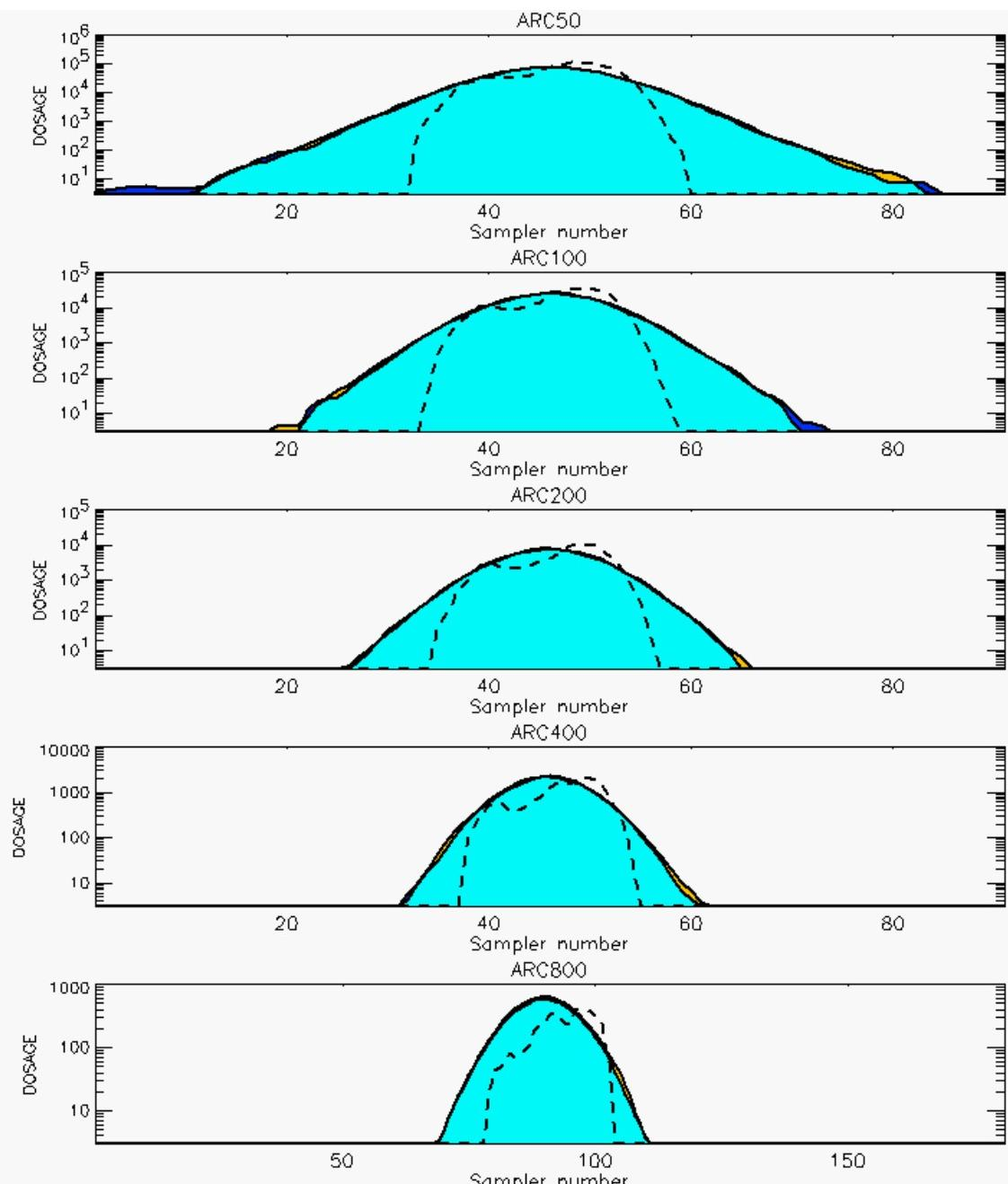
PG Prediction1 to Prediction2 Comparison

PG Trial File: pr_grass_tracer_Experiment_33.txt

PG Prediction File 1: ARAC\sv_vd\pg_33_sv_vd.arac

PG Prediction File 2: ARAC\sv_novd\pg_33_sv_novd.arac

Figure L-25a. NARAC With and Without SO₂ Surface Deposition Predictions to Trial 33 on Linear Scale: Stability Category is 3



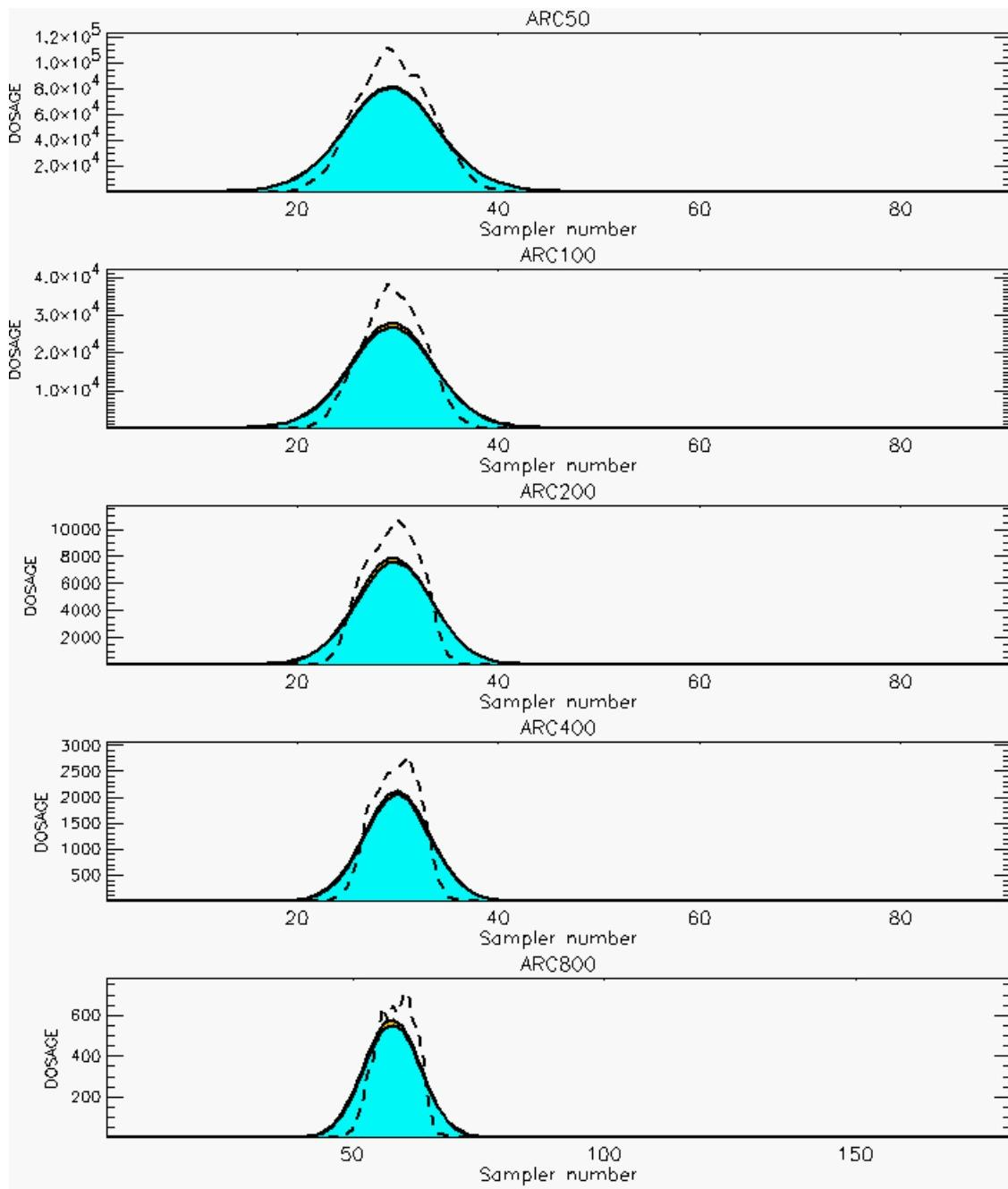
PG Prediction1 to Prediction2 Comparison

PG Trial File: pr_grass_tracer_Experiment_33.txt

PG Prediction File 1: ARAC\sv_vd\pg_33_sv_vd.arac

PG Prediction File 2: ARAC\sv_novd\pg_33_sv_novd.arac

Figure L-25b. NARAC With and Without SO₂ Surface Deposition Predictions to Trial 33 on Logarithmic Scale: Stability Category is 3



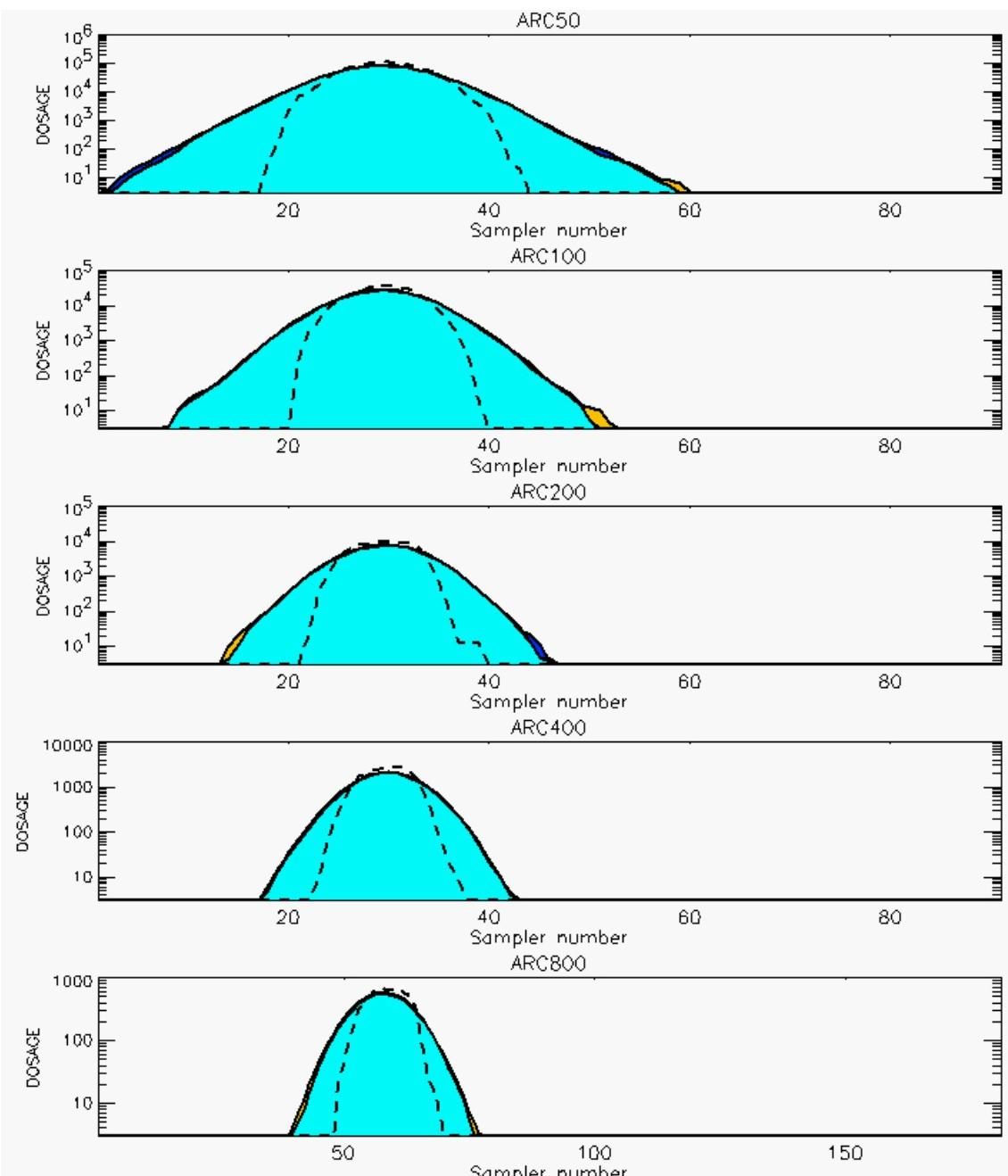
PG Prediction1 to Prediction2 Comparison

PG Trial File: pr_grass_tracer_Experiment_34.txt

PG Prediction File 1: ARAC\sv_vd\pg_34_sv_vd.arac

PG Prediction File 2: ARAC\sv_novd\pg_34_sv_novd.arac

Figure L-26a. NARAC With and Without SO₂ Surface Deposition Predictions to Trial 34 on Linear Scale: Stability Category is 3



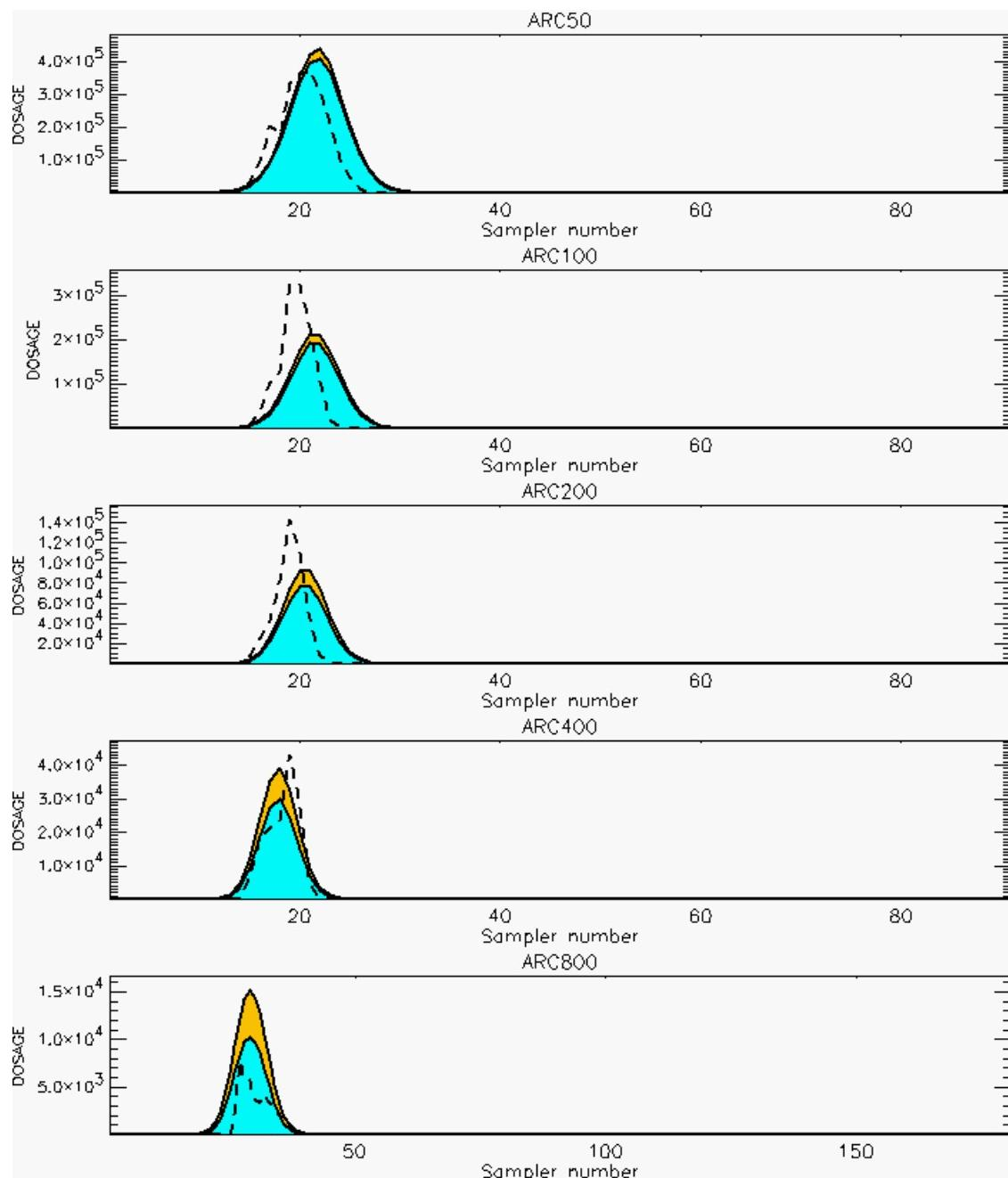
PG Prediction1 to Prediction2 Comparison

PG Trial File: pr_grass_tracer_Experiment_34.txt

PG Prediction File 1: ARAC\sv_vd\pg_34_sv_vd.arac

PG Prediction File 2: ARAC\sv_novd\pg_34_sv_novd.arac

Figure L-26b. NARAC With and Without SO₂ Surface Deposition Predictions to Trial 34 on Logarithmic Scale: Stability Category is 3



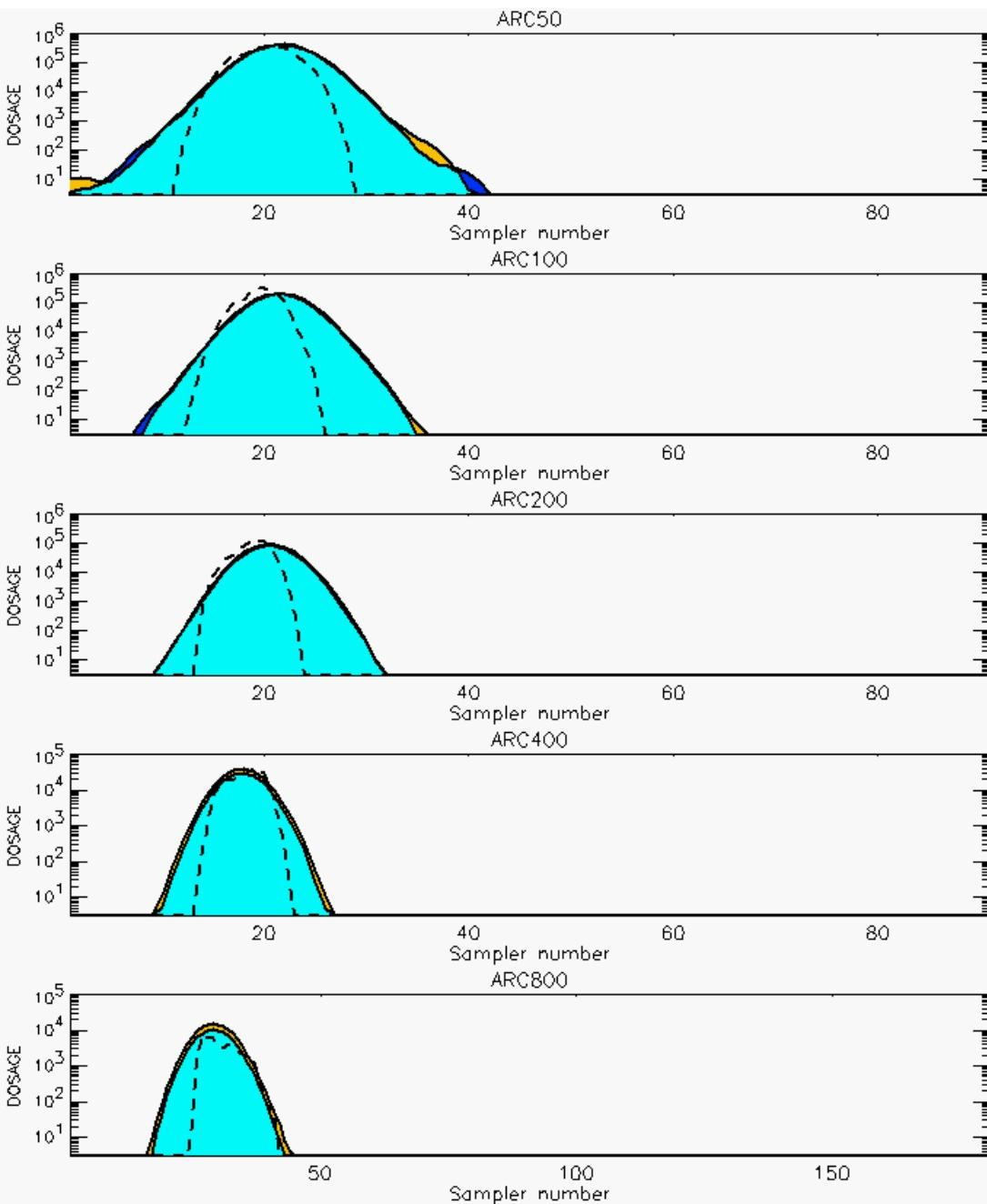
PG Prediction1 to Prediction2 Comparison

PG Trial File: pr_grass_tracer_Experiment_35.txt

PG Prediction File 1: ARAC\sv_vd\pg_35_sv_vd.arac

PG Prediction File 2: ARAC\sv_novd\pg_35_sv_novd.arac

Figure L-27a. NARAC With and Without SO₂ Surface Deposition Predictions to Trial 35 on Linear Scale: Stability Category is 6



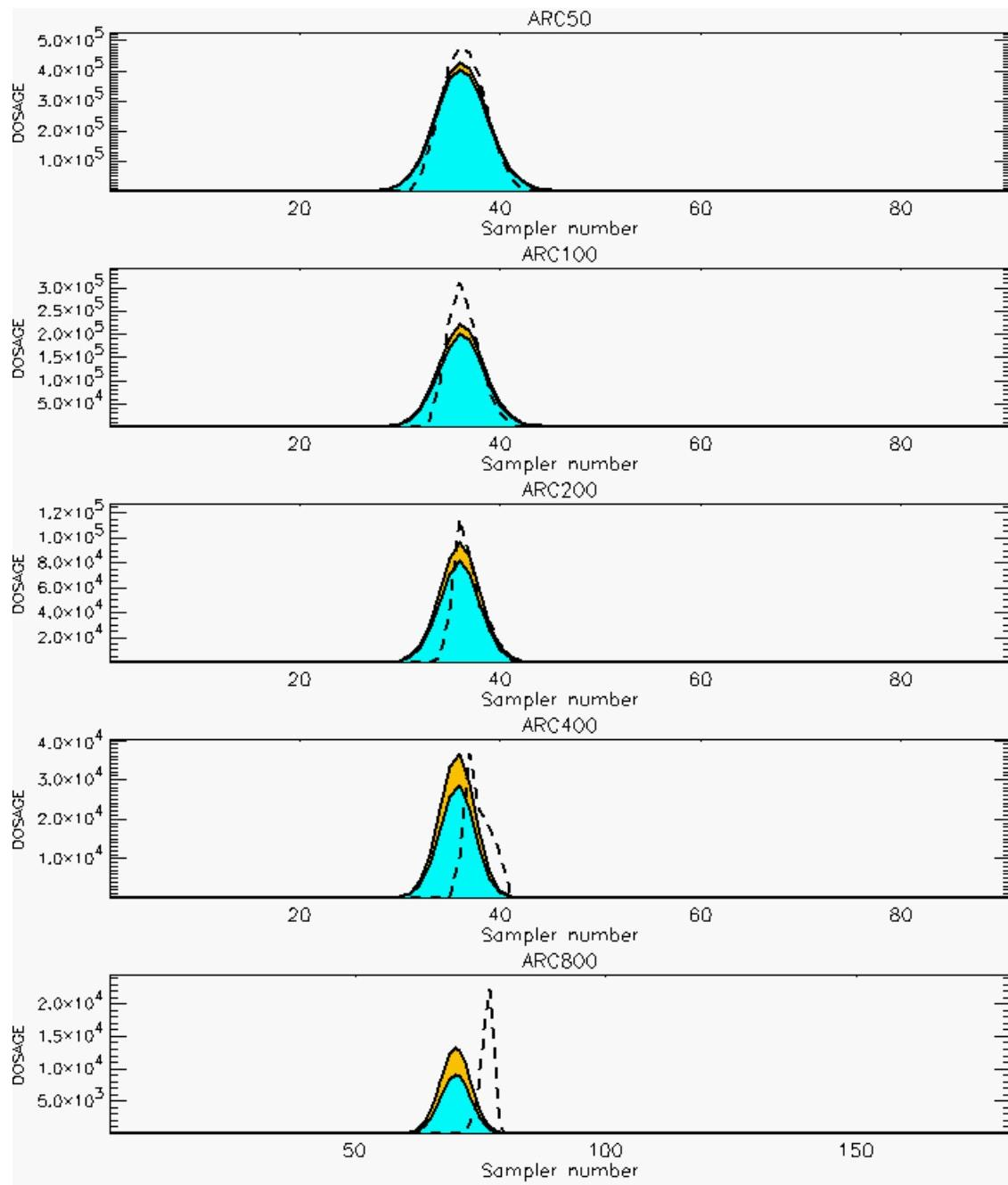
PG Prediction1 to Prediction2 Comparison

PG Trial File: pr_grass_tracer_Experiment_35.txt

PG Prediction File 1: ARAC\sv_vd\pg_35_sv_vd.arac

PG Prediction File 2: ARAC\sv_novd\pg_35_sv_novd.arac

Figure L-27b. NARAC With and Without SO₂ Surface Deposition Predictions to Trial 35 on Logarithmic Scale: Stability Category is 6



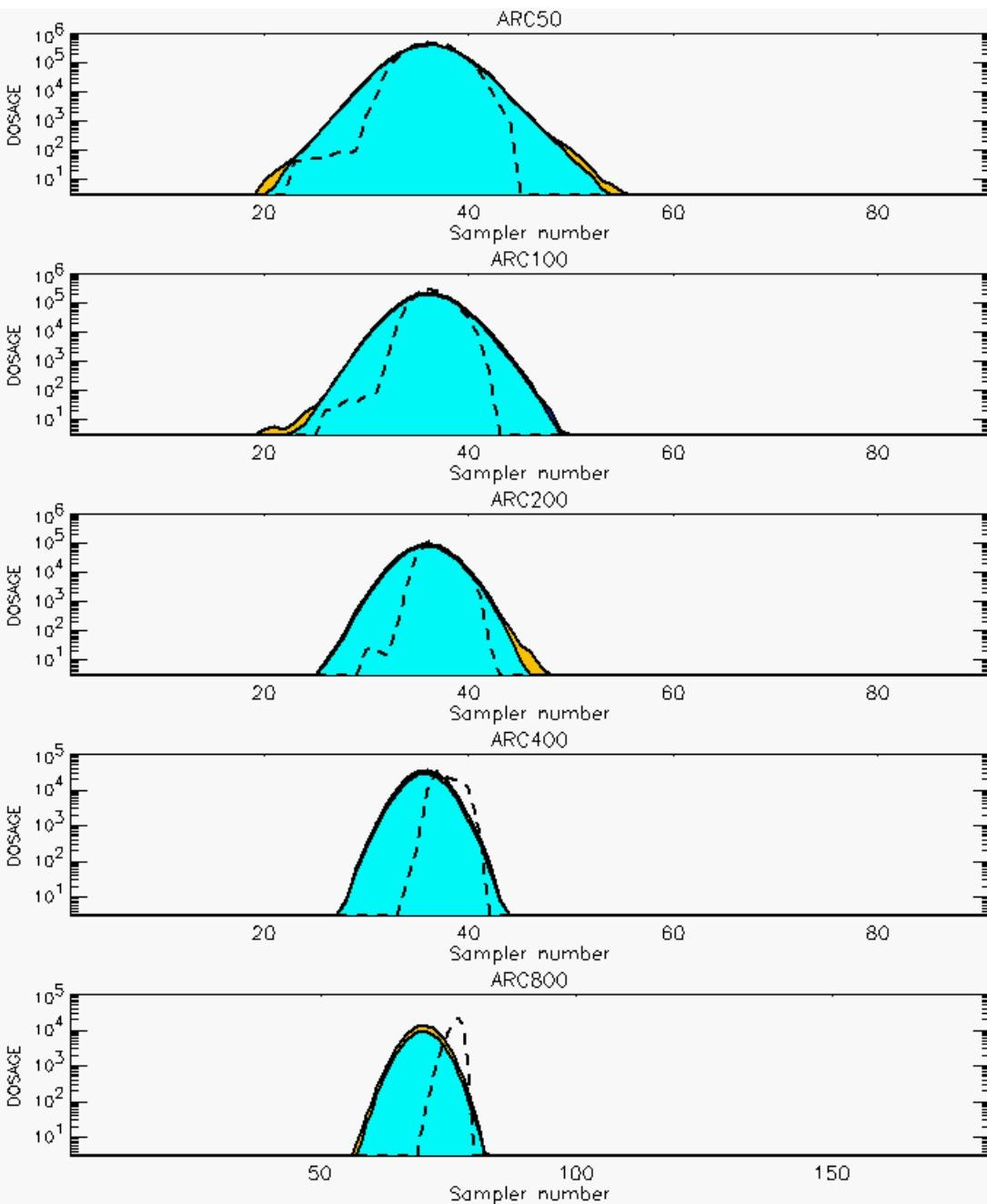
PG Prediction1 to Prediction2 Comparison

PG Trial File: pr_grass_tracer_Experiment_36.txt

PG Prediction File 1: ARAC\sv_vd\pg_36_sv_vd.arac

PG Prediction File 2: ARAC\sv_novd\pg_36_sv_novd.arac

Figure L-28a. NARAC With and Without SO₂ Surface Deposition Predictions to Trial 36 on Linear Scale: Stability Category is 6



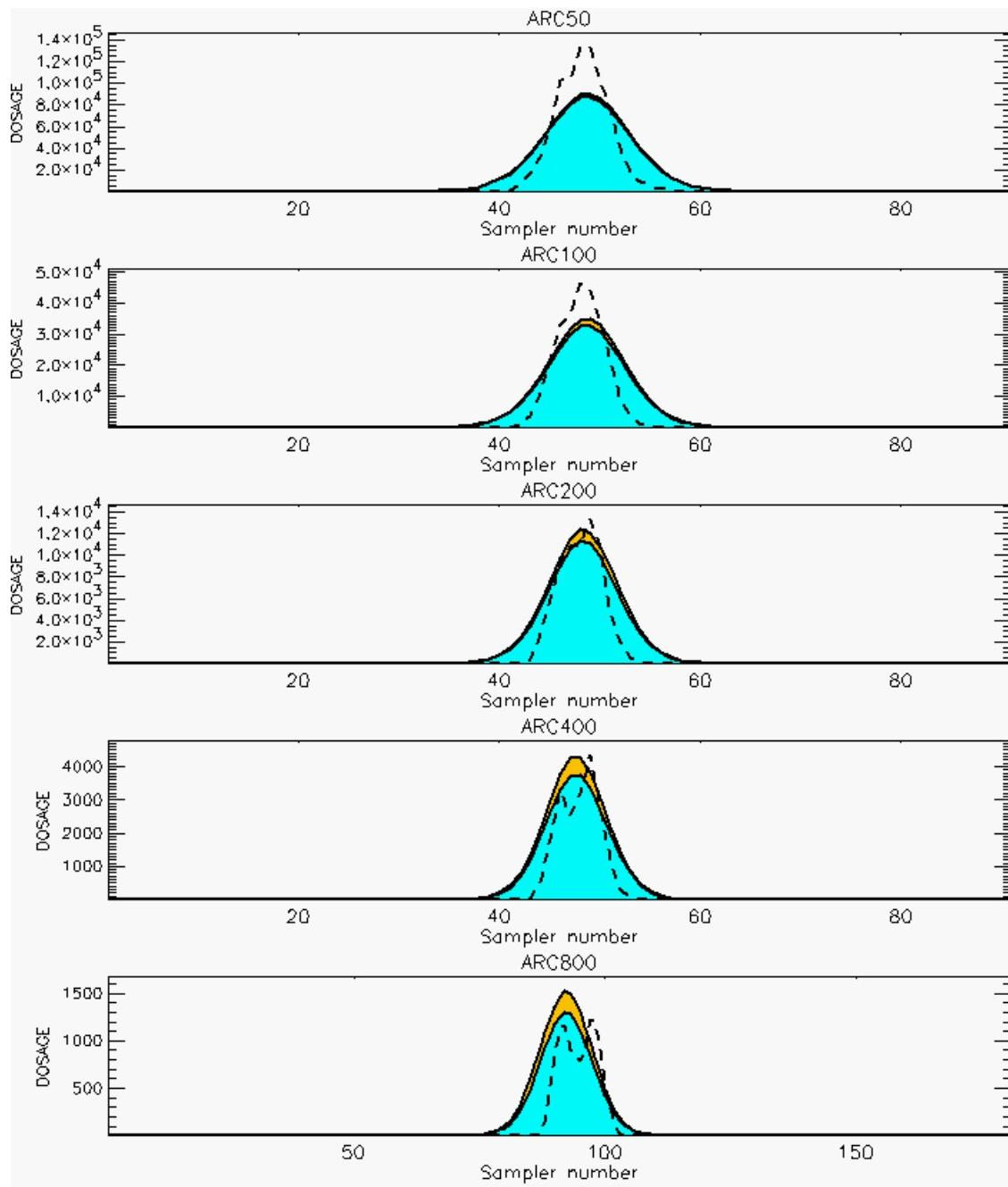
PG Prediction1 to Prediction2 Comparison

PG Trial File: pr_grass_tracer_Experiment_36.txt

PG Prediction File 1: ARAC\sv_vd\pg_36_sv_vd.arac

PG Prediction File 2: ARAC\sv_novd\pg_36_sv_novd.arac

Figure L-28b. NARAC With and Without SO₂ Surface Deposition Predictions to Trial 36 on Logarithmic Scale: Stability Category is 6



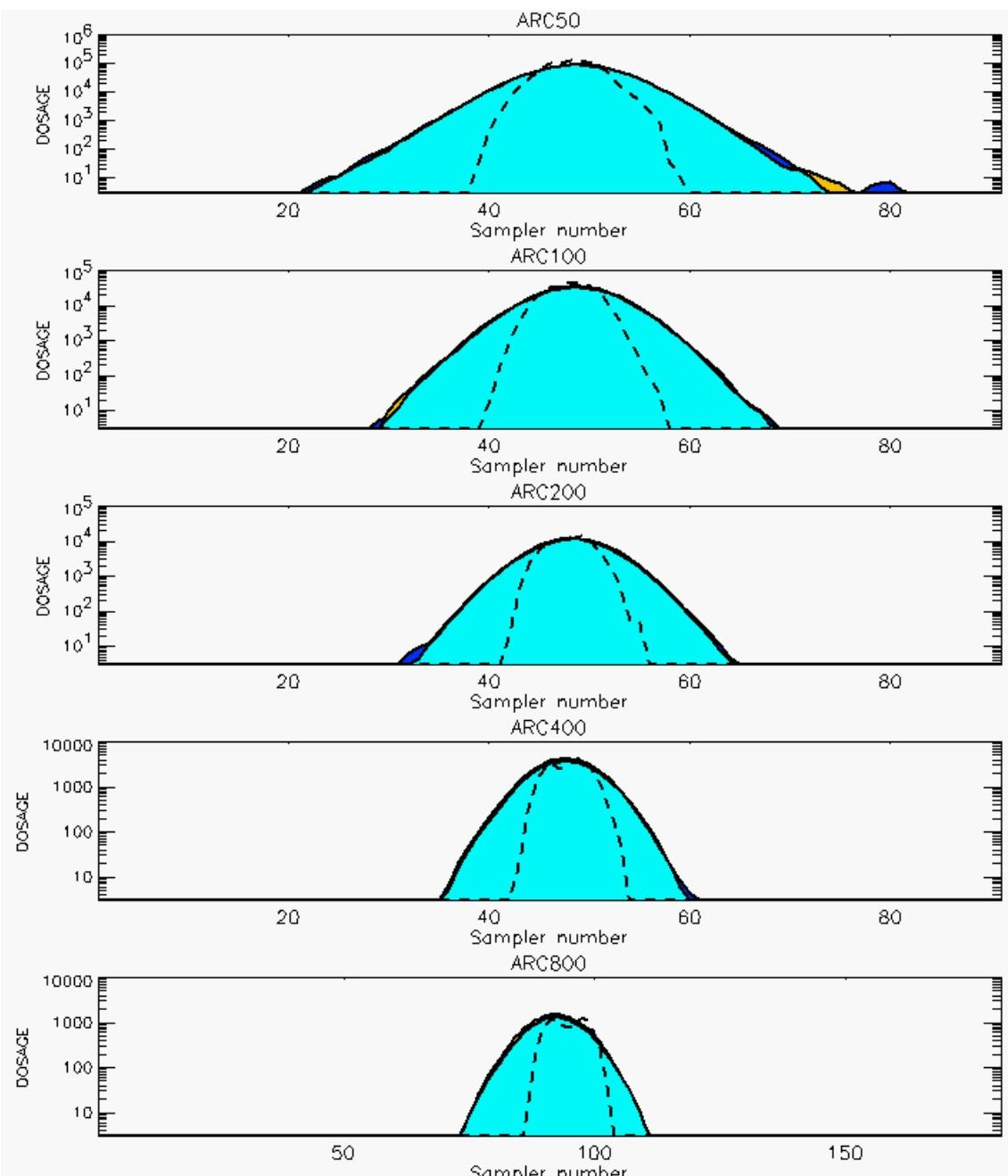
PG Prediction1 to Prediction2 Comparison

PG Trial File: pr_grass_tracer_Experiment_37.txt

PG Prediction File 1: ARAC\sv_vd\pg_37_sv_vd.arac

PG Prediction File 2: ARAC\sv_novd\pg_37_sv_novd.arac

Figure L-29a. NARAC With and Without SO₂ Surface Deposition Predictions to Trial 37 on Linear Scale: Stability Category is 4



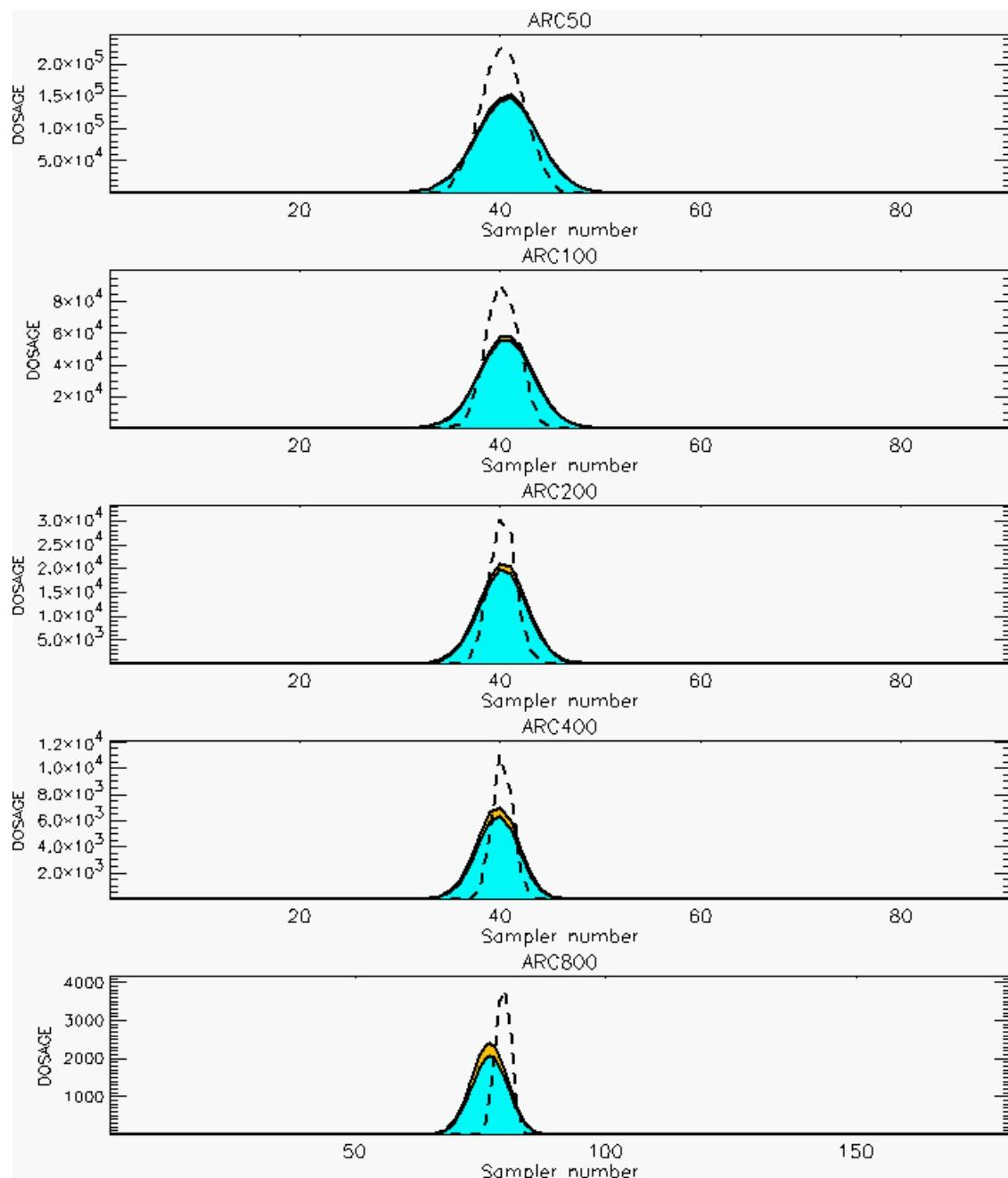
PG Prediction1 to Prediction2 Comparison

PG Trial File: pr_grass_tracer_Experiment_37.txt

PG Prediction File 1: ARAC\sv_vd\pg_37_sv_vd.arac

PG Prediction File 2: ARAC\sv_novd\pg_37_sv_novd.arac

Figure L-29b. NARAC With and Without SO₂ Surface Deposition Predictions to Trial 37 on Logarithmic Scale: Stability Category is 4



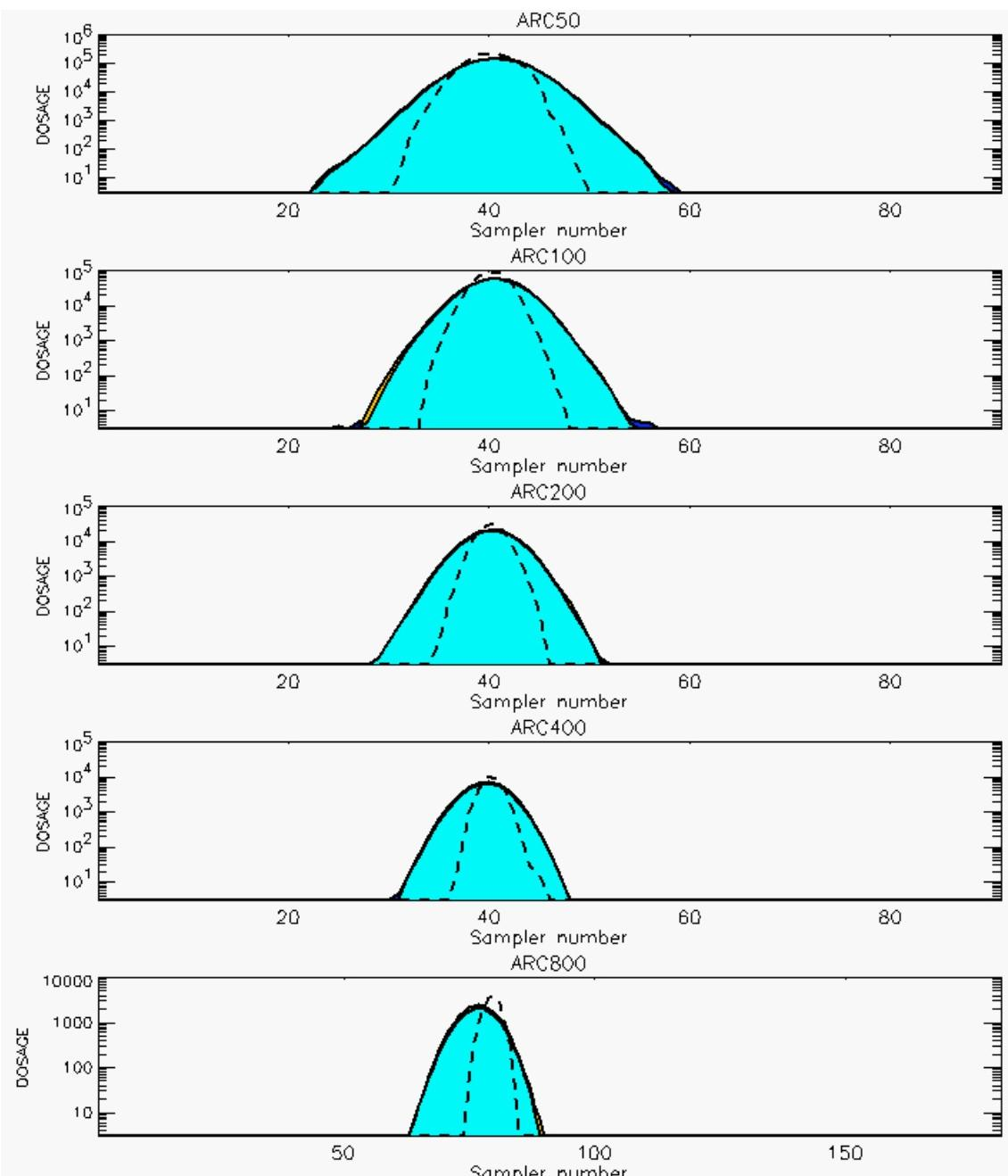
PG Prediction1 to Prediction2 Comparison

PG Trial File: pr_grass_tracer_Experiment_38.txt

PG Prediction File 1: ARAC\sv_vd\pg_38_sv_vd.arac

PG Prediction File 2: ARAC\sv_novd\pg_38_sv_novd.arac

Figure L-30a. NARAC With and Without SO₂ Surface Deposition Predictions to Trial 38 on Linear Scale: Stability Category is 4



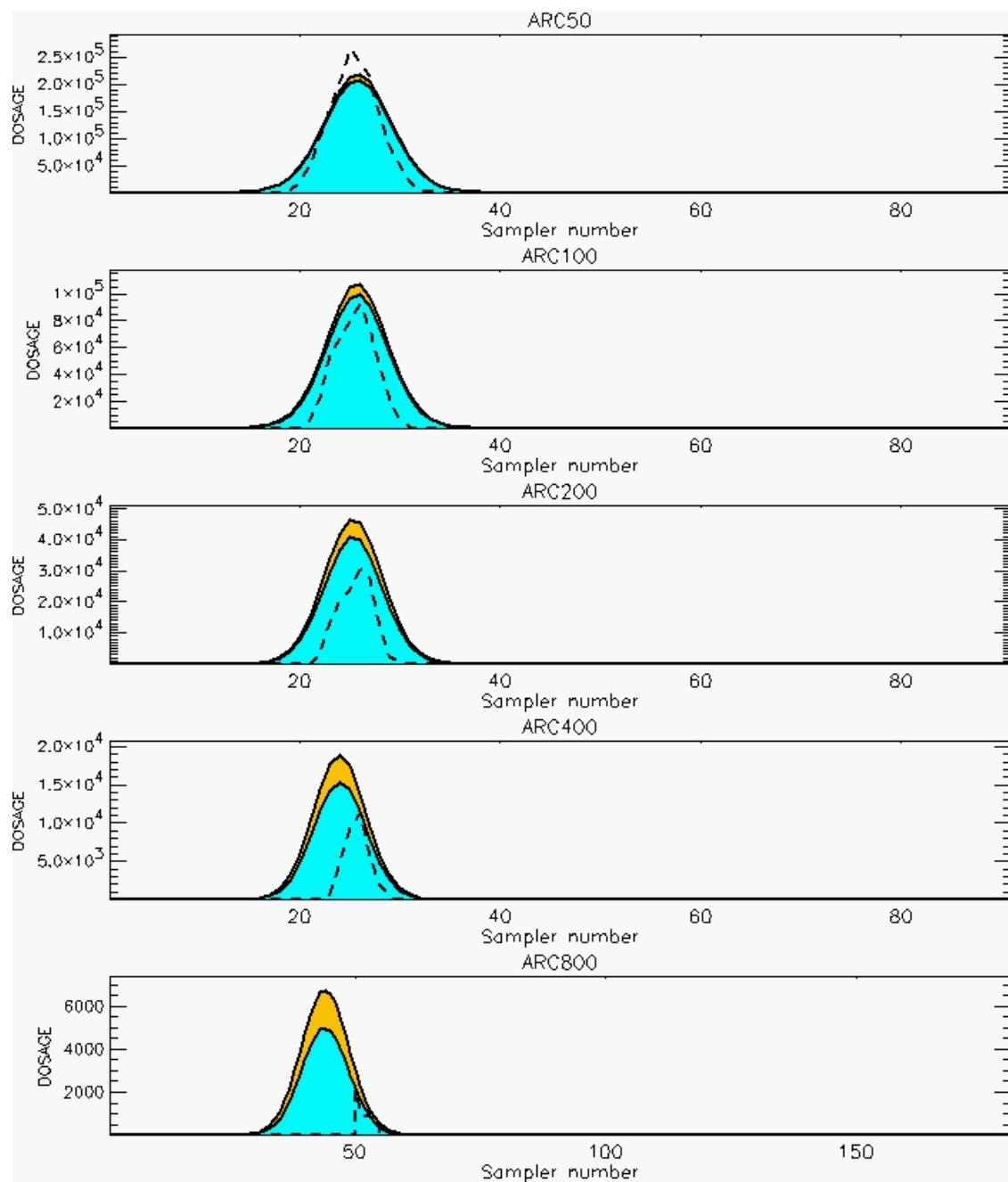
PG Prediction1 to Prediction2 Comparison

PG Trial File: pr_grass_tracer_Experiment_38.txt

PG Prediction File 1: ARAC\sv_vd\pg_38_sv_vd.arac

PG Prediction File 2: ARAC\sv_novd\pg_38_sv_novd.arac

Figure L-30b. NARAC With and Without SO₂ Surface Deposition Predictions to Trial 38 on Logarithmic Scale: Stability Category is 4



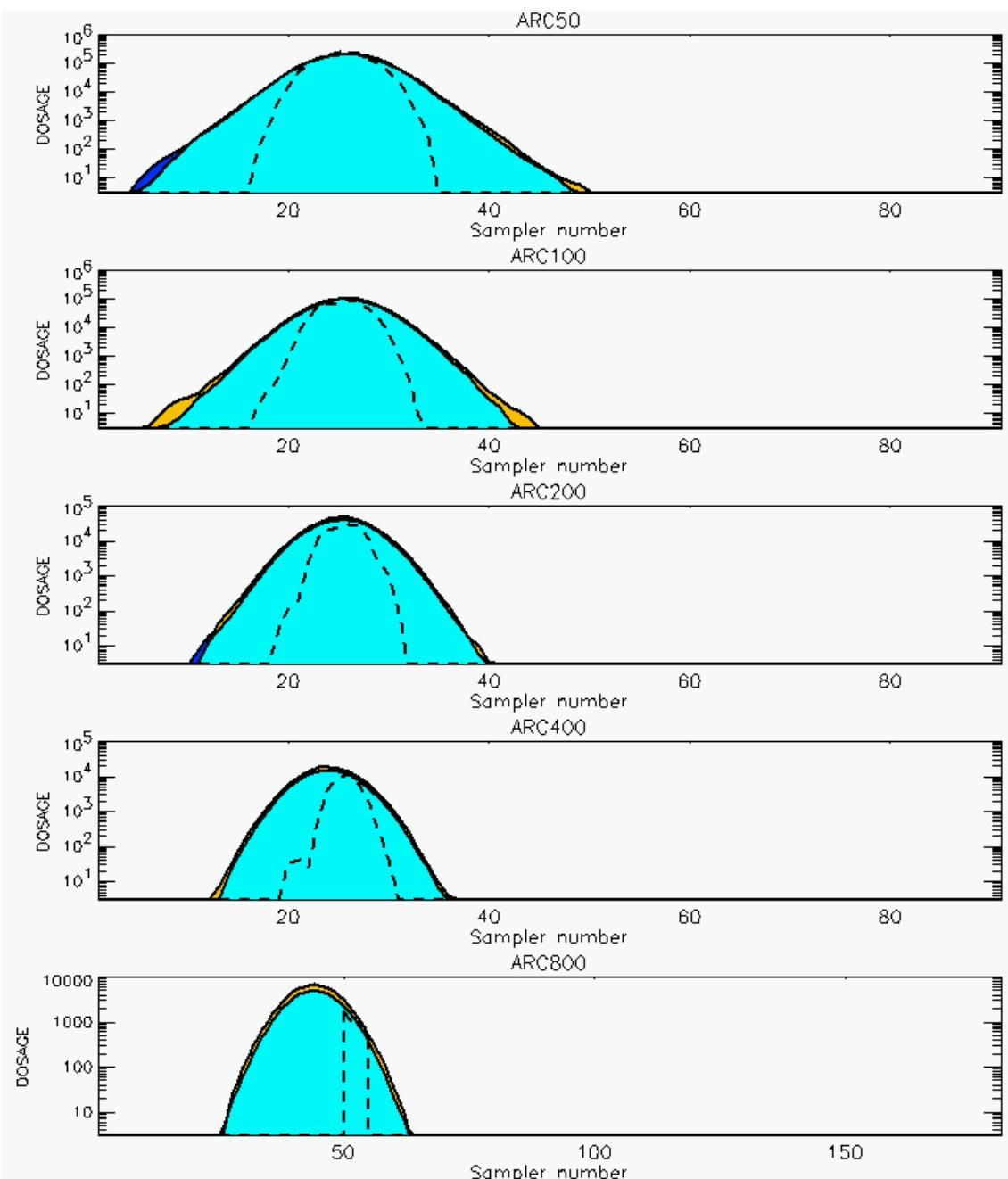
PG Prediction1 to Prediction2 Comparison

PG Trial File: pr_grass_tracer_Experiment_39.txt

PG Prediction File 1: ARAC\sv_vd\pg_39_sv_vd.arac

PG Prediction File 2: ARAC\sv_novd\pg_39_sv_novd.arac

Figure L-31a. NARAC With and Without SO₂ Surface Deposition Predictions to Trial 39 on Linear Scale: Stability Category is 6



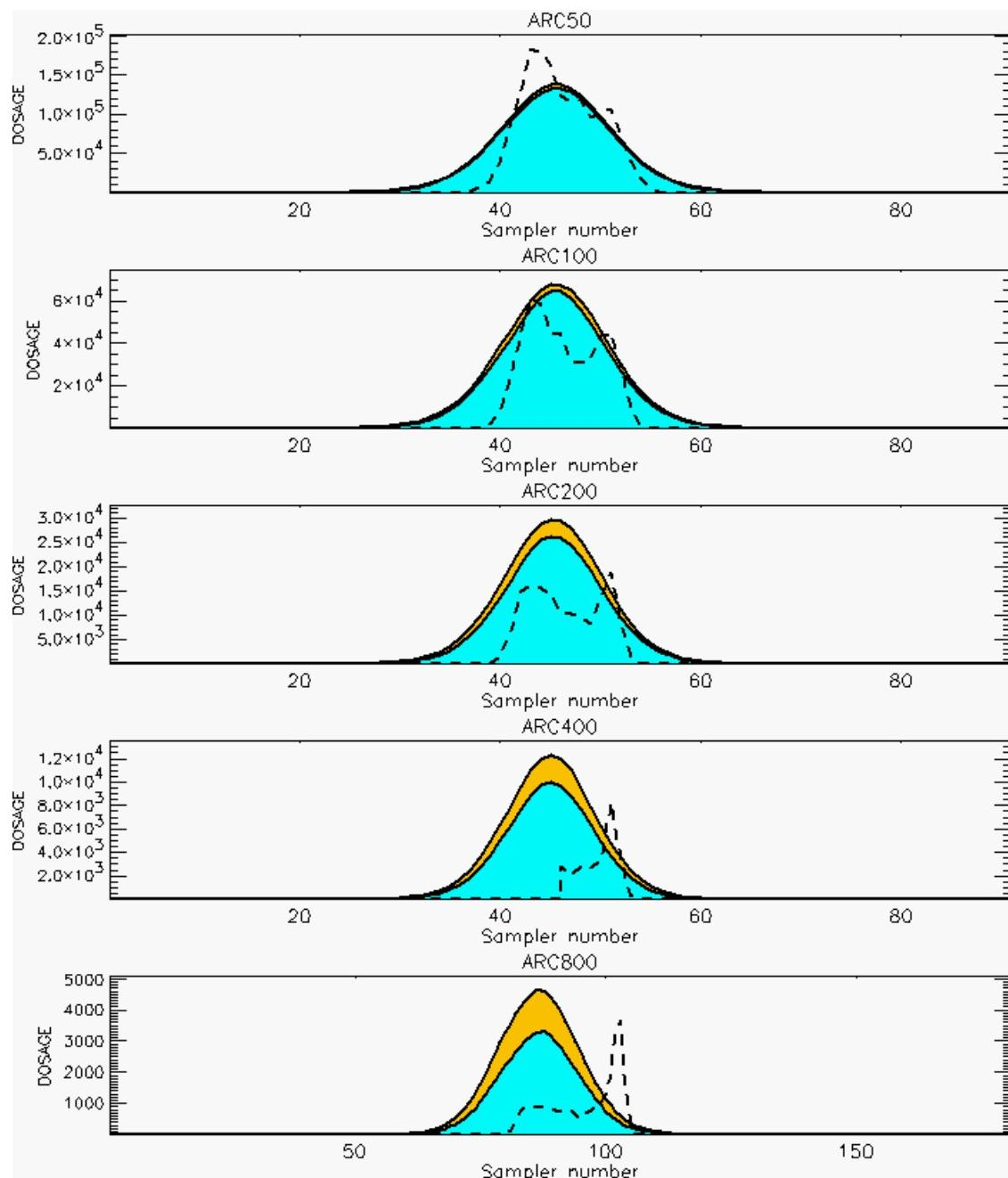
PG Prediction1 to Prediction2 Comparison

PG Trial File: pr_grass_tracer_Experiment_39.txt

PG Prediction File 1: ARAC\sv_vd\pg_39_sv_vd.arac

PG Prediction File 2: ARAC\sv_novd\pg_39_sv_novd.arac

Figure L-31b. NARAC With and Without SO_2 Surface Deposition Predictions to Trial 39 on Logarithmic Scale: Stability Category is 6



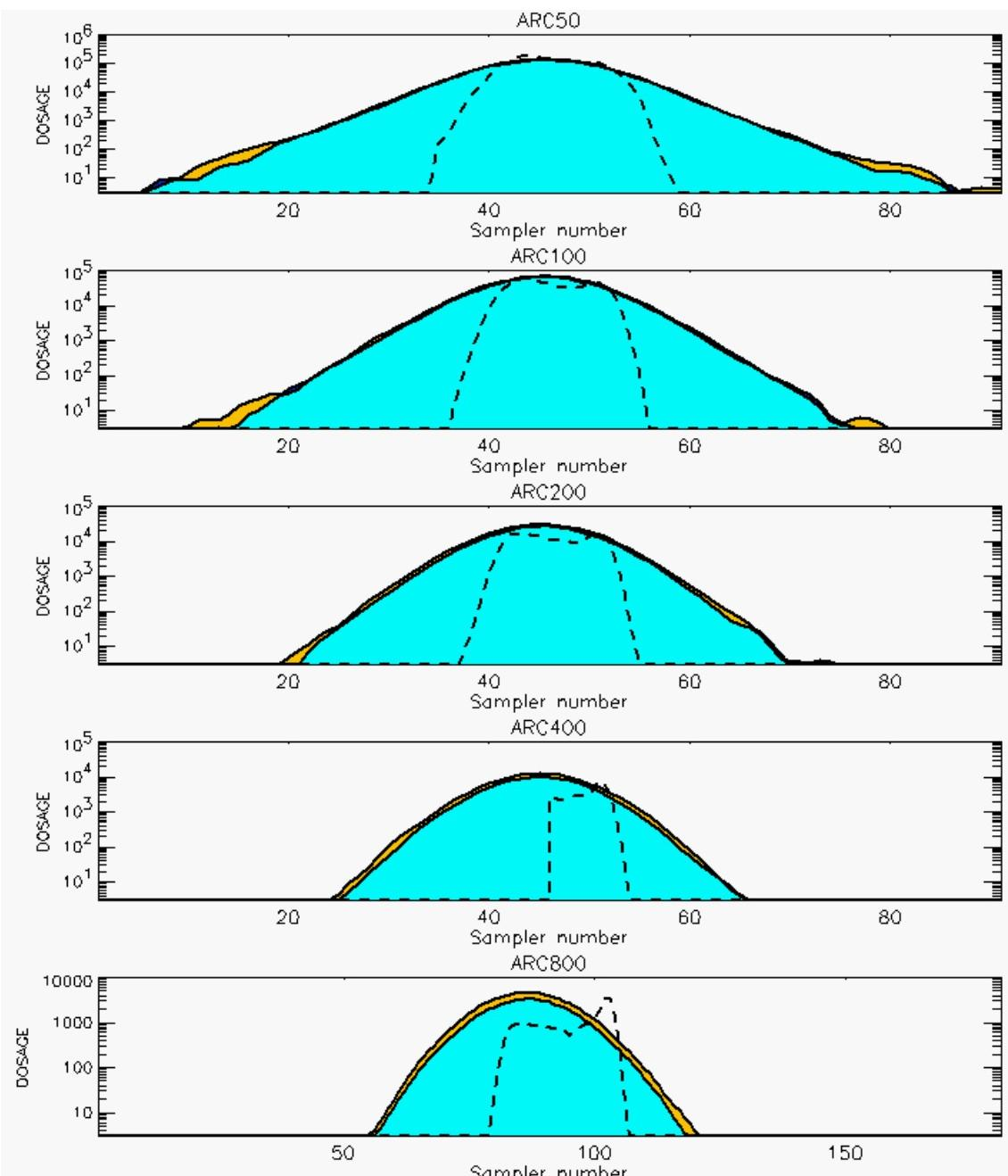
PG Prediction1 to Prediction2 Comparison

PG Trial File: pr_grass_tracer_Experiment_40.txt

PG Prediction File 1: ARAC\sv_vd\pg_40_sv_vd.arac

PG Prediction File 2: ARAC\sv_novd\pg_40_sv_novd.arac

Figure L-32a. NARAC With and Without SO₂ Surface Deposition Predictions to Trial 40 on Linear Scale: Stability Category is 6



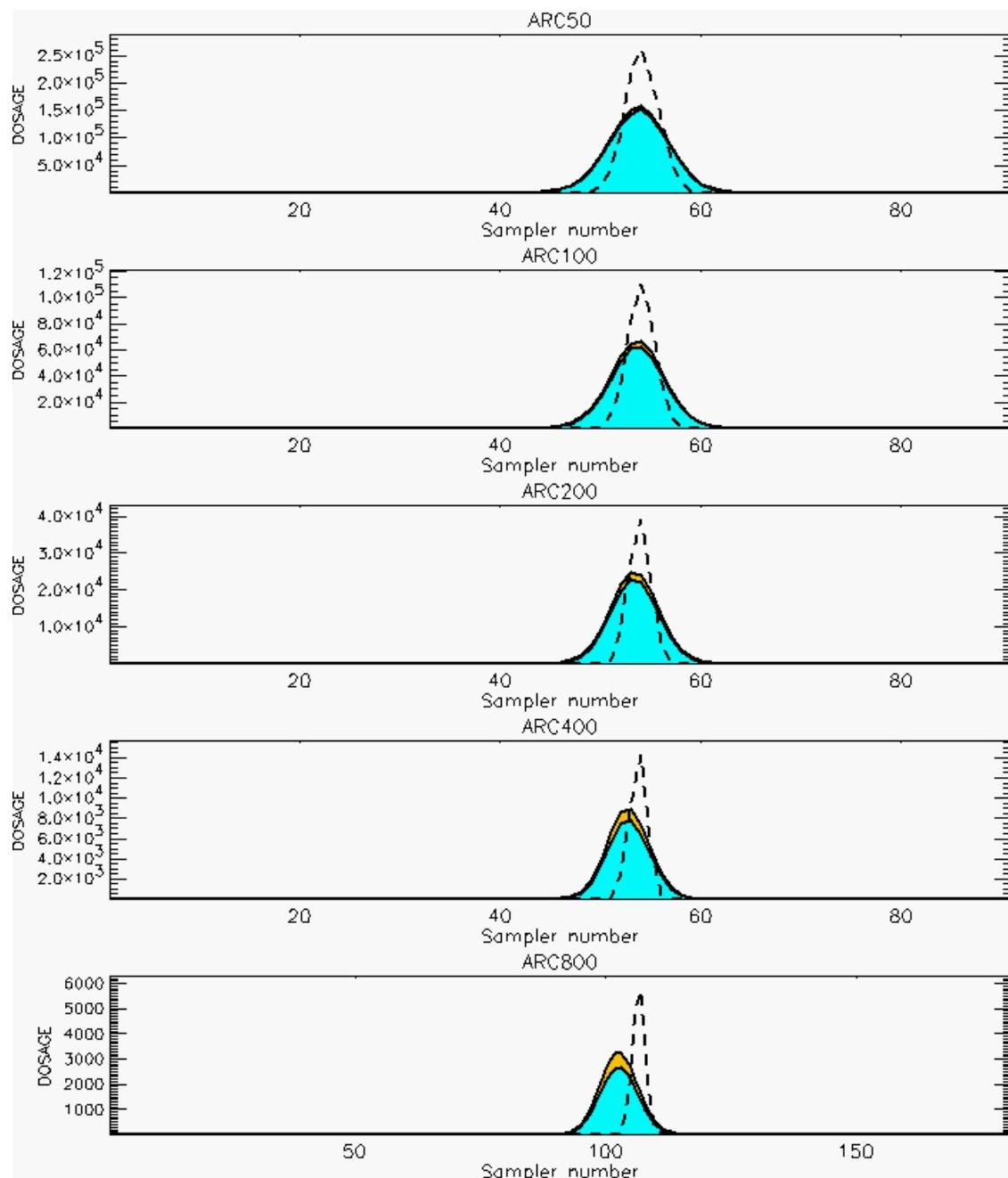
PG Prediction1 to Prediction2 Comparison

PG Trial File: pr_grass_tracer_Experiment_40.txt

PG Prediction File 1: ARAC\sv_vd\pg_40_sv_vd.arac

PG Prediction File 2: ARAC\sv_novd\pg_40_sv_novd.arac

Figure L-32b. NARAC With and Without SO₂ Surface Deposition Predictions to Trial 40 on Logarithmic Scale: Stability Category is 6



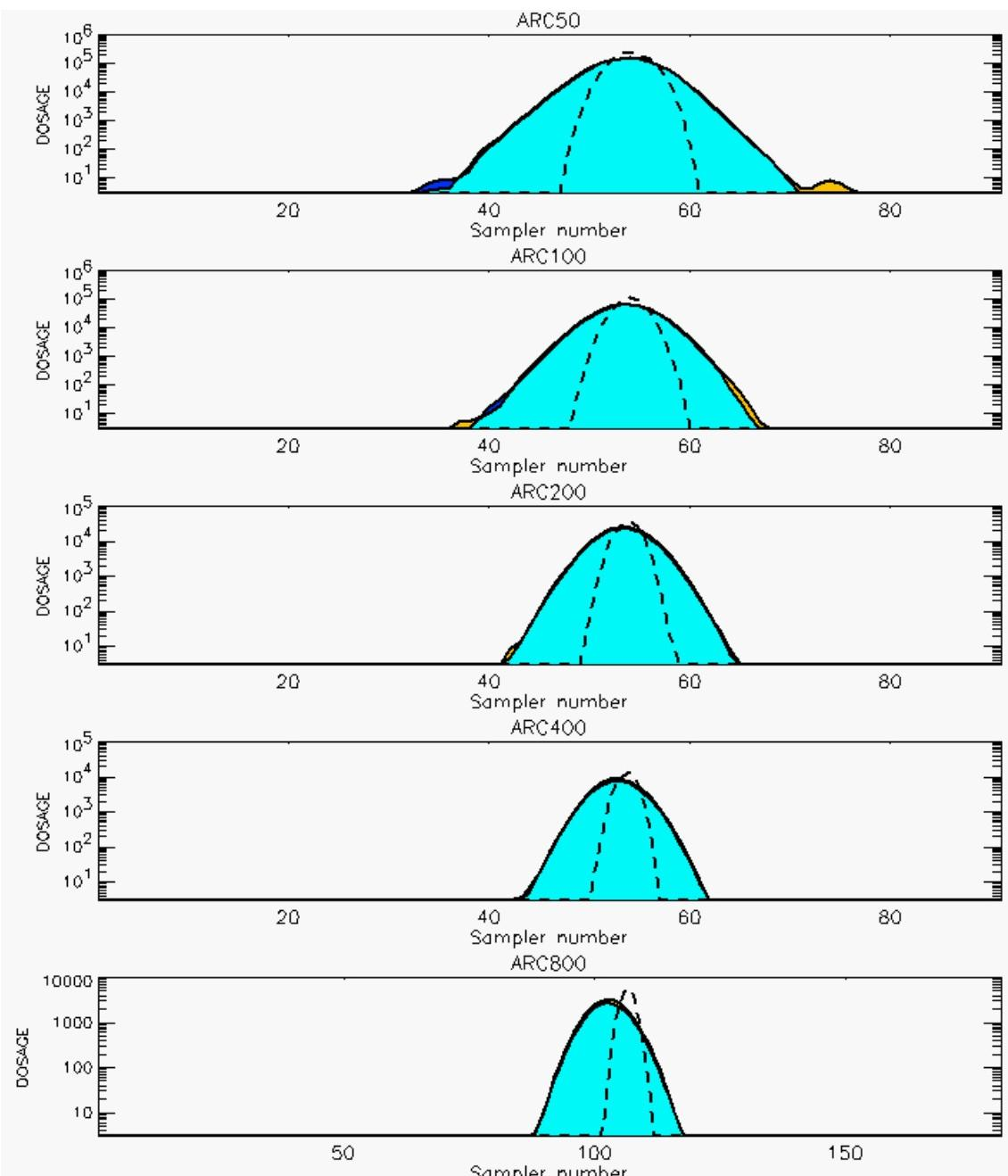
PG Prediction1 to Prediction2 Comparison

PG Trial File: pr_grass_tracer_Experiment_41.txt

PG Prediction File 1: ARAC\sv_vd\pg_41_sv_vd.arac

PG Prediction File 2: ARAC\sv_novd\pg_41_sv_novd.arac

Figure L-33a. NARAC With and Without SO₂ Surface Deposition Predictions to Trial 41 on Linear Scale: Stability Category is 5



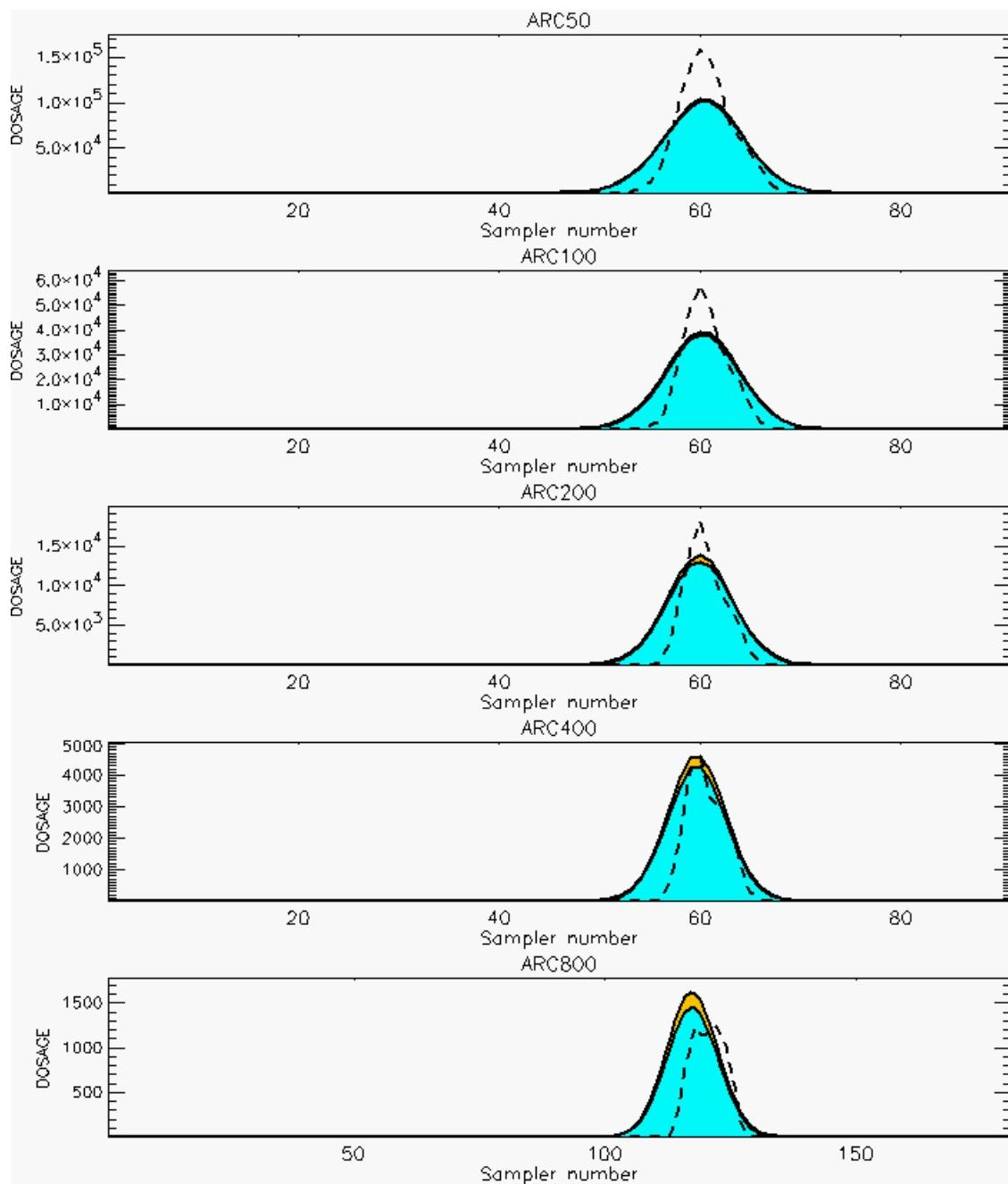
PG Prediction1 to Prediction2 Comparison

PG Trial File: pr_grass_tracer_Experiment_41.txt

PG Prediction File 1: ARAC\sv_vd\pg_41_sv_vd.arac

PG Prediction File 2: ARAC\sv_novd\pg_41_sv_novd.arac

Figure L-33b. NARAC With and Without SO₂ Surface Deposition Predictions to Trial 41 on Logarithmic Scale: Stability Category is 5



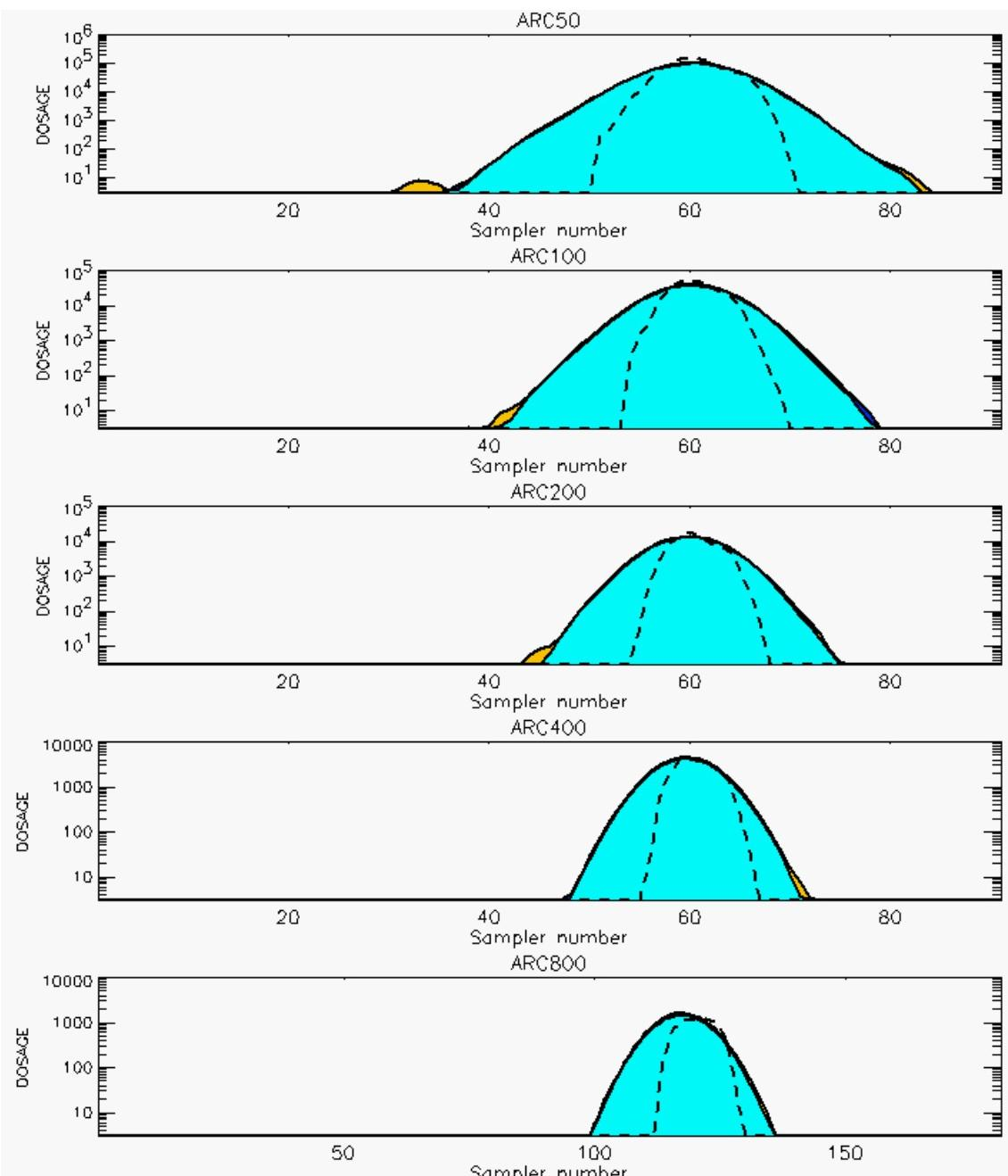
PG Prediction1 to Prediction2 Comparison

PG Trial File: pr_grass_tracer_Experiment_42.txt

PG Prediction File 1: ARAC\sv_vd\pg_42_sv_vd.arac

PG Prediction File 2: ARAC\sv_novd\pg_42_sv_novd.arac

Figure L-34a. NARAC With and Without SO₂ Surface Deposition Predictions to Trial 42 on Linear Scale: Stability Category is 4



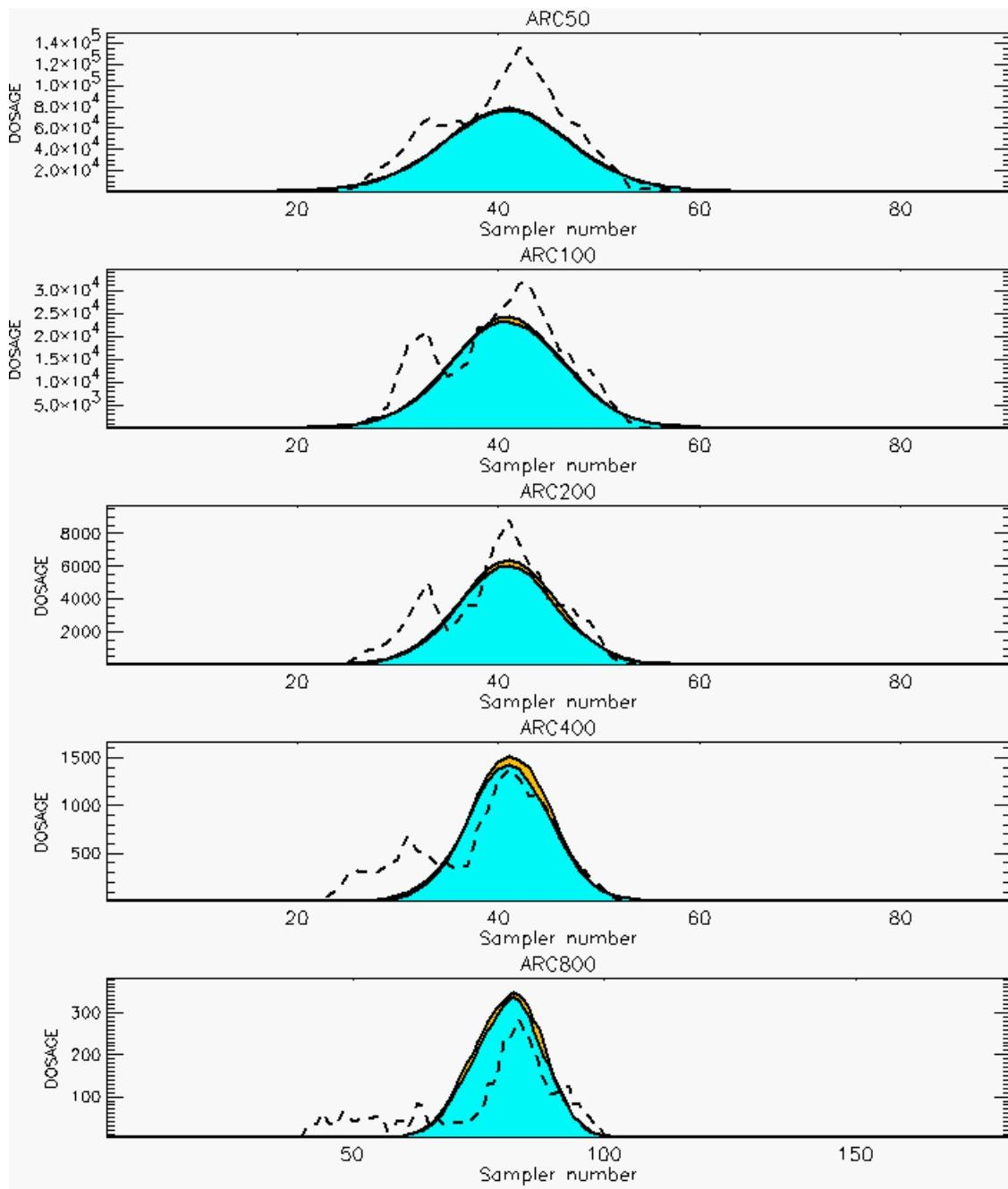
PG Prediction1 to Prediction2 Comparison

PG Trial File: pr_grass_tracer_Experiment_42.txt

PG Prediction File 1: ARAC\sv_vd\pg_42_sv_vd.arac

PG Prediction File 2: ARAC\sv_novd\pg_42_sv_novd.arac

Figure L-34b. NARAC With and Without SO₂ Surface Deposition Predictions to Trial 42 on Logarithmic Scale: Stability Category is 4



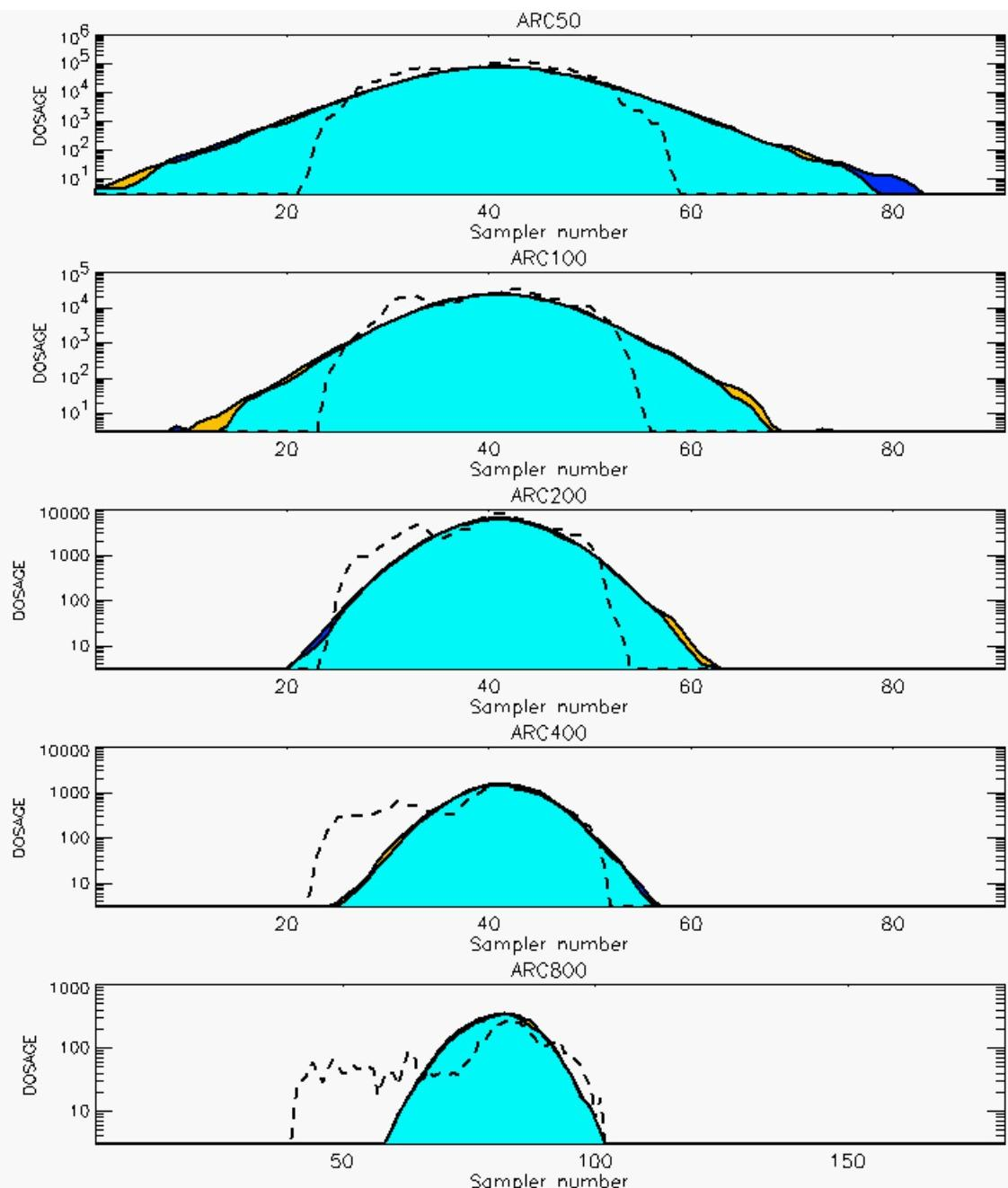
PG Prediction1 to Prediction2 Comparison

PG Trial File: pr_grass_tracer_Experiment_43.txt

PG Prediction File 1: ARAC\sv_vd\pg_43_sv_vd.arac

PG Prediction File 2: ARAC\sv_novd\pg_43_sv_novd.arac

Figure L-35a. NARAC With and Without SO₂ Surface Deposition Predictions to Trial 43 on Linear Scale: Stability Category is 1



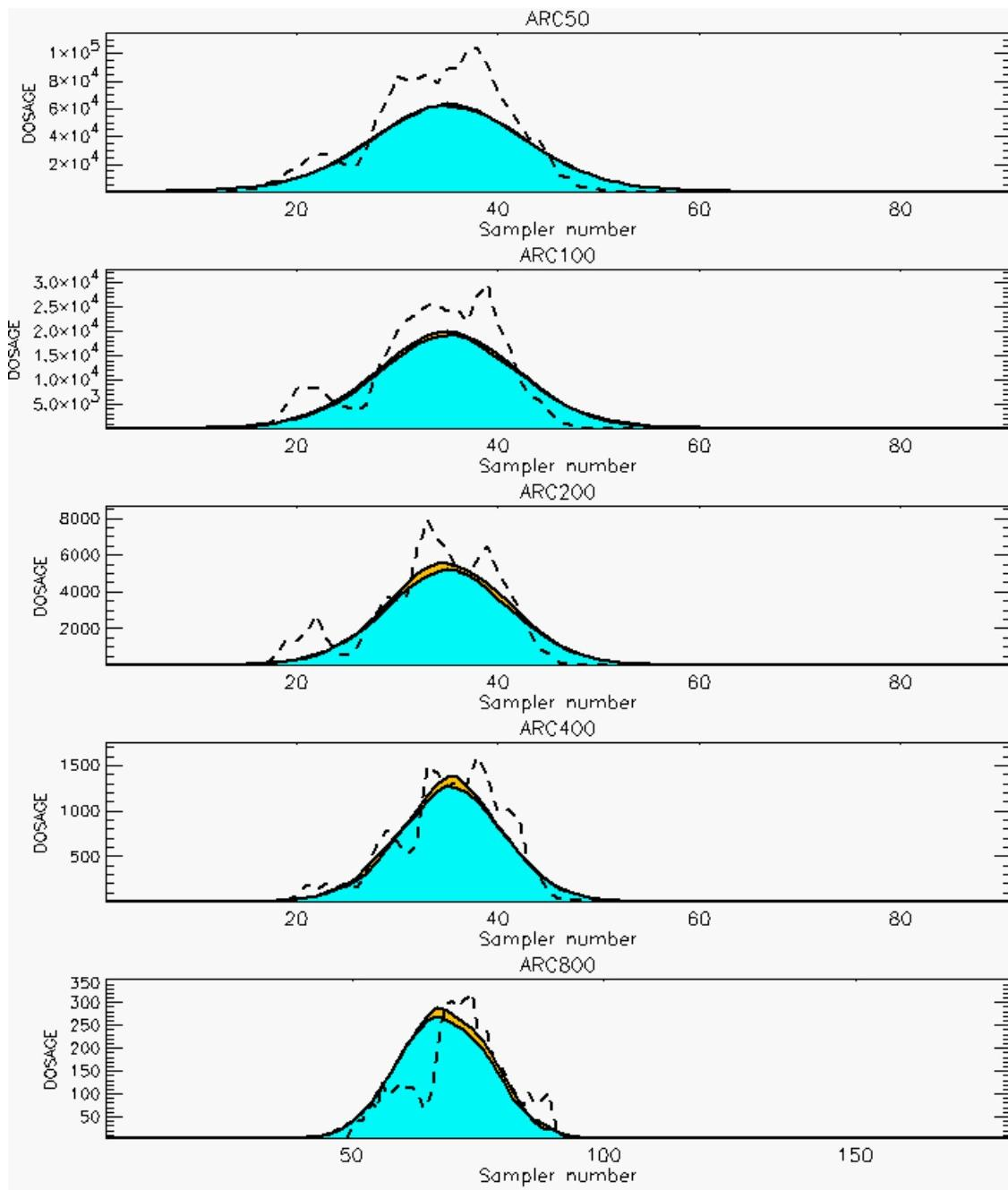
PG Prediction1 to Prediction2 Comparison

PG Trial File: pr_grass_tracer_Experiment_43.txt

PG Prediction File 1: ARAC\sv_vd\pg_43_sv_vd.arac

PG Prediction File 2: ARAC\sv_novd\pg_43_sv_novd.arac

Figure L-35b. NARAC With and Without SO₂ Surface Deposition Predictions to Trial 43 on Logarithmic Scale: Stability Category is 1



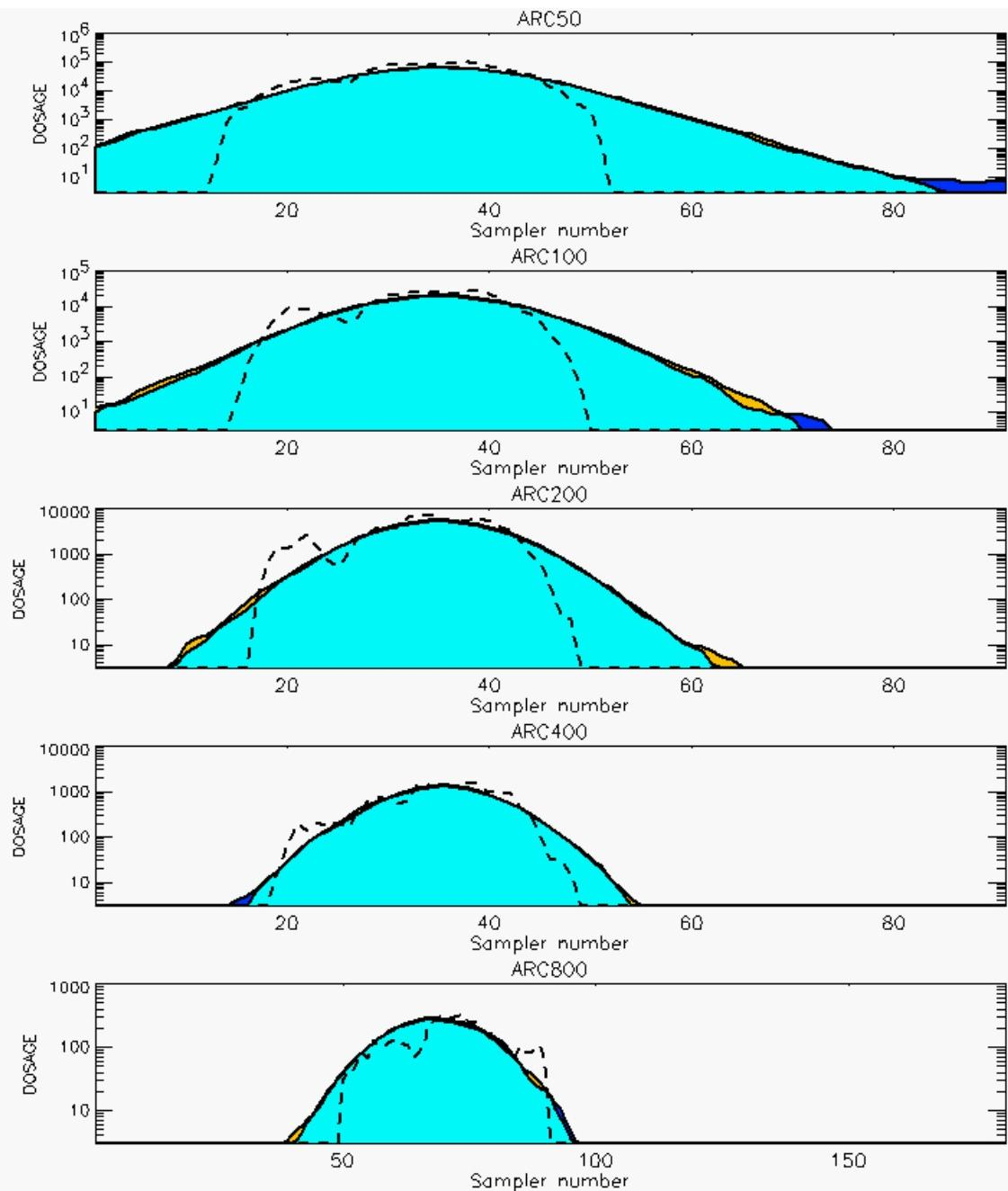
PG Prediction1 to Prediction2 Comparison

PG Trial File: pr_grass_tracer_Experiment_44.txt

PG Prediction File 1: ARAC\sv_vd\pg_44_sv_vd.arac

PG Prediction File 2: ARAC\sv_novd\pg_44_sv_novd.arac

Figure L-36a. NARAC With and Without SO₂ Surface Deposition Predictions to Trial 44 on Linear Scale: Stability Category is 2



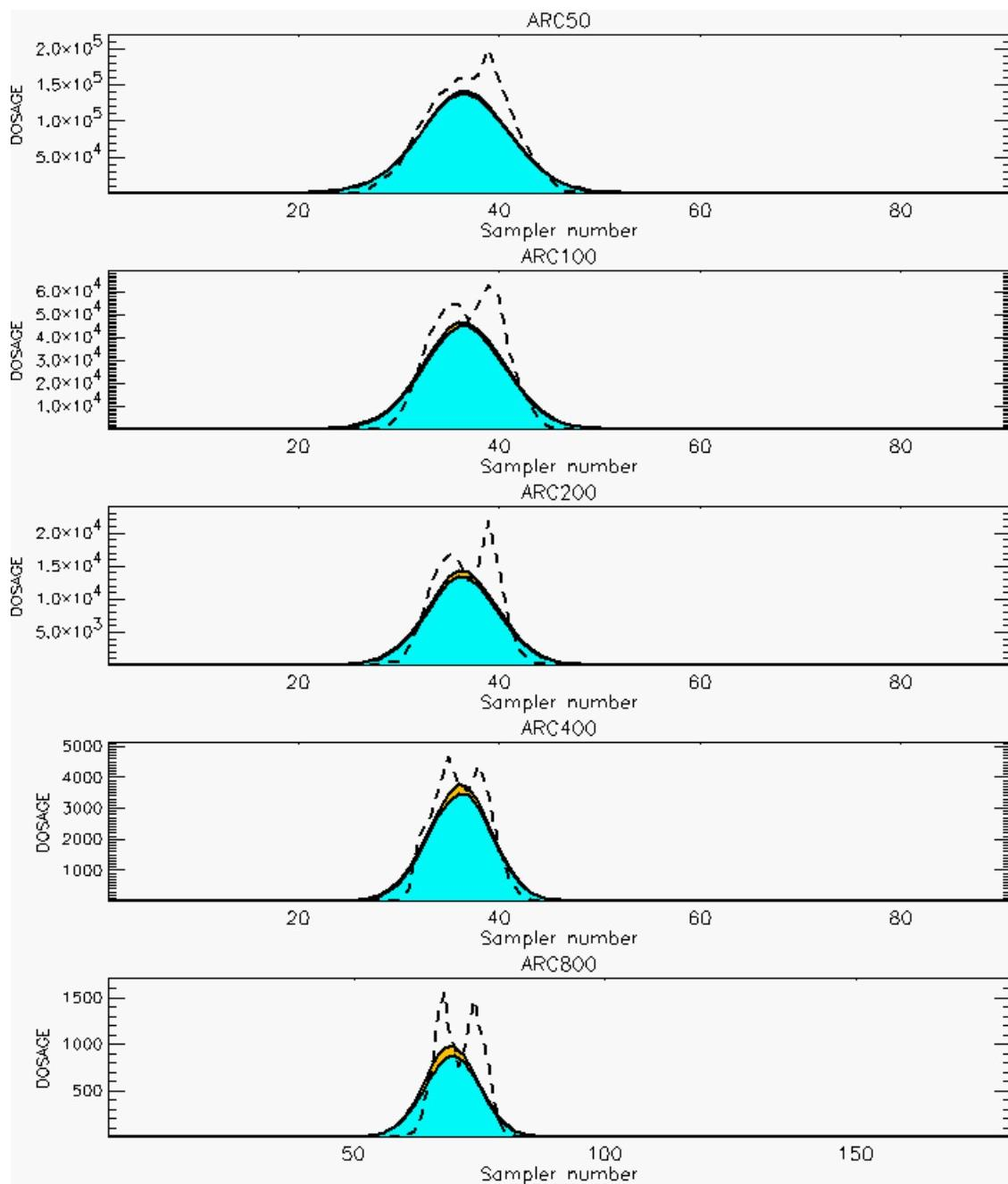
PG Prediction1 to Prediction2 Comparison

PG Trial File: pr_grass_tracer_Experiment_44.txt

PG Prediction File 1: ARAC\sv_vd\pg_44_sv_vd.arac

PG Prediction File 2: ARAC\sv_novd\pg_44_sv_novd.arac

Figure L-36b. NARAC With and Without SO₂ Surface Deposition Predictions to Trial 44 on Logarithmic Scale: Stability Category is 2



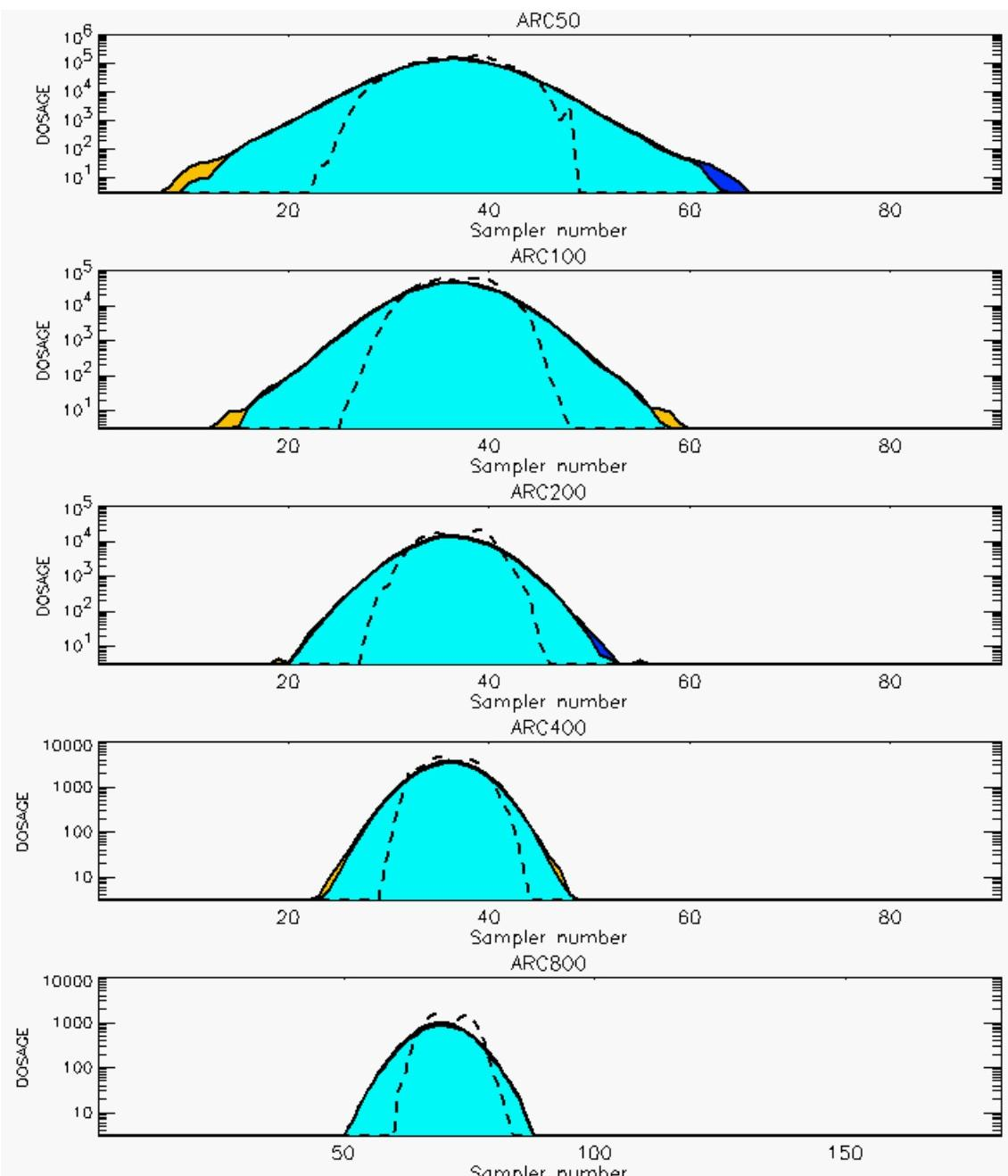
PG Prediction1 to Prediction2 Comparison

PG Trial File: pr_grass_tracer_Experiment_45.txt

PG Prediction File 1: ARAC\sv_vd\pg_45_sv_vd.arac

PG Prediction File 2: ARAC\sv_novd\pg_45_sv_novd.arac

Figure L-37a. NARAC With and Without SO₂ Surface Deposition Predictions to Trial 45 on Linear Scale: Stability Category is 3



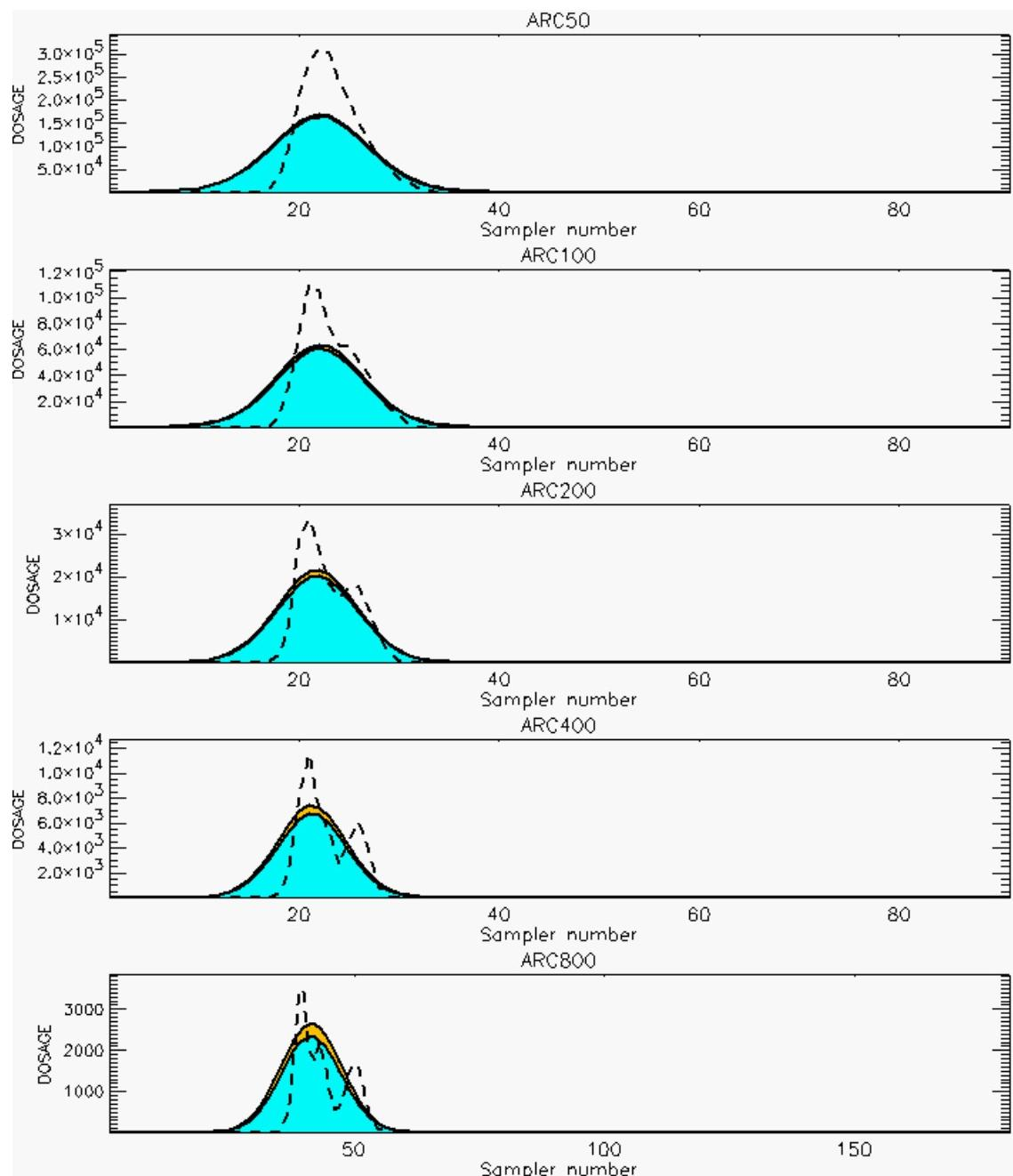
PG Prediction1 to Prediction2 Comparison

PG Trial File: pr_grass_tracer_Experiment_45.txt

PG Prediction File 1: ARAC\sv_vd\pg_45_sv_vd.arac

PG Prediction File 2: ARAC\sv_novd\pg_45_sv_novd.arac

Figure L-37b. NARAC With and Without SO₂ Surface Deposition Predictions to Trial 45 on Logarithmic Scale: Stability Category is 3



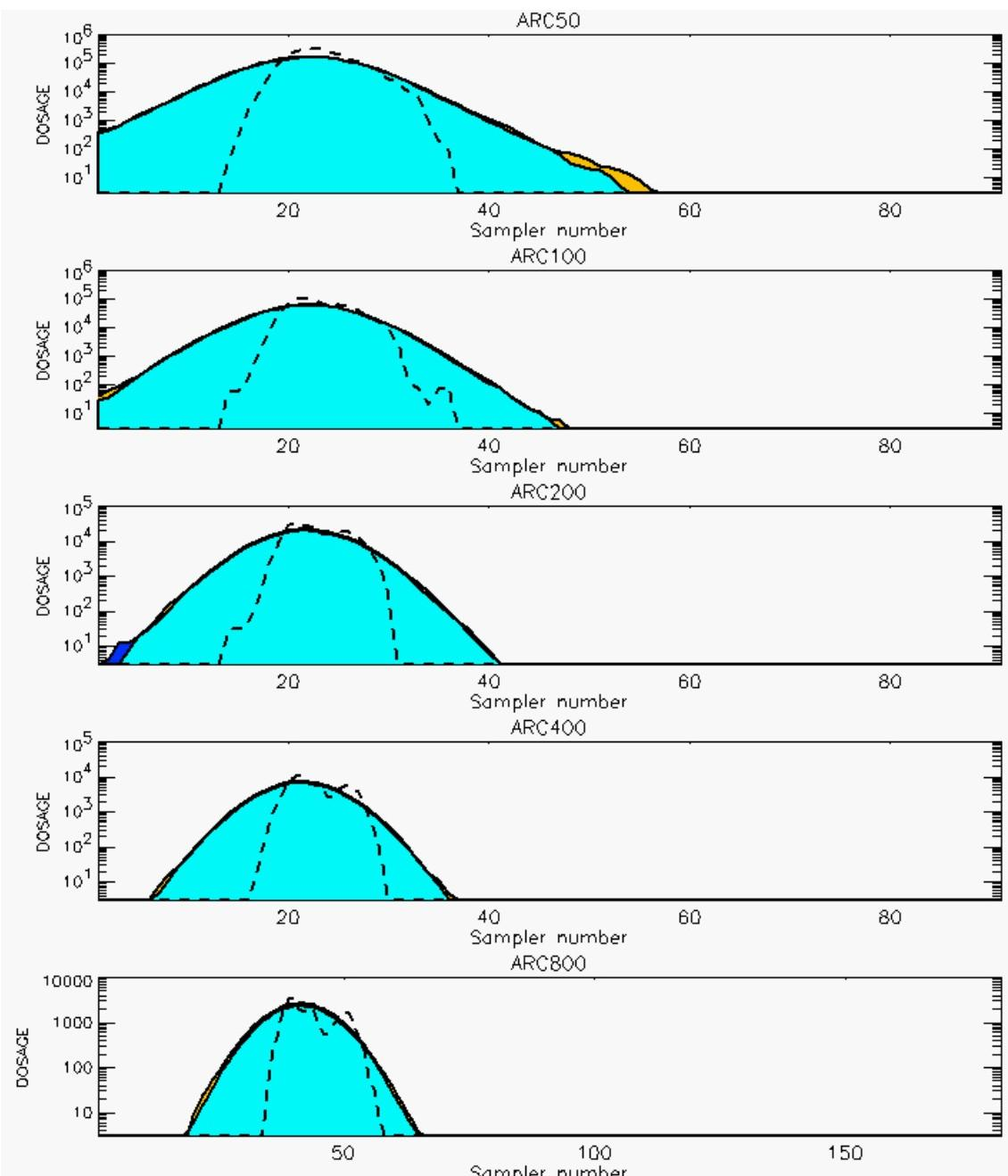
PG Prediction1 to Prediction2 Comparison

PG Trial File: pr_grass_tracer_Experiment_46.txt

PG Prediction File 1: ARAC\sv_vd\pg_46_sv_vd.arac

PG Prediction File 2: ARAC\sv_novd\pg_46_sv_novd.arac

Figure L-38a. NARAC With and Without SO₂ Surface Deposition Predictions to Trial 46 on Linear Scale: Stability Category is 4



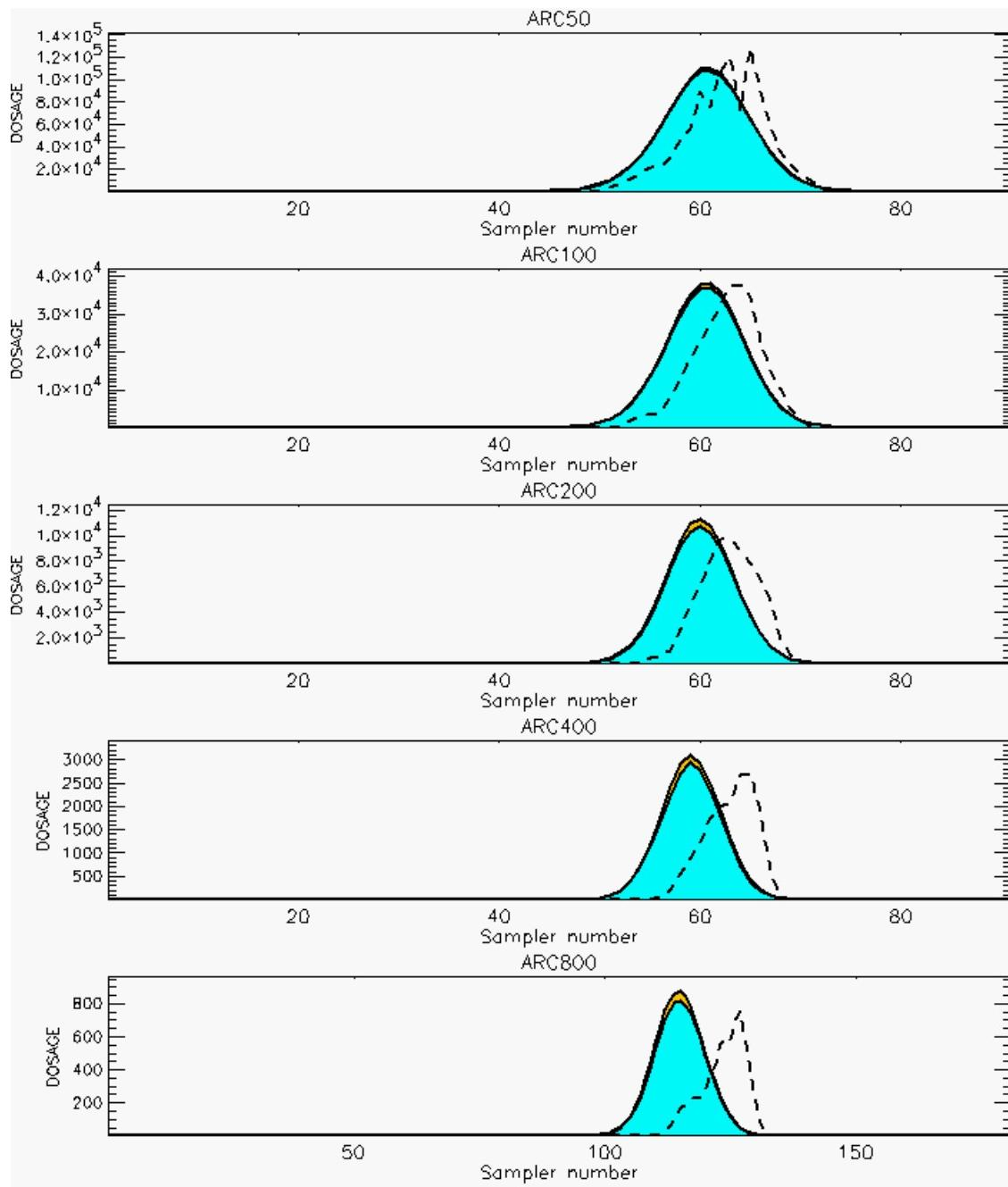
PG Prediction1 to Prediction2 Comparison

PG Trial File: pr_grass_tracer_Experiment_46.txt

PG Prediction File 1: ARAC\sv_vd\pg_46_sv_vd.arac

PG Prediction File 2: ARAC\sv_novd\pg_46_sv_novd.arac

Figure L-38b. NARAC With and Without SO₂ Surface Deposition Predictions to Trial 46 on Logarithmic Scale: Stability Category is 4



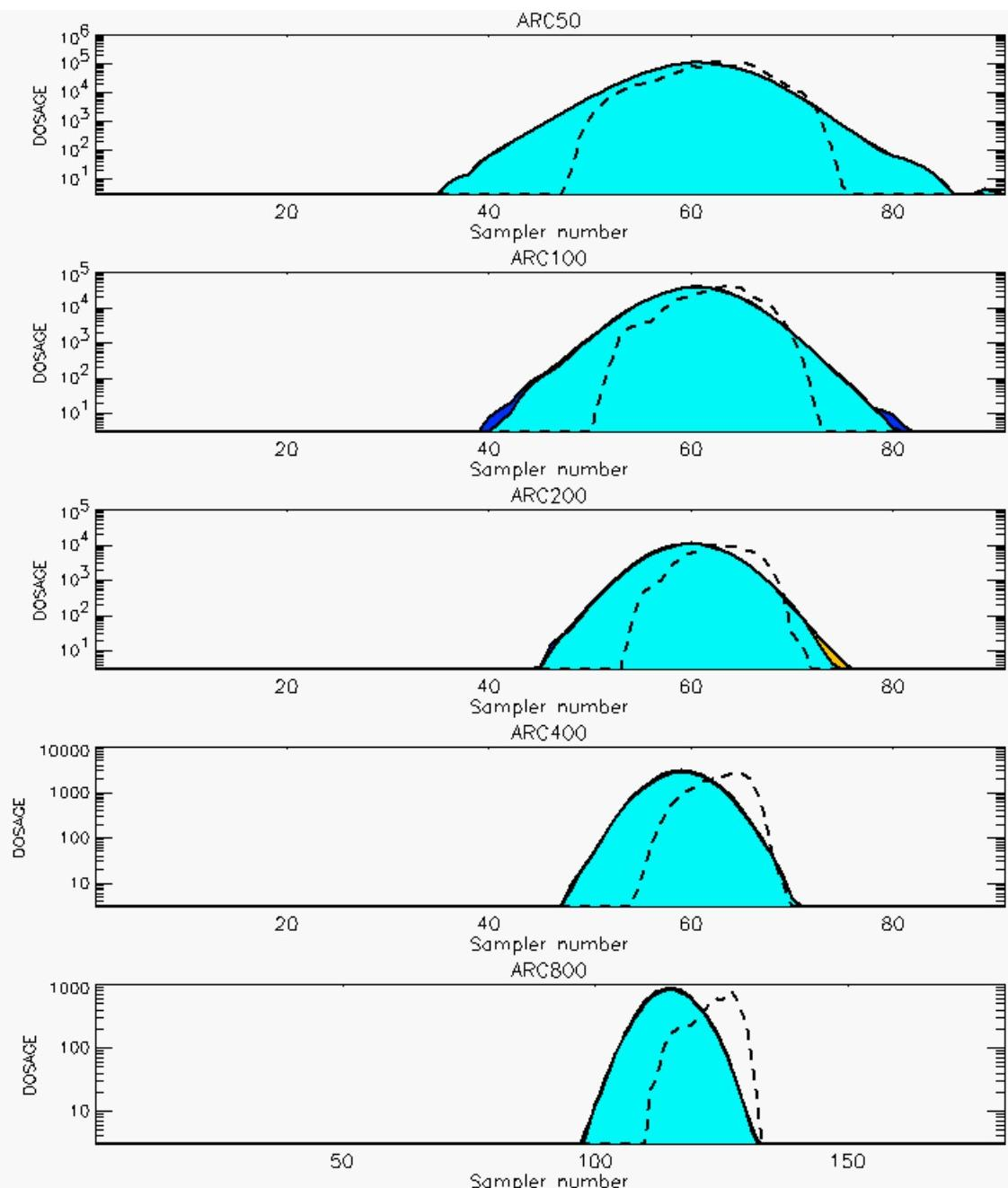
PG Prediction1 to Prediction2 Comparison

PG Trial File: pr_grass_tracer_Experiment_48.txt

PG Prediction File 1: ARAC\sv_vd\pg_48_sv_vd.arac

PG Prediction File 2: ARAC\sv_novd\pg_48_sv_novd.arac

Figure L-39a. NARAC With and Without SO₂ Surface Deposition Predictions to Trial 48 on Linear Scale: Stability Category is 3



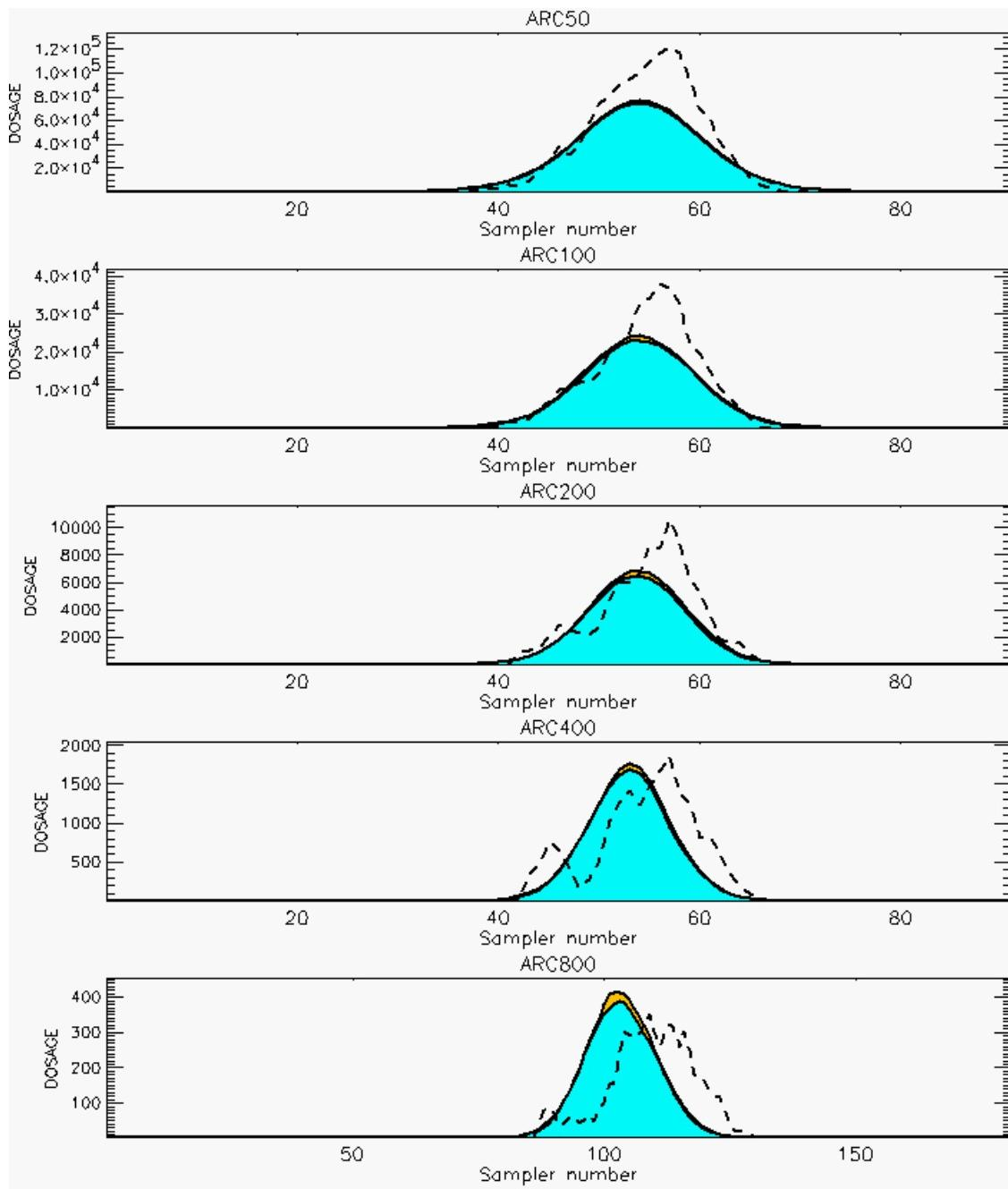
PG Prediction1 to Prediction2 Comparison

PG Trial File: pr_grass_tracer_Experiment_48.txt

PG Prediction File 1: ARAC\sv_vd\pg_48_sv_vd.arac

PG Prediction File 2: ARAC\sv_novd\pg_48_sv_novd.arac

Figure L-39b. NARAC With and Without SO_2 Surface Deposition Predictions to Trial 48 on Logarithmic Scale: Stability Category is 3



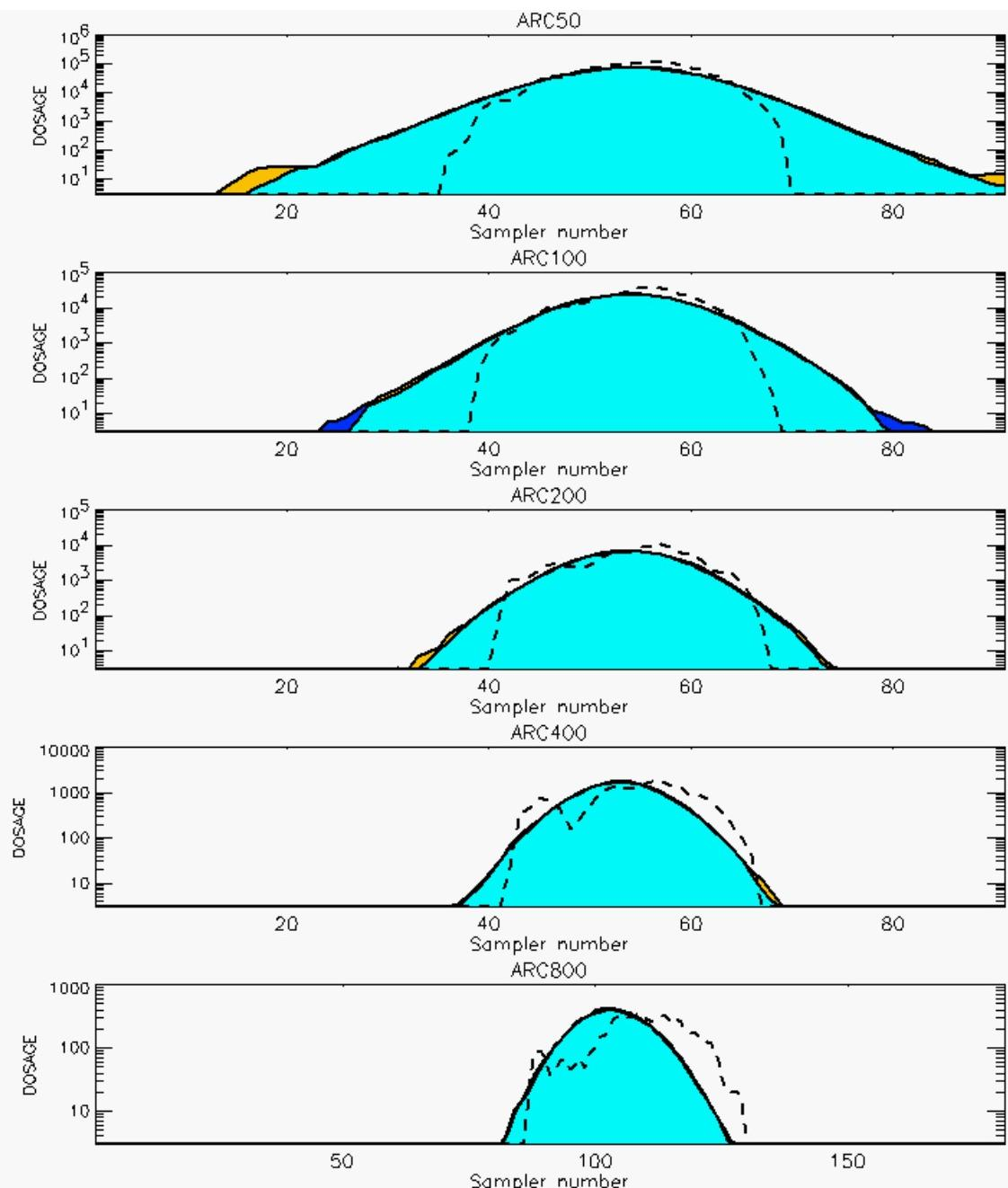
PG Prediction1 to Prediction2 Comparison

PG Trial File: pr_grass_tracer_Experiment_49.txt

PG Prediction File 1: ARAC\sv_vd\pg_49_sv_vd.arac

PG Prediction File 2: ARAC\sv_novd\pg_49_sv_novd.arac

Figure L-40a. NARAC With and Without SO₂ Surface Deposition Predictions to Trial 49 on Linear Scale: Stability Category is 2



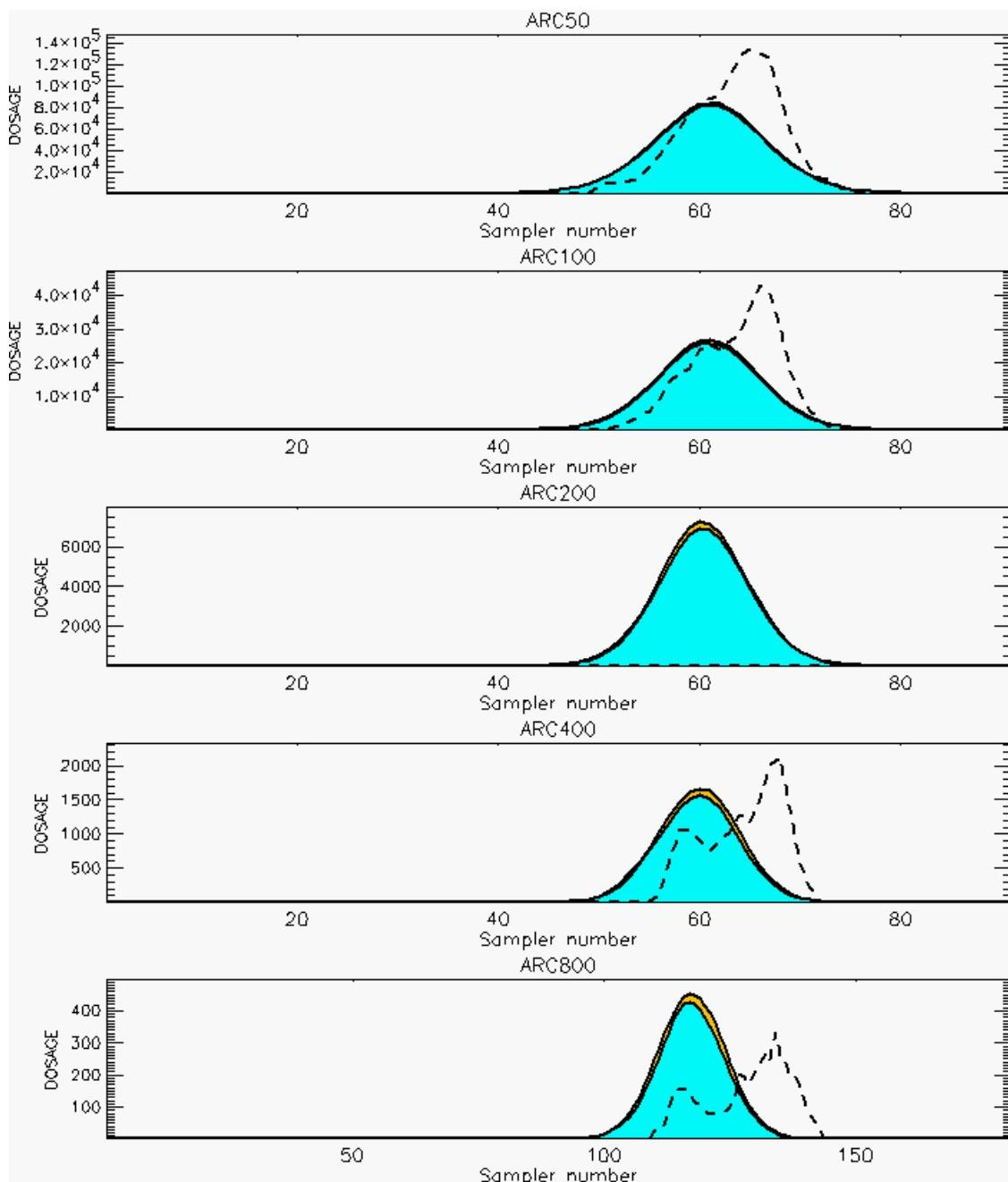
PG Prediction1 to Prediction2 Comparison

PG Trial File: pr_grass_tracer_Experiment_49.txt

PG Prediction File 1: ARAC\sv_vd\pg_49_sv_vd.arac

PG Prediction File 2: ARAC\sv_novd\pg_49_sv_novd.arac

Figure L-40b. NARAC With and Without SO_2 Surface Deposition Predictions to Trial 49 on Logarithmic Scale: Stability Category is 2



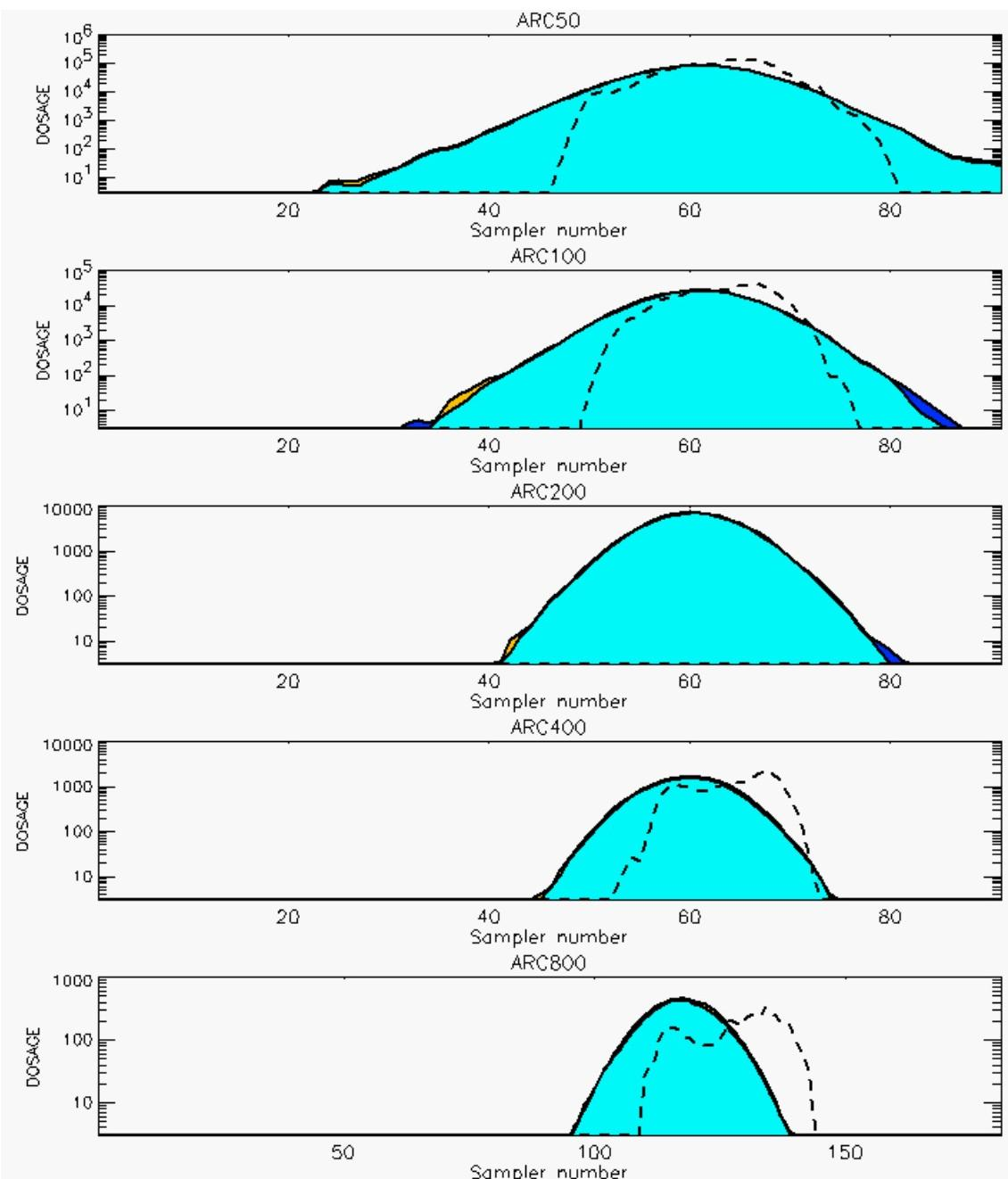
PG Prediction1 to Prediction2 Comparison

PG Trial File: pr_grass_tracer_Experiment_50.txt

PG Prediction File 1: ARAC\sv_vd\pg_50_sv_vd.arac

PG Prediction File 2: ARAC\sv_novd\pg_50_sv_novd.arac

Figure L-41a. NARAC With and Without SO₂ Surface Deposition Predictions to Trial 50 on Linear Scale: Stability Category is 2



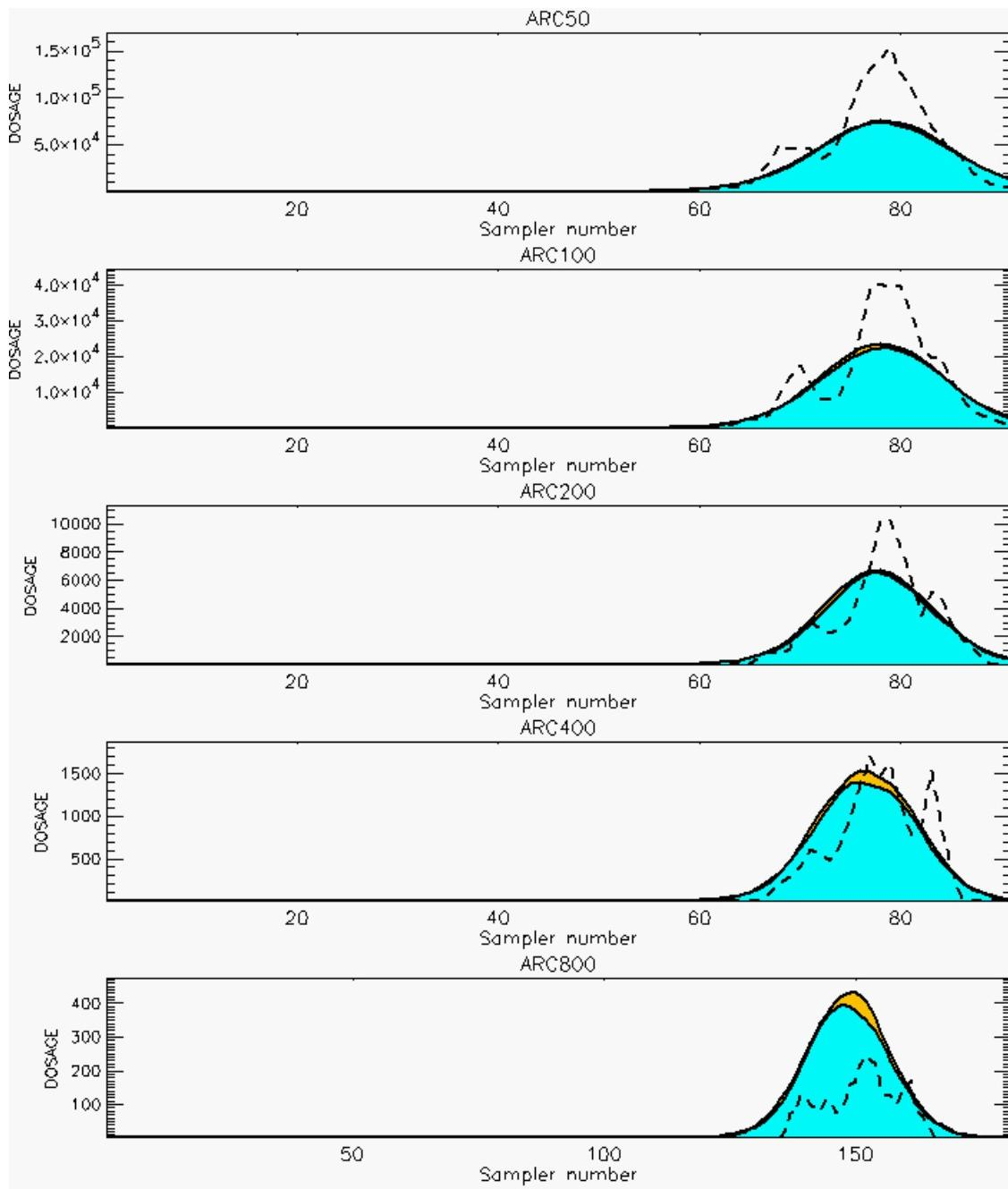
PG Prediction1 to Prediction2 Comparison

PG Trial File: pr_grass_tracer_Experiment_50.txt

PG Prediction File 1: ARAC\sv_vd\pg_50_sv_vd.arac

PG Prediction File 2: ARAC\sv_novd\pg_50_sv_novd.arac

Figure L-41b. NARAC With and Without SO₂ Surface Deposition Predictions to Trial 50 on Logarithmic Scale: Stability Category is 2



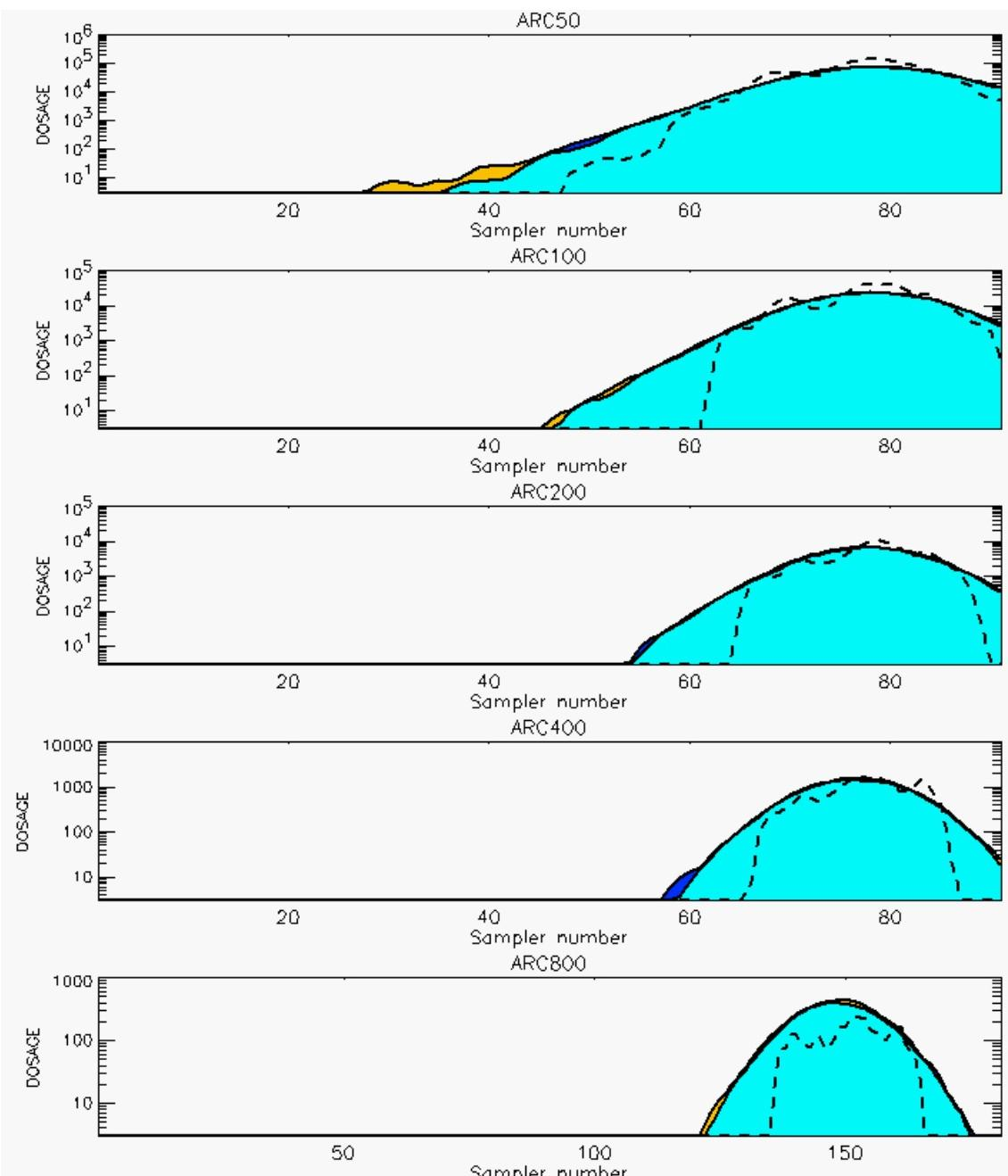
PG Prediction1 to Prediction2 Comparison

PG Trial File: pr_grass_tracer_Experiment_51.txt

PG Prediction File 1: ARAC\sv_vd\pg_51_sv_vd.arac

PG Prediction File 2: ARAC\sv_novd\pg_51_sv_novd.arac

Figure L-42a. NARAC With and Without SO₂ Surface Deposition Predictions to Trial 51 on Linear Scale: Stability Category is 2



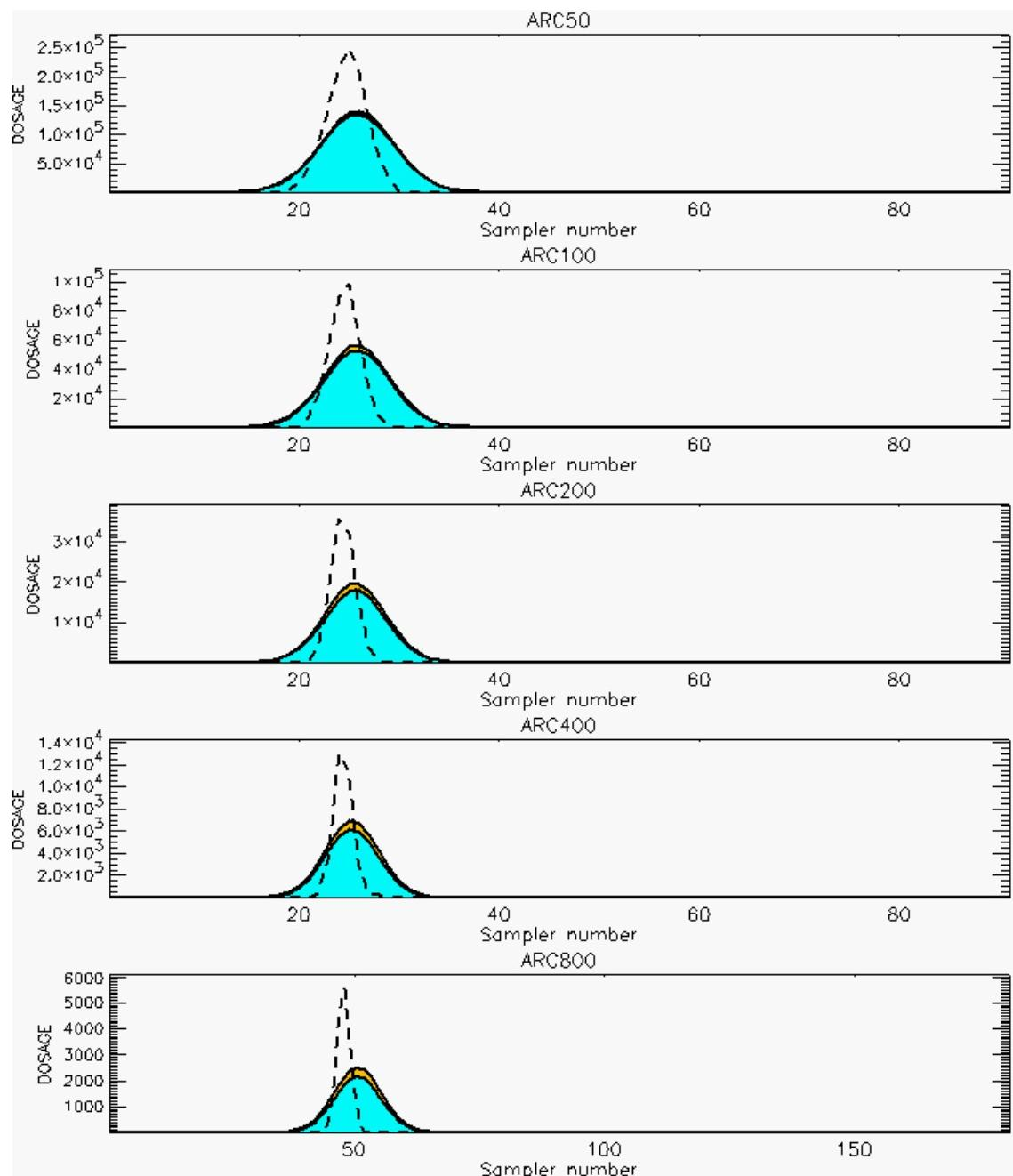
PG Prediction1 to Prediction2 Comparison

PG Trial File: pr_grass_tracer_Experiment_51.txt

PG Prediction File 1: ARAC\sv_vd\pg_51_sv_vd.arac

PG Prediction File 2: ARAC\sv_novd\pg_51_sv_novd.arac

Figure L-42b. NARAC With and Without SO₂ Surface Deposition Predictions to Trial 51 on Logarithmic Scale: Stability Category is 2



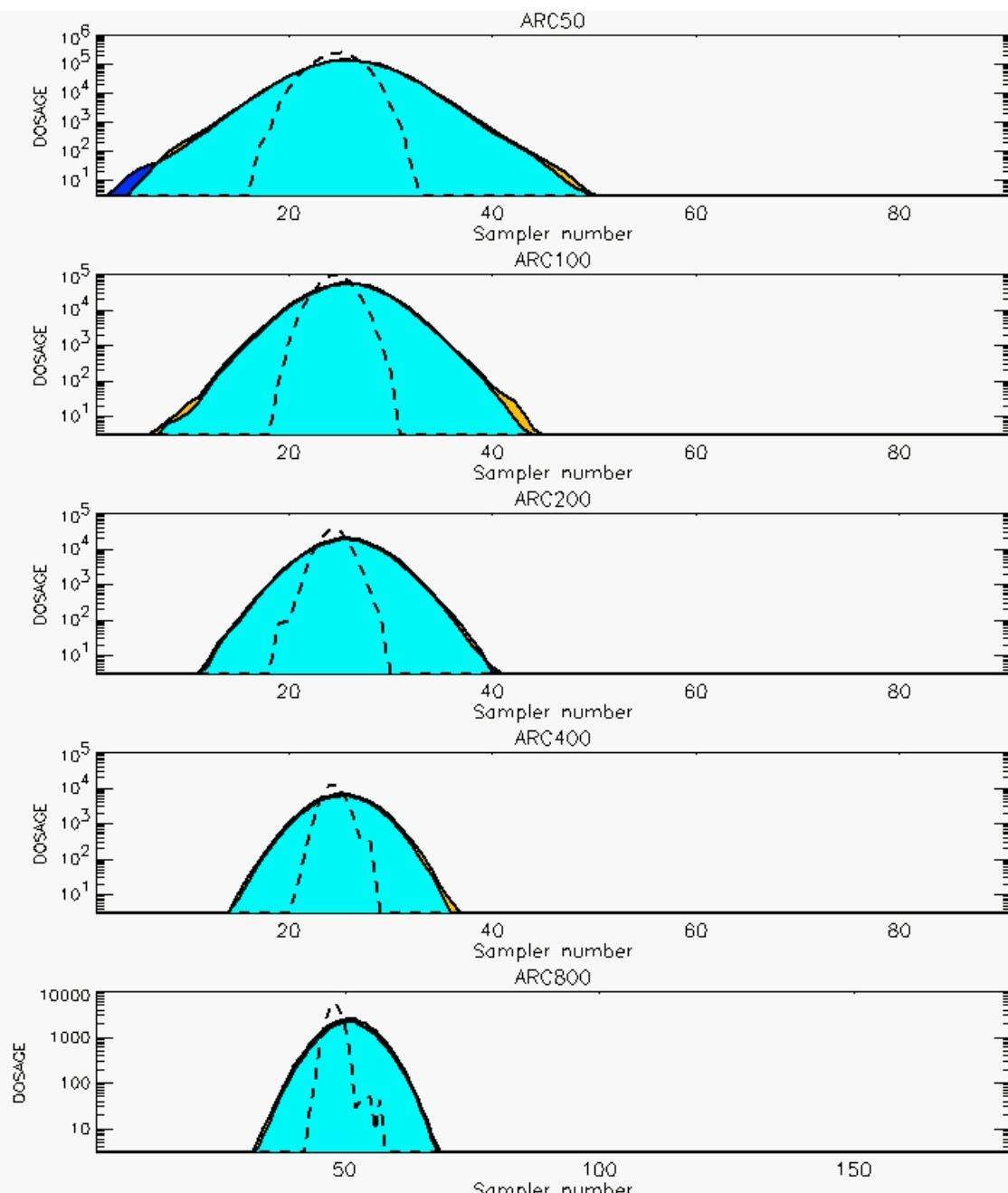
PG Prediction1 to Prediction2 Comparison

PG Trial File: pr_grass_tracer_Experiment_54.txt

PG Prediction File 1: ARAC\sv_vd\pg_54_sv_vd.arac

PG Prediction File 2: ARAC\sv_novd\pg_54_sv_novd.arac

Figure L-43a. NARAC With and Without SO_2 Surface Deposition Predictions to Trial 54 on Linear Scale: Stability Category is 5



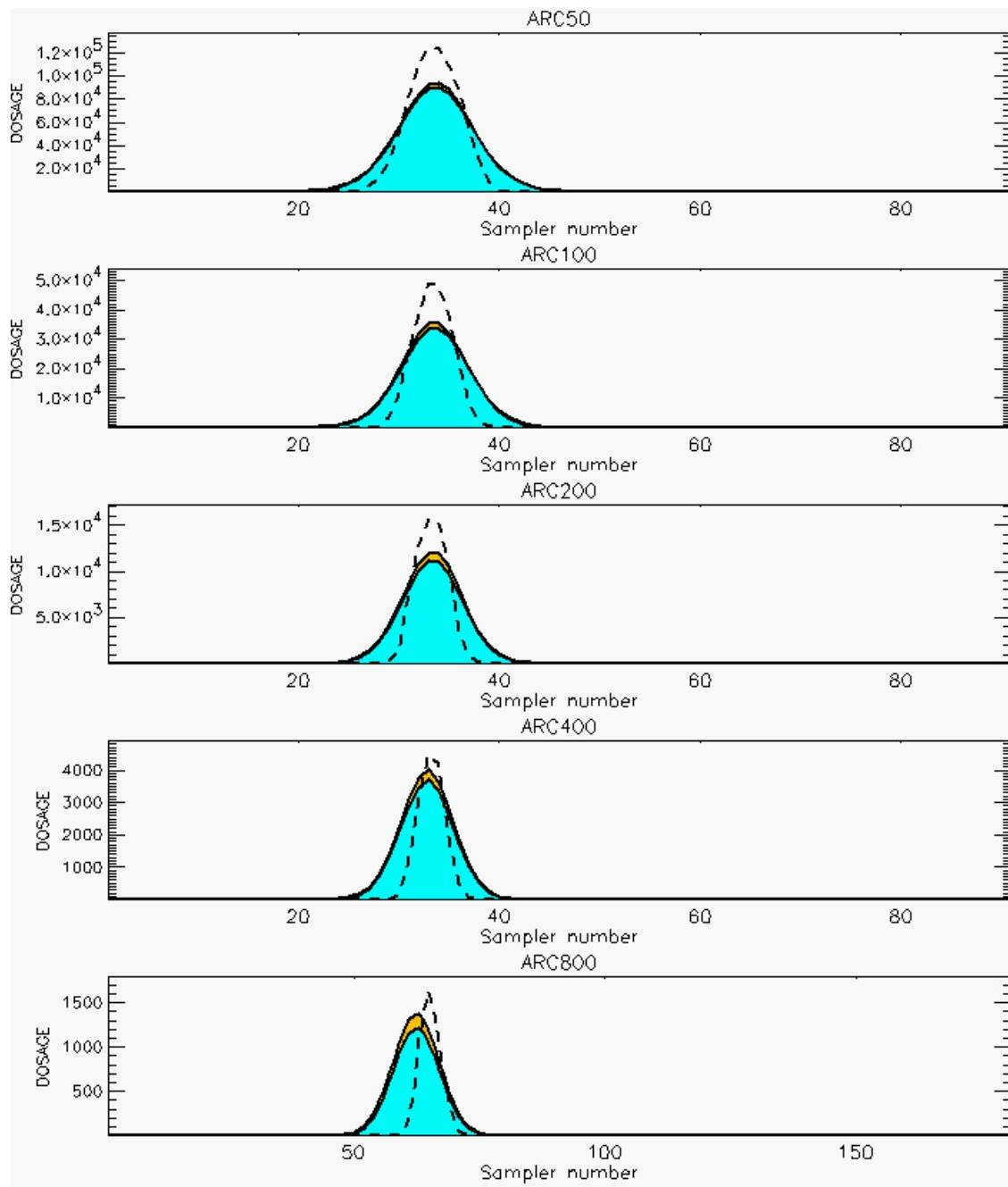
PG Prediction1 to Prediction2 Comparison

PG Trial File: pr_grass_tracer_Experiment_54.txt

PG Prediction File 1: ARAC\sv_vd\pg_54_sv_vd.arac

PG Prediction File 2: ARAC\sv_novd\pg_54_sv_novd.arac

Figure L-43b. NARAC With and Without SO_2 Surface Deposition Predictions to Trial 54 on Logarithmic Scale: Stability Category is 5



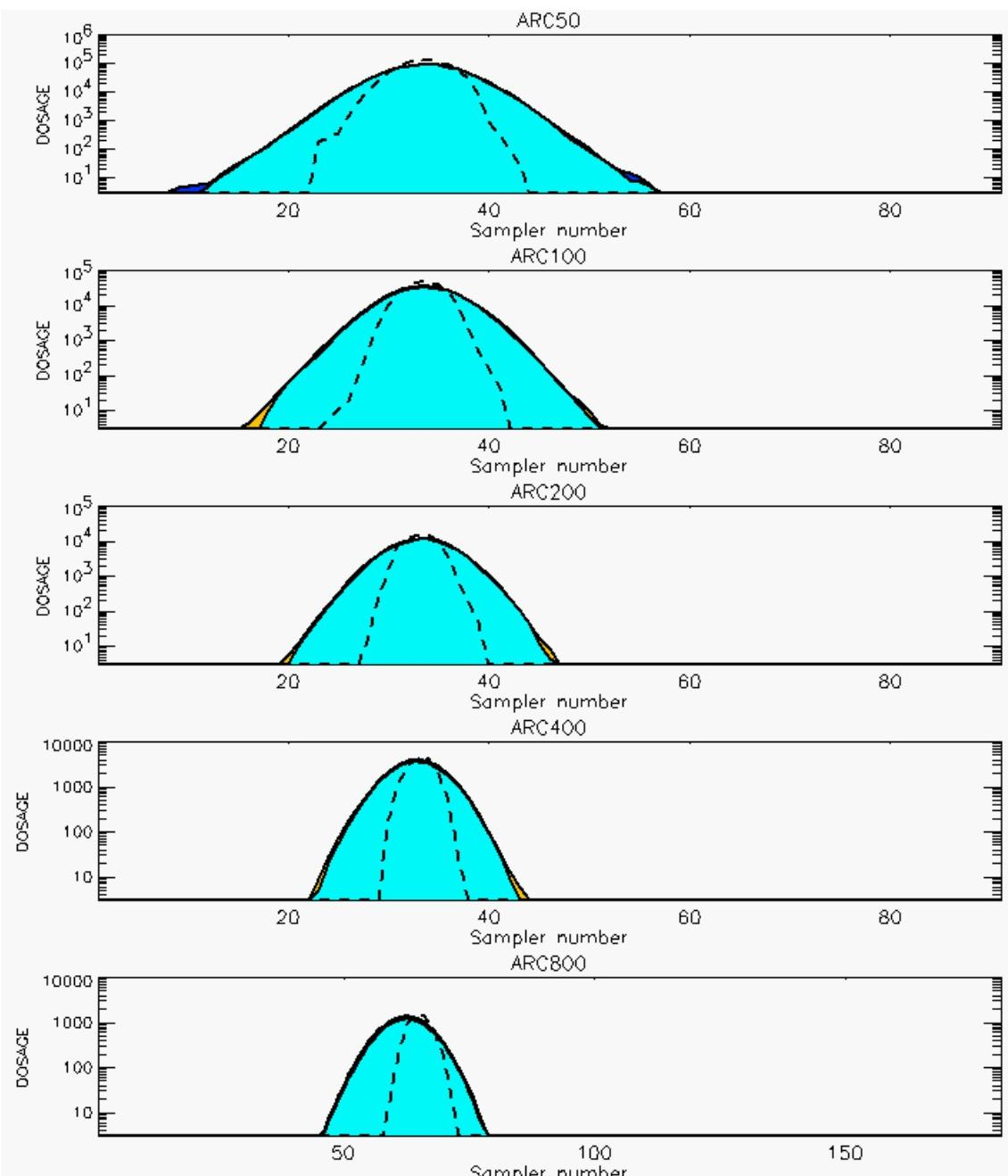
PG Prediction1 to Prediction2 Comparison

PG Trial File: pr_grass_tracer_Experiment_55.txt

PG Prediction File 1: ARAC\sv_vd\pg_55_sv_vd.arac

PG Prediction File 2: ARAC\sv_novd\pg_55_sv_novd.arac

Figure L-44a. NARAC With and Without SO₂ Surface Deposition Predictions to Trial 55 on Linear Scale: Stability Category is 4



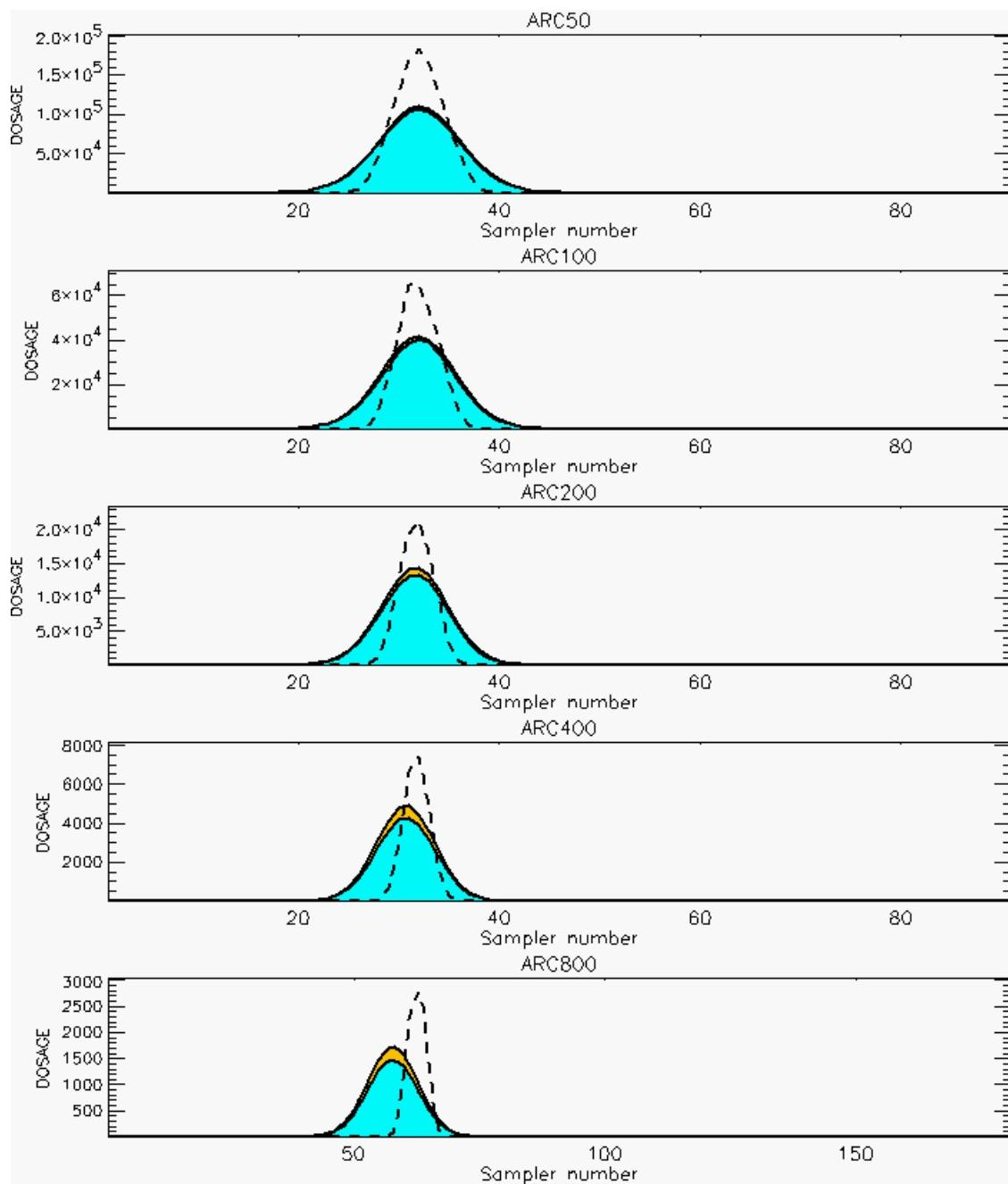
PG Prediction1 to Prediction2 Comparison

PG Trial File: pr_grass_tracer_Experiment_55.txt

PG Prediction File 1: ARAC\sv_vd\pg_55_sv_vd.arac

PG Prediction File 2: ARAC\sv_novd\pg_55_sv_novd.arac

Figure L-44b. NARAC With and Without SO₂ Surface Deposition Predictions to Trial 55 on Logarithmic Scale: Stability Category is 4



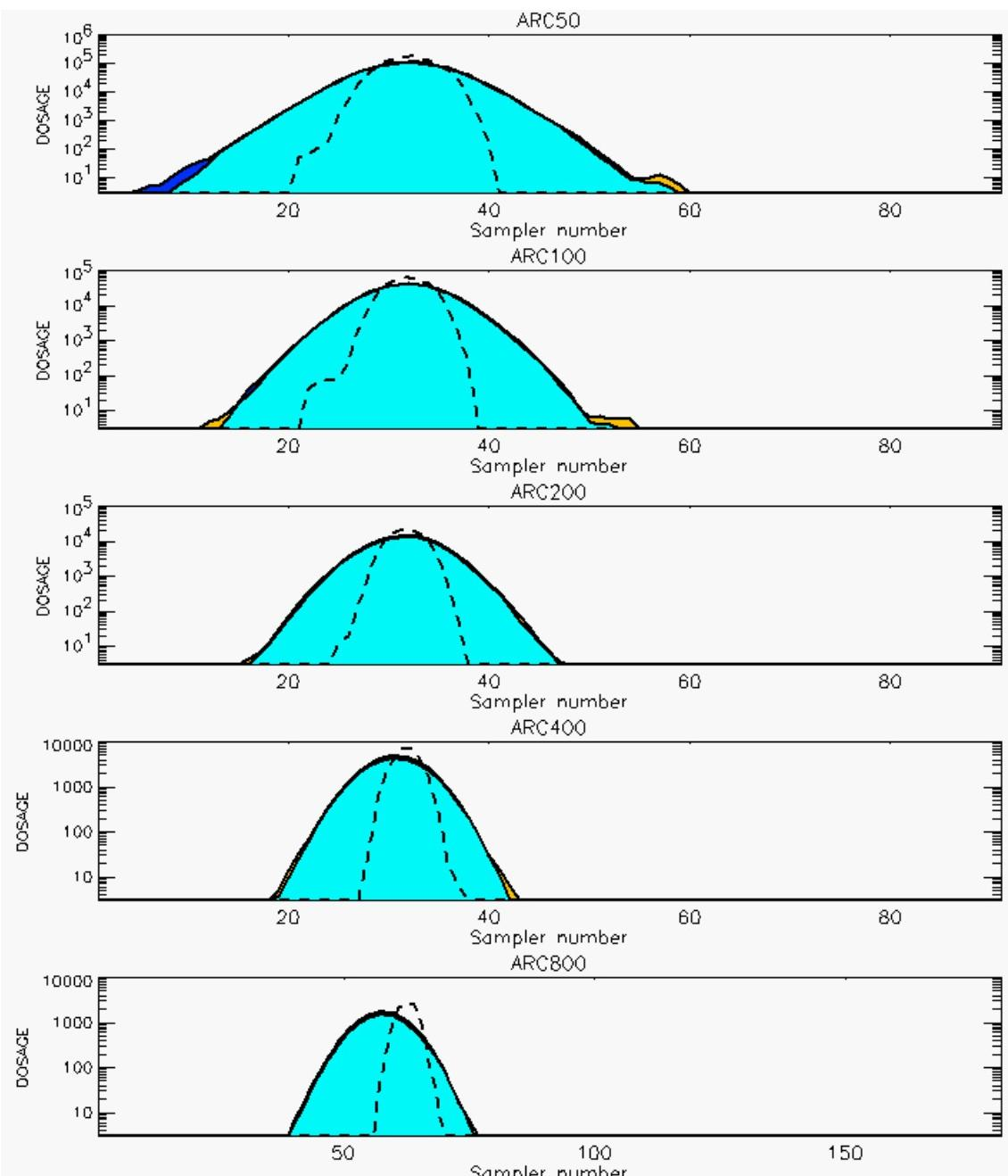
PG Prediction1 to Prediction2 Comparison

PG Trial File: pr_grass_tracer_Experiment_56.txt

PG Prediction File 1: ARAC\sv_vd\pg_56_sv_vd.arac

PG Prediction File 2: ARAC\sv_novd\pg_56_sv_novd.arac

Figure L-45a. NARAC With and Without SO₂ Surface Deposition Predictions to Trial 56 on Linear Scale: Stability Category is 4



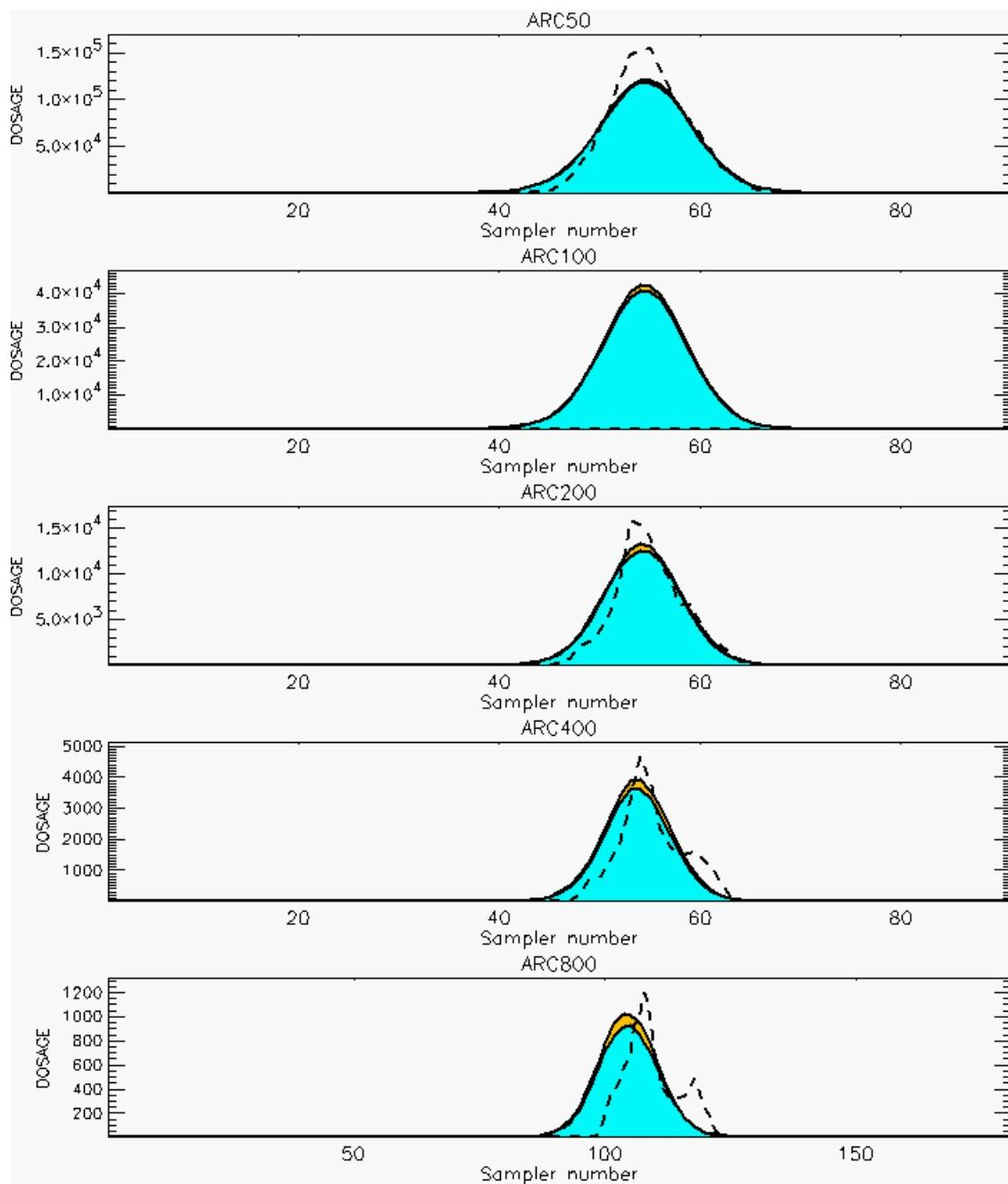
PG Prediction1 to Prediction2 Comparison

PG Trial File: pr_grass_tracer_Experiment_56.txt

PG Prediction File 1: ARAC\sv_vd\pg_56_sv_vd.arac

PG Prediction File 2: ARAC\sv_novd\pg_56_sv_novd.arac

Figure L-45b. NARAC With and Without SO₂ Surface Deposition Predictions to Trial 56 on Logarithmic Scale: Stability Category is 4



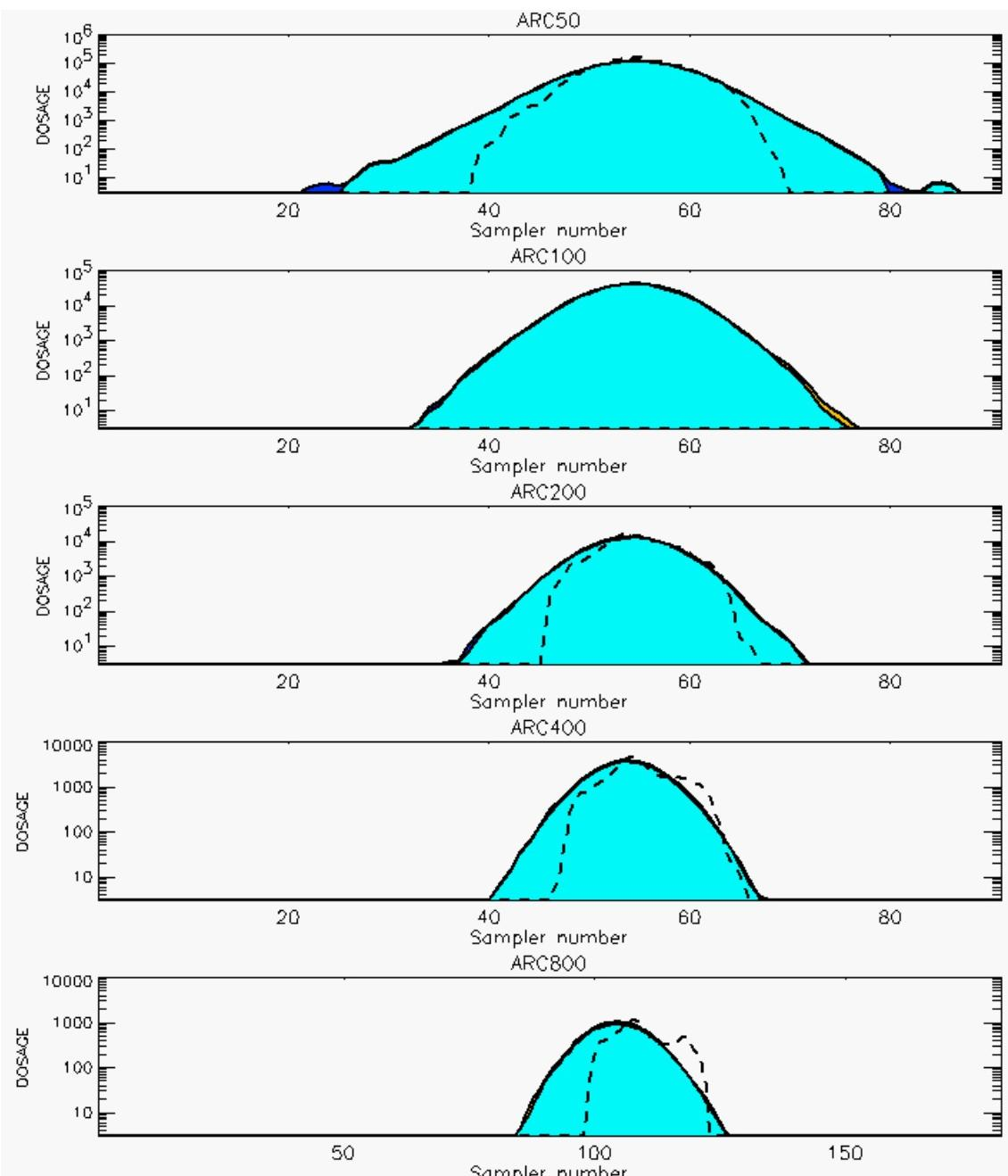
PG Prediction1 to Prediction2 Comparison

PG Trial File: pr_grass_tracer_Experiment_57.txt

PG Prediction File 1: ARAC\sv_vd\pg_57_sv_vd.arac

PG Prediction File 2: ARAC\sv_novd\pg_57_sv_novd.arac

Figure L-46a. NARAC With and Without SO₂ Surface Deposition Predictions to Trial 57 on Linear Scale: Stability Category is 3



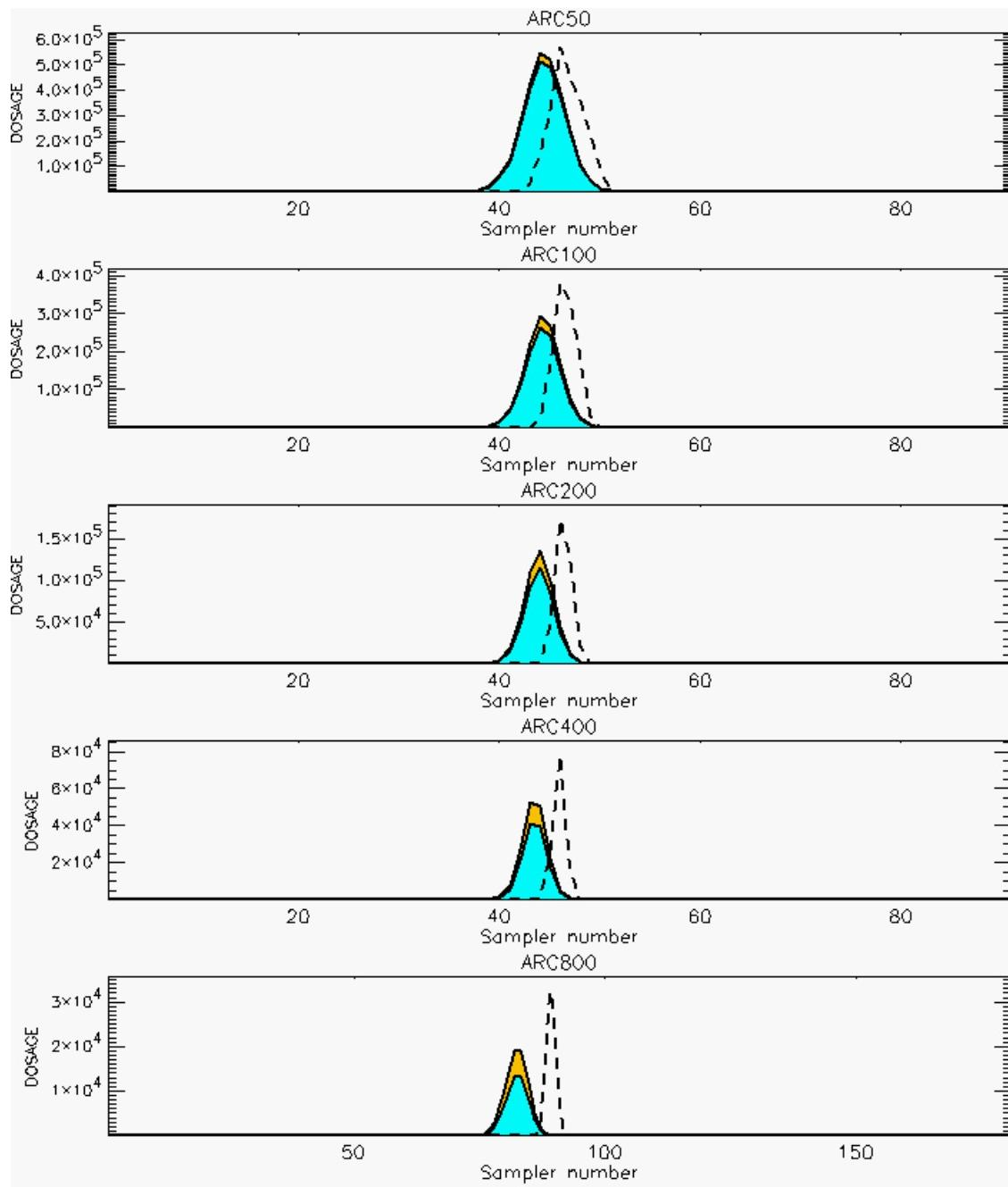
PG Prediction1 to Prediction2 Comparison

PG Trial File: pr_grass_tracer_Experiment_57.txt

PG Prediction File 1: ARAC\sv_vd\pg_57_sv_vd.arac

PG Prediction File 2: ARAC\sv_novd\pg_57_sv_novd.arac

Figure L-46b. NARAC With and Without SO₂ Surface Deposition Predictions to Trial 57 on Logarithmic Scale: Stability Category is 3



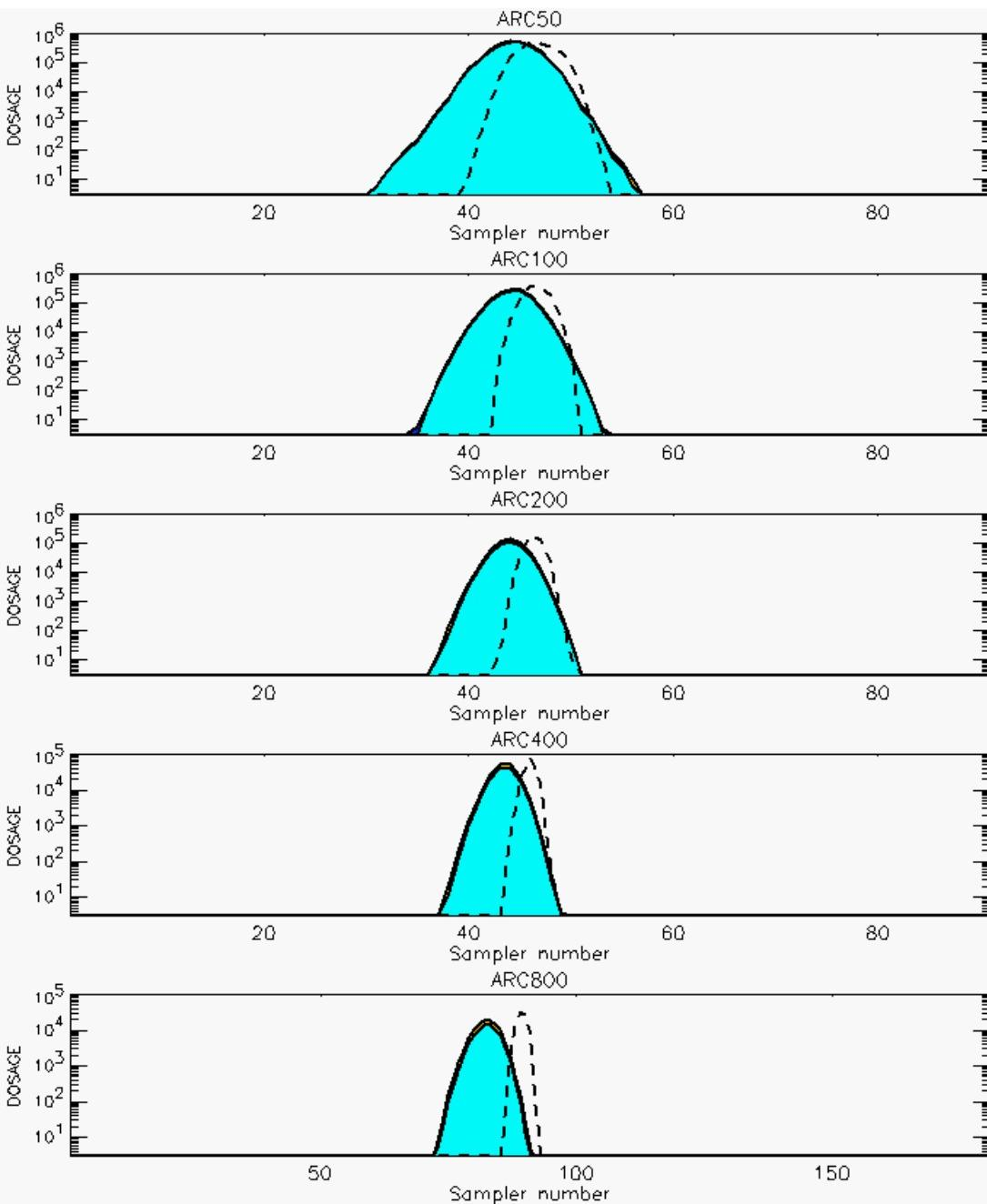
PG Prediction1 to Prediction2 Comparison

PG Trial File: pr_grass_tracer_Experiment_58.txt

PG Prediction File 1: ARAC\sv_vd\pg_58_sv_vd.arac

PG Prediction File 2: ARAC\sv_novd\pg_58_sv_novd.arac

Figure L-47a. NARAC With and Without SO₂ Surface Deposition Predictions to Trial 58 on Linear Scale: Stability Category is 6



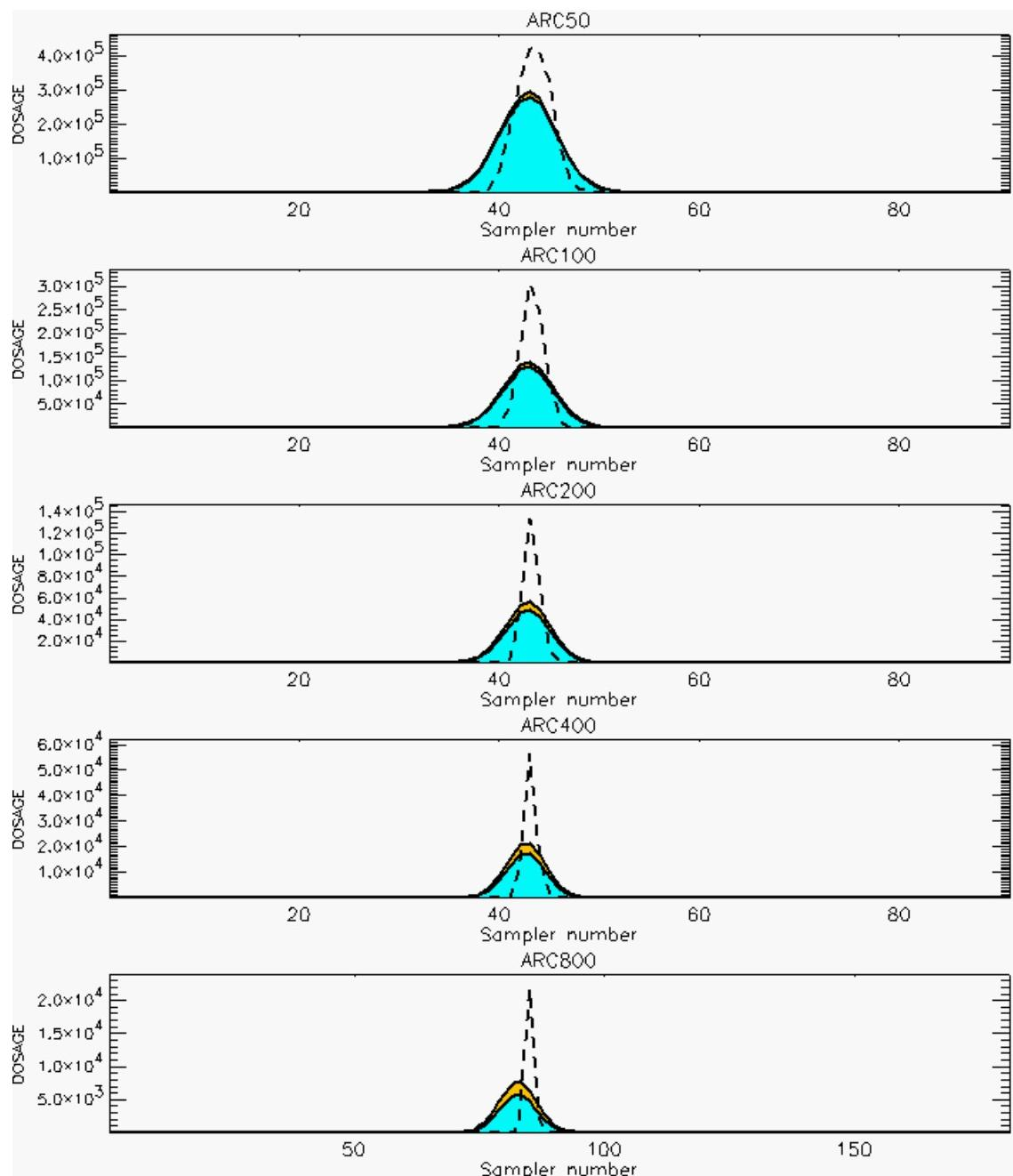
PG Prediction1 to Prediction2 Comparison

PG Trial File: pr_grass_tracer_Experiment_58.txt

PG Prediction File 1: ARAC\sv_vd\pg_58_sv_vd.arac

PG Prediction File 2: ARAC\sv_novd\pg_58_sv_novd.arac

Figure L-47b. NARAC With and Without SO_2 Surface Deposition Predictions to Trial 58 on Logarithmic Scale: Stability Category is 6



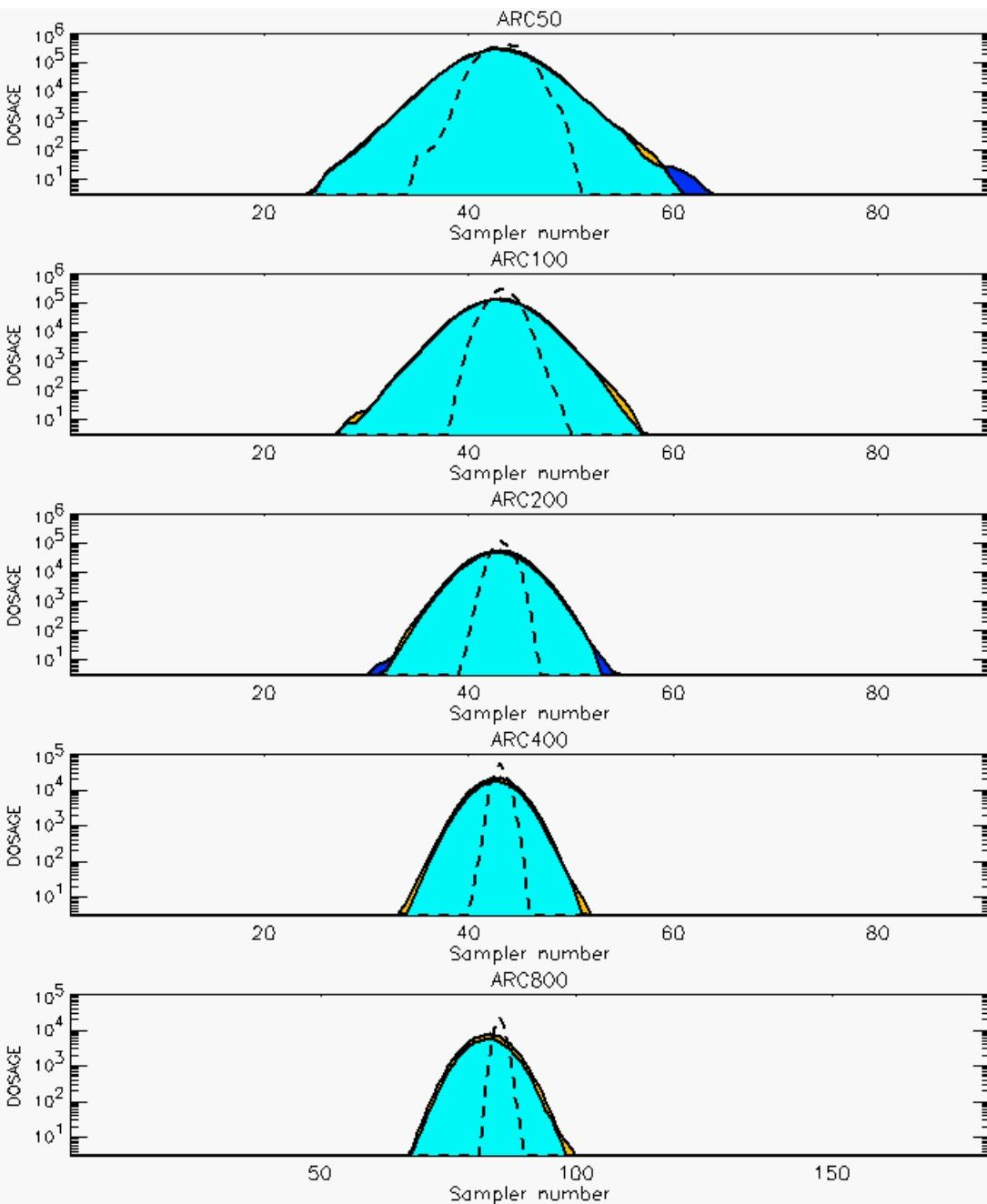
PG Prediction1 to Prediction2 Comparison

PG Trial File: pr_grass_tracer_Experiment_59.txt

PG Prediction File 1: ARAC\sv_vd\pg_59_sv_vd.arac

PG Prediction File 2: ARAC\sv_novd\pg_59_sv_novd.arac

Figure L-48a. NARAC With and Without SO_2 Surface Deposition Predictions to Trial 59 on Linear Scale: Stability Category is 5



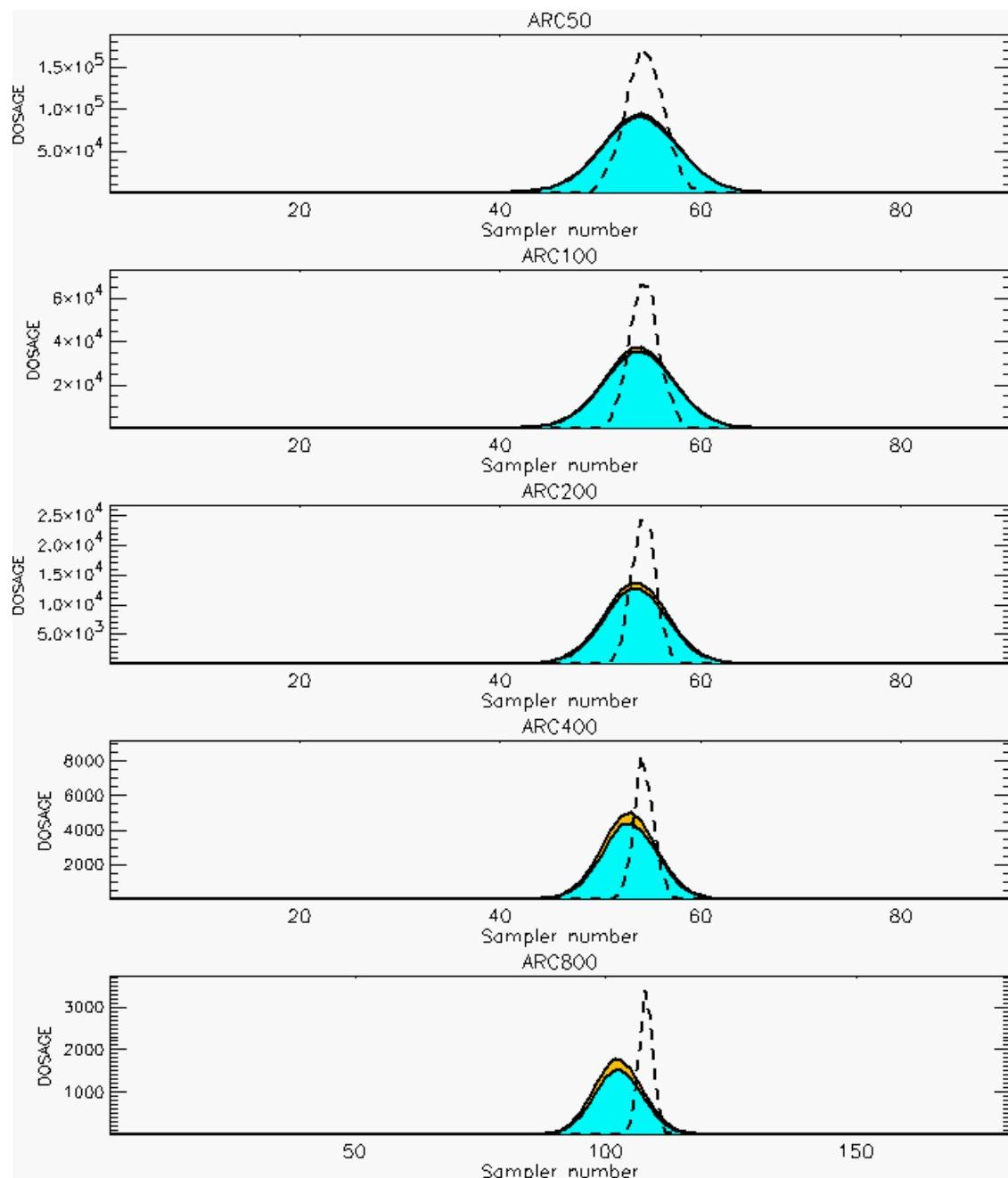
PG Prediction1 to Prediction2 Comparison

PG Trial File: pr_grass_tracer_Experiment_59.txt

PG Prediction File 1: ARAC\sv_vd\pg_59_sv_vd.arac

PG Prediction File 2: ARAC\sv_novd\pg_59_sv_novd.arac

Figure L-48b. NARAC With and Without SO_2 Surface Deposition Predictions to Trial 59 on Logarithmic Scale: Stability Category is 5



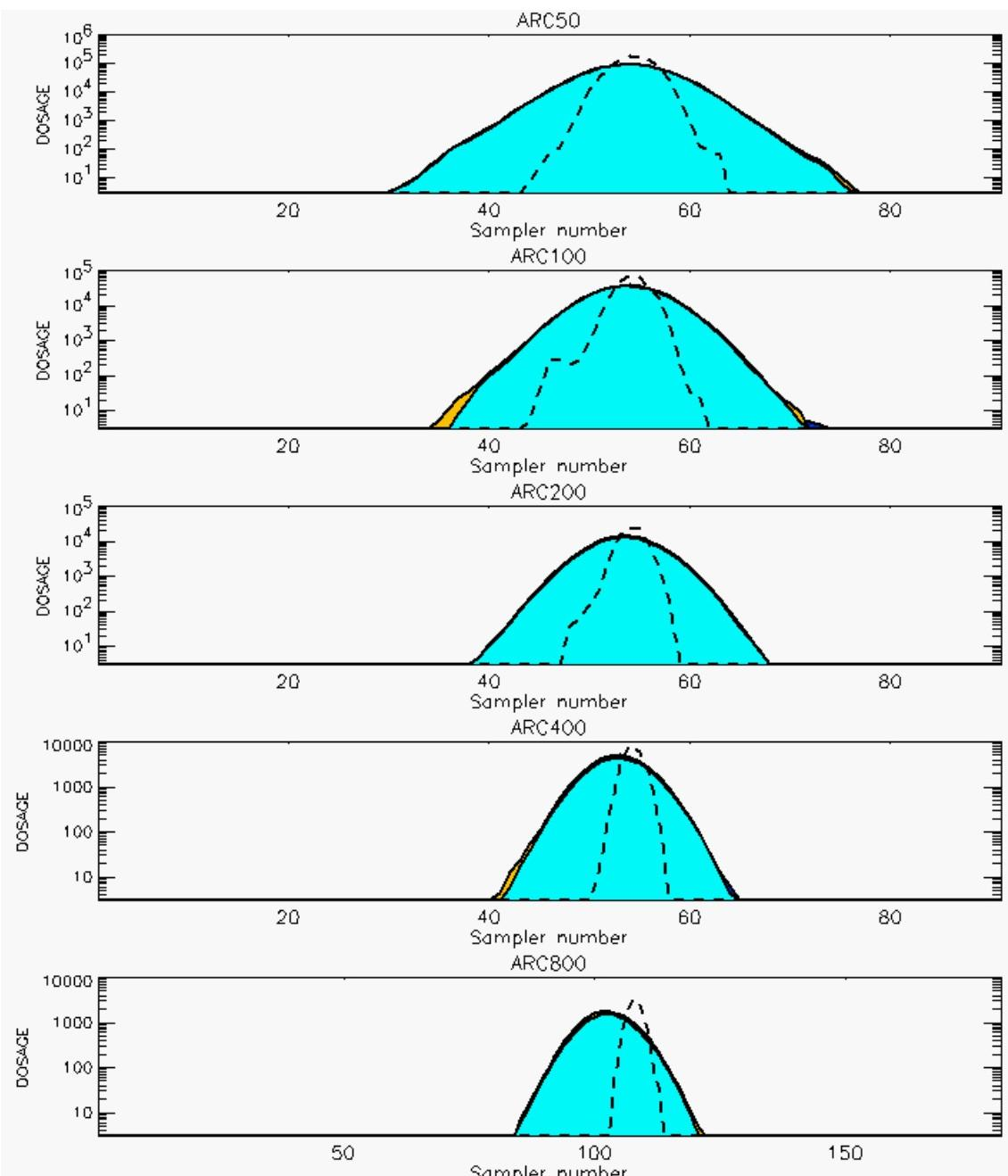
PG Prediction1 to Prediction2 Comparison

PG Trial File: pr_grass_tracer_Experiment_60.txt

PG Prediction File 1: ARAC\sv_vd\pg_60_sv_vd.arac

PG Prediction File 2: ARAC\sv_novd\pg_60_sv_novd.arac

Figure L-49a. NARAC With and Without SO₂ Surface Deposition Predictions to Trial 60 on Linear Scale: Stability Category is 5



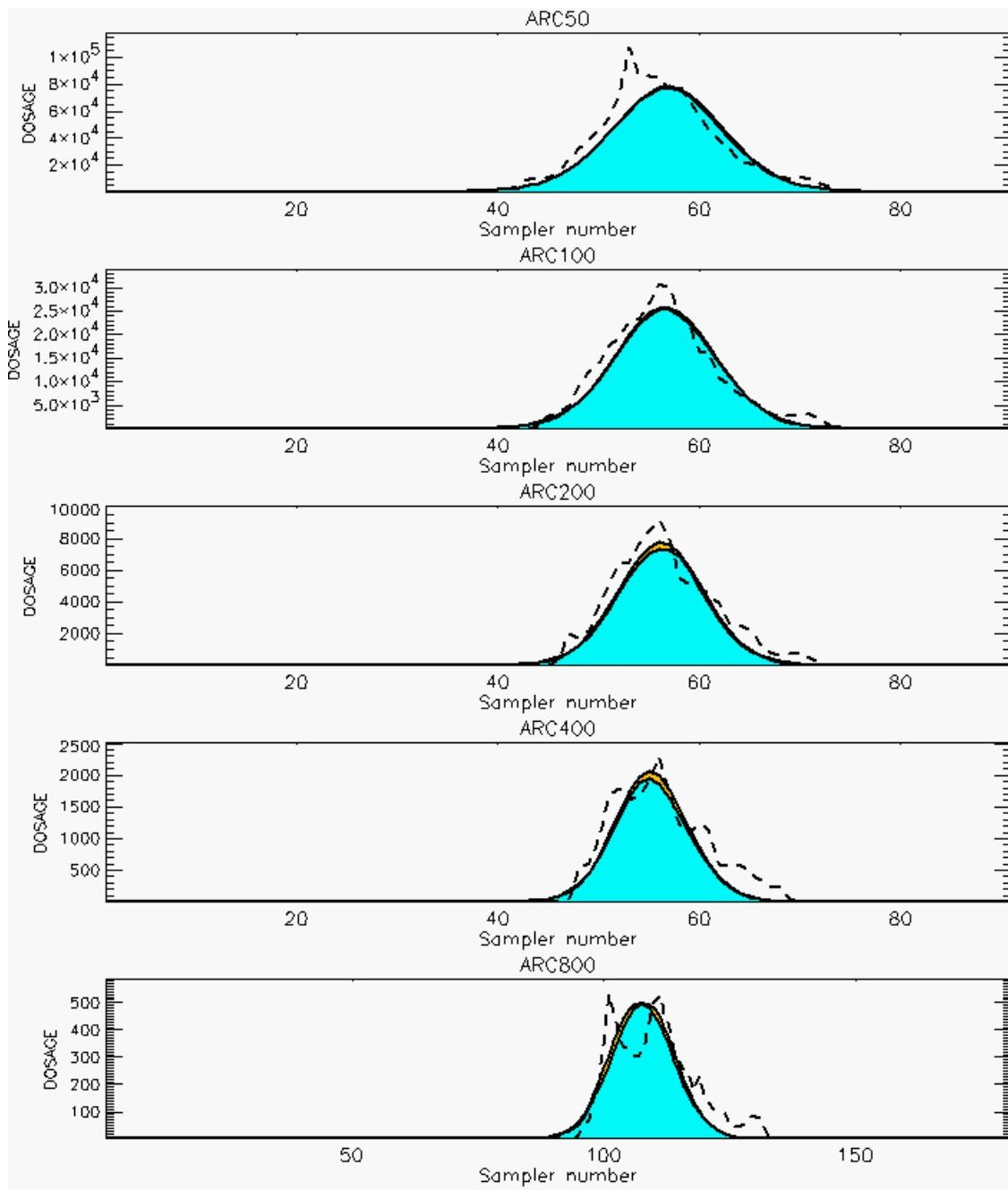
PG Prediction1 to Prediction2 Comparison

PG Trial File: pr_grass_tracer_Experiment_60.txt

PG Prediction File 1: ARAC\sv_vd\pg_60_sv_vd.arac

PG Prediction File 2: ARAC\sv_novd\pg_60_sv_novd.arac

Figure L-49b. NARAC With and Without SO_2 Surface Deposition Predictions to Trial 60 on Logarithmic Scale: Stability Category is 5



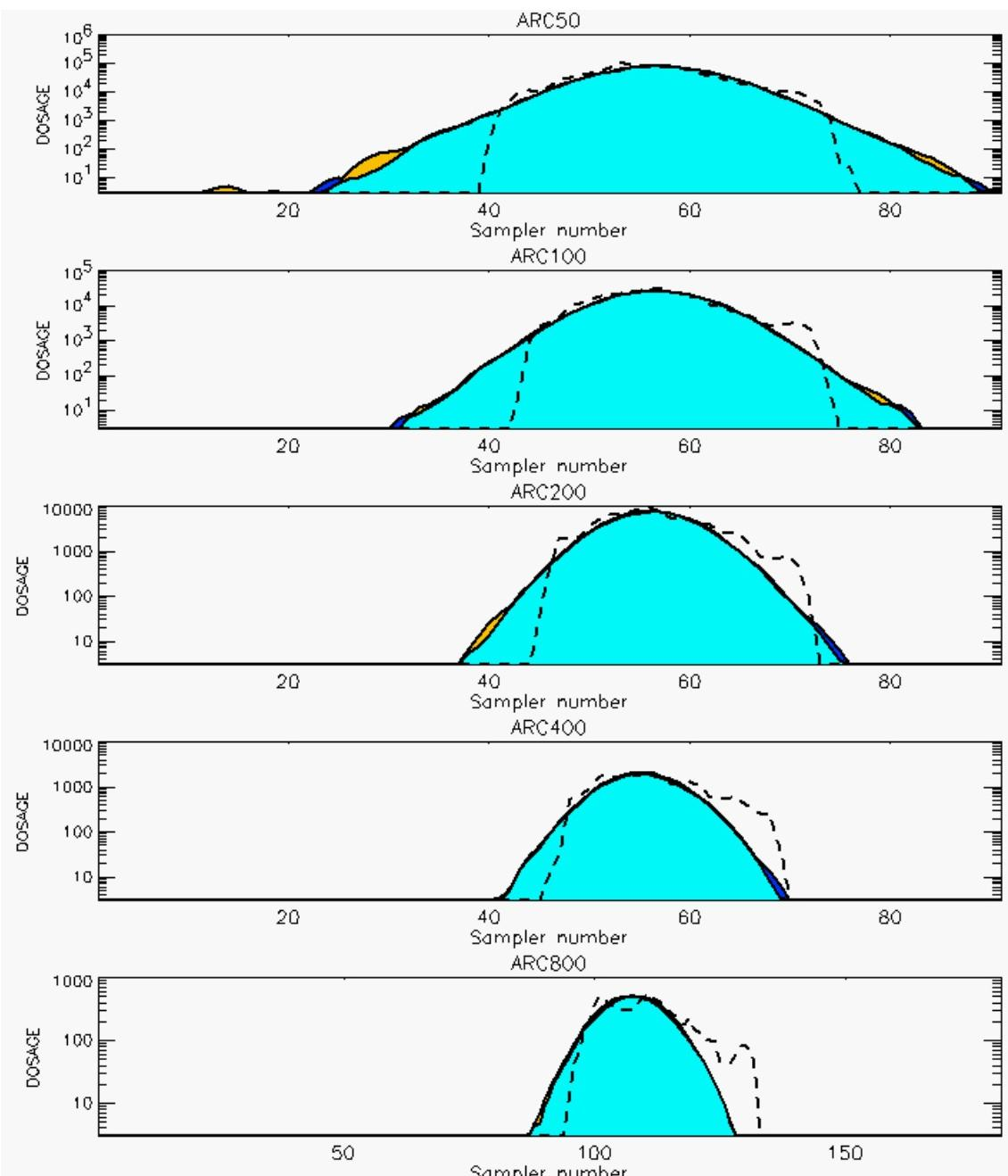
PG Prediction1 to Prediction2 Comparison

PG Trial File: pr_grass_tracer_Experiment_61.txt

PG Prediction File 1: ARAC\sv_vd\pg_61_sv_vd.arac

PG Prediction File 2: ARAC\sv_novd\pg_61_sv_novd.arac

Figure L-50a. NARAC With and Without SO₂ Surface Deposition Predictions to Trial 61 on Linear Scale: Stability Category is 3



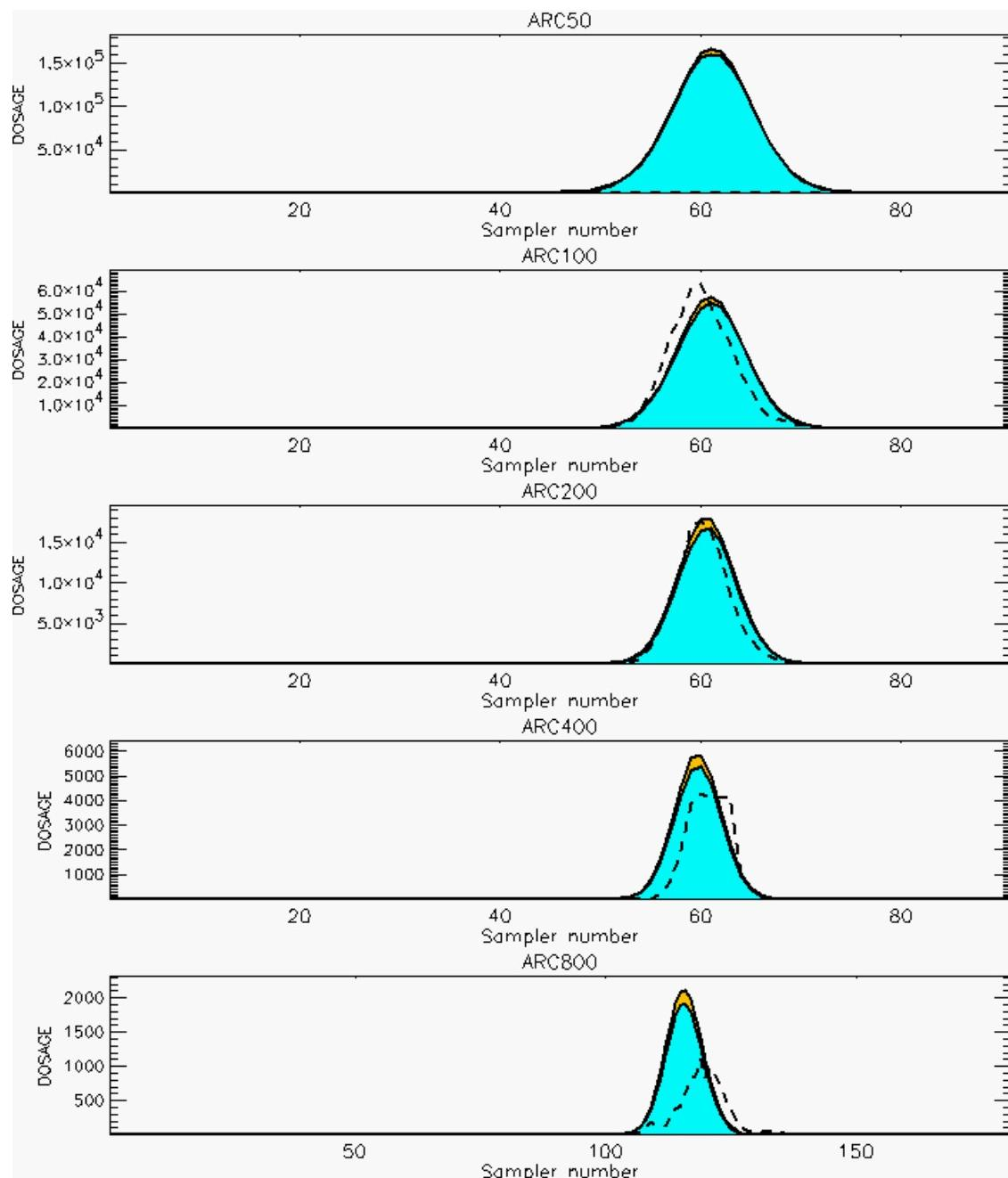
PG Prediction1 to Prediction2 Comparison

PG Trial File: pr_grass_tracer_Experiment_61.txt

PG Prediction File 1: ARAC\sv_vd\pg_61_sv_vd.arac

PG Prediction File 2: ARAC\sv_novd\pg_61_sv_novd.arac

Figure L-50b. NARAC With and Without SO₂ Surface Deposition Predictions to Trial 61 on Logarithmic Scale: Stability Category is 3



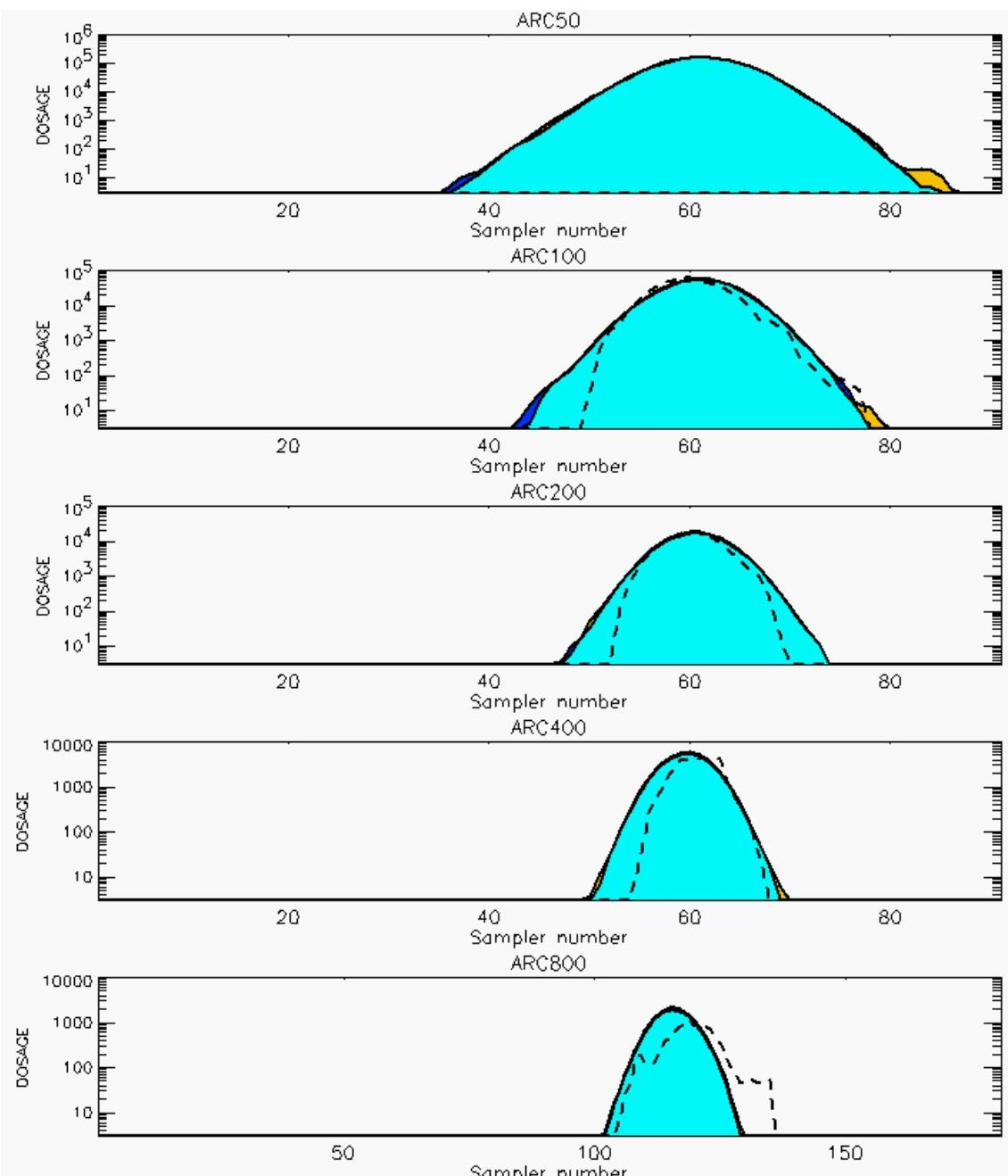
PG Prediction1 to Prediction2 Comparison

PG Trial File: pr_grass_tracer_Experiment_62.txt

PG Prediction File 1: ARAC\sv_vd\pg_62_sv_vd.arac

PG Prediction File 2: ARAC\sv_novd\pg_62_sv_novd.arac

Figure L-51a. NARAC With and Without SO₂ Surface Deposition Predictions to Trial 62 on Linear Scale: Stability Category is 2



PG Prediction1 to Prediction2 Comparison

PG Trial File: pr_grass_tracer_Experiment_62.txt

PG Prediction File 1: ARAC\sv_vd\pg_62_sv_vd.arac

PG Prediction File 2: ARAC\sv_novd\pg_62_sv_novd.arac

Figure L-51b. NARAC With and Without SO₂ Surface Deposition Predictions to Trial 62 on Logarithmic Scale: Stability Category is 2

REFERENCES

- L-1. Barad, M. L. (Editor), *Project Prairie Grass, A Field Program in Diffusion*, Geophysical Research Papers No. 59, Volumes I and II, DTIC #AD-152572/AFCRC-TR-58-235(I), Air Geophysical Laboratory, Hanscom Air Force Base, MA, 1958.
- L-2. Irwin, J. S. and Rosu, M-R., *Comments on a Draft Practice for Statistical Evaluation of Atmospheric Dispersion Models*, Proceedings of the 10th Joint Conference on the Applications of Air Pollution Meteorology. American Meteorological Society, Boston, pp. 6-10, 1998.

APPENDIX M

**COMPARISONS OF NARAC PREDICTIONS: WITH DIFFERENT
VALUES OF DISPERSION (SIGMA-V EXPERIMENTAL AND
SIGMA-V CALCULATED)**

APPENDIX M

COMPARISONS OF NARAC PREDICTIONS: WITH DIFFERENT VALUES OF DISPERSION (SIGMA-v EXPERIMENTAL AND SIGMA-v CALCULATED)

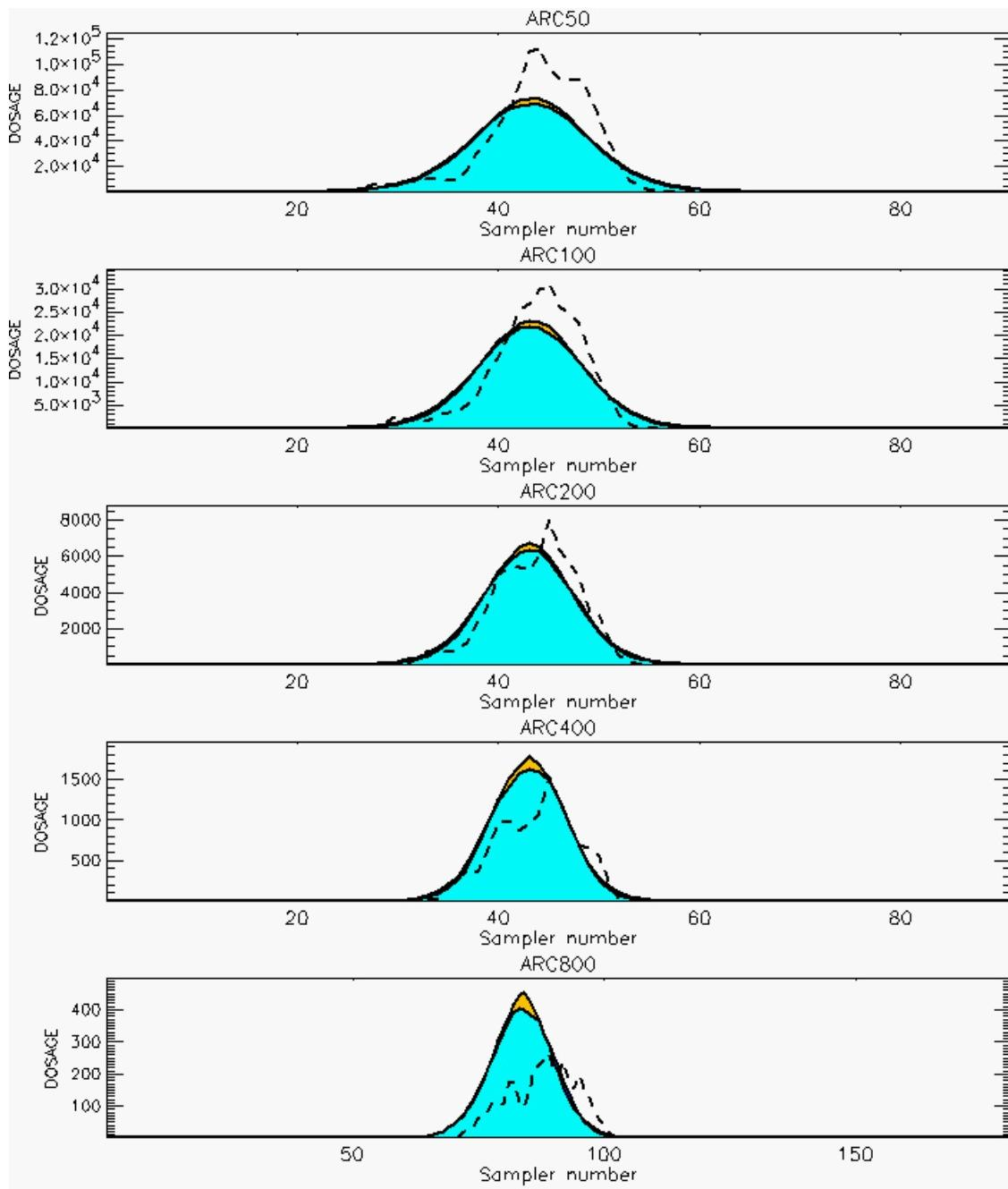
This appendix presents graphical comparisons of NARAC predictions using two different sigma-v values – an experimentally determined value and a calculated value. Vertical plot units are dosage units of mg-sec/m³. The horizontal plot units are sampler numbers as presented in the *Prairie Grass* field trials [Ref. M-1]. Sampler number 1 oriented to the west, the middle sampler (45 or 90) oriented to the north, and the last sampler (91 or 181) is oriented to the east of the SO₂ gas release source. Only data values greater than the cutoff threshold of 3 mg-sec/m³ (0.005 mg/m³) are presented. This cutoff threshold value corresponds to a minimum value reported in *Prairie Grass* field trials.

Comparisons of NARAC predictions are presented on linear and log dosage scales. Each graphical comparison consist of five plots (one for each arc) with the top plot depicting the 50-meter arc, the second plot depicting the 100-meter arc, the third plot depicting the 200-meter arc, and so on. The last panel (just above the figure caption) contains information about the data files used to produce these plots. The *Prairie Grass* field trial file name contains a two-digit number corresponding to the trial number. Prediction file names contain the moniker “novd” denoting that SO₂ surface deposition was not considered and a calculated value for sigma-v was used. The moniker “sv_novd” denotes that SO₂ surface deposition was not considered and an experimentally determined value for sigma-v was used. A one- or two-digit number describes the *Prairie Grass* field trial being predicted. Odd-numbered pages contain figures on the linear dosage scale while even-numbered pages contain figures on the logarithmic dosage scale.

The meanings of the colors used in the plots are described in the below legend:

- Dark Blue — higher dosages for predictions with calculated sigma-v.
- Turquoise — dosages that agree for both predictions.
- Brown — higher dosages for predictions with experimental sigma-v.

The dashed lines depict dosage values actually obtained in the field trial. Irwin stability categories that were used in our analyses are denoted in the figure captions. These stability category assignments are based on Ref. M-2.



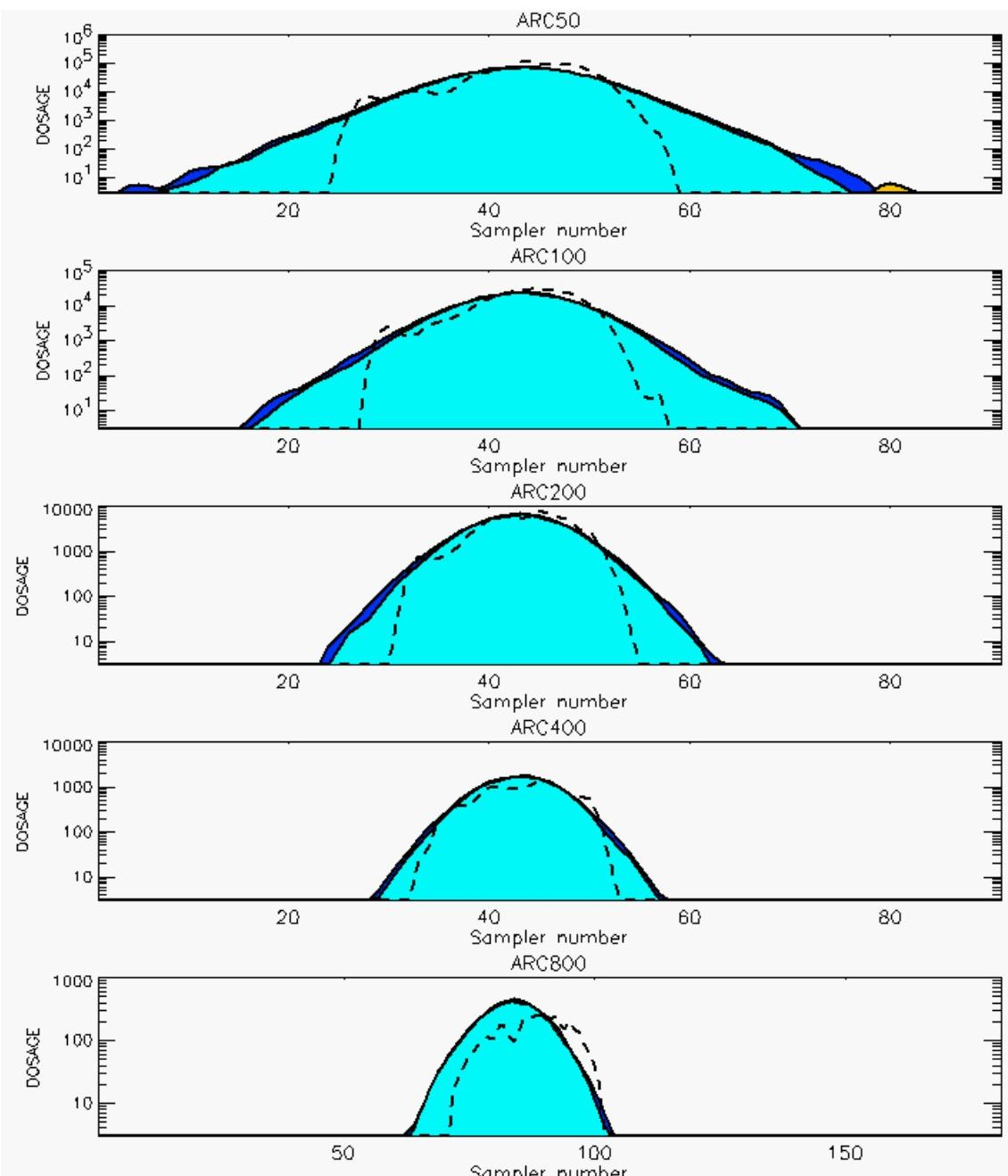
PG Prediction1 to Prediction2 Comparison

PG Trial File: pr_grass_tracer_Experiment_05.txt

PG Prediction File 1: ARAC\nodeposition\pg_5_nozd.arac

PG Prediction File 2: ARAC\sv_nozd\pg_5_sv_nozd.arac

Figure M-1a. NARAC Sigma-v Experimental and Sigma-v Calculated Predictions to Trial 5 on Linear Scale: Stability Category is 2



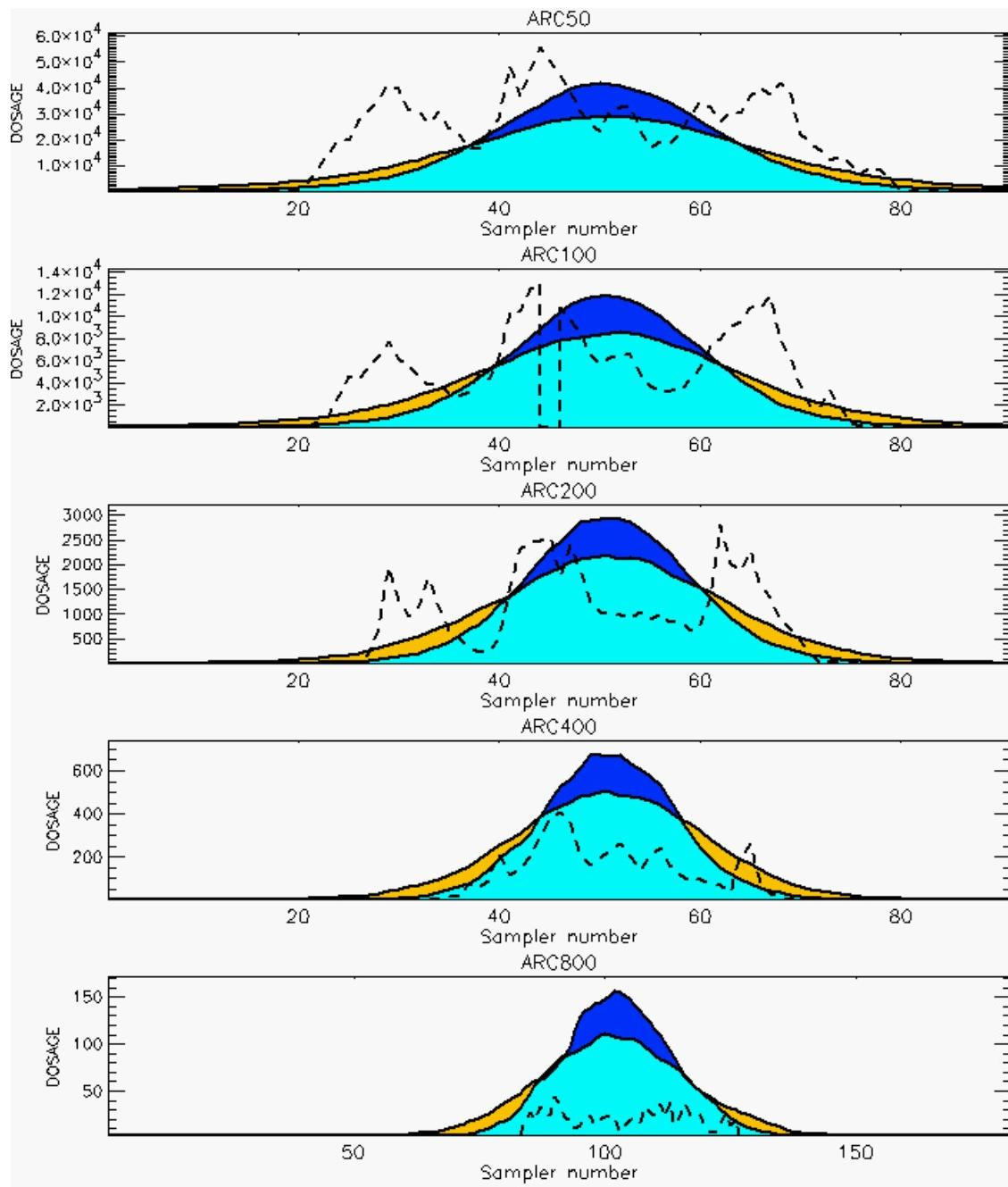
PG Prediction1 to Prediction2 Comparison

PG Trial File: pr_grass_tracer_Experiment_05.txt

PG Prediction File 1: ARAC\nodeposition\pg_5_nozd.arac

PG Prediction File 2: ARAC\sv_nozd\pg_5_sv_nozd.arac

Figure M-1b. NARAC Sigma-v Experimental and Sigma-v Calculated Predictions to Trial 5 on Logarithmic Scale: Stability Category is 2



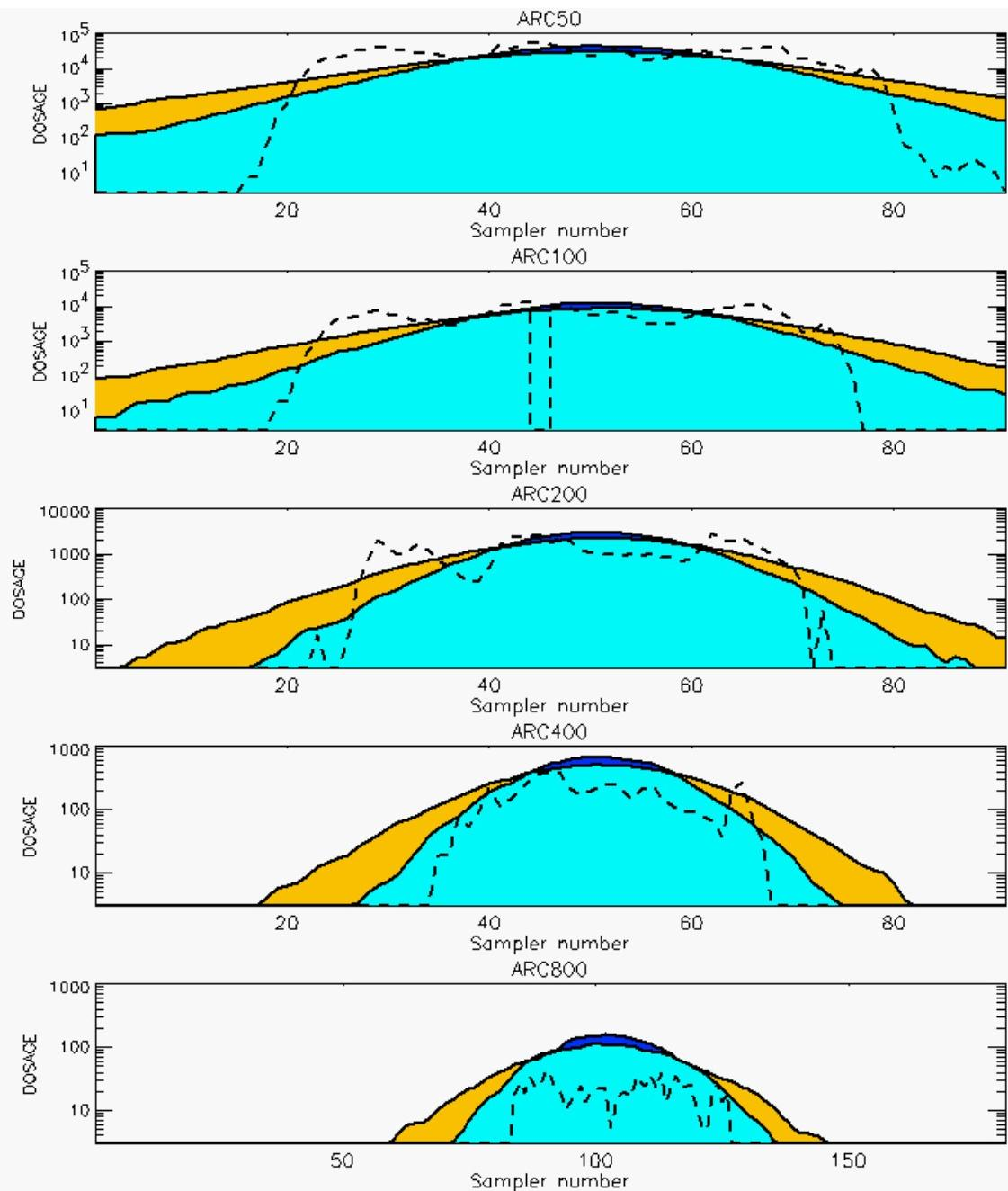
PG Prediction1 to Prediction2 Comparison

PG Trial File: pr_grass_tracer_Experiment_07.txt

PG Prediction File 1: ARAC\nodeposition\pg_7_nozd.arac

PG Prediction File 2: ARAC\sv_nozd\pg_7_sv_nozd.arac

Figure M-2a. NARAC Sigma-v Experimental and Sigma-v Calculated Predictions to Trial 7 on Linear Scale: Stability Category is 1



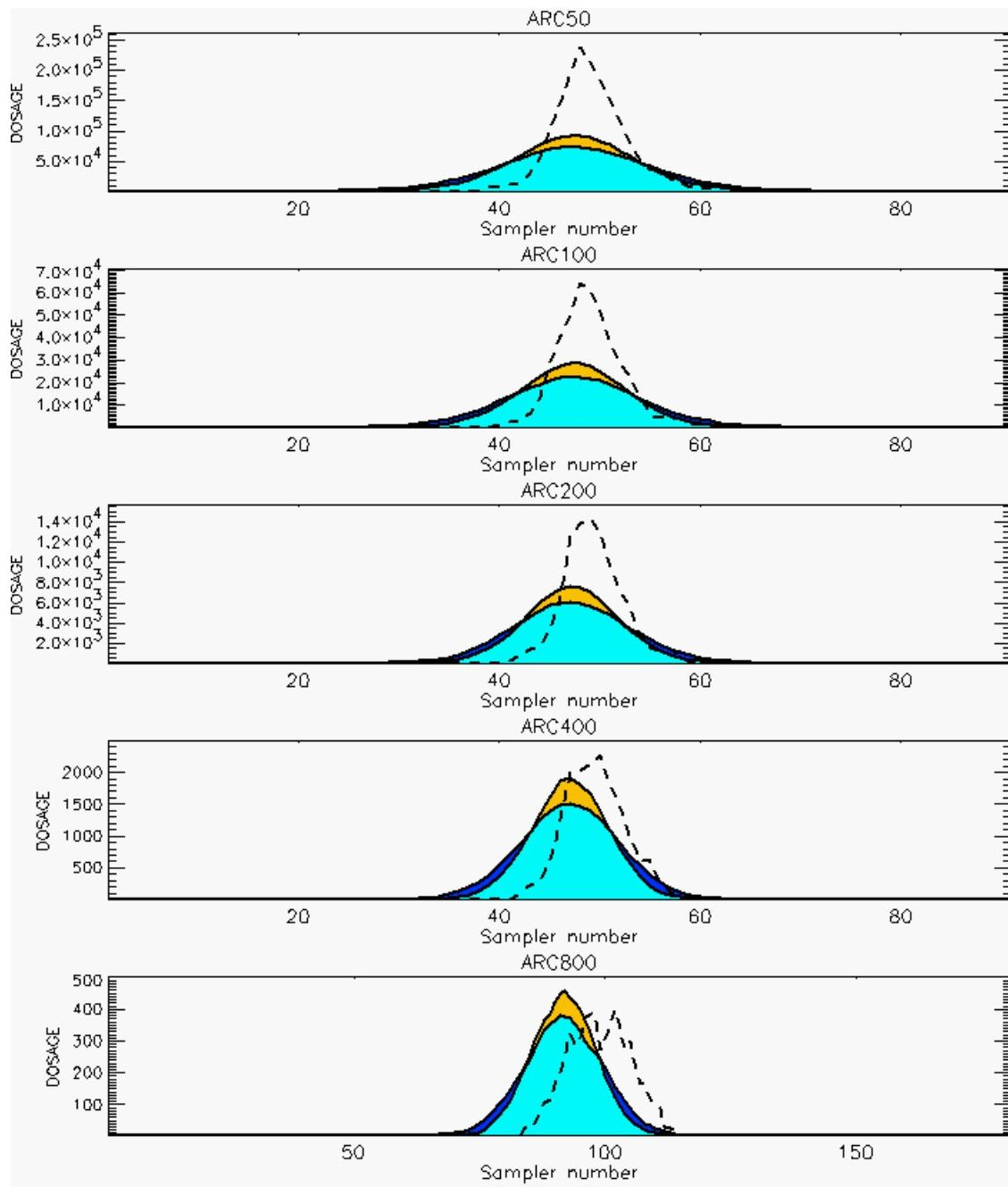
PG Prediction1 to Prediction2 Comparison

PG Trial File: pr_grass_tracer_Experiment_07.txt

PG Prediction File 1: ARAC\nodeposition\pg_7_nozd.arac

PG Prediction File 2: ARAC\sv_nozd\pg_7_sv_nozd.arac

Figure M-2b. NARAC Sigma-v Experimental and Sigma-v Calculated Predictions to Trial 7 on Logarithmic Scale: Stability Category is 1



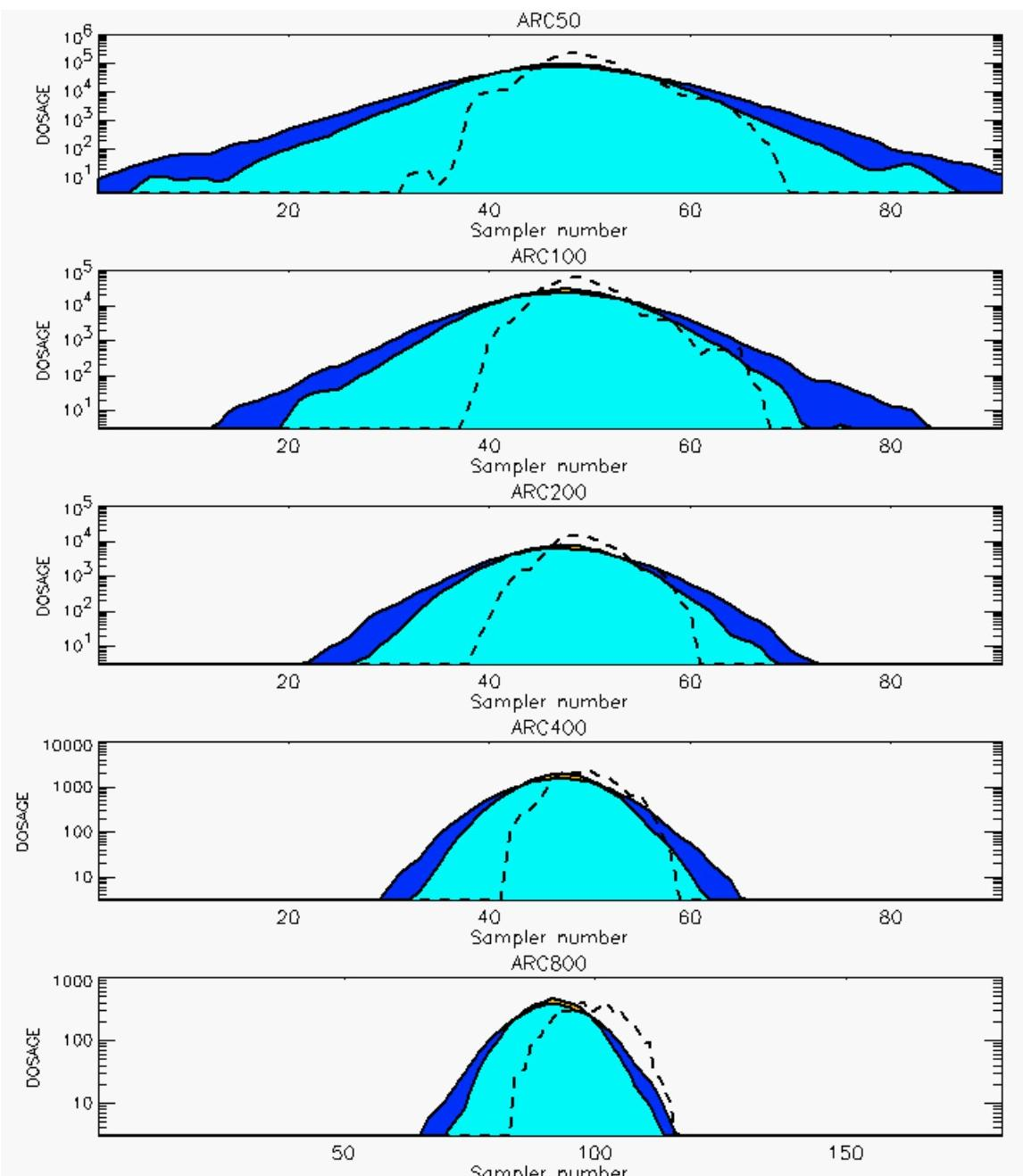
PG Prediction1 to Prediction2 Comparison

PG Trial File: pr_grass_tracer_Experiment_08.txt

PG Prediction File 1: ARAC\nodeposition\pg_8_nozd.arac

PG Prediction File 2: ARAC\sv_nozd\pg_8_sv_nozd.arac

Figure M-3a. NARAC Sigma-v Experimental and Sigma-v Calculated Predictions to Trial 8 on Linear Scale: Stability Category is 2



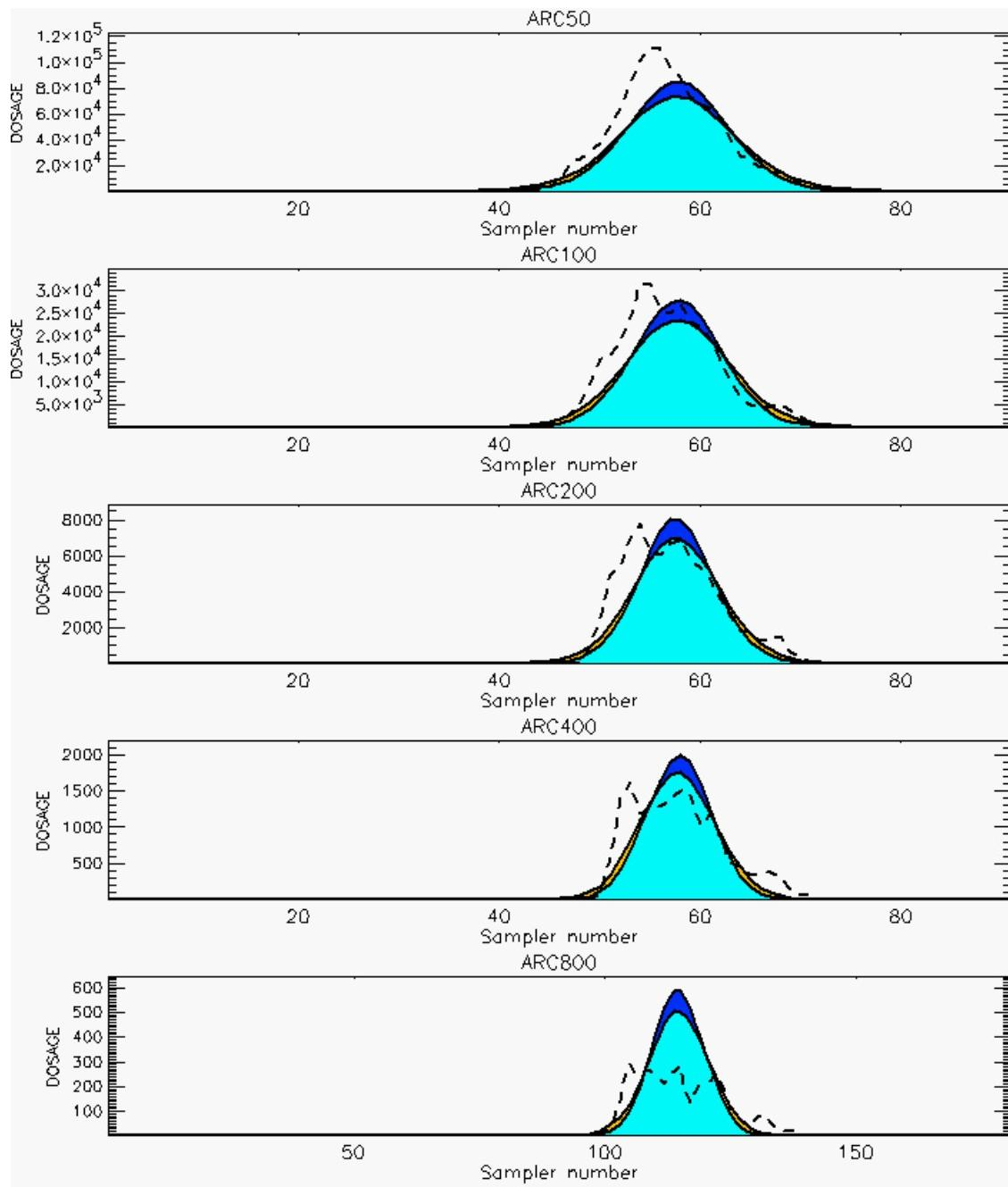
PG Prediction1 to Prediction2 Comparison

PG Trial File: pr_grass_tracer_Experiment_08.txt

PG Prediction File 1: ARAC\nodeposition\pg_8_nozd.arac

PG Prediction File 2: ARAC\sv_nozd\pg_8_sv_nozd.arac

Figure M-3b. NARAC Sigma-v Experimental and Sigma-v Calculated Predictions to Trial 8 on Logarithmic Scale: Stability Category is 2



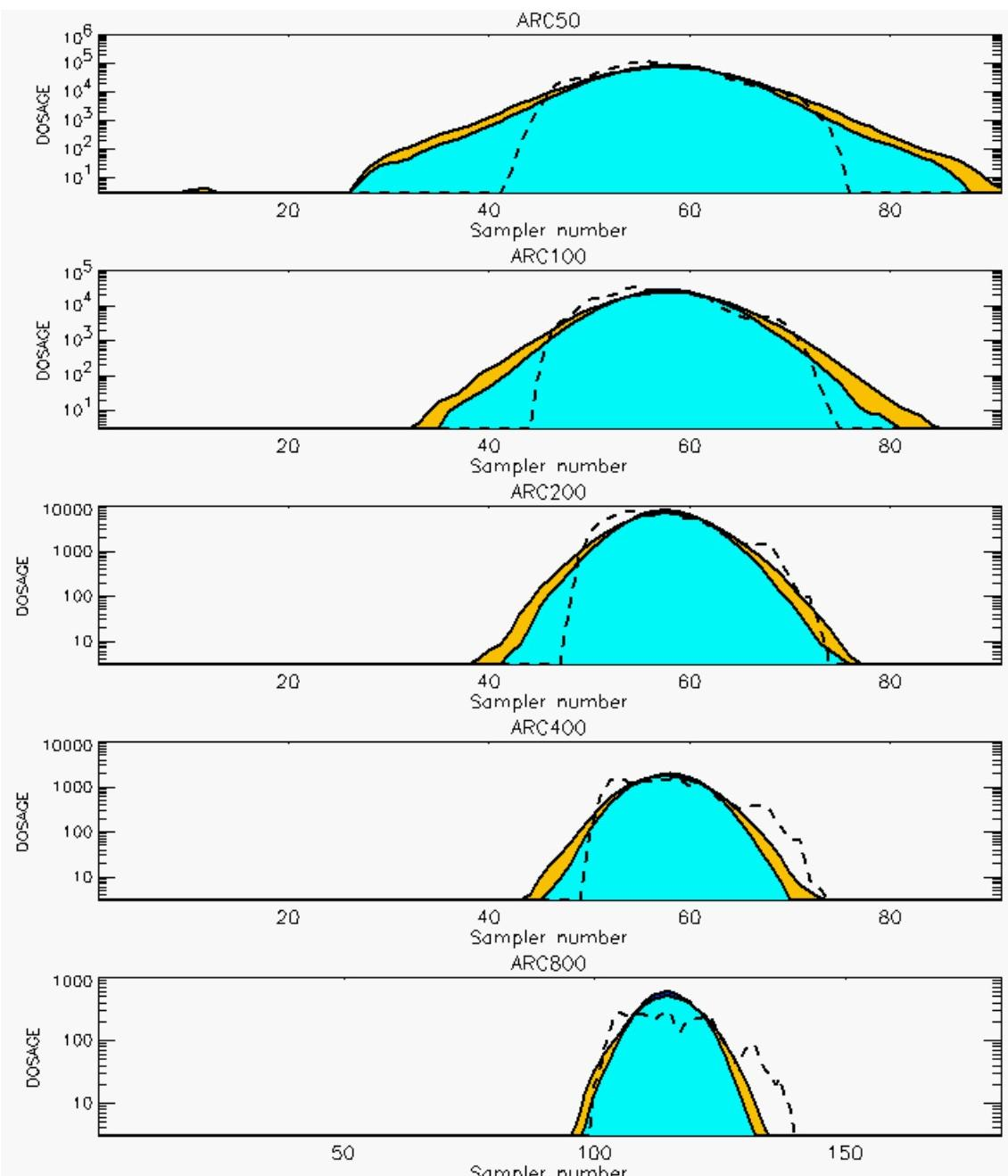
PG Prediction1 to Prediction2 Comparison

PG Trial File: pr_grass_tracer_Experiment_09.txt

PG Prediction File 1: ARAC\nodeposition\pg_9_nozd.arac

PG Prediction File 2: ARAC\sv_nozd\pg_9_sv_nozd.arac

Figure M-4a. NARAC Sigma-v Experimental and Sigma-v Calculated Predictions to Trial 9 on Linear Scale: Stability Category is 2



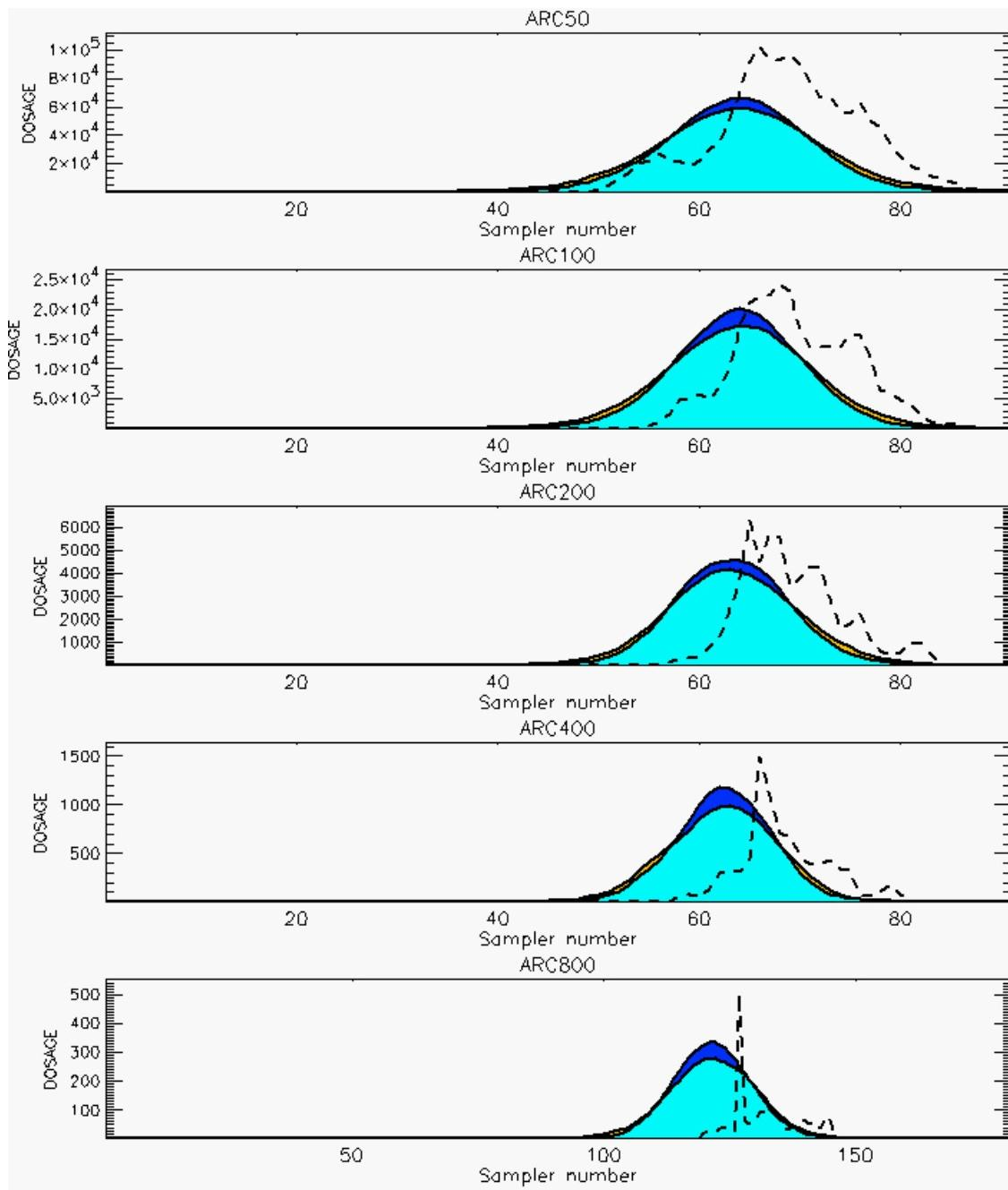
PG Prediction1 to Prediction2 Comparison

PG Trial File: pr_grass_tracer_Experiment_09.txt

PG Prediction File 1: ARAC\nodeposition\pg_9_nozd.arac

PG Prediction File 2: ARAC\sv_nozd\pg_9_sv_nozd.arac

Figure M-4b. NARAC Sigma-v Experimental and Sigma-v Calculated Predictions to Trial 9 on Logarithmic Scale: Stability Category is 2



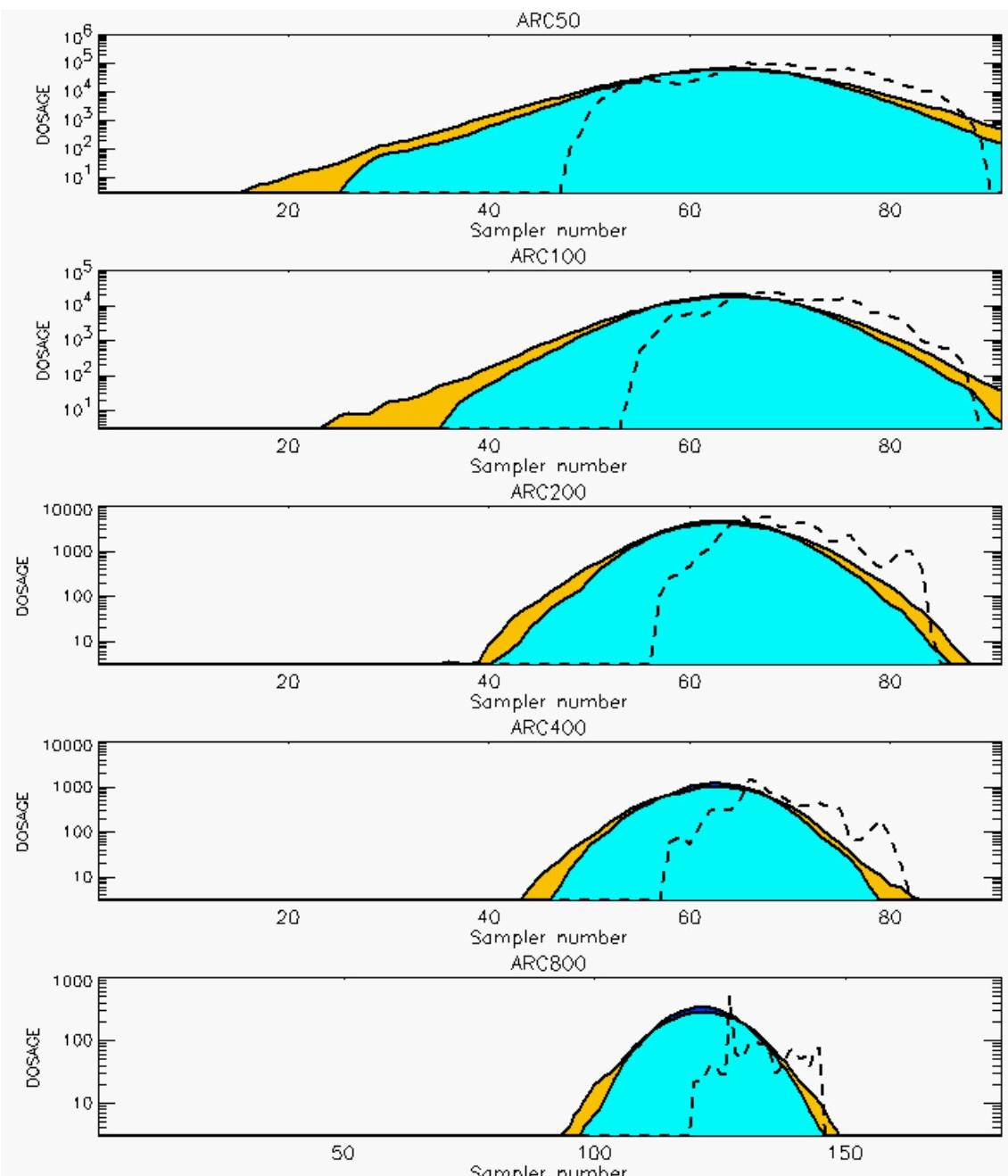
PG Prediction1 to Prediction2 Comparison

PG Trial File: pr_grass_tracer_Experiment_10.txt

PG Prediction File 1: ARAC\nodeposition\pg_10_nozd.arac

PG Prediction File 2: ARAC\sv_nozd\pg_10_sv_nozd.arac

Figure M-5a. NARAC Sigma-v Experimental and Sigma-v Calculated Predictions to Trial 10 on Linear Scale: Stability Category is 1



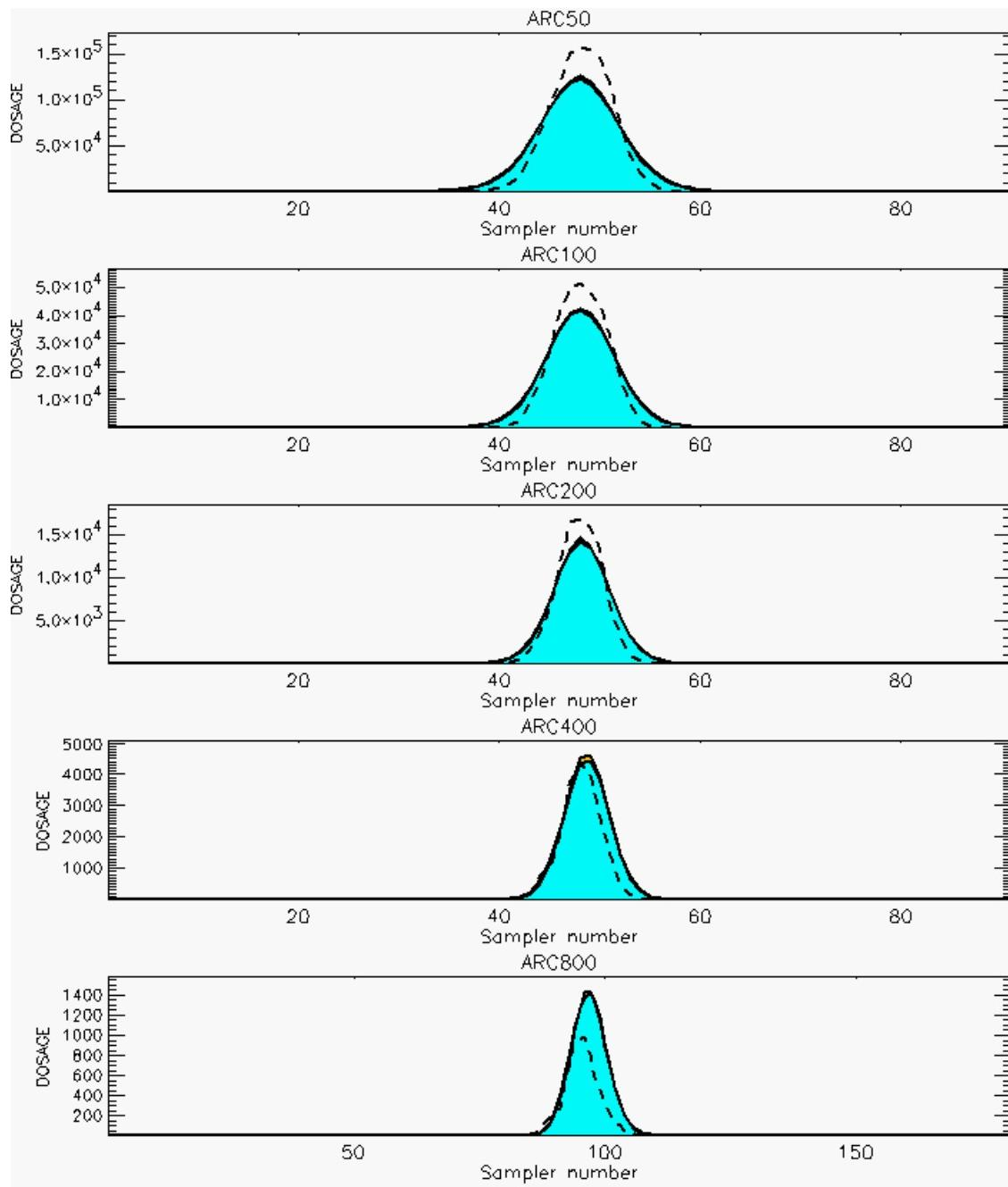
PG Prediction1 to Prediction2 Comparison

PG Trial File: pr_grass_tracer_Experiment_10.txt

PG Prediction File 1: ARAC\nodeposition\pg_10_nozd.arac

PG Prediction File 2: ARAC\sv_nozd\pg_10_sv_nozd.arac

Figure M-5b. NARAC Sigma-v Experimental and Sigma-v Calculated Predictions to Trial 10 on Logarithmic Scale: Stability Category is 1



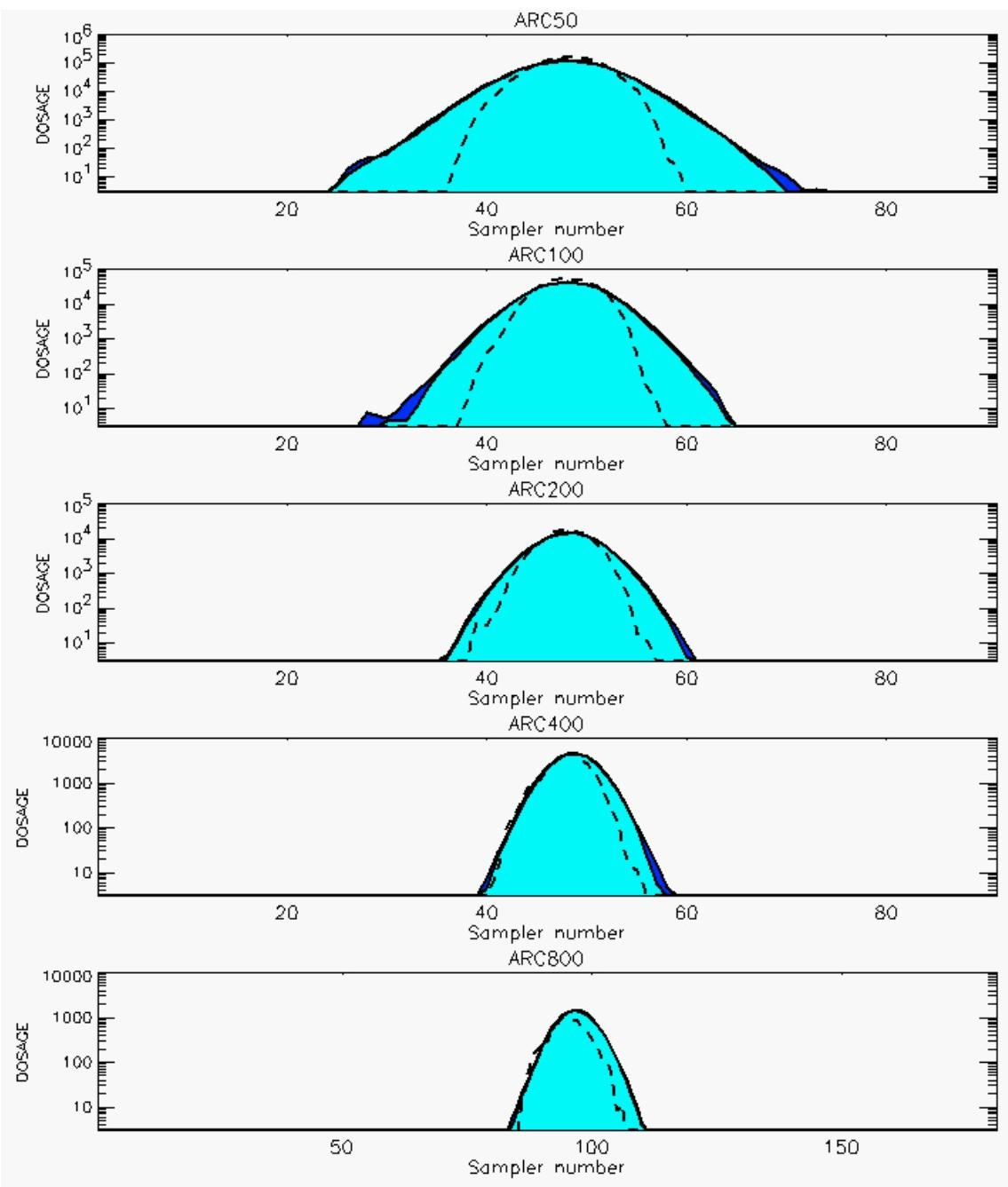
PG Prediction1 to Prediction2 Comparison

PG Trial File: pr_grass_tracer_Experiment_11.txt

PG Prediction File 1: ARAC\nodeposition\pg_11_nozd.arac

PG Prediction File 2: ARAC\sv_nozd\pg_11_sv_nozd.arac

Figure M-6a. NARAC Sigma-v Experimental and Sigma-v Calculated Predictions to Trial 11 on Linear Scale: Stability Category is 3



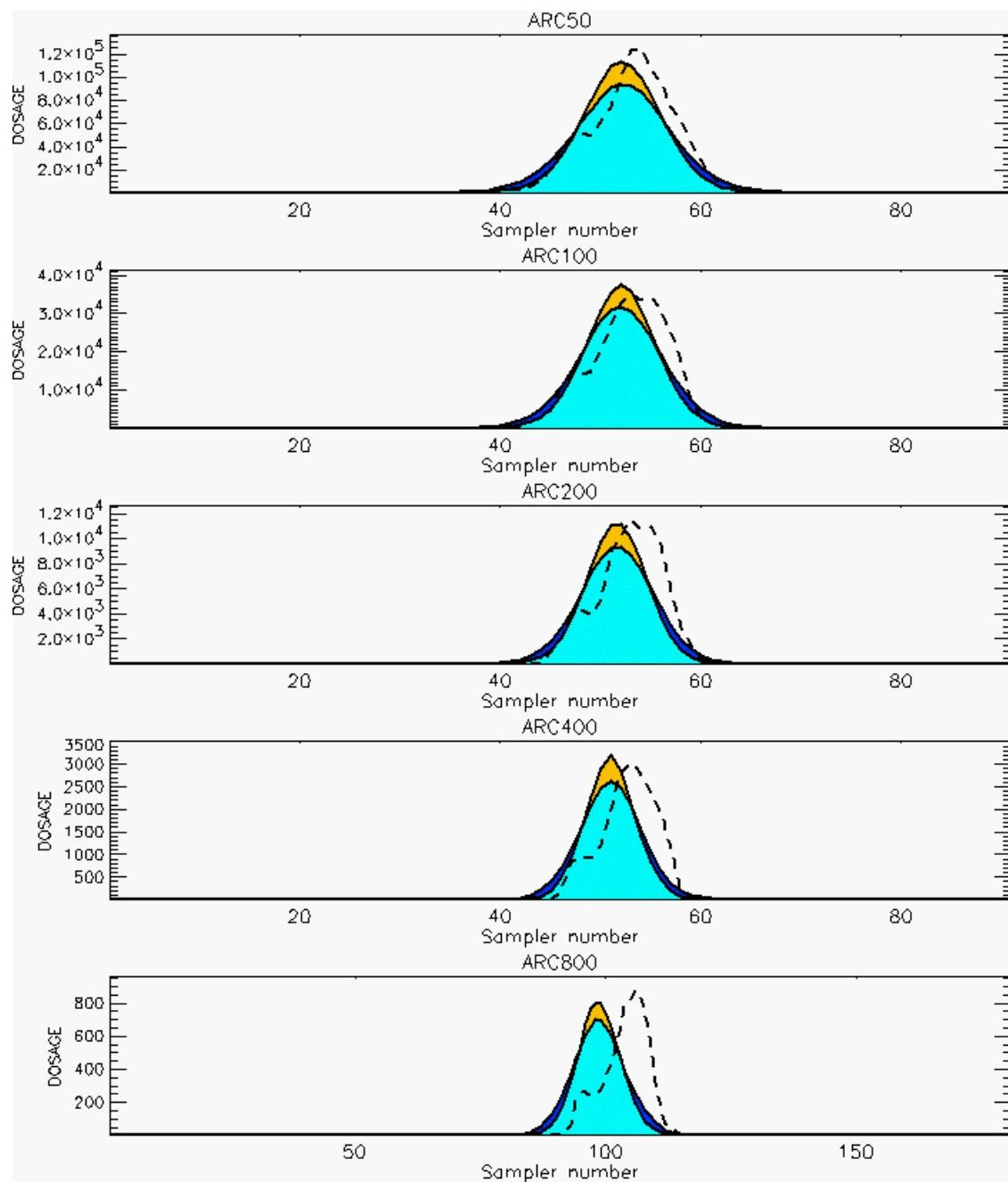
PG Prediction1 to Prediction2 Comparison

PG Trial File: pr_grass_tracer_Experiment_11.txt

PG Prediction File 1: ARAC\nodeposition\pg_11_noxd.arac

PG Prediction File 2: ARAC\sv_noxd\pg_11_sv_noxd.arac

Figure M-6b. NARAC Sigma-v Experimental and Sigma-v Calculated Predictions to Trial 11 on Logarithmic Scale: Stability Category is 3



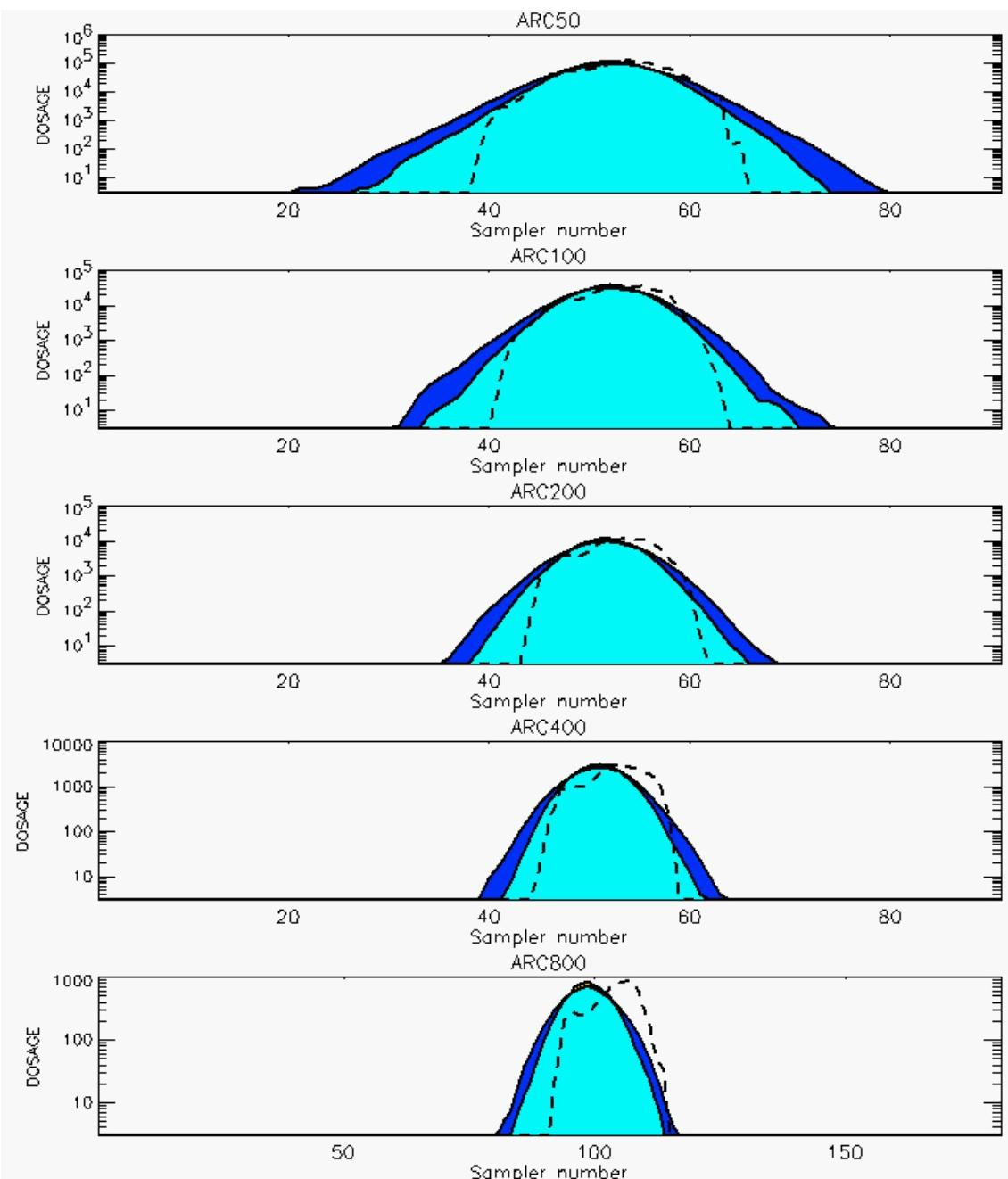
PG Prediction1 to Prediction2 Comparison

PG Trial File: pr_grass_tracer_Experiment_12.txt

PG Prediction File 1: ARAC\nodeposition\pg_12_nozd.arac

PG Prediction File 2: ARAC\sv_nozd\pg_12_sv_nozd.arac

Figure M-7a. NARAC Sigma-v Experimental and Sigma-v Calculated Predictions to Trial 12 on Linear Scale: Stability Category is 3



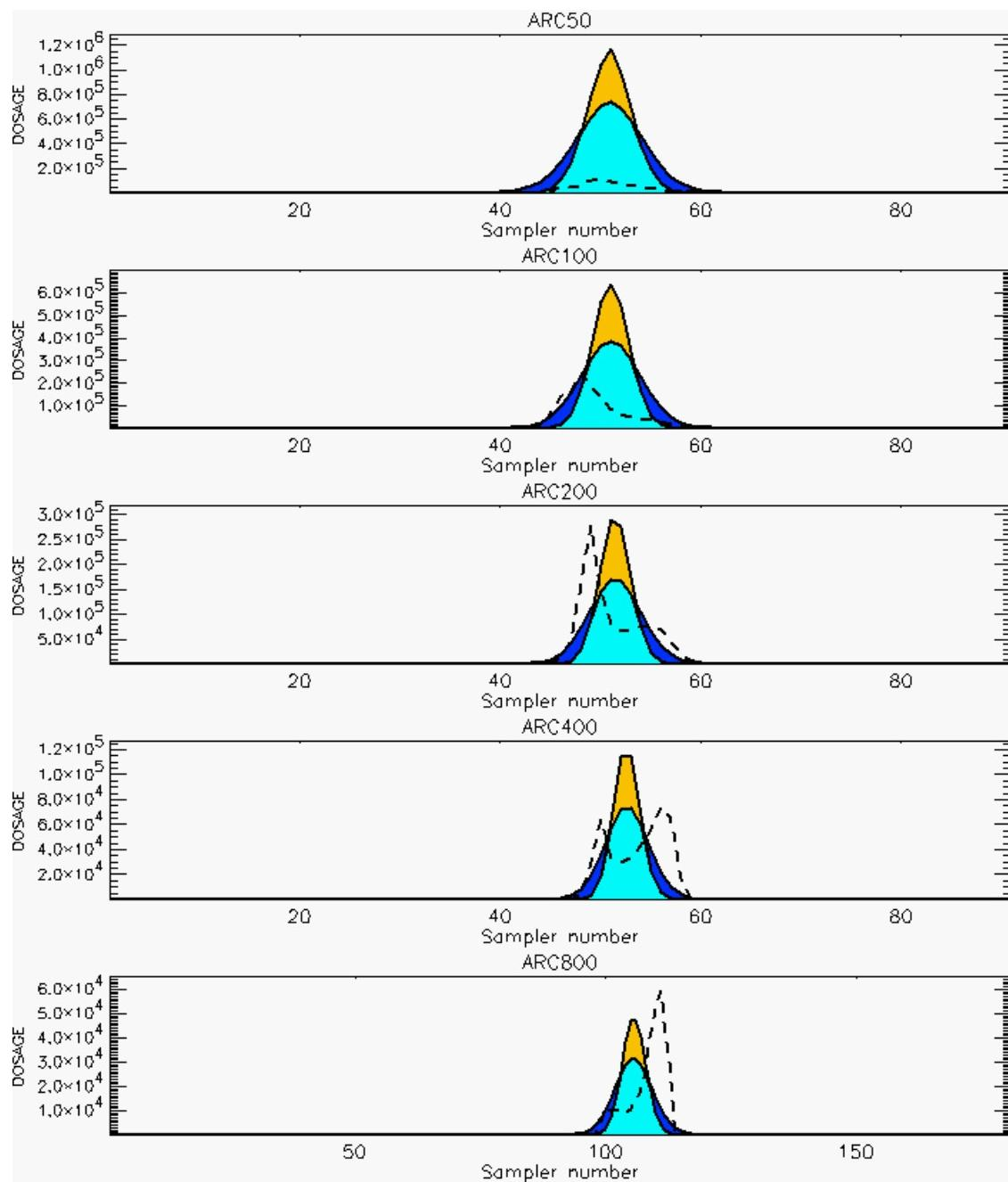
PG Prediction1 to Prediction2 Comparison

PG Trial File: pr_grass_tracer_Experiment_12.txt

PG Prediction File 1: ARAC\nodeposition\pg_12_nozd.arac

PG Prediction File 2: ARAC\sv_nozd\pg_12_sv_nozd.arac

Figure M-7b. NARAC Sigma-v Experimental and Sigma-v Calculated Predictions to Trial 12 on Logarithmic Scale: Stability Category is 3



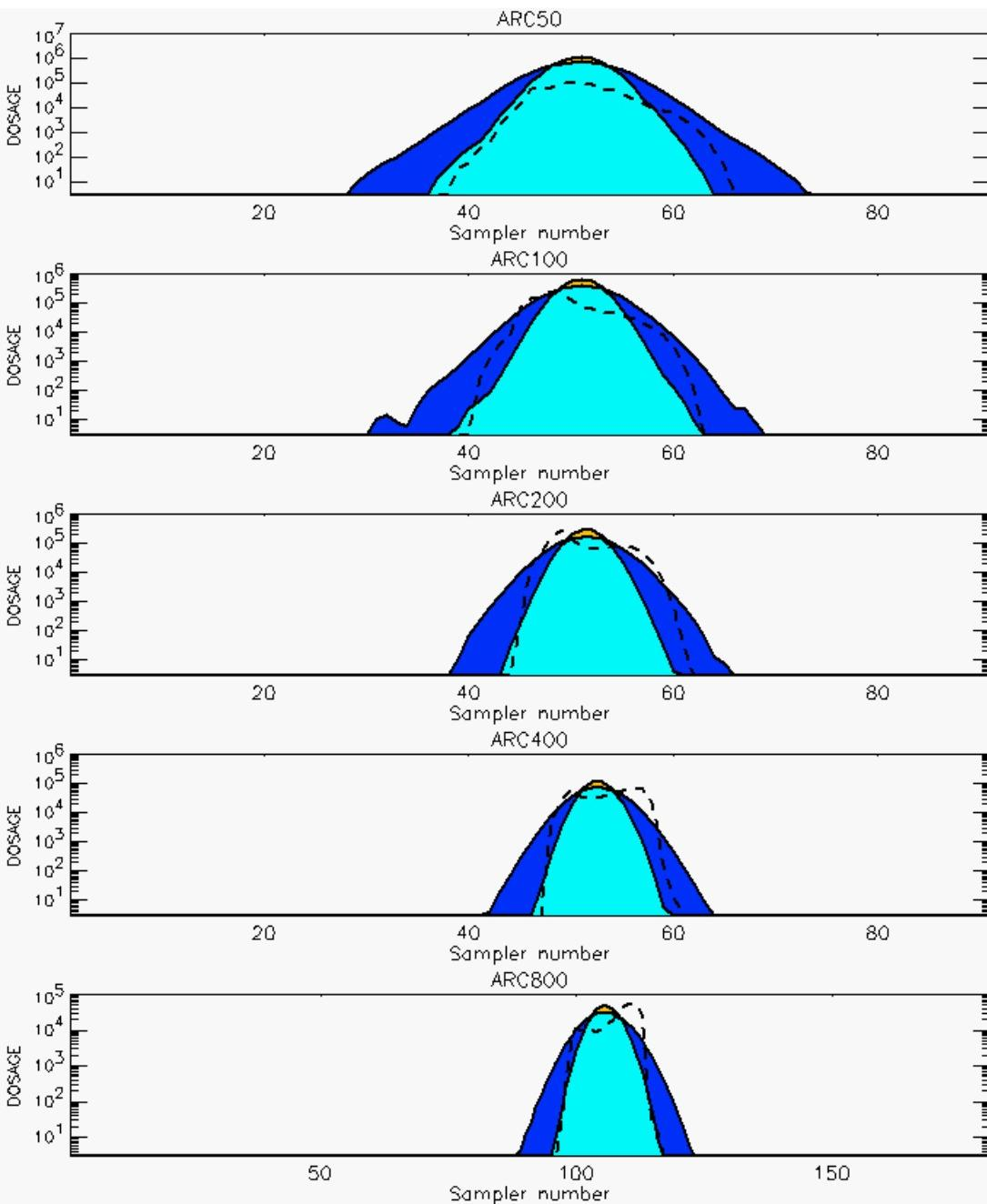
PG Prediction1 to Prediction2 Comparison

PG Trial File: pr_grass_tracer_Experiment_13.txt

PG Prediction File 1: ARAC\nodeposition\pg_13_nozd.arac

PG Prediction File 2: ARAC\sv_nozd\pg_13_sv_nozd.arac

Figure M-8a. NARAC Sigma-v Experimental and Sigma-v Calculated Predictions to Trial 13 on Linear Scale: Stability Category is 7



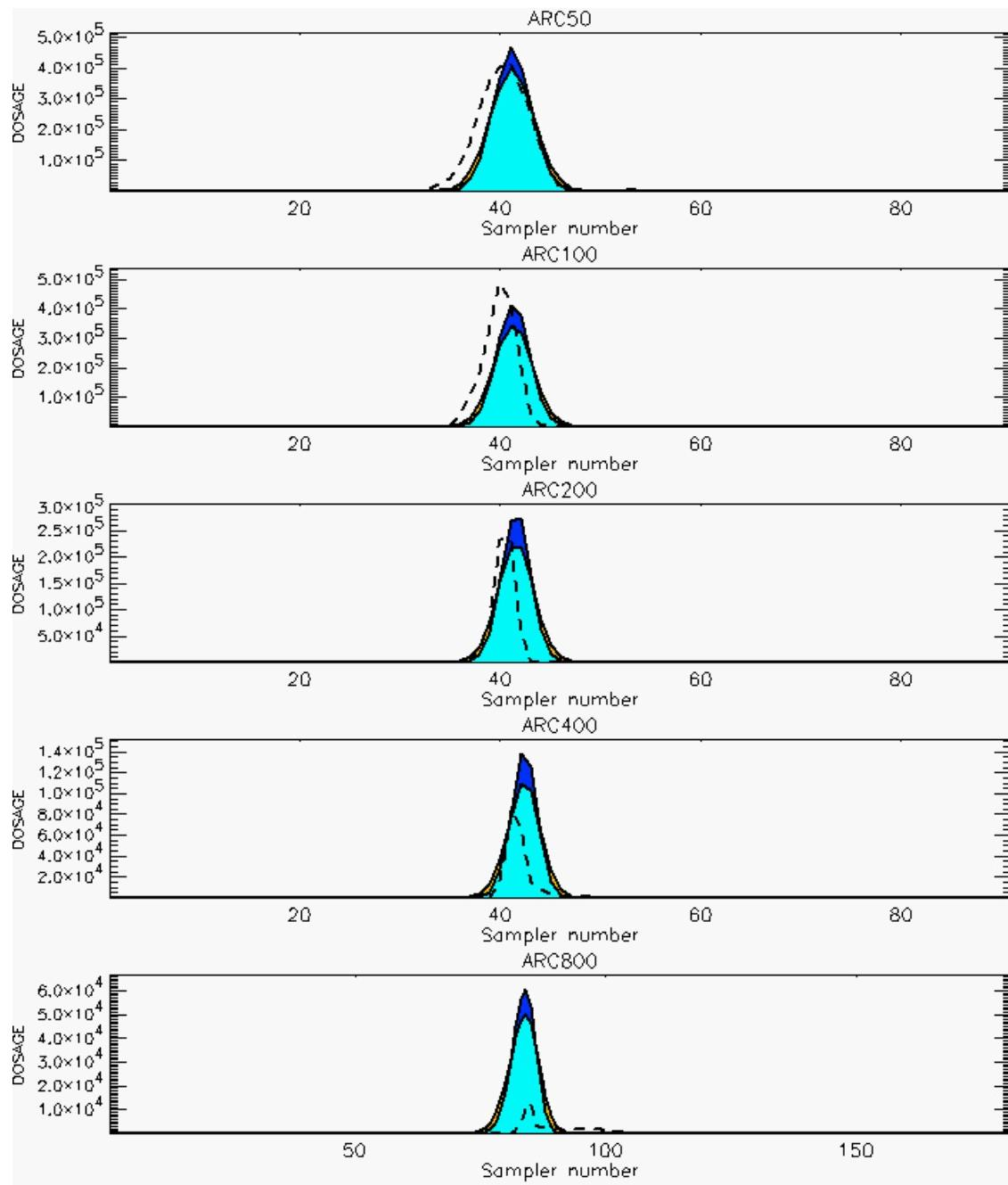
PG Prediction1 to Prediction2 Comparison

PG Trial File: pr_grass_tracer_Experiment_13.txt

PG Prediction File 1: ARAC\nodeposition\pg_13_nozd.arac

PG Prediction File 2: ARAC\sv_nozd\pg_13_sv_nozd.arac

Figure M-8b. NARAC Sigma-v Experimental and Sigma-v Calculated Predictions to Trial 13 on Logarithmic Scale: Stability Category is 7



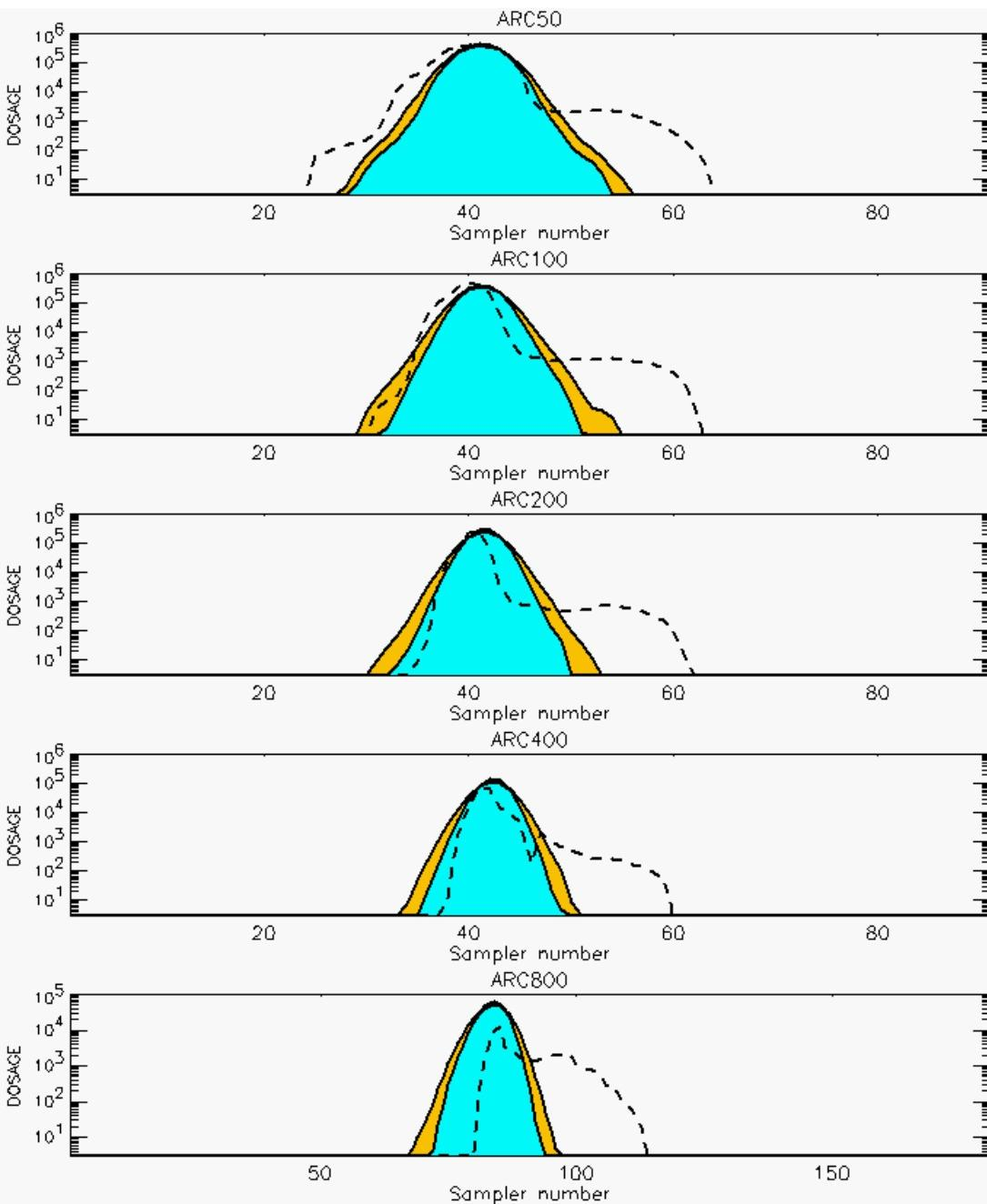
PG Prediction1 to Prediction2 Comparison

PG Trial File: pr_grass_tracer_Experiment_14.txt

PG Prediction File 1: ARAC\nodeposition\pg_14_nozd.arac

PG Prediction File 2: ARAC\sv_nozd\pg_14_sv_nozd.arac

Figure M-9a. NARAC Sigma-v Experimental and Sigma-v Calculated Predictions to Trial 14 on Linear Scale: Stability Category is 7



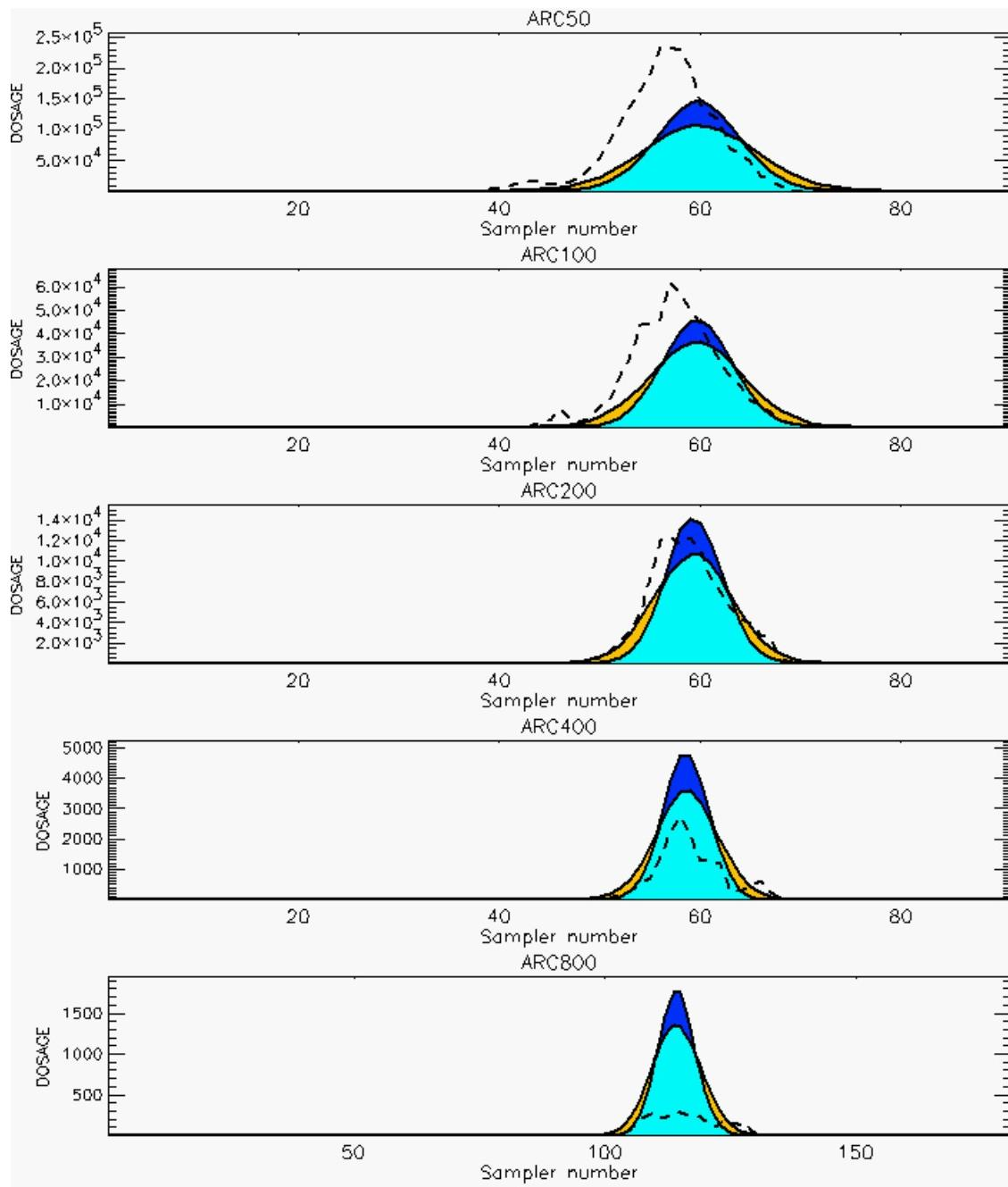
PG Prediction1 to Prediction2 Comparison

PG Trial File: pr_grass_tracer_Experiment_14.txt

PG Prediction File 1: ARAC\nodeposition\pg_14_nozd.arac

PG Prediction File 2: ARAC\sv_nozd\pg_14_sv_nozd.arac

Figure M-9b. NARAC Sigma-v Experimental and Sigma-v Calculated Predictions to Trial 14 on Logarithmic Scale: Stability Category is 7



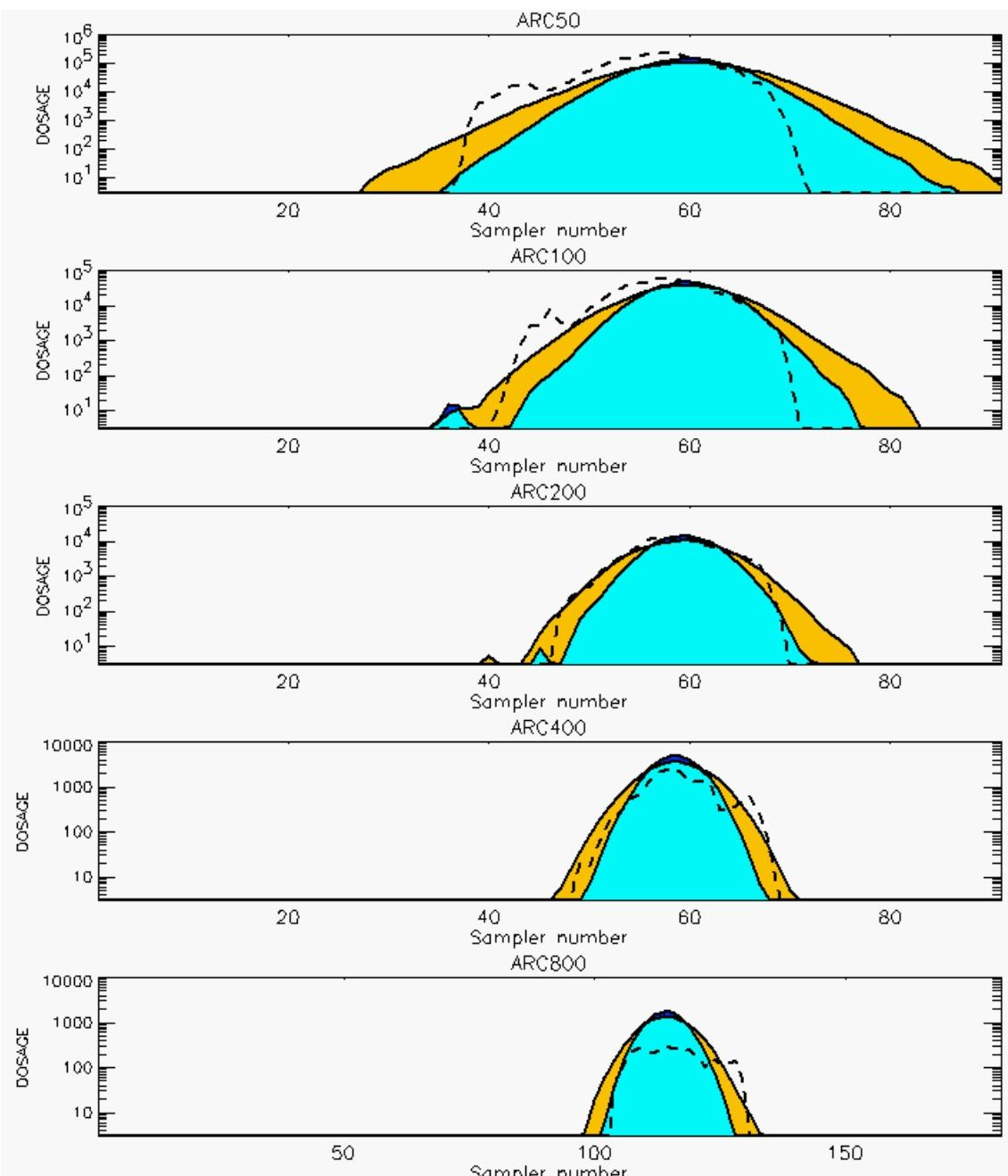
PG Prediction1 to Prediction2 Comparison

PG Trial File: pr_grass_tracer_Experiment_15.txt

PG Prediction File 1: ARAC\nodeposition\pg_15_nozd.arac

PG Prediction File 2: ARAC\sv_nozd\pg_15_sv_nozd.arac

Figure M-10a. NARAC Sigma-v Experimental and Sigma-v Calculated Predictions to Trial 15 on Linear Scale: Stability Category is 1



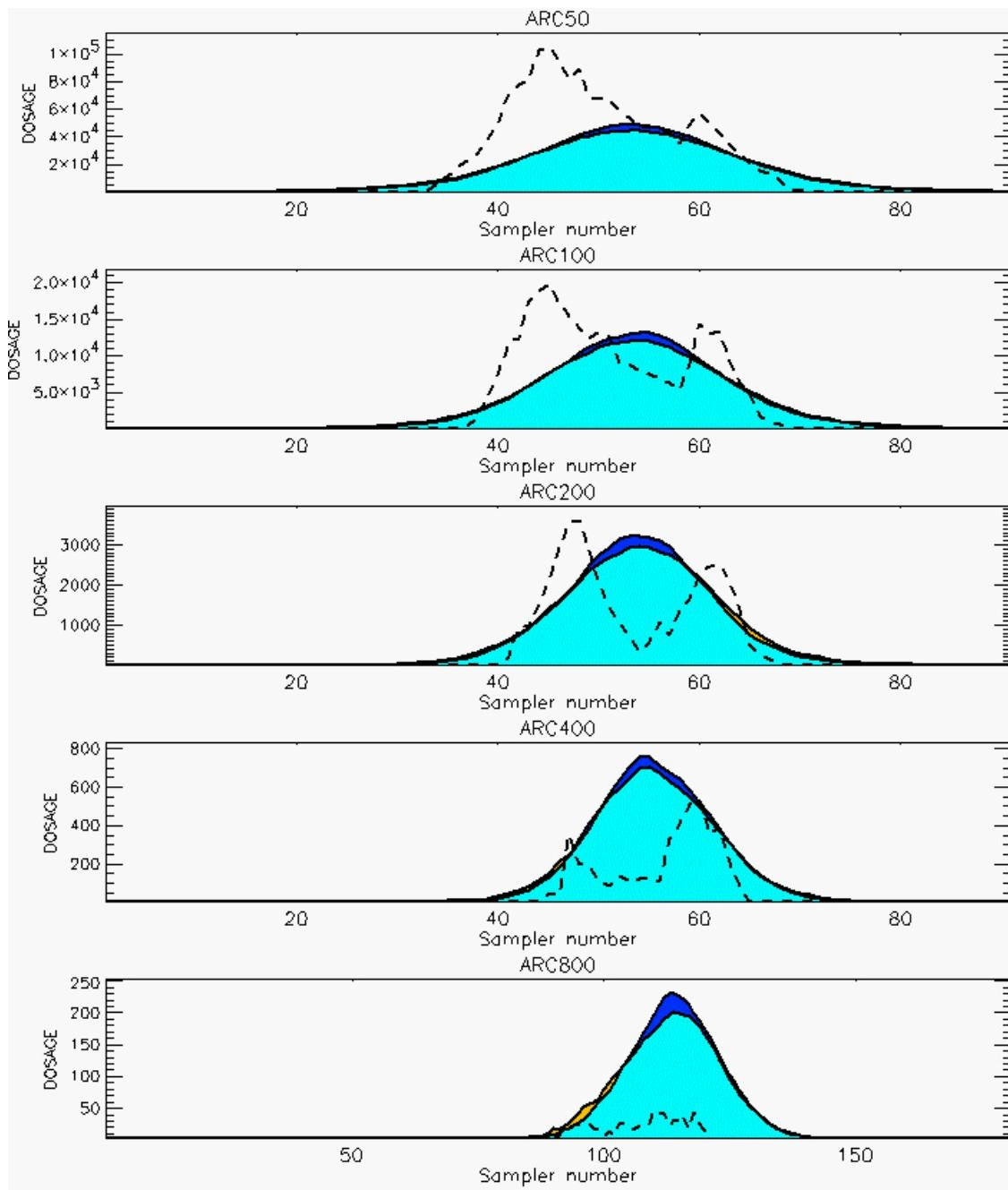
PG Prediction1 to Prediction2 Comparison

PG Trial File: pr_grass_tracer_Experiment_15.txt

PG Prediction File 1: ARAC\nodeposition\pg_15_nozd.arac

PG Prediction File 2: ARAC\sv_nzd\pg_15_sv_nzd.arac

Figure M-10b. NARAC Sigma-v Experimental and Sigma-v Calculated Predictions to Trial 15 on Logarithmic Scale: Stability Category is 1



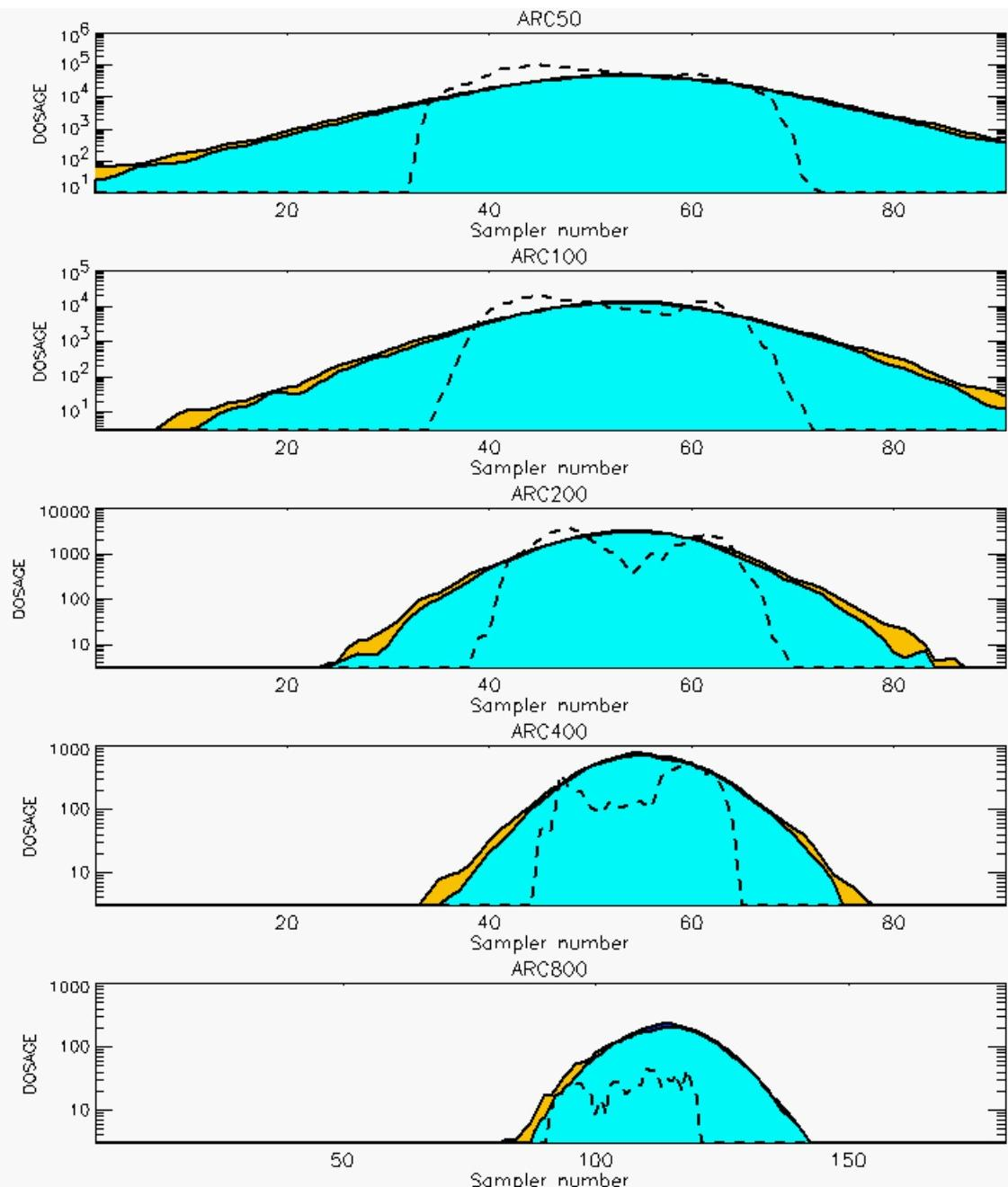
PG Prediction1 to Prediction2 Comparison

PG Trial File: pr_grass_tracer_Experiment_16.txt

PG Prediction File 1: ARAC\nodeposition\pg_16_nozd.arac

PG Prediction File 2: ARAC\sv_nzd\pg_16_sv_nzd.arac

Figure M-11a. NARAC Sigma-v Experimental and Sigma-v Calculated Predictions to Trial 16 on Linear Scale: Stability Category is1



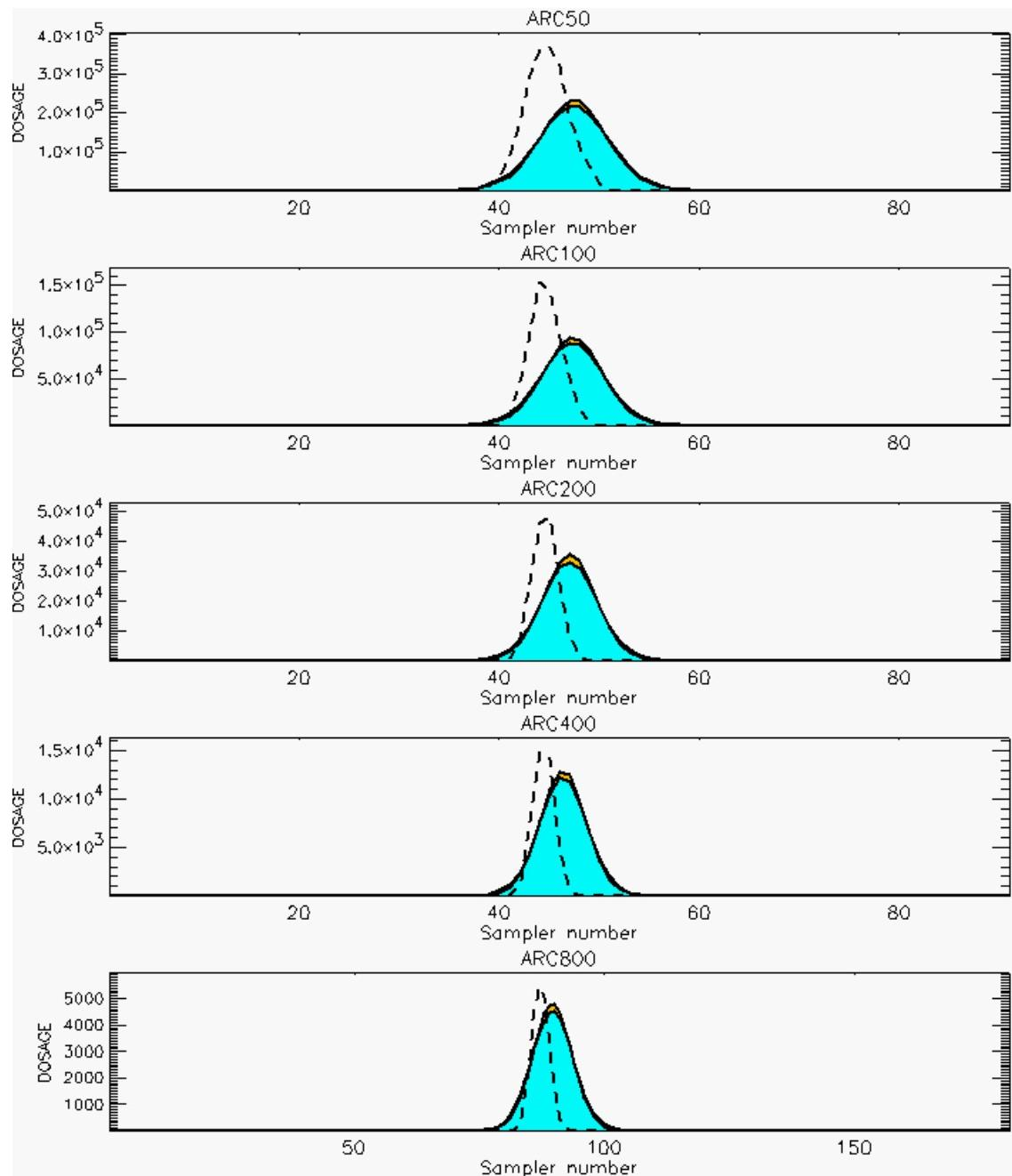
PG Prediction1 to Prediction2 Comparison

PG Trial File: pr_grass_tracer_Experiment_16.txt

PG Prediction File 1: ARAC\nodeposition\pg_16_nozd.arac

PG Prediction File 2: ARAC\sv_nozd\pg_16_sv_nozd.arac

Figure M-11b. NARAC Sigma-v Experimental and Sigma-v Calculated Predictions to Trial 16 on Logarithmic Scale: Stability Category is1



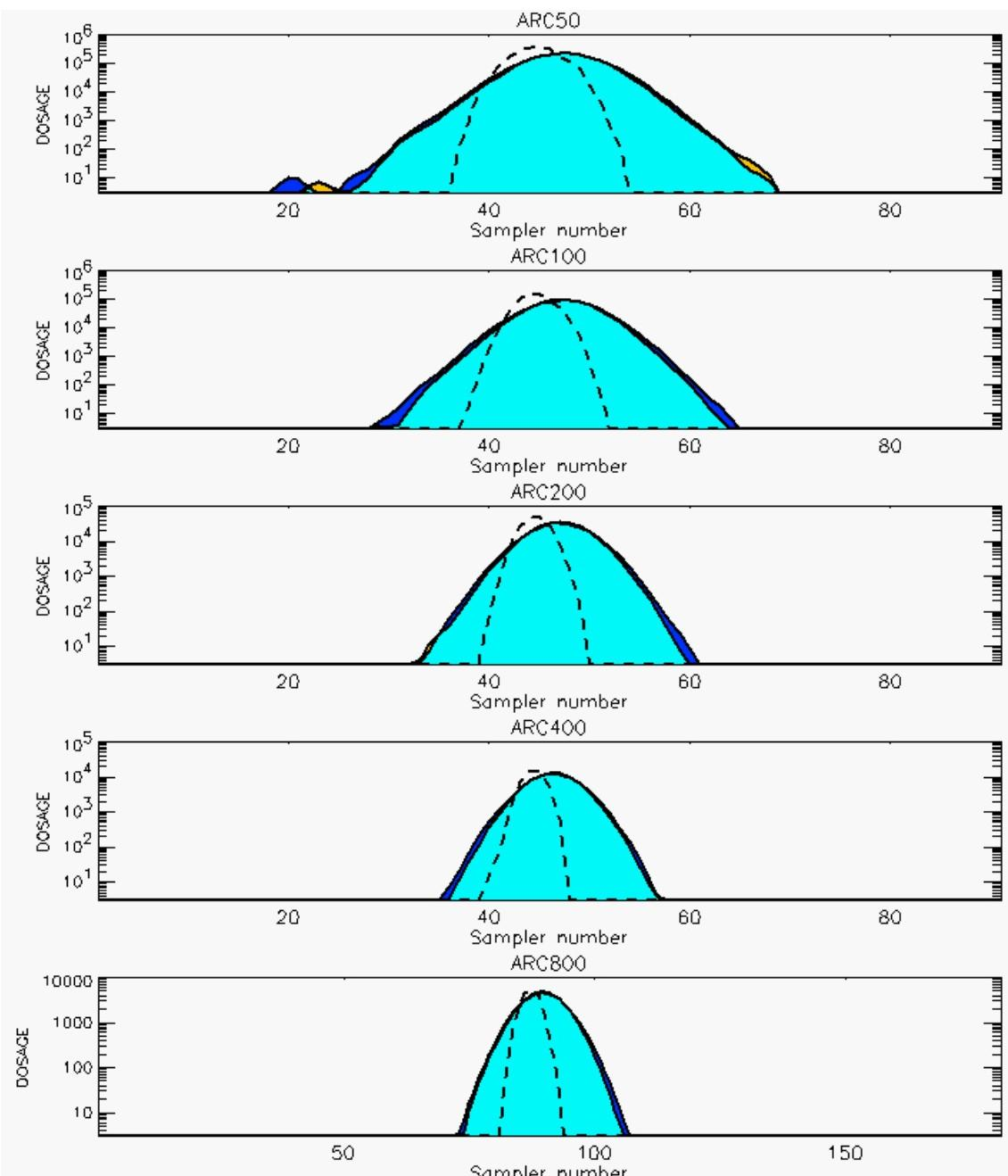
PG Prediction1 to Prediction2 Comparison

PG Trial File: pr_grass_tracer_Experiment_17.txt

PG Prediction File 1: ARAC\nodeposition\pg_17_noxd.arac

PG Prediction File 2: ARAC\sv_noxd\pg_17_sv_noxd.arac

Figure M-12a. NARAC Sigma-v Experimental and Sigma-v Calculated Predictions to Trial 17 on Linear Scale: Stability Category is 5



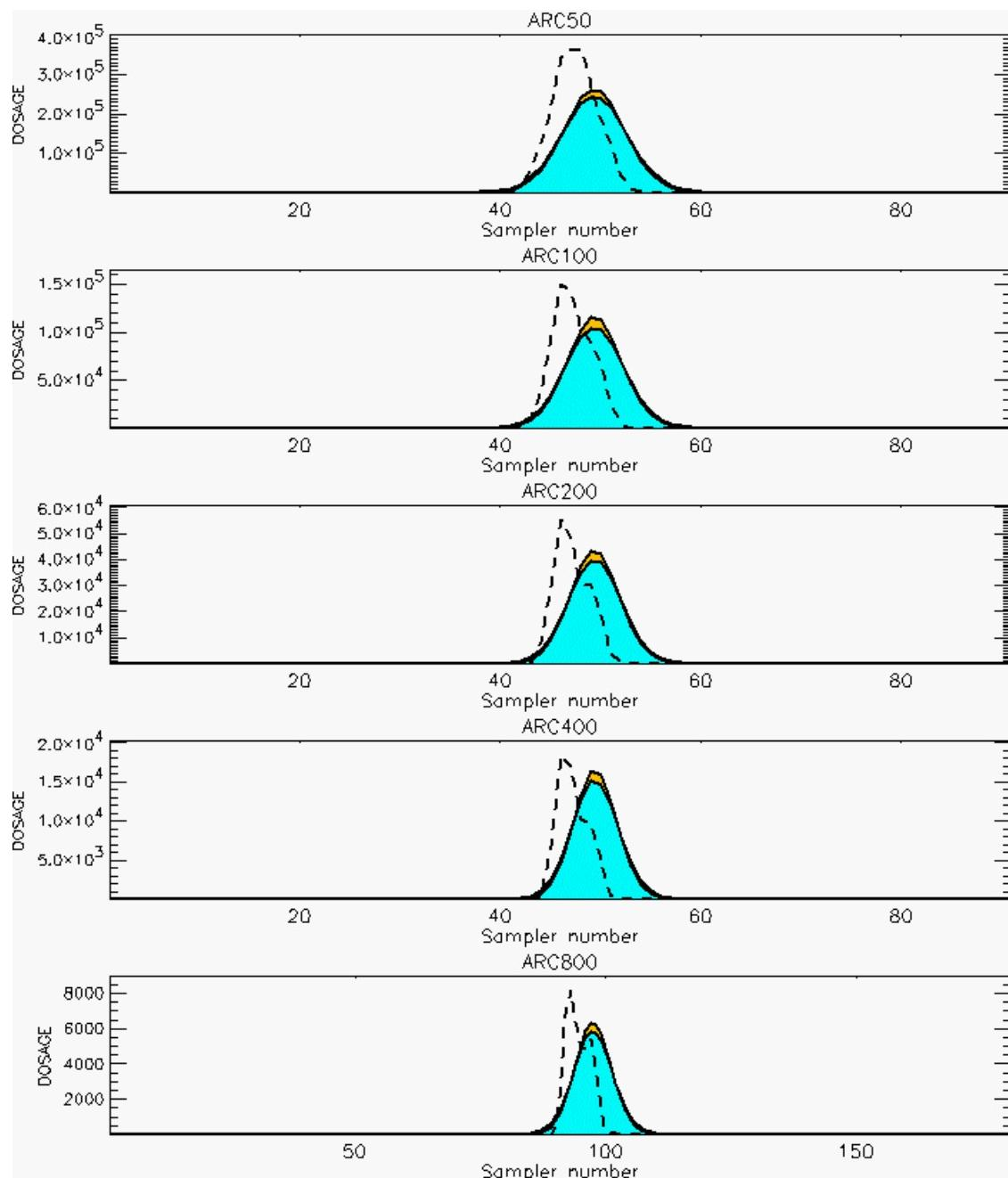
PG Prediction1 to Prediction2 Comparison

PG Trial File: pr_grass_tracer_Experiment_17.txt

PG Prediction File 1: ARAC\nodeposition\pg_17_noxd.arac

PG Prediction File 2: ARAC\sv_noxd\pg_17_sv_noxd.arac

Figure M-12b. NARAC Sigma-v Experimental and Sigma-v Calculated Predictions to Trial 17 on Logarithmic Scale: Stability Category is 5



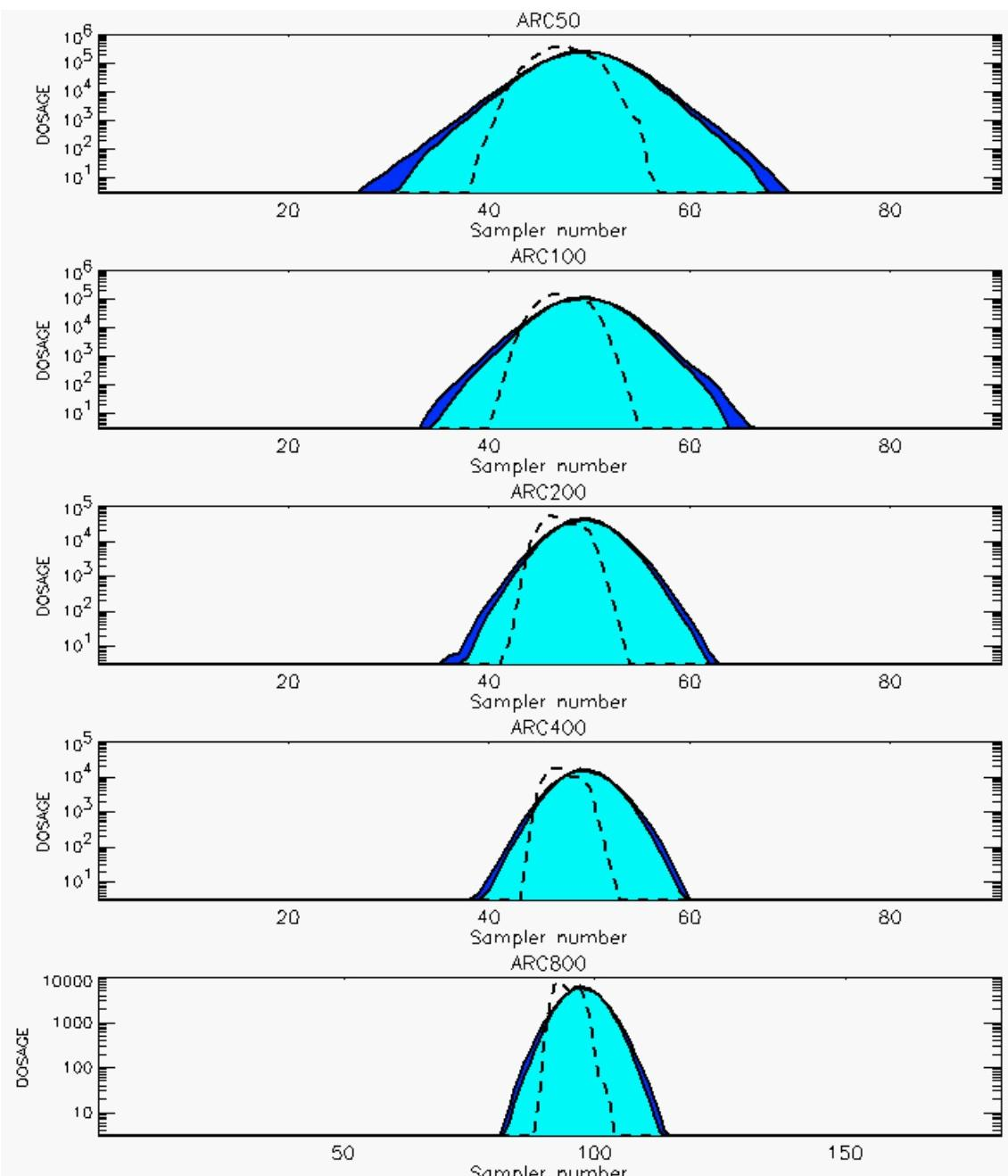
PG Prediction1 to Prediction2 Comparison

PG Trial File: pr_grass_tracer_Experiment_18.txt

PG Prediction File 1: ARAC\nodeposition\pg_18_nozd.arac

PG Prediction File 2: ARAC\sv_nozd\pg_18_sv_nozd.arac

Figure M-13a. NARAC Sigma-v Experimental and Sigma-v Calculated Predictions to Trial 18 on Linear Scale: Stability Category is 5



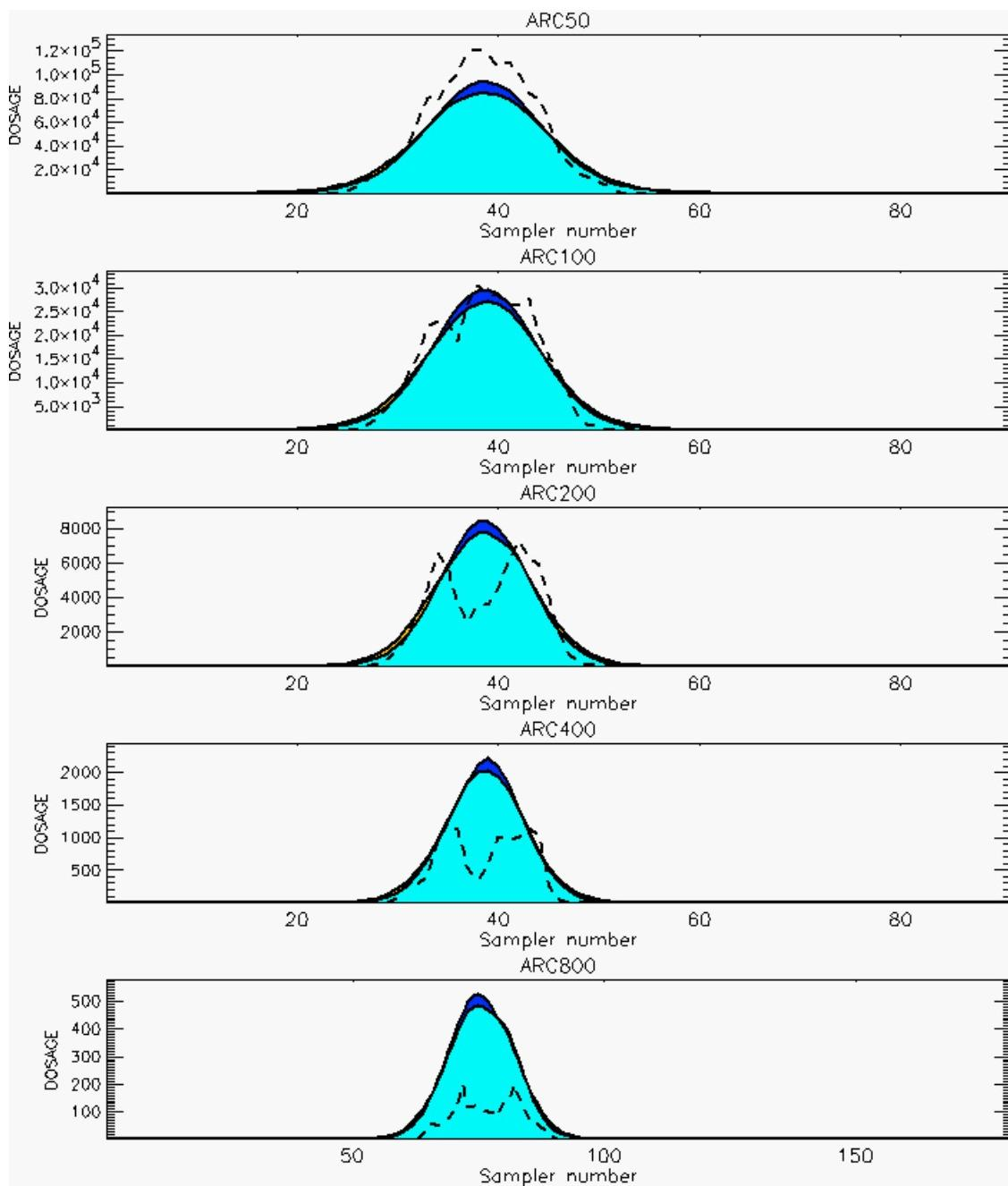
PG Prediction1 to Prediction2 Comparison

PG Trial File: pr_grass_tracer_Experiment_18.txt

PG Prediction File 1: ARAC\nodeposition\pg_18_nozd.arac

PG Prediction File 2: ARAC\sv_nozd\pg_18_sv_nozd.arac

Figure M-13b. NARAC Sigma-v Experimental and Sigma-v Calculated Predictions to Trial 18 on Logarithmic Scale: Stability Category is 5



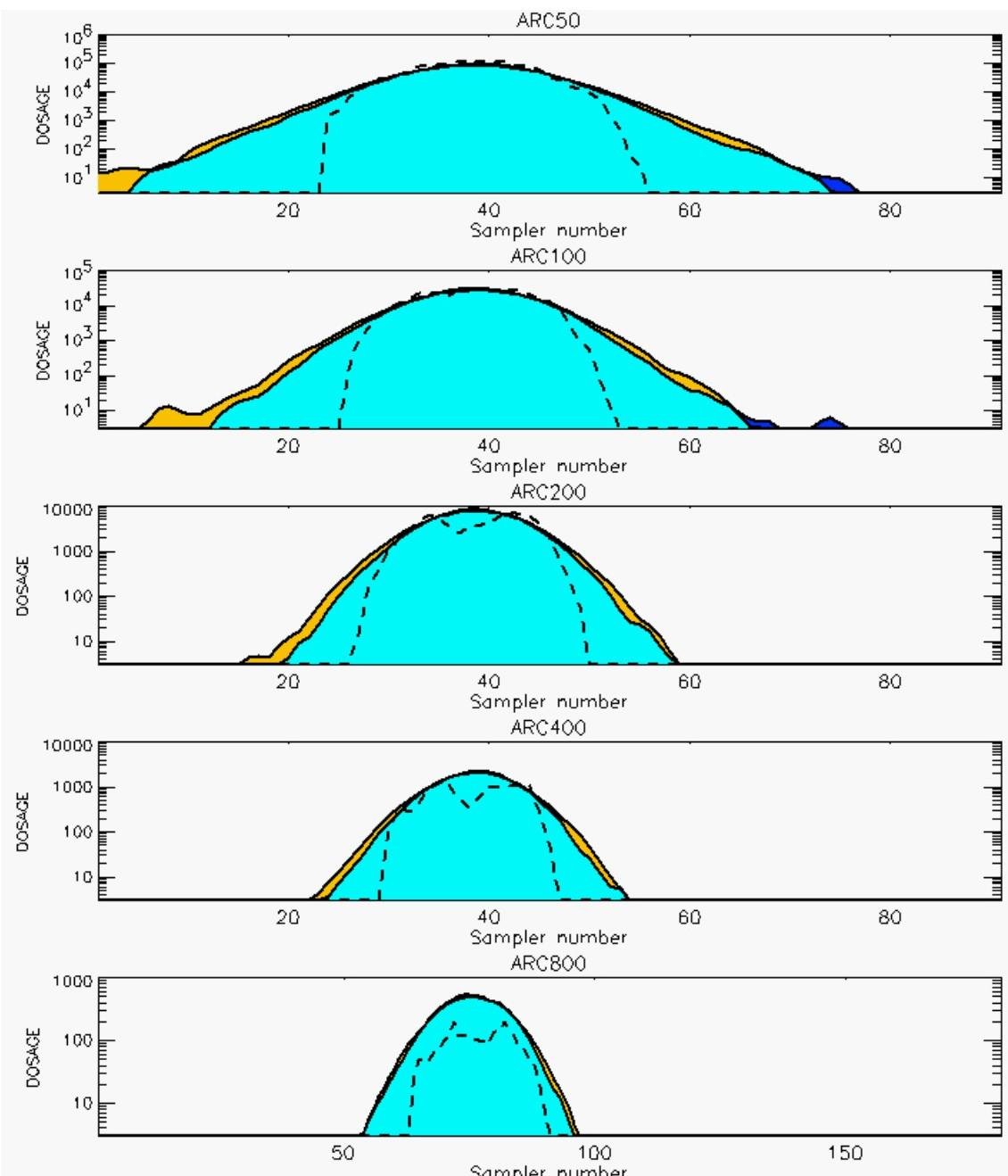
PG Prediction1 to Prediction2 Comparison

PG Trial File: pr_grass_tracer_Experiment_19.txt

PG Prediction File 1: ARAC\nodeposition\pg_19_novd.arac

PG Prediction File 2: ARAC\sv_novd\pg_19_sv_novd.arac

Figure M-14a. NARAC Sigma-v Experimental and Sigma-v Calculated Predictions to Trial 19 on Linear Scale: Stability Category is 2



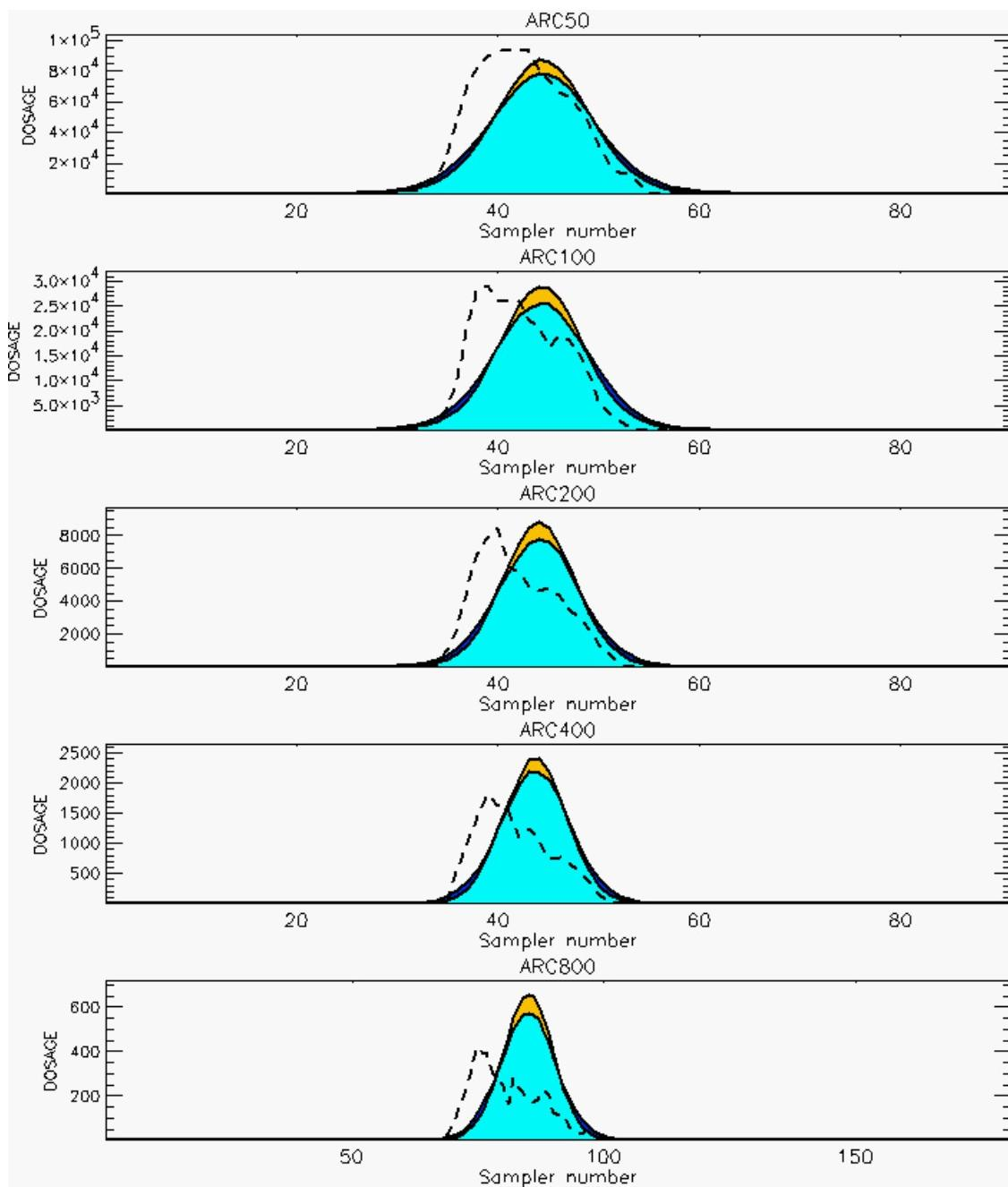
PG Prediction1 to Prediction2 Comparison

PG Trial File: pr_grass_tracer_Experiment_19.txt

PG Prediction File 1: ARAC\nodeposition\pg_19_nozd.arac

PG Prediction File 2: ARAC\sv_nozd\pg_19_sv_nozd.arac

Figure M-14b. NARAC Sigma-v Experimental and Sigma-v Calculated Predictions to Trial 19 on Logarithmic Scale: Stability Category is 2



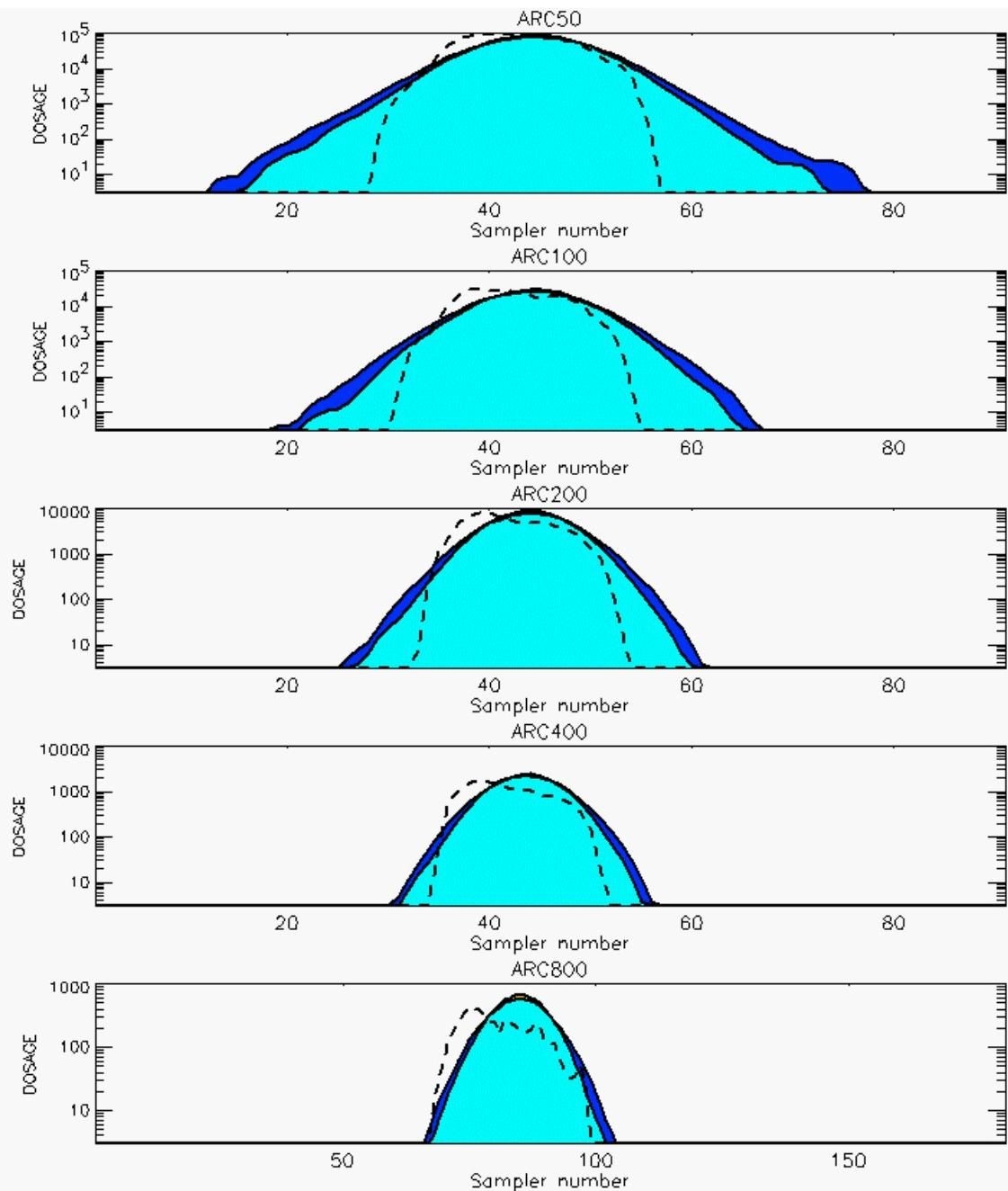
PG Prediction1 to Prediction2 Comparison

PG Trial File: pr_grass_tracer_Experiment_20.txt

PG Prediction File 1: ARAC\nodeposition\pg_20_nozd.arac

PG Prediction File 2: ARAC\sv_nozd\pg_20_sv_nozd.arac

Figure M-15a. NARAC Sigma-v Experimental and Sigma-v Calculated Predictions to Trial 20 on Linear Scale: Stability Category is 3



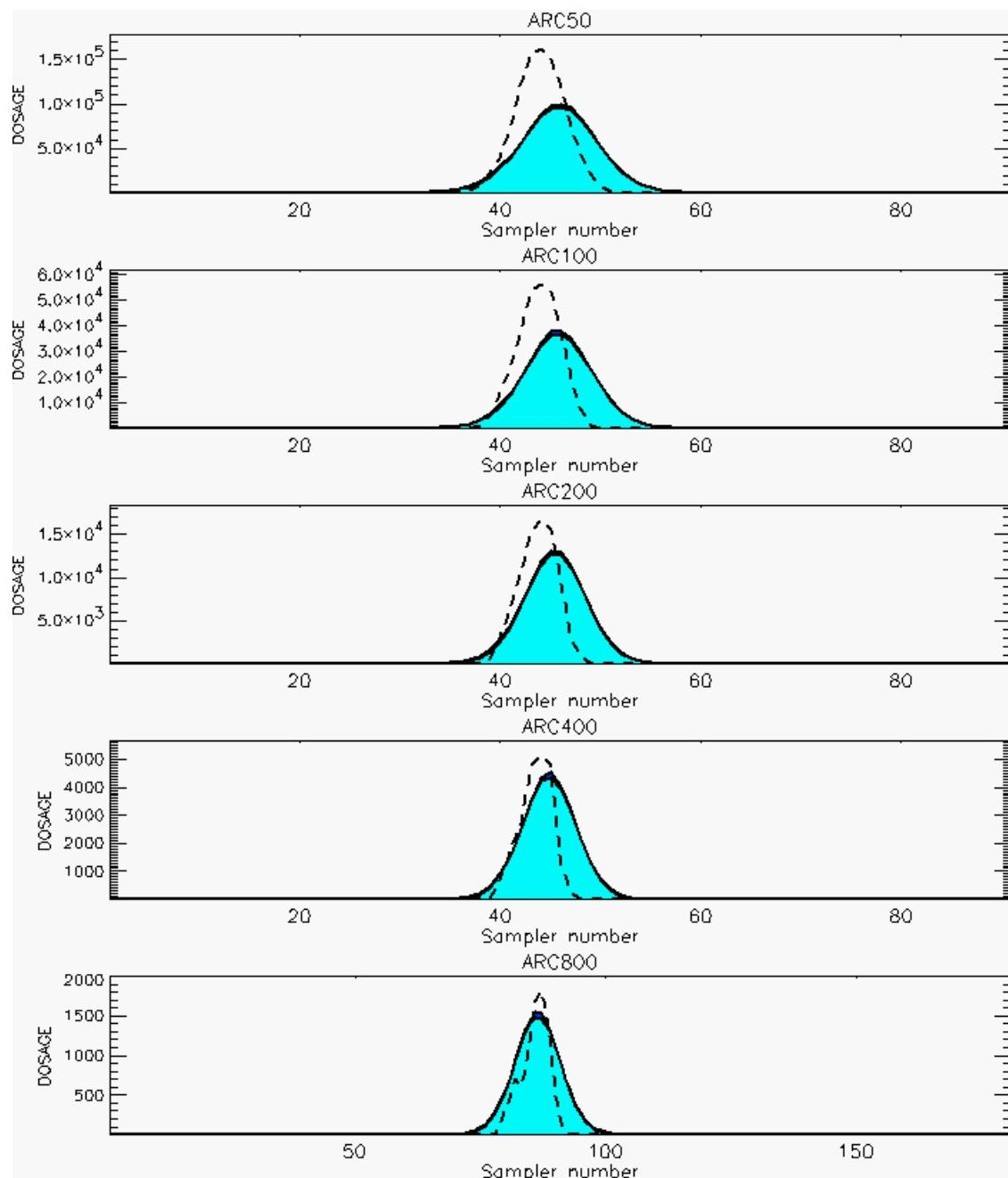
PG Prediction1 to Prediction2 Comparison

PG Trial File: pr_grass_tracer_Experiment_20.txt

PG Prediction File 1: ARAC\nodeposition\pg_20_noxd.arac

PG Prediction File 2: ARAC\sv_noxd\pg_20_sv_noxd.arac

Figure M-15b. NARAC Sigma-v Experimental and Sigma-v Calculated Predictions to Trial 20 on Logarithmic Scale: Stability Category is 3



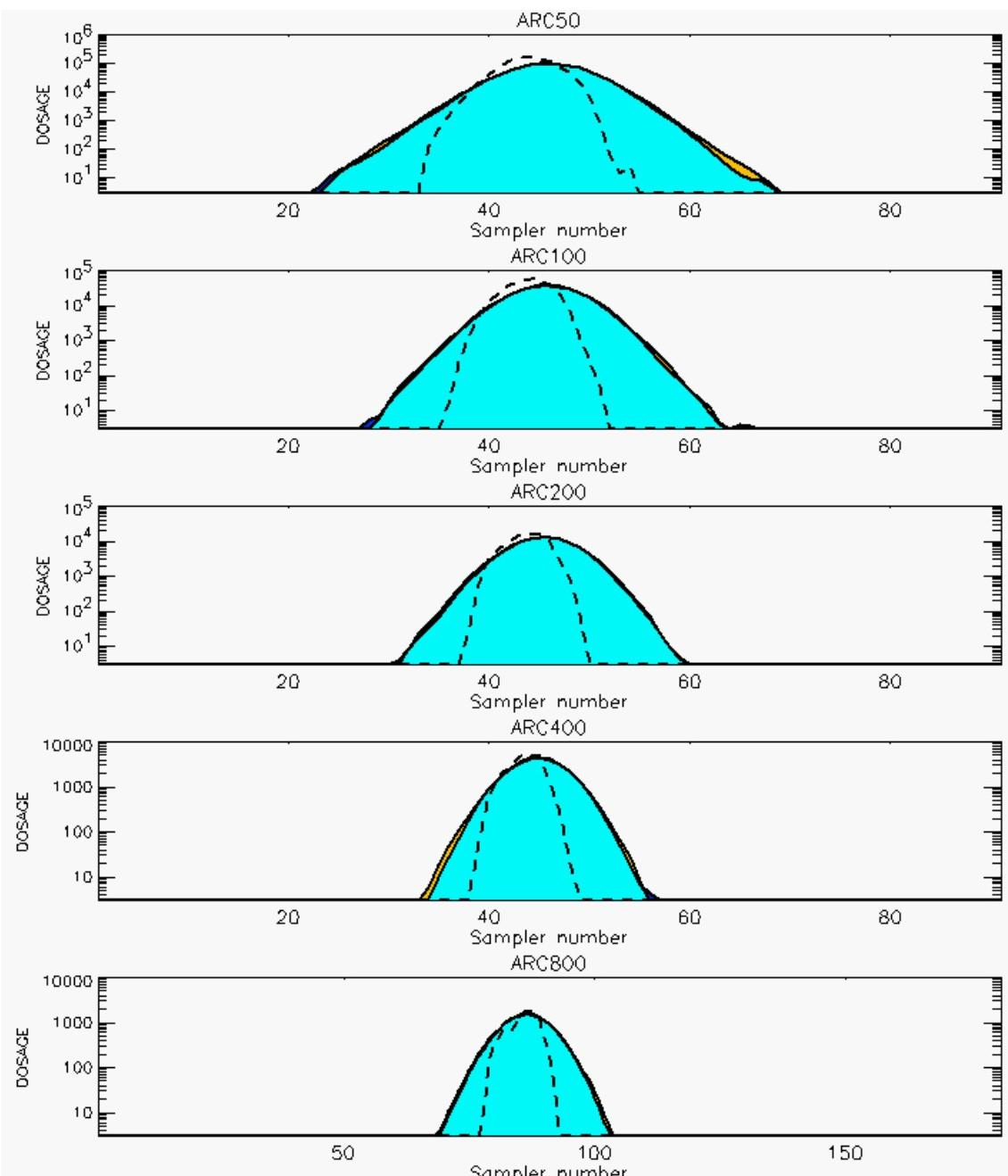
PG Prediction1 to Prediction2 Comparison

PG Trial File: pr_grass_tracer_Experiment_21.txt

PG Prediction File 1: ARAC\nodeposition\pg_21_nozd.arac

PG Prediction File 2: ARAC\sv_nzd\pg_21_sv_nozd.arac

Figure M-16a. NARAC Sigma-v Experimental and Sigma-v Calculated Predictions to Trial 21 on Linear Scale: Stability Category is 4



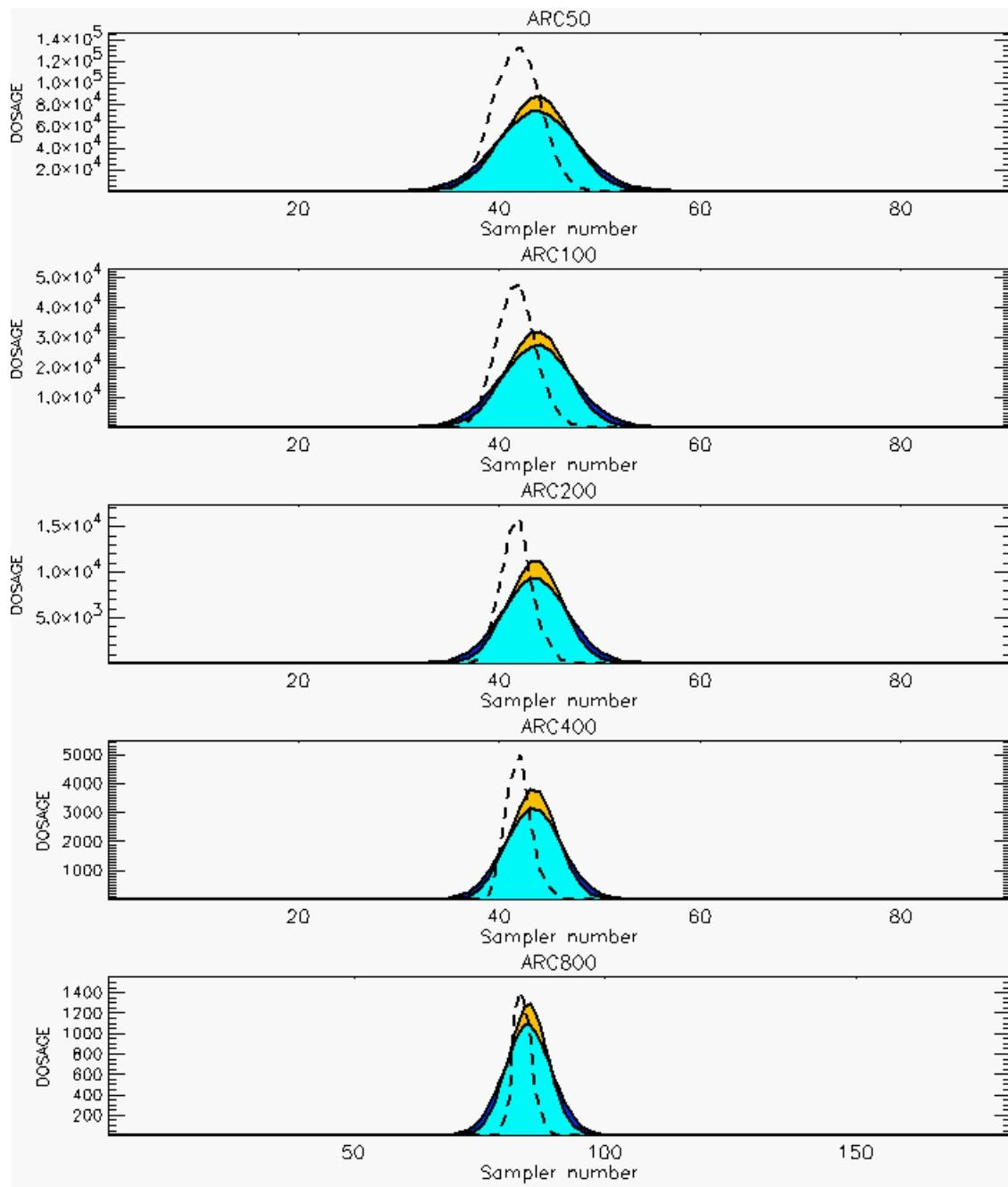
PG Prediction1 to Prediction2 Comparison

PG Trial File: pr_grass_tracer_Experiment_21.txt

PG Prediction File 1: ARAC\nodeposition\pg_21_nozd.arac

PG Prediction File 2: ARAC\sv_nozd\pg_21_sv_nozd.arac

Figure M-16b. NARAC Sigma-v Experimental and Sigma-v Calculated Predictions to Trial 21 on Logarithmic Scale: Stability Category is 4



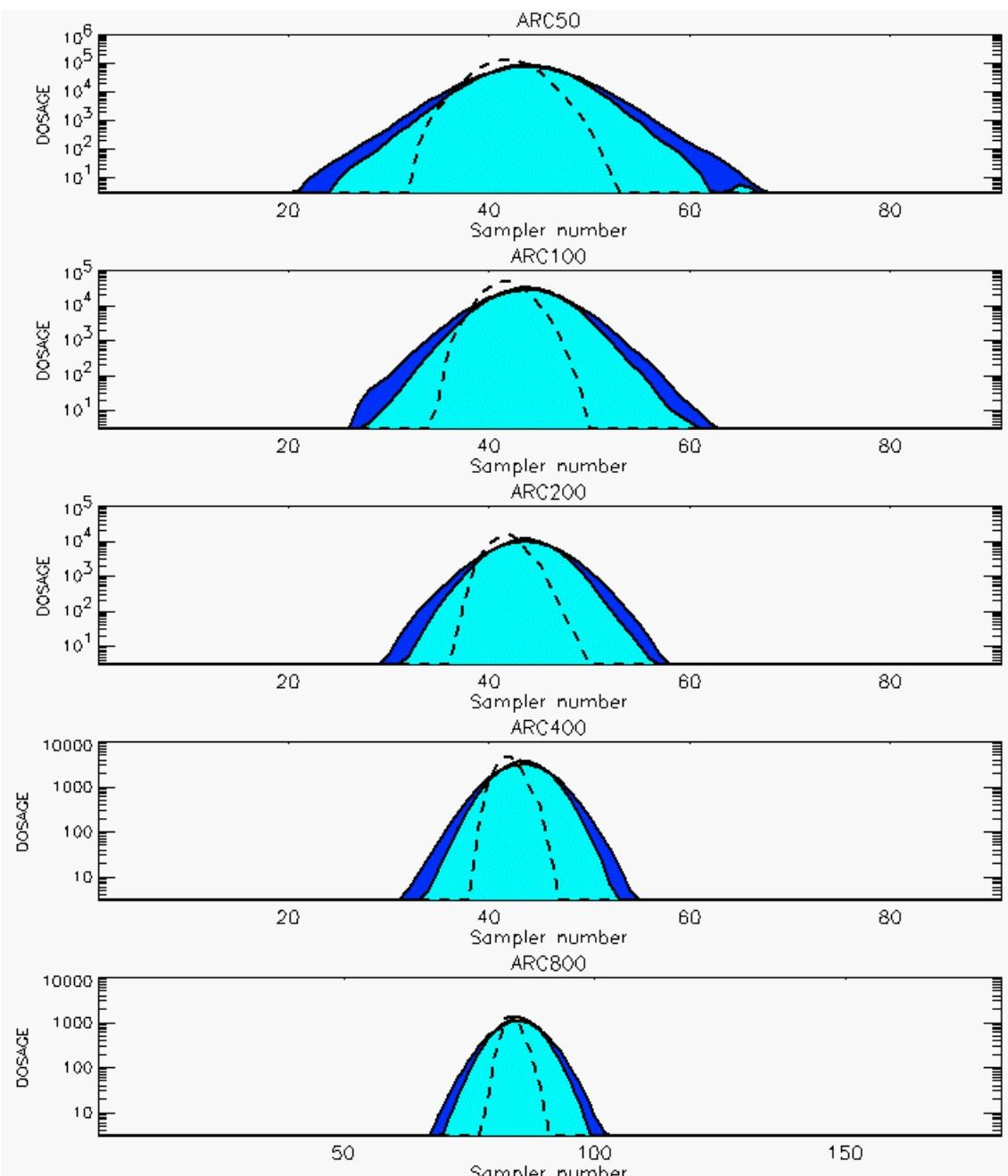
PG Prediction1 to Prediction2 Comparison

PG Trial File: pr_grass_tracer_Experiment_22.txt

PG Prediction File 1: ARAC\nodeposition\pg_22_nozd.arac

PG Prediction File 2: ARAC\sv_nzd\pg_22_sv_nzd.arac

Figure M-17a. NARAC Sigma-v Experimental and Sigma-v Calculated Predictions to Trial 22 on Linear Scale: Stability Category is 4



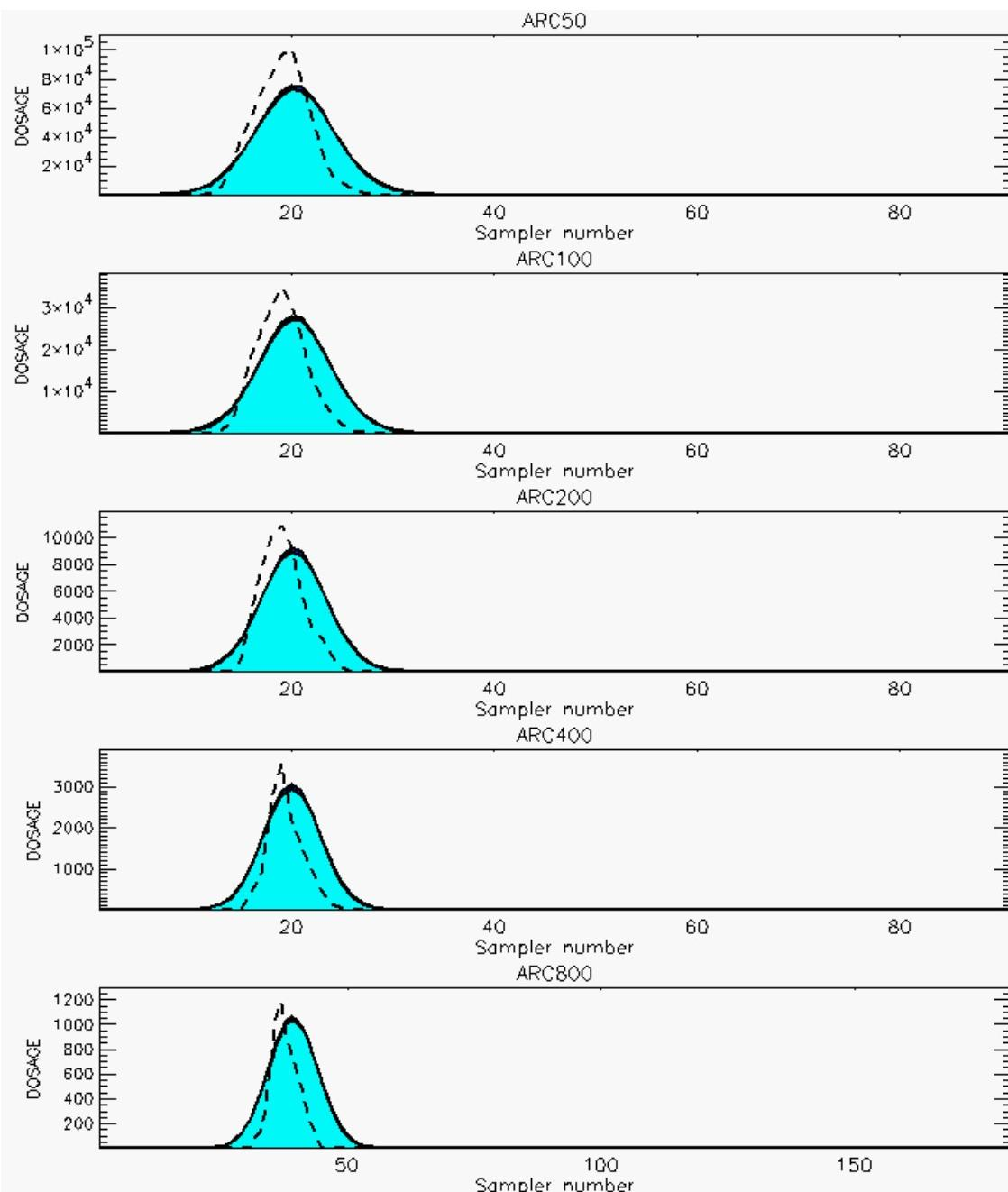
PG Prediction1 to Prediction2 Comparison

PG Trial File: pr_grass_tracer_Experiment_22.txt

PG Prediction File 1: ARAC\nodeposition\pg_22_nozd.arac

PG Prediction File 2: ARAC\sv_nozd\pg_22_sv_nozd.arac

Figure M-17b. NARAC Sigma-v Experimental and Sigma-v Calculated Predictions to Trial 22 on Logarithmic Scale: Stability Category is 4



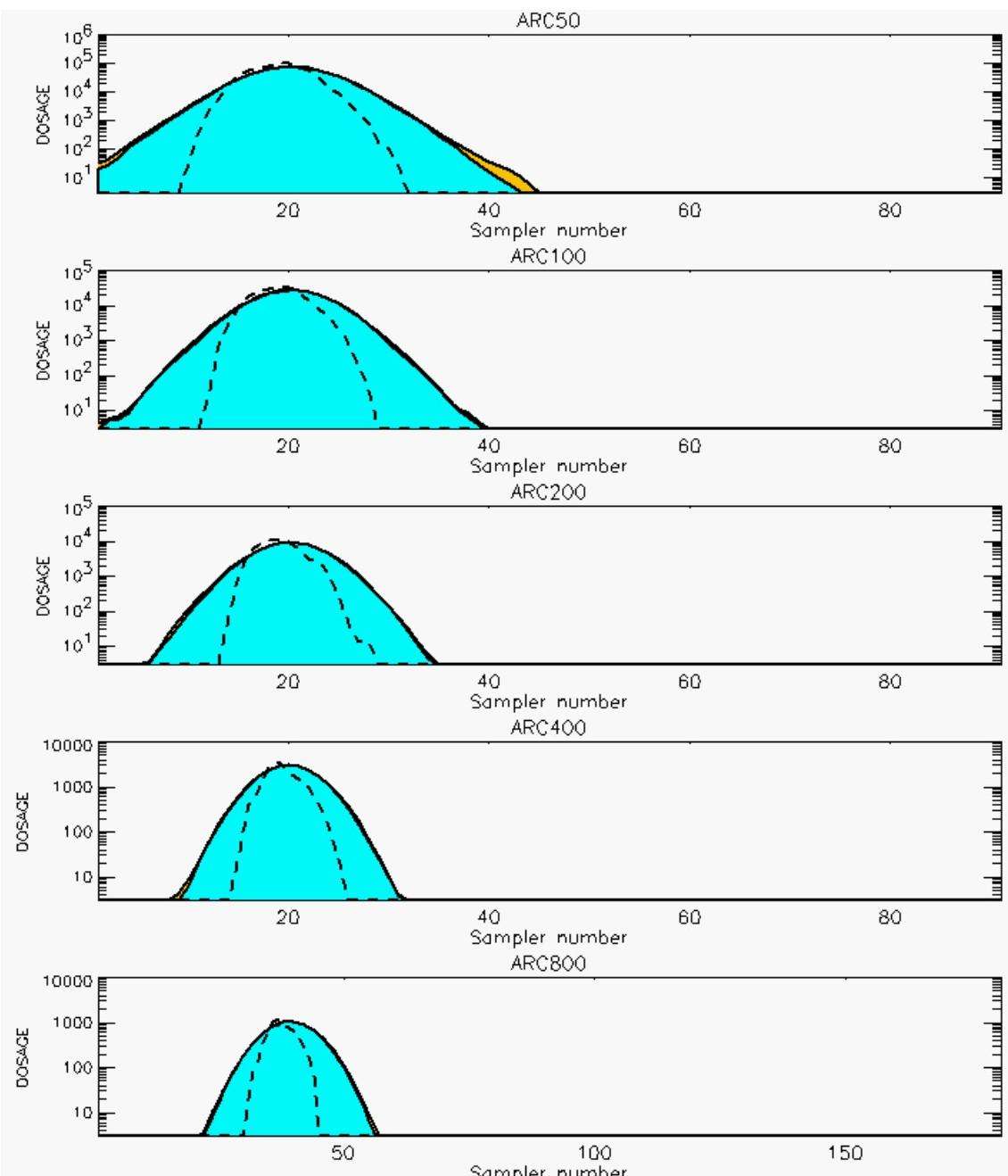
PG Prediction1 to Prediction2 Comparison

PG Trial File: pr_grass_tracer_Experiment_23.txt

PG Prediction File 1: ARAC\nodeposition\pg_23_nozd.arac

PG Prediction File 2: ARAC\sv_nozd\pg_23_sv_nozd.arac

Figure M-18a. NARAC Sigma-v Experimental and Sigma-v Calculated Predictions to Trial 23 on Linear Scale: Stability Category is 4



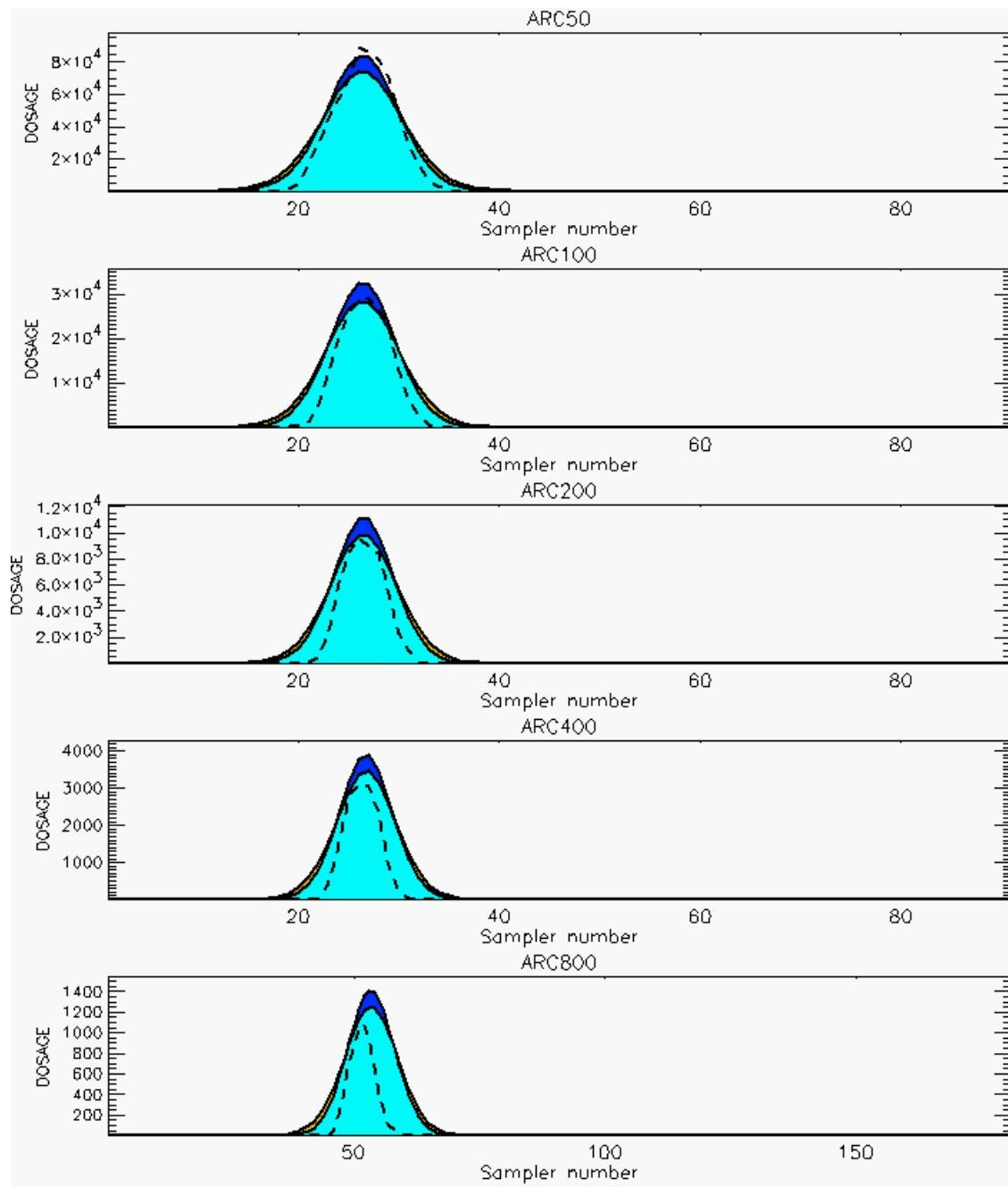
PG Prediction1 to Prediction2 Comparison

PG Trial File: pr_grass_tracer_Experiment_23.txt

PG Prediction File 1: ARAC\nodeposition\pg_23_novd.arac

PG Prediction File 2: ARAC\sv_novd\pg_23_sv_novd.arac

Figure M-18b. NARAC Sigma-v Experimental and Sigma-v Calculated Predictions to Trial 23 on Logarithmic Scale: Stability Category is 4



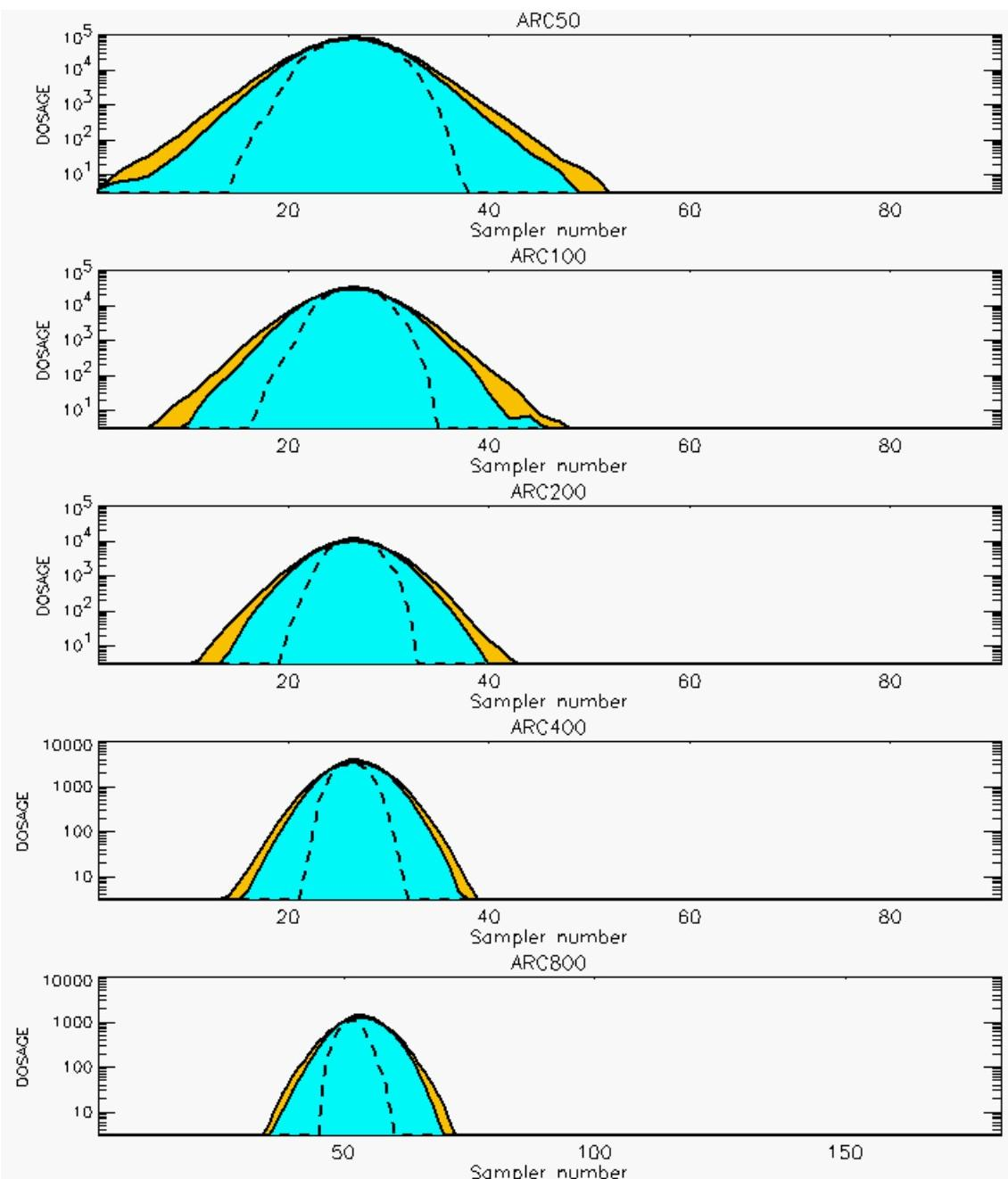
PG Prediction1 to Prediction2 Comparison

PG Trial File: pr_grass_tracer_Experiment_24.txt

PG Prediction File 1: ARAC\nodeposition\pg_24_nozd.arac

PG Prediction File 2: ARAC\sv_nozd\pg_24_sv_nozd.arac

Figure M-19a. NARAC Sigma-v Experimental and Sigma-v Calculated Predictions to Trial 24 on Linear Scale: Stability Category is 4



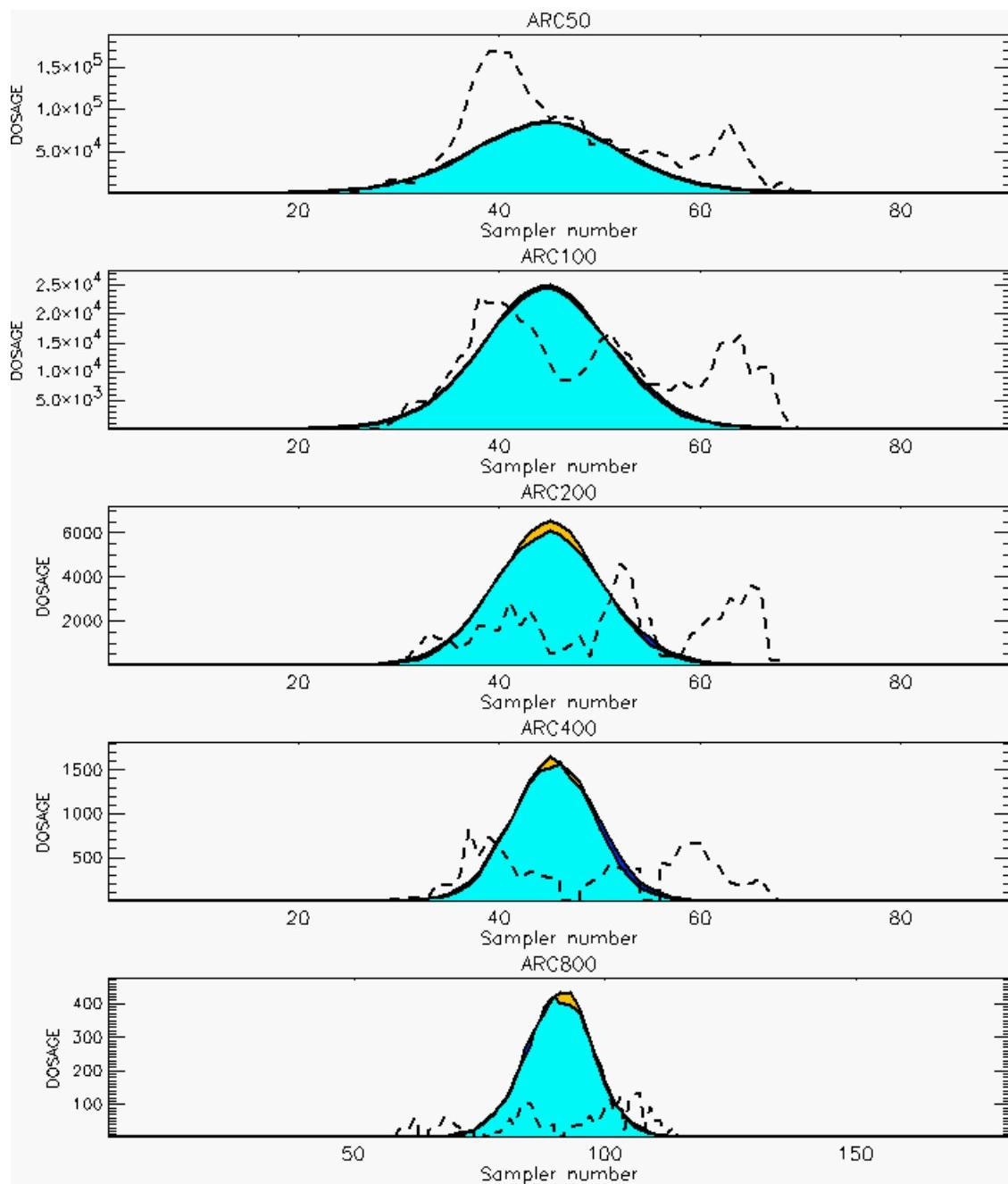
PG Prediction1 to Prediction2 Comparison

PG Trial File: pr_grass_tracer_Experiment_24.txt

PG Prediction File 1: ARAC\nodeposition\pg_24_nozd.arac

PG Prediction File 2: ARAC\sv_nozd\pg_24_sv_nozd.arac

Figure M-19b. NARAC Sigma-v Experimental and Sigma-v Calculated Predictions to Trial 24 on Logarithmic Scale: Stability Category is 4



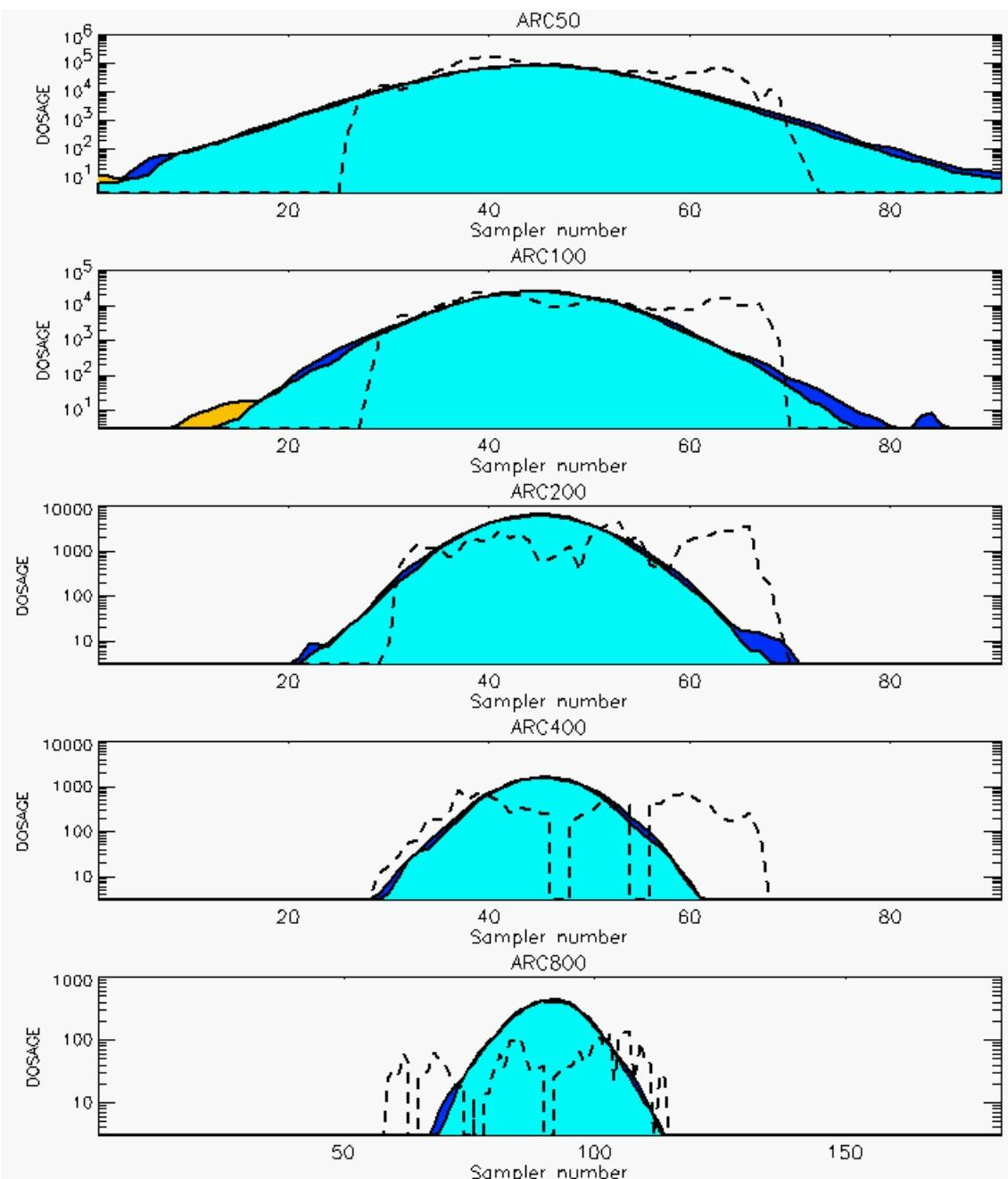
PG Prediction1 to Prediction2 Comparison

PG Trial File: pr_grass_tracer_Experiment_25.txt

PG Prediction File 1: ARAC\nodeposition\pg_25_novd.arac

PG Prediction File 2: ARAC\sv_novd\pg_25_sv_novd.arac

Figure M-20a. NARAC Sigma-v Experimental and Sigma-v Calculated Predictions to Trial 25 on Linear Scale: Stability Category is1



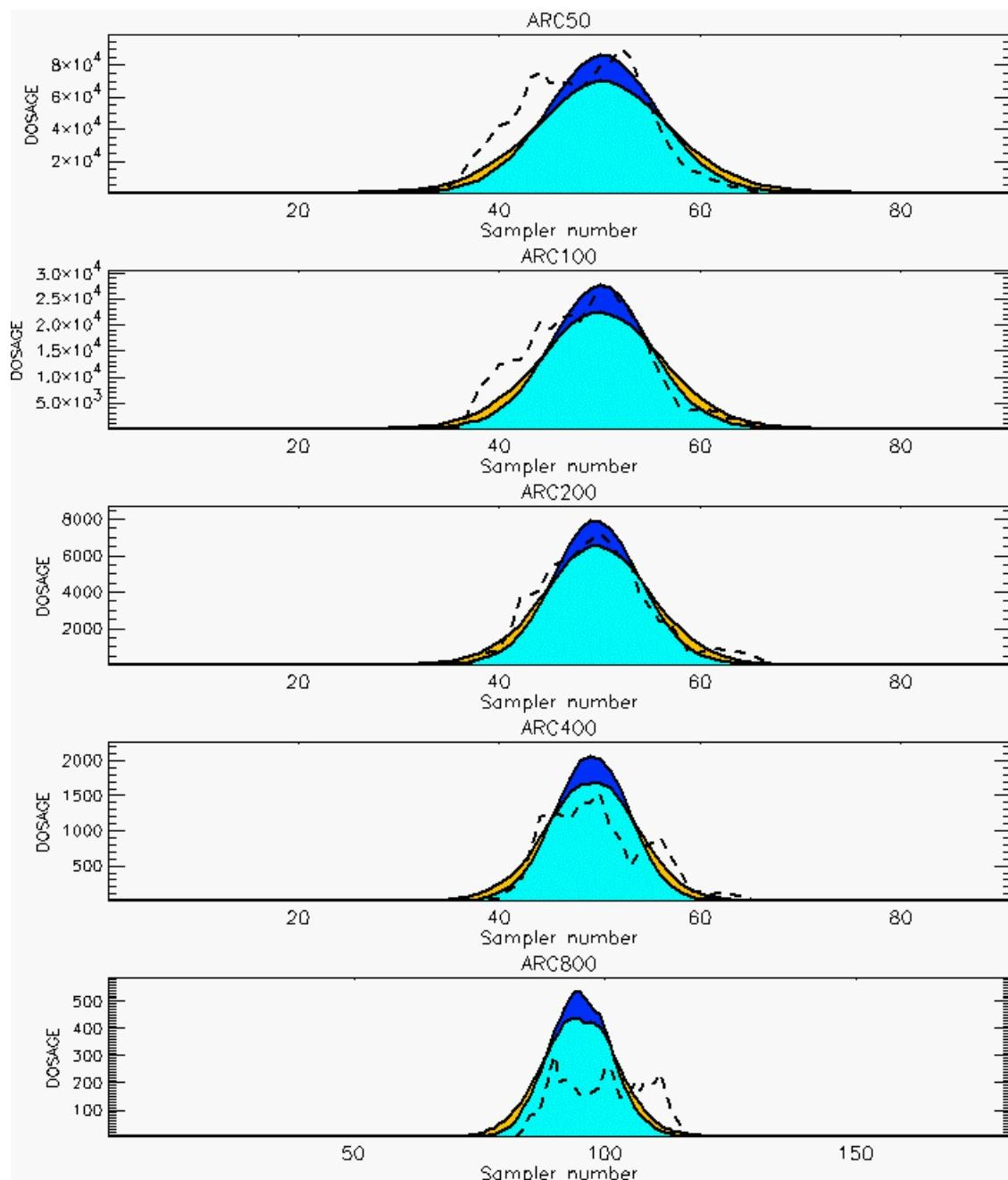
PG Prediction1 to Prediction2 Comparison

PG Trial File: pr_grass_tracer_Experiment_25.txt

PG Prediction File 1: ARAC\nodeposition\pg_25_novd.arac

PG Prediction File 2: ARAC\sv_novd\pg_25_sv_novd.arac

Figure M-20b. NARAC Sigma-v Experimental and Sigma-v Calculated Predictions to Trial 25 on Logarithmic Scale: Stability Category is1



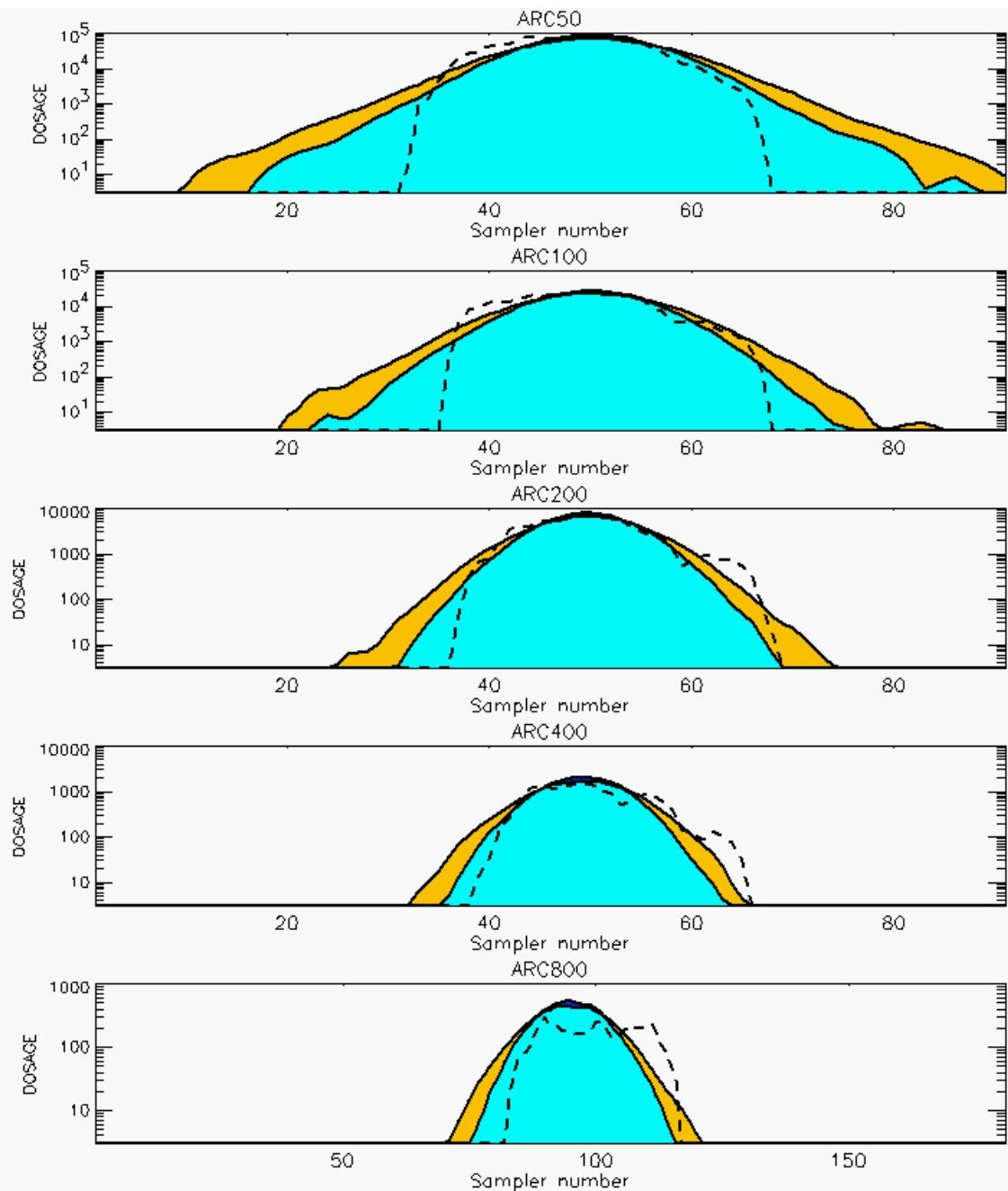
PG Prediction1 to Prediction2 Comparison

PG Trial File: pr_grass_tracer_Experiment_26.txt

PG Prediction File 1: ARAC\nodeposition\pg_26_nozd.arac

PG Prediction File 2: ARAC\sv_nzd\pg_26_sv_nzd.arac

Figure M-21a. NARAC Sigma-v Experimental and Sigma-v Calculated Predictions to Trial 26 on Linear Scale: Stability Category is 2



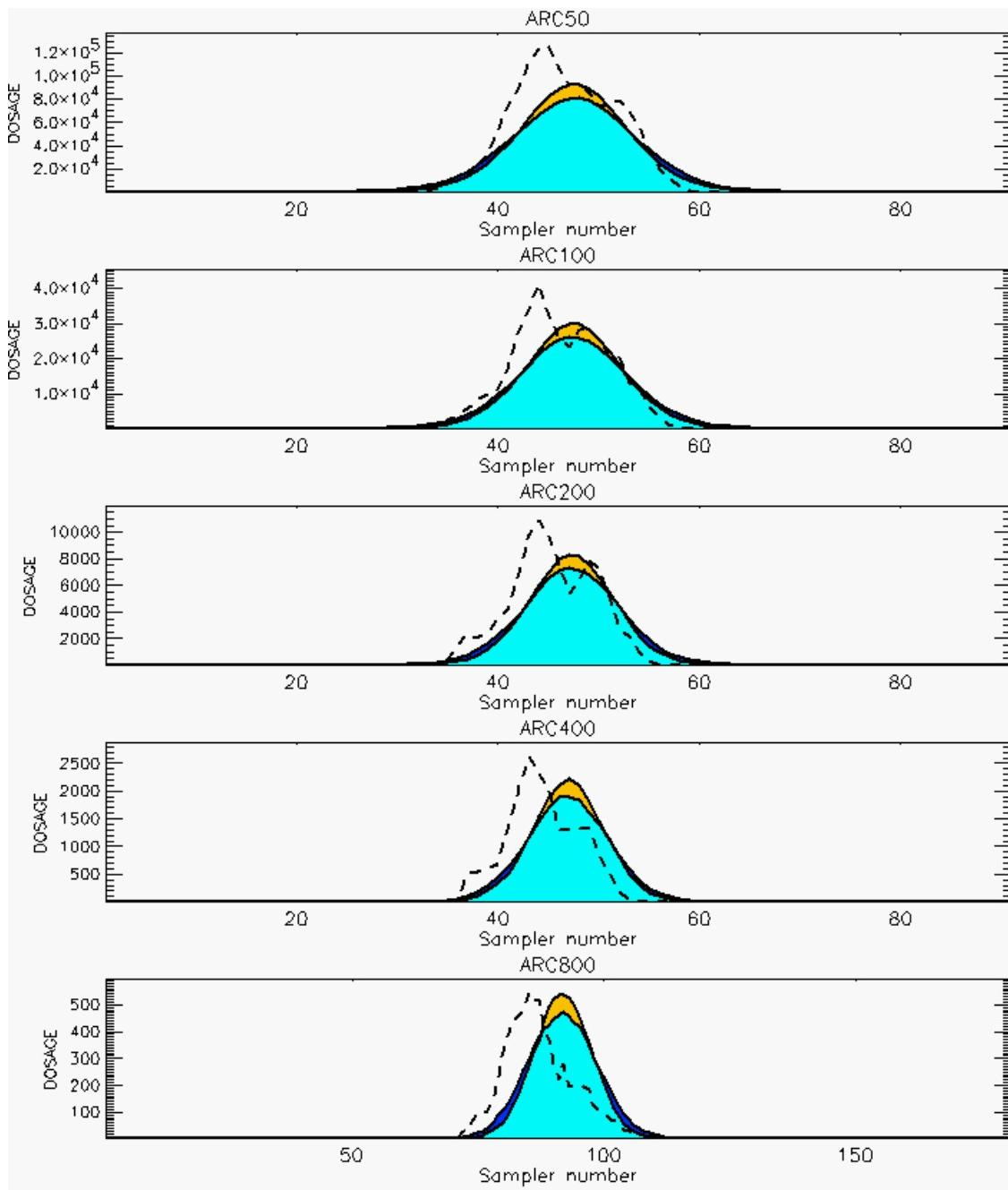
PG Prediction1 to Prediction2 Comparison

PG Trial File: pr_grass_tracer_Experiment_26.txt

PG Prediction File 1: ARAC\nodeposition\pg_26_novd.arac

PG Prediction File 2: ARAC\sv_novd\pg_26_sv_novd.arac

Figure M-21b. NARAC Sigma-v Experimental and Sigma-v Calculated Predictions to Trial 26 on Logarithmic Scale: Stability Category is 2



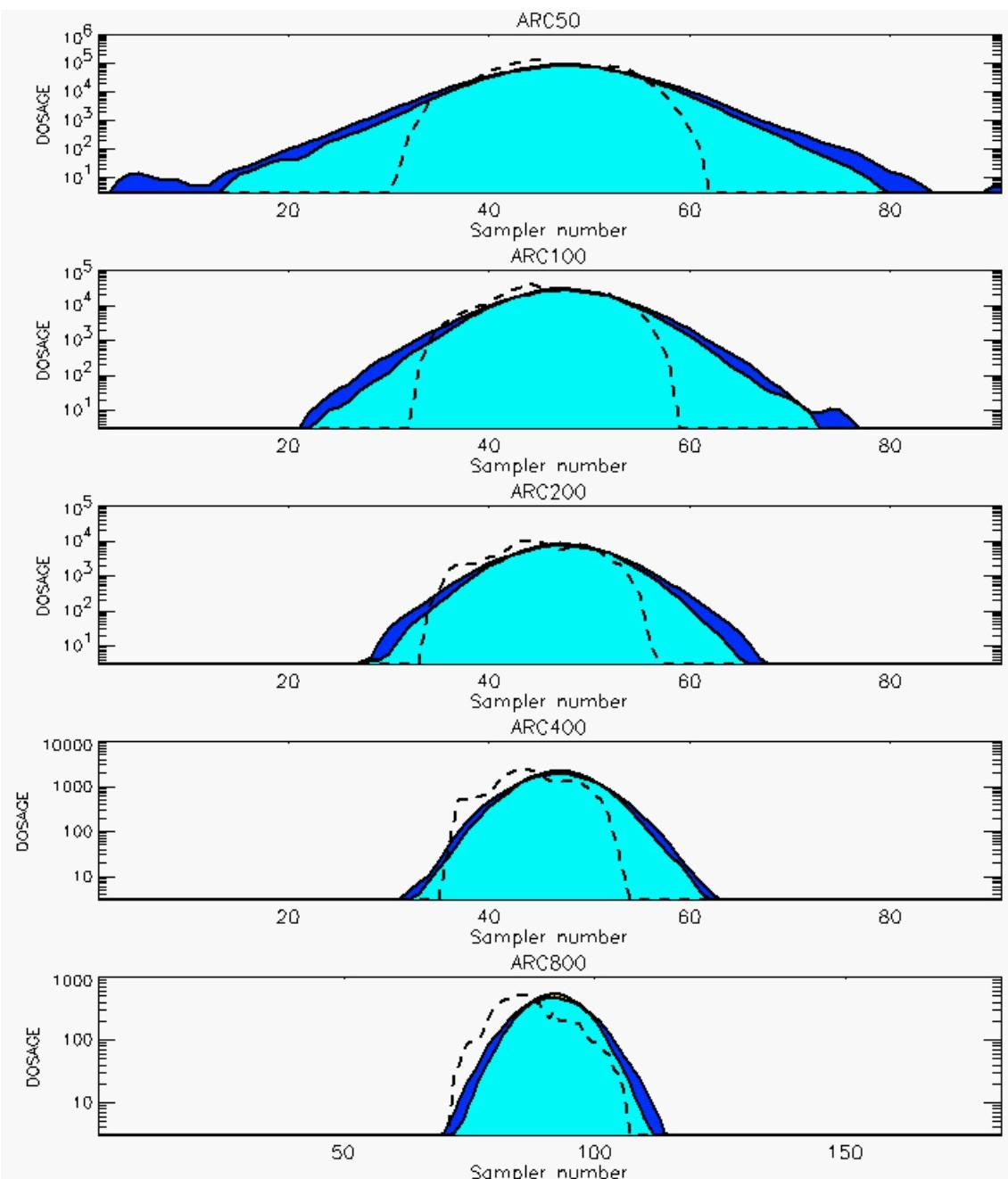
PG Prediction1 to Prediction2 Comparison

PG Trial File: pr_grass_tracer_Experiment_27.txt

PG Prediction File 1: ARAC\nodeposition\pg_27_novd.arac

PG Prediction File 2: ARAC\sv_novd\pg_27_sv_novd.arac

Figure M-22a. NARAC Sigma-v Experimental and Sigma-v Calculated Predictions to Trial 27 on Linear Scale: Stability Category is 2



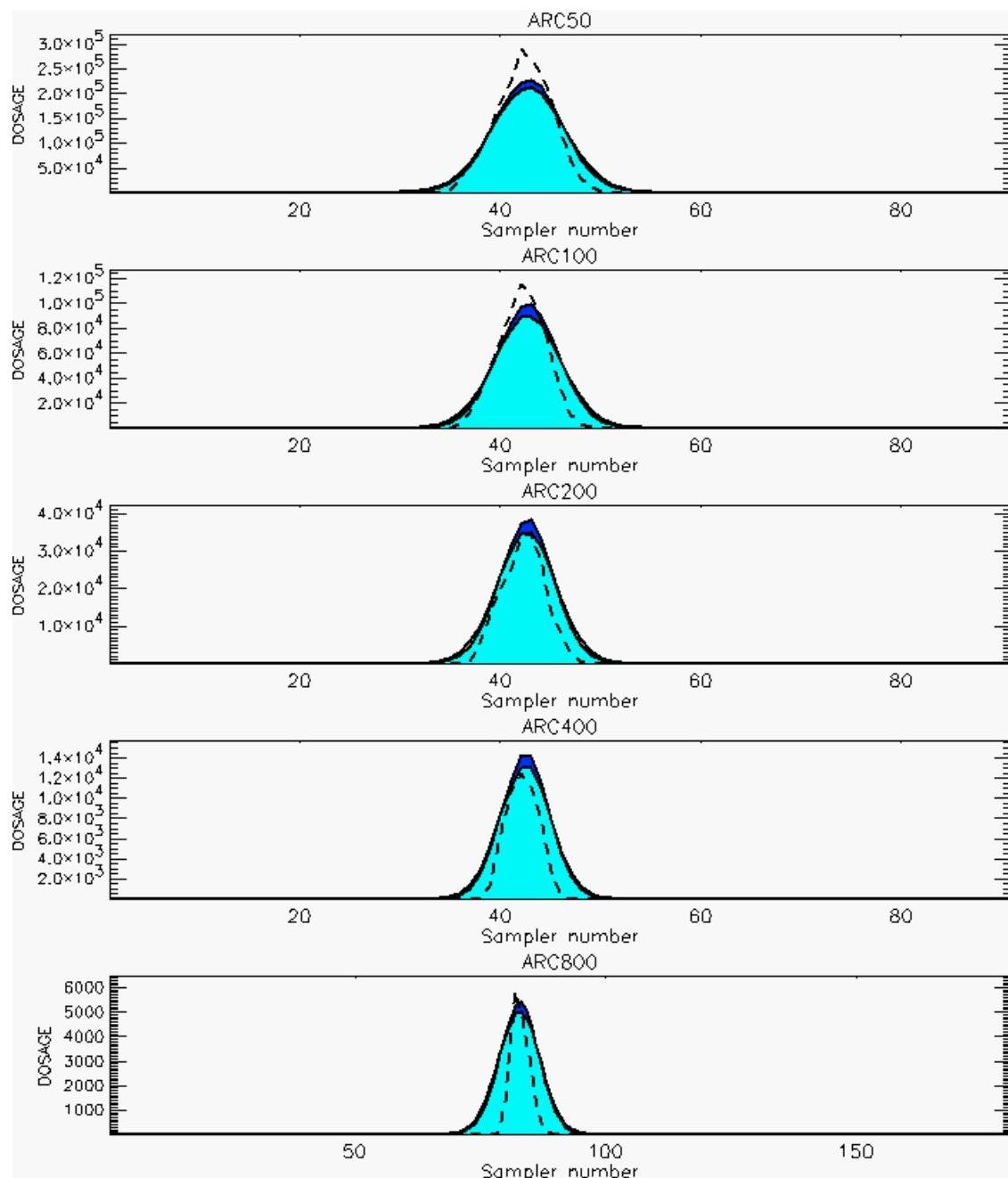
PG Prediction1 to Prediction2 Comparison

PG Trial File: pr_grass_tracer_Experiment_27.txt

PG Prediction File 1: ARAC\nodeposition\pg_27_nozd.arac

PG Prediction File 2: ARAC\sv_nozd\pg_27_sv_nozd.arac

Figure M-22b. NARAC Sigma-v Experimental and Sigma-v Calculated Predictions to Trial 27 on Logarithmic Scale: Stability Category is 2



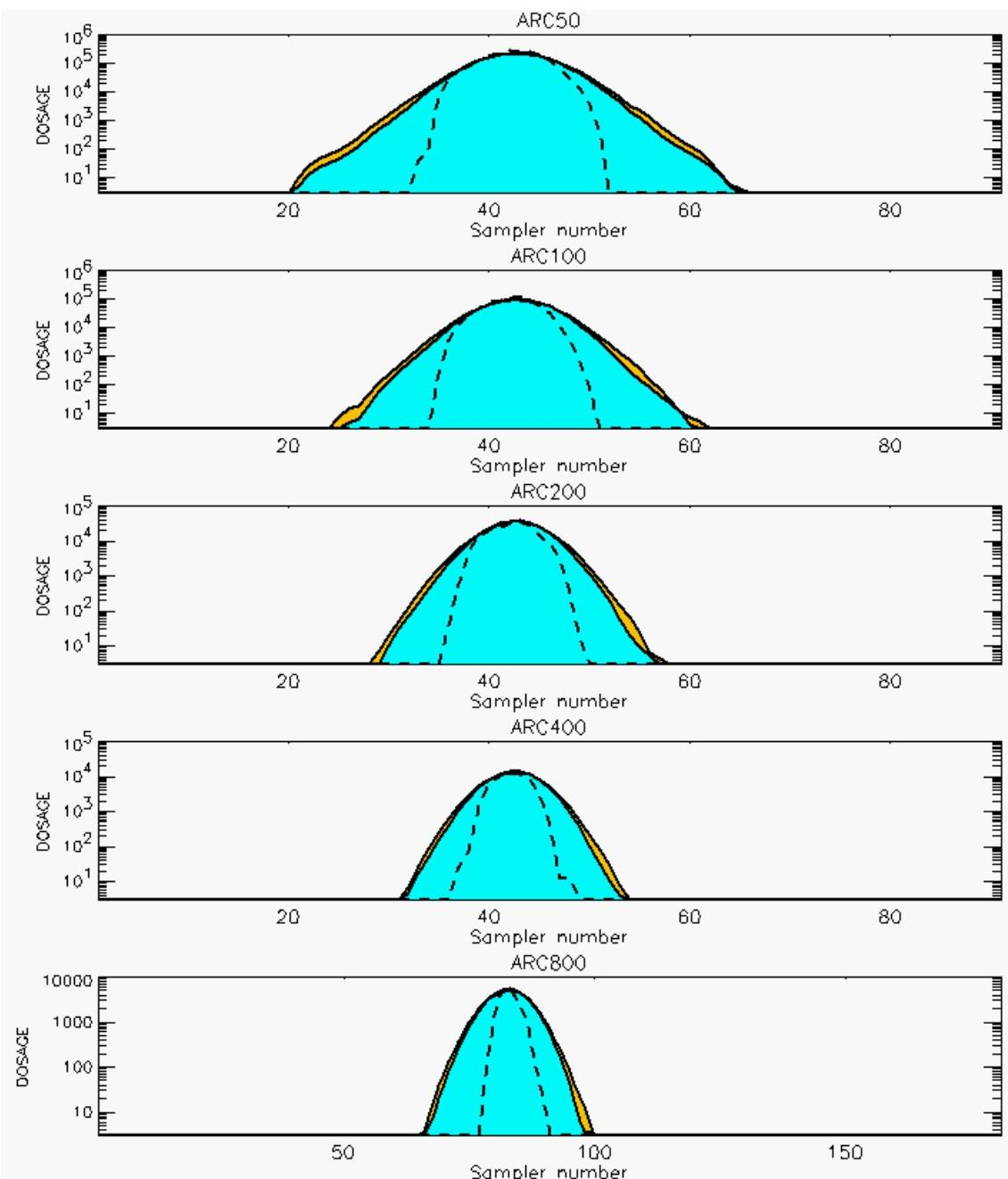
PG Prediction1 to Prediction2 Comparison

PG Trial File: pr_grass_tracer_Experiment_28.txt

PG Prediction File 1: ARAC\nodeposition\pg_28_novd.arac

PG Prediction File 2: ARAC\sv_novd\pg_28_sv_novd.arac

Figure M-23a. NARAC Sigma-v Experimental and Sigma-v Calculated Predictions to Trial 28 on Linear Scale: Stability Category is 5



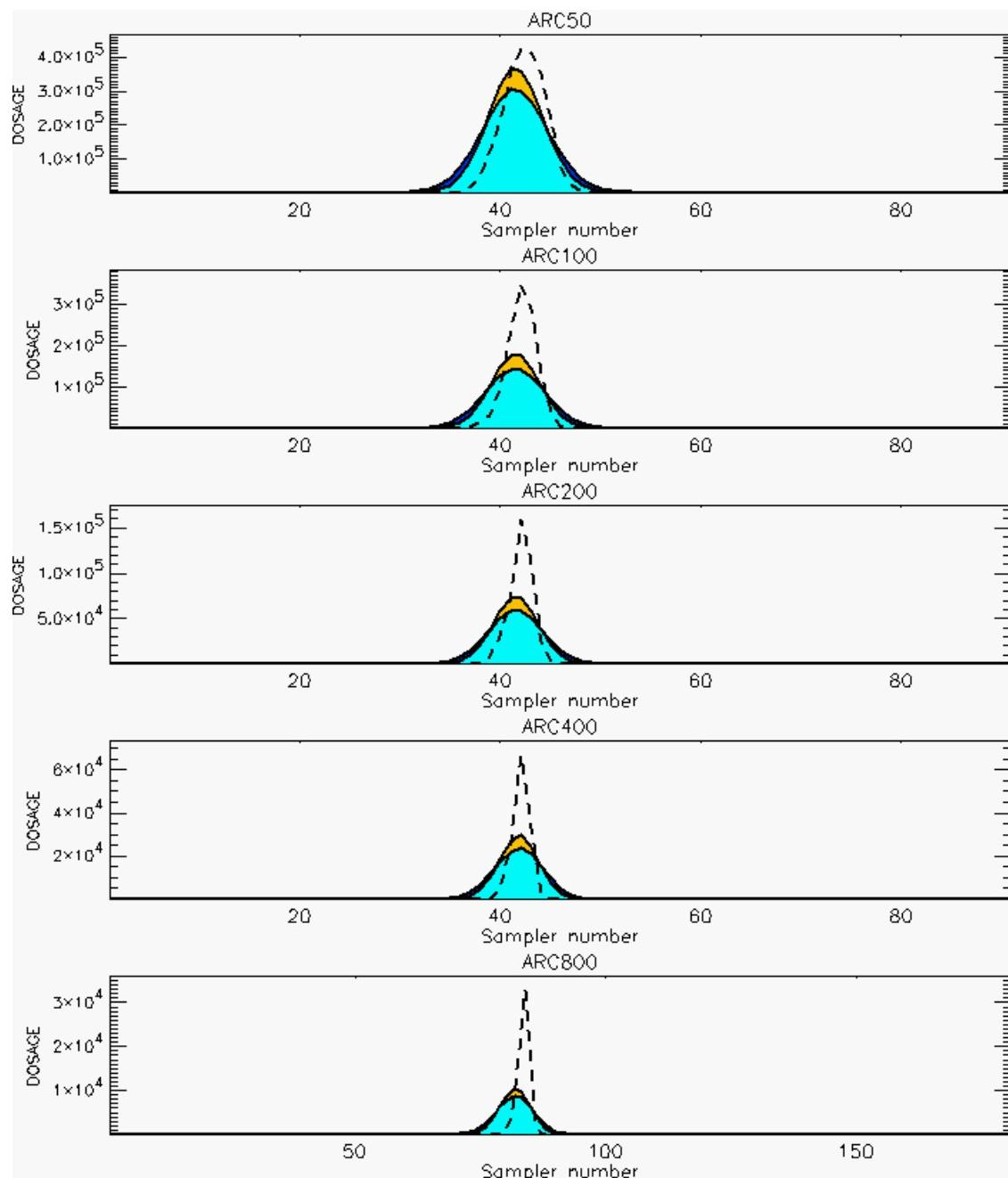
PG Prediction1 to Prediction2 Comparison

PG Trial File: pr_grass_tracer_Experiment_28.txt

PG Prediction File 1: ARAC\nodeposition\pg_28_novd.arac

PG Prediction File 2: ARAC\sv_novd\pg_28_sv_novd.arac

Figure M-23b. NARAC Sigma-v Experimental and Sigma-v Calculated Predictions to Trial 28 on Logarithmic Scale: Stability Category is 5



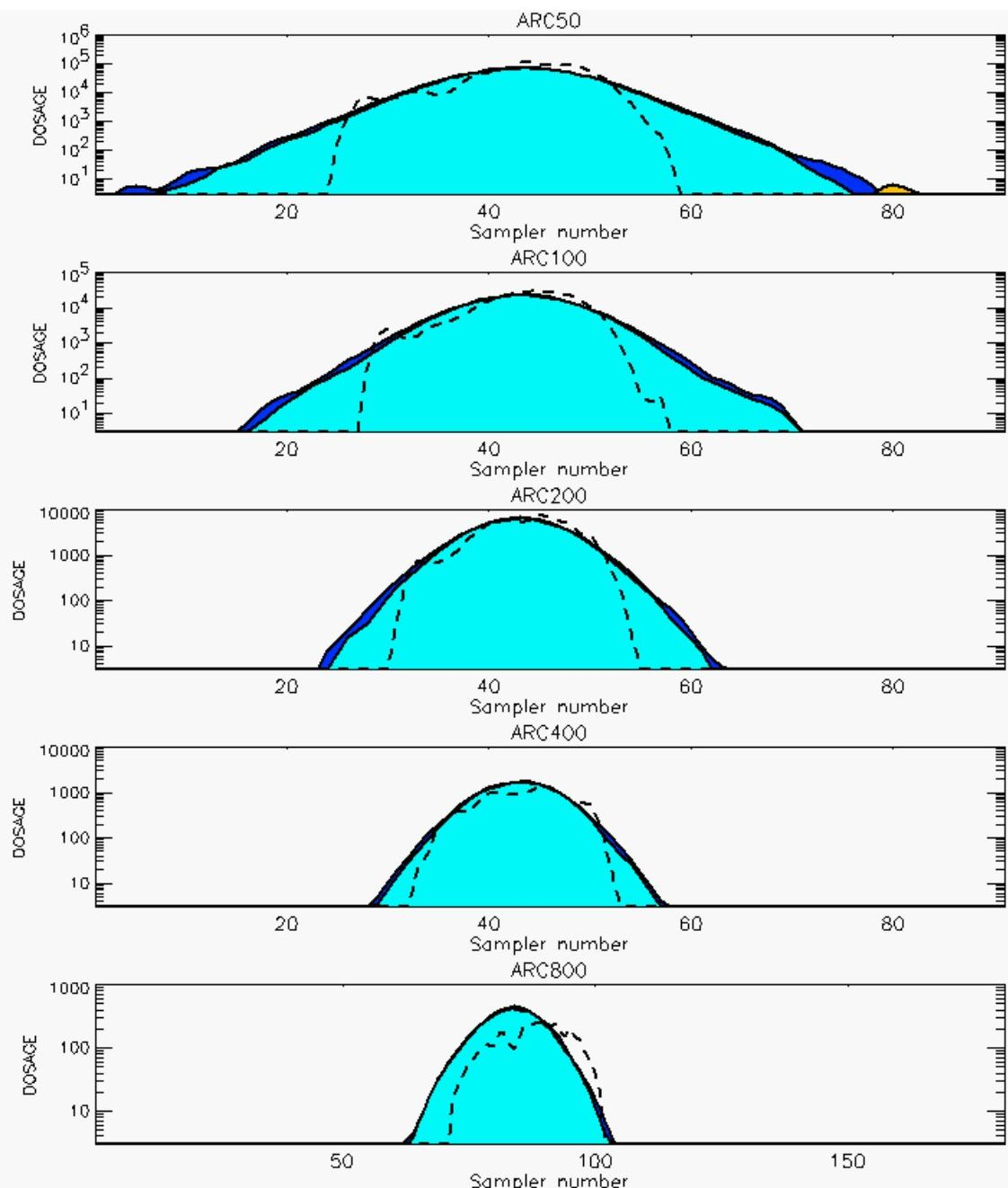
PG Prediction1 to Prediction2 Comparison

PG Trial File: pr_grass_tracer_Experiment_32.txt

PG Prediction File 1: ARAC\nodeposition\pg_32_nozd.arac

PG Prediction File 2: ARAC\sv_nzd\pg_32_sv_nzd.arac

Figure M-24a. NARAC Sigma-v Experimental and Sigma-v Calculated Predictions to Trial 32 on Linear Scale: Stability Category is 6



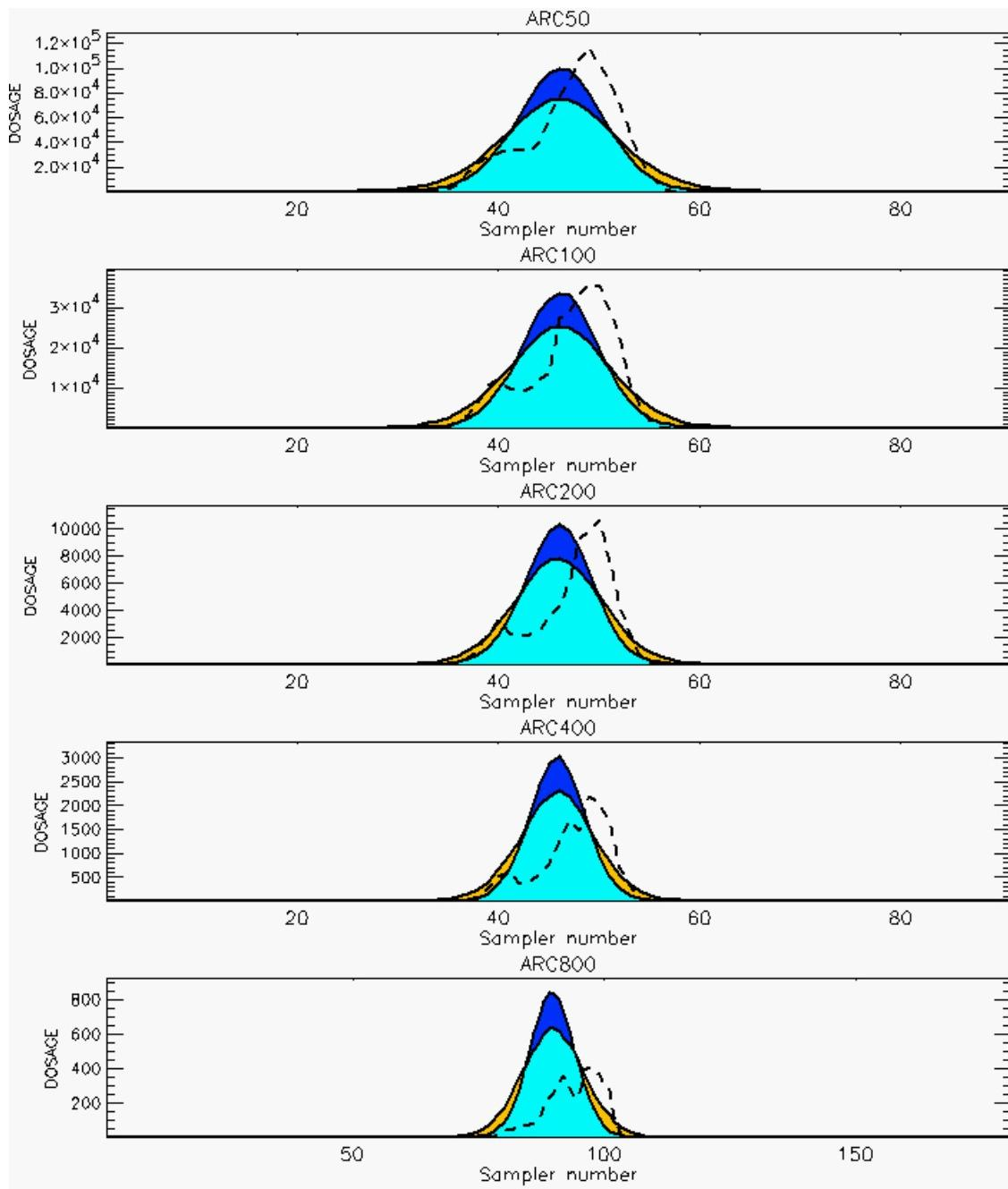
PG Prediction1 to Prediction2 Comparison

PG Trial File: pr_grass_tracer_Experiment_05.txt

PG Prediction File 1: ARAC\nodeposition\pg_5_nozd.arac

PG Prediction File 2: ARAC\sv_nozd\pg_5_sv_nozd.arac

Figure M-24b. NARAC Sigma-v Experimental and Sigma-v Calculated Predictions to Trial 32 on Logarithmic Scale: Stability Category is 6



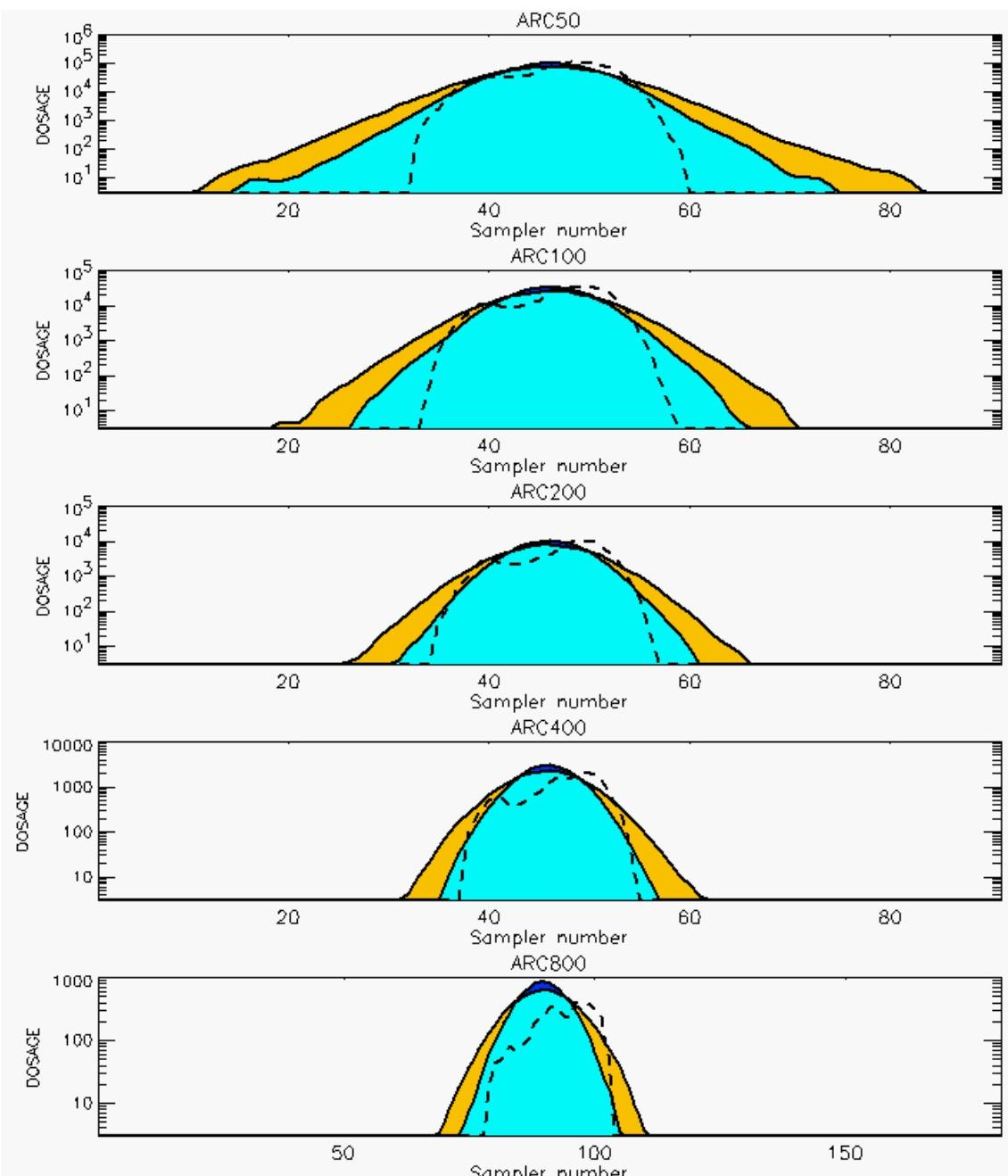
PG Prediction1 to Prediction2 Comparison

PG Trial File: pr_grass_tracer_Experiment_33.txt

PG Prediction File 1: ARAC\nodeposition\pg_33_novd.arac

PG Prediction File 2: ARAC\sv_novd\pg_33_sv_novd.arac

Figure M-25a. NARAC Sigma-v Experimental and Sigma-v Calculated Predictions to Trial 33 on Linear Scale: Stability Category is 3



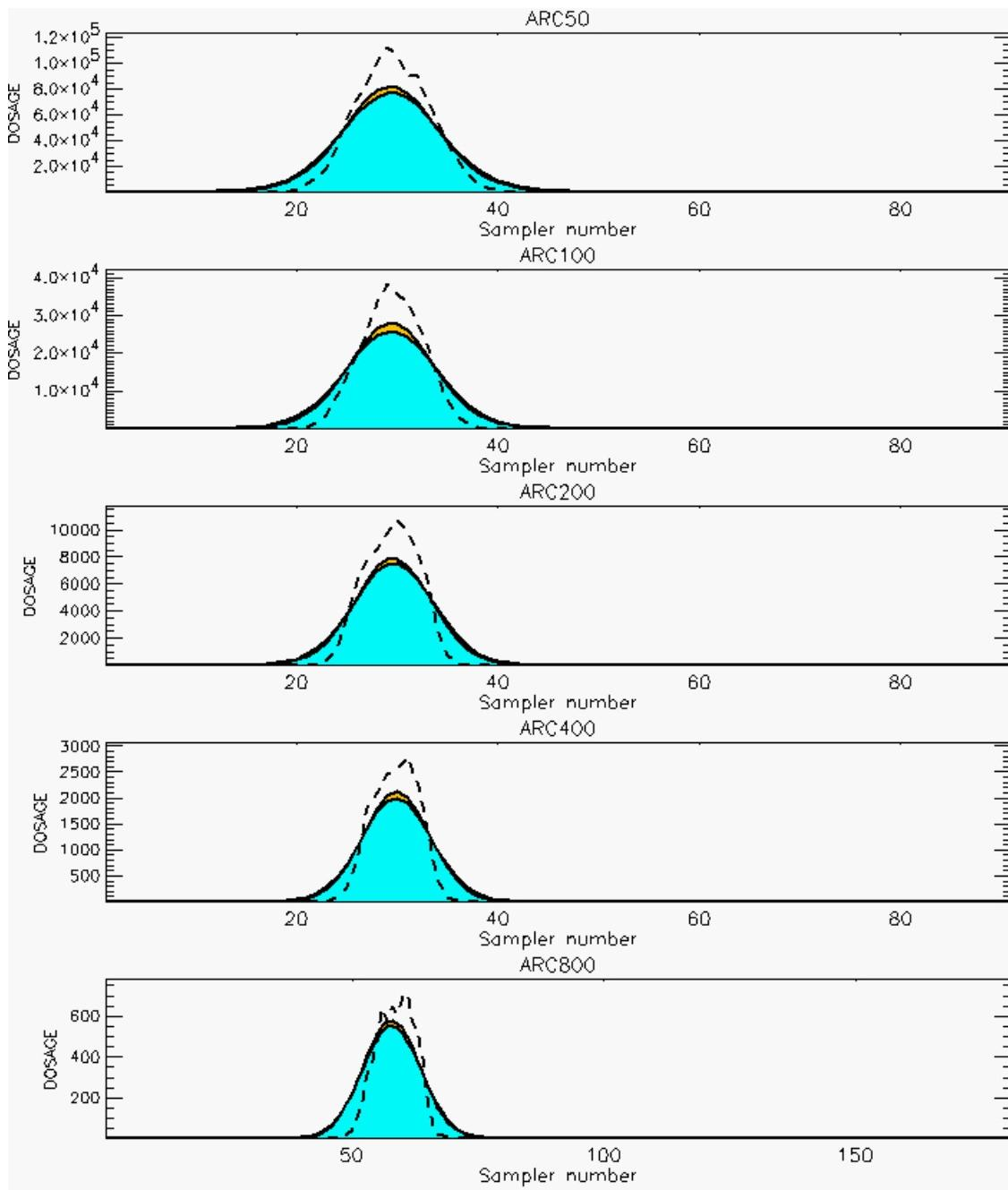
PG Prediction1 to Prediction2 Comparison

PG Trial File: pr_grass_tracer_Experiment_33.txt

PG Prediction File 1: ARAC\nodeposition\pg_33_novd.arac

PG Prediction File 2: ARAC\sv_novd\pg_33_sv_novd.arac

Figure M-25b. NARAC Sigma-v Experimental and Sigma-v Calculated Predictions to Trial 33 on Logarithmic Scale: Stability Category is 3



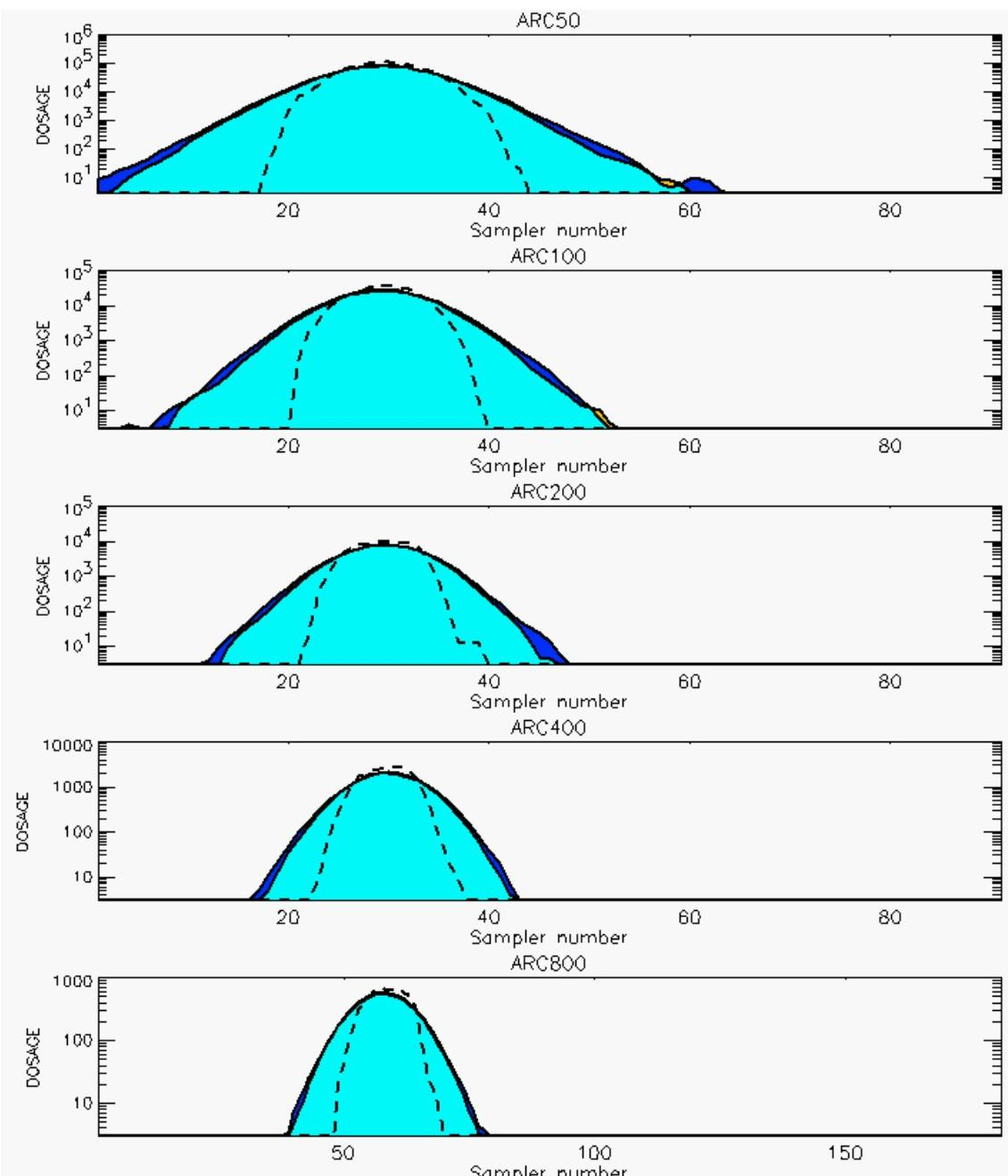
PG Prediction1 to Prediction2 Comparison

PG Trial File: pr_grass_tracer_Experiment_34.txt

PG Prediction File 1: ARAC\nodeposition\pg_34_novd.arac

PG Prediction File 2: ARAC\sv_novd\pg_34_sv_novd.arac

Figure M-26a. NARAC Sigma-v Experimental and Sigma-v Calculated Predictions to Trial 34 on Linear Scale: Stability Category is 3



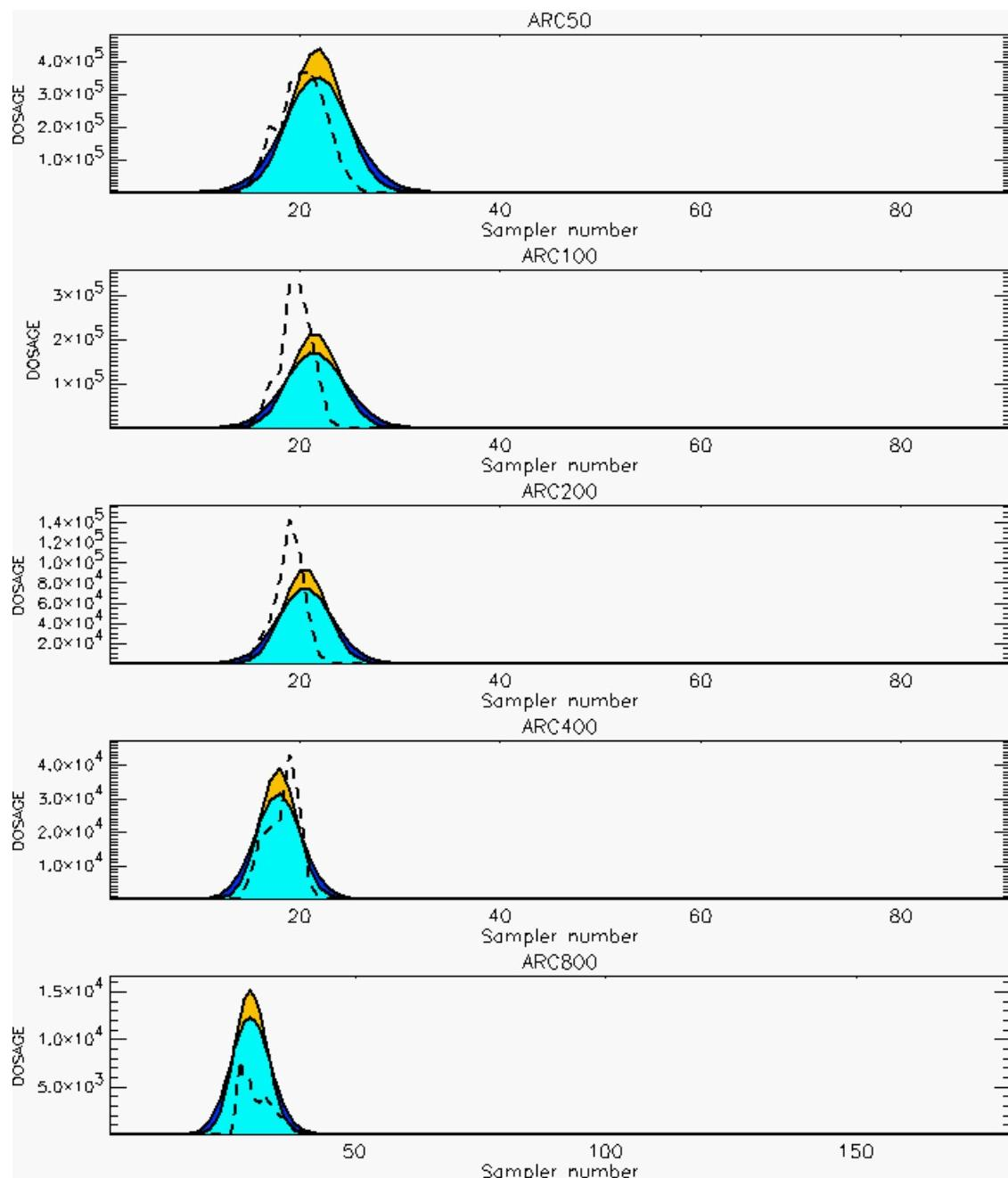
PG Prediction1 to Prediction2 Comparison

PG Trial File: pr_grass_tracer_Experiment_34.txt

PG Prediction File 1: ARAC\nodeposition\pg_34_nozd.arac

PG Prediction File 2: ARAC\sv_nzd\pg_34_sv_nzd.arac

Figure M-26b. NARAC Sigma-v Experimental and Sigma-v Calculated Predictions to Trial 34 on Logarithmic Scale: Stability Category is 3



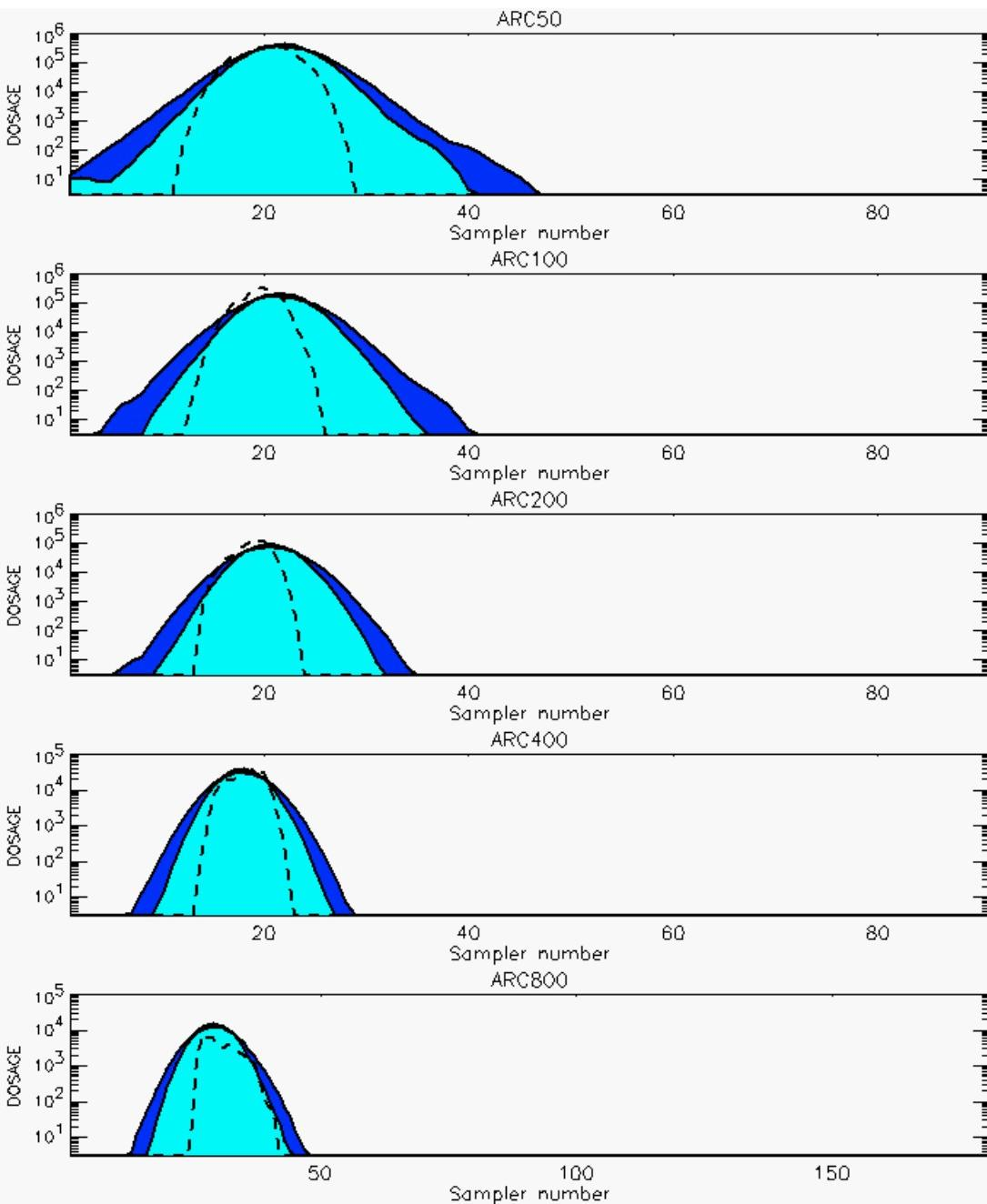
PG Prediction1 to Prediction2 Comparison

PG Trial File: pr_grass_tracer_Experiment_35.txt

PG Prediction File 1: ARAC\nodeposition_replace\pg_35_noxd.arac

PG Prediction File 2: ARAC\sv_noxd\pg_35_sv_noxd.arac

Figure M-27a. NARAC Sigma-v Experimental and Sigma-v Calculated Predictions to Trial 35 on Linear Scale: Stability Category is 6



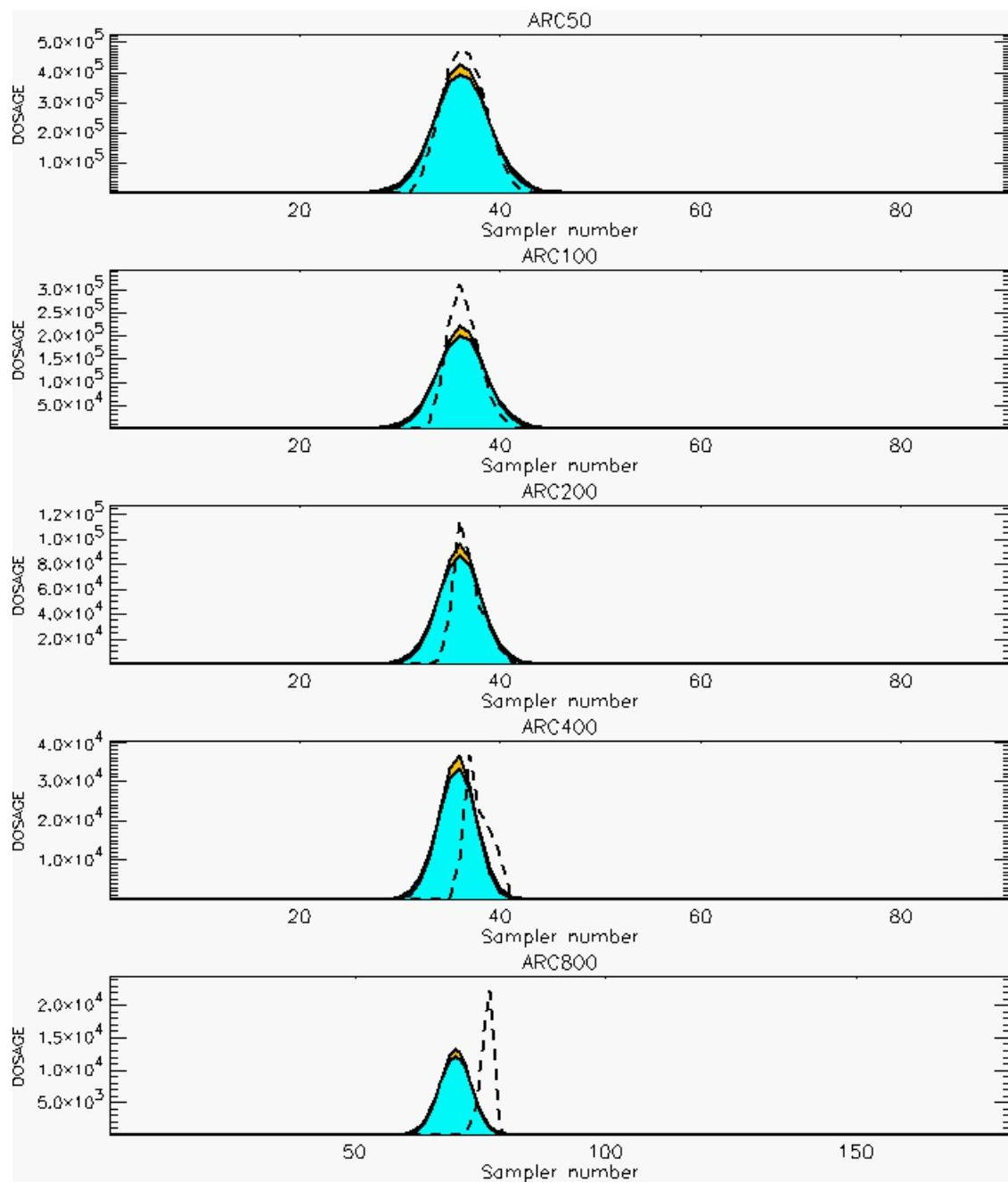
PG Prediction1 to Prediction2 Comparison

PG Trial File: pr_grass_tracer_Experiment_35.txt

PG Prediction File 1: ARAC\nodeposition_replace\pg_35_nozd.arac

PG Prediction File 2: ARAC\sv_nozd\pg_35_sv_nozd.arac

Figure M-27b. NARAC Sigma-v Experimental and Sigma-v Calculated Predictions to Trial 35 on Logarithmic Scale: Stability Category is 6



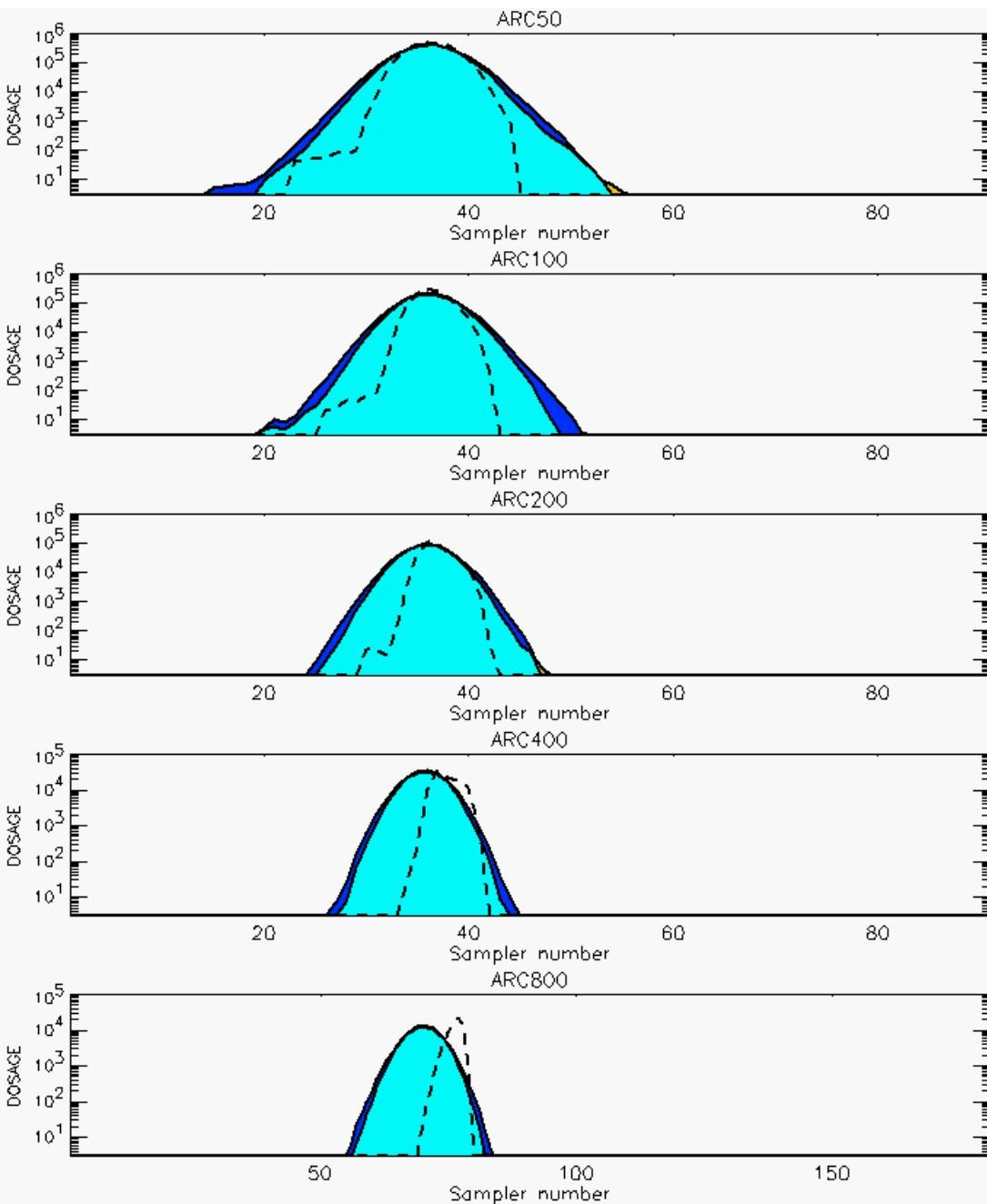
PG Prediction1 to Prediction2 Comparison

PG Trial File: pr_grass_tracer_Experiment_36.txt

PG Prediction File 1: ARAC\nodeposition\pg_36_nozd.arac

PG Prediction File 2: ARAC\sv_nozd\pg_36_sv_nozd.arac

Figure M-28a. NARAC Sigma-v Experimental and Sigma-v Calculated Predictions to Trial 36 on Linear Scale: Stability Category is 6



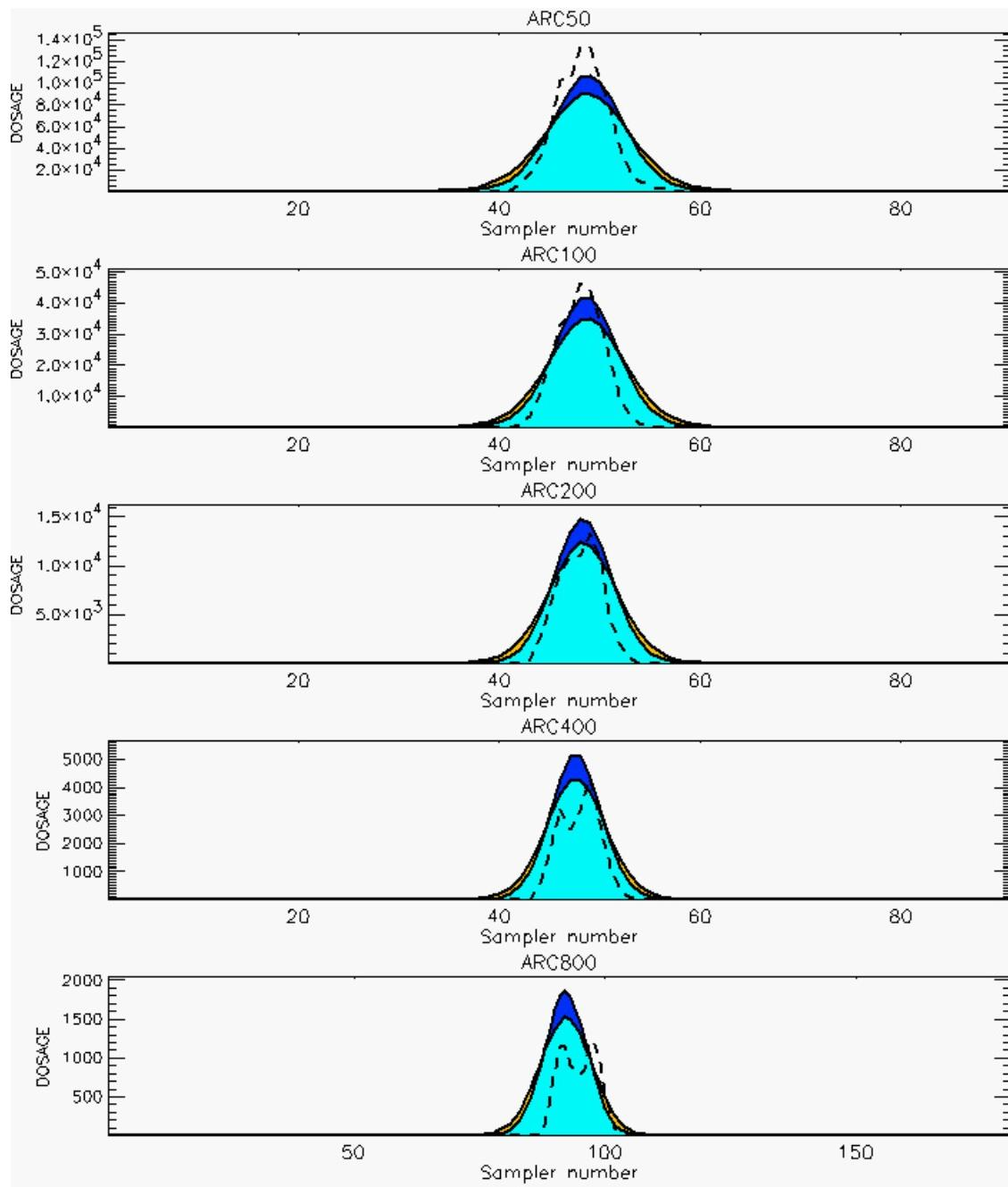
PG Prediction1 to Prediction2 Comparison

PG Trial File: pr_grass_tracer_Experiment_36.txt

PG Prediction File 1: ARAC\nodeposition\pg_36_novd.arac

PG Prediction File 2: ARAC\sv_novd\pg_36_sv_novd.arac

Figure M-28b. NARAC Sigma-v Experimental and Sigma-v Calculated Predictions to Trial 36 on Logarithmic Scale: Stability Category is 6



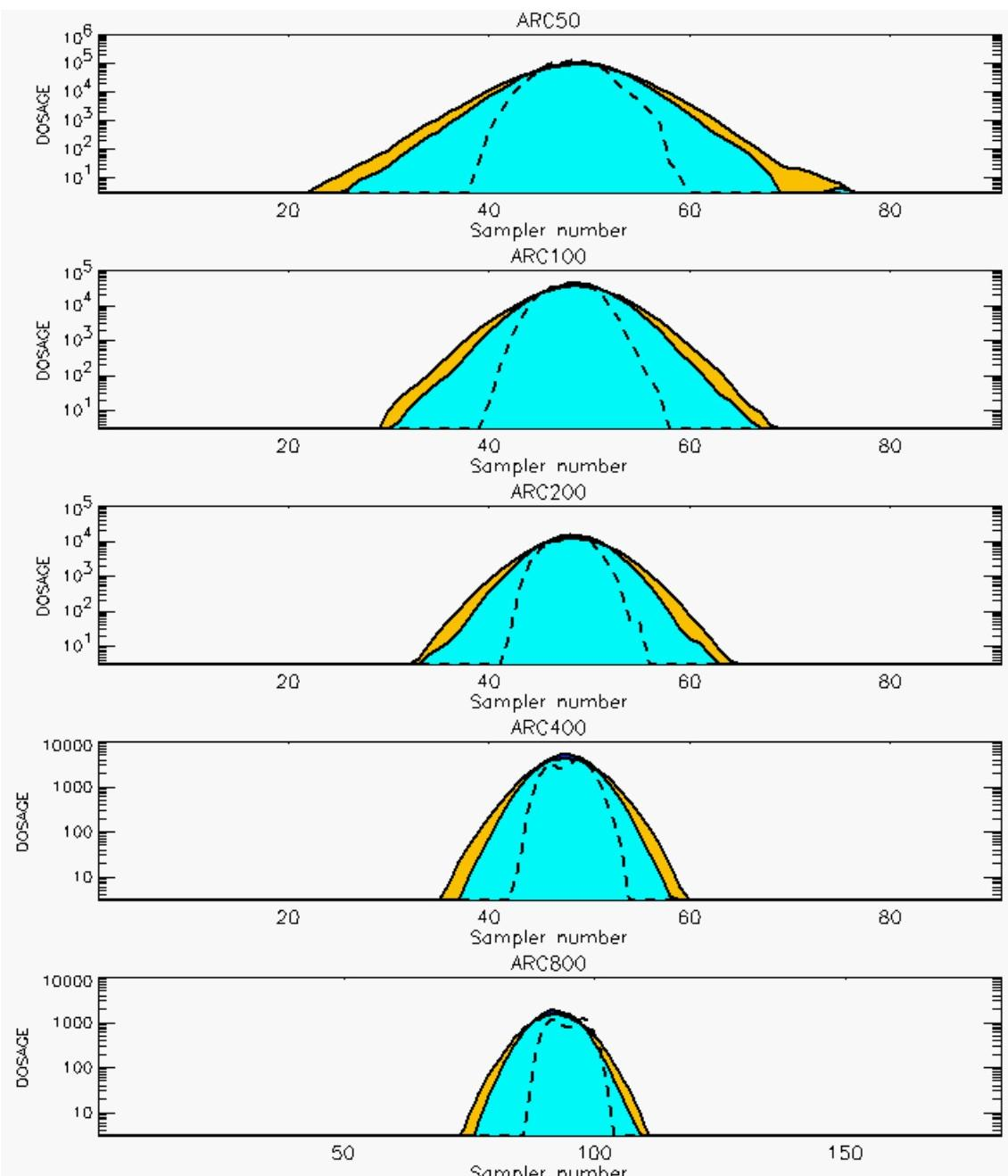
PG Prediction1 to Prediction2 Comparison

PG Trial File: pr_grass_tracer_Experiment_37.txt

PG Prediction File 1: ARAC\nodeposition\pg_37_nozd.arac

PG Prediction File 2: ARAC\sv_nozd\pg_37_sv_nozd.arac

Figure M-29a. NARAC Sigma-v Experimental and Sigma-v Calculated Predictions to Trial 37 on Linear Scale: Stability Category is 4



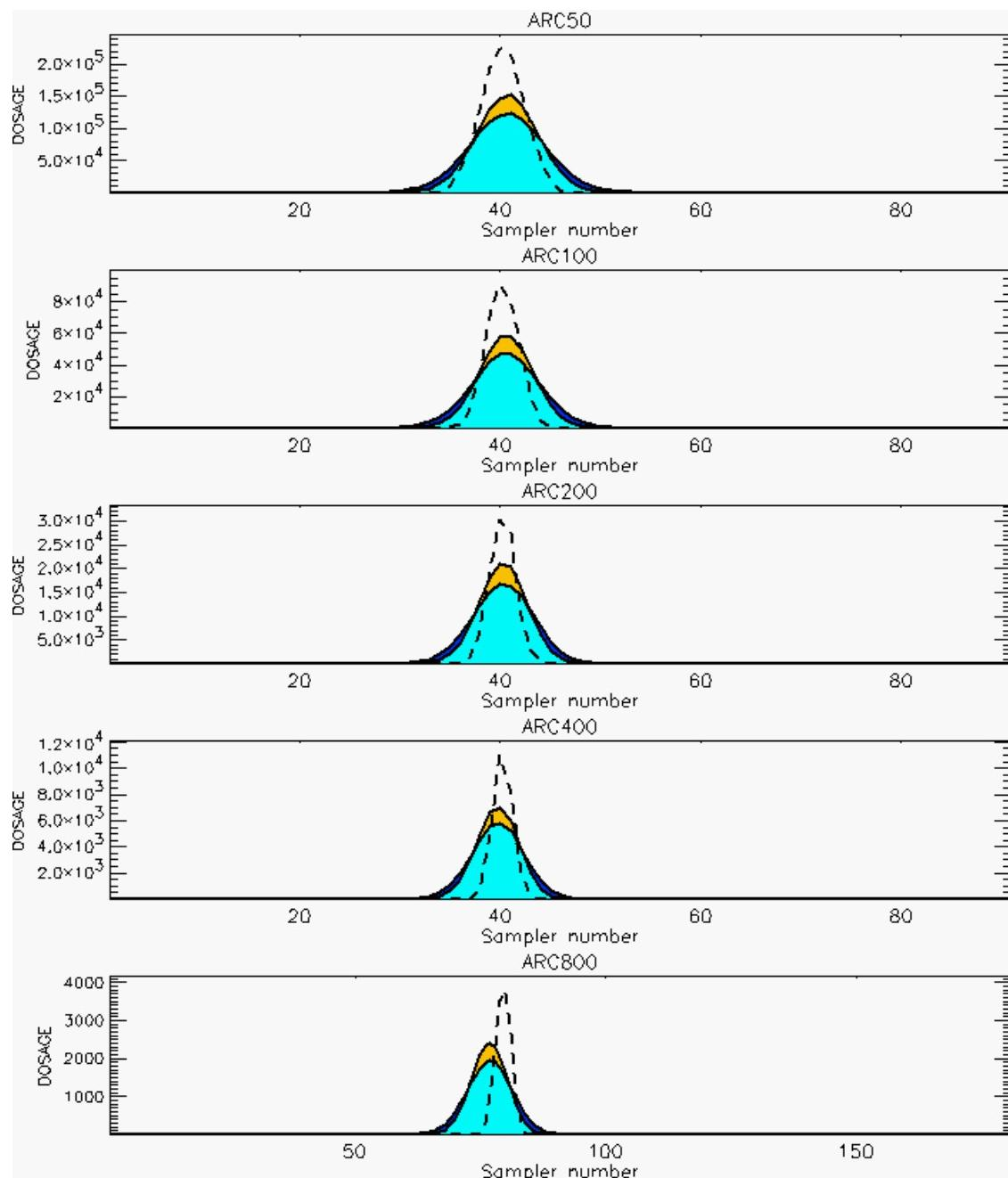
PG Prediction1 to Prediction2 Comparison

PG Trial File: pr_grass_tracer_Experiment_37.txt

PG Prediction File 1: ARAC\nodeposition\pg_37_nozd.arac

PG Prediction File 2: ARAC\sv_nzd\pg_37_sv_nzd.arac

Figure M-29b. NARAC Sigma-v Experimental and Sigma-v Calculated Predictions to Trial 37 on Logarithmic Scale: Stability Category is 4



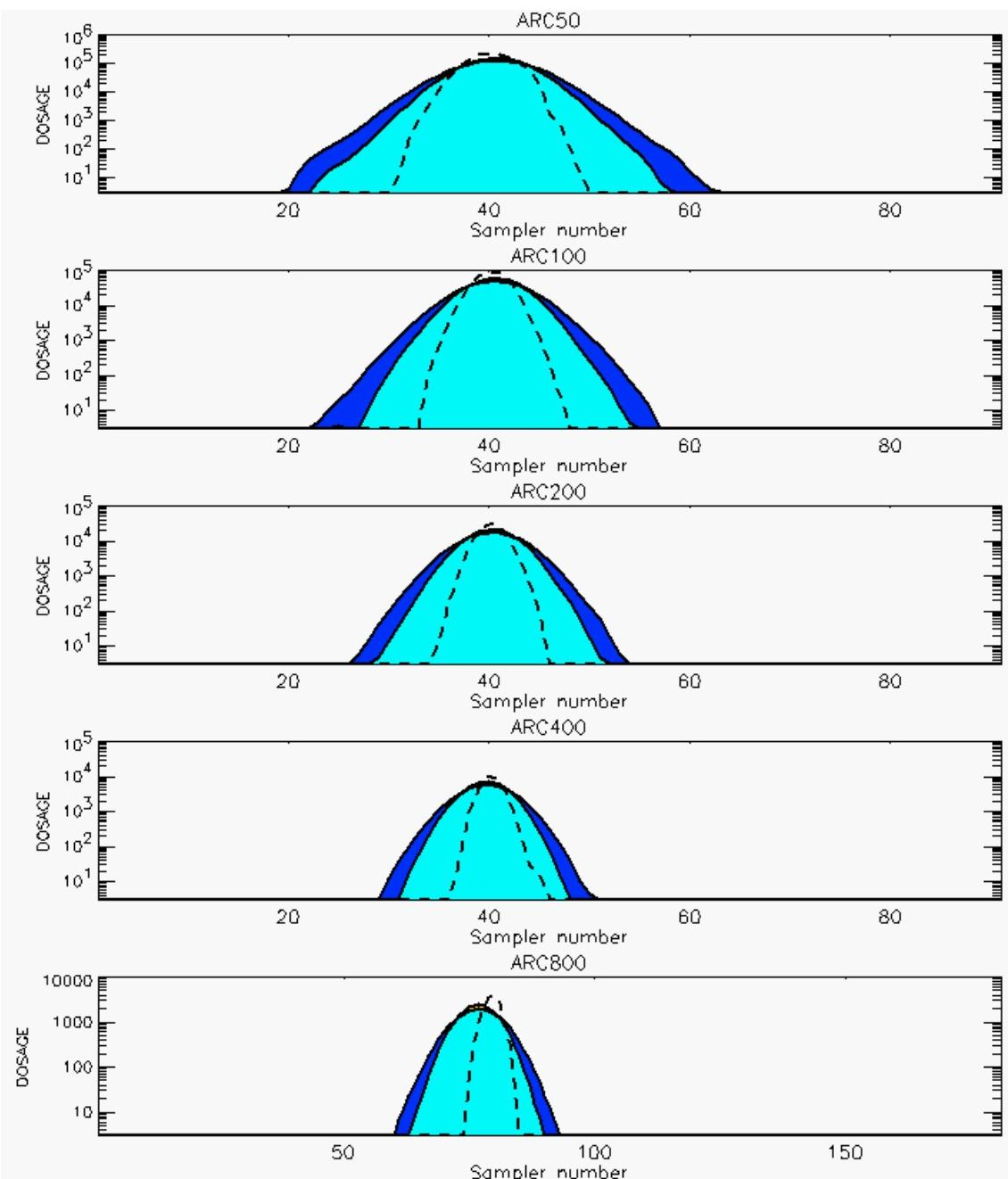
PG Prediction1 to Prediction2 Comparison

PG Trial File: pr_grass_tracer_Experiment_38.txt

PG Prediction File 1: ARAC\nodeposition\pg_38_novd.arac

PG Prediction File 2: ARAC\sv_novd\pg_38_sv_novd.arac

Figure M-30a. NARAC Sigma-v Experimental and Sigma-v Calculated Predictions to Trial 38 on Linear Scale: Stability Category is 4



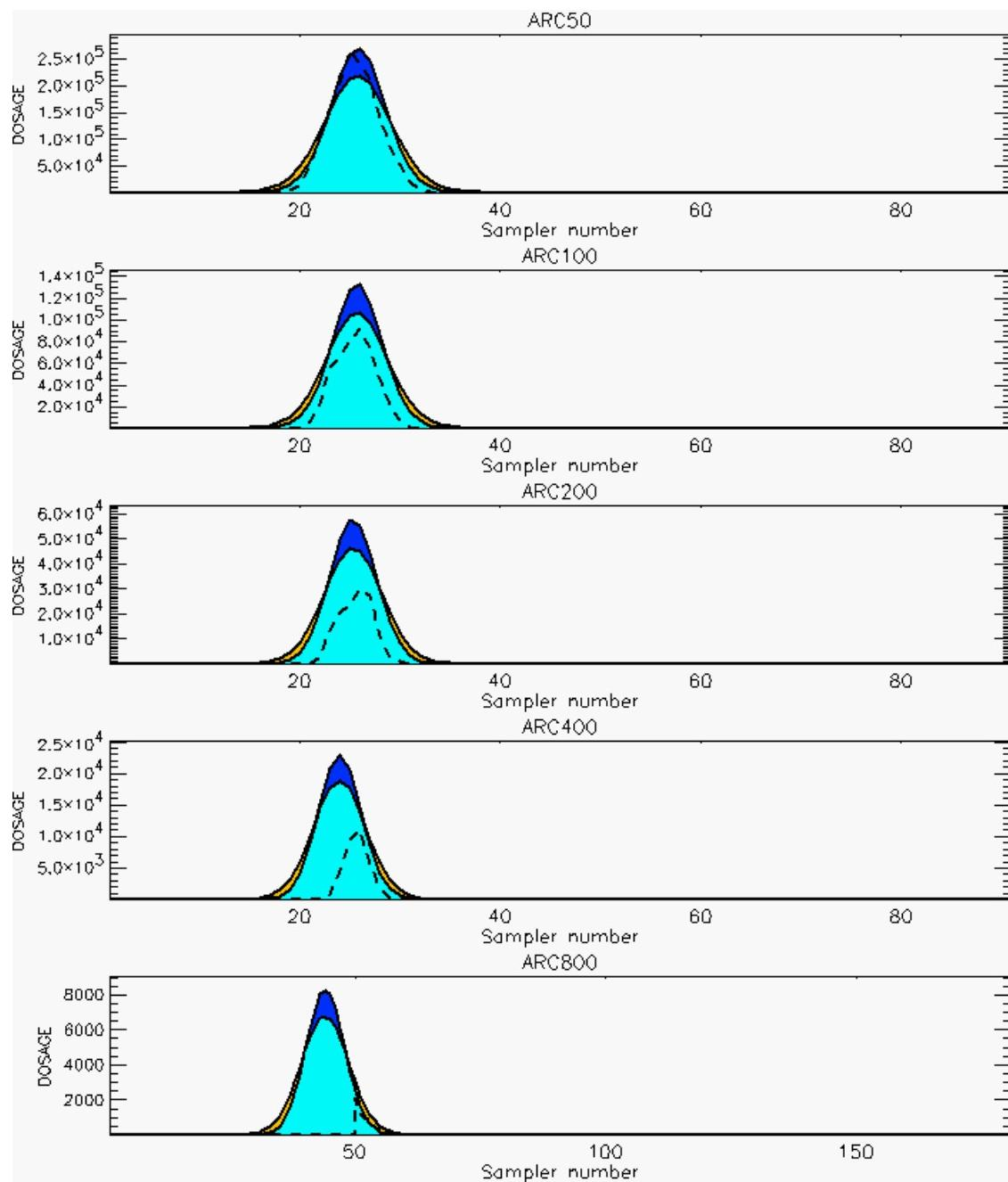
PG Prediction1 to Prediction2 Comparison

PG Trial File: pr_grass_tracer_Experiment_38.txt

PG Prediction File 1: ARAC\nodeposition\pg_38_novd.arac

PG Prediction File 2: ARAC\sv_novd\pg_38_sv_novd.arac

Figure M-30b. NARAC Sigma-v Experimental and Sigma-v Calculated Predictions to Trial 38 on Logarithmic Scale: Stability Category is 4



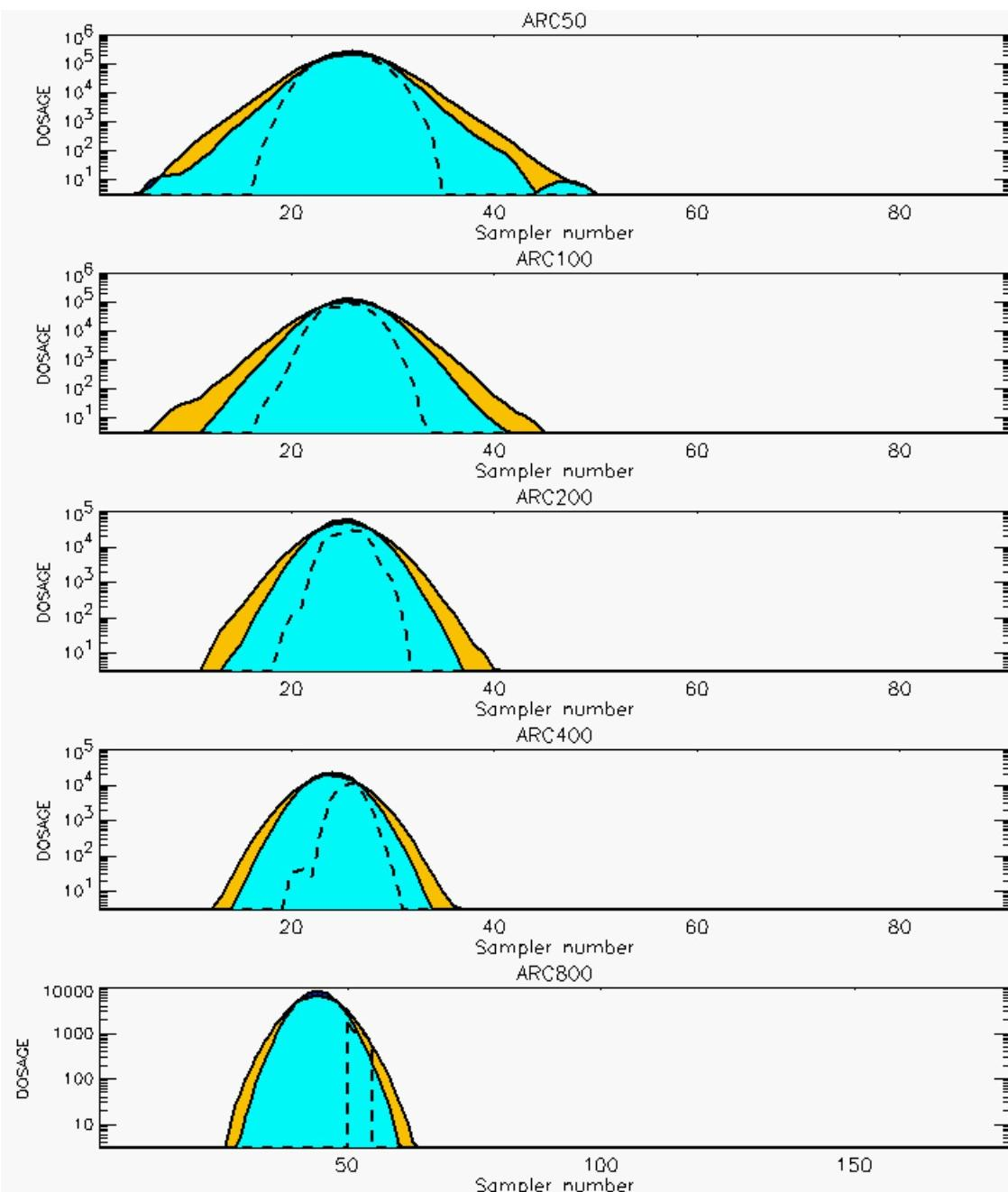
PG Prediction1 to Prediction2 Comparison

PG Trial File: pr_grass_tracer_Experiment_39.txt

PG Prediction File 1: ARAC\nodeposition_replace\pg_39_nozd.arac

PG Prediction File 2: ARAC\sv_nozd\pg_39_sv_nozd.arac

Figure M-31a. NARAC Sigma-v Experimental and Sigma-v Calculated Predictions to Trial 39 on Linear Scale: Stability Category is 6



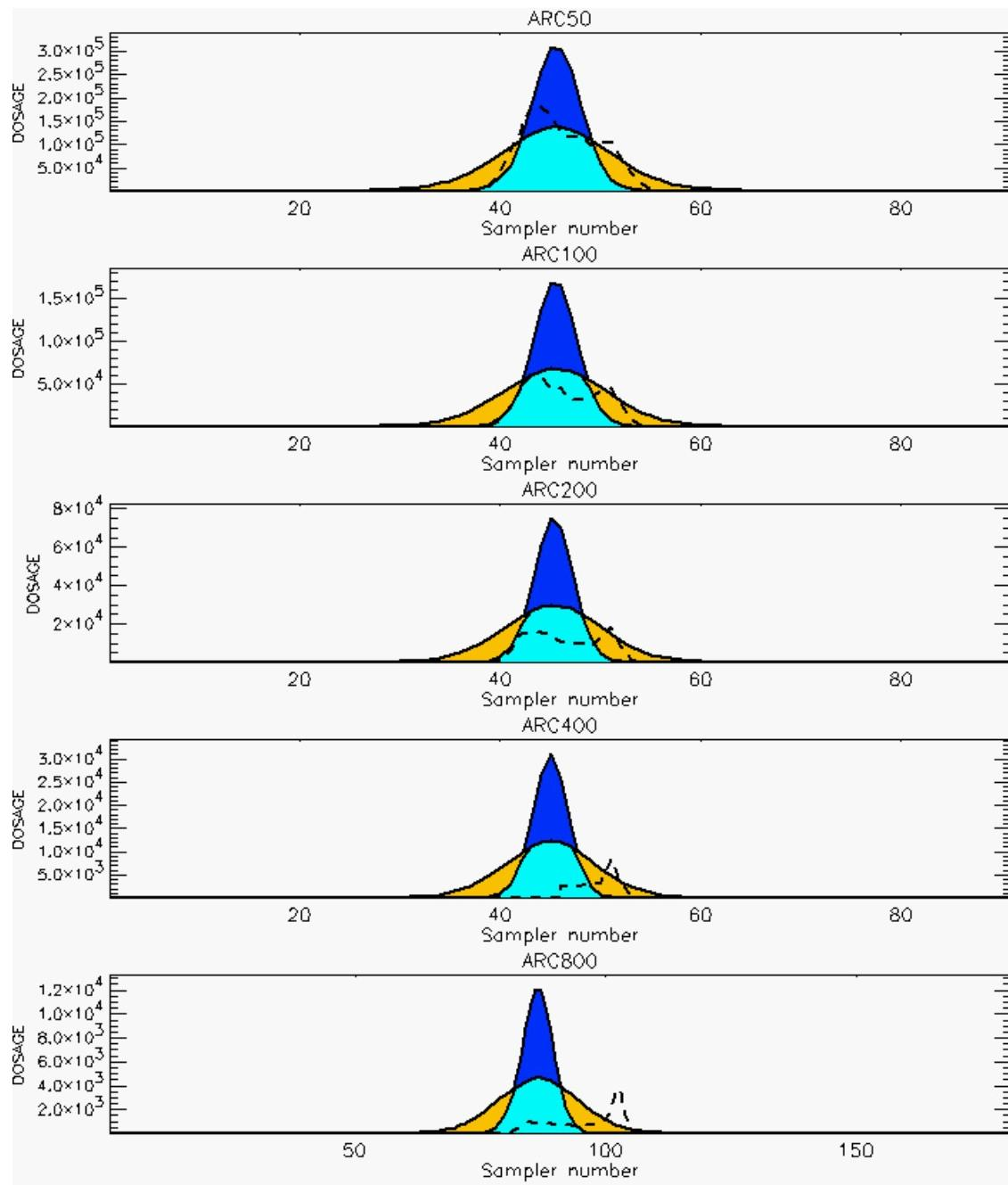
PG Prediction1 to Prediction2 Comparison

PG Trial File: pr_grass_tracer_Experiment_39.txt

PG Prediction File 1: ARAC\nodeposition_replace\pg_39_novd.arac

PG Prediction File 2: ARAC\sv_novd\pg_39_sv_novd.arac

Figure M-31b. NARAC Sigma-v Experimental and Sigma-v Calculated Predictions to Trial 39 on Logarithmic Scale: Stability Category is 6



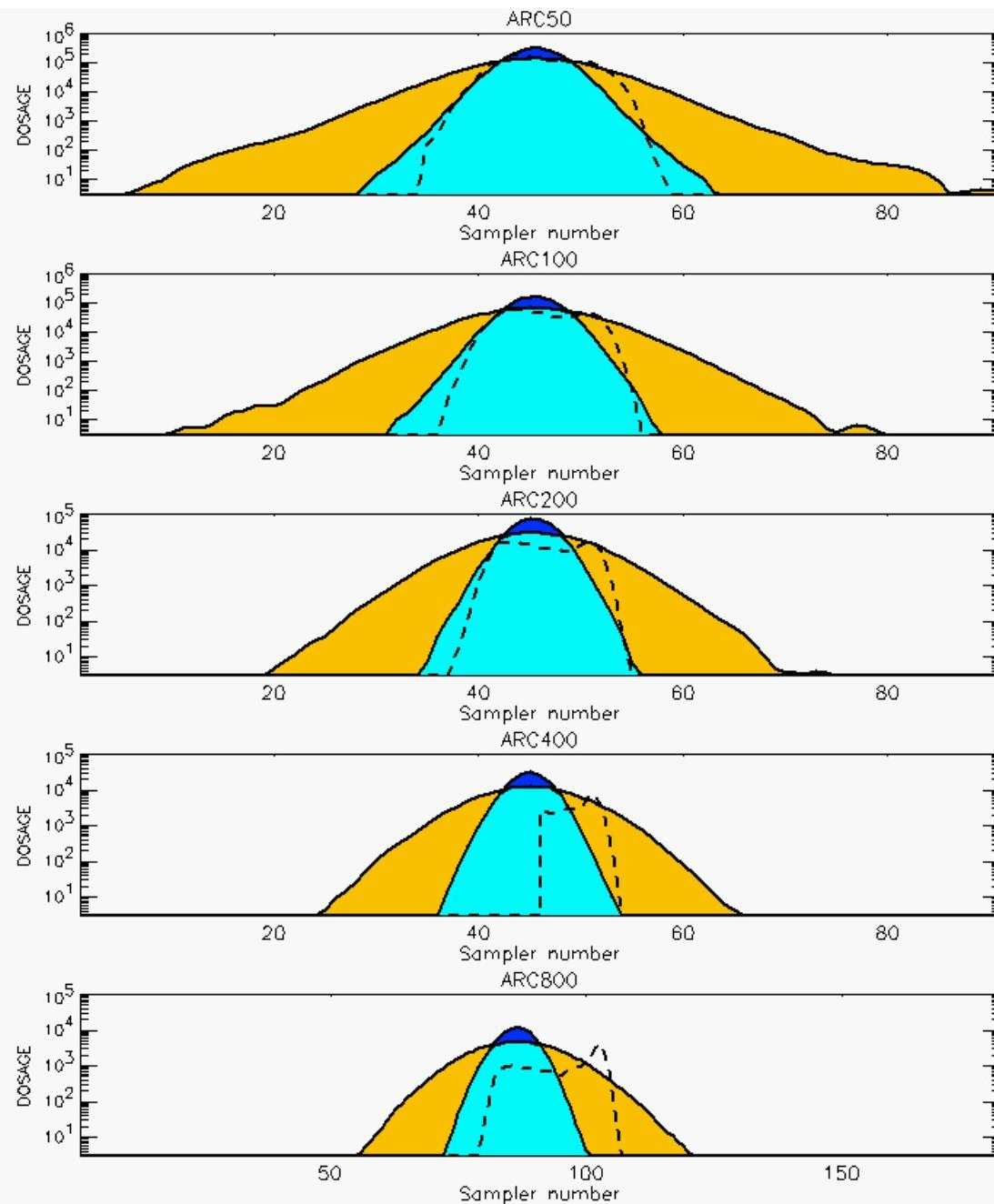
PG Prediction1 to Prediction2 Comparison

PG Trial File: pr_grass_tracer_Experiment_40.txt

PG Prediction File 1: ARAC\nodeposition\pg_40_nozd.arac

PG Prediction File 2: ARAC\sv_nozd\pg_40_sv_nozd.arac

Figure M-32a. NARAC Sigma-v Experimental and Sigma-v Calculated Predictions to Trial 40 on Linear Scale: Stability Category is 6



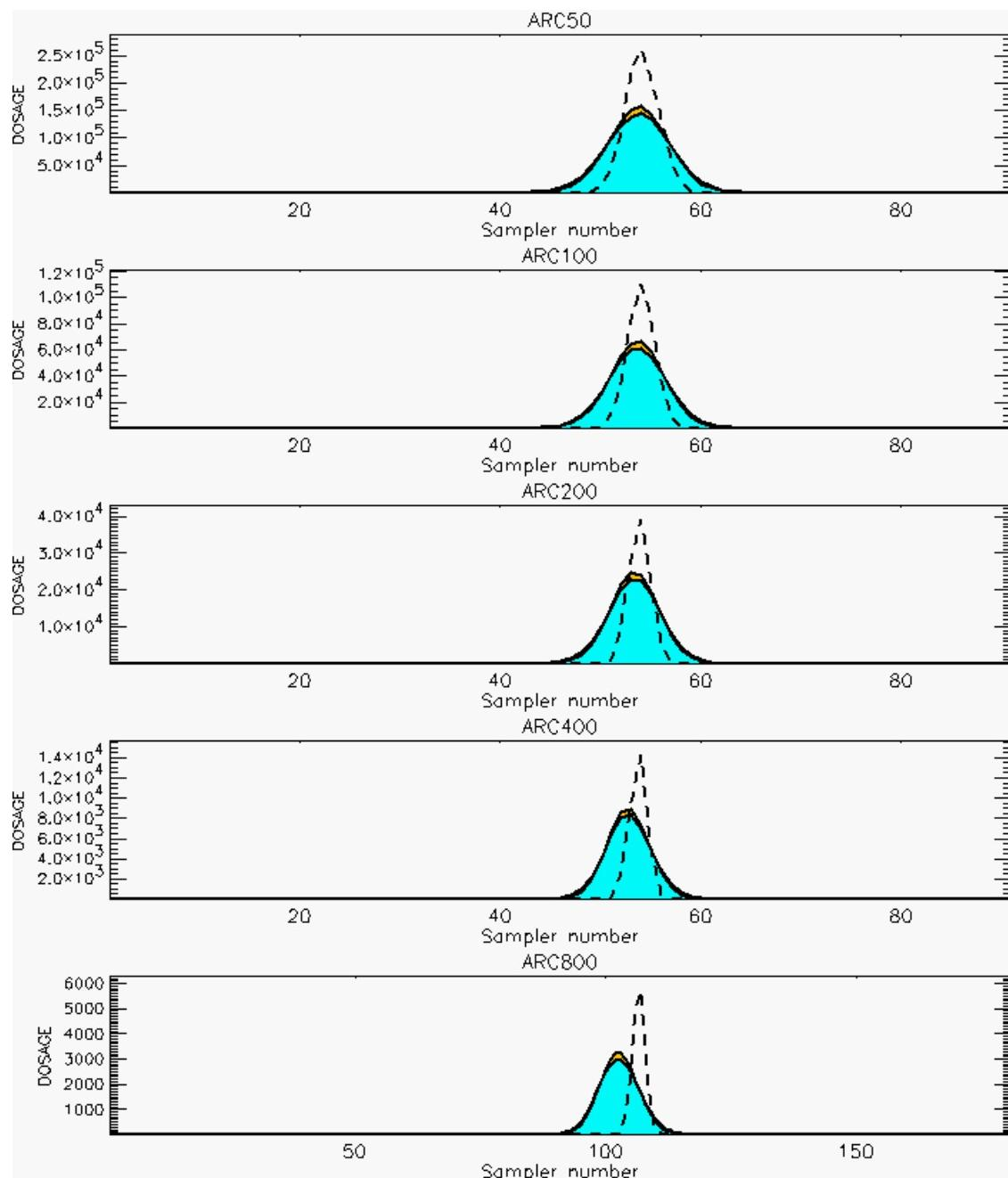
PG Prediction1 to Prediction2 Comparison

PG Trial File: pr_grass_tracer_Experiment_40.txt

PG Prediction File 1: ARAC\nodeposition\pg_40_nozd.arac

PG Prediction File 2: ARAC\sv_nozd\pg_40_sv_nozd.arac

Figure M-32b. NARAC Sigma-v Experimental and Sigma-v Calculated Predictions to Trial 40 on Logarithmic Scale: Stability Category is 6



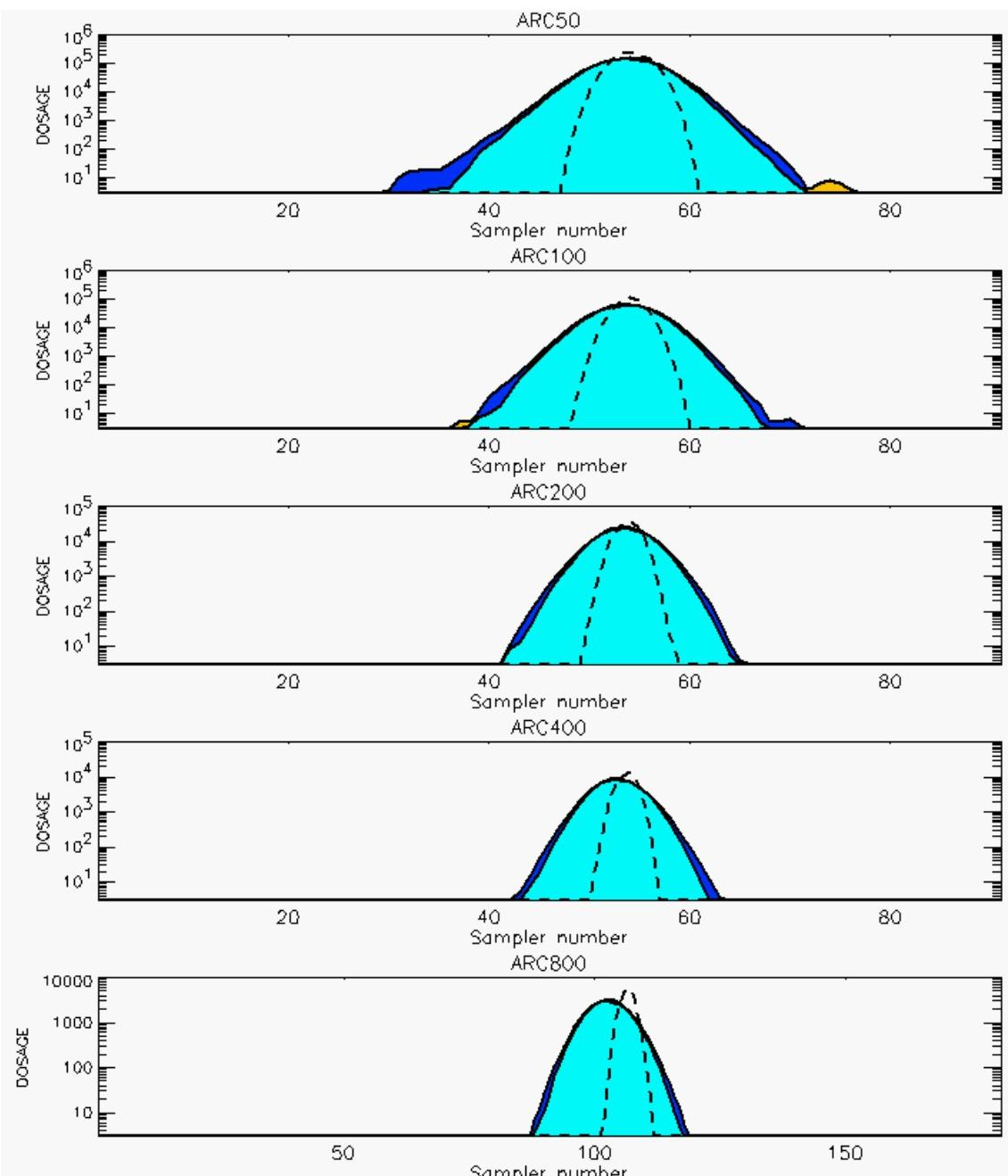
PG Prediction1 to Prediction2 Comparison

PG Trial File: pr_grass_tracer_Experiment_41.txt

PG Prediction File 1: ARAC\nodeposition\pg_41_nozd.arac

PG Prediction File 2: ARAC\sv_nozd\pg_41_sv_nozd.arac

Figure M-33a. NARAC Sigma-v Experimental and Sigma-v Calculated Predictions to Trial 41 on Linear Scale: Stability Category is 5



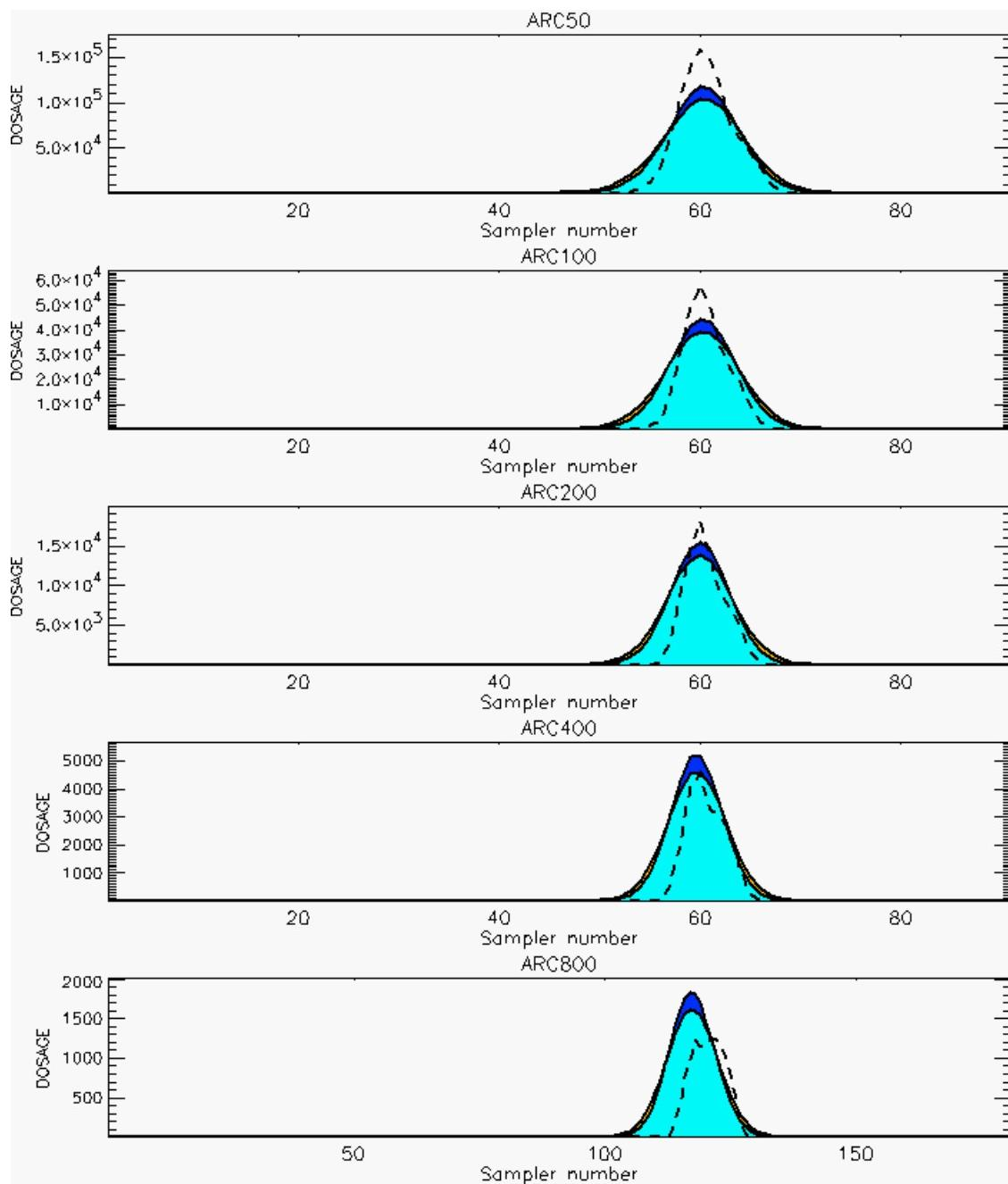
PG Prediction1 to Prediction2 Comparison

PG Trial File: pr_grass_tracer_Experiment_41.txt

PG Prediction File 1: ARAC\nodeposition\pg_41_nozd.arac

PG Prediction File 2: ARAC\sv_nzd\pg_41_sv_nzd.arac

Figure M-33b. NARAC Sigma-v Experimental and Sigma-v Calculated Predictions to Trial 41 on Logarithmic Scale: Stability Category is 5



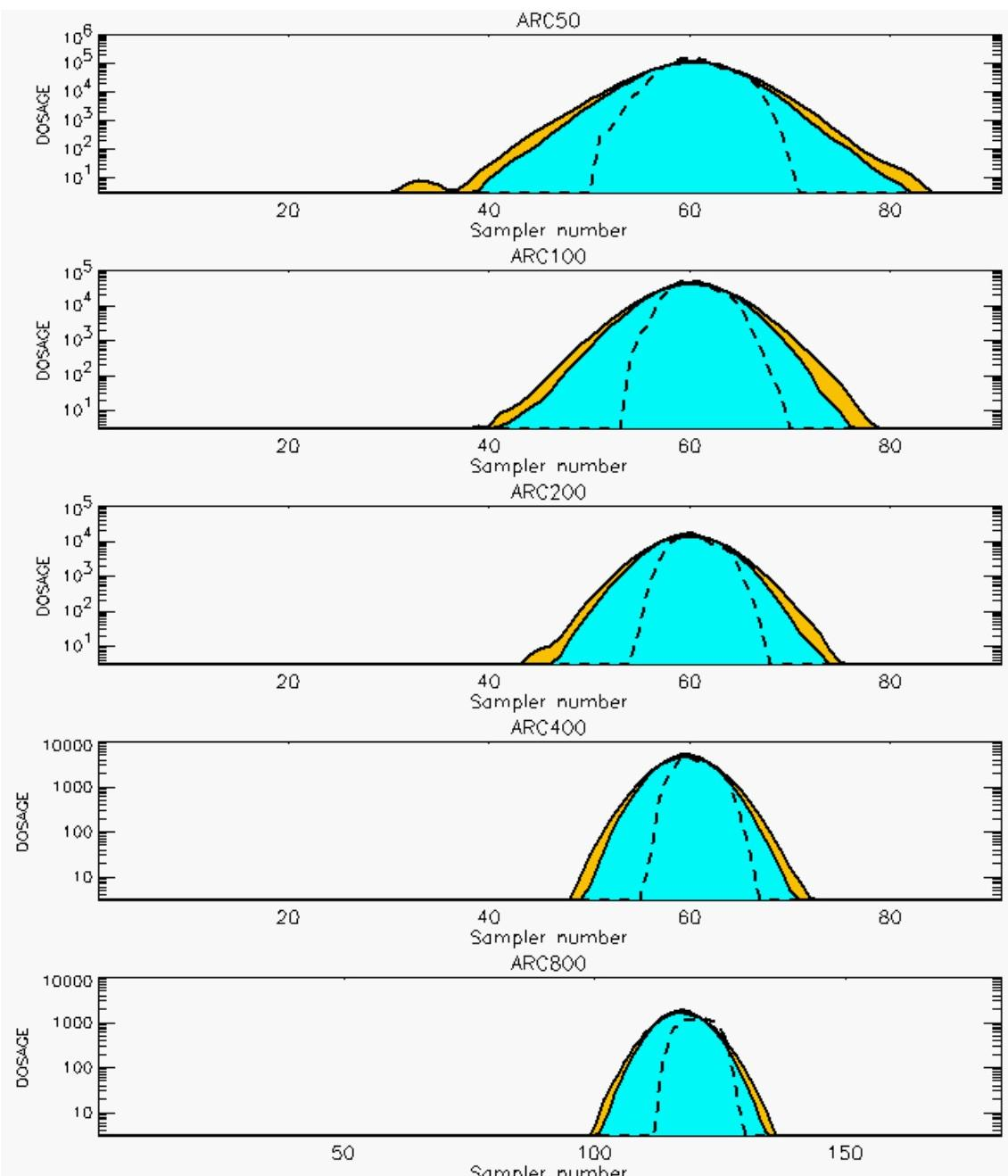
PG Prediction1 to Prediction2 Comparison

PG Trial File: pr_grass_tracer_Experiment_42.txt

PG Prediction File 1: ARAC\nodeposition\pg_42_nozd.arac

PG Prediction File 2: ARAC\sv_nozd\pg_42_sv_nozd.arac

Figure M-34a. NARAC Sigma-v Experimental and Sigma-v Calculated Predictions to Trial 42 on Linear Scale: Stability Category is 4



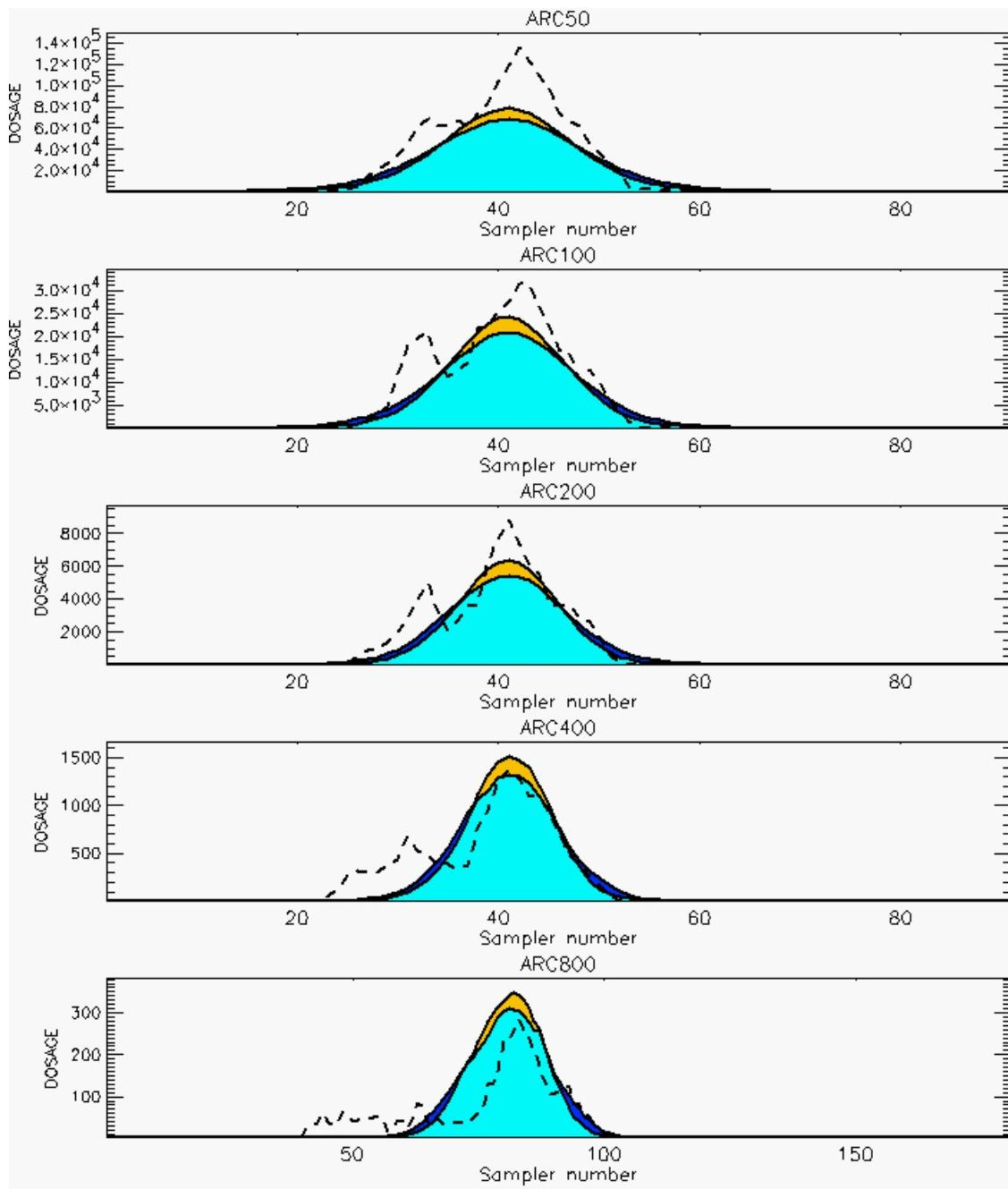
PG Prediction1 to Prediction2 Comparison

PG Trial File: pr_grass_tracer_Experiment_42.txt

PG Prediction File 1: ARAC\nodeposition\pg_42_nozd.arac

PG Prediction File 2: ARAC\sv_nozd\pg_42_sv_nozd.arac

Figure M-34b. NARAC Sigma-v Experimental and Sigma-v Calculated Predictions to Trial 42 on Logarithmic Scale: Stability Category is 4



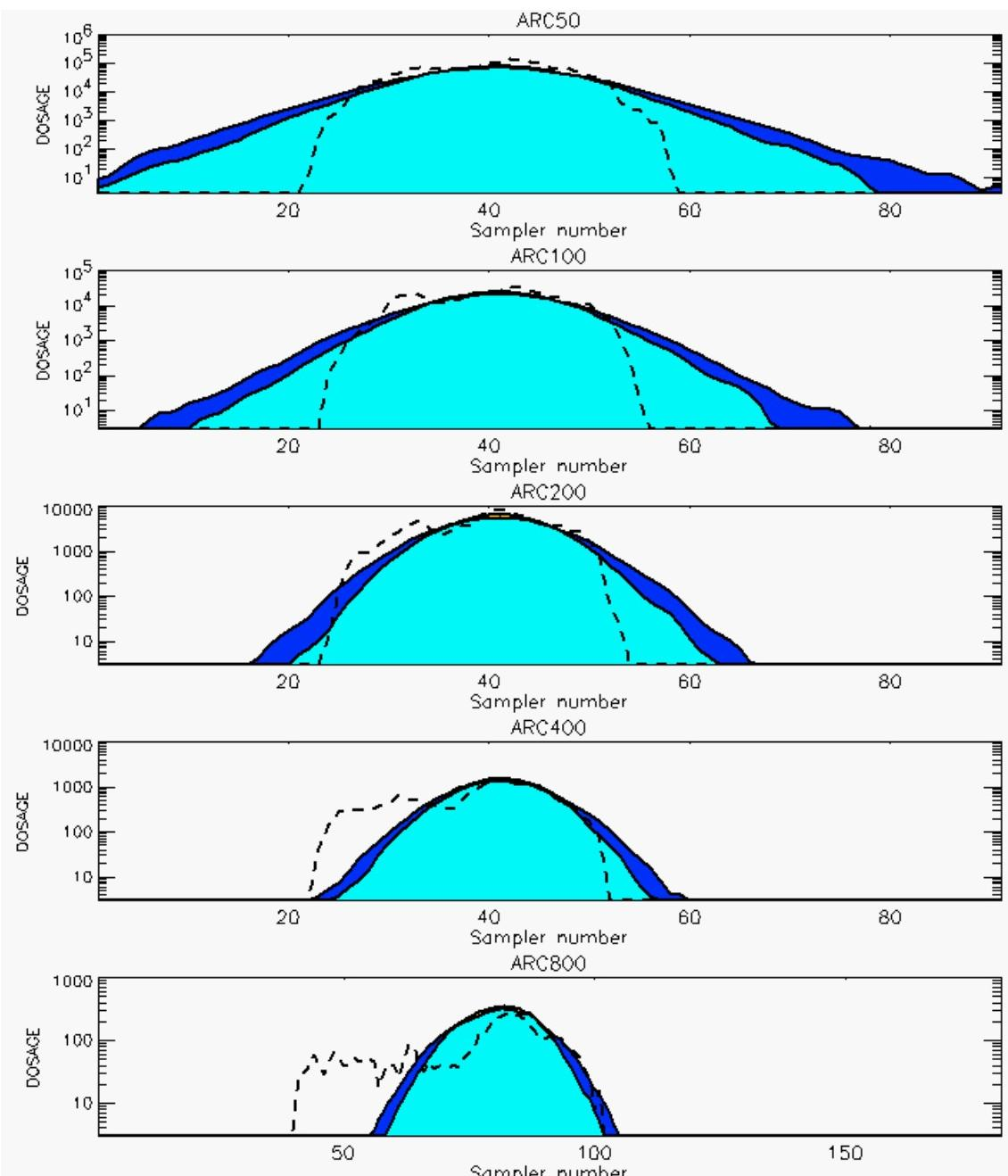
PG Prediction1 to Prediction2 Comparison

PG Trial File: pr_grass_tracer_Experiment_43.txt

PG Prediction File 1: ARAC\nodeposition\pg_43_nozd.arac

PG Prediction File 2: ARAC\sv_nozd\pg_43_sv_nozd.arac

Figure M-35a. NARAC Sigma-v Experimental and Sigma-v Calculated Predictions to Trial 43 on Linear Scale: Stability Category is 1



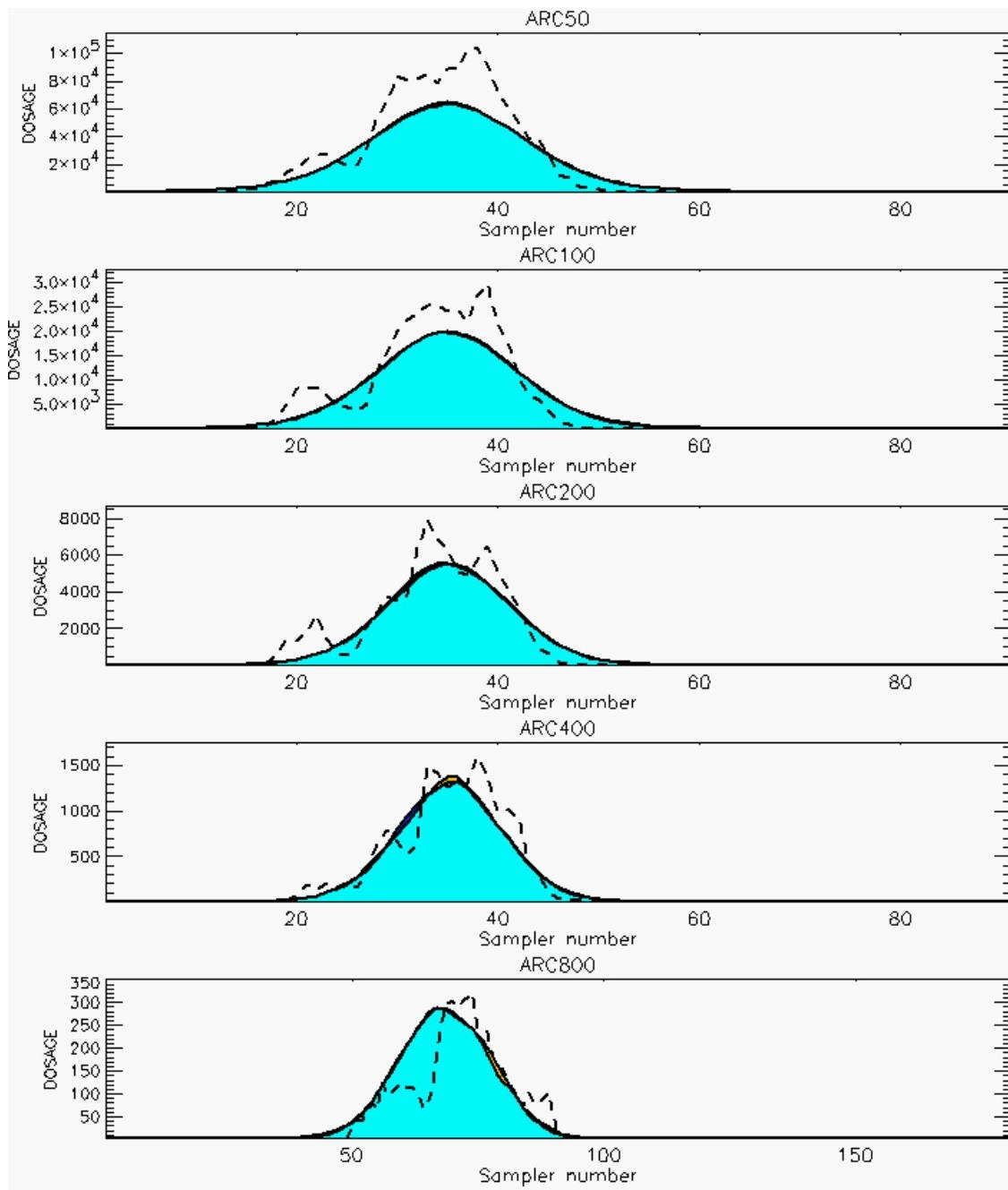
PG Prediction1 to Prediction2 Comparison

PG Trial File: pr_grass_tracer_Experiment_43.txt

PG Prediction File 1: ARAC\nodeposition\pg_43_nozd.arac

PG Prediction File 2: ARAC\sv_nozd\pg_43_sv_nozd.arac

Figure M-35b. NARAC Sigma-v Experimental and Sigma-v Calculated Predictions to Trial 43 on Logarithmic Scale: Stability Category is 1



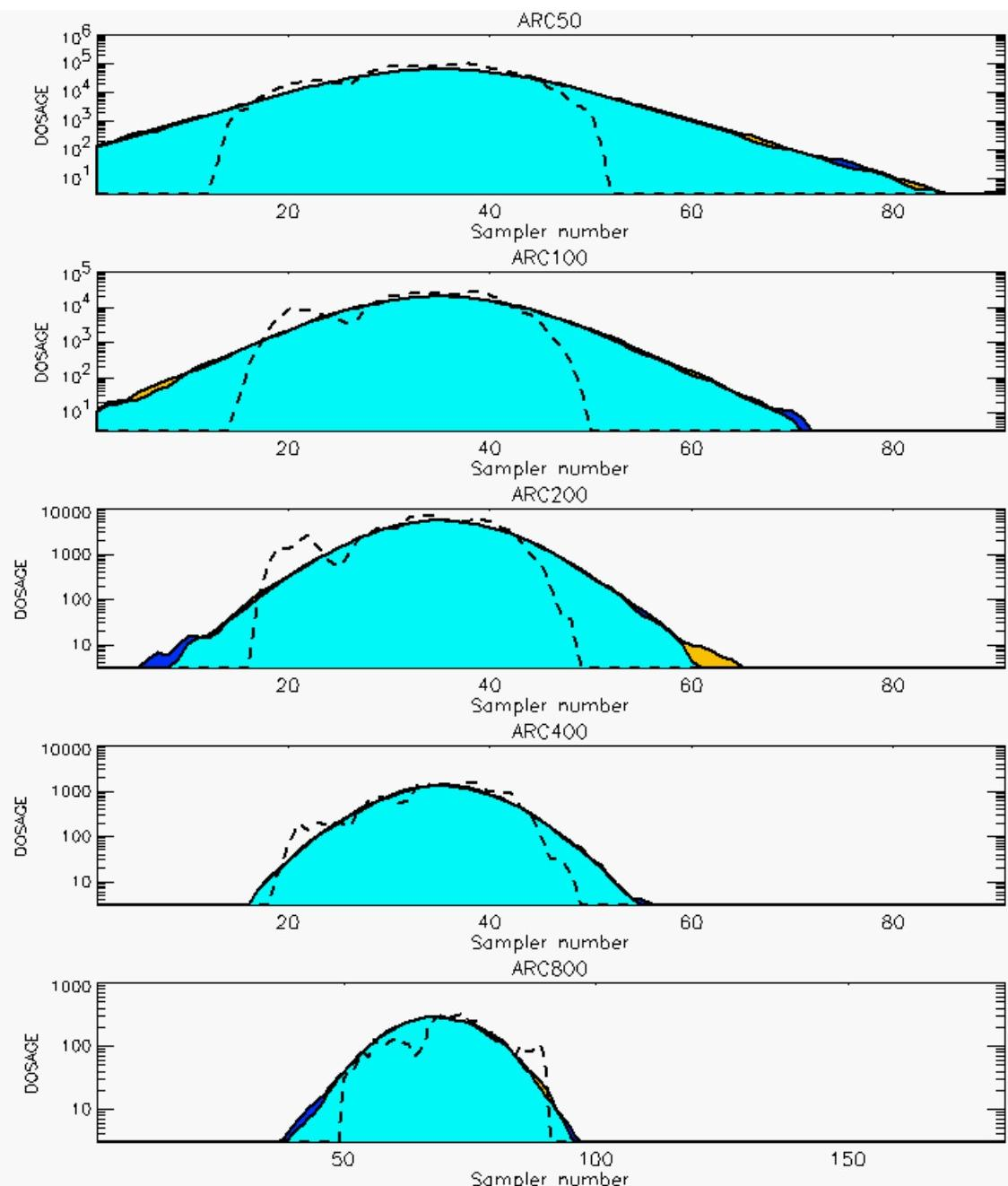
PG Prediction1 to Prediction2 Comparison

PG Trial File: pr_grass_tracer_Experiment_44.txt

PG Prediction File 1: ARAC\nodeposition\pg_44_novd.arac

PG Prediction File 2: ARAC\sv_novd\pg_44_sv_novd.arac

Figure M-36a. NARAC Sigma-v Experimental and Sigma-v Calculated Predictions to Trial 44 on Linear Scale: Stability Category is 2



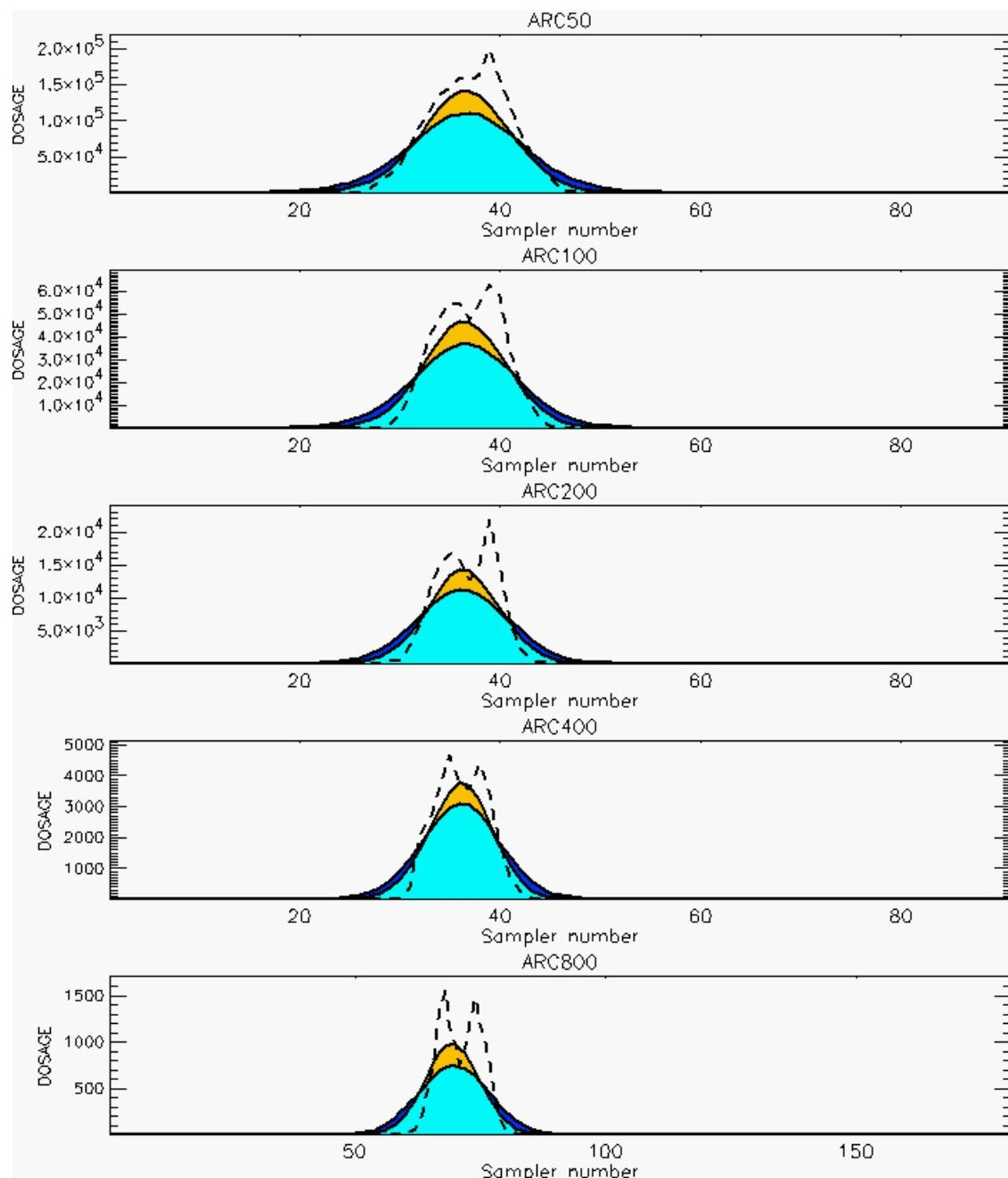
PG Prediction1 to Prediction2 Comparison

PG Trial File: pr_grass_tracer_Experiment_44.txt

PG Prediction File 1: ARAC\nodeposition\pg_44_nozd.arac

PG Prediction File 2: ARAC\sv_nozd\pg_44_sv_nozd.arac

Figure M-36b. NARAC Sigma-v Experimental and Sigma-v Calculated Predictions to Trial 44 on Logarithmic Scale: Stability Category is 2



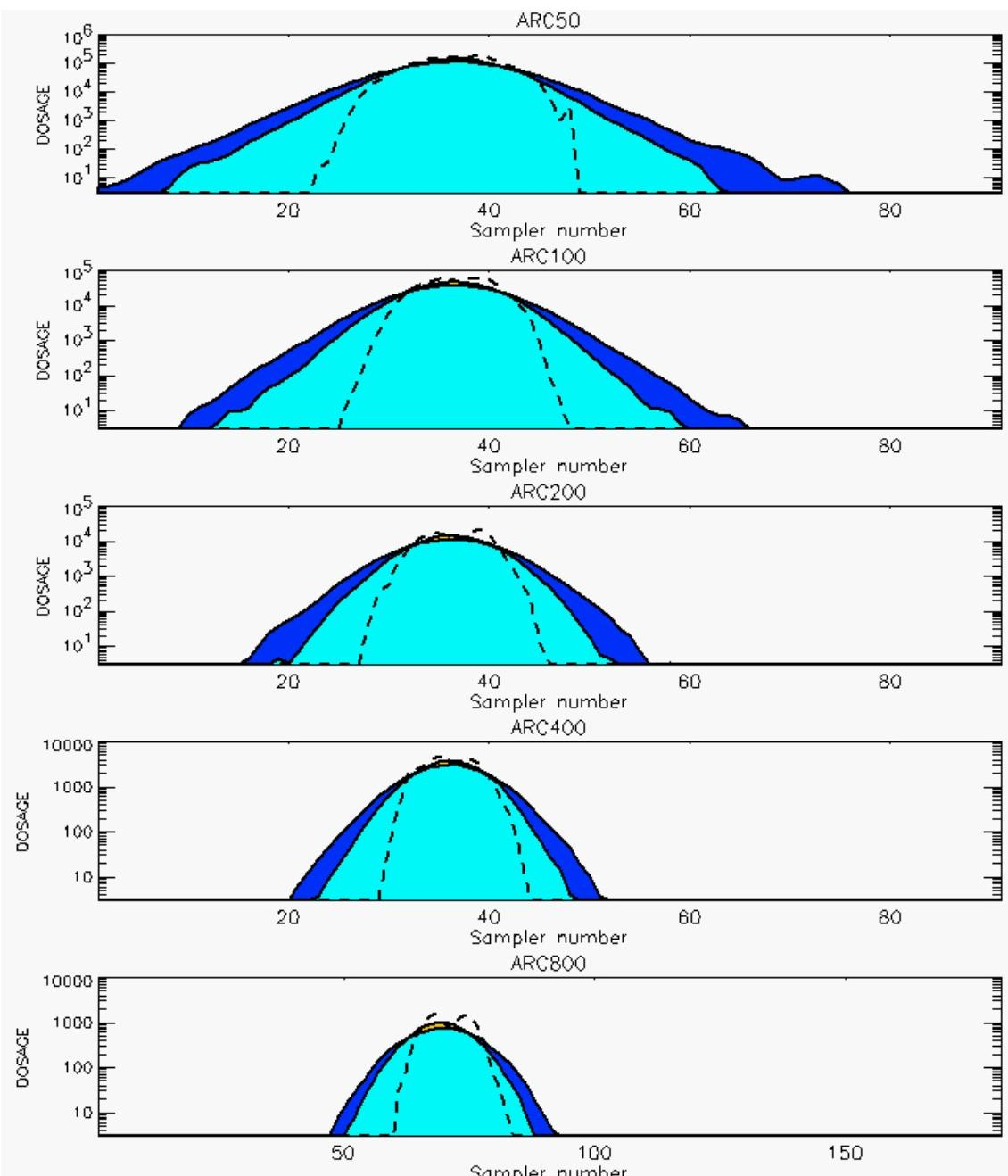
PG Prediction1 to Prediction2 Comparison

PG Trial File: pr_grass_tracer_Experiment_45.txt

PG Prediction File 1: ARAC\nodeposition\pg_45_novd.arac

PG Prediction File 2: ARAC\sv_novd\pg_45_sv_novd.arac

Figure M-37a. NARAC Sigma-v Experimental and Sigma-v Calculated Predictions to Trial 45 on Linear Scale: Stability Category is 3



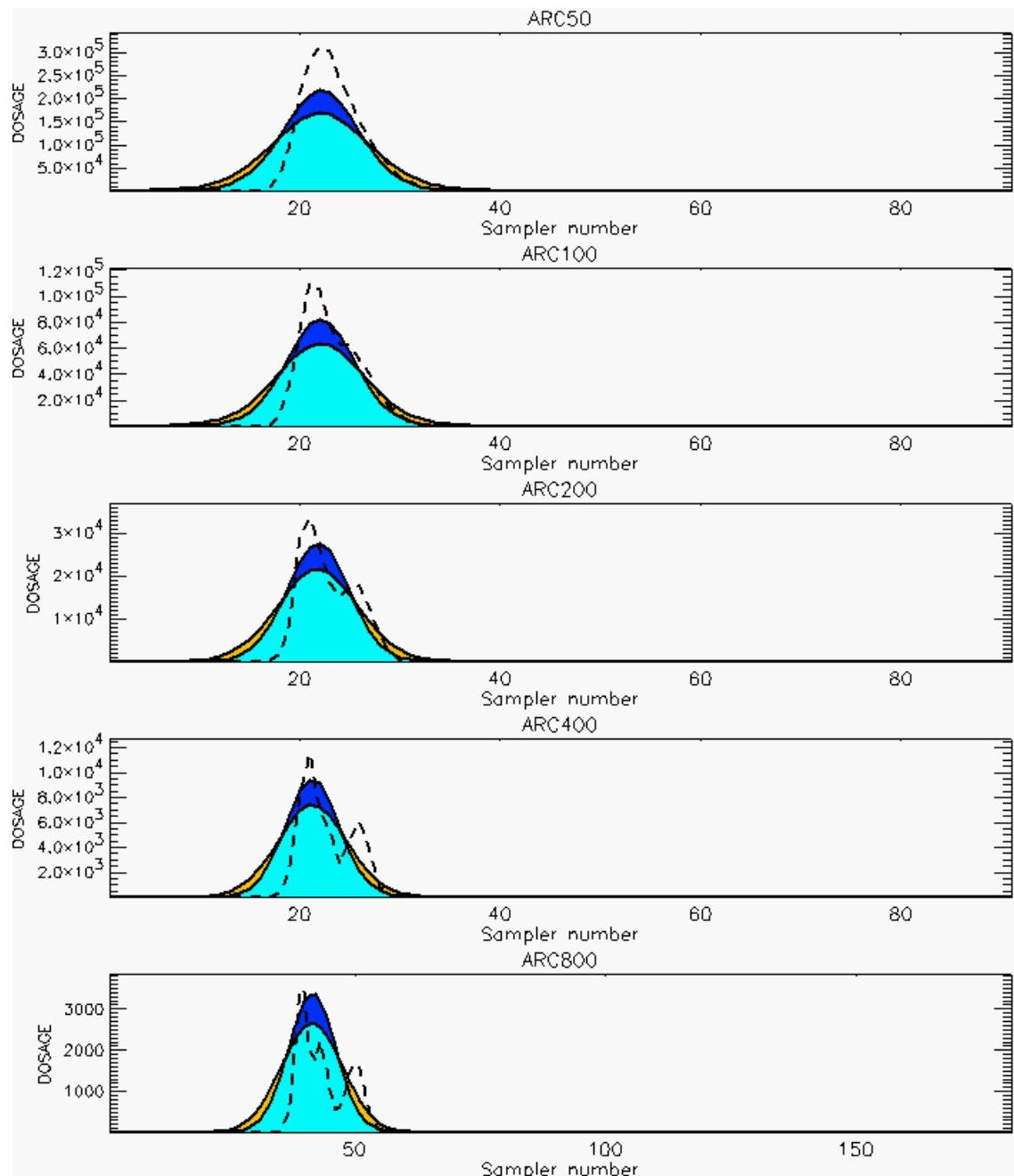
PG Prediction1 to Prediction2 Comparison

PG Trial File: pr_grass_tracer_Experiment_45.txt

PG Prediction File 1: ARAC\nodeposition\pg_45_nozd.arac

PG Prediction File 2: ARAC\sv_nozd\pg_45_sv_nozd.arac

Figure M-37b. NARAC Sigma-v Experimental and Sigma-v Calculated Predictions to Trial 45 on Logarithmic Scale: Stability Category is 3



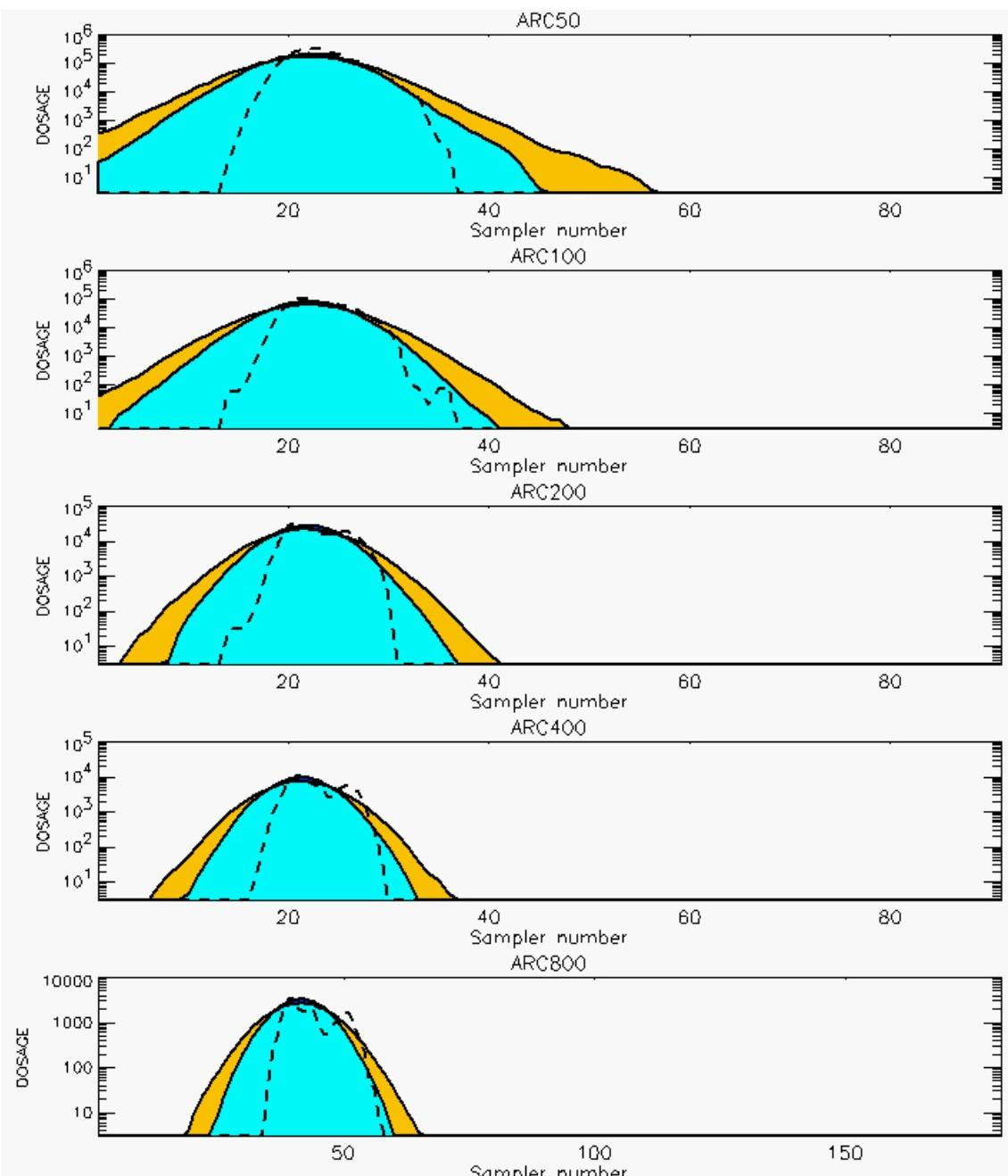
PG Prediction1 to Prediction2 Comparison

PG Trial File: pr_grass_tracer_Experiment_46.txt

PG Prediction File 1: ARAC\nodeposition\pg_46_nozd.arac

PG Prediction File 2: ARAC\sv_nozd\pg_46_sv_nozd.arac

Figure M-38a. NARAC Sigma-v Experimental and Sigma-v Calculated Predictions to Trial 46 on Linear Scale: Stability Category is 4



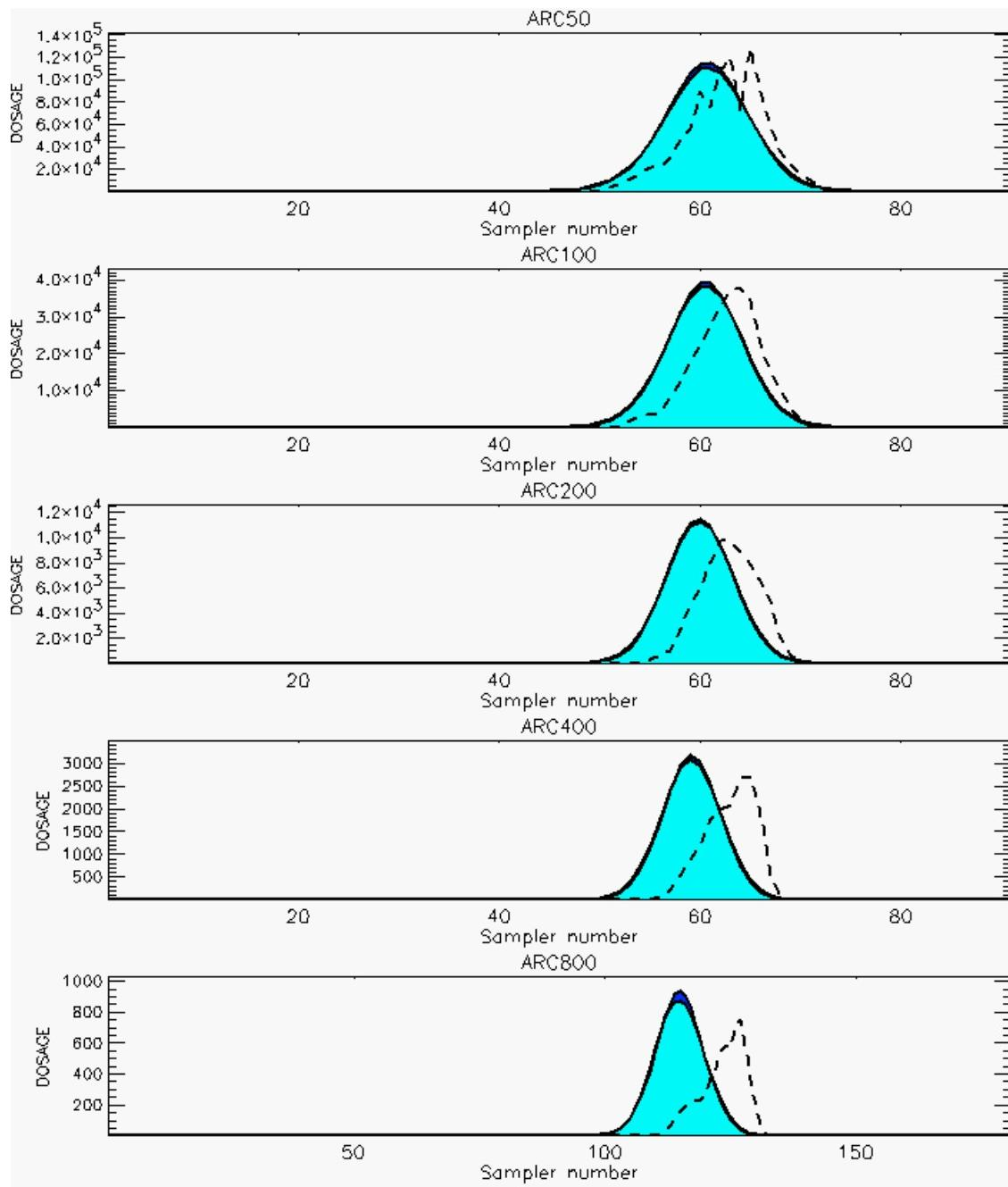
PG Prediction1 to Prediction2 Comparison

PG Trial File: pr_grass_tracer_Experiment_46.txt

PG Prediction File 1: ARAC\nodeposition\pg_46_nozd.arac

PG Prediction File 2: ARAC\sv_nozd\pg_46_sv_nozd.arac

Figure M-38b. NARAC Sigma-v Experimental and Sigma-v Calculated Predictions to Trial 46 on Logarithmic Scale: Stability Category is 4



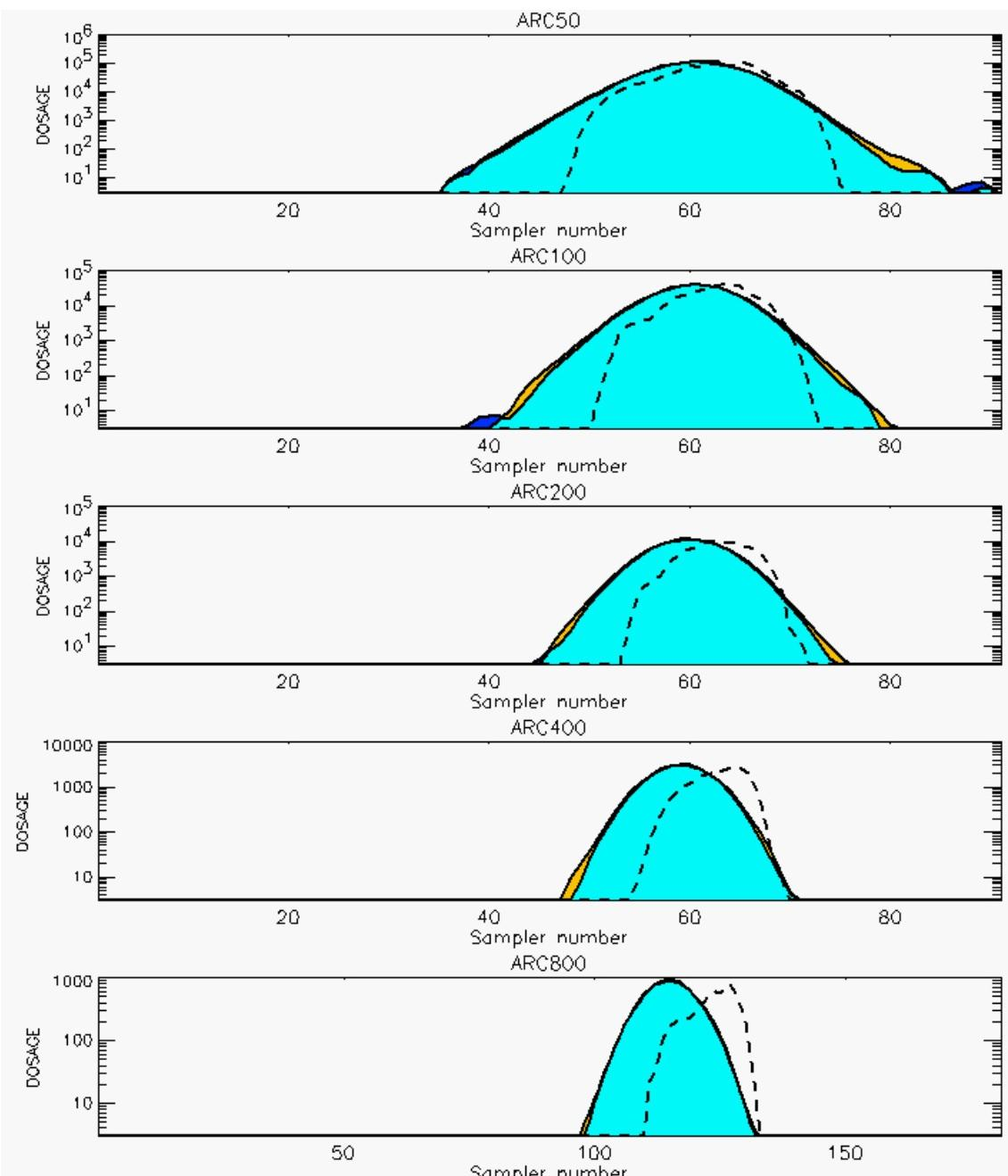
PG Prediction1 to Prediction2 Comparison

PG Trial File: pr_grass_tracer_Experiment_48.txt

PG Prediction File 1: ARAC\nodeposition\pg_48_novd.arac

PG Prediction File 2: ARAC\sv_novd\pg_48_sv_novd.arac

Figure M-39a. NARAC Sigma-v Experimental and Sigma-v Calculated Predictions to Trial 48 on Linear Scale: Stability Category is 3



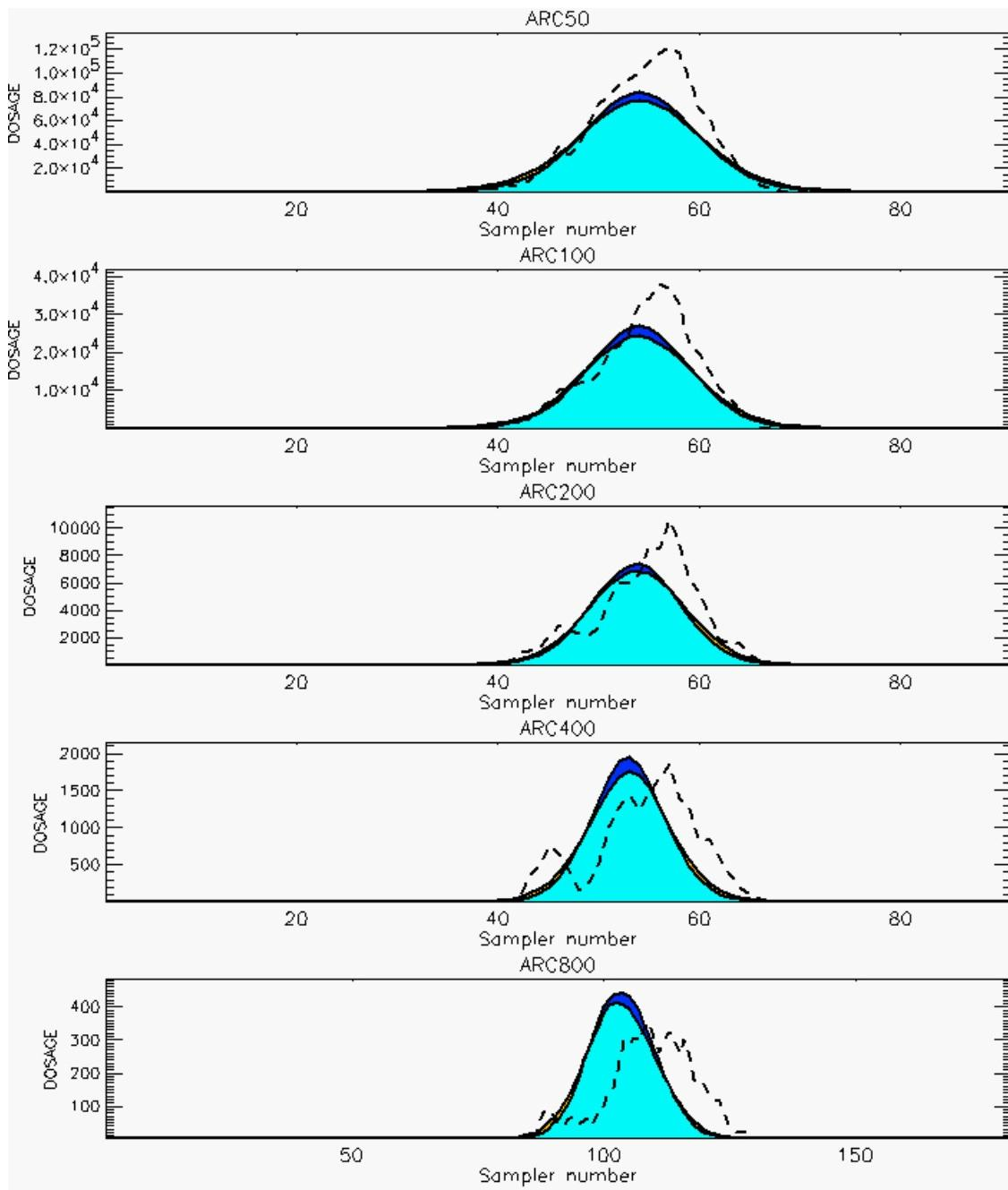
PG Prediction1 to Prediction2 Comparison

PG Trial File: pr_grass_tracer_Experiment_48.txt

PG Prediction File 1: ARAC\nodeposition\pg_48_novd.arac

PG Prediction File 2: ARAC\sv_novd\pg_48_sv_novd.arac

Figure M-39b. NARAC Sigma-v Experimental and Sigma-v Calculated Predictions to Trial 48 on Logarithmic Scale: Stability Category is 3



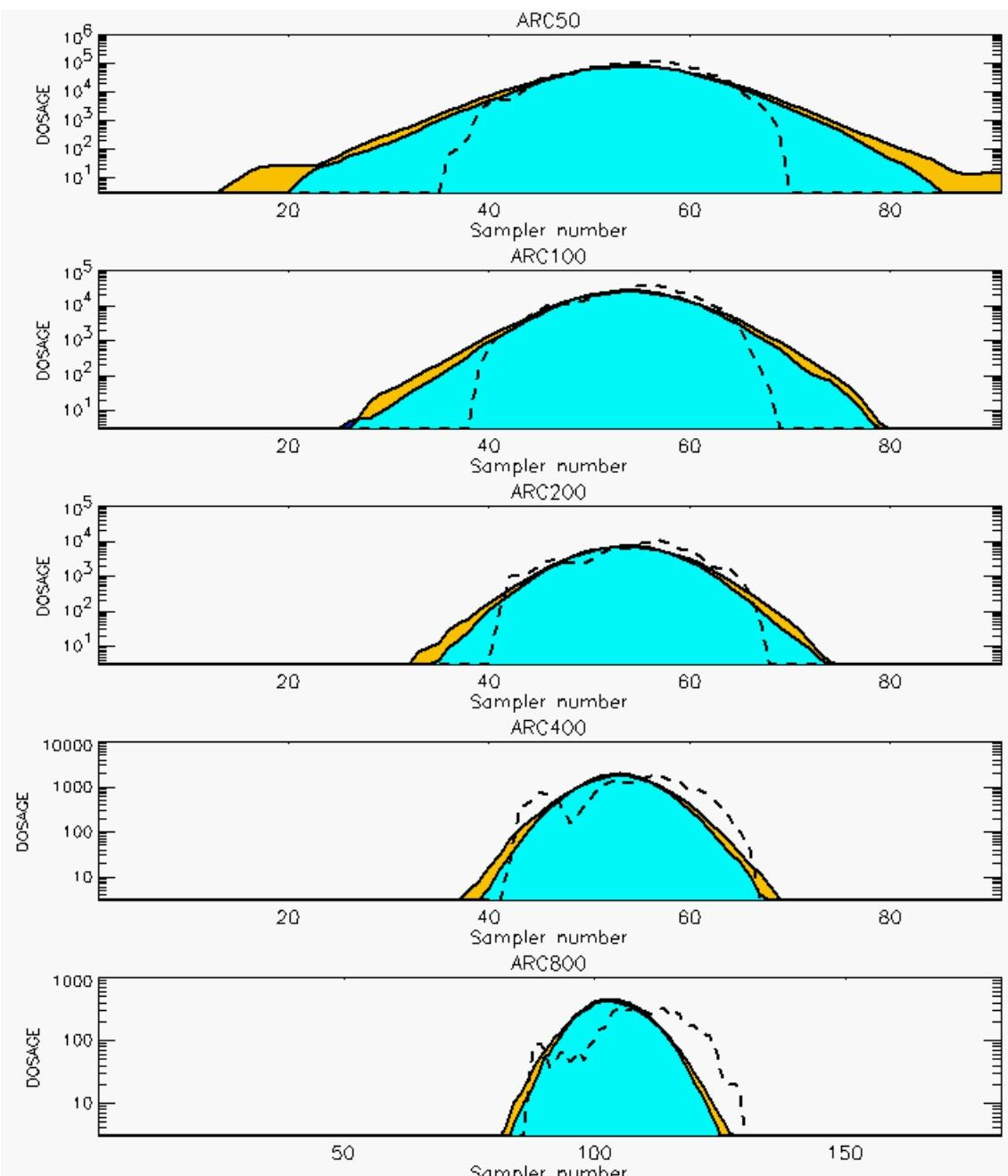
PG Prediction1 to Prediction2 Comparison

PG Trial File: pr_grass_tracer_Experiment_49.txt

PG Prediction File 1: ARAC\nodeposition\pg_49_novd.arac

PG Prediction File 2: ARAC\sv_novd\pg_49_sv_novd.arac

Figure M-40a. NARAC Sigma-v Experimental and Sigma-v Calculated Predictions to Trial 49 on Linear Scale: Stability Category is 2



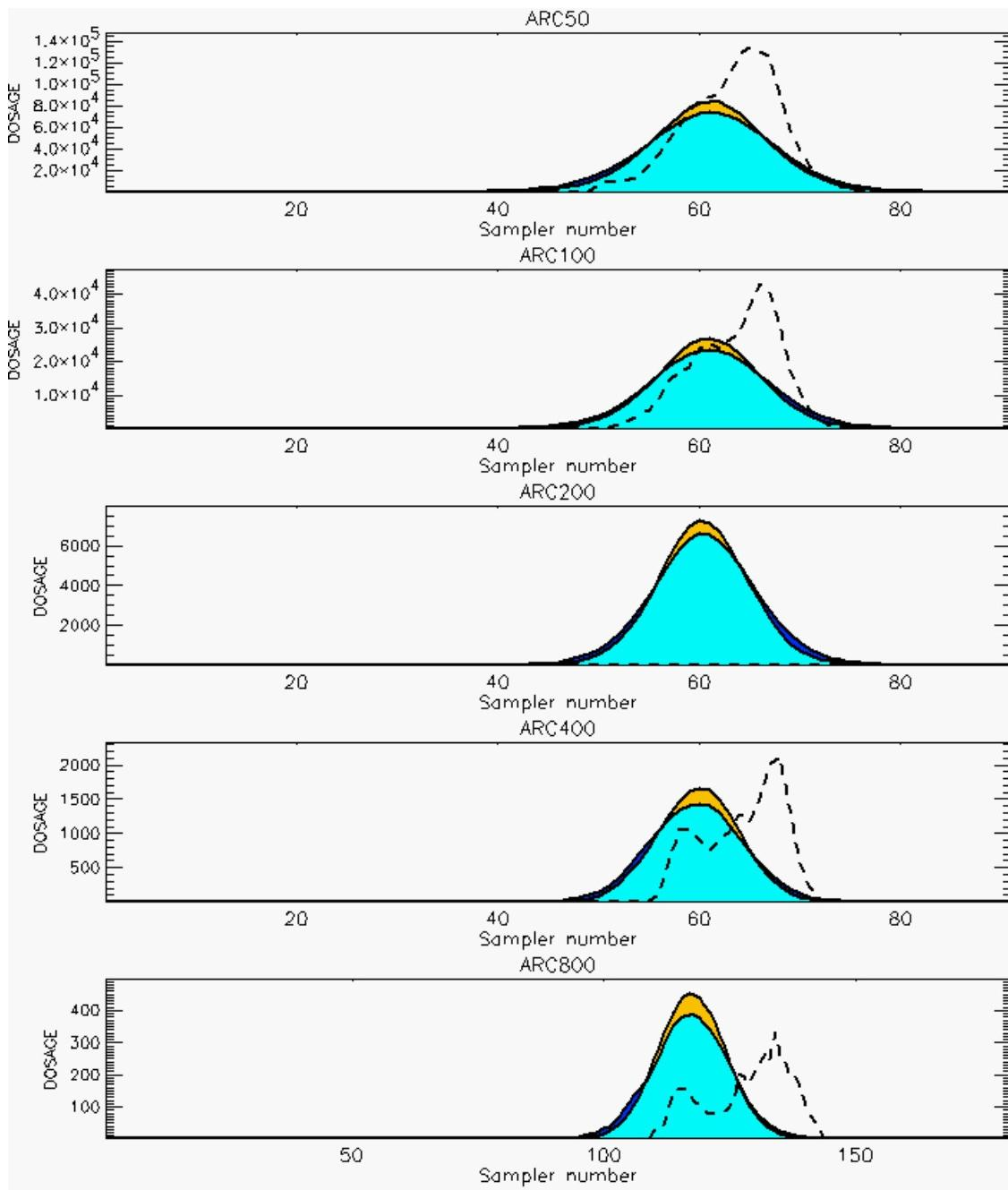
PG Prediction1 to Prediction2 Comparison

PG Trial File: pr_grass_tracer_Experiment_49.txt

PG Prediction File 1: ARAC\nodeposition\pg_49_novd.arac

PG Prediction File 2: ARAC\sv_novd\pg_49_sv_novd.arac

Figure M-40b. NARAC Sigma-v Experimental and Sigma-v Calculated Predictions to Trial 49 on Logarithmic Scale: Stability Category is 2



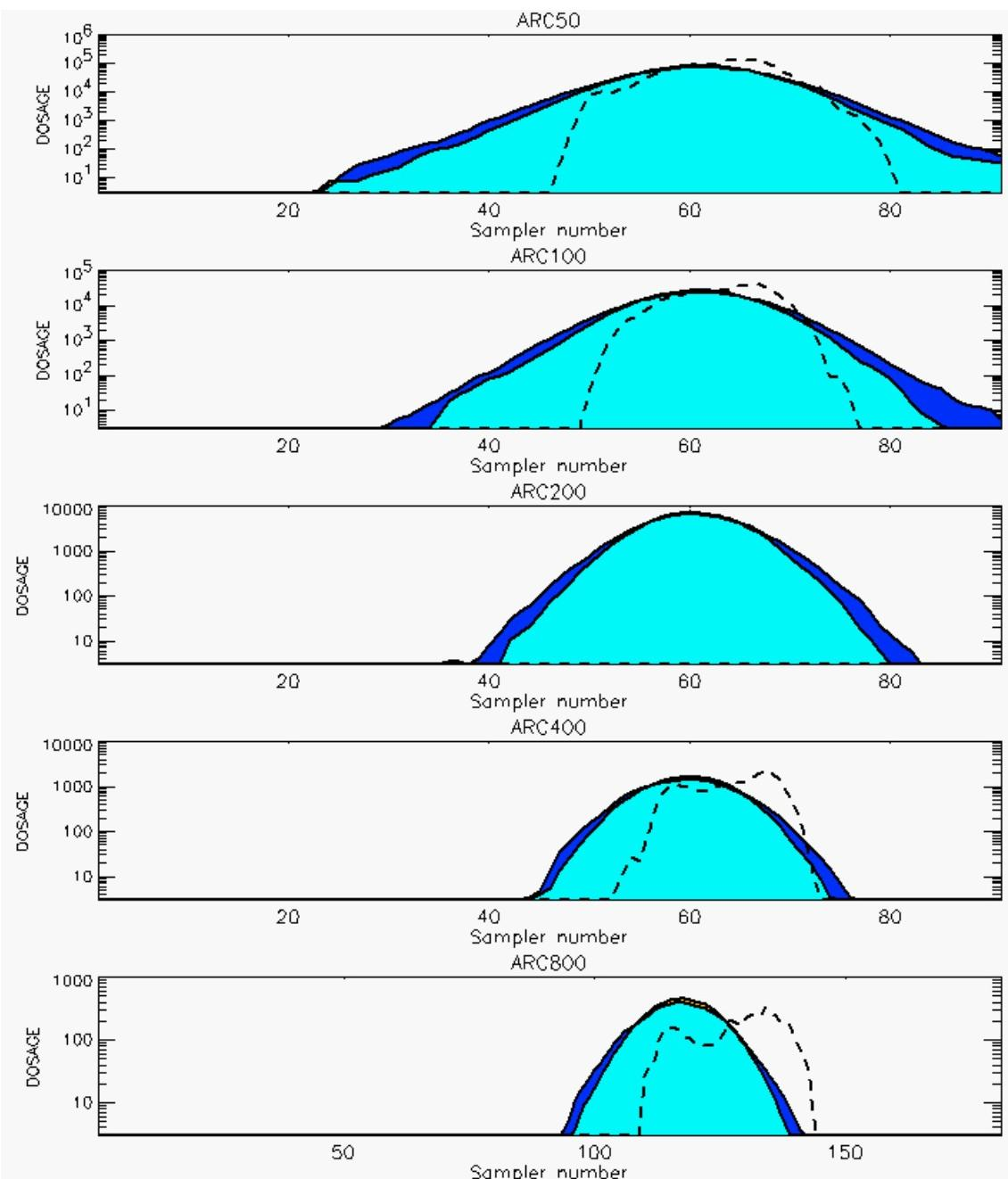
PG Prediction1 to Prediction2 Comparison

PG Trial File: pr_grass_tracer_Experiment_50.txt

PG Prediction File 1: ARAC\nodeposition\pg_50_novd.arac

PG Prediction File 2: ARAC\sv_novd\pg_50_sv_novd.arac

Figure M-41a. NARAC Sigma-v Experimental and Sigma-v Calculated Predictions to Trial 50 on Linear Scale: Stability Category is 2



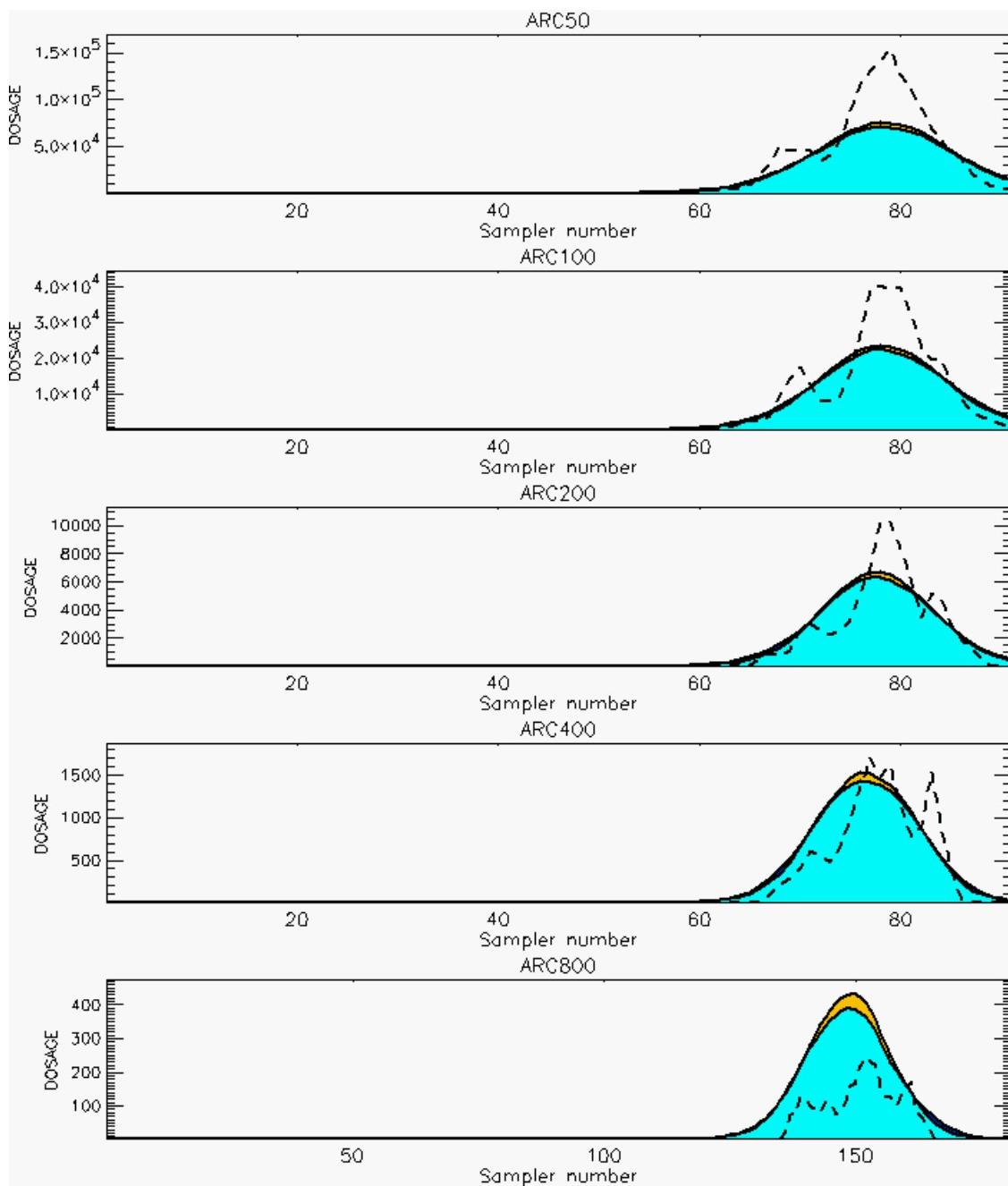
PG Prediction1 to Prediction2 Comparison

PG Trial File: pr_grass_tracer_Experiment_50.txt

PG Prediction File 1: ARAC\nodeposition\pg_50_nozd.arac

PG Prediction File 2: ARAC\sv_nozd\pg_50_sv_nozd.arac

Figure M-41b. NARAC Sigma-v Experimental and Sigma-v Calculated Predictions to Trial 50 on Logarithmic Scale: Stability Category is 2



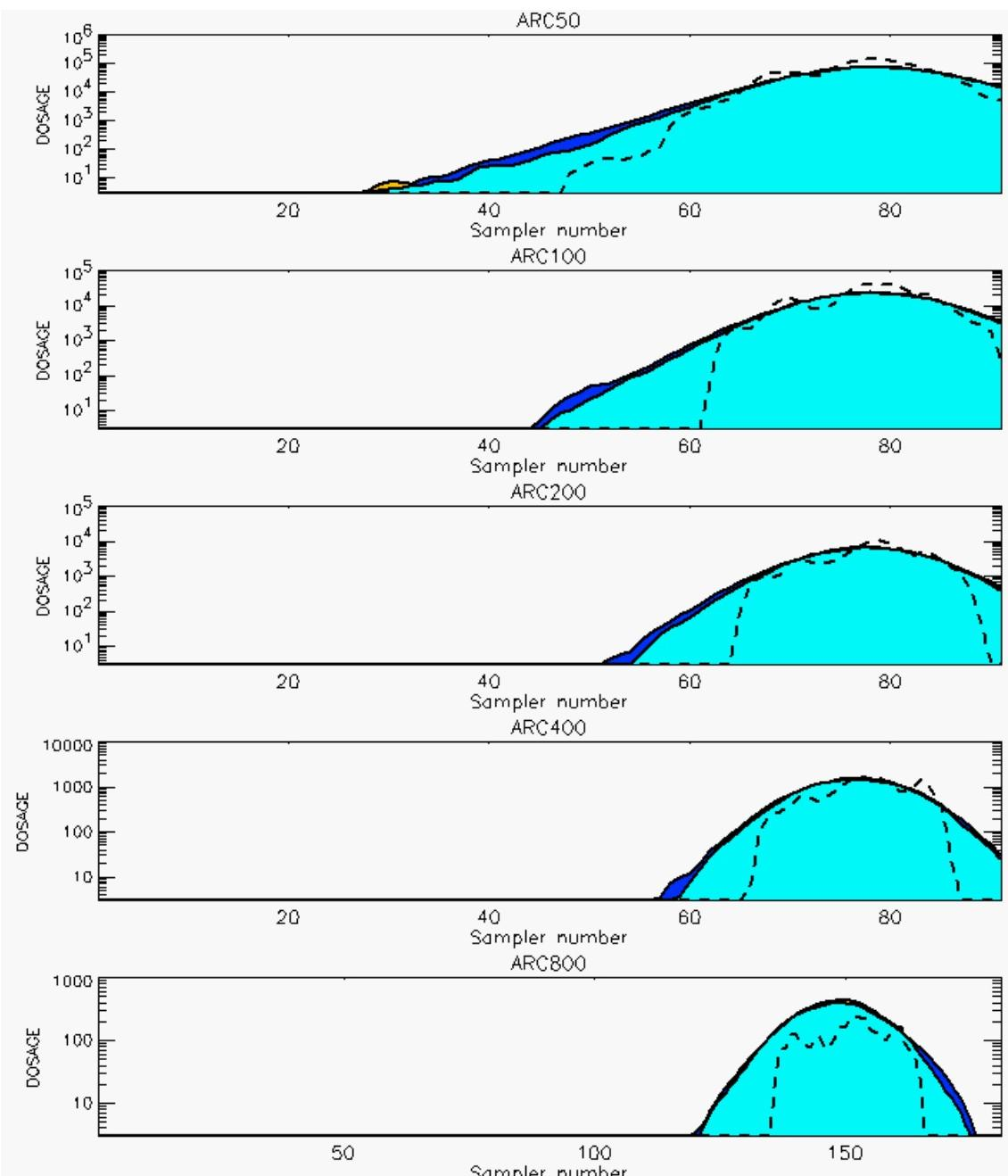
PG Prediction1 to Prediction2 Comparison

PG Trial File: pr_grass_tracer_Experiment_51.txt

PG Prediction File 1: ARAC\nodeposition_replace\pg_51_nozd.arac

PG Prediction File 2: ARAC\sv_nozd\pg_51_sv_nozd.arac

Figure M-42a. NARAC Sigma-v Experimental and Sigma-v Calculated Predictions to Trial 51 on Linear Scale: Stability Category is 2



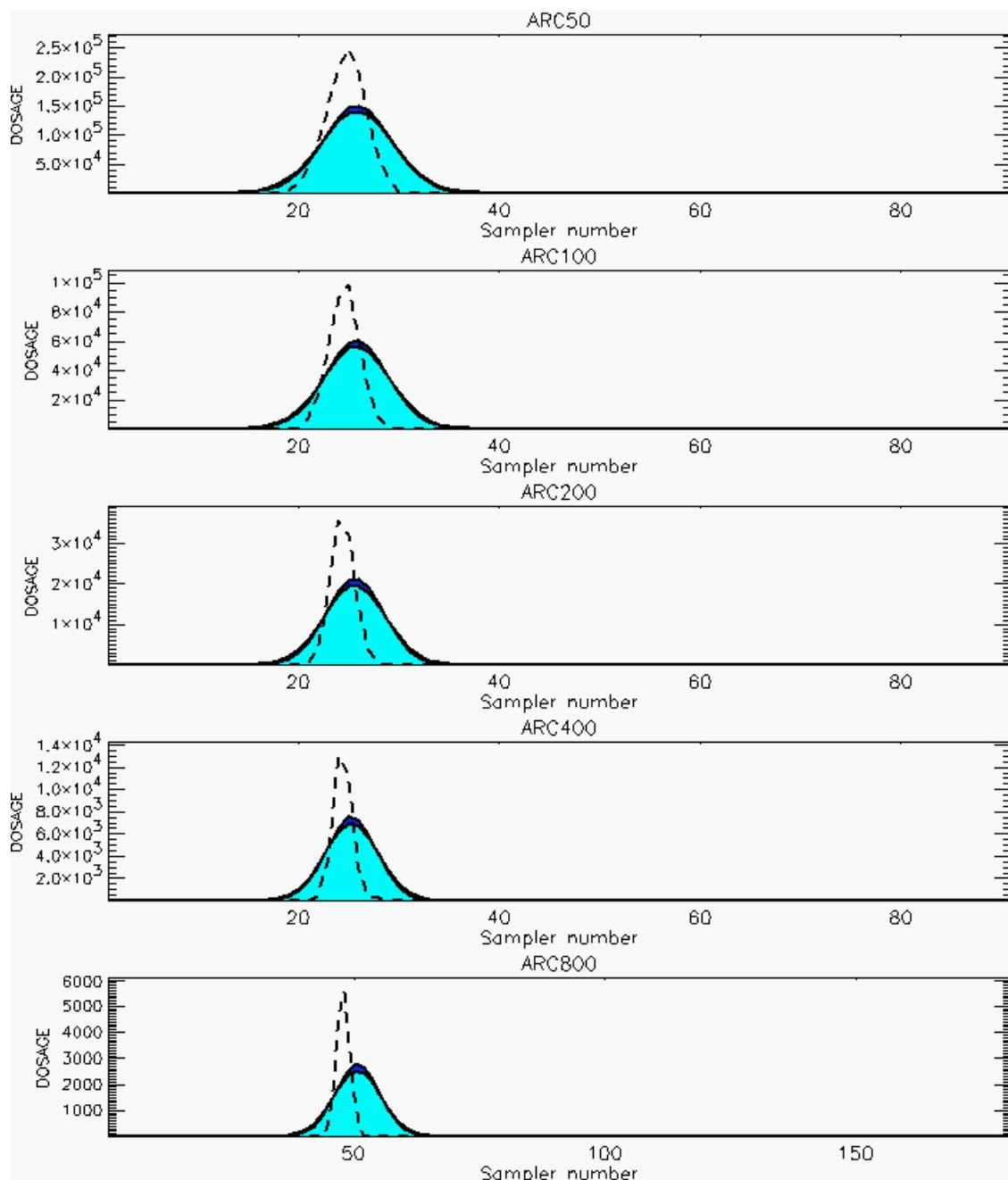
PG Prediction1 to Prediction2 Comparison

PG Trial File: pr_grass_tracer_Experiment_51.txt

PG Prediction File 1: ARAC\nodeposition_replace\pg_51_nozd.arac

PG Prediction File 2: ARAC\sv_nozd\pg_51_sv_nozd.arac

Figure M-42b. NARAC Sigma-v Experimental and Sigma-v Calculated Predictions to Trial 51 on Logarithmic Scale: Stability Category is 2



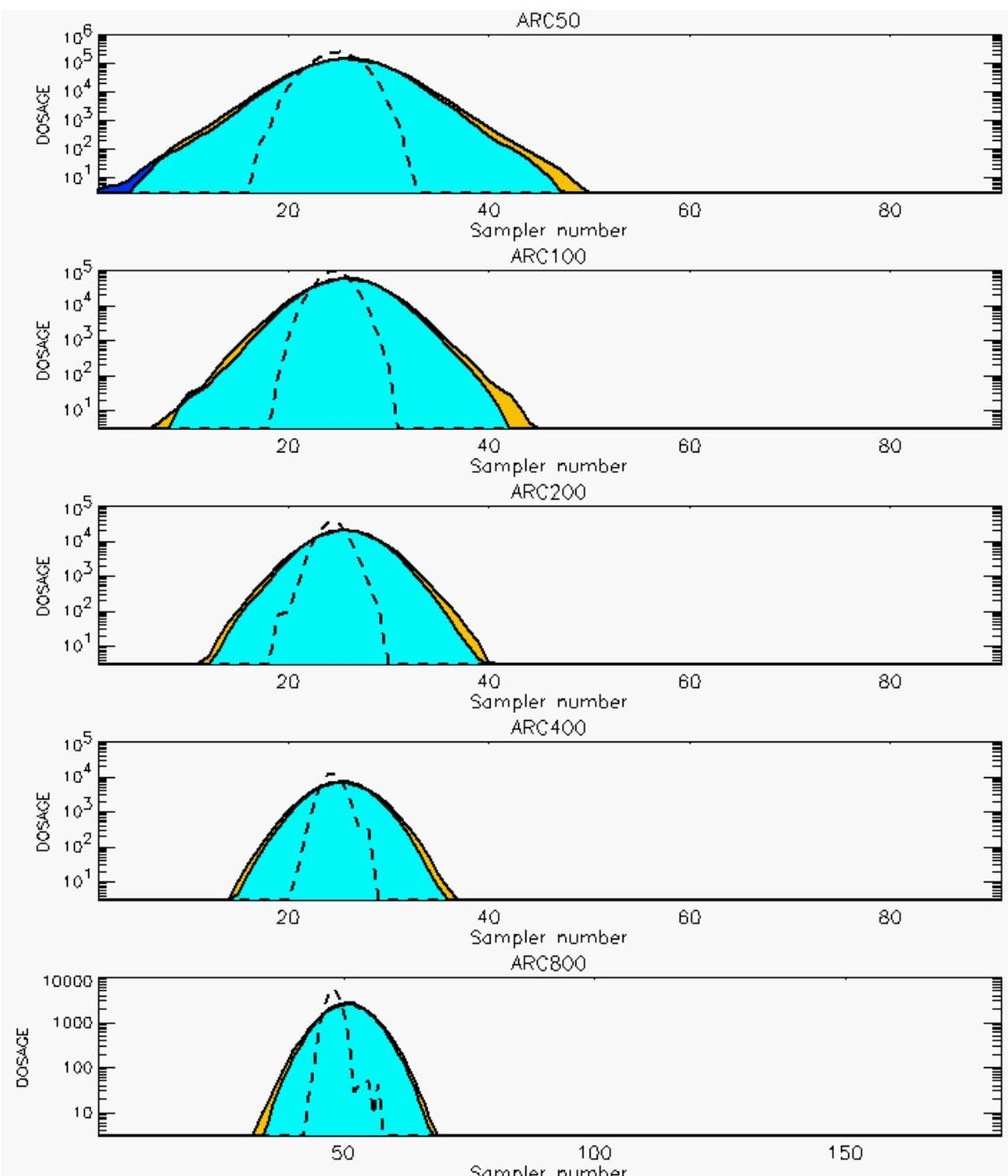
PG Prediction1 to Prediction2 Comparison

PG Trial File: pr_grass_tracer_Experiment_54.txt

PG Prediction File 1: ARAC\nodeposition\pg_54_nozd.arac

PG Prediction File 2: ARAC\sv_nzd\pg_54_sv_nzd.arac

Figure M-43a. NARAC Sigma-v Experimental and Sigma-v Calculated Predictions to Trial 54 on Linear Scale: Stability Category is 5



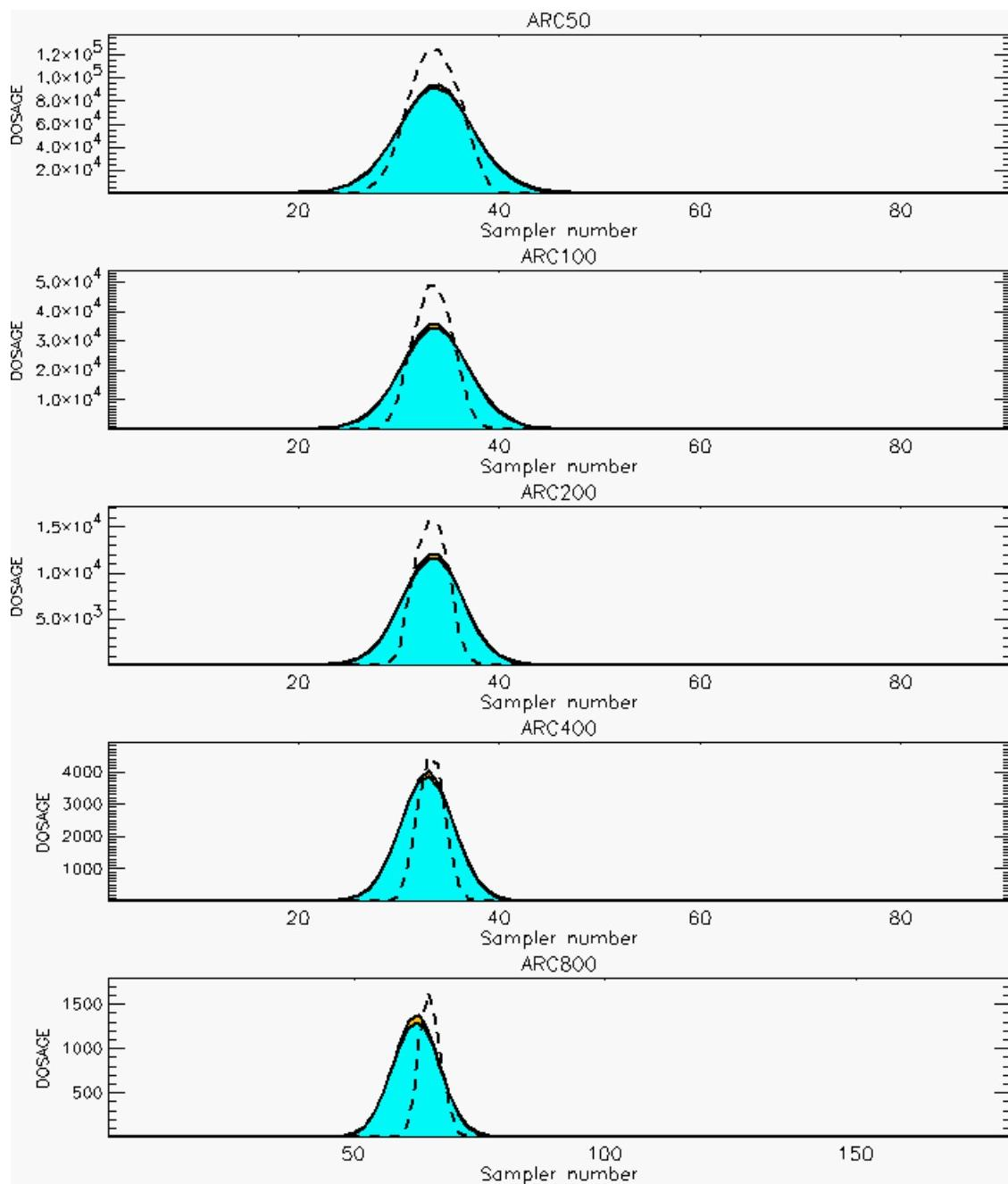
PG Prediction1 to Prediction2 Comparison

PG Trial File: pr_grass_tracer_Experiment_54.txt

PG Prediction File 1: ARAC\nodeposition\pg_54_nozd.arac

PG Prediction File 2: ARAC\sv_nozd\pg_54_sv_nozd.arac

Figure M-43b. NARAC Sigma-v Experimental and Sigma-v Calculated Predictions to Trial 54 on Logarithmic Scale: Stability Category is 5



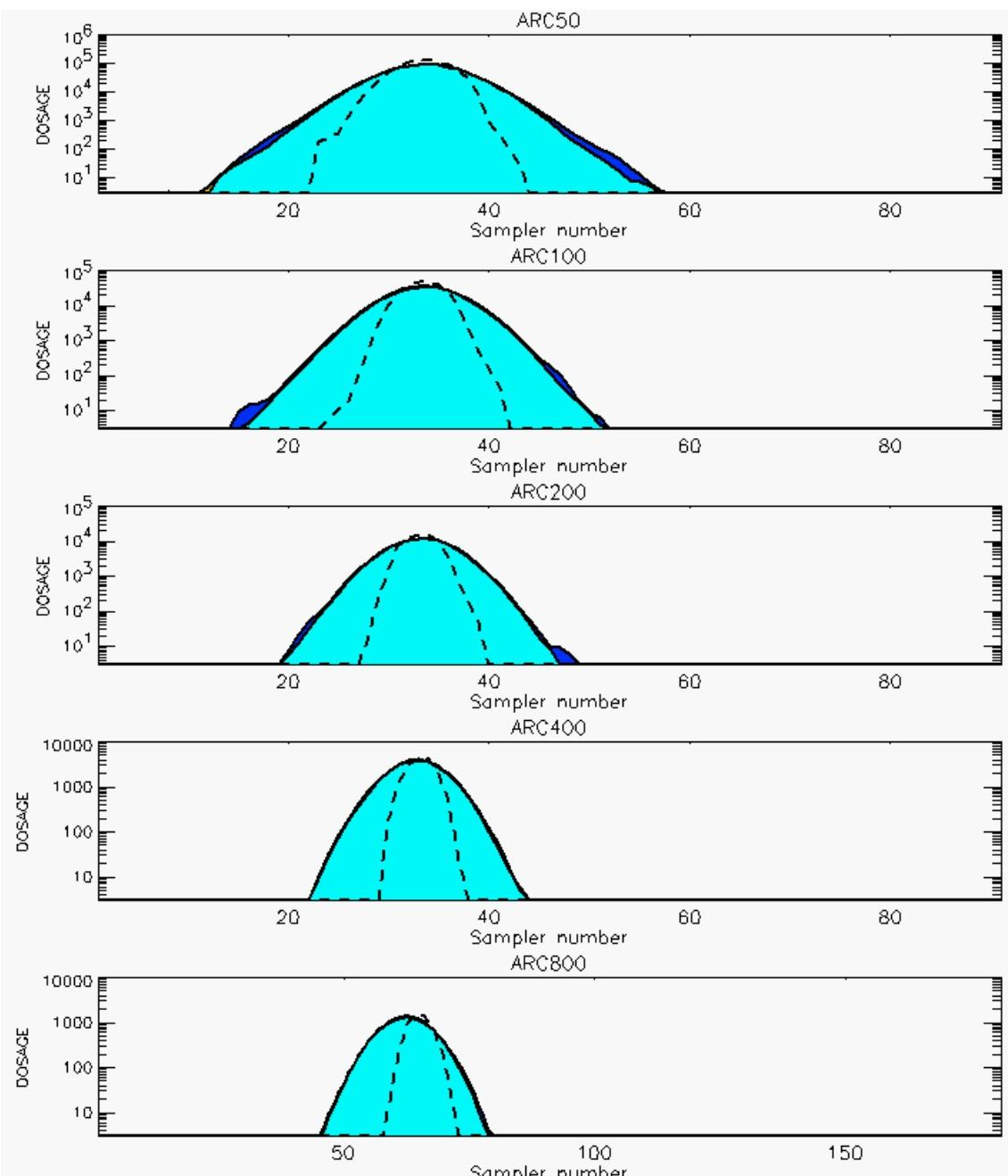
PG Prediction1 to Prediction2 Comparison

PG Trial File: pr_grass_tracer_Experiment_55.txt

PG Prediction File 1: ARAC\nodeposition\pg_55_novd.arac

PG Prediction File 2: ARAC\sv_novd\pg_55_sv_novd.arac

Figure M-44a. NARAC Sigma-v Experimental and Sigma-v Calculated Predictions to Trial 55 on Linear Scale: Stability Category is 4



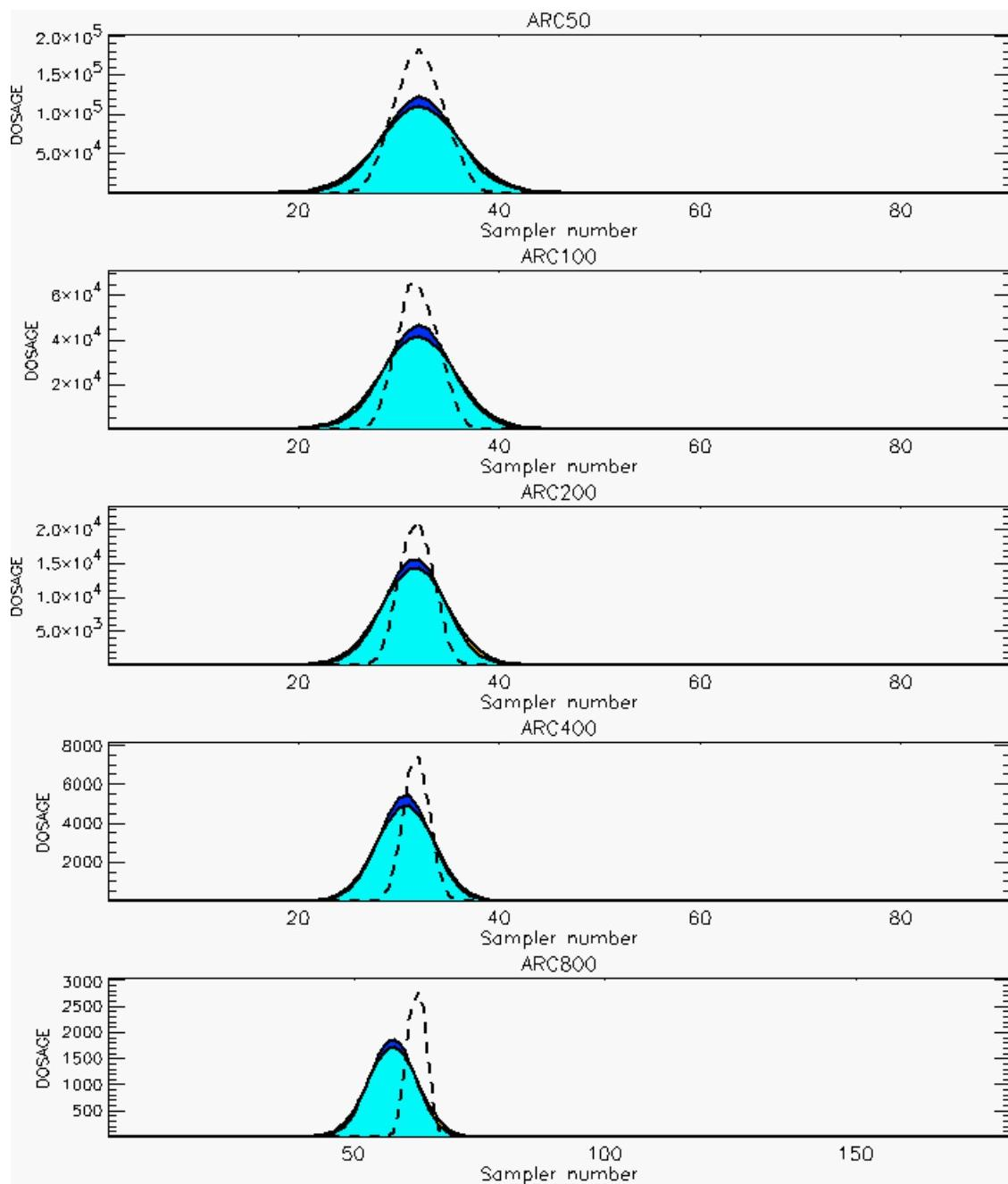
PG Prediction1 to Prediction2 Comparison

PG Trial File: pr_grass_tracer_Experiment_55.txt

PG Prediction File 1: ARAC\nodeposition\pg_55_novd.arac

PG Prediction File 2: ARAC\sv_novd\pg_55_sv_novd.arac

Figure M-44b. NARAC Sigma-v Experimental and Sigma-v Calculated Predictions to Trial 55 on Logarithmic Scale: Stability Category is 4



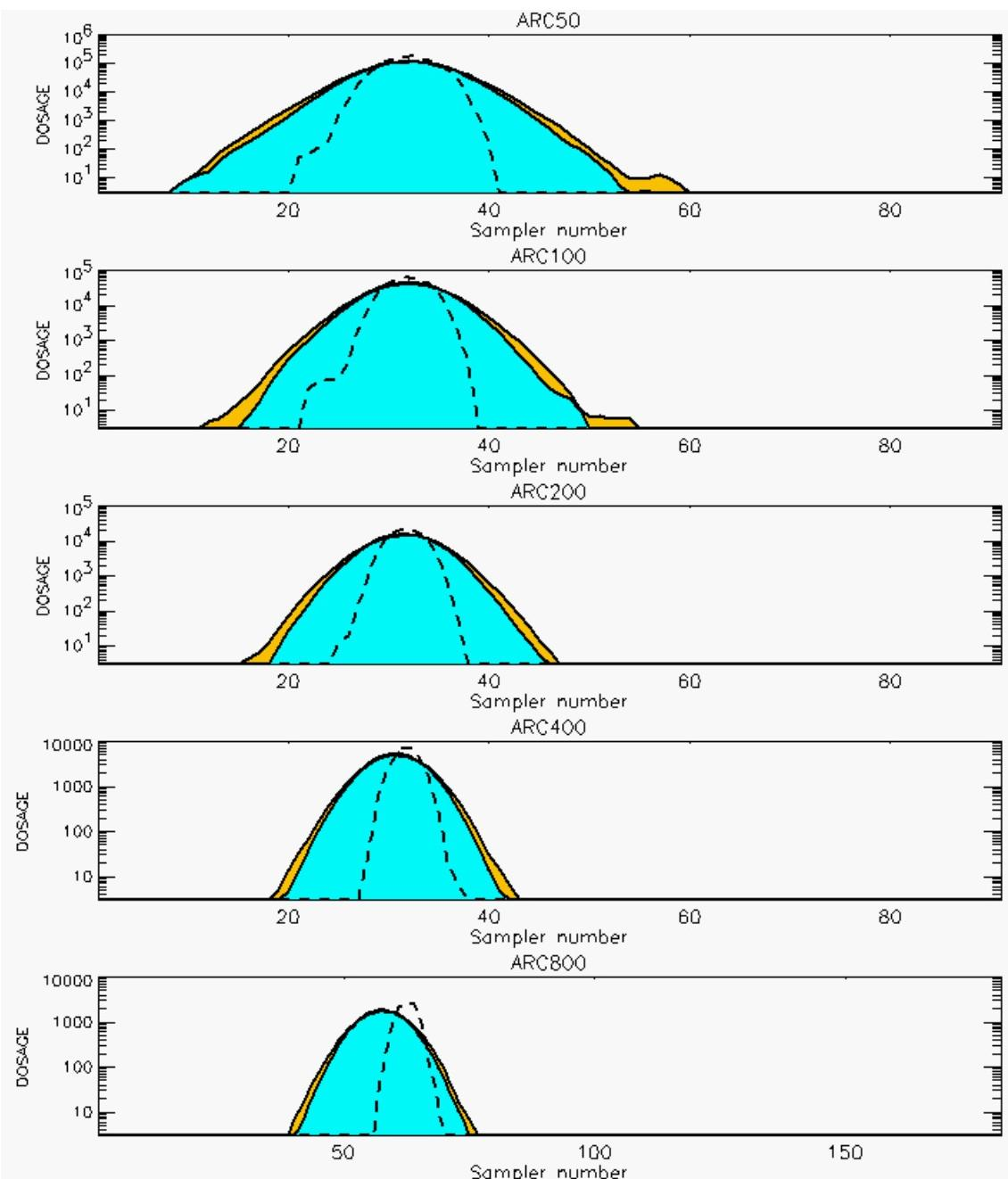
PG Prediction1 to Prediction2 Comparison

PG Trial File: pr_grass_tracer_Experiment_56.txt

PG Prediction File 1: ARAC\nodeposition\pg_56_nozd.arac

PG Prediction File 2: ARAC\sv_nozd\pg_56_sv_nozd.arac

Figure M-45a. NARAC Sigma-v Experimental and Sigma-v Calculated Predictions to Trial 56 on Linear Scale: Stability Category is 4



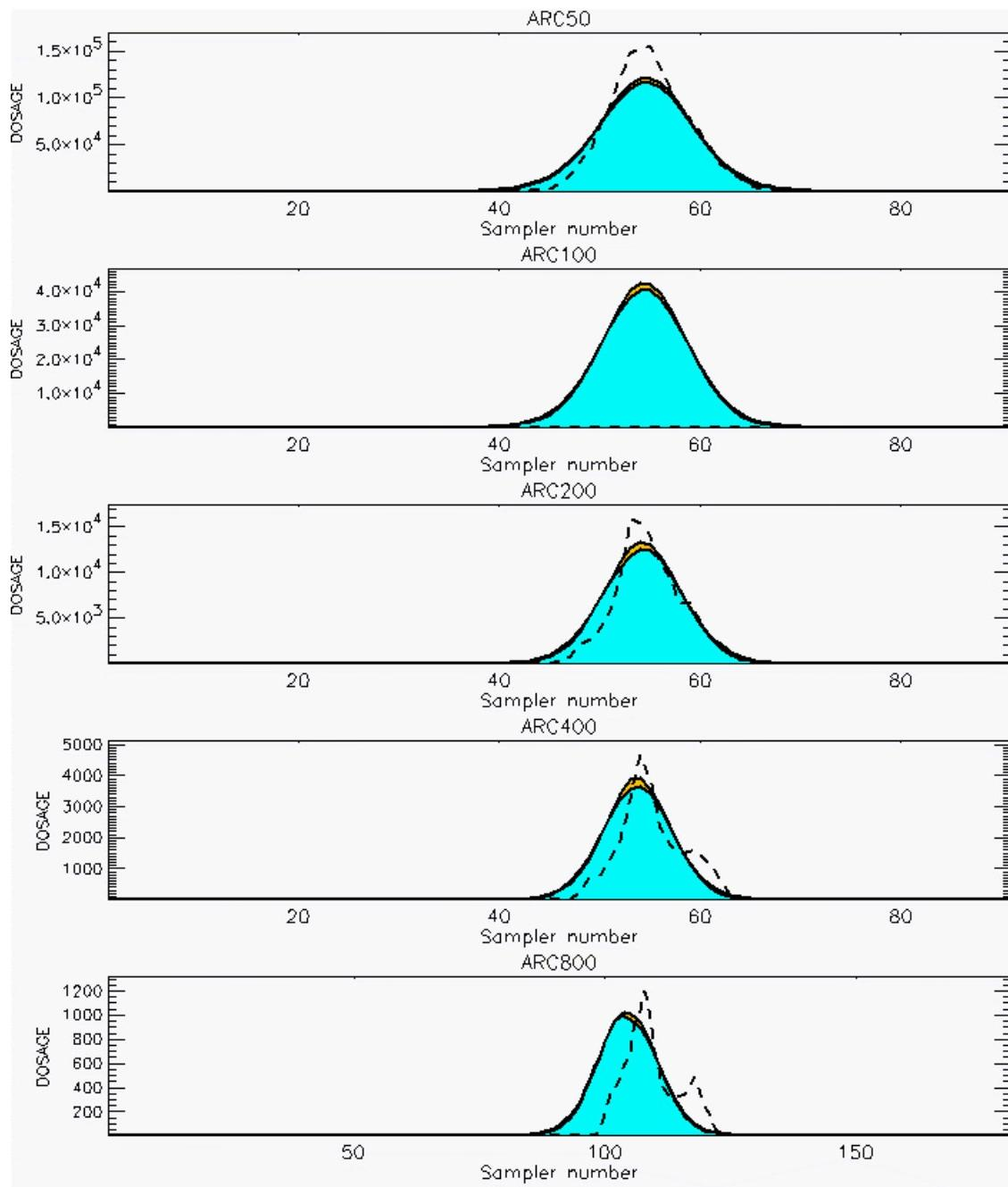
PG Prediction1 to Prediction2 Comparison

PG Trial File: pr_grass_tracer_Experiment_56.txt

PG Prediction File 1: ARAC\nodeposition\pg_56_novd.arac

PG Prediction File 2: ARAC\sv_novd\pg_56_sv_novd.arac

Figure M-45b. NARAC Sigma-v Experimental and Sigma-v Calculated Predictions to Trial 56 on Logarithmic Scale: Stability Category is 4



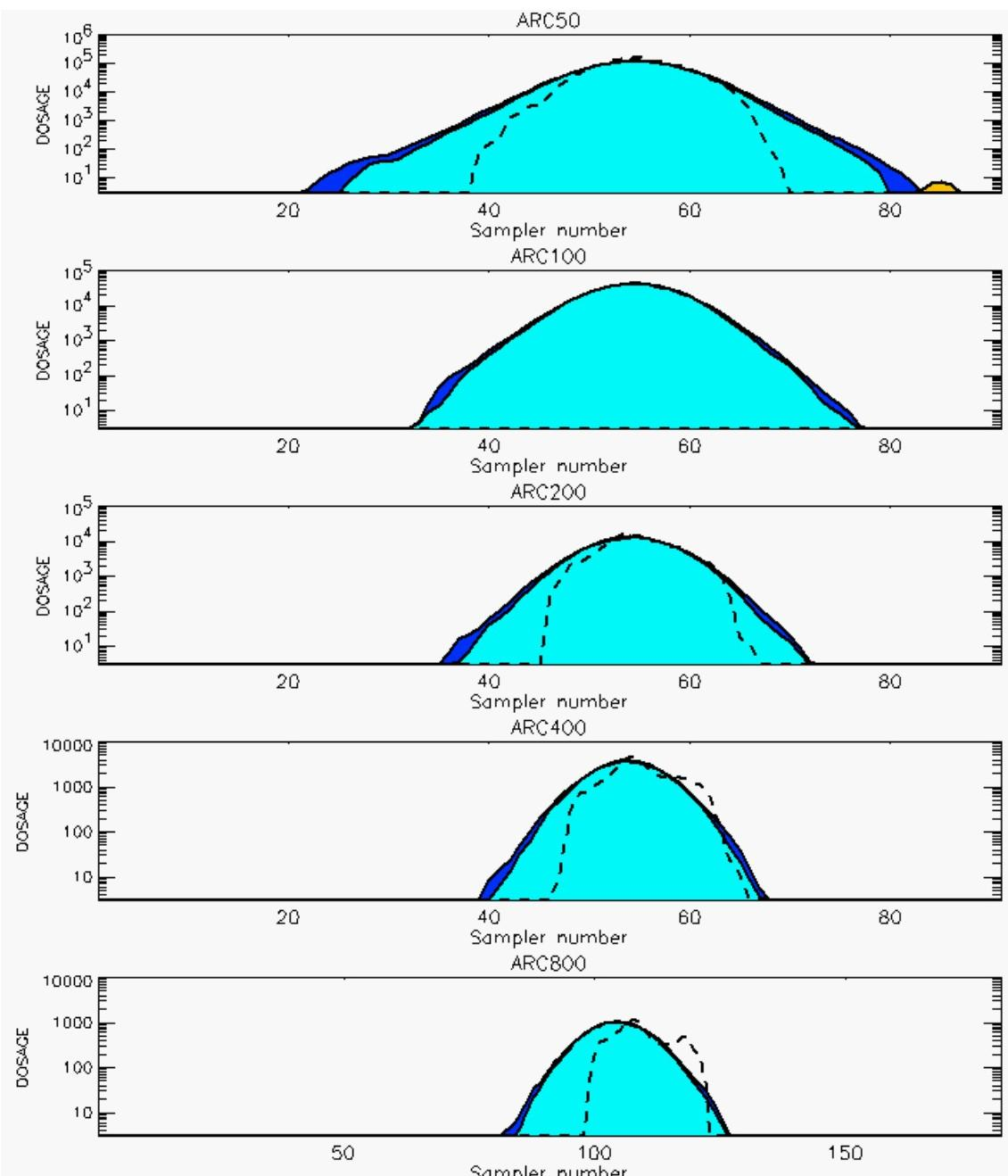
PG Prediction1 to Prediction2 Comparison

PG Trial File: pr_grass_tracer_Experiment_57.txt

PG Prediction File 1: ARAC\nodeposition\pg_57_nozd.arac

PG Prediction File 2: ARAC\sv_nozd\pg_57_sv_nozd.arac

Figure M-46a. NARAC Sigma-v Experimental and Sigma-v Calculated Predictions to Trial 57 on Linear Scale: Stability Category is 3



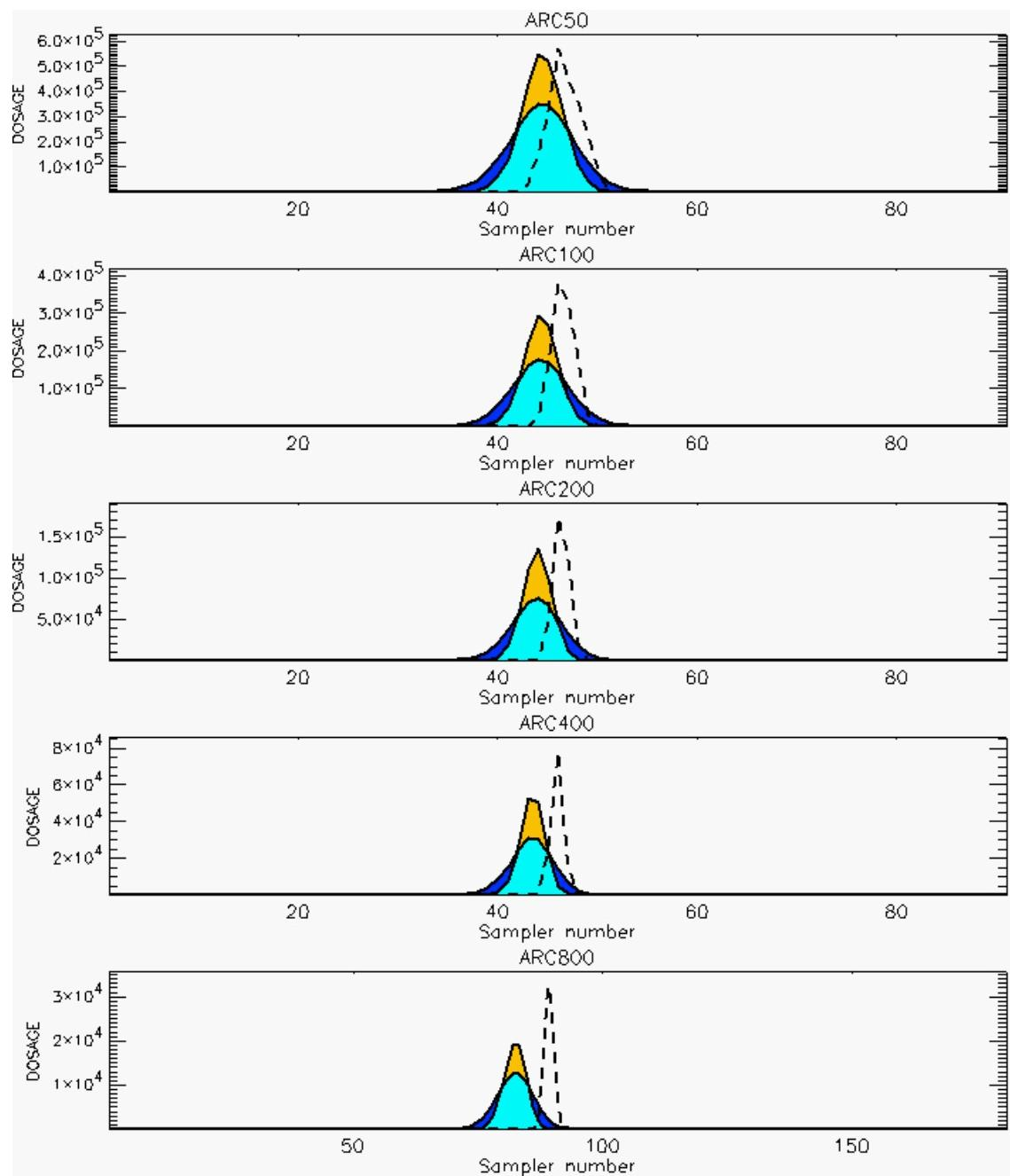
PG Prediction1 to Prediction2 Comparison

PG Trial File: pr_grass_tracer_Experiment_57.txt

PG Prediction File 1: ARAC\nodeposition\pg_57_nozd.arac

PG Prediction File 2: ARAC\sv_nozd\pg_57_sv_nozd.arac

Figure M-46b. NARAC Sigma-v Experimental and Sigma-v Calculated Predictions to Trial 57 on Logarithmic Scale: Stability Category is 3



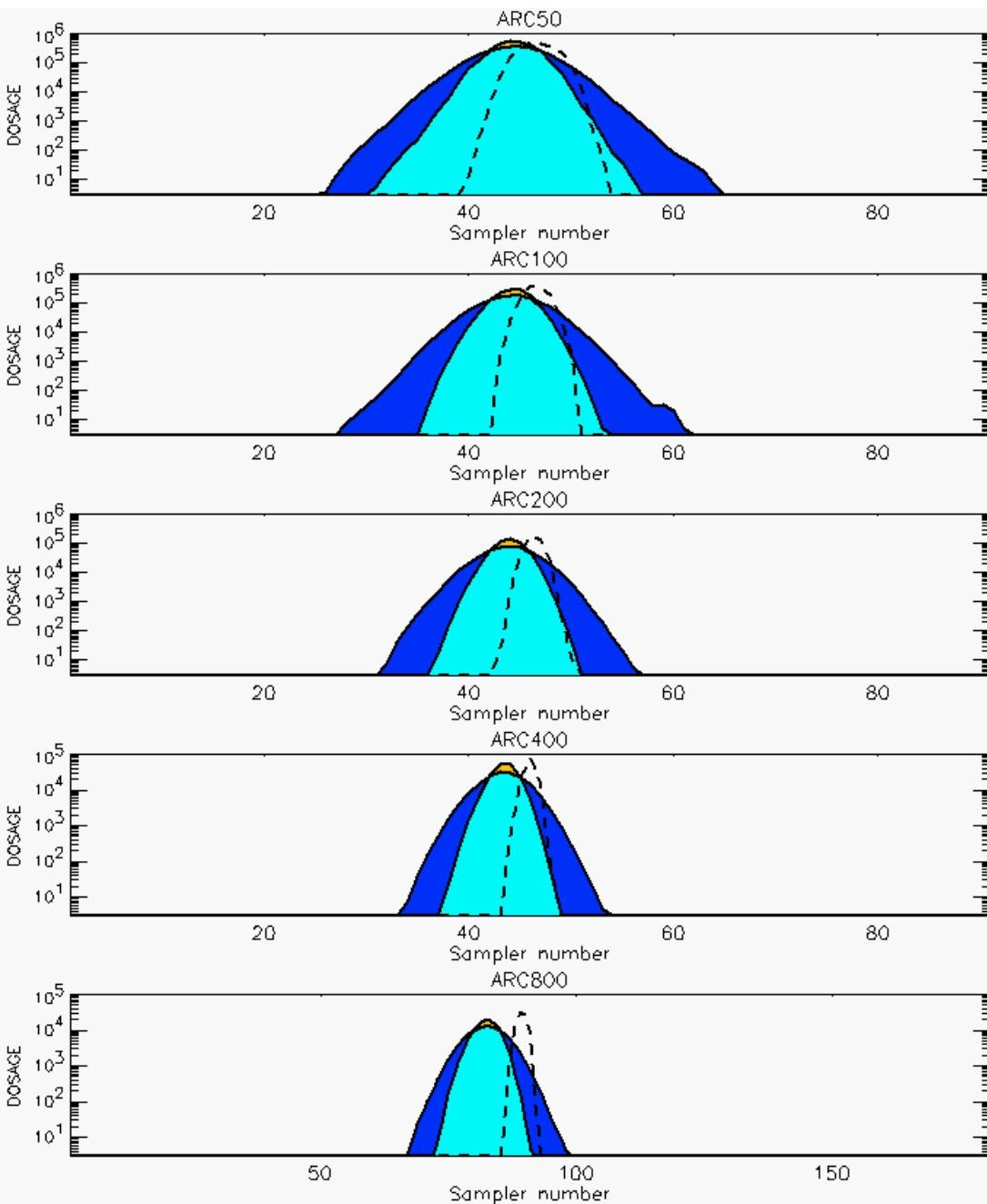
PG Prediction1 to Prediction2 Comparison

PG Trial File: pr_grass_tracer_Experiment_58.txt

PG Prediction File 1: ARAC\nodeposition\pg_58_novd.arac

PG Prediction File 2: ARAC\sv_novd\pg_58_sv_novd.arac

Figure M-47a. NARAC Sigma-v Experimental and Sigma-v Calculated Predictions to Trial 58 on Linear Scale: Stability Category is 6



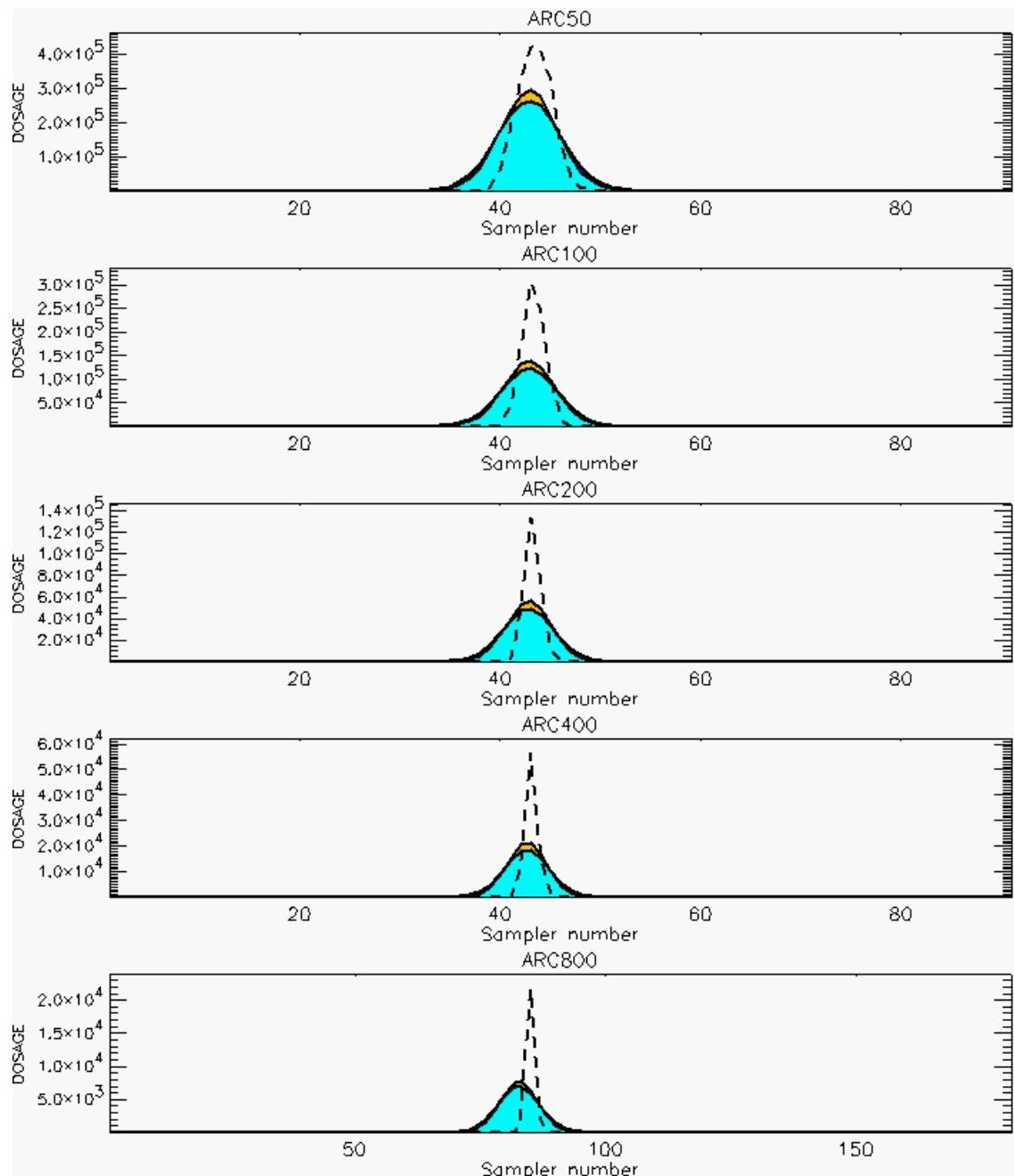
PG Prediction1 to Prediction2 Comparison

PG Trial File: pr_grass_tracer_Experiment_58.txt

PG Prediction File 1: ARAC\nodeposition\pg_58_novd.arac

PG Prediction File 2: ARAC\sv_novd\pg_58_sv_novd.arac

Figure M-47b. NARAC Sigma-v Experimental and Sigma-v Calculated Predictions to Trial 58 on Logarithmic Scale: Stability Category is 6



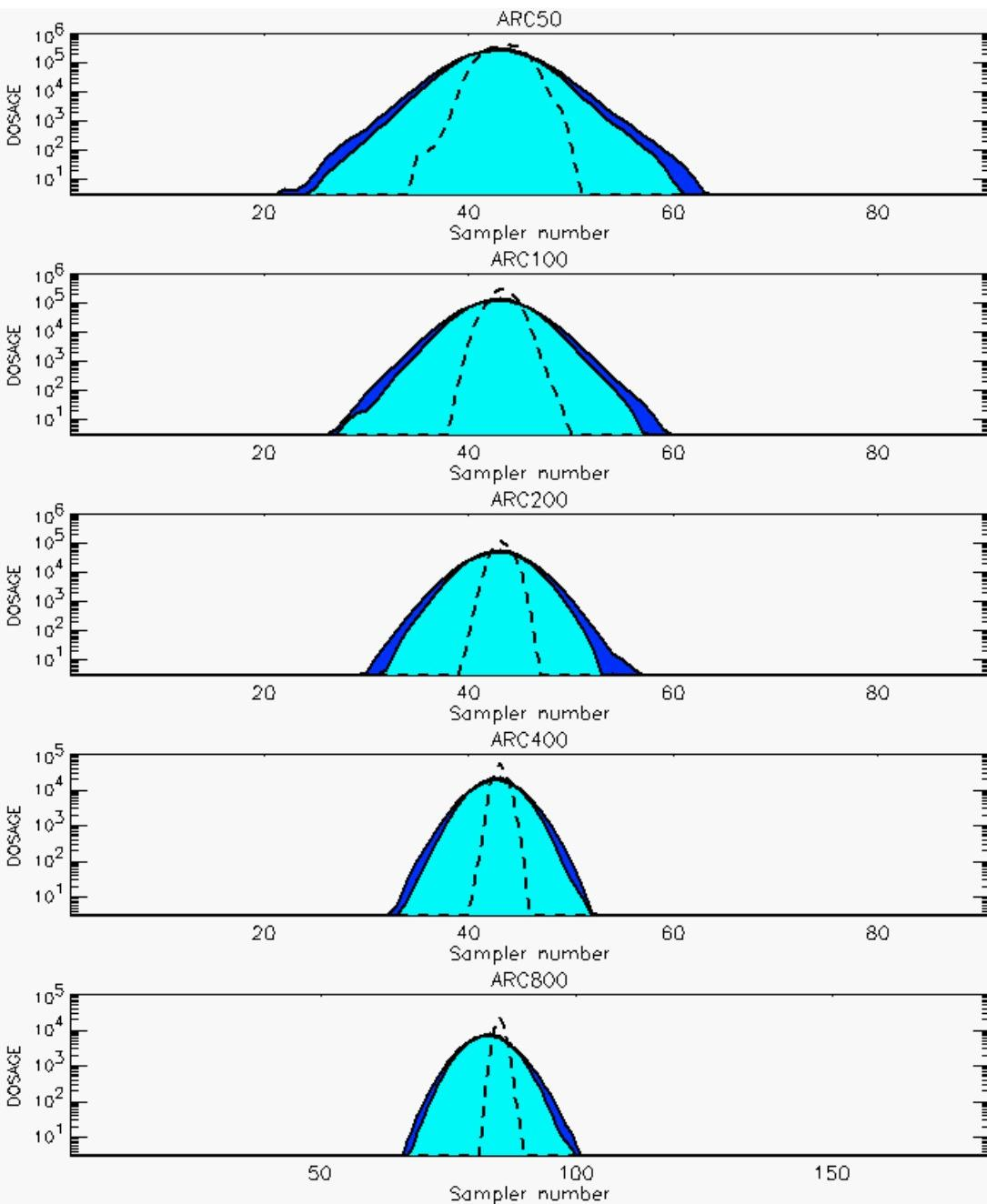
PG Prediction1 to Prediction2 Comparison

PG Trial File: pr_grass_tracer_Experiment_59.txt

PG Prediction File 1: ARAC\nodeposition_replace\pg_59_nozd.arac

PG Prediction File 2: ARAC\sv_nozd\pg_59_sv_nozd.arac

Figure M-48a. NARAC Sigma-v Experimental and Sigma-v Calculated Predictions to Trial 59 on Linear Scale: Stability Category is 5



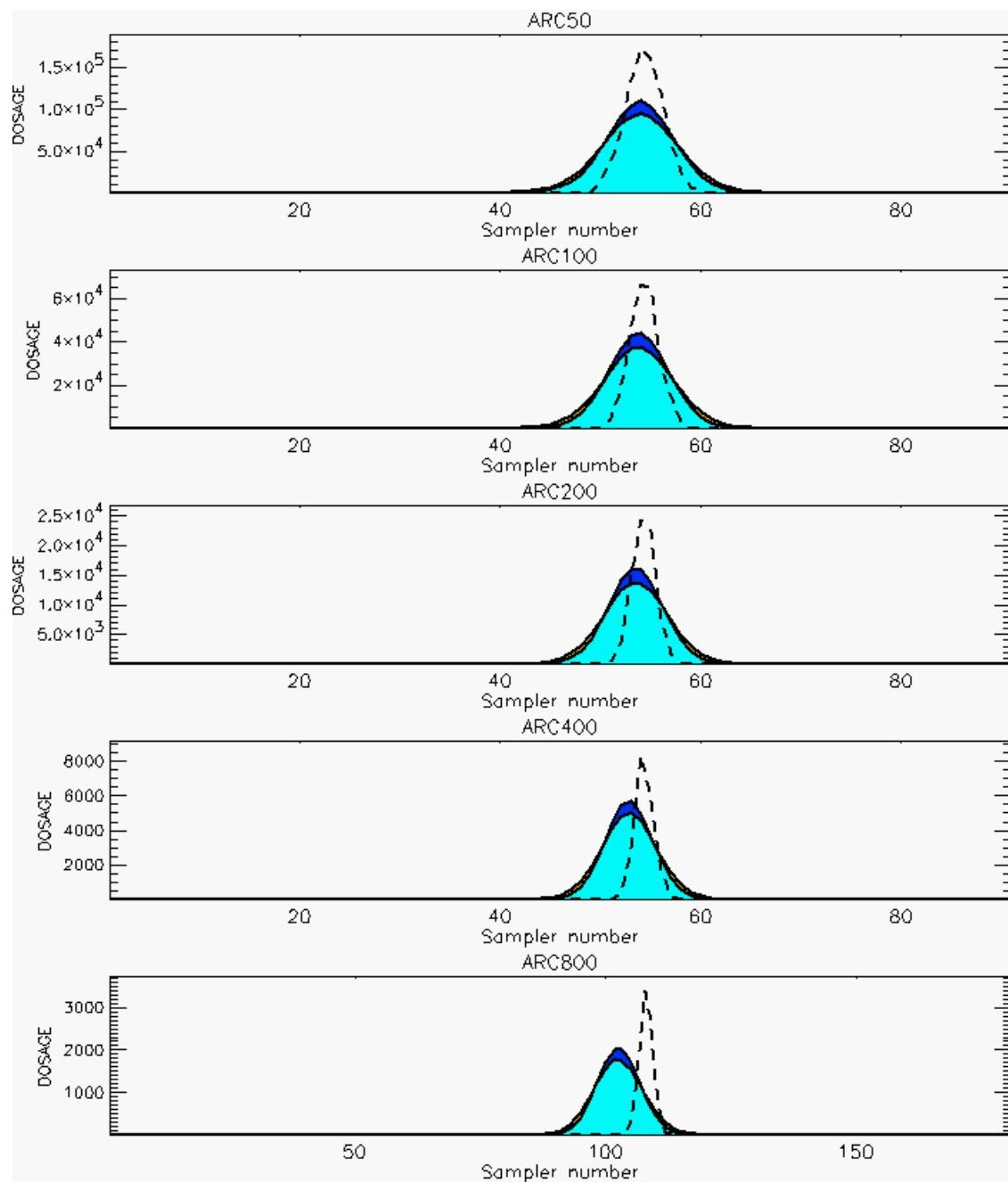
PG Prediction1 to Prediction2 Comparison

PG Trial File: pr_grass_tracer_Experiment_59.txt

PG Prediction File 1: ARAC\nodeposition_replace\pg_59_nozd.arac

PG Prediction File 2: ARAC\sv_nozd\pg_59_sv_nozd.arac

Figure M-48b. NARAC Sigma-v Experimental and Sigma-v Calculated Predictions to Trial 59 on Logarithmic Scale: Stability Category is 5



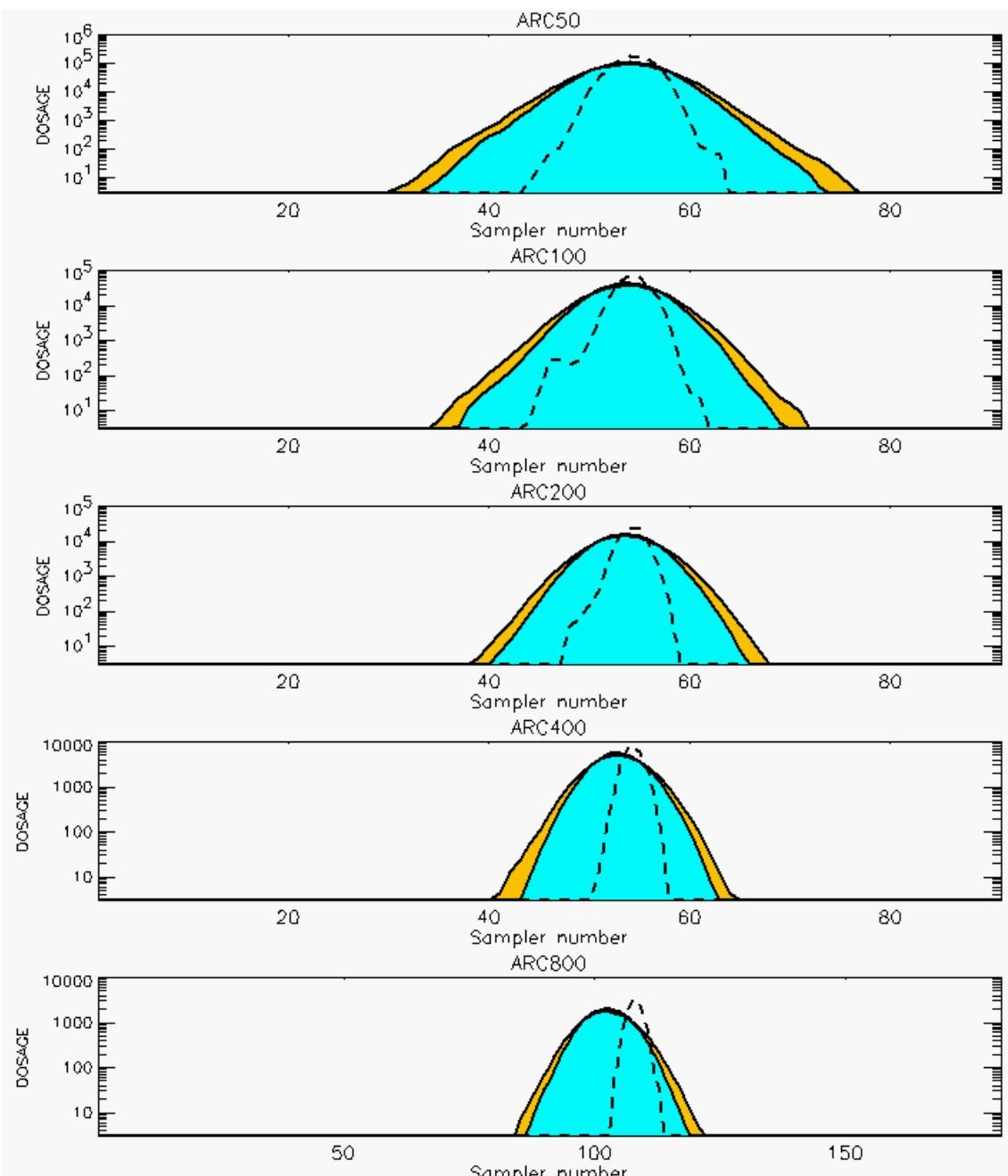
PG Prediction1 to Prediction2 Comparison

PG Trial File: pr_grass_tracer_Experiment_60.txt

PG Prediction File 1: ARAC\nodeposition\pg_60_nozd.arac

PG Prediction File 2: ARAC\sv_nzd\pg_60_sv_nzd.arac

Figure M-49a. NARAC Sigma-v Experimental and Sigma-v Calculated Predictions to Trial 60 on Linear Scale: Stability Category is 5



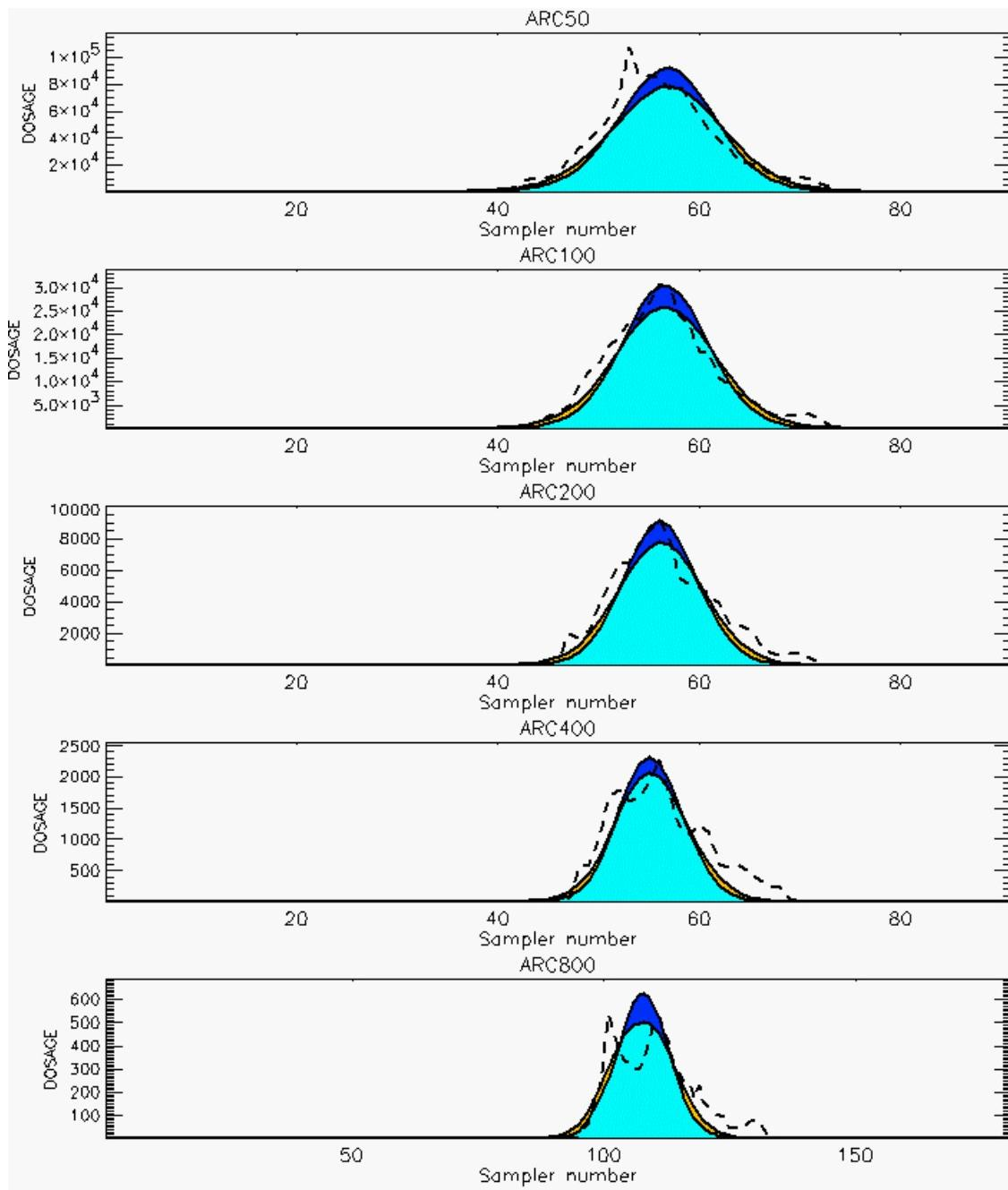
PG Prediction1 to Prediction2 Comparison

PG Trial File: pr_grass_tracer_Experiment_60.txt

PG Prediction File 1: ARAC\nodeposition\pg_60_novd.arac

PG Prediction File 2: ARAC\sv_novd\pg_60_sv_novd.arac

Figure M-49b. NARAC Sigma-v Experimental and Sigma-v Calculated Predictions to Trial 60 on Logarithmic Scale: Stability Category is 5



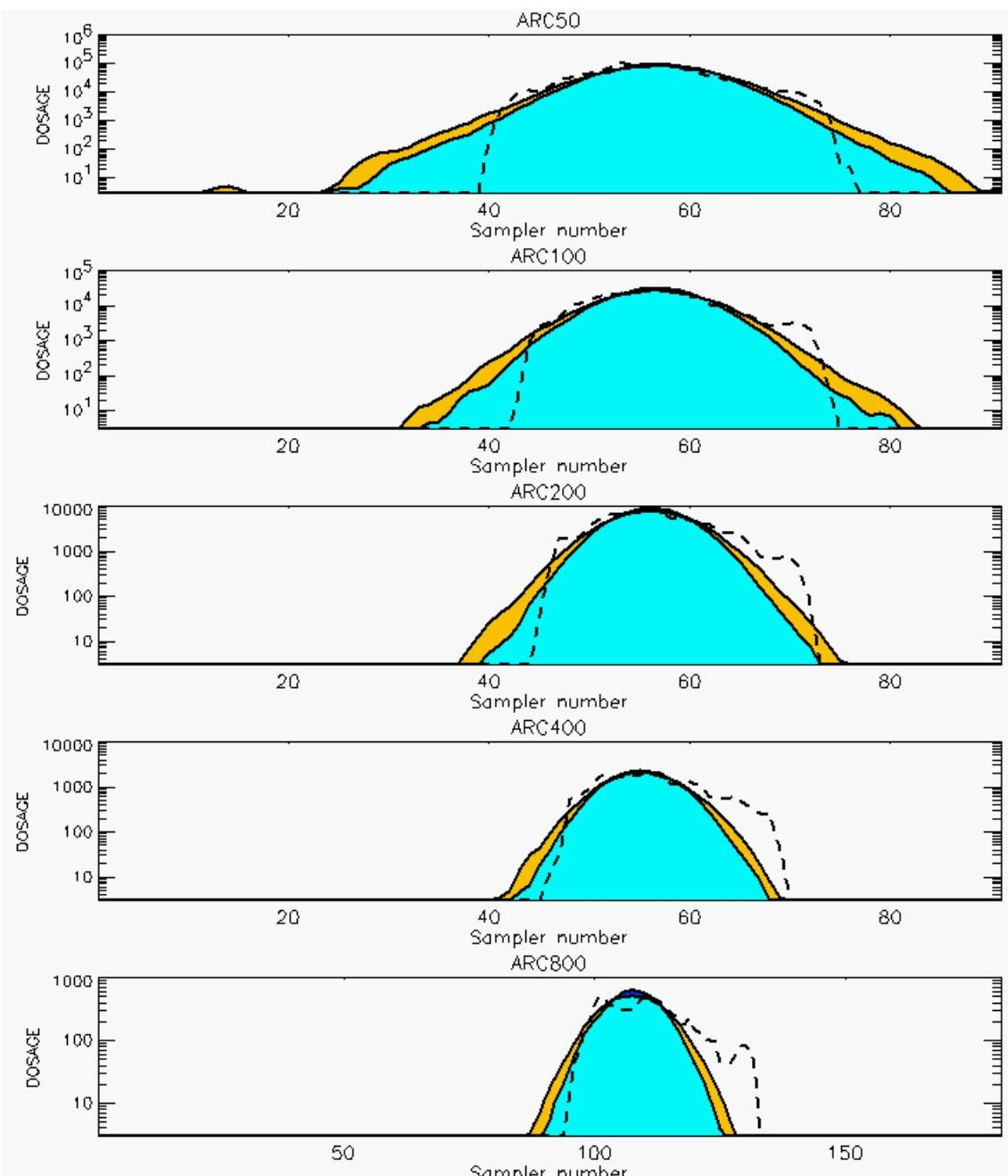
PG Prediction1 to Prediction2 Comparison

PG Trial File: pr_grass_tracer_Experiment_61.txt

PG Prediction File 1: ARAC\nodeposition\pg_61_nozd.arac

PG Prediction File 2: ARAC\sv_nozd\pg_61_sv_nozd.arac

Figure M-50a. NARAC Sigma-v Experimental and Sigma-v Calculated Predictions to Trial 61 on Linear Scale: Stability Category is 3



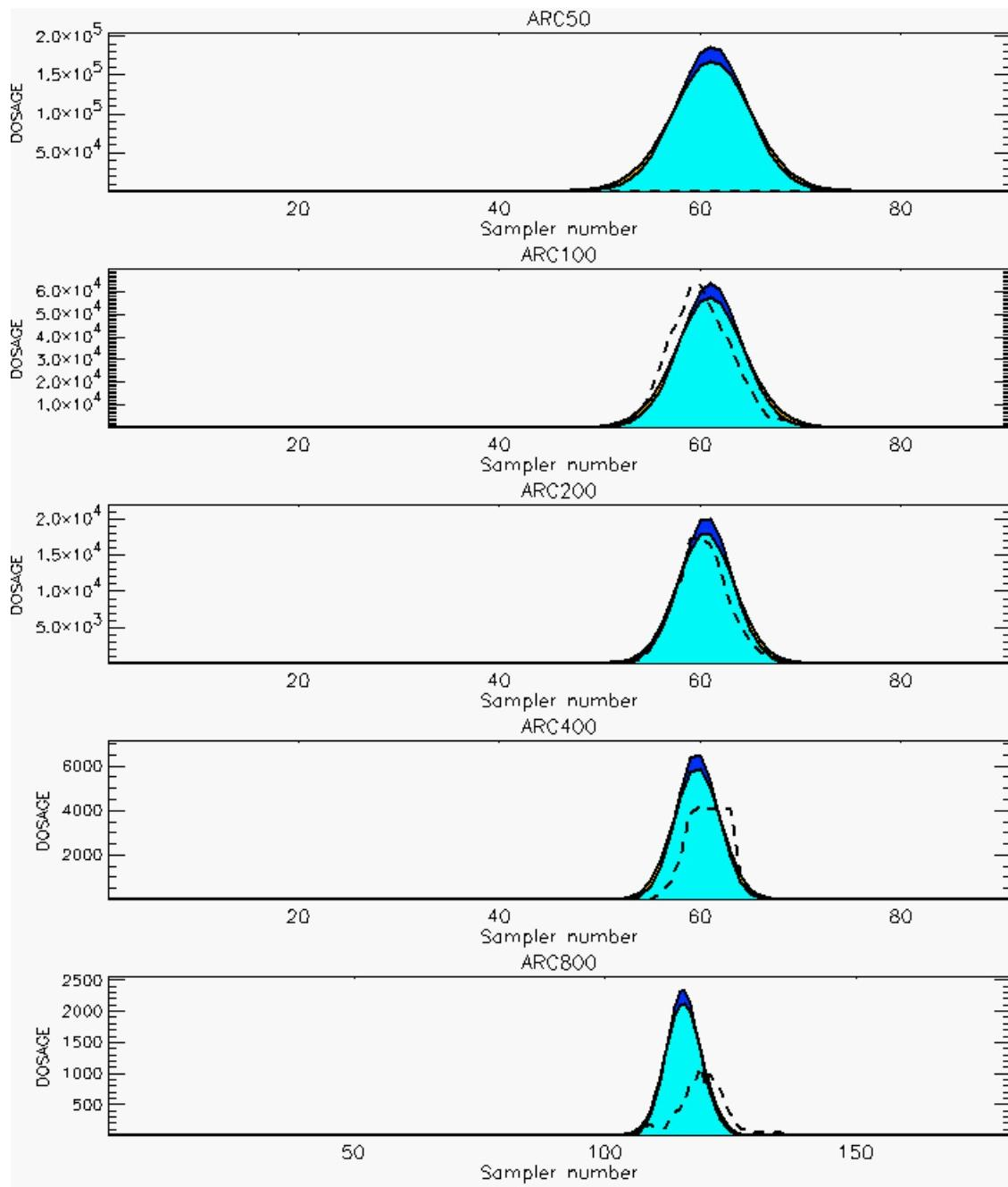
PG Prediction1 to Prediction2 Comparison

PG Trial File: pr_grass_tracer_Experiment_61.txt

PG Prediction File 1: ARAC\nodeposition\pg_61_nozd.arac

PG Prediction File 2: ARAC\sv_nozd\pg_61_sv_nozd.arac

Figure M-50b. NARAC Sigma-v Experimental and Sigma-v Calculated Predictions to Trial 61 on Logarithmic Scale: Stability Category is 3



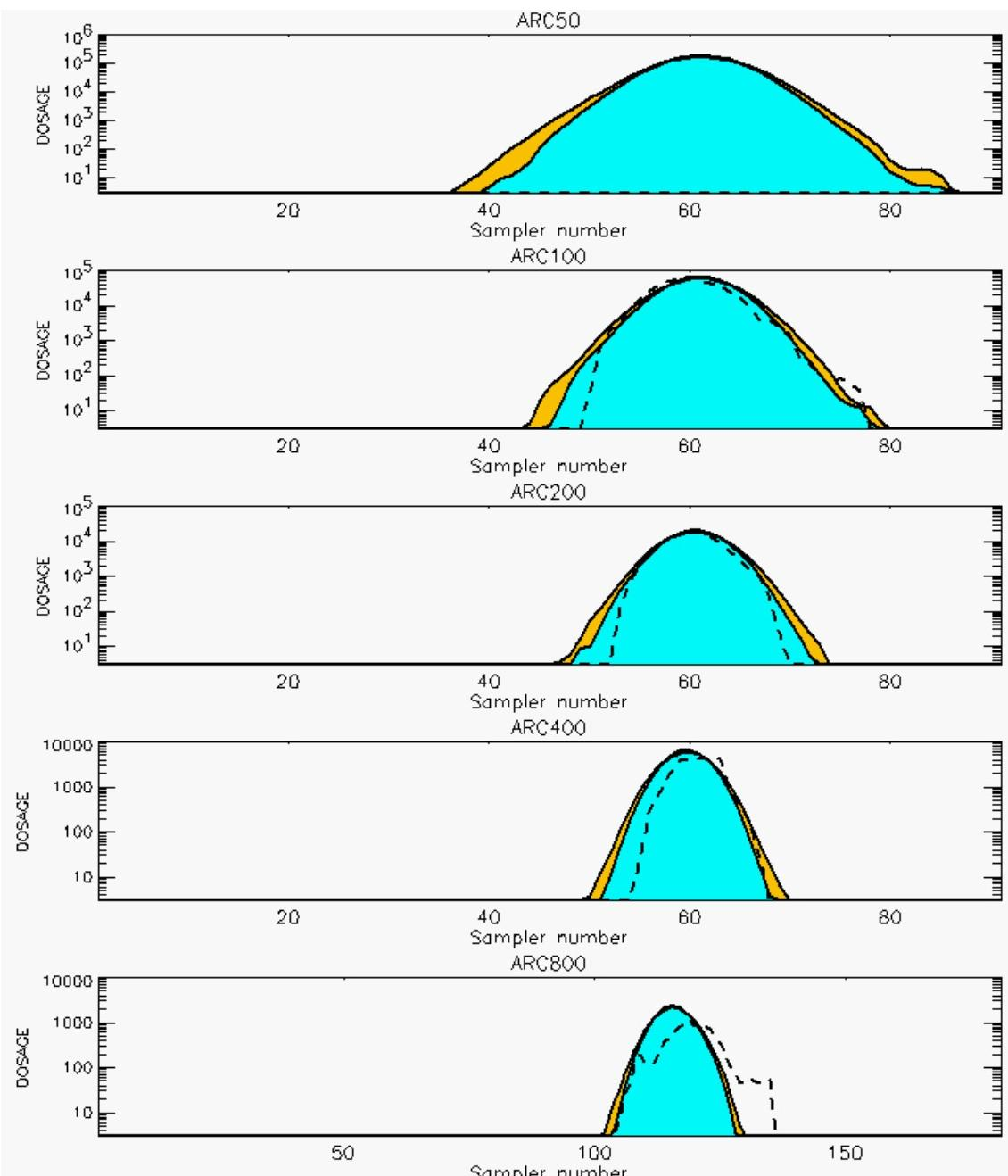
PG Prediction1 to Prediction2 Comparison

PG Trial File: pr_grass_tracer_Experiment_62.txt

PG Prediction File 1: ARAC\nodeposition\pg_62_nozd.arac

PG Prediction File 2: ARAC\sv_nozd\pg_62_sv_nozd.arac

Figure M-51a. NARAC Sigma-v Experimental and Sigma-v Calculated Predictions to Trial 62 on Linear Scale: Stability Category is 2



PG Prediction1 to Prediction2 Comparison

PG Trial File: pr_grass_tracer_Experiment_62.txt

PG Prediction File 1: ARAC\nodeposition\pg_62_nozd.arac

PG Prediction File 2: ARAC\sv_nozd\pg_62_sv_nozd.arac

Figure M-51b. NARAC Sigma-v Experimental and Sigma-v Calculated Predictions to Trial 62 on Logarithmic Scale: Stability Category is 2

REFERENCES

- M-1. Barad, M. L. (Editor), *Project Prairie Grass, A Field Program in Diffusion*, Geophysical Research Papers No. 59, Volumes I and II, DTIC #AD-152572/AFCRC-TR-58-235(I), Air Geophysical Laboratory, Hanscom Air Force Base, MA, 1958.
- M-2. Irwin, J. S. and Rosu, M-R., *Comments on a Draft Practice for Statistical Evaluation of Atmospheric Dispersion Models*, Proceedings of the 10th Joint Conference on the Applications of Air Pollution Meteorology. American Meteorological Society, Boston, pp. 6-10, 1998.

APPENDIX N
TASK ORDER EXTRACT

APPENDIX N

TASK ORDER EXTRACT

DC-9-1797

TITLE: Support for DTRA and LLNL in the Validation Analysis of Hazardous Material Transport and Dispersion Prediction Models

This task order is for work to be performed by the Institute for Defense Analyses (IDA) under Contract DASW01-98-C-0067, for the Defense Threat Reduction Agency (DTRA) in the Department of Defense. This task order authorizes funding for FY 2000.

1. BACKGROUND:

The Hazard Prediction and Assessment Capability (HPAC) is a suite of codes that predicts the effects of hazardous material releases into the atmosphere and their impact on civilian and military populations. The software can use integrated source terms, high-resolution weather forecasts, and particulate transport models to predict hazard areas produced by battlefield or terrorist use of weapons of mass destruction (WMD), by conventional counterforce attacks against WMD facilities, or by military and industrial accidents. HPAC is a forward deployable, counterproliferation and counterforce capability software tool available for government, government-related, or academic use. This tool assists warfighters in selecting weapon mixes for targets containing WMD and in emergency response to hazardous agent release. HPAC's relatively fast-running, physics-based algorithms enable users to model and predict hazard areas and human collateral effects in minutes.

The DTRA Verification and Validation (V&V) Program represents ongoing activities performed in parallel with development of all predictive codes in support of HPAC. One element of V&V is to perform code-on-code comparisons. In this strategy, each code receives the same input. In this manner, differences in the output predictions can lead to the identification of software bugs, or help to assess technical strengths and weaknesses of component algorithms within each code. In addition, a certain amount of credibility for both models is achieved when their predictions agree. When the inputs are simple, such as for fixed winds and simple terrain, the predictions tend to be dominated by the dispersion algorithms. Comparisons at this level of complexity are important to establish fundamental dispersion algorithm veracity, and to help discover software bugs. As more complex terrain and weather is included as input, the number of physical processes

responsible for transport and dispersion increases and the predictions become the result of many interdependent algorithm calculations.

Code-on-code comparisons will be performed using the DTRA code HPAC, the Lawrence Livermore National Laboratory (LLNL) code Atmospheric Release Advisory Capability (ARAC), and, possibly, Sandia-developed codes. These codes represent major national investments in transport and dispersion modeling within their respective applications. The comparisons will provide information from which to validate the HPAC and ARAC models (and perhaps others), as well as provide an opportunity to advance both technologies. The code comparisons will include short, medium, and long-range transport distances. Complex terrain and weather will also be included.

It is very difficult to separate meteorological uncertainty from the transport and dispersion model accuracy when comparing predictions to field-trial validation quality or real-world data. The validation challenge is to assess whether a model performs well over different field trials, and ultimately reflects real-world phenomena. Some codes perform better under certain conditions and specific scenarios. Hazard prediction models are generally developed for a range of user communities and applications. Each user community has a different set of requirements. Thus, the corresponding hazard models tend to be optimized for specific applications. The process of accrediting a model is always couched in terms of the end-user requirements.

Various figures-of-merit (FOM) are used to express model performance relative to observed data. Most FOMs tend to use manifestations of a ratio (geometric or arithmetic) between the predicted and measured quantities. The compared quantities are usually peak, plume-centerline, and off-axis concentration or dosage, as well as crosswind and along-wind spread and area coverage. Other FOMs may include the second-moment of the dosage and concentration values at a sampler location. All these FOMs are reasonable validation performance measures, but none of them explicitly expresses an application-oriented performance measure. A “yardstick” is needed that measures application-oriented model performance. The scale on this yardstick would clearly and directly relate to specific user’s concerns and needs. The pursuit of this “accreditation” performance measure is a new initiative at DTRA.

2. OBJECTIVE:

IDA will conduct independent analysis and special studies associated with verification and validation of the suite of models associated with the Hazard Assessment and Prediction Capability. IDA will support development of user-oriented performance measures of effectiveness (MOE) using validation quality field trial data sets; coordinate scenario definition and arbitration for code-on-code V&V activities; and assist DTRA and the Department of Energy in identifying the V&V parameter space associated with various hazard assessment and collateral effects communities.

The objectives of verification and validation analysis and coordination are: (1) to ensure that a consistent analysis approach is used when comparing model

predictions, and assist DTRA in the implementation of code-on-code analysis, comparisons, and interpretation; and (2) to define measures of effectiveness in terms of user-specific objectives and applications.

The scope of this effort may be expanded to other programs as directed by DTRA.

3. STATEMENT OF WORK:

As required by DTRA technical representatives, IDA will perform the following tasks:

- a. Support the planning, implementation, arbitration, and evaluation of code-on-code comparison activities. The purpose of these activities is to compare the transport and dispersion algorithms and corresponding output predictions between DTRA's suite of models, the DOE ARAC's suite of transport and dispersion models, and other models as called for. IDA will support code-on-code scenario definition, coordinate the identification and implementation of common performance measures, and support development of a common analysis approach. IDA will conduct independent analysis, as needed, to support the code-on-code analysis and interpretation of the results.
- b. Explore validation and accreditation MOEs given a framework that includes quantification of false positive and false negative predictions. This exploration would include the computation of MOE values for various formulations based on short-range comparisons of HPAC and ARAC predictions to field trial data. A key to interpreting the results of this effort will be obtaining a sense for what are the acceptable user requirements. These requirements will differ among potential user groups (military targeting, passive CB defense, civilian first responders, military versus civilian population human effects, etc.).

4. CORE STATEMENT:

This research is consistent with IDA's mission in that it will support specific analytical requirements of the sponsor and will assist the sponsor with planning efforts. Accomplishment of this task order requires an organization with experience in operationally oriented issues from a joint and combined perspective, which IDA, a Federally Funded Research and Development Center, is able to provide. It draws upon IDA's core competencies in Systems Evaluations and Operational Test and Evaluation. Performance of this task order will benefit from and contribute to the long-term continuity of IDA's research program.

REPORT DOCUMENTATION PAGE**Form Approved
OMB No. 0704-0188**

Public reporting burden for this collection of information is estimated to average 1 hour per response, including the time for reviewing instructions, searching existing data sources, gathering and maintaining the data needed, and completing and reviewing the collection of information. Send comments regarding this burden estimate or any other aspect of this collection of information, including suggestions for reducing this burden, to Washington Headquarters Services, Directorate for Information Operations and Reports, 1215 Jefferson Davis Highway, Suite 1204, Arlington, VA 22203-4302, and to the Office of Management and Budget, Paperwork Reduction Project (0704-0188), Washington, DC 20503.

1. AGENCY USE ONLY (Leave blank)		2. REPORT DATE January 2001	3. REPORT TYPE AND DATES COVERED Final: Jan. – Dec. 2000
4. TITLE AND SUBTITLE User-Oriented Measures of Effectiveness for the Evaluation of Transport and Dispersion Models		5. FUNDING NUMBERS DASW01-98-C-0067, OUSD(A) DC-9-1797	
6. AUTHOR(s) Dr. Steve Warner, Dr. Nathan Platt, Dr. James F. Heagy, et al.			
7. PERFORMING ORGANIZATION NAME(S) AND ADDRESS(ES) Institute for Defense Analyses 1801 N. Beauregard St. Alexandria, VA 22311		8. PERFORMING ORGANIZATION REPORT NUMBER IDA Paper P-3554	
9. SPONSORING/MONITORING AGENCY NAME(S) AND ADDRESS(ES) Dr. Allan Reiter Defense Threat Reduction Agency (DTRA) 6801 Telegraph Road Alexandria, VA 22310-3398		10. SPONSORING/MONITORING AGENCY REPORT NUMBER	
11. SUPPLEMENTARY NOTES			
12a. DISTRIBUTION/AVAILABILITY STATEMENT Approved for public release; distribution unlimited. Directorate for Freedom of Information and Security Review, 23 January 2001.		12b. DISTRIBUTION CODE	
13. ABSTRACT (Maximum 200 words) The goal of this task is to improve the verification, validation, and accreditation (VV&A) of hazard prediction and assessment models and capabilities. These studies are part of a larger joint VV&A effort that DTRA and the Department of Energy, via the Lawrence Livermore National Laboratory (LLNL), are conducting. This joint effort includes comparisons of the LLNL and DTRA transport and dispersion modeling systems – National Atmospheric Release Advisory Center (NARAC) and Hazard Prediction and Assessment Capability (HPAC), respectively. The Institute for Defense Analyses' role was to conduct independent analysis and special studies associated with this VV&A effort. This role included conducting comparisons between the models, providing analysis and discussions associated with these examinations, and exploring and developing measures of effectiveness (MOE) that can aid hazard prediction model validation and accreditation. This paper develops novel user-oriented MOEs for the evaluation of hazard prediction models. The usage and interpretation of these MOEs and their resulting values are described for model predictions of the short-range <i>Prairie Grass</i> field trials. NARAC and HPAC predictions of the <i>Prairie Grass</i> field trials are compared and examined with the aid of user-oriented MOEs. In addition, “standard” statistical measures are computed and some comparisons to the proposed MOEs are provided.			
14. SUBJECT TERMS Model validation; hazardous material transport and dispersion; HPAC; NARAC; measures of effectiveness; <i>Prairie Grass</i>			15. NUMBER OF PAGES 856
			16. PRICE CODE
17. SECURITY CLASSIFICATION OF REPORT Unclassified	18. SECURITY CLASSIFICATION OF THIS PAGE Unclassified	19. SECURITY CLASSIFICATION OF ABSTRACT Unclassified	20. LIMITATION OF ABSTRACT Unlimited
NSN 7540-01-280-5500			
Standard Form 298 (Rev. 2-89) Prescribed by ANSI Std. Z39-18 298-102			